

**Redox and Non-Redox Reactions Catalyzed by Biomimetic Flavin-based Organocatalysts
and the Discovery of Selective Oxidation Methods for the Preparation of N-Heterocycles**

by

PAWAN THAPA

**Presented to the Faculty of the Graduate School of
The University of Texas at Arlington in Partial Fulfillment
of the Requirements
for the Degree of**

DOCTOR OF PHILOSOPHY

THE UNIVERSITY OF TEXAS AT ARLINGTON

August 2018

Copyright © by Pawan Thapa 2018 All Rights Reserved



Acknowledgements

I would like to express my deepest sense of gratitude and sincere appreciation to my Supervisor and Professor, Dr. Frank Foss for providing me with an opportunity to work in his lab with project works of my interest. He has been very supportive and helpful throughout. I am highly impressed by his broad knowledge not just in organic chemistry but also in several areas of science, which has certainly inspired me to think and work beyond the comfort zone. He would devote much time with enthusiasm to discuss many problems during the course of this work which resulted into successful solutions to those problems. Dr. Foss will be one of the people behind my every good achievement in future. I will never forget his and his wife Dr. Ann Foss' great hospitality in every get together we had in his home and outside.

I owe my sincere gratitude to Professor Carl J. Lovely, Professor Junha Jeon, Professor Alejandro Bugarin, Professor Jongyun Heo and Dr. William Cleaver for their valuable feedback and constructive criticism in all interactions of research and teaching works we had within the Department. I have learned more than I had ever thought.

Dr. Mohammad Hossain, Dr. Diego Lopez and Dr. Sumit Bhawal are among the people who guided me in initial days to improve my technical skills. I would like to thank them for everything they have tolerated from me. My colleagues Shakar, Mohammad, Akop, Parham, Thiru, Ravi, Enrique, Udaya, Dananjaya, Bikash, Fakrul and Hasmal will always be remembered for all good memories in and outside the Department I have shared with them.

I am truly indebted to my collaborators Professor Brad Pierce and his students Sinjinee Sardar and Philip Palacios without whom, the EPR study would have been impossible. Their suggestions and co-operations are greatly admirable. My undergraduates Trevor, Carlos, Esai, Tam, Elizabeth,

Imaad, Ana, Charleston, Branston, and Maya were my driving force for all the passion they showed in their early age towards research works we shared.

Finally, I owe a debt of gratitude to my mother, wife, sisters and all my relatives for their encouragement and support. They have put up so many days and evenings with patience throughout, without which the successful completion of my study would be impossible. My daughter Priyasha's arrival to the world is the best memory I have ever had during my Ph.D. career and all my life. She is the reason for transforming my stress to enthusiasm. So thank you my daughter from the bottom of my heart. Lastly, I will leave my great respect to God for giving me strength and positive thoughts during every hard time of my life.

August 2018

Abstract

Redox and Non-Redox Reactions Catalyzed by Biomimetic Flavin-based Organocatalysts and the Discovery of Selective Oxidation Methods for the Preparation of N-Heterocycles

Pawan Thapa, Ph. D.

The University of Texas at Arlington, 2018

Supervising Professor: Frank W. Foss, Jr.

In nature, flavoproteins (FMN and FAD) are known to catalyze several chemical transformations which play a vital role in the growth, development, and survival of organisms. They are involved in one-electron and two-electron transfer reactions, photo-induced electron transfer reactions, dehydrogenase reactions, oxidative atom transfer reactions and also rare non-redox reactions. Their enhanced stability and ability to turn over in presence of dioxygen has inspired synthetic chemists, including our group, to perform biomimetic transformations within a range of function of natural flavoproteins.

In **chapter 1**, both intramolecular and intermolecular dehydrogenative coupling between the alpha carbon of tertiary amines and various nitrogen, phosphorus, and carbon-based nucleophiles are reported. This study signifies the flavin dependent oxidase type chemistry promoted by synthetic flavins, rendering the catalytic construction of some sophisticated heterocycles through an atom economical and aerobic approach. Mechanistic studies with different radical probes suggest the involvement of radical intermediates in the reaction cycle. Moreover, intramolecular kinetic isotope studies performed reveal possibility of Hydrogen atom abstraction being rate determining step.

In **chapter 2**, a non-redox type of chemistry is disclosed. A subclass of riboflavin mimics was found to catalyze C-C bond formation by activating small molecules in a new manner. This

approach was successfully applied to synthesize various industrially important dyes and chemical reagents. Additionally, the relationship discovered between molecular structure and catalytic function of riboflavin mimics in these new chemical reactions revealed a plausible explanation for the function of natural riboflavin-dependent *hydroxynitrilase* enzymes in biological system. Mechanistic studies using nuclear magnetic resonance (NMR) spectroscopy, UV-vis spectroscopy and electron paramagnetic resonance (EPR) spectroscopy showed a possible frustrated lewis-pair (FLP) type of interaction between aldehydes and flavin mimics.

In **chapter 3**, studies on benzimidazole synthesis by iron catalysts will be discussed. 1,2-disubstituted benzimidazoles serve as important class of molecules in several area of chemistry including drug discovery, catalysis, etc. Our investigation in this area with redox active iron catalysts revealed *N,N'*-disubstituted-*ortho*-phenylenediamine substrates being superior to *N,N*-disubstituted-*ortho*-phenylenediamines in generating 1,2-disubstituted benzimidazoles. Extensive UV-vis spectroscopy studies and kinetic studies have been performed in addition to EPR spectroscopy to understand the nature of mechanism. Both Lewis acid property and redox active property of iron trichloride are thought to play a significant role in catalysis. Smooth complex formation between *N,N'*-disubstituted-*ortho*-phenylenediamine substrates and iron catalyst provides the driving force for the electron transfer process to form productive iminium intermediate.

A simple method for chemo-selective oxidation of isoindolines to isoindolinones was also studied in **chapter 4**. This method utilizes no catalyst, no additive, mild condition and is highlighted as just solvent mediated transformation. Mechanistic investigation shows hydrogen atom abstraction process leading to isoindole intermediates which further binds to oxygen to give desired isoindolinones products.

Table of Contents

Acknowledgements	iii
Abstract	v
List of Illustrations	ix
List of Tables.....	xiii
Chapter 1 Introduction to flavin and its chemistry.....	1
1.1. Flavoproteins and their functions.....	1
1.1.1. Discovery and structures of flavins	1
1.1.2. Flavin dependent enzymes and their fuctions	2
1.1.3. Flavin catalytic cycle.....	3
1.1.4. Nitroalkane oxidase.....	4
1.1.5. Monoamine oxidases	5
1.1.6. Hydroxynitrile Lyase/Oxynitrilase	7
1.2. Biomimetic organocatalysts.....	8
1.3. Frustrated lewis pairs.....	9
Chapter 2 Flavin-catalyzed Aerobic Cross-dehydrogenative Coupling Reactions.....	11
2.1. Background.....	12
2.2. Results and discussions.....	16
2.3. Conclusion.....	32
Chapter 3 Flavin-catalyzed Green Synthesis of Michler Hydride Derivatives.....	34
3.1. Background.....	34
3.2. Results and discussions.....	35

3.3. Conclusion.....	50
Chapter 4 Iron-catalyzed 1,2-disubstituted Benzimidazole Synthesis by Cross- dehydrogenative Coupling Strategy.....	51
4.1. Background.....	51
4.2. Results and discussions.....	52
4.3. Conclusion.....	68
Chapter 5 Dioxane-mediated Selective Oxidation of Isoindolines to Isoindolinones.....	70
5.1. Background.....	70
5.2. Results and discussions.....	73
5.3. Conclusion.....	83
Appendix A List of abbreviation.....	84
Appendix B General experimental procedure	85
Appendix C NMR spectra of compounds.....	187
Biographical Information	635

List of Illustrations

List of Figures

Figure 1.1 Natural and Non-natural Flavin Catalysts.....	1
Figure 1.2 Catalytic cycle of flavin based on redox function.....	4
Figure 1.3 Reaction cycle for NAO catalyzed oxidation of nitroalkane.....	5
Figure 1.4 Radical mechanism for MAO catalyzed oxidation of amines.....	6
Figure 1.5 Nucleophilic pathway for MAO catalyzed oxidation of amines.....	6
Figure 1.6 Proposed mechanism for activation of carbonyl group by flavin in oxynitrilase.....	7
Figure 1.7 Examples of biomimetic organocatalysts.....	8
Figure 1.8 Report on first metal free reversible H ₂ activation.....	10
Figure 1.9 [Fe]-hydrogenase involved in H ₂ cleavage.....	11
Figure 2.1 Flavin dependent Reticulin oxidase catalyzed reaction.....	12
Figure 2.2 Bond dissociation energy of some sp ³ C-H bonds.....	13
Figure 2.3 Ruthenium catalyzed first aerobic oxidative CDC reaction.....	13
Figure 2.4 Copper catalyzed oxidative CDC reaction.....	13
Figure 2.5 Biomimetic enantioselective oxidative CDC approach.....	14
Figure 2.6.1 Copper catalyzed enantioselective CDC reaction with unactivated aldehyde.....	15
Figure 2.6.2 Metal free enantioselective CDC approach with unactivated ketones.....	15
Figure 2.7 Detection of aldehyde from reaction of trisubstituted substrate 2.1q.....	31
Figure 2.8 ¹ H NMR of fully oxidized THIQ species isolated from crude reaction mixture.....	31
Figure 2.8 Proposed mechanism for artificial flavin mimic catalyzed CDC reaction.....	32
Figure 3.1 Discovery of current method.....	36

Figure 3.2 A (Hydride donors), B (HIV-I Integrase Inhibitor, IC ₅₀ = 50 μM), and C (Ligand for selective recognition of Cu ²⁺ in presence of other metals).....	36
Figure 3.3 Widely accepted mechanism (left); our hypothesized working model (right).....	36
Figure 3.4 UV-vis study for formaldehyde-flavin adduct formation.....	47
Figure 3.5 NMR spectrum of aromatic region for crude mixture.....	47
Figure 3.6 ³¹ P NMR of Et ₃ PO without FLClO ₄	47
Figure 3.7 control reaction with Bronsted acid HClO ₄	47
Figure 3.8 ³¹ P NMR for Ph ₃ PO only (red), and mixture of FLClO ₄ (3equiv.) and Ph ₃ PO.....	48
Figure 3.9 Plausible pathways for flavin catalyzed formaldehyde activation step.....	49
Figure 4.1 Some examples of medicinally important 1,2-disubstituted benzimidazoles.....	51
Figure 4.2 Comparative NMR study for a mixture of isomeric substrate.....	54
Figure 4.3 Spectral time course for <i>N,N'</i> -diethyl- <i>o</i> -phenylenediamine.....	62
Figure 4.4 Spectral time course for <i>N,N</i> -diethyl- <i>o</i> -phenylenediamine	62
Figure 4.5 Spectral time course for Iron (III) chloride at 60 °C.....	62
Figure 4.6 Spectral time course for Copper (II) chloride at 60 °C.....	62
Figure 4.7 Spectral time course for Silver (I) nitrate at 60 °C.....	63
Figure 4.8 Spectral time course for Nickel (II) chloride at 60 °C.....	63
Figure 4.9 Spectral time course at rt and inert condition.....	63
Figure 4.10 spectral time course at rt in inert atmosphere with H ₂ O ₂ additive.....	63
Figure 4.11 Broad scan mode comparison	65
Figure 4.12 Parallel mode comparison.....	65
Figure 4.13 Spectral time course for deuterated and non-deuterated substrate.....	65
Figure 4.14 Plausible reaction mechanism for synthesis of benzimidazole products.....	68

Figure 5.1 Bioactive isoindolinone molecules.....	69
Figure 5.2 Reductive amination/cyclization strategy for isoindolinone synthesis.....	69
Figure 5.3 Selective monoreduction strategy for isoindolinone synthesis.....	70
Figure 5.4 Intramolecular aminative cyclization strategies for isoindolinone synthesis.....	70
Figure 5.5 DMSO mediated tandem cross-dehydrogenative coupling strategy.....	71
Figure 5.6 Bischler-Napieralski type cyclization strategy for isoindolinone synthesis.....	71
Figure 5.7 Palladium catalyzed carbonylation strategies for isoindolinone synthesis.....	72
Figure 5.8 Development of solvent mediated isoindolinone synthesis.....	69
Figure 5.9 Reaction scope at 100 °C for 2 days in open flask.....	74
Figure 5.10 EPR spectra for selected reaction conditions.....	81
Figure 5.11 Proposed reaction pathways.....	83

List of Schemes

Scheme 2.1 Effect of different Bronsted acids on Aza-Henry reaction with THIQ.....	28
Scheme 2.2 Study on radical scavenging effect.....	29
Scheme 2.3 Study on intramolecular kinetic isotope effect.....	29
Scheme 2.4 Evidence for possible hydrolysis of iminium intermediates.....	30
Scheme 2.5 Reaction scope with imine substrate.....	31
Scheme 3.1 A) Scope of benzaldehyde and B) control experiment with CD ₃ CN.....	44
Scheme 3.2 Control reactions with bronsted acid HClO ₄	45
Scheme 3.3 <i>N</i> -Meacridinium iodide catalyzed reaction (A); LUMO level energy of acridinium catalyst and flavinium catalyst (B).....	49
Scheme 4.1 Synthetic strategies for 1,2-disubstitutedbenzimidazoles.....	52
Scheme 4.2 Parallel studies with two isomers in same condition (left); comparative study of two isomers in the mixture.....	53
Scheme 4.3 control reactions.....	61
Scheme 4.4 Scope of mono-imine intermediates.....	66
Scheme 4.5 Attempt on monoimine synthesis.....	66
Scheme 4.6 Effect of base in reaction scope.....	67
Scheme 5.1 Challenges in oxidation of Isoindoline.....	73
Scheme 5.2 Synthetic scope of the method.....	78
Scheme 5.3 Mechanistic investigation.....	80
Scheme 5.4 Study on parallel kinetic isotope effect.....	80

List of Table

Table 2.1 Optimization of reaction conditions for intramolecular C-N bond formation.....	18
Table 2.2 Catalyst screening.....	19
Table 2.3 Substrate scope for intramolecular C-N bond formation in THIQ substrate.....	21
Table 2.4 Substrate scope for C-N bond formation in ortho-phenylenediammine substrate.....	22
Table 2.5 Catalyst screening for C-P bond formation.....	23
Table 2.6 Substrate scope for C-P bond formation.....	24
Table 2.7 Optimization of Reaction condition for C-C bond formation.....	26
Table 2.8 Substrate scope for C-C bond formation.....	27
Table 3.1 Screening amount of HCHO.....	37
Table 3.2 Screening of temperature.....	37
Table 3.3 Screening of solvent.....	38
Table 3.4 Screening of atmosphere.....	38
Table 3.5 Optimization of reaction condition.....	39
Table 3.6 Substrate Scope study.....	42
Table 3.7 Multi-component reaction substrate scope study.....	43
Table 4.1 Screening of catalyst.....	55
Table 4.2 Screening of solvent.....	55
Table 4.3 Screening of reaction condition.....	56
Table 4.4 Substrate scope for <i>N,N'</i> -disubstituted- <i>o</i> -phenylenediammine.....	57
Table 4.5 Substrate scope for <i>N,N</i> -disubstituted- <i>o</i> -phenylenediammine.....	59
Table 4.6 Substrate scope for <i>N</i> -monosubstituted- <i>o</i> -phenylenediammine.....	60
Table 5.1 Screening of solvent.....	74

Table 5.2 Reaction selectivity at optimized condition.....	75
Table 5.3 Substrate Scope.....	77
Table AB1 Gutmann AN values for different acid sources in presence of lewis base Et ₃ PO...170	170
Table AB2 Screening of reaction condition in relation to chapter 5 work.....	183

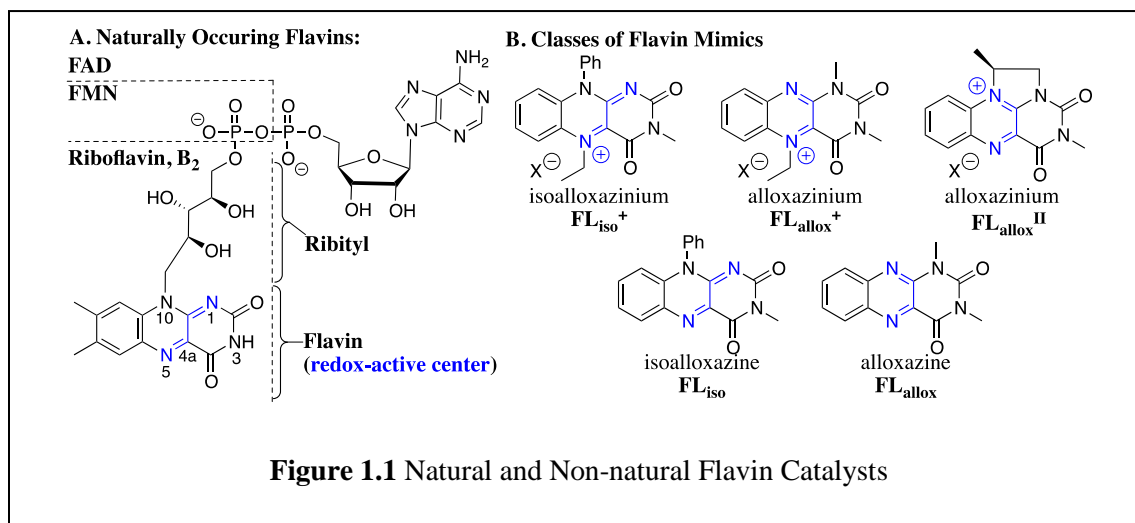
Chapter 1

Introduction to flavin and its chemistry

1.1 Flavoproteins and their functions

1.1.1. Discovery and structures of flavins

In 1879, an English chemist A. Wynter Blyth first isolated riboflavin as a bright yellow pigment from cow milk.¹ He coined the term 'lactochrome'. Later, two scientists Richard Kuhn in 1934² and Paul Karrer in 1935³ provided structural information of the compound. The compound was found to have a ribityl group at *N*-10 position of a tricyclic isoalloxazine and was later discovered as integral component of the coenzymes, flavin adenosine dinucleotide (FAD) and flavin mononucleotide (FMN). FAD differs to FMN in that FAD is condensation product of FMN and AMP (adenosine monophosphate). An isomeric form of tricyclic core isoalloxazine **FL_{iso}** (**IA**) is termed as alloxazine **FL_{allox}** (**A**) (**Figure 1.1**).



1.1.2. Flavin dependent enzymes and their functions

Flavoenzymes are probably the most widely studied enzymes due to their involvement in large variety of chemical transformations, such as, energy production, natural product biosynthesis, biodegradation, DNA repair, protein folding, and neural development. About 1-3% of bacterial

and eukaryotic genomes are known to encode flavin dependent proteins.^{4,5} On the basis of type of reactions they catalyze, flavoenzymes are classified as follows:

General classification	Reaction Classification	Prototype
Redox reactions	Oxidation of carbon-heteroatom bond i. Carbon-Nitrogen oxidation ii. Carbon-Oxygen oxidation iii. Carbon-Sulfur oxidation	Nitroalkane oxidase Lysine specific demethylase Monoamine oxidase Glucose oxidase Prenylcysteine lyase
	Oxidation and reduction of C-C bond	Acyl-CoA dehydrogenase and oxidase
	Thiol/Disulfide chemistry	Glutathione Reductase
	Electron transfer reactions	Cytochrome P450 Reductase
	Oxygen reactions	Tryptophan-7-Halogenase Baeyer-Villiger Monooxygenase Oxidase
Non-redox reactions	Photochemical reactions Hydrolysis and formation of cyanohydrins	DNA Photolyase Oxynitrilase

1.1.3. Flavin catalytic cycle

The majority of flavoproteins perform redox-related transformation and therefore, a number of studies have been performed and an established mechanistic pathway has been proposed. Intensive studies carried out by Bruice, Massey, and Hemmerich on redox mechanisms of flavins and flavoproteins revealed the interesting and versatile roles of flavins as small organocatalysts. Consistent with their collective findings, the general catalytic cycle of flavin in biological system involving redox chemical change is represented in **Figure 1.2**. The oxidized flavin **1.1** undergoes a two-electron reduction process to generate reduced flavin **1.2**. This process is exemplified by

the hydride transfer process in presence of reducing cofactor NADH or NADPH and is especially executed during *oxidase* related functions. Alternatively, **1.1** can perform two one-electron reduction processes sequentially through the semiquinone form of flavin **1.5** to give reduced flavin **1.2**. These single electron reductions are often observed in nature by interactions with metal cofactors. The reduced flavin **1.2** activates molecular oxygen to convert itself to 4a-hydroperoxyflavin FLOOH **1.3**. FLOOH then transfers oxygen to oxidize substrate, which is essentially executed during oxygenase related functions. During this process, 4a-hydroxyflavin FLOH **1.4** is formed, which finally eliminates one molecule of water to regenerate oxidized flavin **1.1**. Alternatively, following reaction with O₂, hydrogen peroxide can be eliminated to reform flavin **1.1**. The H₂O₂ elimination is reversible, and can be taken advantage of to directly activate hydrogen peroxide by addition of **1.1** to form FLOOH **1.3**, this process is specifically known as a peroxide shunt process that avoids the reduction and oxidation of **1.1** to **1.3**.^{6,7}

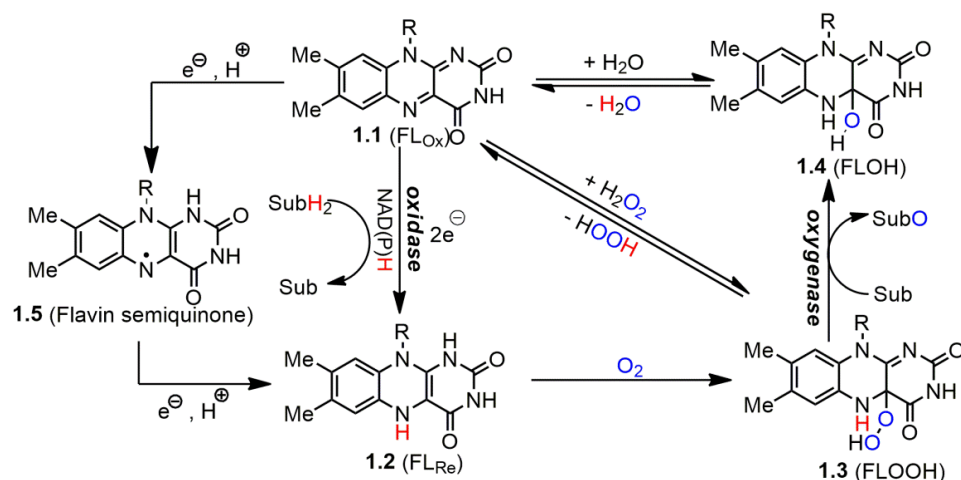


Figure 1.2 Catalytic cycle of flavin based redox function

On the other hand, there is no general mechanism for flavin catalytic cycle for non-redox based transformation and therefore, a specific example of *hydroxynitrile lyase/oxynitrilase* will be discussed here.

1.1.4. Nitroalkane oxidase (NAO)

Flavin dependent nitroalkane oxidase catalyzes oxidative transformation of nitroalkanes to aldehyde/ketone along with generation of nitrite and hydrogen peroxide. Other flavoproteins like 2-nitropropane dioxygenase (2-NPD), nitroalkane dioxygenase, glucose oxidase and *D*-amino acid oxidase are also known to catalyze the process. However, one unique feature of enzyme NAO among other flavoproteins that catalyze the similar reaction is that it requires a neutral substrate and is responsible for normal functioning in biological system.^{8,9,10}

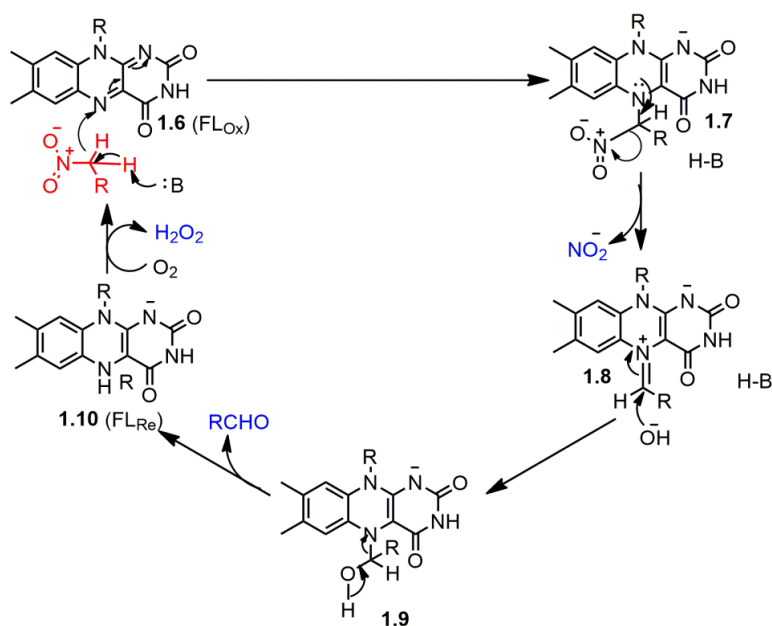


Figure 1.3 Reaction cycle for NAO catalyzed oxidation of nitroalkane

As shown in **Figure 1.3** above, oxidized flavin **1.6** undergoes nucleophilic attack by activated nitroalkane to form adduct **1.7**, which releases nitrite (NO_2^-) to give imminium species **1.8**. Upon nucleophilic attack followed by hydrolysis, the reduced flavin **1.10** is formed. The oxidized flavin **1.6** is regenerated from oxidation of the reduced flavin **1.10** by molecular oxygen releasing hydrogen peroxide during the process.

1.1.5 Monoamine oxidase (MAO)

Monoamine oxidase is involved in catabolism of neurotransmitters like norepinephrine, serotonin, and dopamine. They catalyze the oxidation of primary, secondary, and tertiary alkyl and arylalkyl amines to the corresponding imines. The imines hydrolyze nonenzymatically to aldehyde/ketone. There are two types of MAO. They are MAO A and MAO B which are 70% identical in amino acid sequence. However, they interact with different substrate and therefore are substrate specific.^{11,12,13}

Two different mechanisms are proposed for the oxidation process involving amine to iminium species. The radical mechanism (**Figure 1.4**) involves single electron transfer from amine to flavin giving radical cation species. Upon loss of proton from this species, a carbon-centered radical is formed. The radical finally loses one electron to flavin **1.13** forming iminium species and fully reduced flavin **1.14**. Overall, the mechanism involves electron, proton, and electron transfer process.¹⁴ Alternatively, a direct hydrogen atom transfer from radical cation also gives iminium species, suggesting hydrogen atom transfer process.¹⁵ Another mechanism proposes nucleophilic attack of nitrogen nucleophile to flavin to form C-4a adduct **1.15**. This adduct upon collapsing releases iminium species and reduced flavin **1.14** (**Figure 1.5**).¹⁶

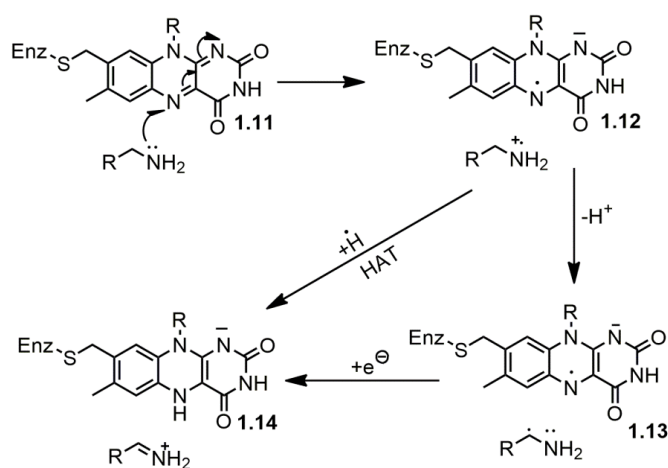


Figure 1.4 Radical mechanism for MAO catalyzed oxidation of amines

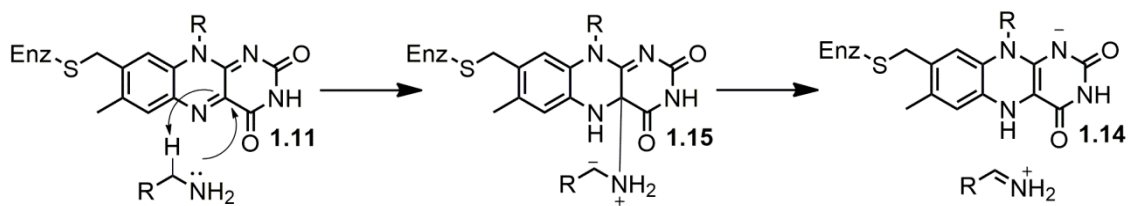


Figure 1.5 Nucleophilic pathway for MAO catalyzed oxidation of amines

1.1.6. Hydroxynitrile lyase/oxynitrilase

Oxynitrilases catalyze the synthesis and cleavage of cyanohydrins. They are widely distributed in plants and are believed to be physiologically responsible for defensive functions upon attack of microbes because the cleavage process releases HCN, which is toxic to the invading microbes.¹⁷

In 1837, Friedrich Wohler first reported its biocatalytic function in almonds, where he observed the cleavage of cyanohydrin to aldehyde and HCN. In one particular case of almond, flavin dependent oxynitrilase is known to catalyze both formation and degradation of mandelonitrile. Oxynitrilases are classified into two groups depending on presence or absence of cofactor FAD. Although the flavin cofactor is not involved in redox catalysis within this enzyme, the enzyme's inactivation due to FAD removal suggests that flavin plays a structural role.¹⁸

Although there is no consensus about how oxynitrilases perform, the most widely accepted mechanism states that the electron rich flavin **1.16** attacks the electron poor carbonyl carbon thus generating flavin-aldehyde adduct **1.17**. The cyanide source then attacks the adduct **1.17** to generate flavin **1.18** and cyanohydrin product.

Oxynitrilase is a potential biocatalyst and has been extensively used in stereoselective synthesis of cyanohydrins in industry. Cyanohydrins are versatile chemical synthons and therefore, there is growing interests in this class of enzyme.¹⁹

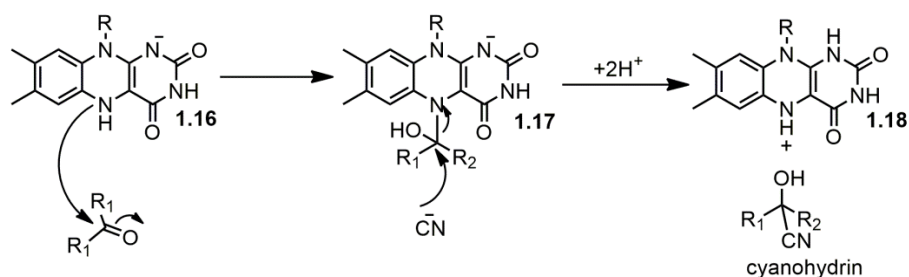


Figure 1.6 Proposed reaction mechanism for the formation of cyanohydrins catalyzed by oxynitrilase

1.2 Biomimetic organocatalysts

Biomimetic chemistry is a field of chemistry where chemists aim to develop new chemical reactions or new processes using key principles and concepts of biological systems. In general, biomimetic chemistry is a chemistry inspired by biology. However, the biomimetic chemist does not necessarily use materials or building blocks from nature. Three component features required while developing enzyme mimics are high substrate-enzyme binding, high turnover numbers, and substantial rate enhancement compared to non-catalyzed reactions.^{20,21,22}

Biomimetic organocatalysts are often low-molecular weight organic molecules that resemble natural component of enzymes and mimic general chemical transformation adopted by natural enzyme. Organocatalysts are normally superior to biocatalysts due to their broad scope for substrates, easy of handling, scalability, and relative high stability and comparative low cost. They are also often better than their more abundant metal and organometallic catalysts in regards to cost effectiveness and environment friendliness. Organocatalysts, including biomimetic catalysts have served as co-catalytic systems for synergistic catalysis and sequential catalysis along with other catalytic systems. Their unique selectivity for a given transformation as inspired by natural catalysts has potential to complement or even excel over the predominant transition metal catalysis.²³ Biomimetic organocatalysis, therefore, has the dual advantage of providing a basis for a chemical method to understand complex biological system and developing sustainable

chemical transformation. An often overlooked benefit to organocatalytic systems is their ability to be immobilized on a variety of solid surfaces. Some of the examples of biomimetic organocatalysts are presented in **Figure 1.7**.

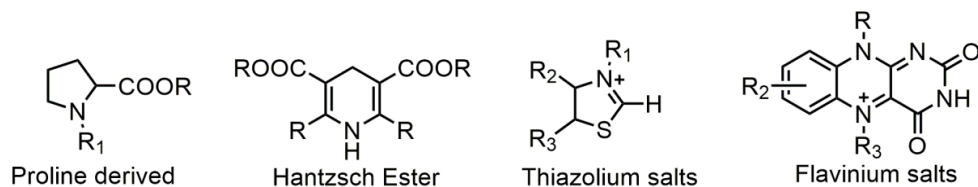


Figure 1.7 Examples of biomimetic organocatalysts

Proline and its derivatives have been extensively used in several chemical transformations. They have been resources to unnatural aminoacids²⁴ and catalysts for asymmetric synthesis. Major success has been achieved in the field of asymmetric aldol reactions leading to one of the powerful methods for building desired stereochemistry.^{25,26} Similarly, Hantzsch esters have also found use in several biomimetic approaches for asymmetric transfer hydrogenation reactions.²⁷ Thiazolium and structurally related salts have emerged to be a powerful molecular tools for various condensation and other reactions since the pioneering work of Ronald Breslow.^{28,29}

Artificial flavoprotein catalysis is currently involved in oxidation reactions, most of which are within the boundary of monooxygenase type activity but are providing wide variety of substrate scope in mild condition. Flavin structures with tunable structural moieties have inspired researchers to use them successfully as drugs,³⁰ drug carrier,³¹ photocatalyst,³² dye degrader,³³ etc. Involvement of natural flavin in a wide range of biological functions, easy manipulation of tricyclic core of synthetic flavins to tune the electronic and steric feature of the molecule, and excellent tolerance to non-natural conditions should inspire chemists to develop efficient functional flavin derivatives, catalysts and processes.

1.3 Frustrated Lewis pair (FLP)

Lewis put forward the concept of acids as electron pair acceptors and bases as electron pair donors in 1923. These acids and bases combine and form acid-base adducts. However, sterically demanding substituents and geometric constraints in Lewis pairs can deter the formation of such adducts. One exceptional feature of these sterically encumbered pairs is that they can incorporate small molecules and electronically polarize them, causing the splitting of relatively strong bonds in small molecules.^{34,35} The first successful use of the concept of a frustrated lewis pair (FLP) dated back to 2006 where Stephen *et al.* reported the first metal free approach to heterogeneously cleave H₂ with the use of sterically demanding Lewis pairs derived from a boron acid and a phosphorus base (**Figure 1.8**).³⁶ Today the concept of FLP has emerged as a powerful tool to activate and alter the chemical properties of several functional molecules. Initial research works focusing on H₂ activation in relation to reduction chemistry has now been expanded to C-C bond formation, C-H activation, hydrosilylation, etc.^{37,38} Recently a new strategy called inverse-FLP has paved a more sustainable approach in the field of FLP chemistry. One such example is use of readily available strong organosuperbase and weak Lewis acid like 9-BBN or BPh₃, etc. for H₂ activation.³⁹

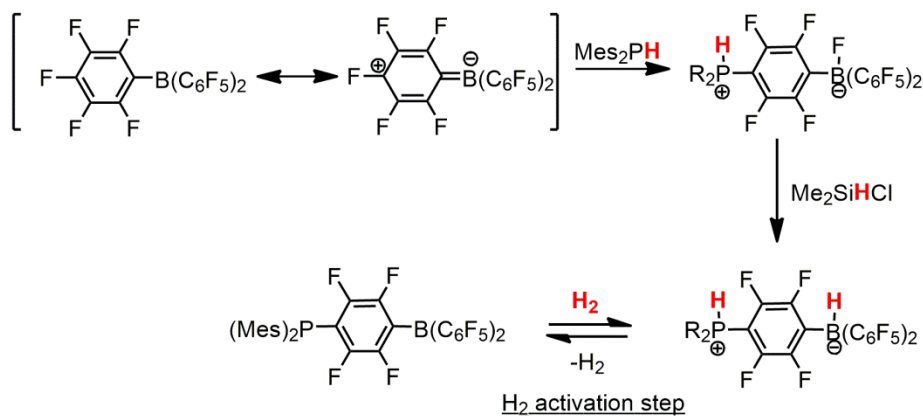


Figure 1.8 Report on first metal free reversible H₂ activation

FLP concept of molecule activation is relevant to enzyme models too. Enzymes like [Fe]-hydrogenase reversibly oxidizes H_2 to reduce its substrate in highly selective manner in the presence of Fe-guanylylpyridinol cofactor. Both metal center and enzyme matrix are involved in this process (**Figure 1.9**).⁴⁰ One chemical model reaction studied by Meyer *et al.* showed that a Lewis basic [Ru]-metalate in presence of imidazolium salt could split H_2 heterolytically. Hydride addition to the imidazolium and protonation of the [Ru]-metalate process clearly indicated H_2 cleavage similar to [Fe]-hydrogenase's activity.⁴¹

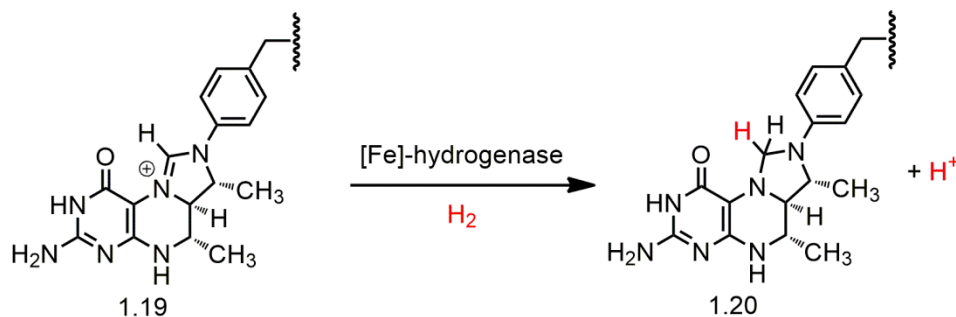


Figure 1.9 [Fe]-hydrogenase involved in H_2 cleavage

Chapter 2

Flavin catalyzed Aerobic Cross-Dehydrogenative Coupling Reactions

2.1. Background

Riboflavins, water-soluble cofactors crucial for enzymatic reactions, are pertinent to both redox and non-redox applications.⁴² Flavoprotein-mediated redox reactions contribute to proper functioning in biological systems; the conversion of (*S*)-reticuline to (*S*)-scoulerine (**Figure 2.1**), catalyzed by the enzyme *reticuline oxidase* during the biosynthesis of morphine, a secondary metabolite in a species of opium, is one such example.⁴³ While enzymatic functions are unique to a given substrate, concomitant to a high degree of site specificity, use of closely related artificial mimics of cofactors could entail broader scope of substrates and wider opportunity, both for potential application in synthesis and for understanding the relevant mechanism of related enzymatic reaction. Therefore, search for such artificial bioorganic mimics for their role in real world application is highly demanded.⁴⁴

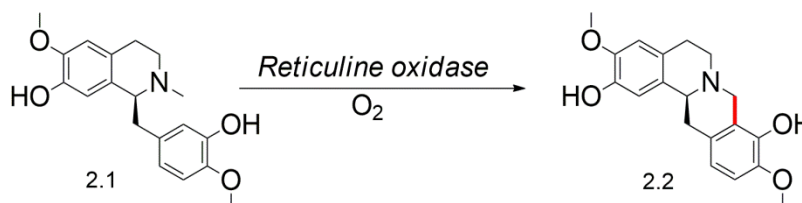


Figure 2.1 Flavin dependent Reticulin oxidase catalyzed reaction

In the presence of oxidizing agents, sp^3 C-H bonds adjacent to nitrogen and oxygen, found in tetrahydroisoquinoline and other related molecular structures, are susceptible to undergo oxidation due to their increased reactivity (**Figure 2.2**). Oxidative cross dehydrogenative coupling (CDC) reactions procure a strategic approach concerning coupling of two molecules; coupling performance is initiated by the oxidation of sp^3 C-H bonds alpha to heteroatoms like

nitrogen, generating an electrophilic center, and is subsequently coupled with various nucleophilic species.^{45,46}

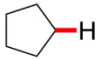
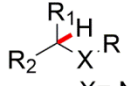
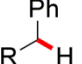
sp ³ C-H	BDE (Kcal/mol)
	95-96
 X = N, O, S	80-97
 R = Ph, H	84-90

Figure 2.2 Bond dissociation energy of some sp³ C-H bonds

The first report on aerobic oxidative cross coupling reaction was presented by Murahashi group in 2003 using a ruthenium catalyst (**Figure 2.3**).⁴⁷ Later in 2004, the Li group revealed more practical CDC approach using a copper catalyst and TBHP oxidant (**Figure 2.4**).⁴⁸ This work was extended with a broader nucleophile scope in 2009 by the same group.⁴⁹ Both ruthenium and copper catalyzed works was pioneer in oxidative CDC approach.

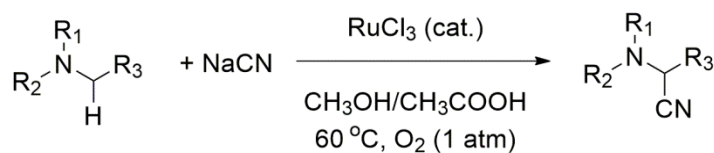


Figure 2.3 Ruthenium catalyzed first aerobic oxidative CDC reaction

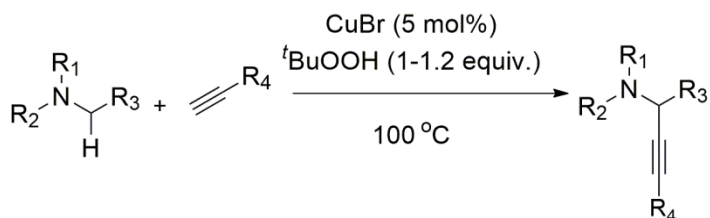


Figure 2.4 Copper catalyzed oxidative CDC reaction

Inspired by these findings, Backvall *et al.* in 2005 put forward an enantioselective aerobic oxidative CDC approach using an unactivated aldehyde as nucleophilic source.⁵⁰ This synergistic approach utilized proline as organocatalyst to activate aldehyde. Quinone was used as co-oxidant. This was the first biomimetic CDC approach that resembled nature's unique way of merging two separate biochemical pathways for the biosynthesis of complex molecules (**Figure 2.5**).

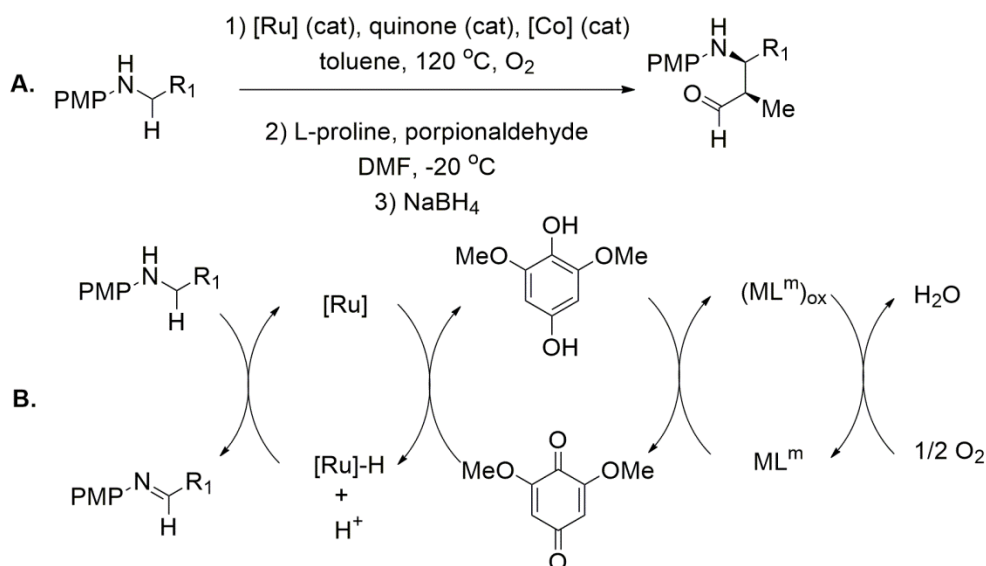


Figure 2.5 Biomimetic enantioselective oxidative CDC approach

The scope of earliest oxidative CDC work with electron rich nucleophiles was extended with the use of unactivated ketones and aldehydes as nucleophilic partner. In 2009, Klussman group reported use of ketone as nucleophiles in vanadium catalyzed oxidative CDC. This was possible due to synergistic organocatalysis approach using proline as organocatalyst.⁵¹ Furthermore, enantioselective methods were later reported with the use of both metal⁵² (**Figure 2.6.1**) and metal free⁵³ approach, both operating under synergistic catalysis with chiral amine catalysts (**Figure 2.6.2**).

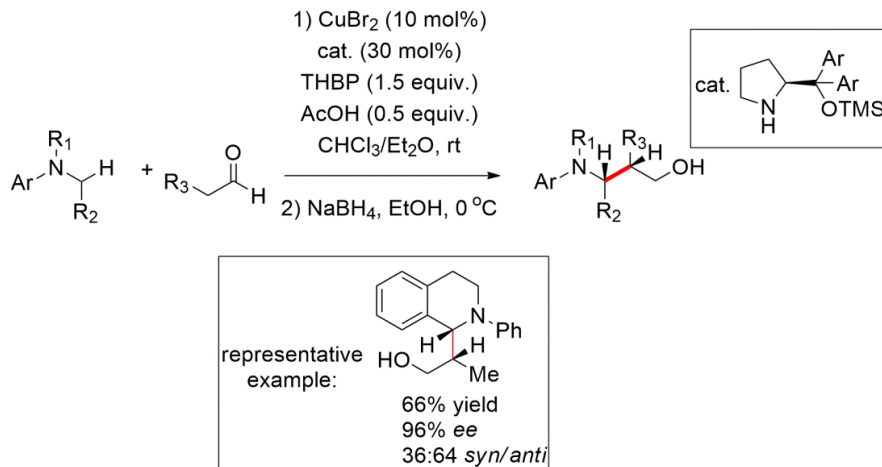


Figure 2.6.1 Copper catalyzed enantioselective CDC reaction with unactivated aldehyde

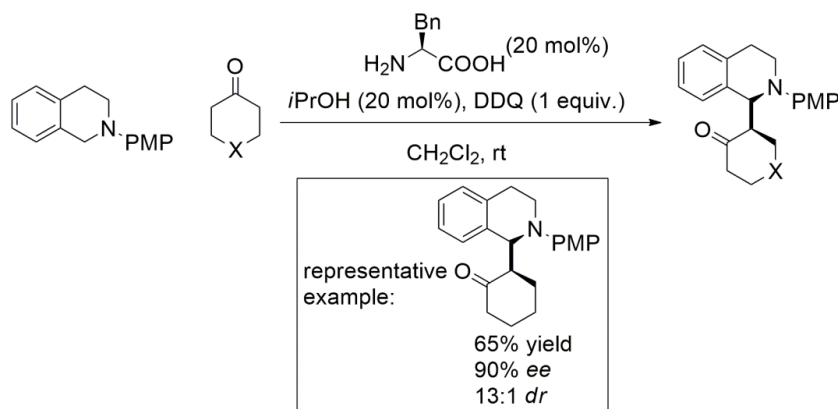


Figure 2.6.2 Metal free enantioselective CDC approach with unactivated ketones

In addition to metal catalyzed transformations, a number of organocatalysts have been utilized in similar transformations. Notable examples are reactions catalyzed by AIBN and DDQ,⁵⁴ iodine,⁵⁵ SO₂Cl₂,⁵⁶ photoinduced electron transfer,⁵⁷⁻⁶¹ and Brønsted acid catalyzed processes.^{62,63} Moreover, oxidant-free⁶⁴ and catalyst-free⁶⁵ approaches have also been reported invoking a CDC approach.

Although there has been significant development in oxidative CDC reactions, the scope of biomimetic organocatalysis in this field is rarely tested-especially for ground state aerobic organocatalysis.^{66,67,68} To the best of our knowledge, artificial riboflavin mimics have not been

used as catalysts for CDC approach. Subsequently, this present research endeavors to further investigate oxidation reactions induced by artificial riboflavin mimics, as well as examine both intramolecular and intermolecular oxidative cross dehydrogenative couplings to maximize formation efficacy of C-N, C-P, and C-C bonding, utilizing readily oxidizable tetrahydroisoquinoline substrates.

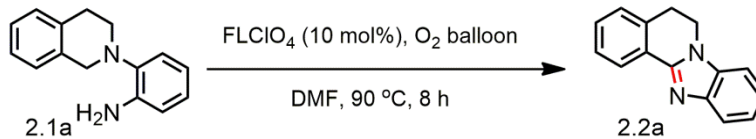
Notable accomplishments within the field of flavin-catalyzed oxidation include sulfur, nitrogen, Baeyer-Villager, and Dakin oxidations.⁶⁸⁻⁷² The synthesis of diverse groups of artificial riboflavin mimics have been long-withstanding amongst present researchers, specifically regarding applicability towards organocatalysis⁶⁶ and (photo)electrocatalysis,^{73, 74} ensuing motivation for further investigation of artificial riboflavin mimic's roles in oxidizable, tertiary amine substrates, such as tetrahydroisoquinoline (THIQ), in CDC reactions. We envisioned that electron poor flavin derivatives could possibly be reduced by our desired substrates with high oxidation potential like tertiary amines. Towards this end, the electron transfer could be facilitated through increase in temperature or oxygen pressure.⁷⁵ On the other hand, an ionic mechanism involving lewis acid-base complex formation between amines and lewis acidic flavin mimics could not be overlooked too.⁷⁶

2.2. Results and Discussions

To begin, an intramolecular CDC reaction for C-N bond formation was initiated, leading to polycyclic benzimidazole moieties. Synthesis of starting material **2.1a** and its derivatives were conducted via nucleophilic aromatic substitution, followed by reduction of resulting nitro derivatives.⁷⁷ Subjection of **2.1a** to 5 mol % of FLCIO₄ catalyst in DMF solvent at 90 °C at atmospheric oxygen (**Table 2.1**, entry 1) yielded **2.2a**, the desired product, with 72% NMR yield. Doubling catalyst concentration increased the yield to 83% (entry 2). Under inert conditions,

lowered activity was observed (entry 3). Toluene, a non-polar solvent, was ineffective, yielding only trace quantities of desired product over eight-hour span (entry 4), likely due to catalyst insolubility. Use of anhydrous DMF yielded similar results (entry 5). Notably, product was observed in trace amounts in the absence of catalyst, even under prolonged time conditions (entry 6). Subjection of oxidant to open air conditions slightly reduced yield, totaling 64% (entry 7). At lower temperature 60 °C, only 48% NMR yield was observed (entry 8). Radical scavengers, such as butylated hydroxytoluene (BHT) and TEMPO, reduced the yields as shown in entries 9-10. Under dark conditions, desired product reached a 66% NMR yield (entry 11), indicating a ground-state reactivity of flavinium catalyst. Presence of base additive greatly reduced the reaction yield (entry 12), indicating favorable acidic medium prevalent in flavinium species.

Table 2.1 Optimization of reaction conditions for intramolecular C-N bond formation.



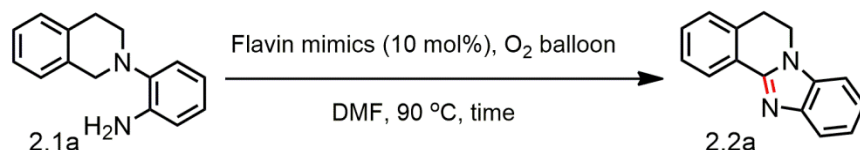
Entry	Yield (%) ^b
1 ^c	72
2	83 (76)
3 ^d	11
4 ^e	trace
5 ^f	76
6 ^g	trace
7 ^h	64
8 ⁱ	48
9 ^j	33
10 ^k	50
11 ^l	66
12 ^m	7

^a **Reaction conditions:** **1a** (0.045 mmol), **FLCIO₄** (10 mol%), **DMF** (0.11M), O₂ balloon; ^bNMR yield, 1 equiv. of CH₂Br₂ as I.S added after the stoppage of reaction, isolated yield in parenthesis; ^c**FLCIO₄** (5 mol%); ^din Argon; ^eToluene was used as solvent; ^fanhydrous DMF as solvent; ^gNo catalyst, 24 h; ^hair instead of O₂ balloon; ⁱ60 °C, 20 h; ^j**BHT** (1 equiv. was used); ^k20 % **TEMPO**; ^lreaction was performed in dark; ^m1 equiv. of KO^tBu was used.

Enhanced activity was not observed upon screening other flavinium catalysts, apart from **IA1/FLCIO₄**. Alloxazinium peroxy catalysts trended toward catalytic activity (**Table 2.2**, entries 1-3). Electron-deficient, peroxy flavinium catalyst, **A4-OOH**, indicated little effect when compared to electron-rich catalysts, **A1-OOH** and **A2-OOH**. The efficacy of alloxazinium-based catalysts was notably lower than isoalloxazinium-based catalysts, **IA1-Cl** and **IA**. Catalyst **IA1-**

Cl differing only in counteranion to **IA1**, displayed similar catalytic activity (entry 5). This observation is indicative that little to no anionic effect exists regarding observed catalytic activity of flavinium based organocatalysts. A lower yield of 69% was observed in **BC2** catalyst (entry 4).

Table 2.2 Catalyst screening^a



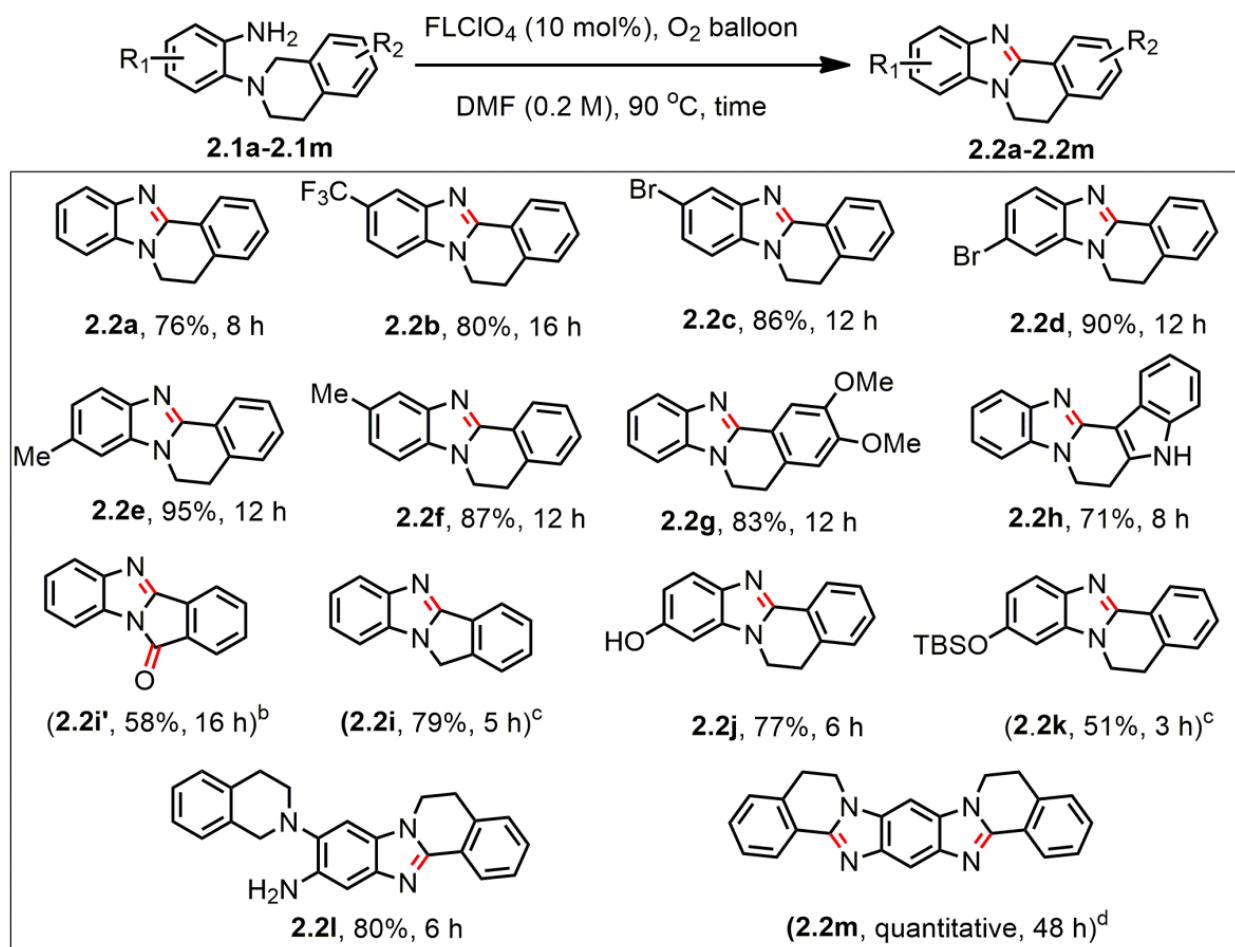
Entry	Structure	Time (hr.)	Yield (%)
A4-OOH		24	16
A2-OOH		24	71
A1-OOH		16	77
BC2		8	69
IA1-Cl		8	81
IA1		8	83

^a**1a** (0.045 mmol), **catalyst** (10 mol%), **DMF** (0.2 M)

Various substrates were tested utilizing the optimized conditions observed during catalytic screening and optimization reactions. Results indicated that substrates containing

electron-withdrawing, or electron-donating, substituents underwent efficient C-N bonding reactions, producing high yields. Electron-withdrawing group $-\text{CF}_3$ (**2.1b**) took relatively longer to procure an isolated product yield of 80%. Significant differences were not observed between substrates containing identical substituents but differing substituent location (substrates **2.1c** vs. **2.1d**, and **2.1e** vs. **2.1f**). A slightly reduced yield of 77% was observed for phenolic substrate **2.1j**, while a rather high yield of 83% was observed in substrate **2.1g**, a tetrahydroisoquinoline moiety bearing a methoxy substituent. Substrate **2.1h**, bearing a carbazole substituent, provided an effective yield of 71% over 8 hours. In merely 5 hours, isoindoline substrate **2.1i** produced an oxidized product with a greater yield of 79%. However, reduced yield was observed when substrate **2.1i** was subjected to wet DMSO solvent which could be due to over-oxidation resulting in formation of product **2.2h**; yet with prolonged time a decent yield of 58% was achieved. Similarly, -OTBS substituents reacted well under anhydrous conditions, yet reduced yield of 42% was observed when subjected to wet DMSO solvent at same time interval. Doubly oxidizable substrate **2.1l** produced a mono-oxidized product, in 6 hours, with an 80% product yield. The resulting compound when subjected to open-air conditions, allowing the acquisition of the fully oxidized product in quantitative yield; this further oxidation required an additional 48 hours to complete.

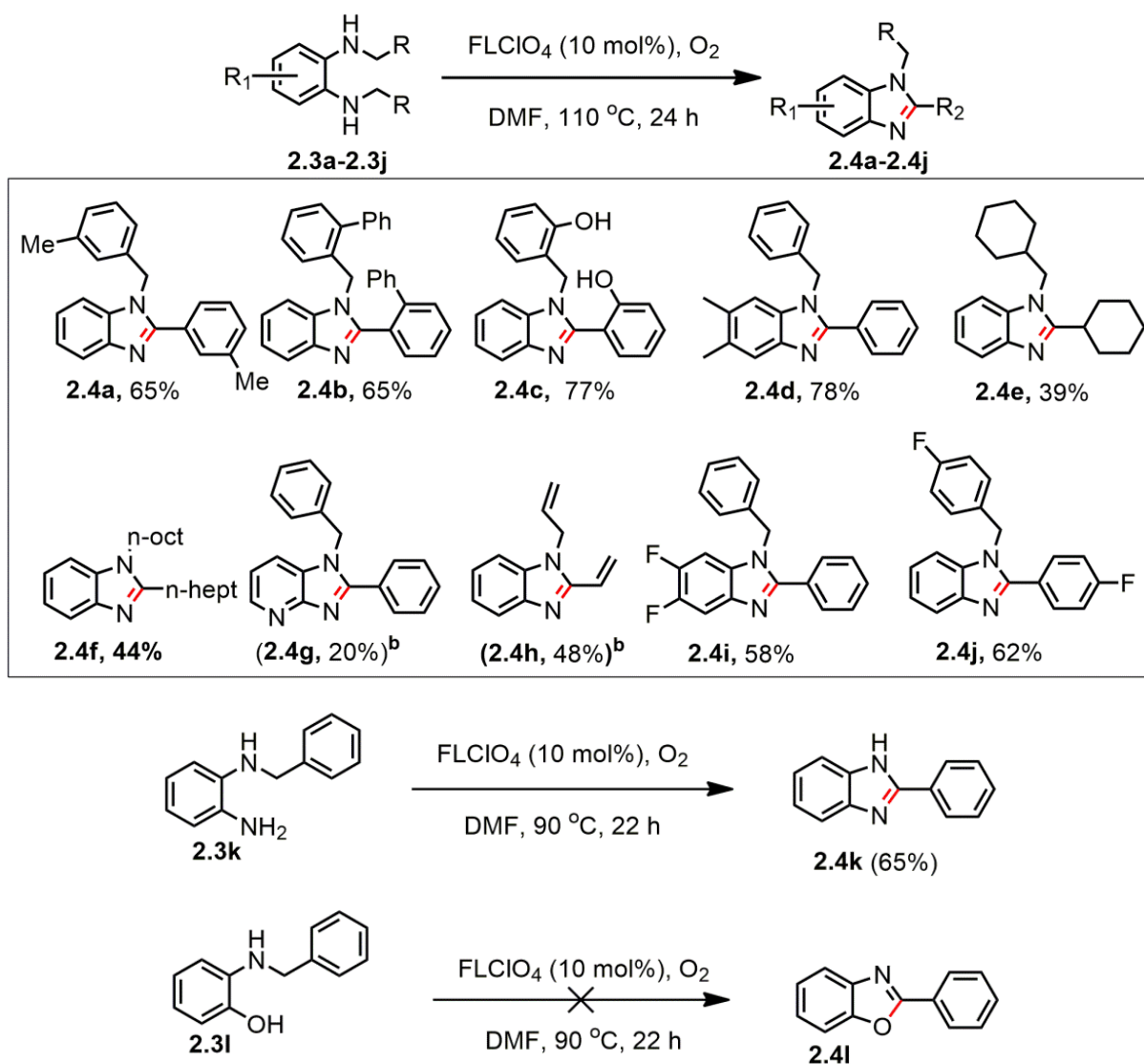
Table 2.3: Substrate scope for intramolecular C-N bond formation in THIQ substrate^a



^aReaction conditions: **2.1a-2.1m** (0.5 mmol), FLClO_4 (0.05 mmol), DMF (0.2 M); ^bwet DMSO as solvent; ^cdry DMSO as solvent; ^d0.2 mmol scale and obtained from **2.2l** and under open-air conditions.

Expansion of substrate scope was performed for intramolecular, oxidative CDC to non-THIQ substrate, *N,N'*-dialkyl-*o*-phenylenediamine. *N,N'*-dialkyl-*o*-phenylenediamine substrates (**2.3a** to **2.3j**) were less effective than THIQ substrates; however, corresponding products (**2.4a** to **2.4j**) were achieved in moderate yields, with the exception of pyridine-bearing compound **2.4g** which attained only a 20% NMR yield in 36 hours. In addition, it was observed that monosubstituted-*o*-phenyldiamine substrate possessing a benzyl substituent (**2.3n**) exhibited the ability to oxidize, and thus cyclize, to yield 2-phenylbenimidazole. In contrast, *N*-benzylaminophenol substrate (**2.3o**) underwent no activity during reaction procedures.

Table 2.4: Substrate scope for C-N bond formation in ortho-phenylenediamine substrate^a

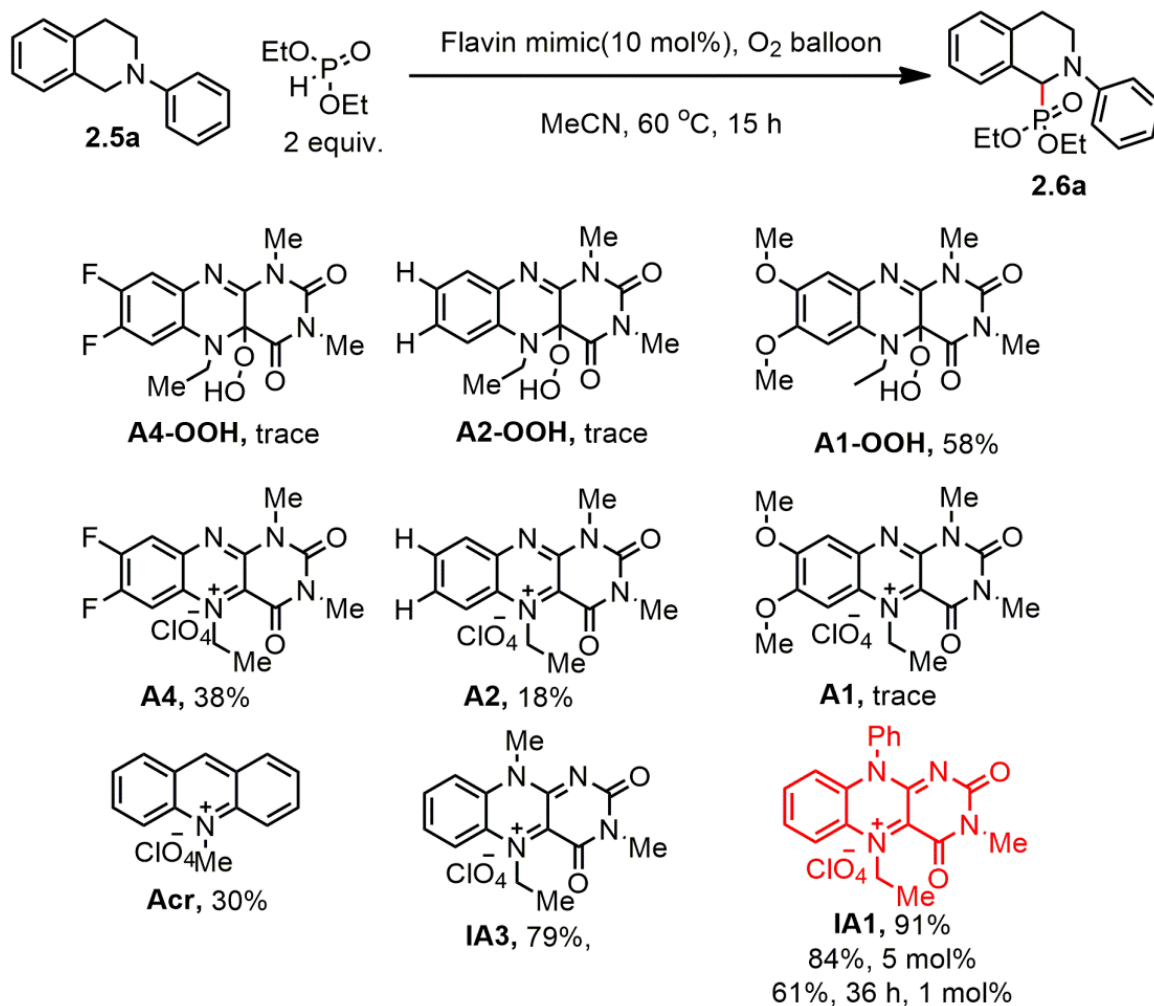


^aReaction conditions: 2.3a-2.3l (0.5 mmol), FLClO_4 (0.05 mmol), DMF (0.2 M); ^bNMR yields.

Intermolecular coupling reactions pose a greater challenge than intramolecular, as the former requires coupling of two molecules to produce one due to entropy factor. Further optimization of reaction conditions was performed for the intermolecular oxidative coupling between *N*-substituted tetrahydroisoquinoline and nucleophilic phosphites. A lower temperature of 60 °C with low boiling, aprotic-solvent acetonitrile, were observed as ideal conditions for intermolecular coupling. Catalytic screening displayed similar activity observed previously,

although lower catalyst loading was observed to be equally effective for product-conversion efficacy (**Table 2.5**).

Table 2.5: Catalyst screening for C-P bond formation^a

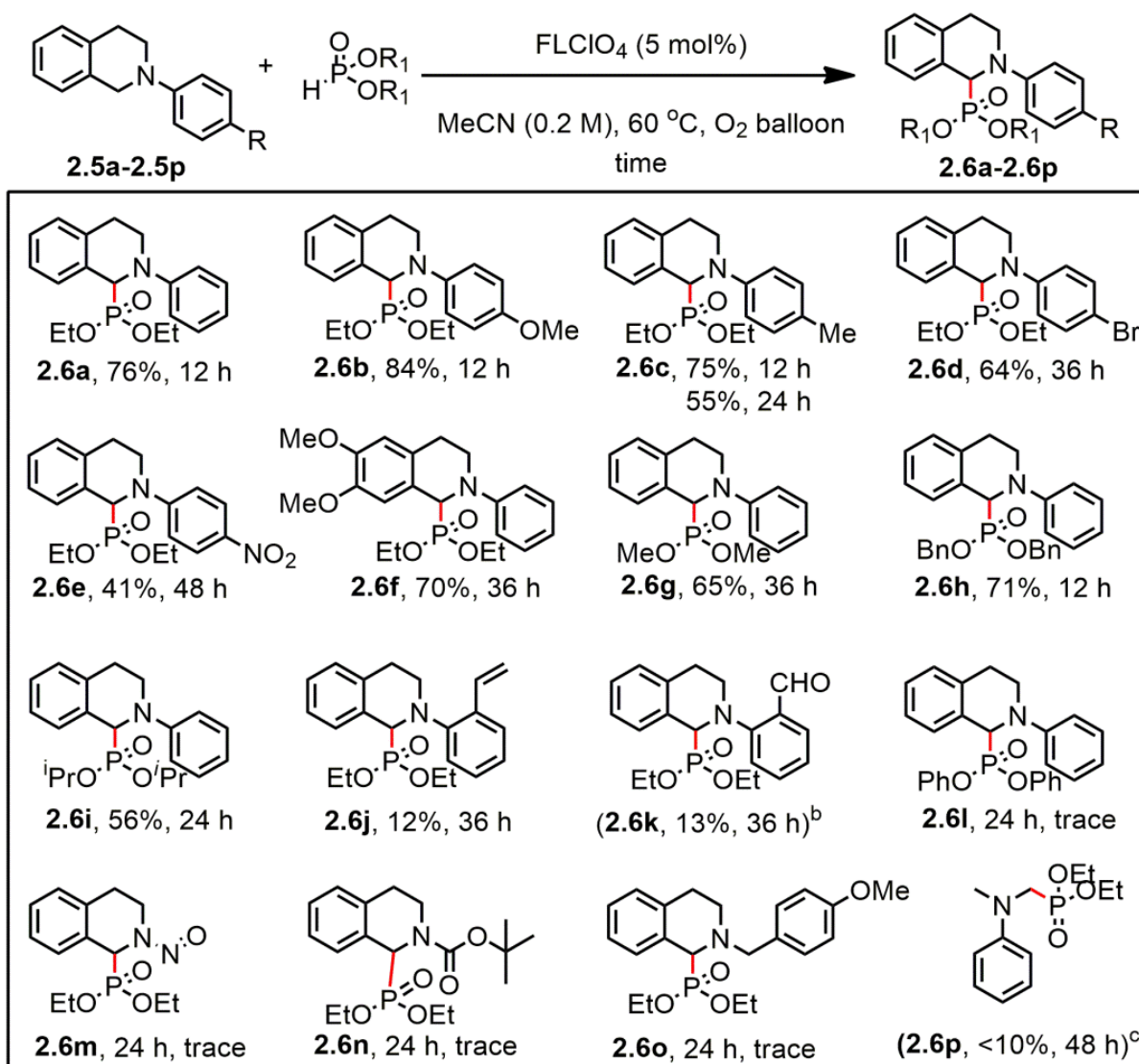


^a**Reaction conditions:** **2.5a** (0.1 mmol), **Dialkyl phosphite** (0.2 mmol), **FLClO₄** (0.01 mmol), **MeCN** (0.2 M)

Substrate scope results indicate that electron-donating groups possessed by substituents (e.g., -Me and -OMe) in the para position relative to nitrogen are more efficient than substrates with electron-withdrawing groups. For example, substrate **2.5e**, which possessed a -NO₂ group, reacted in 48 hours yielding 41% product, contrasting to a yield of 84% in 12 hours for substrate **2.5b**, which contained an -OMe group. Phosphite nucleophiles were also observed as compatible

with optimized reaction conditions. Substrate scope study indicated a reactivity trend, decreasing in order from diethyl phosphate (entry **2.6a**), dibenzyl phosphate (entry **2.6h**), dimethyl phosphate (entry **2.6g**), diisopropyl phosphate (entry **2.6i**), to diphenyl phosphate (entry **2.6l**). Addition of diphenyl phosphite to THIQ substrate yielded insufficient results, as both ortho-styryl (**2.5j**) and ortho-carbaldehyde (**2.5k**) yielded roughly 12% product, and *N,N*-dimethylaniline (**2.5p**) procured less than 10% NMR yield in 48 hours. Other THIQ substrates with alkyl or amine substituents were indicated as ineffective candidates for intermolecular coupling; the involvement of THIQ in conducted reactions yielded only trace quantities of product (entries **2.6m**, **2.6n**, and **2.6o**).

Table 2.6: Substrate scope for C-P bond formation^a

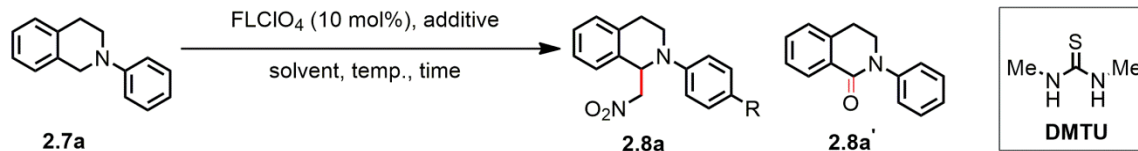


^a**Reaction conditions:** **2.5a-2.5p** (0.5 mmol), **Dialkyl phosphite** (1.0 mmol), **FLClO₄** (0.025 mmol), **MeCN** (0.2 M); ^b4 equivalent of Diethylphosphite and 2.5 mol% **FLClO₄** were used; ^cNMR yield

To undergo scope expansion for CDC reactions generating formation of C-C bonds, several carbon-based pro-nucleophiles and nucleophiles were examined. Despite exiguous results regarding conversion observation, study of aza-Henry reaction, nitroalkane with *N*-phenyltetrahydroisoquinoline in the presence of **FLClO₄** catalyst yielded some advantageous results. 2 equivalents of nitromethane in dichloromethane solvent had an observed yield of 51%

desired product, obtained in 48 hours (**Table 2.6**, entry 1). An increase of nitromethane to 20 equivalents generated slight improvement (entry 2), although quantity of byproduct **2.8a'** also increased from a yield of 9% to 13%. Replacement of dichloromethane solvent with acetonitrile did improve product yield (**Table 2.6**, entry 3), but not significantly. Usage of pro-nucleophile as solvent was determined to yield the resulting byproduct as a major product, with no coupling of desired product observed (entry 5). However, a reduction in reaction time allotted to 24 hours procured a 92% yield of desired product, with no byproduct formation (entry 6).

To determine if the product conversion of **2.8a** to amide **2.8a'** was peroxide driven, a control reaction was performed on substrate **2.8a** using 100 mol% hydrogen peroxide at 100 °C. The reaction yielded amide **2.8a'** quantitatively in 3 hours. Among few additives tested to determine selectivity of desired product over byproduct **2.8a'**, only urea based DMTU was found to be effective. In this case only trace amounts of byproduct were detected even under a prolonged reaction time of 72 hours (entry 7). Further investigation on substrate scope was carried out using the best condition among tested ones.

Table 2.7: Optimization of Reaction condition for C-C bond formation^a

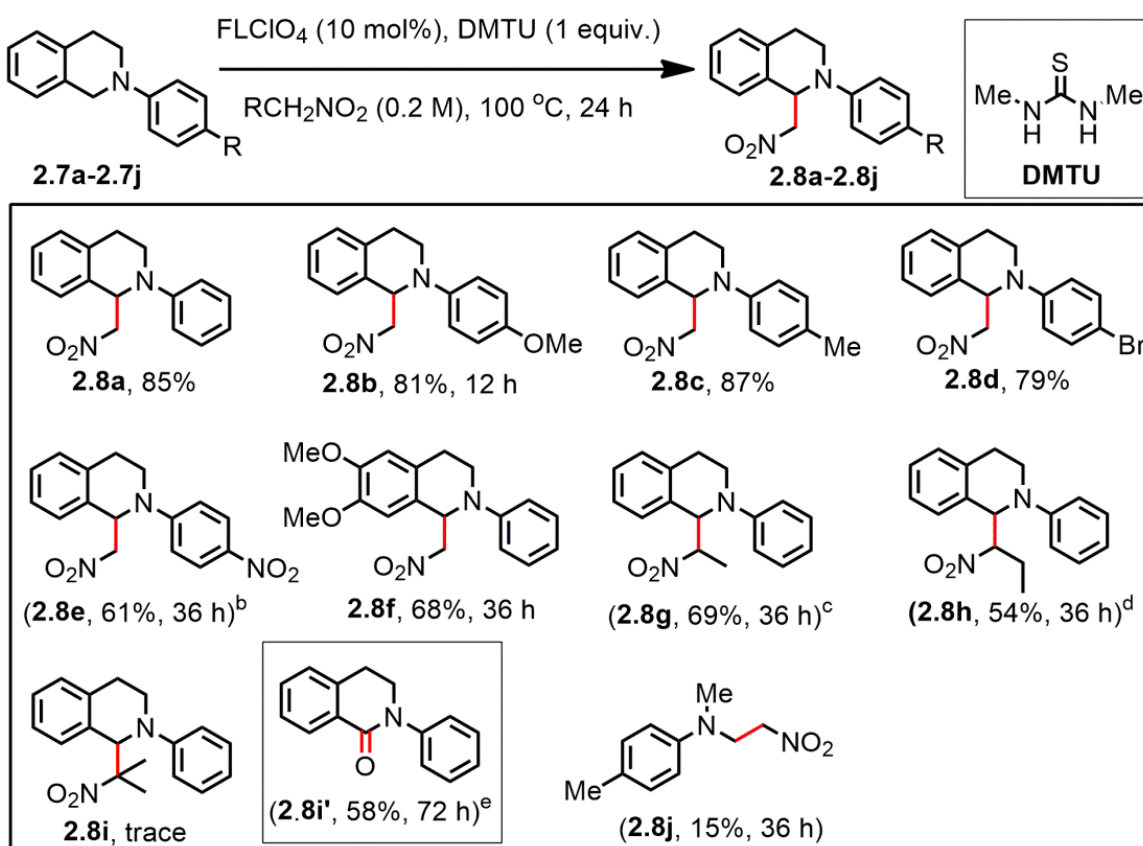
Entry	Equiv. of MeNO_2	Additive (1 equiv.)	solvent	Temp ($^\circ\text{C}$)	Time	Yield for 2.8a	Yield for 2.8a'
1	2	-	DCM	80	48 h	51%	9%
2	20	-	DCM	80	48 h	58%	13%
3	20	-	MeCN	80	48 h	63%	10%
4	>100	-	MeCN	80	48 h	69%	16%
5	>100	-	-	100	48 h	trace	71%
6	>100	-	-	100	24 h	92%	trace
7	>100	DMTU	-	100	72 h	82%	trace
8	>100	DMTU	-	100	24 h	87%	trace

^aReaction condition: 7a (0.05 mmol), FLClO_4 (0.005 mmol), DMTU (0.05 mmol)

Extension of aza-Henry reaction scope to varying THIQ derivatives and nitroalkanes was performed. All THIQ derivatives observed reacted smoothly, yielding desired coupling products (table 2.7). However, electron-withdrawing groups, for instance $-\text{NO}_2$, attained a moderate yield of 61% in 36 hours, even with 20% catalyst loading (entry 2.8e). Nitroethane subsequently had an observed product yield of 68%, despite longer time allowance necessary for conversion to occur (entry 2.8g). Nitropropane, as a nucleophilic partner, had a fair NMR yield of 54% (entry

2.8h), while no formation of product incurred with 2-nitropropane (entry **2.8i**). In the absence of DMTU, substrate provisioned amide product in moderate yield of 58% in 72 hours (entry **2.8i'**). Poor conversion was observed for *N,N*-dimethylaniline, with a meager 15% yield in 36 hours (entry **2.8j**), similar to observed yield in aforementioned C-P bond formation.

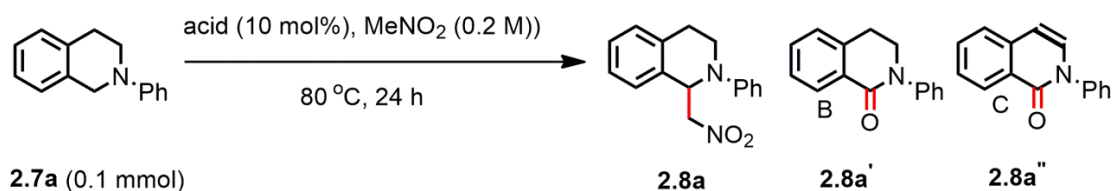
Table 2.8: Substrate scope for C-C bond formation^a



^a**Reaction conditions:** **2.7a-2.7j** (0.5 mmol), **FLClO₄** (0.05 mmol), **DMTU** (0.5 mmol), **RCH₂NO₂** (0.2 M); ^b20 mol% catalyst was used; ^cdr. 3:2; ^dyield represented are NMR yields; ^eNo DMTU additive was used.

Further investigation regarding the role of several Brønsted acid catalysts as control reactions for the aza-Henry reaction was performed, as flavinium catalysts release protons during turnover^{6,7} and literature reports on redox-based catalysis by Brønsted acids^{62,63}. As shown in **scheme 2.1**, strong acids yielded full consumption of amine starting material **2.1a** within 24 hours. Only 20%

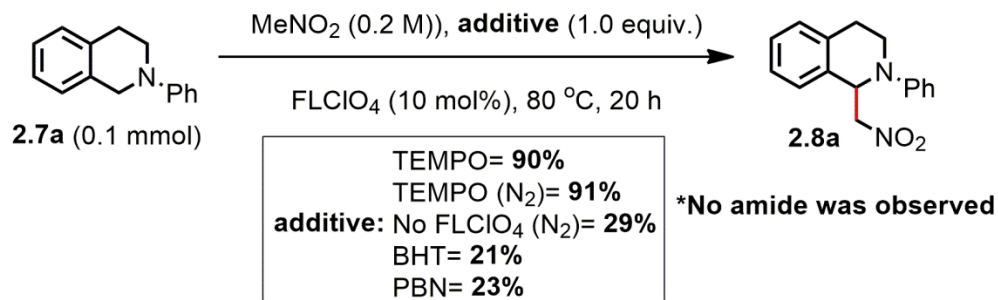
product formation was observed for the strong acid, HClO₄, while with methanesulfonic acid, two over-oxidized products were observed in addition to CDC product. Identical byproducts were observed in trifluoroacetic acid, although observation of desired product was absent. Acetic acid converted product relatively well, although observed conversion rate was low. Sufficient evidence for an ionic reaction mechanism was not provisioned; however the supportive role of in-situ generated acids during reaction cycling in CDC reactions cannot be neglected.



Acid catalyst (conversion based on consumption of 2.7a)	Yield of 2.8a	Yield of 2.8a'	Yield of 2.8a''
HClO ₄ (100%)	20	trace	trace
MeSO ₃ H (100%)	21	23	8
CF ₃ COOH (100%)	trace	30	20
CH ₃ COOH (48%)	40	trace	trace

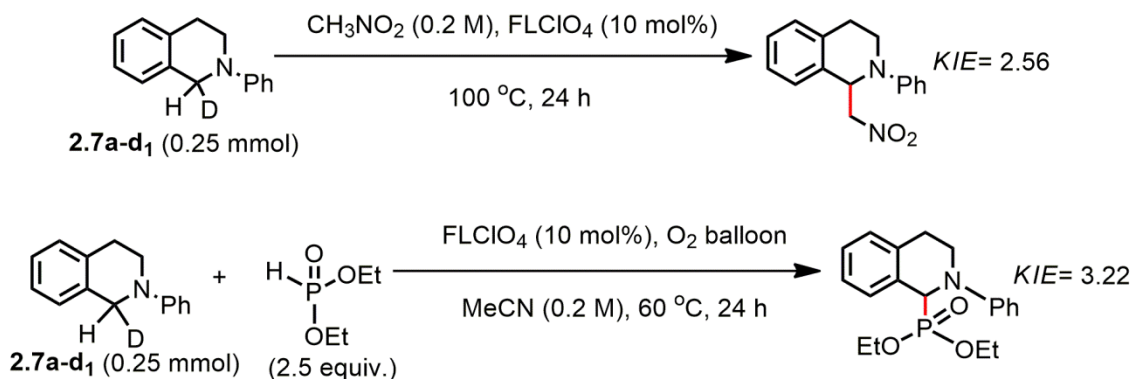
Scheme 2.1 Effect of different Brønsted acids on Aza-Henry reaction with THIQ

To investigate involvement of radical intermediates in reaction mechanism, radical probe experiments with varying radical probes were performed (**scheme 2.2**). TEMPO additive in both aerobic and anaerobic condition produced over 90% NMR yield. However, in both BHT and PBN, reduced yield of 21% and 23% were detected respectively. These results are indicative of a radical-based mechanism although the exact reason for TEMPO promoting the reaction is yet to be determined.



Scheme 2.2 Study on radical scavenging effect

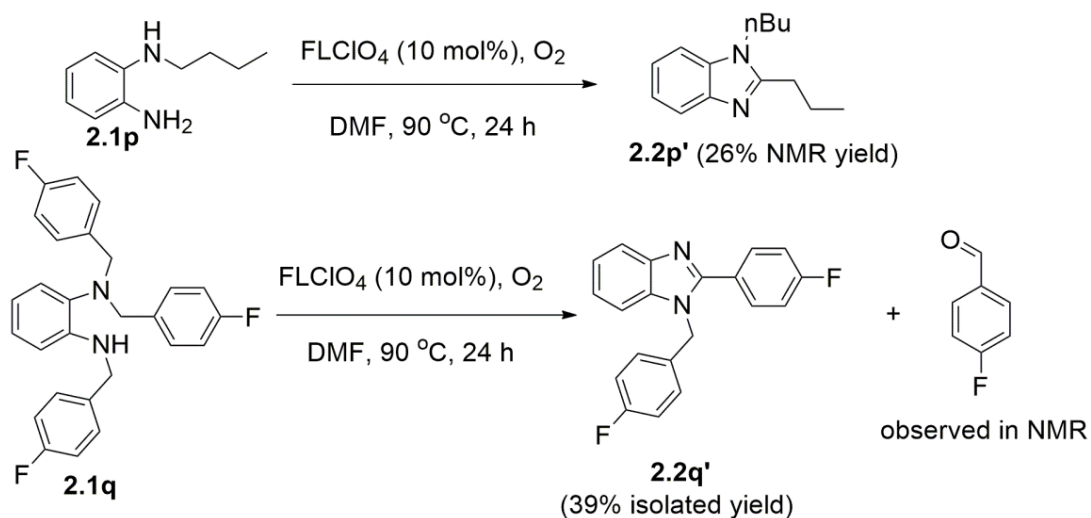
Intramolecular kinetic experiments conducted in H/D substrate in both aza-Henry and phosphonation hinted at the H atom abstraction step being rate determining step in overall mechanism. Primary kinetic isotope effect values of 2.56 in aza-Henry reaction and 3.22 in oxidative phosphonation were suggestive of Hydrogen atom abstraction step being the rate determining step of the reaction.⁷⁸



Scheme 2.3 Study on intramolecular kinetic isotope effect

Consistent with higher reduction potential of isoalloxazinium based flavin mimics⁷⁹ and above preliminary results, a radical mechanism involving single electron transfer from **substrate** amine to flavin mimic **FLClO₄** is proposed (**Figure 2.9**). This process results into radical cation amine species **2.9** and fairly stable **FL** radical. Upon combination of **FL** radical with oxygen, oxygen based radical **FLOO** could be formed, which could abstract hydrogen atom from **2.9** to afford reactive iminium species **2.10**. Concomitantly, **FLOOH** is formed which could provide oxidized

flavinium species **FLClO₄** ready for another catalytic cycle, although this step is normally rate limiting for isoalloxazinium based catalyst like **FLClO₄**⁸⁰. In case of iminium species **2.10**, a nucleophilic attack could result into formation of desired **product**. Supporting evidences for imine/iminium species come from observation of hydrolysis of benzylic site from substrate **2.1p** and **2.1q** (**scheme 2.4**). The former gave 1,2-disubstituted benzimidazole product **2.2p'** through hydrolysis of one of the alkyl chains. In case of **2.1q**, corresponding benzaldehyde was observed in crude NMR spectrum (**Figure 2.7**). In addition, imine substrate **2.9a** readily gave desired benzimidazole product. We were also able to isolate fully oxidized quinolium species ($m/z = 206$) of parent substrate **2.7a** in trace yield during purification of the corresponding nitro product (**Figure 2.8**).



Scheme 2.4 Evidence for possible hydrolysis of iminium intermediates

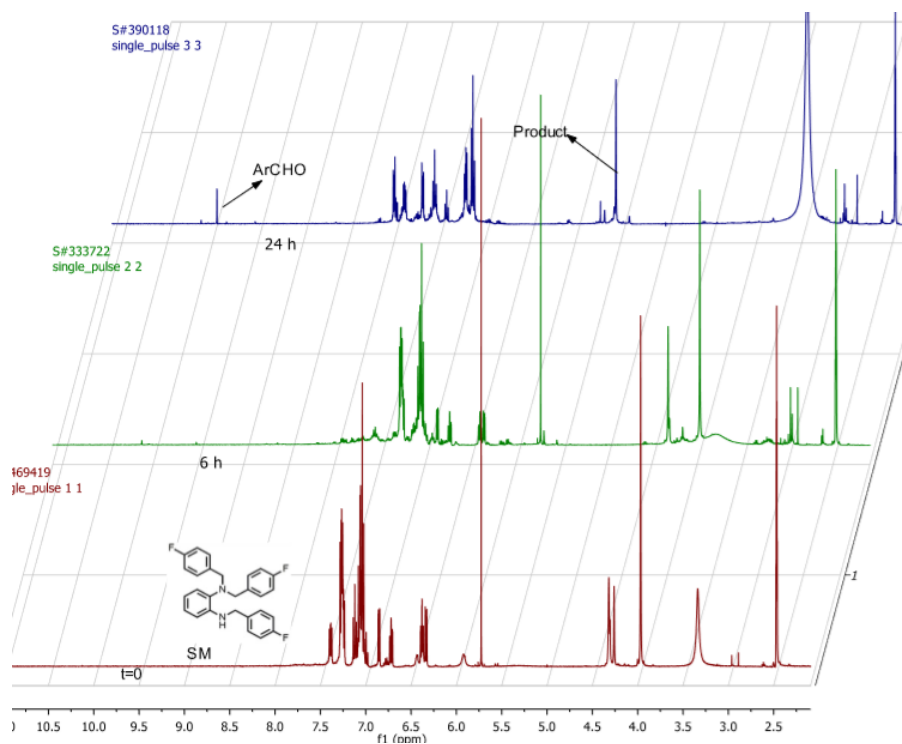
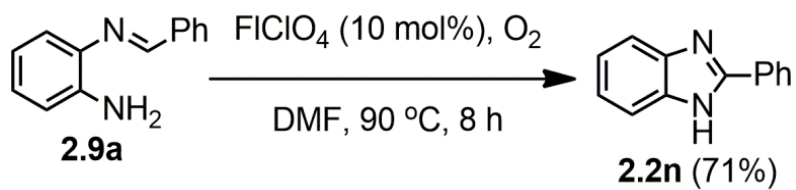


Figure 2.7 Detection of aldehyde from reaction of trisubstituted substrate **2.1q**



Scheme 2.5 Reaction scope with imine substrate

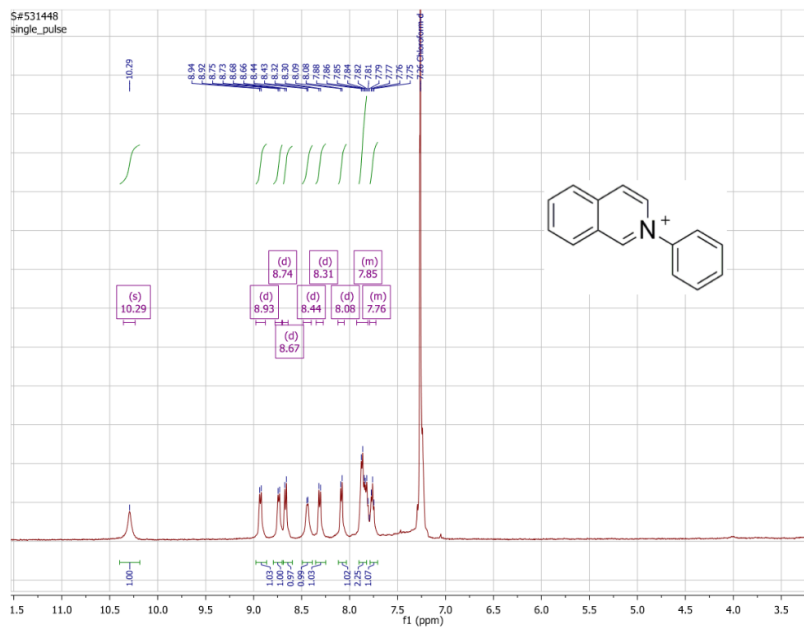


Figure 2.8 ^1H NMR spectrum of fully oxidized THIQ species isolated from crude reaction mixture

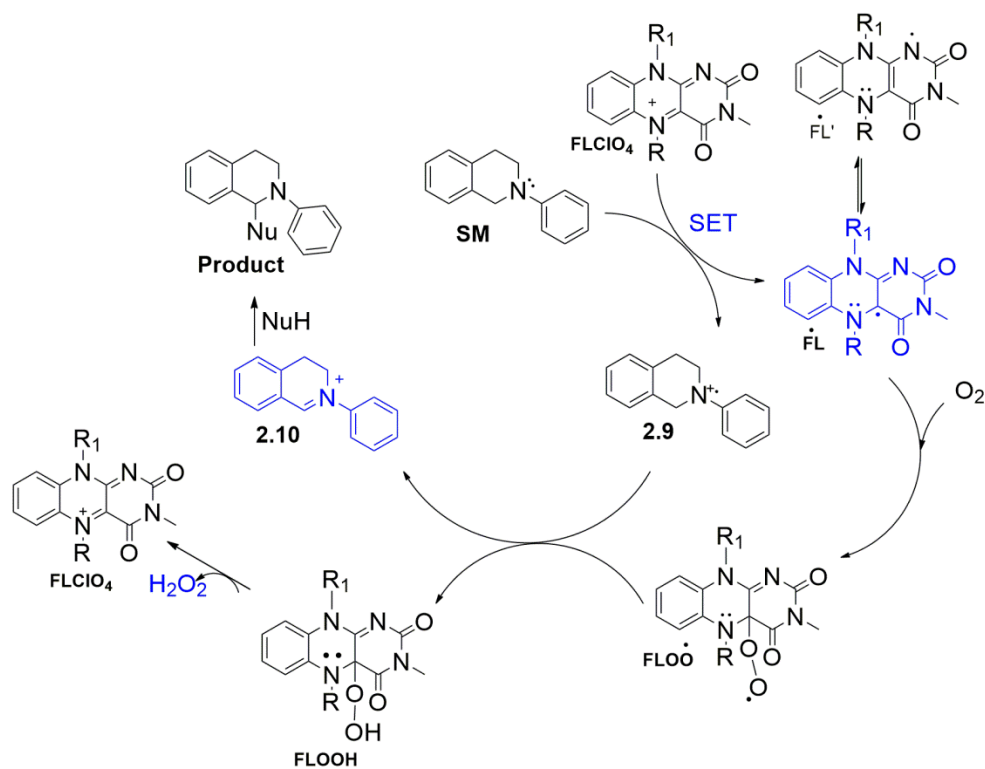


Figure 2.9 Proposed reaction mechanism for artificial flavin mimic catalyzed oxidative CDC reaction

2.3. Conclusion

This work introduces the first application of artificial riboflavin mimics in oxidative CDC reactions. Notably, these catalysts perform CDC reactions in mild conditions with just air or oxygen as oxidant. Also, relative reactivity of various flavin based catalysts showed that electron poor isoalloxazine catalyst facilitates the reaction. During the course of the study, it was found that the urea based additives allow selective CDC nitro-Mannich reaction presumably due to inhibitory effect on peroxide formed during catalyst turnover. Anion effects with different bronsted acids ruled out the purely acid mediated process. Reactions with different radical probes indicated radical-based mechanism. Intramolecular kinetic isotope effect studies provided a useful insight for being hydrogen atom abstraction as a rate limiting process. Furthermore, unlike THIQ substrates, hydrolysable C-N bond containing substrates afforded hydrolyzed product.

Future investigations will be targeted towards design and synthesis of more effective flavin based catalysts. Nucleophilic scope will also be further extended by screening more reactive nucleophilic partners like enamines, enols, etc. More effectively, incorporating synergistic catalysis through proline based catalyst to activate carbonyls for C-C bond formation will be a high target, both for normal and stereoselective transformation. Many oxidizable substrates towards oxidation and oxidative application will also be studied to increase the scope of biomimetic flavinium catalysis.

Chapter 3

Flavin-catalyzed Green Synthesis of Michler Hydride Derivatives

3.1. Background

Activation of small molecules and subsequent formation of C-C bonds are of growing interest in organic syntheses because this approach allows construction of both simple and complex organic molecules in fewer steps.⁸¹⁻⁸⁶ Several multi-component reactions (MCRs) utilize this strategy for synthesis of various drugs and dyes.⁸⁷⁻⁹¹ Moreover, sterically encumbered Lewis acids/base pairs for activation of small molecules and subsequent C-C bond formations have attracted considerable attention in recent years.^{34,35} New avenues in related areas involve carbon based Lewis acids to activate small molecules like H₂, CO₂, etc.³⁴ Ongoing research work has been contributing significantly towards development of water tolerant Lewis acids/bases and/or conditions to circumvent the specific problem of catalyst deactivation by aqueous environments.⁹²⁻⁹⁶ Therefore, a search for a system able to tolerate water and catalyze the organic reactions is strongly desirable.

Artificial riboflavin mimics have structural and functional similarities to naturally occurring riboflavin cofactors. They have been widely used to mimic both redox and non-redox functions of natural riboflavin. Biomimetic studies on functional ability of artificial riboflavin mimics related to non-redox property, however, remain under develop.⁶⁶ In biological system, flavin dependent enzymes like *oxynitrilase* and *hydroxynitrile lyase* are known to catalyze C-C bond formation leading to formation of cyanohydrins compounds and hydrolysis of those cyanohydrins back to aldehyde respectively, the processes especially adapted by organisms for defense mechanism against predation. Widely studied biocatalytic systems have shown that carbonyl compounds are activated through condensation with electron rich reduced flavin,

enabling through either radical or ionic mechanism, and concomitant attack of cyanide group thus leading to formation of cyanohydrin compounds which are very important building blocks for versatile functional group manipulation.⁹⁷⁻¹⁰¹ While this model remains dominant in scientific community, activation of electron rich carbonyl oxygen by oxidized flavin could not be ignored, especially when the oxidized flavin core is more electron deficient through H-bonding effects or similar effects of different amino acids in proximity of the substrate in biological systems. Towards this end, flavin mimics' work as Lewis acid has been rarely tested, although many studies involving their electrophilic effects are known and have been discussed thoroughly in mechanistic studies including their redox properties.⁷⁹

3.2. Results and Discussions

During the course in exploring the chemistry of flavin mimics in oxidation reaction, we found that oxidized and electron poor flavin mimics are capable of catalyzing Mannich type reaction between formaldehyde and aromatic nucleophiles, providing Michler hydride type diarylmethane derivative. This was unexpectedly discovered while studying additive effects in oxidation reaction (**Figure 3.1**). Initially, we supposed it was caused by generation of acid in situ due to deprotonation of the pseudobase FLOH (pH 8.0) by amine bases, studied earlier by other research group.¹⁰² However, the reaction worked in a buffer system at pH 7.5 without significant change in pH of the solution. Several Michler hydride type molecules are significant towards various applications. For example, they are widely used as initiator in radical chain polymerization reaction.¹⁰³ In addition, they are bioactive and their structural motif in organometallic chemistry provide interesting feature for selective recognition of metal ions (**Figure 3.2**).^{104,105} Together, scope of Michler hydride type molecules and unique catalytic scope of flavinium species, both motivated us to further research on these systems.

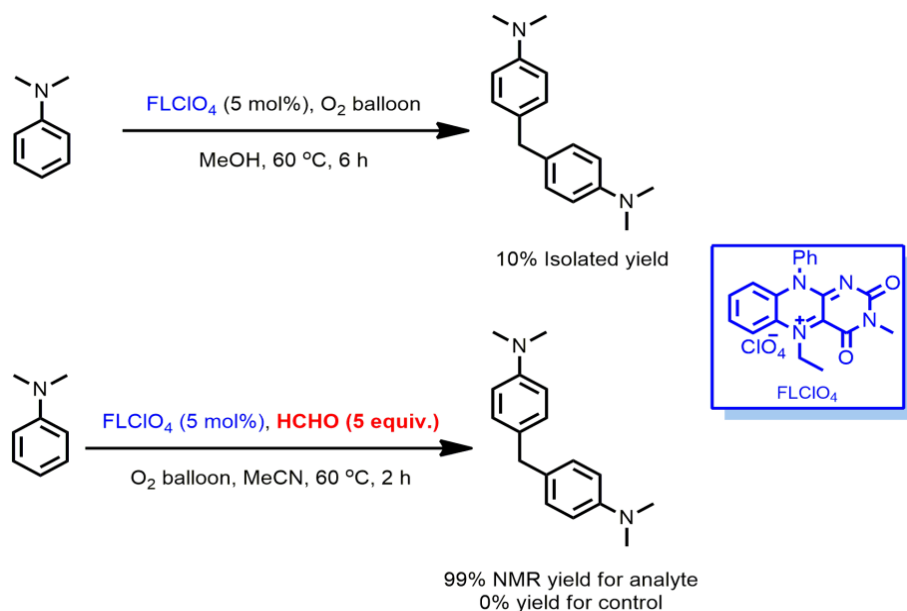


Figure 3.1 Discovery of current method

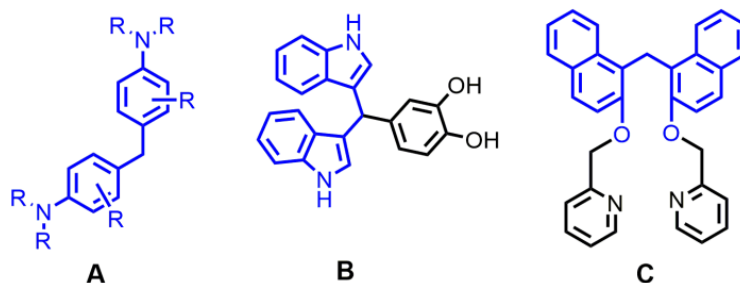


Figure 3.2 A (Hydride donors), B (HIV-I Integrase Inhibitor, IC_{50} = 50 μ M), and C (Ligand for selective recognition of Cu^{2+} in presence of other metals)

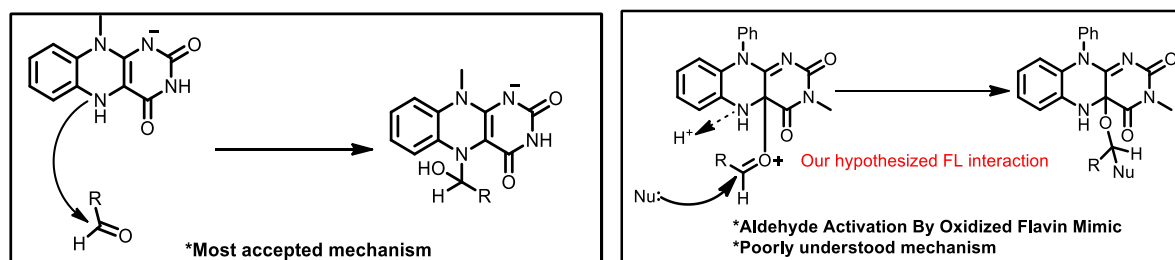


Figure 3.3 Widely accepted mechanism (left); our hypothesized working model (right)

We began our study by optimizing the reaction conditions based on amount of formaldehyde (**table 3.1**), temperature (**table 3.2**), solvent (**table 3.3**), and various external conditions (**table 3.4**). Relatively high concentration of HCHO was required (table 1, entry 4). In case of solvent

screening, methanol was not found effective at all (table 3, entry 3), which could be due to catalyst deactivation by the nucleophilic solvent. However, ethanolic solvent showed some improvement in yield (table 3, entry 4). A control reaction with Brønsted acid catalyst HClO₄ in methanol solvent however provided excellent yield (table 3, entry 5). Acetonitrile proved to be the best solvent giving more than 95% yield in only 2 h reaction time (table 3, entry 2). Temperature screening showed slower rate at lower temperature, delivering only 26% yield at room temperature (table 2, entry 1). On the other hand, higher temperatures were very effective giving more than 90% NMR yield in only 3 hours. Moreover, no significant difference in yield was observed at 45 °C and 75 °C (table 2, entry 2 and 3).

Table 3.1 Screening amount of HCHO

Entry	HCHO (Equiv.)	% NMR yield
1 ^a	0.5	50
2	1	60
3	2	61
4	5	99
	^a = 3h time	

Table 3.2 Screening of temperature

Entry	temp. (°C)	% NMR yield
1	rt	26
2	45	95
3	70	99
4 ^a	rt	71
	^a = ON reaction	

Table 3.3 Screening of solvent

Entry	solvent	% NMR yield
1 ^a	H ₂ O	66, 56, 59
2	MeCN	99
3	MeOH	Trace
4	EtOH	44
5 ^b	MeOH	98
	^a 4 h; ^b HClO ₄ (5 mol%) was used as catalyst	

Table 3.4 Screening of atmosphere

Entry	atmosphere	% NMR yield
1	air	99
2	Argon	94
3	O ₂	95
4 ^a	air	90
	^a = No light	

Table 3.5: Optimization of reaction condition:^a

Entry	Catalyst (mol%)	% NMR Yield	Entry	Catalyst (mol%)	base additive	% NMR yield
1	FLOOH (5)	0	12	FLClO ₄ (5)	NaHCO ₃	trace
2	TEMPO (10)	0	13	FLClO ₄ (5)	TEA	trace
3	FLClO ₄ (5)	95	14	FLClO ₄ (5)	DABCO	trace
4	NaClO ₄ (10)	0	15	H ₂ O ₂ (10)		0
5	-	0	16	TBAI ^c (10)		0
6	FLClO ₄ (2)	41	17 ^f	FLClO ₄ (5)		70
7	A2 (5)	0	18 ^g	FLClO ₄ (5)		71
8	IA2 (5)	94	19	<i>N</i> 10-PhIsoalloxazine (10)		0
9 ^b	FLClO ₄ (5)	93	20	<i>N</i> -Methylpyridinium Iodide (10)		0
10	TBAP (5)	0	21 ^h	FLClO ₄ (5)		9
11 ^c	FLClO ₄ (5)	91	22 ⁱ	FLClO ₄ (5)		70
12	TBAA ^d (10)	0	23 ^j	FLOOH (5)		20

^aReaction Conditions: **3.1a** (0.155 mmol), HCHO (5 equiv.), MeCN (0.5 ml). ^bBHT (2 equiv.). ^cCD₃CN solvent. ^dTetrabutylammoniumacetate. ^eTetrabutylammoniumiodide. ^fParaformaldehyde was used (5 equiv.) as formaldehyde source, 6 h. ^gParaformaldehyde (5 equiv.), distilled and degassed solvent, 6 h. ^hM.S. 4Å. ⁱM.S. 4Å and F₃CCH₂OH (2 equiv.) ^j10 h, thioanisole (10 mol%)

While most of the artificial flavin mimics catalyzed reactions require terminal oxidant source like peroxide, oxygen, etc, these reactions worked equally well in presence or absence of oxidant (**table 4**). Interestingly, the reactions worked equally effectively in argon atmosphere and also in

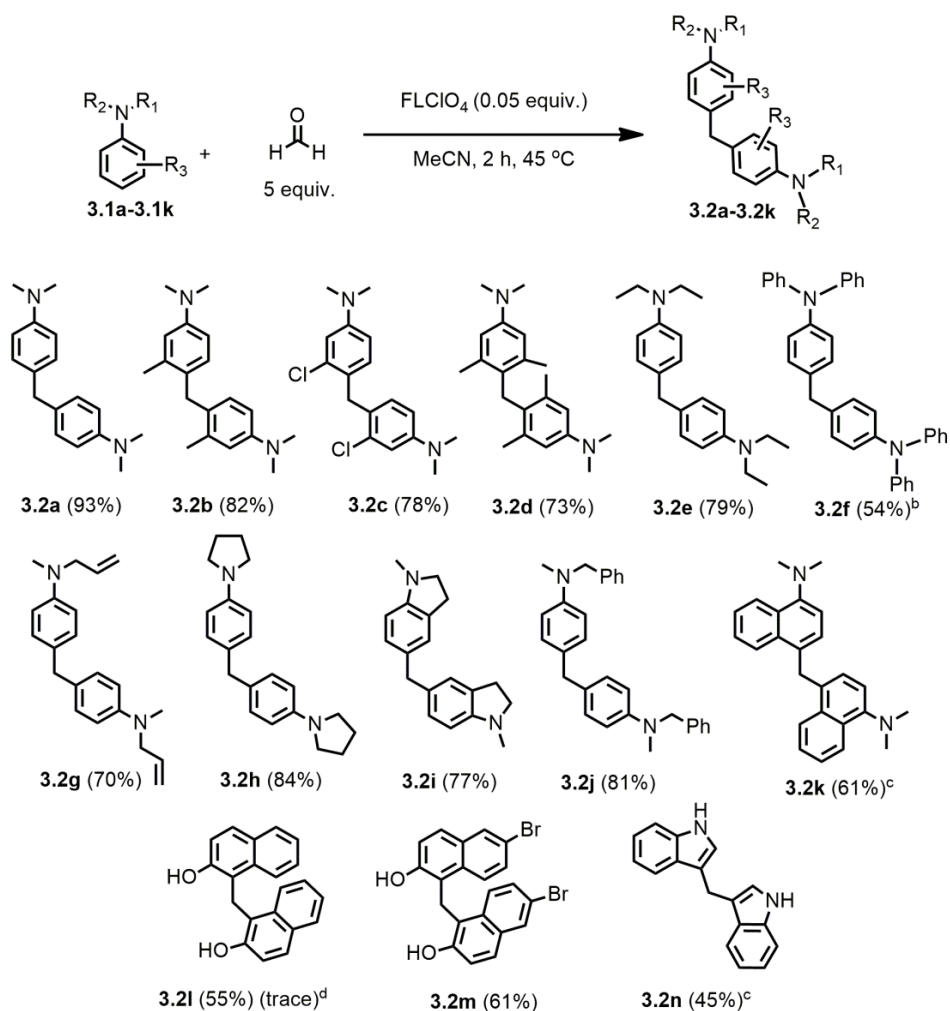
absence of light (entry 2 and 4, table 4), which indicated that reagents involved for catalyst turnover was other than normal oxidants like peroxide and oxygen.

Further screenings were carried out with respect to counter anion sources, other catalysts, and additives (**table 3.5**). The role of ClO_4^- ions in reaction was investigated through the use of additives like NaClO_4 and Bu_4NClO_4 in reaction mixture. Both perchlorate sources were unable to generate product (entry 10, 12). To understand the role of flavin mimics as phase transfer catalysts, several phase transfer catalysts were tested but none of them were found effective as catalysts (entry 10, 12 and 16). No products and conversion were detected in NMR. As predicted, pre-catalyst of *N*3-Methyl-*N*10-PhenylIsoalloxazinium catalyst was found ineffective. Interestingly, alloxazinium based catalyst **A2** was not effective at all and full starting material was recovered (entry 7). Isoalloxazinium catalyst **IA2** bearing phenyl group in *N*3 position was as effective as **FLClO₄** (entry 8). Furthermore, base like NaHCO_3 , TEA, and DABCO all had negative impact on the scope; providing trace amount of yield (entry 12, 13 and 14), indicative of acid catalyzed process. In order to know the effect of water in reaction scope, paraformaldehyde was chosen as a source of formaldehyde was used as solvent. In this case, reduced NMR yield of 71 % in 6 hour period was found (entry 17, 18). The yield was not affected when freshly distilled and degassed solvent was used (entry 18). However, the use of molecular sieves greatly suppressed the reaction progress providing only 9% NMR yield in 1 day period (entry 21), indicating a positive role of water in reaction cycle. These observations suggested that water played a crucial role in the reaction cycle. With this information in hand, we wondered if water could be used as solvent. Interestingly, a good NMR yield of 70% was obtained when water was used as a solvent. Gratifyingly, the aqueous solution after organic solvent extraction of desired product, byproducts and remaining starting material, could still be used without adding extra

catalyst for at least three reaction cycles without any significant change in NMR yields (**table 3**, entry 1).

With an optimized condition in hand, a number of ortho-, meta- and para- substituted *N,N*-dimethylanilines were studied. Ortho-substituted substrates did not work at all which could be due to steric stress provided by ortho group in proximity of a lone-pair of electrons in nitrogen.¹⁴ In case of meta-substituted substrate, all gave a decent isolated yield ranging from 75% to 85%. Para substituted substrate did not afford any ortho coupled product. With respect to substituents on the nitrogen atom, we tried ethyl, allylic, benzyl, phenyl, indolyl, and pyrrolidinyl substituted aniline. In all case, we obtained excellent results (entry **3.2e-j**). More notable examples include *N,N*-diphenyl substituted aniline (entry **3.2f**) and indolyl substituted aniline (entry **3.2i**), both of which did not polymerize. Previous studies have shown that these substrates were challenging as they were found to polymerize and reduce the scope of desired Michler hydride type molecules.¹⁰⁶ Furthermore, the substrate scope was broadened to naphthyl amine, 2-naphthol and indole molecules. All of these substrates provided moderate yields for the respective coupled products. Unfortunately, substrates like *o*-substituted aniline, *p*-substituted, phenol, anisole and *N*-phenyltetrahydroisoquinoline did not work at all. Two arguments could be made from these undesired results. The first one being requirement of higher nucleophilicity on aromatic ring and other, the steric demand that comes from the most acidic or activated C4a position in flavin catalysts.¹⁰⁷ Higher oxidation potential could be responsible for lower nucleophilicity in case of substrate *N*-phenyltetrahydroisoquinoline.^{45,108}

Table 3.6 Substrate Scope study^a



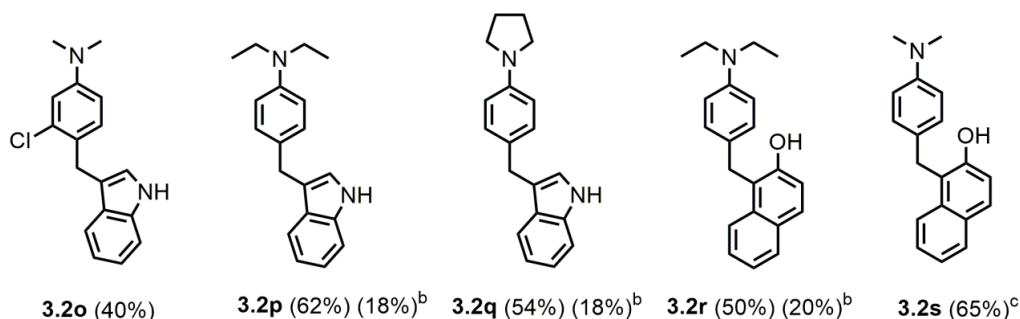
^a reaction conditions: **3.1a-3.1n** (0.5 mmol), HCHO (2.5 mmol), FLClO_4 (0.0025 mmol), MeCN (1.0 mL), 2 hours, $45\text{ }^\circ\text{C}$; ^b $70\text{ }^\circ\text{C}$; ^c6 hour reaction time; ^dNMR yield of control reaction

Multicomponent reaction involving two different nucleophilic components is useful for construction of two different C-C bonds in the same molecule.¹⁰⁹ We applied the optimized condition from above screening studies for this strategy. However, initially poor yields were obtained leading to different byproducts. With few more trials with respect to different mode of addition of reagents, we found that dropwise addition of one nucleophilic component in the mixture of another component and formaldehyde afforded better yields. The results are presented

in **Figure 3.4**. As shown in the table, various different nucleophiles were coupled. However, in each case Michler hydride derived from aniline as byproduct could not be avoided. Nevertheless, effective conversions were observed in all cases. As shown in entry **3.2s**, we were unable to separate two different Michler Hydride products and therefore, combined isolated yield was reported.

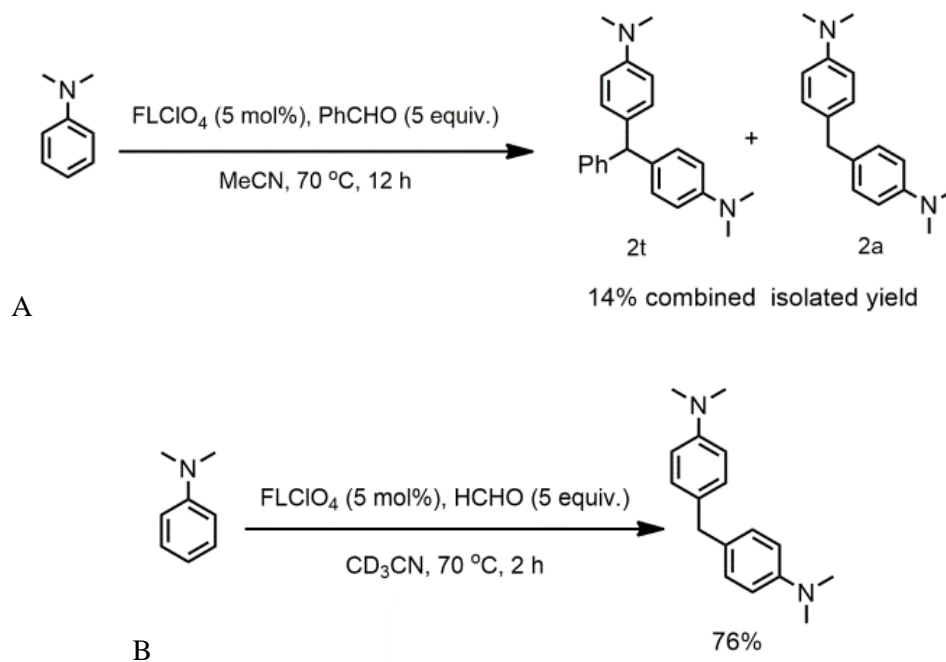
To further investigate the catalytic activity of flavin mimic FLClO_4 for other aldehyde source, we employed benzaldehyde in the reaction condition (**Scheme 3.1**, entry a). Unfortunately, desired corresponding coupling product was obtained in poor yield. Additionally, Michler hydride product **3.2a** was also observed. A control experiment in CD_3CN solvent (**Scheme 3.1**, entry b) ruled out that the methylene ($-\text{CH}_2$) group in the byproduct **3.2a** was derived from the acetonitrile solvent as Michler hydride **3.2a** was observed in good yield and no deuterated MH product was observed. Nevertheless, the formation of product **3.2a** in the case of benzaldehyde supports our observation of *N*-demethylation type reaction during initial study.

Figure 3.4 Multi-component reaction substrate scope study^a

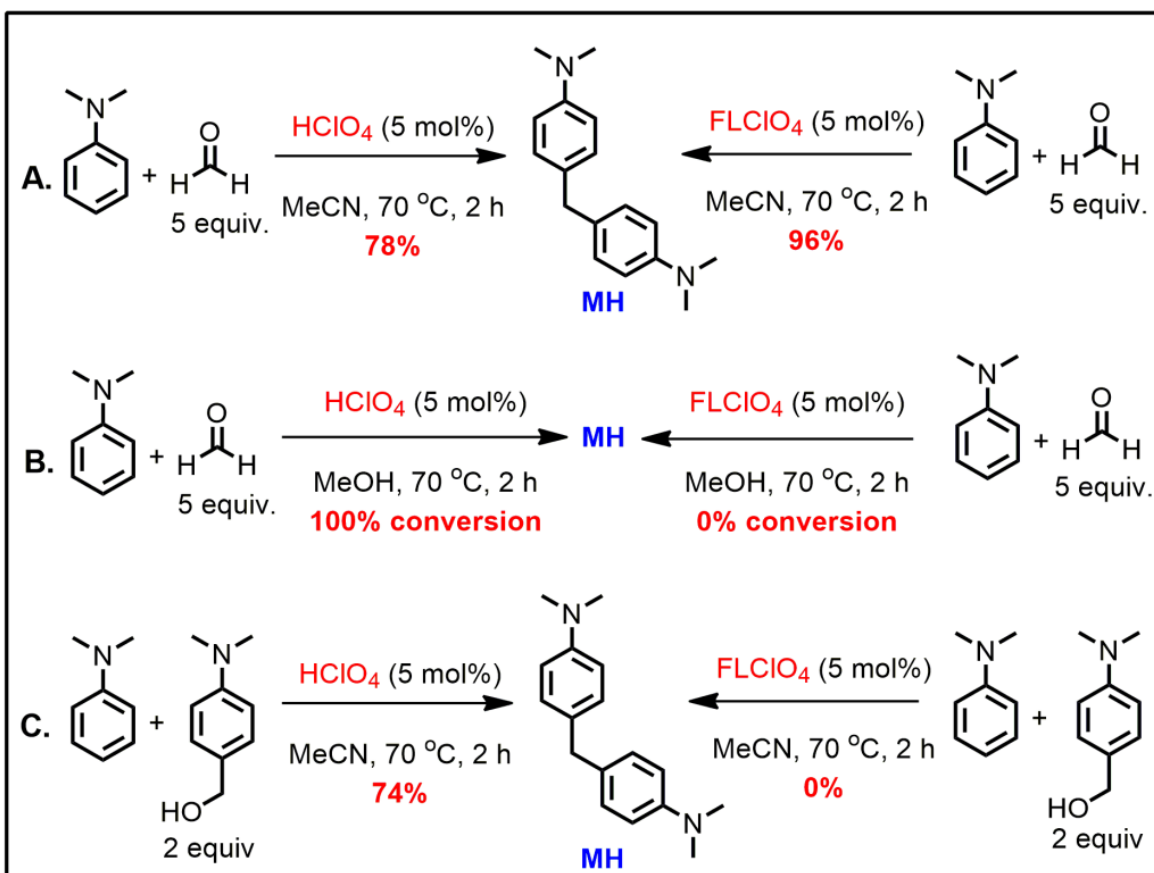


^areaction conditions: **3.1a** or **3.1e** or **3.1h** (0.5 mmol) and **indole** or **naphthol** (0.5 mmol), HCHO (0.5 mmol) added dropwise in the reaction mixture, FLClO_4 (0.0025 mmol), MeCN (1.0 mL), 12 hours, 60°C ;
^bisolated yield of Michler hydride product derived from aniline partner only; ^ccombined isolated yield

Scheme 3.1: A) Scope of benzaldehyde and B) control experiment with CD₃CN



Amine sources are known to facilitate adduct formation with water resulting in formation of proton source.¹⁰⁷ To investigate if proton source is responsible for the scope of the reaction but not flavin catalyst, control reactions using Brønsted acid with same counter anion ClO₄⁻ was tested. Control reactions represented in **scheme 3.2** gave some useful insights for comparative analysis of Brønsted acid and Lewis acidic flavinium species. In acetonitrile, both acids gave good yields (entry A) although flavin catalyst worked better than bronsted acid catalyst. However, in methanolic solvent, only bronsted acid was effective (entry B) and no conversion were found in case of flavin catalyst. Similarly, using flavin catalyst, when alcohol derivative of aniline was used as coupling partner for coupling reaction with aniline, no effect was seen. However, bronsted acid effectively catalyzed the same coupling reaction to afford Michler hydride in very good yield (entry C).



Scheme 3.2 Control reactions with bronsted acid HClO₄

Activation of formaldehyde through FLP interaction with sterically encumbered Lewis acid/base pair have been reported in few literatures.^{94,95} Sufficient evidence has come from isolation and characterization of the adduct formed between Lewis acid/base pair with formaldehyde. Our initial trials during study for the formation of adduct of flavinium species and selected base with formaldehyde in different solvents were unsuccessful. Furthermore, we tried a number of UV-vis experiment to understand the adduct formation with different formaldehyde source in different solvent and conditions. However, all trials were inconclusive. On the other hand, sequential NMR studies revealed a unique feature of shielding effect on aromatic protons of flavinium species after addition of formaldehyde in solution of flavinium species and internal standard in CD₃CN. Interestingly, no such effect was observed or at least not significant as former in case of

internal standard and its aromatic protons. Since, proton (^1H) and carbon (^{13}C) NMR studies for FLP interaction are limited due to low abundance and thus less sensitivity for these nuclei, we wondered if the effects could be significant and thus quantitative in more abundant nucleus like Phosphorus (^{31}P). Initially, we chose triphenyl phosphine oxide (PPh_3O) as lewis base source to observe effect of lewis acidic flavinium species on ^{31}P NMR of the selected base similar to Gutmann-Beckett experiment which is widely used for understanding lewis acidity of lewis acid in FLP chemistry.⁹² Phosphorus peak broadening and deshielding effect, both were observed in case of mixture of Phosphine oxide with flavin in CD_3CN (**Figure 3.8**). Negative control reaction without catalyst showed no change in both chemical shift and peak shape (**Figure 3.6**). Positive control reaction with bronsted acid HClO_4 , however, led to larger deshielding effect without peak broadening effect, leading to strong acid-base adduct formation (**Figure 3.7**). Further investigation with usual Gutmann-Beckett experiment involving triethylphosphine oxide (Et_3PO) also affected similarly like PPh_3O . However, in case of Et_3PO , overall lower deshielding effect was found as predicted with stronger base Et_3PO (Figures and Table will be represented in **Appendix B** separately, including for other flavinium catalysts). Overall, these observations with peak broadening and deshielding effects are suggestive of FLP interaction between Flavinium species FLClO_4 and phosphine oxide source.

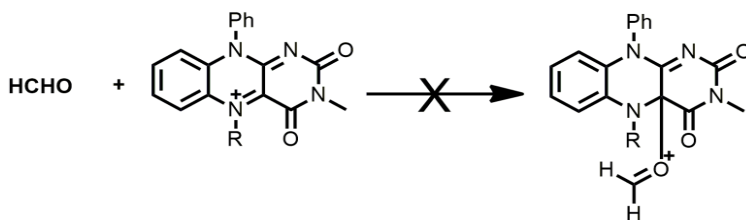


Figure 3.5 UV-vis study for formaldehyde-flavin adduct formation

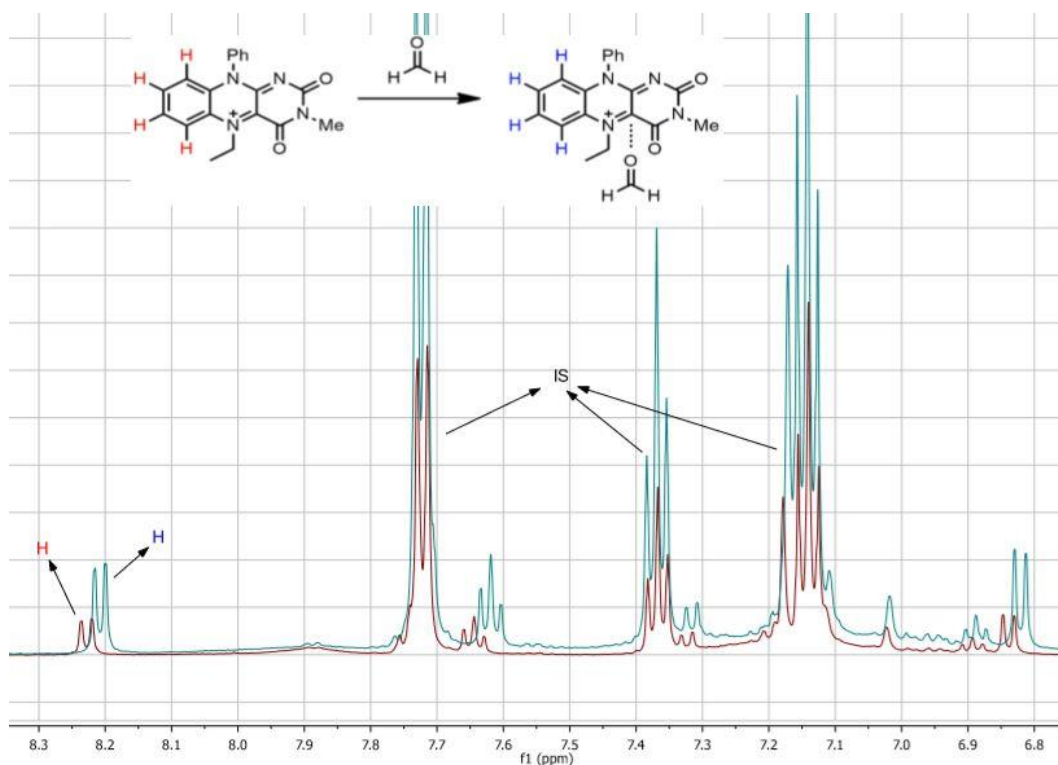


Figure 3.6 NMR spectrum of aromatic region for crude mixture of flavin (used as catalyst), Internal standard (Iodobenzene) and formaldehyde; red (before adding formaldehyde) and blue (after adding formaldehyde)

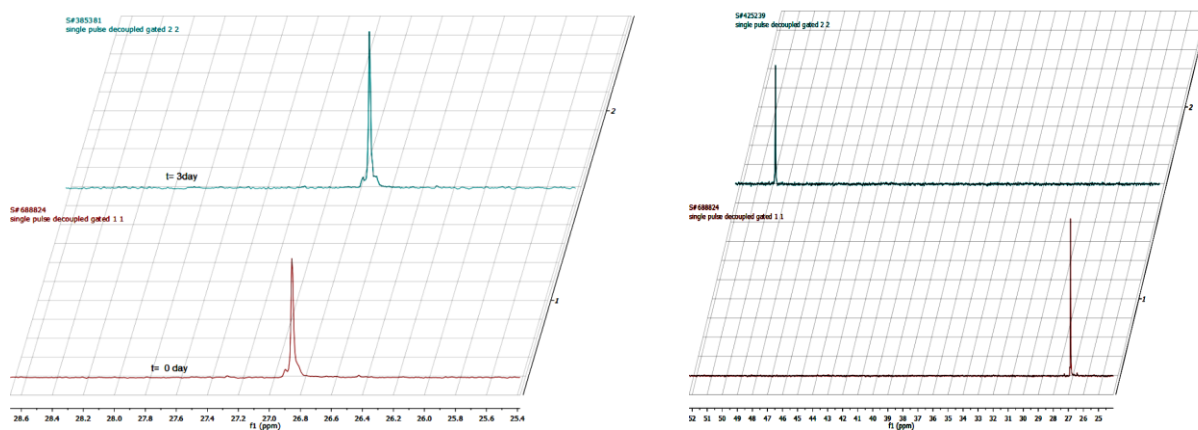


Figure 3.6 ^{31}P NMR of Et_3PO without FLClO_4 ; HClO_4 ;

Figure 3.7 control reactions with Bronsted acid

Ph_3PO only (red); mixture of HClO_4 (3 equiv.) and Ph_3PO (blue)

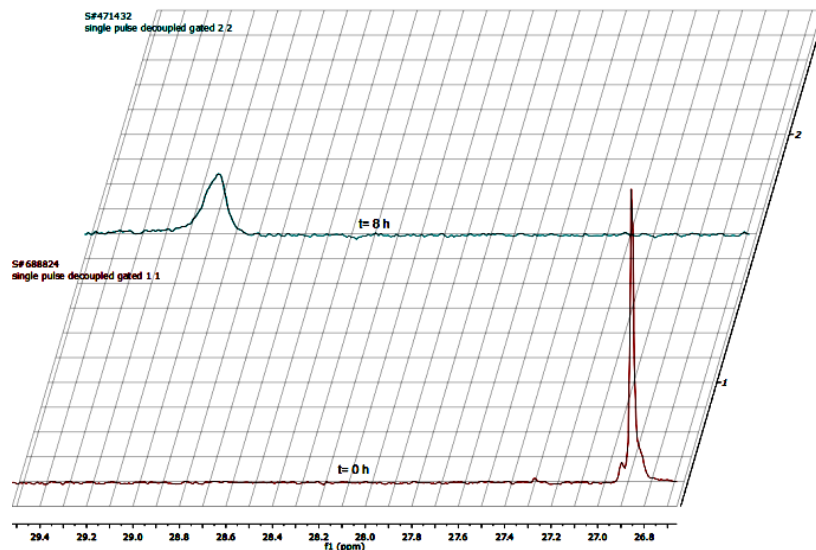
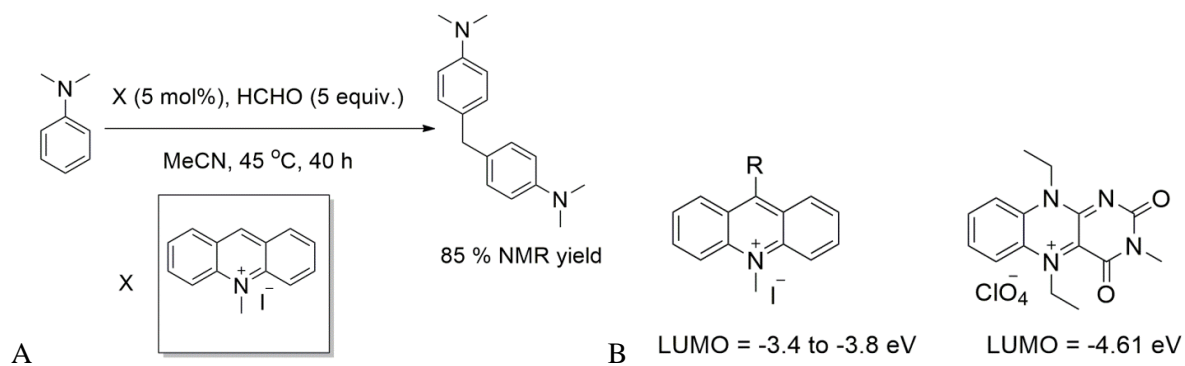


Figure 3.8 ^{31}P NMR for Ph_3PO only (red), and mixture of FLClO_4 (3equiv.) and Ph_3PO (blue)

Based on all the previously described results, a catalytic cycle has been proposed as shown in **figure 3.9**. Formaldehyde could be activated at C-4a position (the most lewis acidic position) of electrol poor flavin **FLClO₄**. Nucleophilic attack of amine would result into adduct formation. Deprotonation on this adduct results into formation of **FLOH** along with azaquinone methide, the active intermediate for Michler hydride product. In the presence of base, **FLOH** with low pK_a value¹¹⁰ could be deprotonated and could result into resting state **FLO⁻** as this could not turn over. However, in absence of base, **FLOH** could provide **FL⁺** which could be available for activation of formaldehyde for another reaction cycle. Lower electrophilic characters of alloxazinium flavin catalysts could be responsible for inability of these catalysts for activation of formaldehydes.⁷⁹ The acridinium catalyst could still give the product in good yield of 85% but in longer duration of 40 hours, possibly due to higher LUMO level of these catalysts as compared to isoalloxazinium flavin catalyst.^{111a,111b} In other words, acridinium catalyst and formaldehyde could possibly have lower HOMO-LUMO interaction than isoalloxazinium flavin catalyst and formaldehyde.



Scheme 3.3 N-Meacridinium iodide catalyzed reaction (A); LUMO level energy of acridinium catalyst and flavinium catalyst (B)

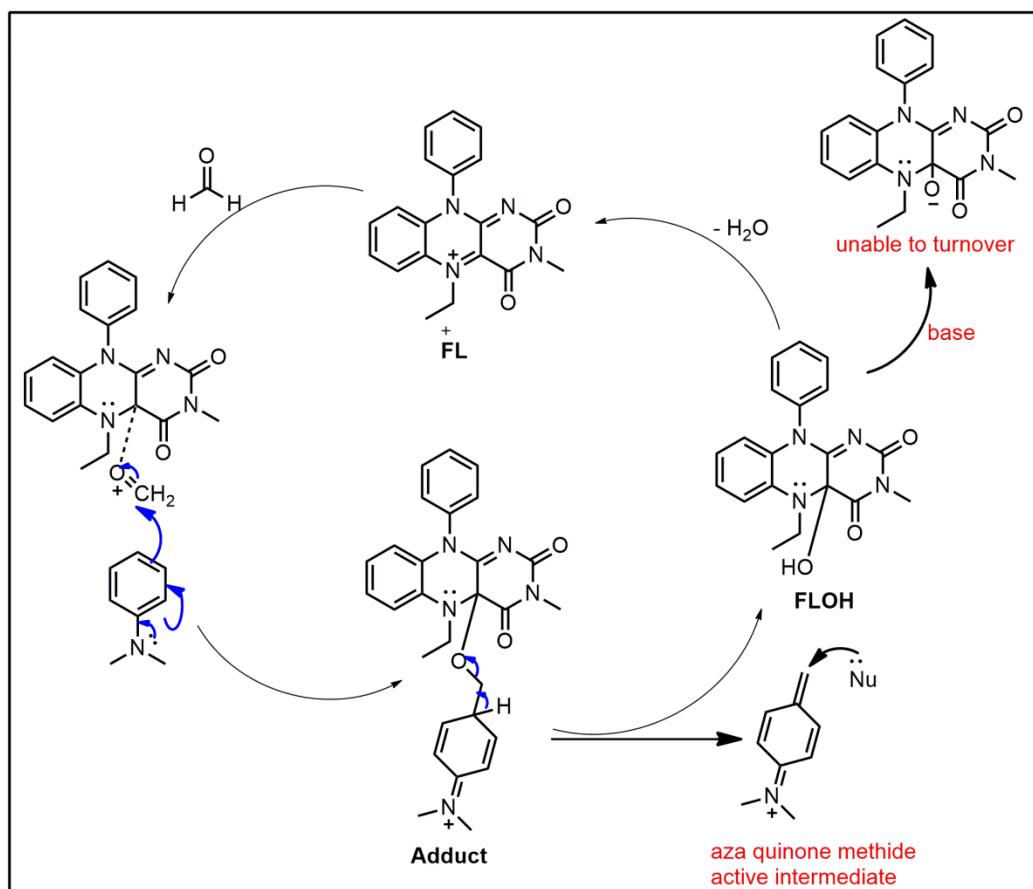


Figure 3.9 Plausible pathways for flavin catalytic cycle including formaldehyde activation step

3.3. Conclusion

In conclusion, in this chapter, a completely new paradigm of flavinium species especially isoalloxazinium based flavin catalysts was introduced. They were found to activate small aldehydes like formaldehyde sufficiently enough to allow coupling with different nucleophilic components like aniline derivatives, indoles and naphthols. This chemistry reveals the first non-redox based chemistry afforded by artificial flavin mimics. In future, focus on activation of other small molecules like H_2 , CO_2 , etc. for the relevant chemistry will be extended. In addition, cyanohydrins synthesis will also be tested, which could possibly serve as synthetic model studies for hydroxynitrilase involved biochemical reactions.

Chapter 4

Iron-catalyzed 1,2-disubstituted benzimidazoles Synthesis by Cross-dehydrogenative Coupling Strategy

4.1. Background

Iron trichloride is a valuable catalyst in organic synthesis—available and applicable to a growing number of transformations.^{112,113} FeCl₃ performs primarily Lewis acid catalysis,¹¹⁴ including addition,¹¹⁵ substitution,^{116,117} and cross-coupling reactions.¹¹⁸⁻¹²⁰ Recently, FeCl₃ in presence of enantiopure ligands was used to catalyze hydroaminations,^{121,122} hydrosilylations,^{123,124} and various enantioselective transformations.¹²⁵ Because FeCl₃ is appealing for sustainable chemical methodologies, we often evaluate its potential activity for reactions of interest.¹²⁶

Benzimidazoles are heteroaromatic compounds, well known for their medical and material applications.¹²⁷ Specifically, 1,2-disubstituted benzimidazoles have significant pharmacological utility (**Figure 4.1**), such as antihypertensive telmisartan (**1**),¹²⁸ non-sedating antihistamine drug mizolastine (**2**),¹²⁹ and GABA_A agonist (**3**).¹³⁰ A wide range of applications has been reported in the realm of medicines, dyes, polymers, ligands and also as organocatalysts.

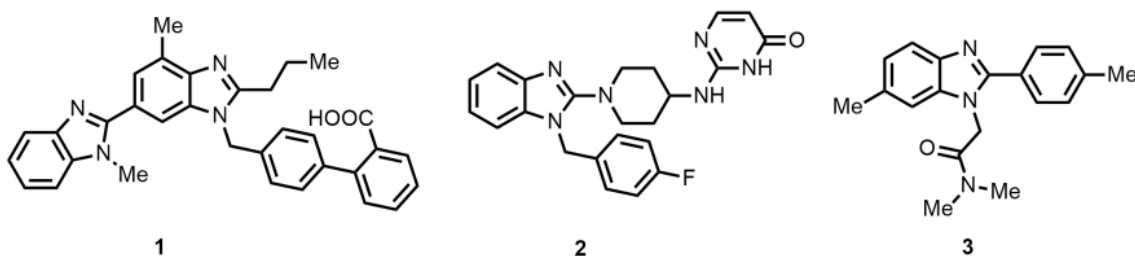
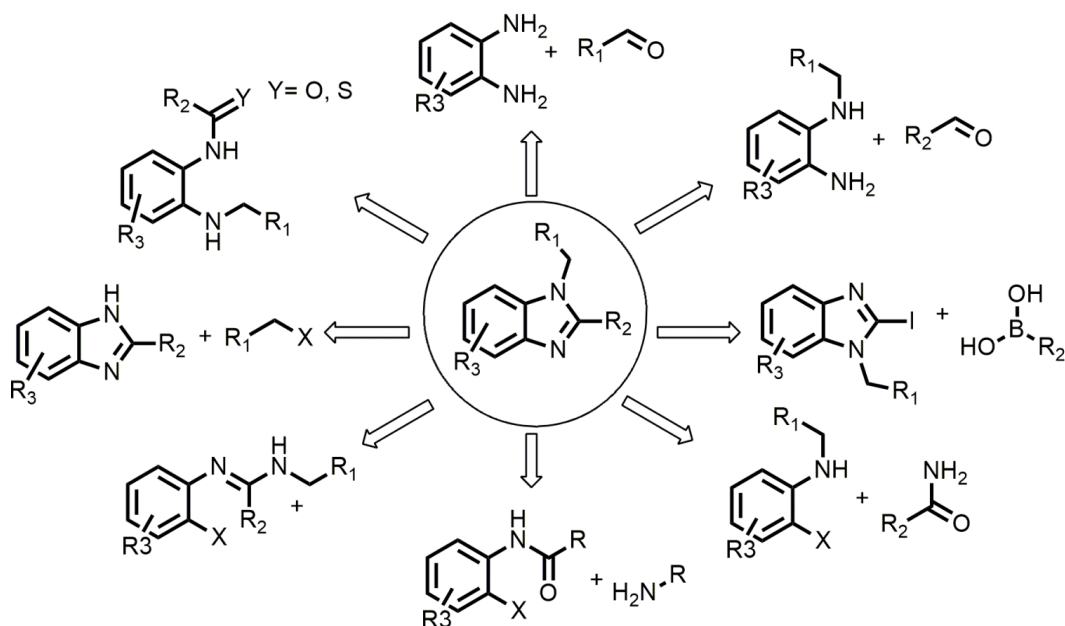


Figure 4.1 Some examples of medicinally important 1,2-disubstituted benzimidazoles

Benzimidazoles, are classically synthesized by cyclocondensation reactions between *ortho*-phenylenediamines (OPD) and highly-oxidized functional groups (e.g. carboxylic acids, nitriles, ortho esters) in presence of strong Brønsted acids under heat or microwave conditions.^{131,132,133} Milder cyclocondensation conditions were achieved by a variety of reagents, including: DDQ,¹³⁴

KHSO₄,¹³⁵ Sc(OTf)₃,¹³⁶ Cu(OTf)₂,¹³⁷ and CeCl₃·7H₂O/CuI.¹³⁸ Our laboratory previously reported mild flavin-catalyzed oxidative cyclizations with O₂ as a terminal oxidant.¹³⁹ Recently, benzimidazoles were created by direct C-N bond construction via intramolecular cross-dehydrogenative-coupling (CDC) approaches.¹⁴⁰⁻¹⁴³ CDC reactions formally remove α-hydrides of amines, ethers, and thiols to generate reactive intermediates (e.g. imines), reminiscent of dehydrogenations performed by metallo- and flavo-protein oxygenases. Recently, aerobic CDC approaches were applied to prepare 2-substituted benzimidazoles,¹⁴⁴⁻¹⁴⁷ with Cu-, Pd-, and Co-based catalysts at elevated temperatures.¹⁴⁸⁻¹⁵⁰ In this work, we show that relatively inexpensive and less toxic FeCl₃·6H₂O catalyzes CDC alpha to the 2° or 3° amines of N-substituted OPDs, to efficiently prepare many 1,2-disubstituted benzimidazoles (**Scheme 4.1**).

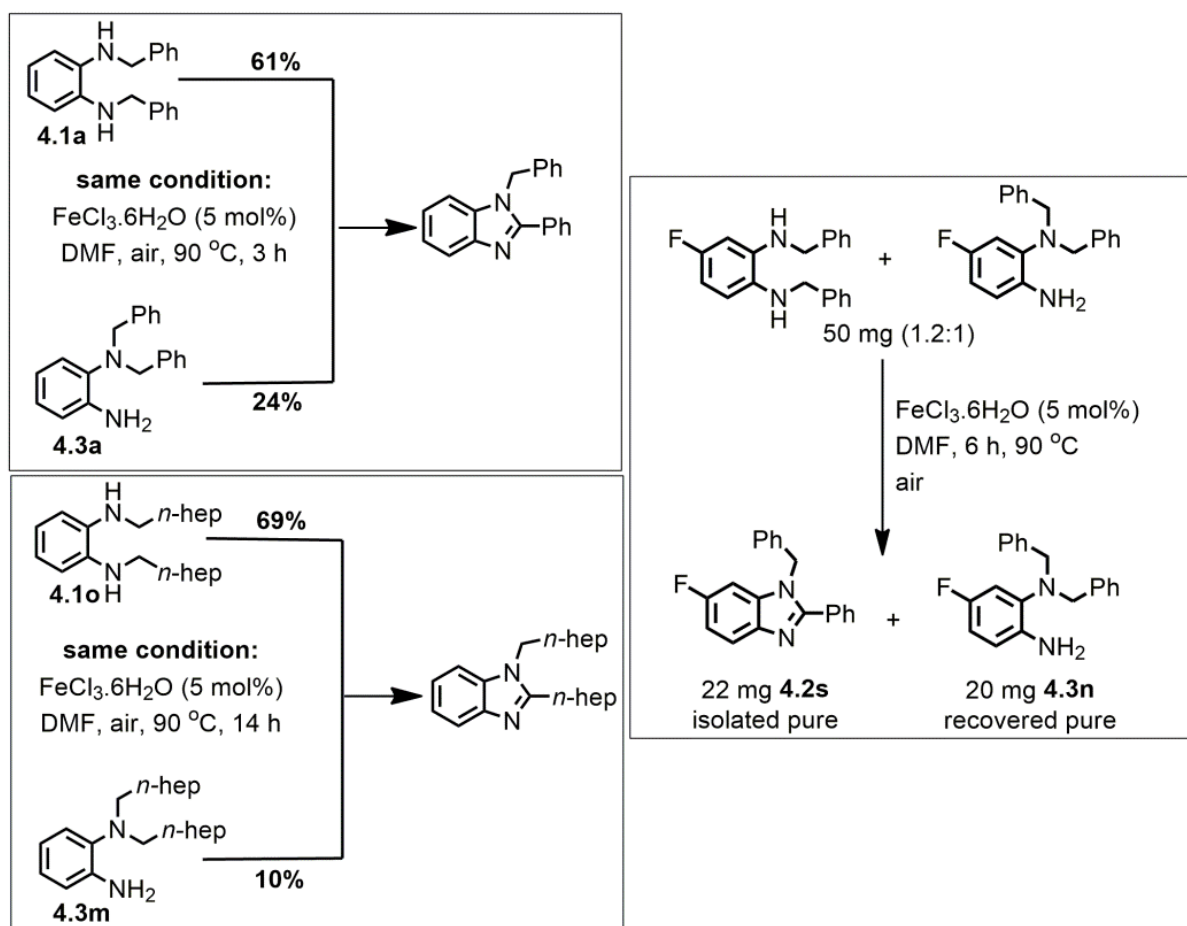


Scheme 4.1 Synthetic strategies for 1,2-disubstituted benzimidazoles

4.2. Results and Discussions

Our effort began with a comparative study on 1,2-disubstituted benzimidazole formation from *N,N'*-disubstituted-OPD and *N,N*-disubstituted-OPD similar to the conditions of Doyle and coworkers¹⁵¹ (**Scheme 4.2**). Whether investigating dioctyl (**4.1o** vs. **4.1l**) or dibenzyl-OPDs (**4.1a**

vs. **4.3a**), the *N,N'*-system, bearing two 2° amines, reacted faster and reached greater yields compared to their *N,N*-disubstituted-OPDs. In another experiment, a mixture of *N,N*-OPD and *N,N'*-OPD when reacted under the similar condition rendered corresponding 1,2-disubstituted benzimidazole **4.2s** product in excellent yield along with 89% recovered *N,N*-OPD starting material **4.3n**. Furthermore, time dependent NMR experiment conducted for a mixture of *N,N*-OPD and *N,N'*-OPD clearly revealed the conversion of the later to the product while the former being intact as clearly seen in **figure 4.2**. Reaction conditions were then improved for the *N,N'*-disubstituted substrate.



Scheme 4.2 Parallel studies with two isomers in same condition (left); comparative study of two isomers in the mixture

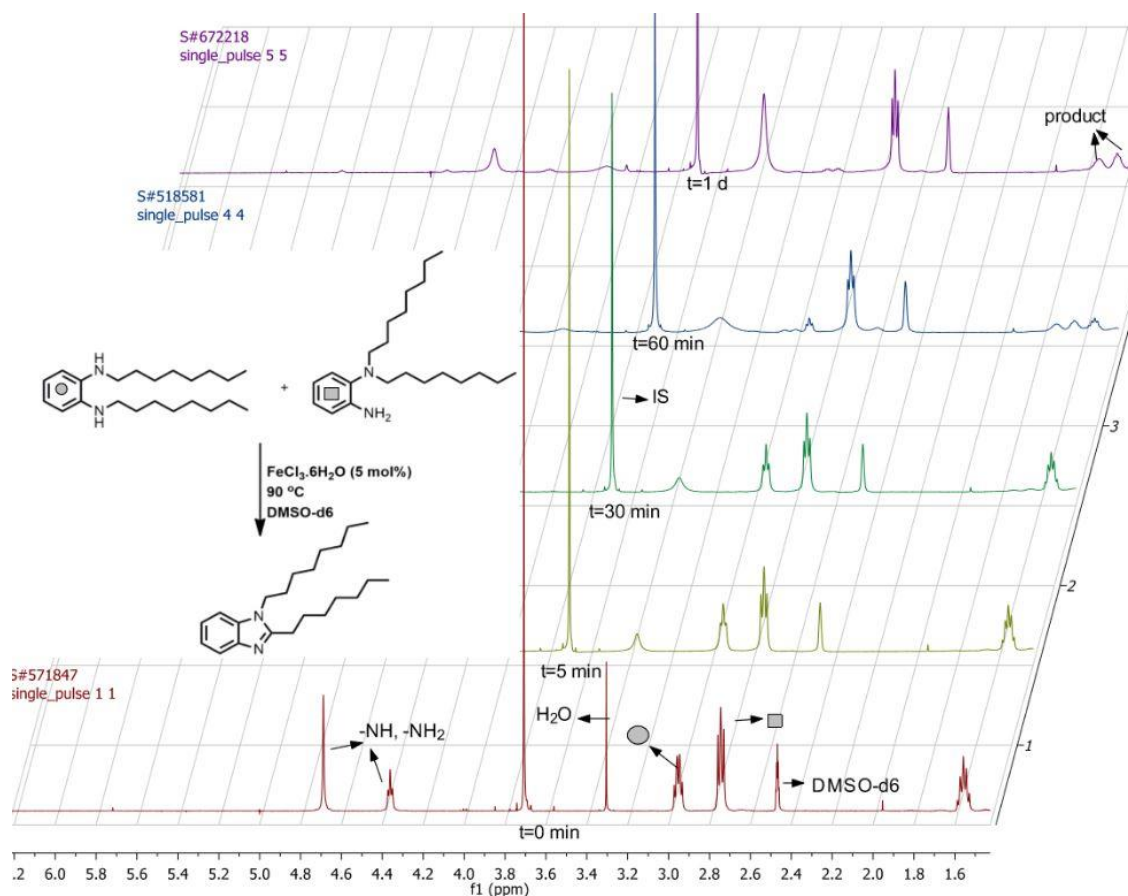


Figure 4.2 Comparative NMR study for a mixture of isomeric substrate

In a monovariate manner, solvents, oxidants, and additives were analyzed for their effects on the reaction yield. Polar aprotic solvents were preferred to non-polar solvents (**table 4.1-4.3**). Various O₂-containing atmospheres were investigated. Interestingly, open-air vessels appear superior to higher concentrations of O₂ (either under balloon or in a capped vessel). Oxidant *t*-BuOOH may perform benzylic oxidations in the presence of FeCl₃, however, this additive performed relatively poorly (25% yield) and led to multiple byproducts. Additives such as butylated hydroxytoluene (BHT), K₂CO₃, and TEMPO were also tested. BHT resulted in diminished yields. Basic conditions (K₂CO₃) resulted in poor yield with only trace amount of product observed. Surprisingly, the addition of TEMPO had no visible effect on the reaction outcome.

Screening of Reaction Conditions^a

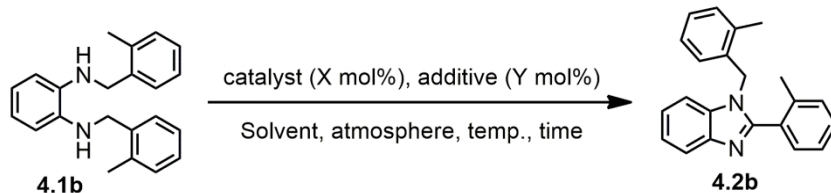


Table 4.1: Screening of catalyst

Table 4.2: Screening of solvent

Entry	Cat. (mol%)	% NMR yield	Entry	solvent	% NMR yield
1	FeCl₃.6H₂O (5)	90	1	DMSO	78
2	FeNO ₃ (5)	40	2	MeCN	41
3	AlCl ₃ (5)	24	3	Benzene	20
4	Fe ₂ (SO ₄) ₃ (5)	10	4	Pyridine	33
5	CuCl ₂ (5)	-	5	DME	15
6	AgNO ₃ (5)	-	6	DMF	90
7	FeCl ₃ (5)	78	7	Toluene	63
8	FeCl ₂ (5)	74			
9	FeCl ₂ .4H ₂ O (5)	75			
10	Hemin (5)	54			

Table 4.3 Screening of reaction condition

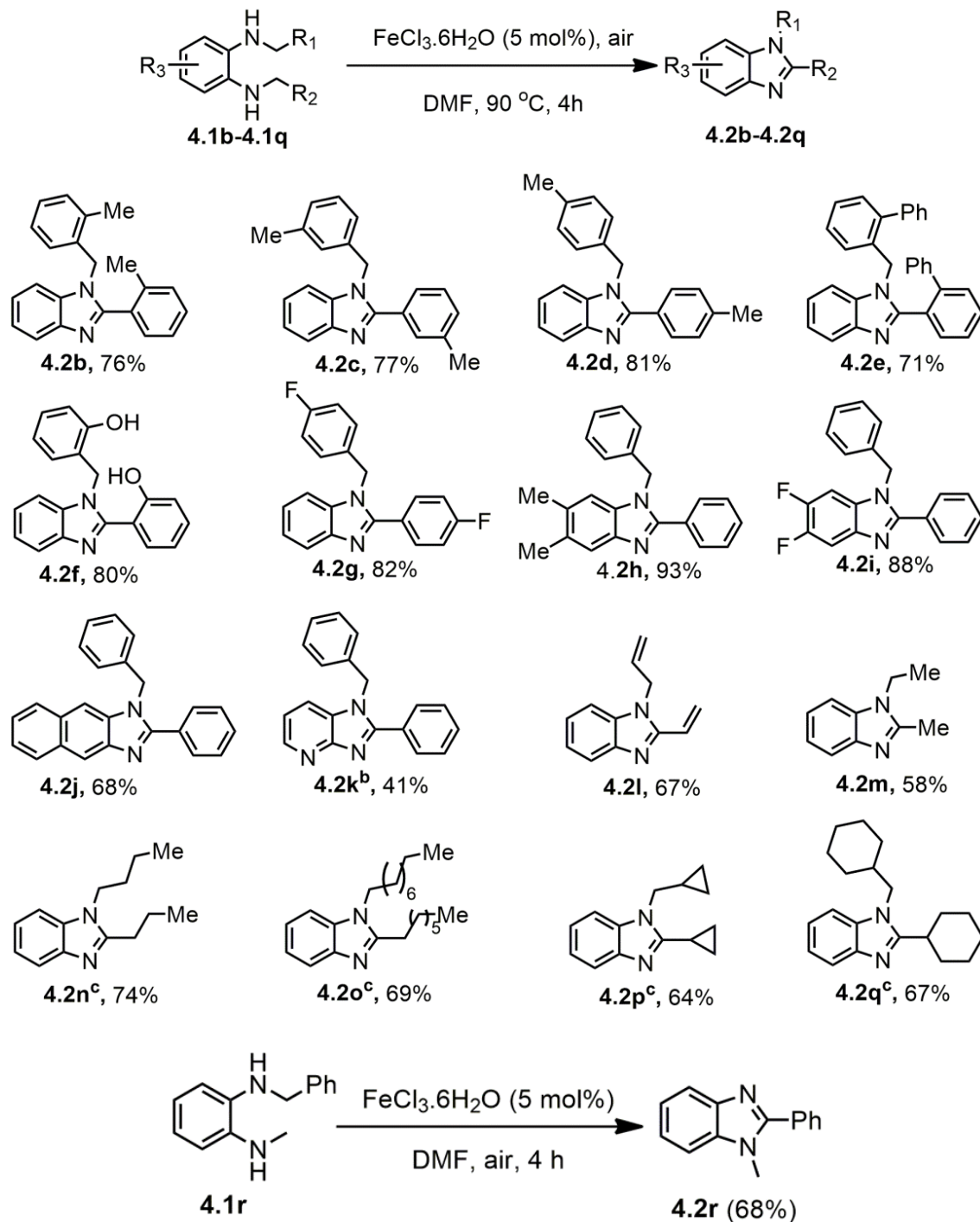
Entry	Cat. (mol%), atmosphere	Additive (Equiv.)	% NMR yield
1	FeCl ₃ (5), air	-	90
2	none, air	-	-
3 ^b	FeCl ₃ (5) air	-	86
4	FeCl ₃ (5) Ar	-	-
5	AlCl ₃ (5) air	-	24%
6 ^c	FeCl ₃ (5) air	-	78
7	FeCl ₃ (5) air	K ₂ CO ₃ (1 equiv.)	-
8	FeCl ₃ (5) air	TEMPO(1 equiv.)	72 ^d
9	FeCl ₃ (5) air	BHT (1 equiv.)	61
10	FeCl ₃ (5) capped vial	-	25
11	FeCl ₃ (2.5) air	-	57
12	FeCl ₃ (5) O ₂ balloon	-	58 ^e
13	FeCl ₃ (5) air	^t BuOOH (2 eq)	25
14 ^f	FeCl ₃ (1)	-	60

^aAll reactions were performed on **4.1b** (20 mg, 0.2 M) scale for 3 h, with CH₂Br₂ as an internal standard; ^bdark; ^c60 °C; ^disolated yield performed on 100 mg scale; ^e12% unreacted material and 5-10% imine; ^f24 h

Various substrates were tested with the improved reaction system (**Table 4.4**). In most cases, good yields were obtained in short reaction times. (Control reactions provided only trace products, which could not be detected by NMR but appeared visible by TLC analysis.) Substituent effects appear to play only a minor role in the turnover rate and yield of *N,N'*-dibenzyl-OPDs (**4.2a-4.2k**). Steric effects can be observed for the *ortho*-substituted series (**4.2a**,

4.2c, 4.2e) and the *ortho*-, *meta*-, *para*-substituted series (**4.2b, 4.2c, 4.2d**); however, these changes are relatively small based on end point analysis of the reactions. electron-deficient OPD derivative **4.1k** gave only 41% isolated yield. The naphthyl substrate gave lower yields, and though the reaction mixture was fully soluble, starting material remained unreacted. To our delight, *N,N'*-diallylic and *N,N'*-dialiphatic substrates (**4.1l-4.1o**) also provided useful yields. In most cases, no starting materials were detected. Similarly, unsymmetrical substrate **4.1r** was also highly productive and provided corresponding product **4.2r** in good yield as only benzimidazole product.

Table 4.4: Substrate scope for *N,N'*-disubstituted-*o*-phenylenediammine^a



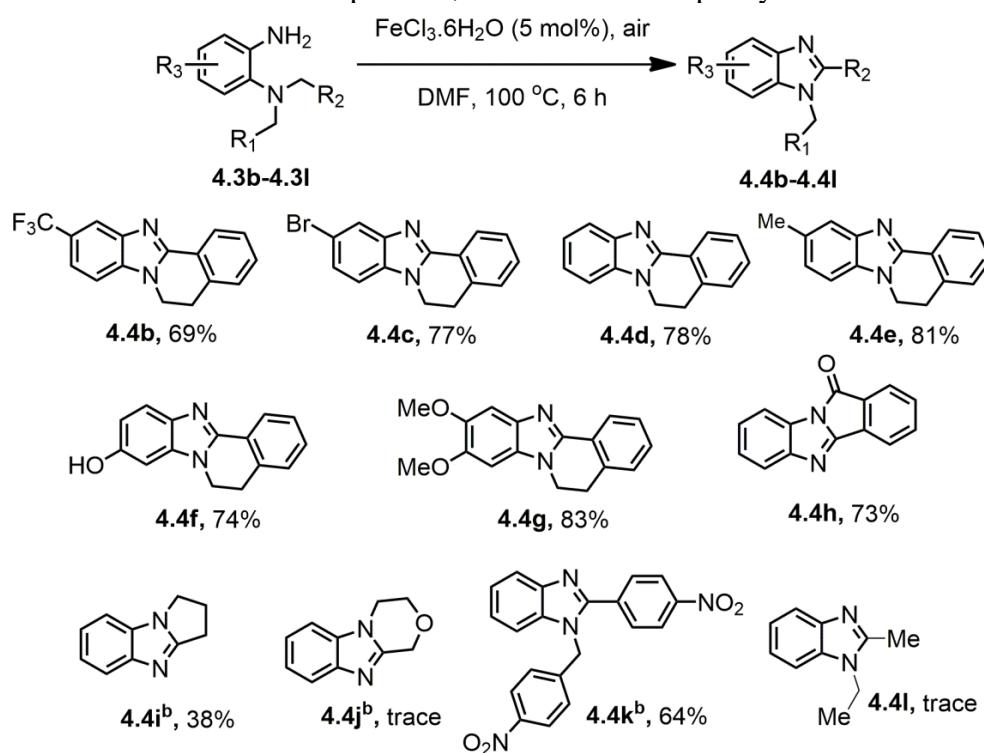
^aReaction conditions:**4.1b-4.1r** (0.3 mmol), DMF (0.5 M).^b16 h reaction.^cOvernight reaction

With these results in hand, isomeric substrates *N,N*-disubstituted-OPDs, including tetrahydroisoquinoline (THIQ) derivatives, were investigated (**Table 4.5**). Comparatively, *N,N*-

disubstituted substrates in **Table 4.5** reacted slower than the *N,N'*-disubstituted substrates above. Nonetheless, most of the substrates showed good scope, especially those associated with THIQ moieties.

An apparent electronic effect was consistent with formation of an amine radical cation. Electron deficient OPDs (**4.3b** and **4.3c**) had lower yields than the parent or electron rich OPDs (**4.3e** and **4.3g**). Isoindoline substrate (**4.3h**) resulted in over-oxidation, giving a cyclic amide, albeit with slightly lower yield. The production of **4.3h**, however, occurred faster than the THIQ substrate, with full conversion of starting materials. A plausible explanation for further oxidation involves trapping an iminium ion intermediate with H₂O₂ (or H₂O), followed by oxidation and tautomerization.¹⁵² *N,N'*-disubstituted-OPDs with benzylic substituents provided good yields. However, highly reduced yields were seen for non-THIQ heterocycle containing substrates (**4.3i-4.3j**). In fact substrate **4.3j** gave only trace yields presumably due to presence of oxygen atom which could bind to and deactivate the catalyst for the desired transformation. It is worth noting that substrate **4.3l** and **4.1m**, both containing same aliphatic groups, had different reactivity. The former provided only trace products, while the latter proved to be a very efficient substrate. This signifies the improved scope of *N,N'*-disubstituted substrates for formation of 1,2-disubstituted benzimidazoles. Overall, polysubstituted benzimidazoles were synthesized in useful yields from aerobic iron trichloride catalyst system for the substrates represented in **Table 4.5**.

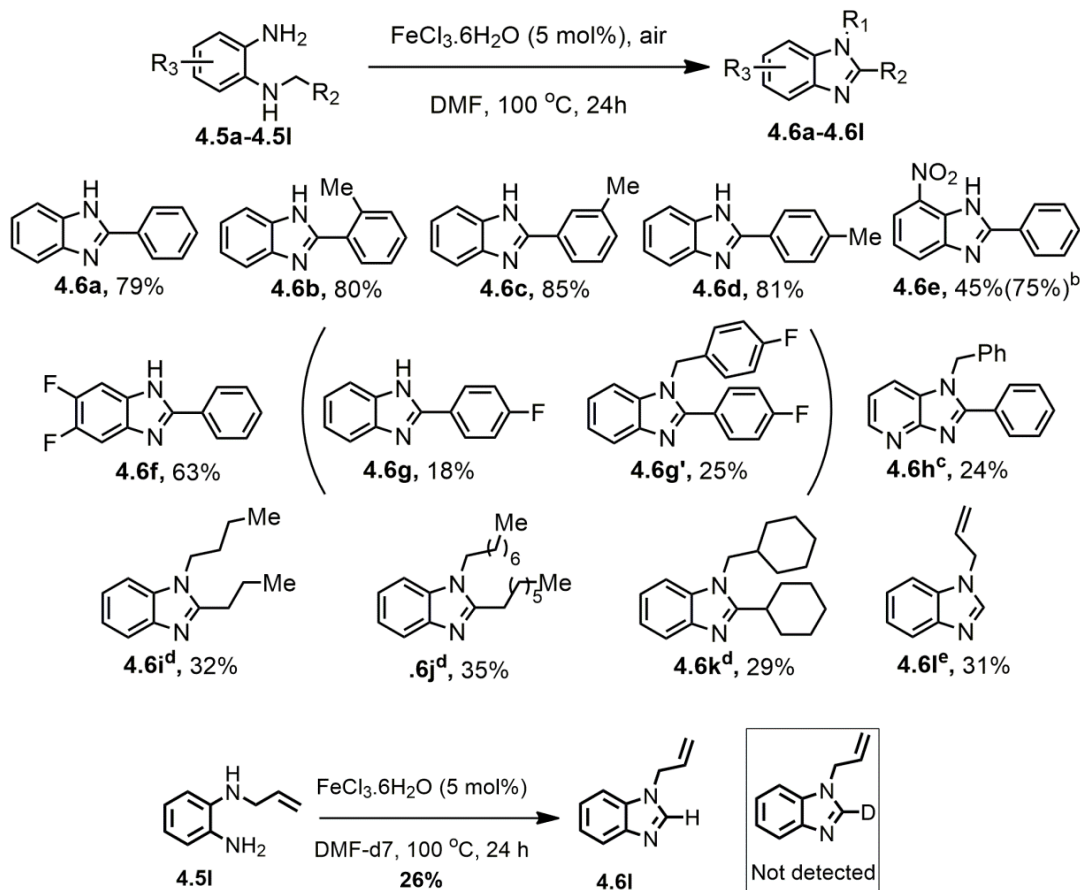
Table 4.5: Substrate scope for *N,N*-disubstituted-*o*-phenylenediammine^a



^aReaction conditions: 4.3a-4.3l (0.3 mmol), DMF (0.5 M solution). ^b24 hour reaction

The synthesis of mono-substituted benzimidazoles was investigated (Table 4.6). Mono-substituted OPDs containing benzyl groups (4.5a-4.5f) were successful. However, the 4-fluorobenzyl substrate, 4.5g, experienced intermolecular group transfer, leading to a mixture of products. The major product was a 1,2-disubstituted benzimidazole, 4.2g. Substrates with aliphatic substituents (4.5h-4.5i) or electron poor substrates (4.5k) also provided 1,2-disubstituted benzimidazoles through alkyl or benzyl group transfer.^{19a} These observations suggest that electron withdrawing groups and aliphatic groups have greater tendency for imine hydrolysis or transfer—after formation of the oxidized, but acyclic imine intermediate. Interestingly, allylic substituted substrate 4.5h afforded 1-allylbenzimidazole, presumably due to radical cleavage of the 2-vinyl group after formation of 1,2-diallyl-OPD.^{153,154}

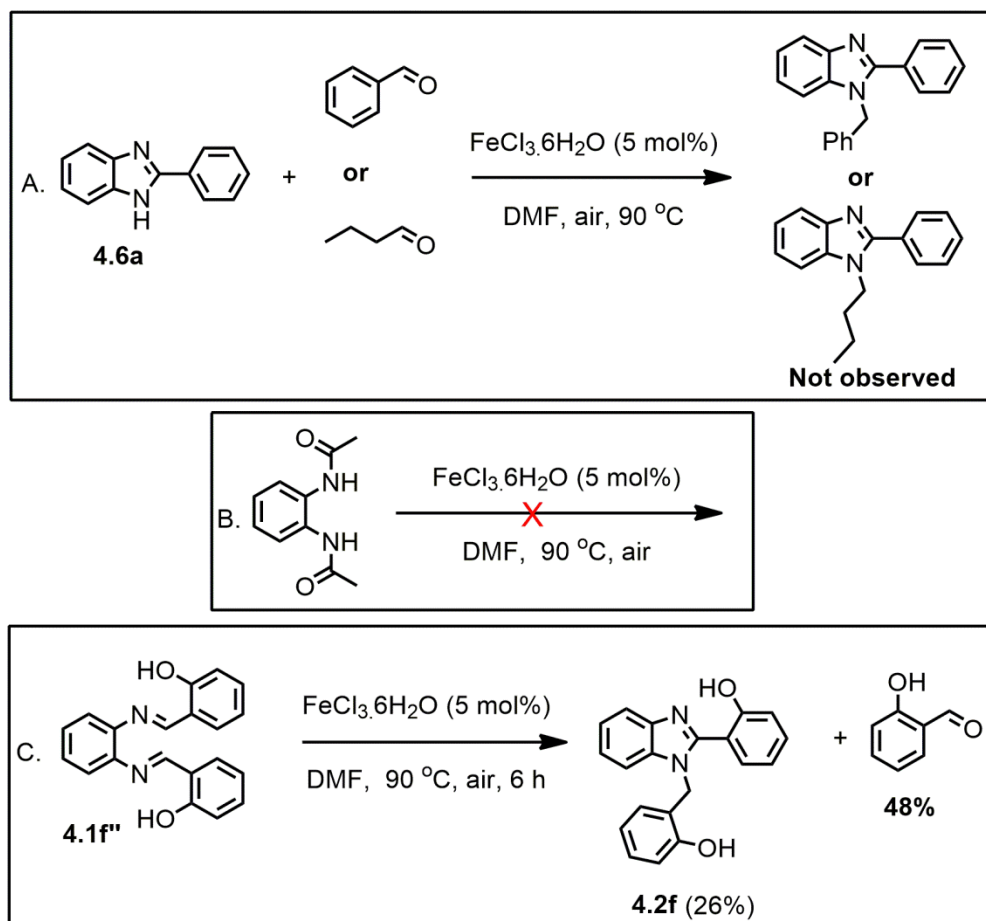
Table 4.6: Substrate scope for *N*-monosubstituted-*o*-phenylenediammine^a



^a**4.5a-4.5i** (0.3 mmol), DMF (0.5 M); ^bYields in parenthesis represent NMR yield; ^c48 h reaction; ^d16 h reaction; ^e24 h reaction

Since imine and iminium ions are prone to hydrolysis,¹⁵⁵ we wondered if the 1,2-disubstituted benzimidazoles generated from monosubstituted OPDs were formed from reductive amination of the hydrolyzed product. When 2-phenylbenzimidazole was reacted with both aliphatic and aromatic aldehyde (**Scheme 4.3**, entry A), no disubstituted product was observed, providing evidence that *N*-alkylation of 2-substituted benzimidazole does not occur following hydrolysis of alkyl chains. Furthermore, bisimine substrate **4.1f'** when treated under similar conditions did not provide comparative yield and only 26 % yield of desired product and 48% byproduct salicylaldehyde were formed (**entry C**). These results indicated that the double dehydrogenation

leading to bisimine intermediate and finally to product transformation may not a productive pathway. In addition diacetamide substrate also failed to react and no conversion was observed at all (**entry B**).



Scheme 4.3 control reactions

To investigate the coordination of substrate to ligand and understand the mechanism further, UV-vis experiments were performed to visualize complexation. The *N,N'*-dialkyl- OPD **4.1m** substrate was selected because they react on a timescale that is useful for studying via UV-Vis experiments. At low temperature $-78\text{ }^\circ\text{C}$, electronic band at 485 and 525 nm were observed which are consistent with LMCT band (**Figure 4.5, trace blue**).¹⁵⁶ At room temperature, however, an additional band at ca. 800 nm was observed (**Figure 4.3**). A time course study at

heated condition (60 °C) showed disappearance of all three bands and appearance of a new band at 365 nm corresponding to the product peak as confirmed by separate study performed with spectroscopically pure product and iron (III) chloride in same condition (**Figure 4.5**). Interestingly, no such electronic bands were observed in case of isomeric substrate *N,N'*-diethyl-*o*-phenylenediammine **4.3I** (**Figure 4.4**). A small shoulder around 500 nm was ruled out to be charge transfer band with substrate, confirmed by a UV experiment conducted with iron (III) chloride and DMF only which showed the exact curve.

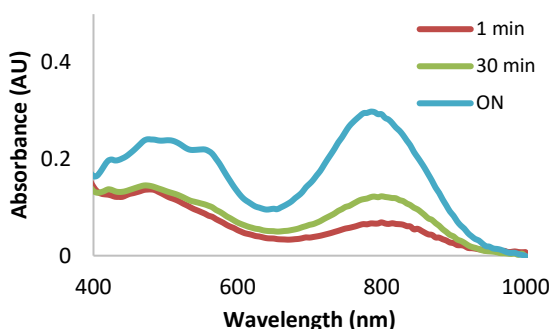


Figure 4.3 Spectral time course for *N,N'*-diethyl-*o*-phenylenediammine w/FeCl₃ at rt and aerobic conditions

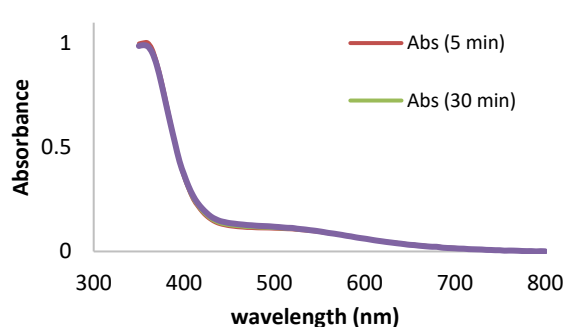


Figure 4.4 Spectral time course for *N,N'*-diethyl-*o*-phenylenediammine w/FeCl₃ at rt and aerobic condition
Curve matches FeCl₃ + solvent spectrum

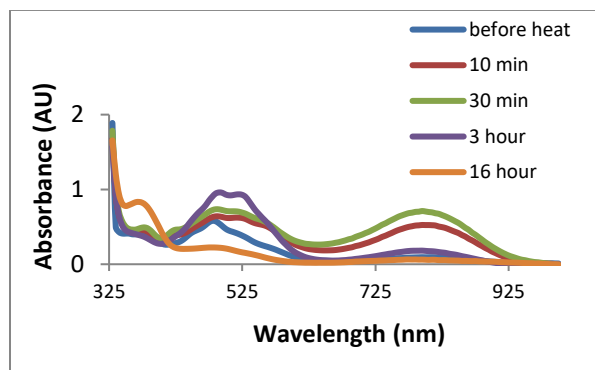


Figure 4.5 Spectral time course for Iron (III) chloride at 60 °C

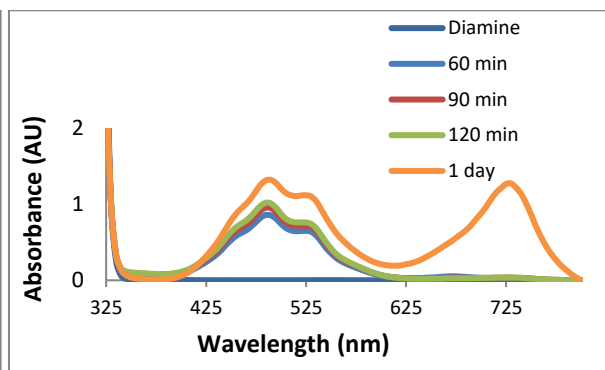


Figure 4.6 Spectral time course for Copper (II) chloride at 60 °C

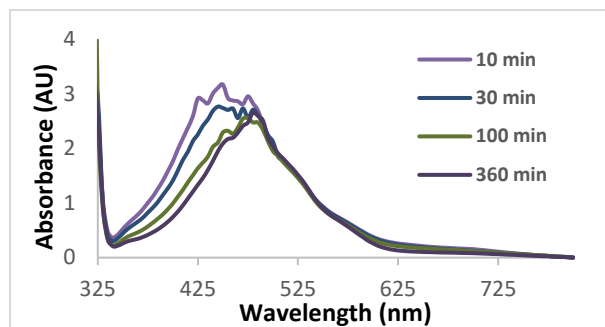


Figure 4.7 Spectral time course for Silver (I) nitrate at 60 °C

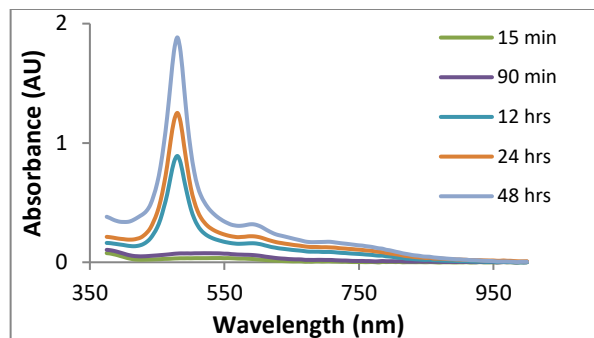


Figure 4.8 Spectral time course for Nickel (II) chloride at 60 °C

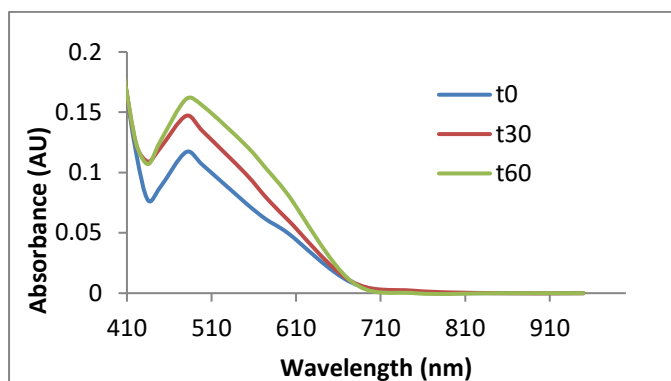


Figure 4.9 Spectral time course at rt and inert condition (FeCl_3 solution purged with Ar and degassed solvent)

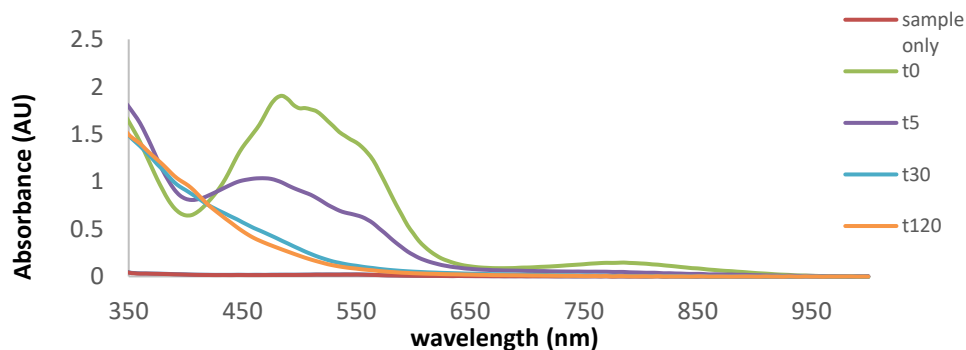


Figure 4.10 spectral time course at rt in inert atmosphere with H_2O_2 (10 equiv.) additive

Comparative studies at elevated temperature (60 °C) were performed with four different metal salts namely $\text{FeCl}_3 \cdot 6\text{H}_2\text{O}$, CuI , AgCl , and $\text{NiCl}_6 \cdot 2\text{H}_2\text{O}$. In all cases, we saw similar characteristic LMCT bands around 500 nm. However, no 800 nm band was observed or at least not so significant as Iron in case of copper, silver and nickel. In case of CuI , the higher band around 750 nm was observed only after 24 hours. It is to be noted that molar extinction coefficients for the observed bands around 500nm of different metal complex are different.

To get insight into 800 nm, UV experiments in presence of degassed solvent and inert condition were performed. Interestingly, no 800 nm was observed, presumably due to absence of O₂ and thus O₂ bound iron complex (**Figure 4.9**). Furthermore, H₂O₂ as additive in inert condition showed similar 800 nm peak (**Figure 4.10**). These UV results indicated potential oxygen bound species at higher wavelength but the exact nature and fate of such species remains unknown. While the presence of oxygen bound iron species are well characterized in Raman spectroscopy (esp. Fe-O stretch and O-O stretch),¹⁵⁷ our attempt to confirm presence of Iron oxo type complexes in Raman was not successful.

Similarly, an EPR study conducted in aerobic and anaerobic conditions could not verify the presence of such species. However, presence of Fe(II) high spin state was confirmed with epr study as revealed from the signals that were recorded in Parallel-mode EPR. We observed g~at 8.8 and g~9.2 which are indicative of a S = 2 spin-system which can arise from a high-spin Fe(II) species (**Figure 4.12**).¹⁵⁸ This signal is, however, present in both the aerobic (top curve) and anaerobic samples (bottom curve). The signal at g~4.3 is attributed to Fe(III) of S= 3/2 spin state (**Figure 4.11**).¹⁵⁹ However, the sharp signal at g~2.0 with spin state of S=1/2 is quite possible coming from organic radical species although its exact properties are yet to be determined. All these EPR results are indicative of one electron reduction of Fe(III) to Fe(II). The fact that both aerobic and anaerobic samples having similar epr bands reflects that oxygen does not play a significant role before the single electron transfer event occurs.

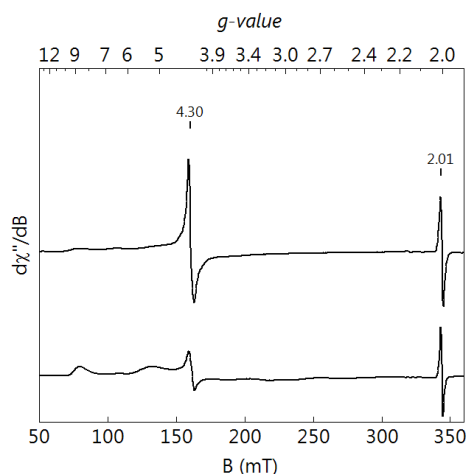


Figure 4.11 Broad scan mode comparison

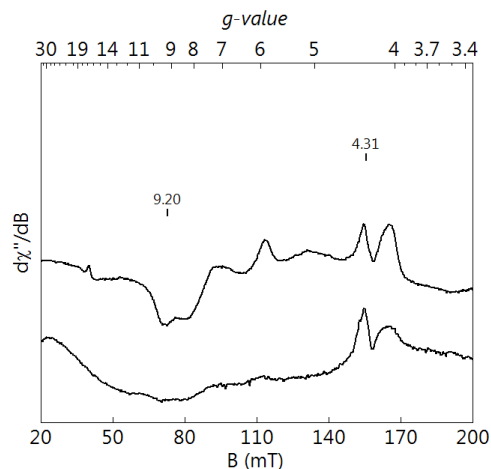


Figure 4.12 Parallel mode comparison

Furthermore, normal kinetic isotope effect represented by KIE value 1.0 ± 0.13 showed no bias on deuterated and non-deuterated substrate (**4.1m**) for the formation of product. However, the rate of formation of 800 nm band species was found to be different in two isotopic substrates. In this case, deuterated substrate gave the band at higher rate. Interestingly, it degraded much faster than the non-deuterated in longer time although the fate of these species is unknown.

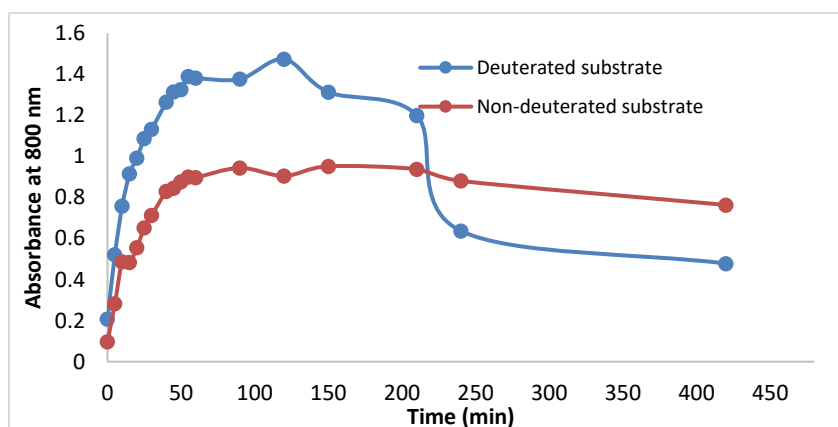
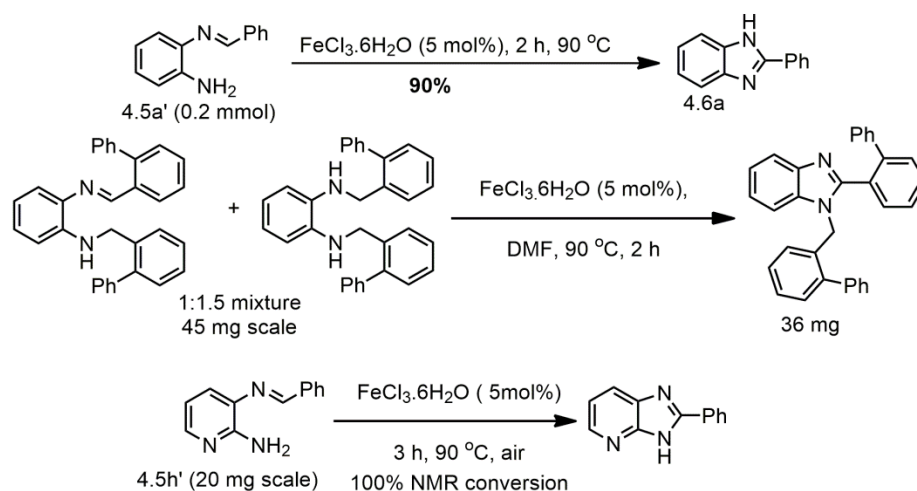


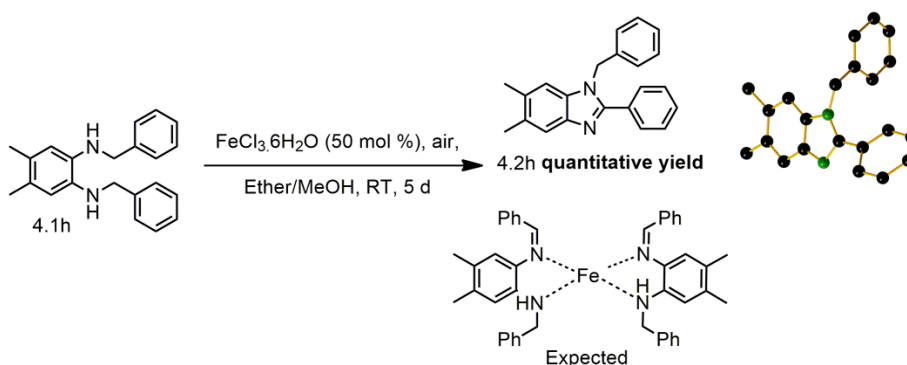
Figure 4.13 Spectral time course for deuterated and non-deuterated substrate for 800 nm peak at 60 °C (average of two runs)

The scope of imine substrates was tested for both 2-substituted benzimidazole and 1,2-disubstituted benzimidazole (**Scheme 4.4**). Substrate **4.5a'** reacted smoothly to give 90% of the corresponding 2-phenylbenzimidazole product in 2 hours under the same condition. In another

instance, 45 mg of a mixture of monoimine substrate **4.1e'** and substrate **4.1e** gave 1,2-disubstituted product **4.2e** in about 80% yield. The later result demonstrates the increased scope of monoimine substrate towards 1,2-disubstituted benzimidazole and therefore it being the productive intermediate in overall transformation of amine to benzimidazole product. In an effort to synthesize the monoamine intermediate, a reaction trial similar to the published literature was performed.¹⁶⁰ However, 1,2-disubstituted benzimidazole was isolated in quantitative yield and the structure was further confirmed by X-ray crystallography (**Scheme 4.5**).



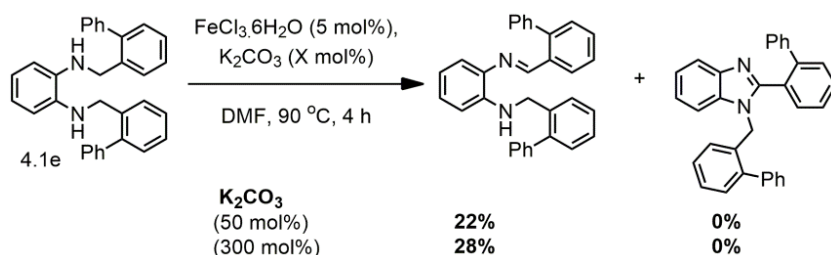
Scheme 4.4 Scope of mono-imine intermediates



Scheme 4.5 Attempt on monoimine synthesis

In further investigation towards base effect in the reaction scope, substoichiometric and excess concentration of base K_2CO_3 was added and closely monitored through NMR. As shown in

Scheme 4.6, in both cases, no desired benzimidazole product was detected. However, reaction afforded monoimine product. These results indicate the role of iron catalyst as Lewis acid, which in the presence of base gets deactivated and thus, shuts down the cyclization process for the formation of benzimidazole product. In other words, once the monoimine is formed through a redox mechanism, the iron catalyst simply acts as a Lewis acid to give benzoimidazolium intermediate which upon oxidative aromatization gives benzimidazole product.



Scheme 4.6 Effect of base in reaction scope

With respect to all preliminary investigations done in this work, a reaction mechanism is proposed as shown in **Figure 4.13**. A single electron transfer process from OPD to Fe(III) leads to formation of OPD radical cation along with reduced iron species Fe(II) as confirmed from EPR data. Although the exact role of oxygen is not known, the hydrogen atom abstraction (HAT) from α -carbon to radical cation by oxygen bound iron species (detected in UV) could give highly electrophilic iminium species which upon nucleophilic attack by nitrogen provides cyclized species. Dehydrogenation of this species could readily give final benzimidazole product. Additionally, the coordination of *N,N'*-disubstituted OPD substrate to Fe(III) should be strongly favored. Whether SET process occurs with OPD bound Fe or in an intermolecular fashion as shown in **Figure 4.13** is less certain. However, this process could be the rate determining step since the following HAT process is less susceptible to rate limiting step confirmed from KIE study.^{151, 160}

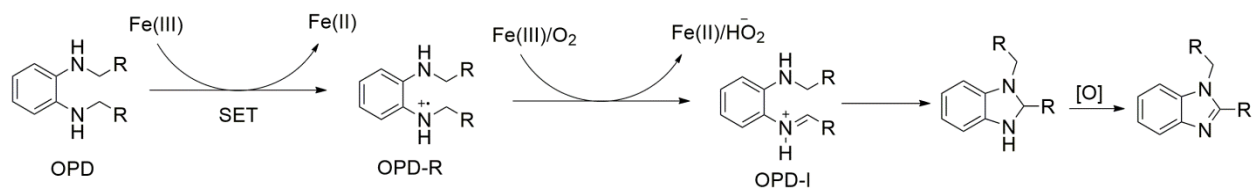


Figure 4.14 Plausible reaction mechanism for synthesis of benzimidazole products

4.3. Conclusion

In conclusion, we have investigated untested substrates for ready access to 1,2-disubstituted benzimidazoles. During the course of study, we discovered different reactivity of two isomeric substrates; *N,N'*-disubstituted being more efficient than *N,N*-disubstituted. This milder protocol was also used to prepare polycyclic benzimidazoles, which bear very interesting applications. With convenient access available to both isomers, through orthogonal chemistry, we believe this work provides a platform for unveiling strong counterpart of several underlying substrates in organic syntheses especially with a use of commodious catalysts. Future works include a detailed mechanistic survey of this study.

Chapter 5

Dioxane-mediated Selective Oxidation of Isoindolines to Isoindolinones

5.1. Background

Isoindolinones are heterocycles that belong to the family of benzofused lactams. They are privileged group of nitrogen containing heterocycles and find structural motifs in various natural products. Closely related members of this family are fully oxidized phthalimides, fully reduced isoindolines, and fully aromatic isoindoles. Several natural compounds and synthetic compounds with isoindolinone structure are well known for their biological activity; for e.g. indoprofen, lactonamycin, hericinone, etc. are some of the bioactive isoindolinone derivatives.¹⁶¹⁻¹⁶⁸

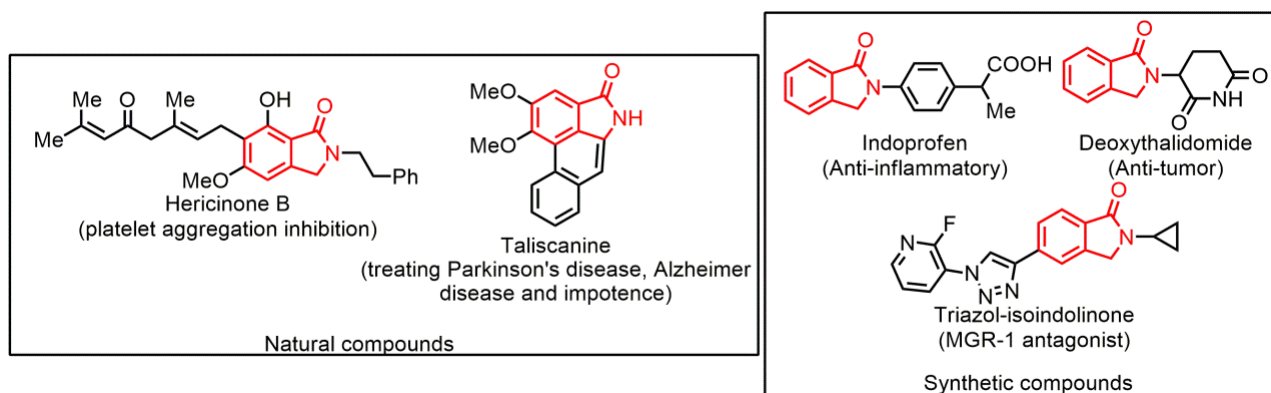


Figure 5.1 Bioactive isoindolinone molecules

Synthesis of isoindolinone derivatives have been realized by a number of methods. Traditional methods to synthesize isoindolinones use reductive amination/cyclization strategy involving condensation of 2-formylbenzoic acid or its derivatives with amines in presence of reducing agents like NaBH_4 .¹⁶⁹⁻¹⁷¹

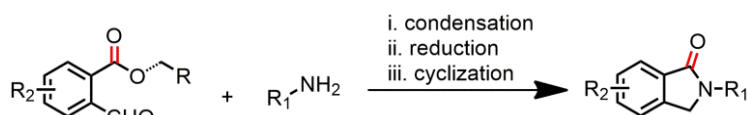


Figure 5.2 Reductive amination/cyclization strategy for isoindolinone synthesis

Other method includes selective reduction of phthalimides. However, several other reducing products limit this strategy being from practical. Nevertheless, a selective reduction method was discovered by Beller group in which they used TBAF (tetrabutylammonium fluoride) as catalyst and PMHS (polymethylhydrosiloxane) as reducing agent although other silanes also afford to give products. In general this method is highlighted due to operationally simplicity and mild reduction technique.¹⁷²

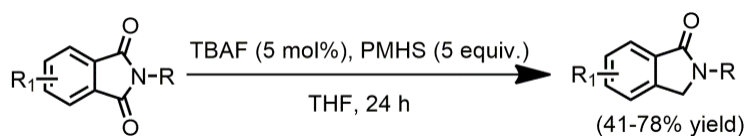


Figure 5.3 Selective monoreduction strategy for isoindolinone synthesis

Both intramolecular and intermolecular C-H aminative cyclization strategies have also been employed targeting synthesis of isoindolinone. Two different groups independently reported intramolecular $\text{sp}^3\text{C-H}$ aminative cyclization method using similar substrate 2-alkyl-*N*-substituted benzamides. While one method focused on metal free approach using molecular iodine, base, and ditertiarybutylperoxide (DTBP) as oxidant,¹⁷³ the other method utilized copper catalyst and DTBP as oxidant.¹⁷⁴ Various functional groups were tolerated. The highlight of this method is smooth synthesis of 3-alkyl-2-phenylisoindolinone in addition to simple 2-phenylisoindolinones.

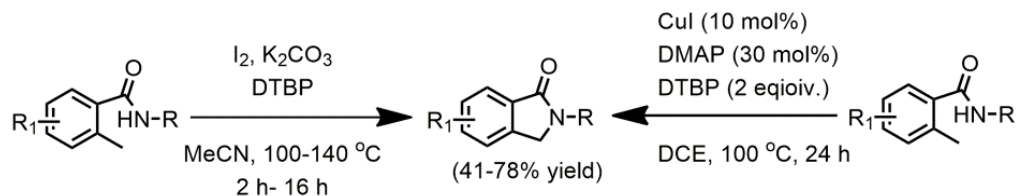


Figure 5.4 Intramolecular aminative cyclization strategies for isoindolinone synthesis

Other methods reported for isoindolinones are Bischler-Napieralsky type cyclization¹⁷⁵ and DMSO mediated tandem CDC¹⁷⁶. The former approach was successfully employed in late stage synthesis in total synthesis of Lactanomycin.¹⁷⁷ In case of CDC approach, C-3 methylene group incorporated from DMSO and amides were used as amine sources.

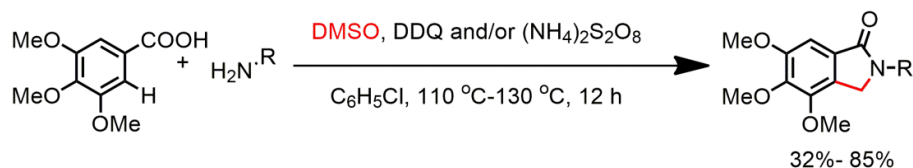


Figure 5.5 DMSO mediated tandem cross-dehydrogenative coupling strategy for isoindolinone synthesis

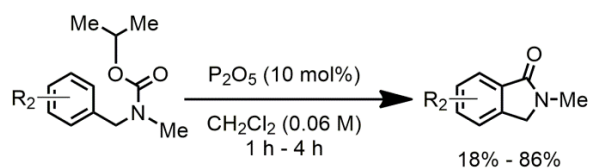


Figure 5.6 Bischler-Napieralski type cyclization strategy for isoindolinone synthesis

Cross coupling technique is another widely developed strategy in isoindolinone synthesis. Among them, carbonylation reaction using palladium catalysts have been studied the most. A slight change in oxidant from $\text{Cu}(\text{OAc})_2$ to $\text{Cu}(\text{OTf})_2$ has been found to be effective with respect to using free amine as amine source. Otherwise majority of such methods used either protected amine or directing group.¹⁷⁸⁻¹⁸²

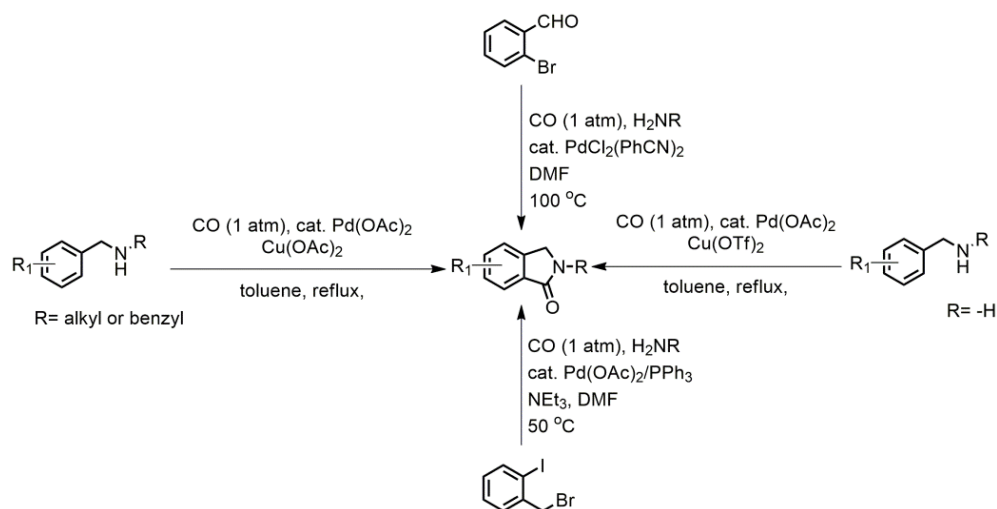
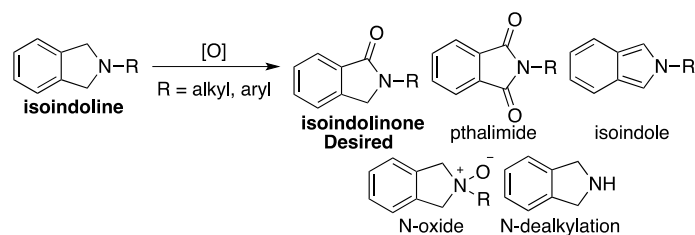


Figure 5.7 Palladium catalyzed carbonylation strategies for isoindolinone synthesis

Several other reports are known for isoindolinone synthesis. Slight variant to above methods includes synthesis of 2,3-disubstituted isoindolinones. For these specific isoindolinones, methods like rhodium¹⁸³, ruthenium¹⁸⁴, and cobalt catalyzed carbonylation¹⁸⁵, and carbonylation with *o*-lithiated aromatic imines and amides.¹⁸⁶⁻¹⁸⁸

Although there has been a significant development in reaction scope for isoindolinones synthesis, requirement of specific type of substrate, presence of transition metals, strong oxidizing agents, etc, and harsh reaction condition present big drawbacks. In fact, thermodynamically controlled transformation of isoindolinones favors isoindoles, which could further lead to several undesired byproducts in regard to isoindole's unusual instability.^{189,190} Furthermore, highly activated C-H bonds pose great challenge in C-H oxidation, especially when more than one such C-H bonds are present in a molecule and fate of oxidation is uncontrollable.¹⁹¹ In isoindolines also, oxidative conditions could promote formation of *N*-oxide, *N*-dealkylation product, isoindoles, and fully oxidized phthalimide (**Scheme 5.1**).



Scheme 5.1 Challenges in oxidation of Isoindoline

5.2 Results and Discussions

Based on the previous observation in intramolecular CDC approach (Chapter 2, table 2.3, entry 2.2i'), it was surmised if isoindoline could be fully oxidized to phthalimide under the similar condition. Although phthalimide was the target, oxidation of only a single benzylic site in the tested isoindoline **1i** was detected in the NMR and no fully oxidized phthalimide product was observed even at prolonged time and high temperature. Interestingly, a control reaction in absence of catalyst performed the oxidative transformation equally well (**Figure 5.8**). This result along with no report on the selective oxidative transformation of isoindoline to isoindolinone prompted us to screen different solvents for the observed oxidation reaction. Among several solvents screened, all polar aprotic solvents except acetonitrile afforded positive results albeit in different yield (**Table 5.1**). The best solvent studied was found to be dioxane providing 91% NMR yield in 8 hours. No conversion was observed in neat condition. A number of metal and non-metal oxidants used in both catalytic and stoichiometric amount did not surpass the best yield (**Table AB2**). Moreover, both acid and base additives were found ineffective in reaction scope. Oxygen concentration was found to affect the reaction rate directly but not effectively. Since, dioxanes are known as peroxidizable chemicals, the effect of other peroxides for reaction screening was considered in both dioxane and other solvents. Unfortunately, none of the selected peroxide sources performed better than dioxane alone (**Table AB2**). Of all peroxide additives

tested in dioxane, 1 mol% NBS at room temperature provided 77% NMR yield in 24 h without any observed byproduct. This result indicated that NBS can also be used in low catalyst loading to afford selectively oxidized isoindolinone product.

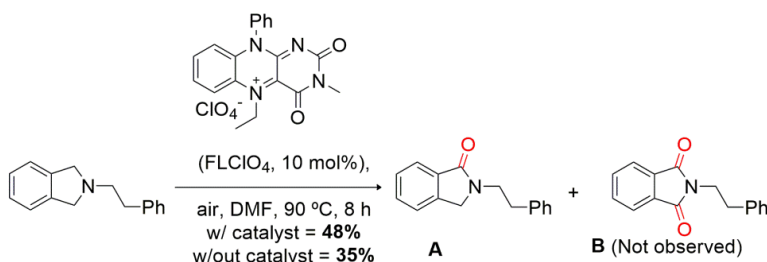
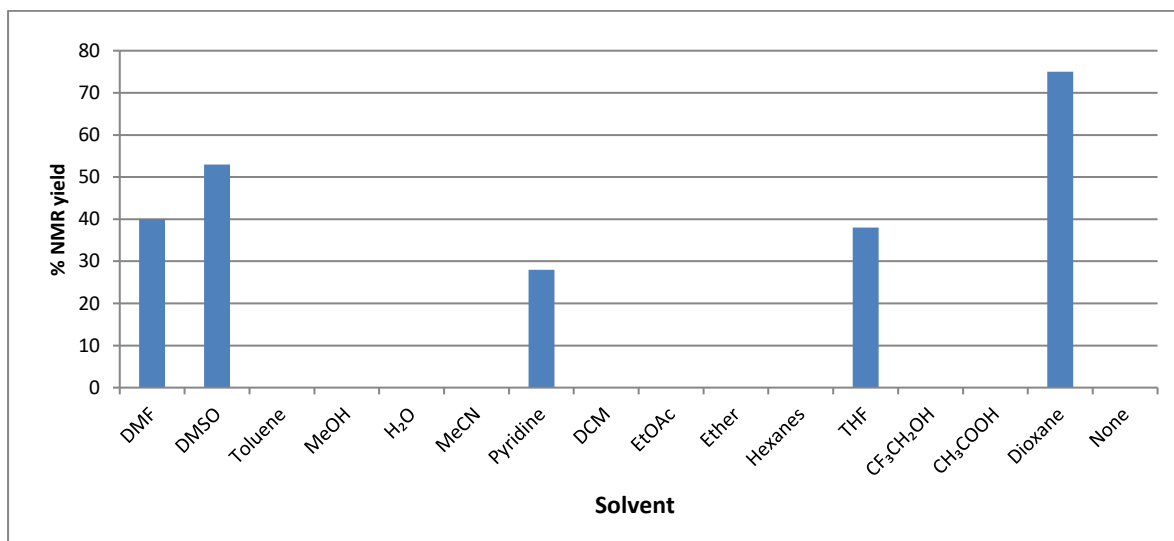
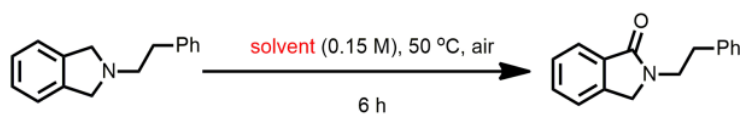


Figure 5.8 Development of solvent mediated isoindolinone synthesis

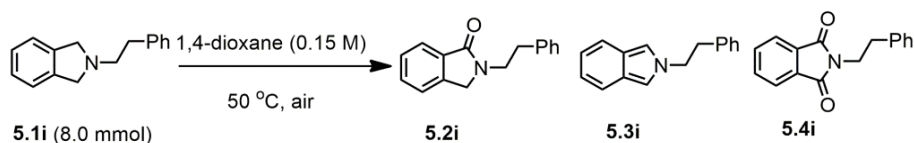
Table 5.1 Screening of solvent



Next, the effect of different grade of dioxane in reaction scope was studied. ACS grade dioxane from Acros and Sigma Aldrich had a similar outcome (**see Appendix for details**). The dioxane solvent was heated to study degradation of dioxane by peroxide contents. However, no other

detectable chemicals than dioxane were found even after 7 days at 70 °C. To study the selective scope of the reaction, two parallel reactions were performed. In each condition, 8.0 mmol of **5.1i** was heated at 50 °C and stopped at two time points of 6 hours and 120 hours. As indicated in **table 5.2**, even at prolonged time, over-oxidized phthalimide **5.4i** and isoindole **5.3i** were formed in trace amounts. In addition, a solution of **5.2i** with dioxane was heated at 100 °C for 2 days in open air condition. To our delight, only trace amount of byproduct was observed with major product being desired isoindolinone product (**figure 5.9**).

Table 5.2 Reaction selectivity at optimized condition



Reaction Time	Conversion	Isolated yield of 5.2i	Isolated yield of 5.3i	Isolated yield of 5.4i
6 h	75%	59	5	0
120 h	100%	68	1	3

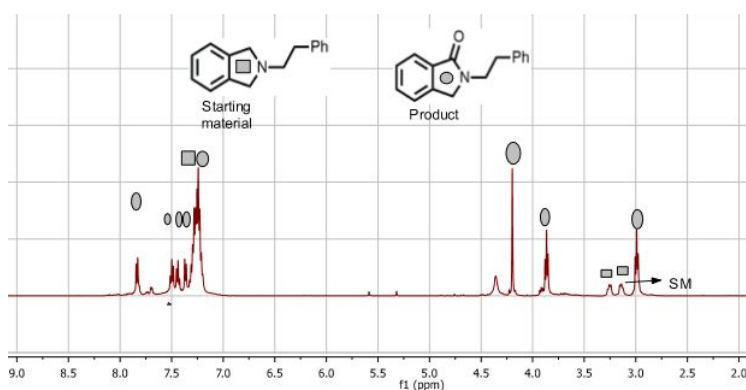
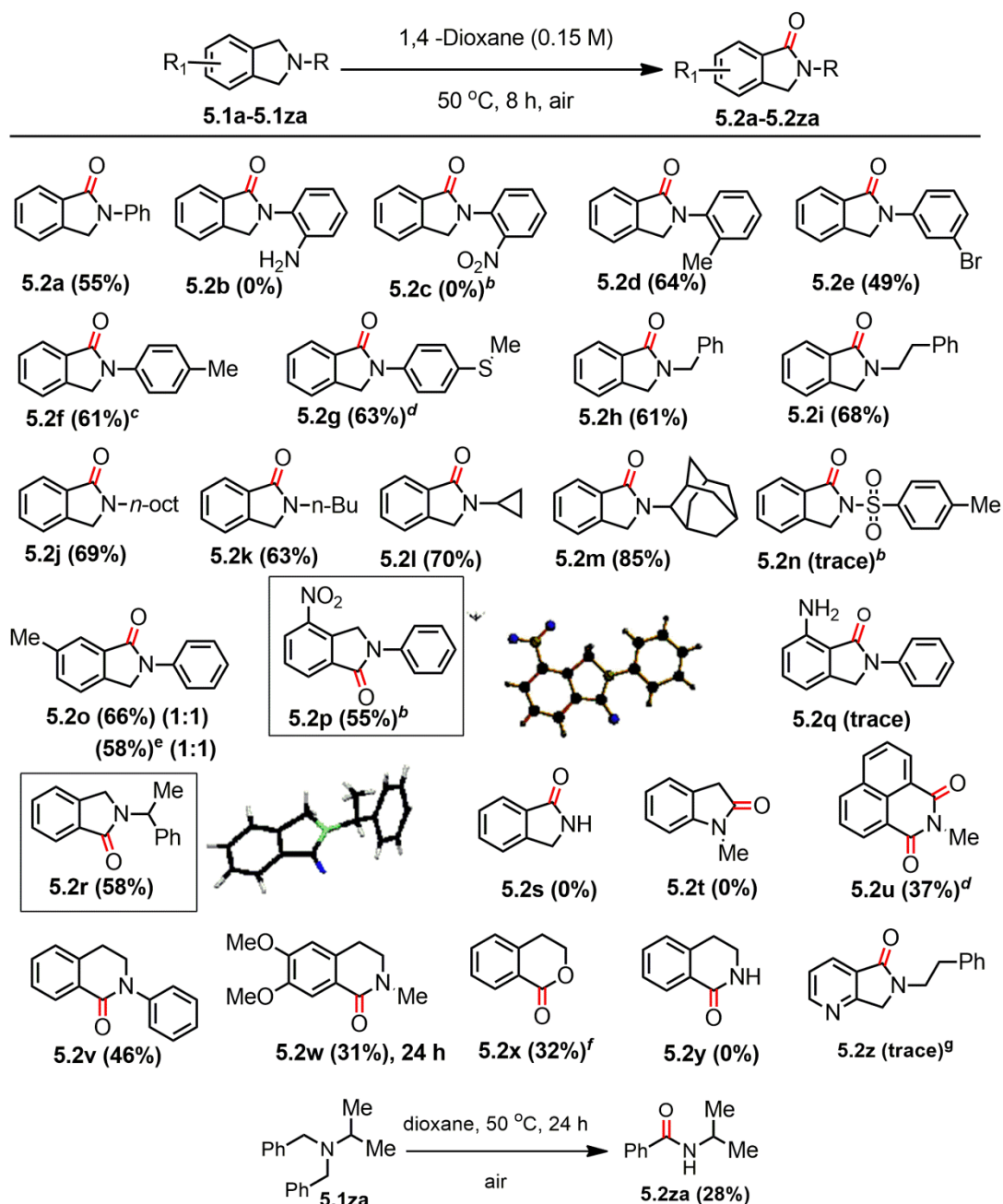


Figure 5.9 Reaction scope at 100 °C for 2 days in open flask

Several substrates were selected for selective oxidative transformation using the optimized condition. All *N*-aliphatic substituted substrates (entry **5.2h-5.2m**) provided very good yields. *N*-phenyl substituted substrates (entry **5.2a-5.2g**) in comparison provided moderate yields. However, no significant conversion was observed with electron poor substrates containing electron withdrawing group eg. -nitro group (entry **5.2c**) and tosyl group (entry **5.2n**). In contrary, 2-aminophenyl substituted substrate, being electronically rich (entry **5.2b**) also afforded trace amount of product. To test if the observed poor reactivity is due to ortho effect in the substrate, 2-orthomethylphenyl substituted substrate (entry **5.2d**) was introduced. An isolated yield of 64% was obtained, which could potentially rule out the presence of ortho effect in the observed reactivity with 2-(ortho-substituted phenyl) isoindoline derivatives.

Table 5.3 Substrate Scope^a

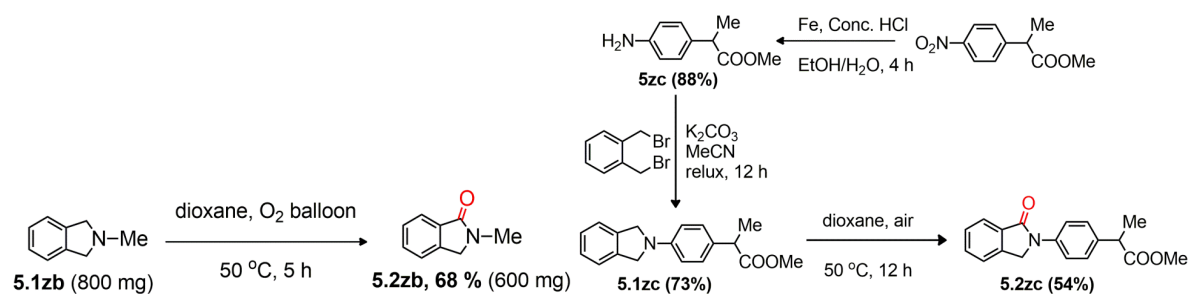


^a**Reaction conditions:** Isoindoline **1a-y** (0.25 mmol), isolated yield in parenthesis. ^bO₂ balloon, 12 h. ^cO₂ balloon, 4 h. ^d0.5 mmol scale. ^eIn 1 mol% NBS; ^f68 h, 80 °C. ^g30% Isoindole product was observed in NMR

The substrate scope was further expanded to different 5-substituted isoindolines. Contrary to 2-nitrophenyl substituent, 4-nitrosubstituted isoindoline (entry **5.2p**) gave isoindolinone product in moderate yield, affording a chemoselectively oxidized isoindolinone product. 5-methyl

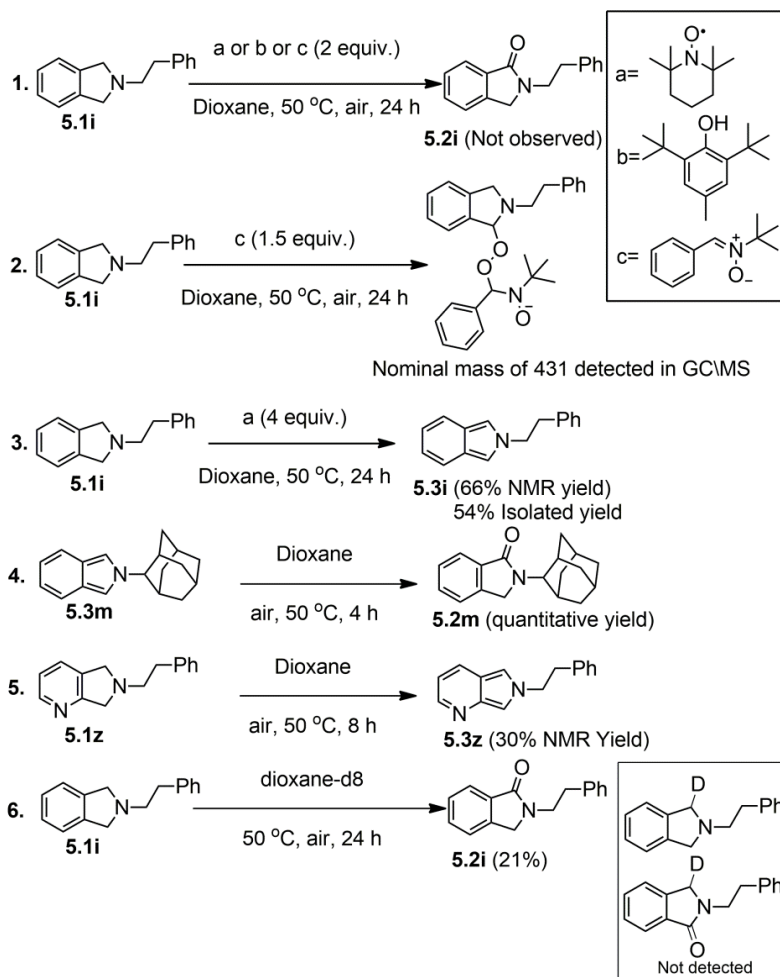
substituted isoindoline (entry **5.2o**), unlike 4-nitro substituted isoindoline, gave 1:1 regioisomer. In contrary, 4-amino substituted isoindoline (entry **5.2q**) like 2-aminophenyl substituted isoindoline was not reactive under the condition. To study the scope of secondary amines containing both benzylic and non-benzylic CHs as well as tertiary amines with non-benzylic substrate, substrates (entry **5.2s**, **5.2t** and **5.2y**) were introduced into the selected optimized condition. However, none of the substrates were found to give desired product. In all case, no conversion was observed. These results indicate high selectivity of dioxane towards benzylic C-H bond alpha to tertiary amines, even better towards aliphatic substituents. Also, tetrahydroisoquinoline derived substrates like *N*-phenyl tetrahydroisoquinoline (entry **5.2v**) and *N*-methyl tetrahydroisoquinoline (entry **5.2w**) gave oxidized product in low yields. However, in both cases, increased temperature and time were required. Similarly, isochroman substrate (entry **5.2x**) required higher temperature and more time to afford the oxidized product in only 32% isolated yield. Interestingly, acyclic tertiary amine **5.1za** when reacted under dioxane condition resulted dealkylation product **5.2za** in poor yield of 28%.

Next, the synthetic utility of the method was tested. 6.0 mmols of *N*-methylisoindoline (**5.1zb**) reacted efficiently in presence of dioxane and oxygen atmosphere to give 68% of isolated yield of *N*-methylIsoindolinone (**5.2zb**) in 5 hours (**Scheme 5.2**). The formal synthesis of indoprofen ester was performed utilizing selective oxidation process as a late stage process. The selective oxidative transformation afforded 54% isolated yield of the indoprofen ester **5.2zc**.

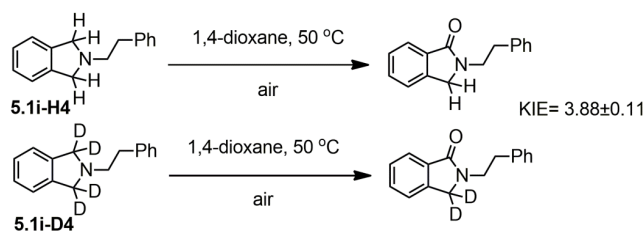


Scheme 5.2 Synthetic scope of the method

To understand reaction mechanism, chemical studies involving reactions of substrate **5.2i** with radical scavengers like TEMPO, BHT and PBN were performed. In all cases, no desired product was observed, which clearly indicated towards the possibility of involvement of radical intermediates in the reaction and therefore, a possible radical pathway in the reaction (**scheme 5.3**, entry 1). While effort taken to isolate possible radical adduct formed between radical species failed, nominal mass (m/z 431) of peroxy adduct of substrate **5.2i** and PBN was observed during GC/MS study of crude reaction mixture (entry 2). Use of excess TEMPO reagent switched the reaction scope to isoindole product **5.3i** (entry 3), potentially due to hydrogen abstraction from the resulting peroxy adduct. Isoindole **5.3m** gave full conversion to isoindolinone **5.2m** quantitatively within 4 hour (entry 4). Also, electron poor substrate **5.1z** gave isoindole product **5.2z** in 30% NMR yield. Moreover, no deuterium incorporation was observed in the product when the reaction was conducted in dioxane- d_8 solvent suggesting a surprisingly level of fidelity to the radical process (entry 6). In addition, parallel KIE study performed on H/D substrates indicated breakage of labeled bond in rate determining step. KIE value of 3.88 ± 0.11 was consistent with primary kinetic isotopic effect (**Scheme 5.4**).¹⁹²



Scheme 5.3 Mechanistic investigation



Scheme 5.4 Study on parallel kinetic isotope effect

The involvement of a radical species was confirmed by a series of EPR experiments illustrated in **Figure 5.9**. Initially, the analysis of radical was carried out in a reaction involving only the dioxane heated for one hour in open air. In this case, no radical species were detected (trace **A**). Consistent with this, no paramagnetically shifted peaks were observed by NMR. Reactions

carried out in the presence of excess (0.09 M) spin-trap, *N*-tert-butyl- α -phenylnitrone (PBN) in dioxane, formation of a radical was verified when the solution was heated. The characteristic ^{14}N -triplet ($I = 1$; 40.5 MHz) centered at a g -value of 2.007 (trace **B**) is typical of the nitrogen-centered PBN-radical.¹⁹³ Control reactions were performed in solvents where product formation was not observed (ethyl acetate). As expected, no PBN-radicals were observed under equivalent conditions (trace **C**). When a reaction mixture containing substrate **5.1i** (0.022 mmol), dioxane (0.3 mL), and spin trap PBN (0.028 mmol) were heated together, an EPR analysis of aliquots taken from the reaction showed the PBN-radical. As compared to similar reactions performed at room temperature, the amount of PBN-radical is greatly increased for elevated temperature reactions. To illustrate, (traces **D**) shows the EPR spectra observed for an aliquot taken from 50 °C reactions. The equivalent reaction aliquot taken from an ambient temperature reaction is shown in (trace **E**). Double integration of these spectra indicates that the amount of PBN-radical formed at room temperature is attenuated by nearly 85% relative to 50 °C reactions. Collectively, these observations are consistent with the formation of radical reaction intermediates; however, the exact identity of this species has yet to be determined.

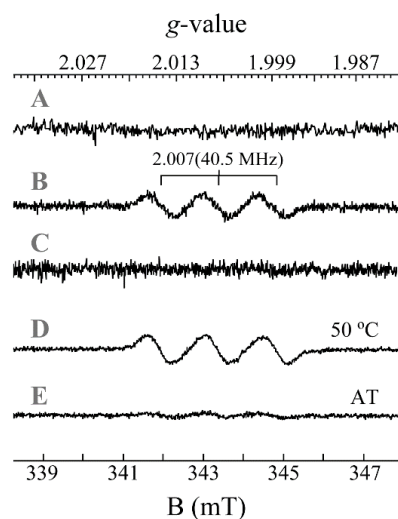


Figure 5.10 EPR spectra for selected reaction conditions. (**A**) dioxane at 50 °C; (**B**) dioxane and PBN at 50 °C; (**C**) ethyl acetate and PBN at 50 °C; (**D**) dioxane, isoindoline, and PBN at 50 °C; (**E**) dioxane, isoindoline, and PBN at ambient temperature (AT). Instrumental conditions: frequency, 9.65 GHz; modulation power, 20 mW; modulation frequency, 0.3 mT.

It is proposed that the autooxidation of dioxane releases active radical species which facilitates hydrogen atom abstraction from isoindoline, thereby generating fairly stable benzylic radical in isoindoline. This species upon reaction with oxygen gives another peroxy radical. Upon another Hydrogen atom abstraction followed by O-O cleavage, the desired isoindolinone is formed (Figure 5.11).¹⁹⁴

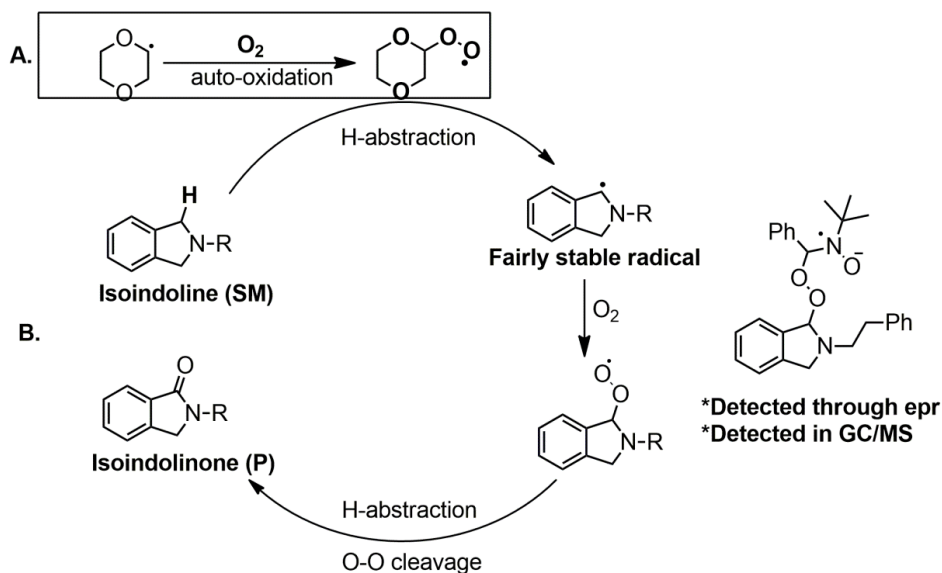


Figure 5.11 Proposed reaction pathways

5.3. Conclusion

In conclusion, a simple yet useful solvent mediated method was discovered to selectively oxidize highly activated benzylic C-H bond in isoindolines to afford various isoindolinone derivatives. NBS loading of 1 mol% was also found to be effective for similar transformation although limited substrate scope were presented. Therefore, a future work with catalytic process will be studied in relation to selective oxidation process in relevant molecules. Mechanistic studies clearly showed the radical dominant processes. Overall, this is the first report on oxidation of isoindoline to isoindolinone

Appendix A

List of Abbreviation

AMP	Adenosine monophosphate
BHT	Butylated hydroxytoluene
CDC	Cross dehydrogenative coupling
DABCO	1,4-diazabicyclooctane
DMF	<i>N,N</i> -dimethyl formamide
DMSO	Dimethyl sulfoxide
EPR	Electron paramagnetic resonance
Et ₃ PO	Triethylphosphine oxide
ESI	Electron spray ionization
FAD	Flavin adenosine dinucleotide
FLP	Frustrated lewis pair
FMN	Flavin mononucleotide
GCMS	Gas chromatography mass spectrometry
HAT	Hydrogen atom transfer
Hz	Hertz
IR	Infra-red
KIE	Kinetic isotope effect
MAO	Monoamine oxidase
MCR	Multi-component reaction
mp	Melting point
NADH	Nicotinamide adenine dinucleotide
NAO	Nitroalkane oxidase
NMR	Nuclear magnetic resonance
OPD	Orthophenylene diamine
PBN	<i>N</i> -tert-Butyl- α -phenylnitron
PPh ₃ O	Triphenylphosphine oxide
rt	room temperature
TBHP	Tertiarybutyl hydrogen peroxide
TEA	Triethyl amine
TEMPO	(2,2,6,6-tetramethylpiperidin-1-yl)oxy
THIQ	Tetrahydroisoquinoline
UV-vis	Ultraviolet visible

Appendix B

General Experimental Procedure

A. General procedure for synthesis of bridged flavinium catalysts (**BC1-BC5**):

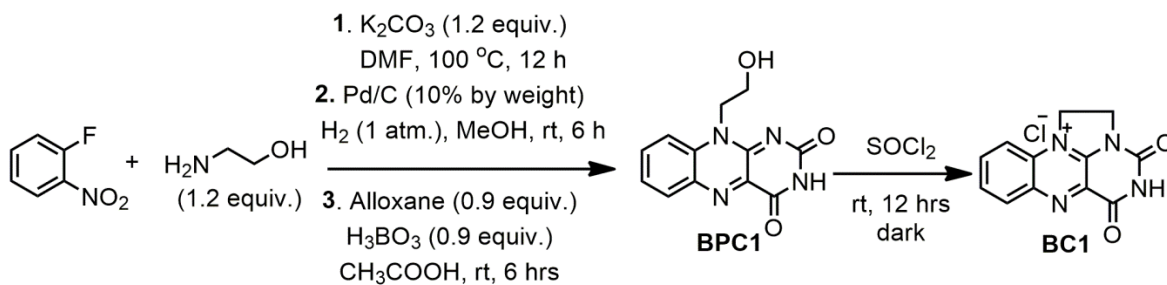
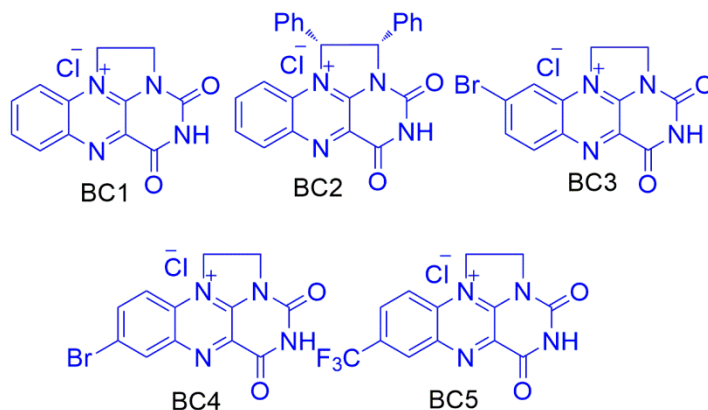


Figure Synthetic scheme for bridged flavinium catalyst **BC1**

In a representative example for the synthesis of **BPC1**, ethanolamine (12.0 mmol) and 2-fluoronitrobenzene (1.41 g, 10 mmol) were added to a solution of potassium carbonate (1.65 g, 12 mmol) in DMF (20 mL). The reaction mixture was stirred at 100 °C for 12 hours. The solution was cooled at room temperature and diluted with distilled water (40 mL). The mixture was extracted with ethyl acetate (30 mL \times 3). The combined organic layer was dried over anhydrous MgSO_4 and dried under reduced pressure. The crude residue was dissolved in methanol (40 mL) followed by careful addition of Pd/C (10 % by weight). The resulting mixture was hydrogenated (1 atm) at room temperature for 6 hours. The mixture was filtered through celite pad and washed with methanol (10 mL). The crude product was concentrated under reduced pressure. Without further purification, the crude product was added into the mixture of alloxane (9.0 mmol) and boric acid (9.0 mmol) in 10 mL acetic acid. The resulting solution was stirred for 6 hours. The yellow precipitate was filtered off and washed with 2 mL acetic acid followed by ether. The yellow solid was dried under vacuum to obtain 1.67 grams, 65% yield over three steps.

Synthesis of **BC1** from **BPC1** was carried out according to published literature. **BPC1** (1 mmol, 258 mg) was added into round bottom flask flushed with argon. 2 mL of thionyl chloride was added slowly over dropwise under argon and the solution was stirred for 12 hours at room temperature in dark. The precipitate was filtered and washed thoroughly with dichloromethane.

The crude solid was dissolved in small volume of formic acid and reprecipitated by adding diethyl ether. The precipitate thus formed was washed with ether and dried under high vacuum which gave 70% of **BC1**.



1,10-Ethylenedioxy-1H-benzo[1,2-a]pteridin-12-ium chloride (**BC1**)¹⁰⁷:

Yield 70% (193 mg); Yellow solid; **mp** 214-215 °C (lit. mp 216-219 °C)¹⁹⁶; **¹H NMR** (500 MHz, DMSO-*d*₆) δ 12.88 (s, 1H), 8.59 (d, *J* = 8.3 Hz, 1H), 8.39 (m, 1H), 8.27 (d, *J* = 8.4 Hz, 1H), 8.14 (m, 1H), 5.39 (t, *J* = 9.3 Hz, 2H), 4.67 (t, *J* = 9.4 Hz, 3H); **¹³C NMR** (125 MHz, DMSO-*d*₆) δ 157.9, 146.4, 144.4, 139.1, 138.3, 134.6, 132.2, 131.1, 128.6, 117.9, 50.6, 44.9; **IR** (neat, cm⁻¹): **HRMS**: 241.0711 [*M*⁺], predicted 241.0720; **UV/Vis (H₂O)** λ_{max} = 365, 410 nm.

4,6-Dioxo-1,2-diphenyl-2,4,5,6-tetrahydro-1H-benzo[1,2-a]pteridin-12-ium chloride (**BC2**)¹⁹⁷:

Yield 64% (274 mg); Yellow bright solid; **mp** 280-283 °C; **¹H NMR** (500 MHz, DMSO-*d*₆) δ 12.97 (s, 1H), 8.60 (d, *J* = 7.5 Hz, 1H), 8.09 (t, *J* = 7.3 Hz, 1H), 8.02 (t, *J* = 7.5 Hz, 1H), 7.70 (dd, *J* = 7.2, 2.2 Hz, 2H), 7.68 – 7.62 (m, 2H), 7.53 – 7.46 (m, 7H), 7.01 (d, *J* = 7.7 Hz, 1H), 5.90 (d, *J* = 7.7 Hz, 1H); **¹³C NMR** (125 MHz, DMSO-*d*₆) δ 158.1, 145.7, 144.1, 139.7, 137.4, 135.7, 135.2, 134.7, 132.7, 130.8, 130.5, 129.8, 129.5, 129.0, 128.0, 127.6, 127.3, 117.4, 70.3, 39.5; **IR** (neat, cm⁻¹): 3368, 3065, 2900, 1723, 1619, 1587, 1363; **HRMS**: 393.1345 [*M*⁺], predicted

393.1346; **UV/Vis (H₂O)** λ_{max} = 370, 405 nm; $[\alpha]_D +207.9^\circ$ (c 0.15, CH₃OH) {Ref: +206.2° (c 0.15, CH₃OH)}

10-Bromo-4,6-dioxo-2,4,5,6-tetrahydro-1H-benzo[g]imidazo[1,2,3-ij]pteridin-12-ium

(BC3):

Yield 58% (205 mg); Yellow solid; **mp** 160-163 °C; **¹H NMR** (500 MHz, DMSO-d₆) δ 12.92 (s, 1H), 8.90 (s, 1H), 8.55 (d, J = 8.3 Hz, 1H), 8.24 (d, J = 9.0 Hz, 1H), 5.39 (t, J = 8.5 Hz, 2H), 4.66 (t, J = 9.5 Hz, 2H); **¹³C NMR** (125 MHz, DMSO-d₆) δ 158.2, 146.8, 145.1, 140.9, 140.1, 136.4, 134.4, 128.4, 124.1, 120.2, 51.3, 45.5; **IR** (neat, cm⁻¹): 3368, 3071. 3007; 1728, 1613, 1443; **HRMS**: 318.9688 [M⁺], predicted 318.9680; **UV/Vis (H₂O)** λ_{max} = 340, 430 nm.

9-Bromo-4,6-dioxo-2,4,5,6-tetrahydro-1H-benzo[g]imidazo[1,2,3-ij]pteridin-12-ium

(BC4):

Yield 69% (245 mg); Yellow solid; **mp** decomposed at 310 °C; **¹H NMR** (500 MHz, DMSO-d₆) δ 12.91 (s, 1H), 8.66 (s, 1H), 8.49 (d, J = 8.5 Hz, 1H), 8.29 (d, J = 8.2 Hz, 1H), 5.34 (t, J = 9.3 Hz, 2H), 4.67 (t, J = 9.1 Hz, 2H); **¹³C NMR** (125 MHz, DMSO-d₆) δ 158.3, 146.8, 145.3, 138.5, 135.3, 134.9, 134.0, 133.1, 129.8, 121.4, 51.4, 45.5; **IR** (neat, cm⁻¹): 3345, 3070, 2930, 1731, 1624, 1369; **HRMS**: 318.9822 [M⁺], predicted 318.9825; **UV/Vis (H₂O)** λ_{max} = 404 nm

4,6-Dioxo-9-(trifluoromethyl)-2,4,5,6-tetrahydro-1H-benzo[g]imidazo[1,2,3-ij]pteridin-12-ium **(BC5)**¹⁰⁷:

Yield 79% (271 mg); Bright yellow solid; **mp** 190 °C; **¹H NMR** (500 MHz, CD₃COOD) δ 10.66 (bs, 1H), 8.74 (s, 1H), 8.41 (s, 1H), 8.16 (s, 1H), 5.54 (bs, 2H), 4.96 (bs, 2H); **¹³C NMR** (125 MHz, CD₃COOD) δ 160.1, 147.6, 146.6, 142.4, 138.1, 136.63 (q, J = 32.5 Hz, C-CF₃), 135.4, 133.1, 132.8, 125.4 (q, J = 275 Hz, CF₃), 120.5, 54.5, 48.3; **¹⁹F NMR** (282 MHz, CD₃COOD) δ -

65.5; **IR** (neat, cm^{-1}): 3354, 3021, 2913, 1730, 1715, 1642, 1453; **HRMS**: 309.0584 [M^+], predicted 309.0594; **UV/Vis** (H_2O) $\lambda_{\text{max}} = 400 \text{ nm}$

10-(2-hydroxyethyl)benzo[g]pteridine-2,4(3H,10H)-dione (**BPC1**)¹⁹⁶:

Yield 65% (838 mg at 5.0 mmol scale); Yellow solid; **mp** decomposed at 315 °C (lit. mp 312-315 °C)¹⁹⁶; **HRMS**: 259.0820 [$\text{M}+\text{H}$]⁺, predicted 259.0826; NMR spectra not reported due to unresolved peaks.

10-(2-hydroxy-1,2-diphenylethyl)benzo[g]pteridine-2,4(3H,10H)-dione (**BPC2**)¹⁹⁷:

Yield 59% (484 mg at 2.0 mmol scale); Yellow solid; **mp** decomposed at 255 °C ; **¹H NMR** (500 MHz, DMSO-d_6) δ 11.49 (s, 1H), 7.93 (d, $J = 8.0 \text{ Hz}$, 1H), 7.67 (d, $J = 8.1 \text{ Hz}$, 3H), 7.58 (s, 1H), 7.49 (t, $J = 7.3 \text{ Hz}$, 1H), 7.38 (t, $J = 7.5 \text{ Hz}$, 2H), 7.31 (t, $J = 7.3 \text{ Hz}$, 1H), 7.05 (s, 1H), 6.99 (dt, $J = 20.9, 7.1 \text{ Hz}$, 3H), 6.43 (s, 1H), 5.91 (s, 1H); **¹³C NMR** (125 MHz, DMSO-d_6) δ 159.2, 155.2, 151.6, 140.3, 138.0, 136.6, 134.8, 133.9, 131.8, 131.4, 128.6, 128.4, 127.8, 127.5, 127.2, 126.6, 125.9, 118.7, 73.2, 61.5; **IR** (neat, cm^{-1}): 3336, 3168, 3059, 1709, 1674, 1551, 1267; **$[\alpha]_D^{-69.7^\circ}$ (c 0.1, CH_3OH)** {*Ref*: -68.9° (c 0.1, CH_3OH)}¹⁹⁷

8-Bromo-10-(2-hydroxyethyl)benzo[g]pteridine-2,4(3H,10H)-dione (**BPC3**):

Yield 67% (1.12 g at 5.0 mmol scale); Yellow solid; **mp** decomposed at 261 °C ; **¹H NMR** (500 MHz, DMSO-d_6) δ 11.48 (s, 1H), 8.33 (d, $J = 2.1 \text{ Hz}$, 1H), 8.09 – 7.96 (m, 2H), 4.94 (t, $J = 5.8 \text{ Hz}$, 1H), 4.66 (t, $J = 5.8 \text{ Hz}$, 2H), 3.80 (t, $J = 5.9 \text{ Hz}$, 2H); **¹³C NMR** (125 MHz, DMSO-d_6) δ 159.4, 155.5, 150.6, 139.6, 136.7, 135.5, 132.9, 132.9, 119.3, 117.6, 57.4, 46.8, 40.2; **IR** (neat, cm^{-1}): 3399, 3156, 3015, 1713, 1650, 1538; **HRMS**: 336.9912 [$\text{M}+\text{H}$]⁺, predicted 336.9931

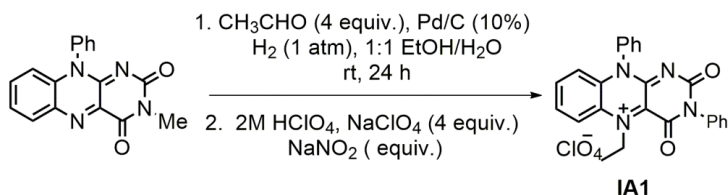
7-bromo-10-(2-hydroxyethyl)benzo[g]pteridine-2,4(3H,10H)-dione (**BPC4**):

Yield 72% (1.2 g at 5.0 mmol scale); Yellow solid; **mp** decomposed at 270 °C; **¹H NMR** not reported due to unresolved peaks; **¹³C NMR** (125 MHz, DMSO-d_6) δ 159.9, 155.8, 151.0, 139.1,

134.8, 134.0, 133.3, 129.3, 128.7, 120.2, 57.8, 47.2; **IR** (neat, cm^{-1}): 3456, 3163, 3045, 2825, 1735, 1642, 1535, 1278; **HRMS**: 336.9930 $[\text{M}+\text{H}]^+$, predicted 336.9931

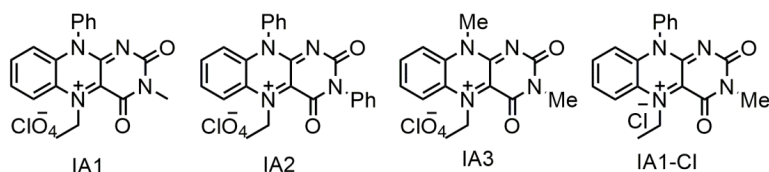
10-(2-hydroxyethyl)-7-(trifluoromethyl)benzo[*g*]pteridine-2,4(3*H*,10*H*)-dione (**BPC5**)¹⁰⁷:
Yield 70% (1.15 g at 5.0 mmol scale); Yellow solid; **mp** decomposed at 262 °C ; **¹H NMR** (500 MHz, DMSO-d_6) δ 11.57 (s, 1H), 8.47 (s, 1H), 8.21 (dt, $J = 9.1, 5.4$ Hz, 2H), 4.97 (s, 1H), 4.70 (t, $J = 5.7$ Hz, 2H), 3.83 (t, $J = 5.5$ Hz, 2H); **¹³C NMR** (125 MHz, DMSO-d_6) δ 159.8, 156.0, 151.6, 140.8, 136.5, 134.4, 130.3 (q, $J = 3.7$ Hz), 129.1 (q, $J = 3.7$ Hz), δ 126.2 (q, $J = 33.2$ Hz), 124.0 (q, $J = 272.2$ Hz), 119.4, 57.9, 47.3; **¹⁹F NMR** (282 MHz, DMSO-d_6) δ -60.5; **IR** (neat, cm^{-1}): 3296, 3098, 2996, 1677, 1556; **HRMS**: 327.0691 $[\text{M}+\text{H}]^+$, predicted 327.0700

A. General procedure for synthesis of bridged flavinium catalysts (**IA1**, **IA3**, **IA1-Cl**, and **A1-A5**):



In a typical experiment, *N3*-Methyl-*N10*-phenylisoalloxazine (304 mg, 1.0 mmol) and Pd/C (31 mg) were added into flame dried round bottom flask. The flask was evacuated and back filled with argon. Degassed 1:1 ethanol-water mixture (25 mL), acetaldehyde (1.77 g, 4 mmol), and conc. HCl (2.0 mL) were then added into the flask through syringe. The solution was degassed one more time using freeze-pump-thaw technique. Hydrogen balloon was inserted and the mixture was stirred vigorously at room temperature for 24 hours. The solution was filtered through celite pad under argon to remove palladium and other residues. The filtrate was concentrated under reduced pressure to remove most of the solvent. The concentrated solution was added successively with 4.5 mL 2M HClO_4 solution, NaClO_4 (1.35 g, 10 mmol), and NaNO_2

(0.45 g, 10 mmol) at 0 °C. The resulting solution was stirred at 0 °C for 2 hours. The purple color precipitate was filtered off and washed with cold water and ether. The crude product was dissolved in minimum volume of acetonitrile and reprecipitated with ether. The precipitate was washed with cold acetonitrile and ether to obtain 73% of desired product **IA1** as purple solid.



IA1⁷⁹

Yield 73% (315 mg); Purple solid; **mp** decomposed >300 °C; **¹H NMR** (500 MHz, DMSO-*d*₆) δ 7.67 (d, *J* = 1.2 Hz, 1H), 7.56 (d, *J* = 5.4 Hz, 2H), 7.44 (d, *J* = 12.6 Hz, 1H), 7.27 (d, *J* = 7.9 Hz, 1H), 7.20 – 7.14 (m, 2H), 6.86 (t, *J* = 7.4 Hz, 1H), 6.35 (d, *J* = 7.9 Hz, 1H), 3.74 (m, 1H), 3.57 (m, 1H), 3.15 (s, 3H), 1.23 (t, *J* = 6.6 Hz, 3H); **¹³C NMR** (125 MHz, DMSO-*d*₆) δ 166.1, 159.3, 154.6, 138.0, 132.6, 130.5, 130.4, 130.1, 129.1, 128.2, 125.2, 120.9, 117.9, 117.3, 74.7, 43.7, 28.1, 14.0; **IR** (neat, cm⁻¹): 3089, 2993, 1712, 1665, 1552; **HRMS**: 333.1345 [M⁺], predicted 333.1346; **UV/Vis (DMSO)** λ_{max} = 352 nm

IA2:

Yield 66% (260.7 mg); Purple solid; **mp** decomposed at 188 °C; **¹H NMR** (500 MHz, DMSO-*d*₆) δ 7.71 – 7.65 (m, 1H), 7.64 – 7.53 (m, 2H), 7.53 – 7.37 (m, 4H), 7.30 – 7.16 (m, 5H), 6.86 (t, *J* = 8.7 Hz, 1H), 6.36 (d, *J* = 7.7 Hz, 1H), 3.87 – 3.77 (m, 1H), 3.65 – 3.56 (m, 1H), 1.30 (t, *J* = 7.1 Hz, 3H); **¹³C NMR** (125 MHz, DMSO-*d*₆) δ 166.0, 159.2, 154.0, 137.8, 136.0, 132.5, 130.3, 129.1, 129.0, 128.9, 128.5, 128.2, 128.0, 126.1, 125.2, 120.2, 117.2, 116.7, 75.6, 43.2, 13.9; **IR** (neat, cm⁻¹): 3068, 2987, 1713, 1663, 1553; **HRMS**: 395.1500 [M⁺], predicted 395.1503; **UV/Vis (CH₃CN)** λ_{max} = 394, 551 nm.

IA3⁷⁹:

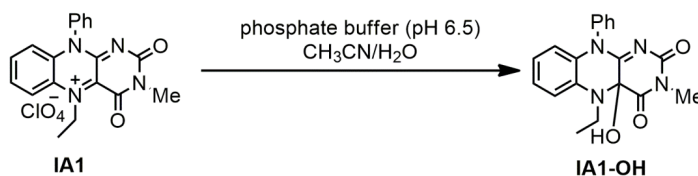
Yield 69% (255 mg); Purple solid; **mp** decomposed at 158 °C; **¹H NMR** (500 MHz, DMSO-d₆) δ 7.42 (d, *J* = 7.7 Hz, 1H), 7.28 – 7.13 (m, 2H), 7.07 (d, *J* = 3.5 Hz, 1H), 3.62 (s, 2H), 3.70 – 3.42 (m, 4H), 3.17 (s, 2H), 1.14 (t, *J* = 6.2 Hz, 3H); **¹³C NMR** (125 MHz, DMSO-d₆) δ 166.1, 158.3, 154.5, 132.7, 128.8, 125.1, 121.0, 117.4, 116.4, 74.4, 43.2, 32.1, 28.0, 13.8; **IR** (neat, cm⁻¹): 3080, 2987, 1714, 1662, 1560; **HRMS**: 271.1188 [M⁺], predicted 271.1190; **UV/Vis** (CH₃CN) λ_{max} = 391, 545 nm.

IA1-Cl:

4M HCl solution, NaCl (4 mmol) and NaNO₂ (4 mmol) were used instead of HClO₄ and NaClO₄. Other procedure was similar to general procedure **B**.

Yield 53% (195 mg); Brown solid; **mp** >320 °C; **¹H NMR** (500 MHz, DMSO-d₆) δ 8.18 – 7.95 (m, 4H), 7.86 (d, *J* = 7.7 Hz, 1H), 7.69 (d, *J* = 7.7 Hz, 1H), 7.58 (t, *J* = 6.5 Hz, 1H), 7.28 (t, *J* = 7.1 Hz, 1H), 6.76 (d, *J* = 7.7 Hz, 1H), 4.29 – 3.91 (m, 2H), 2.92 (s, 3H), 1.65 (t, *J* = 6.6 Hz, 3H); **LRMS**: 333.13 [M⁺], predicted 333.13

B.1. General Procedure for synthesis of IA1-OH¹⁹⁸

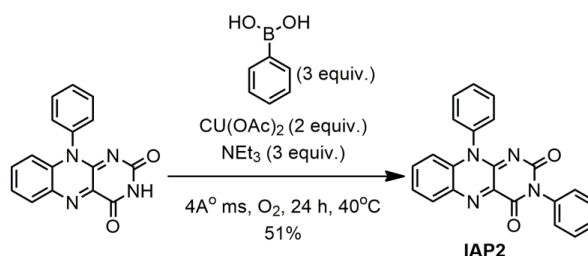


IA1 (102 mg, 0.26 mmol) was added with 1 mL of CH₃CN/H₂O (10:1 v/v) followed by 7.5 mL of phosphate buffer (pH 6.5). The resulting mixture was stirred for 15 minutes at room temperature. The resulting greenish precipitate was filtered off, washed with 20 mL of water and dried under vacuum to afford 79% (71.9 mg) of **IA1-OH**

Yield 79% (71.9 mg); Green solid; **mp** 125-127 °C; **¹H NMR** (500 MHz, CDCl₃) δ 7.58 (d, *J* = 7.6 Hz, 1H), 7.52 – 7.41 (m, 3H), 7.28 (d, *J* = 7.6 Hz, 1H), 7.23 – 7.13 (m, 1H), 7.01 (d, *J* = 9.3

Hz, 1H), 6.99 – 6.90 (m, 1H), 6.60 (d, $J = 8.1$ Hz, 1H), 3.57 (q, $J = 13.9, 6.8$ Hz, 2H), 3.37 (s, 3H), 1.17 (t, $J = 6.9$ Hz, 3H); $^{13}\text{C NMR}$ (126 MHz, CD_2Cl_2) δ 167.1, 158.5, 154.8, 138.7, 132.5, 130.8, 129.7, 129.4, 128.2, 125.8, 123.1, 121.0, 118.9, 74.6, 45.8, 28.7, 14.3; **IR** (neat, cm^{-1}): 3179, 3070, 2994, 1724, 1647, 1548, 1278; **HRMS**: 351.0697 $[\text{M}+\text{H}]^+$, predicted 351.0705; **UV/Vis** (CH_3CN) $\lambda_{\text{max}} = 345, 440$ nm.

B2. General procedure for synthesis of **IAP2**¹⁹⁹:

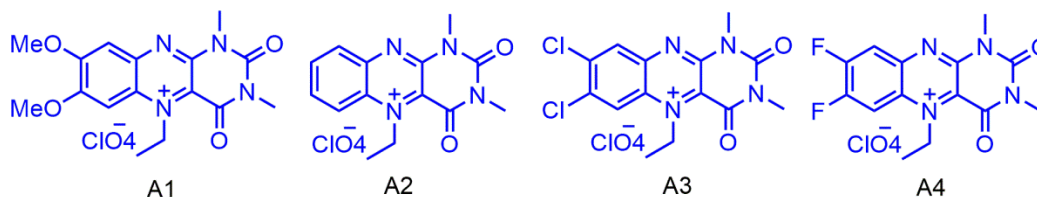


A flame dried round bottom flask was added with 4 Å molecular sieves, phenylboronic acid (365.7 mg, 3 mmol), $\text{Cu}(\text{OAc})_2$ (363 mg, 2 mmol) and *N*₁₀-phenylisoalloxazine (290.2 mg, 1 mmol) under argon atmosphere. The flask was evacuated and back filled with oxygen for two cycles. Then triethylamine (303.5 mg, 3 mmol) and dry CH_2Cl_2 (10 mL) were added via syringe. The resulting solution was stirred for 24 hours at 40 °C in oxygen atmosphere. After most of the starting material was consumed as indicated by TLC, the solution was diluted with 10 mL of dichloromethane and washed with 5 mL water. The organic phase was dried under anhydrous Na_2SO_4 and concentrated in rotary evaporator. The crude product was purified in column chromatography in silica gel (100% DCM) to afford 51% (208 mg) of desired product.

Yield 186 mg (51%); Yellow solid; **mp** 317-320 °C; $^1\text{H NMR}$ (500 MHz, DMSO-d_6) δ 8.58 (d, $J = 9.3$ Hz, 1H), δ 8.34 (d, $J = 7.6$ Hz, 1H), 8.30 (d, $J = 8.8$ Hz, 2H), 8.27 (dd, $J = 8.1, 0.9$ Hz, 1H), 8.21 (d, $J = 8.0$ Hz, 1H), 8.15 (s, 2H), 8.09 (t, $J = 7.6$ Hz, 1H), 7.92 (d, $J = 8.0$ Hz, 1H), 7.82 – 7.78 (m, 1H), 7.75 (t, $J = 7.6$ Hz, 2H), 7.67 (dd, $J = 14.2, 7.2$ Hz, 2H), 7.49 (d, $J = 7.4$ Hz, 2H), 6.84 (d, $J = 8.5$ Hz, 1H), 5.86 (s, 2H); $^{13}\text{C NMR}$ (125 MHz, DMSO-d_6) δ 159.6, 154.9,

150.7, 138.9, 135.8, 135.1, 135.1, 134.0, 131.5, 130.8, 130.5, 130.4, 130.2, 130.0, 129.8, 127.8, 127.6, 127.6, 127.3, 127.0, 126.3, 126.2, 125.3, 125.2, 124.6, 124.2, 123.9, 123.8, 123.0, 116.8, 42.5; **IR** (neat, cm^{-1}): 3058, 1713, 1654, 1584, 1537; **HRMS**: 505.0890 $[\text{M}+\text{H}]^+$, predicted 505.0895.

A1-A4:



For the synthesis of alloxazinium catalysts **A1-A4**, acetic acid was used as solvent instead of ethanol-water mixture. Also, for catalyst **A4**, hydrogen pressure was maintained at 4 atmosphere. For all other catalysts, procedures were followed as described in general procedure **B**.

A1:

Yield 83% (356 mg); Yellow solid; **mp** 255-256 °C; **$^1\text{H NMR}$** (500 MHz, CD_3CN) δ 7.57 (s, 1H), 7.45 (s, 1H), 6.00 (s, 1H), 5.22 (s, 1H), 4.23 (s, 3H), 4.16 (s, 3H), 3.78 (s, 3H), 3.49 (s, 3H), 1.74 (t, $J = 7.1$ Hz, 3H); **$^{13}\text{C NMR}$** (125 MHz, CD_3CN) δ 160.5, 159.9, 157.0, 150.1, 148.1, 147.6, 131.0, 116.6, 107.7, 97.5, 59.1, 58.6, 51.6, 31.1, 30.3, 14.8; **IR** (neat, cm^{-1}): 3071, 2991, 1712, 1668, 1492; **HRMS**: 331.1395 $[\text{M}^+]$, predicted 331.1401; **UV/Vis** (CH_3CN) $\lambda_{\text{max}} = 412$ nm.

A2²⁰⁰:

Yield 69% (255 mg); yellow solid; **mp** 244-247 °C; **$^1\text{H NMR}$** (500 MHz, CD_3CN) δ 8.56 (d, $J = 9.1$ Hz, 1H), 8.39 – 8.19 (m, 3H), 5.83 (bs, 2H), 3.83 (s, 3H), 3.52 (s, 3H), 1.80 (t, $J = 7.2$ Hz, 3H); **$^{13}\text{C NMR}$** (125 MHz, CD_3CN) δ 156.4, 149.7, 148.7, 148.0, 137.8, 137.1, 131.1, 122.5,

120.7, 52.9, 31.5, 30.7, 15.6; **IR** (neat, cm^{-1}): 3069, 2994, 1721, 1676, 1553; **HRMS**: 271.1190 $[\text{M}^+]$, predicted 271.1190; **UV/Vis** (CH_3CN) $\lambda_{\text{max}} = 378, 454 \text{ nm}$.

A3²⁰⁰:

Yield 67% (293 mg); Yellow solid; **mp** 216-218 °C (lit. mp 227-231); **¹H NMR** (500 MHz, CD_3CN) δ 8.78 (s, 1H), 8.55 (s, 1H), 6.07 (s, 1H), 5.26 (s, 1H), 3.79 (s, 3H), 3.50 (s, 3H), 1.77 (t, $J = 7.1 \text{ Hz}$, 3H); **¹³C NMR** (125 MHz, CD_3CN) δ 156.0, 149.5, 149.4, 146.5, 142.8, 141.6, 131.2, 129.9, 123.4, 122.0, 53.5, 31.7, 30.8, 15.6; **HRMS**: 340.9579 $[\text{M}^+]$, predicted 340.9577; **UV/Vis** (CH_3CN) $\lambda_{\text{max}} = 387, 461 \text{ nm}$.

A4²⁰⁰:

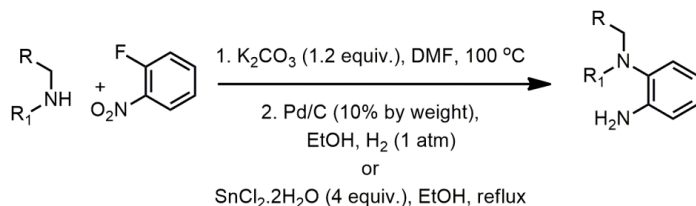
Yield 46% (17.5 mg at 0.1 mmol scale); Yellow solid; **mp** 205-208 °C (lit. mp 195-198 °C); **¹H NMR** (500 MHz, CD_3CN) δ 8.51 (dd, $J = 11.2, 7.3 \text{ Hz}$, 1H), 8.21 (dd, $J = 9.5, 8.1 \text{ Hz}$, 1H), 3.78 (s, 3H), 3.49 (s, 3H), 1.76 (t, $J = 7.2 \text{ Hz}$, 3H); **¹³C NMR** (125 MHz, CD_3CN) δ 157.4 (d, $J = 16.7 \text{ Hz}$), 156.8 (d, $J = 16.3 \text{ Hz}$), 155.2, 148.8, 148.3, 145.7 (d, $J = 13.0 \text{ Hz}$), 128.5 (d, $J = 8.2 \text{ Hz}$), 122.1, 116.0 (d, $J = 18.2 \text{ Hz}$), 107.9 (d, $J = 25.3 \text{ Hz}$), 52.9, 30.7, 29.8, 14.4; **¹⁹F NMR** (282 MHz, CD_3CN) δ -117.75 – -118.45 (m), -118.67 – -119.33 (m); **IR** (neat, cm^{-1}): 3070, 2944, 1728, 1679, 1563; **HRMS**: 307.0996 $[\text{M}^+]$, predicted 307.1001; **UV/Vis** (CH_3CN) $\lambda_{\text{max}} = 362, 441 \text{ nm}$.

7,8-dimethoxy-*NI,N3*-dimethylalloxazine (**API**):

Yield 81% (2.44 g at 10 mmol scale); Yellow solid; **mp** decomposed > 299 °C; **¹H NMR** (500 MHz, CDCl_3) δ 7.56 (s, 1H), 7.25 (s, 1H), 4.10 (s, 3H), 4.03 (s, 3H), 3.78 (s, 3H), 3.58 (s, 3H); **¹³C NMR** (125 MHz, CDCl_3) δ 160.4, 156.7, 152.7, 150.9, 144.8, 141.9, 137.5, 126.5, 107.6, 105.0, 56.8, 56.6, 29.5, 29.1; **IR** (neat, cm^{-1}): 3007, 2941, 1711, 1661, 1547, 1486; **HRMS(ESI)**: 303.1080 $[\text{M}+\text{H}]^+$, Predicted 303.1088

Note: Catalysts **A1-OOH** and other peroxyflavinium catalysts were synthesized by previous graduate student Dr. Shuau Chen and were used as they were.

B. General procedure for synthesis of starting materials 2.1a-2.1h, 2.1j, 2.1l, and 4.3a-4.3g:



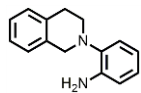
Amine (10.0 mmol) and 2-fluoronitrobenzene (1.41 g, 10.0 mmol) were added to a solution of potassium carbonate (1.65 g, 12 mmol) in DMF (15 mL). The reaction mixture was stirred at 100 °C until the reaction was complete as indicated by TLC. The solution was cooled at room temperature and diluted with distilled water (50 mL). The mixture was extracted with ethyl acetate (30 mL×3). The combined organic layer was dried over anhydrous MgSO₄ and concentrated under reduced pressure. The crude residue was dissolved in ethanol (40 mL) followed by careful addition of Pd/C (10 % by weight). The resulting mixture was hydrogenated (1 atm) at room temperature for 14 h. The mixture was filtered through celite pad and washed with methanol (10 mL). The crude product was concentrated under reduced pressure. The crude product was purified by flash column chromatography over silica gel using hexanes and ethyl acetate as eluants to obtain 60–87% of desired products.

In case of substrate **2.1l**, corresponding amine and potassium carbonate were used twice the equivalent mentioned above in 5.0 mmol scale with respect to nitro derivative starting material.

In case of substrate **2.1c** and **2.1d**, 4 equivalent of SnCl₂·2H₂O was used as reducing agent in ethanol solvent. The solution was refluxed until the starting material was consumed. The solution was slowly added with 10% sodium bicarbonate solution until it was slightly basic. The residue was filtered off and the filtrate was extracted with ethyl acetate (30 mL× 3), dried under

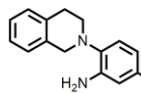
anhydrous MgSO₄ and concentrated under reduced pressure. The crude product was purified with column chromatography in silica gel using 2:1 hexanes:ethyl acetate.

2-(3,4-dihydroisoquinolin-2(1H)-yl)aniline (**2.1a/4.3d**):



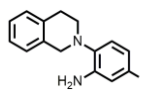
Yield 79% (1.7 g), White solid; **mp** 108-110 °C (lit. mp 110-112 °C)¹⁴³; **¹H NMR** (500 MHz, CDCl₃) δ 7.21 – 7.16 (m, 3H), 7.11 – 7.05 (m, 2H), 6.99 (td, *J* = 7.9, 1.4 Hz, 1H), 6.80 – 6.75 (m, 2H), 4.15 (s, 2H), 3.30 (t, *J* = 5.7 Hz, 2H), 3.03 (t, *J* = 5.5 Hz, 2H); **¹³C NMR** (125 MHz, CDCl₃) δ 141.8, 135.0, 134.2, 129.1, 129.0, 126.5, 125.9, 125.3, 120.3, 118.7, 115.6, 53.8, 49.3, 29.5; **IR** (neat, cm⁻¹): 3427, 3339, 3018, 2923, 1605, 1581, 1496, 1379, 1266, 1111.

2-(3,4-dihydroisoquinolin-2(1H)-yl)-5-(trifluoromethyl)aniline (**2.1b/4.3b**):



Yield 75% (2.2 g); White solid; **mp** 98-100 °C (lit. mp 97-99 °C)¹⁴³; **¹H NMR** (500 MHz, CDCl₃) δ 7.19 (d, *J* = 4.5 Hz, 3H), 7.09 (d, *J* = 8.0 Hz, 2H), 7.01 (d, *J* = 8.3 Hz, 1H), 6.97 (s, 1H), 4.12 (s, 2H), 4.12 (bs, 2H), 3.27 (t, *J* = 5.8 Hz, 2H), 3.02 (t, *J* = 5.7 Hz, 2H); **¹³C NMR** (125 MHz, CDCl₃) δ 142.0, 141.8, 134.8, 134.1, 129.0, 126.7, 126.5, 126.5, 125.9, 124.7 (q, *J* = 276.0 Hz), 120.0, 115.4 (q, *J* = 4.0 Hz), 111.6 (q, *J* = 4.0 Hz), 53.4, 48.9, 29.6; **¹⁹F NMR** (282 MHz, CDCl₃) δ -62.0; **IR** (neat, cm⁻¹): 3446, 3355, 3011, 2958, 1616, 1439, 1257, 1148.

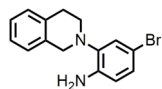
5-Bromo-2-(3,4-dihydroisoquinolin-2(1H)-yl)aniline (**2.1c/4.3c**):



Yield 76% (2.3 g); White solid; **mp** 107-109 °C; **¹H NMR** (500 MHz, CDCl₃) δ 7.23 – 7.16 (m, 3H), 7.10 – 7.07 (m, 1H), 6.92 – 6.84 (m, 3H), 4.08 (s, 2H), 3.23 (t, *J* = 5.7 Hz, 2H), 3.01 (t, *J* = 5.7 Hz, 2H); **¹³C NMR** (125 MHz, CDCl₃) δ 143.3, 137.8, 134.8, 134.1, 129.0, 126.6, 126.5, 126.0, 121.8, 121.2, 118.0, 117.8, 53.8, 49.3, 29.5; **IR** (neat, cm⁻¹): 3427, 3340,

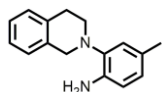
3067, 3018, 2953, 1605, 1581, 1427, 1288, 1144, 1083; **HRMS**: 303.0488 [M+H]⁺, predicted 303.0491

4-Bromo-2-(3,4-dihydroisoquinolin-2(1H)-yl)aniline (**2.1d**):



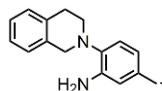
Yield 71% (2.1 g), White solid; **mp** 80-82 °C (lit. mp 76.8–79.3 °C)¹⁴³; **¹H NMR** (500 MHz, CDCl₃) δ 7.22 – 7.16 (m, 1H), 7.14 (d, *J* = 2.2 Hz, 1H), 7.08 (dd, *J* = 8.4, 2.2 Hz, 1H), 6.65 (d, *J* = 8.4 Hz, 1H), 4.11 (s, 1H), 3.25 (t, *J* = 5.8 Hz, 1H), 3.03 (t, *J* = 5.8 Hz, 1H); **¹³C NMR** (125 MHz, CDCl₃) δ 140.6, 134.4, 133.9, 129.0, 127.9, 126.6, 126.5, 126.0, 123.5, 116.8, 110.1, 53.7, 49.3, 29.5;

2-(3,4-dihydroisoquinolin-2(1H)-yl)-4-methylaniline (**2.1e**):



Yield 81% (1.9 g); White solid; **mp** 77-79 °C (lit. mp 79.2-81.9 °C)¹⁴³; **¹H NMR** (500 MHz, CDCl₃) δ 7.29 – 7.24 (m, 3H), 7.17 (d, *J* = 6.5 Hz, 1H), 6.99 (d, *J* = 1.7 Hz, 1H), 6.88 (ddd, *J* = 7.9, 1.9, 0.7 Hz, 1H), 6.76 (d, *J* = 7.9 Hz, 1H), 4.18 (s, 2H), 3.97 (bs, 2H), 3.32 (t, *J* = 5.8 Hz, 2H), 3.11 (t, *J* = 5.7 Hz, 2H), 2.38 (s, 3H); **¹³C NMR** (125 MHz, CDCl₃) δ 139.2, 139.1, 135.4, 134.3, 128.9, 127.9, 126.5, 126.3, 125.7, 125.2, 120.7, 115.3, 53.8, 49.4, 30.0, 20.8; **IR** (neat, cm⁻¹): 3436, 3345, 3013, 2962, 2929, 1614, 1509, 1453, 1149.

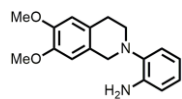
2-(3,4-dihydroisoquinolin-2(1H)-yl)-5-methylaniline (**2.1f/4.3e**):



Yield 73% (1.7 g); White solid; **mp** 80-82 °C; **¹H NMR** (300 MHz, CDCl₃) δ 7.27 – 7.17 (m, 3H), 7.12 (d, *J* = 4.8 Hz, 1H), 6.94 (s, 1H), 6.83 (d, *J* = 7.9 Hz, 1H), 6.72 (d, *J* = 7.8 Hz, 1H), 4.12 (s, 2H), 3.85 (bs, 1H), 3.27 (t, *J* = 5.5 Hz, 2H), 3.06 (t, *J* = 5.3 Hz, 2H), 2.32 (s, 3H); **¹³C NMR** (75 MHz, CDCl₃) δ 139.4, 139.1, 135.6, 134.4, 129.0, 128.0, 126.5, 126.3, 125.7,

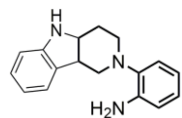
125.1, 120.8, 115.3, 53.9, 49.5, 30.1, 20.9; **IR** (neat, cm^{-1}): 3425, 3335, 3021, 2922, 1578, 1509;
HRMS: 261.1300 $[\text{M}+\text{Na}]^+$, predicted 261.1362

6,7-Dimethoxy-2-phenyl-1,2,3,4-tetrahydroisoquinoline (**2.1g/4.3g**):



Yield 60% (1.7 g); **White solid**; **mp** 130-132 °C (lit. mp 126.2-126.8 °C)¹⁴³; **¹H NMR** (500 MHz, CDCl_3) δ 7.05 (dd, $J = 7.7, 1.4$ Hz, 1H), 7.00 – 6.96 (m, 1H), 6.79 – 6.74 (m, 2H), 6.66 (s, 1H), 6.57 (s, 1H), 4.05 (s, 2H), 3.87 (s, 3H), 3.85 (s, 3H), 3.25 (t, $J = 5.6$ Hz, 2H), 2.92 (t, $J = 5.3$ Hz, 2H); **¹³C NMR** (125 MHz, CDCl_3) δ 147.7, 147.4, 141.8, 138.6, 126.9, 126.0, 125.1, 120.3, 118.7, 115.5, 111.6, 109.2, 56.0, 56.0, 53.4, 49.3, 29.1; **IR** (neat, cm^{-1}): 3364, 3292, 3100, 3060, 2982, 2919, 1556, 1468, 1382, 1131.

2-(3,4,4a,5-tetrahydro-1H-pyrido[4,3-b]indol-2(9bH)-yl)aniline (**2.1h**):

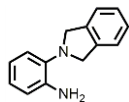


Yield 62% (164 mg at 1.0 mmol scale reaction); **Pale brown solid**; **mp** 215-217 °C; **¹H NMR** (500 MHz, DMSO-d_6) δ 10.80 (bs, 1H), 7.40 (d, $J = 7.7$ Hz, 1H), 7.30 (d, $J = 8.0$ Hz, 1H), 7.04 – 6.99 (m, 2H), 6.99 – 6.94 (m, 1H), 6.84 (td, $J = 7.8, 1.2$ Hz, 1H), 6.72 (dd, $J = 7.8, 1.3$ Hz, 1H), 6.56 (td, $J = 7.6, 1.4$ Hz, 1H), 4.78 (s, 2H), 4.07 (s, 2H), 3.19 (t, $J = 5.2$ Hz, 2H), 2.80 (t, $J = 5.4$ Hz, 2H); **¹³C NMR** (125 MHz, DMSO-d_6) δ 142.6, 138.0, 135.8, 133.1, 126.8, 124.2, 120.3, 119.9, 118.3, 117.3, 116.6, 114.5, 110.9, 106.5, 49.0, 47.9, 21.8; **LRMS**: 264.0 $[\text{M}+\text{H}]^+$, Predicted 264.0

C.1. General procedure for synthesis of 2-(isoindolin-2-yl)aniline (**2.1i/4.3h**)¹⁴³:

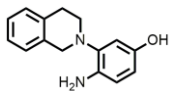
2.1i is prepared as following: α,α' -dibromo-*o*-xylene (500 mg, 1.76 mmol) and *o*-phenylenediamine (190 mg, 1.76 mmol) were dissolved in 10 mL acetonitrile. Potassium carbonate (690 mg, 5 mmol) was then added to the reaction mixture. This resulting mixture was

heated at 60 °C for 18 hours under Argon atmosphere. After the completion of reaction as indicated by TLC analysis, the precipitate was filtered and the residue was washed with 5 mL of acetonitrile. The filtrate solution was concentrated under reduced pressure, giving the crude product, which was purified by column chromatography (SiO₂; hexanes: ethyl acetate; 1:5) which afforded 54% (199 mg) of **2-(isoindolin-2-yl)aniline** as white solid.



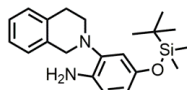
Yield 54% (199 mg); White solid; **mp** 100-101 °C (lit. mp 101-103 °C)¹⁴³; **¹H NMR** (500 MHz, CDCl₃) δ 7.32 – 7.29 (m, 4H), 7.17 (dd, *J* = 7.9, 1.3 Hz, 1H), 6.99 (ddd, *J* = 7.9, 7.3, 1.4 Hz, 1H), 6.81 – 6.79 (m, 1H), 6.77 (ddd, *J* = 7.9, 7.3, 1.5 Hz, 1H), 4.55 (s, 4H); **¹³C NMR** (125 MHz, CDCl₃) δ 142.1, 139.0, 127.3, 127.15, 125.3, 122.4, 120.4, 118.8, 116.2, 57.2; **IR** (neat, cm⁻¹): 3414, 3329, 1614, 1500, 1469, 1296, 1188; **HRMS**: 211.1222 [M+H]⁺, Predicted: 211.1230

4-Amino-3-(3,4-dihydroisoquinolin-2(1H)-yl)phenol (**2.1j/4.3f**)²⁰¹:



Yield 66% (1.58 g); Pale brown solid; **mp** 180-183 °C (lit. mp 186.8-190.3 °C)¹⁴³; **¹H NMR** (500 MHz, DMSO-d₆) δ 8.45 (s, 1H), 7.15 – 7.06 (m, 4H), 6.54 (d, *J* = 8.4 Hz, 1H), 6.45 (d, *J* = 2.6 Hz, 1H), 6.30 (dd, *J* = 8.4, 2.7 Hz, 1H), 4.15 (bs, 2H), 3.97 (s, 2H), 3.09 (t, *J* = 5.8 Hz, 2H), 2.92 (t, *J* = 5.7 Hz, 2H); **¹³C NMR** (125 MHz, DMSO-d₆) δ 149.0, 139.1, 135.2, 134.3, 134.2, 128.7, 126.4, 126.1, 125.5, 115.4, 110.3, 107.0, 52.8, 48.4, 29.1; **IR** (neat, cm⁻¹): 3364, 3292, 3100, 3060, 2982, 1556, 1468, 1382, 1234, 1170.

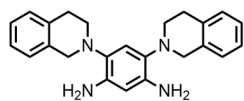
4-((tert-butyldimethylsilyl)oxy)-2-(3,4-dihydroisoquinolin-2(1H)-yl)aniline (**2.1k**):



Yield 55% (194 mg); White solid; **mp** 74-76 °C; **¹H NMR** (500 MHz, CDCl₃) δ 7.19 – 7.15 (m, 1H), 7.10 – 7.07 (m, 1H), 6.63 (d, *J* = 8.4 Hz, 1H), 6.58 (d, *J* = 2.6 Hz, 1H), 6.48

(dd, $J = 8.4, 2.6$ Hz, 1H), 4.07 (s, 2H), 3.23 (t, $J = 5.9$ Hz, 2H), 3.00 (t, $J = 5.7$ Hz, 2H), 0.96 (s, 9H), 0.14 (s, 6H); $^{13}\text{C NMR}$ (125 MHz, CDCl_3) δ 148.3, 139.9, 135.5, 135.32, 134.3, 129.0, 126.5, 126.3, 125.8, 115.9, 115.8, 112.5, 53.8, 49.2, 29.8, 29.6, 25.8, 18.3, -4.3; **IR** (neat, cm^{-1}): 3417, 3331, 2952, 2926, 2906, 2854, 2817, 2787, 1610, 1585, 1505, 1462, 1239, 1174, 1110; **HRMS**: 355.2207 $[\text{M}+\text{H}]^+$, Predicted: 355.2200

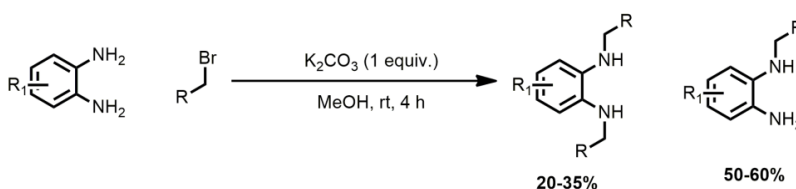
4,6-Bis(3,4-dihydroisoquinolin-2(1H)-yl)benzene-1,3-diamine (**2.1l**):



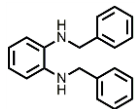
Yield 60 % (1.1 g), Pale brown solid; **mp** 187-191 °C; $^1\text{H NMR}$ (500 MHz, CDCl_3) δ 7.19 – 7.15 (m, 6H), 7.06 (d, $J = 6.5$ Hz, 2H), 6.88 (s, 1H), 6.25 (s, 1H), 4.04 (s, 2H), 3.18 (t, 2H), 3.01 (t, 2H); $^{13}\text{C NMR}$ (125 MHz, CDCl_3) δ 139.6, 135.47, 134.3, 130.5, 128.9, 126.5, 126.3, 125.8, 113.2, 102.4, 54.8, 50.2, 30.0; **IR** (neat, cm^{-1}): 3410, 3324, 3020, 2921, 1570, 1510; **HRMS**: 371.1950 $[\text{M}+\text{H}]$, Predicted: 371.2230

C. General procedure for synthesis of *N,N'*-dialkyl-*o*-phenylenediammine (**2.1n-2.1q**, **2.4a-2.4j**, and **4.1a-4.1q**)

O-phenylenediammine (40.0 mmol) and K_2CO_3 (5.52 g, 40 mmol) were added with 40 mL methanol in a flame dried round bottom flask. Alkyl or Aryl bromide (30.0 mmol) was added drop-wise into the reaction vessel. The resulting mixture was stirred for 4 hours at room temperature. When most of the starting materials were consumed as indicated by TLC, 15 mL of water was added, and the solution was extracted with dichloromethane (3 mL \times 20). The organic phase was dried in anhydrous Na_2SO_4 . The solution was concentrated under reduced pressure and the crude products were purified with column chromatography in silica gel.

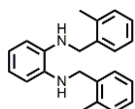


N,N'-dibenzylbenzene-1,2-diamine (**4.1a**):



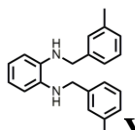
Yield 29% (2.5 g); Colorless oil; **¹H NMR** (500 MHz, CDCl₃) δ 7.53 – 7.44 (m, 8H), 7.43 – 7.37 (m, 2H), 6.93 (dd, *J* = 5.8, 3.4 Hz, 2H), 6.84 (dd, *J* = 5.7, 3.5 Hz, 2H), 4.42 (s, 4H), 3.77 (bs, 2H); **¹³C NMR** (125 MHz, CDCl₃) δ 139.5, 137.1, 128.68, 127.8, 127.3, 119.5, 112.0, 48.8; **IR** (neat, cm⁻¹): 3334, 3059, 3023, 2917, 1597, 1451, 1262, 1155, 1054; **HRMS**: 289.1580 [M+H]⁺, Predicted: 289.1583

N,N'-bis(2-methylbenzyl)benzene-1,2-diamine (**4.1b**):



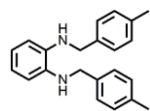
Yield 35% (3.3 g); White solid; **mp** 108-109 °C; **¹H NMR** (300 MHz, CDCl₃) δ 7.32 (d, *J* = 6.6 Hz, 2H), 7.25 – 7.10 (m, 6H), 6.86 (dd, *J* = 5.3, 3.5 Hz, 2H), 6.82 – 6.72 (m, 2H), 4.27 (s, 4H), 3.52 (bs, 2H), 2.38 (s, 6H); **¹³C NMR** (75 MHz, CDCl₃) δ 137.3, 137.1, 136.7, 130.5, 128.7, 127.6, 126.2, 119.5, 111.9, 46.9, 19.0; **IR** (neat, cm⁻¹): 3299, 3054, 3074, 1611, 1448, 1358, 1224, 1128; **HRMS**: 317.1880 [M+H]⁺, Predicted: 317.1885

N,N'-bis(3-methylbenzyl)benzene-1,2-diamine (**2.4a/4.1c**):



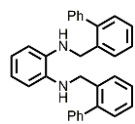
Yield 30% (2.8 g); White solid; **mp** 115-117 °C; **¹H NMR** (300 MHz, CDCl₃) δ 7.34 – 7.24 (m, 6H), 7.17 (d, *J* = 7.2 Hz, 2H), 6.90 – 6.85 (m, 2H), 6.84 – 6.78 (m, 2H), 4.34 (s, 4H), 3.69 (bs, 2H), 2.43 (s, 6H); **¹³C NMR** (75 MHz, CDCl₃) δ 139.5, 138.3, 137.3, 128.7, 128.6, 128.1, 125.0, 119.4, 111.9, 48.9, 21.5; **IR** (neat, cm⁻¹): 3353, 3024, 2916, 1598, 1434, 1260, 1127; **HRMS**: 317.1882 [M+H]⁺, Predicted: 317.1885

N,N'-bis(4-methylbenzyl)benzene-1,2-diamine (**4.1d**):



Yield 27% (2.56 g); White solid; **mp** 116-118 °C; **¹H NMR** (300 MHz, CDCl₃) δ 7.28 (d, *J* = 8.0 Hz, 4H), 7.15 (d, *J* = 7.8 Hz, 4H), 6.84 – 6.73 (m, 4H), 4.29 (s, 4H), 2.35 (s, 6H); **¹³C NMR** (75 MHz, CDCl₃) δ 137.1, 135.6, 129.3, 128.9, 128.1, 120.1, 113.3, 48.9, 21.2; **IR** (neat, cm⁻¹): 3334, 3046, 3019, 2918, 1599, 1437, 1255, 1052; **HRMS**: 317.1878 [M+H]⁺, Predicted: 317.1885

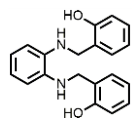
N,N'-bis([1,1'-biphenyl]-2-ylmethyl)benzene-1,2-diamine (**2.4b/4.1e**):



Yield 25% (3.3 g); Yellow crystal; **mp** 130-132 °C; **¹H NMR** (500 MHz, CDCl₃) δ 7.55 – 7.46 (m, 2H), 7.43 – 7.28 (m, 16H), 6.71 (dd, *J* = 5.6, 3.5 Hz, 2H), 6.57 – 6.48 (m, 2H), 4.21 (s, 4H); **¹³C NMR** (125 MHz, CDCl₃) δ 142.0, 140.9, 136.3, 130.3, 129.1, 129.0, 128.3, 127.8, 127.4, 127.2, 121.2, 119.5, 112.4, 46.6; **IR** (neat, cm⁻¹): 3352, 3094, 1590, 1469, 1253, 1047; **HRMS**: 441.2132 [M+H]⁺, Predicted: 441.2130

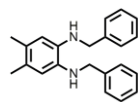
D.1. General procedure for synthesis of 2,2'-((1,2-phenylenebis(azanediyl))bis(methylene))diphenol (**2.4c/4.1f**)²⁰²:

O-phenylenediamine (1.08 g, 10.0 mmol) and salicaldehyde (2.44 g, 20.0 mmol) were added in 25 mL of Methanol. The resulting mixture was refluxed until orange colored precipitates were observed. The solution was cooled to room temperature and sodium borohydride (1.45 g, 5 equiv.) was added in portion wise until yellow transparent solution was obtained. The reaction mixture was poured into 50 mL of distilled water and allowed to stand until white precipitates were formed. The resulting solid was filtered and was successively washed with cold water and cold diethyl ether (5 mL) to obtain 81% (2.59 g) of desired product.



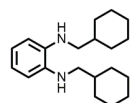
Yield 81% (2.6 g); White solid; **mp** 115-116 °C (lit. mp 98 °C)¹⁴²; **¹H NMR** (300 MHz, CDCl₃) δ 7.89 (bs, 2H), 7.31 – 7.16 (m, 4H), 6.99 – 6.82 (m, 8H), 4.41 (s, 4H), 3.74 (bs, 2H); **¹³C NMR** (75 MHz, CD₃OD) δ 155.4, 137.2, 128.8, 127.7, 125.4, 119.2, 119.0, 114.7, 112.8, 44.3; **IR** (neat, cm⁻¹): 3355, 3284, 3052, 2925, 1594, 1488, 1234, 1024. **HRMS**: 321.1460 [M+H]⁺, Predicted: 321.1463

N,N'-dibenzyl-4,5-dimethylbenzene-1,2-diamine (**2.4d/4.1h**):



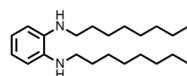
Yield 33% (3.1 g); Pale brown solid; **mp** 82-84 °C (lit. mp 88-90 °C)²⁰²; **¹H NMR** (500 MHz, CDCl₃) δ 7.49 (d, *J* = 7.6 Hz, 4H), 7.47 – 7.41 (m, 4H), 7.37 (t, *J* = 7.2 Hz, 2H), 6.65 (s, 2H), 4.38 (s, 4H), 3.67 (bs, 2H), 2.28 (s, 6H); **¹³C NMR** (125 MHz, CDCl₃) δ 139.7, 135.2, 128.6, 127.9, 127.2, 126.9, 114.4, 49.2, 19.3; **IR** (neat, cm⁻¹): 3299, 3054, 3074, 1611, 1448, 1224, 1025; **HRMS**: 317.1879 [M+H]⁺, Predicted: 317.1885

N,N'-bis(cyclohexylmethyl)benzene-1,2-diamine (**2.4e/4.1q**):



Yield 20% (1.8 g); Colorless liquid; **¹H NMR**(300 MHz, CDCl₃) δ 6.78 (dd, *J* = 5.6, 3.5 Hz, 2H), 6.67 (dd, *J* = 5.6, 3.5 Hz, 2H), 2.93 (d, *J* = 6.6 Hz, 4H), 1.89 – 1.73 (m, 8H), 1.72 – 1.61 (m, 4H), 1.33 – 1.18 (m, 6H), 1.07 – 0.97 (m, 4H); **¹³C NMR** (75 MHz, CDCl₃) δ 137.6, 119.0, 111.8, 51.30, 37.6, 31.6, 26.7, 26.1; **IR** (diamond-ATR) γ/cm⁻¹: 3305, 3077, 2957, 1597, 1255; **HRMS**: 301.2504 [M+H]⁺, Predicted: 301.2500

N,N'-dioctylbenzene-1,2-diamine (**2.4f/4.1o**):

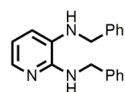


Yield 22% (2.2 g); Pale brown liquid; **¹H NMR** (300 MHz, CDCl₃) δ 6.84 (dd, *J* = 5.7, 3.5 Hz, 2H), 6.73 (dd, *J* = 5.7, 3.5 Hz, 2H), 3.21 (bs, 2H), 3.13 (t, *J* = 7.1 Hz, 4H), 1.79 –

1.66 (m, 4H), 1.54 – 1.31 (m, 20H), 0.96 (t, $J = 9.4$ Hz, 6H); ^{13}C NMR (75 MHz, CDCl_3) δ 137.5, 119.0, 111.5, 44.6, 32.0, 29.9, 29.6, 29.4, 27.5, 22.8, 14.2; IR (neat, cm^{-1}): 3365, 2922, 2852, 1600, 1512, 1457, 1253; HRMS: 333.3133 $[\text{M}+\text{H}]^+$, Predicted: 333.3133

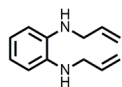
D.2. General procedure for synthesis of *N2,N3*-dibenzylpyridine-2,3-diamine (2.4g/4.1k)²⁰³:

2,3-diaminopyridine (0.82 g, 7.5 mmol), molecular sieves (2.5 g, 4 Å), and benzaldehyde (0.9 mL, 9 mmol) were added in benzene (50 mL). The resulting mixture was refluxed for 3 h, after which the mixture was brought to room temperature and continued stirring for another 20 h. The solid was filtered and washed with cold ether (5 mL). The filtrate was concentrated under reduced pressure and the crude product was dissolved in 50 mL of ethanol followed by portion wise addition of sodium borohydride (2 g). The mixture was refluxed for another 18 h. The reaction mixture was then cooled to room temperature and quenched with water (50 mL). The aqueous solution was extracted with methylene chloride (20 mL \times 2), dried with anhydrous Na_2SO_4 and concentrated under reduced pressure. The crude product was purified with flash column chromatography using ethyl acetate and acetone as eluants to obtain 54% (1.17 g) of desired product.



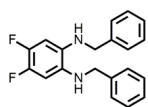
Yield 54% (1.17 g); Brown solid; **mp** 71-73 °C (lit. mp 76 °C)²⁰³; ^1H NMR (300 MHz, CDCl_3) δ 7.77 (dd, $J = 5.1, 1.5$ Hz, 1H), 7.46 – 7.27 (m, 10H), 6.82 (dd, $J = 7.6, 1.5$ Hz, 1H), 6.64 (dd, $J = 7.6, 5.1$ Hz, 1H), 4.64 (s, 2H), 4.40 (bs, 1H), 4.27 (s, 2H), 3.45 (bs, 1H); ^{13}C NMR (125 MHz, CDCl_3) δ 140.9, 138.1, 129.0, 128.7, 128.6, 128.5, 128.2, 127.5, 127.5, 117.0, 116.5, 114.2, 113.7, 48.0, 46.1; IR (neat, cm^{-1}): 3320, 3058, 2960, 1583, 1481, 1378, 1247, 1025; HRMS: 290.1538 $[\text{M}+\text{H}]^+$, Predicted: 290.1539

N,N'-diallylbenzene-1,2-diamine (2.4h/4.1l):



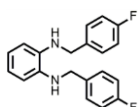
Yield 24% (1.35 g); Brown liquid; **¹H NMR** (500 MHz, CDCl₃) δ 6.86 (dd, *J* = 5.8, 3.4 Hz, 2H), 6.75 (dd, *J* = 5.7, 3.5 Hz, 2H), 6.08 (ddt, *J* = 17.2, 10.3, 5.5 Hz, 2H), 5.36 (dq, *J* = 17.2, 1.7 Hz, 2H), 5.24 (dq, *J* = 10.3, 1.5 Hz, 2H), 3.81 (dt, *J* = 5.5, 1.5 Hz, 4H), 3.50 (bs, 2H); **¹³C NMR** (125 MHz, CDCl₃) δ 137.1, 135.8, 119.5, 116.5, 112.2, 47.1; **IR** (neat, cm⁻¹): 3260, 3100, 2876, 1599, 1508, 1439, 1253, 1142; **HRMS**: 189.1317 [M+H]⁺, Predicted: 189.1317

N,N'-dibenzyl-4,5-difluorobenzene-1,2-diamine (**2.4i/4.1i**):



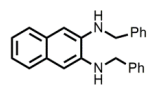
Yield 29% (2.8 g); White solid; **mp** 88-92 °C; **¹H NMR** (300 MHz, CD₃OD) δ 7.39 – 7.19 (m, 10H), 6.30 (t, *J* = 10.4 Hz, 2H), 4.20 (s, 4H); **¹³C NMR** (75 MHz, CD₃OD) δ 144.0 (dd, *J* = 234.8, 15.1 Hz), 140.6, 134.4 (dd, *J* = 4.9, 4.9 Hz), 129.4, 128.4, 128.0, 101.6 (dd, *J* = 12.8, 10.3 Hz), 49.3; **IR** (neat, cm⁻¹): 3400, 3048, 2908, 1518, 1428, 1186; **HRMS**: 325.1379 [M+H]⁺, Predicted: 325.1380

N,N'-bis(4-fluorobenzyl)benzene-1,2-diamine (**2.4j/4.1g**):



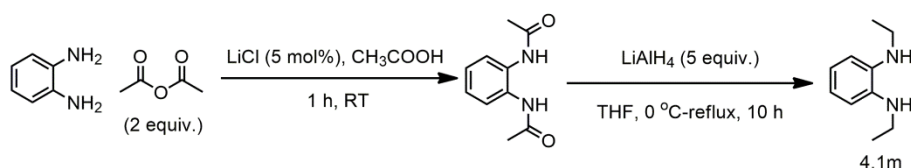
Yield 25% (2.4 g); Yellow viscous liquid; **¹H NMR** (500 MHz, CDCl₃) δ 7.37 – 7.31 (m, 4H), 7.02 (t, *J* = 8.7 Hz, 4H), 6.80 (dd, *J* = 5.8, 3.4 Hz, 2H), 6.69 (dd, *J* = 5.8, 3.5 Hz, 2H), 4.28 (s, 4H), 3.61 (bs, 2H); **¹³C NMR** (125 MHz, CDCl₃) δ 162.1 (d, *J* = 245.0 Hz), 137.0, 135.1 (d, *J* = 3.1 Hz), 129.4 (d, *J* = 7.9 Hz), 119.7, 115.5 (d, *J* = 21.5 Hz), 112.2, 48.2; **¹⁹F NMR** (470 MHz, CDCl₃) δ -115.3; **IR** (neat, cm⁻¹): 3355, 3066, 3041, 2921, 1598, 1505, 1218; **HRMS**: 325.1370 [M+H]⁺, Predicted: 325.1379

N2,N3-dibenzyl-naphthalene-2,3-diamine (**4.1j**):

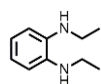


Yield 25% (253 mg at 3.0 mmol scale of benzyl bromide); Brown solid; **¹H NMR** (500 MHz, CDCl₃) δ 7.60 (dd, *J* = 6.1, 3.3 Hz, 2H), 7.47 – 7.44 (m, 4H), 7.40 – 7.35 (m, 5H), 7.31 (ddd, *J* = 7.4, 5.9, 1.3 Hz, 2H), 7.26 – 7.22 (m, 3H), 7.02 (s, 2H), 4.45 (s, 4H); **¹³C NMR** (125 MHz, CDCl₃) δ 138.5, 137.4, 129.3, 128.81, 128.2, 127.6, 126.1, 123.3, 107.7, 49.1; **IR** (neat, cm⁻¹): 3374, 3027, 2922, 1624, 1524, 1449, 1274; **HRMS**: 339.1709 [M+H]⁺, Predicted: 339.1715

D.3. General procedure for synthesis of *N,N'*-diethylbenzene-1,2-diamine (**4.1m**)²⁰⁴:

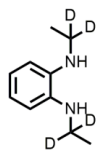


A mixture of *ortho*-phenylenediamine (9.2 mmol, 1 g) and acetic anhydride (18.5 mmol, 1.9 g) in 2 mL acetic acid was added with LiCl (0.46 mmol, 20 mg) at room temperature. The solution was stirred for 1 hour. A white solid immediately formed. The solution was diluted with 5 mL water and the solid was filtered off, washed with 10 mL water and dried under vacuum to afford 80% of diamide product. This product (384 mg, 2 mmol) was reduced with LiAlH₄ (10 mmol, 380 mg) in dry THF (15 mL) to obtain **4.1m** in 66% (216 mg).



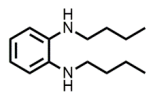
Yield 66% (216 mg); Pale pink liquid; **¹H NMR** (500 MHz, CDCl₃) δ 6.95 – 6.88 (m, 2H), 6.84 – 6.75 (m, 2H), 3.24 (q, *J* = 7.1 Hz, 4H), 3.23 (b, 2H), 1.41 (t, *J* = 7.1 Hz, 6H); **¹³C NMR** (125 MHz, CDCl₃) δ 137.3, 119.0, 111.3, 38.8, 15.0; **IR** (neat, cm⁻¹): 3369, 3080, 2989, 2900, 1550, 1500, 1440, 1250, 1110; **HRMS**: 165.1320 [M+H]⁺, Predicted: 165.1322

4.1m-D4:



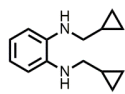
Yield 76% (128 mg from 1.0 mmol scale of corresponding diamide in 4 equivalent of LiAlD₄); Pale red liquid; **¹H NMR** (500 MHz, CDCl₃) δ 6.84 – 6.79 (dd, *J* = 5.5, 3.6 Hz, 2H), 6.71 (dd, *J* = 5.5, 3.6 Hz, 2H), 3.31 (bs, 2H), 1.30 (s, 6H); **¹³C NMR** (125 MHz, CDCl₃) δ 137.0, 119.46, 112.0, 14.7; **IR** (neat, cm⁻¹): 3336, 3044, 2966, 1598, 1431, 1348, 1263, 1056; **HRMS**: 169.1643 [M+H]⁺, predicted 169.1660

N,N'-dibutylbenzene-1,2-diamine (**4.1m**):



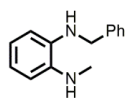
Yield 26% (1.7 g); Pale brown liquid; **¹H NMR** (300 MHz, CDCl₃) δ 6.89-6.82 (m, 2H), 6.76 – 6.70 (m, 2H), 3.14 (t, *J* = 7.1 Hz, 4H), 1.78 – 1.64 (m, 4H), 1.52 (dq, *J* = 14.2, 7.2 Hz, 4H), 1.03 (t, *J* = 7.3 Hz, 6H); **¹³C NMR** (75 MHz, CDCl₃) δ 137.4, 118.9, 111.3, 44.1, 31.8, 20.4, 14.0; **IR** (neat, cm⁻¹): 3339, 3053, 3041, 2956, 2927, 2859, 1600, 1513, 1441, 1249; **HRMS**: 221.1922 [M+H]⁺, Predicted: 221.1923

N,N'-bis(cyclopropylmethyl)benzene-1,2-diamine (**4.1p**)²⁰⁴:



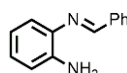
Yield 68% (146 mg obtained from 1 mmol scale of corresponding diamide following general procedure as **4.1m**); Colorless liquid; **¹H NMR** (500 MHz, CDCl₃) δ 6.78 (dd, *J* = 5.8, 3.4 Hz, 2H), 6.66 (dd, *J* = 5.7, 3.5 Hz, 2H), 2.96 (d, *J* = 6.9 Hz, 4H), 1.23 – 1.14 (m, 2H), 0.62 – 0.55 (m, 4H), 0.30 – 0.23 (m, 4H); **¹³C NMR** (125 MHz, CDCl₃) δ 137.3, 119.2, 111.6, 49.8, 11.0, 3.7; **IR** (neat, cm⁻¹): 3337, 3076, 3001, 2819, 1599, 1507, 1434, 1250, 1127; **HRMS**: 217.1610 [M+H]⁺, Predicted: 217.1614

N-benzyl-*N'*-methylbenzene-1,2-diamine (**4.1r**):



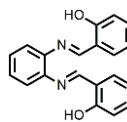
Yield 19% (1.0 mmol scale of benzyl bromide); Brown liquid; **¹H NMR** (500 MHz, CDCl₃) δ 7.33 (dd, *J* = 3.9, 1.9 Hz, 5H), 7.04 (d, *J* = 7.6 Hz, 1H), 6.96 – 6.92 (m, 1H), 6.78 – 6.72 (m, 2H), 4.00 (s, 2H), 2.57 (s, 3H); **¹³C NMR** (125 MHz, CDCl₃) δ 141.8, 138.9, 129.0, 128.8, 128.4, 127.2, 124.7, 130.0, 118.6, 115.3, 60.1, 40.6; **IR** (neat, cm⁻¹): 3441, 3346, 3060, 3027, 2926, 1607, 1499, 1364, 1098.

N-benzylidenebenzene-1,2-diamine (**2.3k'**):



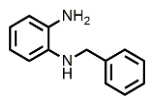
Yield 55% (obtained from reaction of **2.3k** with FeCl₃ in presence of excess base K₂CO₃); Yellow oil; **¹H NMR** (500 MHz, CDCl₃) δ 8.55 (s, 1H), 7.92 (dd, *J* = 6.6, 2.9 Hz, 2H), 7.47 (dd, *J* = 4.1, 2.3 Hz, 3H), 7.08 (dd, *J* = 12.6, 4.7 Hz, 2H), 6.77 (dd, *J* = 15.3, 7.6 Hz, 2H); **¹³C NMR** (125 MHz, CDCl₃) δ 157.6, 142.3, 137.3, 136.6, 131.2, 128.8, 128.8, 127.8, 118.6, 117.3, 115.5; **IR** (neat, cm⁻¹): 3412, 3351, 3045, 2926, 1610, 1457, 1261, 1144.

1,2-Phenylenebis(azanylylidene))bis(methanylylidene))diphenol (**4.1f''**):



Yellow crystalline solid; **mp** 166-168 °C; **¹H NMR** (500 MHz, CDCl₃) δ 13.08 (s, 1H), 8.62 (s, 1H), 7.37 (ddd, *J* = 6.6, 1.8, 1.2 Hz, 2H), 7.36 – 7.32 (m, 2H), 7.22 (dd, *J* = 5.9, 3.4 Hz, 1H), 7.05 (d, *J* = 8.0 Hz, 1H), 6.92 (td, *J* = 7.5, 1.1 Hz, 1H); **¹³C NMR** (125 MHz, CDCl₃) δ 163.8, 161.4, 142.6, 133.4, 132.4, 127.8, 119.8, 119.3, 119.1, 117.6; **IR** (neat, cm⁻¹): 3409, 3071, 2926, 1608, 1558, 1478, 1274, 1188, 1103.

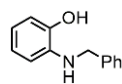
N-benzylbenzene-1,2-diamine (**2.3k**)¹⁴²:



Yield 50% (2.9 g); brown liquid; **¹H NMR** (300 MHz, CD₃OD) δ 7.36 (d, *J* = 7.1 Hz, 2H), 7.27 (t, *J* = 7.1 Hz, 2H), 7.19 (t, *J* = 7.2 Hz, 1H), 6.71 (d, *J* = 5.8 Hz, 1H), 6.64 – 6.57 (m,

1H), 6.52 (t, $J = 7.6$ Hz, 2H), 4.30 (s, 2H); ^{13}C NMR (75 MHz, CDCl_3) δ 139.4, 137.6, 134.2, 128.6, 127.8, 127.3, 120.7, 118.8, 116.5, 112.0, 48.6; IR (neat, cm^{-1}): 3360, 3278, 3026, 1604, 1505, 1452, 1310, 1261.

2-(benzylamino)phenol (**2.3l**)¹⁴²:



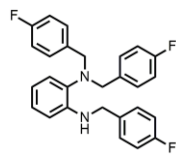
Yield 65% (129 mg from 1.0 mmol scale of 2-aminophenol); Pale yellow solid; **mp** 70-72 °C; ^1H NMR (300 MHz, CDCl_3) δ 7.47 – 7.27 (m, 5H), 6.90 – 6.58 (m, 4H), 4.35 (s, 2H); ^{13}C NMR (125 MHz, CDCl_3) δ 143.6, 139.4, 136.8, 128.7, 127.7, 127.3, 121.8, 118.0, 114.4, 112.7, 48.7.

N-butylbenzene-1,2-diamine (**2.3m/4.5h**)¹⁴²:



Yield 58% (2.8 g); Brown liquid; ^1H NMR (300 MHz, DMSO-d_6) δ 6.57 – 6.45 (m, 2H), 6.43 – 6.35 (m, 2H), 4.47 (bs, 2H), 4.30 (bs, 1H), 2.99 (t, $J = 6.1$ Hz, 2H), 1.58 (dt, $J = 14.4$, 7.0 Hz, 2H), 1.49 – 1.30 (m, 2H), 0.93 (t, $J = 7.3$ Hz, 3H); ^{13}C NMR (75 MHz, DMSO-d_6) δ 136.1, 135.0, 117.5, 116.6, 114.0, 109.6, 43.1, 31.0, 20.0, 13.9; IR (neat, cm^{-1}): 3382, 3355, 3283, 2927, 1602, 1451, 1339,, 1255, 1142.

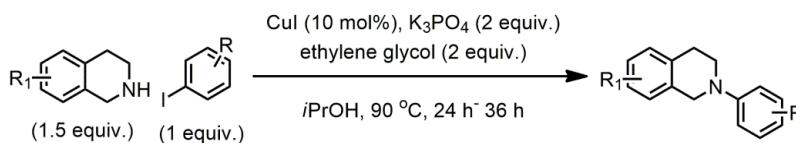
N1,N1,N2-tris(4-fluorobenzyl)-*o*-phenylenediammine (**2.3n**):



Yield 11% (47.5 mg from 3 mmol of corresponding benzyl bromide); Yellow oil; ^1H NMR (500 MHz, CDCl_3) δ 7.21 (dd, $J = 7.9$, 5.6 Hz, 2H), 7.16 (dd, $J = 7.9$, 5.8 Hz, 4H), 7.10 – 6.94 (m, 8H), 6.68 (td, $J = 7.5$, 1.4 Hz, 1H), 6.57 – 6.51 (m, 1H), 5.29 (bs, 1H), 4.29 (s, 2H), 4.03 (s, 4H); ^{13}C NMR (126 MHz, CDCl_3) δ 163.05 (d, $J = 9.5$ Hz), 161.10 (d, $J = 9.0$ Hz), 143.9, 136.0, 135.48 (d, $J = 2.7$ Hz), 133.8, 130.71 (d, $J = 4.8$ Hz), 128.71 (d, $J = 7.7$ Hz), 125.9, 123.3, 116.7, 115.47 (d, $J = 21.3$ Hz), 115.13 (d, $J = 21.2$ Hz), 110.6, 56.6, 47.3; IR (neat, cm^{-1}):

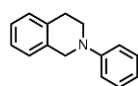
3405, 3092, 2910, 1599, 1505, 1218, 1154, 1014; [HRMS]: 433.1871 [M+H]⁺, Predicted: 433.1815

D. General procedure for synthesis of **(2.5a-2.5f/2.7a-2.7f)**^{48, 62, 78}:



In a representative example, CuI (95 mg, 0.5 mmol), K₃PO₄ (2.1 g, 10 mmol), and a stirbar were charged into a flame-dried (100 mL) round-bottom flask. The flask was evacuated and back filled with argon. This process was repeated three times. At room temperature, 5 mL of isopropanol, ethylene glycol (560 μL, 10 mmol), tetrahydroisoquinoline (1.0 g, 950 μL, 7.5 mmol) and iodobenzene (1.0 g, 557 μL, 5 mmol) were then added successively via syringe. The reaction mixture was heated to 90 °C and stirred for a day. After completion of the reaction, 10 mL diethyl ether followed by 10 mL water was added to the reaction flask. The aqueous layer was extracted by Et₂O (2x10 mL). The combined organic phase was washed with brine solution, dried over anhydrous MgSO₄, filtered and then concentrated under reduced pressure. The crude residue was purified by column chromatography (SiO₂; hexanes: ethyl acetate, 15:1; R_f = 0.33) to afford 82% (857 mg, 4.1 mmol) of *N*-phenyl-1,2,3,4-tetrahydroisoquinoline (**1v**) as colorless liquid.

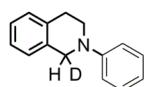
N-phenyl-1,2,3,4-tetrahydroisoquinoline (**2.5a/2.7a**)^{48, 62, 78}:



Yield 82% (857 mg); Clear oil; **¹H NMR** (500 MHz, CDCl₃) δ 7.31 (m, 2H), 7.22 – 7.16 (m, 4H), 7.00 (d, *J* = 8.6 Hz, 2H), 6.85 (m, 1H), 4.43 (s, 2H), 3.58 (t, *J* = 5.7 Hz, 2H), 3.01 (t, *J* = 5.9 Hz, 2H); **¹³C NMR** (125 MHz, CDCl₃) δ 150.6, 135.0, 134.6, 129.3, 128.6, 126.6, 126.4, 126.1, 118.7, 115.2, 50.8, 46.6, 29.2.

2.5a-D⁷⁸:

Solution of *N*-Phenyl-3,4-dihydroisoquinolinium dichlorocuprate (**2.5a-Cu**, 342.5 mg, 1.0 mmol) in methanol (20 mL) was cooled to 0 °C and added portion wise with NaBD₄ (50.2 mg, 1.2 mmol). The resulting solution was stirred for 15 minutes after which the solution was quenched with aq. NaHCO₃, and extracted with CH₂Cl₂ (3 x 10 mL). The organic fractions were dried over anhydrous Na₂SO₄ and concentrated under reduced pressure and purified by column chromatography over silica using 15:1 hexanes and ethyl acetate to afford 95% of desired product as white solid.

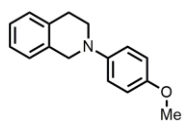


Yield 95% (200 mg); White solid; **mp** 44-48 °C; **¹H NMR** (500 MHz, CDCl₃) δ 7.36 (dd, *J* = 8.6, 7.4 Hz, 2H), 7.27 – 7.20 (m, 4H), 7.05 (d, *J* = 8.0 Hz, 2H), 6.90 (t, *J* = 7.3 Hz, 1H), 4.45 (s, 1H), 3.68 – 3.56 (m, 2H), 3.04 (t, *J* = 5.8 Hz, 2H); **¹³C NMR** (125 MHz, CDCl₃) δ 150.6, 135.0, 134.5, 129.3, 128.6, 126.6, 126.4, 126.1, 118.7, 115.2, 50.8, 50.4 (t, *J* = 20 Hz, C-D), 46.5, 29.1; **IR** (neat, cm⁻¹): 3053, 2905, 2068, 1596, 1500; **HRMS**: 210.1251 [M+H]⁺, Predicted: 210.1277

2.5a-Cu⁷⁸

¹H NMR (500 MHz, CDCl₃) δ 9.41 (s, 1H), 8.20 (d, *J* = 7.6 Hz, 1H), 7.84 (dd, *J* = 14.7, 7.5 Hz, 3H), 7.72 – 7.55 (m, 4H), 7.49 (d, *J* = 7.5 Hz, 1H), 4.68 (t, *J* = 7.9 Hz, 2H), 3.59 (t, *J* = 7.9 Hz, 2H); **HRMS**: 208.1102[M]⁺, Predicted: 208.1121

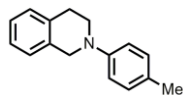
2-(4-methoxyphenyl)-1,2,3,4-tetrahydroisoquinoline (**2.5b/2.7b**)^{48, 62, 78}:



Yield 78% (932 mg); White solid; **mp** 91-93 °C; **¹H NMR** (500 MHz, CDCl₃) δ 7.19 – 7.12 (m, 4H), 7.00 (d, *J* = 9.0 Hz, 2H), 6.88 (d, *J* = 9.1 Hz, 2H), 4.31 (s, 2H), 3.79 (s, 3H),

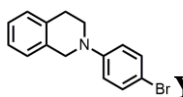
3.46 (t, $J = 5.9$ Hz, 2H), 3.00 (t, $J = 5.8$ Hz, 2H); ^{13}C NMR (125 MHz, CDCl_3) δ 153.7, 145.2, 134.6, 128.8, 126.6, 126.4, 126.0, 118.2, 114.7, 55.7, 52.8, 48.6, 29.1.

2-(p-tolyl)-1,2,3,4-tetrahydroisoquinoline (**2.5c/2.7c**)^{48, 62, 78}:



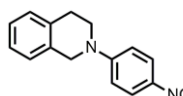
Yield 72% (802 mg); White solid; **mp** 37-39 °C; ^1H NMR (500 MHz, CDCl_3) δ 7.29 – 7.22 (m, 4H), 7.21 (d, $J = 8.7$ Hz, 2H), 7.02 (d, $J = 8.6$ Hz, 2H), 4.45 (s, 2H), 3.60 (t, $J = 5.9$ Hz, 2H), 3.07 (t, $J = 5.9$ Hz, 2H), 2.39 (s, 3H); ^{13}C NMR (125 MHz, CDCl_3) δ 148.6, 134.8, 134.6, 129.8, 128.6, 128.4, 126.6, 126.3, 126.0, 115.9, 51.5, 47.3, 29.1, 20.5.

2-(4-bromophenyl)-1,2,3,4-tetrahydroisoquinoline (**2.5d/2.7d**)^{48, 62, 78}:



Yield 61% (875 mg); Pale brown solid; **mp** 68-70 °C; ^1H NMR (500 MHz, CDCl_3) δ 7.36 (d, $J = 9.1$ Hz, 2H), 7.23 – 7.14 (m, 4H), 6.85 (d, $J = 9.0$ Hz, 2H), 4.38 (s, 2H), 3.54 (t, $J = 5.9$ Hz, 2H), 2.99 (t, $J = 5.9$ Hz, 2H); ^{13}C NMR (125 MHz, CDCl_3) δ 149.4, 134.7, 134.0, 132.0, 128.6, 126.6, 126.6, 126.3, 116.7, 110.7, 50.6, 46.5, 28.9.

2-(4-nitrophenyl)-1,2,3,4-tetrahydroisoquinoline (**2.6e/2.7e**)^{48, 62, 78}:

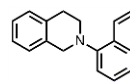


Yield 54% (685 mg), Orange solid; **mp** 144-148 °C; ^1H NMR (500 MHz, CDCl_3) δ 8.16 (d, $J = 9.4$ Hz, 2H), 7.27 – 7.18 (m, 4H), 6.83 (d, $J = 9.5$ Hz, 2H), 4.58 (s, H), 3.70 (t, $J = 5.9$ Hz, 2H), 3.02 (t, $J = 5.9$ Hz, 2H); ^{13}C NMR (125 MHz, CDCl_3) δ 153.8, 137.7, 135.0, 133.1, 128.2, 127.3, 126.8, 126.6, 126.3, 111.4, 48.9, 44.9, 29.0.

D.1. General synthesis of 2-(2-vinylphenyl)-1,2,3,4-tetrahydroisoquinoline (**2.5j**)²⁰⁵:

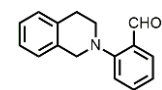
Substrate **2.5j** was synthesized according to published literature. $\text{CH}_3\text{PPh}_3\text{Br}$ (5 mmol) and $\text{KO}t\text{-Bu}$ (5.0 mmol) were added into 30 mL dry THF. The mixture was stirred at 0 °C for 1 hour, after which **2.5k** (4.5 mmol) was added at the same temperature. The resulting solution was stirred at

room temperature for 14 hours. The solvent was removed under reduced pressure and the crude product was purified by column chromatography (hexane/EtOAc = 10:1) over silica gel to give **2.5j** as pale yellow oil.

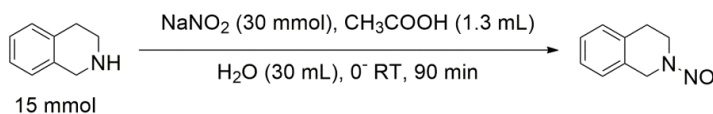
 **Yield** 72% (761 mg); Pale yellow oil; **¹H NMR** (500 MHz, CDCl₃) δ 7.54 (dd, *J* = 7.6, 1.2 Hz, 1H), 7.31 – 7.25 (m, 1H), 7.18 (dd, *J* = 8.7, 5.8 Hz, 3H), 7.14 – 7.05 (m, 4H), 5.73 (dd, *J* = 17.7, 1.4 Hz, 1H), 5.25 (dd, *J* = 11.0, 1.2 Hz, 1H), 4.18 (s, 2H), 3.30 (t, *J* = 5.8 Hz, 2H), 3.02 (t, *J* = 5.8 Hz, 2H); **¹³C NMR** (125 MHz, CDCl₃) δ 135.2, 134.6, 134.4, 132.5, 129.0, 128.6, 126.8, 126.5, 126.3, 125.8, 123.1, 119.0, 113.7, 54.5, 50.7, 29.5; **IR** (neat, cm⁻¹): 3062, 3022, 2918, 1691, 1594, 1482.

2-(3,4-dihydroisoquinolin-2(1H)-yl)benzaldehyde (**2.5k**):

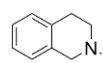
Following first half of nucleophilic aromatic substitution described in general procedure A, **2.5k** was synthesized in 74% yield as pale yellow solid

 **Yield** 74% (1.75 g); Pale yellow solid; **mp** 70-72 °C (lit. mp 72-74 °C)²⁰⁶; **¹H NMR** (500 MHz, CDCl₃) δ 10.35 (s, 1H), 7.87 (dd, *J* = 7.7, 1.5 Hz, 1H), 7.61 – 7.47 (m, 1H), 7.25 – 7.20 (m, 4H), 7.16 – 7.11 (m, 2H), 4.35 (s, 2H), 3.47 (t, *J* = 5.8 Hz, 2H), 3.08 (t, *J* = 5.8 Hz, 2H); **¹³C NMR** (125 MHz, CDCl₃) δ 191.4, 155.2, 134.9, 134.2, 134.1, 130.0, 129.0, 128.6, 126.6, 126.4, 126.1, 122.3, 119.0, 54.8, 53.6, 29.1; **IR** (neat, cm⁻¹): 3049, 2970, 2839, 1676, 1590.

D.2. General procedure for synthesis of 2-nitroso-1,2,3,4-tetrahydroisoquinoline (**2.5m**)²⁰⁷:



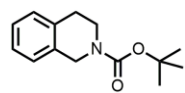
1,2,3,4-tetrahydroisoquinoline (2.00 g, 15.0 mmol) and sodium nitrite (2.0 g, 30.0 mmol) were mixed in 30 mL H₂O. To this solution at 0 °C, was added AcOH (1.30 mL, 22.7 mmol) slowly. The mixture was stirred at room temperature for 90 min. The reaction mixture was first diluted with 10 mL EtOAc and then separated. The combined organic layer was washed with 5 mL saturated aqueous NaHCO₃, 5 mL brine and dried over MgSO₄. The solution was concentrated under reduced pressure and the crude product was purified by silica gel column chromatography (hexane/EtOAc = 5:1) to afford 1.73 g of a colorless oil.



Yield 71% (1.73 g); White solid; **mp** 36-37 °C; **¹H NMR** (500 MHz, CDCl₃) δ 7.36 – 7.08 (m, 4H), 4.81 (s, 2H), 4.52 (t, *J* = 5.9 Hz, 2H), 3.09 (t, *J* = 5.9 Hz, 2H); **IR** (neat, cm⁻¹): 3023, 2992, 1419, 1339; **HRMS**: 163.0858 [M+H]⁺, Predicted: 163.0866

D.3. General procedure for synthesis of tert-butyl 3,4-dihydroisoquinoline-2(1H)-carboxylate (2.5n)²⁰⁸:

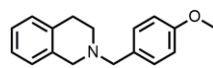
1,2,3,4-tetrahydroisoquinoline (1 g, 7.5 mmol), triethylamine (1.6 mL, 11.3 mmol) and 4-(*N,N*-dimethyl)aminopyridine (0.180 g, 1.5 mmol, 0.1 equiv.) were dissolved in 5 mL dichloromethane. Di-tert-butyl dicarbonate (2.45 g, 11.3 mmol) was added slowly and the reaction mixture stirred at room temperature for 24 h. The reaction mixture was diluted with 20 mL dichloromethane and washed with 25 mL of water. The organic phase was dried with anhydrous MgSO₄ and concentrated under reduced pressure. The crude product was purified by column chromatography (3:1 ethyl acetate:hexanes) to give the amine **2.5n** as yellow oil (1.75 g, 99%).



Yield 99% (1.75 g); Yellow oil; **¹H NMR** (500 MHz, CDCl₃) δ 7.22 – 7.05 (m, 4H), 4.58 (s, 2H), 3.65 (t, 2H), 2.84 (t, *J* = 5.6 Hz, 2H), 1.50 (s, 9H); **¹³C NMR** (126 MHz,

CDCl_3) δ 155.0, 134.8, 133.8, 128.7, 126.4, 126.2, 79.8, 45.8, 41.4, 28.5; **IR** (neat, cm^{-1}): 3016, 2979, 1676, 1420, 1156.

2-(4-methoxybenzyl)-1,2,3,4-tetrahydroisoquinoline (**2.5o**)²⁰⁹:

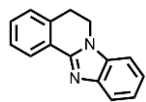


Yield 81% (205 mg, obtained from 1.0 mmol scale of 1,2,3,4-tetrahydroisoquinoline); Pale yellow oil; **$^1\text{H NMR}$** (500 MHz, CDCl_3) δ 7.36 (d, $J = 8.7$ Hz, 2H), 7.17 – 7.11 (m, 3H), 7.02 (dd, $J = 8.1, 1.0$ Hz, 1H), 6.92 (d, $J = 8.7$ Hz, 2H), 3.84 (s, 3H), 3.67 (s, 2H), 3.66 (s, 2H), 2.93 (t, $J = 5.9$ Hz, 2H), 2.77 (t, $J = 5.9$ Hz, 2H); **$^{13}\text{C NMR}$** (125 MHz, CDCl_3) δ 158.8, 135.0, 134.5, 130.4, 130.3, 128.7, 126.7, 126.1, 125.6, 113.7, 62.2, 56.1, 55.3, 50.5, 29.2.

E. General Procedure for synthesis of product **2.2a-2.2m** and **2.4a-2.4j**:

Amine derivative (0.5 mmol) and **FLClO_4** (0.05 mmol) were dissolved in DMF (0.2 M) in 2 dram vial fitted with magnetic stirbar. The resulting solution was heated at 90 °C or 110 °C for a given amount of time. After the reaction was complete, the solution was added with 1 mL water and extracted with ethyl acetate (3 x 4 mL). The combined organic phase was washed with brine, dried under MgSO_4 and concentrated under reduced pressure. The crude product was purified using column chromatography over silica gel.

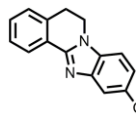
5,6-Dihydrobenzo[4,5]imidazo[2,1-a]isoquinoline (**2.2a**):



Yield 76% (83 mg); White solid; **mp** 142-144 °C (lit. 145-147 °C)¹⁴³; **$^1\text{H NMR}$** (500 MHz, CDCl_3) δ 8.33 (d, $J = 6.5$ Hz, 1H), 7.84 (dd, $J = 6.4, 2.7$ Hz, 1H), 7.43 – 7.35 (m, 3H), 7.34 – 7.27 (m, 3H), 4.35 (t, $J = 6.9$ Hz, 2H), 3.30 (t, $J = 6.8$ Hz, 2H); **$^{13}\text{C NMR}$** (125 MHz, CDCl_3) δ 149.1, 143.8, 134.7, 134.3, 130.3, 128.2, 127.8, 126.6, 125.8, 122.8, 122.6, 119.8,

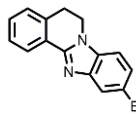
109.1, 40.5, 28.3; **IR** (neat, cm^{-1}): 3100, 1481, 1447, 1407, 1325; **HRMS**: 221.1093 $[\text{M}+\text{H}]^+$, Predicted: 221.1102

10-(trifluoromethyl)-5,6-dihydrobenzo[4,5]imidazo[2,1-a]isoquinoline (**2.2b**):



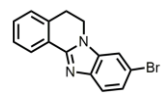
Yield 80% (115 mg); White solid; **mp** 187-189 °C (lit. 185-188 °C)¹⁴³; **¹H NMR** (500 MHz, CDCl_3) δ 8.34 (d, $J = 5.7$ Hz, 1H), 8.11 (s, 1H), 7.54 (d, $J = 8.1$ Hz, 1H), 7.45 (dd, $J = 6.3, 2.7$ Hz, 3H), 7.38 – 7.33 (m, 1H), 4.39 (t, $J = 6.8$ Hz, 2H), 3.34 (t, $J = 6.7$ Hz, 2H); **¹³C NMR** (125 MHz, CDCl_3) δ 150.9, 142.8, 136.5, 134.5, 131.2, 128.3, 128.1, 126.3, 125.8 (q, $J = 272.0$ Hz), 125.1 (q, $J = 31.0$ Hz), 123.8, 119.9 (q, $J = 3.4$ Hz), 117.3 (q, $J = 4.2$ Hz), 109.6, 40.8, 28.2; **¹⁹F NMR** (283 MHz, CDCl_3) δ -60.6; **IR** (neat, cm^{-1}): 3069, 2950, 1457, 1401, 1321, 1249, 1220, 1158, 1048, 937; **HRMS**: 289.0937 $[\text{M}+\text{H}]^+$, Predicted: 289.0940

10-Bromo-5,6-dihydrobenzo[4,5]imidazo[2,1-a]isoquinoline (**2.2c**):



Yield 86% (128 mg); White solid; **mp** 182-184 °C; **¹H NMR** (500 MHz, CDCl_3) δ 8.28 – 8.24 (m, 1H), 7.94 – 7.93 (d, $J = 1.5$ Hz, 1H), 7.43 – 7.38 (m, 2H), 7.35 (dd, $J = 8.5, 1.8$ Hz, 1H), 7.33 – 7.28 (m, 1H), 7.21 (d, $J = 8.5$ Hz, 1H), 4.29 (t, $J = 6.9$ Hz, 2H), 3.28 (t, $J = 6.9$ Hz, 2H); **¹³C NMR** (125 MHz, CDCl_3) δ 149.9, 144.5, 134.3, 133.5, 130.8, 128.2, 128.0, 126.0, 125.9, 125.8, 122.3, 115.6, 110.4, 40.6, 28.1; **IR** (neat, cm^{-1}): 3077, 2900, 2868, 1610, 1524, 1486, 1450, 1399, 1040; **HRMS**: 299.0187 $[\text{M}+\text{H}]^+$, Predicted: 299.0178

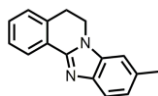
9-Bromo-5,6-dihydrobenzo[4,5]imidazo[2,1-a]isoquinoline (**2.2d**):



Yield 90% (135 mg); White solid; **mp** 187-189 °C (lit. 180-183 °C)¹⁴³; **¹H NMR** (500 MHz, CDCl_3) δ 8.29 (dd, $J = 5.3, 3.7$ Hz, 1H), 7.67 (d, $J = 8.6$ Hz, 1H), 7.52 (d, $J = 1.7$ Hz,

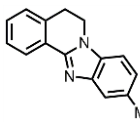
1H), 7.44 – 7.40 (m, 2H), 7.38 (dd, $J = 8.6, 1.8$ Hz, 1H), 7.34 – 7.29 (m, 1H), 4.30 (t, $J = 6.9$ Hz, 2H), 3.29 (t, $J = 6.9$ Hz, 2H); $^{13}\text{C NMR}$ (125 MHz, CDCl_3) δ 149.6, 142.1, 135.5, 134.3, 130.9, 128.3, 128.0, 126.2, 126.1, 120.7, 116.2, 112.2, 40.7, 28.1; **IR** (neat, cm^{-1}): 3350, 3022, 2924, 1597, 1477, 1449, 1401, 1239, 1024, 933, 841, 806, 774, 733, 700; **HRMS**: 299.0176 $[\text{M}+\text{H}]^+$, Predicted: 299.0178.

9-Methyl-5,6-dihydrobenzo[4,5]imidazo[2,1-a]isoquinoline (**2.2e**):



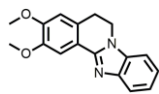
Yield 95% (111 mg); White solid, **mp** 100-102 °C (lit. 98-100 °C)¹⁴³; $^1\text{H NMR}$ (500 MHz, CDCl_3) δ 8.25 (dd, $J = 7.5, 1.0$ Hz, 1H), 7.68 (d, $J = 8.9$ Hz, 1H), 7.38 – 7.29 (m, 2H), 7.23 (d, $J = 7.2$ Hz, 1H), 7.07 (d, $J = 7.6$ Hz, 2H), 4.18 (t, $J = 6.9$ Hz, 2H), 3.17 (t, $J = 6.8$ Hz, 2H), 2.47 (s, 3H); $^{13}\text{C NMR}$ (125 MHz, CDCl_3) δ 148.5, 141.8, 134.7, 134.1, 132.6, 129.9, 128.0, 127.5, 126.6, 125.3, 124.0, 119.0, 109.0, 40.2, 28.1, 21.8; **HRMS**: 235.1233 $[\text{M}+\text{H}]^+$, Predicted: 235.1230

10-Methyl-5,6-dihydrobenzo[4,5]imidazo[2,1-a]isoquinoline (**2.2f**):



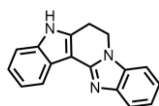
Yield 87% (101 mg); White solid; **mp** 178-180 °C (lit. 174.5-177 °C)¹⁴³; $^1\text{H NMR}$ (500 MHz, CDCl_3) δ 8.39 – 8.18 (m, 1H), 7.60 (s, 1H), 7.43 – 7.34 (m, 2H), 7.32 – 7.27 (m, 1H), 7.23 (d, $J = 8.2$ Hz, 1H), 7.10 (dd, $J = 8.2, 0.9$ Hz, 1H), 4.27 (t, $J = 6.9$ Hz, 2H), 3.25 (t, $J = 6.9$ Hz, 2H), 2.49 (s, 2H); $^{13}\text{C NMR}$ (125 MHz, CDCl_3) δ 149.0, 144.0, 134.2, 132.7, 132.3, 130.1, 128.1, 127.81, 126.7, 125.7, 124.3, 119.5, 108.6, 40.5, 28.3, 21.7; **IR** (neat, cm^{-1}): 3050, 2921, 2889, 1606, 1489, 1315, 1265, 1227; **HRMS**: 235.1227 $[\text{M}+\text{H}]^+$, Predicted: 235.1230

2,3-Dimethoxy-5,6-dihydrobenzo[4,5]imidazo[2,1-a]isoquinoline (**2.2g**):



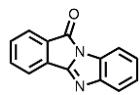
Yield 83% (116 mg); White solid; **mp** 185-187 °C (lit. 151-153 °C)¹⁴³; **¹H NMR** (500 MHz, CDCl₃) δ 7.84 – 7.76 (m, 2H), 7.35 – 7.30 (m, 1H), 7.29 – 7.23 (m, 2H), 6.79 (s, 1H), 4.30 (t, *J* = 7.0 Hz, 2H), 4.01 (s, 3H), 3.94 (s, 3H), 3.22 (t, *J* = 6.9 Hz, 2H); **¹³C NMR** (125 MHz, CDCl₃) δ 150.9, 149.3, 148.7, 143.6, 134.6, 127.6, 122.6, 122.5, 119.2, 118.9, 110.8, 108.9, 108.2, 56.4, 56.1, 40.6, 27.9; **IR** (neat, cm⁻¹): 3081, 2950, 2921, 1608, 1458, 1391, 1206, 1138, 1052; **HRMS**: 281.1282 [M+H]⁺, Predicted: 281.1285

6,7-Dihydro-5H-benzo[4',5']imidazo[1',2':1,2]pyrido[4,3-b]indole (**2.2h**):



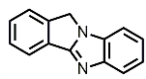
Yield 71% (93 mg); Pale brown solid; **mp** decomposed at 230 °C; **¹H NMR** (500 MHz, CDCl₃) δ 11.85 (s, 1H), 7.73 (d, *J* = 7.9 Hz, 1H), 7.60 (d, *J* = 8.0 Hz, 1H), 7.49 – 7.38 (m, 3H), 7.36 (dd, *J* = 11.2, 4.0 Hz, 1H), 7.30 – 7.26 (m, 1H), 7.15 (t, *J* = 7.4 Hz, 1H), 4.53 (t, *J* = 7.6 Hz, 2H), 3.50 (t, *J* = 7.6 Hz, 2H); **¹³C NMR** (125 MHz, CDCl₃) δ 144.8, 140.5, 138.4, 134.1, 125.8, 124.7, 123.7, 123.4, 123.2, 120.5, 119.4, 118.3, 114., 112.94, 109.6, 42.2, 20.6; **HRMS**: 260.1189 [M+H]⁺, Predicted: 260.1182

11H-benzo[4,5]imidazo[2,1-a]isoindol-11-one (**2.2i'**)²¹⁰:



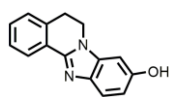
Yield 58% (64 mg); Yellow solid; **mp** 216-217 °C (lit. 211-216 °C)²¹⁰; **¹H NMR** (500 MHz, CDCl₃) δ 7.90 – 7.84 (m, 2H), 7.81 (d, *J* = 7.8 Hz, 1H), 7.71 (d, *J* = 7.9 Hz, 1H), 7.66 (t, *J* = 7.5 Hz, 1H), 7.54 (t, *J* = 7.7 Hz, 1H), 7.36 (t, *J* = 7.2 Hz, 1H), 7.33 – 7.28 (m, 1H); **¹³C NMR** (125 MHz, CDCl₃) δ 161.1, 156.8, 149.3, 135.2, 134.9, 132.5, 131.8, 129.9, 126.6, 126.0, 125.2, 122.5, 121.4, 112.8.

11H-benzo[4,5]imidazo[2,1-a]isoindole (**2.2i**)¹⁴²:



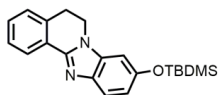
Yield 79% (87 mg); White solid; **mp** 214-215 °C (lit. mp 211-213 °C)¹⁴²; **¹H NMR** (500 MHz, CDCl₃) δ 8.04 (dd, *J* = 6.7, 0.8 Hz, 1H), 7.84 – 7.81 (m, 1H), 7.56 – 7.53 (m, 1H), 7.52 – 7.49 (m, 1H), 7.48 – 7.45 (m, 1H), 7.43 – 7.40 (m, 1H), 7.28 – 7.25 (m, 2H), 5.00 (s, 2H); **¹³C NMR** (125 MHz, CDCl₃) δ 158.6, 148.5, 143.6, 132.8, 129.6, 129.5, 128.8, 123.9, 122.8, 122.3, 122.1, 120.6, 109.4, 47.3.

5,6-Dihydrobenzo[4,5]imidazo[2,1-a]isoquinolin-9-ol (**2.2j**):



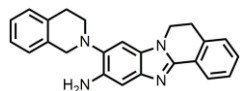
Yield 77% (91 mg); Pale brown solid; **mp** 214-216 °C (lit. mp 275-278 °C)¹⁴³; **¹H NMR** (500 MHz, DMSO-d₆) δ 9.32 (s, 1H), 8.03 – 7.96 (m, 1H), 7.42 (dd, *J* = 8.6, 0.4 Hz, 1H), 7.39 – 7.33 (m, 3H), 6.85 – 6.80 (m, 1H), 6.68 (dd, *J* = 8.6, 2.3 Hz, 1H), 4.23 (t, *J* = 6.9 Hz, 2H), 3.20 (t, *J* = 6.8 Hz, 2H); **¹³C NMR** (125 MHz, DMSO-d₆) δ 153.8, 147.1, 137.0, 135.5, 134.6, 129.4, 128.4, 127.2, 126.6, 124.2, 119.3, 111.8, 95.1, 39.7, 27.4; **IR** (neat, cm⁻¹): 3053, 2935, 2859, 2802, 1619, 1459, 1411, 1233, 1102; **HRMS**: 235.0876 [M+H]⁺, Predicted: 235.0877

9-((tert-butyl dimethylsilyl)oxy)-5,6-dihydrobenzo[4,5]imidazo[2,1-a]isoquinoline (**2.2k**):



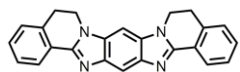
Yield 51% (89 mg); White solid; **mp** 138-140 °C; **¹H NMR** (500 MHz, CDCl₃) δ 8.31 (dd, *J* = 6.9, 1.8 Hz, 1H), 7.67 (d, *J* = 8.7 Hz, 1H), 7.43 – 7.36 (m, 2H), 7.30 (d, *J* = 6.7 Hz, 1H), 6.83 (dd, *J* = 8.6, 2.1 Hz, 1H), 6.80 (d, *J* = 2.0 Hz, 1H), 4.27 (t, *J* = 6.9 Hz, 2H), 3.28 (t, *J* = 6.8 Hz, 2H), 1.02 (s, 9H), 0.23 (s, 6H); **¹³C NMR** (125 MHz, CDCl₃) δ 152.6, 148.3, 137.4, 135.0, 134.0, 130.3, 128.2, 128.0, 126.0, 125.8, 119.6, 117.0, 100.0, 40.6, 28.2, 25.8, 18.3, -4.3; **IR** (neat, cm⁻¹): 3045, 2948, 2927, 1620, 1258, 836, 778; **HRMS**: 351.1868 [M+H]⁺, Predicted: 351.1877

9-(3,4-dihydroisoquinolin-2(1H)-yl)-5,6-dihydrobenzo[4,5]imidazo[2,1-a]isoquinolin-10-amine (**2.2l**):



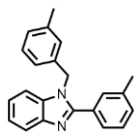
Yield 80% (146 mg); Brown solid; **mp** decomposed at 289 °C; **¹H NMR** (500 MHz, CDCl₃) δ 8.32 – 8.13 (m, 1H), 7.41 – 7.33 (m, 2H), 7.28 (dd, *J* = 7.3, 0.8 Hz, 1H), 7.22 – 7.16 (m, 4H), 7.11 (d, *J* = 6.9 Hz, 1H), 7.05 (s, 1H), 4.25 (t, *J* = 6.9 Hz, 2H), 4.16 (s, 2H), 3.31 (s, 2H), 3.25 (t, *J* = 6.9 Hz, 2H), 3.08 (s, 2H); **¹³C NMR** (125 MHz, CDCl₃) δ 148.4, 141.2, 138.8, 137.9, 135.4, 134.3, 133.3, 129.6, 129.0, 128.5, 128.0, 127.7, 127.0, 126.5, 126.4, 125.8, 125.2, 104.2, 100.6, 54.7, 50.2, 40.5, 30.1, 28.4; **IR** (neat, cm⁻¹): 3410, 3325, 3019, 2906, 1510; **HRMS**: 367.1927 [M+H]⁺, Predicted: 367.1917

(**2.2m**):



Yield >99% (72 mg); Brown solid; **mp** decomposed at 310 °C; **¹H NMR** (500 MHz, DMSO-d₆) δ 8.14 (dd, *J* = 5.0, 2.7 Hz, 2H), 7.91 (s, 1H), 7.73 (s, 1H), 7.47 – 7.41 (m, 6H), 4.43 (t, *J* = 6.8 Hz, 4H); **¹³C NMR** (125 MHz, DMSO-d₆) δ 148.7, 140.8, 135.0, 132.8, 129.9, 128.5, 127.3, 126.5, 124.6, 107.2, 89.3, 27.4; **IR** (neat, cm⁻¹): 3056, 3016, 2921, 1581; **HRMS**: 363.1445 [M+H]⁺, Predicted: 363.1451

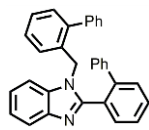
1-(3-methylbenzyl)-2-(m-tolyl)-1H-benzo[d]imidazole (**2.4a**)²¹¹:



Yield 65% (101 mg); White solid; **mp** 136-138 °C; **¹H NMR** (300 MHz, CD₃OD) δ 7.75 (d, *J* = 7.9 Hz, 1H), 7.48 – 7.17 (m, 8H), 7.09 (d, *J* = 4.0 Hz, 2H), 6.95 (dd, *J* = 7.6, 3.8 Hz, 1H), 6.51 (d, *J* = 7.6 Hz, 1H), 5.27 (s, 2H), 2.09 (s, 3H), 2.05 (s, 3H); **¹³C NMR** (75 MHz, CD₃OD) δ 155.1, 143.1, 139.5, 136.4, 136.2, 135.4, 131.6, 131.4, 130.9, 130.7, 128.6, 127.1,

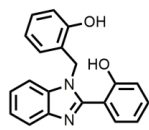
126.8, 124.4, 123.9, 119.8, 112.1, 46.5, 19.7, 19.0; **IR** (neat, cm^{-1}) : 3080, 2980, 1454, 1386, 1327, 1244, 1161, 982; **HRMS**: 313.1693 $[\text{M}+\text{H}]^+$, Predicted:313.1699

2-([1,1'-biphenyl]-3-yl)-1-([1,1'-biphenyl]-3-ylmethyl)-1H-benzo[d]imidazole (**2.4b**):



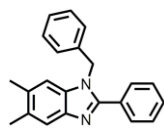
Yield 65% (141 mg); White solid; **mp** 160-162 °C; **$^1\text{H NMR}$** (300 MHz, CD_3OD) δ 7.72 (d, $J = 8.0$ Hz, 1H), 7.57 (dd, $J = 7.6, 1.1$ Hz, 1H), 7.47 – 6.90 (m, 18H), 6.80 (d, $J = 7.1$ Hz, 2H), 6.33 (d, $J = 7.7$ Hz, 1H), 4.90 (s, 2H); **$^{13}\text{C NMR}$** (75 MHz, CD_3OD) δ 155.2, 143.0, 142.8, 142.1, 141.3, 140.9, 136.3, 134.8, 132.4, 131.7, 131.1, 130.8, 130.2, 129.6, 129.5, 129.5, 129.4, 128.6, 128.5, 128.3, 127.1, 124.3, 123.8, 119.7, 111.6, 46.1; **IR** (neat, cm^{-1}): 3061, 2956, 1448, 1428, 1386, 1351, 1243, 1156; **HRMS**: 437.2031 $[\text{M}+\text{H}]^+$, Predicted: 437.2012.

2-(1-(2-hydroxybenzyl)-1H-benzo[d]imidazol-2-yl)phenol (**2.4c**)²¹²:



Yield 77% (122 mg); White solid; **mp** 203-205 °C (lit. mp 207 °C)²¹²; **$^1\text{H NMR}$** (300 MHz, $\text{DMSO}-d_6$) δ 11.05 (s, 1H), 9.92 (s, 1H), 7.71 (dd, $J = 6.3, 1.7$ Hz, 1H), 7.48 – 7.30 (m, 4H), 7.28 – 7.15 (m, 2H), 7.03 (t, $J = 5.8$ Hz, 2H), 6.89 (t, $J = 7.5$ Hz, 1H), 6.81 (d, $J = 8.0$ Hz, 1H), 6.58 (t, $J = 7.4$ Hz, 1H), 6.38 (d, $J = 7.5$ Hz, 1H), 5.40 (s, 2H); **$^{13}\text{C NMR}$** (75 MHz, $\text{DMSO}-d_6$) δ 156.3, 154.4, 152.1, 141.8, 135.2, 131.4, 130.3, 128.3, 126.7, 122.6, 122.5, 122.0, 119.0, 119.0, 118.7, 116.4, 116.2, 115.0, 110.8, 43.2; **IR** (neat, cm^{-1}) : 3250, 3072, 2929, 1594, 1453, 1393, 1243, 1023, 1002; **HRMS**: 317.1285 $[\text{M}+\text{H}]^+$, Predicted: 317.1225

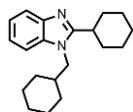
1-Benzyl-5,6-dimethyl-2-phenyl-1H-benzo[d]imidazole (**2.4d**):



Yield 78% (122 mg); White solid; **mp** 190-192 °C; **$^1\text{H NMR}$** (500 MHz, CDCl_3) δ 7.66 (d, $J = 6.5$ Hz, 1H), 7.51 – 7.39 (m, 1H), 7.33 (d, $J = 6.1$ Hz, 1H), 7.18 – 7.06 (m, 1H), 6.98

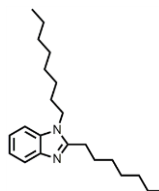
(s, 1H), 5.41 (s, 1H), 2.39 (s, 1H), 2.33 (s, 1H); ^{13}C NMR(125 MHz, CDCl_3) δ 153.3, 141.5, 136.7, 134.6, 132.5, 131.8, 130.1, 129.8, 129.2, 129.1, 128.8, 127.7, 125.9, 119.9, 110.7, 48.3, 20.7, 20.43; **IR** (neat, cm^{-1}): 3052, 2945, 1455, 1384, 1177, 1051; **HRMS**: 313.1690 $[\text{M}+\text{H}]^+$, Predicted: 313.1699

2-Cyclohexyl-1-(cyclohexylmethyl)-1H-benzo[d]imidazole (**2.4e**)²¹³:



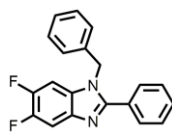
Yield 39% (58 mg); **White solid**; **mp** 92-94 °C (lit. mp 91-92 °C)²¹³; **^1H NMR** (300 MHz, CD_3OD) δ 7.57 (dd, $J = 6.3, 2.6$ Hz, 1H), 7.44 (dd, $J = 6.3, 2.4$ Hz, 1H), 7.28 – 7.15 (m, 2H), 4.07 (d, $J = 7.5$ Hz, 2H), 2.95 (tt, $J = 11.7, 3.1$ Hz, 1H), 1.99 – 1.64 (m, 12H), 1.63 – 1.35 (m, 5H), 1.31 – 1.03 (m, 5H); ^{13}C NMR (75 MHz, CD_3OD) δ 160.8, 142.9, 136.1, 123.2, 123.0, 118.9, 111.5, 50.4, 40.0, 37.4, 33.2, 31.8, 27.3, 26.9, 26.9; **IR** (neat, cm^{-1}): 3060, 3052, 2924, 2849, 1502, 1457, 1347, 1271; **HRMS**: 297.2326 $[\text{M}+\text{H}]^+$, Predicted: 297.2325

2-Heptyl-1-octyl-1H-benzo[d]imidazole (**2.4f**)²¹¹:



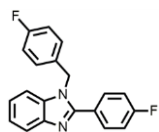
Yield 44% (75 mg); **Brown viscous liquid**; **^1H NMR** (500 MHz, CDCl_3) δ 7.77 – 7.72 (m, 1H), 7.33 – 7.29 (m, 1H), 7.25 – 7.21 (m, 2H), 4.14 – 4.05 (t, $J = 7.5$ Hz, 2H), 2.92 – 2.83 (m, 2H), 1.91 (dt, $J = 15.5, 7.7$ Hz, 2H), 1.84 – 1.75 (m, 2H), 1.45 (dt, $J = 14.9, 7.0$ Hz, 2H), 1.40 – 1.24 (m, 16H), 0.88 (t, $J = 7.0, 2.8$ Hz, 3H), 0.87 (t, $J = 7.0, 2.8$ Hz, 3H); ^{13}C NMR (125 MHz, CDCl_3) δ 155.0, 141.8, 134.8, 122.2, 122.1, 119.0, 109.5, 43.9, 31.8, 31.8, 30.0, 29.6, 29.3, 29.2, 29.1, 28.0, 27.5, 27.0, 22.7, 22.7, 14.2, 14.1; **IR** (neat, cm^{-1}): 2953, 2923, 2853, 1509, 1408, 1375, 1283, 1008; **HRMS**: 329.2947 $[\text{M}+\text{H}]^+$, Predicted: 329.2951

1-Benzyl-5,6-difluoro-2-phenyl-1H-benzo[d]imidazole (**2.4i**):



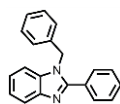
Yield 58% (93 mg); **White solid**; **mp** 132-134 °C; **¹H NMR** (500 MHz, CD₃OD) δ 7.65 (d, *J* = 7.0 Hz, 2H), 7.60 – 7.48 (m, 4H), 7.35 – 7.23 (m, 4H), 7.01 (d, *J* = 7.4 Hz, 2H), 5.50 (s, 2H); **¹³C NMR** (125 MHz, CD₃OD) δ 157.2, 150.5 (dd, *J* = 15.3, 11.5 Hz), 148.5 (dd, *J* = 15.4, 9.5 Hz), 138.7 (d, *J* = 9.6 Hz), 137.2, 132.5 (d, *J* = 11.0 Hz), 131.6 (s), 130.4 (s), 130.3, 130.1, 130.0, 129.0, 127.2, 107.1 (d, *J* = 20.2 Hz), 100.5 (d, *J* = 23.5 Hz); **IR** (neat, cm⁻¹): 3031, 1522, 1481, 1399, 1363, 1178, 1159, 1122, 1027; **HRMS**: 321.1990 [M+H]⁺, Predicted: 321.1998

1-(4-fluorobenzyl)-2-(4-fluorophenyl)-1H-benzo[d]imidazole (**2.4j/2.2q'**)²¹²:



Yield 62% (99 mg); **White solid**; **mp** 106-108 °C (lit. mp 111 °C)²¹²; **¹H NMR** (500 MHz, CDCl₃) δ 7.88 – 7.84 (m, 1H), 7.64 (dd, *J* = 8.9, 5.3 Hz, 2H), 7.33 (ddd, *J* = 8.3, 7.1, 1.3 Hz, 1H), 7.26 (ddd, *J* = 8.2, 7.1, 1.1 Hz, 2H), 7.22 – 7.19 (m, 1H), 7.15 (t, *J* = 8.7 Hz, 2H), 7.08 – 6.99 (m, 4H), 5.40 (s, 2H); **¹³C NMR** (125 MHz, CDCl₃) δ 164.1 (d, *J* = 188.2 Hz), 162.1 (d, *J* = 184.2 Hz), 153.2, 143.2, 136.0, 132.0 (d, *J* = 3.1 Hz), 131.3 (d, *J* = 8.5 Hz), 127.7 (d, *J* = 8.2 Hz), 126.3 (d, *J* = 3.3 Hz), 123.4, 123.0, 120.2, 116.3 (d, *J* = 14.2 Hz), 116.1 (d, *J* = 14.4 Hz), 110.4, 47.8; **¹⁹F NMR** (471 MHz, CDCl₃) δ -109.9, -113.9; **IR** (neat, cm⁻¹): 2921, 2851, 1604, 1508, 1479, , 1381, 1220, 1155, 1095, 1213; **HRMS**: 321.1176 [M+H]⁺, Predicted: 321.1155

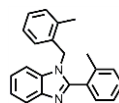
1-Benzyl-2-phenyl-1H-benzo[d]imidazole (**4.2a**)²¹³:



Yield 61%; **White solid**; **mp** 131-133 °C (lit. mp 130-132 °C)²¹³; **¹H NMR** (500 MHz, CDCl₃) δ 7.88 (d, *J* = 8.0 Hz, 1H), 7.73 – 7.67 (m, 2H), 7.51 – 7.43 (m, 3H), 7.37 – 7.29 (m, 4H), 7.26 – 7.19 (m, 2H), 7.11 (d, *J* = 7.0 Hz, 2H), 5.47 (s, 2H); **¹³C NMR** (125 MHz, CDCl₃) δ

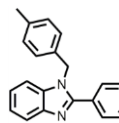
154.2, 143.2, 136.5, 136.1, 130.0, 129.4, 129.2, 128.9, 127.9, 126.1, 123.1, 122.8, 120.1, 110.6, 48.5; **IR** (neat, cm^{-1}): 3011, 2899, 1520, 1448, 1428, 1386, 1351, 1243, 1156; **HRMS**: 285.1387 $[\text{M}+\text{H}]^+$, Predicted: 285.1386

1-(2-methylbenzyl)-2-(o-tolyl)-1H-benzo[d]imidazole (**4.2b**):



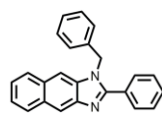
Yield 76%; White solid, **mp** 137-139 °C; **$^1\text{H NMR}$** (500 MHz, CDCl_3) δ 7.89 (dd, $J = 8.0, 0.6\text{Hz}$, 1H), 7.39 – 7.11 (m, 10H), 7.05 – 7.00 (m, 1H), 6.64 (d, $J = 7.7\text{ Hz}$, 1H), 5.19 (s, 2H), 2.25 (s, 3H), 2.15 (s, 3H); **$^{13}\text{C NMR}$** (125 MHz, CDCl_3) δ 153.9, 142.9, 138.4, 135.0, 134.9, 134.0, 130.7, 130.4, 129.9, 129.9, 129.7, 127.6, 126.4, 126.1, 125.7, 123.0, 122.5, 120.0, 110.6, 45.8, 19.9, 19.1; **IR** (neat, cm^{-1}): 3061, 3023, 2976, 2944, 2923, 2856, 1454, 1386, 1244, 1161; **HRMS**: 285.1568 $[\text{M}+\text{H}]^+$, Predicted: 285.1570

1-(4-methylbenzyl)-2-(p-tolyl)-1H-benzo[d]imidazole (**4.2d**)²¹²:



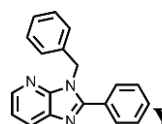
Yield 81%; Brown solid; **mp** 116-118 °C (lit. mp 130 °C)²¹²; **$^1\text{H NMR}$** (500 MHz, CDCl_3) δ 7.91 (d, $J = 8.1\text{ Hz}$, 1H), 7.63 (d, $J = 8.1\text{ Hz}$, 2H), 7.35 – 7.31 (m, 1H), 7.28 (d, $J = 8.0\text{ Hz}$, 2H), 7.23 (dt, $J = 8.5, 3.8\text{ Hz}$, 2H), 7.15 (d, $J = 8.0\text{ Hz}$, 2H), 7.01 (d, $J = 8.0\text{ Hz}$, 2H), 5.43 (s, 2H), 2.42 (s, 3H), 2.35 (s, 3H); **$^{13}\text{C NMR}$** (125 MHz, CDCl_3) δ 154.1, 142.4, 140.4, 137.6, 135.9, 133.3, 129.8, 129.5, 129.2, 126.6, 125.9, 123.1, 122.8, 119.6, 110.6, 48.3, 21.5, 21.1; **IR** (neat, cm^{-1}): 3025, 2947, 1919, 1611, 1455, 1380, 1160, 1019; **HRMS**: 313.1700 $[\text{M}+\text{H}]^+$, Predicted: 313.1699

1-Benzyl-2-phenyl-1H-naphtho[2,3-d]imidazole (**4.2j**):



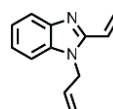
Yield 68%; Brown solid; **mp** 196-198 °C; **¹H NMR** (500 MHz, CDCl₃) δ 8.56 (s, 1H), 8.04 (dd, *J* = 6.3, 3.4 Hz, 1H), 7.87 (dd, *J* = 13.1, 5.9 Hz, 4H), 7.71 (s, 1H), 7.62 (t, *J* = 7.4 Hz, 1H), 7.56 (t, *J* = 7.6 Hz, 3H), 7.51 – 7.45 (m, 3H), 7.39 (tt, *J* = 7.8, 3.7 Hz, 4H), 7.16 (dd, *J* = 7.8, 1.3 Hz, 2H), 5.65 (s, 2H); **¹³C NMR** (125 MHz, CDCl₃) δ 156.7, 135.3, 131.8, 131.2, 131.1, 129.7, 129.5, 129.4, 128.9, 128.7, 128.3, 127.7, 126.0, 125.3, 124.7, 116.1, 107.4, 49.1; **IR** (neat, cm⁻¹): 3056, 3031, 2922, 1493, 1394, 1366, 1310; **HRMS**: 335.1546 [M+H]⁺, Predicted: 335.1543

3-Benzyl-2-phenyl-3H-imidazo[4,5-b]pyridine (**4.2k**):



Yield 41%; Brown solid; **mp** 115-117 °C; **¹H NMR** (500 MHz, CDCl₃) δ 8.60 (d, *J* = 4.9 Hz, 1H), 7.79 (d, *J* = 7.2 Hz, 2H), 7.76 (d, *J* = 8.0 Hz, 1H), 7.59 – 7.53 (m, 1H), 7.50 (t, *J* = 7.4 Hz, 2H), 7.40 – 7.34 (m, 3H), 7.33 – 7.29 (m, 1H), 7.12 – 7.07 (m, 2H), 5.61 (s, 2H); **¹³C NMR** (75 MHz, CD₃OD) δ 156.6, 149.6, 145.5, 138.1, 135.8, 131.9, 130.7, 130.3, 130.0, 129.8, 128.7, 128.2, 127.6, 120.4, 47.6; **IR** (neat, cm⁻¹): 3059, 2922, 2852, 1596, 1496, 1156, 1106, 1074; **HRMS**: 286.1338 [M+H]⁺, Predicted: 286.1339

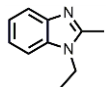
1-Allyl-2-vinyl-1H-benzo[d]imidazole (**4.2l**):



Yield 67%; Brown viscous liquid; **¹H NMR** (500 MHz, CDCl₃) δ 7.80 – 7.77 (m, 1H), 7.33 – 7.23 (m, 2H), 6.75 (dd, *J* = 17.2, 11.0 Hz, 1H), 6.59 (dd, *J* = 17.2, 1.4 Hz, 1H), 5.96 (ddt, *J* = 17.1, 10.4, 4.8 Hz, 1H), 5.72 (dd, *J* = 11.0, 1.4 Hz, 1H), 5.23 (dtd, *J* = 10.4, 1.8, 0.7 Hz, 1H), 4.98 (dtd, *J* = 17.1, 1.9, 0.7 Hz, 1H), 4.81 (dt, *J* = 4.8, 1.8 Hz, 1H); **¹³C NMR** (125 MHz, CDCl₃)

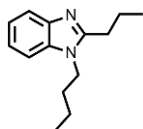
δ 150.4, 142.5, 135.1, 131.8, 123.8, 123.1, 122.9, 122.8, 119.72, 117.6, 109.7, 45.7; **IR** (neat, cm^{-1}): 3066, 2956, 1500, 1454, 1423, 1329; **HRMS**: 185.1075 $[\text{M}+\text{H}]^+$, Predicted: 185.1073

1-Ethyl-2-methyl-1H-benzo[d]imidazole (**4.2m**)¹⁴³:



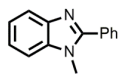
Yield 58%; Brown liquid; **¹H NMR** (500 MHz, CDCl_3) δ 7.73 – 7.68 (m, 1H), 7.33 – 7.30 (m, 1H), 7.26 – 7.23 (m, 2H), 4.18 (q, $J = 7.3$ Hz, 2H), 2.63 (s, 3H), 1.42 (t, $J = 7.3$ Hz, 3H); **¹³C NMR** (125 MHz, CDCl_3) δ 151.1, 134.6, 122.2, 122.1, 119.0, 109.1, 38.7, 15.0, 13.7; **IR** (neat, cm^{-1}): 3048, 2966, 1505, 1478, 1355, 1245; **HRMS**: 161.0990 $[\text{M}+\text{H}]^+$, Predicted: 161.0999

1-Butyl-2-propyl-1H-benzo[d]imidazole (**2.2p'**/**4.2n**)²¹³:



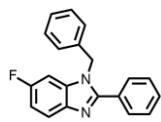
Yield 74%; White solid; **mp** 125-127 °C (lit. mp 128-130 °C); **¹H NMR** (300 MHz, CD_3OD) δ 7.57 (dd, $J = 6.4, 2.4$ Hz, 1H), 7.43 (dd, $J = 6.5, 2.2$ Hz, 1H), 7.31 – 7.14 (m, 2H), 4.20 (t, $J = 7.4$ Hz, 2H), 2.88 (t, $J = 7.6$ Hz, 2H), 1.96 – 1.83 (m, 2H), 1.83 – 1.71 (m, 2H), 1.47 – 1.31 (m, 2H), 1.05 (t, $J = 7.4$ Hz, 3H), 0.96 (t, $J = 7.3$ Hz, 3H); **¹³C NMR** (75 MHz, CD_3OD) δ 156.4, 142.9, 136.0, 123.3, 123.1, 118.9, 111.0, 44.3, 33.0, 29.8, 22.3, 21.0, 14.2, 14.1; **IR** (neat, cm^{-1}): 3050, 2959, 1507, 1457, 1329, 1284; **HRMS**: 217.1706 $[\text{M}+\text{H}]^+$, Predicted: 217.1699

1-Methyl-2-phenyl-1H-benzo[d]imidazole (**4.2r**)¹⁴³:



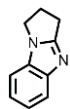
Yield 68% (42.5 mg); Brown solid; **mp** 92-94 °C; **¹H NMR** (500 MHz, CDCl_3) δ 7.83 (dd, $J = 6.3, 2.3$ Hz, 1H), 7.78 (dd, $J = 7.8, 1.6$ Hz, 2H), 7.56 – 7.50 (m, 3H), 7.41 (dd, $J = 6.4, 2.3$ Hz, 1H), 7.36 – 7.29 (m, 2H); **¹³C NMR** (125 MHz, CDCl_3) δ 153.8, 143.0, 136.6, 130.2, 129.8, 129.5, 128.7, 122.9, 122.5, 119.9, 109.7, 31.8; **IR** (neat, cm^{-1}): 3048, 2950, 2850, 1467, 1327, 1276, 1128, 1018; **HRMS**: 209.1079 $[\text{M}+\text{H}]^+$, Predicted: 209.1073

1-Benzyl-6-fluoro-2-phenyl-1H-benzo[d]imidazole (**4.2s**)²¹⁴:



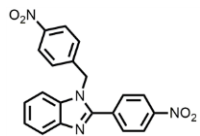
Yield 81% (22 mg from mixture of isomer); **White solid**; **mp** 132-134 °C (lit. mp 133-135 °C)²¹⁴; **¹H NMR** (500 MHz, CDCl₃) δ 7.79 (dd, *J* = 8.8, 4.8 Hz, 1H), 7.69 – 7.66 (m, 2H), 7.50 – 7.43 (m, 3H), 7.37 – 7.31 (m, 3H), 7.09 (dd, *J* = 8.0, 1.4 Hz, 2H), 7.06 (ddd, *J* = 9.7, 8.8, 2.5 Hz, 1H), 6.88 (dd, *J* = 8.6, 2.4 Hz, 1H), 5.42 (s, 2H); **¹³C NMR** (125 MHz, CDCl₃) δ 159.9 (d, *J* = 240 Hz), 154.9 (d, *J* = 3 Hz), 139.3, 136.2 (d, *J* = 13.2 Hz), 135.8, 130.2, 129.7, 129.3, 129.3, 128.9, 128.1, 126.0, 120.7 (d, *J* = 10 Hz), 111.3 (d, *J* = 25 Hz), 97.4 (d, *J* = 27.5 Hz), 48.7; **¹⁹F NMR** (470 MHz, CDCl₃) δ -117.8; **IR** (diamond-ATR) γ/cm^{-1} : 3059, 2947, 1601, 1470, 1449, 1366, 1248, 1142; **HRMS**: 303.2416 [M+H]⁺, Predicted: 303.2410

2,3-Dihydro-1H-benzo[d]pyrrolo[1,2-a]imidazole (**4.4i**)¹⁴³:



Yield 38% (18 mg); **Brown liquid**; **¹H NMR** (500 MHz, CDCl₃) δ 7.75 – 7.72 (m, 1H), 7.35 – 7.32 (m, 1H), 7.27 (dd, *J* = 6.9, 3.3 Hz, 2H), 4.17 (t, *J* = 7.1 Hz, 2H), 3.17 (t, *J* = 7.7 Hz, 2H), 2.81 – 2.73 (m, 2H); **¹³C NMR** (125 MHz, CDCl₃) δ 160.51, 146.16, 131.65, 122.78, 122.76, 118.96, 110.03, 43.42, 26.10, 23.71; **IR** (neat, cm⁻¹): 3056, 2889, 1673, 1552, 1448, 1300, 1280, 1215, 1004; **HRMS**: 159.0915 [M+H]⁺, Predicted: 159.0917

1-(4-nitrobenzyl)-2-(4-nitrophenyl)-1H-benzo[d]imidazole (**4.4k**)^{211, 212, 213}:



Yield 64% (74.5 mg); **White solid**; **mp** 214-216 °C; **¹H NMR** (500 MHz, CDCl₃) δ 8.37 – 8.31 (m, 2H), 8.27 – 8.22 (m, 2H), 7.95 (d, *J* = 8.0 Hz, 1H), 7.86 (d, *J* = 8.7 Hz, 2H), 7.43 (t, *J* = 7.7 Hz, 1H), 7.36 (t, *J* = 7.7 Hz, 1H), 7.28 (d, *J* = 8.8 Hz, 2H), 7.22 (d, *J* = 8.1 Hz, 1H), 5.60 (s, 2H); **¹³C NMR** (125 MHz, CDCl₃) δ 151.3, 148.8, 147.9, 142.8, 135.9, 135.6,

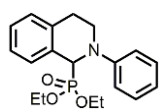
130.1, 126.8, 124.7, 124.3, 124.0, 120.8, 110.3, 48.1; **IR** (neat, cm^{-1}): 3200, 2955, 2850, 1600, 1510, 1342, 1109, 1012; **HRMS**: 375.1036 $[\text{M}+\text{H}]^+$, Predicted: 375.1022

F. General procedure for synthesis of phosphonate product 2.6a-2.6k and nitro product 2.8a-2.8g and 2.8j:

Amine derivative (0.5 mmol) and flavin catalyst (0.025 mmol) were added into 2 dram vial fitted with magnetic stirbar and oxygen balloon. The vial was purged with O_2 before adding dialkyl phosphate (1.0 mmol) and 0.2 M acetonitrile (nitroalkane for nitro-Mannich reaction). The resulting solution was heated at 60 $^\circ\text{C}$ for a given amount of time (100 $^\circ\text{C}$ for nitro-Mannich reaction). After the reaction was complete, the solution was directly concentrated under reduced pressure. The crude product was purified using column chromatography over silica gel.

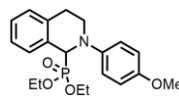
In case of nitro product, an additive DMTU (1 equiv.) was added and the resulting mixture was heated at 100 $^\circ\text{C}$ in air for a given amount of time. After the completion of reaction, the solution was directly concentrated under reduced pressure and purified using column chromatography over silica.

Diethyl(2-phenyl-1,2,3,4-tetrahydroisoquinolin-1-yl)phosphonate (**2.6a**)⁵⁵:



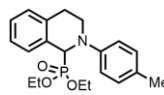
Yield 76% (131 mg), Clear oil; **$^1\text{H NMR}$** (500 MHz, CDCl_3) δ 7.37 (d, $J = 7.0$ Hz, 1H), 7.28 – 7.23 (m, 2H), 7.22 – 7.14 (m, 3H), 6.99 (d, $J = 8.3$ Hz, 2H), 6.80 (t, $J = 7.3$ Hz, 1H), 5.19 (d, $J = 20.0$ Hz, 1H), 4.12 – 3.85 (m, 5H), 3.66 – 3.60 (m, 1H), 3.67 – 3.59 (m, 1H), 3.11 – 2.97 (m, 2H), 1.25 (t, $J = 7.1$ Hz, 3H), 1.14 (t, $J = 7.1$ Hz, 3H); **$^{13}\text{C NMR}$** (125 MHz, CDCl_3) δ 149.5 (d, $J = 5.6$ Hz), 136.5 (d, $J = 5.6$ Hz), 130.7, 129.3, 128.9 (d, $J = 2.6$ Hz), 128.3 (d, $J = 4.6$ Hz), 127.3 (d, $J = 3.4$ Hz), 126.0 (d, $J = 2.8$ Hz), 118.7, 114.9, 63.5 (d, $J = 7.2$ Hz), 62.5 (d, $J = 7.6$ Hz), 58.9 (d, $J = 159.3$ Hz), 43.6, 26.8, 16.6 (d, $J = 5.4$ Hz), 16.5 (d, $J = 5.8$ Hz); **$^{31}\text{P NMR}$** (122 MHz, CDCl_3) δ 22.7.

Diethyl(2-(4-methoxyphenyl)-1,2,3,4-tetrahydroisoquinolin-1-yl)phosphonate (**2.6b**)⁵⁵:



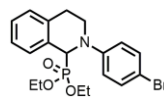
Yield 69% (157 mg); Yellow oil; **¹H NMR** (500 MHz, CDCl₃) δ 7.41 – 7.37 (m, 1H), 7.20 – 7.15 (m, 2H), 7.15 – 7.11 (m, 1H), 6.93 (d, *J* = 9.1 Hz, 2H), 6.81 (d, *J* = 9.1 Hz, 2H), 5.02 (d, *J* = 21.5 Hz, 1H), 4.14 – 3.92 (m, 5H), 3.75 (s, 3H), 3.54 (dt, *J* = 12.7, 5.0 Hz, 1H), 2.93 (m, 2H), 1.25 (t, *J* = 7.1 Hz, 3H), 1.16 (t, *J* = 7.1 Hz, 3H); **¹³C NMR** (125 MHz, CDCl₃) δ 153.2, 144.2 (d, *J* = 8.2 Hz), 136.4 (d, *J* = 5.8 Hz), 130.5, 129.0 (d, *J* = 2.5 Hz), 128.3 (d, *J* = 4.4 Hz), 127.4 (d, *J* = 3.5 Hz), 125.9 (d, *J* = 2.9 Hz), 117.7, 114.6, 63.4 (d, *J* = 7.2 Hz), 62.3 (d, *J* = 7.6 Hz), 59.5 (d, *J* = 158.7 Hz), 55.7, 44.8, 26.2, 16.6 (d, *J* = 5.5 Hz), 16.5 (d, *J* = 5.9 Hz); **³¹P NMR** (122 MHz, CDCl₃) δ 22.8.

Diethyl(2-(p-tolyl)-1,2,3,4-tetrahydroisoquinolin-1-yl)phosphonate (**2.6c**)⁵⁵:



Yield 75% (134 mg); Pale yellow oil; **¹H NMR** (500 MHz, CDCl₃) δ 7.37 (d, *J* = 6.8 Hz, 1H), 7.17 (t, *J* = 6.4 Hz, 2H), 7.14 – 7.11 (m, 1H), 7.05 (d, *J* = 8.3 Hz, 2H), 6.89 (d, *J* = 8.5 Hz, 2H), 5.11 (d, *J* = 20.8 Hz, 1H), 4.12 – 3.89 (m, 5H), 3.63 – 3.57 (m, 1H), 3.03 – 2.93 (m, 2H), 2.25 (s, 3H), 1.25 (t, *J* = 7.1 Hz, 3H), 1.15 (t, *J* = 7.1 Hz, 3H); **¹³C NMR** (125 MHz, CDCl₃) δ 147.4 (d, *J* = 7.2 Hz), 136.5 (d, *J* = 5.7 Hz), 130.6, 129.7, 129.4, 128.9 (d, *J* = 2.6 Hz), 128.3 (d, *J* = 4.2 Hz), 127.5 (d, *J* = 3.4 Hz), 125.9 (d, *J* = 2.9 Hz), 115.5, 63.5 (d, *J* = 7.2 Hz), 62.4 (d, *J* = 7.7 Hz), 59.2 (d, *J* = 159.5 Hz), 44.0, 26.5, 20.4, 16.6 (d, *J* = 5.5 Hz), 16.5 (d, *J* = 5.9 Hz); **³¹P NMR** (122 MHz, CDCl₃) δ 22.7.

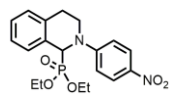
Diethyl(2-(4-bromophenyl)-1,2,3,4-tetrahydroisoquinolin-1-yl)phosphonate (**2.6d**)²¹⁵:



Yield 64% (135 mg); yellow oil; **¹H NMR** (301 MHz, CDCl₃) δ 7.39 – 7.28 (m, 3H), 7.23 – 7.14 (m, 3H), 6.84 (d, *J* = 9.0 Hz, 2H), 5.10 (d, *J* = 19.1 Hz, 1H), 4.14 – 3.81 (m,

5H), 3.60 – 3.48 (m, 1H), 3.21 – 2.91 (m, 2H), 1.24 (t, $J = 7.0$ Hz, 3H), 1.14 (t, $J = 7.0$ Hz, 3H); $^{13}\text{C NMR}$ (75 MHz, CDCl_3) δ 148.3 (d, $J = 4.9$ Hz), 136.4 (d, $J = 5.4$ Hz), 131.9, 130.4, 128.7 (d, $J = 2.6$ Hz), 128.22 (d, $J = 4.8$ Hz), 127.7 (d, $J = 3.4$ Hz), 126.1 (d, $J = 2.7$ Hz), 116.2, 110.4, 63.43 (d, $J = 7.4$ Hz), 62.60 (d, $J = 7.7$ Hz), 58.8 (d, $J = 159.7$ Hz), 43.7, 27.0, 16.58 (d, $J = 5.7$ Hz), 16.49 (d, $J = 6.1$ Hz); $^{31}\text{P NMR}$ (122 MHz, CDCl_3) δ 22.4.

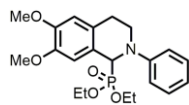
Diethyl(2-(4-nitrophenyl)-1,2,3,4-tetrahydroisoquinolin-1-yl)phosphonate (**2.6e**)²¹⁶:



Yield 41% (80 mg); Yellow gummy solid; $^1\text{H NMR}$ (500 MHz, CDCl_3) δ 8.16 (d, $J = 9.5$ Hz, 2H), 7.35 (dd, $J = 7.5, 2.2$ Hz, 1H), 7.30 – 7.26 (m, 1H), 7.23 (t, $J = 6.4$ Hz, 1H), 6.94 (d, $J = 9.5$ Hz, 2H), 5.31 (d, $J = 17.4$ Hz, 1H), 4.09 – 3.96 (m, 3H), 3.95 – 3.79 (m, 2H), 3.68 – 3.59 (m, 1H), 3.47 – 3.38 (m, 1H), 3.02 (dt, $J = 11.3, 5.3$ Hz, 1H), 1.21 (t, $J = 7.1$ Hz, 3H), 1.13 (t, $J = 7.1$ Hz, 3H); $^{13}\text{C NMR}$ (125 MHz, CDCl_3) δ 153.2 (d, $J = 2.1$ Hz), 138.2, 136.0 (d, $J = 4.9$ Hz), 130.0, 128.5 (d, $J = 2.9$ Hz), 128.3 (d, $J = 3.5$ Hz), 128.2 (d, $J = 5.3$ Hz), 126.5 (d, $J = 2.8$ Hz), 125.9, 112.0, 63.3 (d, $J = 7.4$ Hz), 63.0 (d, $J = 7.7$ Hz), 58.1 (d, $J = 159.1$ Hz), 44.0, 27.6, 16.5 (d, $J = 5.5$ Hz), 16.4 (d, $J = 5.8$ Hz); $^{31}\text{P NMR}$ (202 MHz, CDCl_3) δ 21.4; **IR (neat)**: 3033, 2979, 1591, 1309, 1229;

Diethyl (6,7-dimethoxy-2-phenyl-1,2,3,4-tetrahydroisoquinolin-1-yl)phosphonate

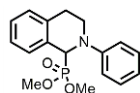
(**2.6f**)⁶⁵:



Yield 70% (141 mg); Yellow oil, $^1\text{H NMR}$ (500 MHz, CDCl_3) δ 7.24 (dd, $J = 8.8, 7.3$ Hz, 2H), 6.97 (d, $J = 8.0$ Hz, 2H), 6.93 (s, 1H), 6.79 (t, $J = 7.3$ Hz, 1H), 6.62 (s, 1H), 5.09 (d, $J = 20.2$ Hz, 1H), 4.16 – 3.98 (m, 4H), 3.95 – 3.89 (m, 1H), 3.86 (s, 3H), 3.85 (s, 3H), 3.72 – 3.64 (m, 1H), 2.97 – 2.82 (m, 2H), 1.28 (t, $J = 7.1$ Hz, 3H), 1.16 (t, $J = 7.1$ Hz, 3H); $^{13}\text{C NMR}$ (125 MHz, CDCl_3) δ 149.7 (d, $J = 7.1$ Hz), 148.44 (d, $J = 3.3$ Hz), 147.19 (d, $J = 2.8$ Hz), 129.3,

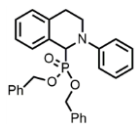
128.7 (d, $J = 6.2$ Hz), 122.1, 118.8, 115.3, 111.63 (d, $J = 2.5$ Hz), 111.1 (d, $J = 3.5$ Hz), 63.5 (d, $J = 7.1$ Hz), 62.1 (d, $J = 7.6$ Hz), 58.5 (d, $J = 160.0$ Hz), 56.0, 55.9, 43.5, 26.0, 16.6 (d, $J = 2.9$ Hz), 16.6 (d, $J = 3.5$ Hz); ^{31}P NMR (122 MHz, CDCl_3) δ 22.9.

Dimethyl (2-phenyl-1,2,3,4-tetrahydroisoquinolin-1-yl)phosphonate (**2.6g**)⁵⁵:



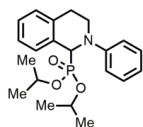
Yield 65% (103 mg); Pale yellow oil, ^1H NMR (500 MHz, CDCl_3) δ 7.35 (d, $J = 6.8$ Hz, 1H), 7.29 – 7.23 (m, 2H), 7.23 – 7.14 (m, 3H), 6.98 (d, $J = 8.2$ Hz, 2H), 6.81 (t, $J = 7.2$ Hz, 1H), 5.20 (d, $J = 20.0$ Hz, 1H), 4.06 – 3.95 (m, 1H), 3.65 (t, $J = 10.2$ Hz, 6H), 3.14 – 2.95 (m, 2H); ^{13}C NMR (125 MHz, CDCl_3) δ 149.3 (d, $J = 6.0$ Hz), 136.5 (d, $J = 5.6$ Hz), 130.5, 129.4, 129.0 (d, $J = 2.5$ Hz), 128.0 (d, $J = 4.6$ Hz), 127.7 (d, $J = 3.5$ Hz), 126.2 (d, $J = 2.9$ Hz), 118.8, 114.9, 58.9 (d, $J = 159.6$ Hz), 54.1 (d, $J = 7.1$ Hz), 53.1 (d, $J = 7.7$ Hz), 43.7, 26.8; ^{31}P NMR (122 MHz, CDCl_3) δ 25.0.

Dibenzyl (2-phenyl-1,2,3,4-tetrahydroisoquinolin-1-yl)phosphonate (**2.6h**)⁵⁵:



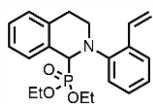
Yield 71% (166 mg), Pale yellow solid, **mp** 96-98 °C, ^1H NMR (500 MHz, CDCl_3) δ 7.35 – 7.28 (m, 4H), 7.26 – 7.19 (m, 8H), 7.17 – 7.10 (m, 4H), 6.97 (d, $J = 8.1$ Hz, 2H), 6.80 (t, $J = 7.3$ Hz, 1H), 5.28 (d, $J = 19.7$ Hz, 1H), 5.05 – 4.72 (m, 4H), 4.02 (ddd, $J = 12.9, 7.6, 4.7$ Hz, 1H), 3.66 – 3.57 (m, 1H), 3.10 – 2.94 (m, 2H); ^{13}C NMR (125 MHz, CDCl_3) δ 149.3 (d, $J = 5.6$ Hz), 136.6 (d, $J = 5.6$ Hz), 136.4 (d, $J = 5.9$ Hz), 136.3 (d, $J = 6.1$ Hz), 130.5, 129.3, 128.9 (d, $J = 2.5$ Hz), 128.8 (d, $J = 2.5$ Hz), 128.6, 128.5, 128.4, 128.3, 128.2, 128.1, 128.0, 127.7 (d, $J = 3.5$ Hz), 126.1 (d, $J = 2.8$ Hz), 68.7 (d, $J = 7.3$ Hz), 67.8 (d, $J = 7.8$ Hz), 59.1 (d, $J = 158.1$ Hz), 43.7, 26.9; ^{31}P NMR (122 MHz, CDCl_3) δ 23.5.

Diisopropyl(2-phenyl-1,2,3,4-tetrahydroisoquinolin-1-yl)phosphonate (**2.6i**)⁵⁵:



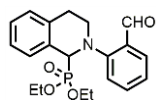
Yield 56% (104 mg); Clear oil; **¹H NMR** (500 MHz, CDCl₃) δ 7.40 (d, *J* = 7.0 Hz, 1H), 7.26 – 7.11 (m, 5H), 6.96 (d, *J* = 8.5 Hz, 2H), 6.77 (t, *J* = 7.0 Hz, 1H), 5.13 (d, *J* = 21.1 Hz, 1H), 4.68 – 4.56 (m, 2H), 4.11 – 4.01 (m, 1H), 3.69 – 3.60 (m, 1H), 3.06 – 2.93 (m, 2H), 1.30 (d, *J* = 6.2 Hz, 3H), 1.28 (d, *J* = 6.2 Hz, 3H), 1.16 (d, *J* = 6.2 Hz, 3H), 0.94 (d, *J* = 6.2 Hz, 3H); **¹³C NMR** (125 MHz, CDCl₃) δ 149.6 (d, *J* = 6.5 Hz), 136.5 (d, *J* = 5.6 Hz), 130.9, 129.1, 128.8 (d, *J* = 2.5 Hz), 128.5 (d, *J* = 4.5 Hz), 127.4 (d, *J* = 3.5 Hz), 125.7 (d, *J* = 2.8 Hz), 118.5, 115.2, 72.3 (d, *J* = 7.8 Hz), 71.0 (d, *J* = 8.1 Hz), 58.9 (d, *J* = 161.0 Hz), 43.6, 26.6, 24.7 (d, *J* = 2.8 Hz), 24.2 (d, *J* = 2.8 Hz), 23.8 (d, *J* = 5.6 Hz), 23.4 (d, *J* = 5.6 Hz); **³¹P NMR** (122 MHz, CDCl₃) δ 21.5.

Diethyl (2-(2-vinylphenyl)-1,2,3,4-tetrahydroisoquinolin-1-yl)phosphonate (**2.6j**):



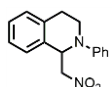
Yield 12% (22 mg); Yellow oil; **¹H NMR** (500 MHz, CDCl₃) δ 7.53 – 7.46 (m, 2H), 7.22 (dd, *J* = 5.6, 3.5 Hz, 3H), 7.14 – 7.08 (m, 3H), 7.03 (t, *J* = 7.2 Hz, 1H), 6.84 (d, *J* = 7.9 Hz, 1H), 5.72 (dd, *J* = 17.8, 1.5 Hz, 1H), 5.27 (dd, *J* = 11.0, 1.5 Hz, 1H), 4.85 (d, *J* = 24.4 Hz, 1H), 4.09 – 3.97 (m, 4H), 3.93 – 3.85 (m, 2H), 3.35 – 3.27 (m, 1H), 2.82 – 2.71 (m, 1H), 2.61 (d, *J* = 16.5 Hz, 1H), 1.22 (t, *J* = 7.1 Hz, 3H), 1.13 (t, *J* = 7.1 Hz, 3H); **¹³C NMR** (125 MHz, CDCl₃) δ 149.5 (d, *J* = 10.8 Hz), 136.6 (d, *J* = 6.0 Hz), 134.4, 132.7, 130.4, 129.5 (d, *J* = 2.3 Hz), 128.4, 128.2 (d, *J* = 3.7 Hz), 127.2 (d, *J* = 3.4 Hz), 126.8, 125.9 (d, *J* = 3.1 Hz), 123.6, 122.2, 114.1, 62.97 (d, *J* = 7.3 Hz), 62.21 (d, *J* = 6.9 Hz), 59.7 (d, *J* = 153.8 Hz), 46.5, 25.5, 16.54 (d, *J* = 6.1 Hz), 16.49 (d, *J* = 6.4 Hz); **³¹P NMR** (122 MHz, CDCl₃) δ 23.3; **IR** (neat, cm⁻¹): 3060, 2977, 1663, 1239; **HRMS(ESI)**: 374.1715 [M+H]⁺, Predicted 374.1723

diethyl (2-(2-formylphenyl)-1,2,3,4-tetrahydroisoquinolin-1-yl)phosphonate (**2.6k**):



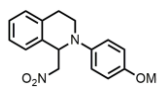
Yield 13% (24 mg); Yellow oil; **¹H NMR** (500 MHz, CDCl₃) δ 10.42 (s, 1H), 7.84 (dd, *J* = 7.7, 1.6 Hz, 1H), 7.53 – 7.48 (m, 1H), 7.44 – 7.38 (m, 1H), 7.26 – 7.22 (m, 2H), 7.18 – 7.11 (m, 2H), 6.98 (d, *J* = 8.1 Hz, 1H), 4.91 (d, *J* = 24.3 Hz, 1H), 4.28 (ddd, *J* = 13.4, 11.4, 4.1 Hz, 1H), 4.08 – 3.97 (m, 2H), 3.97 – 3.83 (m, 2H), 3.40 – 3.34 (m, 1H), 2.84 (ddd, *J* = 20.7, 11.0, 4.9 Hz, 1H), 2.74 – 2.64 (m, 1H), 1.21 (t, *J* = 7.1 Hz, 3H), 1.13 (t, *J* = 7.1 Hz, 3H); **¹³C NMR** (125 MHz, CDCl₃) δ 191.9, 155.1 (d, *J* = 10.7 Hz), 136.0 (d, *J* = 6.2 Hz), 134.9, 129.8, 129.5, 129.5 (d, *J* = 2.4 Hz), 129.3, 128.1 (d, *J* = 3.7 Hz), 127.5 (d, *J* = 3.5 Hz), 126.2 (d, *J* = 3.1 Hz), 123.6, 122.8, 63.0 (d, *J* = 7.2 Hz), 62.4 (d, *J* = 7.2 Hz), 60.3 (d, *J* = 156.1 Hz), 50.3 (s), 25.7, 16.5 (d, *J* = 5.5 Hz), 16.4 (d, *J* = 5.8 Hz); **³¹P NMR** (122 MHz, CDCl₃) δ 22.5; **IR** (neat, cm⁻¹): 3064, 2980, 2851, 2742, 1741, 1210; **HRMS(ESI)**: 374.1510 [M+H]⁺, Predicted 374.1516

1-(Nitromethyl)-2-phenyl-1,2,3,4-tetrahydroisoquinoline (**2.8a**)⁶²:



Yield 85% (114 mg); Yellow oil; **¹H NMR** (300 MHz, CDCl₃) δ 7.33 – 7.11 (m, 6H), 6.99 (d, *J* = 8.2 Hz, 2H), 6.85 (t, *J* = 7.3 Hz, 1H), 5.56 (t, *J* = 7.2 Hz, 1H), 4.88 (dd, *J* = 11.8, 7.8 Hz, 2H), 4.57 (dd, *J* = 11.8, 6.6 Hz, 2H), 3.74 – 3.58 (m, 2H), 3.16 – 3.03 (m, 1H), 2.80 (dt, *J* = 16.3, 5.0 Hz, 1H); **¹³C NMR** (75 MHz, CDCl₃) δ 148.5, 135.4, 133.0, 129.6, 129.3, 128.3, 127.1, 126.8, 119.5, 115.2, 78.9, 58.3, 42.2, 26.6.

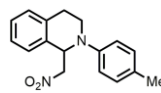
2-(4-Methoxyphenyl)-1-(nitromethyl)-1,2,3,4-tetrahydroisoquinoline (**2.8b**)⁶²:



Yield 81% (120 mg); Yellow oil; **¹H NMR** (500 MHz, CDCl₃) δ 7.23 (td, *J* = 7.1, 1.4 Hz, 2H), 7.18 – 7.12 (m, 2H), 6.91 (d, *J* = 9.0 Hz, 2H), 6.81 (d, *J* = 9.0 Hz, 2H), 5.39 (dd, *J* = 9.0, 5.9 Hz, 1H), 4.83 (dd, *J* = 12.0, 8.6 Hz, 1H), 4.56 (dd, *J* = 12.0, 5.9 Hz, 1H), 3.75 (s, 3H),

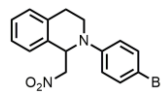
3.61 – 3.51 (m, 2H), 3.01 (ddd, $J = 16.3, 9.6, 6.5$ Hz, 1H), 2.69 (dt, $J = 16.3, 3.8$ Hz, 1H); ^{13}C NMR (125 MHz, CDCl_3) δ 154.1, 143.2, 135.6, 133.0, 129.6, 128.0, 127.1, 126.8, 119.0, 114.8, 79.1, 59.1, 55.7, 43.3, 25.9.

1-(Nitromethyl)-2-(p-tolyl)-1,2,3,4-tetrahydroisoquinoline (**2.8c**)⁶²:



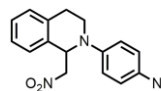
Yield 87% (122 mg); Yellow oil; ^1H NMR (500 MHz, CDCl_3) δ 7.27 – 7.12 (m, 4H), 7.08 (d, $J = 8.3$ Hz, 2H), 6.89 (d, $J = 8.6$ Hz, 2H), 5.50 (t, $J = 7.2$ Hz, 1H), 4.86 (dd, $J = 11.8, 8.1$ Hz, 1H), 4.56 (dd, $J = 11.8, 6.4$ Hz, 1H), 3.70 – 3.54 (m, 2H), 3.13 – 3.01 (m, 1H), 2.76 (dt, $J = 16.4, 4.5$ Hz, 1H), 2.27 (s, 3H); ^{13}C NMR (125 MHz, CDCl_3) δ 146.5, 135.5, 133.1, 130.1, 129.4, 129.2, 128.1, 127.1, 126.76, 116.0, 78.9, 58.5, 42.4, 26.3, 20.5.

2-(4-Bromophenyl)-1-(nitromethyl)-1,2,3,4-tetrahydroisoquinoline (**2.8d**)⁶²:



Yield 79% (137 mg); Yellow oil; ^1H NMR (500 MHz, CDCl_3) δ 7.34 (d, $J = 7.1$ Hz, 2H), 7.26 – 7.11 (m, 4H), 6.84 (d, $J = 7.1$ Hz, 2H), 5.48 (dd, $J = 7.0$ Hz, 1H), 4.85 (dd, $J = 14.5, 5.5$ Hz, 1H), 4.57 (dd, $J = 11.5, 6.2$ Hz, 1H), 3.73 – 3.51 (m, 2H), 3.13 – 3.01 (m, 1H), 2.79 (dt, $J = 15.2, 5.2$ Hz, 1H); ^{13}C NMR (125 MHz, CDCl_3) δ 147.6, 135.1, 132.5, 132.3, 129.4, 128.4, 127.1, 126.9, 116.9, 111.7, 78.7, 58.2, 42.2, 26.3.

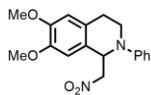
2-(4-Nitrophenyl)-1-(nitromethyl)-1,2,3,4-tetrahydroisoquinoline (**2.8e**)⁶²:



Yield 61% (95 mg); Yellow oil; ^1H NMR (500 MHz, CDCl_3) δ 8.16 (d, $J = 9.5$ Hz, 2H), 7.34 – 7.28 (m, 1H), 7.28 – 7.23 (m, 2H), 7.19 – 7.14 (m, 1H), 6.96 (d, $J = 9.5$ Hz, 2H), 5.71 (t, $J = 7.2$ Hz, 1H), 4.88 (dd, $J = 12.1, 7.2$ Hz, 1H), 4.63 (dd, $J = 12.1, 7.2$ Hz, 1H), 3.75 (t, $J = 6.2$ Hz, 1H), 3.16 (dt, $J = 16.2, 6.2$ Hz, 1H), 2.96 (dt, $J = 16.2, 6.0$ Hz, 1H); ^{13}C NMR (125

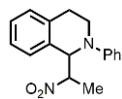
MHz, CDCl₃) δ 152.7, 139.1, 134.6, 132.1, 129.2, 129.0, 127.4, 127.2, 126.4, 112.1, 78.2, 57.6, 42.4, 27.1.

6,7-dimethoxy-1-(nitromethyl)-2-phenyl-1,2,3,4-tetrahydroisoquinoline (**2.8f**)²¹⁵:



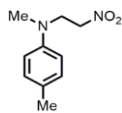
Yield 68% (111 mg); Yellow oil; **¹H NMR** (500 MHz, CDCl₃) δ 7.28 – 7.24 (m, 2H), 6.97 (d, *J* = 8.1 Hz, 2H), 6.84 (t, *J* = 7.3 Hz, 1H), 6.64 (s, 1H), 6.60 (s, 1H), 5.46 (t, *J* = 7.2 Hz, 1H), 4.85 (dd, *J* = 11.8, 8.0 Hz, 1H), 4.56 (dd, *J* = 11.8, 6.4 Hz, 1H), 3.85 (s, 3H), 3.85 (s, 3H), 3.70 – 3.54 (m, 2H), 3.06 – 2.93 (m, 1H), 2.67 (dt, *J* = 16.2, 4.6 Hz, 1H); **¹³C NMR** (125 MHz, CDCl₃) δ 148.9, 148.7, 147.8, 129.6, 127.6, 124.7, 119.7, 115.6, 111.8, 109.7, 78.9, 58.1, 56.2, 56.0, 42.2, 25.9.

1-(1-Nitroethyl)-2-phenyl-1,2,3,4-tetrahydroisoquinoline (**2.8g**)⁶²:



Yield 69% (97 mg); Yellow oil; **¹H NMR** (500 MHz, CDCl₃, 3:2 mixture of diastereoisomers) δ 7.31 – 7.08 (m, 6H), 7.03 – 6.97 (m, 2H), 6.86 – 6.80 (m, 1H), [5.26 (d, *J* = 8.9 Hz), 5.24 (d, *J* = 8.4 Hz), 1H], [5.06 (dq, *J* = 8.3, 6.7 Hz), 4.89 (dq, *J* = 8.8, 6.8 Hz), 1H], [3.90 – 3.79 (m), 3.64 – 3.53 (m), 2H], 3.12 – 3.01 (m, 1H), 2.97 – 2.84 (m, 1H), [1.71 (d, *J* = 6.8 Hz), 1.55 (d, *J* = 6.6 Hz), 3H]; **¹³C NMR** (125 MHz, CDCl₃, 3:2 mixture of diastereoisomers) δ 149.1, 149.0, 135.7, 134.9, 133.9, 132.2, 129.6, 129.5, 129.2, 128.8, 128.5, 128.3, 127.4, 126.7, 126.3, 119.5, 118.9, 115.6, 114.6, 89.1, 85.6, 62.9, 61.3, 43.7, 42.8, 26.9, 26.5, 17.6, 16.5.

N,4-dimethyl-N-(2-nitroethyl)aniline (**2.8j**)⁵⁵:



Yield 15% (14.5 mg); Yellow oil; **¹H NMR** (500 MHz, CDCl₃) δ 7.08 (d, *J* = 8.4 Hz, 1H), 6.67 (d, *J* = 8.6 Hz, 1H), 4.56 (t, *J* = 6.4 Hz, 1H), 3.97 (t, *J* = 6.4 Hz, 1H), 2.95 (s, 2H), 2.27 (s, 2H); **¹³C NMR** (125 MHz, CDCl₃) δ 145.9, 130.1, 127.6, 113.3, 72.7, 51.1, 39.1, 20.3.

G. General procedure for synthesis of *N*-protected anilines from *N*-methyl anilines (**3.1g** and **3.1j**)

Following general procedure described in literature²¹⁸, 25 mL of DMSO was added to a reaction mixture containing *N*-methyl aniline (5.0 mmol) and KOH (10.0 mmol). The resulting mixture was stirred at room temperature followed by addition of alkyl bromide (10.0 mmol). The reaction mixture was heated at 50 °C and the reaction progress was monitored by TLC. When most of the starting materials were consumed, the reaction was quenched with 10 mL of water and extracted with (3x10 mL) ethyl acetate. Combined organic phase was dried over anhydrous MgSO₄ and concentrated under reduced pressure. The residue was purified with column chromatography with silica gel (hexanes/ethyl acetate).

Substrate **3.1t** was synthesized from reductive amination of corresponding 2-aminostyrene with paraformaldehyde in presence of base K₂CO₃ and reducing agent NaBH₄.

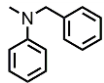
Substrate **3.1u** was synthesized from acetylation reaction using acetic anhydride and *N*-methylaniline.

N-allyl-*N*-methylaniline (**3.1g**)²¹⁷:



Yield 79% (580 mg); Brown oil; **¹H NMR** (500 MHz, CDCl₃) δ 7.24 (dd, *J* = 6.8, 4.7 Hz, 1H), 6.54 (d, *J* = 9.0 Hz, 1H), 5.78 (ddt, *J* = 17.0, 10.1, 4.9 Hz, 1H), 5.30 – 4.37 (m, 1H), 3.86 (dd, *J* = 3.3, 1.6 Hz, 1H), 2.89 (s, 2H); **¹³C NMR** (125 MHz, CDCl₃) δ 148.2, 132.9, 131.5, 116.1, 113.7, 108.0, 55.0, 38.0

N-benzyl-*N*-methylaniline (**3.1j**)²¹⁷:



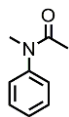
Yield 85% (837 mg); Brown oil; **¹H NMR** (500 MHz, CDCl₃) δ 7.44 (t, *J* = 7.0 Hz, 1H), 7.39 – 7.31 (m, 2H), 7.08 – 6.71 (m, 1H), 4.65 (s, 1H), 3.13 (s, 1H); **¹³C NMR** (125 MHz, CDCl₃) δ 149.5, 138.8, 129.0, 128.3, 126.6, 126.5, 116.3, 112.1, 56.4, 38.3.

N,N-dimethyl-2-vinylaniline (**3.1t**)²¹⁸:



Yield 75% (551 mg); Yellow oil; **¹H NMR** (500 MHz, CDCl₃) δ 7.58 (d, *J* = 7.4 Hz, 1H), 7.33 (t, *J* = 7.5 Hz, 1H), 7.18 (dd, *J* = 17.7, 11.0 Hz, 1H), 7.14 – 7.07 (m, 2H), 5.78 (d, *J* = 17.7 Hz, 1H), 5.35 (d, *J* = 11.0 Hz, 1H), 2.82 (s, 6H); **¹³C NMR** (125 MHz, CDCl₃) δ 151.8, 135.0, 131.9, 128.4, 126.9, 122.3, 118.0, 113.1, 44.6

N-methyl-*N*-phenylacetamide (**3.1u**)²¹⁹:



Yield 91% (678 mg); White solid; **mp** 98-100 °C (lit. mp 101-103 °C)²¹⁹; **¹H NMR** (500 MHz, CDCl₃) δ 7.41 (t, *J* = 7.6 Hz, 2H), 7.33 (t, *J* = 7.3 Hz, 1H), 7.18 (d, *J* = 7.5 Hz, 2H), 3.26 (s, 3H), 1.86 (s, 3H); **¹³C NMR** (125 MHz, CDCl₃) δ 170.6, 144.7, 129.8, 127.8, 127.2, 37.2, 22.5

I.1. General procedure for synthesis of 1-phenylpyrrolidine **3.1h**:

Following the procedure described in literature²²⁰, with slight modification, iodobenzene (1.0 mmol), pyrrolidine (1.0 mmol) and KOH (2.5 mmol) were charged into pressure tube under Argon atmosphere. 5 mL of dry DMSO was added into the tube under argon. The reaction mixture was stirred in an oil bath at 120 °C for 3 days. The mixture was then quenched with 5 mL of saturated NH₄Cl and extracted with (3x5mL) EtOAc. Organic phase was dried over anhydrous MgSO₄ and concentrated under reduced pressure. The crude residue was purified with

column chromatography with silica gel (20:1; hexanes: ethyl acetate) to afford desired product as colorless liquid in 82% (120.7 mg) isolated yield.

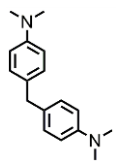
¹H NMR (500 MHz, CDCl₃) δ 7.37 (t, *J* = 7.8 Hz, 2H), 6.81 (t, *J* = 7.2 Hz, 1H), 6.71 (d, *J* = 8.1 Hz, 2H), 3.45 – 3.34 (m, 4H), 2.15 – 2.08 (m, 4H); **¹³C NMR** (125 MHz, CDCl₃) δ 147.9, 129.1, 115.3, 111.6, 47.5, 25.5.

H. General procedure for synthesis of 4,4'-diaminodiphenylmethanes (**3.2a** – **3.2i**), 4,4'-bisnaphthylmethane (**3.2j**), 1,1'-bisnaphthalylmethane (**3.2l** and **3.2m**), and 3,3'-bisindolylmethane (**3.2n**):

2 dram vial fitted with stirbar was added with aniline or indole or 2-naphthol or 1-naphthol (0.5 mmol), 37% HCHO solution (2.5 mmol) and 500 μL MeCN. The reaction mixture was stirred at 45 °C or 70 °C and the reaction progress was monitored by TLC. After the starting material is consumed, the solvent was removed under reduced pressure and the crude product was purified with column chromatography with silica gel.

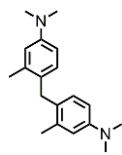
Products **3.2e**, **3.2k**, **3.2l**, and **3.2m** were purified by recrystallization of corresponding crude precipitates present in reaction mixture using diethylether. Crystallized products were washed with cold ether followed by cold pentane.

4,4'-Methylenebis(*N,N*-dimethylaniline) (**3.2a**)²²¹:



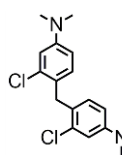
Yield 93% (59.0 mg); White crystal; **mp** 84-85 °C; **¹H NMR** (500 MHz, CDCl₃) δ 7.07 (d, *J* = 8.7 Hz, 4H), 6.70 (d, *J* = 8.6 Hz, 4H), 3.82 (s, 2H), 2.91 (s, 12H); **¹³C NMR** (125 MHz, CDCl₃) δ 149.1, 130.6, 129.5, 113.2, 41.1, 40.0; **HRMS (ESI)**: 255.1852 [M+H]⁺, Predicted 255.1852

4,4'-Methylenebis(*N,N*,3-trimethylaniline) (**3.2b**)²²¹:



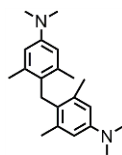
Yield 82% (58 mg); White solid; **mp** 85-86 °C; **¹H NMR** (300 MHz, CD₃OD) δ 6.82 (d, *J* = 8.6 Hz, 2H), 6.74 (d, *J* = 2.6 Hz, 2H), 6.59 (dd, *J* = 8.6, 2.7 Hz, 2H), 3.92 (s, 2H), 2.88 (s, 12H); **¹³C NMR** (75 MHz, CD₃OD) δ 150.8, 137.9, 130.7, 129.8, 116.8, 112.8, 41.6, 35.9, 20.1; **HRMS (ESI)**: 283.1417 [M+H]⁺, Predicted 283.1422

4,4'-Methylenebis(3-chloro-*N,N*-dimethylaniline) (**3.2c**)²²¹:



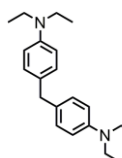
Yield 78% (63 mg), White solid, **mp** 96-98 °C; **¹H NMR** (300 MHz, CD₃OD) δ 6.82 (d, *J* = 8.6 Hz, 1H), 6.74 (d, *J* = 2.6 Hz, 2H), 6.59 (dd, *J* = 8.6, 2.7 Hz, 1H), 2.88 (s, 7H); **¹³C NMR** (125 MHz, CD₃OD) δ 151.7, 135.6, 131.9, 126.6, 114.1, 112.6, 40.7, 35.6; **HRMS (ESI)**: 323.0349 [M]⁺, Predicted 323.0344

4,4'-Methylenebis(*N,N*,3,5-tetramethylaniline) (**3.2d**):



Yield 73% (56.5 mg); White solid; **mp** 131-134 °C; **¹H NMR** (300 MHz, CDCl₃) δ 6.42 (s, 1H), 3.92 (s, 1H), 2.89 (s, 3H), 2.12 (s, 3H); **¹³C NMR** (75 MHz, CDCl₃) δ 148.6, 137.5, 127.4, 113.6, 41.0, 30.0, 21.5; **IR** (neat, cm⁻¹): 3030, 2970, 2914, 1601; **HRMS (ESI)**: 311.1714 [M+H]⁺, Predicted 311.1719

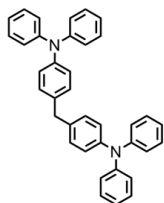
4,4'-Methylenebis(*N,N*-diethylaniline) (**3.2e**)²¹⁷:



Yield 79% (61 mg); yellow oil; **¹H NMR** (300 MHz, CDCl₃) δ 7.03 (d, *J* = 8.4 Hz, 4H), 6.62 (d, *J* = 8.4 Hz, 4H), 3.77 (s, 2H), 3.31 (q, *J* = 6.9 Hz, 8H), 1.13 (t, *J* = 7.0 Hz, 12H);

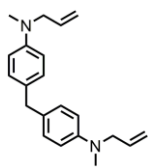
^{13}C NMR (125 MHz, CD_3CN) δ 147.0, 130.2, 118.3, 131.1, 45.0, 40.3, 12.7; **HRMS (ESI):** 311.1724 $[\text{M}+\text{H}]^+$, Predicted 311.1724

4,4'-Methylenebis(*N,N*-diphenylaniline) (**3.2f**):



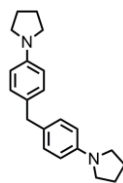
Yield 54% (68 mg); White solid; **mp** 158-161 °C; ^1H NMR (500 MHz, CDCl_3) δ 7.25 – 7.21 (m, 6H), 7.18 – 7.04 (m, 11H), 7.04 – 6.92 (m, 8H), 3.89 (s, 2H); ^{13}C NMR (125 MHz, CDCl_3) δ 148.0, 145.9, 135.8, 129.8, 129.3, 129.3, 124.5, 124.3, 124.3, 124.0, 122.8, 122.6, 40.7; **IR** (neat, cm^{-1}): 3025, 2977, 1583, 1503; **HRMS (ESI):** 437.2031 $[\text{M}+\text{H}]^+$, Predicted: 437.2028

4,4'-Methylenebis(*N*-allyl-*N*-methylaniline) (**3.2g**)²¹⁷:



Yield 70% (53.5 mg); clear oil; ^1H NMR (500 MHz, CDCl_3) δ 7.07 – 7.02 (m, 4H), 6.68 – 6.64 (m, 4H), 5.84 (ddt, $J = 17.1, 10.3, 5.2$ Hz, 2H), 5.19 – 5.11 (m, 4H), 3.89 – 3.86 (m, 4H), 3.79 (s, 2H), 2.89 (s, 6H); ^{13}C NMR (125 MHz, CDCl_3) δ 147.9, 134.2, 130.1, 129.5, 116.2, 112.8, 55.7, 39.9, 38.2; **HRMS (ESI):** 307.1298 $[\text{M}+\text{H}]^+$, Predicted 307.1299

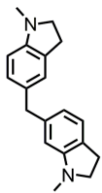
Bis(4-(pyrrolidin-1-yl)phenyl)methane (**3.2h**)²¹⁷:



Yield 84% (64.3 mg); Purple solid; **mp** 65-68 °C; ^1H NMR (300 MHz, CDCl_3) δ 7.04 (d, $J = 7.6$ Hz, 4H), 6.50 (d, $J = 7.6$ Hz, 4H), 3.80 (s, 2H), 3.24 (t, 8H), 1.97 (t, $J = 5.0$ Hz, 8H);

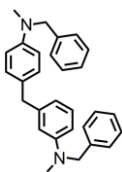
^{13}C NMR (125 MHz, CDCl_3) δ 129.4, 129.1, 129.0, 111.6, 47.6, 39.8, 25.2; **HRMS (ESI)**: 307.2158 $[\text{M}+\text{H}]^+$, Predicted: 307.2159

1-Methyl-6-((1-methylindolin-5-yl)methyl)indoline (**3.2i**)²¹⁷:



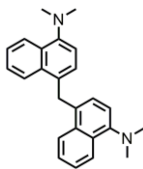
Yield 77% (53.5 mg); Pale yellow viscous liquid; ^1H NMR (500 MHz, CDCl_3) δ 6.91 (d, $J = 5.2$ Hz, 4H), 6.41 (d, $J = 8.3$ Hz, 4H), 3.77 (s, 2H), 3.24 (t, $J = 8.0$ Hz, 4H), 2.88 (t, $J = 8.0$ Hz, 4H), 2.72 (s, 6H); ^{13}C NMR (125 MHz, CDCl_3) δ 151.7, 131.8, 130.8, 127.6, 125.0, 107.2, 56.6, 40.9, 36.8, 28.9; **HRMS (ESI)**: 279.1108 $[\text{M}+\text{H}]^+$, Predicted 279.1111

4,4'-Methylenebis(*N*-benzyl-*N*-methylaniline) (**3.2j**)²¹⁷:



Yield 81% (82.0 mg); Pale yellow solid; **mp** 42-44 °C; ^1H NMR (500 MHz, CDCl_3) δ 7.37 – 7.31 (m, 4H), 7.27 (dd, $J = 9.8, 4.4$ Hz, 6H), 7.07 (d, $J = 8.5$ Hz, 4H), 6.71 (d, $J = 8.6$ Hz, 6H), 4.52 (s, 4H), 3.82 (s, 2H), 3.00 (s, 6H); ^{13}C NMR (125 MHz, CDCl_3) δ 148.2, 139.4, 130.2, 129.6, 128.6, 126.9, 126.9, 112.7, 57.0, 40.0, 38.7; **HRMS (ESI)**: 407.1432 $[\text{M}+\text{H}]^+$, Predicted 407.1439

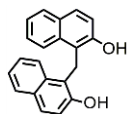
4,4'-Methylenebis(*N,N*-dimethylnaphthalen-1-amine) (**3.2k**)²¹⁷:



Yield 61% (54 mg); White solid; **mp** 180-182 °C; ^1H NMR (500 MHz, CDCl_3) δ 8.33 (dd, $J = 8.1, 1.3$ Hz, 2H), 8.03 (dd, $J = 7.9, 1.2$ Hz, 2H), 7.52 (ddd, $J = 8.4, 6.8, 1.4$ Hz, 2H), 7.47 (ddd, $J = 8.2, 6.8, 1.5$ Hz, 2H), 6.97 (dd, $J = 19.3, 7.7$ Hz, 4H), 4.70 (s, 2H), 2.96 (s, 12H);

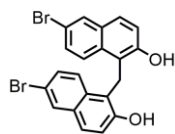
^{13}C NMR (125 MHz, CDCl_3) δ 149.8, 133.4, 131.0, 129.2, 127.1, 125.9, 125.0, 124.8, 124.6, 113.9, 45.5, 35.3; **HRMS (ESI):** 355.1457 $[\text{M}+\text{H}]^+$, Predicted 355.1459

1,1'-Methylenebis(naphthalen-2-ol) (**3.2l**)²²²:



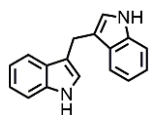
Yield 55% (41.2 mg); White solid; **mp** 200-202 °C (lit. mp 200 °C)²²²; ^1H NMR (500 MHz, CDCl_3) δ 8.22 (d, J = 8.6 Hz, 2H), 7.78 (d, J = 8.0 Hz, 2H), 7.65 (d, J = 8.8 Hz, 2H), 7.50 – 7.41 (m, 2H), 7.33 (t, J = 7.4 Hz, 2H), 7.05 (d, J = 8.8 Hz, 2H), 6.36 (bs, 2H), 4.81 (s, 2H); ^{13}C NMR (125 MHz, CD_3OD) δ 152.9, 135.5, 130.6, 129.1, 128.7, 126.5, 125.2, 123.3, 120.9, 118.7, 21.8; **HRMS (ESI):** 299.1077 $[\text{M}-\text{H}]^+$, Predicted: 299.1078

1,1'-Methylenebis(6-bromonaphthalen-2-ol) (**3.2m**):



Yield 61% (69.8 mg); White solid; **mp** 212-214 °C; ^1H NMR (500 MHz, $\text{DMSO}-d_6$) δ 10.38 (bs, 2H), 8.08 (d, J = 9.1 Hz, 2H), 7.92 (s, 2H), 7.61 (d, J = 8.8 Hz, 2H), 7.29 (t, J = 9.5 Hz, 4H), 4.66 (s, 2H); ^{13}C NMR (125 MHz, $\text{DMSO}-d_6$) δ 152.3, 132.2, 129.8, 129.7, 128.2, 127.0, 126.0, 119.5, 119.2, 115.1, 20.2; **IR** (diamond-ATR) γ/cm^{-1} : 3332, 3056, 2924, 1589; **HRMS (ESI):** 454.9279 $[\text{M}-\text{H}]^+$, Predicted: 454.9288

Di(1H-indol-3-yl)methane (**3.2n**)²²³:



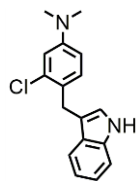
Yield 45% (27.7 mg); Pale red solid; **mp** 145-146 °C (lit. mp 147-148 °C)²²³; ^1H NMR (500 MHz, CDCl_3) δ 7.90 (bs, 2H), 7.63 (d, J = 7.9 Hz, 2H), 7.36 (d, J = 8.1 Hz, 2H), 7.22 – 7.17 (m, 2H), 7.12 – 7.08 (m, 2H), 6.94 (s, 2H), 4.25 (s, 2H); ^{13}C NMR (125 MHz, CDCl_3) δ

136.5, 127.7, 122.3, 122.0, 119.3, 119.3, 115.8, 111.1, 21.3; **HRMS (ESI):** 247.0558 [M+H]⁺, Predicted 247.0555

J.1. General procedure for synthesis of 3.2o-3.2s:

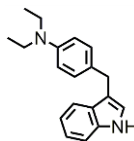
2 dram vial fitted with stirbar was added with aniline derivative (0.5 mmol) and indole/naphthol (0.5 mmol) followed by 700 μ L of acetonitrile solvent. 0.5 mmol of 37% HCHO solution was added separately in 100 μ L of acetonitrile. The latter solution was added dropwise over 5 minutes in the reaction mixture. The resulting mixture was heated to 70 °C. Upon completion of reaction, the solvent was removed under reduced pressure and the crude product was purified under column chromatography with silica gel.

4-((1H-indol-3-yl)methyl)-3-chloro-N,N-dimethylaniline (**3.2o**):



Yield 40% (57 mg); Red viscous oil; **¹H NMR** (500 MHz, CD₂Cl₂) δ 8.08 (s, 1H), 7.54 (d, J = 7.9 Hz, 1H), 7.36 (d, J = 8.1 Hz, 1H), 7.16 (t, J = 7.5 Hz, 1H), 7.05 (dd, J = 7.9, 5.0 Hz, 2H), 6.95 (s, 1H), 6.76 (s, 1H), 6.55 (d, J = 6.6 Hz, 1H), 4.10 (s, 2H), 2.90 (s, 6H); **¹³C NMR** (125 MHz, CD₂Cl₂) δ 150.6, 137.0, 134.8, 131.3, 127.9, 126.5, 123.1, 122.3, 119.7, 119.5, 115.5, 113.4, 111.8, 111.6, 40.8, 28.5; **IR** (neat, cm⁻¹): 3412, 3053, 2887, 1607, 1549; **HRMS (ESI):** 285.0465 [M+H]⁺, Predicted 285.0460

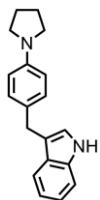
4-((1H-indol-3-yl)methyl)-N,N-diethylaniline (**3.2p**):



Yield 62% (86.2 mg); White solid; **mp** 140-142 °C; **¹H NMR** (300 MHz, CDCl₃) δ 7.94 (bs, 1H), 7.59 (d, J = 7.7 Hz, 1H), 7.40 – 7.34 (m, 1H), 7.24 – 7.06 (m, 4H), 6.93 (d, J = 2.3 Hz, 1H), 6.66 (d, J = 6.9 Hz, 2H), 4.04 (s, 2H), 3.34 (q, J = 7.0 Hz, 4H), 1.16 (t, J = 7.0 Hz, 6H);

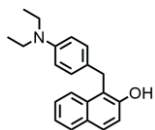
^{13}C NMR (125 MHz, CD_2Cl_2) δ 146.7, 137.1, 129.8, 128.7, 128.0, 122.6, 122.3, 121.8, 119.6, 117.2, 112.5, 111.5, 44.9, 30.9, 12.8; **IR** (neat, cm^{-1}): 3377, 3056, 2963, 1610; **HRMS (ESI)**: 279.1143 $[\text{M}+\text{H}]^+$, Predicted 279.1140

3-(4-(pyrrolidin-1-yl)benzyl)-1H-indole (**3.2q**):



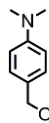
Yield 54% (74.5 mg); White solid; **mp** 174-177 $^\circ\text{C}$; ^1H NMR (300 MHz, CDCl_3) δ 7.90 (bs, 1H), 7.56 (d, $J = 7.8$ Hz, 1H), 7.34 (d, $J = 8.1$ Hz, 1H), 7.16 (d, $J = 8.5$ Hz, 3H), 7.08 (t, $J = 7.5$ Hz, 1H), 6.88 (s, 1H), 6.53 (d, $J = 8.4$ Hz, 2H), 4.03 (s, 2H), 3.27 (t, $J = 6.4$ Hz, 4H), 1.99 (t, $J = 6.5$ Hz, 4H); ^{13}C NMR (75 MHz, CDCl_3) δ 146.5, 136.5, 129.5, 128.0, 127.6, 122.2, 121.9, 119.4, 119.3, 117.1, 111.8, 111.0, 47.8, 30.7, 25.5; **IR** (neat, cm^{-1}): 3253, 3057, 2064, 1614, 1514; **HRMS (ESI)**: 277.0943 $[\text{M}+\text{H}]^+$, Predicted 277.0940

1-(4-(diethylamino)benzyl)naphthalen-2-ol (**3.2r**):



Yield 50% (76.4 mg); Purple solid; **mp** 130-134 $^\circ\text{C}$; ^1H NMR (300 MHz, CDCl_3) δ 7.99 (d, $J = 8.5$ Hz, 1H), 7.80 (d, $J = 8.1$ Hz, 1H), 7.70 (d, $J = 8.8$ Hz, 1H), 7.50 – 7.42 (m, 1H), 7.37 – 7.30 (m, 1H), 7.13 (d, $J = 8.8$ Hz, 1H), 7.06 (d, $J = 8.4$ Hz, 2H), 6.59 (d, $J = 7.4$ Hz, 2H), 5.12 (bs, 1H), 4.34 (s, 2H), 3.29 (q, $J = 7.0$ Hz, 4H), 1.11 (t, $J = 7.0$ Hz, 6H); ^{13}C NMR (75 MHz, CDCl_3) δ 151.6, 146.6, 133.8, 130.0, 129.5, 129.1, 128.6, 128.3, 126.6, 123.4, 123.2, 118.8, 118.2, 112.4, 44.5, 29.8, 12.6; **IR** (neat, cm^{-1}): 3315, 3057, 2967, 1612, 1513; **HRMS (ESI)**: 306.1017 $[\text{M}+\text{H}]^+$, Predicted 306.1017

(4-(dimethylamino)phenyl)methanol²²⁴:



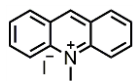
$^1\text{H NMR}$ (300 MHz, CDCl_3) δ 7.25 (d, $J = 7.4$ Hz, 1H), 6.73 (d, $J = 8.6$ Hz, 1H), 4.57 (d, $J = 5.7$ Hz, 1H), 2.95 (s, 3H), 1.46 (t, $J = 5.8$ Hz, 1H); $^{13}\text{C NMR}$ (125 MHz, CDCl_3) δ 150.5, 128.9, 128.8, 112.7, 65.5, 40.7

1-methylpyridin-1-ium iodide²²⁵:



White solid; $^1\text{H NMR}$ (500 MHz, D_2O) δ 8.78 (d, $J = 5.8$ Hz, 1H), 8.53 (t, $J = 7.8$ Hz, 1H), 8.05 (t, $J = 6.4$ Hz, 1H), 4.39 (s, 2H); $^{13}\text{C NMR}$ (125 MHz, D_2O) δ 145.3, 145.1, 128.1, 48.2.

10-methylacridin-10-ium iodide⁹²:

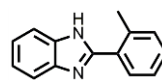


Red solid; $^1\text{H NMR}$ (500 MHz, CD_3OD) δ 10.07 (s, 1H), 8.74 (d, $J = 9.2$ Hz, 2H), 8.62 (d, $J = 8.3$ Hz, 2H), 8.50 – 8.44 (m, 2H), 8.08 – 7.99 (m, 2H), 4.93 (s, 3H); $^{13}\text{C NMR}$ (125 MHz, CD_3OD) δ 152.1, 143.2, 140.5, 133.0, 129.0, 128.2, 119.5, 39.1.

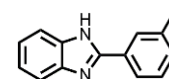
I. General Procedure for synthesis of **4.2a-4.2q**, **4.4a-4.4m**, **4.6a-4.6l**:

N-alkyl-*o*-phenylenediammine or *N,N*-dialkyl-*o*-phenylenediammine or *N,N'*-dialkyl-*o*-phenylenediammine (0.3 mmol) was added in a oven dried 1.5dram vial fitted with magnetic stirbar followed by addition of $\text{FeCl}_3 \cdot 6\text{H}_2\text{O}$ (0.015 mmol) and DMF (0.2 M solution). The reaction mixture was stirred at a given temperature with open cap until all starting material was consumed as indicated by TLC. The reaction mixture was diluted with 3.0 mL of H_2O and extracted with ethyl acetate (5 mL \times 3). The combined organic layer was dried with anhydrous Na_2SO_4 and was concentrated under reduced pressure. The crude product was purified by column chromatography using hexanes and ethyl acetate as eluents.

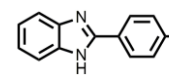
2-(*o*-tolyl)-1H-benzo[d]imidazole (**4.6b**)²²⁶:

 **Yield** 80% (50 mg); White solid; **mp** 220-222 °C (lit. mp 223-224 °C)²²⁶; **¹H NMR** (300 MHz, CD₃OD) δ 7.60 (d, *J* = 6.6 Hz, 3H), 7.42 – 7.21 (m, 5H), 2.49 (s, 3H); **¹³C NMR** (75 MHz, CD₃OD) δ 154.0, 138.5, 132.0, 131.5, 130.9, 130.9, 127.0, 123.7, 20.5; **IR** (diamond-ATR) γ/cm⁻¹: 3061, 2955, 2935, 1477, 1341, 1278.

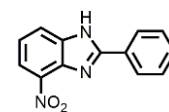
2-(m-tolyl)-1H-benzo[d]imidazole (**4.6c**)²²⁷:

 **Yield** 85% (53 mg); White solid; **mp** 194-196 °C (lit. mp 212-214 °C)²²⁷; **¹H NMR** (300 MHz, CD₃OD) δ 7.93 (s, 1H), 7.88 (d, *J* = 7.5 Hz, 1H), 7.60 (s, 2H), 7.42 (t, *J* = 7.6 Hz, 1H), 7.33 (d, *J* = 7.5 Hz, 1H), 7.29 – 7.21 (m, 2H), 2.46 (s, 3H); **¹³C NMR** (75 MHz, CD₃OD) δ 153.5, 140.1, 132.0, 130.9, 130.0, 128.3, 124.9, 123.8, 112.7, 21.4; **IR** (neat, cm⁻¹): 3051, 2968, 2918, 1444, 1313, 1273,

2-(p-tolyl)-1H-benzo[d]imidazole (**4.6d**)²²⁶:

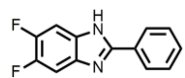
 **Yield** 81% (50.5 mg); White solid; **mp** 267-260 °C (lit. mp 273-275 °C)²²⁷; **¹H NMR** (500 MHz, DMSO-d₆) δ 13.7 (bs, 1H), 8.05 – 8.01 (m, 2H), 7.54 (d, *J* = 54.7 Hz, 2H), 7.33 (d, *J* = 7.8 Hz, 2H), 7.15 (d, *J* = 4.8 Hz, H), 2.35 (s, 3H); **¹³C NMR** (125 MHz, DMSO-d₆) δ 151.9, 140.1, 130.0, 127.9, 126.9, 122.1, 119.2, 111.6, 21.5; **IR** (neat, cm⁻¹): 3066, 2971, 2928, 1484, 1301, 1288.

4-Nitro-2-phenyl-1H-benzo[d]imidazole (**4.6e**):

 **Yield** 45% (32 mg); Brown solid; **mp** 198-200 °C; **¹H NMR** (300 MHz, CD₃OD) δ 8.24 – 8.15 (m, 3H), 8.05 (d, *J* = 7.9 Hz, 1H), 7.61 – 7.53 (m, 3H), 7.43 (dd, *J* = 8.1 Hz, 1H); **¹³C NMR** (75 MHz, CD₃OD) δ 155.7.0, 134.0, 130.9, 128.8, 128.7, 128.6, 127.7, 124.9, 124.6,

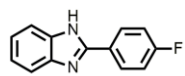
121.7, 119.0; **IR** (neat, cm^{-1}): 3200, 2955, 2850, 1600, 1510, 1342, 1109, 1012; **HRMS**: 262.0576 $[\text{M}+\text{Na}]^+$, Predicted 262.0587.

5,6-Difluoro-2-phenyl-1H-benzo[d]imidazole (**4.6f**)¹⁴²:



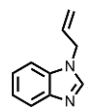
Yield 63% (43.5 mg); Pale brown solid; **mp** 235-237 °C; **^1H NMR** (300 MHz, CD_3OD) δ 8.03 (dd, $J = 7.5, 2.0$ Hz, 2H), 7.57 – 7.49 (m, 3H), 7.48 – 7.38 (m, 2H); **^{13}C NMR** (75 MHz, CD_3OD) δ 154.0, 150.9 (d, $J = 15.0$ Hz), 147.7 (d, $J = 15.4$ Hz), 130.3, 129.1, 128.8, 126.3, 106.1, 100.2; **IR** (neat, cm^{-1}): 3033, 2925, 1605, 1397, 1255, 1145.

2-(4-fluorophenyl)-1H-benzo[d]imidazole (**4.6ga**)²²⁶:



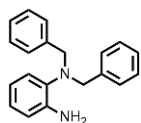
Yield 18% (11.5 mg); White solid; **mp** 248-250 °C; **^1H NMR** (500 MHz, DMSO-d_6) δ 8.24 – 8.18 (m, 2H), 7.60 (dd, $J = 6.0, 3.2$ Hz, 2H), 7.41 (t, $J = 8.8$ Hz, 2H), 7.22 (dd, $J = 6.0, 3.1$ Hz, 2H); **^{13}C NMR** (125 MHz, DMSO-d_6) 163.31 (d, $J = 248.0$ Hz), 150.6, 132.0, 129.04 (d, $J = 8.7$ Hz), 126.4, 123.2, 116.17 (d, $J = 22.0$ Hz), 115.6, 111.7; **^{19}F NMR** (470 MHz, CDCl_3) δ -106.43; **IR** (neat, cm^{-1}): 3050, 2915, 1623, 1497, 1397, 1226, 1154, 1011, 966.

1-Allyl-1H-benzo[d]imidazole (**4.6l**)²²⁸:



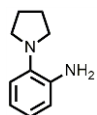
Yield 31% (13.5 mg); Brown liquid; **^1H NMR** (500 MHz, CDCl_3) δ 8.16 (s, 1H), 7.84 (ddd, $J = 4.3, 2.8, 0.7$ Hz, 1H), 7.41 (ddd, $J = 8.3, 3.3, 1.7$ Hz, 1H), 7.35 – 7.30 (m, 2H), 6.02 (ddt, $J = 17.1, 10.3, 5.6$ Hz, 1H), 5.32 (dtd, $J = 10.3, 1.5, 0.9$ Hz, 1H), 5.22 (dtd, $J = 17.1, 1.7, 0.9$ Hz, 1H), 4.84 (dt, $J = 5.6, 1.6$ Hz, 2H); **^{13}C NMR** (125 MHz, CDCl_3) δ 142.6, 142.4, 133.5, 131.6, 123.4, 122.8, 119.9, 119.1, 110.3, 47.7; **IR** (neat, cm^{-1}): 3046, 2936, 1492, 1457, 1263, 1198, 990; **HRMS**: 159.0917 $[\text{M}+\text{H}]^+$, Predicted: 159.0917

N,N-dibenzylbenzene-1,2-diamine (**4.3a**)¹⁴³:



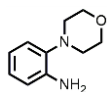
¹H NMR (500 MHz, CDCl₃) δ 7.31 – 7.23 (m, 10H), 6.95 – 6.87 (m, 2H), 6.75 (dd, *J* = 7.8, 1.4 Hz, 1H), 6.66 (ddd, *J* = 7.9, 7.3, 1.5 Hz, 1H), 4.10 (s, 4H); **¹³C NMR** (125 MHz, CDCl₃) δ 142.1, 137.9, 136.7, 129.1, 128.2, 127.2, 125.2, 123.3, 118.3, 115.6, 56.5; **IR** (neat, cm⁻¹): 3410, 3385, 3026, 2945, 1606, 1496, 1265, 1189, 1028.

2-(pyrrolidin-1-yl)aniline (**4.3i**)¹⁴³:



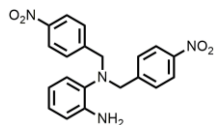
Yield 79% (640 mg from 5.0 mmol scale of 2-fluoronitrobenzene using general procedure D); Brown liquid; **¹H NMR** (500 MHz, CDCl₃) δ 7.03 (dd, *J* = 7.8, 1.4 Hz, 1H), 6.93 (td, *J* = 7.6, 1.4 Hz, 1H), 6.82 – 6.73 (m, 2H), 3.97 (bs, 2H), 3.16 – 3.03 (m, 4H), 2.02 – 1.90 (m, 4H); **¹³C NMR** (125 MHz, CDCl₃) δ 141.4, 137.5, 123.6, 118.7, 118.6, 115.6, 77.5, 77.2, 76.9, 51.0, 24.2; **IR** (neat, cm⁻¹): 3420, 3386, 3033, 2963, 1608, 1498, 1285, 1192.

2-Morpholinoaniline (**4.3j**)¹⁴³:



Yield 70% (623 mg from 5.0 mmol scale of 2-fluoronitrobenzene using general procedure D); Brown liquid; **¹H NMR** (500 MHz, CDCl₃) δ 7.02 (dd, *J* = 8.2, 1.4 Hz, 1H), 6.99 – 6.95 (m, 1H), 6.82 – 6.74 (m, 2H), 3.92 – 3.83 (m, 4H), 2.99 – 2.90 (m, 4H); **¹³C NMR** (125 MHz, CDCl₃) δ 141.1, 138.9, 125.2, 119.9, 119.1, 115.8, 67.6, 51.7; **IR** (neat, cm⁻¹): 3386, 3332, 2922, 1595, 1506, 1455, 1267, 1147.

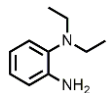
N,N-bis(4-nitrobenzyl)benzene-1,2-diamine (**4.3k**):



Yield 51% (192 mg from 1 mmol scale of OPD in excess 4-nitrobenzyl bromide); Brown solid; **mp** 215-219 °C ; **¹H NMR** (500 MHz, CD₃OD) δ 8.13 – 8.08 (m, 4H),

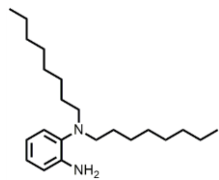
7.51 (dd, $J = 9.0, 2.1$ Hz, 4H), 6.88 (dd, $J = 7.9, 1.3$ Hz, 1H), 6.84 (ddd, $J = 7.9, 7.3, 1.4$ Hz, 1H), 6.72 (dd, $J = 7.9, 1.5$ Hz, 1H), 6.54 (ddd, $J = 7.9, 7.3, 1.5$ Hz, 1H), 4.21 (s, 4H); $^{13}\text{C NMR}$ (125 MHz, CD_3OD) δ 147.2, 145.9, 142.9, 135.1, 129.61, 125.3, 122.9, 122.6, 117.6, 115.7, 56.1; **IR** (neat, cm^{-1}): 3503, 3478, 3075, 2924, 1596, 1506, 1338, 1106.

N,N-diethylbenzene-1,2-diamine (**4.3l**)¹⁴³:



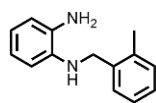
Yield 74% (606 mg from 5.0 mmol scale of 2-fluoronitrobenzene using general procedure D); Brown liquid; $^1\text{H NMR}$ (500 MHz, CDCl_3) δ 7.04 (dd, $J = 7.7, 1.4$ Hz, 1H), 6.95 (ddd, $J = 7.8, 7.3, 1.5$ Hz, 1H), 6.77 – 6.72 (m, 2H), 4.11 (bs, 2H), 2.97 (q, $J = 7.1$ Hz, 4H), 1.01 (t, $J = 7.1$ Hz, 6H); $^{13}\text{C NMR}$ (125 MHz, CDCl_3) δ 144.2, 137.1, 124.9, 123.0, 118.2, 115.1, 47.8, 12.7; **IR** (neat, cm^{-1}): 3426, 3385, 3055, 2968, 1605, 1497, 1377, 1228.

N,N-dioctylbenzene-1,2-diamine (**4.3m**):



Yield 68% (2.2 g following general procedure E); Brown liquid; $^1\text{H NMR}$ (500 MHz, CDCl_3) δ 7.07 (dd, $J = 7.8, 1.4$ Hz, 1H), 6.97 – 6.93 (m, 1H), 6.77 – 6.72 (m, 2H), 4.09 (s, 2H), 2.89 (dd, $J = 8.3, 6.7$ Hz, 4H), 1.48 – 1.40 (m, 4H), 1.33 – 1.24 (m, 23H), 0.91 (t, $J = 7.0$ Hz, 6H); $^{13}\text{C NMR}$ (125 MHz, CDCl_3) δ 143.8, 138.0, 124.7, 122.9, 118.2, 115.1, 54.2, 32.0, 29.6, 29.4, 27.6, 27.5, 22.8, 14.2; **IR** (neat, cm^{-1}): 3467, 3357, 2953, 2922, 2853, 1606, 1498, 1457.

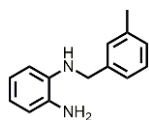
N-(2-methylbenzyl)benzene-1,2-diamine (**4.5b**):



Yield 56% (1.2 g from 10.0 mmol scale of corresponding benzyl bromide); White solid; **mp** 85-87 °C; $^1\text{H NMR}$ (300 MHz, CDCl_3) δ 7.36 (d, $J = 6.2$ Hz, 1H), 7.30 – 7.14 (m,

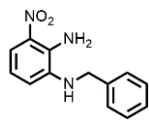
3H), 6.91 – 6.80 (m, 1H), 6.79 – 6.69 (m, 3H), 4.28 (s, 2H), 3.34 (bs, 3H), 2.41 (s, 3H); ¹³C NMR (75 MHz, CDCl₃) δ 137.8, 137.1, 136.7, 134.2, 130.52, 128.6, 127.5, 126.2, 120.8, 118.9, 116.5, 111.9, 46.7, 19.0; IR (neat, cm⁻¹): 3339, 3257, 3019, 2966, 1603, 1506, 1312, 1261, 759.

N-(3-methylbenzyl)benzene-1,2-diamine (**4.5c**)²²⁹:



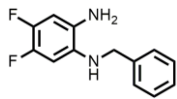
Yield 60% (636 mg from 5.0 mmol scale of corresponding benzyl bromide); Brown liquid; ¹H NMR (300 MHz, CDCl₃) δ 7.34 – 7.20 (m, 3H), 7.14 (d, *J* = 7.1 Hz, 1H), 6.90 – 6.81 (m, 1H), 6.81 – 6.68 (m, 3H), 4.30 (s, 2H), 3.41 (s, 1H), 2.40 (s, 3H); ¹³C NMR (75 MHz, CDCl₃) δ 139.4, 138.3, 137.8, 134.2, 128.7, 128.6, 128.1, 124.9, 120.8, 118.8, 116.5, 112.0, 48.7, 21.5; IR (neat, cm⁻¹): 3394, 3328, 3020, 2916, 1595, 1452, 1312, 1223, 1141, 1055.

N-benzyl-6-nitrobenzene-1,2-diamine (**4.5d**)²³⁰:



Yield 50% (642 mg from 5.0 mmol scale of corresponding benzyl bromide); Brown solid; **mp** 83-84 °C; ¹H NMR (300 MHz, CD₃OD) δ 7.46 (d, *J* = 8.7 Hz, 1H), 7.41 – 7.20 (m, 5H), 6.65 (d, *J* = 7.4 Hz, 1H), 6.54 – 6.46 (m, 1H), 4.38 (s, 2H); ¹³C NMR (75 MHz, CDCl₃) δ 138.2, 137.7, 136.6, 133.4, 128.9, 128.0, 127.9, 117.9, 117.1, 116.7, 49.3; IR (neat, cm⁻¹): 3456, 3351, 3095, 2924, 1621, 1518, 1378, 1330, 1251, 1218; **HRMS**: 243.0887[M-H]⁺, Predicted: 243.0882

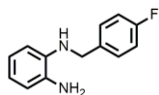
N-benzyl-4,5-difluorobenzene-1,2-diamine (**4.5e**)¹⁴²:



Yield 53% (620 mg from 5.0 mmol scale of corresponding benzyl bromide); Brown solid; **mp** 79-80 °C; ¹H NMR (300 MHz, DMSO-*d*₆) δ 7.40 – 7.27 (m, 4H), 7.24 (ddd, *J* = 6.6, 3.9, 1.9 Hz, 1H), 6.51 (dd, *J* = 12.7, 8.3 Hz, 1H), 6.24 (dd, *J* = 13.5, 8.1 Hz, 1H), 5.27 (t, *J*

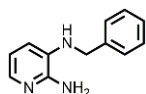
= 5.4 Hz, 1H), 4.77 (s, 2H), 4.26 (d, $J = 5.7$ Hz, 2H); $^{13}\text{C NMR}$ (75 MHz, DMSO- d_6) δ 139.68, 132.29, 132.19, 132.02, 131.94, 128.34, 127.30, 126.79, 101.94, 101.66, 98.91, 98.61, 47.06; **IR** (neat, cm^{-1}): 3407, 3334, 3033, 2874, 2846, 1615, 1523, 1437, 1223, 1182, 1066

N-(4-fluorobenzyl)benzene-1,2-diamine (**4.5f**)¹⁴²:



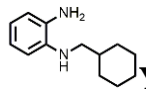
Yield 55% (594 mg from 5.0 mmol scale of corresponding benzyl bromide); Yellow liquid; $^1\text{H NMR}$ (500 MHz, CDCl_3) δ 7.39 – 7.33 (m, 2H), 7.04 (t, $J = 8.7$ Hz, 2H), 6.81 (ddd, $J = 7.8, 7.2, 1.8$ Hz, 1H), 6.73 (dtd, $J = 8.9, 7.6, 1.5$ Hz, 2H), 6.65 (dd, $J = 7.8, 1.2$ Hz, 1H), 4.29 (s, 2H), 3.36 (bs, 1H); $^{13}\text{C NMR}$ (125 MHz, CDCl_3) δ 162.19 (d, $J = 245.0$ Hz), 137.6, 135.20 (d, $J = 3.1$ Hz), 134.2, 129.41 (d, $J = 8.1$ Hz), 120.8, 119.0, 116.7, 115.54 (d, $J = 21.4$ Hz), 112.1, 48.0; $^{19}\text{F NMR}$ (471 MHz, CDCl_3) δ -115.4; **IR** (neat, cm^{-1}): 3400, 3326, 3256, 3060, 2849, 1621, 1504, 1452, 1341, 1267.

*N*3-benzylpyridine-2,3-diamine (**4.5g**)¹⁴²:



Yield 67% (133 mg from reduction of corresponding imine); Brown liquid; $^1\text{H NMR}$ (300 MHz, CDCl_3) δ 7.56 (ddd, $J = 5.1, 1.4, 0.8$ Hz, 1H), 7.39 – 7.34 (m, 4H), 7.34 – 7.28 (m, 1H), 6.79 (dd, $J = 7.7, 0.5$ Hz, 1H), 6.67 (dd, $J = 5.1, 0.8$ Hz, 1H), 6.65 (dd, $J = 5.1, 0.9$ Hz, 1H), 4.53 (bs, 2H), 4.31 (d, $J = 3.6$ Hz, 2H), 3.89 (bs, 1H); $^{13}\text{C NMR}$ (125 MHz, CDCl_3) δ 148.7, 138.5, 135.5, 132.1, 128.8, 127.7, 127.6, 117.4, 115.8, 48.2; **IR** (neat, cm^{-1}): 3448, 3356, 3297, 3217, 3013, 1640, 1575, 1229, 1068.

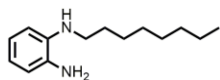
N-(cyclohexylmethyl)benzene-1,2-diamine (**4.5i**)¹⁴²:



Yield 51% (520 mg from 5.0 mmol scale of benzyl bromide); Brown liquid; $^1\text{H NMR}$ (300 MHz, CDCl_3) δ 6.84 (m, 1H), 6.76 – 6.65 (m, 3H), 3.40 (bs, 3H), 2.97 (d, $J = 6.6$ Hz, 2H),

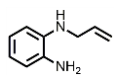
1.96 – 1.84 (m, 2H), 1.83 – 1.59 (m, 4H), 1.39 – 1.17 (m, 3H), 1.14 – 0.94 (m, 2H); ^{13}C NMR (75 MHz, CDCl_3) δ 138.0, 134.2, 120.89, 118.4, 116.6, 111.9, 51.0, 37.6, 31.5, 26.7, 26.1; **IR** (neat, cm^{-1}): 3401, 3348, 3265, 3038, 2944, 1599, 1496, 1448, 1261, 1226, 1110.

N-octylbenzene-1,2-diamine (**4.5j**)²³¹:



Yield 51% (561 mg from 5.0 mmol scale of octyl bromide); Brown liquid; ^1H NMR (500 MHz, CDCl_3) δ 6.90 – 6.86 (m, 1H), 6.76 – 6.70 (m, 3H), 3.37 (bs, 3H), 3.16 – 3.11 (m, 2H), 1.71 (dt, $J = 14.7, 7.2$ Hz, 2H), 1.48 (dt, $J = 15.1, 7.0$ Hz, 2H), 1.43 – 1.32 (m, 9H), 0.96 (t, $J = 7.0$ Hz, 3H); ^{13}C NMR (125 MHz, CDCl_3) δ 138.1, 134.0, 120.7, 118.3, 116.6, 111.6, 44.3, 31.9, 29.7, 29.5, 29.3, 27.3, 22.7, 14.3; **IR** (neat, cm^{-1}): 3409, 3324, 3071, 2974, 1614, 1501, 1410, 1372, 1272, 1108, 1033.

N-allylbenzene-1,2-diamine (**4.5k**)²³⁰:



Yield 59% (436 mg from 5.0 mmol scale of corresponding allyl bromide); Brown liquid; ^1H NMR (500 MHz, CDCl_3) δ 6.83 (m, 1H), 6.76 – 6.66 (m, 3H), 6.03 (ddt, $J = 17.2, 10.3, 5.5$ Hz, 1H), 5.32 (dq, $J = 17.2, 1.7$ Hz, 1H), 5.20 (dq, $J = 10.3, 1.5$ Hz, 1H), 3.79 (dt, $J = 5.6, 1.6$ Hz, 2H), 3.48 (s, 3H); ^{13}C NMR (125 MHz, CDCl_3) δ 137.2, 135.5, 134.5, 120.7, 119.1, 116.7, 116.6, 112.5, 47.0; **IR** (neat, cm^{-1}): 3379, 3345, 3288, 3077, 2957, 1610, 1379, 1275, 1130.

J. General Procedure for the Synthesis of Substrates **5.1a-5.1zc**:

K.1. Nucleophilic Substitution Strategy:

Substrates **5.1a-5.1m**, **5.1r** and **5.1zc** were synthesized utilizing nucleophilic substitution reaction strategy using α,α' -dibromo-*o*-xylene and primary amine derivatives in presence of base potassium carbonate.

In a representative example, α,α' -dibromo-*o*-xylene (500 mg, 1.76 mmol) and aniline (164 mg, 1.76 mmol) were dissolved in 10 mL acetonitrile. Potassium carbonate (690 mg, 5 mmol) was then added to the reaction mixture. This resulting mixture was heated at 60 °C for 18 hours under Argon atmosphere. After the completion of reaction as indicated by TLC analysis, the precipitate was filtered and the residue was washed with 5 mL of acetonitrile. The filtrate solution was concentrated under reduced pressure, giving the crude product, which was purified by column chromatography (SiO₂; hexanes: ethyl acetate; 1:5; $R_f = 0.4$) which afforded 74% (254 mg, 1.30 mmol) of *N*-phenylisoindoline (**5.1a**) as white solid.

K.2. Phthalimide Reduction Strategy:

Substrates **5.1f**, **5.1g**, **5.1n**, **5.1o**, **5.1p**, **5.1q**, **5.1u**, **5.1z**, and **5.1zb** were synthesized by reducing 2-arylphthalimide with BH₃ in THF.

In a representative example, 5-methyl-*N*-phenylphthalimide (474 mg, 2.0 mmol) was dissolved in 10 mL distilled THF and stirred in an ice/water bath at 0 °C. Over five minutes, 6 mL of 1M BH₃ in THF (8 mmol) was added dropwise, to the reaction. The resulting solution was heated under reflux for 6 hours. After cooling the reaction mixture to room temperature, methanol was added until the residual solid was dissolved. The resulting solution was diluted with 10 mL ethyl acetate. The combined organic solution was washed with brine solution, dried with anhydrous sodium sulfate and concentrate under reduced pressure. The crude product was purified by column chromatography (SiO₂; hexanes: ethyl acetate; 10:1; $R_f = 0.41$) which afforded 63% (263 mg, 1.26 mmol) of 2-phenyl-5-methylisoindoline (**5.1o**) as white solid.

K.3. Synthesis of Substrate 5.1q:

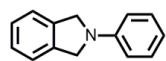
To a cold solution of 2-phenyl-4-nitrophthalimide (536 mg, 2.0 mmol) in dry THF (15 mL), was added lithium aluminum hydride (304 mg, 8.0 mmol) in small portion. The resulting mixture was

refluxed under nitrogen. After the completion of reaction in 4 hours, the reaction mixture was quenched with water (0.5 mL) and saturated Na₂CO₃ solution (1 mL). The white precipitate so formed was filtrated out and the filtrate was concentrated under reduced pressure. The crude product was purified by column chromatography (SiO₂; hexanes: ethyl acetate; 5:1; R_f =0.34) which afforded 58% (243.9 mg, 1.16 mmol) of 2-phenyl-4-aminoIsoindoline (**5.1q**) as brown solid.

K.4. Synthesis of Substrate **5.1w**:

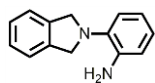
To a mixture of 2-(3,4-dimethoxyphenyl)-*N*-methylethanamine (975 mg, 5 mmol) and 37% aqueous solution of formaldehyde (1.4 mL, 29 mmol), was added 5 mL formic acid at room temperature. The resulting mixture was heated at 100 °C for 4 hours. The solution was poured into ice-water and adjusted to pH =11 by the addition of 2M sodium hydroxide solution. The solid formed was extracted with dichloromethane (15 mL x 2). The combined organic phase was dried with anhydrous Na₂SO₄ and concentrated under reduced pressure. The crude product was purified with column chromatography using silica gel to afford 88% (910 mg, 4.4 mmol) of (**5.1w**) as pale yellow solid.

2-phenylisoindoline (**5.1a**)²³²:



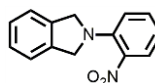
White solid; **mp** 160-162 °C; **¹H NMR** (500 MHz, CDCl₃) δ 7.39 – 7.31 (m, 6H), 6.79 (t, *J* = 7.1 Hz, 1H), 6.72 (d, *J* = 8.2 Hz, 2H), 4.68 (s, 4H); **¹³C NMR** (125 MHz, CDCl₃) δ 147.2, 138.0, 129.5, 127.2, 122.7, 116.2, 111.6, 53.8; **IR** (neat, cm⁻¹): 3038, 3040, 2923, 1588, 1463, 1181, 1091.

2-(2-amino)phenylisoindoline (**5.1b**)¹⁴²:



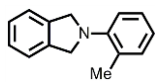
Pale brown solid; **mp** 100-101 °C; **¹H NMR** (500 MHz, CDCl₃) δ 7.34 – 7.24 (m, 5H), 7.21 (dd, *J* = 8.3, 1.3 Hz, 1H), 6.99 – 6.95 (m, 1H), 6.83 – 6.76 (m, 2H), 4.48 (s, 4H), 3.99 (bs, 2H); **¹³C NMR** (125 MHz, CDCl₃) δ 142.4, 139.9, 136.9, 127.0, 124.5, 122.4, 121.4, 120.5, 118.9, 115.8, 56.5; **IR** (neat, cm⁻¹): 3414, 3392, 2802, 1614, 1500, 1469.

2-(2-nitro)phenylisoindoline (**5.1c**)¹⁴²:



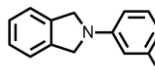
Orange solid; **mp** 105-107 °C; **¹H NMR** (500 MHz, CDCl₃) δ 7.70 (dd, *J* = 8.1, 1.7 Hz, 1H), 7.44 (ddd, *J* = 8.7, 7.1, 1.7 Hz, 1H), 7.29 (s, 4H), 7.02 (dd, *J* = 8.6, 1.0 Hz, 1H), 6.79 (ddd, *J* = 8.2, 7.1, 1.1 Hz, 1H), 4.66 (s, 4H); **¹³C NMR** (125 MHz, CDCl₃) δ 141.4, 138.08, 136.5, 133.0, 127.6, 126.7, 122.3, 116.4, 55.6; **IR** (neat, cm⁻¹): 3055, 2922, 2902, 1512, 1512, 1463, 1377, 1255, 1174.

2-(2-methyl)phenylisoindoline (**5.1d**)²³³:



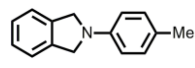
White solid; **mp** 114-115 °C; **¹H NMR** (300 MHz, CDCl₃) δ 7.40 – 7.32 (m, 4H), 7.30 – 7.24 (m, 2H), 7.14 (d, *J* = 8.0 Hz, 1H), 6.99 (t, *J* = 7.2 Hz, 1H), 4.69 (s, 4H), 2.53 (s, 3H); **¹³C NMR** (75 MHz, CDCl₃) δ 148.3, 139.2, 132.2, 129.4, 127.1, 126.8, 122.4, 121.2, 117.3, 56.6, 21.1; **IR** (neat, cm⁻¹): 3043, 2911, 2852, 1520, 1371, 1254, 1163.

2-(3-bromophenyl)isoindoline (**5.1e**):

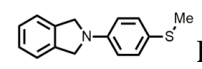


Pale yellow liquid; **¹H NMR** (500 MHz, CDCl₃) δ 7.36 – 7.30 (m, 4H), 7.14 (t, *J* = 8.0 Hz, 1H), 6.85 (d, *J* = 7.8 Hz, 1H), 6.80 (s, 1H), 6.58 (d, *J* = 6.7 Hz, 1H), 4.63 (s, 4H); **¹³C NMR** (125 MHz, CDCl₃) δ 148.3, 137.5, 134.7, 130.6, 127.4, 122.7, 119.0, 114.4, 110.3, 53.8; **IR** (neat, cm⁻¹): 3045, 2966, 1589, 1489, 1479, 1467, 1388, 1217, 993; **HRMS**: 274.0232 [M+H]⁺, Predicted: 274.0226

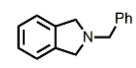
2-(4-methyl)phenylisoindoline (**5.1f**)²³²:

 White solid; **mp** 120-121 °C; **¹H NMR** (300 MHz, CDCl₃) δ 7.38 – 7.28 (m, 4H), 7.13 (d, *J* = 8.3 Hz, 2H), 6.64 (d, *J* = 8.4 Hz, 2H), 4.65 (s, 4H), 2.30 (s, 3H); **¹³C NMR** (75 MHz, CDCl₃) δ 145.1, 142.1, 138.1, 130.0, 127.2, 122.6, 111.9, 54.3, 20.4; **IR** (neat, cm⁻¹): 3045, 2914, 2854, 1523, 1371, 1255, 1165.

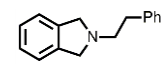
2-(4-thiomethyl)phenylisoindoline (**5.1g**):

 Pale yellow solid; **mp** 210-211 °C; **¹H NMR** (500 MHz, CDCl₃) δ 7.40 – 7.29 (m, 6H), 6.67 (d, *J* = 8.2 Hz, 2H), 4.66 (s, 4H), 2.44 (s, 3H); **¹³C NMR** (125 MHz, CDCl₃) δ 146.0, 137.6, 132.0, 127.4, 123.7, 122.7, 112.6, 54.3, 19.5; **IR** (neat, cm⁻¹): 3043, 2846, 2825, 1608, 1502, 1467, 1377, 1249, 1166; **HRMS**: 241.0803 [M+H]⁺, Predicted: 241.0812

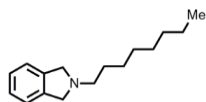
2-Benzylisoindoline (**5.1h**)²³³:

 Pale brown liquid; **¹H NMR** (500 MHz, CDCl₃) δ 7.45 (d, *J* = 7.3 Hz, 2H), 7.38 – 7.34 (m, 2H), 7.31 (dt, *J* = 4.5, 1.8 Hz, 1H), 7.21 – 7.17 (m, 4H), 4.01 (s, 4H), 3.96 (s, 2H); **¹³C NMR** (125 MHz, CDCl₃) δ 140.3, 139.2, 128.9, 128.5, 127.2, 126.7, 122.4, 60.4, 59.0; **IR** (neat, cm⁻¹): 3044, 2962, 1505, 1361, 1135.

2-Phenethylisoindoline (**5.1i**)²³⁴:

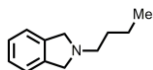
 White solid; **mp** 60-61 °C; **¹H NMR** (300 MHz, CDCl₃-D) δ 7.85 (dd, *J* = 6.8, 1.0 Hz, 1H), 7.51 (td, *J* = 7.3, 1.4 Hz, 1H), 7.45 (td, *J* = 7.4, 0.9 Hz, 1H), 7.37 (d, *J* = 7.4 Hz, 1H), 7.33 – 7.21 (m, 5H), 4.21 (s, 2H), 3.91 – 3.84 (m, 2H), 3.04 – 2.97 (m, 2H); **¹³C NMR** (125 MHz, CDCl₃) δ 140.3, 140.1, 128.7, 128.5, 126.7, 126.1, 122.3, 59.2, 58.0, 35.8; **IR** (neat, cm⁻¹): 3026, 2949, 2882, 1495, 1357, 1120.

2-Octylisoindoline (**5.1j**)²³⁵:



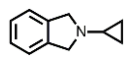
Pale brown liquid; $^1\text{H NMR}$ (500 MHz, CDCl_3) δ 7.19 (m, 4H), 3.95 (s, 4H), 2.74 – 2.70 (m, 2H), 1.63 – 1.57 (m, 2H), 1.40 – 1.25 (m, 10H), 0.89 (t, $J = 7.0$ Hz, 3H); $^{13}\text{C NMR}$ (125 MHz, CDCl_3) δ 139.8, 126.9, 122.4, 59.2, 56.4, 31.9, 29.7, 29.4, 28.8, 27.5, 22.8, 14.2; **IR** (neat, cm^{-1}): 3027, 2926, 2854, 1465, 1364, 1324, 1149.

2-Butylisoindoline (**5.1k**)²³⁶:



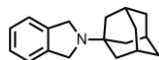
Pale brown liquid; $^1\text{H NMR}$ (500 MHz, CDCl_3) δ 7.20 – 7.17 (m, 4H), 3.92 (s, 4H), 2.74 – 2.69 (m, 2H), 1.62 – 1.55 (m, 2H), 1.42 (m, 2H), 0.96 (t, $J = 7.4$ Hz, 3H); $^{13}\text{C NMR}$ (125 MHz, CDCl_3) δ 140.35, 126.7, 122.3, 59.2, 56.1, 31.2, 20.7, 14.2; **IR** (neat, cm^{-1}): 3038, 2955, 2929, 1463, 1325, 1152.

2-Cyclopropylisoindoline (**5.1l**)²³⁷:



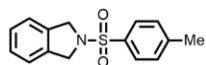
Colorless liquid; $^1\text{H NMR}$ (300 MHz, CDCl_3) δ 7.19 (d, $J = 0.8$ Hz, 4H), 4.06 (s, 4H), 2.08 – 1.99 (m, 1H), 0.58 – 0.49 (m, 4H); $^{13}\text{C NMR}$ (75 MHz, CDCl_3) δ 140.3, 126.8, 122.5, 58.9, 35.6, 6.1; **IR** (neat, cm^{-1}): 3082, 3007, 2935, 2796, 1462, 1348, 1016.

2-Adamantylisoindoline (**5.1m**)²³⁶:



White solid; **mp** 202-203 °C; $^1\text{H NMR}$ (500 MHz, CDCl_3) δ 7.23 – 7.16 (m, 4H), 4.11 (s, 4H), 2.14 (m, 3H), 1.82 (d, $J = 2.7$ Hz, 6H), 1.74 – 1.63 (m, 6H); $^{13}\text{C NMR}$ (125 MHz, CDCl_3) δ 139.6, 126.6, 122.6, 53.2, 50.2, 44.3, 39.2, 37.0, 36.3, 29.8, 29.5; **IR** (neat, cm^{-1}): 2900, 2846, 2770, 1486, 1356, 1282, 1149, 1081.

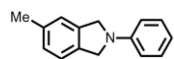
2-Tosylisoindoline (**5.1n**)²³⁸:



White solid; **mp** 174-175 °C; $^1\text{H NMR}$ (500 MHz, CDCl_3) δ 7.77 (d, $J = 8.3$ Hz, 2H), 7.31 (d, $J = 8.5$ Hz, 2H), 7.25 – 7.21 (m, 2H), 7.19 – 7.15 (m, 2H), 4.62 (s, 4H), 2.40 (s,

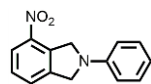
3H); ^{13}C NMR(125 MHz, CDCl_3) δ 143.8, 136.2, 133.8, 129.9, 127.8, 127.7, 122.7, 53.8, 21.6; **IR** (neat, cm^{-1}): 3074, 2974, 1720, 1469, 1344, 1170, 1080.

5-Methyl-2-phenylisoindoline (**5.1o**)²³²:



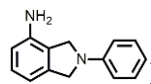
White solid; **mp** 136-138 °C; ^1H NMR (500 MHz, CDCl_3) δ 7.31 (t, $J = 7.9$ Hz, 2H), 7.23 (d, $J = 7.6$ Hz, 1H), 7.16 (s, 1H), 7.12 (d, $J = 8.0$ Hz, 1H), 6.75 (t, $J = 7.3$ Hz, 1H), 6.68 (d, $J = 8.0$ Hz, 2H), 4.62 (s, 4H), 2.40 (s, 3H); ^{13}C NMR(125 MHz, CDCl_3) δ 147.3, 138.2, 137.0, 135.0, 129.5, 128.1, 123.3, 122.4, 116.1, 111.6, 53.7, 53.6, 21.5; **IR** (diamond-ATR) γ/cm^{-1} : 3060, 2951, 2853, 1596, 1496, 1374, 1160.

2-Phenyl-5-nitroIsoindoline (**5.1p**)²³²:



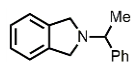
Orange solid; **mp** 128-130 °C; ^1H NMR (300 MHz, CDCl_3) δ 8.19 (d, $J = 8.6$ Hz, 1H), 7.74 – 7.61 (m, 1H), 7.53 (m, 1H), 7.34 (m, 2H), 6.89 – 6.67 (m, 3H), 5.10 (s, 2H), 4.74 (s, 2H); ^{13}C NMR (75 MHz, CDCl_3) δ 146.4, 141.9, 135.1, 130.0, 129.6, 128.8, 123.0, 122.7, 117.0, 111.8, 55.1, 53.4; **IR** (neat, cm^{-1}): 3053, 3036, 2953, 2922, 1692, 1593, 1524, 1489, 1381, 1344, 1297, 1276; **HRMS**: 241.0976 $[\text{M}+\text{H}]^+$, Predicted: 241.0972

2-Phenylisoindolin-5-amine (**5.1q**):



Brown solid; **mp**120-122 °C; ^1H NMR (500 MHz, CDCl_3) δ 7.43 – 7.38 (m, 2H), 7.20 (t, $J = 7.7$ Hz, 1H), 6.85 (dd, $J = 15.8, 7.5$ Hz, 2H), 6.74 (dd, $J = 8.7, 0.9$ Hz, 2H), 6.65 (dd, $J = 7.9, 0.7$ Hz, 1H), 4.66 (s, 2H), 4.51 (s, 2H), 3.64 (bs, 2H); ^{13}C NMR (125 MHz, CDCl_3) δ 147.1, 141.2, 139.1, 129.3, 128.5, 123.0, 116.0, 113.4, 112.7, 111.5, 54.1, 51.4; **IR** (neat, cm^{-1}): 3422, 3374, 3203, 3047, 3020, 2805, 1592, 1458, 1377, 1342, 1155; **HRMS**: 211.1124 $[\text{M}+\text{H}]^+$, Predicted: 211.1120.

(S)-2-(1-phenylethyl)isoindoline (**5.1r**):



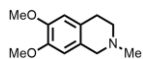
Pale pink solid; **mp** 42-44 °C; **¹H NMR** (500 MHz, CDCl₃) δ 7.46 (d, *J* = 7.3 Hz, 2H), 7.38 (t, *J* = 7.5 Hz, 2H), 7.31 (t, *J* = 7.3 Hz, 1H), 7.22 – 7.16 (m, 4H), 3.98 (d, *J* = 11.3 Hz, 2H), 3.84 (d, *J* = 11.3 Hz, 2H), 3.67 (q, *J* = 6.5 Hz, 1H), 1.53 (d, *J* = 6.6 Hz, 3H); **¹³C NMR** (125 MHz, CDCl₃) δ 145.3, 140.1, 128.6, 127.4, 127.2, 126.7, 122.4, 65.5, 58.1, 23.4; **IR** (neat, cm⁻¹): 3025, 2970, 2928, 1598, 1366, 1077; **HRMS**: 224.1434 [M+H]⁺, Predicted: 224.1434; [α]_D -35 (c 0.5, CH₂Cl₂)

2-Methyl-2,3-dihydro-1H-benzo[de]isoquinoline (**5.1u**)²³⁹:



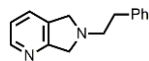
Pale brown solid; **mp** 60-61 °C; **IR** **¹H NMR** (500 MHz, CDCl₃) δ 7.70 (d, *J* = 8.2 Hz, 2H), 7.40 (dd, *J* = 8.1, 7.1 Hz, 2H), 7.21 (d, *J* = 6.8 Hz, 2H), 3.93 (s, 4H), 2.60 (s, 3H); **¹³C NMR** (125 MHz, CDCl₃) δ 133.3, 133.2, 127.8, 126.3, 125.7, 122.1, 58.7, 45.5; **IR** (neat, cm⁻¹): 3065, 2988, 2886, 1591, 1465, 1400, 1371, 1280.

6,7-Dimethoxy-2-methyl-1,2,3,4-tetrahydroisoquinoline (**5.1w**)²⁴⁰:



Pale yellow solid; **mp** 70-71 °C; **¹H NMR** (500 MHz, CDCl₃) δ 6.57 (s, 1H), 6.48 (s, 1H), 3.81 (s, 3H), 3.80 (s, 3H), 3.49 (s, 2H), 2.82 (t, *J* = 5.8 Hz, 2H), 2.64 (t, *J* = 5.9 Hz, 2H), 2.43 (s, 3H); **¹³C NMR** (125 MHz, CDCl₃) δ 147.5, 147.1, 126.4, 125.6, 111.3, 109.2, 57.5, 55.9, 55.9, 52.9, 46.0, 28.7; **IR** (neat, cm⁻¹): 3045, 2968, 1485, 1375, 1220, 1004.

6-Phenethyl-6,7-dihydro-5H-pyrrolo[3,4-b]pyridine (**5.1z**):

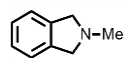


Yellow viscous oil; **¹H NMR** (500 MHz, CDCl₃) δ 8.39 (d, *J* = 4.6 Hz, 1H), 7.49 (d, *J* = 7.5 Hz, 1H), 7.33 – 7.25 (m, 4H), 7.22 (t, *J* = 7.1 Hz, 1H), 7.10 (dd, *J* = 7.5, 5.1 Hz, 1H), 4.06 (s, 2H), 4.04 (s, 2H), 3.06 – 3.00 (m, 2H), 2.97 – 2.86 (m, 2H); **¹³C NMR** (125 MHz, CDCl₃) δ 161.4, 148.1, 140.0, 133.5, 130.2, 128.7, 128.5, 126.3, 121.8, 59.6, 57.9, 57.6, 35.4; **HRMS**: 225.1295 [M+H]⁺, Predicted: 225.1292

N,N-Dibenzylpropan-2-amine (**5.1aa**):

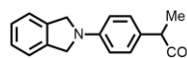
White solid; **mp** 38-40 °C; **¹H NMR** (500 MHz, CDCl₃) δ 7.42 (dd, *J* = 7.9, 1.0 Hz, 4H), 7.33 – 7.30 (m, 4H), 7.25 – 7.20 (m, 2H), 3.59 (s, 4H), 3.01 – 2.90 (m, 1H), 1.09 (d, *J* = 6.6 Hz, 6H); **¹³C NMR** (75 MHz, CDCl₃) δ 141.1, 128.6, 128.2, 126.6, 53.3, 48.2, 17.6; **IR** (neat, cm⁻¹): 3081, 3023, 2963, 2928, 1599, 1362.

2-MethylIsoindoline (**5.1ab**)²³⁴:



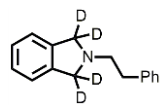
Brown liquid; **IR** (diamond-ATR) γ/cm^{-1} : 3029, 2945, 2919, 1466, 1354, 1177; **¹H NMR** (500 MHz, CDCl₃) δ 7.18 (s, 4H), 3.89 (s, 4H), 2.58 (s, 3H); **¹³C NMR** (125 MHz, CDCl₃) δ 140.5, 126.4, 121.9, 60.7, 42.1

Methyl 2-(4-(isoindolin-2-yl)phenyl)propanoate (**5.1ac**):



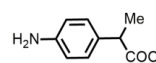
White solid; **mp** 124-126 °C; **¹H NMR** (500 MHz, CDCl₃) ¹H NMR (500 MHz, CDCl₃) δ 7.37 – 7.33 (m, 2H), 7.33 – 7.29 (m, 2H), 7.26 (d, *J* = 8.5 Hz, 2H), 6.65 (d, *J* = 8.6 Hz, 2H), 4.65 (s, 2H), 3.68 (q, 1H), 3.67 (s, 3H), 1.51 (d, *J* = 7.2 Hz, 3H); **¹³C NMR** (125 MHz, CDCl₃) δ 175.8, 146.3, 138.0, 128.5, 128.1, 127.3, 122.7, 111.7, 53.9, 52.0, 44.6, 18.8; **IR** (neat, cm⁻¹): 3041, 2978, 2944, 1726, 1520, 1373, 1159, 1067; **HRMS**: 282.1485 [M+H]⁺, Predicted: 282.1489.

1,1,3,3-tetradeuterated-2-phenethylIsoindoline (**5.1i-D4**):

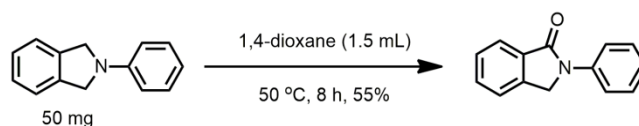


White solid; **mp** 71-72 °C; **¹H NMR** (500 MHz, CDCl₃) δ 7.41 – 7.27 (m, 4H), 3.12 – 3.03 (m, 2H), 3.02 – 2.95 (m, 2H); **¹³C NMR** (125 MHz, CDCl₃) δ 140.1, 139.7, 128.8, 128.5, 126.9, 126.3, 122.4, 57.9, 35.6; **IR** (neat, cm⁻¹): 3057, 2948, 2901, 2387, 2171, 1600, 1454, 1303, 1260; **HRMS**: 228.1677 [M+H]⁺, Predicted: 228.1690.

methyl 2-(4-aminophenyl)propanoate (**5.4ac**)¹⁷³:


 White solid; $^1\text{H NMR}$ (500 MHz, CDCl_3) δ 7.09 (d, $J = 8.4$ Hz, 2H), 6.65 (d, $J = 8.4$ Hz, 2H), 3.76 – 3.56 (q, $J = 7.2$ Hz, 1H), 3.64 (s, 3H), 3.63 (bs, 2H), 1.45 (d, $J = 7.2$ Hz, 3H); $^{13}\text{C NMR}$ (125 MHz, CDCl_3) δ 175.6, 145.3, 130.7, 128.4, 115.4, 52.0, 44.6, 18.7.

K. General procedure for synthesis of Isoindolinone derivative (**5.2a-5.2zc**):

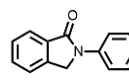


In a representative example, starting material **5.1a** (50 mg, 0.25 mmol) in flame dried 10 mL RB flask was added with 1.5 mL 1,4-dioxane. The reaction mixture was heated for 8 hours at 50 °C in open air. After the completion of reaction, the reaction mixture was directly concentrated under reduced pressure. The crude product was purified by column chromatography (SiO_2 ; hexanes: ethyl acetate, 10:1; $R_f=0.25$) to afford 55% (28 mg, 0.14 mmol) of 2-phenylisoindolin-1-one (**5.2a**) as white solid.

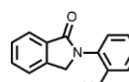
The reaction under O_2 balloon was set up similar to the procedure described above except that the flask was purged with O_2 for three cycles and sealed properly with the septum.

For a gram scale reaction with substrate **5.1i**, **5.1i** (1.78 g, 8 mmol) was added into flame-dried 100 mL round bottom flask. 50 mL of 1,4-dioxane was added in the flask. The resulting solution was then heated in oil bath at 50 °C in open air for 6 hours. The solution was concentrated under reduced pressure and the crude product was purified by column chromatography (SiO_2 ; hexanes: ethyl acetate; 5:1; $R_f=0.1$) to afford 59% (1.12 g, 4.72 mmol) of 2-phenethylisoindolin-1-one (**5.2i**) as white solid.

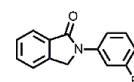
2-Phenylisoindolin-1-one (**5.2a**)¹⁷³:

 **Yield** 55%; $R_f=0.25$ (SiO₂; hexanes: ethyl acetate, 10:1); White solid; **mp** 161-162 °C; **¹H NMR** (500 MHz, CDCl₃) δ 7.93 (d, $J = 7.4$ Hz, 1H), 7.87 (dd, $J = 8.8, 1.1$ Hz, 2H), 7.62 – 7.58 (m, 1H), 7.53 – 7.49 (m, 2H), 7.45 – 7.41 (m, 2H), 7.18 (tt, $J = 7.6, 1.1$ Hz, 1H), 4.87 (s, 2H); **¹³C NMR** (125 MHz, CDCl₃) δ 167.6, 140.2, 139.5, 133.3, 132.1, 129.2, 128.4, 124.5, 124.2, 122.7, 119.5, 50.8; **IR** (neat, cm⁻¹): 3042, 2924, 1683, 1594, 1491, 1329, 1265, 1222, 1151.

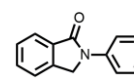
2-(o-tolyl)isoindolin-1-one (**5.2d**)¹⁷³:

 **Yield** 64%; $R_f=0.28$ (SiO₂; hexanes: ethyl acetate; 10:1); White solid; **mp** 129-130 °C; **¹H NMR** (300 MHz, CDCl₃) δ 7.95 (dd, $J = 7.1, 1.2$ Hz, 1H), 7.60 (ddd, $J = 6.9, 6.5, 1.3$ Hz, 1H), 7.55 – 7.48 (m, 2H), 7.33 – 7.23 (m, 4H), 4.72 (s, 2H), 2.25 (s, 3H); **¹³C NMR** (75 MHz, CDCl₃) δ 167.7, 141.6, 137.0, 136.4, 132.5, 131.7, 131.3, 128.3, 128.3, 127.5, 126.9, 124.3, 122.9, 53.1, 18.3; **IR** (neat, cm⁻¹): 3053, 2955, 2924, 1685, 1602, 1451, 1388, 1302, 1213, 1123.

2-(3-bromophenyl)isoindolin-1-one (**5.2e**)¹⁷³:

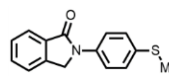
 **Yield** 49%; $R_f=0.41$ (SiO₂; hexanes: ethyl acetate; 10:1); Pale brown solid; **mp** 178-180 °C; **¹H NMR** (500 MHz, CDCl₃) δ 8.07 – 8.04 (m, 1H), 7.92 (dd, $J = 8.0, 1.4$ Hz, 1H), 7.89 (dt, $J = 6.8, 2.2$ Hz, 1H), 7.64 – 7.60 (m, 1H), 7.54 – 7.50 (m, 2H), 7.31 – 7.28 (m, 2H), 4.84 (s, 2H); **¹³C NMR** (125 MHz, CDCl₃) δ 167.6, 140.9, 139.9, 132.9, 132.5, 130.5, 128.6, 127.3, 124.4, 123.0, 122.7, 122.0, 117.7, 50.6; **IR** (neat, cm⁻¹): 3113, 3044, 2950, 1689, 1561, 1432, 1374, 1299, 1197, 1091.

2-(p-tolyl)isoindolin-1-one (**5.2f**)²⁴¹:

 **Yield** 61%; $R_f=0.24$ (SiO₂; hexanes: ethyl acetate; 10:1); White solid; **mp** 125-126 °C **¹H NMR** (500 MHz, CDCl₃) δ 7.92 (d, $J = 7.3$ Hz, 1H), 7.74 (d, $J = 8.5$ Hz, 2H), 7.62 – 7.56

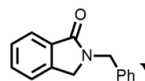
(m, 1H), 7.53 – 7.48 (m, 2H), 7.23 (d, $J = 8.3$ Hz, 2H), 4.84 (s, 2H), 2.36 (s, 3H); ^{13}C NMR (125 MHz, CDCl_3) δ 167.4, 140.2, 137.0, 134.3, 133.4, 132.0, 129.7, 128.4, 124.2, 122.6, 119.7, 50.9, 20.9; ; **IR** (neat, cm^{-1}): 3140, 2918, 1660, 1512, 1390, 1305.

2-(4-(methylthio)phenyl)isoindolin-1-one (**5.2g**)¹⁷³:



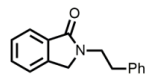
Yield 63%; $R_f = 0.19$ (SiO_2 ; hexanes: ethyl acetate; 5:1); Pale yellow solid; **mp** 168-170 °C; ^1H NMR (500 MHz, CDCl_3) δ 7.92 (dd, $J = 6.8, 1.7$ Hz, 1H), 7.81 (d, $J = 8.9$ Hz, 2H), 7.62 – 7.58 (m, 1H), 7.51 (m, 2H), 7.34 (d, $J = 8.9$ Hz, 2H), 4.84 (s, 1H), 2.51 (s, 1H); ^{13}C NMR (125 MHz, CDCl_3) δ 167.5, 140.1, 137.2, 134.0, 133.3, 132.2, 128.5, 128.1, 124.2, 122.7, 120.1, 50.8, 16.7; **IR** (neat, cm^{-1}): 2922, 1685, 1492, 1440, 1386, 1336, 1222, 1155, 1060.

2-Benzylisoindolin-1-one (**5.2h**)¹⁷²:



Yield 61%; $R_f = 0.15$ (SiO_2 ; hexanes: ethyl acetate; 10:1); White solid; **mp** 86-87 °C; ^1H NMR (500 MHz, CDCl_3) δ 7.90 (d, $J = 7.5$ Hz, 1H), 7.52 (td, $J = 7.5, 1.0$ Hz, 1H), 7.47 (t, $J = 7.3$ Hz, 1H), 7.38 (d, $J = 7.4$ Hz, 1H), 7.35 – 7.27 (m, 5H), 4.81 (s, 2H), 4.27 (s, 2H); ^{13}C NMR (125 MHz, CDCl_3) δ 168.6, 141.3, 137.1, 132.7, 131.4, 128.9, 128.3, 128.1, 127.8, 124.0, 122.8, 49.5, 46.5; **IR** (neat, cm^{-1}): 3028, 2977, 1670, 1567, 1494, 1316, 1255, 1158.

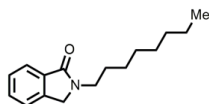
2-Phenethylisoindolin-1-one (**5.2i**)²⁴²:



Yield 68%; $R_f = 0.1$ (SiO_2 ; hexanes: ethyl acetate; 5:1); White solid; **mp** 93-95 °C; ^1H NMR (300 MHz, CDCl_3) δ 7.85 (d, $J = 7.2$ Hz, 1H), 7.51 (td, $J = 7.3, 1.4$ Hz, 1H), 7.45 (t, $J = 7.1$ Hz, 1H), 7.37 (d, $J = 7.3$ Hz, 1H), 7.33 – 7.21 (m, 5H), 4.21 (s, 2H), 3.88 (t, $J = 7.3$ Hz, 2H), 3.00 (t, $J = 7.3$ Hz, 2H); ^{13}C NMR (125 MHz, CDCl_3) δ 168.6, 141.2, 138.9, 133.0, 131.3, 128.8, 128.7,

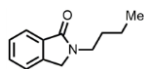
128.1, 126.6, 123.7, 122.7, 50.7, 44.2, 35.0; **IR** (neat, cm^{-1}): 3059, 2913, 1671, 1448, 1409, 1303, 1211, 1127.

2-Octylisoindolin-1-one (**5.2j**)¹⁸²:



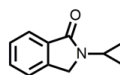
Yield 69%; $R_f=0.2$ (SiO_2 ; hexanes: ethyl acetate; 5:1); Pale yellow liquid; **^1H NMR** (500 MHz, CDCl_3) δ 7.84 (dd, $J = 7.4, 1.0$ Hz, 1H), 7.51 (td, $J = 7.5, 1.2$ Hz, 1H), 7.46 – 7.42 (m, 2H), 3.60 (t, $J = 7.4$ Hz, 2H), 1.71 – 1.60 (m, 2H), 1.34 – 1.23 (m, 10H), 0.86 (t, $J = 7.0$ Hz, 3H); **^{13}C NMR** (125 MHz, CDCl_3) δ 168.5, 141.2, 133.2, 131.1, 128.0, 123.7, 122.7, 50.0, 42.5, 31.9, 29.4, 29.3, 28.5, 27.0, 22.7, 14.2; **IR** (neat, cm^{-1}): 3038, 2923, 1680, 1468, 1226, 1105.

2-Butylisoindolin-1-one (**5.2k**)²³⁶:



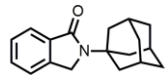
Yield 63%; $R_f=0.2$ (SiO_2 ; hexanes: ethyl acetate; 5:1); Pale yellow liquid; **^1H NMR** (500 MHz, CDCl_3) δ 7.84 (dd, $J = 7.5, 2.2$ Hz, 1H), 7.52 (td, $J = 7.5, 1.2$ Hz, 1H), 7.47 – 7.42 (m, 2H), 4.37 (s, 2H), 3.62 (t, $J = 7.3$ Hz, 2H), 1.70 – 1.59 (m, 2H), 1.44 – 1.32 (m, 2H), 0.95 (t, $J = 7.4$ Hz, 3H); **^{13}C NMR** (125 MHz, CDCl_3) δ 168.5, 141.2, 133.2, 131.2, 128.1, 123.7, 122.7, 50.0, 42.2, 30.6, 20.2, 13.9; **IR** (neat, cm^{-1}): 3047, 2957, 1675, 1469, 1377, 1210, 1172, 1094.

2-Cyclopropylisoindolin-1-one (**5.2l**)²³⁶:



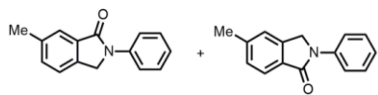
Yield 70%; $R_f=0.28$ (SiO_2 ; hexanes: ethyl acetate; 5:1); Pale yellow solid; **mp** 51-52 °C; **^1H NMR** (500 MHz, CDCl_3) δ 7.81 (d, $J = 7.6$ Hz, 1H), 7.50 (td, $J = 7.4, 1.2$ Hz, 1H), 7.45 – 7.38 (m, 2H), 4.31 (s, 2H), 2.96 – 2.90 (m, 1H), 0.94 – 0.89 (m, 2H), 0.88 – 0.83 (m, 2H); **^{13}C NMR** (75 MHz, CDCl_3) δ 169.8, 141.1, 133.3, 131.4, 128.1, 123.6, 122.7, 50.5, 25.2, 5.7; **IR** (neat, cm^{-1}): 3088, 3014, 2914, 2868, 1678, 1409, 1371, 1213, 1155, 1056.

2-(adamantan-1-yl)isoindolin-1-one (**5.2m**):



Yield 85%; R_f =0.18 (SiO₂; hexanes: ethyl acetate; 5:1); White solid; **mp** 221-222 °C; **¹H NMR** (500 MHz, CDCl₃) δ 7.78 (d, J = 7.5 Hz, 1H), 7.49 (td, J = 7.4, 1.2 Hz, 1H), 7.41 (m, 2H), 4.46 (s, 2H), 2.31 (d, J = 2.7 Hz, 6H), 2.18 – 2.14 (m, 3H), 1.80 – 1.69 (m, 6H); **¹³C NMR** (125 MHz, CDCl₃) δ 168.9, 141.0, 134.8, 130.9, 127.9, 123.3, 122.4, 55.6, 47.6, 40.2, 36.5, 29.7; **IR** (neat, cm⁻¹): 2940, 2892, 1688, 1483, 1402, 1330; **HRMS**: 290.1509 [M+Na]⁺, Predicted: 290.1515

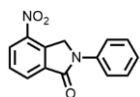
5(6)-Methyl-2-phenylisoindolin-1-one (**5.2o**)¹⁷³:



Yield 66% (45:55); R_f =0.38 (SiO₂; hexanes: ethyl acetate; 5:1); White solid; **IR** (neat, cm⁻¹): 3060, 3041, 2923, 1679, 1620, 1493, 1453, 1375, 1294, 1165, 1122; **I: 6-methyl-2-phenylisoindolin-1-one**: **¹H NMR** (500 MHz, CDCl₃) δ 7.89 – 7.85 (m, 2H), 7.73 (s, 1H), 7.45 – 7.41 (m, 4H), 7.20 – 7.15 (m, 1H), 4.82 (s, 2H), 2.49 (s, 3H); **¹³C NMR** (125 MHz, CDCl₃) δ 167.8, 139.8, 138.5, 137.4, 133.5, 133.2, 129.5, 124.4, 124.4, 122.4, 119.5, 50.7, 22.1.

II: 5-methyl-2-phenylisoindolin-1-one: **¹H NMR** (500 MHz, CDCl₃) δ 7.89 – 7.85 (m, 2H), 7.81 (d, J = 8.2 Hz, 1H), 7.40 (s, 2H), 7.31 (d, J = 6.4 Hz, 2H), 7.20 – 7.15 (m, 1H), 4.82 (s, 2H), 2.47 (s, 3H); **¹³C NMR** (125 MHz, CDCl₃) δ 167.7, 142.9, 140.6, 139.7, 130.8, 129.2, 124.5, 124.1, 123.2, 120.4, 119.5, 50.7, 21.5.

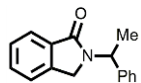
6-Nitro-2-phenylisoindolin-1-one (**5.2p**):



Yield 55%; R_f =0.22 (SiO₂; hexanes: ethyl acetate; 5:1); Orange solid; **mp** 142-143 °C; **¹H NMR** (500 MHz, CDCl₃) δ 8.47 (d, J = 8.0 Hz, 1H), 8.28 (d, J = 7.5 Hz, 1H), 7.91 (d, J =

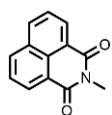
7.8 Hz, 2H), 7.76 (t, $J = 7.8$ Hz, 1H), 7.48 (t, $J = 8.0$ Hz, 2H), 7.25 (t, $J = 7.4$ Hz, 2H), 5.35 (s, 2H); ^{13}C NMR (125 MHz, CDCl_3) δ 164.9, 138.6, 136.7, 135.9, 130.5, 130.2, 129.5, 127.4, 126.7, 125.5, 119.9, 51.9; IR (neat, cm^{-1}): 3051, 3036, 2919, 2851, 1692, 1523, 1344, 1145; HRMS: 255.0763 $[\text{M}+\text{H}]^+$, Predicted: 255.0764

2-(1-phenylethyl)isoindolin-1-one (**5.2r**)²⁴³:



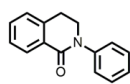
Yield 58%; $R_f = 0.18$ (SiO_2 ; hexanes: ethyl acetate; 5:1); Pale brown solid; **mp** 144-145 °C; ^1H NMR (500 MHz, CDCl_3) δ 7.88 (d, $J = 7.4$ Hz, 1H), 7.50 (td, $J = 7.4, 1.3$ Hz, 1H), 7.45 (t, $J = 7.3$ Hz, 1H), 7.39 – 7.32 (m, 5H), 7.28 (dt, $J = 4.7, 2.1$ Hz, 1H), 5.82 (q, $J = 7.3$ Hz, 1H), 4.33 (d, $J = 17.0$ Hz, 1H), 4.00 (d, $J = 17.0$ Hz, 1H), 1.70 (d, $J = 7.1$ Hz, 3H); ^{13}C NMR (125 MHz, CDCl_3) δ 168.2, 141.4, 140.8, 133.0, 131.3, 128.8, 128.1, 127.7, 127.2, 123.9, 122.9, 49.2, 45.7, 17.4; IR (neat, cm^{-1}): 3087, 2986, 1668, 1497, 1347, 1161; $[\alpha]_D -167$ (c 0.1, CH_2Cl_2) {Ref: -161.3 (c 1.33, CHCl_3)}

2-Methyl-1H-benzo[de]isoquinoline-1,3(2H)-dione (**5.2u**)²⁴⁴:



Yield 37%; $R_f = 0.3$ (SiO_2 ; hexanes: ethyl acetate; 5:1); White solid; **mp** 206-207 °C; ^1H NMR (500 MHz, CDCl_3) δ 8.61 (dd, $J = 7.3, 1.1$ Hz, 2H), 8.21 (dd, $J = 8.4, 1.0$ Hz, 2H), 7.76 (dd, $J = 8.2, 7.2$ Hz, 2H), 3.57 (s, 3H); ^{13}C NMR (125 MHz, CDCl_3) δ 164.6, 134.1, 131.7, 131.3, 128.1, 127.0, 122.7, 27.1; IR (neat, cm^{-1}): 3070, 2954, 1697, 1588, 1439, 1397, 1279, 1232, 1201, 1182, 1033.

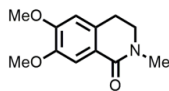
2-Phenyl-3,4-dihydroisoquinolin-1(2H)-one (**5.2v**)²⁴⁵:



Yield 46%; $R_f = 0.13$ (SiO_2 ; hexanes: ethyl acetate; 5:1); Pale brown solid; **mp** 100-101 °C; ^1H NMR (500 MHz, CDCl_3) δ 8.16 (d, $J = 7.7$ Hz, 1H), 7.47 (td, $J = 7.5, 1.3$ Hz, 1H),

7.44 – 7.36 (m, 5H), 7.28 – 7.23 (m, 2H), 3.99 (t, $J = 6.5$ Hz, 2H), 3.14 (t, $J = 6.5$ Hz, 2H); ^{13}C NMR (125 MHz, CDCl_3) δ 164.3, 143.2, 138.4, 132.1, 129.8, 129.0, 128.8, 127.2, 127.0, 126.3, 125.4, 49.5, 28.7; IR (neat, cm^{-1}): 3059, 3036, 2926, 1647, 1594, 1466, 1456, 1407, 1316, 1307, 1276, 1254, 1220, 1169, 1064.

6,7-Dimethoxy-2-methyl-3,4-dihydroisoquinolin-1(2H)-one (**5.2w**)²⁴⁶:



Yield 31%; $R_f = 0.15$ (SiO_2 ; hexanes: ethyl acetate; 2:1); White solid; **mp** 123-125 °C; ^1H NMR (301 MHz, CDCl_3) δ 7.59 (s, 1H), 6.62 (s, 1H), 3.92 (s, 3H), 3.91 (s, 3H), 3.54 (t, $J = 6.8$ Hz, 2H), 3.13 (s, 3H), 2.93 (t, $J = 6.7$ Hz, 2H); ^{13}C NMR (125 MHz, CDCl_3) δ 165.1, 151.8, 148.0, 131.7, 121.9, 110.6, 109.3, 56.2, 56.1, 48.5, 35.4, 27.6; IR (neat, cm^{-1}): 2924, 2886, 1640, 1508, 1435, 1275, 1016.

Isochroman-1-one (**5.2x**)²⁴⁷:



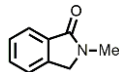
Yield 32%; $R_f = 0.35$ (SiO_2 ; hexanes: ethyl acetate; 5:1); Pale yellow liquid; ^1H NMR (500 MHz, CDCl_3) δ 8.09 (dd, $J = 7.8, 1.3$ Hz, 1H), 7.53 (td, $J = 7.5, 1.4$ Hz, 1H), 7.41 – 7.36 (m, 1H), 7.26 (d, $J = 7.6$ Hz, 1H), 4.55 – 4.51 (m, 2H), 3.06 (t, $J = 6.0$ Hz, 2H); ^{13}C NMR (125 MHz, CDCl_3) δ 165.2, 139.6, 133.7, 130.5, 127.8, 127.3, 125.4, 67.4, 27.9; IR (neat, cm^{-1}): 3071, 2990, 1714, 1605, 1470, 1391, 1291, 1193, 1118, 1089.

N-isopropylbenzamide (**5.2aa**)²⁴⁸:



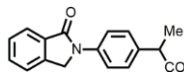
Yield 28%; $R_f = 0.1$ (SiO_2 ; hexanes: ethyl acetate; 5:1); White solid; **mp** 100-101 °C; ^1H NMR (500 MHz, CDCl_3) δ 7.75 (d, $J = 7.2$ Hz, 2H), 7.49 (t, $J = 7.3$ Hz, 1H), 7.42 (t, $J = 7.4$ Hz, 2H), 4.34 – 4.26 (m, 1H), 1.27 (d, $J = 6.6$ Hz, 6H); ^{13}C NMR (125 MHz, CDCl_3) δ 166.8, 135.1, 131.4, 128.6, 126.9, 42.0, 23.0; IR (neat, cm^{-1}): 3292, 3029, 2930, 1627, 1577, 1346, 1168.

2-Methylisoindolin-1-one (**5.2ab**)¹⁷²:



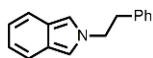
Yield 68% (0.6 mmol scale); R_f = 0.18 (SiO₂; hexanes: ethyl acetate; 2:1); Pale brown solid; **mp** 106-108 °C;; **¹H NMR** (500 MHz, CDCl₃) δ 7.83 (d, J = 7.5 Hz, 1H), 7.52 (td, J = 7.4, 1.2 Hz, 1H), 7.46 – 7.41 (m, 2H), 4.37 (s, 2H), 3.20 (s, 3H); **¹³C NMR** (125 MHz, CDCl₃) δ 168.8, 141.1, 133.0, 131.3, 128.1, 123.7, 122.7, 52.1, 29.6; **IR** (neat, cm⁻¹): 3053, 2953, 2918, 1665, 1590, 1480, 1396, 1275, 1053.

Methyl 2-(4-(1-oxoisoindolin-2-yl)phenyl)propanoate (**5.2ac**)¹⁷³:



Yield 54%; R_f = 0.16 (SiO₂; hexanes: ethyl acetate; 2:1); Pale brown solid; **mp** 120-122 °C; **¹H NMR** (500 MHz, CDCl₃) δ 7.92 (dd, J = 7.5, 1.2 Hz, 1H), 7.83 (d, J = 8.7 Hz, 2H), 7.62 – 7.58 (m, 1H), 7.53 – 7.49 (m, 2H), 7.36 (d, J = 8.5 Hz, 2H), 4.85 (s, 2H), 3.74 (q, J = 7.2 Hz, 1H), 3.67 (s, 3H), 1.52 (d, J = 7.2 Hz, 3H); **¹³C NMR** (125 MHz, CDCl₃) δ 175.1, 167.6, 140.2, 138.6, 136.7, 133.2, 132.2, 128.5, 128.3, 124.3, 122.7, 119.8, 52.2, 50.8, 44.9, 18.6; **IR** (neat, cm⁻¹): 3039, 2978, 2950, 1730, 1683, 1608, 1513, 1467, 1442, 1245, 1015.

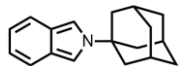
2-Phenethylisoindole (**5.3i**):



Yield 54%; R_f = 0.9 (SiO₂; hexanes: ethyl acetate; 5:1); Pale brown liquid; **¹H NMR** (500 MHz, CDCl₃) δ 7.50 (dd, J = 6.4, 3.1 Hz, 2H), 7.32 – 7.22 (m, 3H), 7.12 – 7.07 (m, H), 7.04 (s, 2H), 6.91 (dd, J = 6.6, 3.0 Hz, 2H), 4.40 (t, J = 7.5 Hz, 2H), 3.19 (t, J = 7.4 Hz, 2H); **¹³C NMR** (125 MHz, CDCl₃) δ 128.7, 128.7, 126.9, 124.4, 123.3, 120.7, 119.6, 110.6, 52.7, 38.7; **GC/MS**: t_R = 7.89 min, 221.0 m/z

Note: This compound is highly sensitive to heat, light, and moisture. As such, other analytical data were not presented due to inconsistent result.

2-((3s,5s,7s)-Adamantan-1-yl)-2H-isoindole (**5.3m**):



Substrate **5.3m** was obtained in first fraction during column chromatography during preparation of substrate **5.1m** by following general procedure described in **L.1**.

Pale pink solid; **mp** 170-172 °C; **¹H NMR** (300 MHz, CDCl₃) δ 7.54 (dd, *J* = 6.4, 3.0 Hz, 2H), 7.33 (s, 2H), 6.91 (dd, *J* = 6.5, 2.9 Hz, 2H), 2.25 (m, 9H), 1.82 (m, 6H); **¹³C NMR** (75 MHz, CDCl₃) δ 123.5, 120.4, 119.7, 106.8, 44.4, 40.1, 36.3, 29.8; **IR** (neat, cm⁻¹): 3058, 2915, 2848, 1627, 1585, 1458, 1347, 1154.

General Procedure for Gutmann-Beckett Experiment and Child's Method Experiment

*Gutmann-Beckett Method Measurements*⁹²

Triphenylphosphine oxide (5mg, 0.0179 mmol) was dissolved in CD₃CN (1cm³) in a NMR tube. Flavin **FLClO₄** (0.0539mmol, 3 equiv.) was added and allowed to dissolve, and the spectra were recorded. The ³¹P{¹H} (Pure Ph₃PO δ26.85ppm in red, equilibrium mixture δ28.94ppm in Blue) spectra indicate broadening as well as down-field shift of the phosphorus resonance. This type of behavior is generally observed for an equilibrium state between Lewis acid and Lewis base. The overall Δδ was found to be 2.09ppm.

Similar procedure was followed for Triethylphosphine oxide lewis base (0.0179 mmol) and Flavin lewis acid.

*Childs' Method Type Measurement using Formaldehyde*⁹²

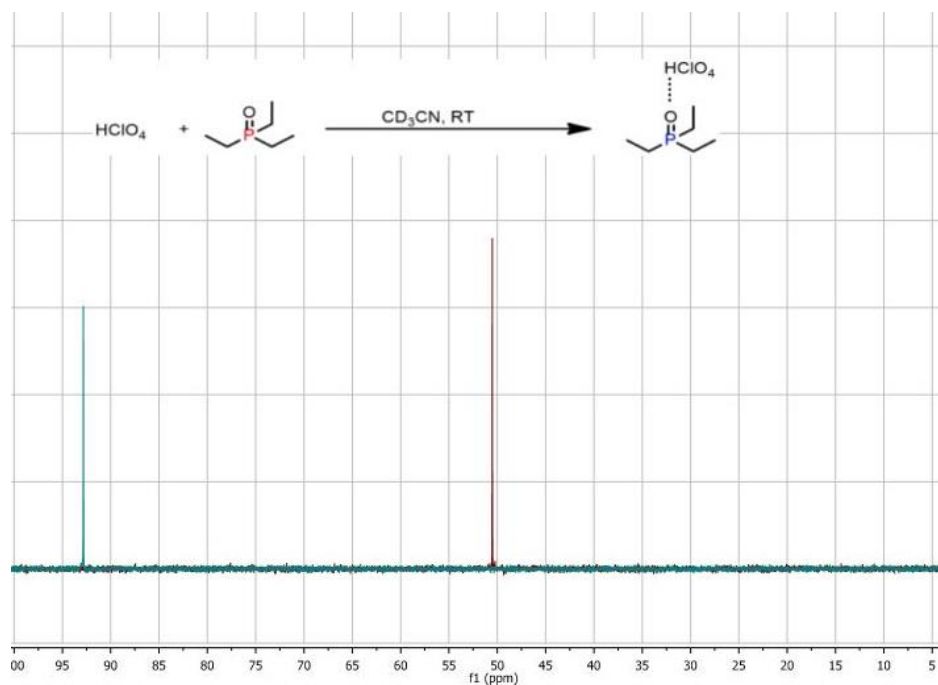
Flavin mimics (3.0 mg, 0.0074mmol) was dissolved in CD₃CN (1 cm³) followed by addition of iodobenzene as internal standard (5μl, 0.03878mmol) and the ¹H NMR was rerecorded. Formaldehyde (12.1μl, 0.03878mmol) was added and the ¹H NMR spectra were again recorded. An upfield shift in the H signal was observed for all peaks associated with Flavin while not with internal standard. For example, δ8.20 ppm peak has been shifted upfield to 8.22 ppm, indicating a very weak acid-base interaction between Flavinium species and formaldehyde.

Table AB1: Gutmann AN values for different acid sources in presence of lewis base Et₃PO

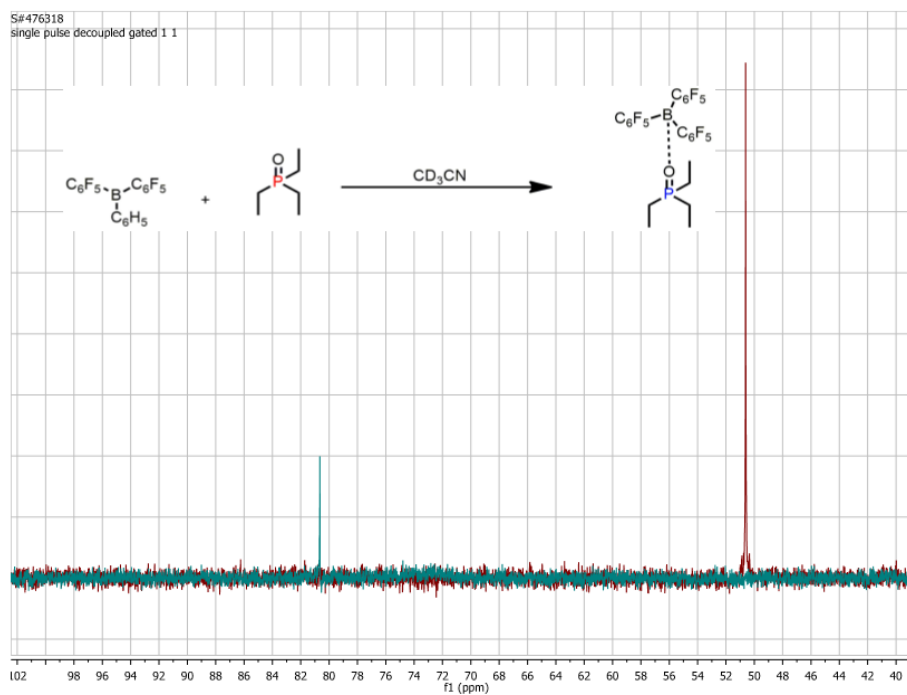
Entry	Acidic sources	Acceptor Number	Gutmann AN AN= 2.21($\delta_{\text{sample}} - 41$)
1	HClO ₄	94.3	114.6
2	B(C ₆ H ₅) ₃	66.7	87.5
3	N-MeAcridinium Iodide (Acr)	0.4	21.2
4	7,8-Dimethoxy-N ₁ ,N ₃ - Dimethylalloxazinium perchlorate (A1)	1.3	21.8
5	N ₁ ,N ₃ -Dimethylalloxazinium perchlorate (A2)	13.4	34.2
6	7,8-Dichloro-N ₁ ,N ₃ - Dimethylalloxazinium perchlorate (A3)	16.3	36.2
7	Bridgedalloxazinium chloride (BC1)	0.61 (0.56) ^a	21.61
8	8-Br-bridgedalloxazinium chloride (BC3)	31.6 (29.9) ^a	52.1
9	7-CF ₃ -bridgedalloxazinium chloride (BC5)	3.7 (1.9) ^a	24.7
10	N ₃ ,N ₁₀ -DimethylIsoalloxazinium perchlorate (IA3)	34.0	54.8
11	N ₃ -Me-N ₁₀ -PhIsoalloxazinium perchlorate (IA1)	45.3	66.0
12	FLOOH	0	20.7
13	-	0	20.7 (18.9) ^b

^aIn DMSO solvent; ^bActual value from original Gutmann experiment²⁴⁹

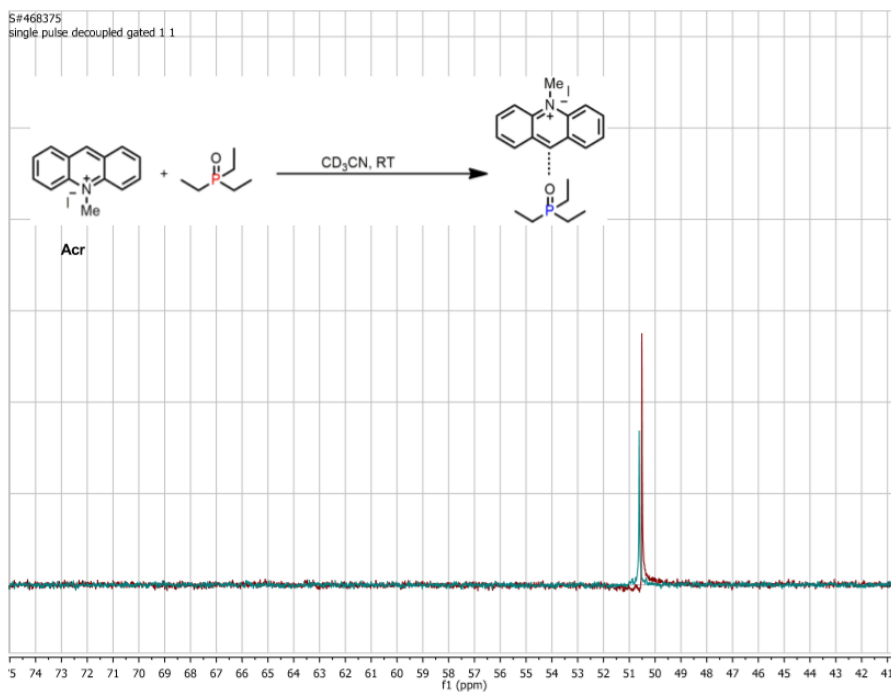
NMR overlay spectra for selected lewis acids and triethylphosphine oxide:



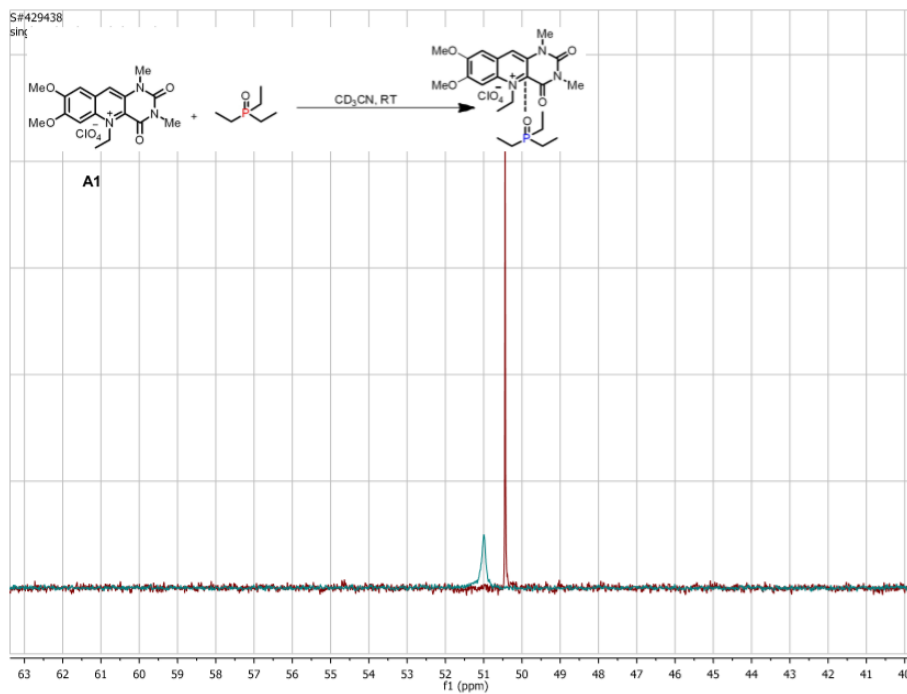
HClO_4 and Et_3PPO



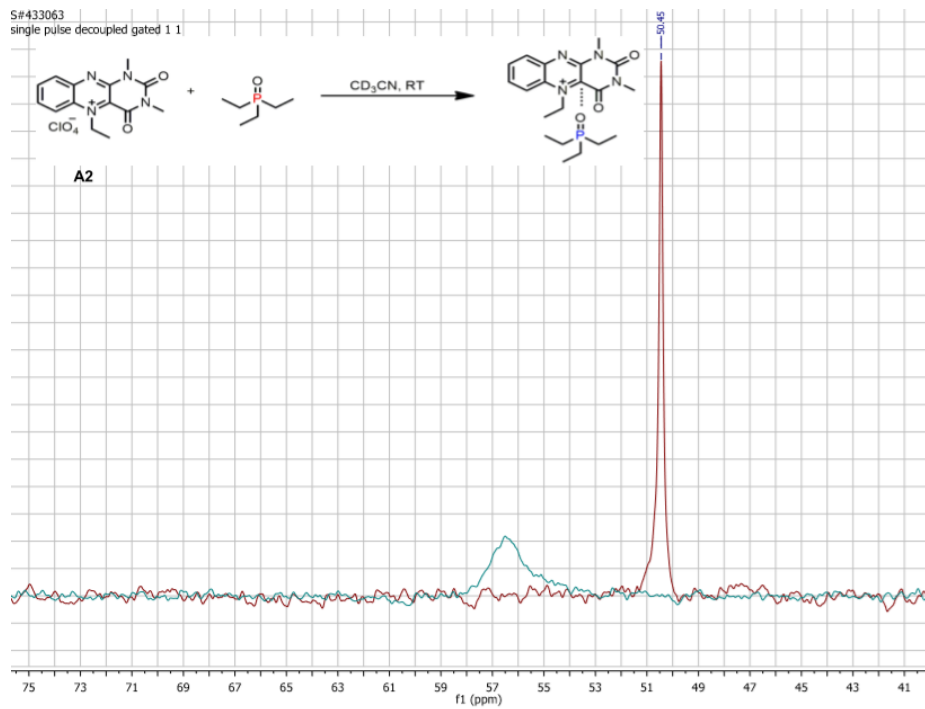
$\text{B}(\text{C}_6\text{F}_5)_3$ and Et_3PPO



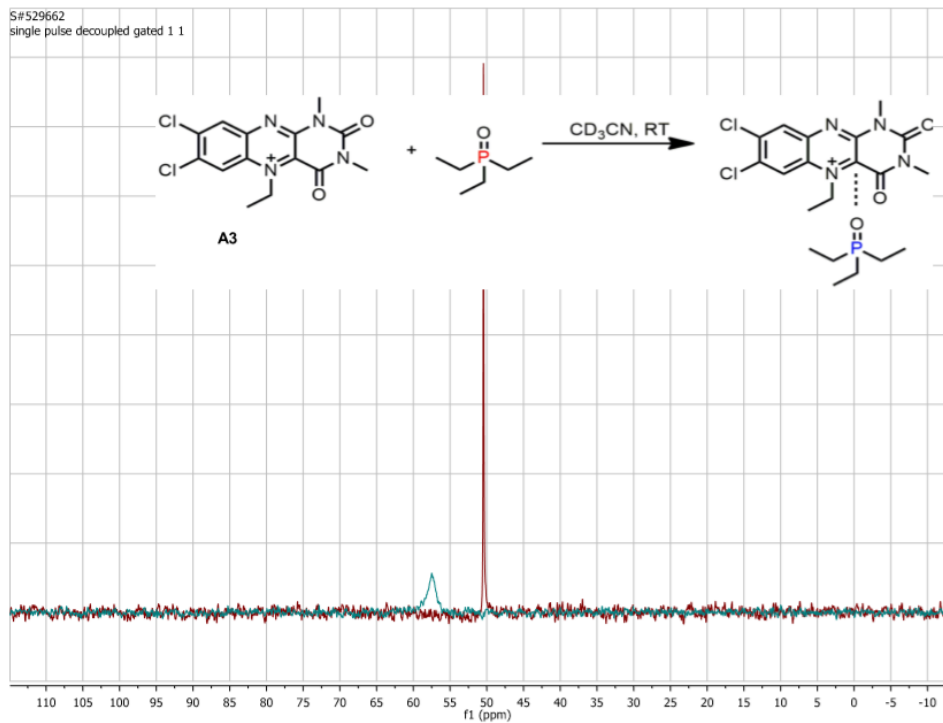
N-MeAcridinium and Et₃PPO



A1 and Et₃PPO



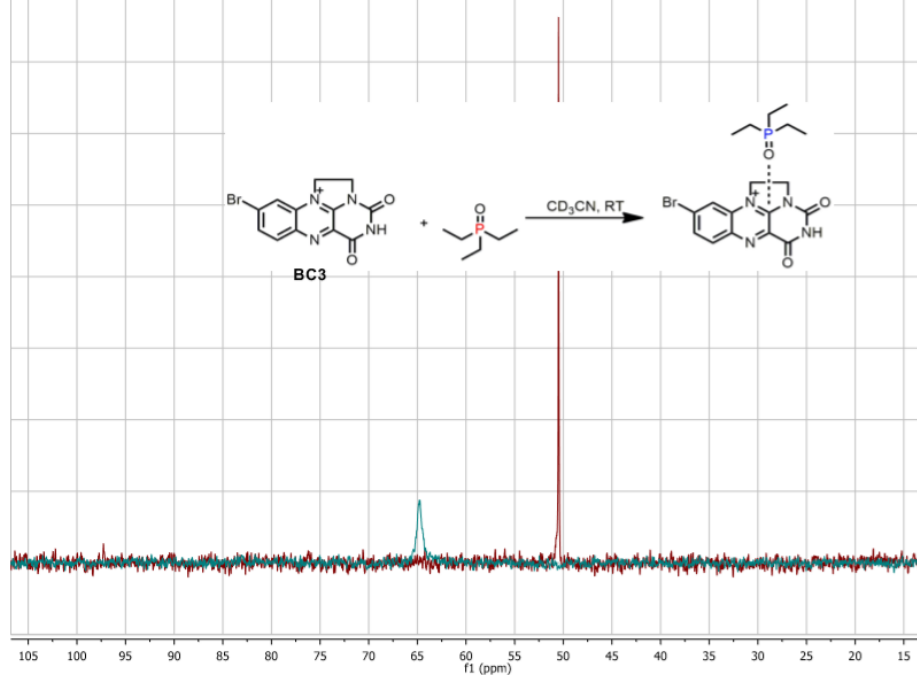
A2 and Et₃PPO



A3 and Et₃PPO

S#579110

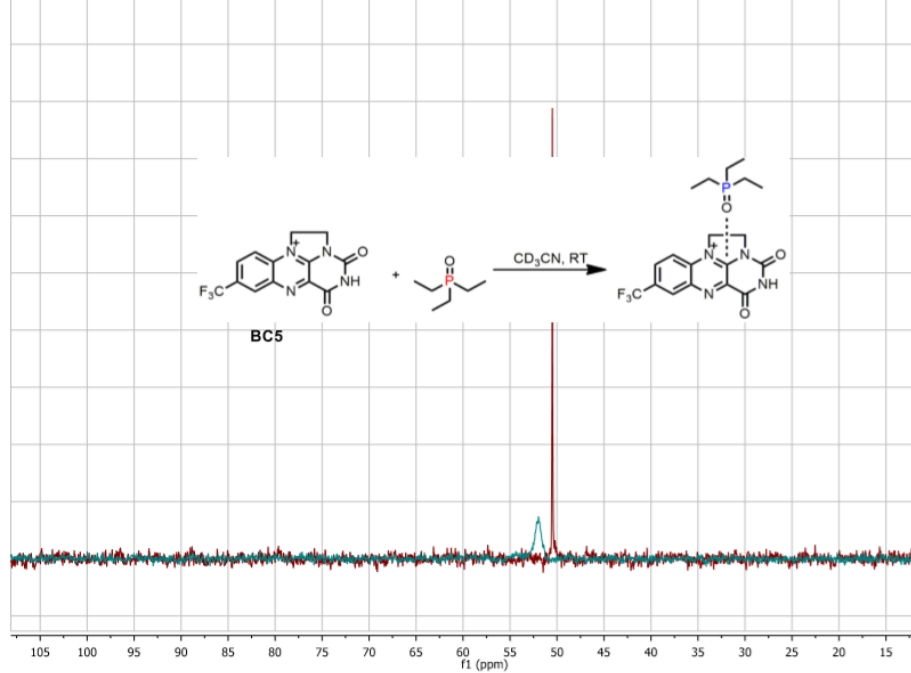
single pulse decoupled gated 1 1



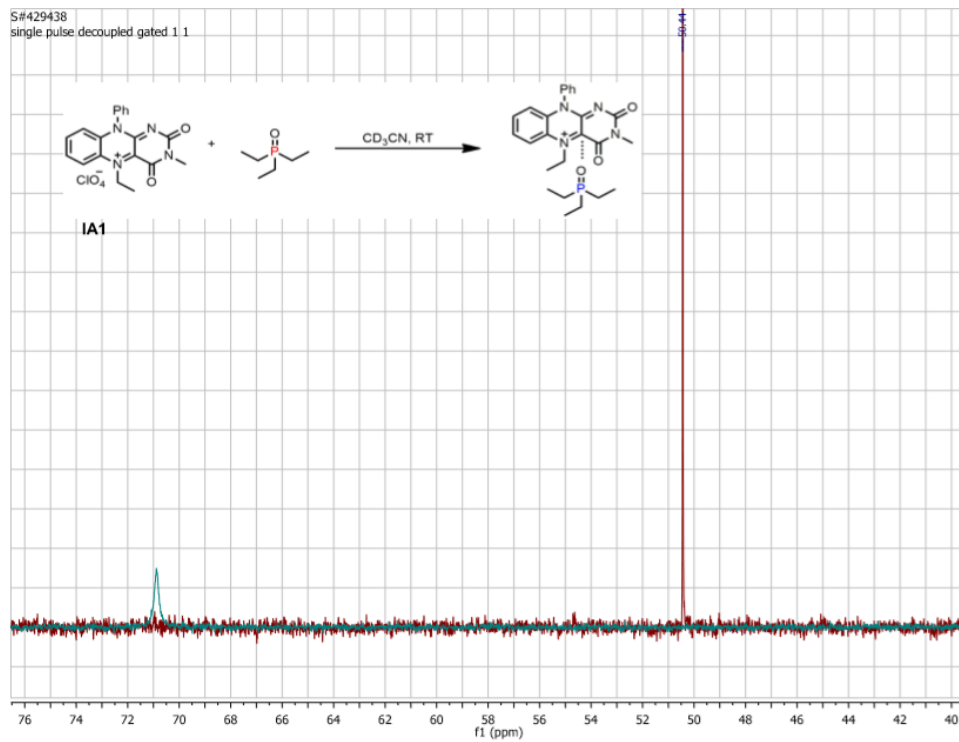
BC3 and Et₃PPO

S#587010

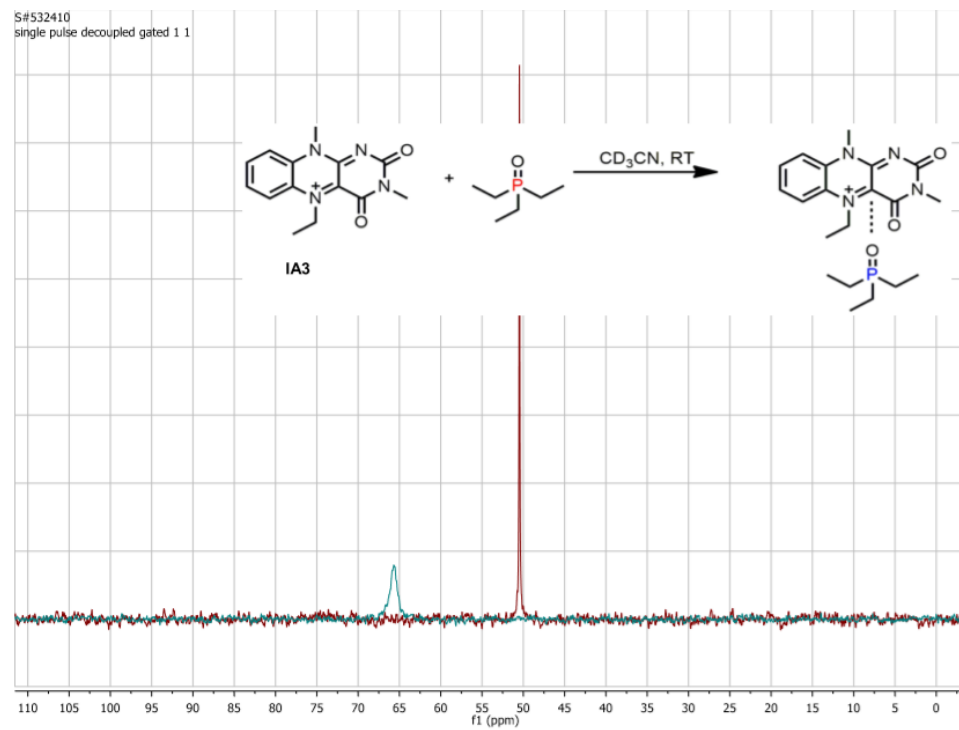
single pulse decoupled gated 1 1



BC5 and Et₃PPO

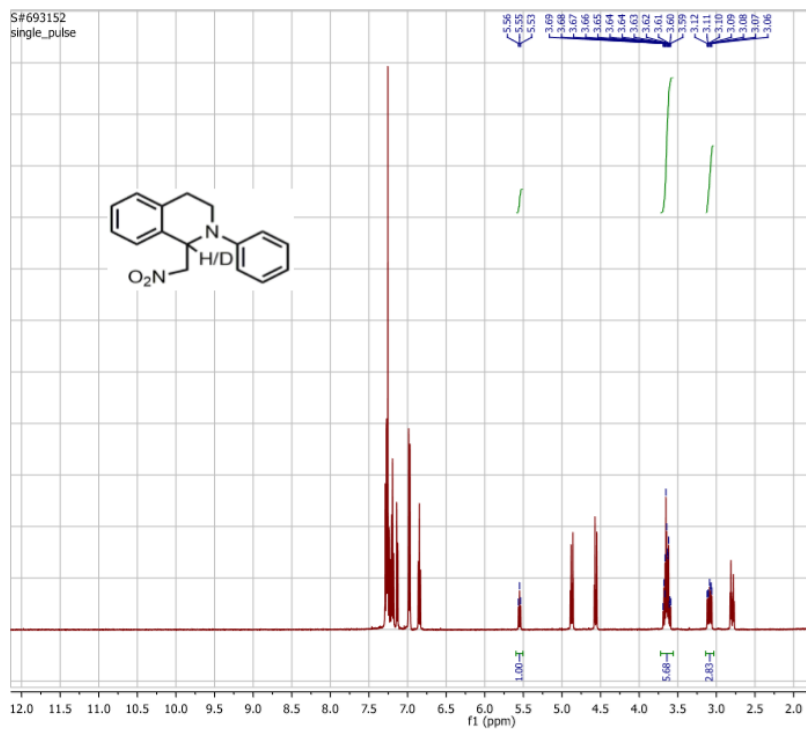


IA1 and Et₃PPO

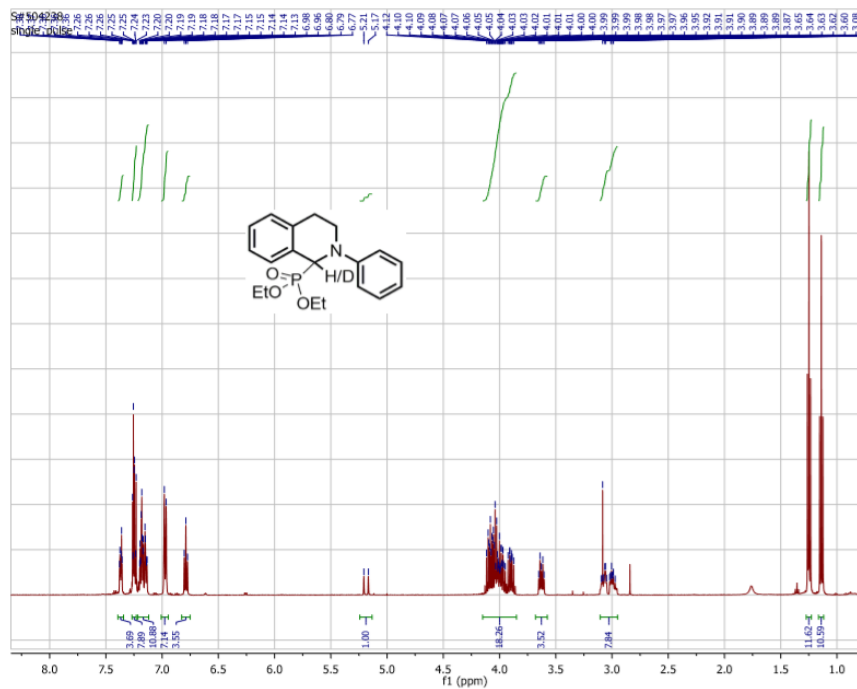


IA3 and Et₃PPO

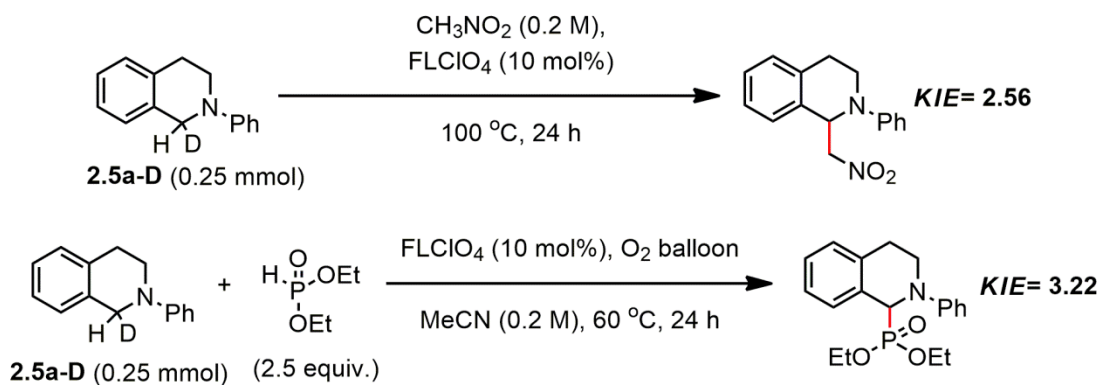
General procedure for measuring Kinetic Isotopic Effect in relation to Chapter 2 work



2.81-H/D



2.6a-H/D



After full conversion of the amine 2.5a-D, the ratio of the signal intensity in the 1-position relative to reference signals in the 3- and 4-position was considered for the KIE values. It should be noted that starting material amine was only 90% pure, and therefore KIE values were calculated based on 90% deuterium enrichment of the starting material.

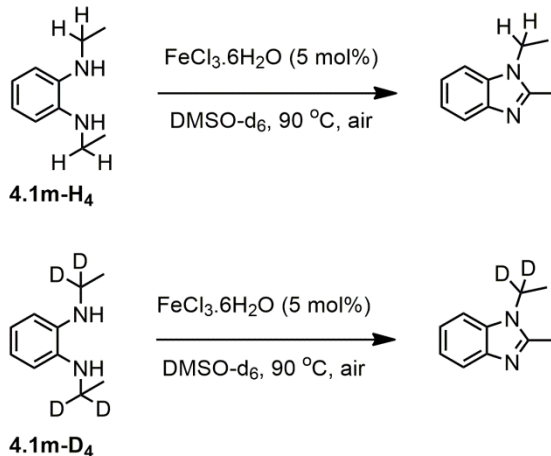
The respective values for reaction 1 and 2 are:

Reaction 1: Nitromethane as Nucleophile: 2.62 and 2.50; average value= 2.56

Reaction 2: Diethyl phosphate as Nucleophile: 3.34 and 3.10; average value= 3.22

Each KIE value obtained was the result of two experiments.

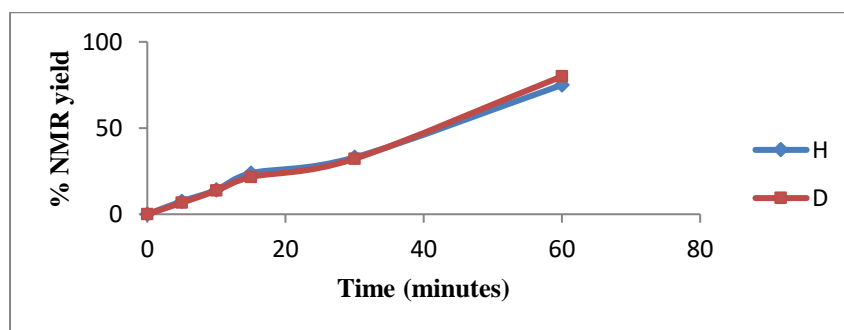
General procedure for measuring Kinetic Isotopic Effect in relation to Chapter 3 work



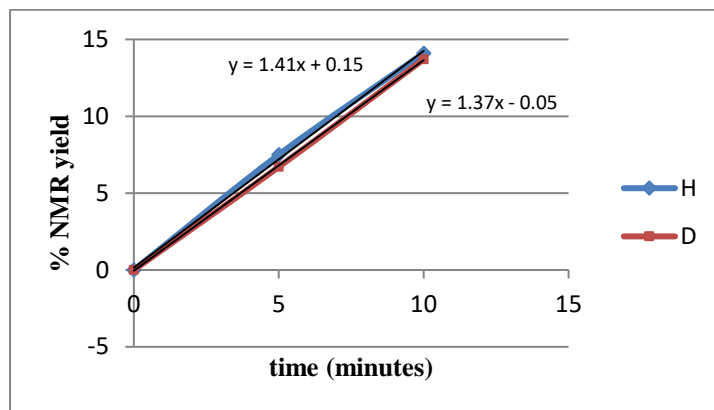
0.3 mmol of each substrate **4.1m-H₄** and **4.1m-D₄** were added in two separate 1.5-dram vial. Each vial was added with a stir-bar and 1.5 mL of DMSO-d₆ at room temperature. The solution in each vial was divided equally into three 1.5-dram vial.

To get the NMR conversion, 0.05 mL of aliquot was taken from each vial at different time scale. Time t₀ refers to solution before heating. Time t₅, time t₁₀, time t₁₅, time t₃₀, and time t₆₀ refer to 5 minute, 10 minute, 15 minute, 30 minute, and 60 minute respectively. Each NMR sample was prepared by adding 0.05 mL aliquot with 0.5 mL of stock solution of DMSO-d₆ containing internal standard CH₂Br₂. The % NMR yield for each aliquot was measured comparing integration value of peak at 7.75 ppm against internal standard peak at 5.3 ppm.

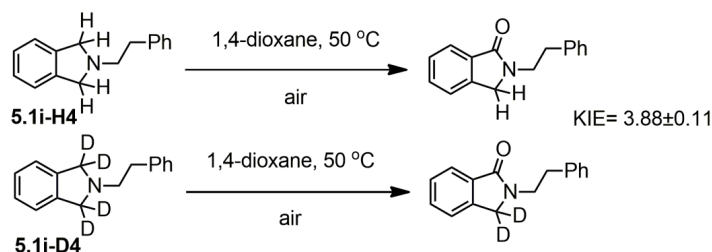
A plot of average % NMR yields from two runs of product vs time was drawn which is as shown below:



t0, t5, and t10 data were selected for studying initial rate. KIE value was found from the ratio of slope of line for product (H) to slope of line for product (D). The plot for initial rate and slope for each curve is shown below:

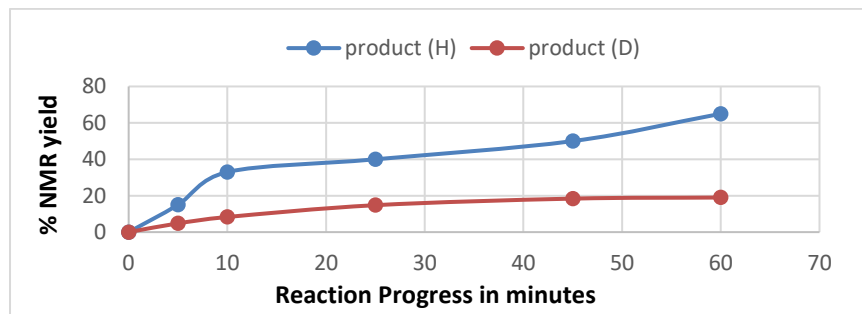


General Procedure for measuring Kinetic Isotopic Effect in relation to Chapter 5 work



Substrate **5.1i-H₄** and **5.1i-D₄** each 0.1 mmol in 0.6 mL of 1,4-dioxane was mixed in 1.5-dram vial fitted with stirbar at room temperature. Each resulting solution was divided between two 1.5-dram vials. 0.05 mL of aliquot was taken from each vial before heating the reaction mixture for time 0 ¹H NMR study. Similarly, time 5 min (t5), time 10 min (t10), time 25 min (t25), time 45 min (t45) and time 60 min (t60) aliquots were studied after the reaction mixture was heated to 50 °C. To each 0.05 mL aliquot was added with 0.5 mL of stock solution of CDCl₃ containing internal standard dibromomethane (CH₂Br₂). The % NMR yield for each aliquot was measured comparing integration value of peak at 7.75 ppm against internal standard peak at 5.3 ppm.

A plot of % NMR yield of Isoindolinone product vs time was drawn which is as shown below:



Initial rate was taken into consideration for measuring KIE. For this t_0 , t_5 and t_{10} data were considered. KIE value was found from the ratio of slope of curve for product (H) to slope of curve for product (D). The plot for initial rate and slope for each line is shown below:

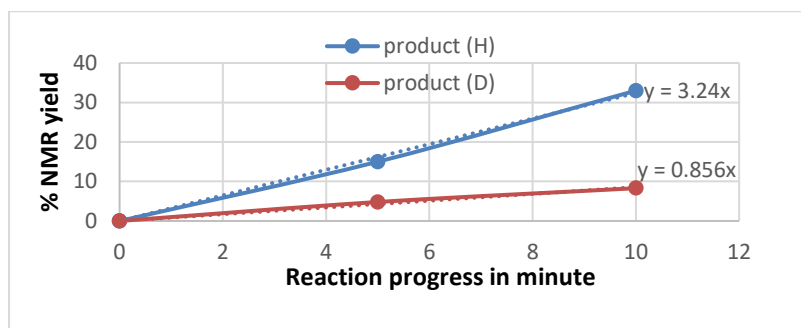
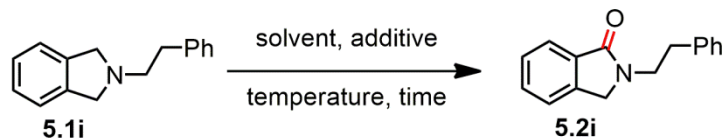


Table AB2: Screening of reaction condition in relation to chapter 5 work



Entry	solvent	time (h)	temp. (°C)	additive (mol%)	conversion NMR (%)	yield by NMR (%) ^a
1	DMF	6	50		86	40
2	DMSO	6	50		100	53
3	Toluene	6	50		20	ND
4	MeOH	6	50		50	ND
5	H ₂ O	6	50		25	ND
6	MeCN	6	50		35	ND
7	Pyridine	6	50		NA	28
8	DCM	6	50		0	ND
9	EtOAc	6	50		0	ND
10	DMSO	8	50	H ₂ O (100)	68	23
11	Diethylether	8	50		0	-
12	Hexanes	8	50		0	-
13	THF	8	50		43	38
14	CF ₃ CH ₂ OH	4	60		0	-
15	MeNO ₂	8	50		0	-
16	CH ₃ COOH	4	60		0	-
17	Dioxane	4	50		70	55
18	Dioxane	6	50		80	75
19	Dioxane	8	50		100	91^b, 86^c, 83^d
20	Dioxane	6	50		0	0 ^e
21	Dioxane	6	50		41	40 ^f
22	Dioxane	48	100		82	NA
23	-	6	50		0	-
24	Dioxane	8	50	Et ₃ N (200)	0	-
25	Dioxane	6	50	^t BuOOH (200)	50	48
26	Dioxane	8	rt		NA	21
27	Dioxane	6	50	TEMPO (200)	NA	0
28	Dioxane	6	50	BHT (120)	NA	0
29	Dioxane	2	50		100	61 ^g
30	Dioxane	4	50	H ₂ O (200)	0	-
31	Dioxane	4	50	H ₂ O ₂ (200)	NA	-
32	Dioxane	4	50	H ₂ O ₂ (100)	NA	-

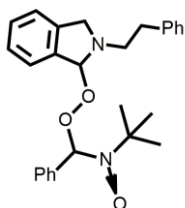
33	MeCN	16	70	<i>o</i> -salicylic acid (20)	0	-
34	MeCN	16	70	TEMPO (100)	NA	0
35	MeCN	16	rt	NIS (300), K ₂ CO ₃ (200)	100	ND
36	MeCN	4	50	NBS (5)	NA	trace
37	Dioxane	4	50	NBS (5)	NA	78
38	Dioxane	4	50	NBS (1)	70	66
39	Dioxane	24	50	NBS (1)	100	77 ^h
40	Dioxane	4	50	NBS (5), K ₂ CO ₃ (20)	NA	trace
41	DMSO	4	50	NBS (5)	NA	46
42	THF	4	50	NBS (5)	NA	42
43	Dioxane	8	50	PBN ⁱ (100)	NA	0
44	Dioxane	8	50	^t BuOK (10)	NA	0
45	Dioxane	8	50	FeCl ₃ .6H ₂ O (5)	NA	trace
46	MeCN	8	50	Na ₂ WO ₄ .2H ₂ O (10)	0	-
47	Dioxane	8	50	Na ₂ WO ₄ .2H ₂ O (10)	0	-
48	DMF	8	50	Mg(NO ₂) ₂ (200)	0	-
49	Dioxane	8	50	CuI (10)	NA	trace
50	Dioxane	8	50	K ₂ S ₂ O ₈ (10)	NA	55
51	Dioxane	8	50	<i>m</i> -CPBA (7.5)	NA	trace
52	Dioxane	8	50	P ₂ O ₅ (10)	NA	43
53	Dioxane	48	50	K ₂ S ₂ O ₈ (10)	100	19 ^j

^aall reaction was performed with substrate **5.1i** (0.2 mmol) in given solvent (0.15 M) at given condition with CH₂Br₂ as internal standard added after the reaction was complete; ^bACS grade Acros Organics dioxane; ^cACS grade Sigma Aldrich dioxane; ^dextra dry Alfa Aesar dioxane; ^eIn Argon atmosphere; ^fIn dark; ^gIn O₂ balloon; ^hin capped vial ⁱPBN= *N*-tert-butyl- α -phenylnitron; ^j65% phthalimide product was observed. NA= Not Available, ND= Not determined

Study on adduct formation with spin trap reagent in relation to chapter 5 work

Reaction sample was prepared by heating a mixture of substrate **1i** (0.1 mmol) and PBN reagent (0.15 mmol) in 1 mL of dioxane for 24 hour at 50 °C. The reaction mixture was concentrated in rotary evaporator, dissolved in 1 mL dichloromethane, diluted and immediately analyzed through GC/MS.

1. PBN adduct with Peroxy species:



GCMS: $t_R = 7.99$ min, m/z 431 $[(M^+, 10)]$, 355 (25), $[(1-H)^+, 5]$, 281 (20), 147 (33) and 73 (100)

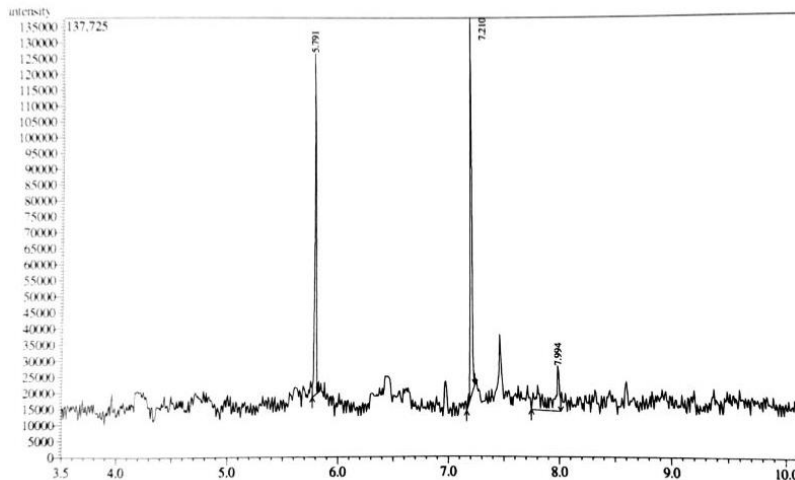


Figure A1 GC data for reaction mixture of substrate **1i** and PBN in dioxane

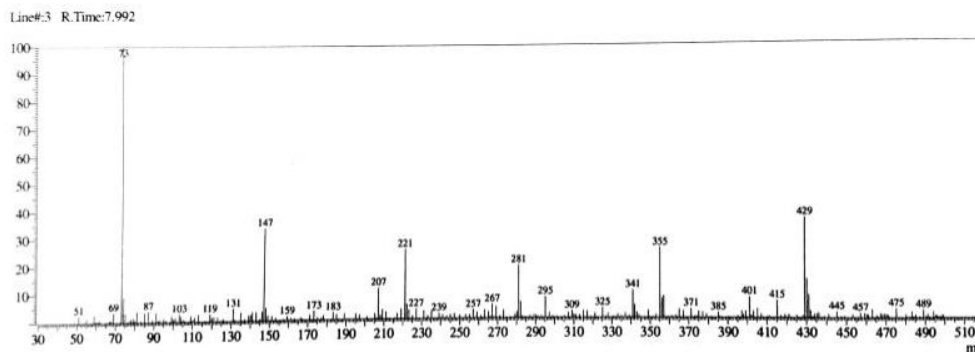


Figure A2 MS data for peak corresponding to retention time 7.99 in GC data above

General Procedure for UV-visible experiments:

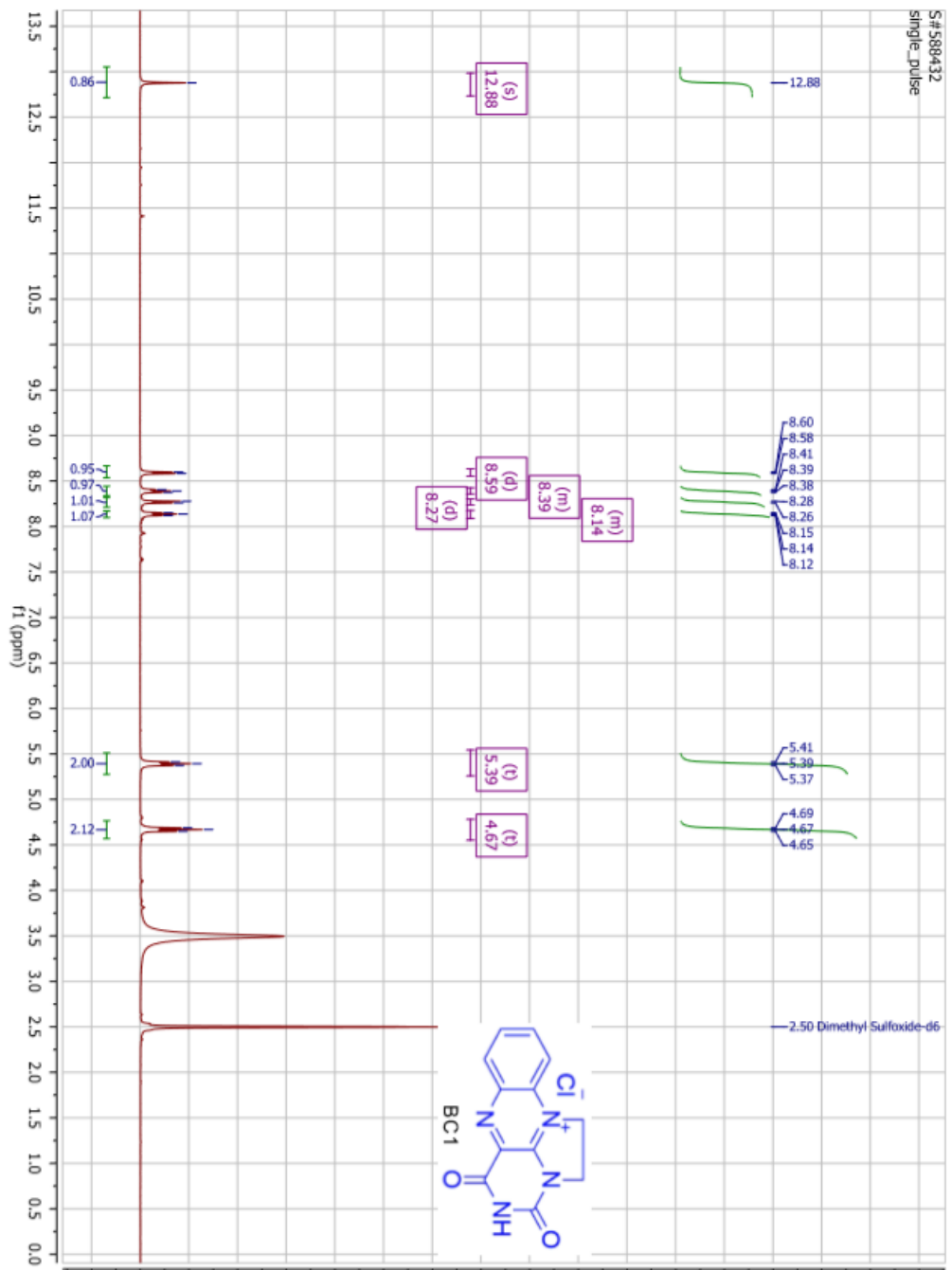
All UV-visible measurements were performed on a Cary WinUV instrument. All measurements were made in Q-10-S-Screw Cap and Septum Quartz cuvettes (Parameters: Cell Material Optical Quartz Top Type Screw Cap Typed Light Path 10 mm, Cell Volume 3.5 mL, Outside Dimensions 45mm × 12.5mm × 12.5mm and Spectral range 190-2000 nm). Spectra collected in kinetic mode used a 5 minute interval between measurements for the first 60 minutes.

In a typical UV-visible experiment, DMF (4 mL) was added to the substrate **1m** (5 mg, 0.03 mmol) followed by 10 mol% catalyst. The solution in cuvette was purged with oxygen for 5 minute and the cuvette was immediately capped. A solution of only DMF was used as a blank solution the UV-visible spectrometer.

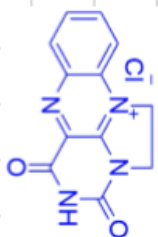
Sample preparation for EPR study in relation to Chapter 5 work

Substrate **5.1i** (5 mg, 0.022 mmol) and *N*-tert-butyl- α -phenylnitron (5 mg, 0.028 mmol) were added with 0.3 mL of 1,4-dioxane at room temperature. The resulting solution was heated at 50 °C for 1 hour in open air. 20 μ L of aliquot was added into capillary tube which was immediately placed inside epr tube. The reaction mixture was immediately analyzed by epr instrument.

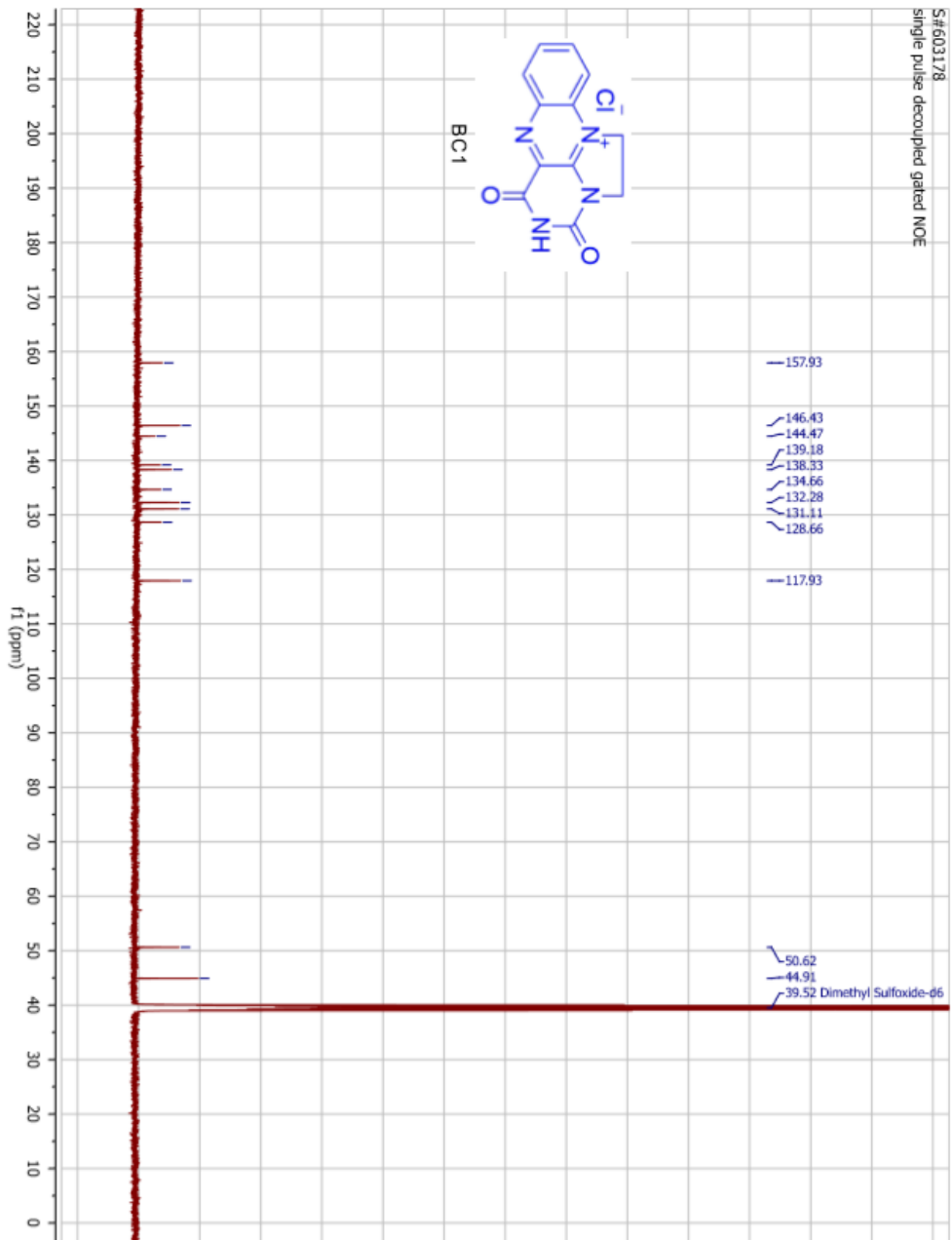
Appendix C
NMR Figures

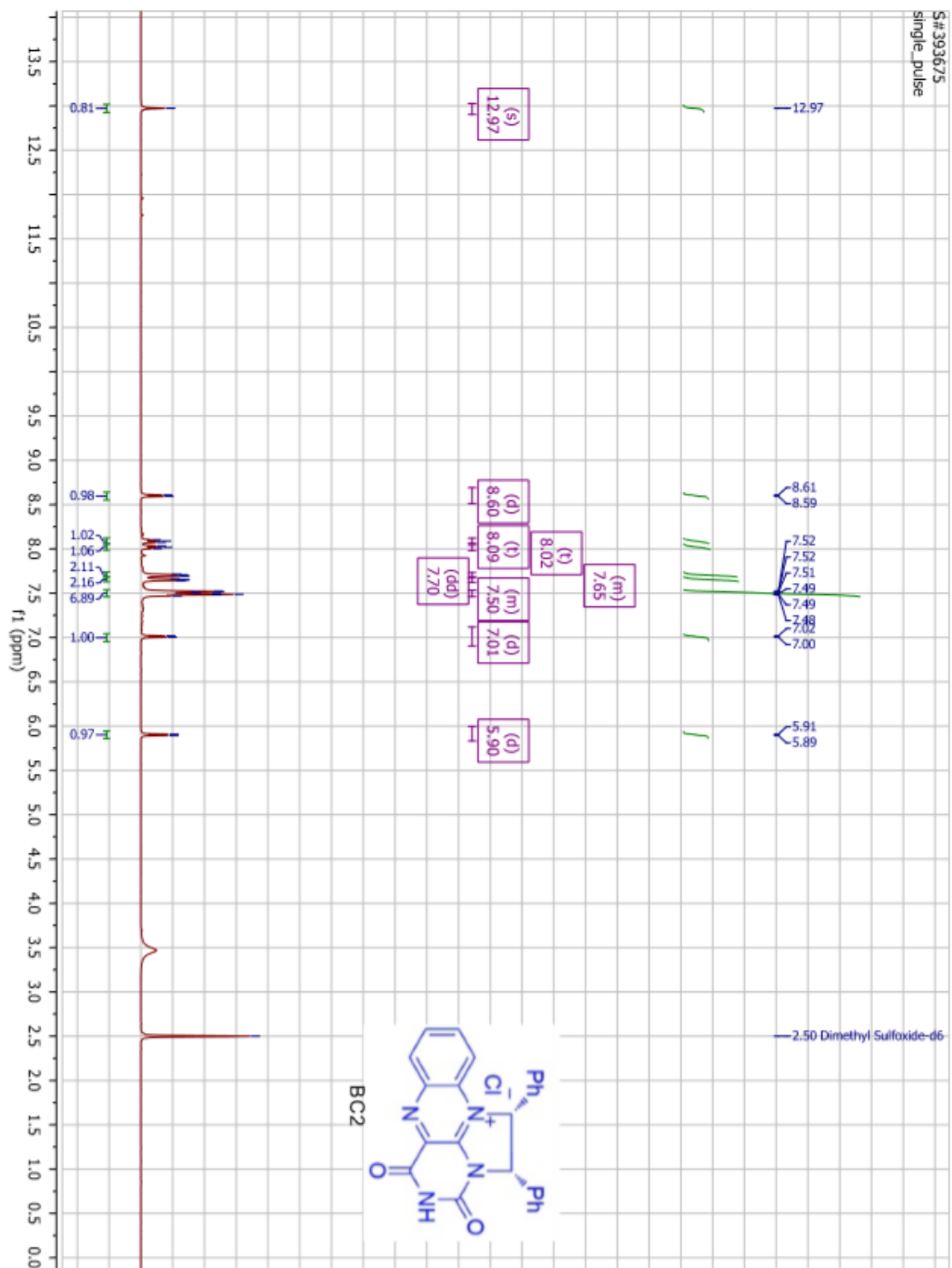


S#603178
single pulse decoupled gated NOE

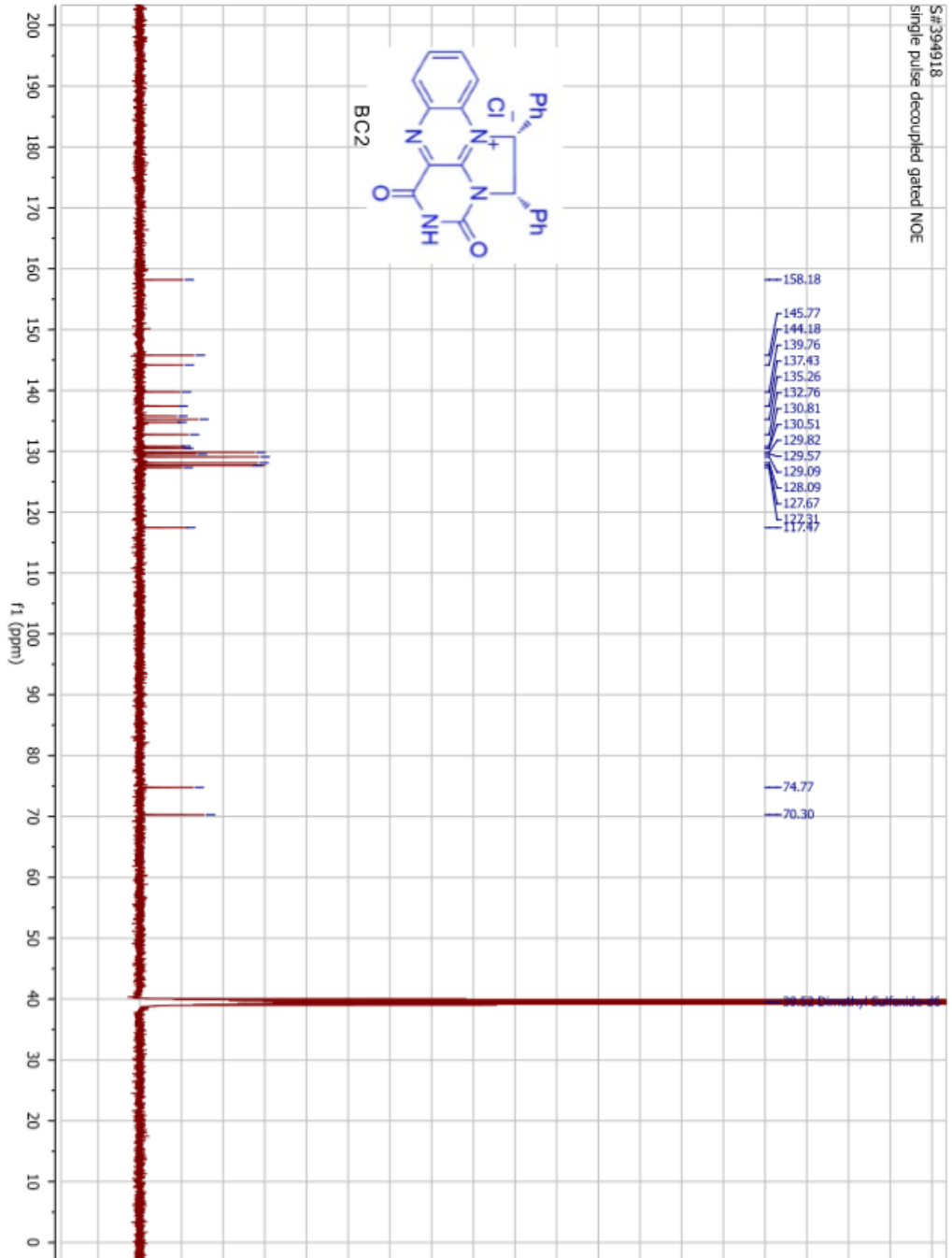
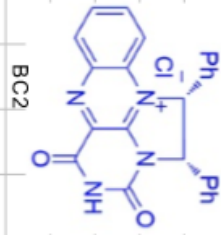


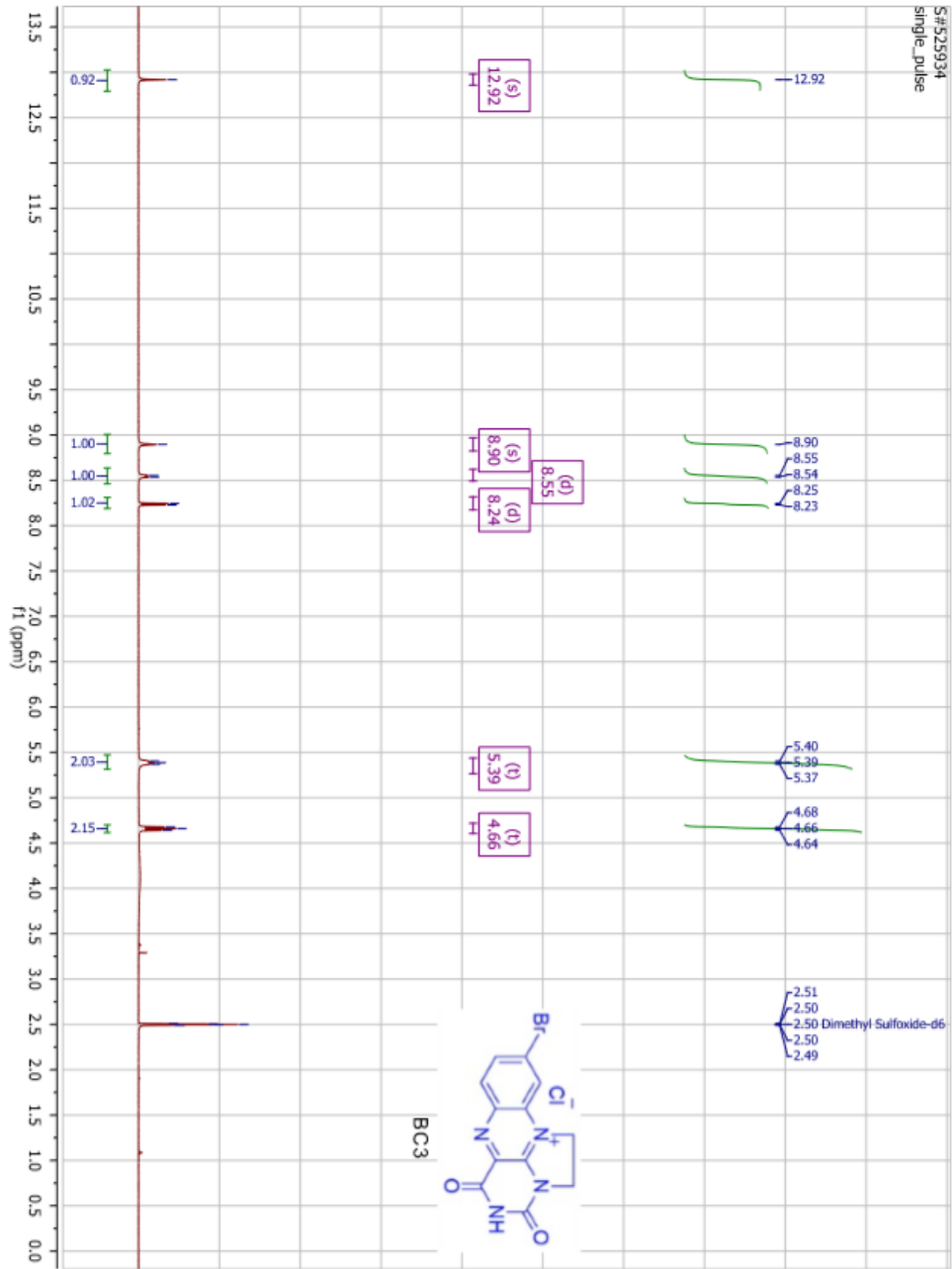
BC1

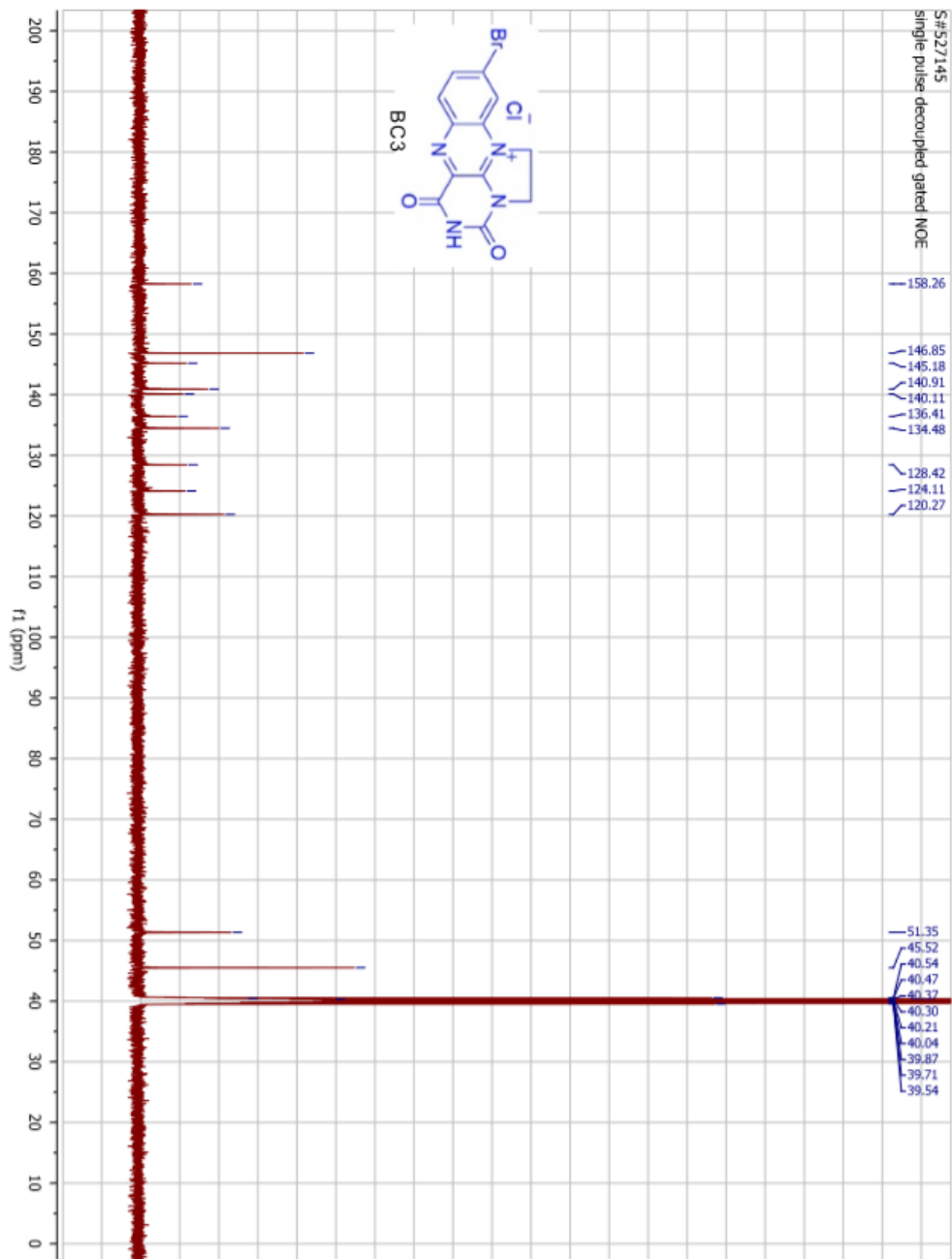




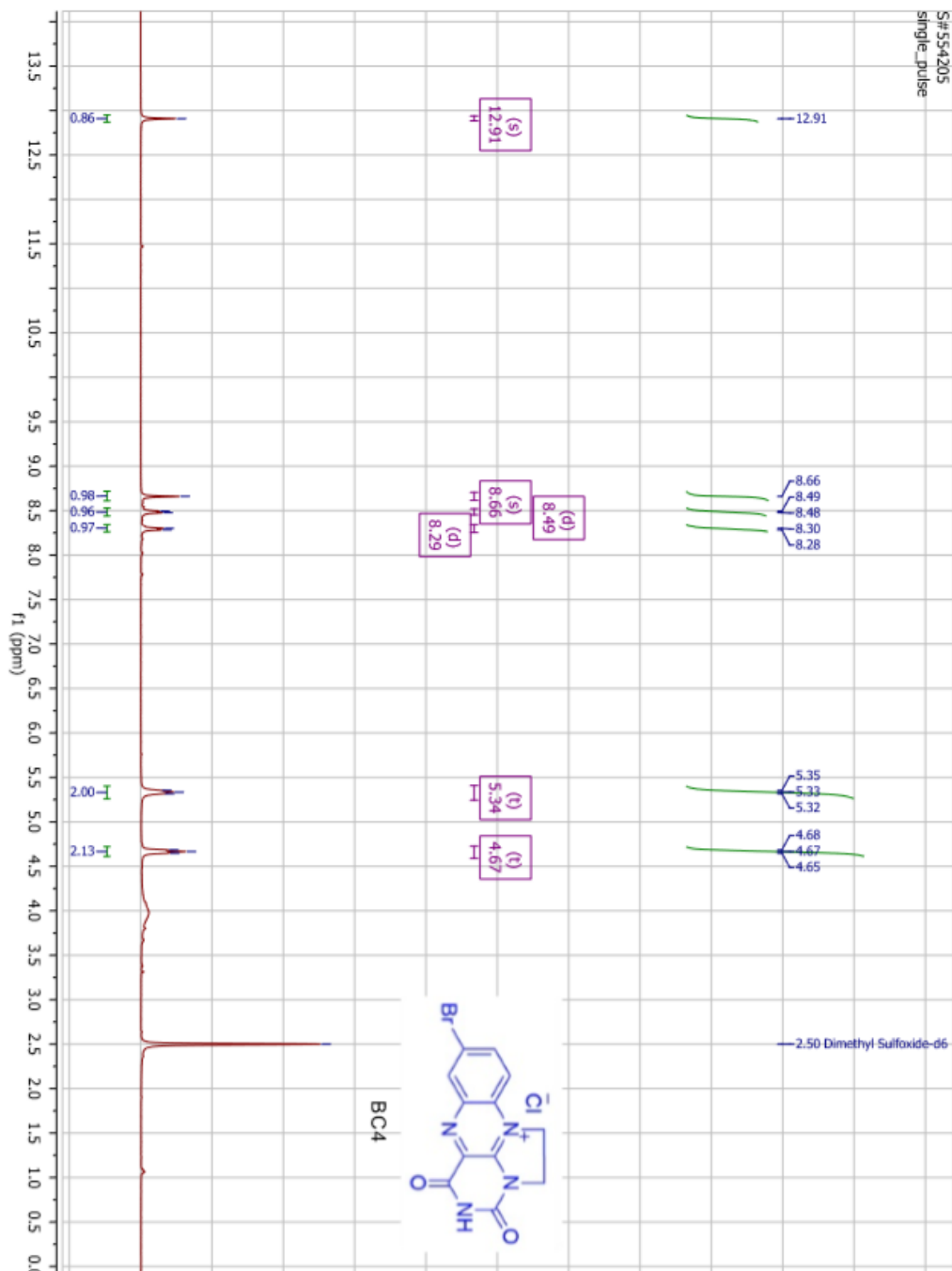
S#394918
single pulse decoupled gated NOE

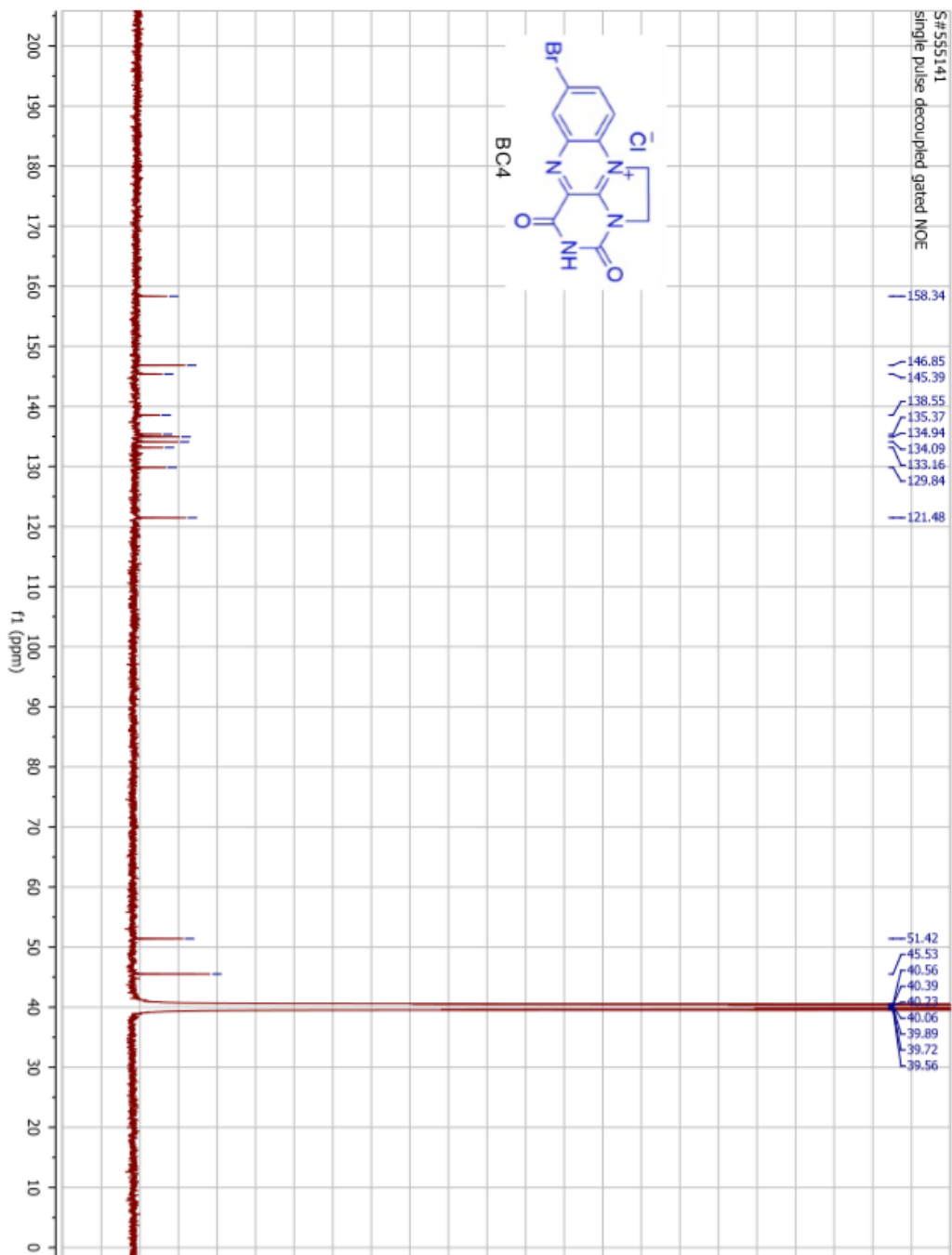


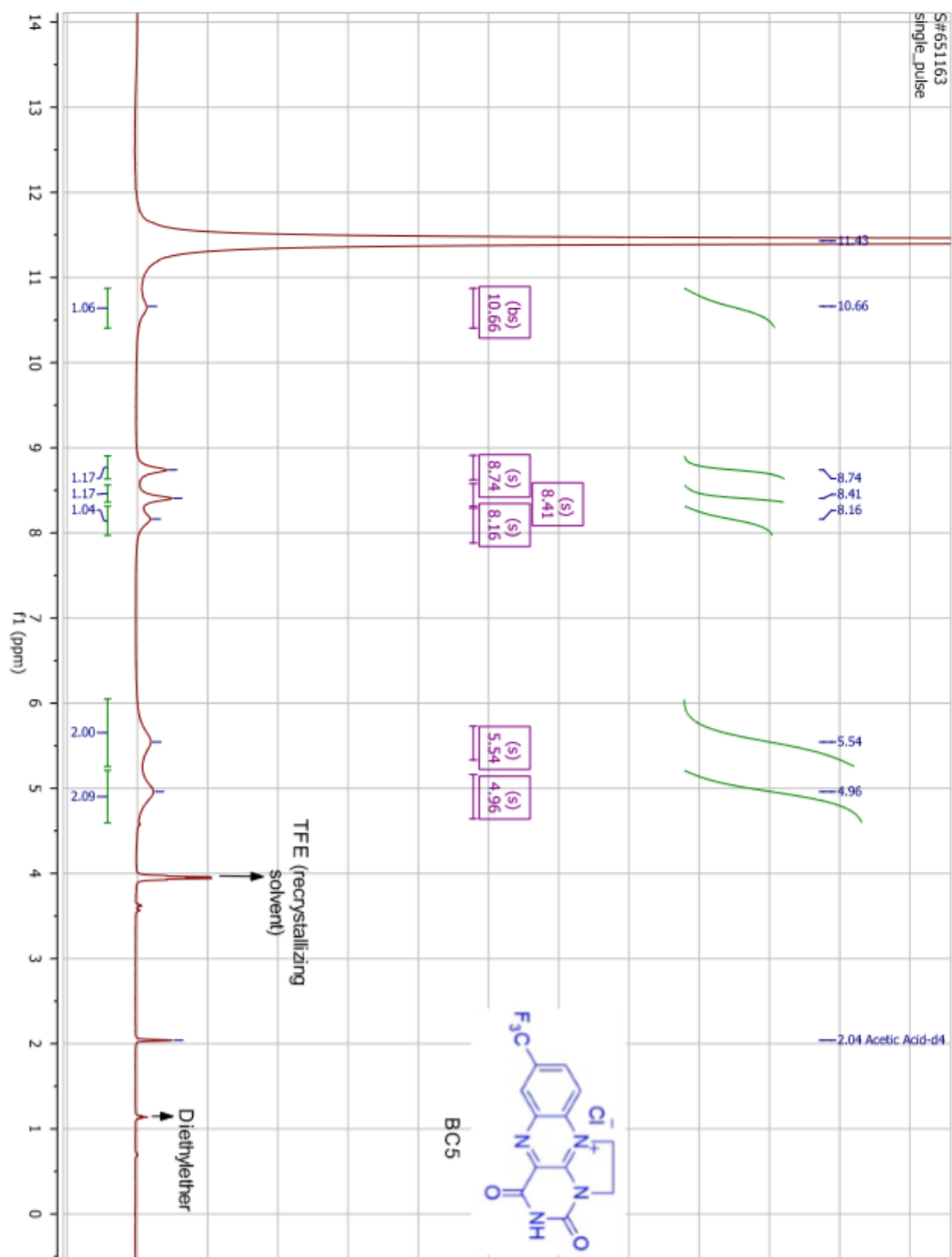


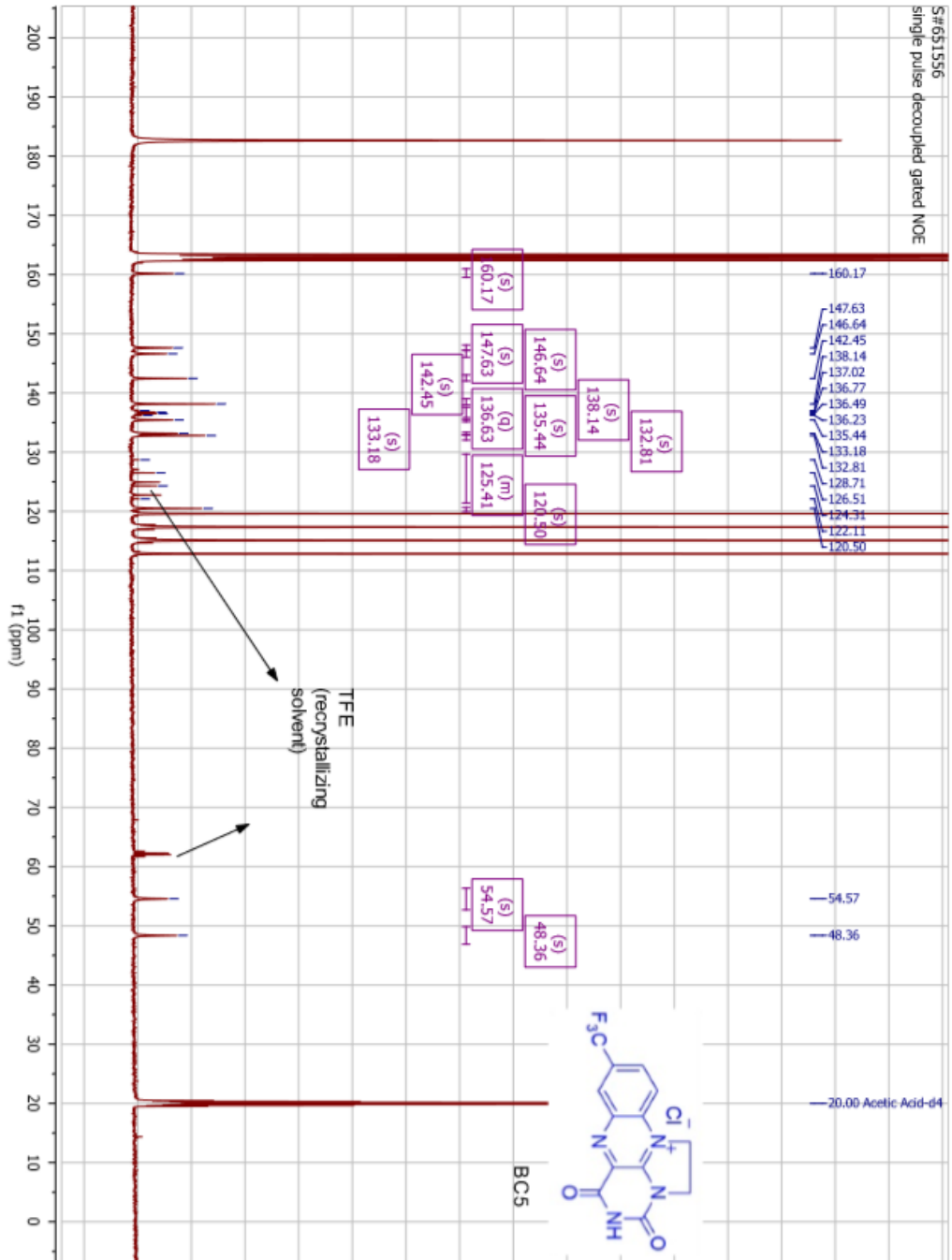


S# 554205
single_pulse

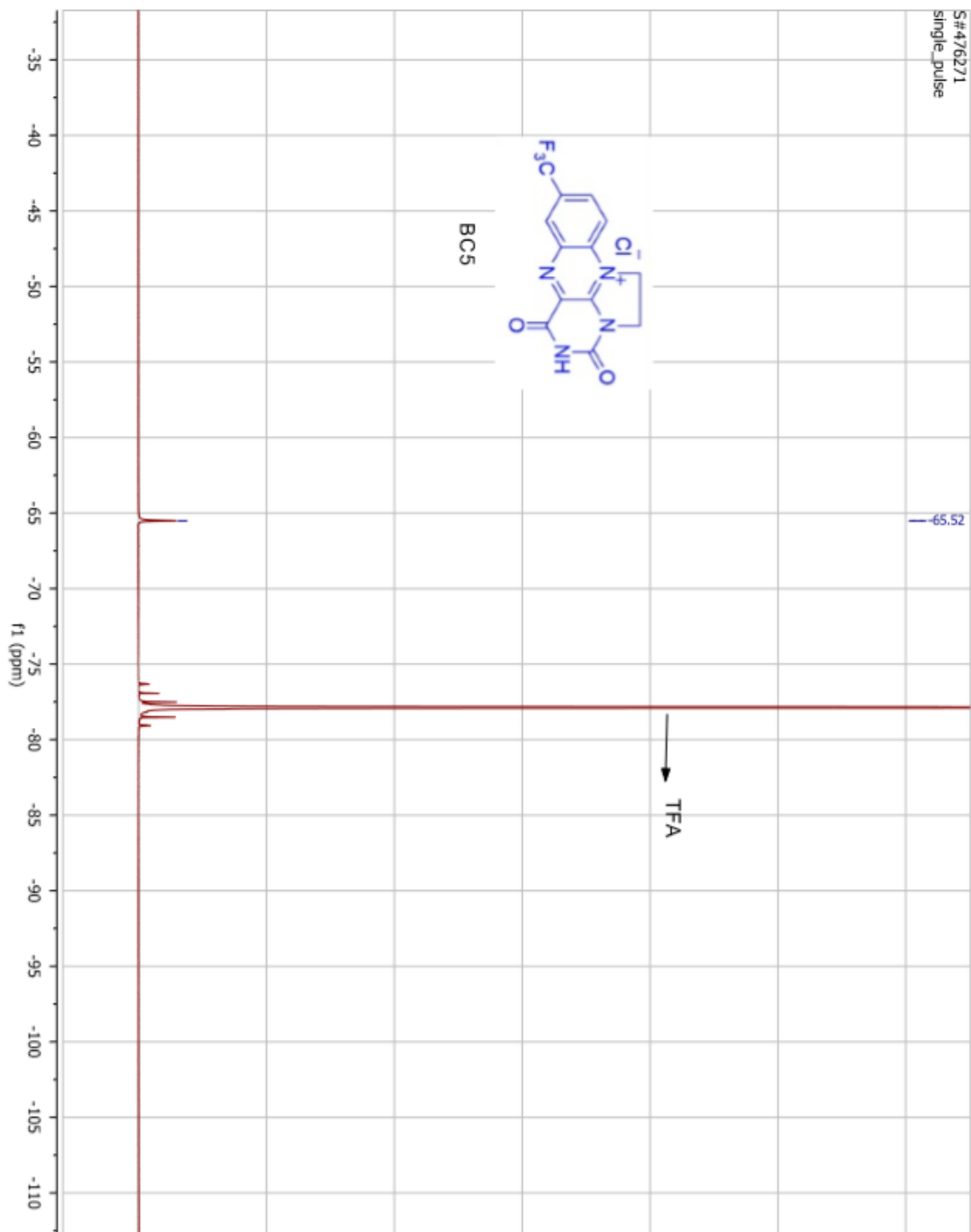




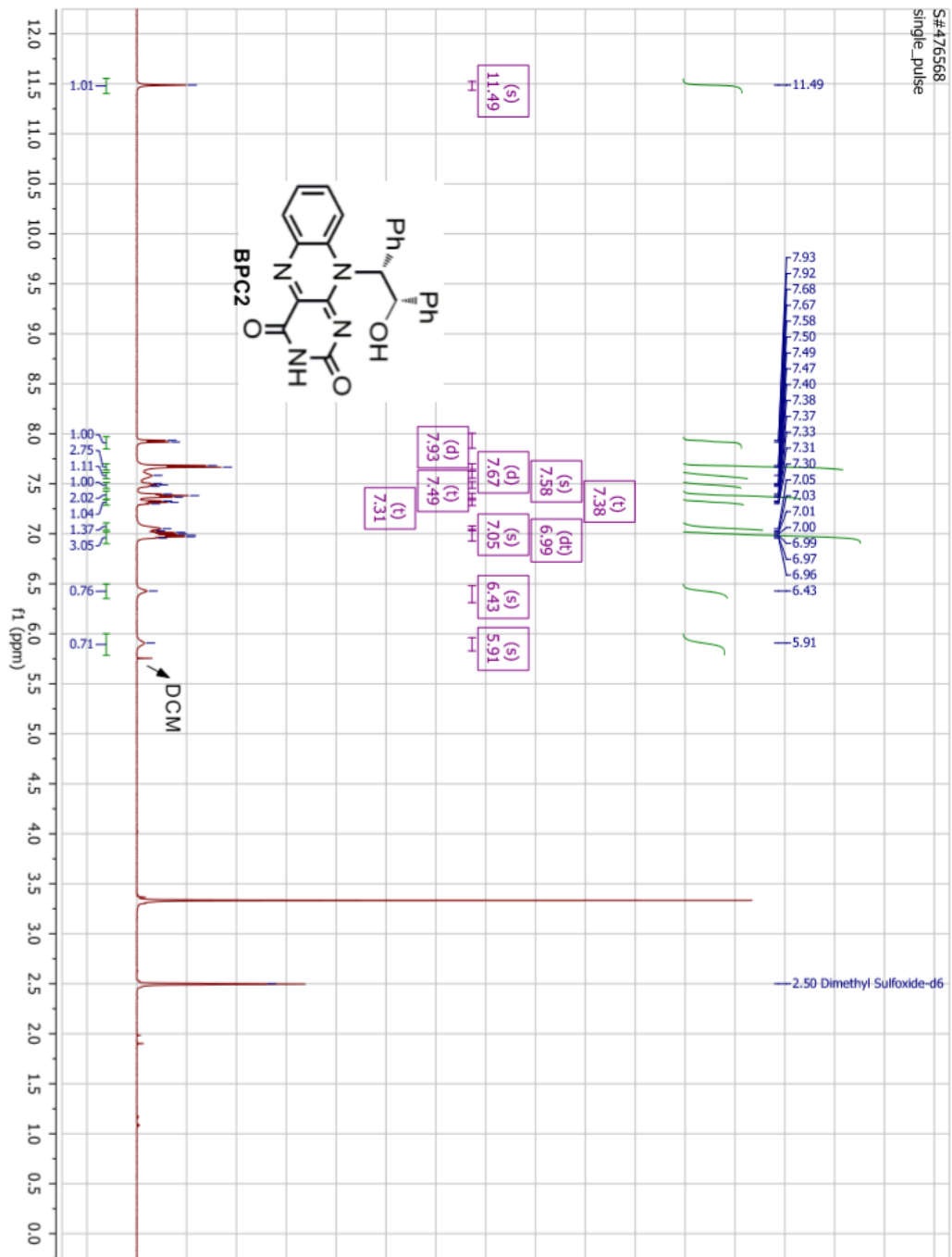




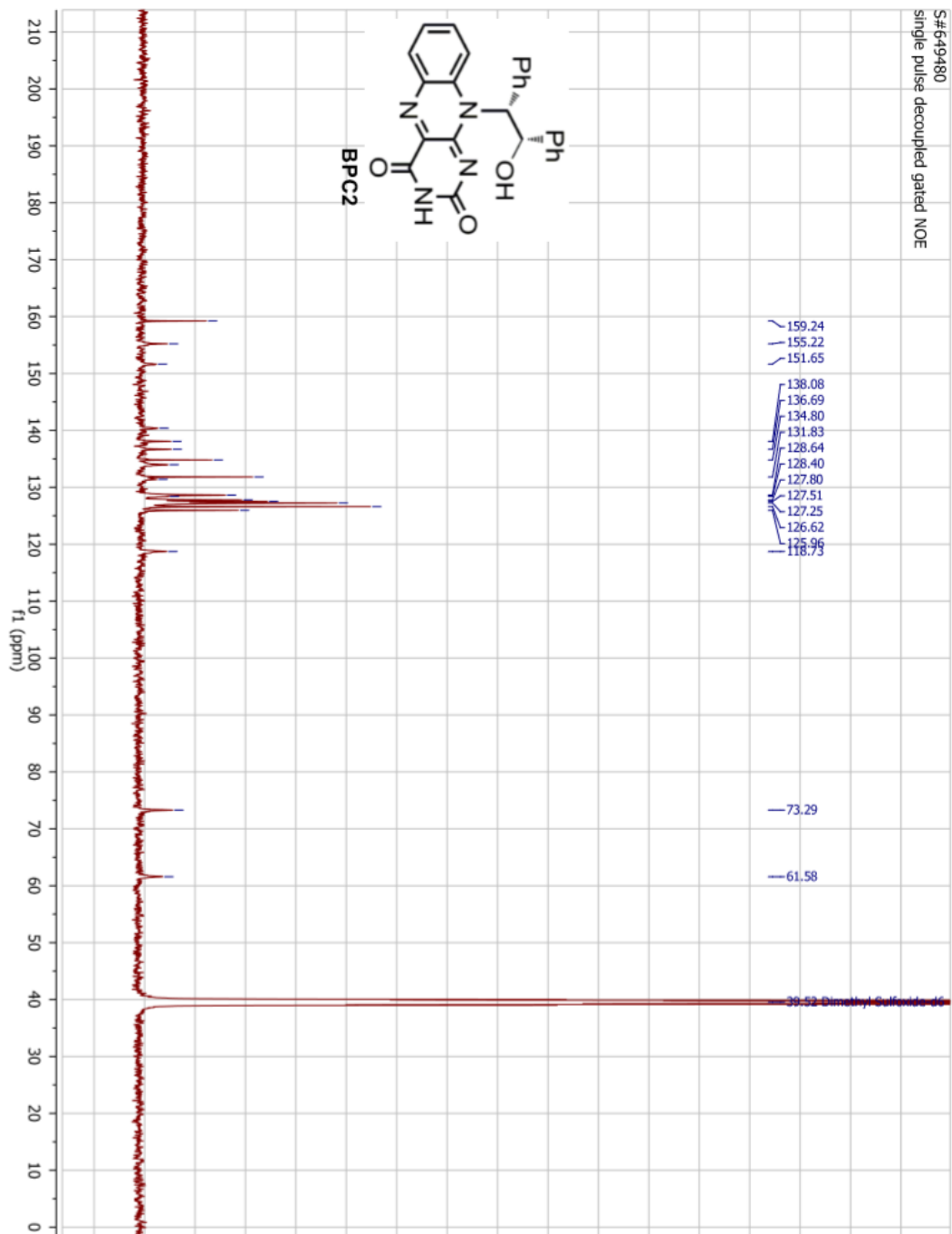
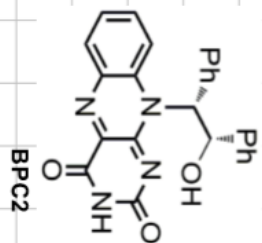
S#476271
single_pulse



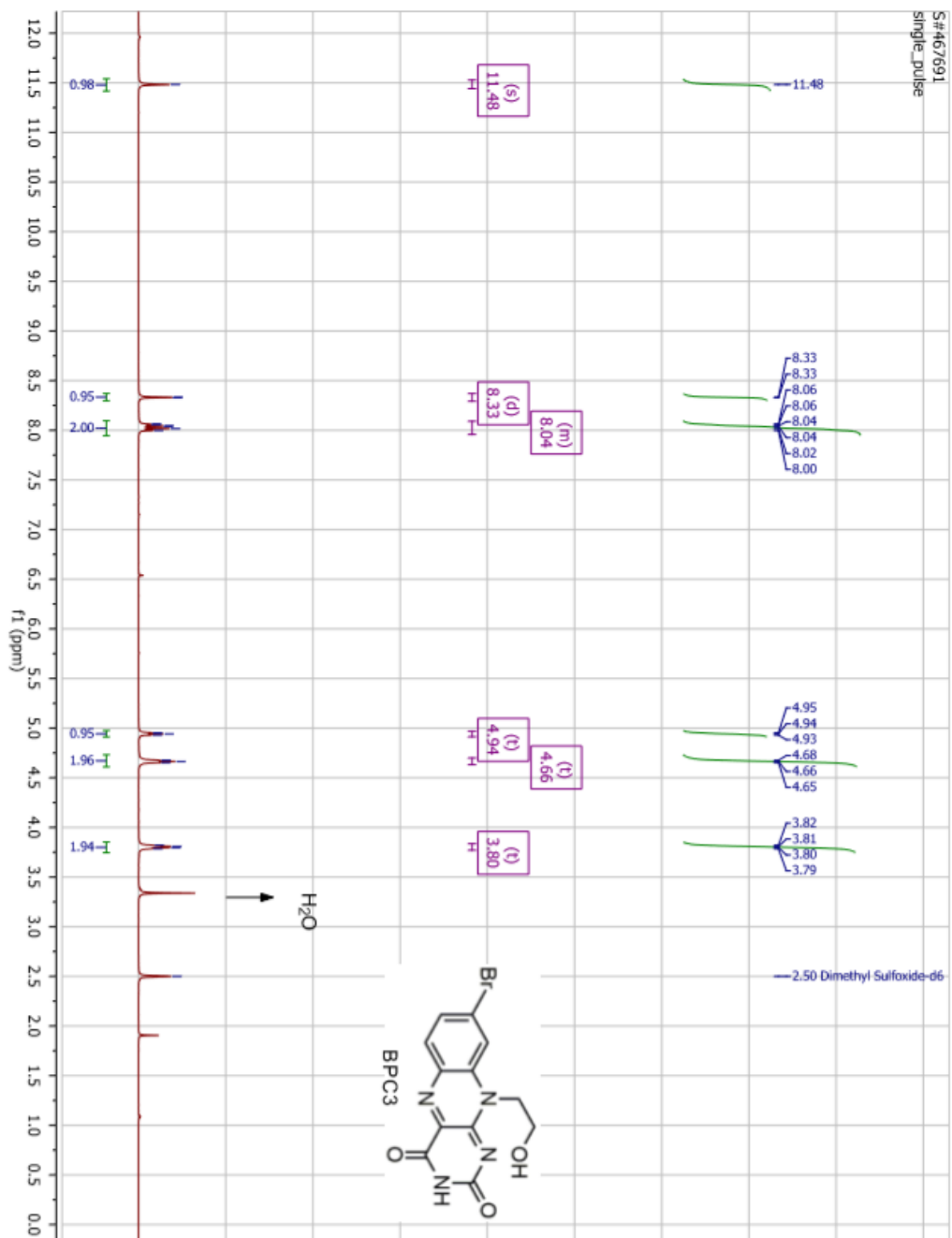
S#476568
single_pulse



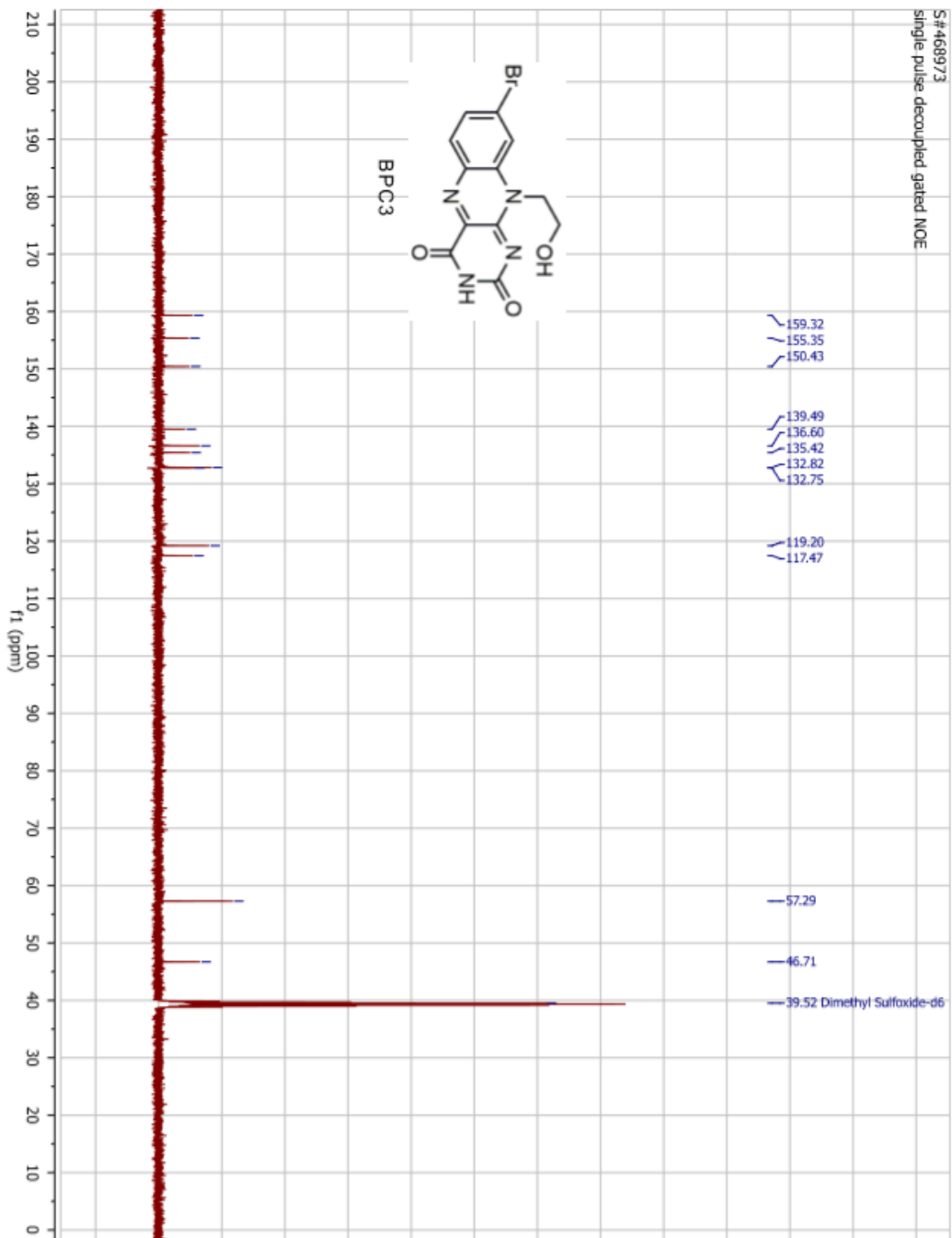
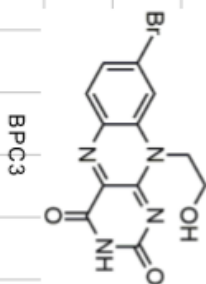
S#649480
single pulse decoupled gated NOE



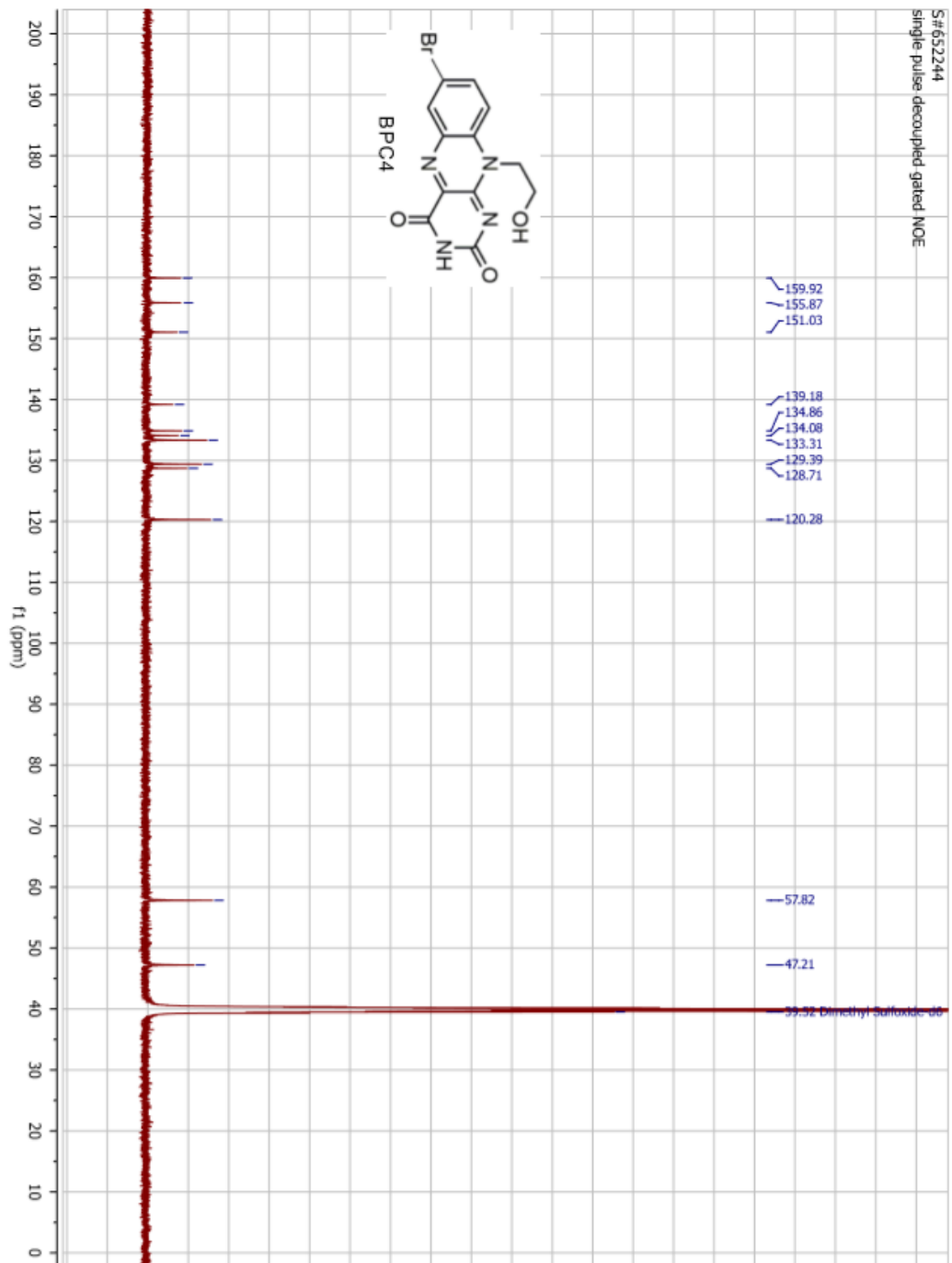
S#467691
single_pulse



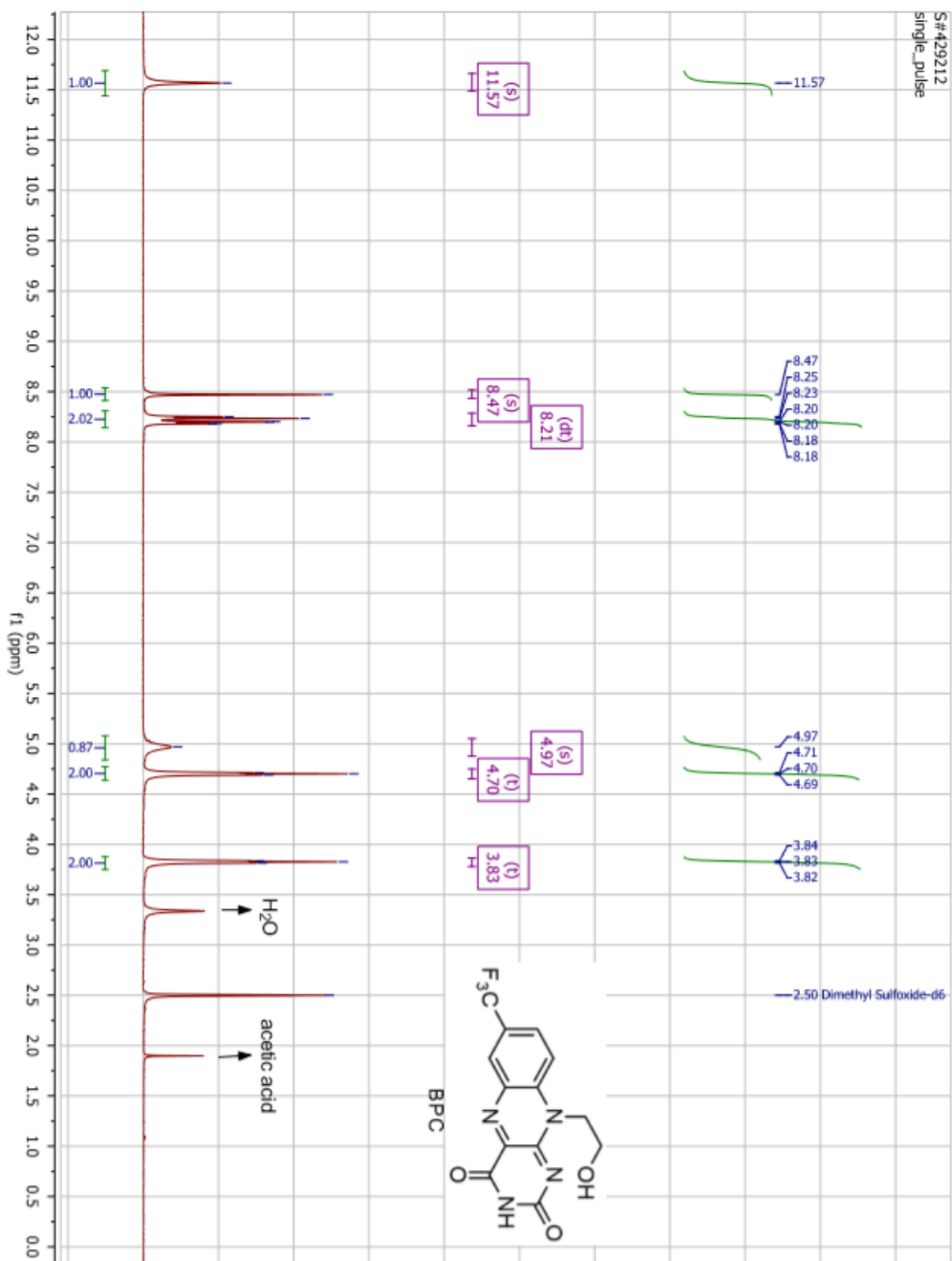
S#468973
single pulse decoupled gated NOE

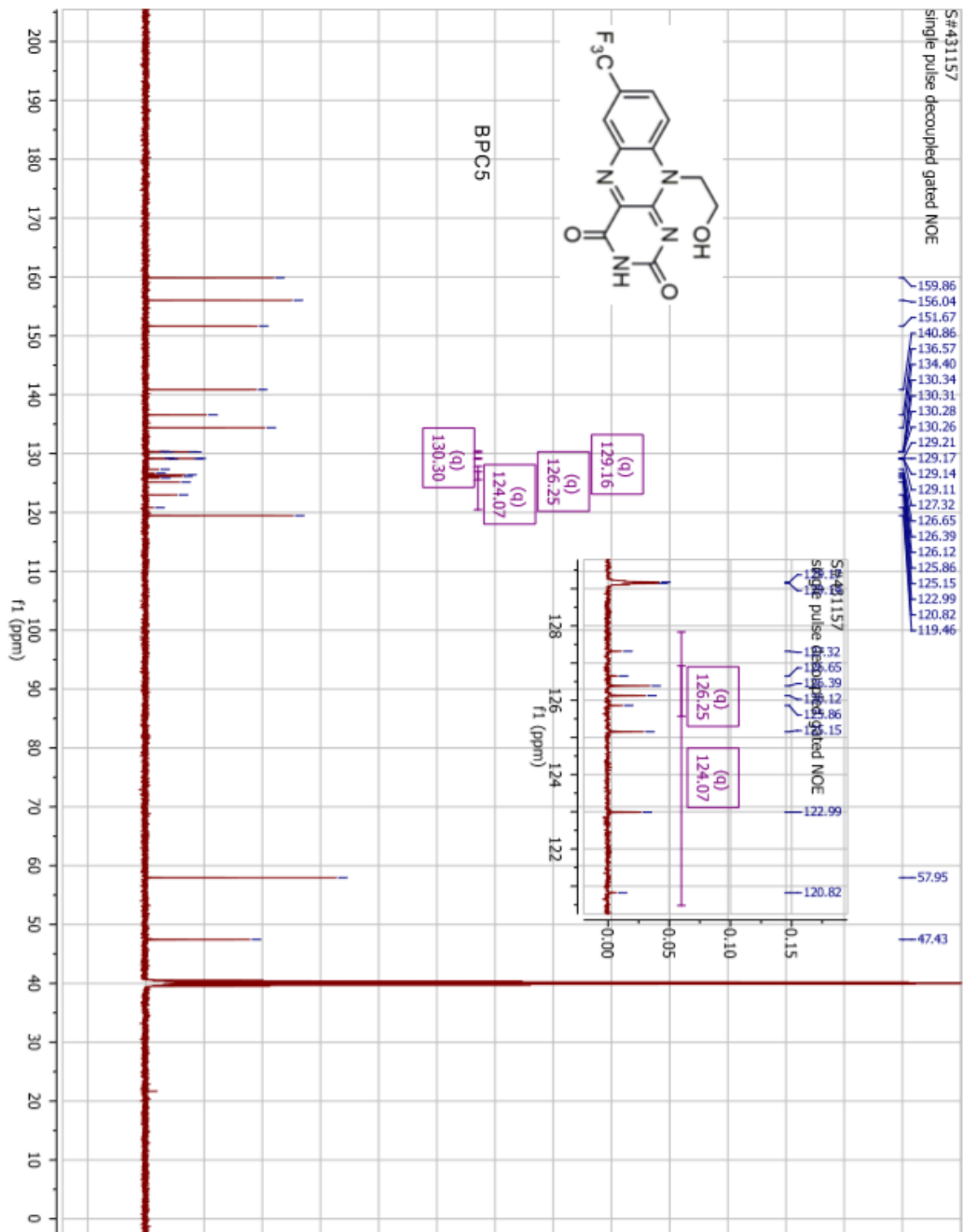


S#652244
Single pulse decoupled gated NOE

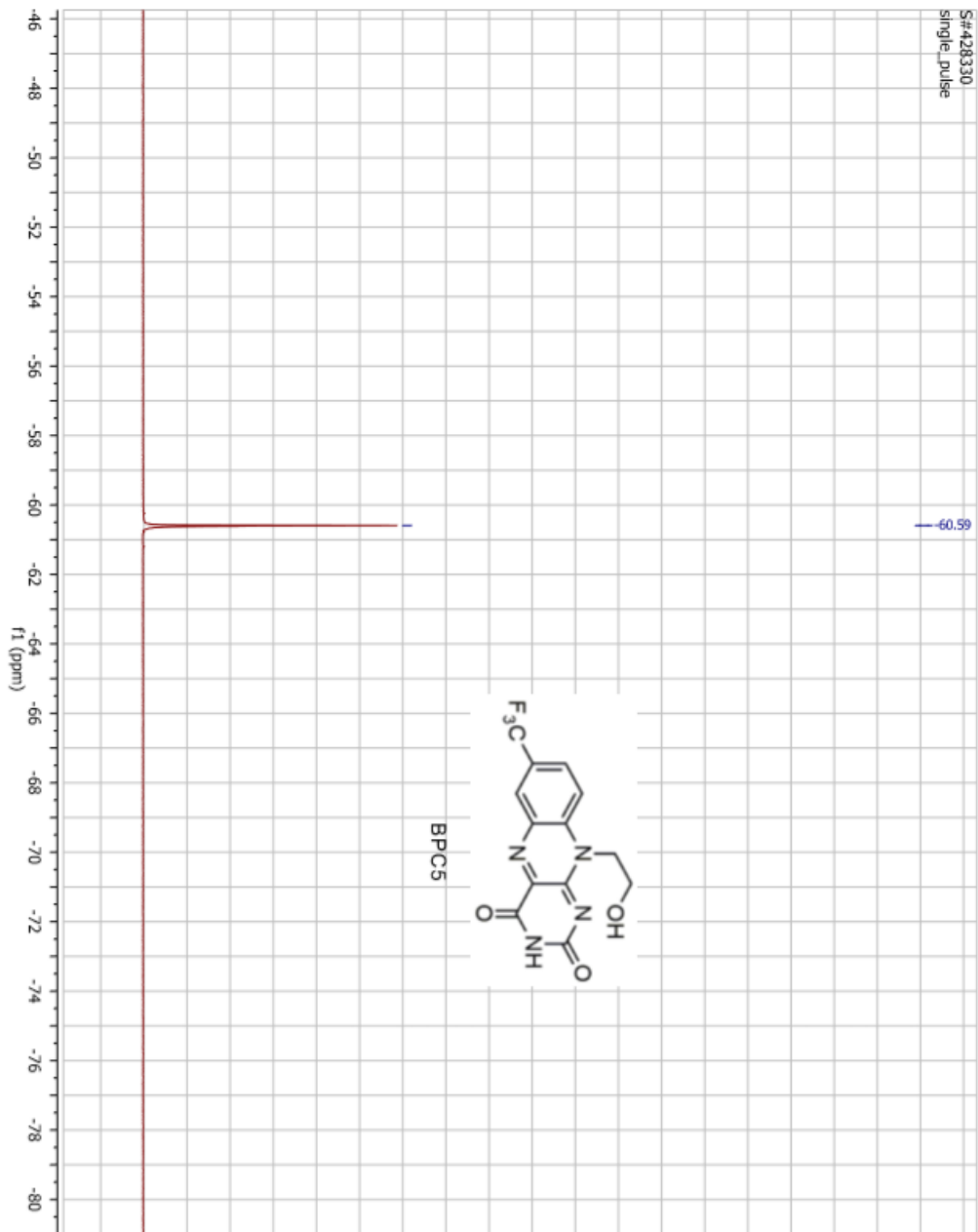


S#429212
single_pulse

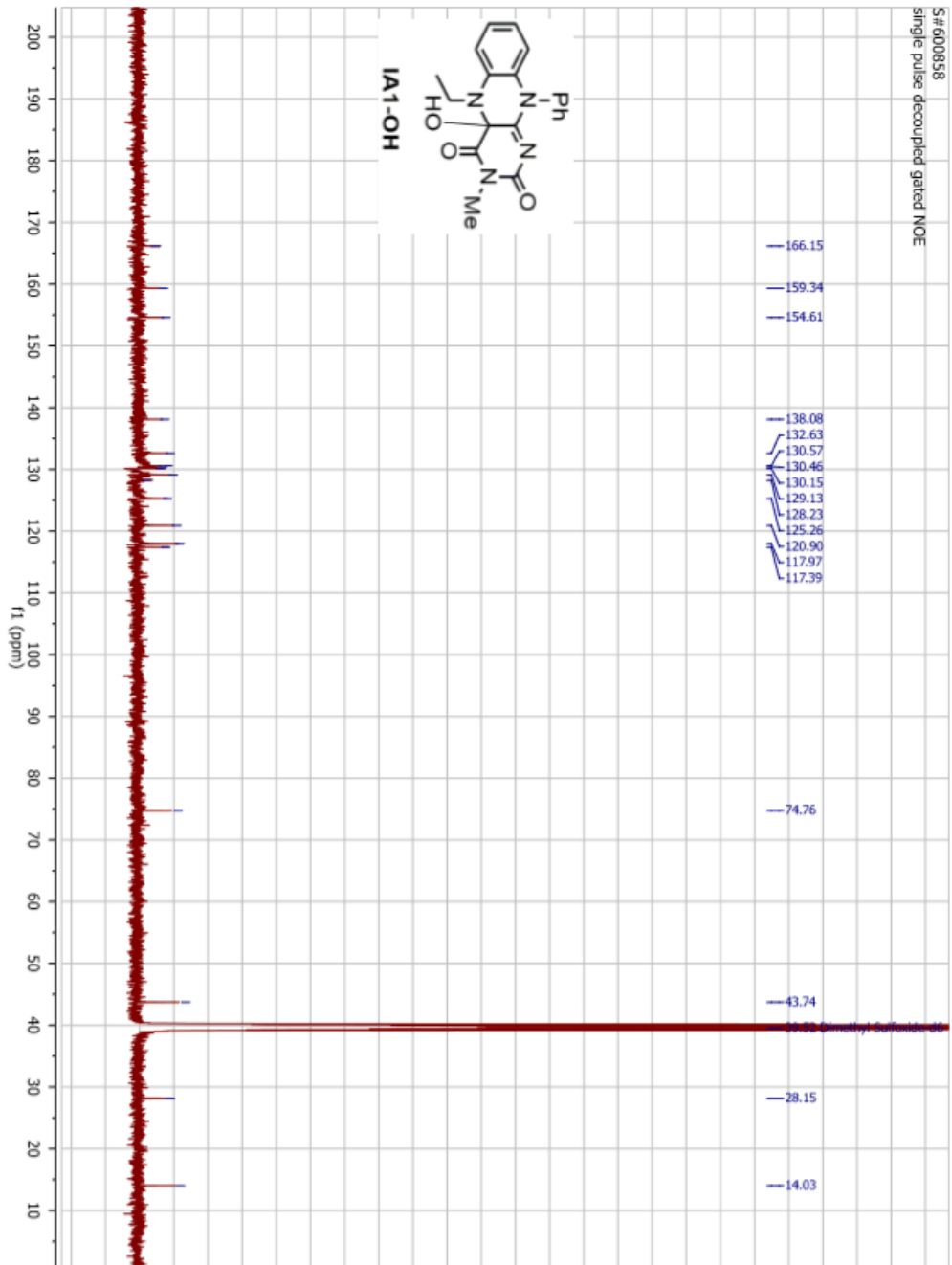
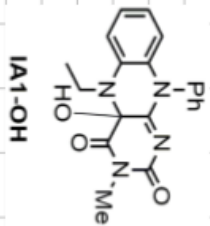


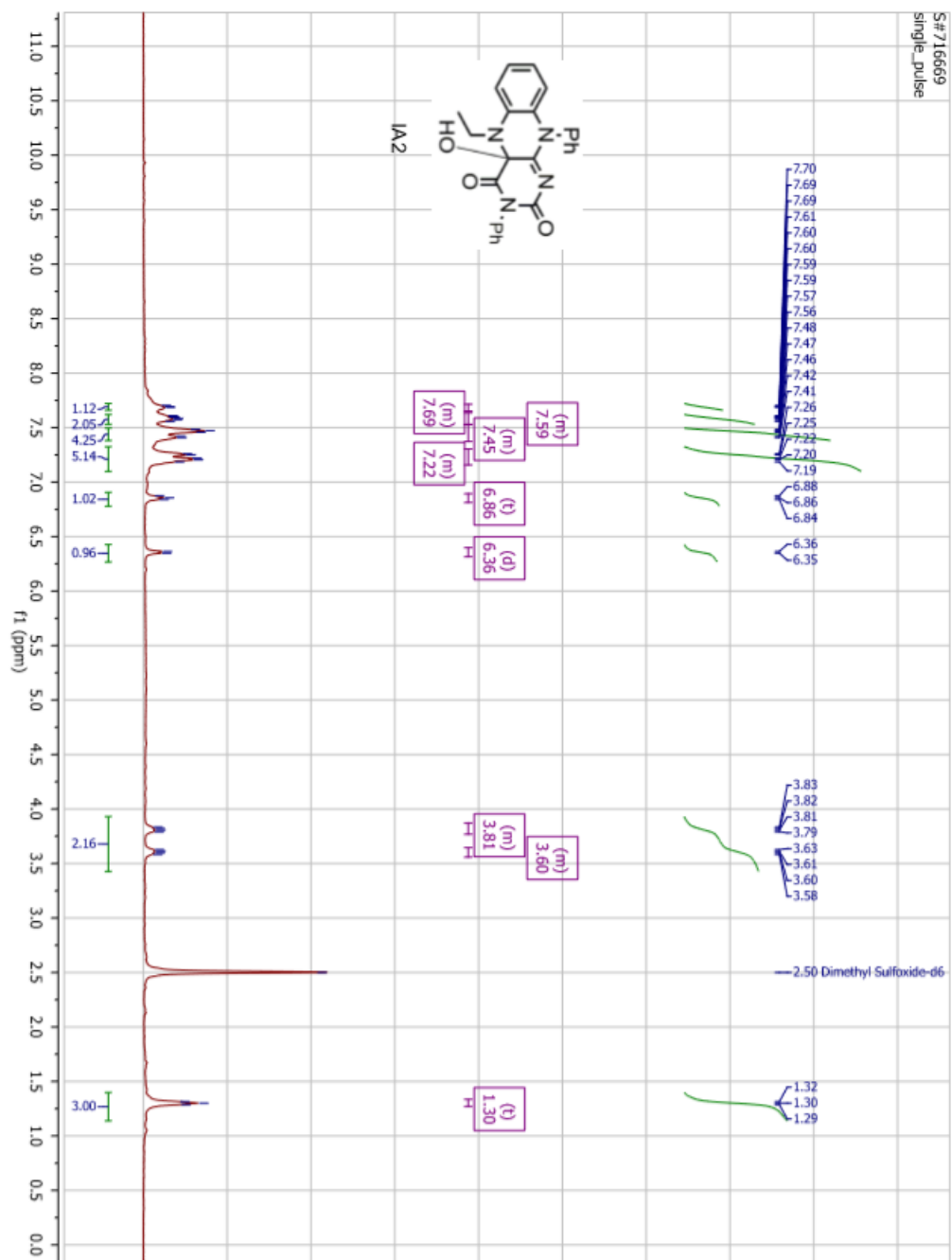


S#A28330
single_pulse

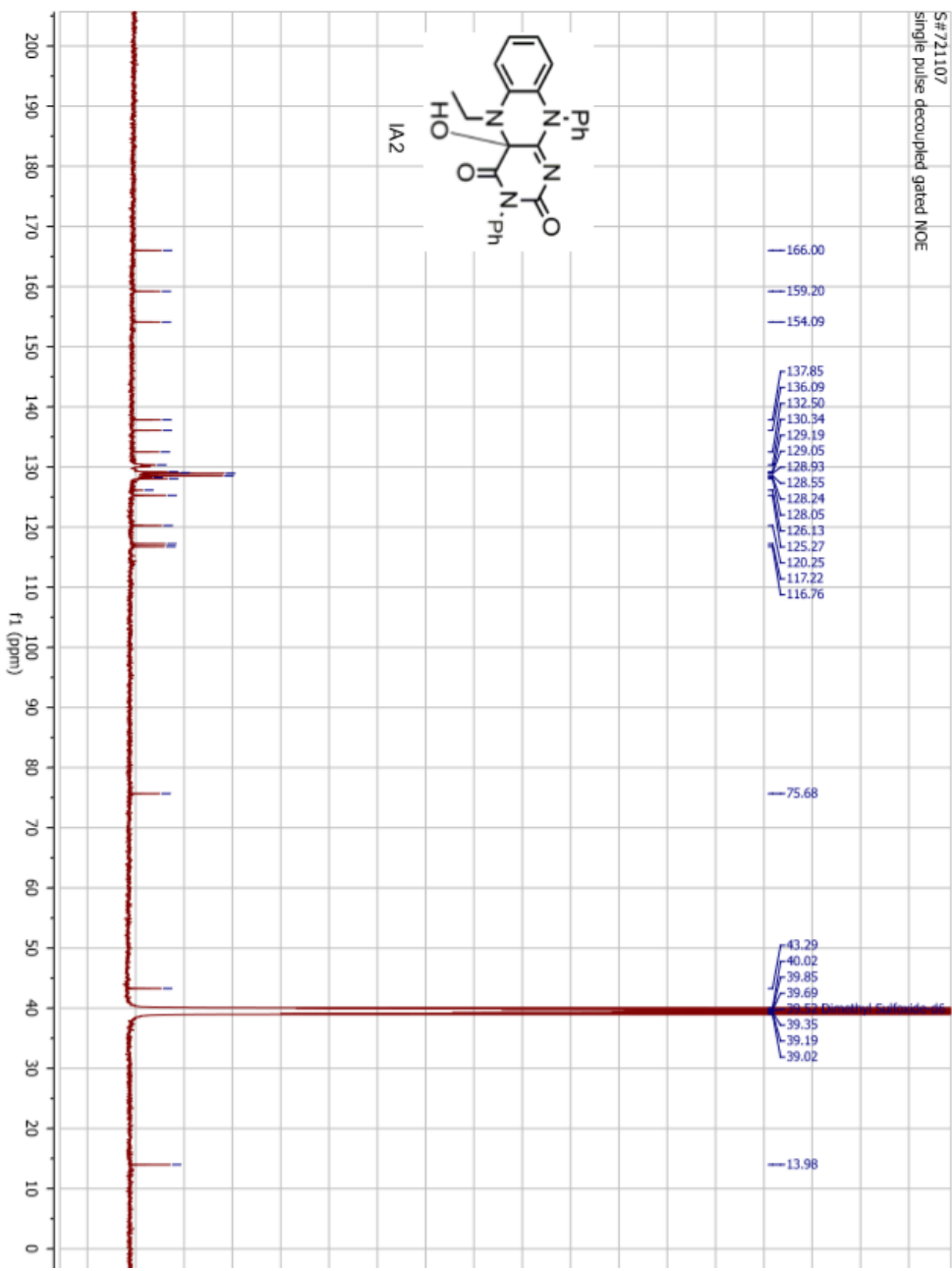
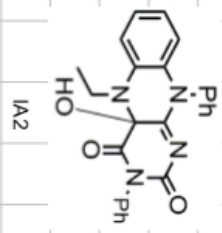


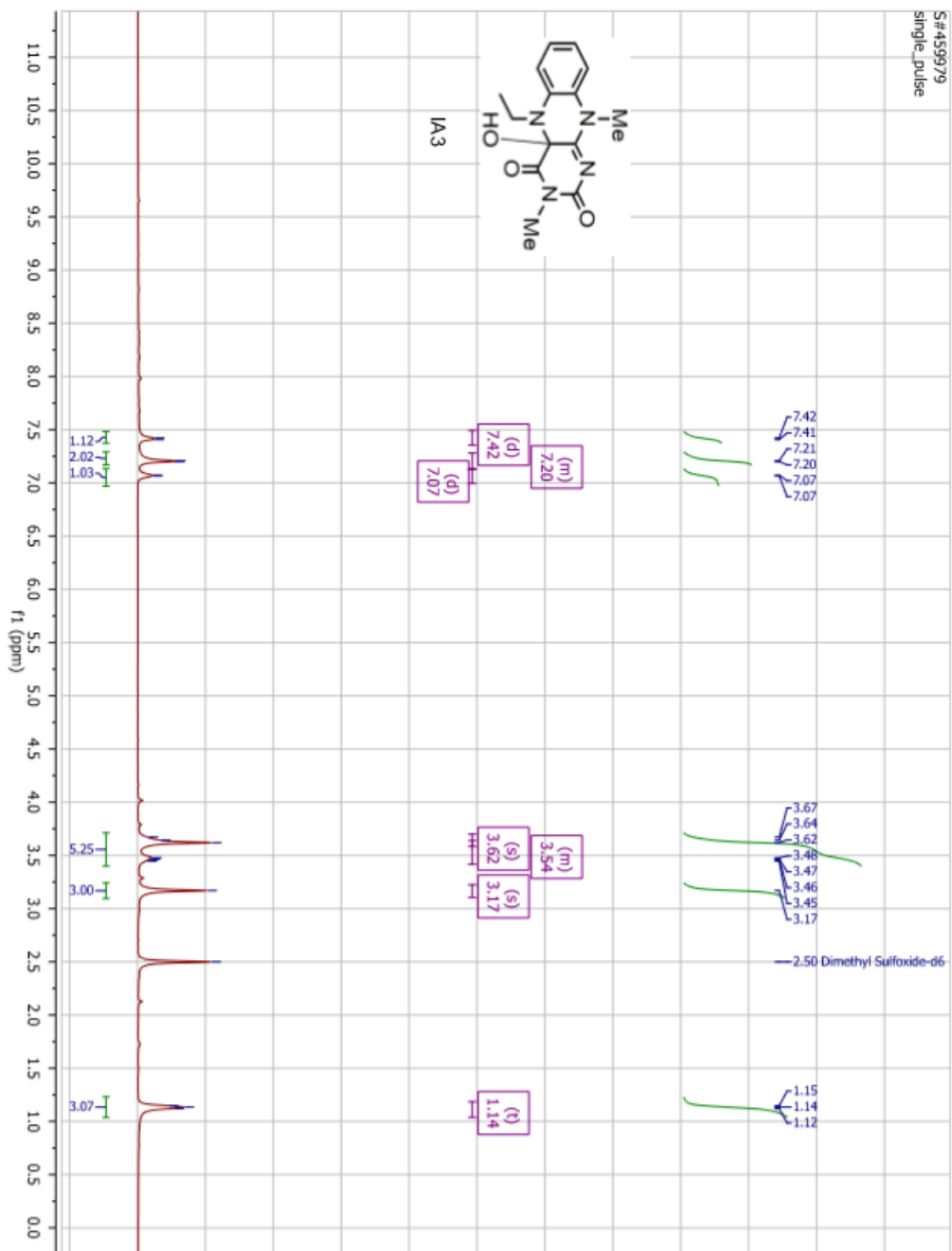
S#600858
single pulse decoupled gated NOE

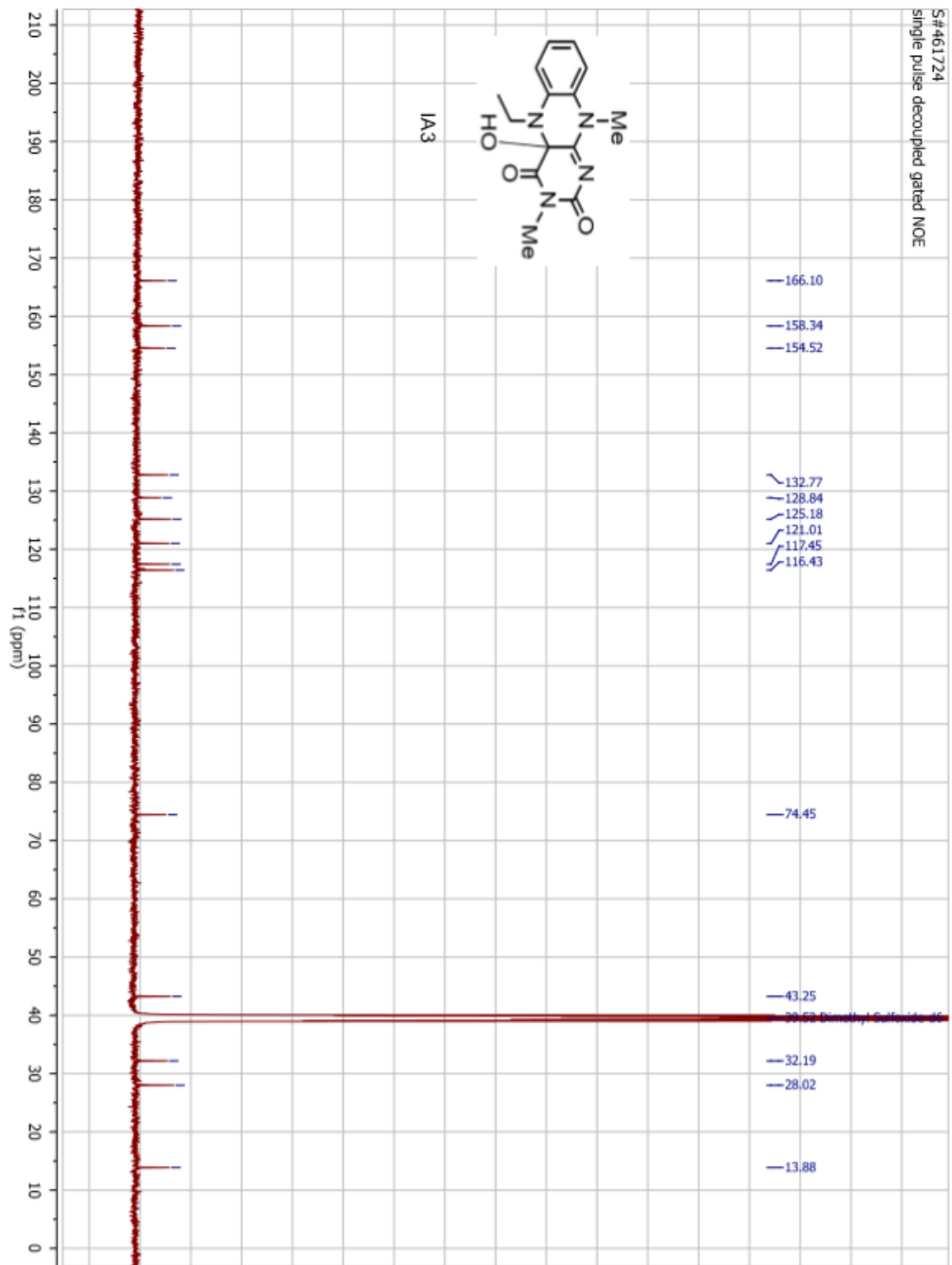


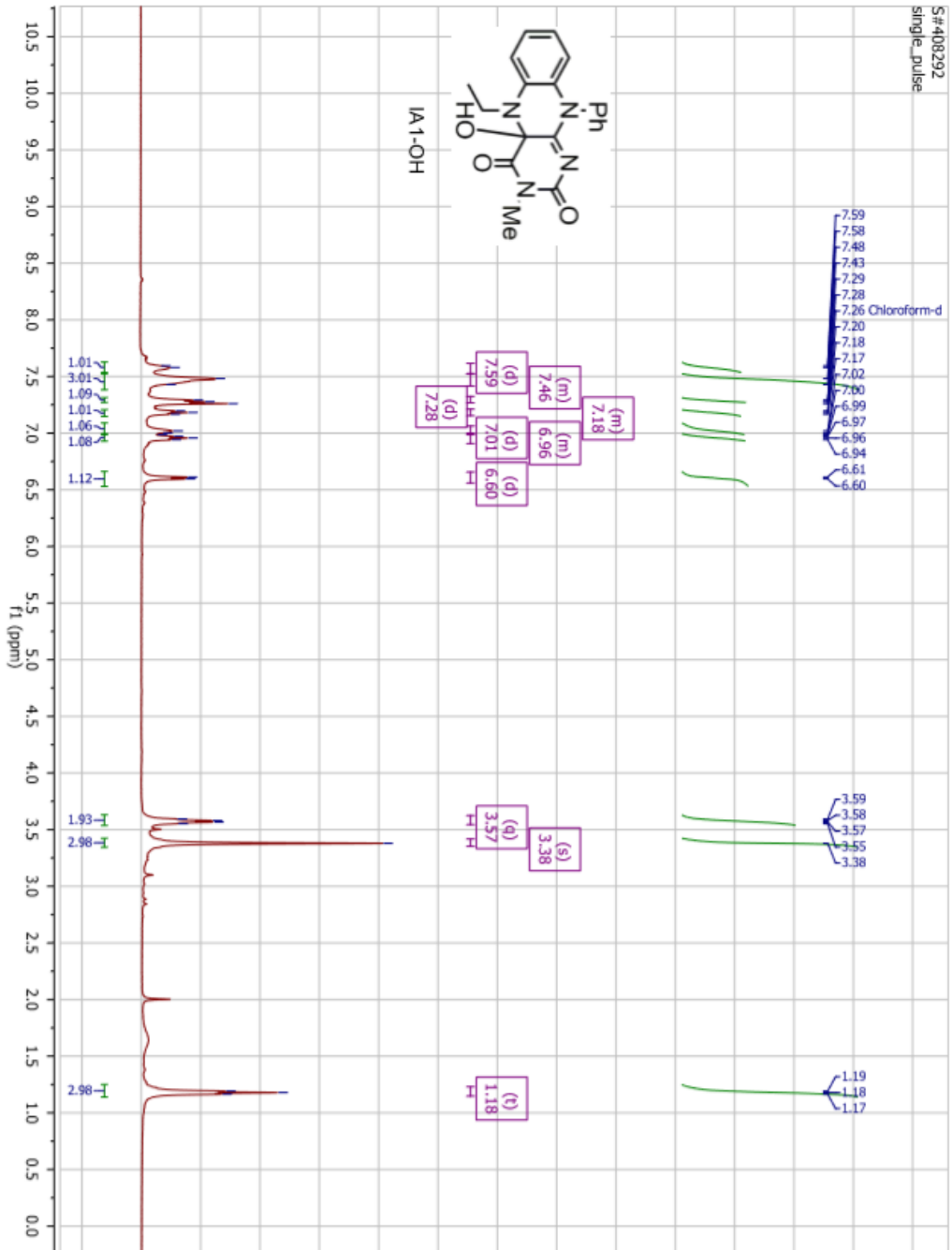


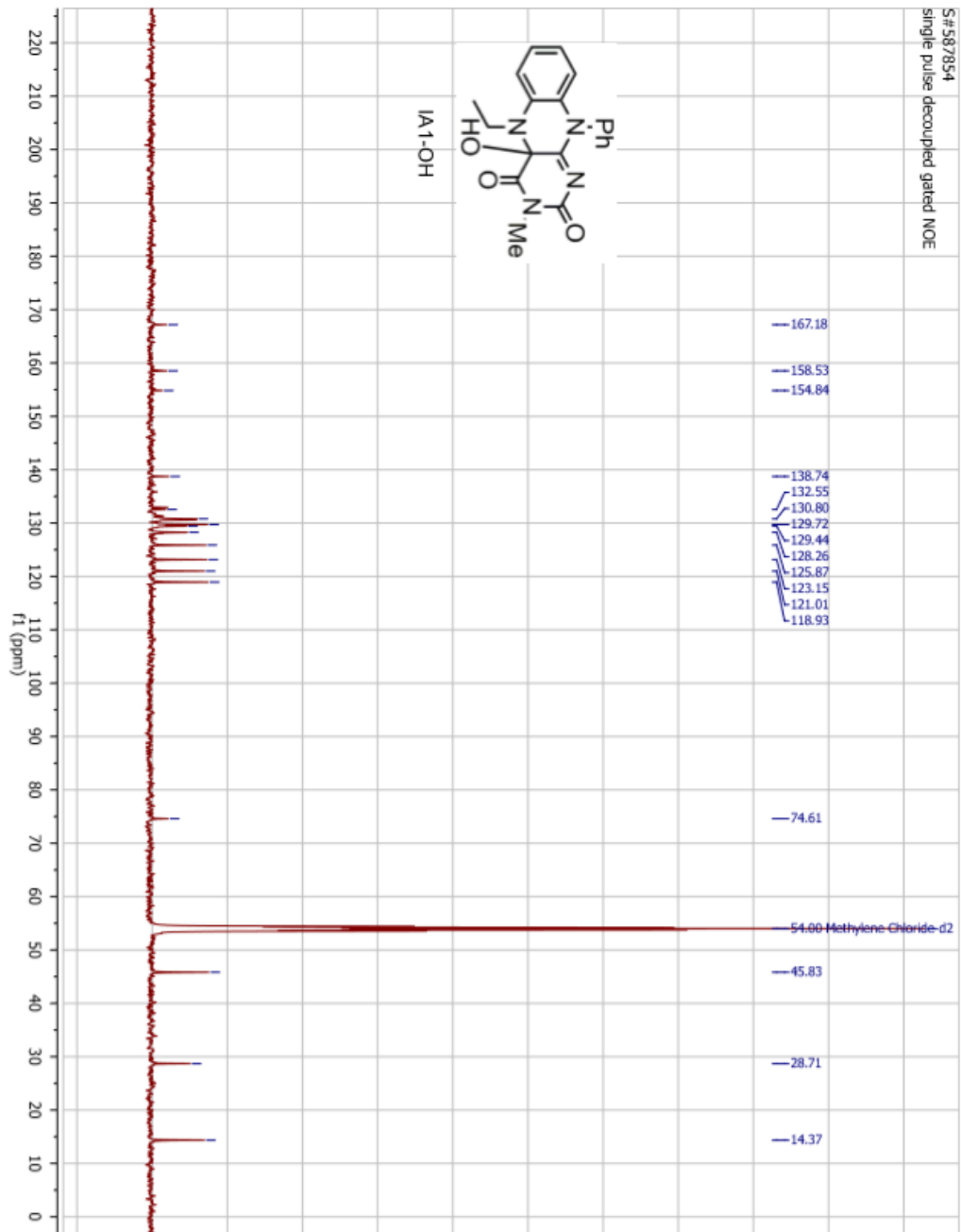
S#721107
single pulse decoupled gated NOE

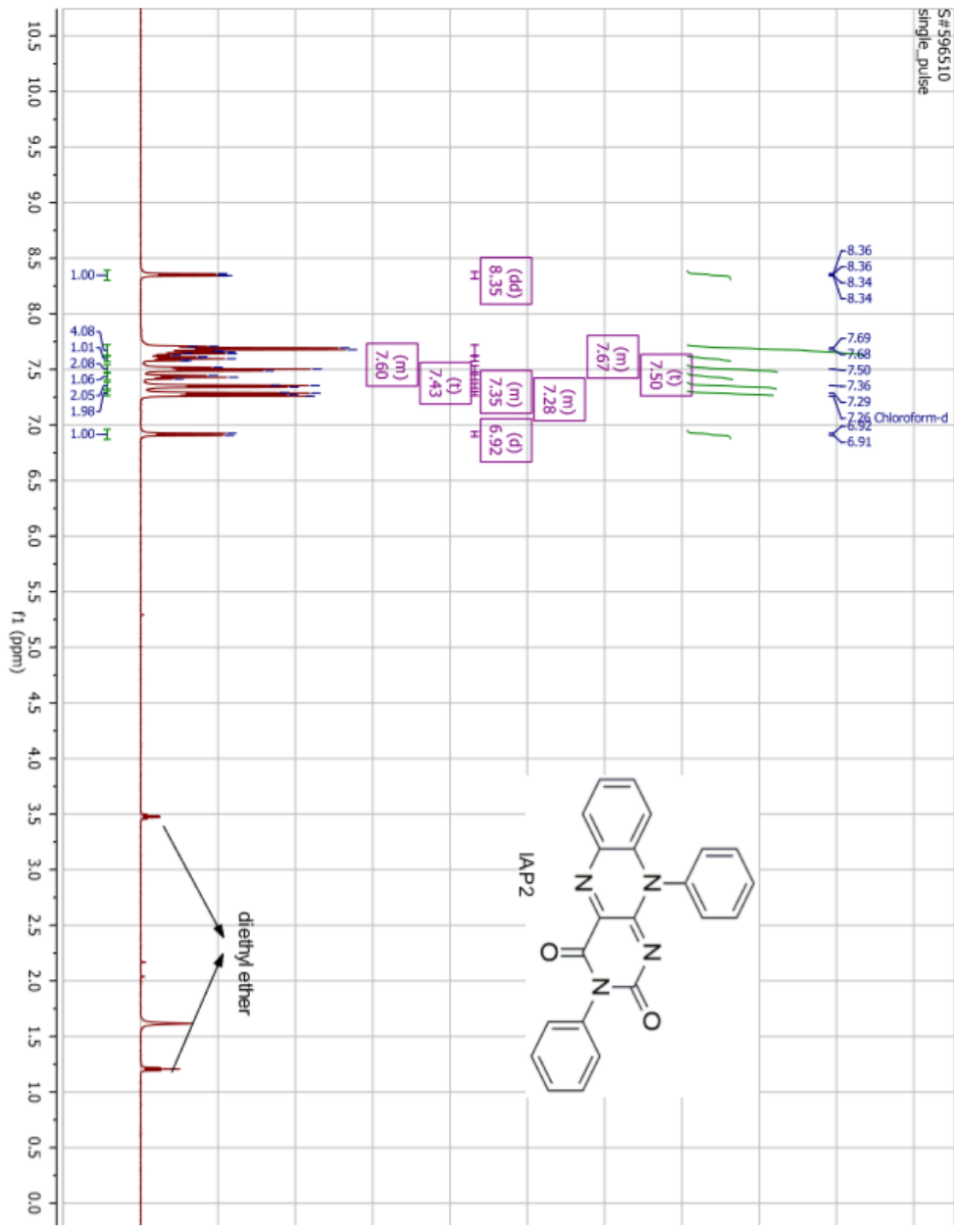


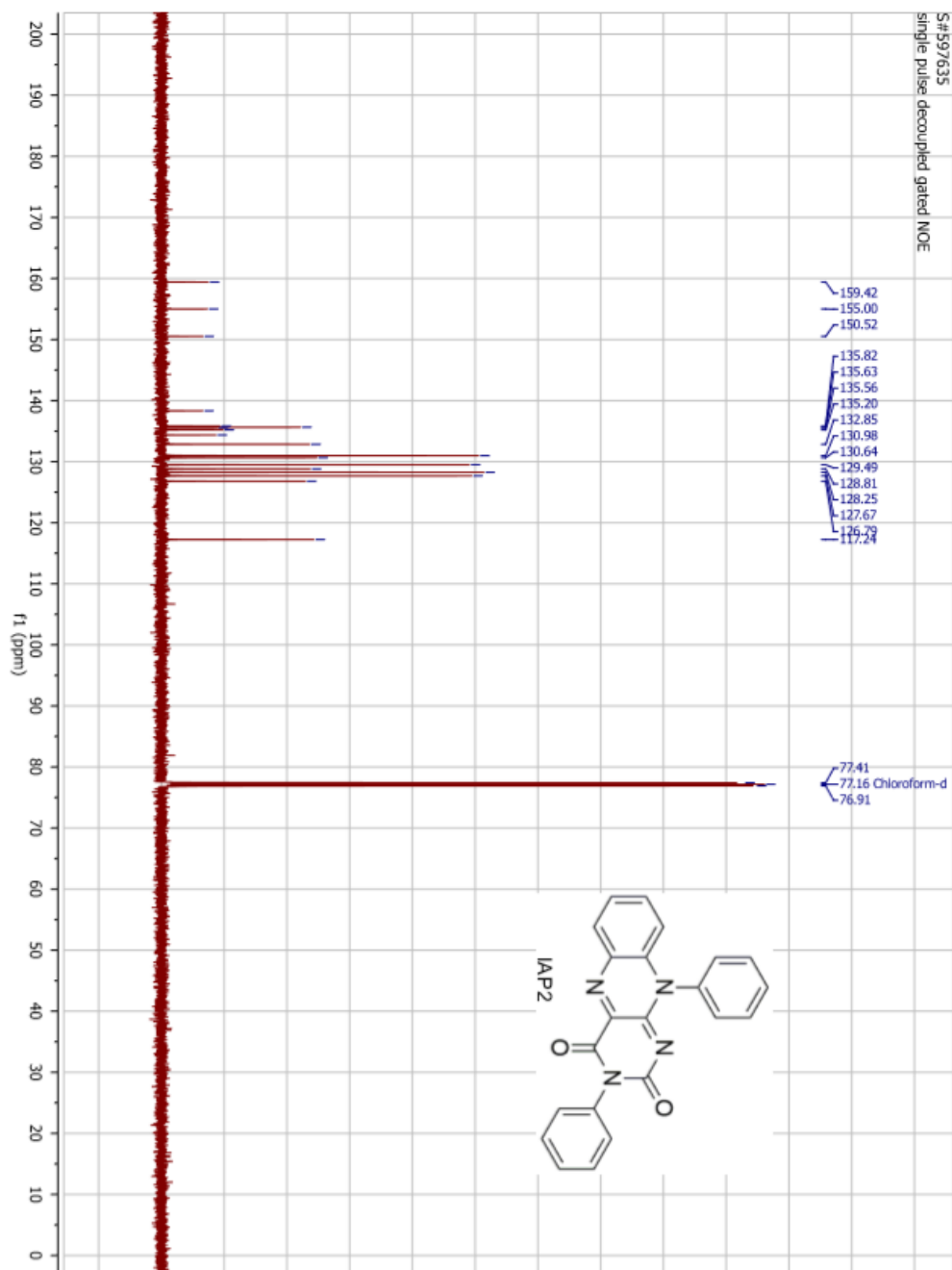




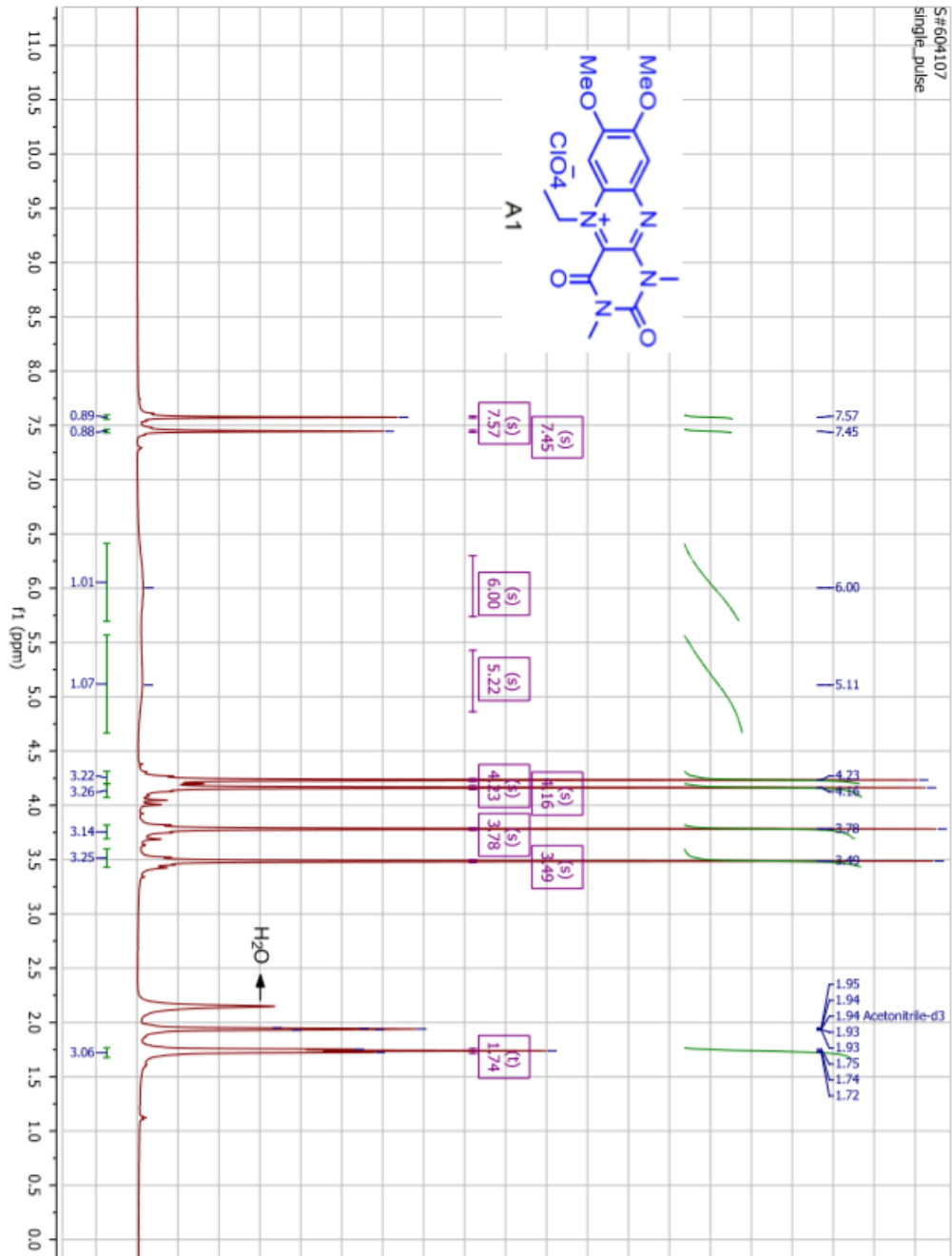


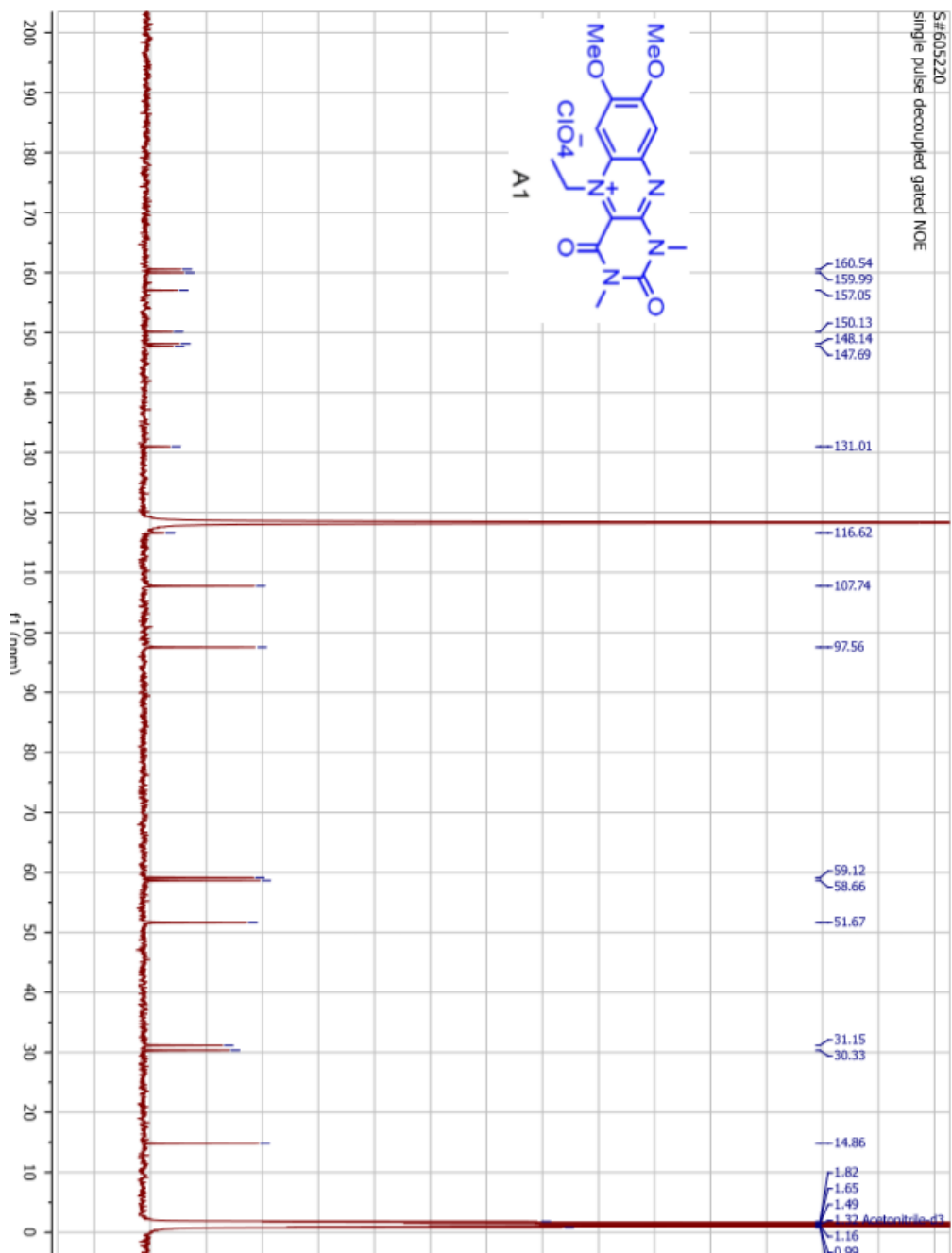




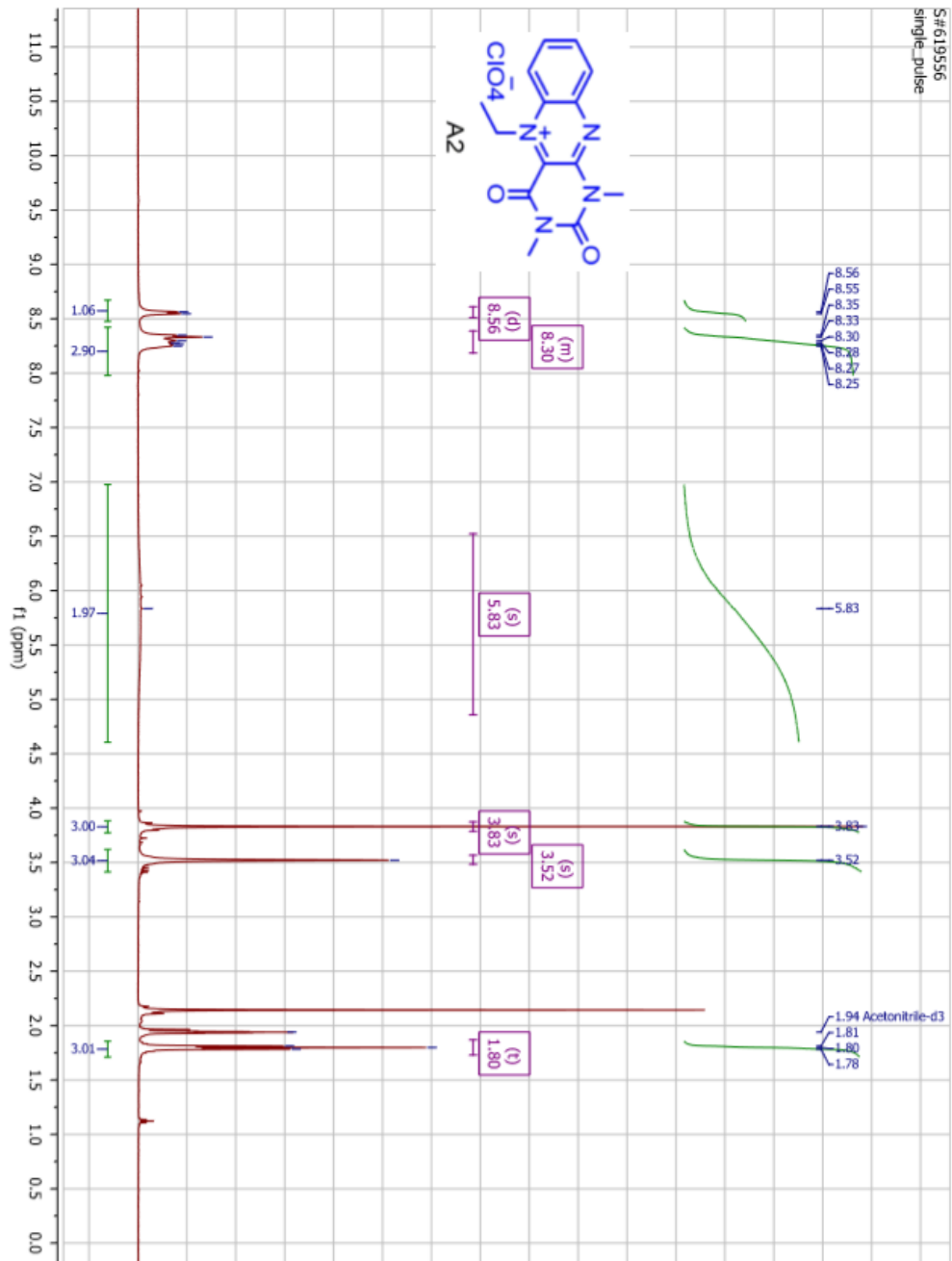


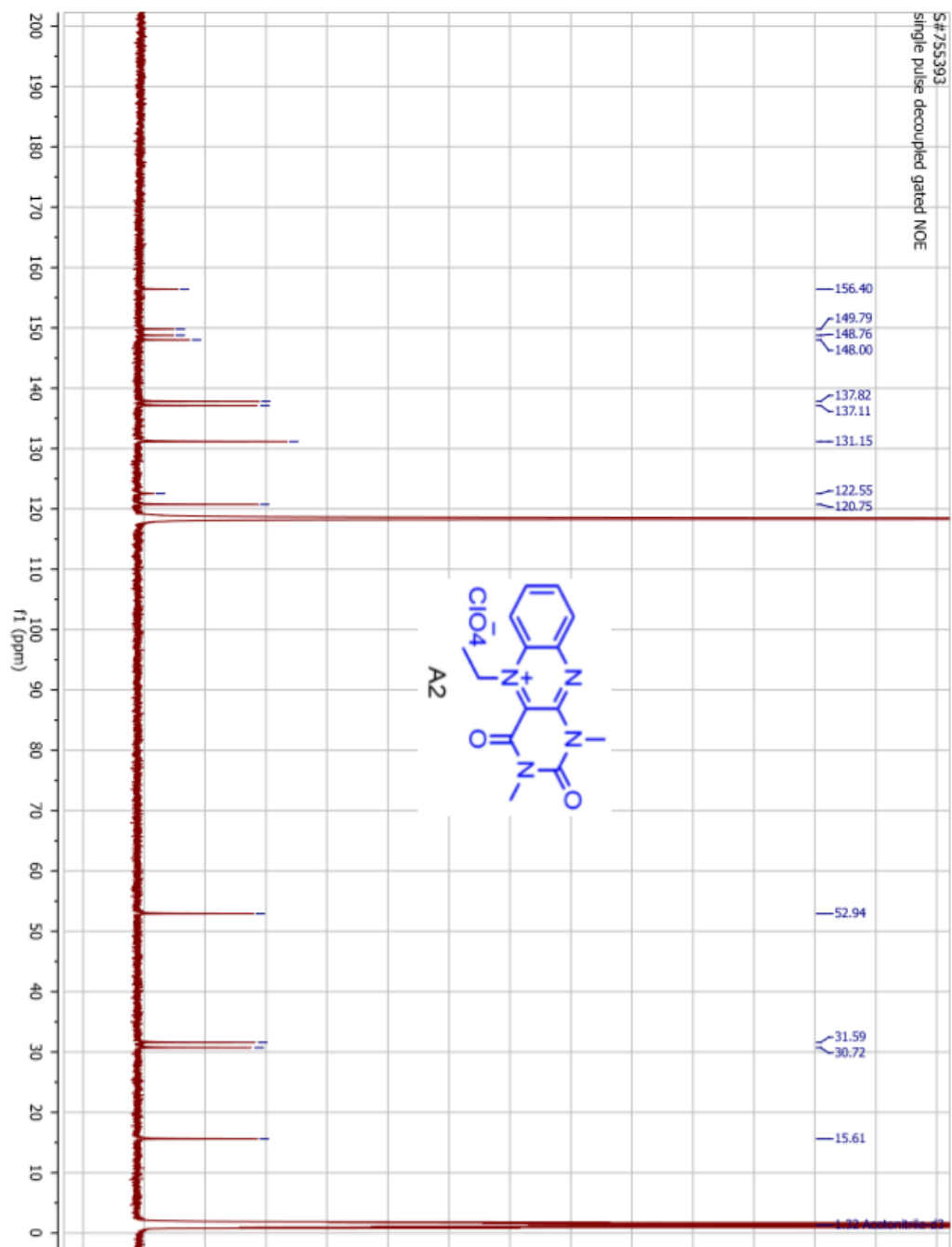
S#604107
single_pulse



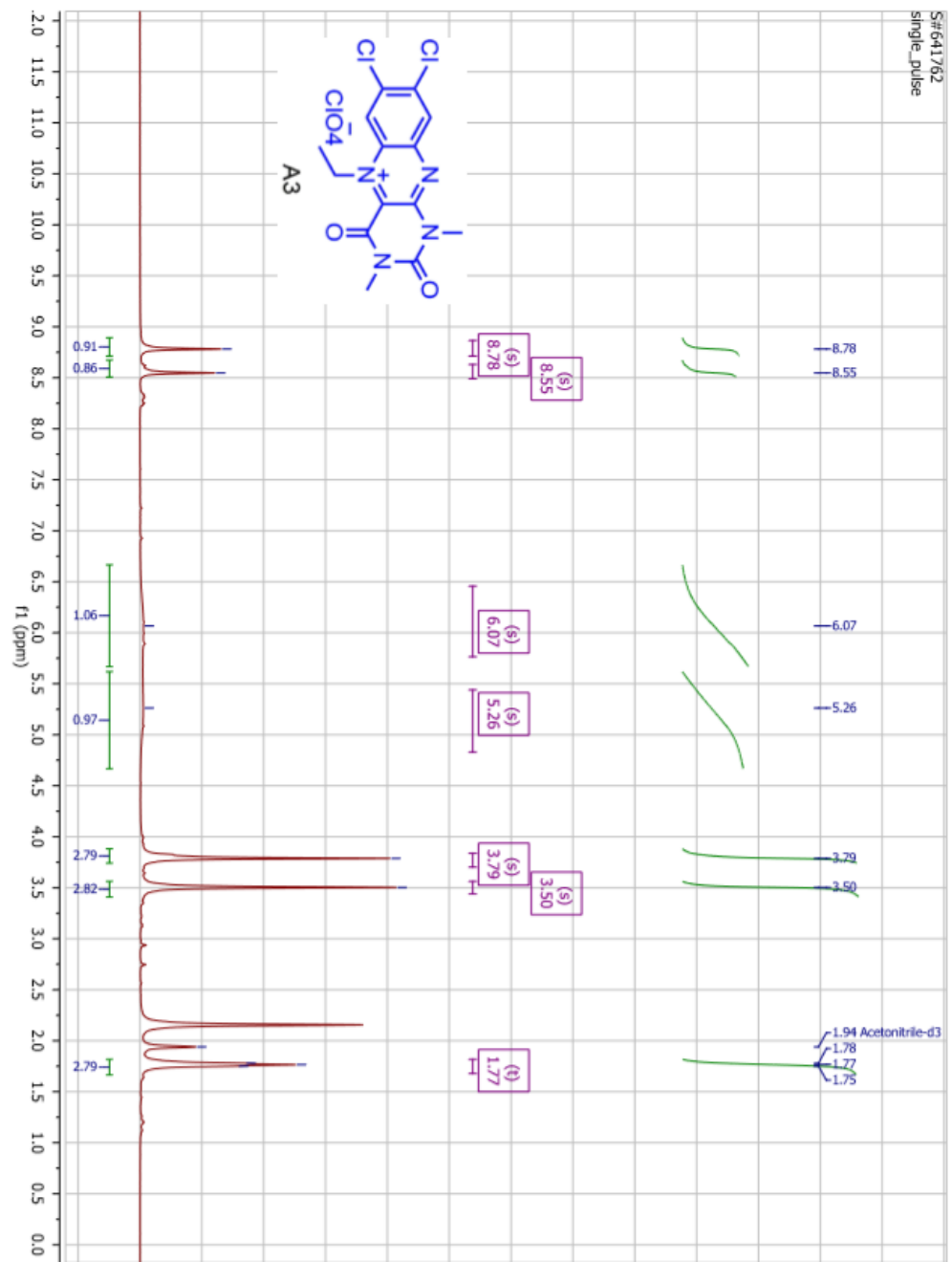


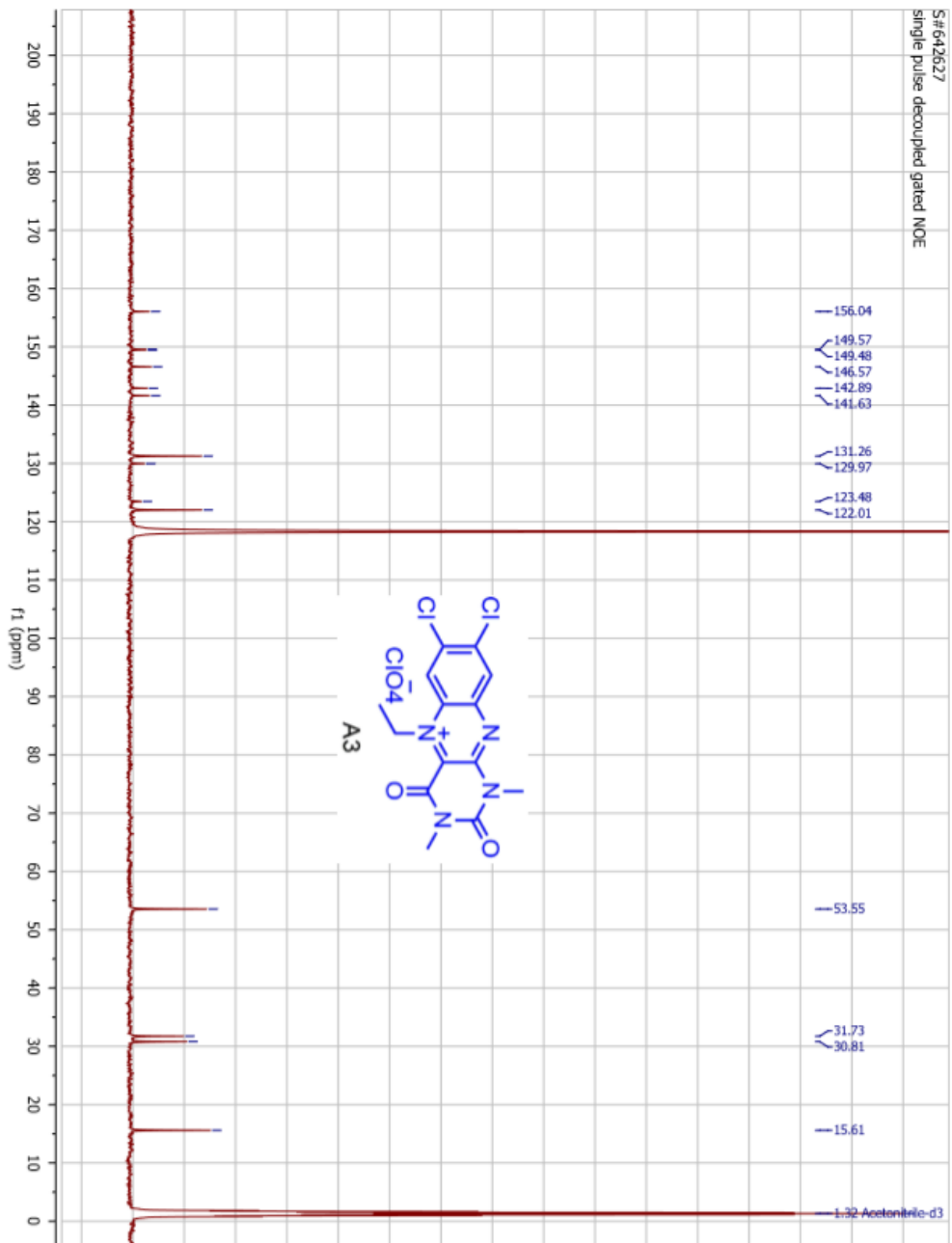
S#619556
single_pulse



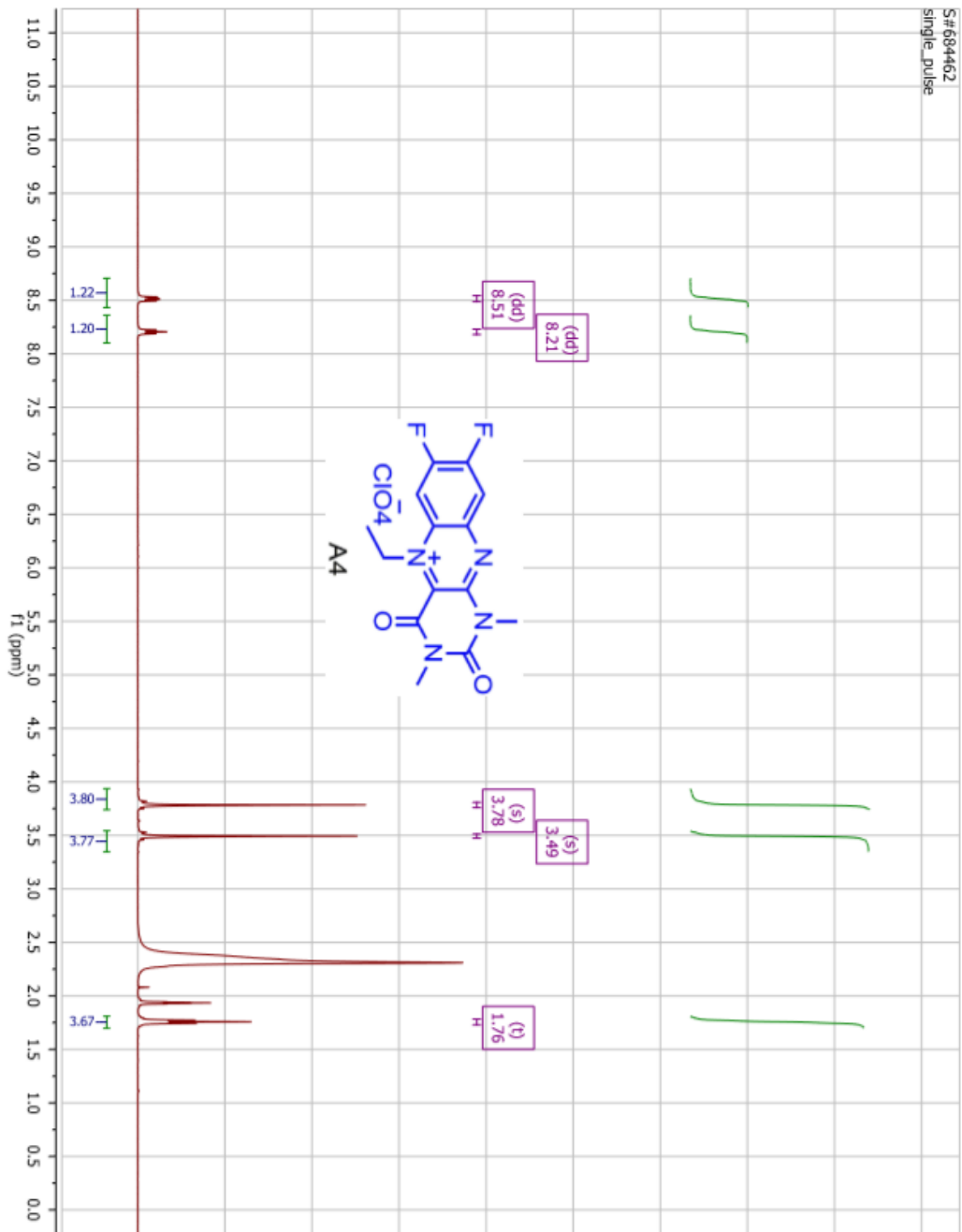


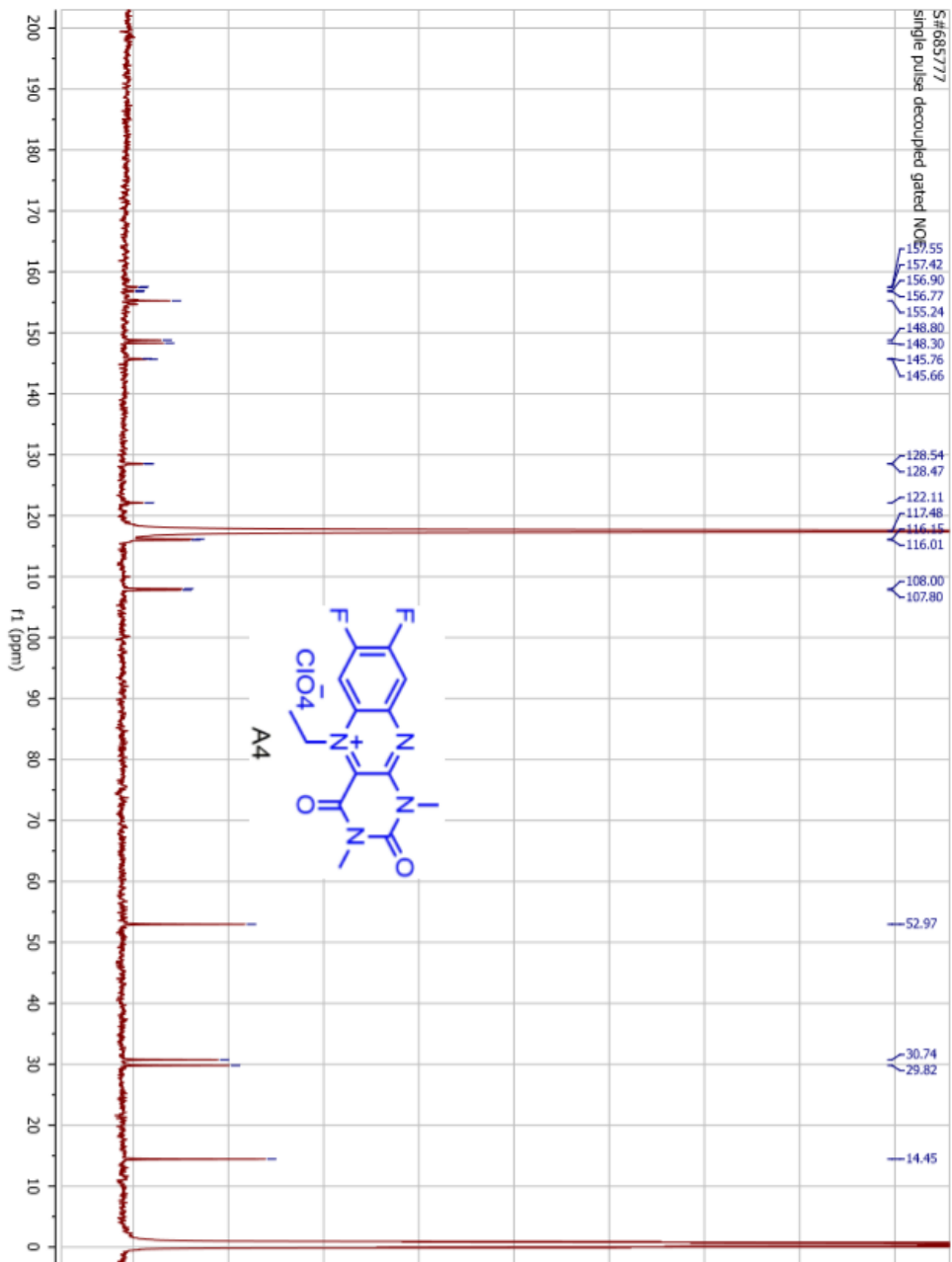
S#641762
single_pulse



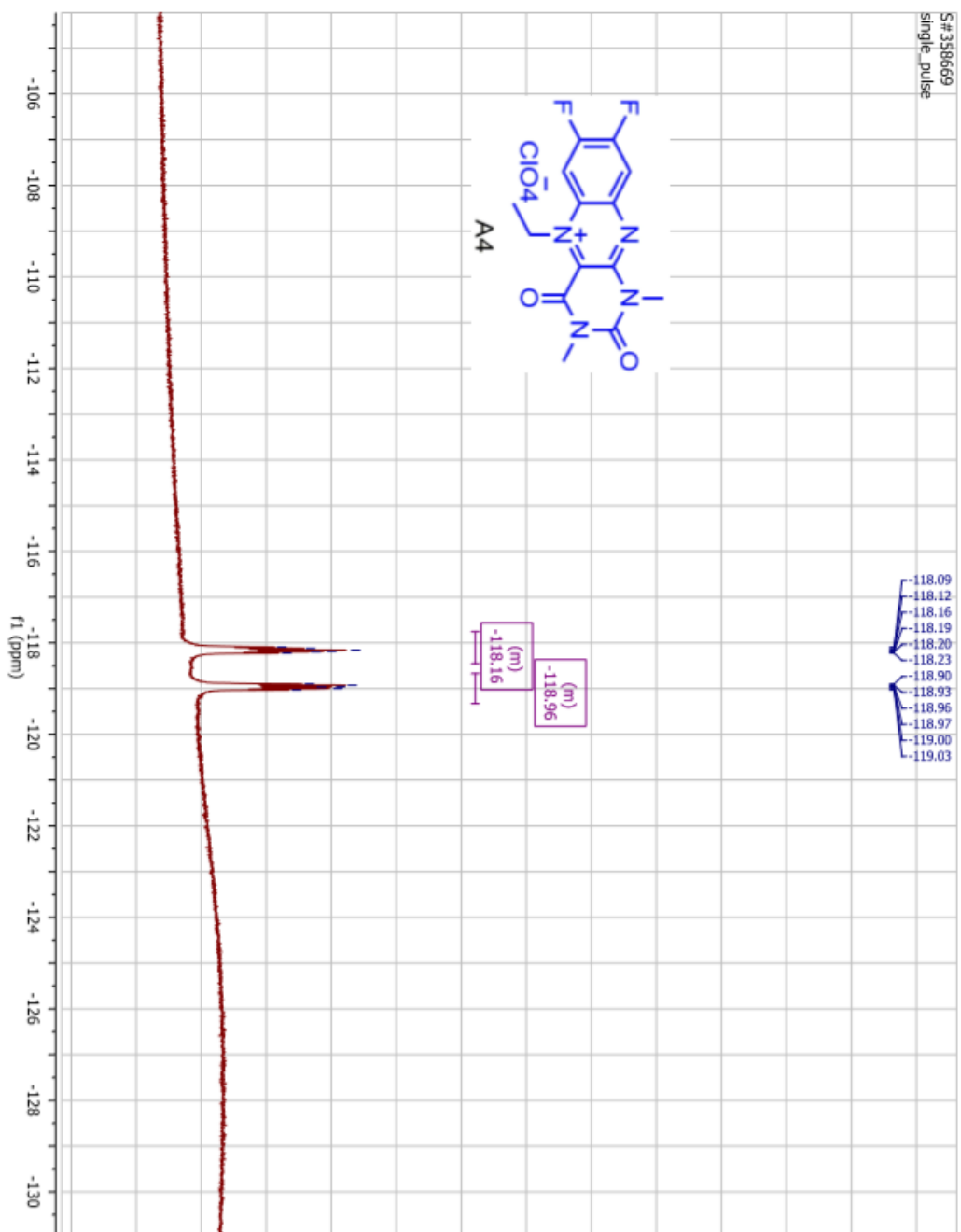
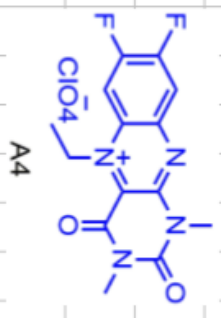


S#684462
single_pulse

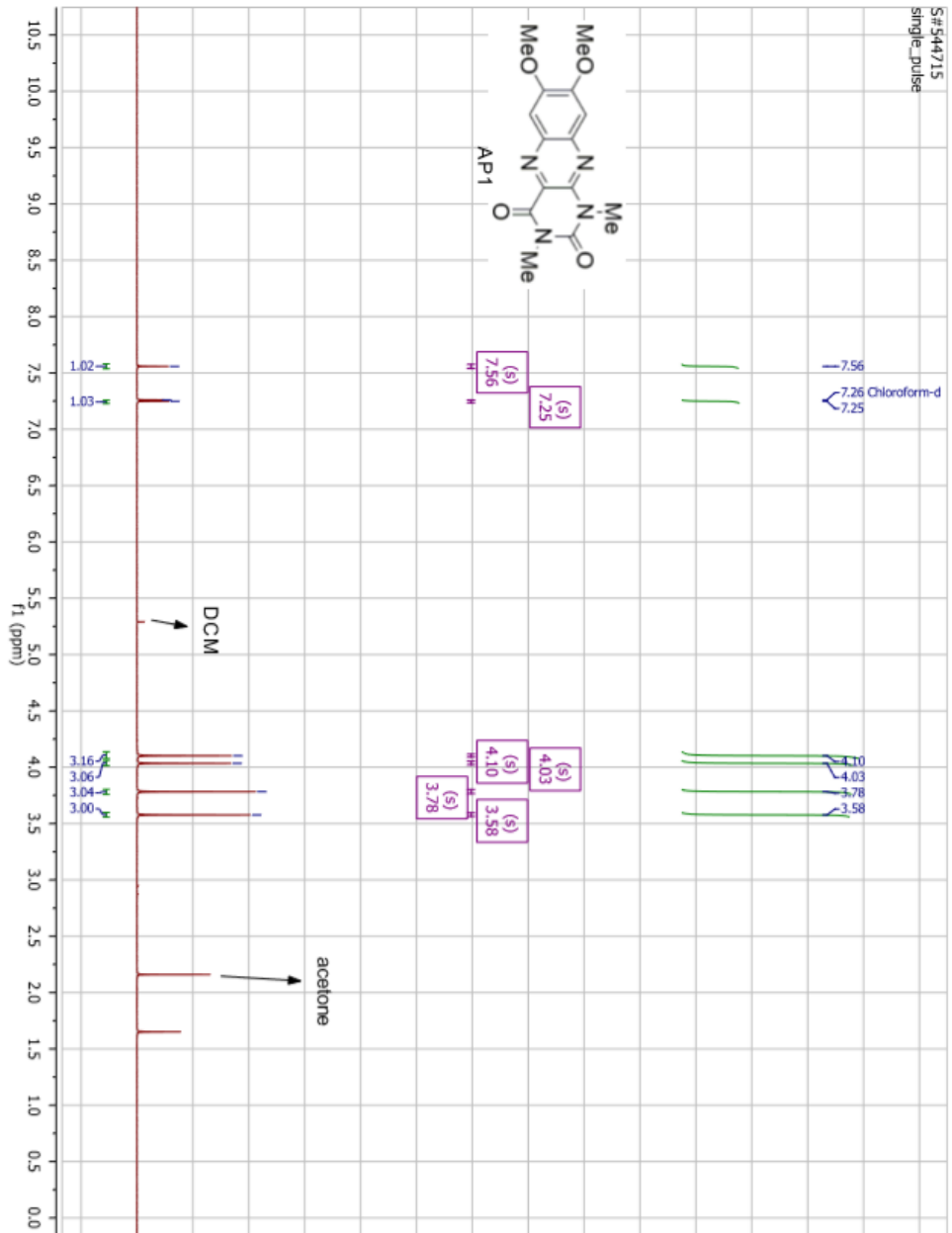


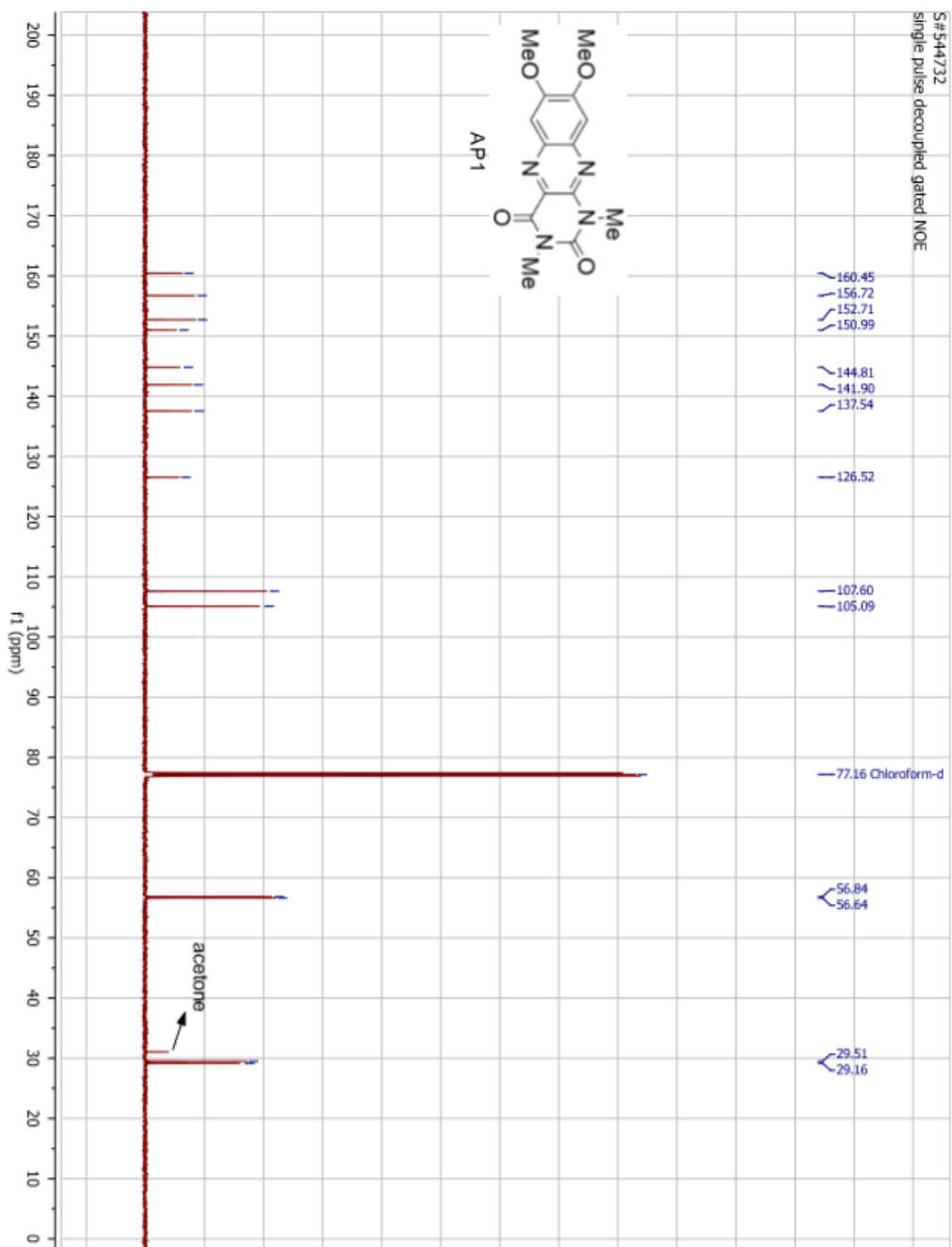


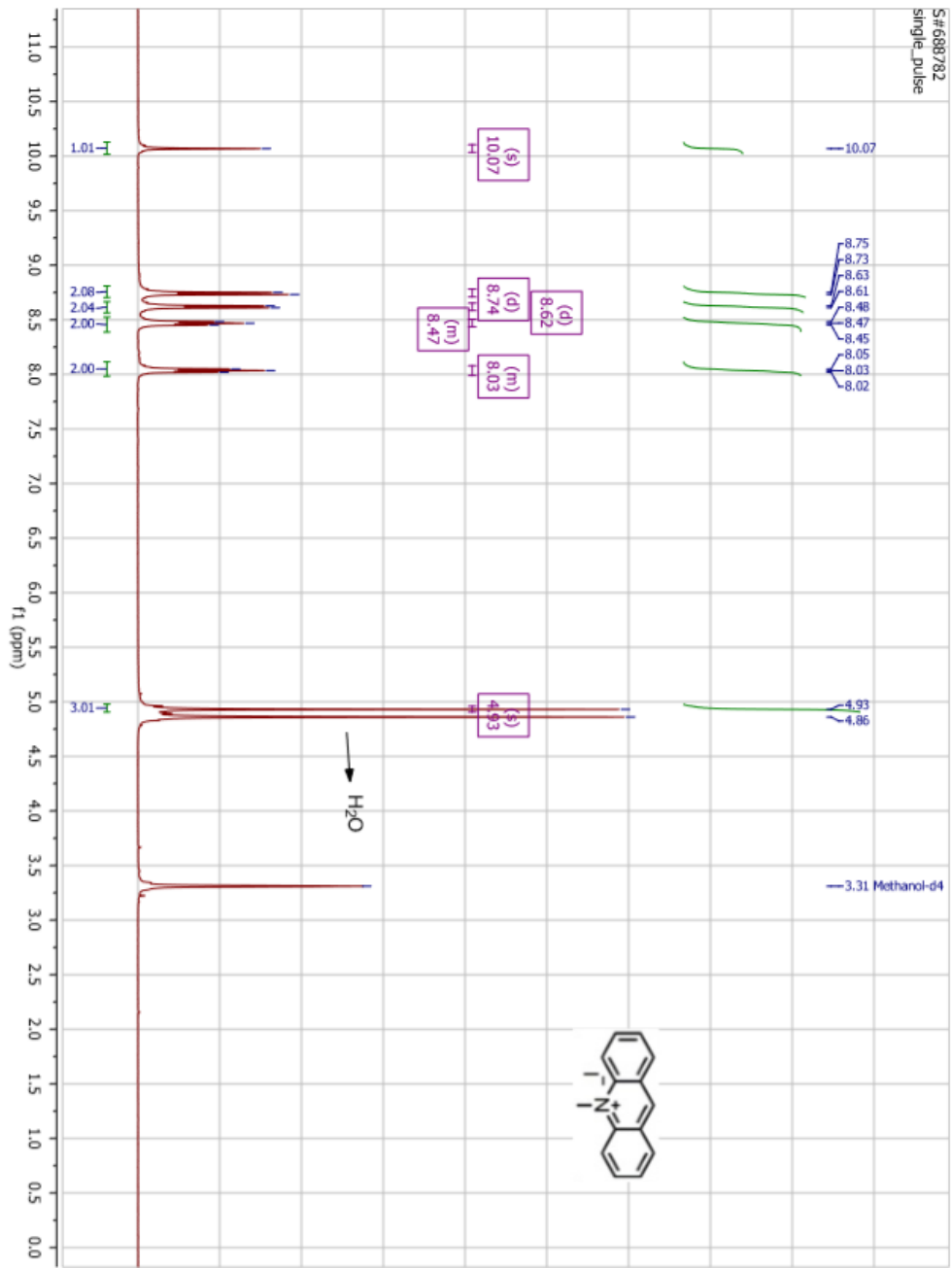
S#358669
single_pulse

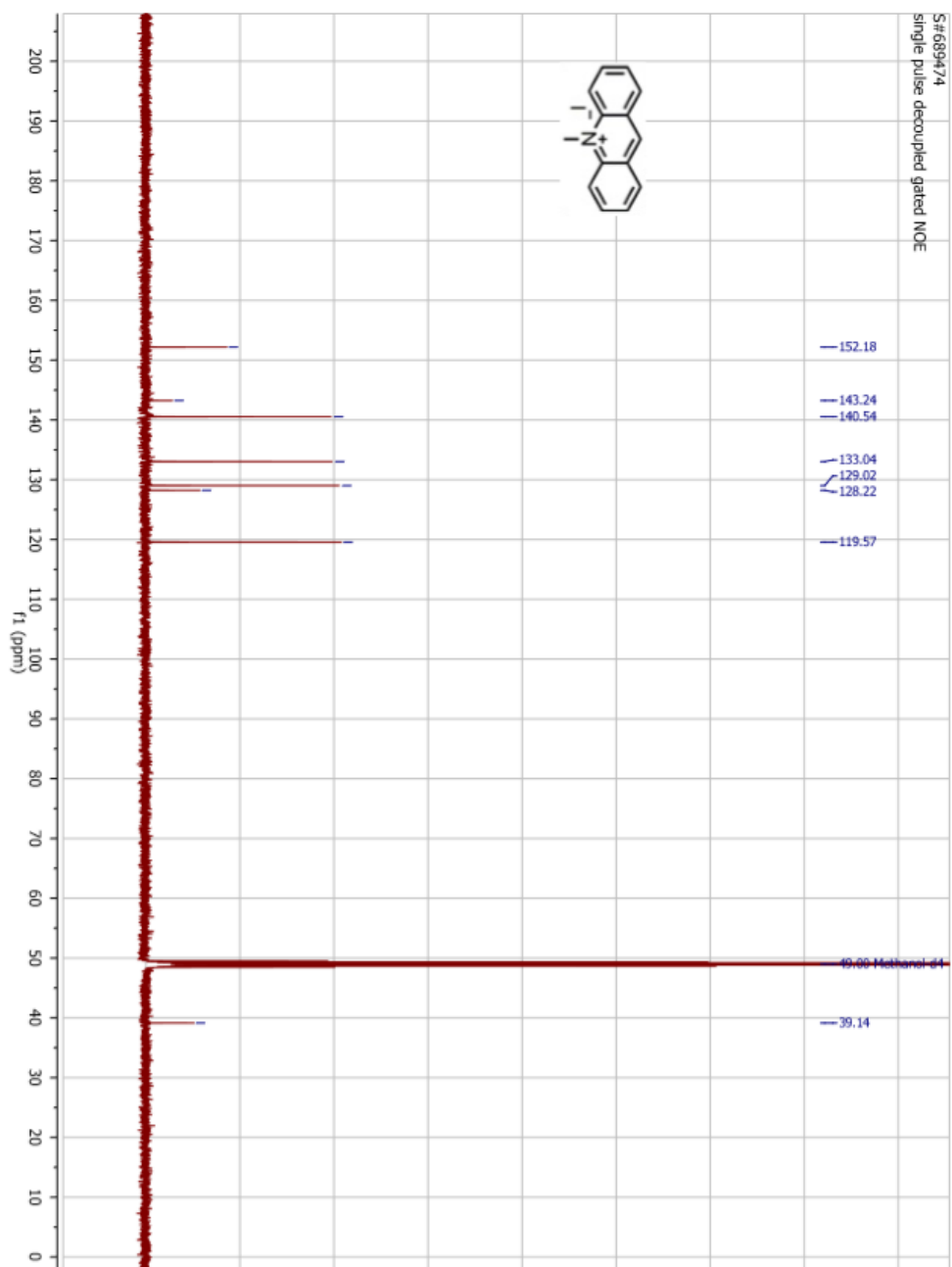


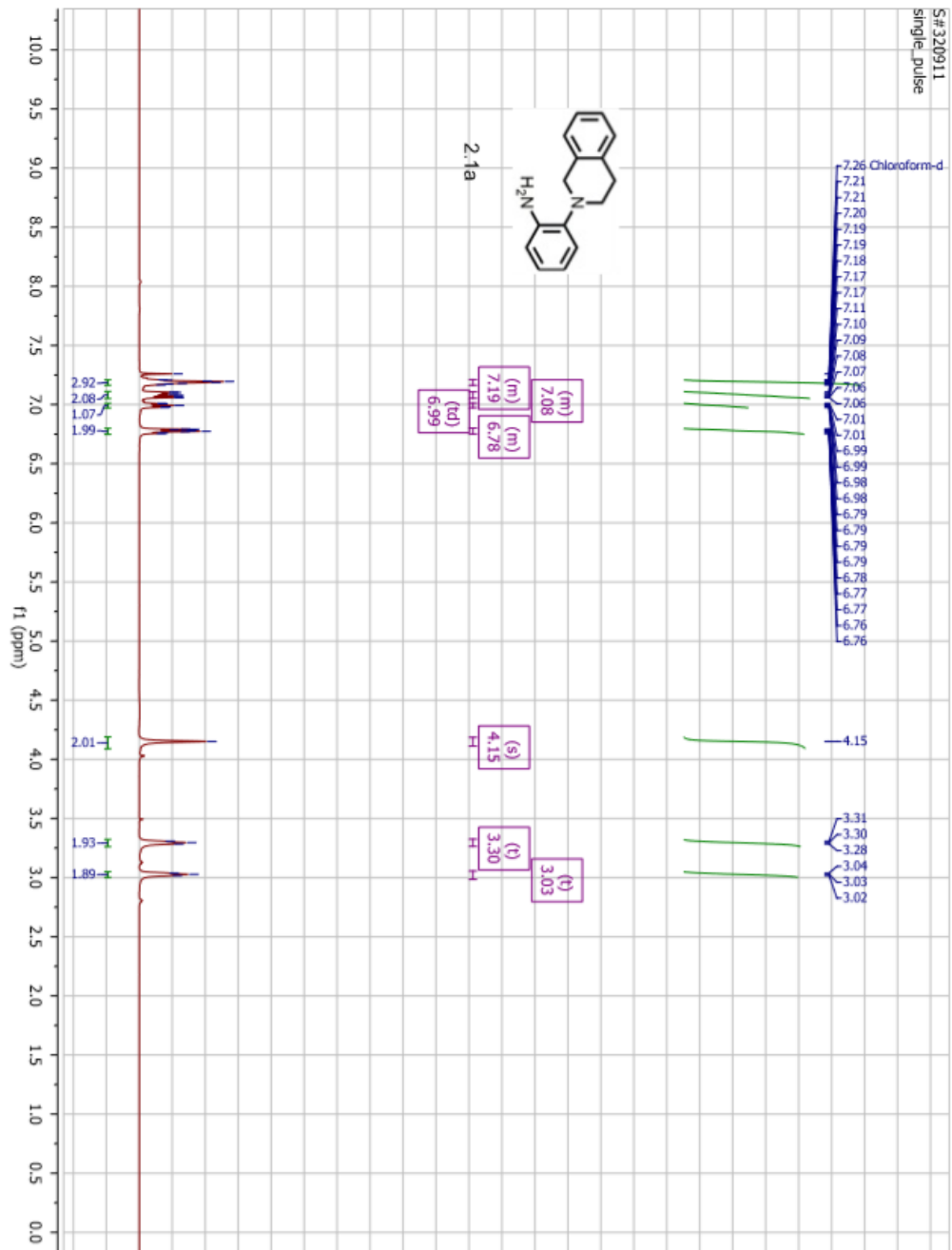
S# 544715
single_pulse

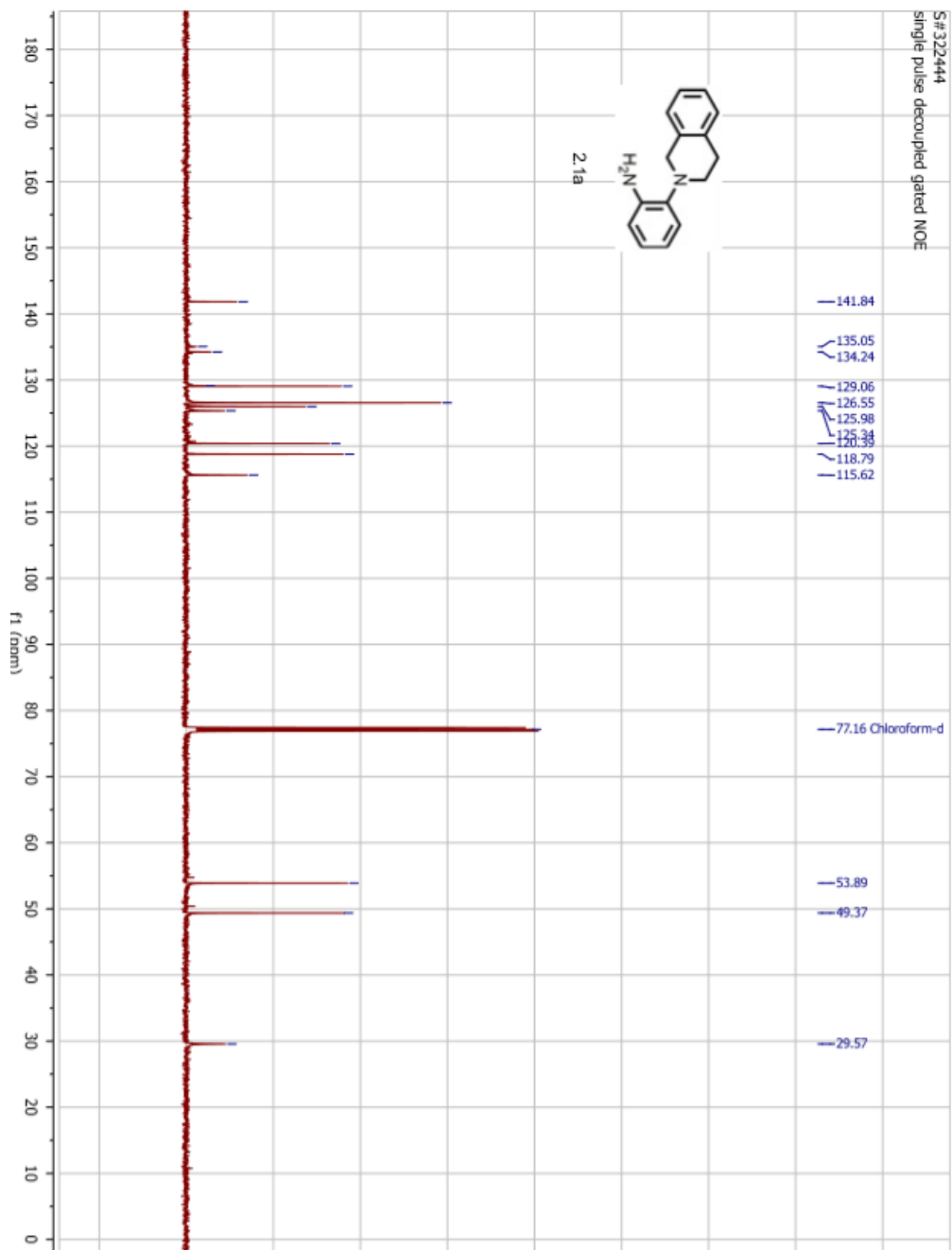




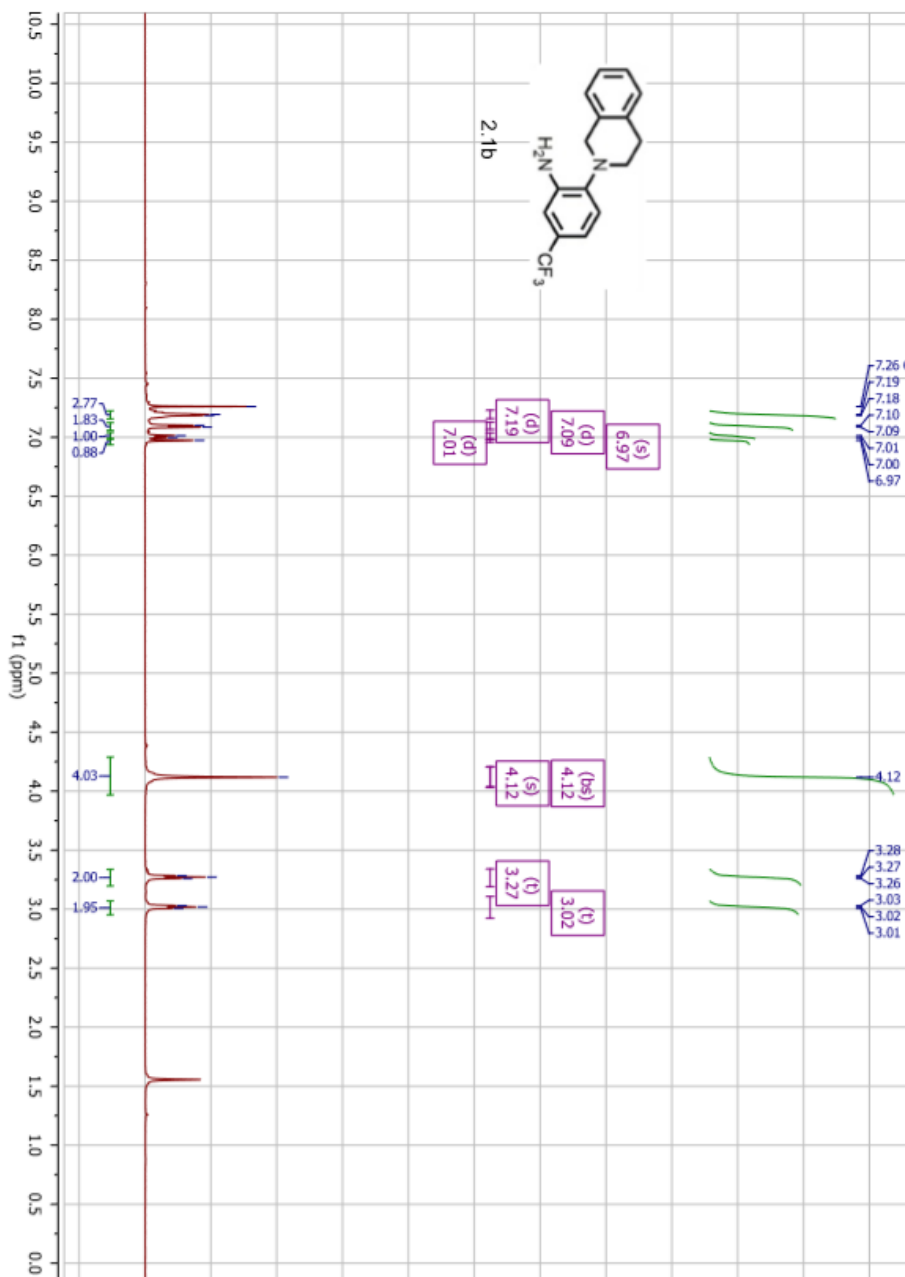


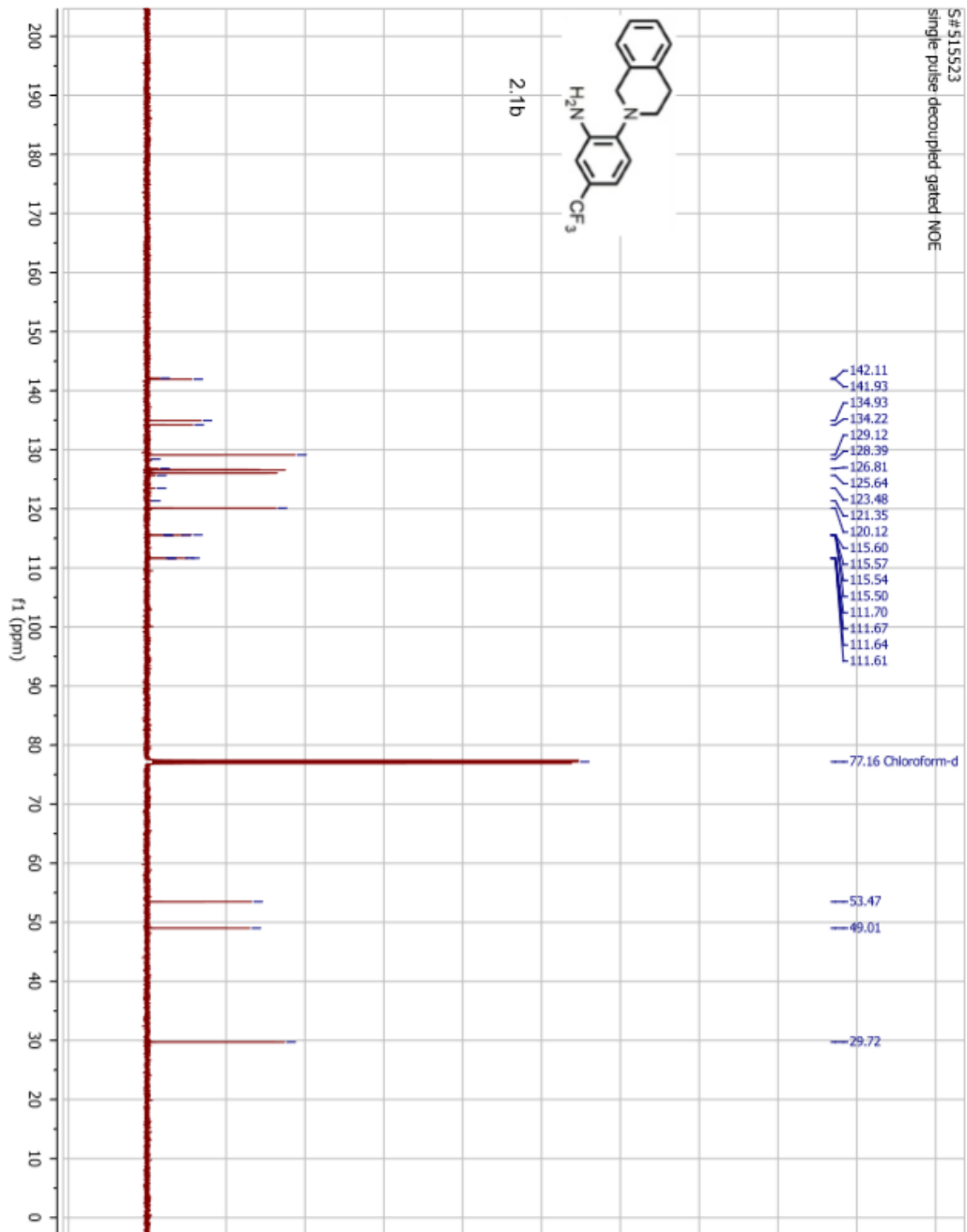


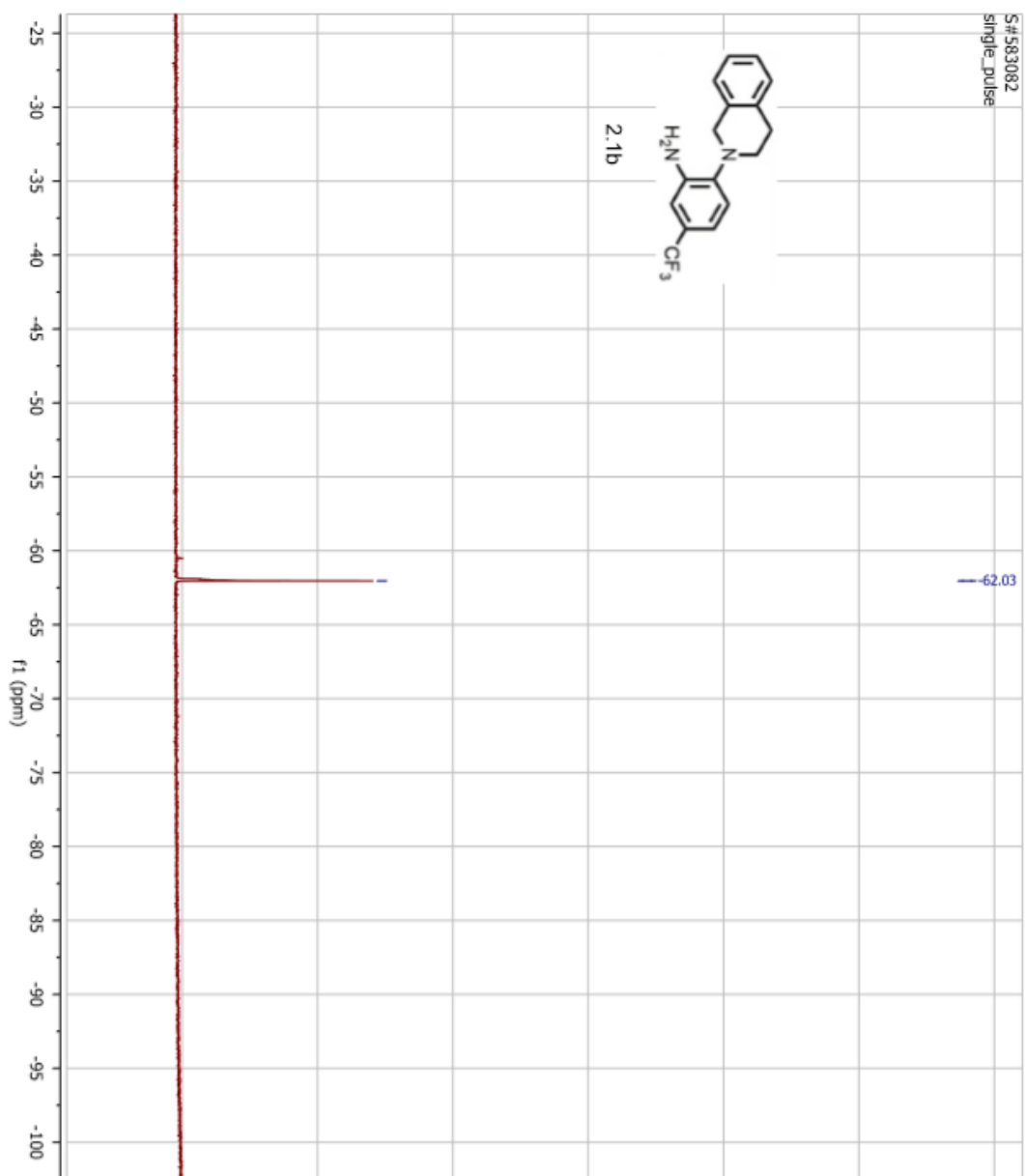


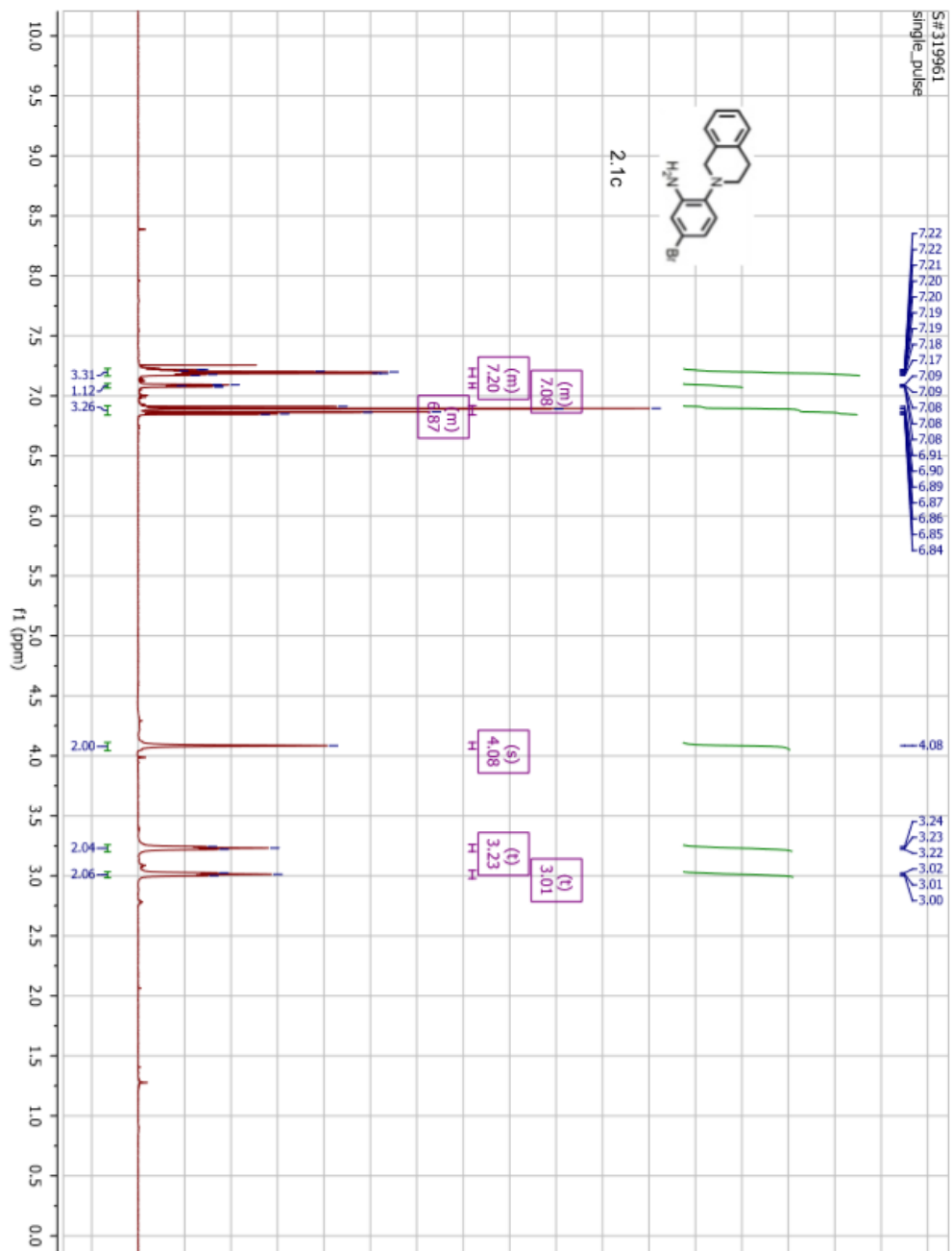


S# 514872
single_pulse

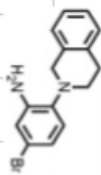




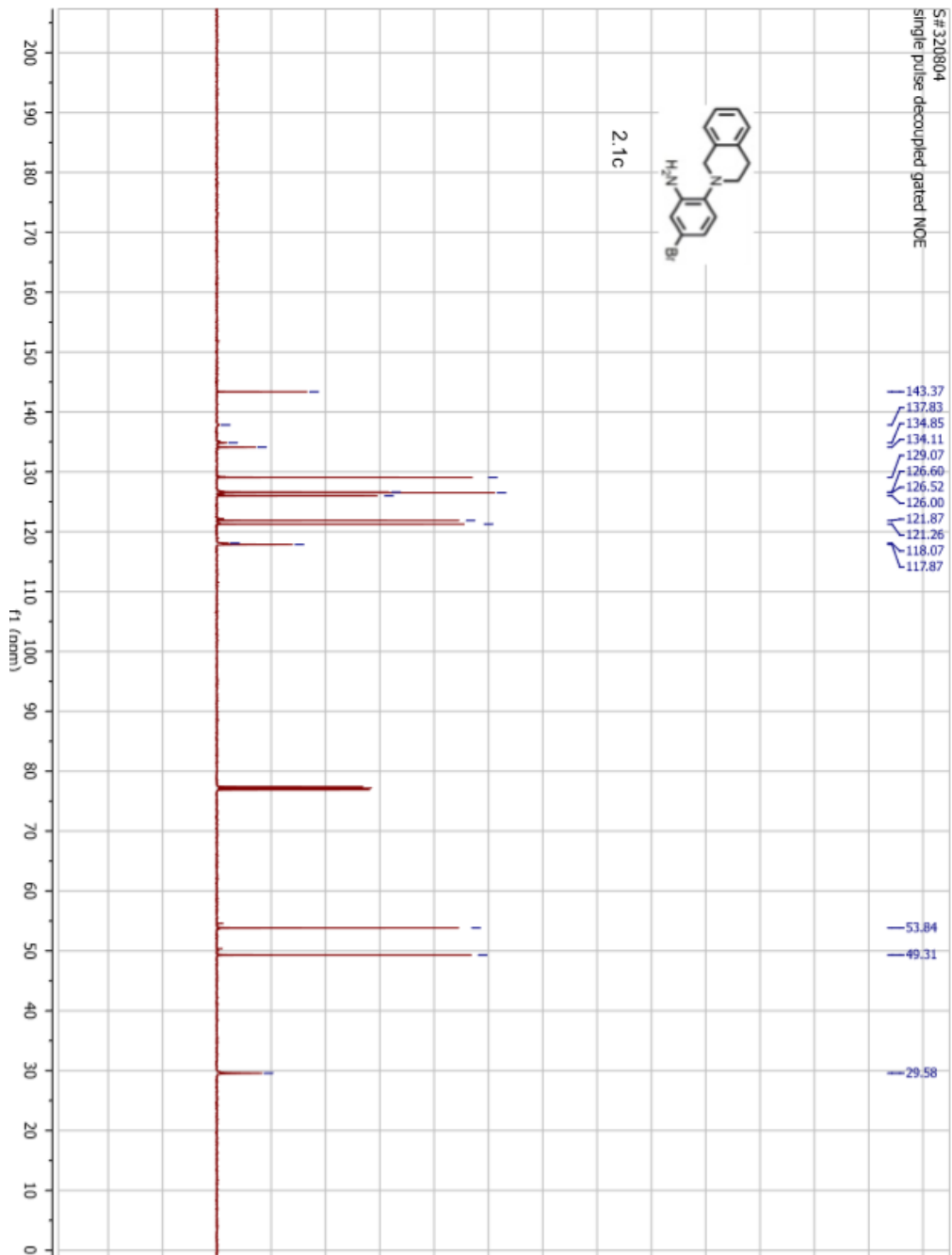


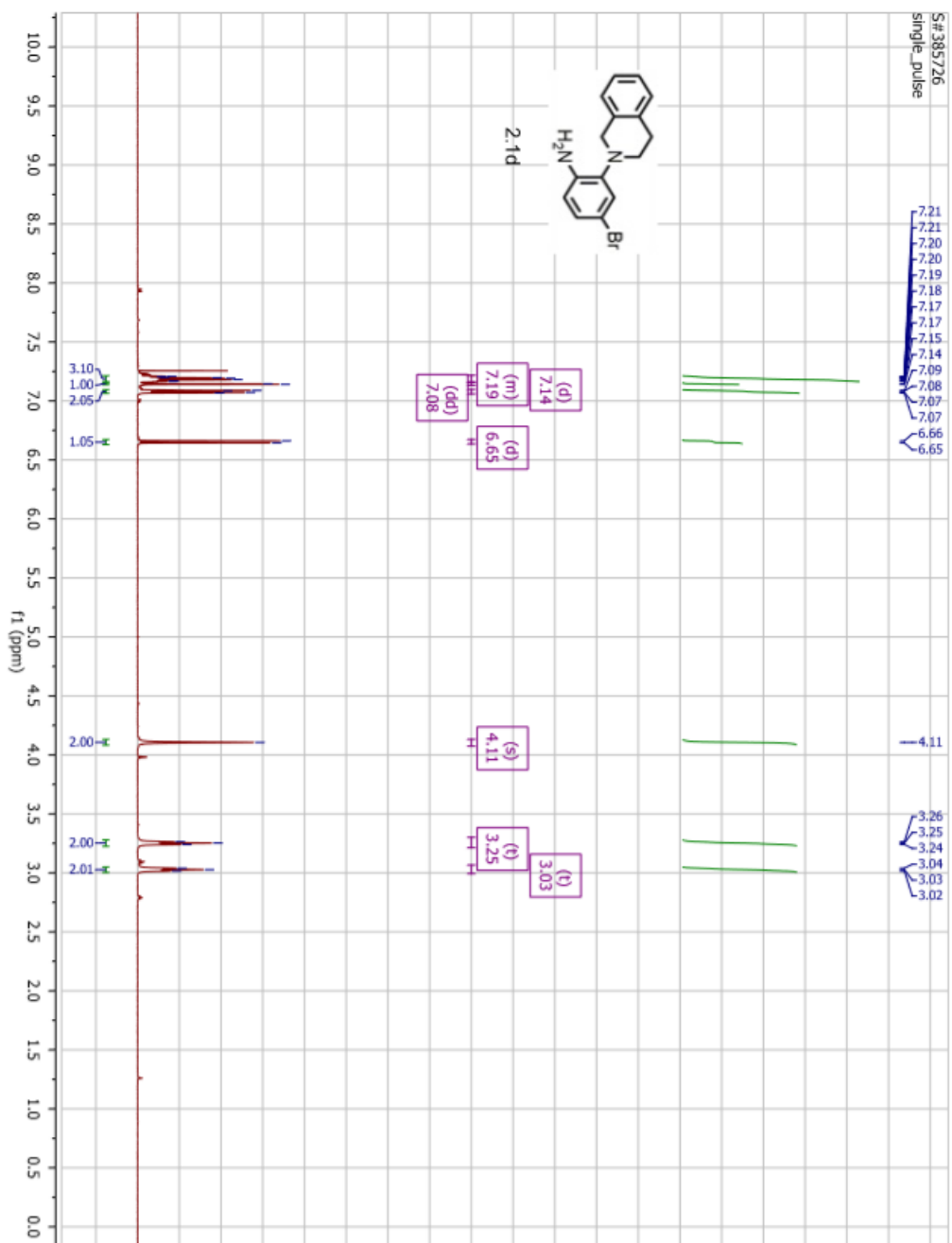


S# 320804
single pulse decoupled gated NOE

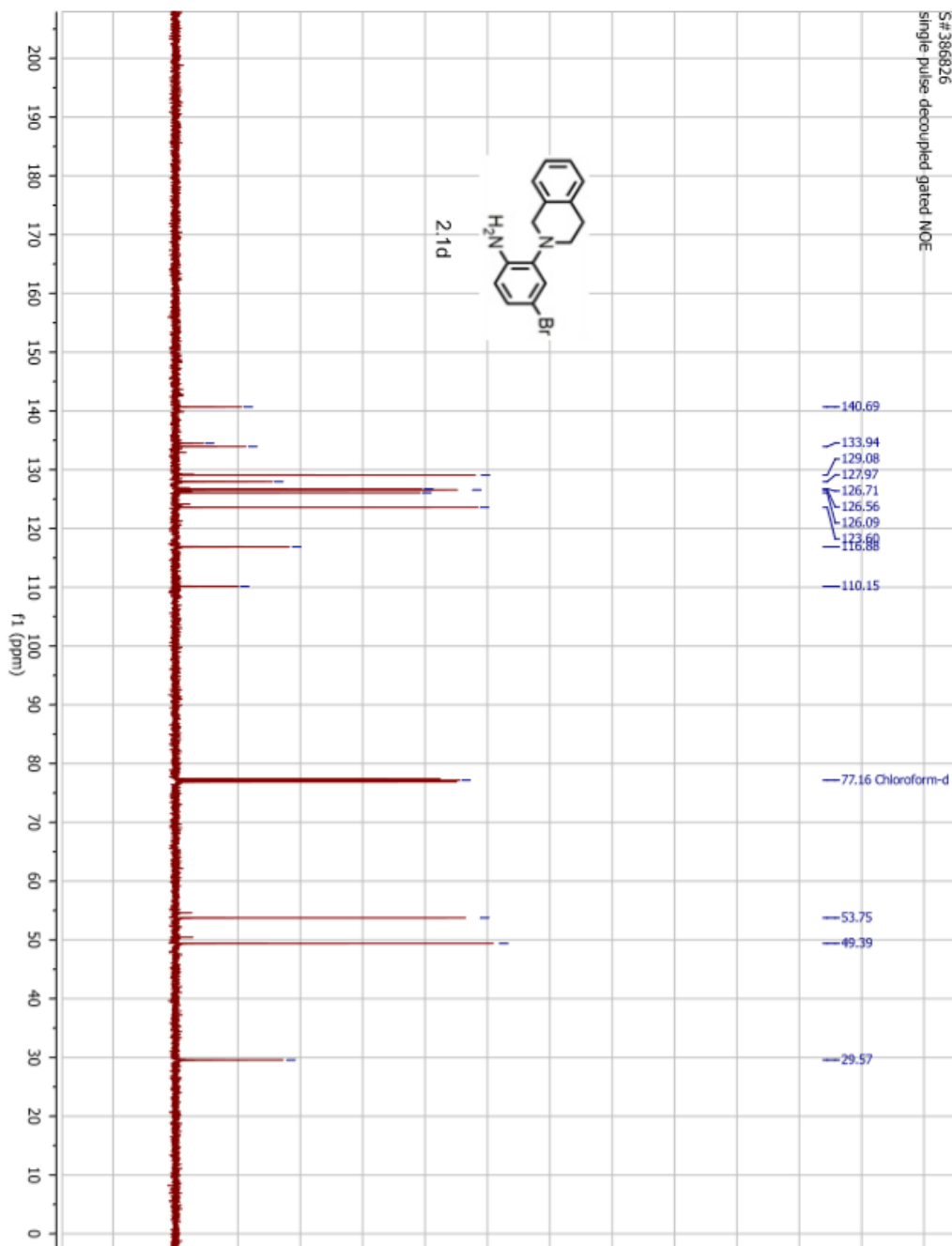


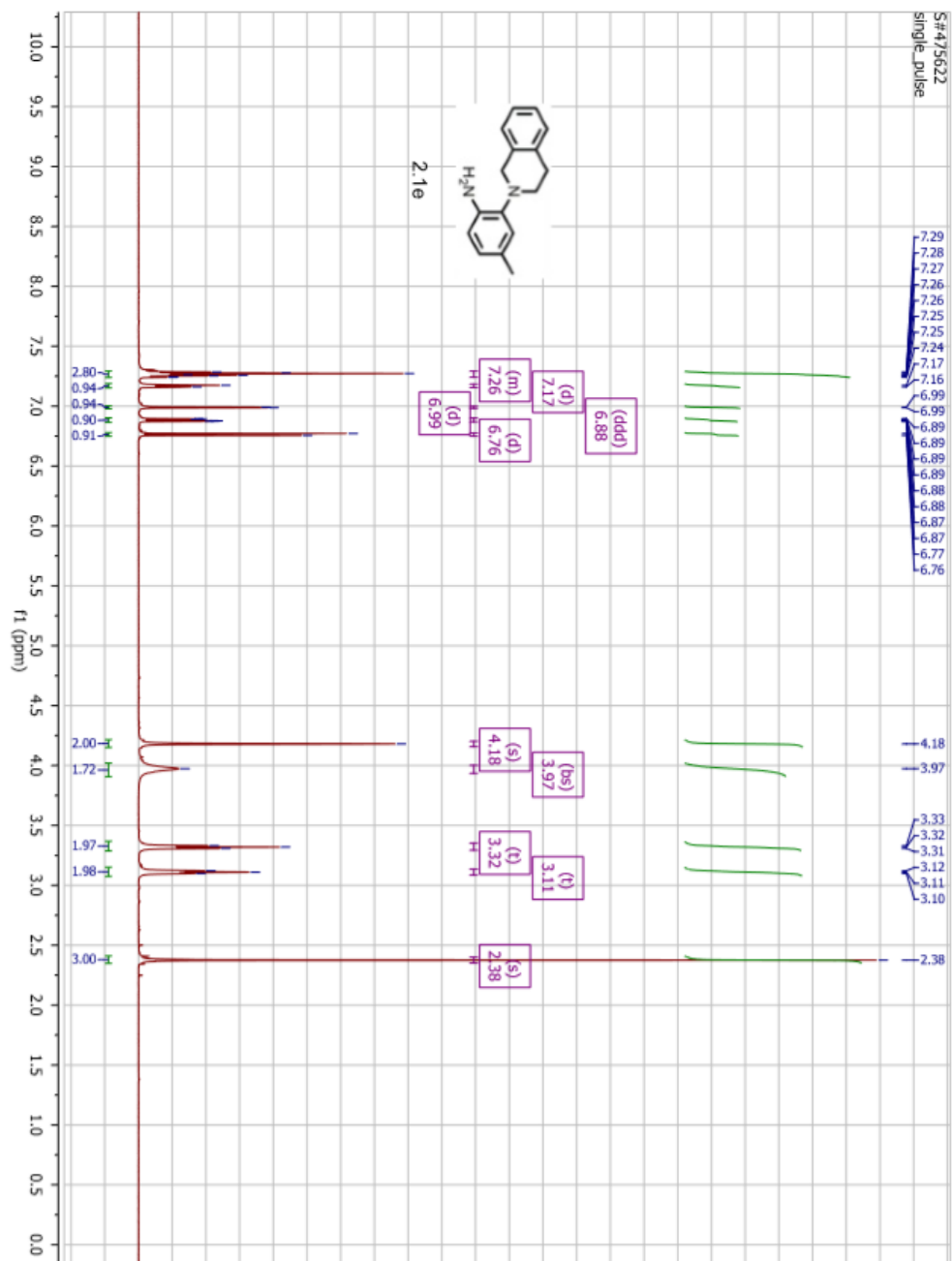
2.1c



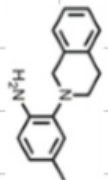


S# 386826
single pulse decoupled gated NOE

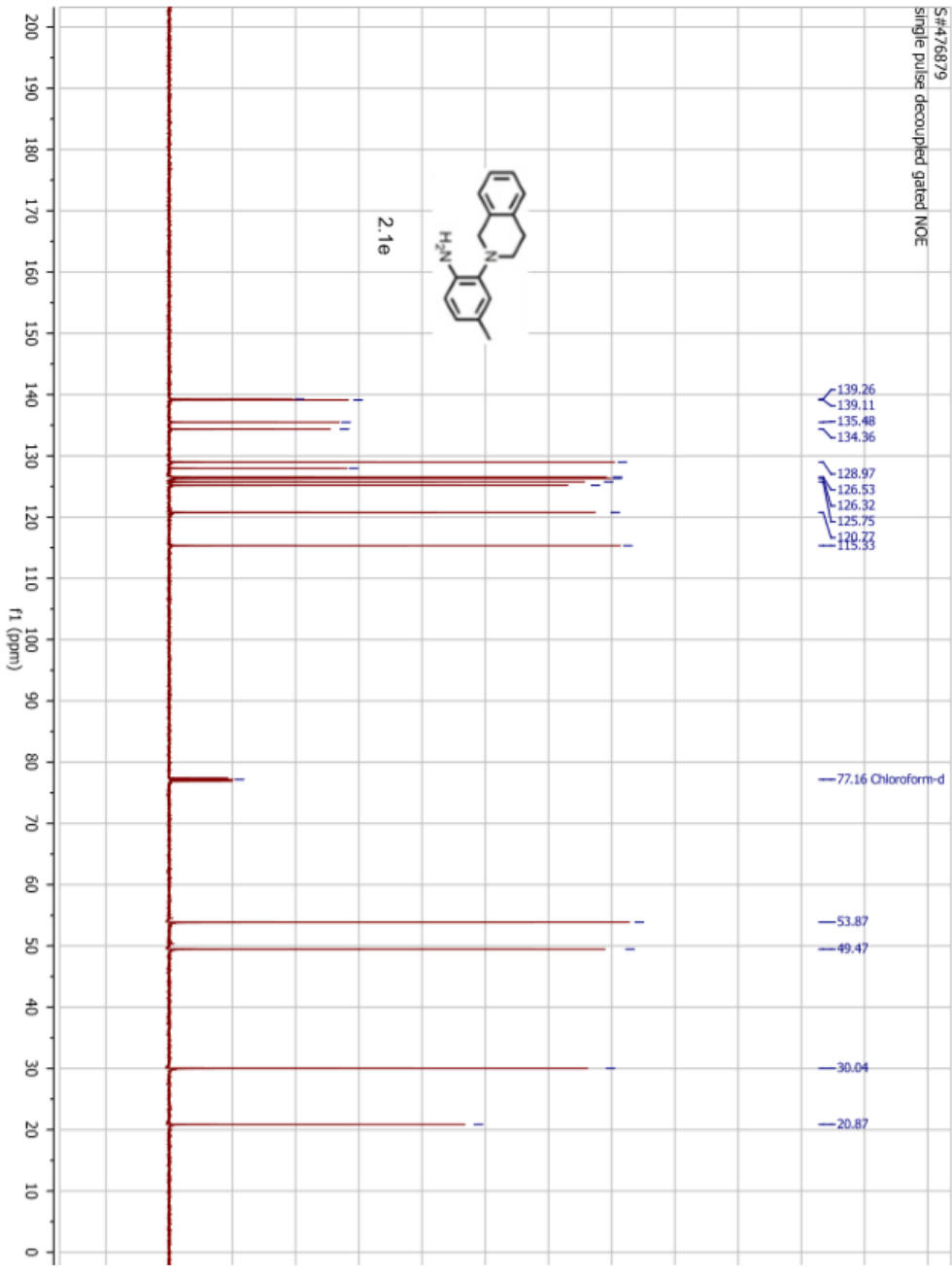


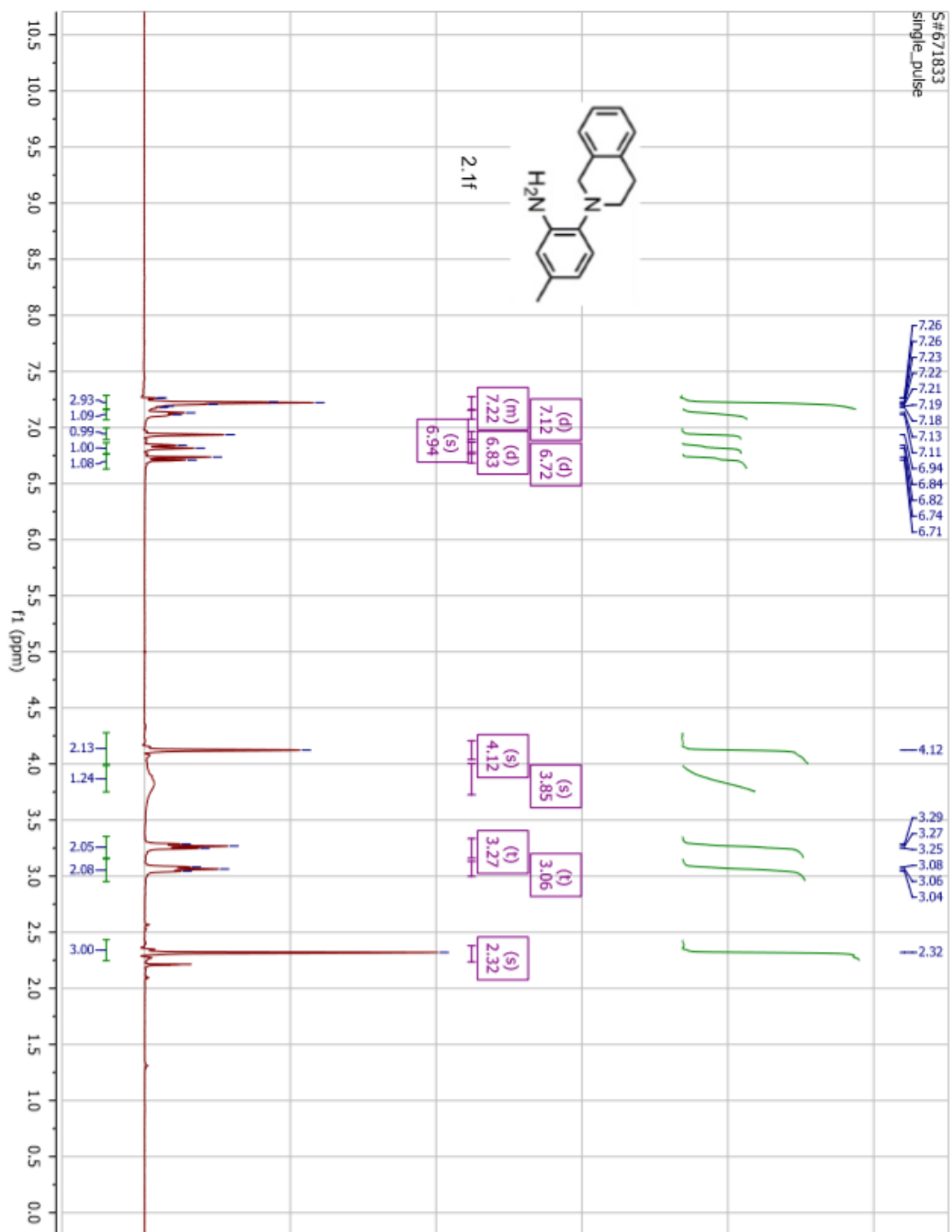


S#476879
single pulse decoupled gated NOE

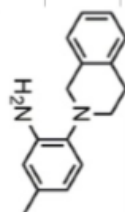


2.1e

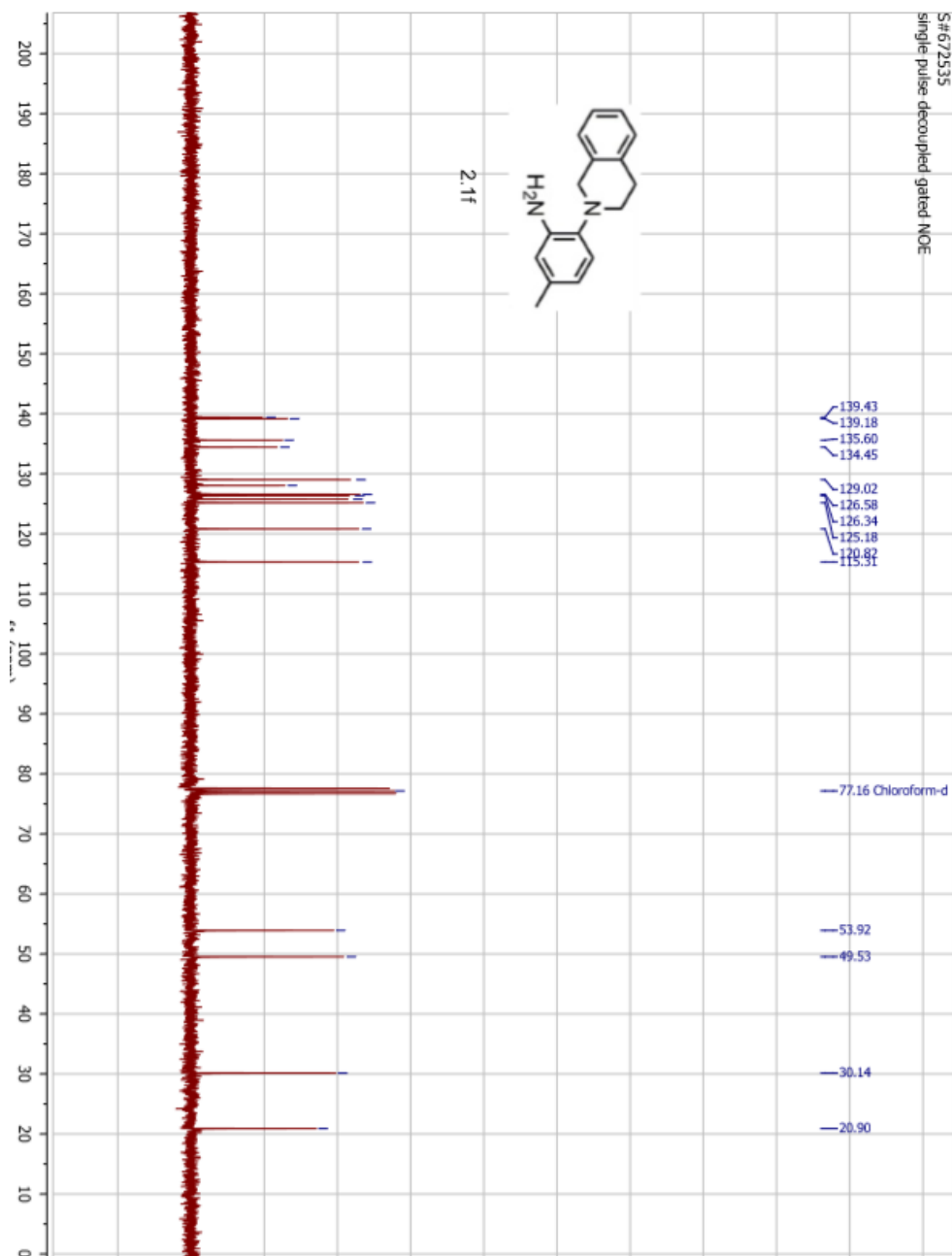




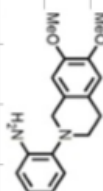
S#672535
single pulse decoupled gated NOE



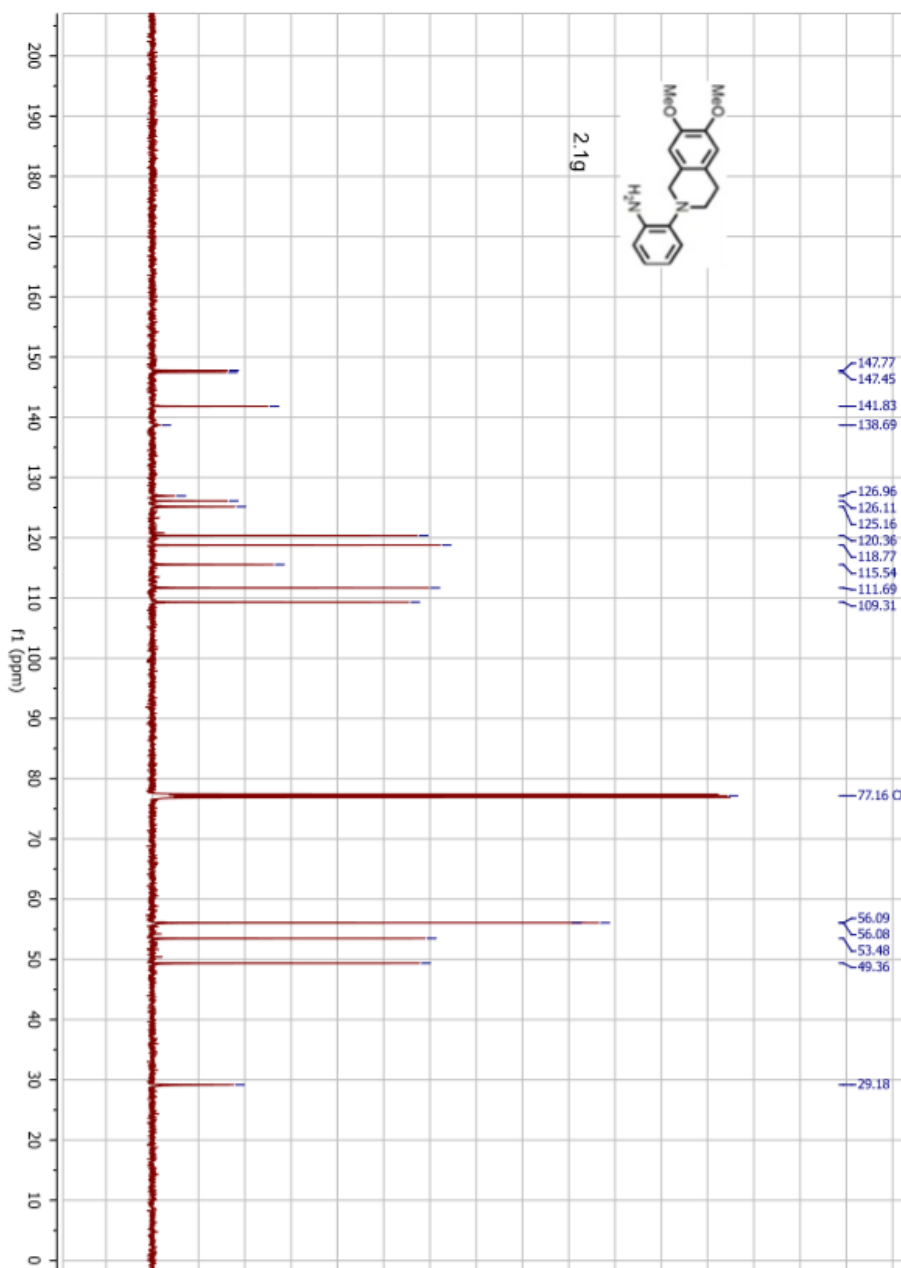
2.1f

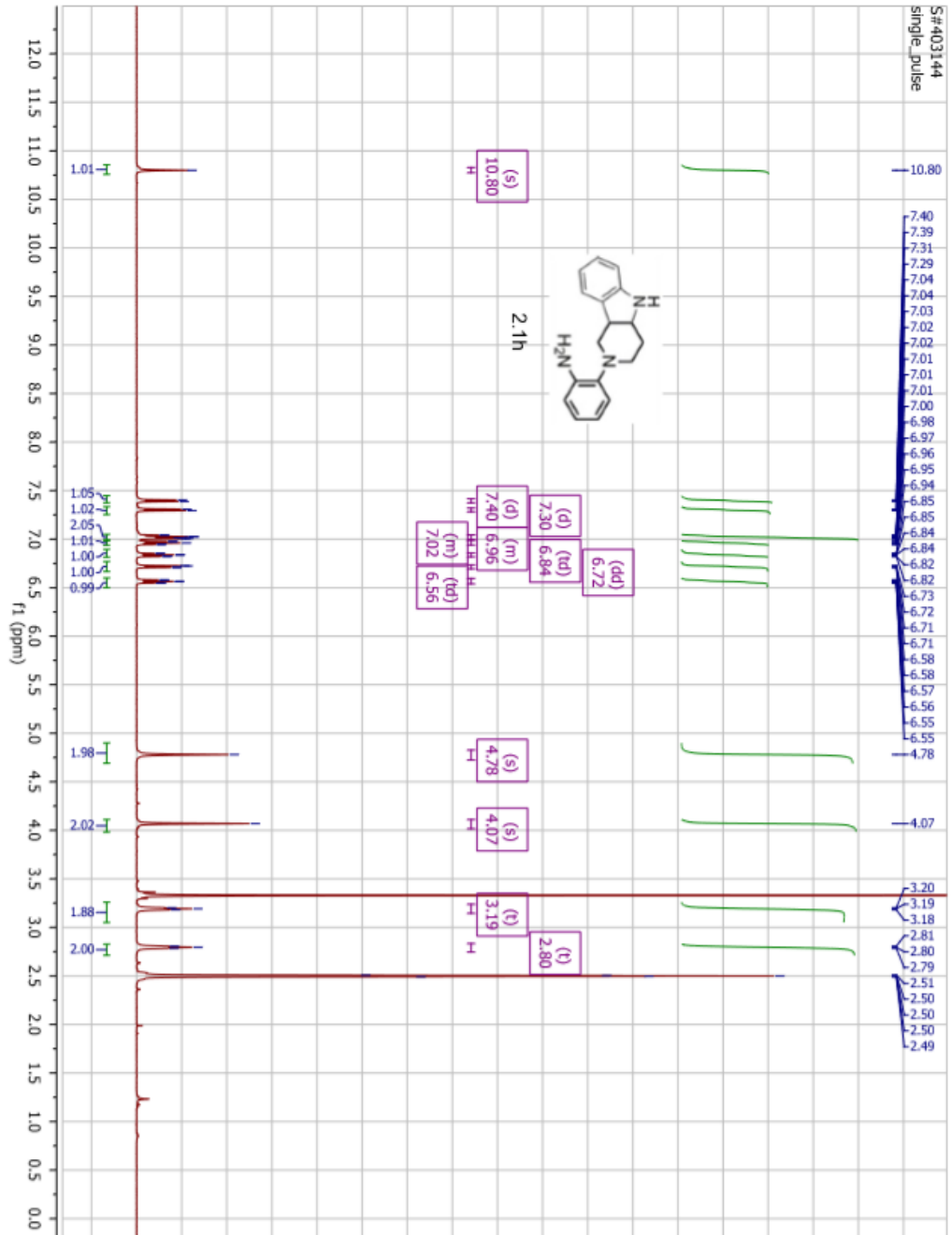


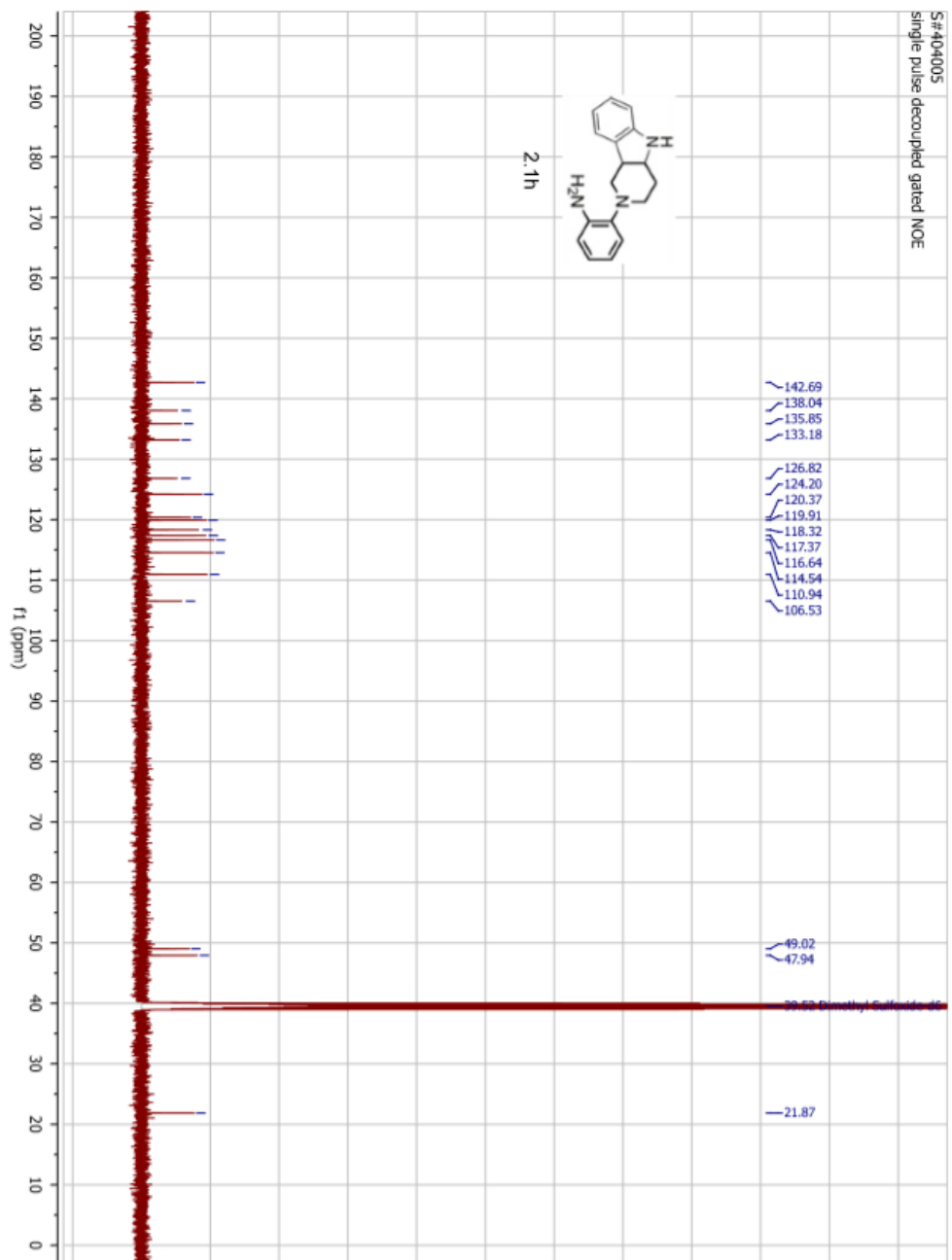
S#444456
single pulse decoupled gated NOE

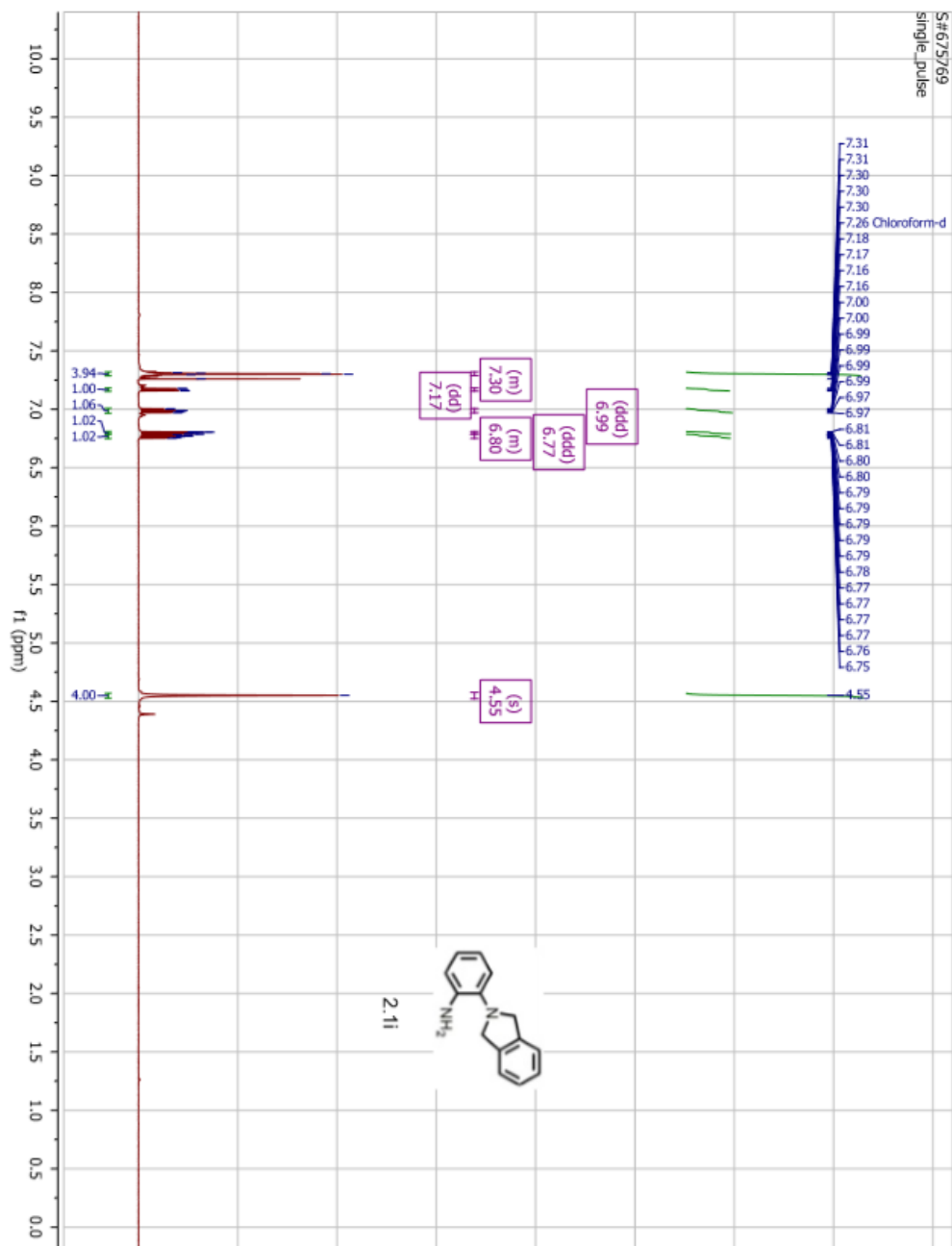


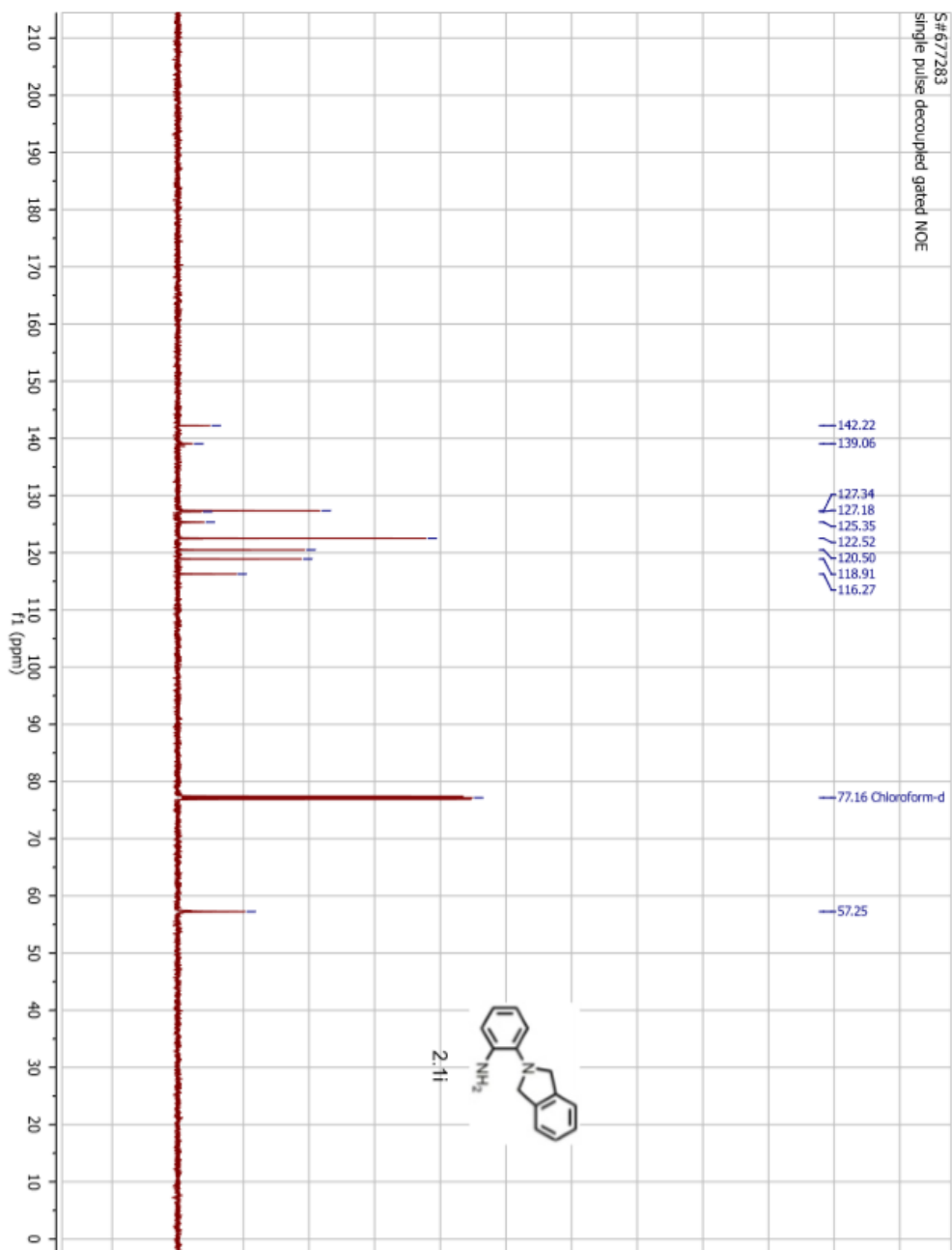
2.1g



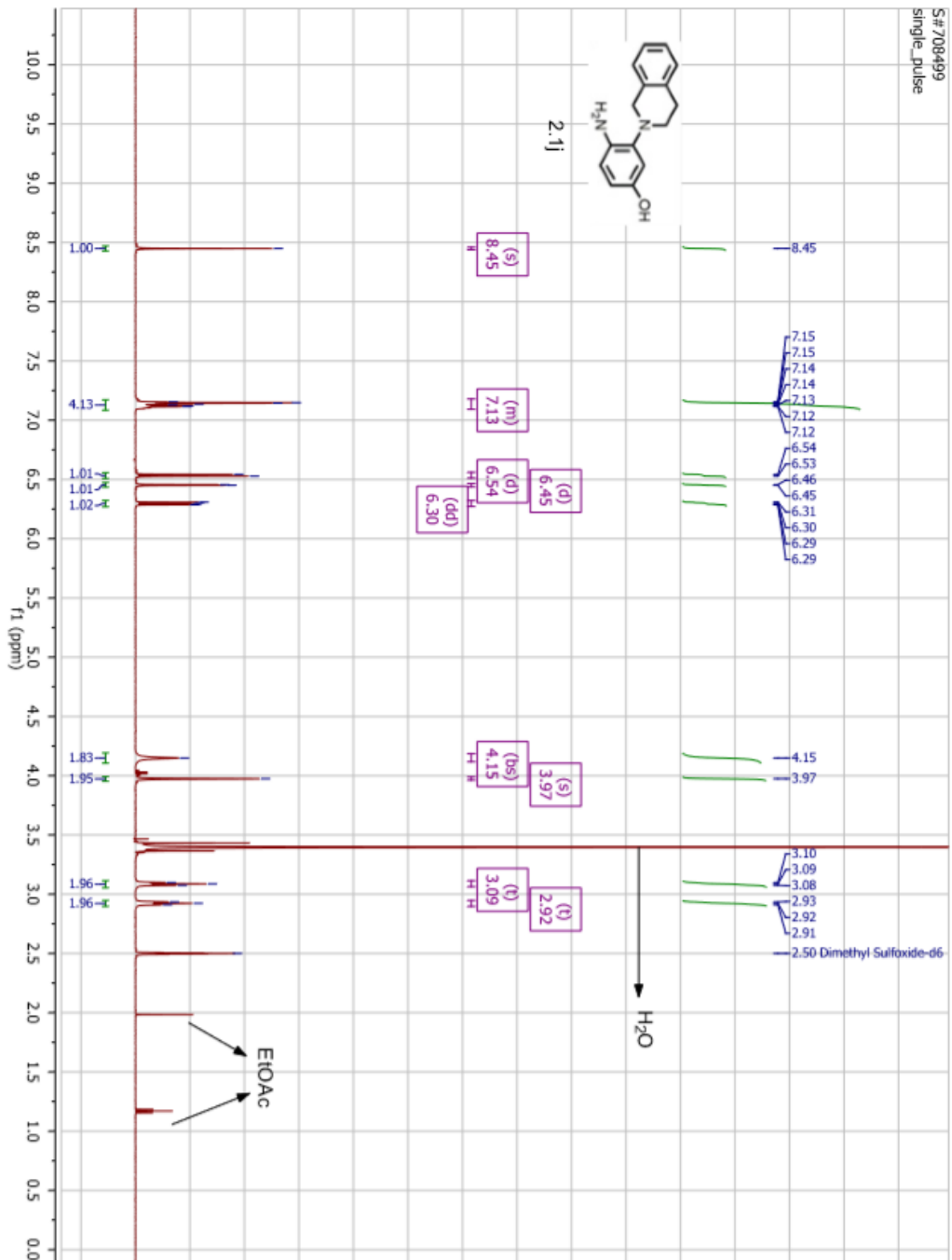




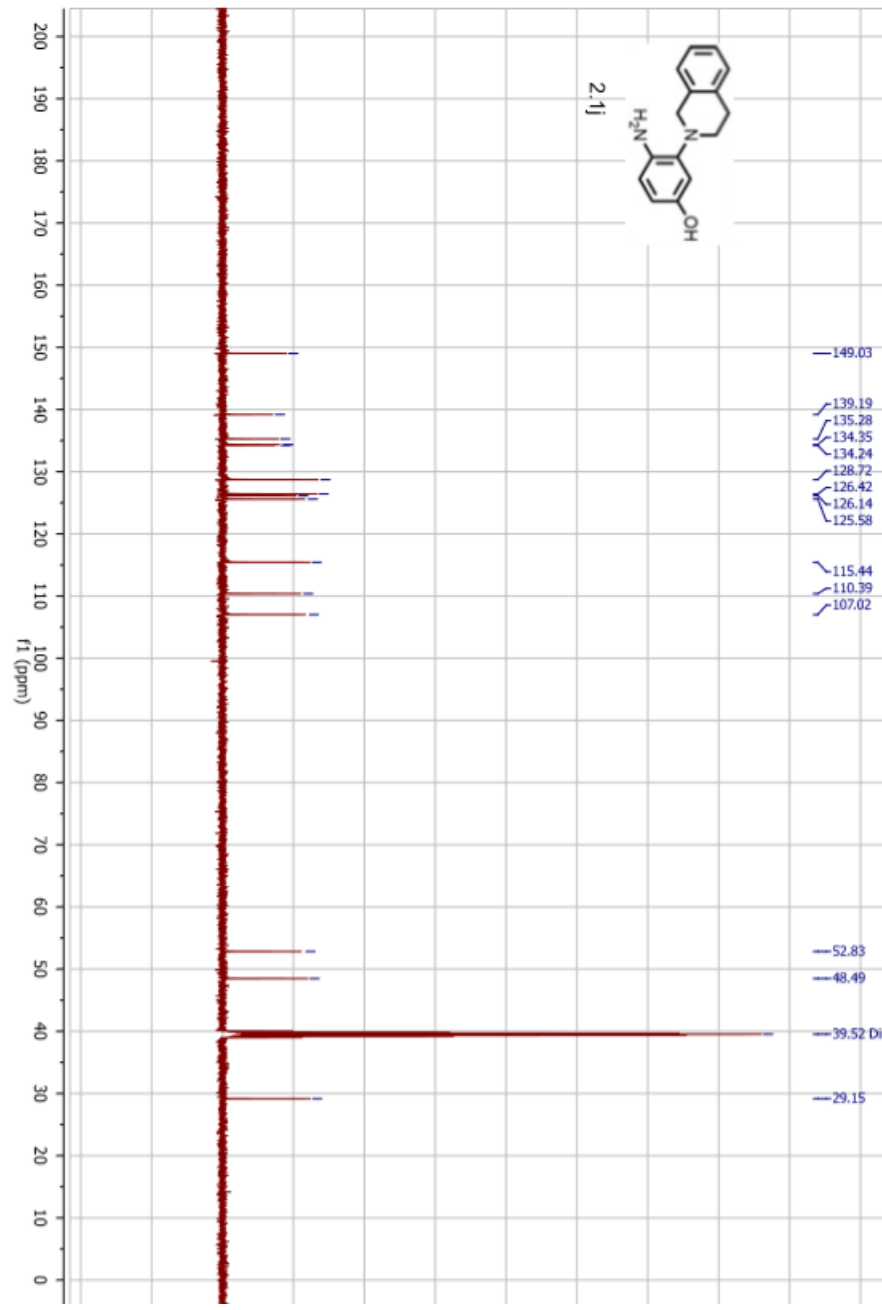
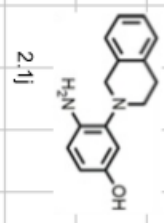


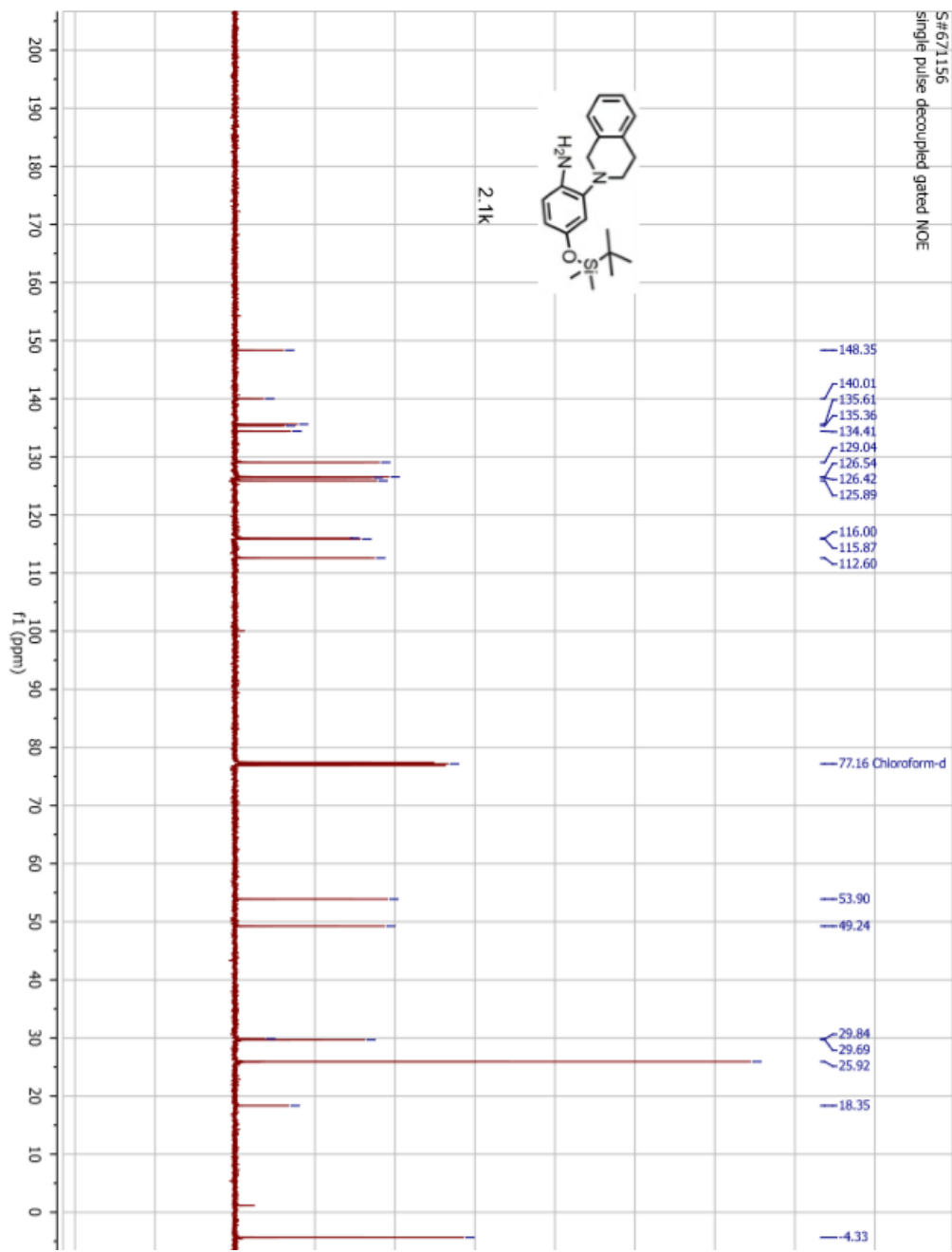


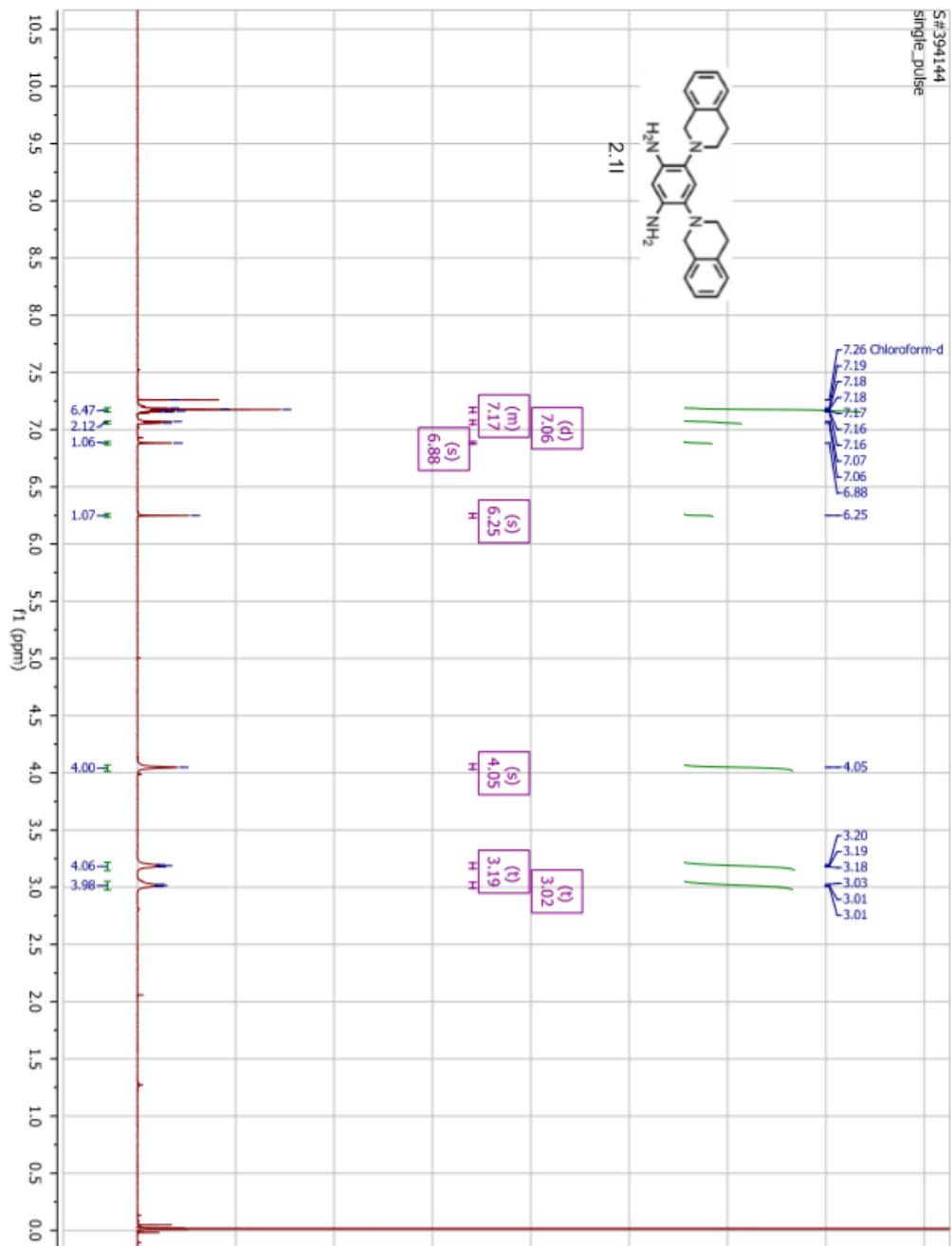
S#708499
single_pulse



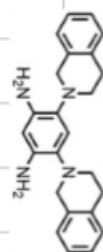
S# 709339
single pulse decoupled gated NOE



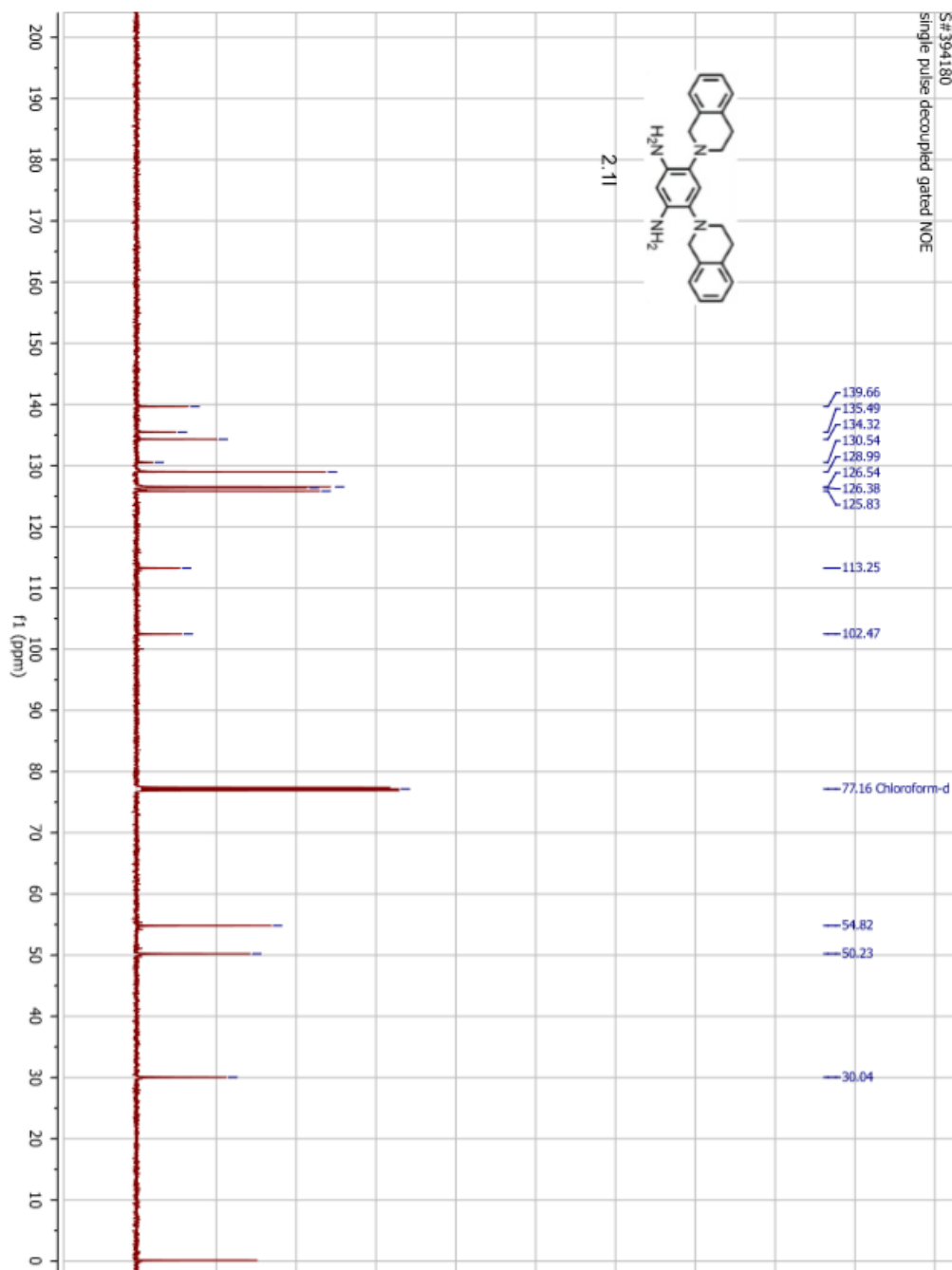


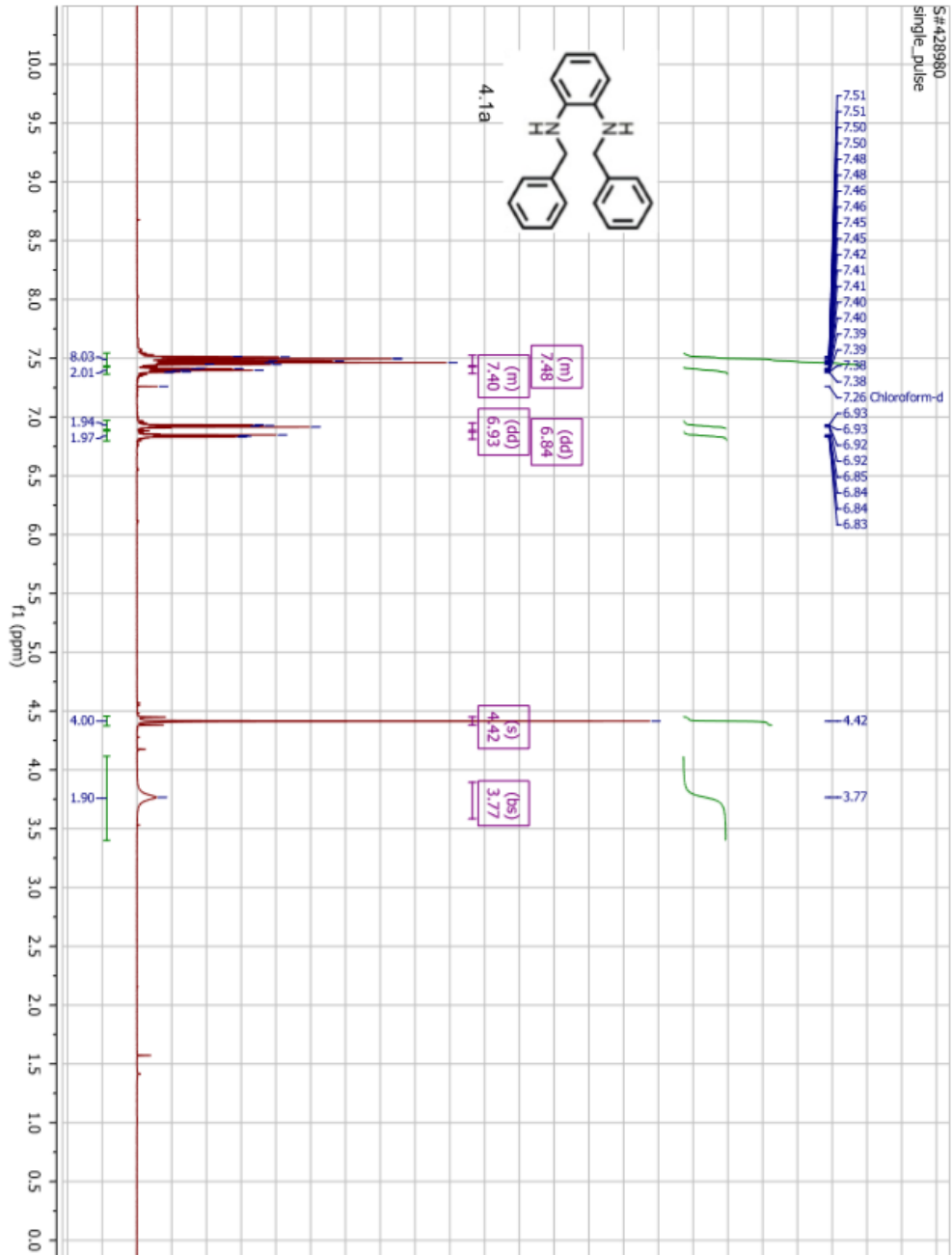


S#394180
single pulse decoupled gated NOE

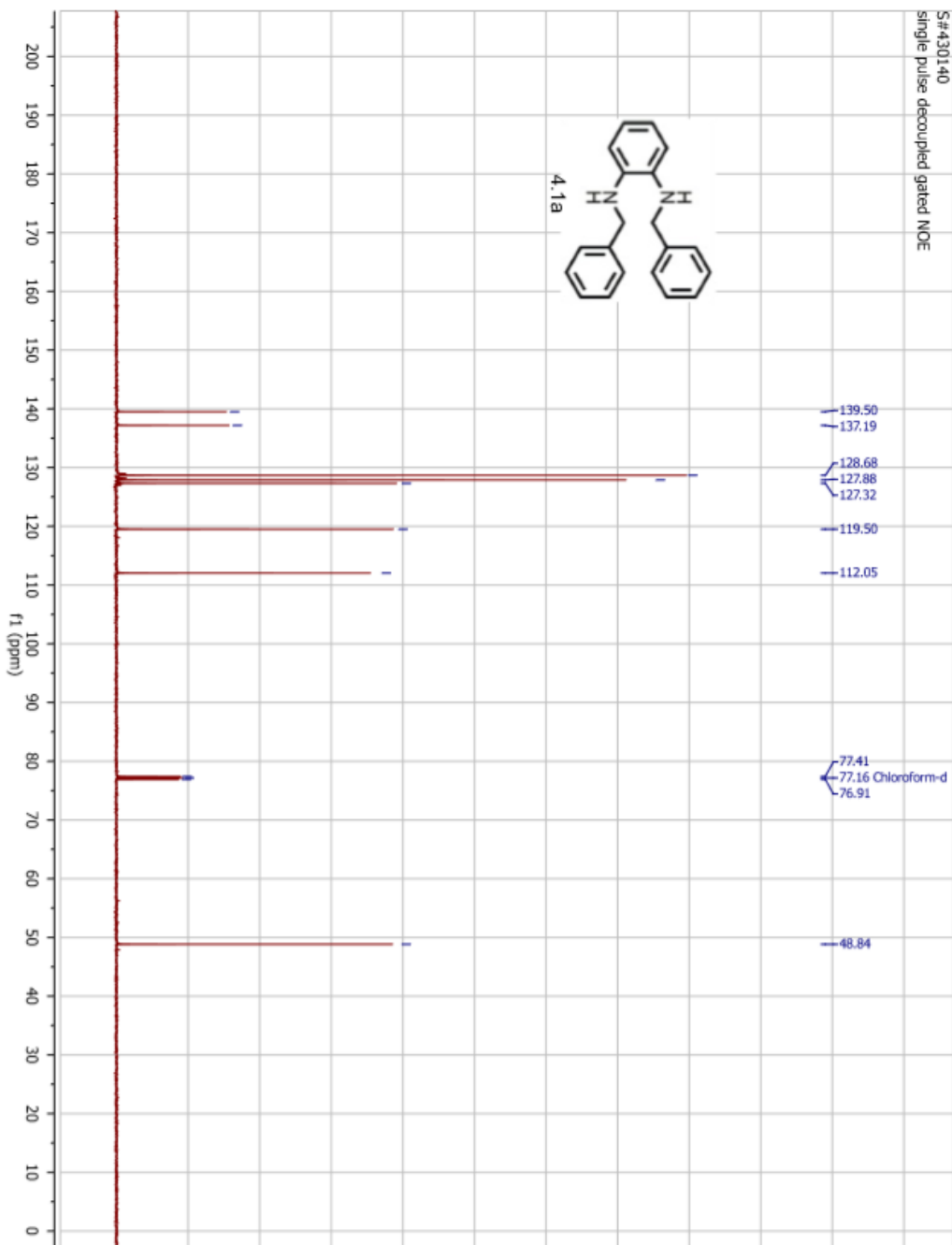
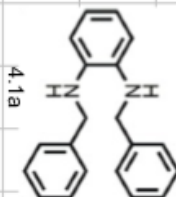


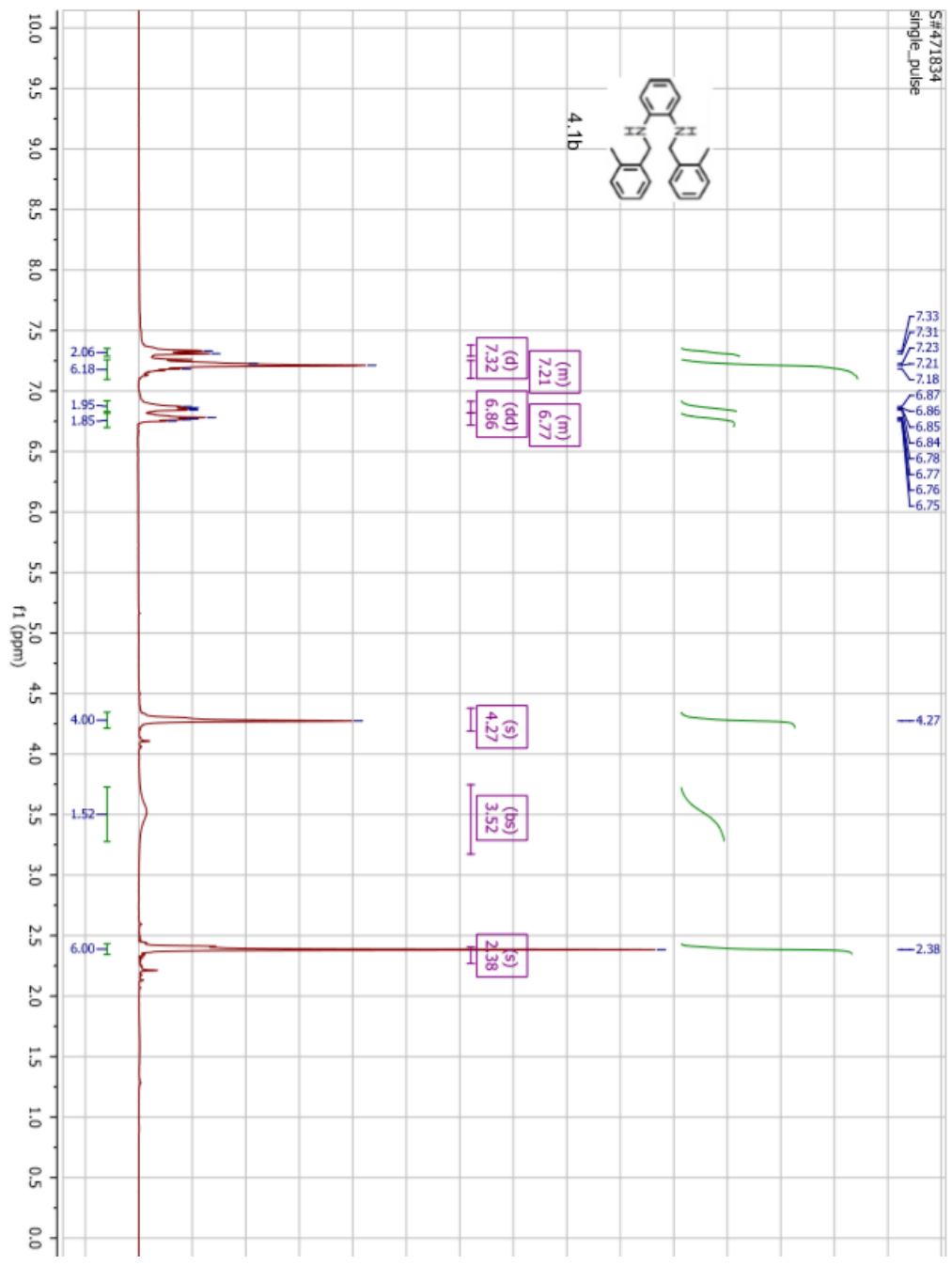
2.11



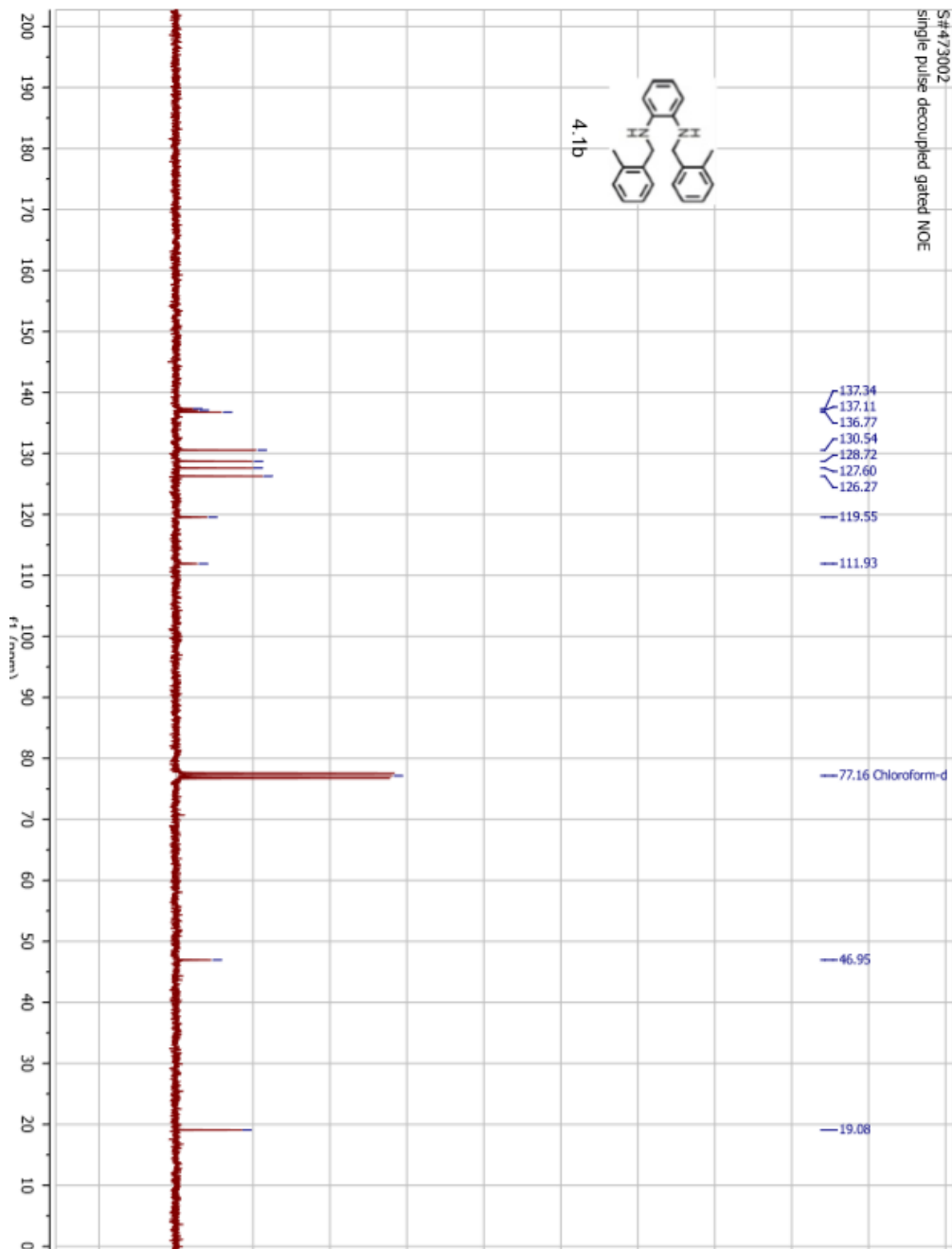
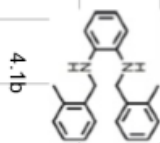


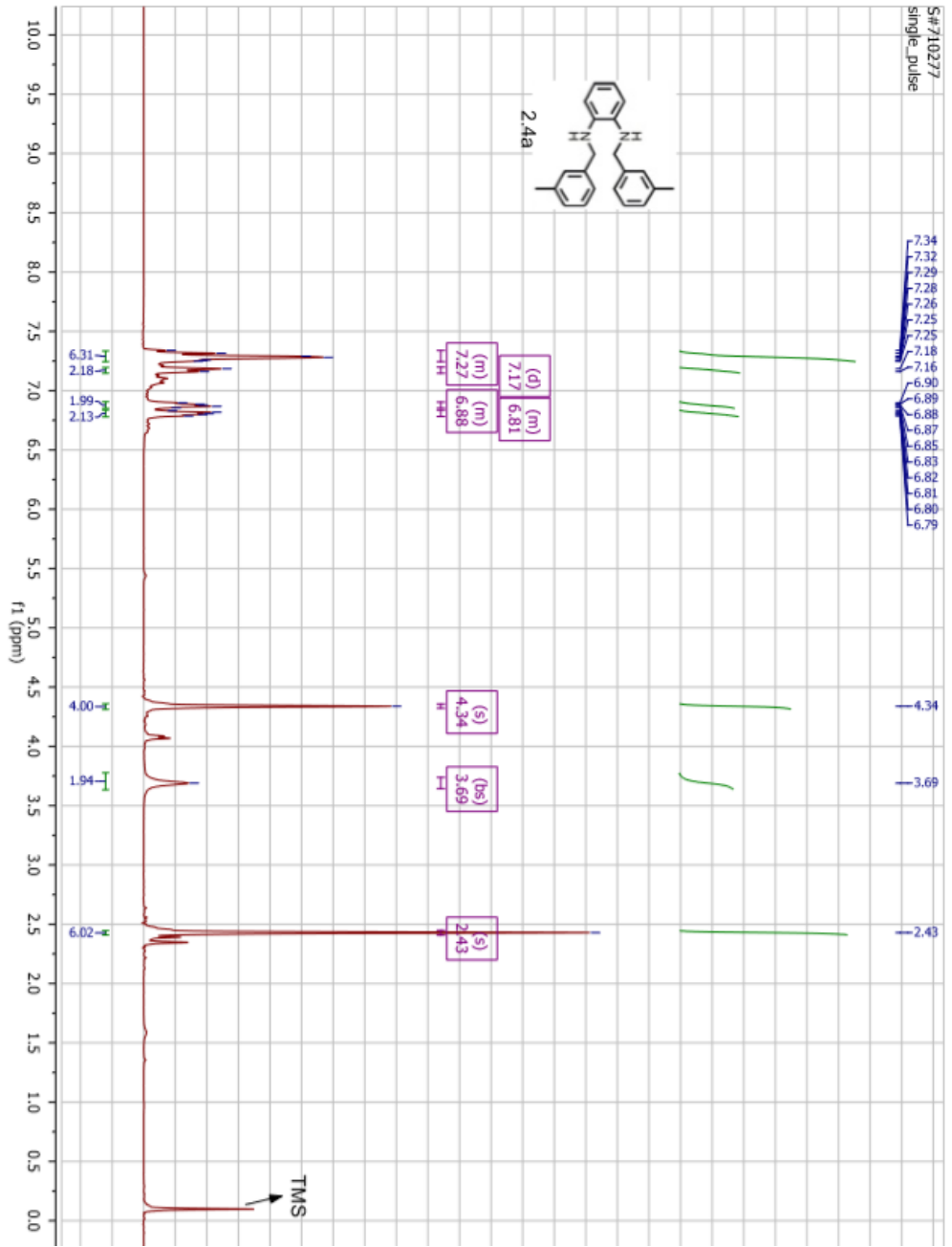
S#430140
single pulse decoupled gated NOE



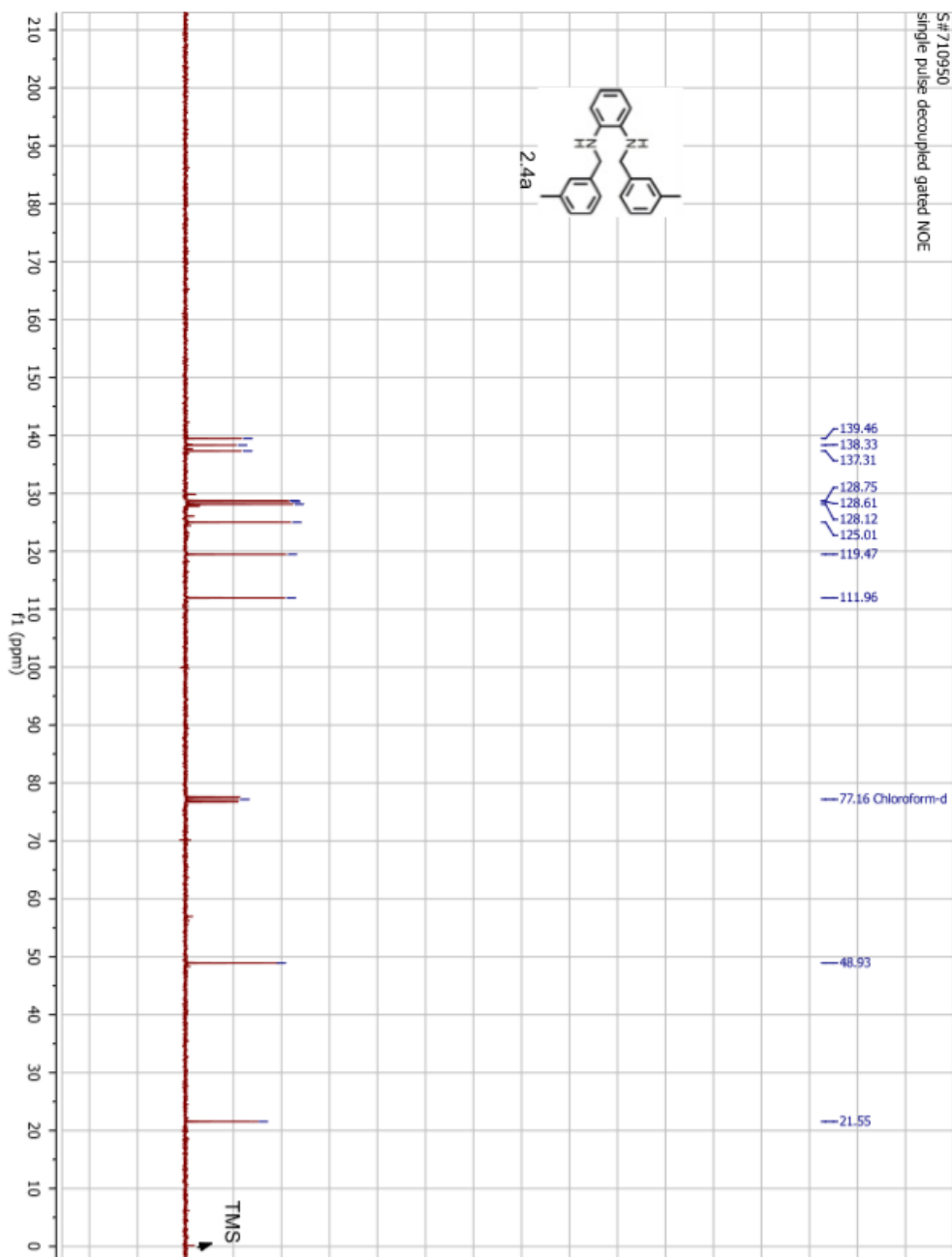
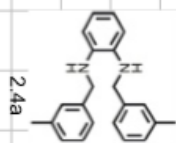


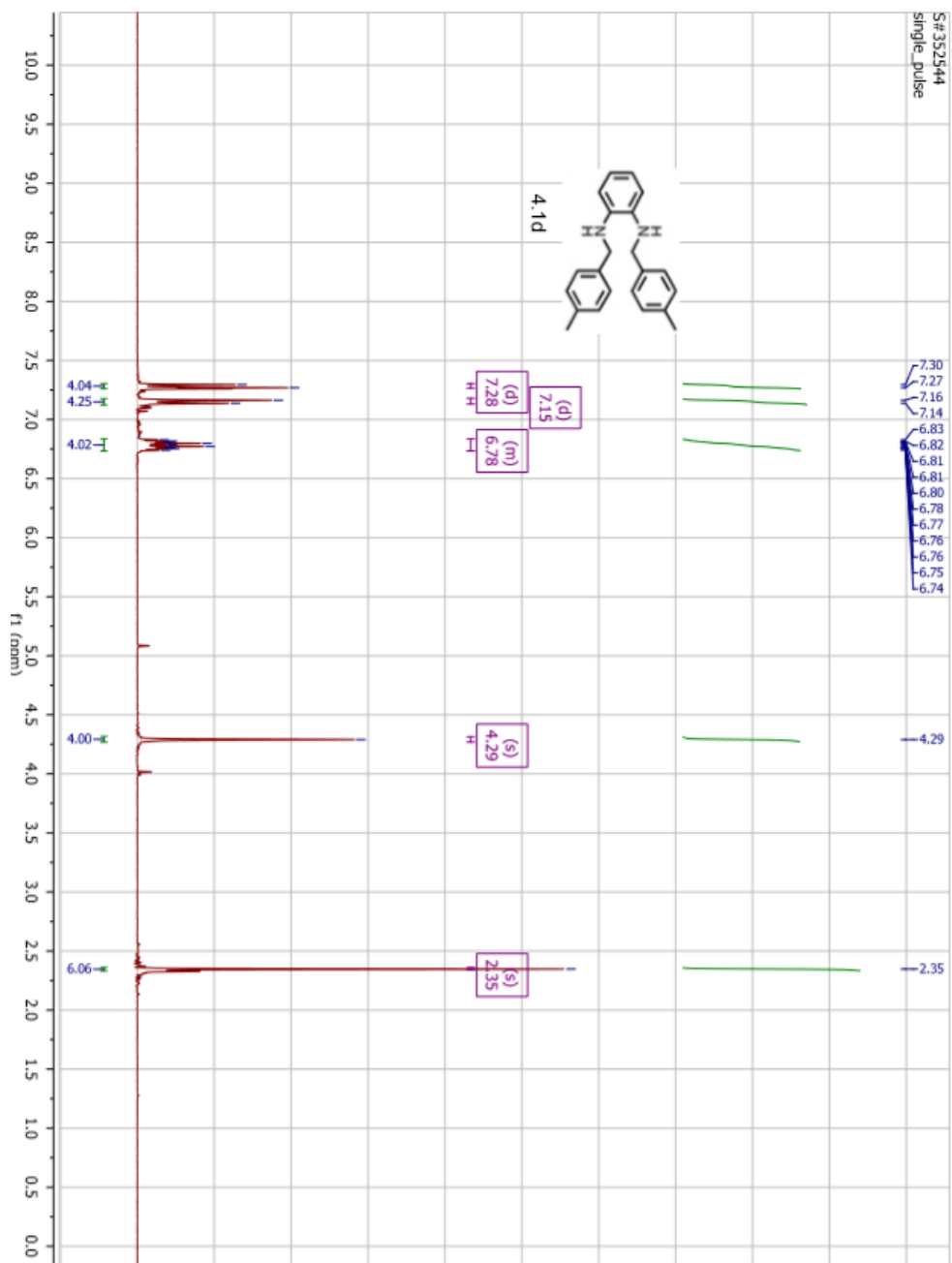
S#473002
single pulse decoupled gated NOE



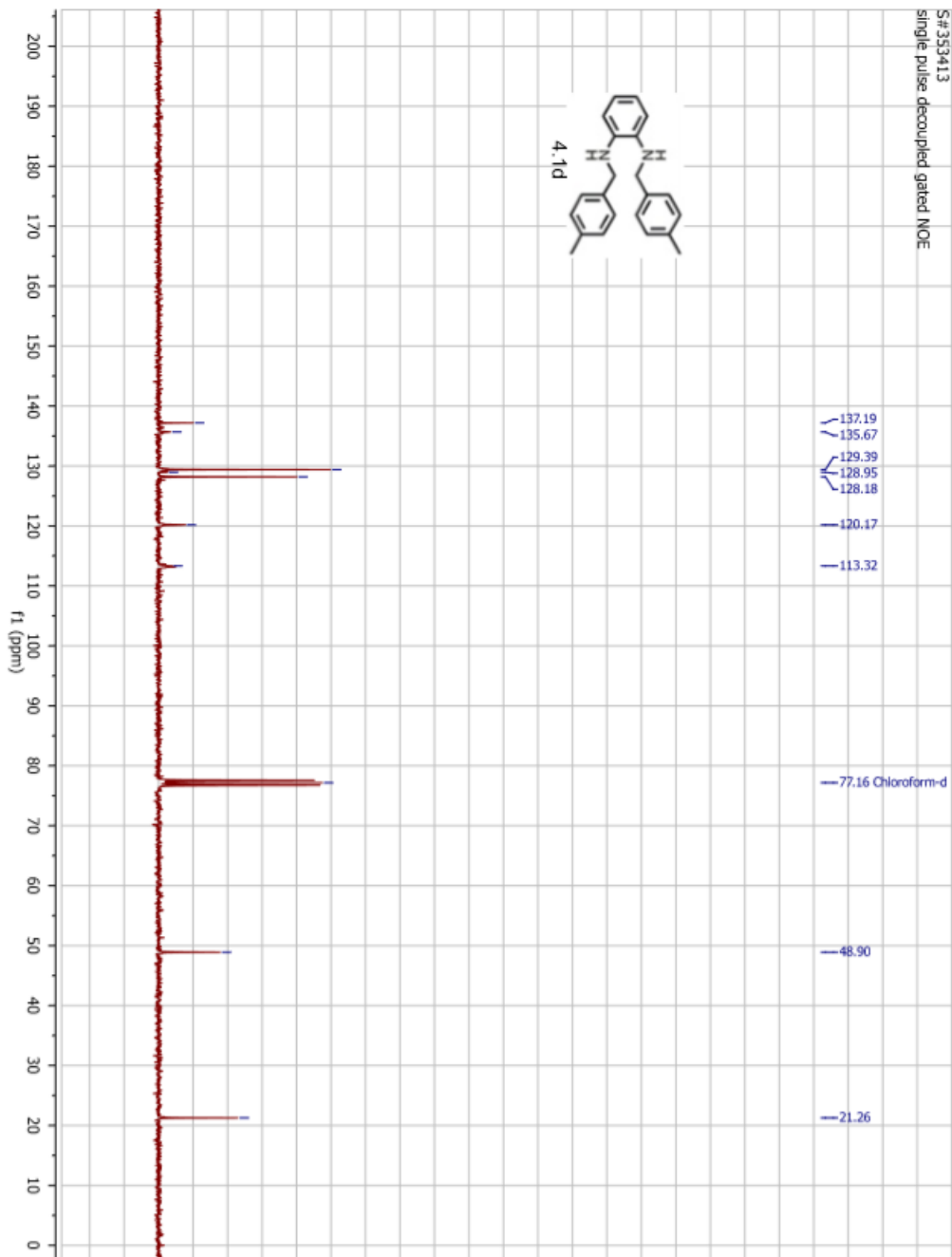
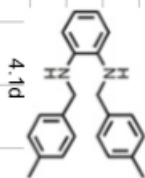


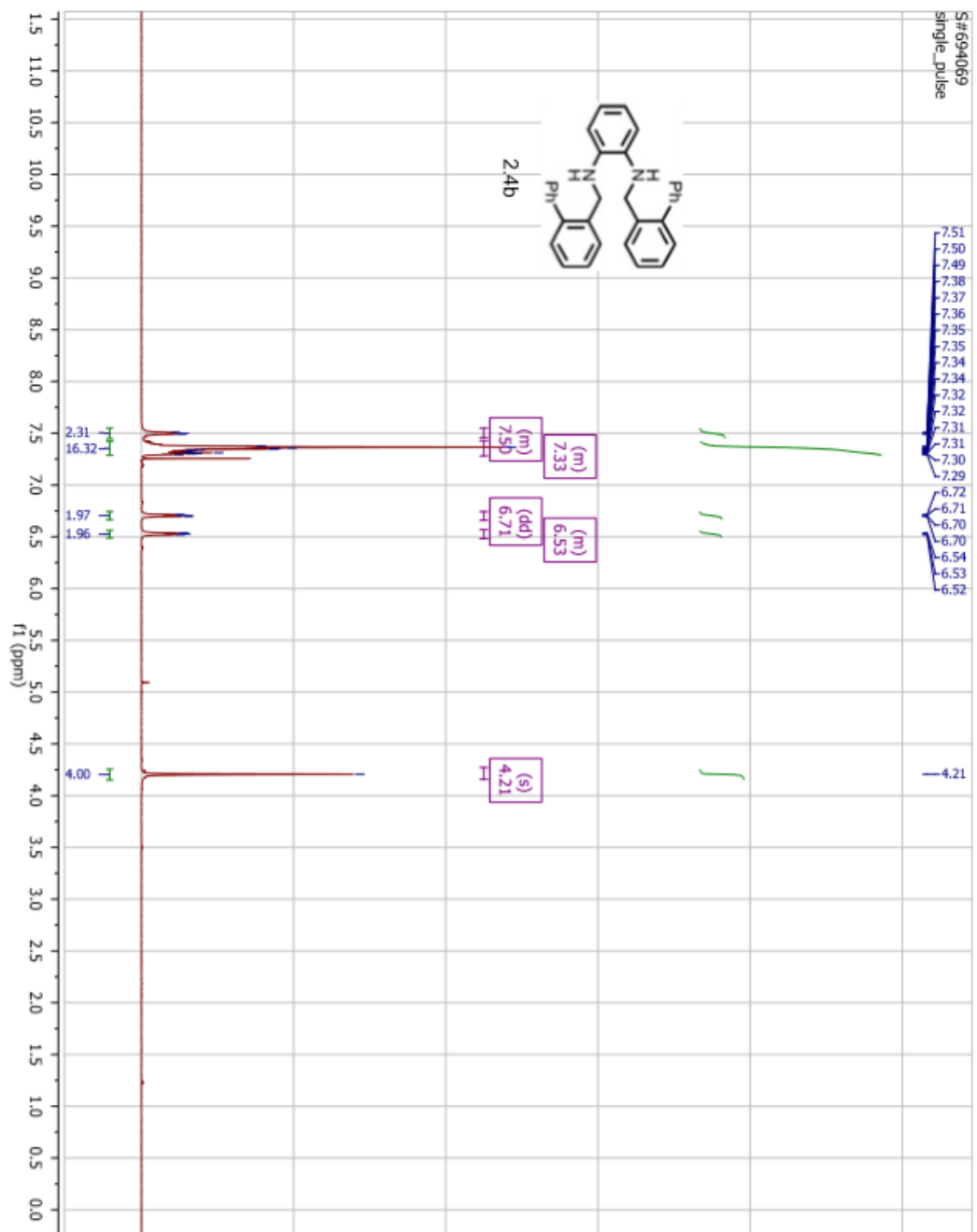
S#710950
single pulse decoupled gated NOE

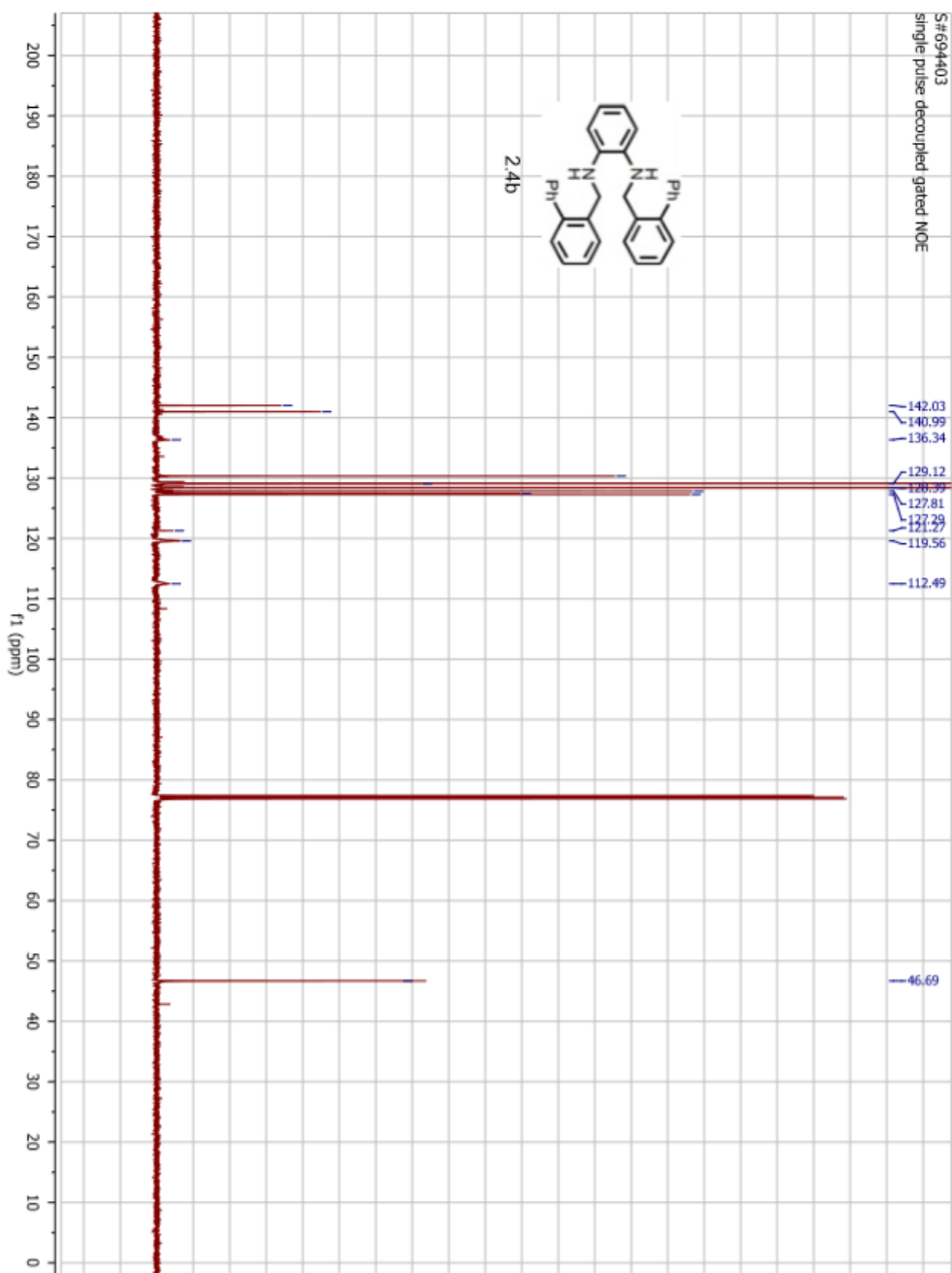


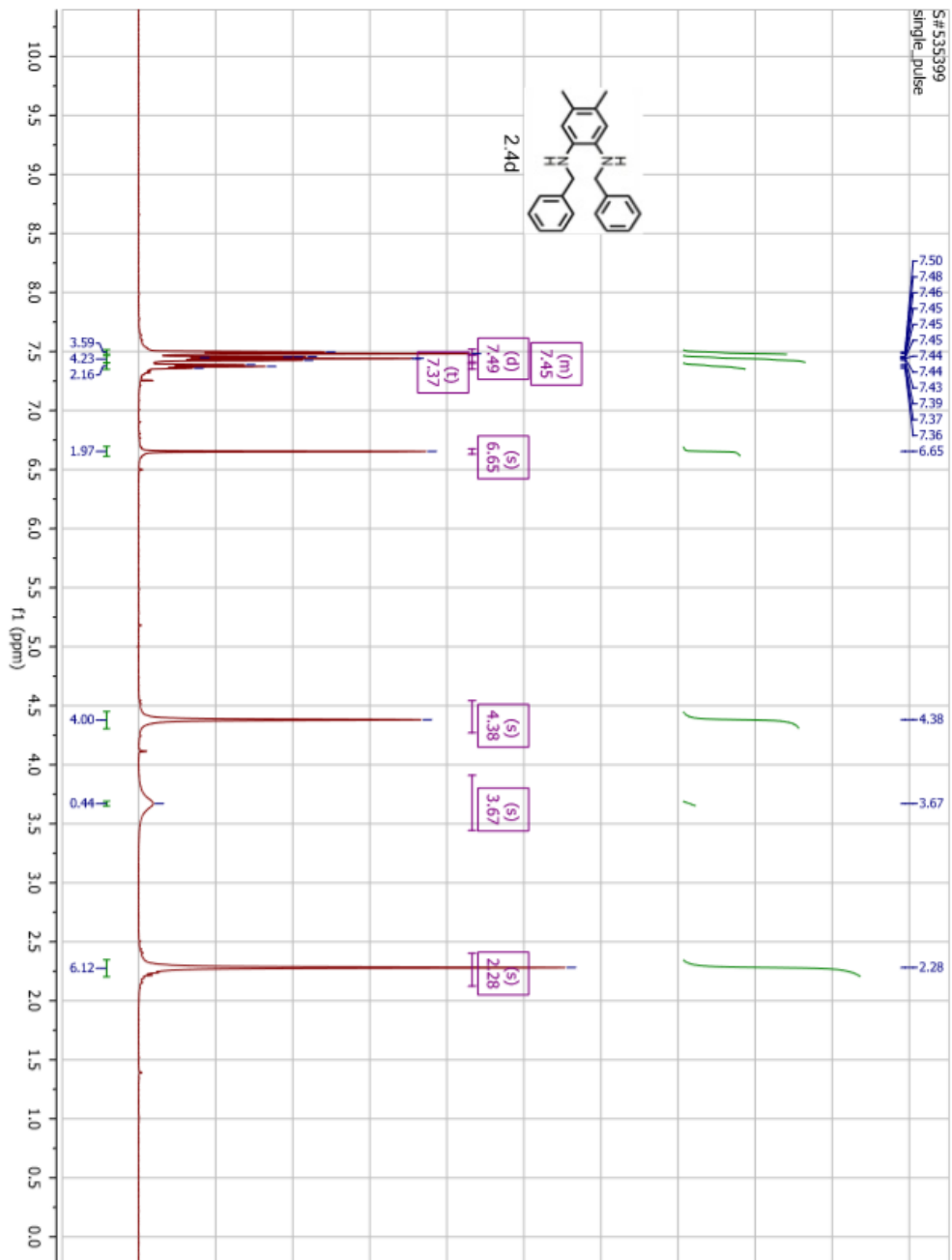


S#353413
Single pulse decoupled gated NOE

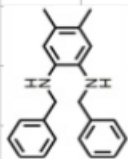




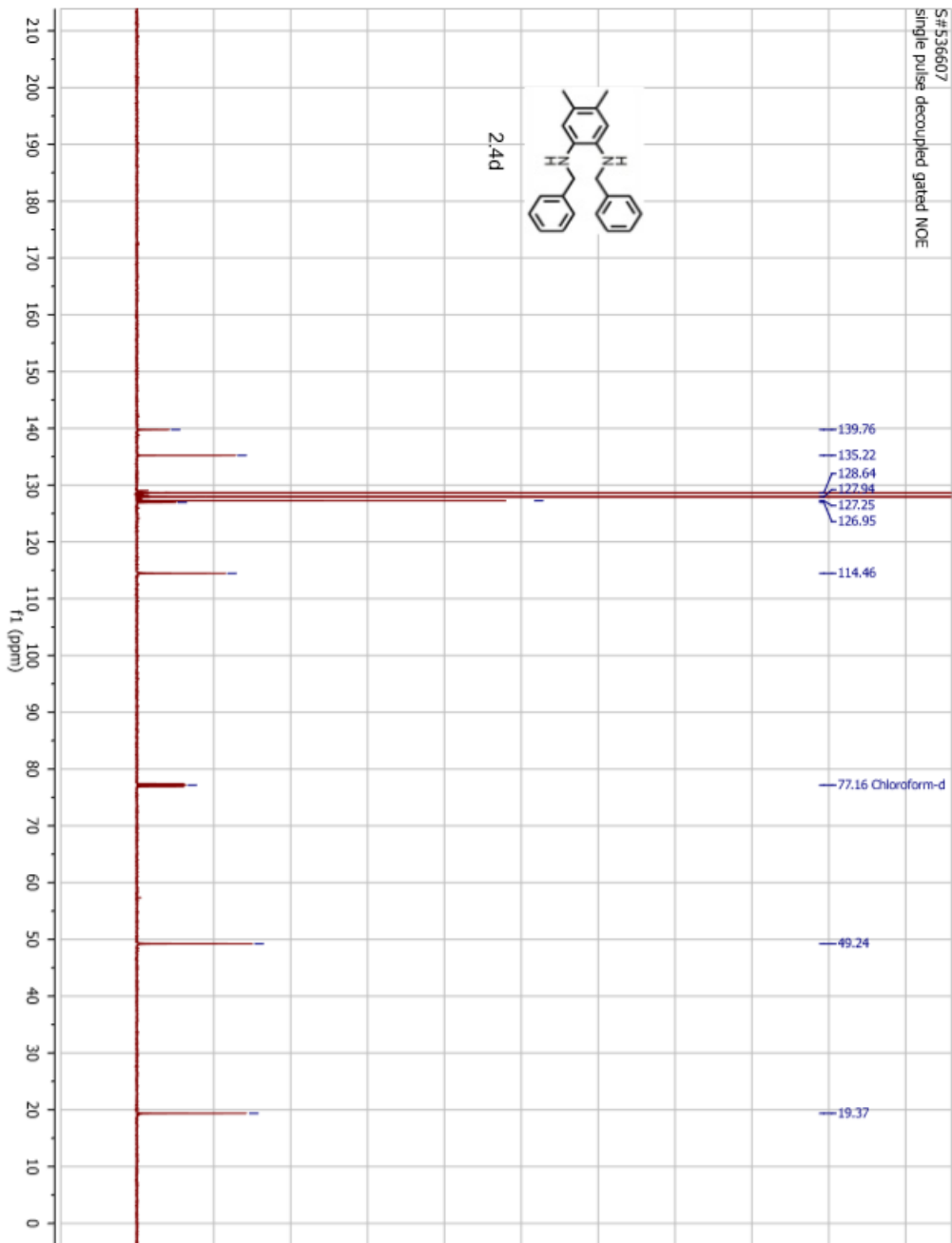




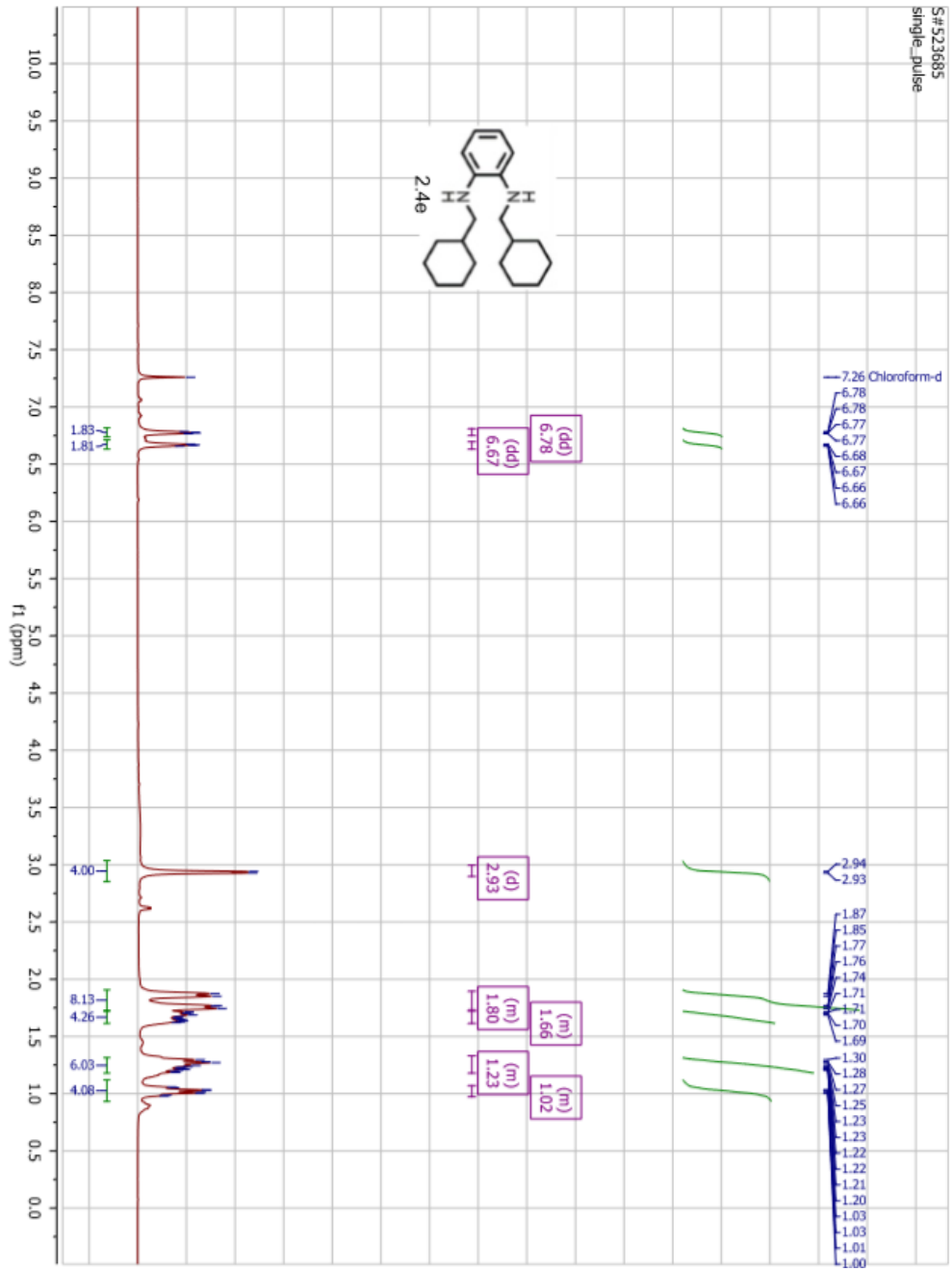
S#536607
single pulse decoupled gated NOE



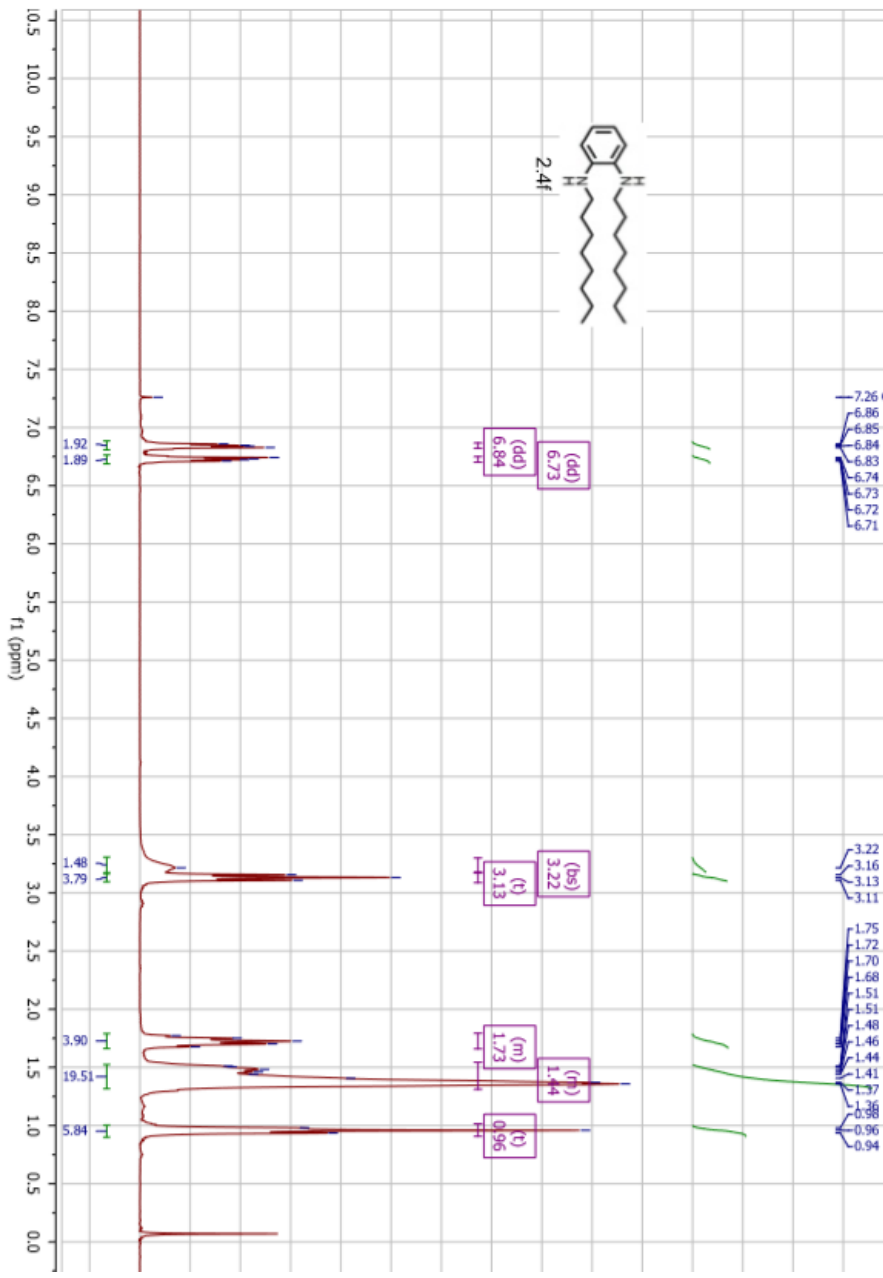
2.4d

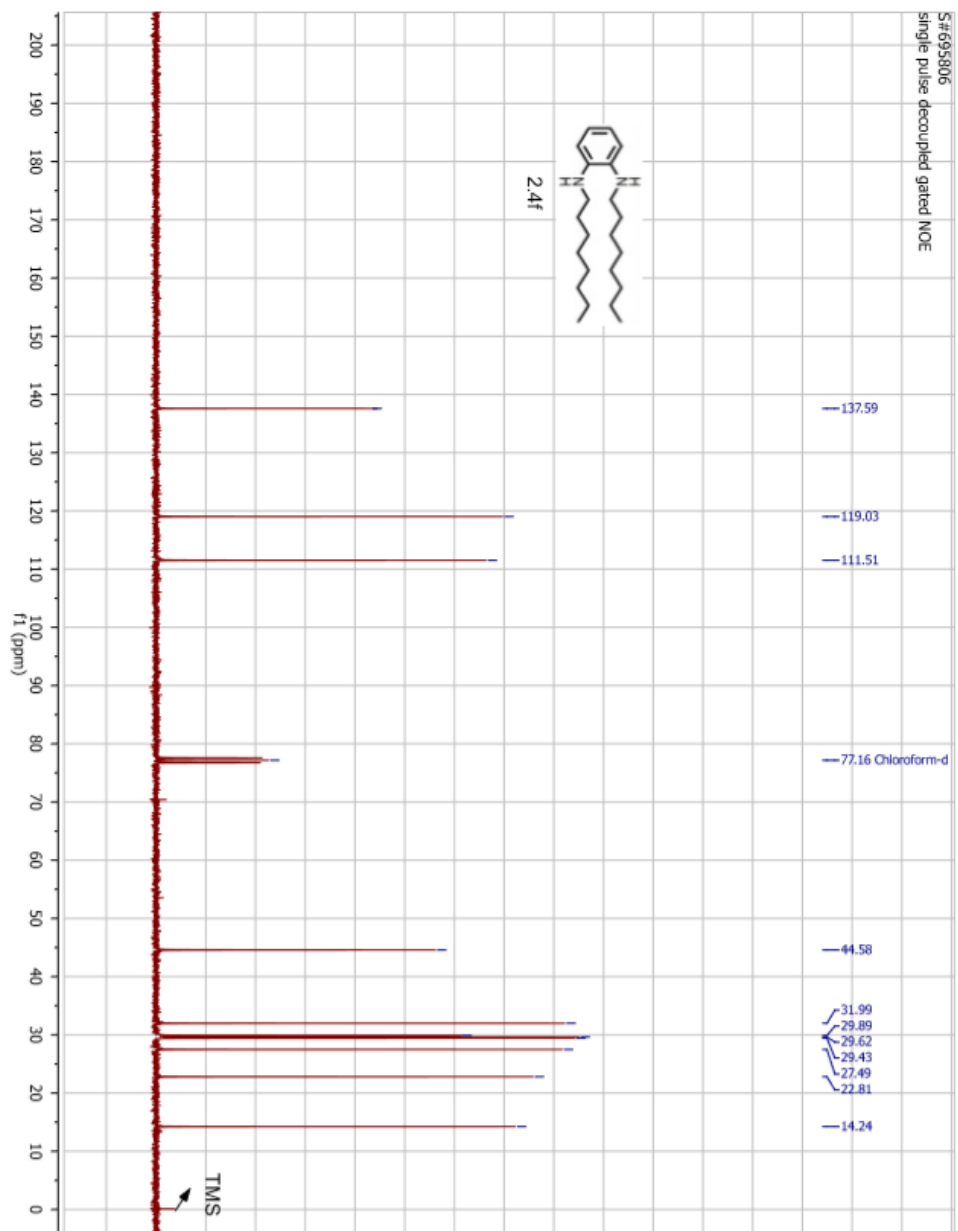


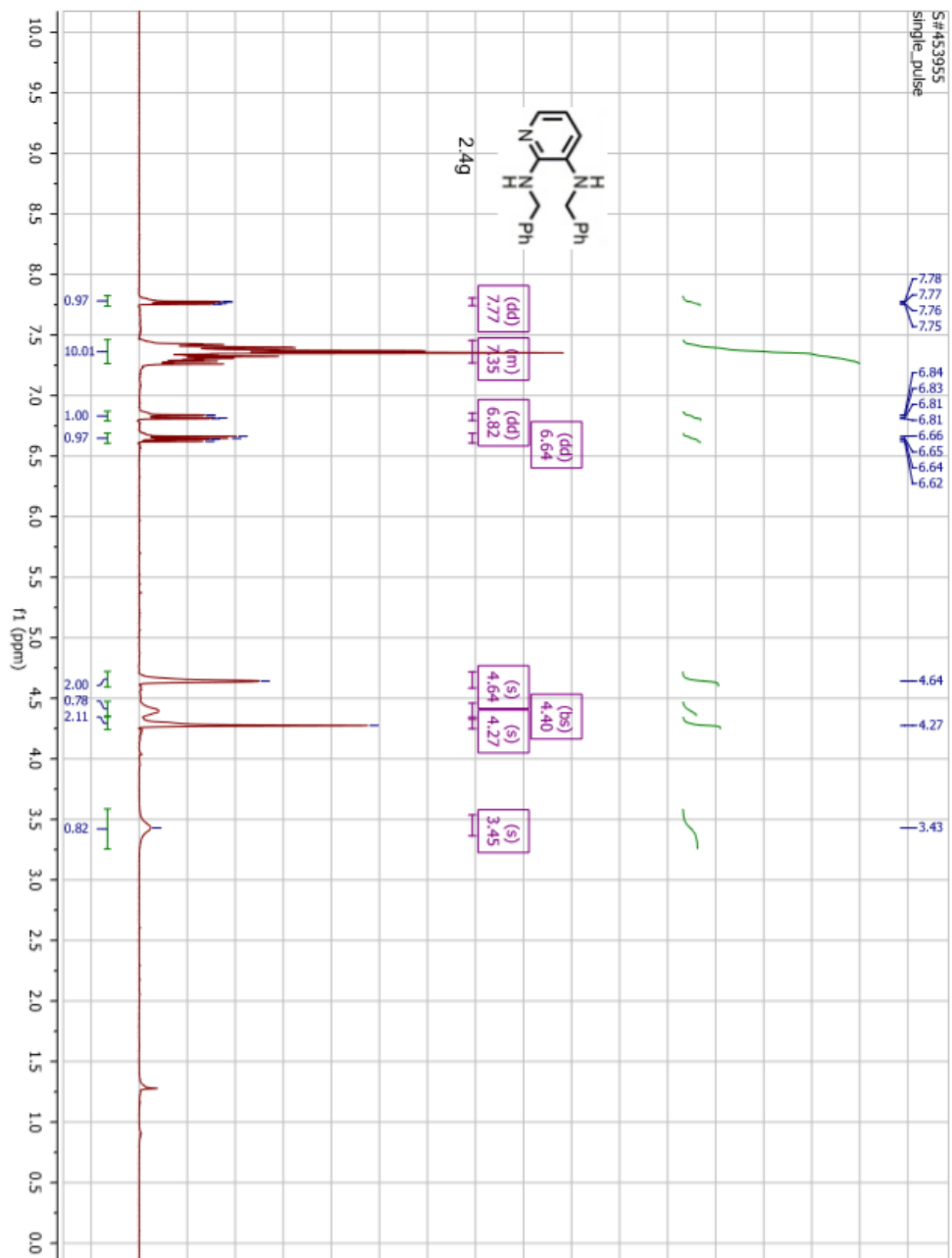
S#523685
single_pulse

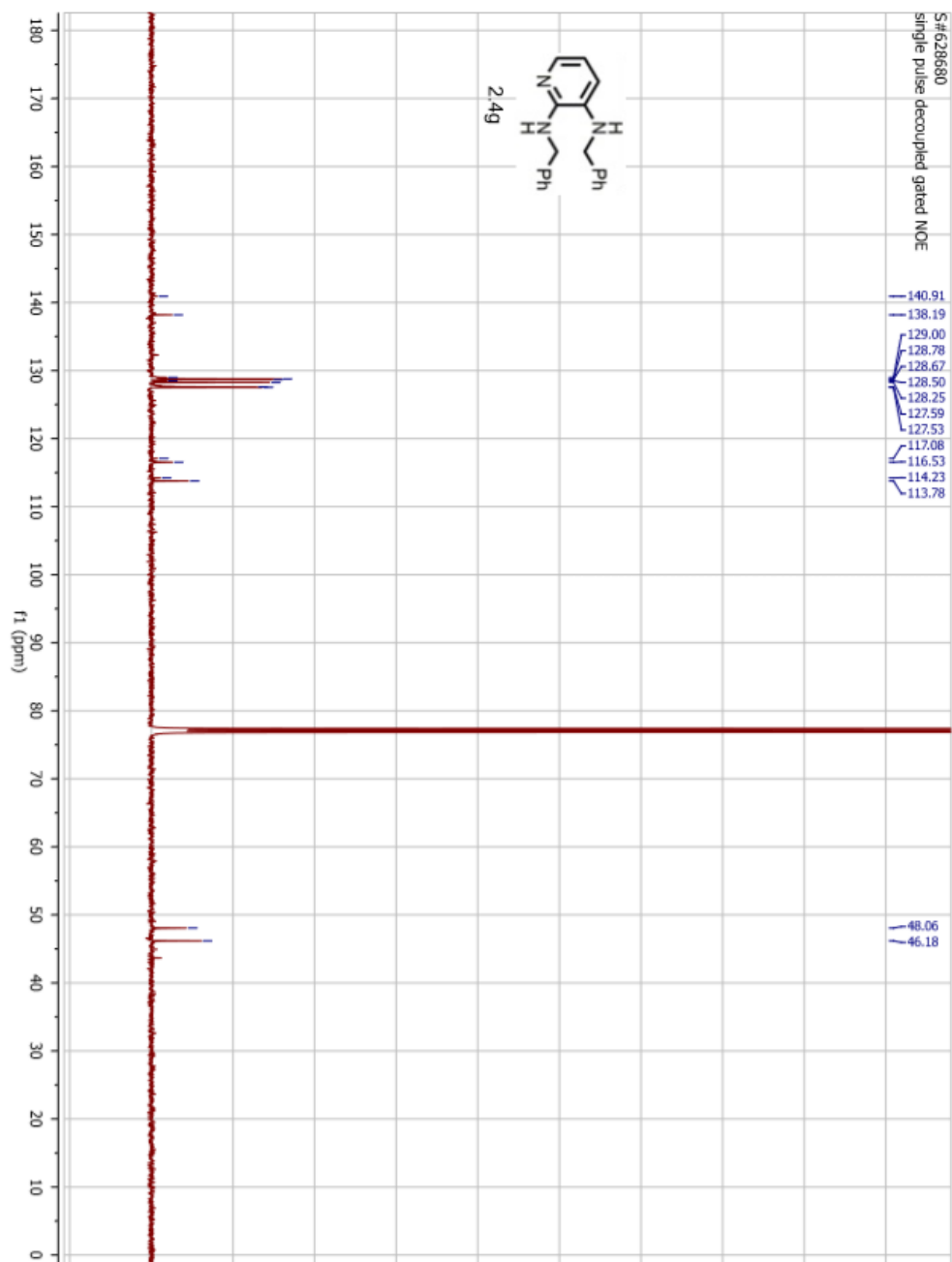


S#694510
single_pulse

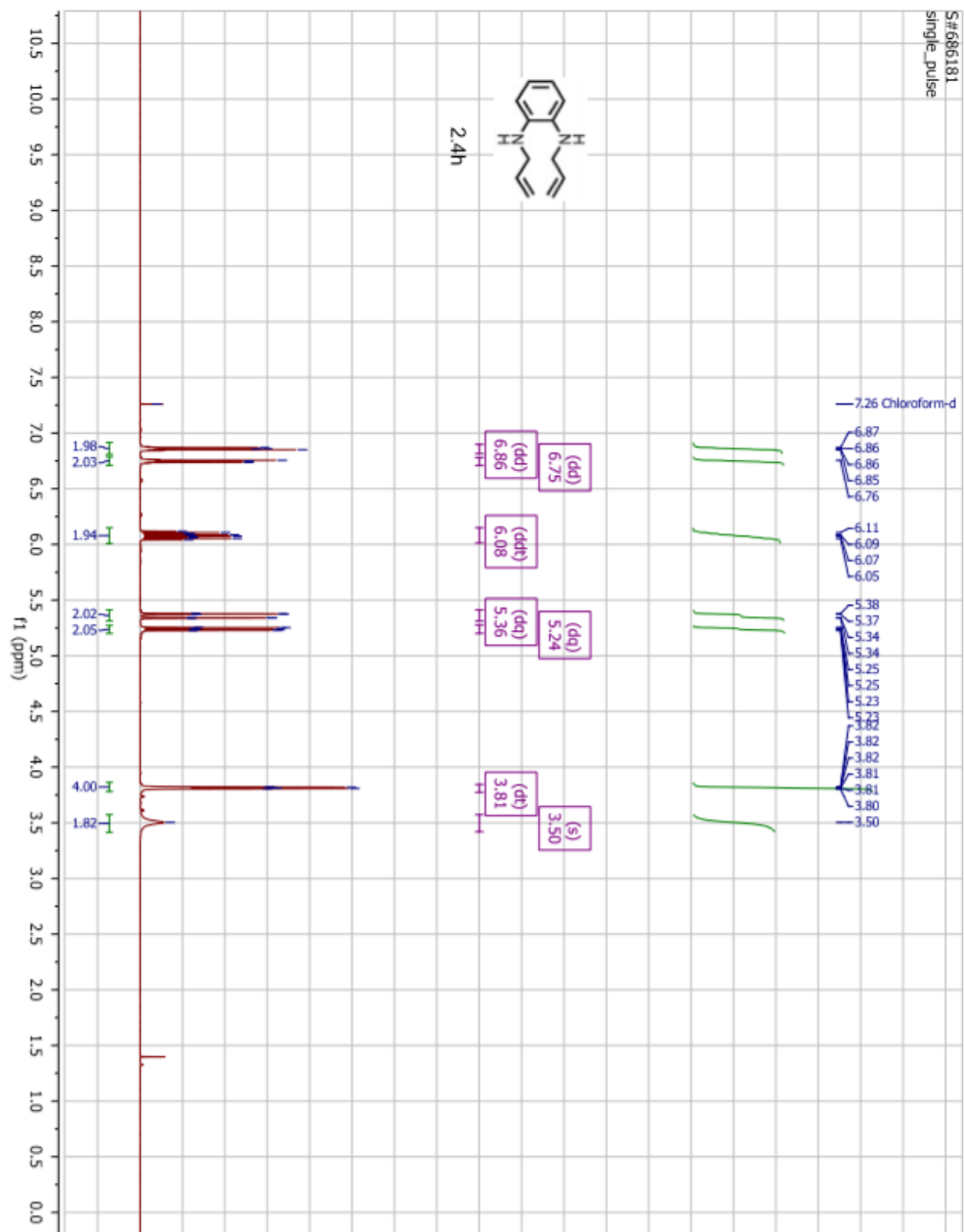




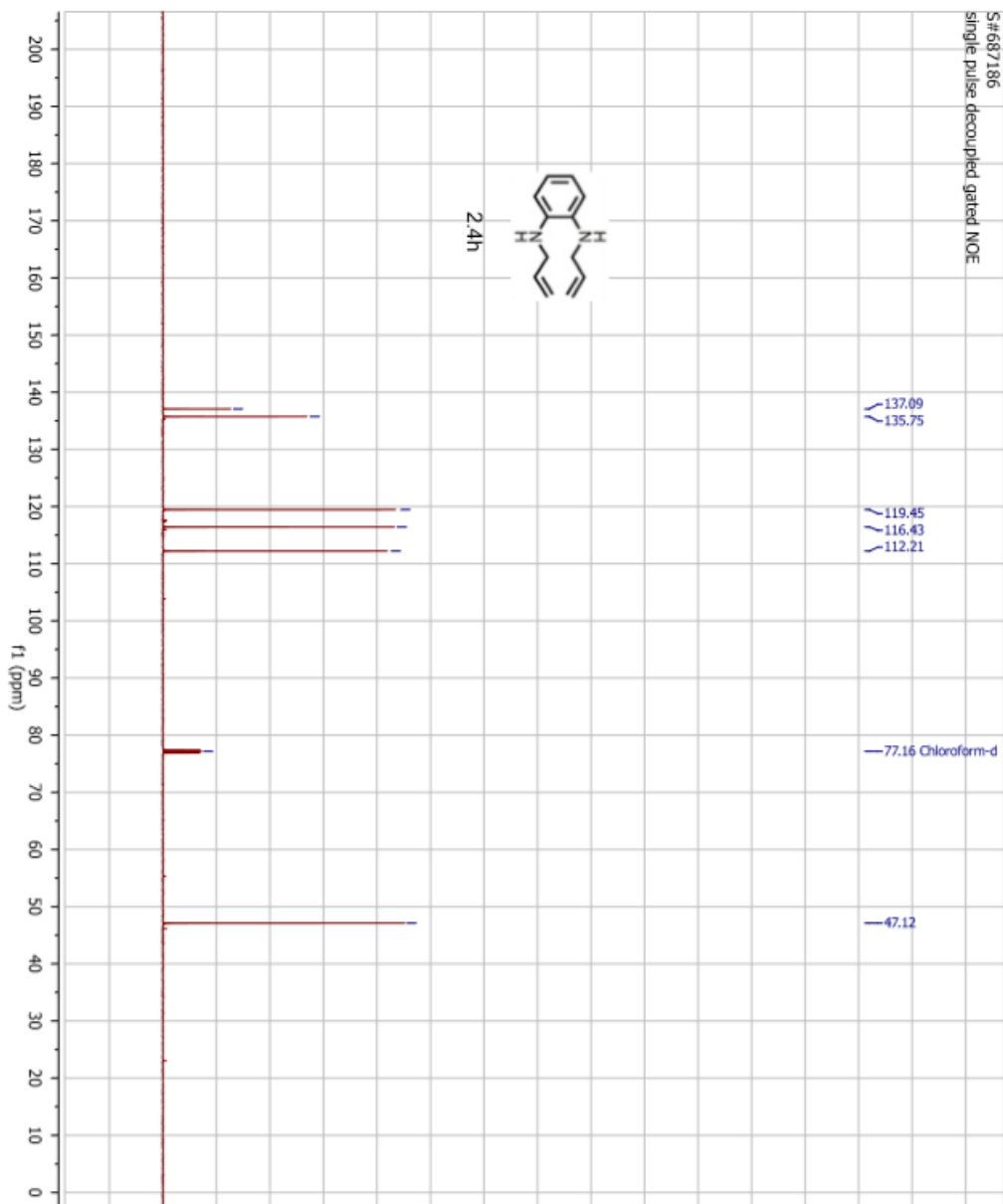
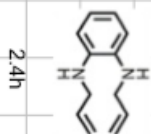


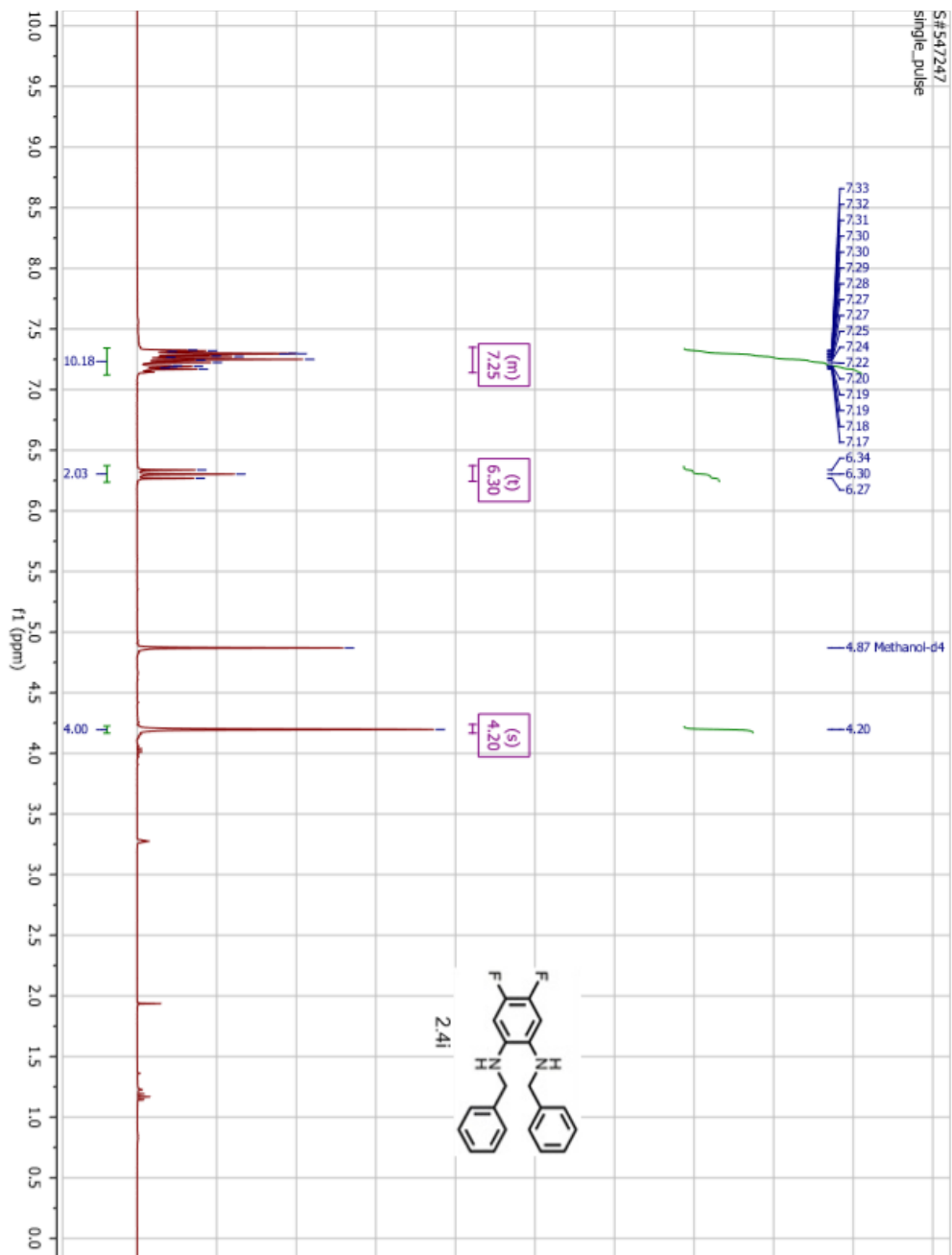


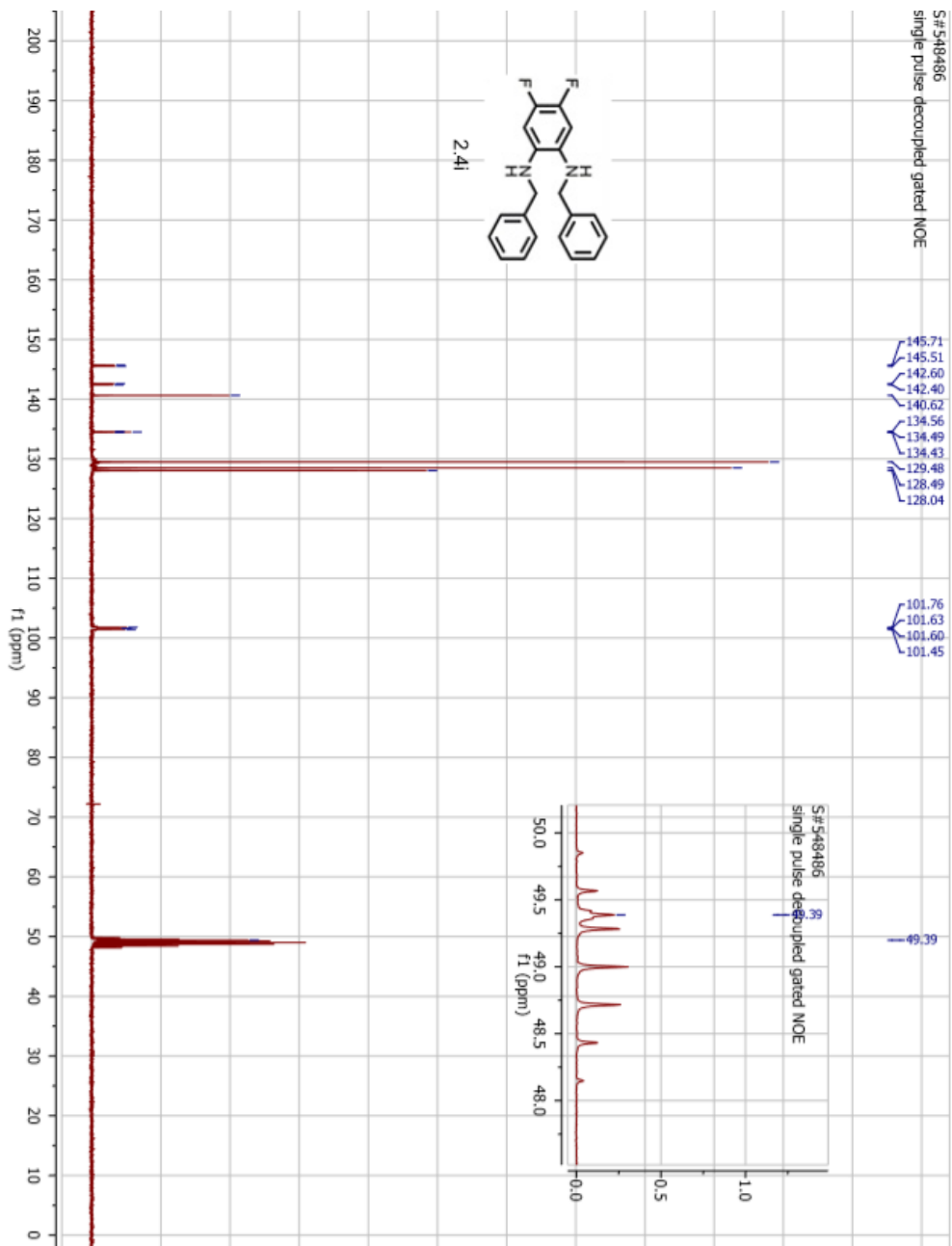
S#586181
single_pulse

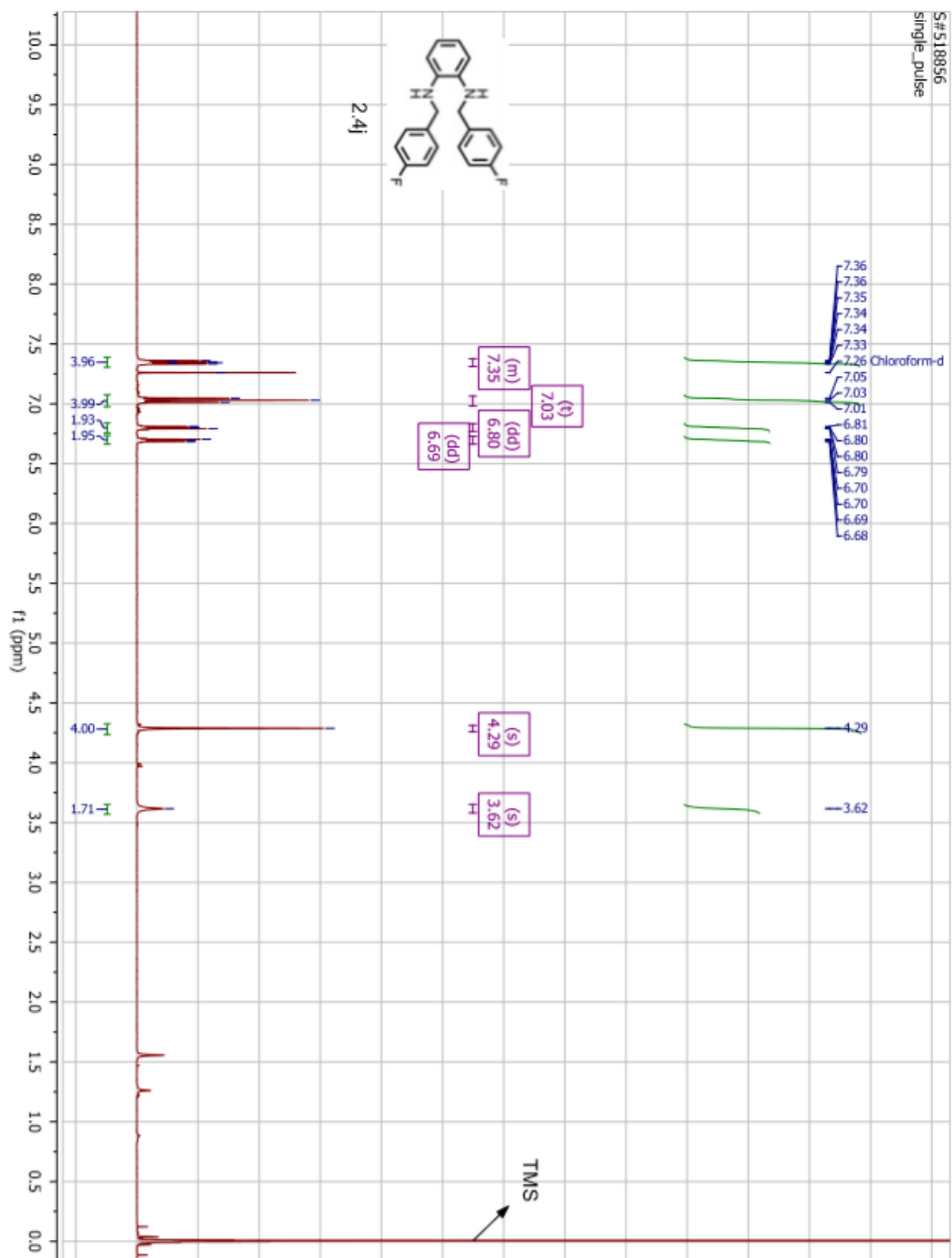


S#687186
single pulse decoupled gated NOE

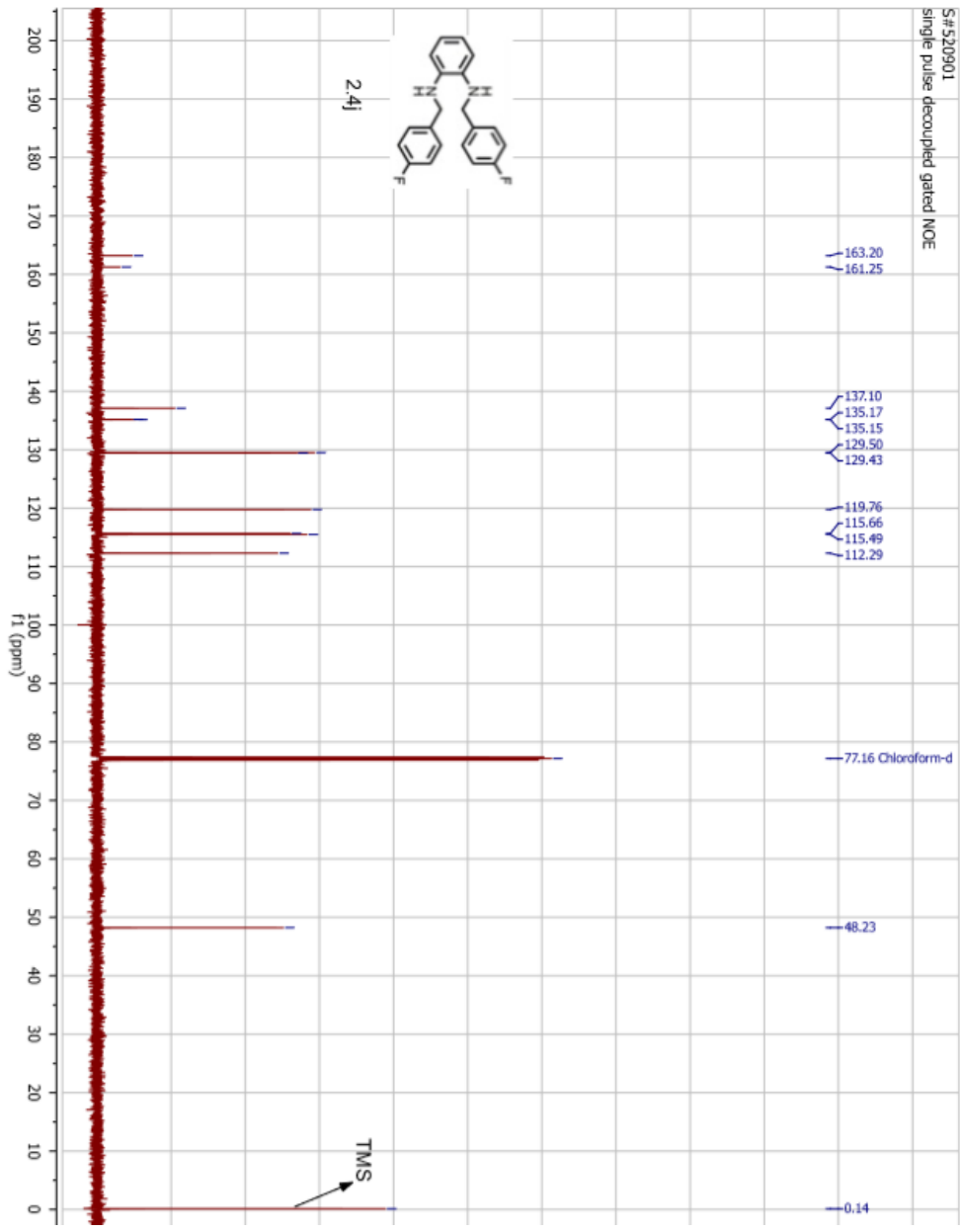
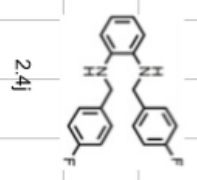


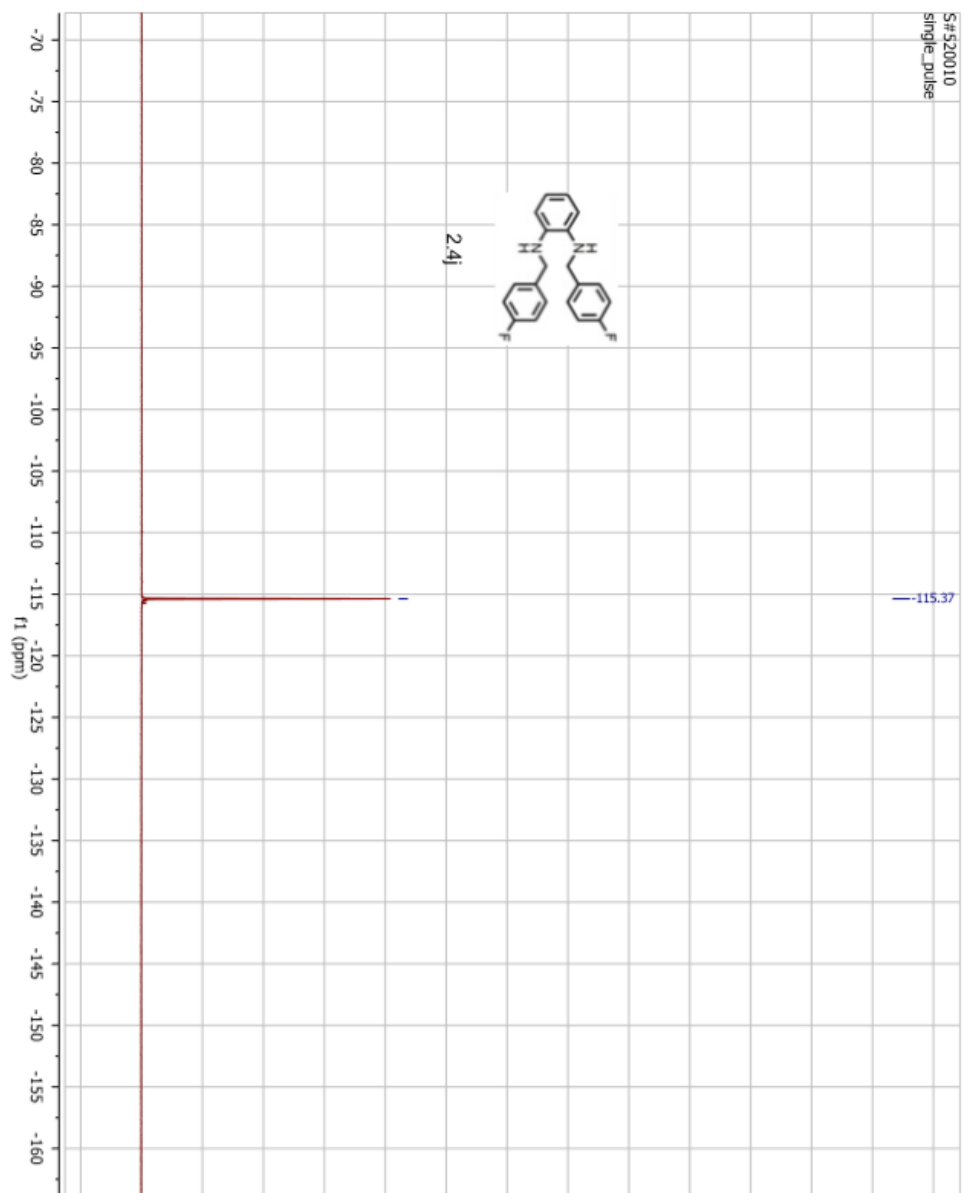


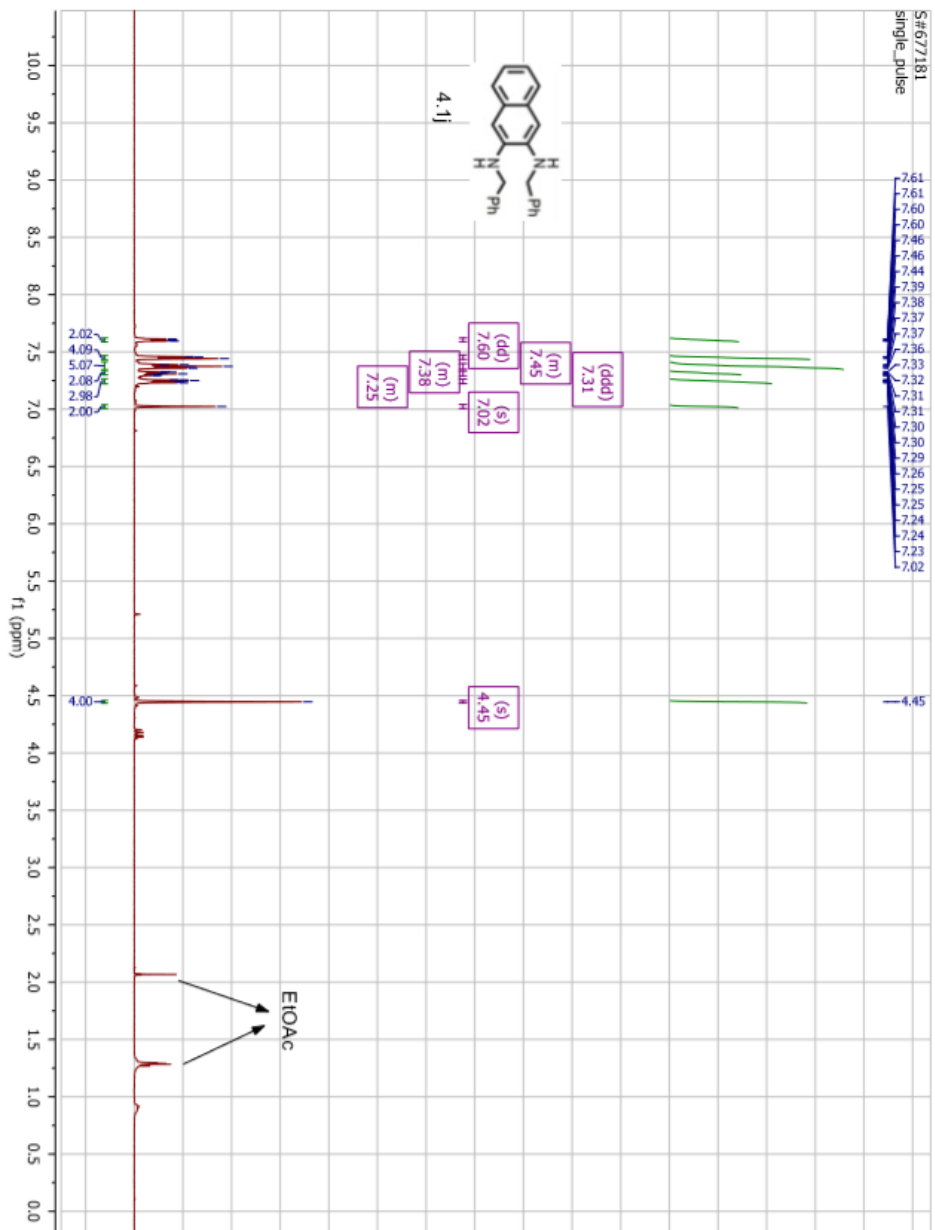




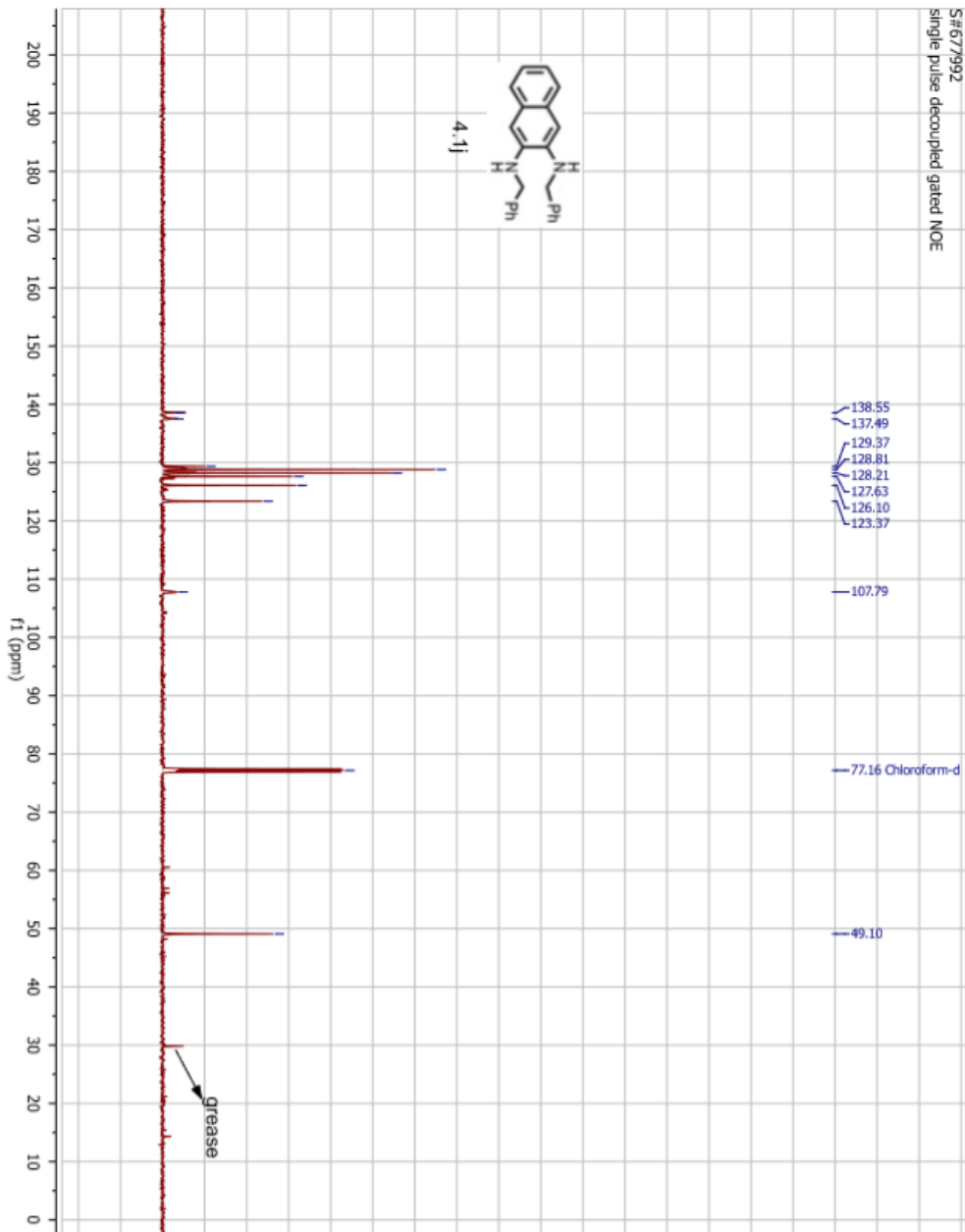
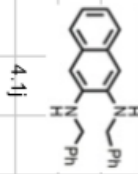
S#520901
single pulse decoupled gated NOE

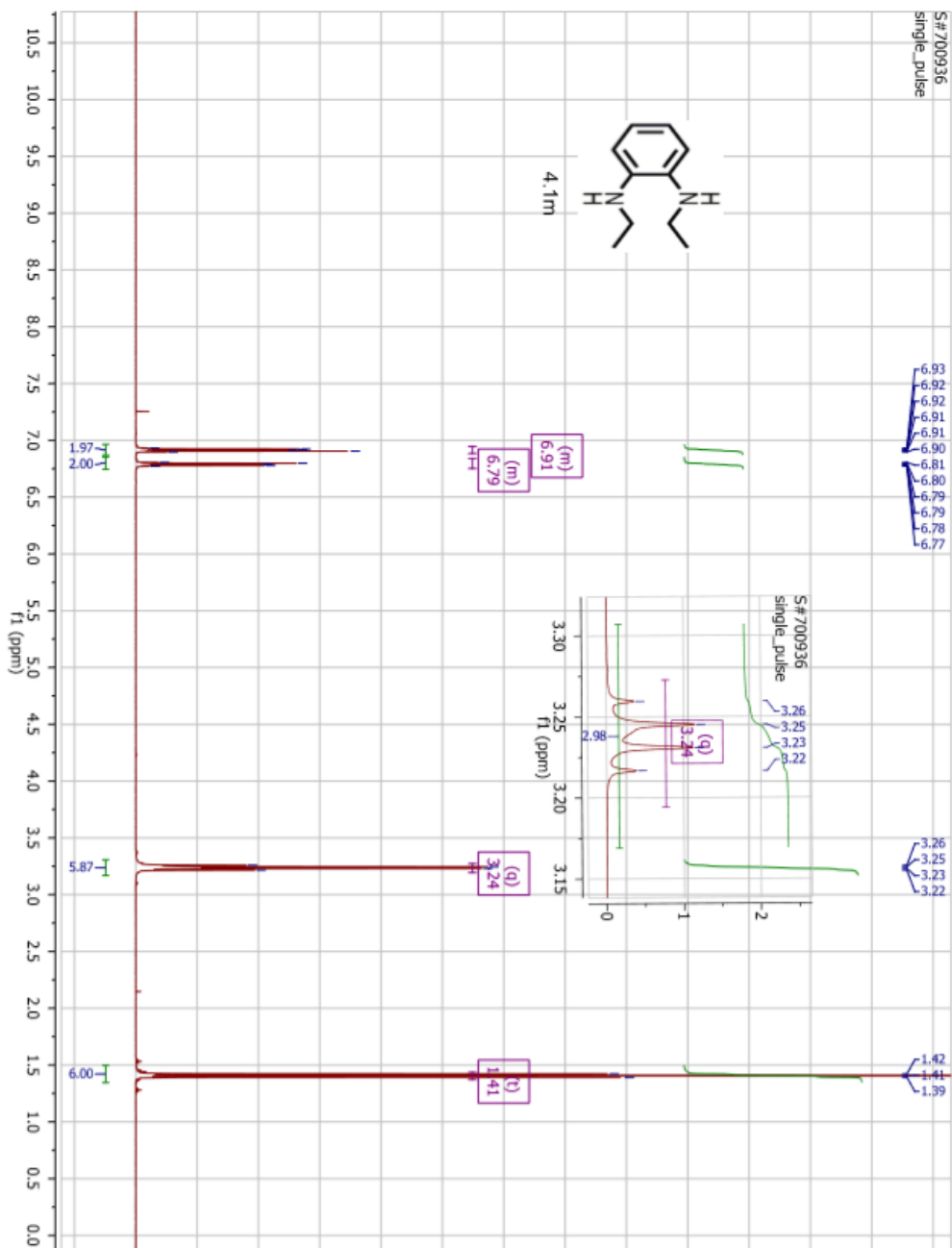




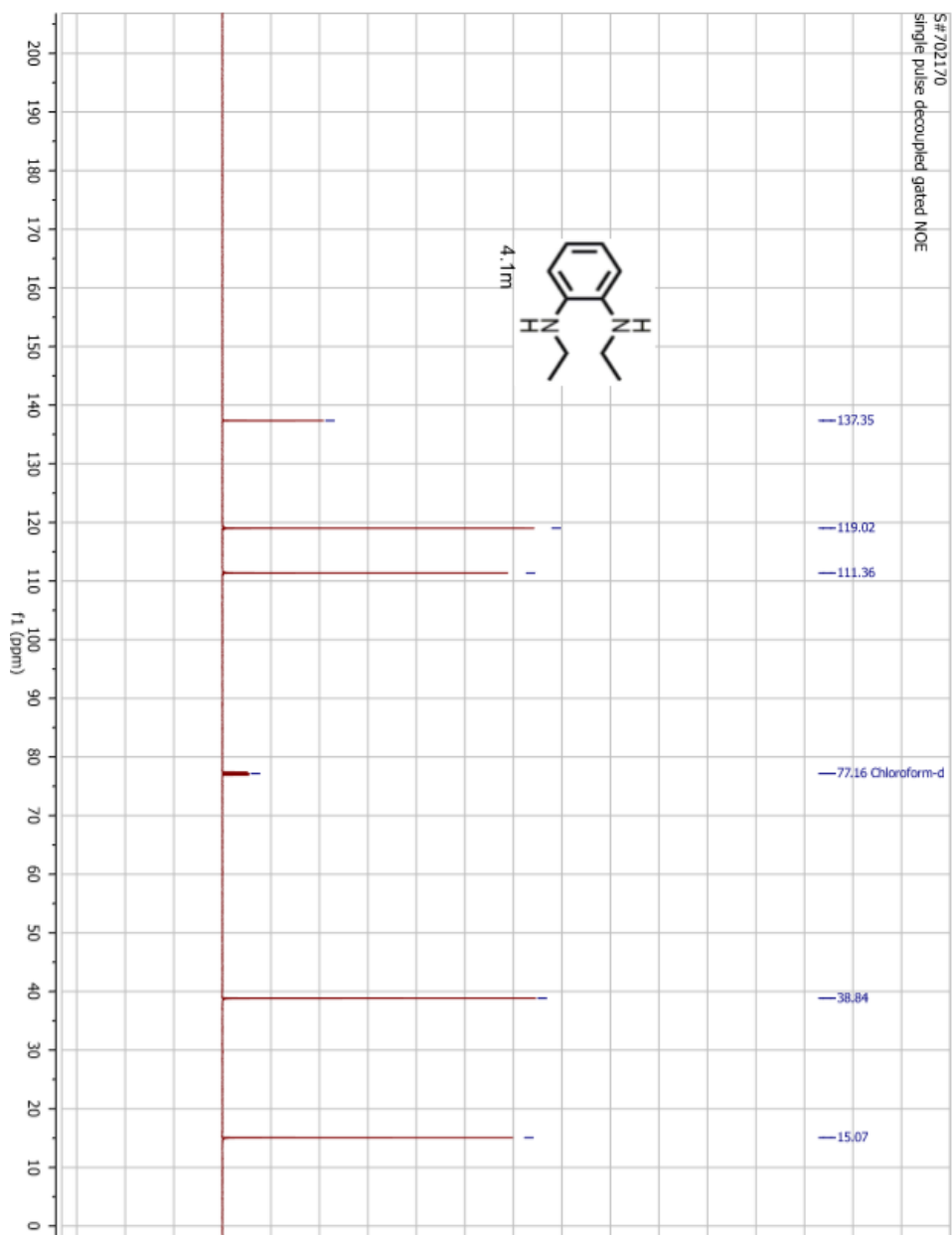
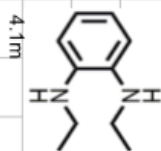


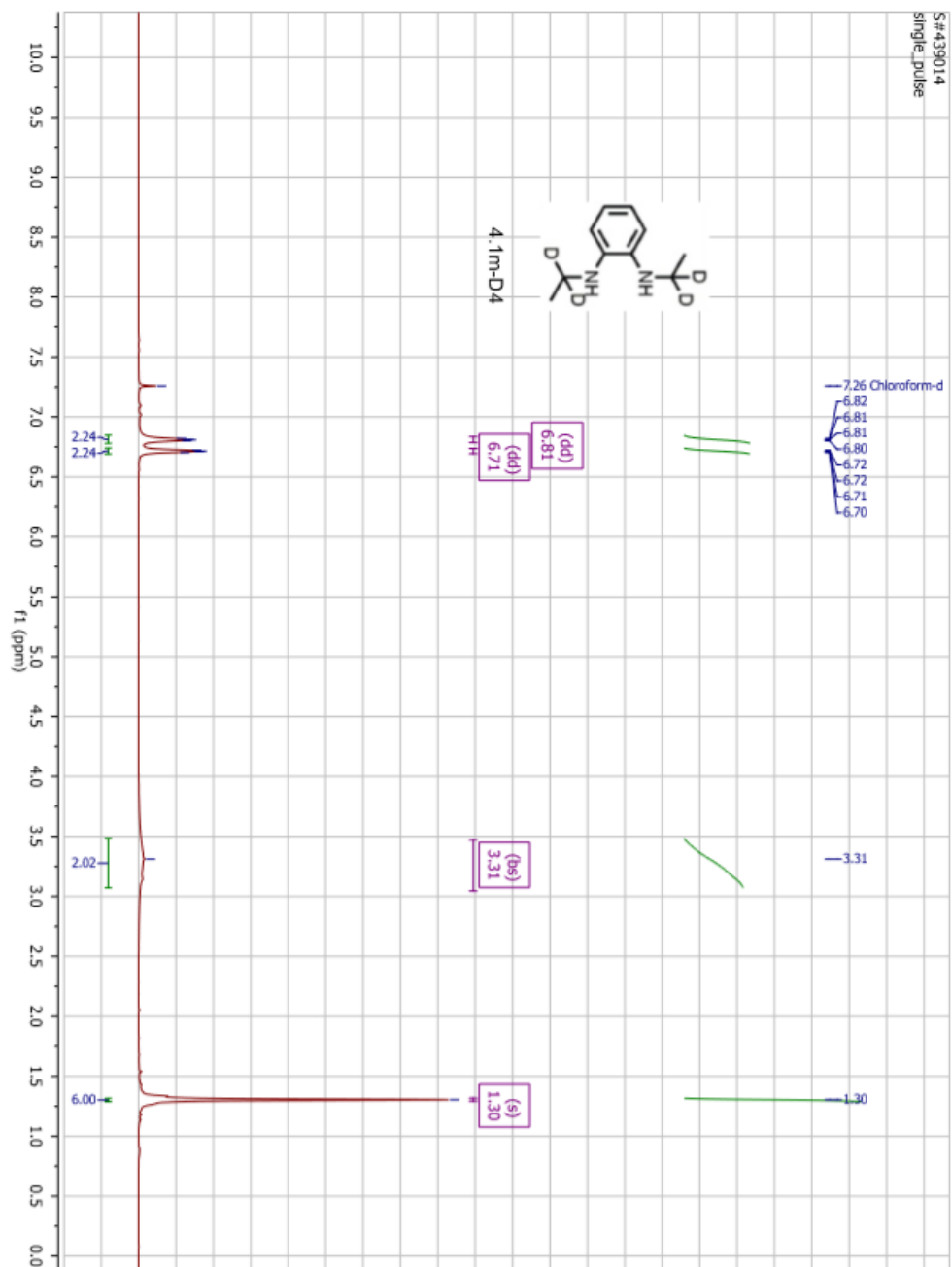
S#677992
Single pulse decoupled gated NOE



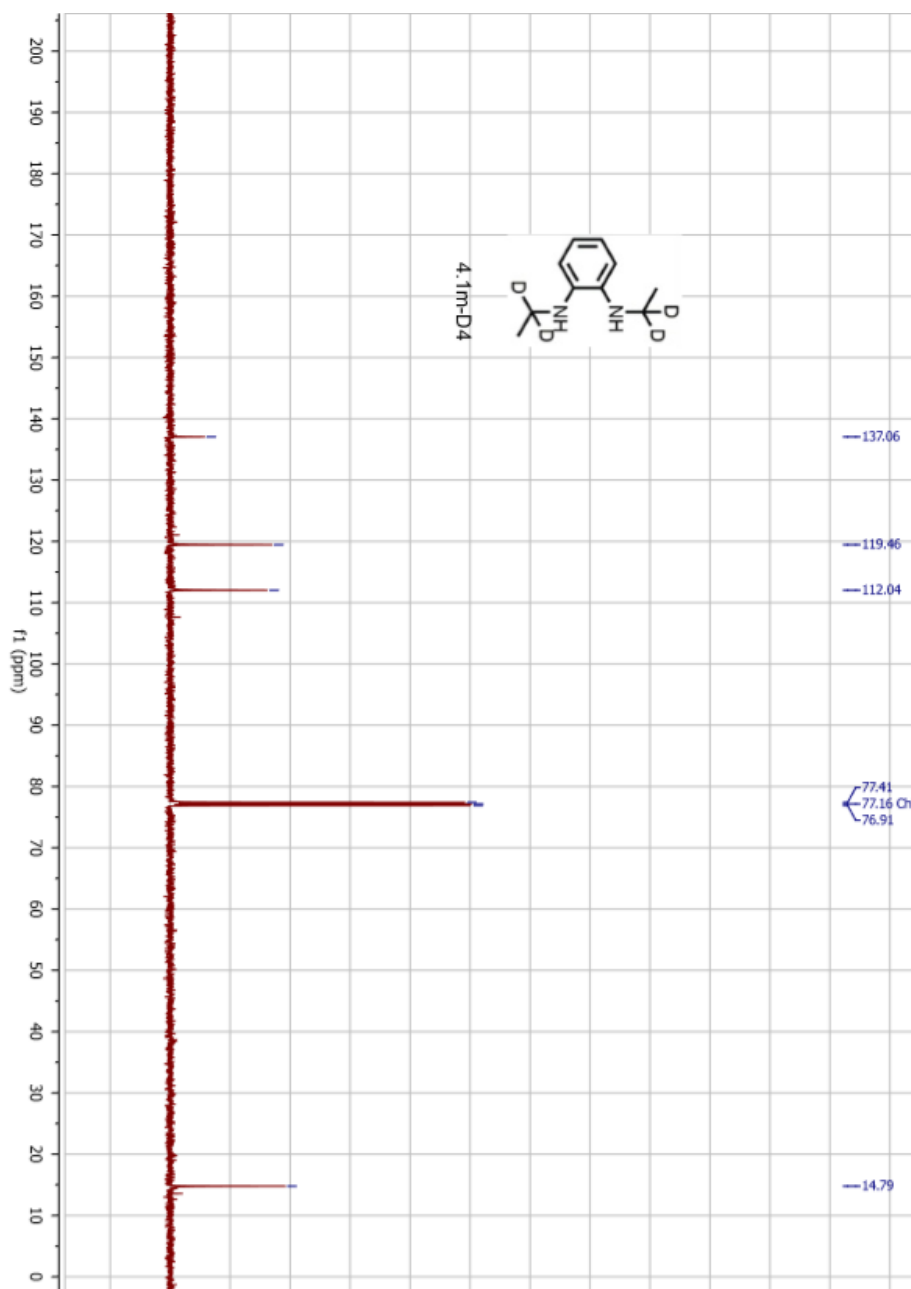


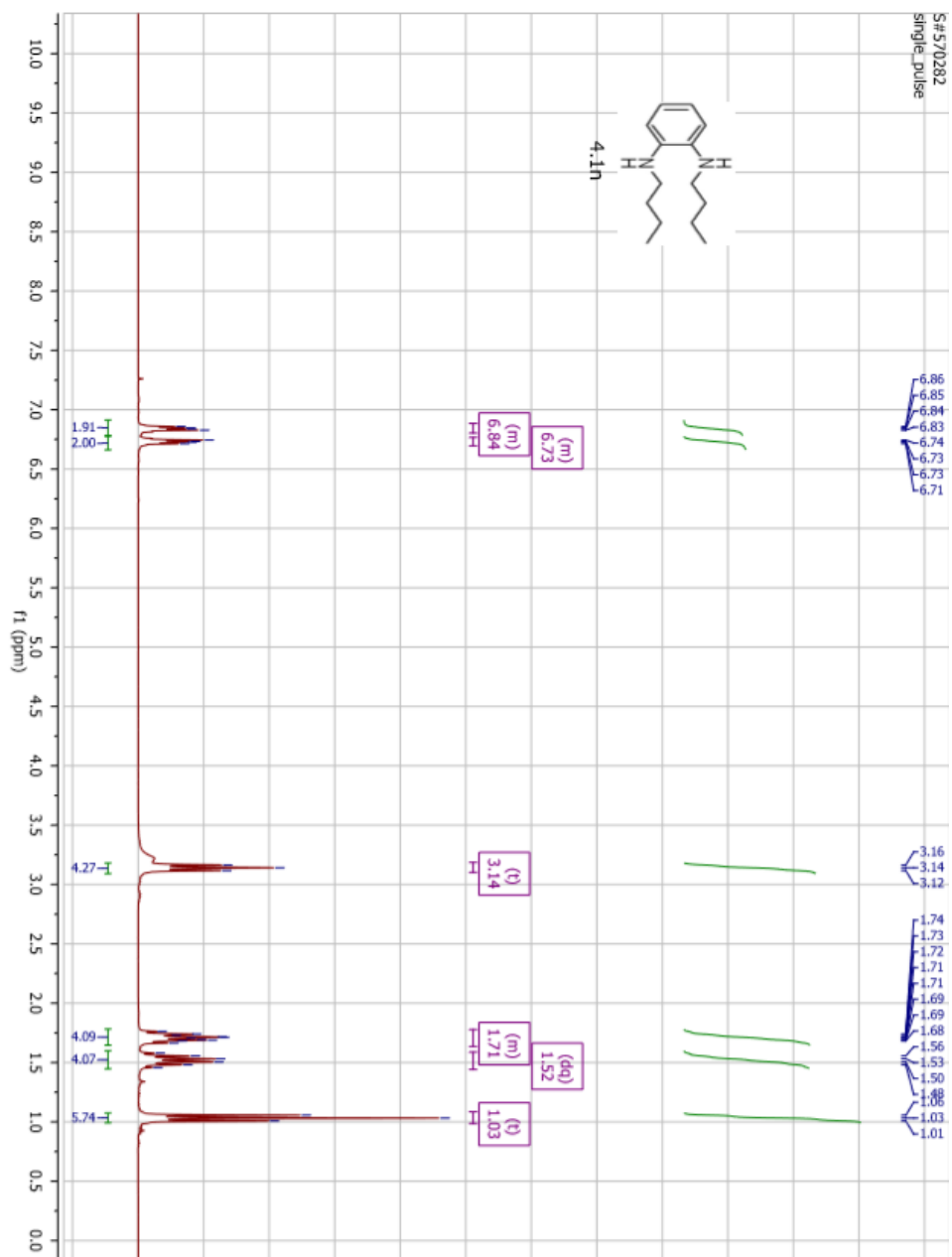
S#702170
single pulse decoupled gated NOE



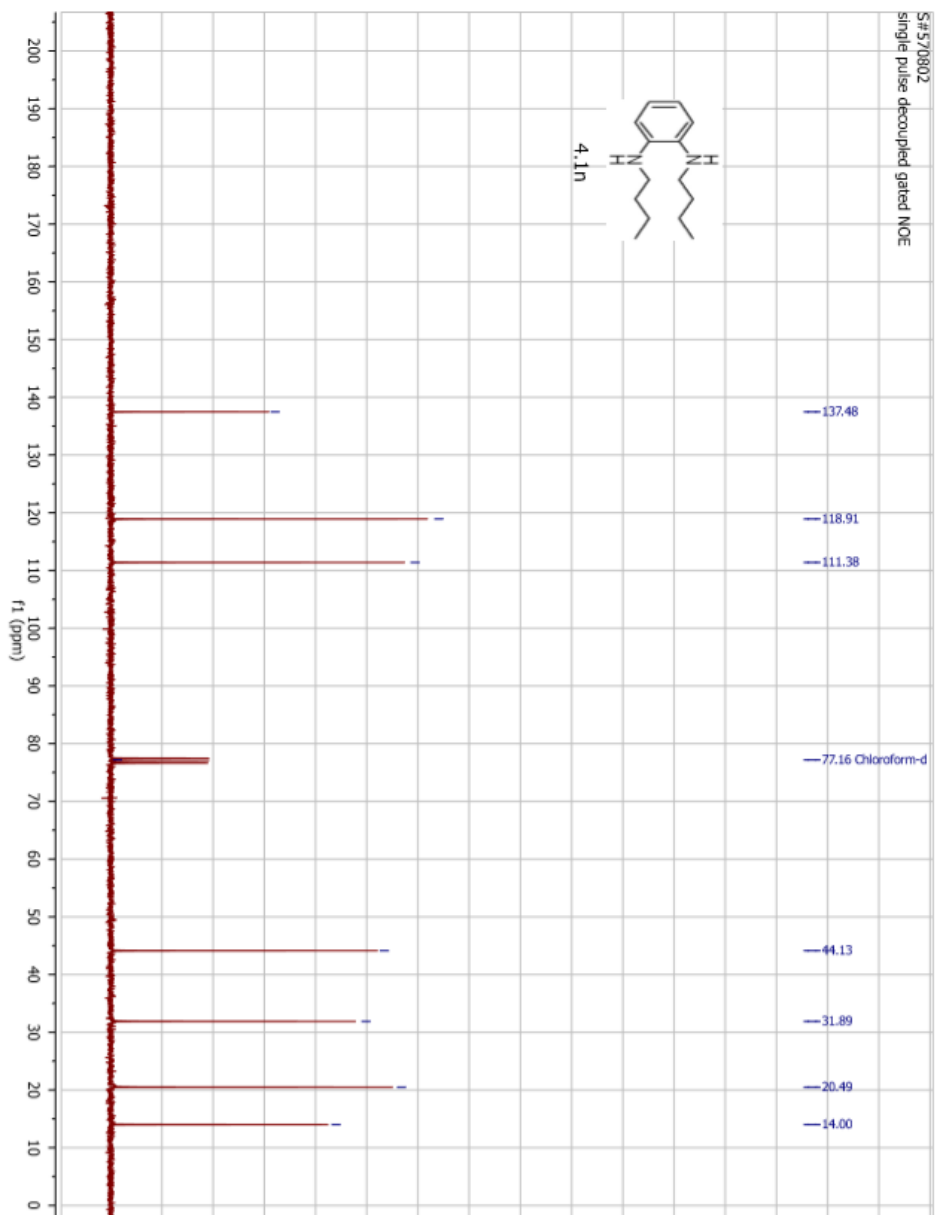
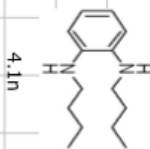


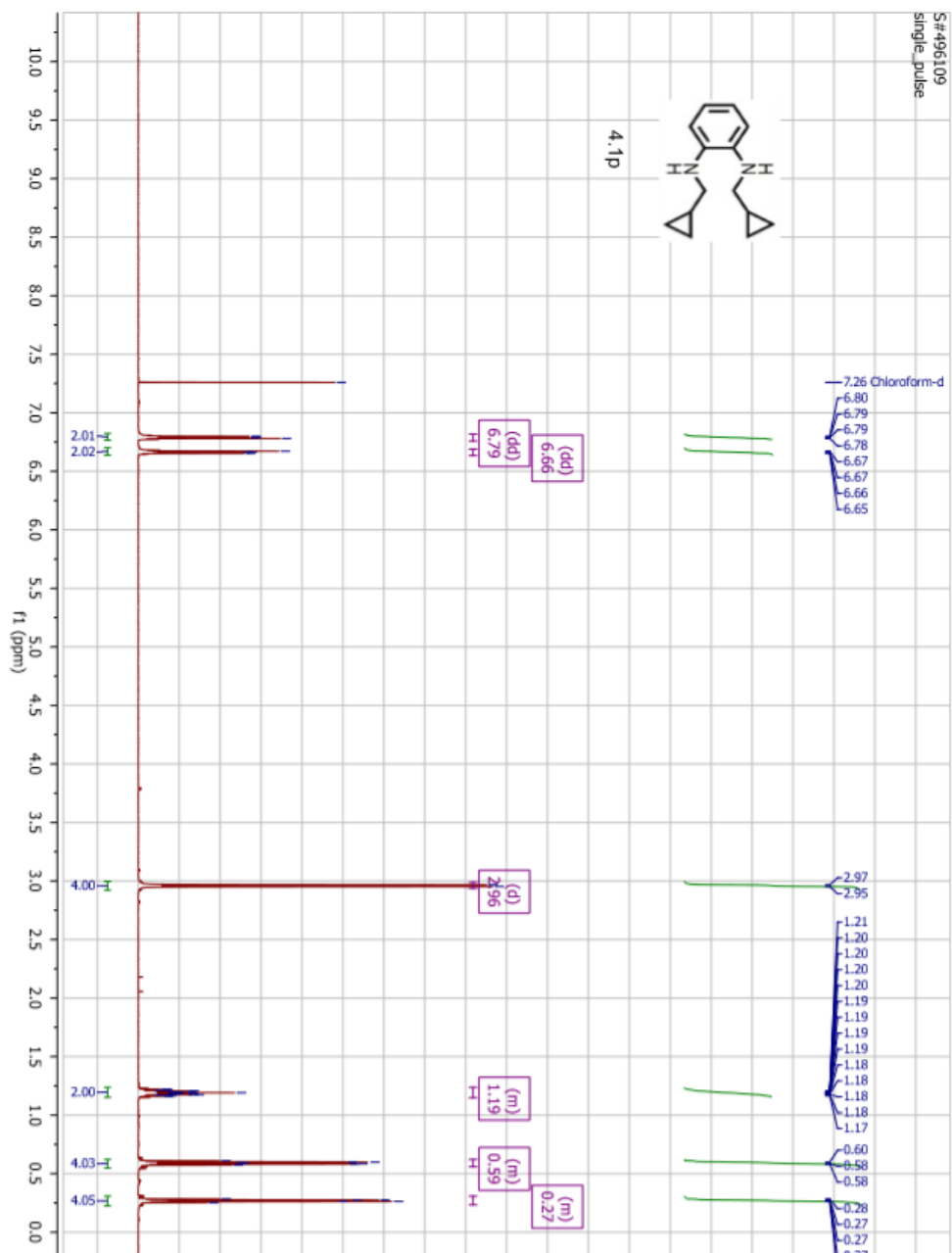
S#440129
single pulse decoupled gated NOE



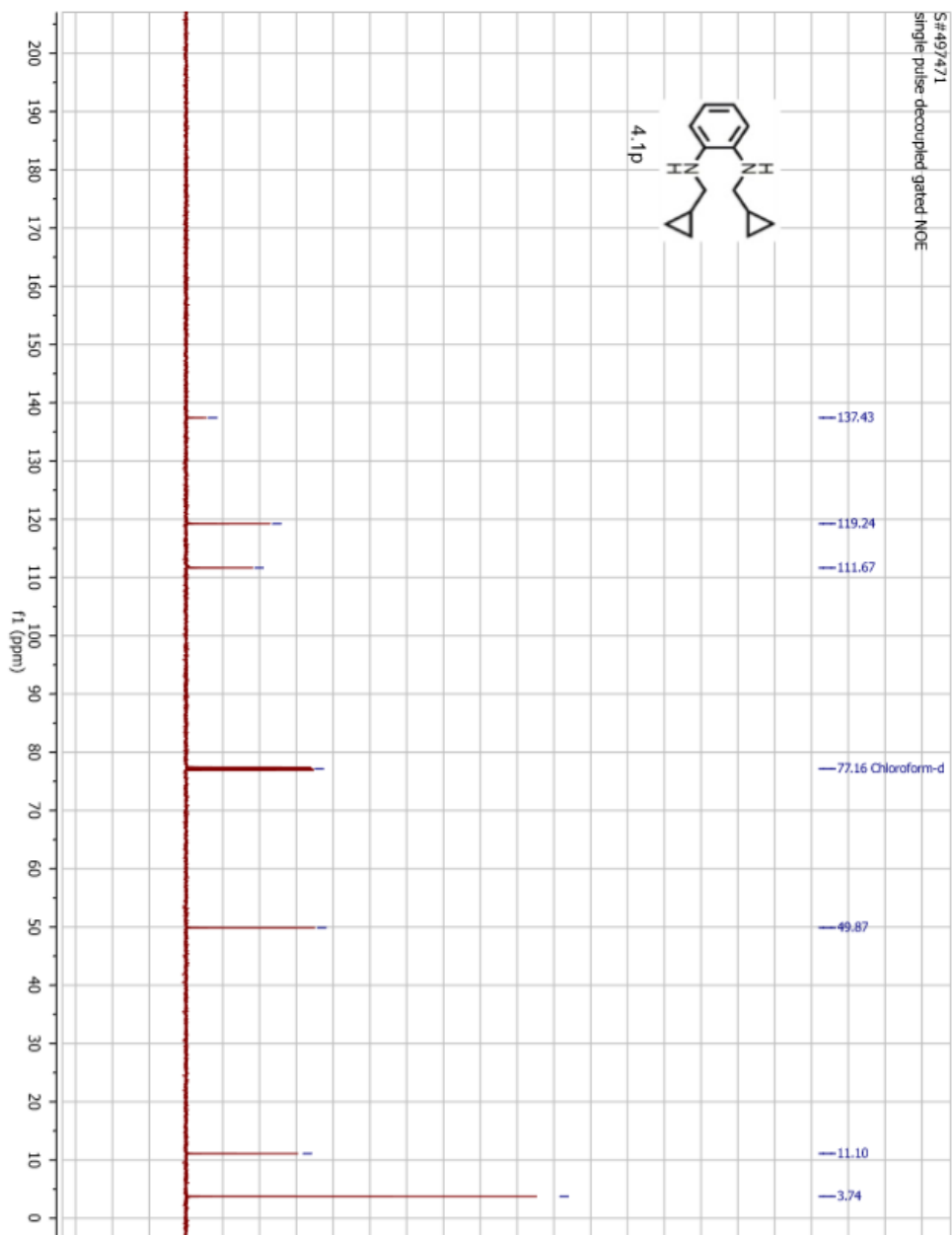
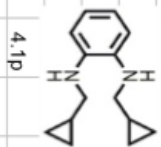


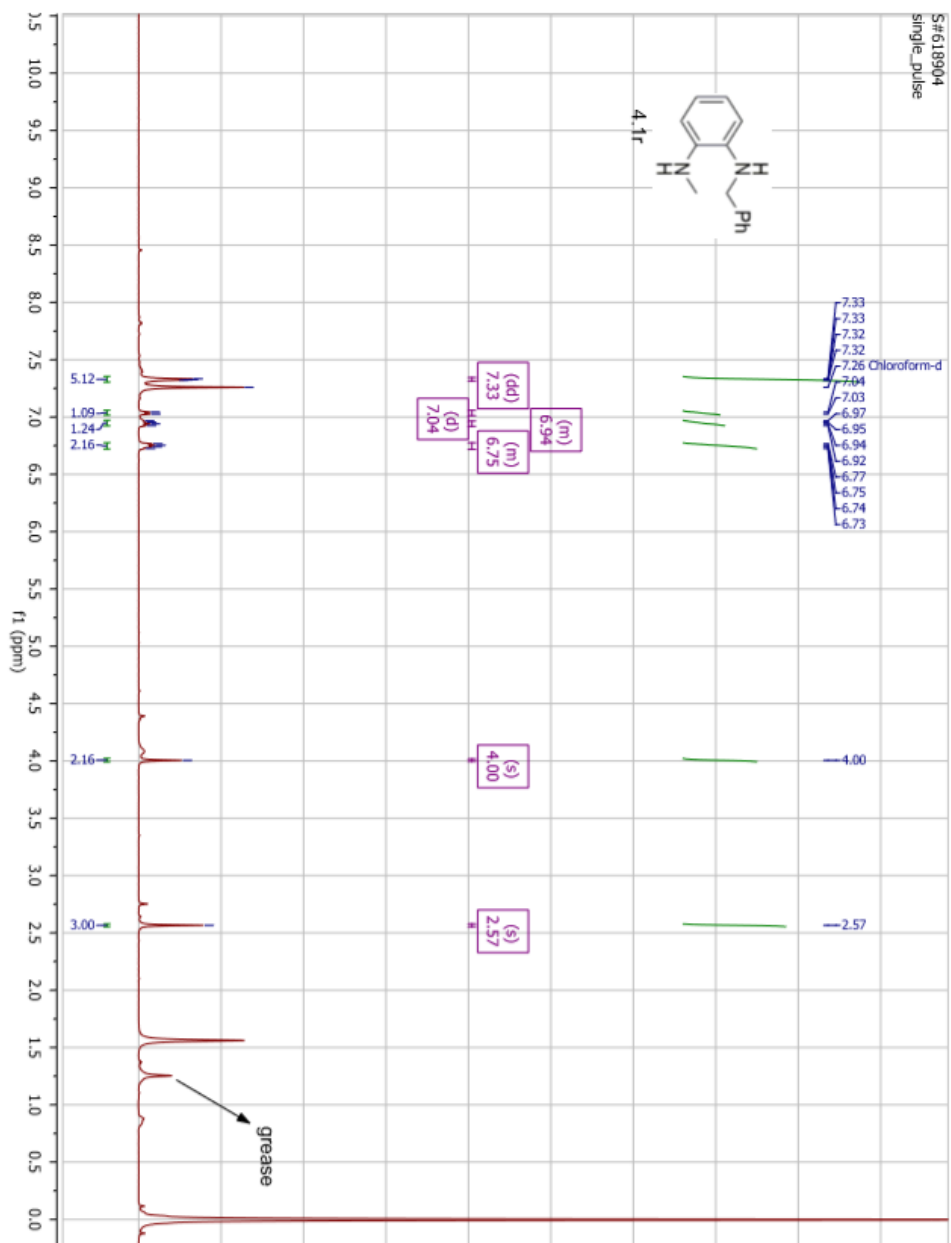
S# 570802
single pulse decoupled gated NOE



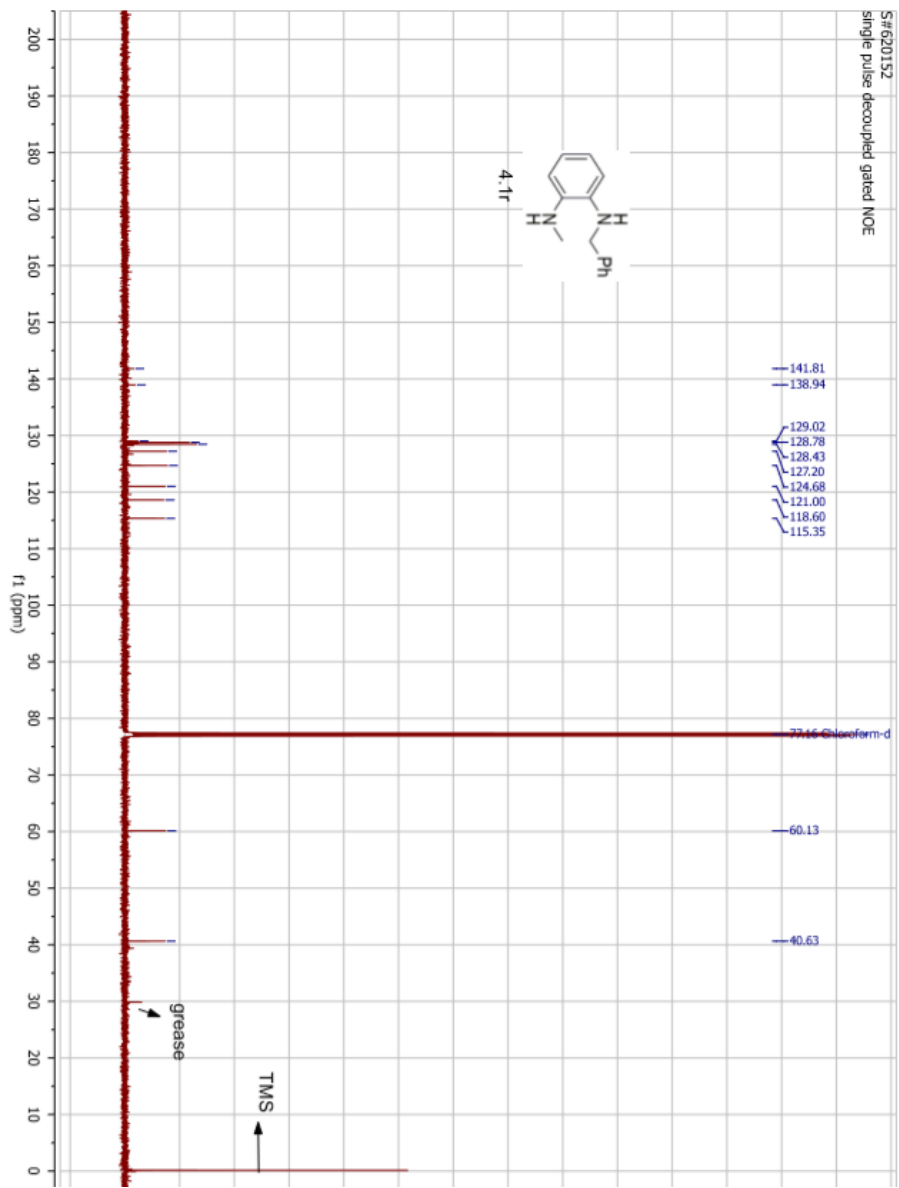
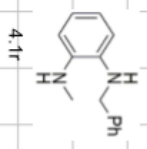


S#497471
single-pulse decoupled gated NOE

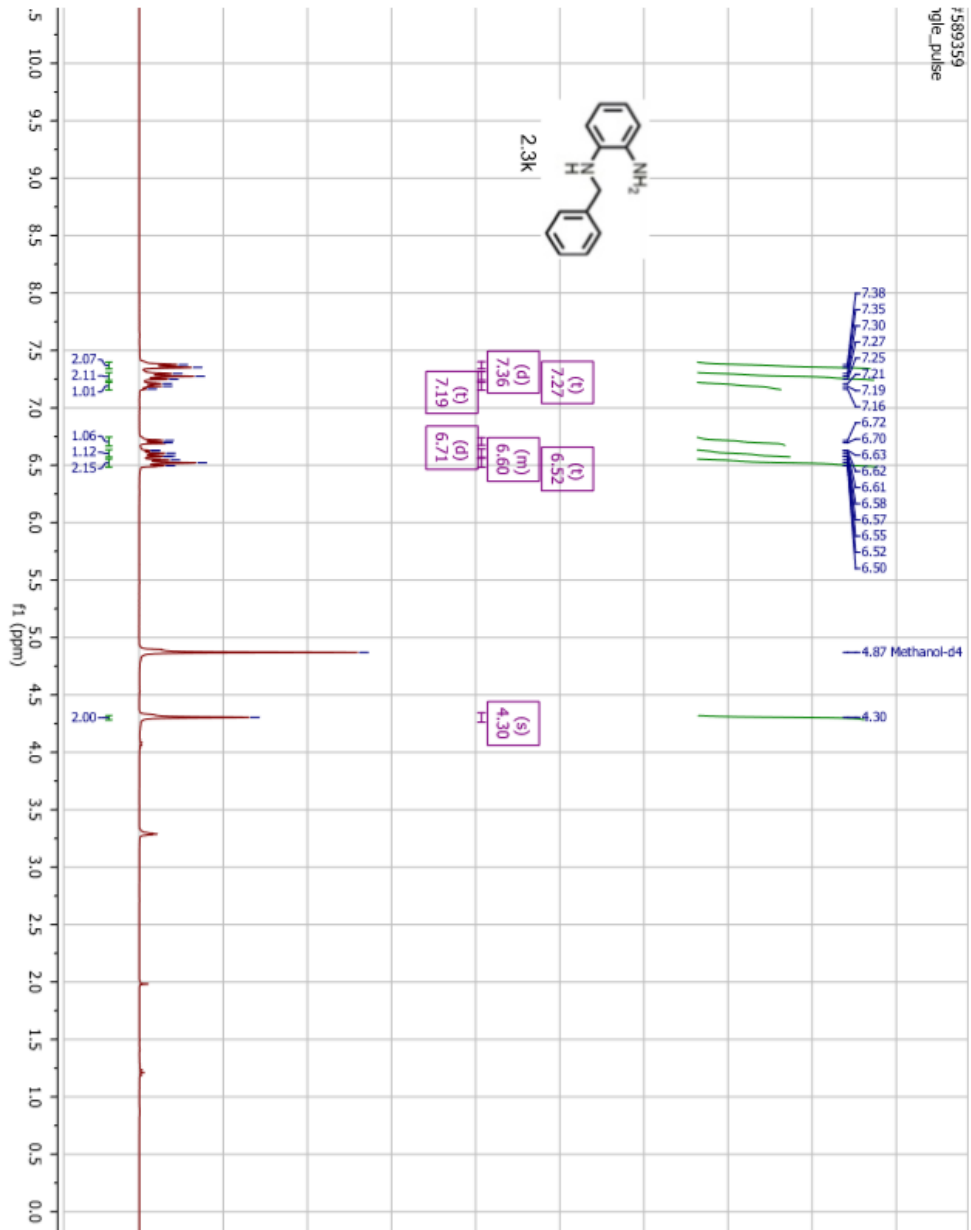
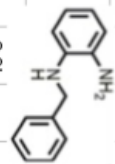




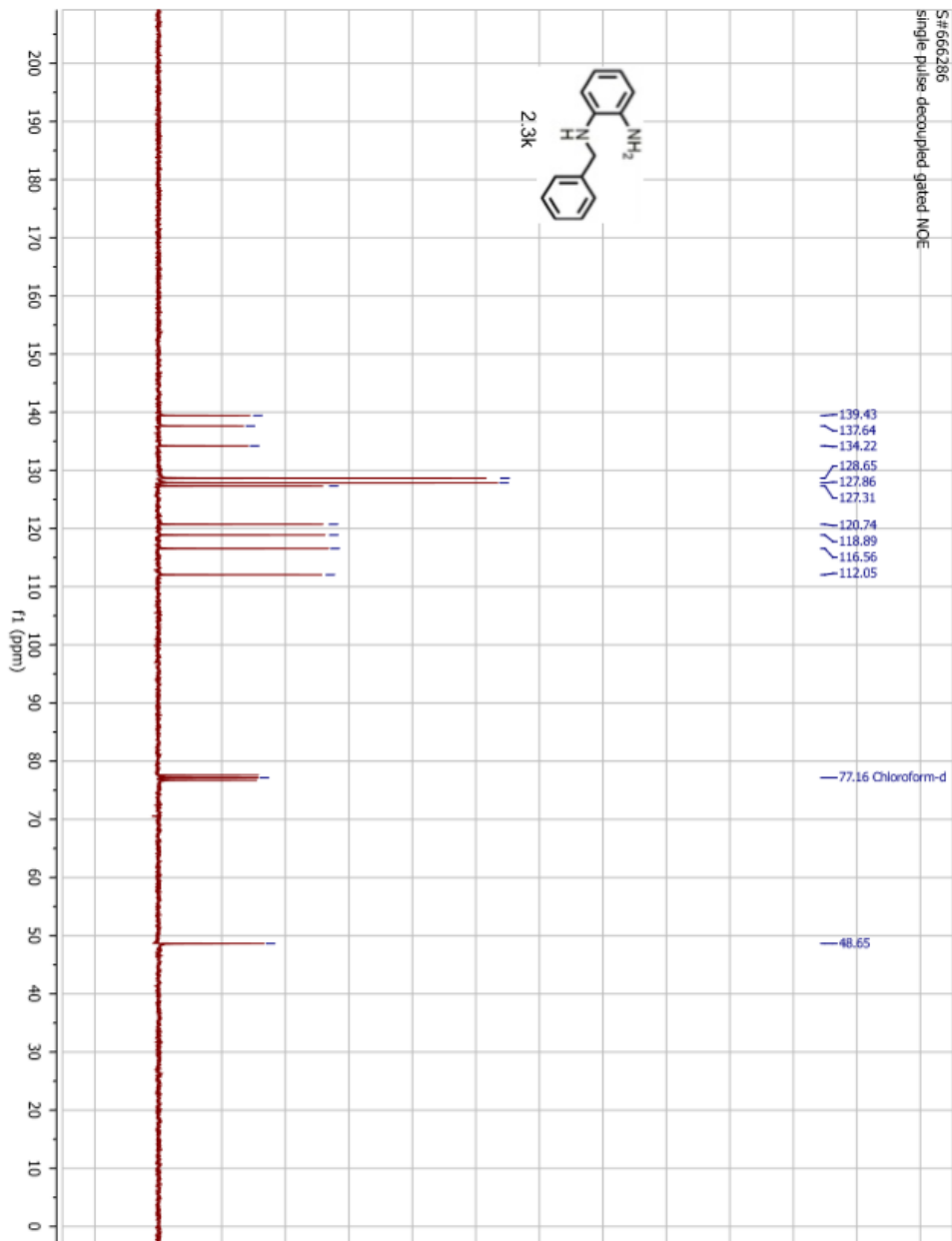
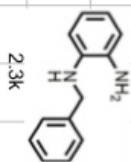
S# 620152
single pulse decoupled gated NOE

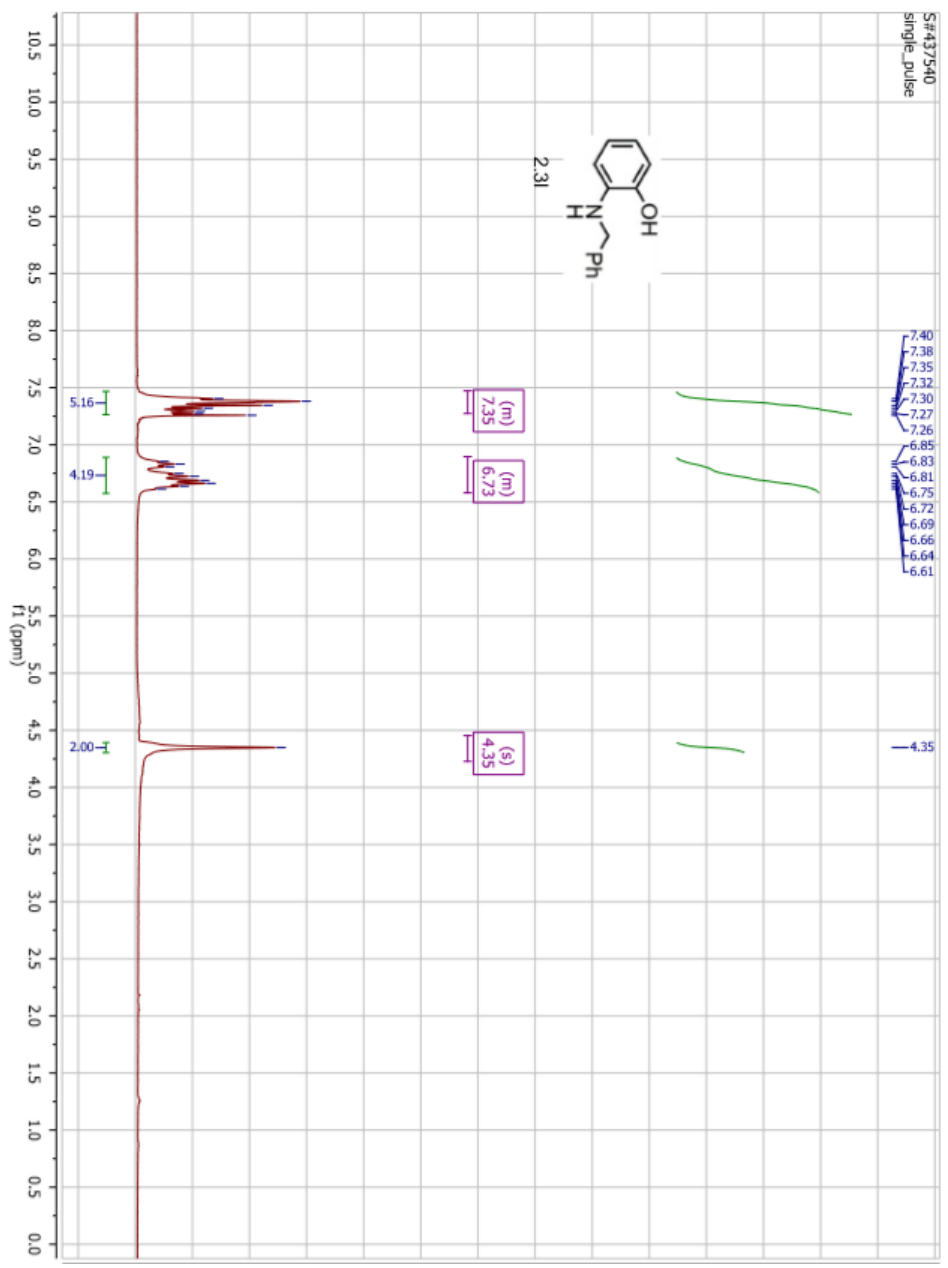


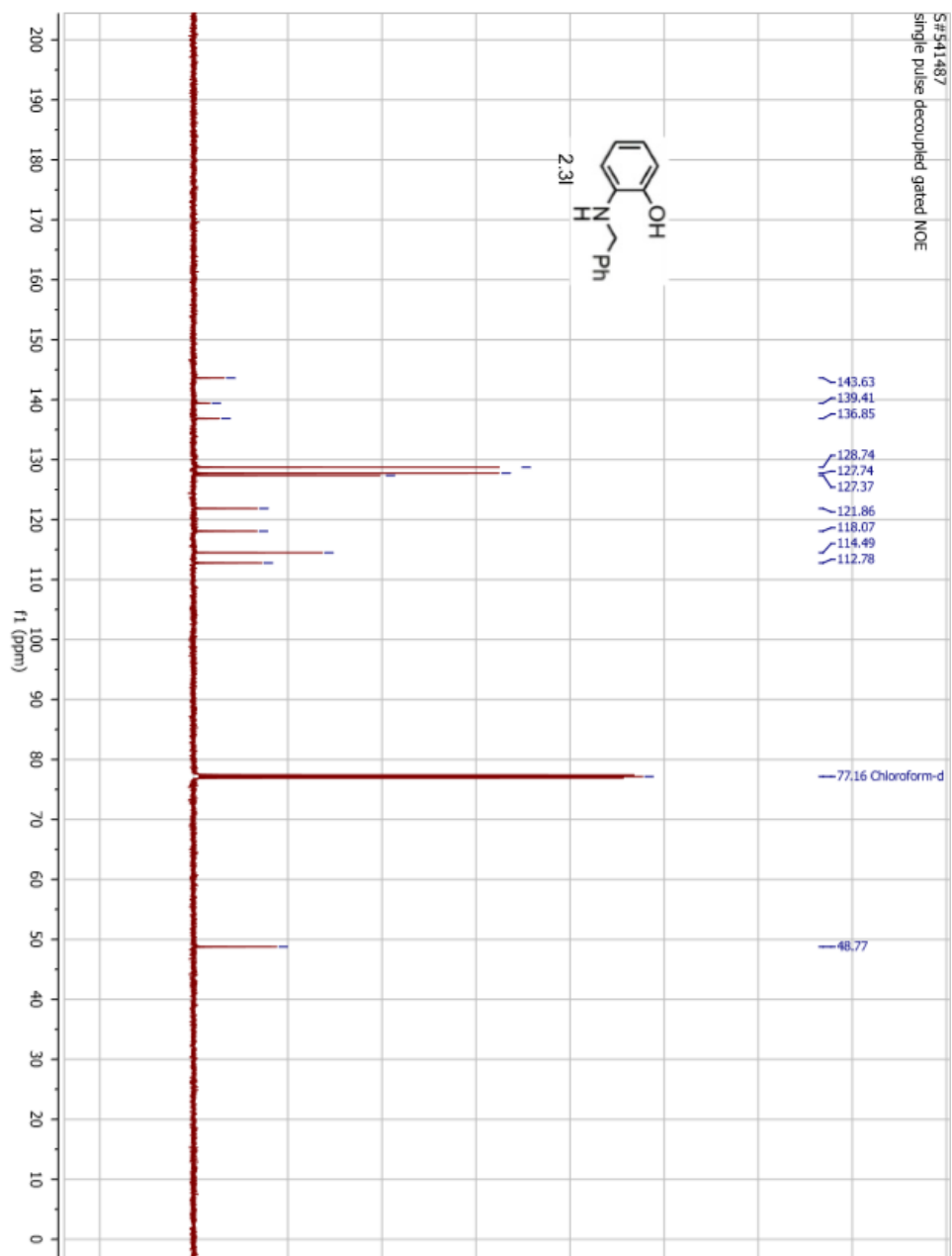
7589339
tgle_pulse



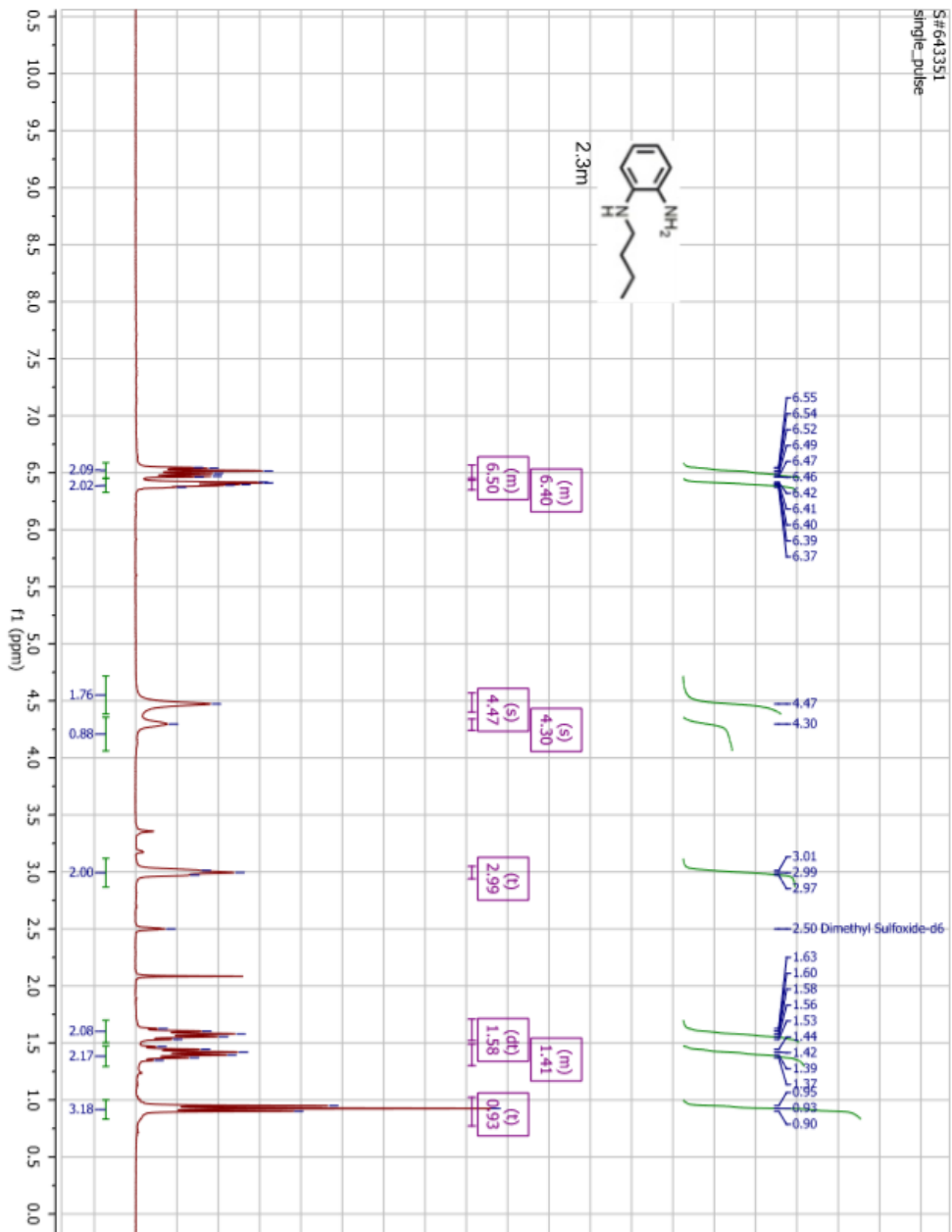
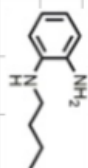
S#666286
single pulse decoupled gated NOE



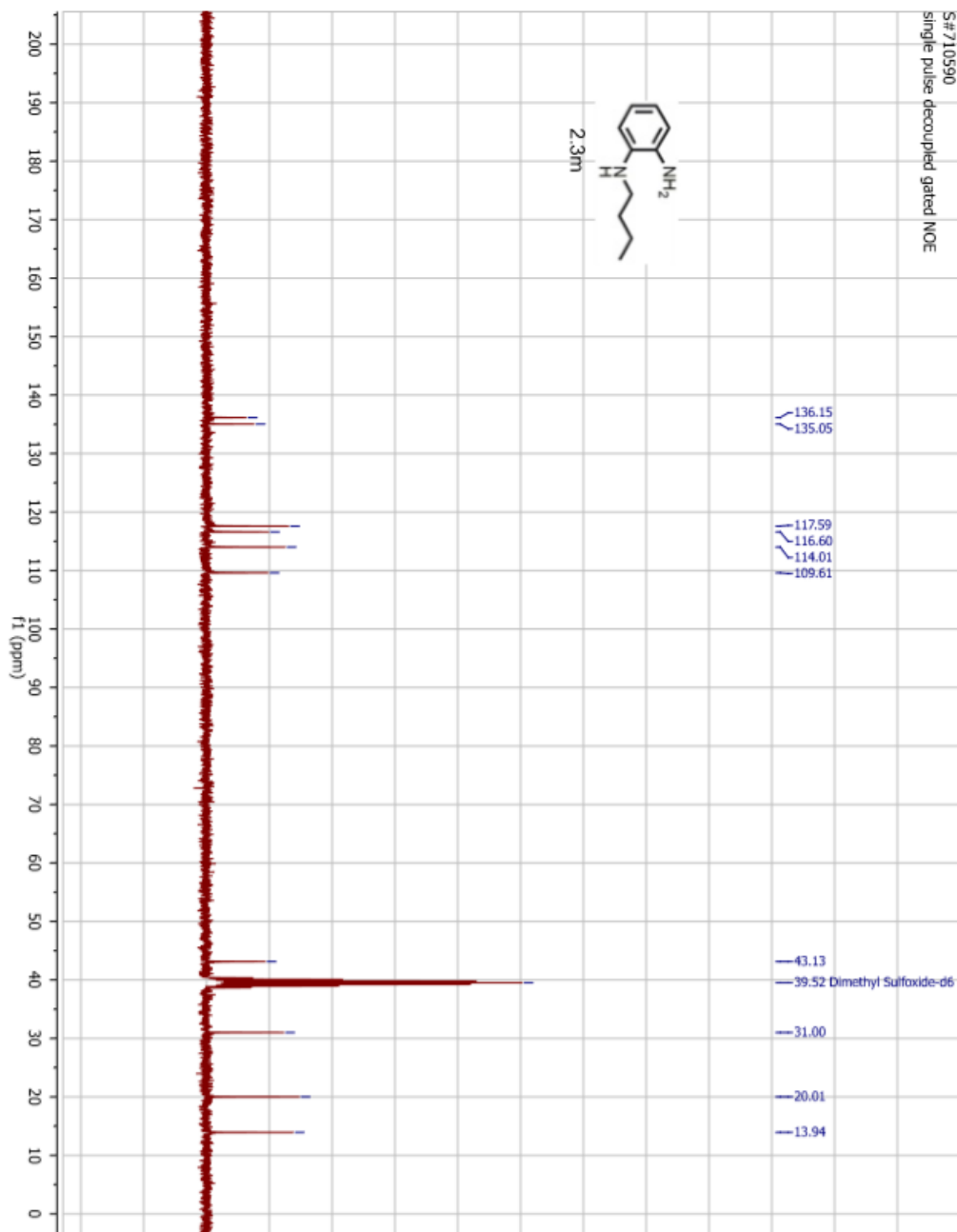
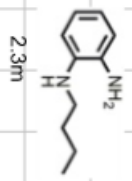


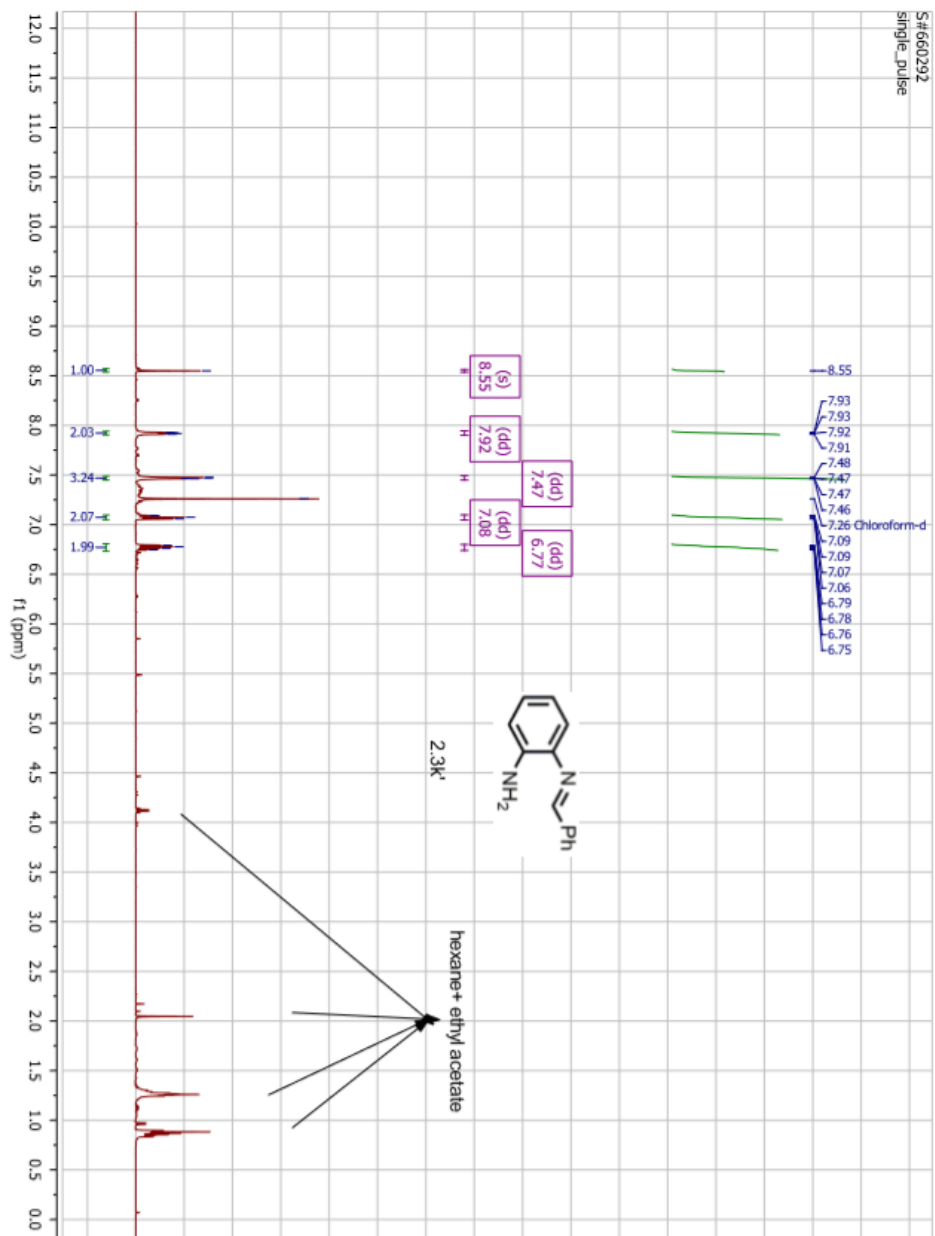


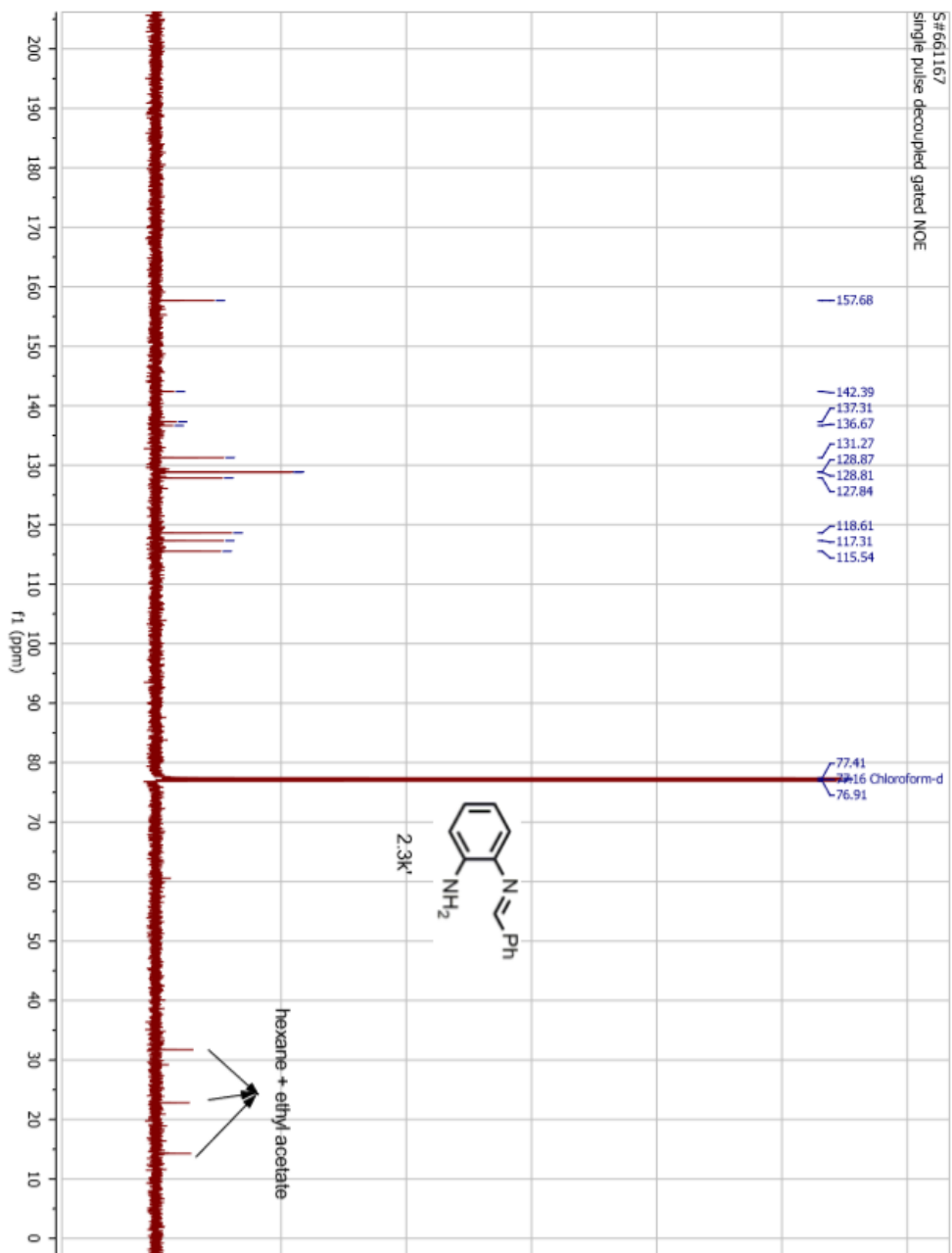
S#643351
single_pulse

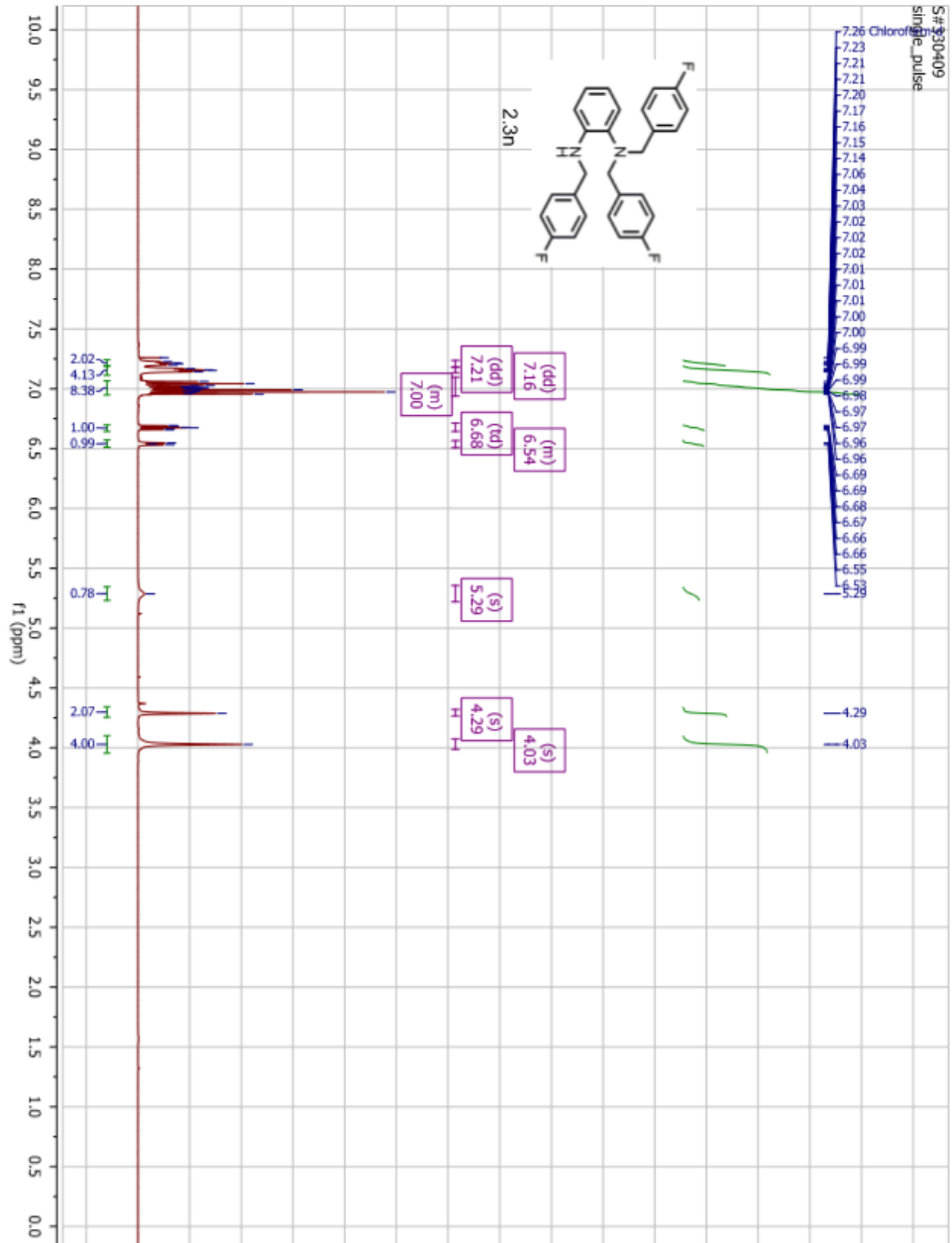


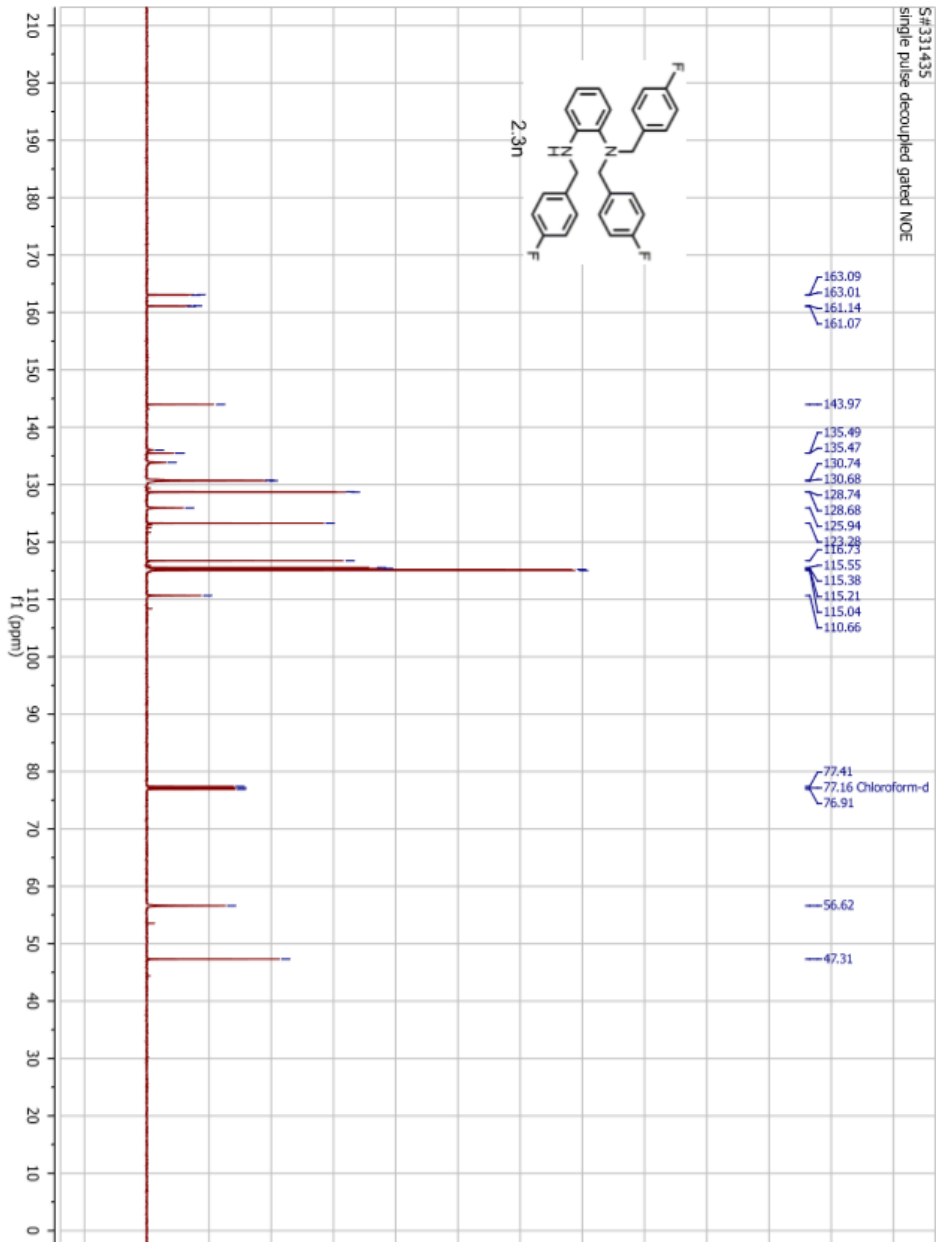
S#710590
single pulse decoupled gated NOE



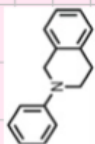




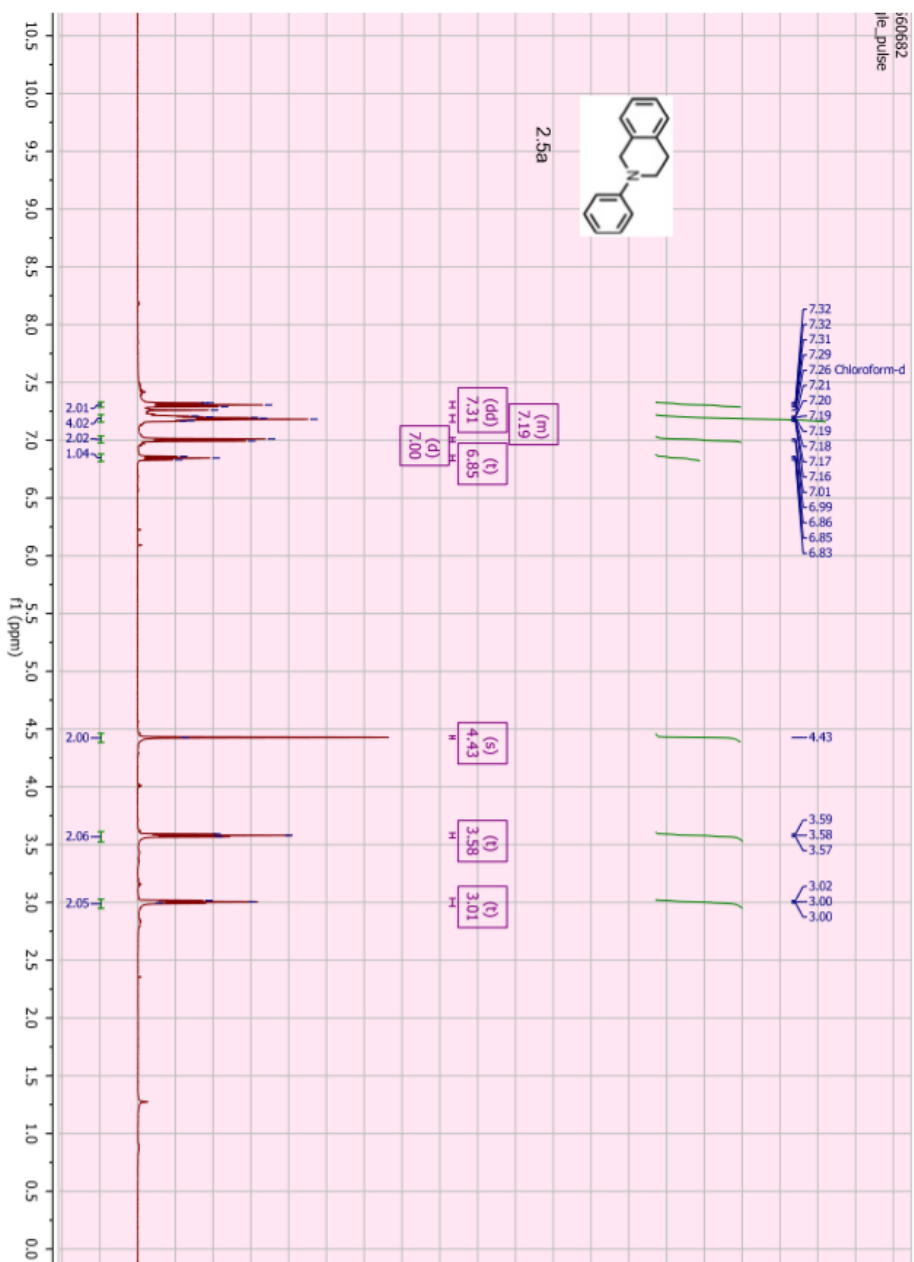


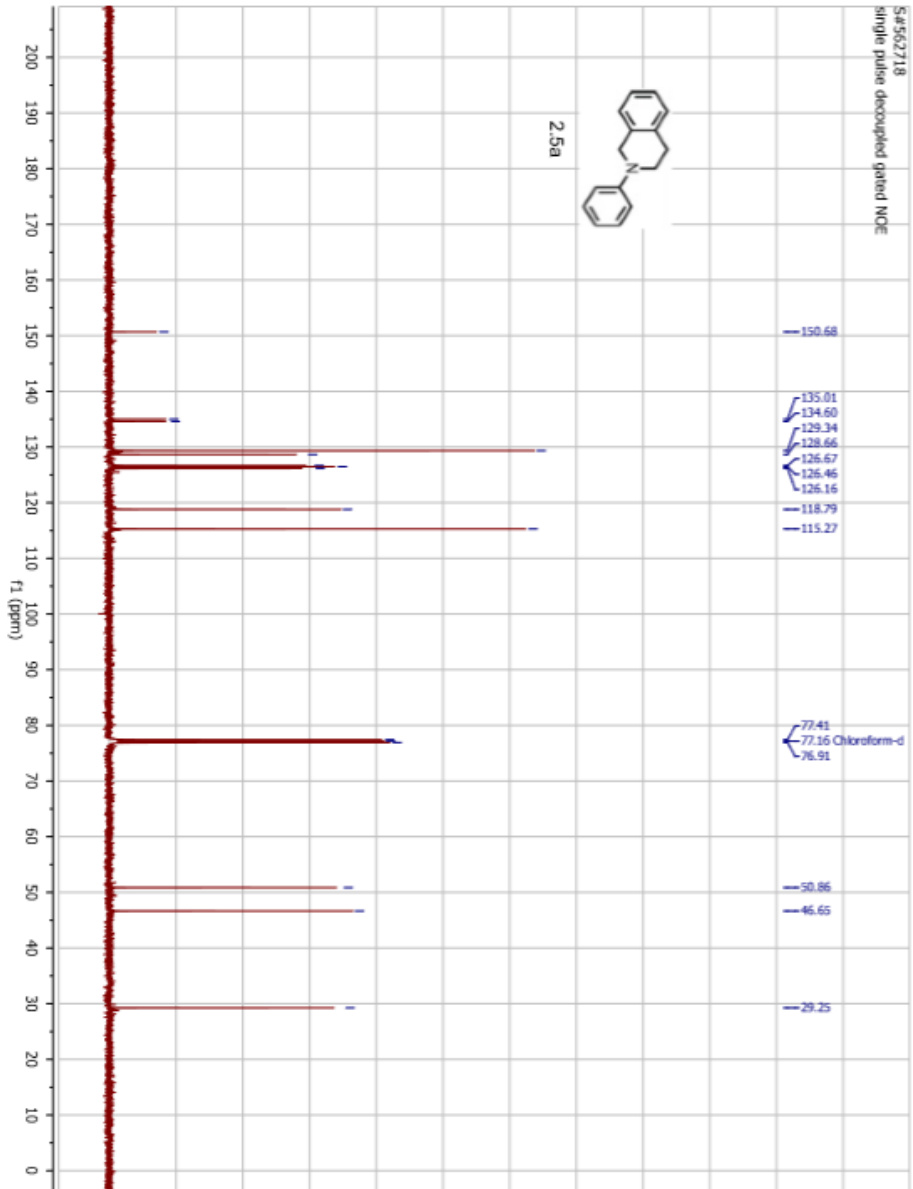


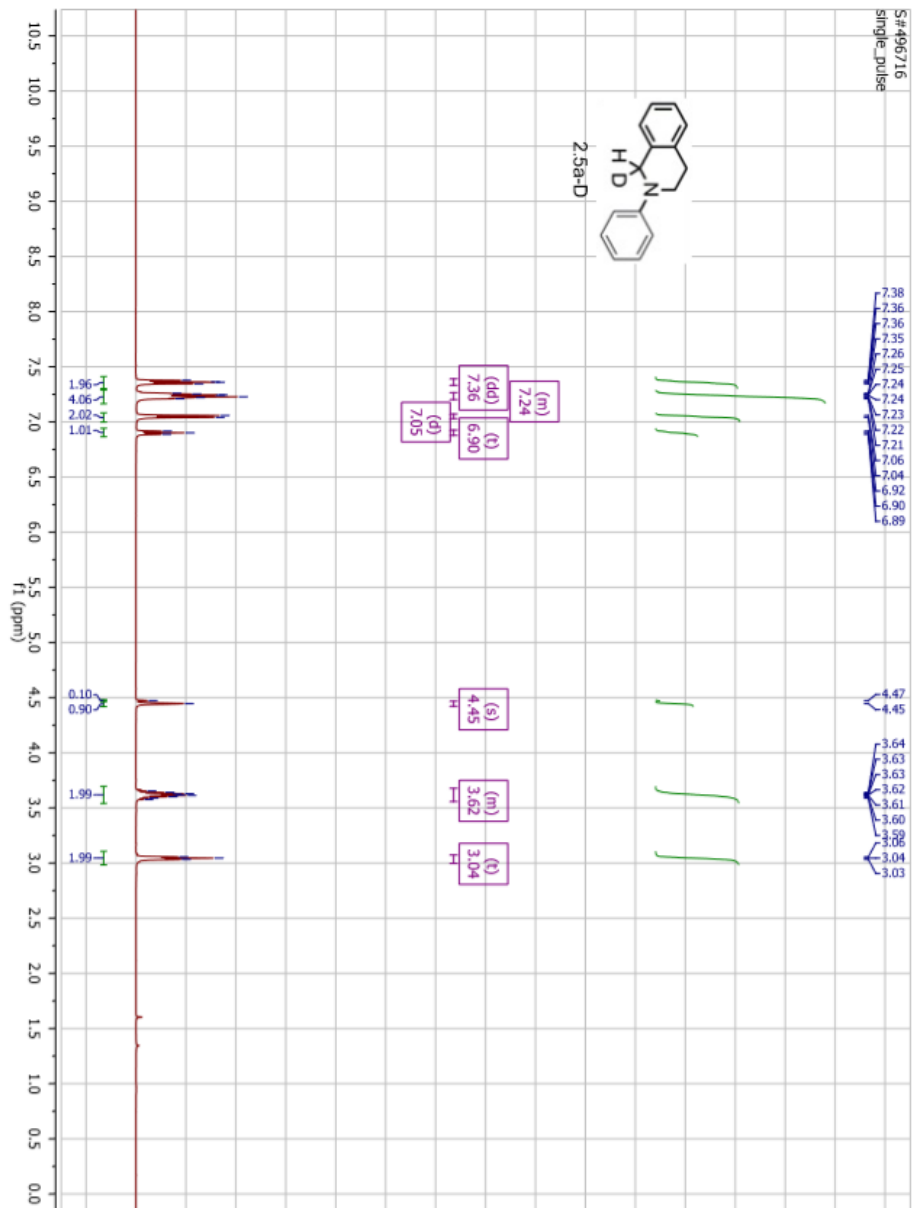
160682
1H pulse



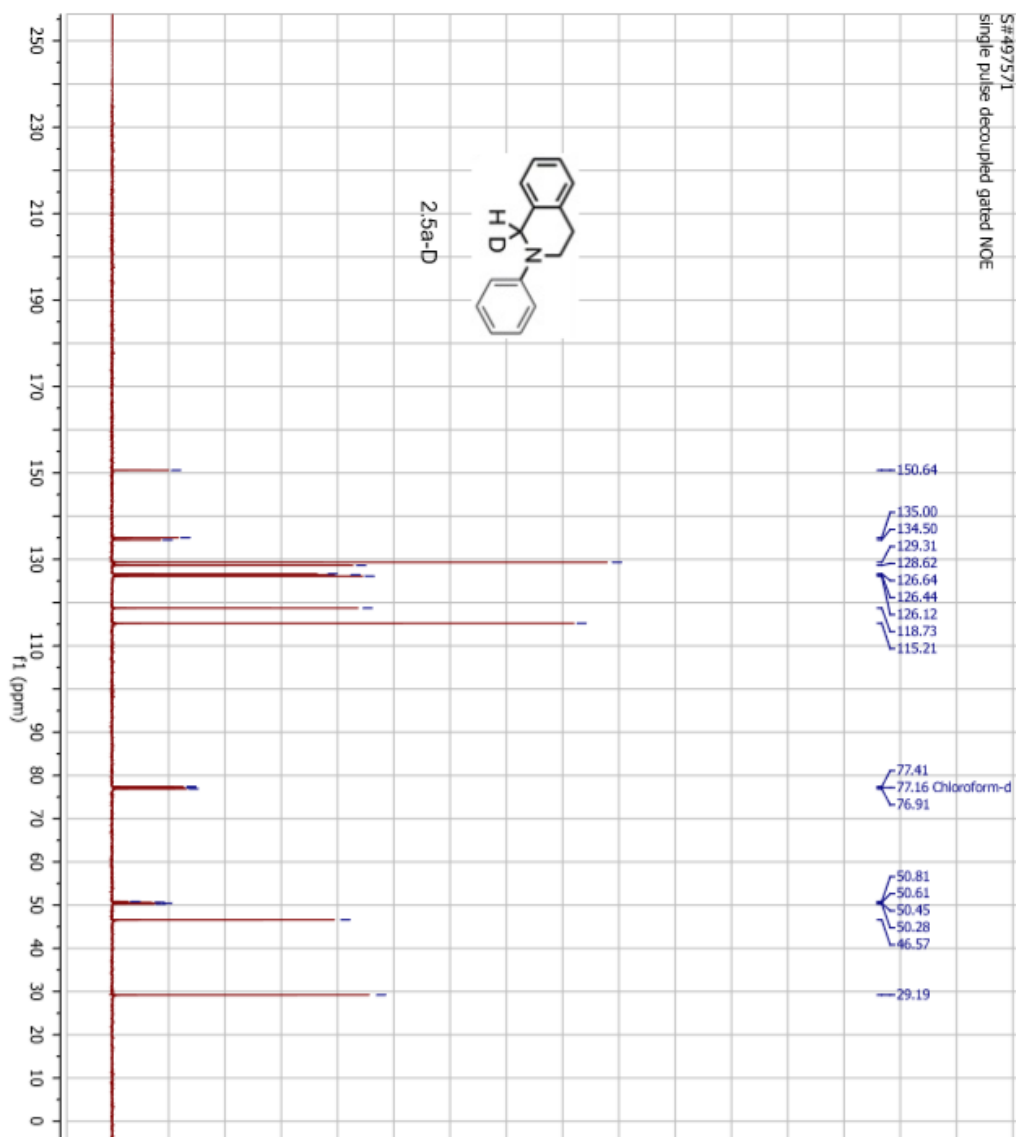
2.5a

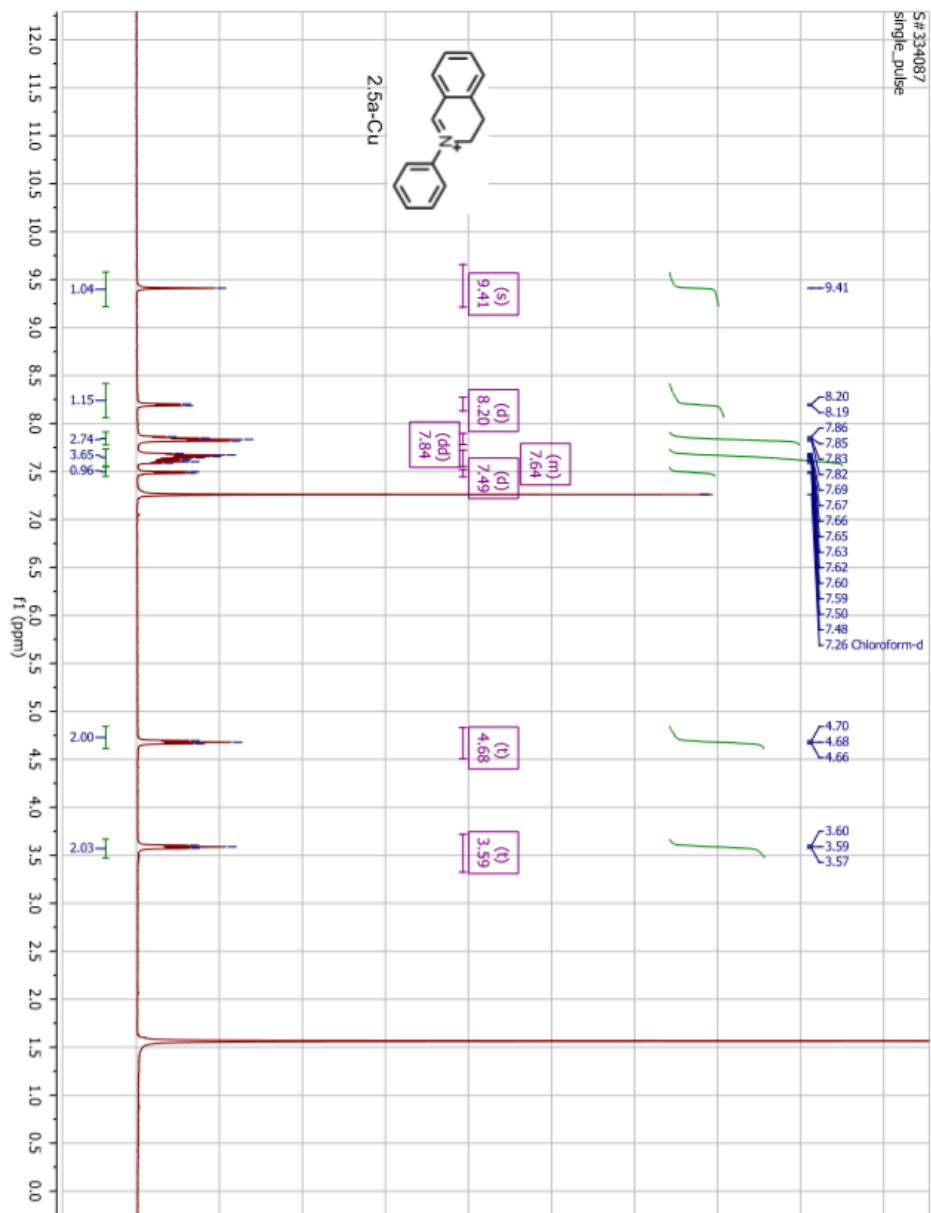


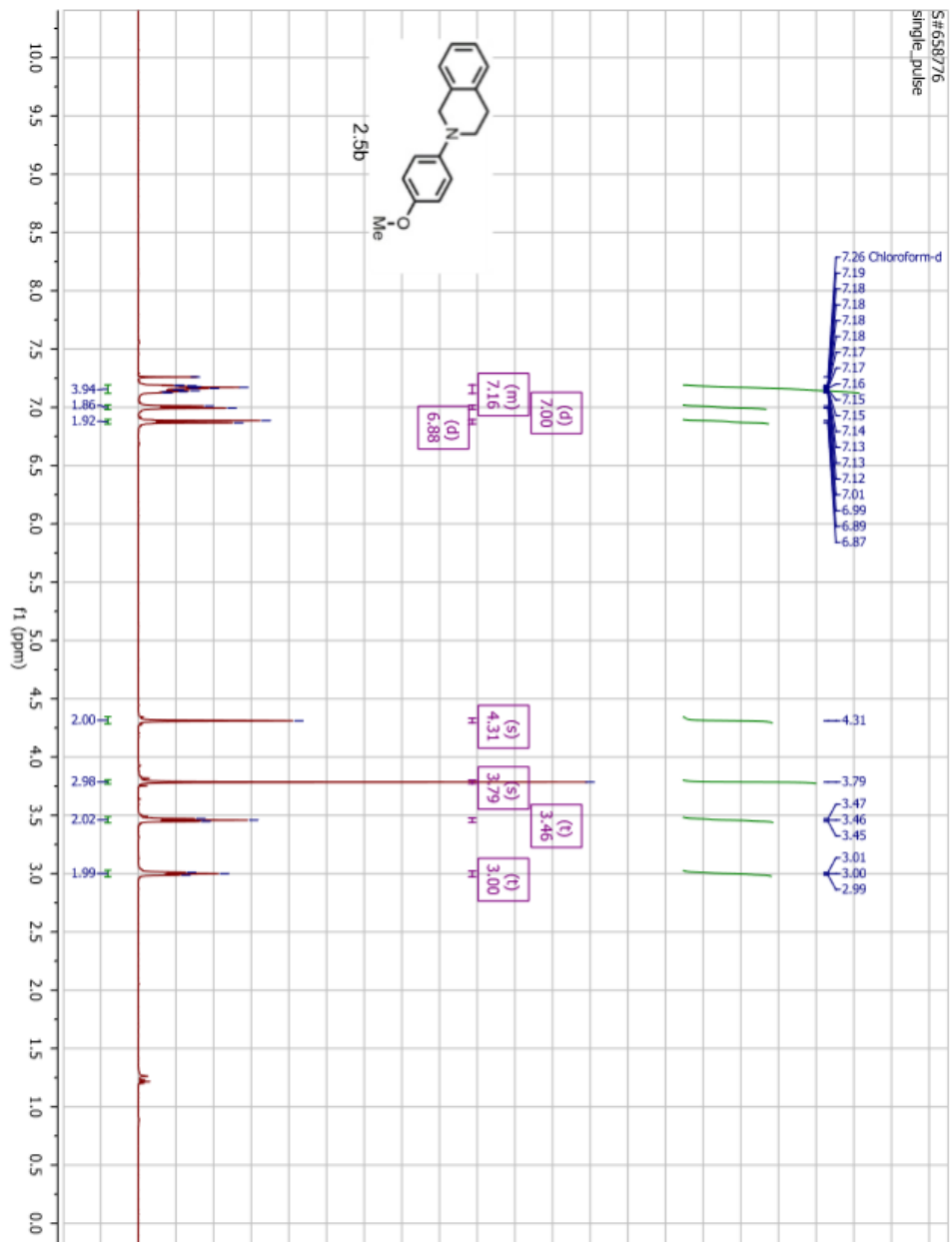


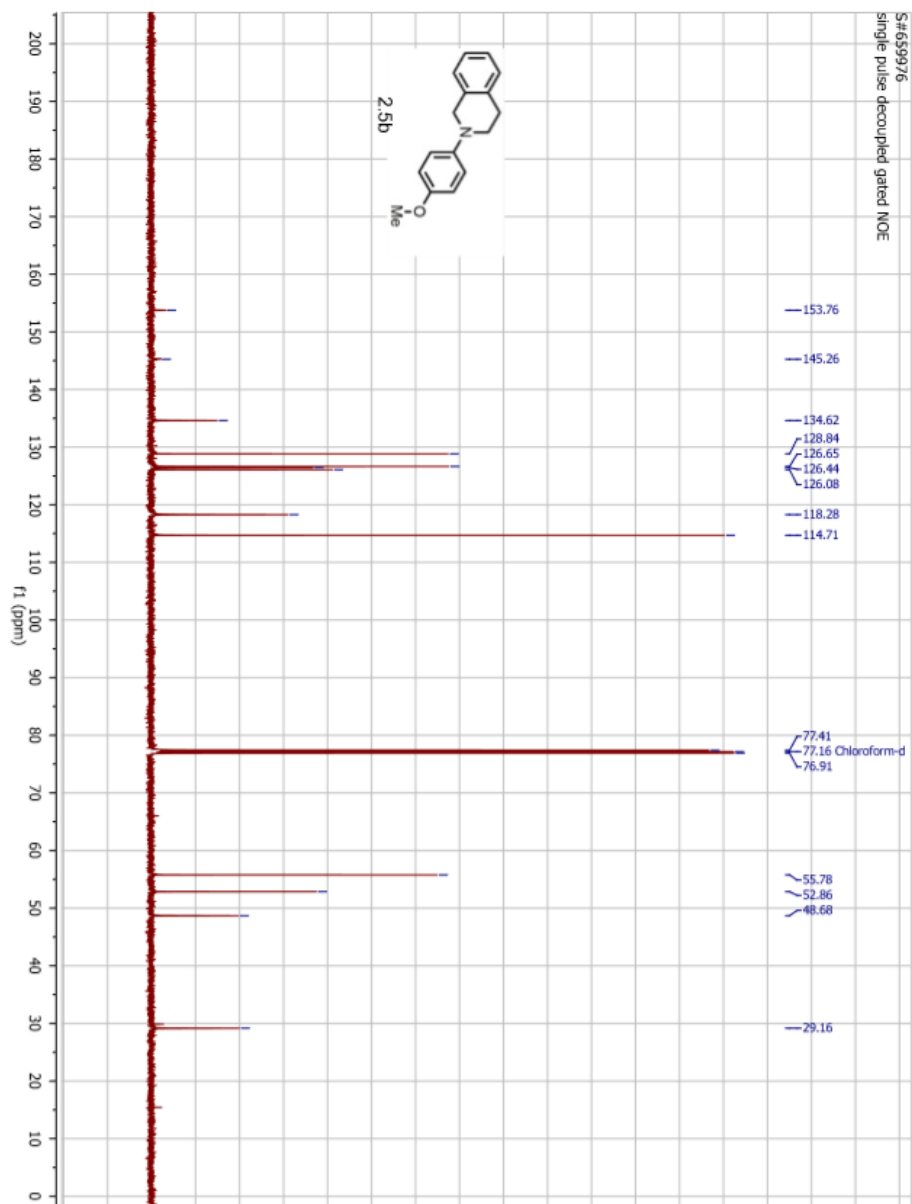


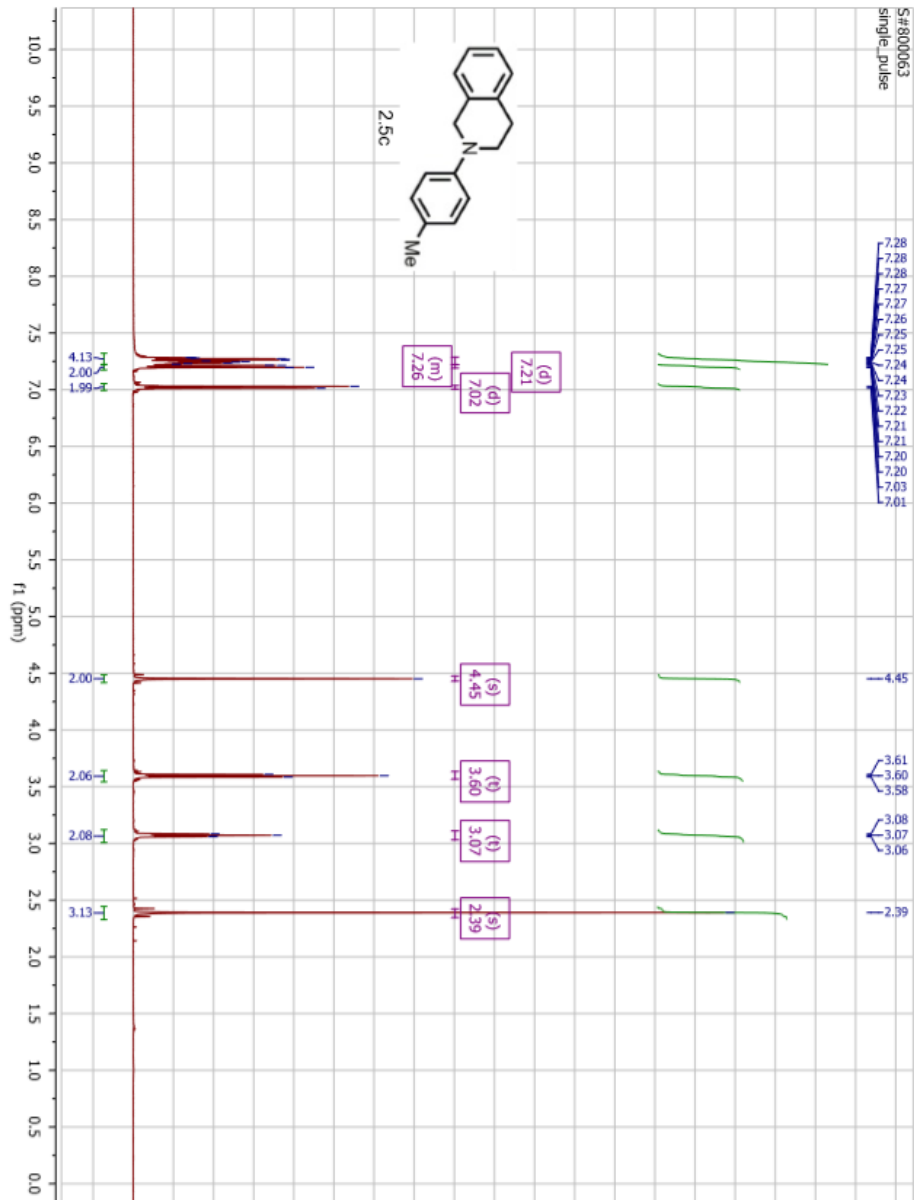
S#497571
single pulse decoupled gated NOE



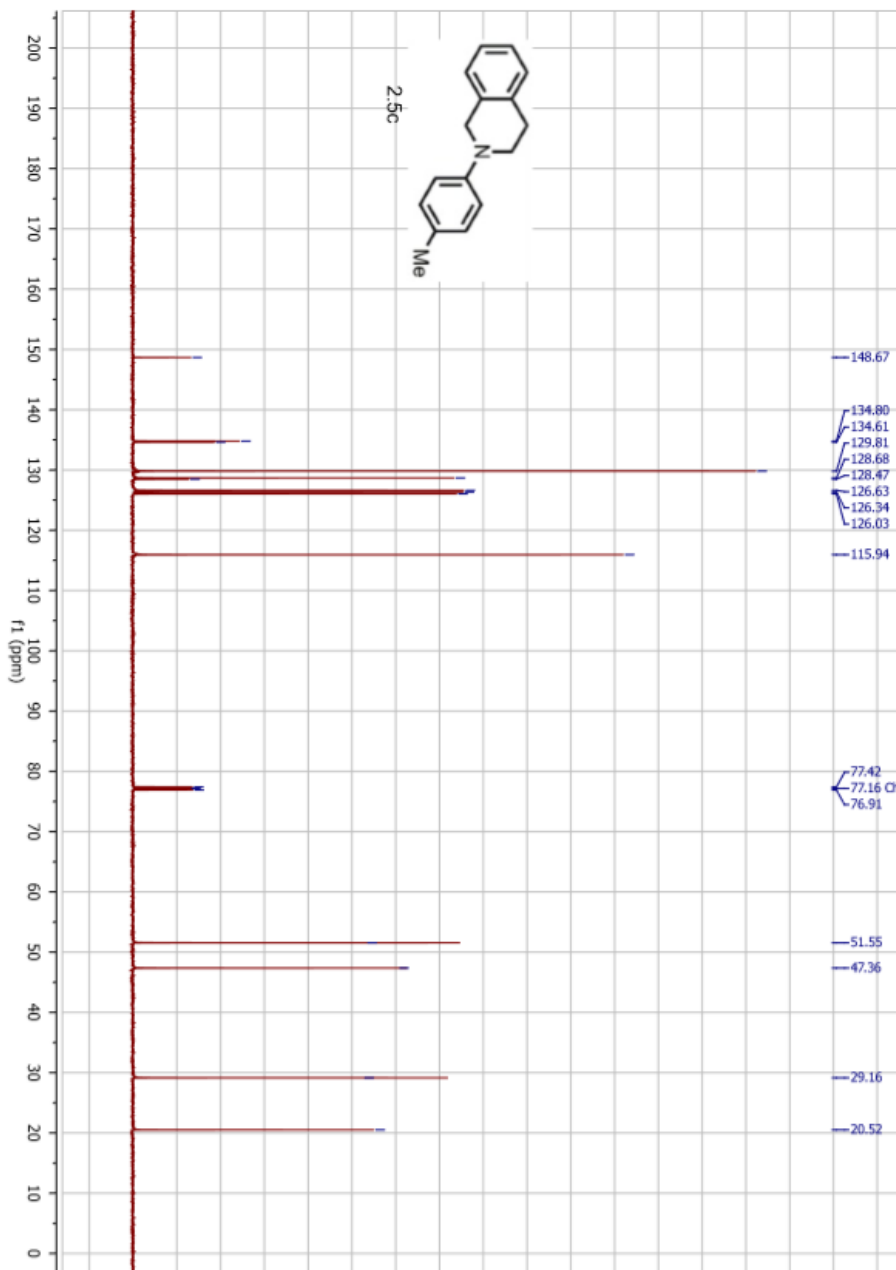
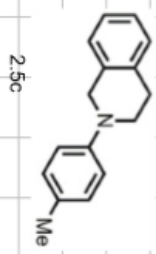


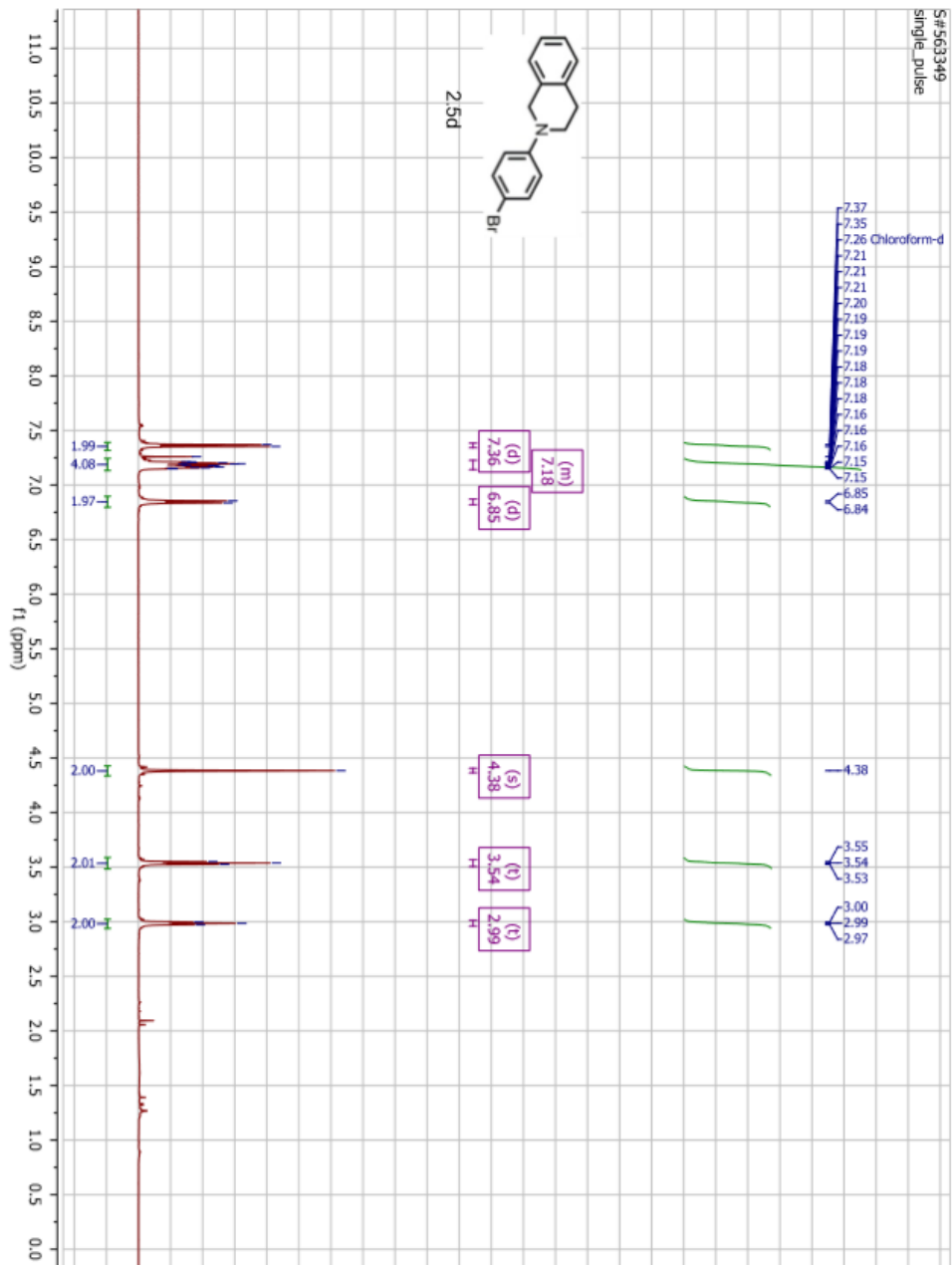


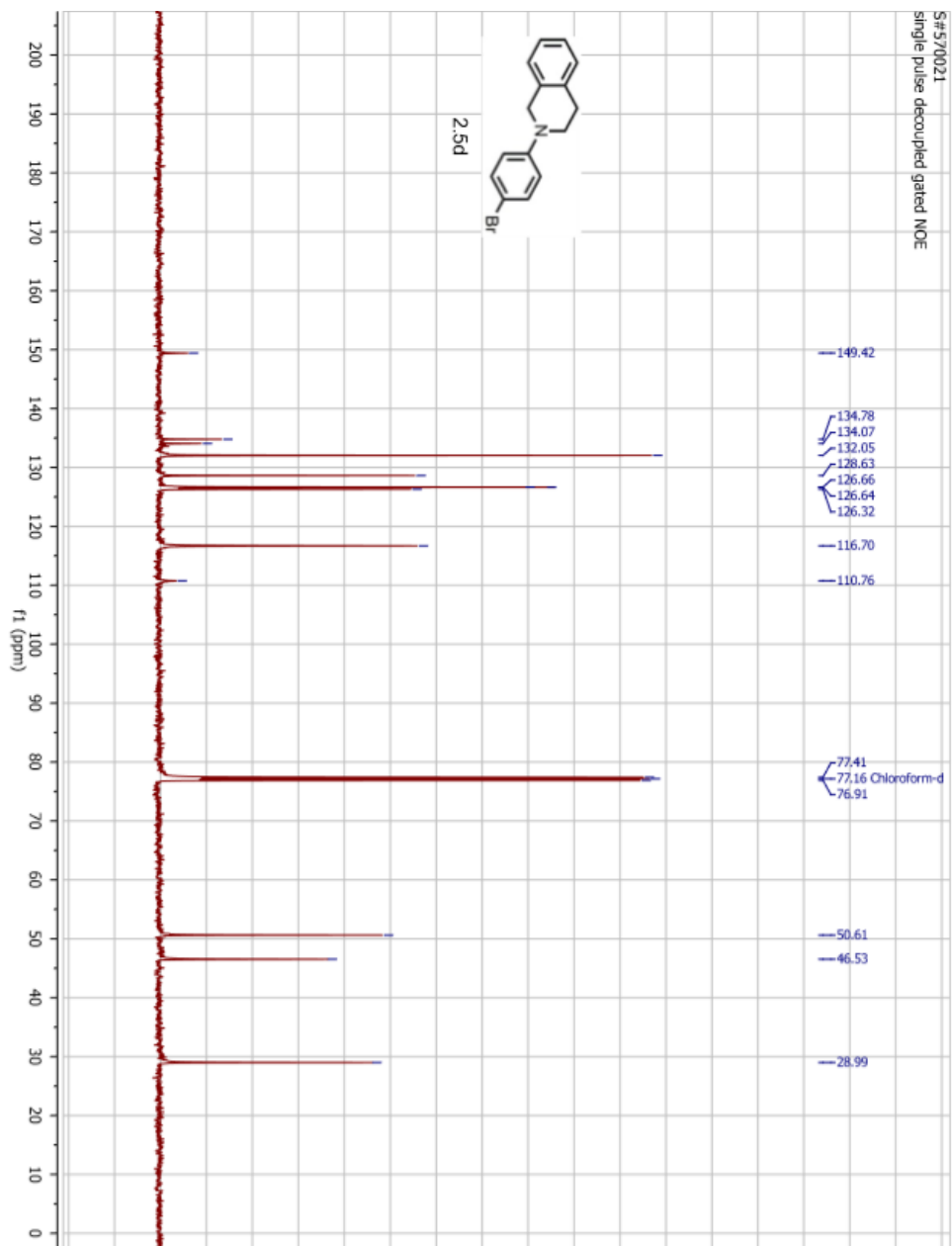


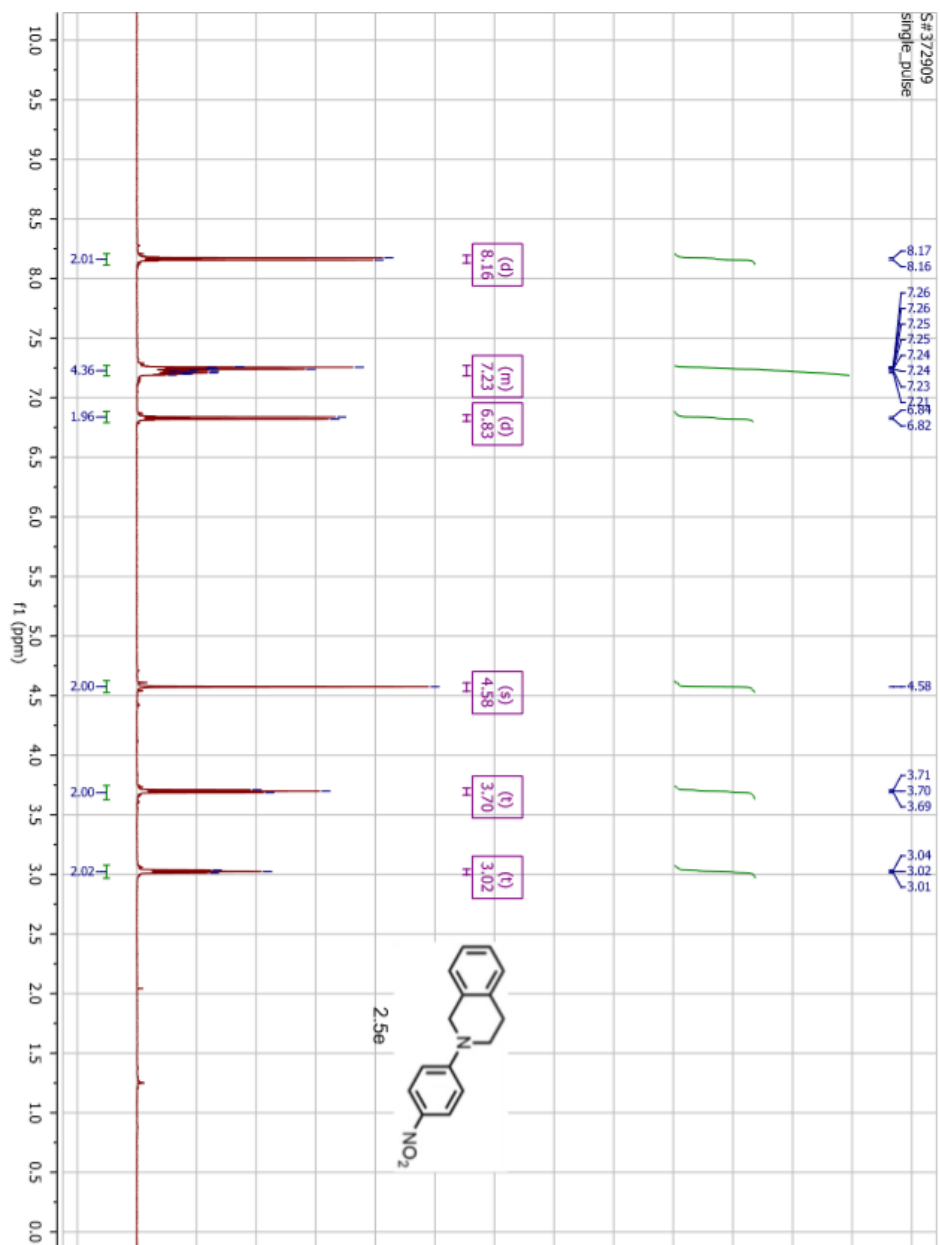


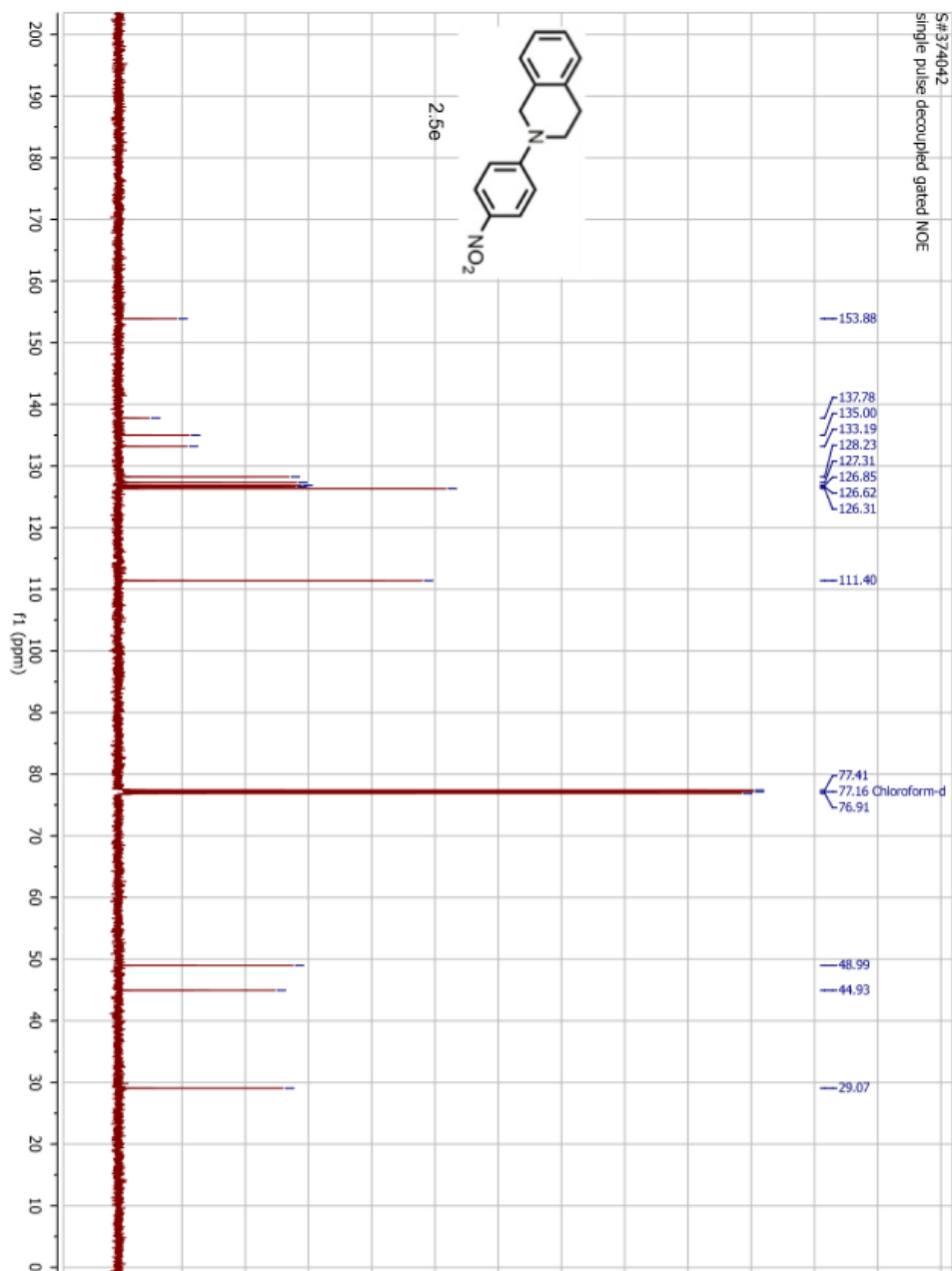
S#801531
single pulse decoupled gated NOE

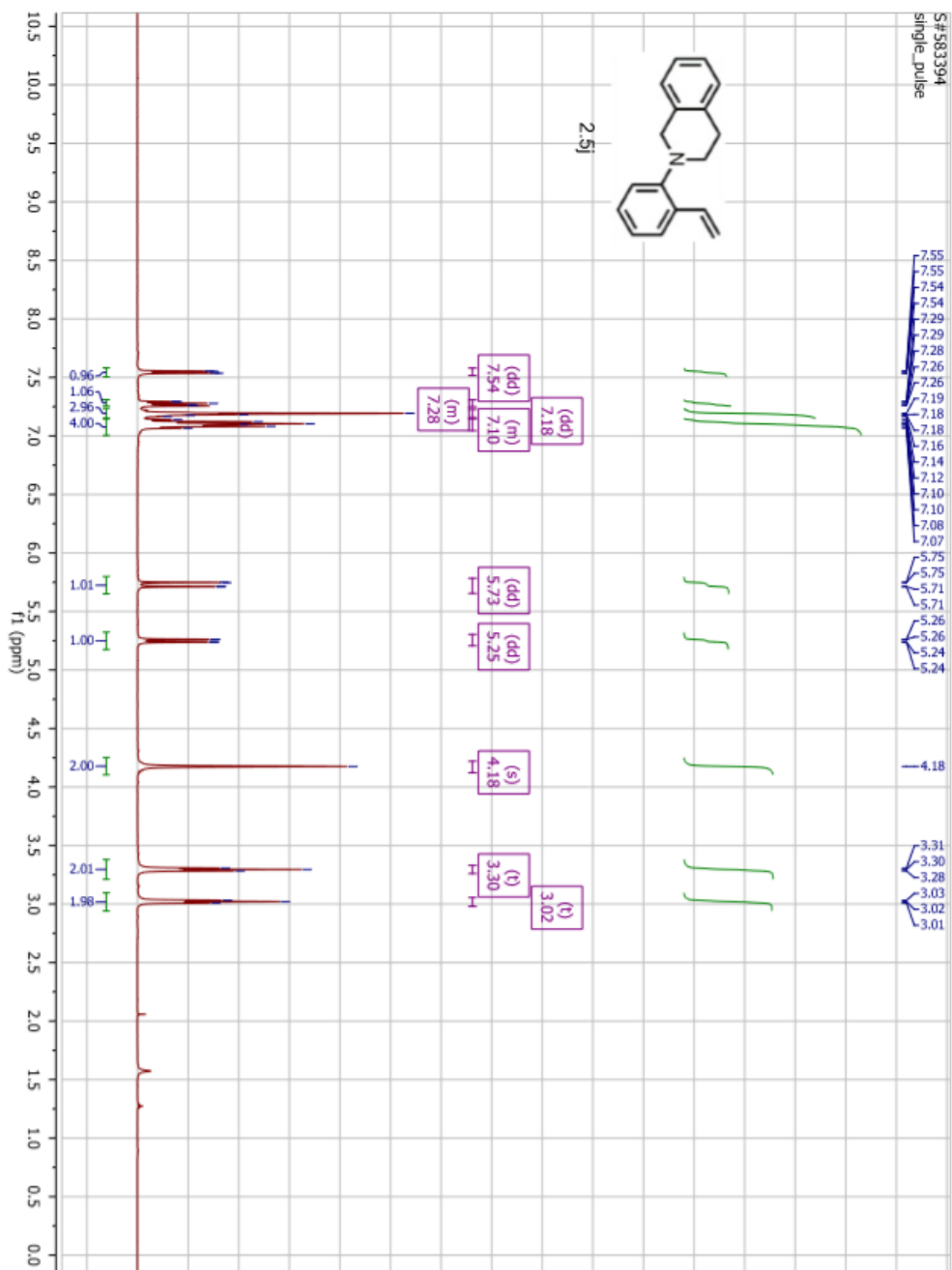


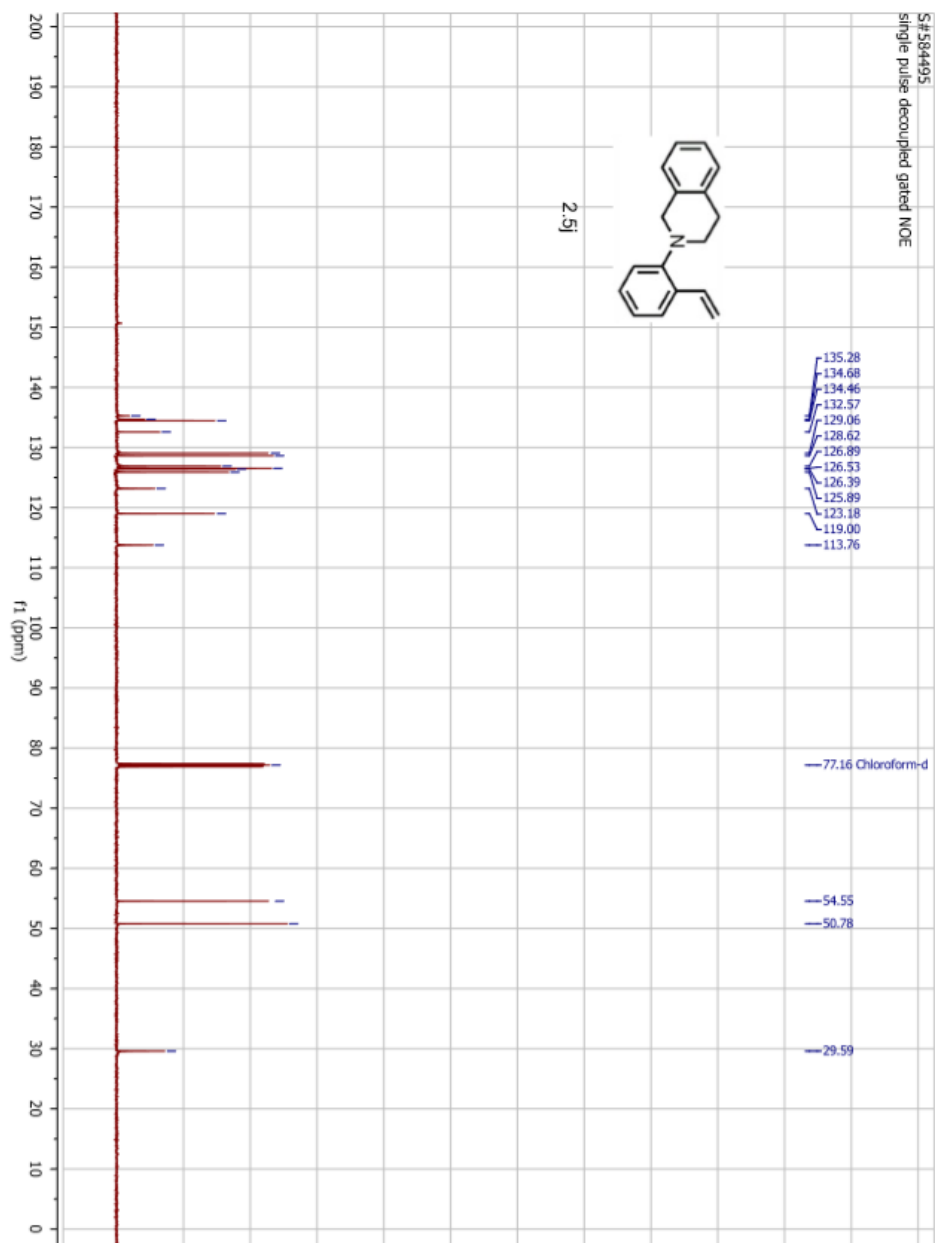


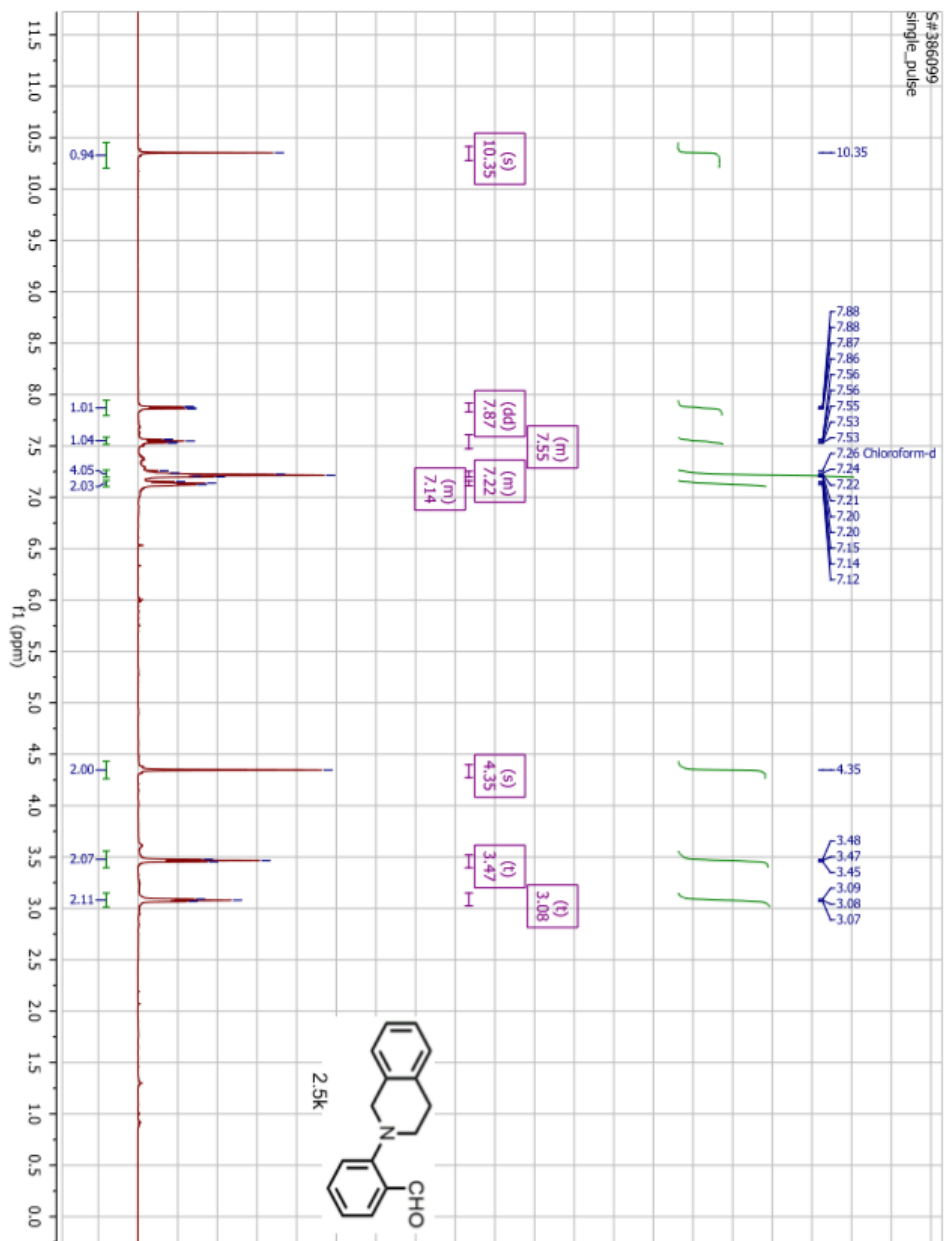


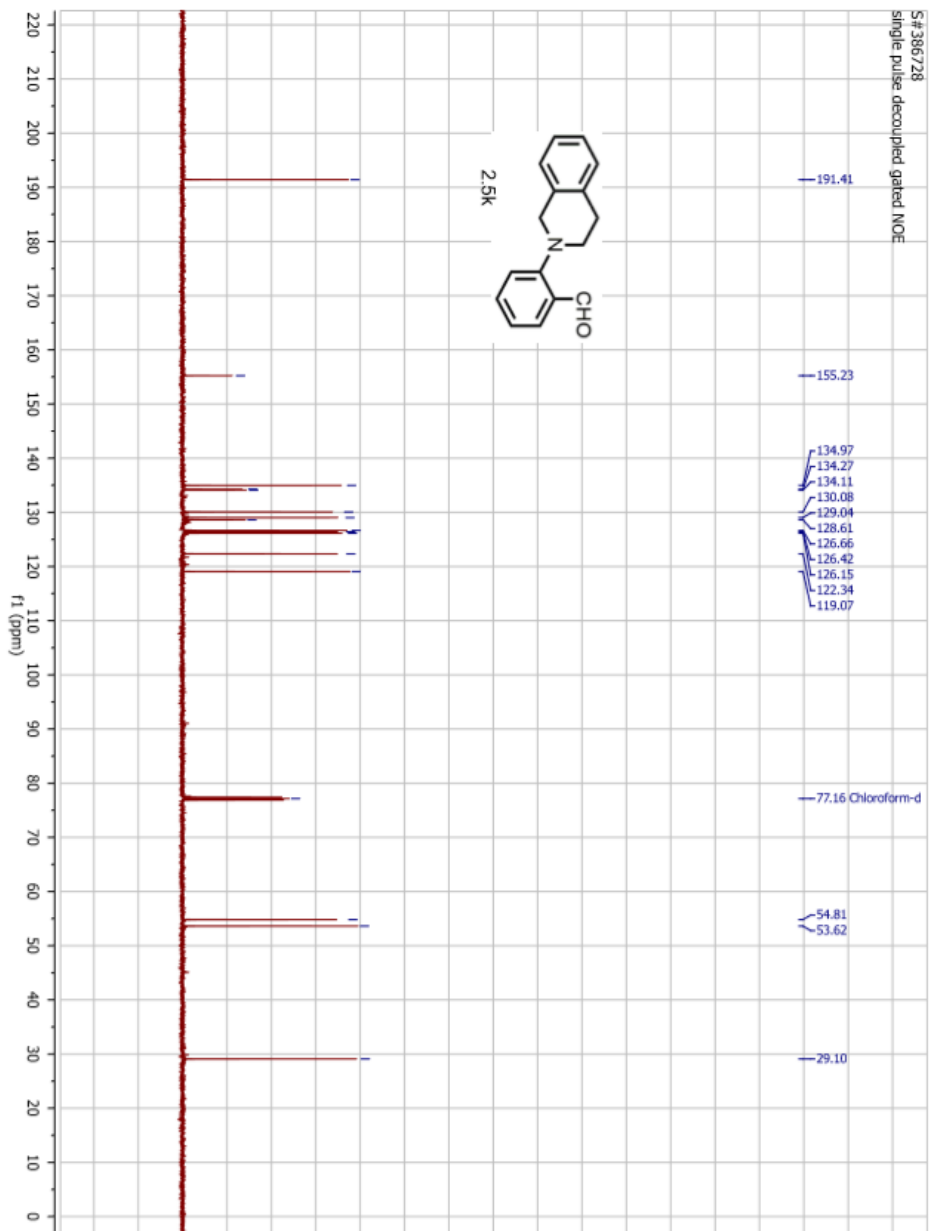


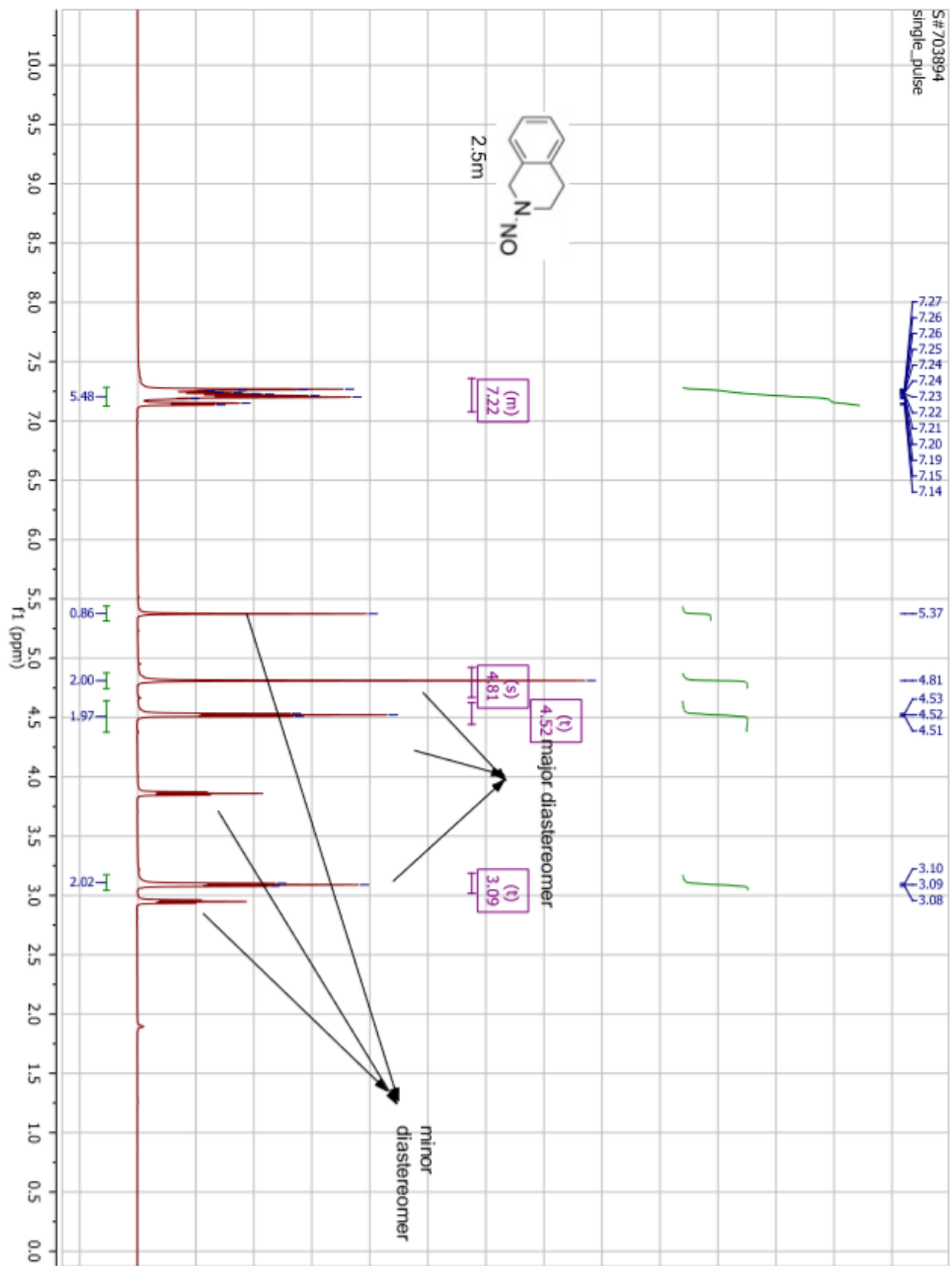




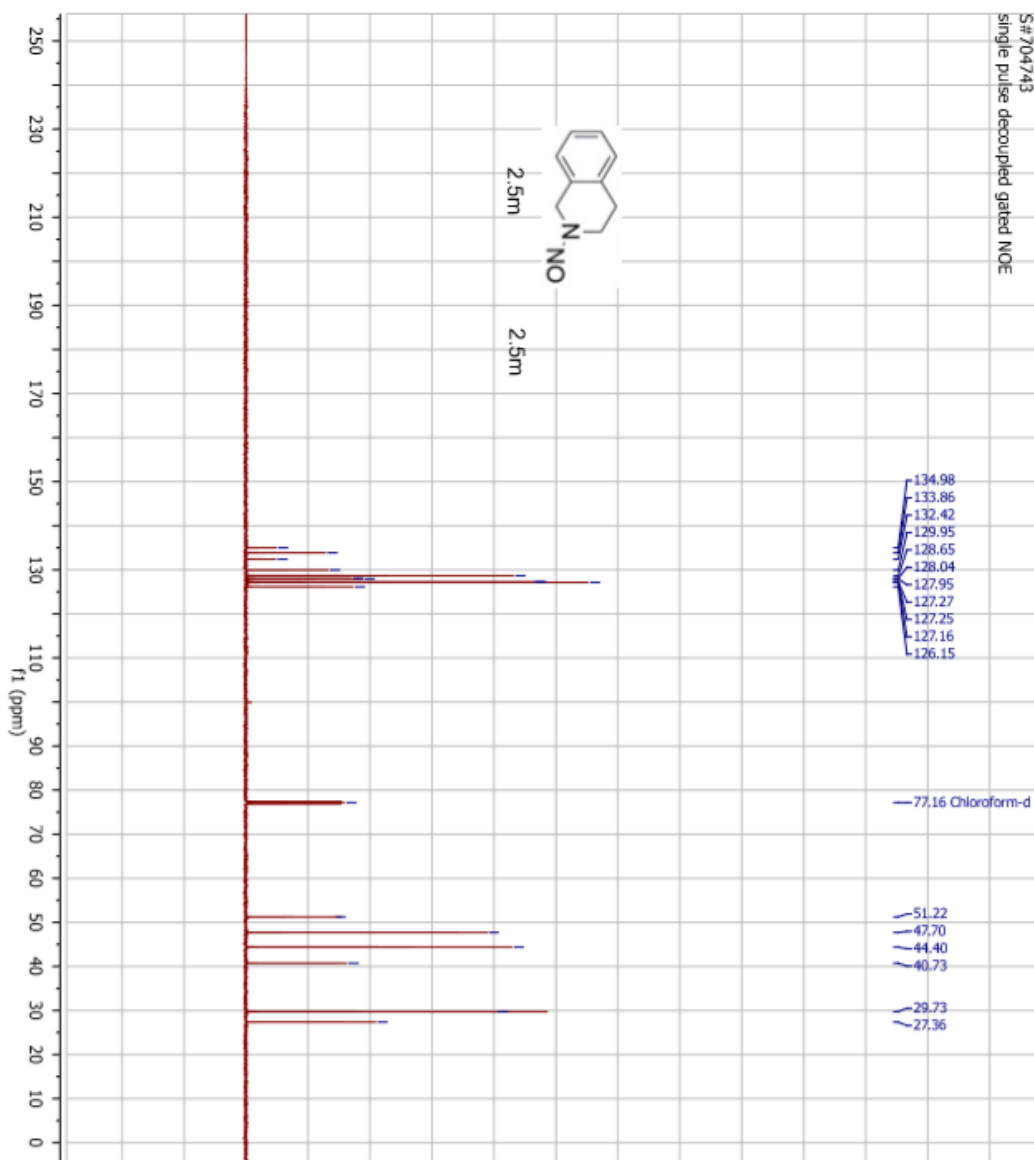


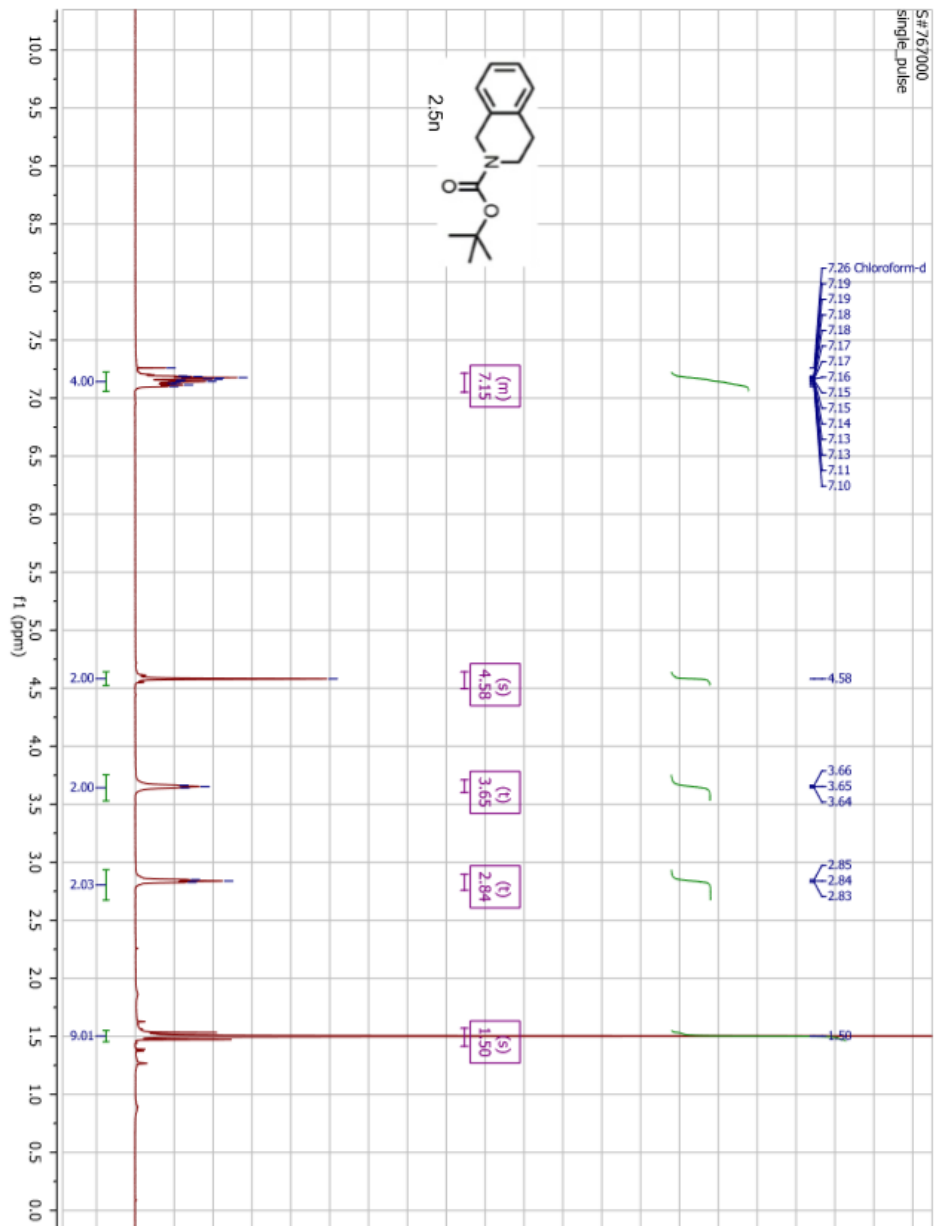


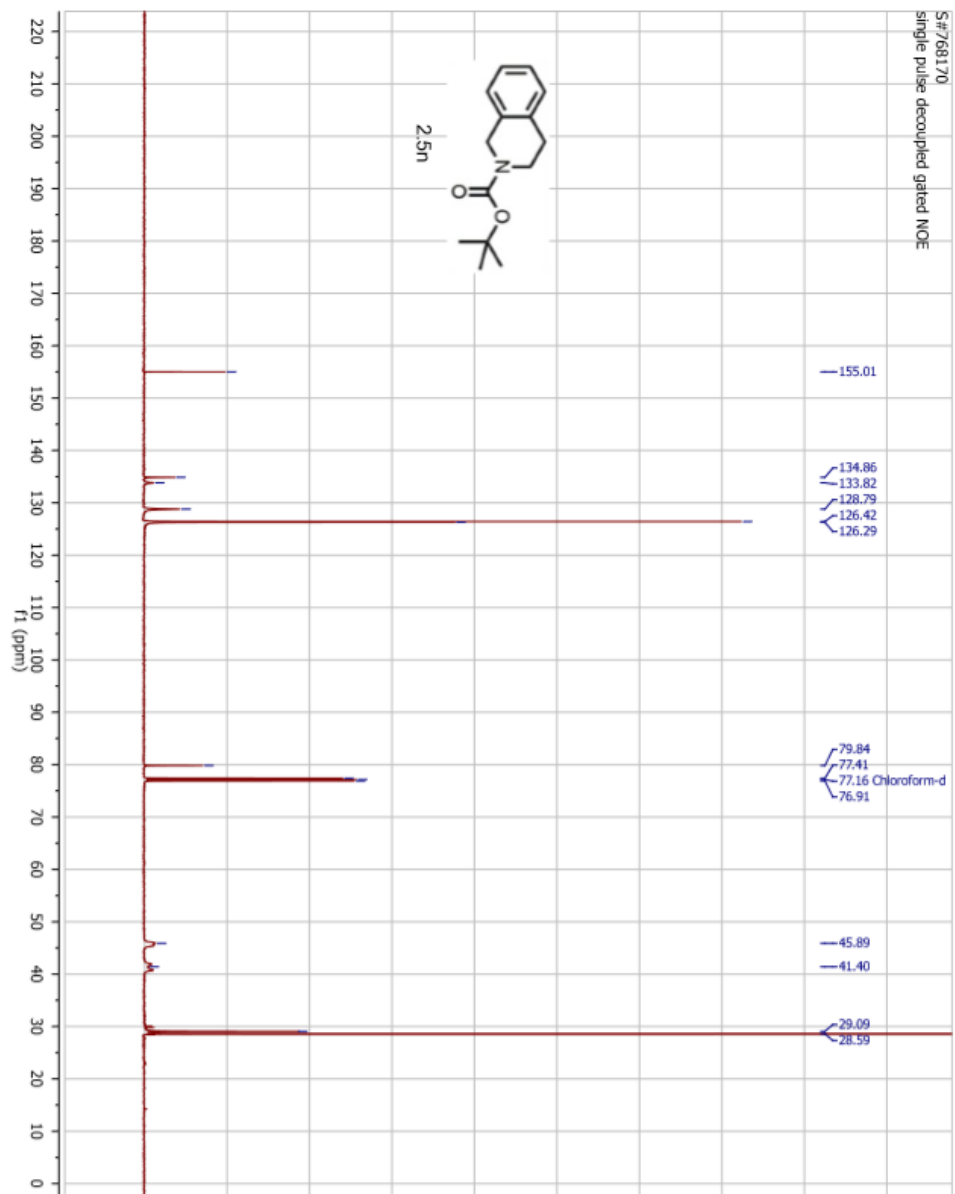


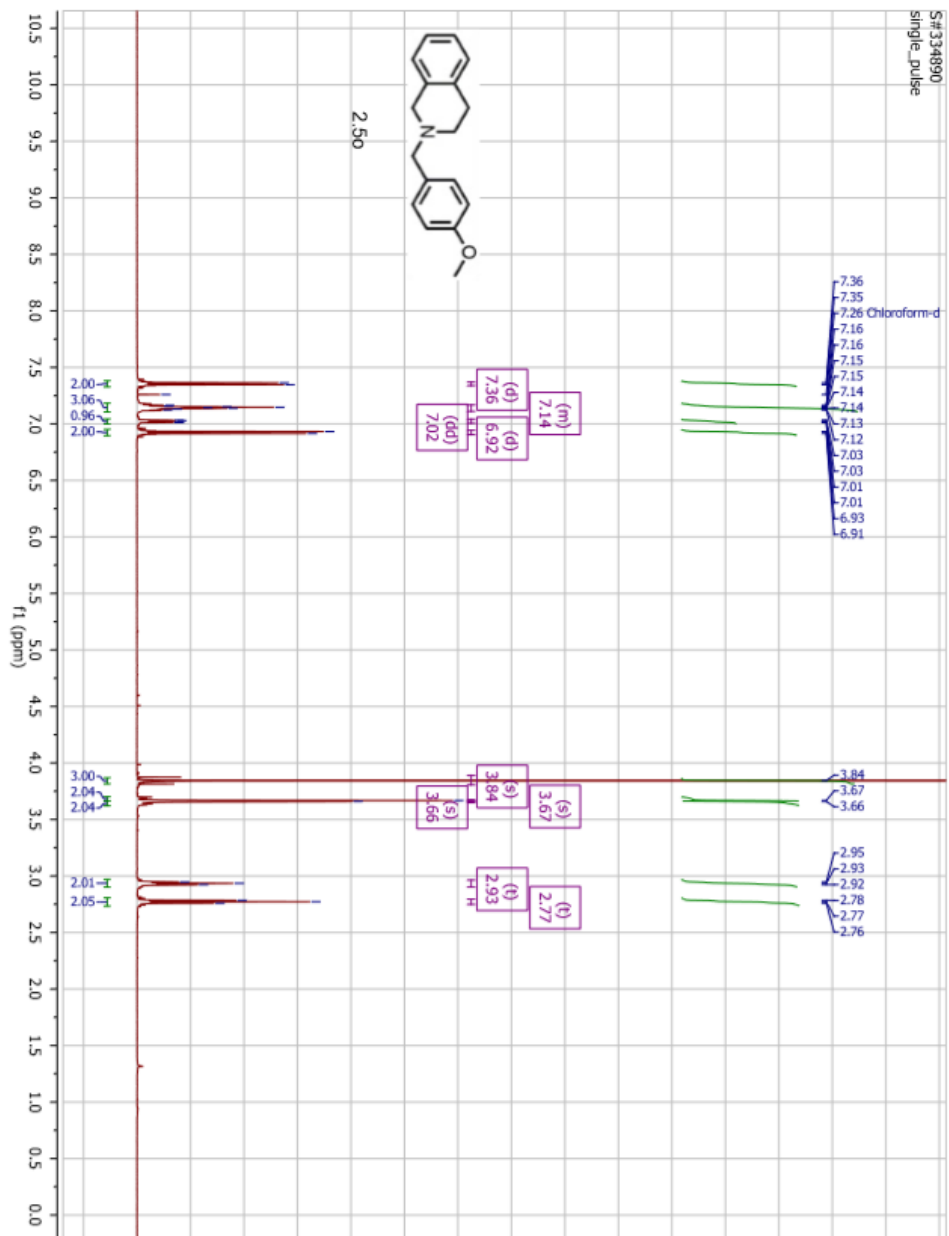


S#704743
single pulse decoupled gated NOE

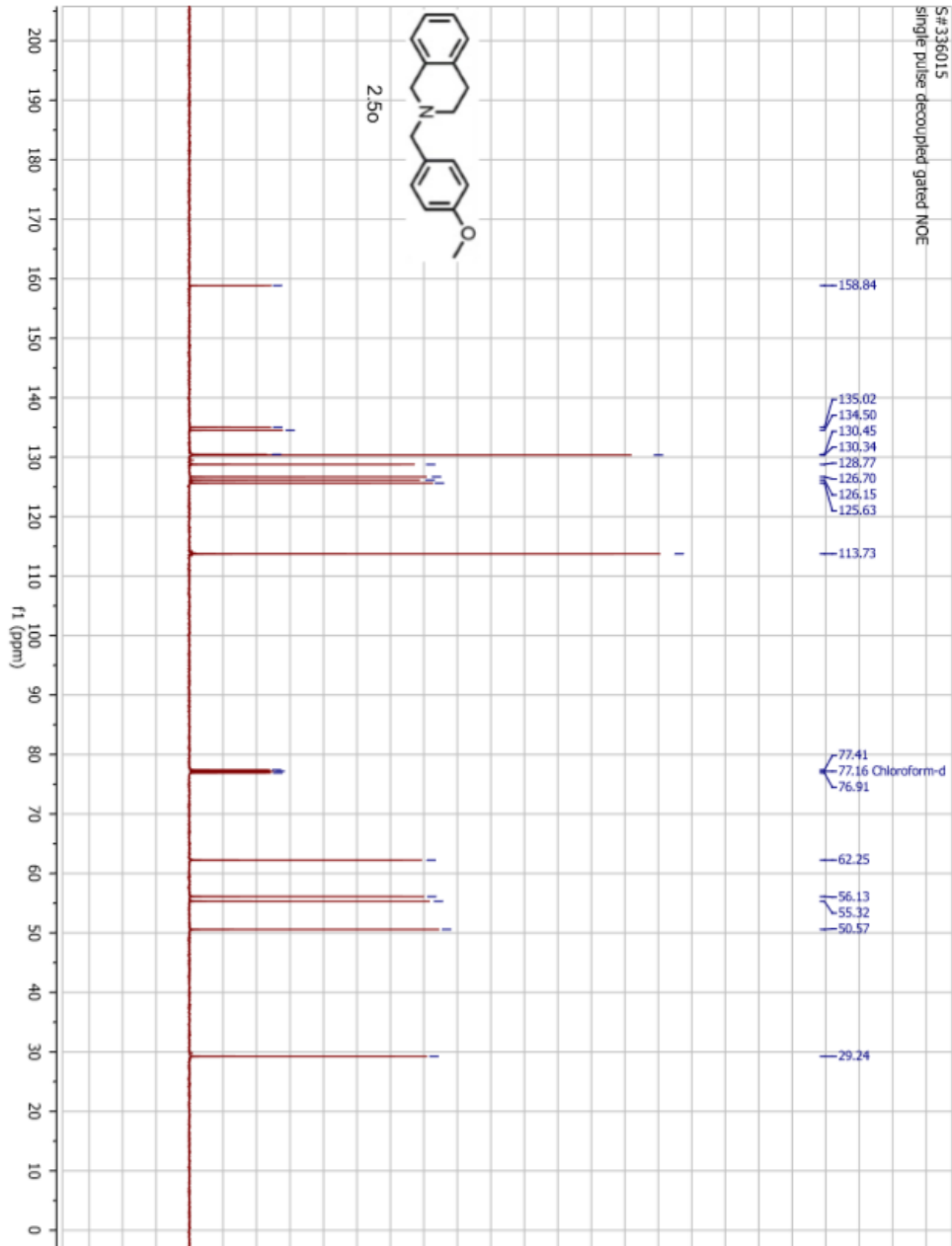
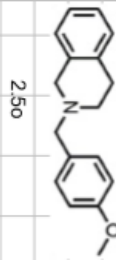


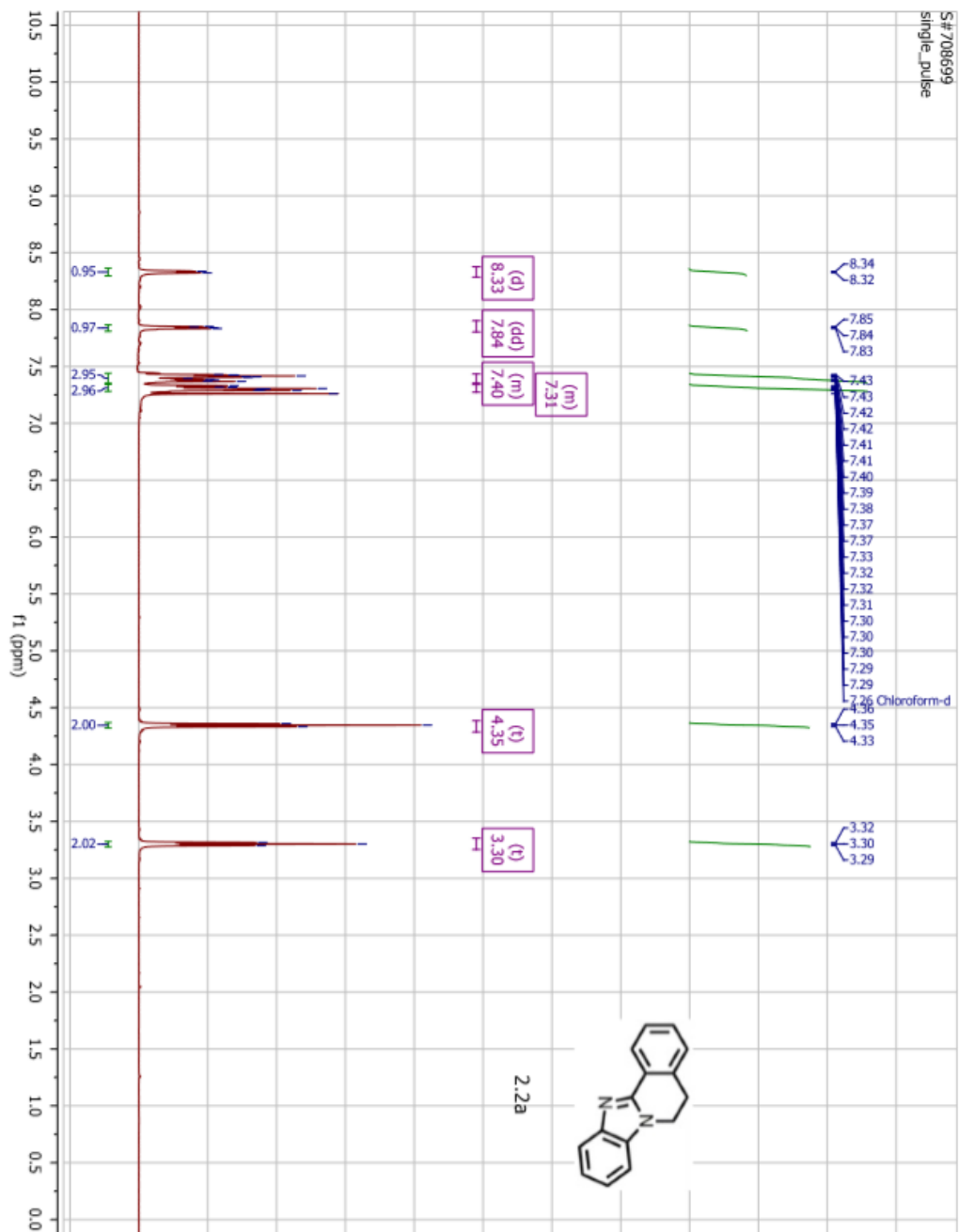




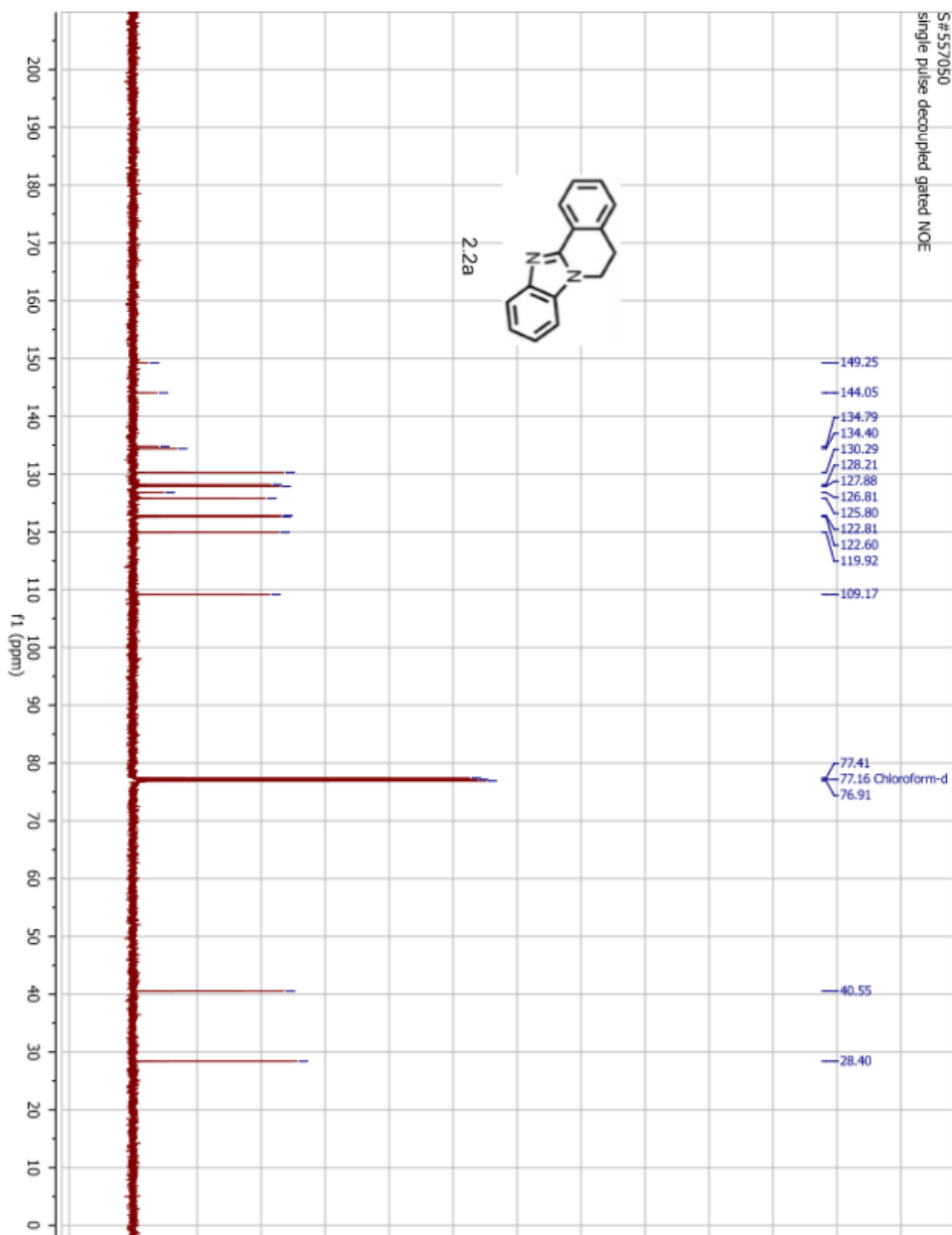


S# 336015
single pulse decoupled gated NOE

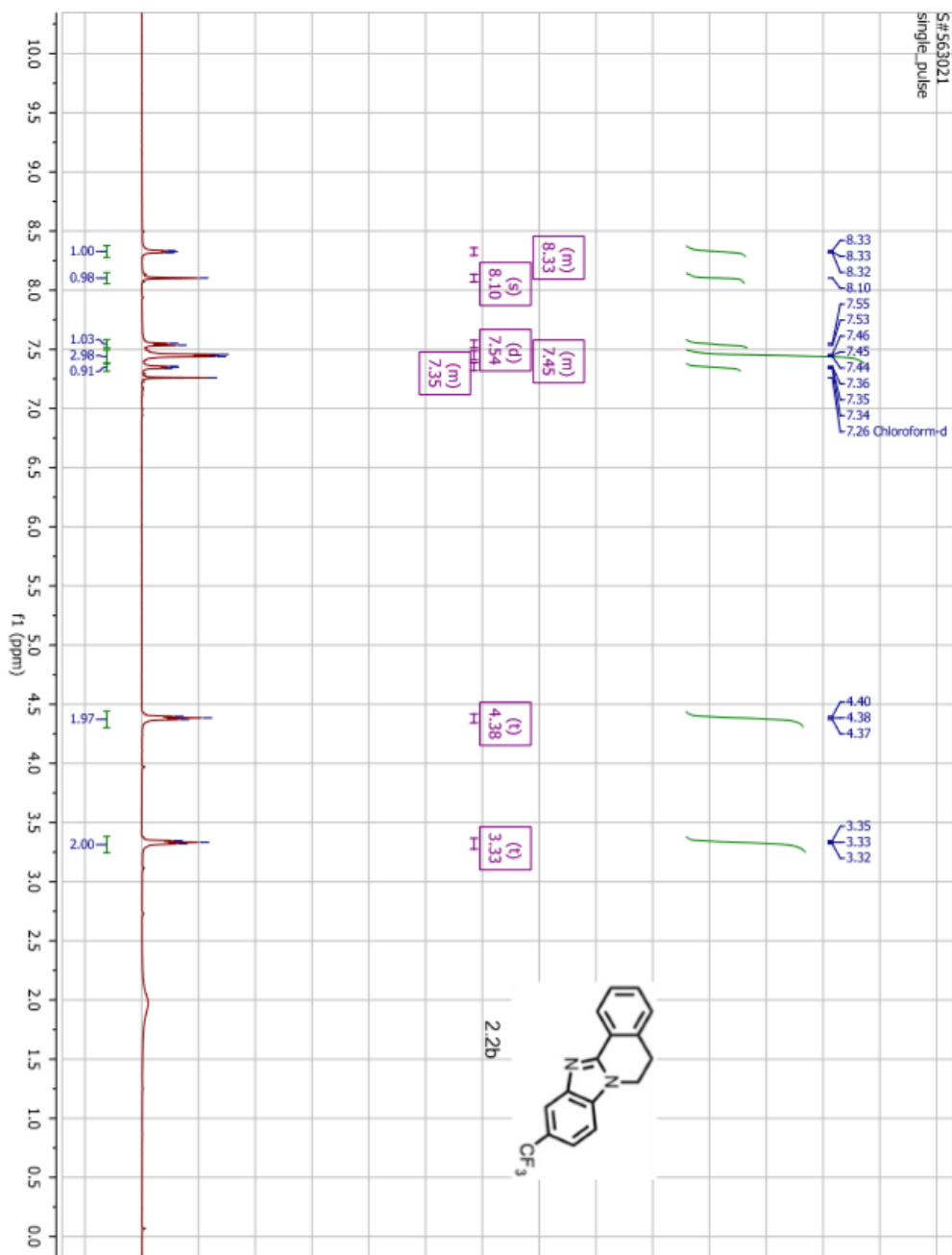


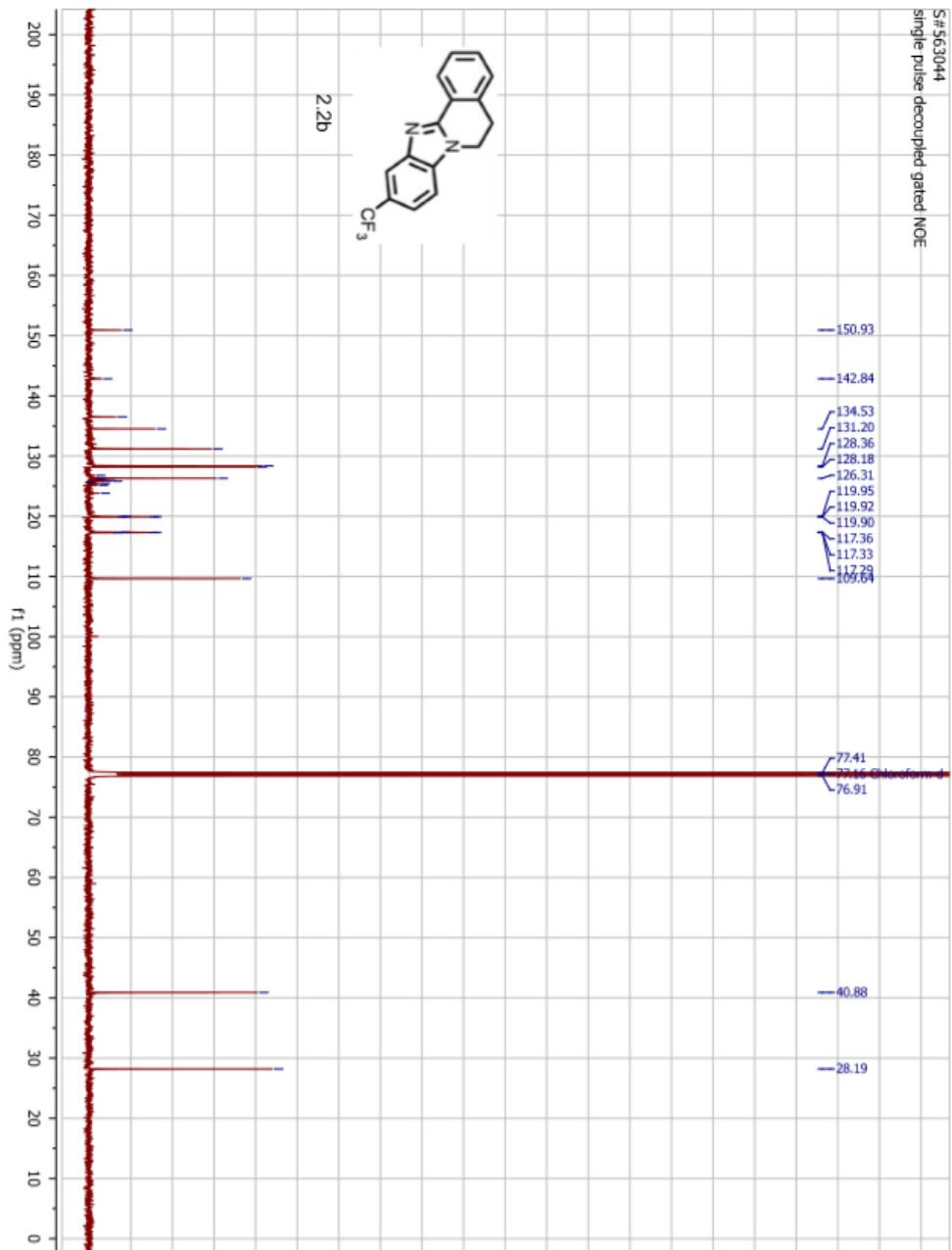


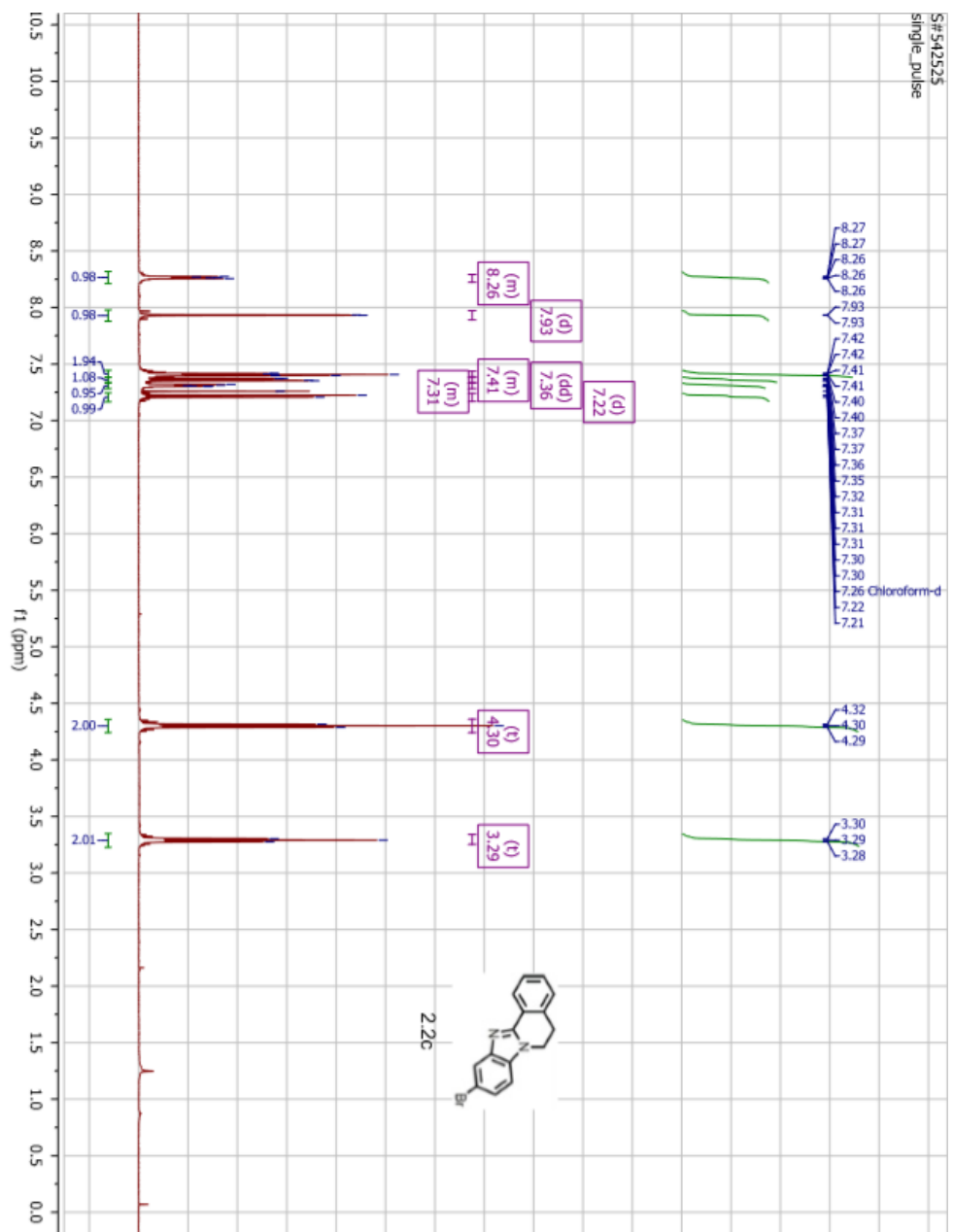
S# 557050
single pulse decoupled gated NOE

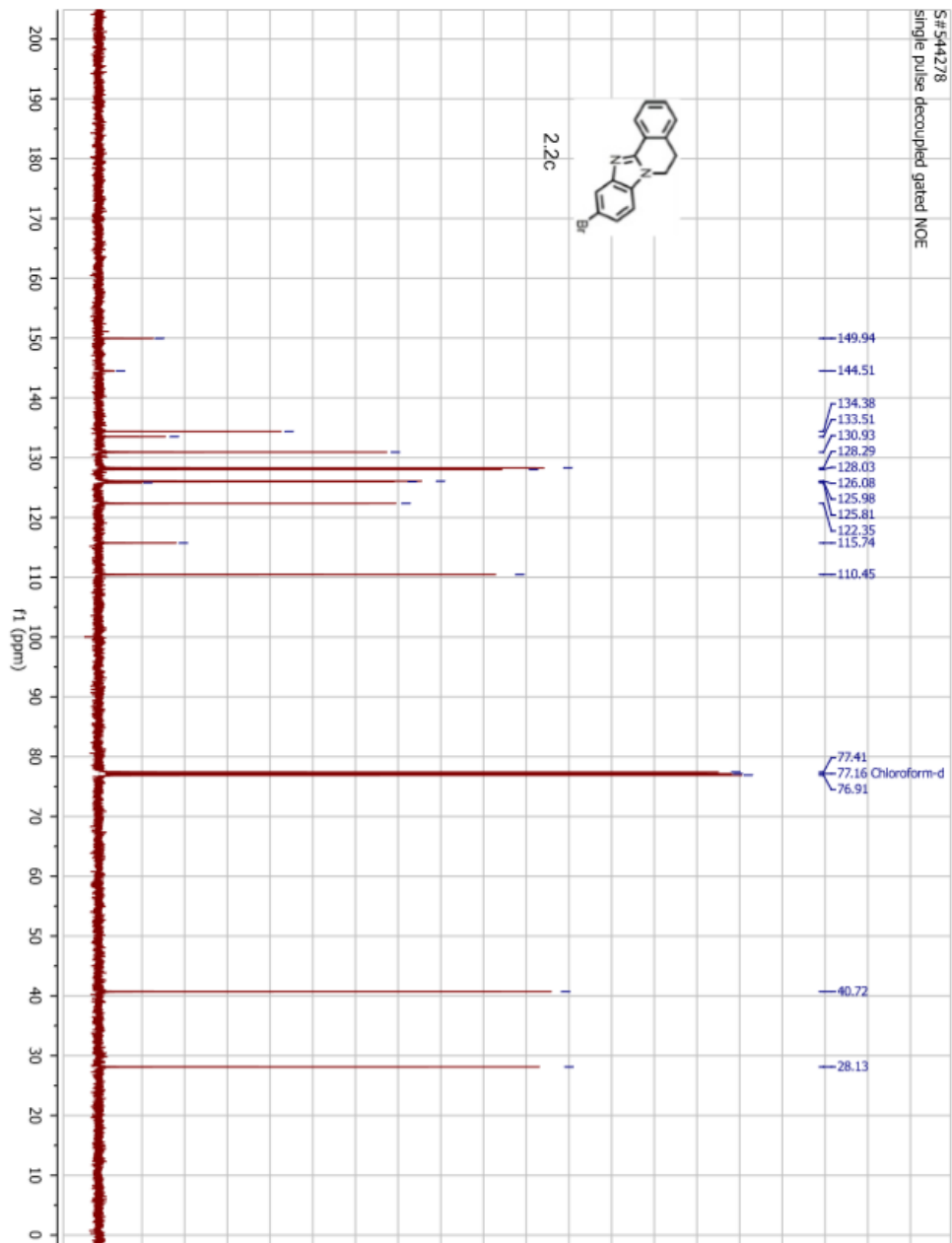


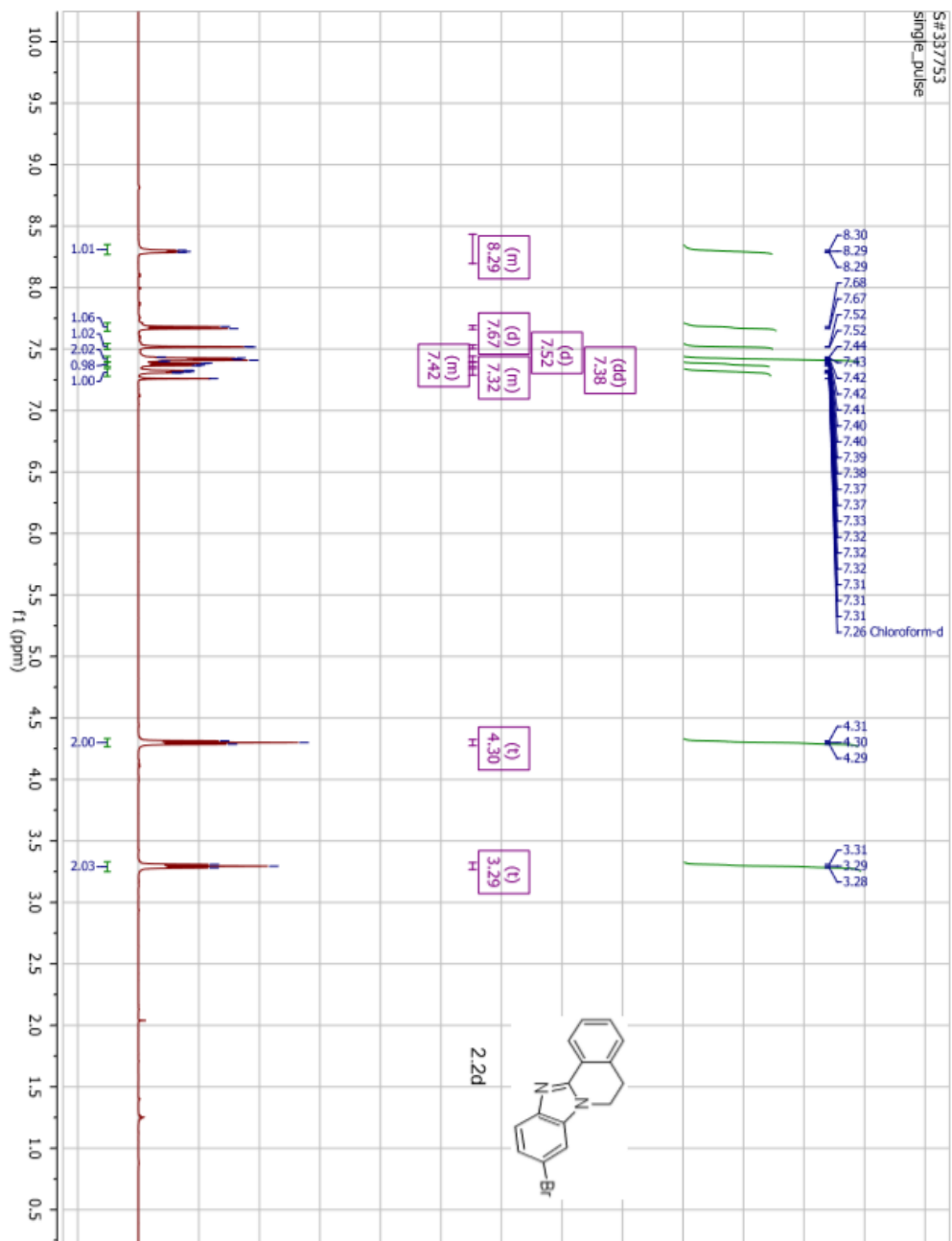
S#563021
single_pulse



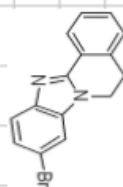




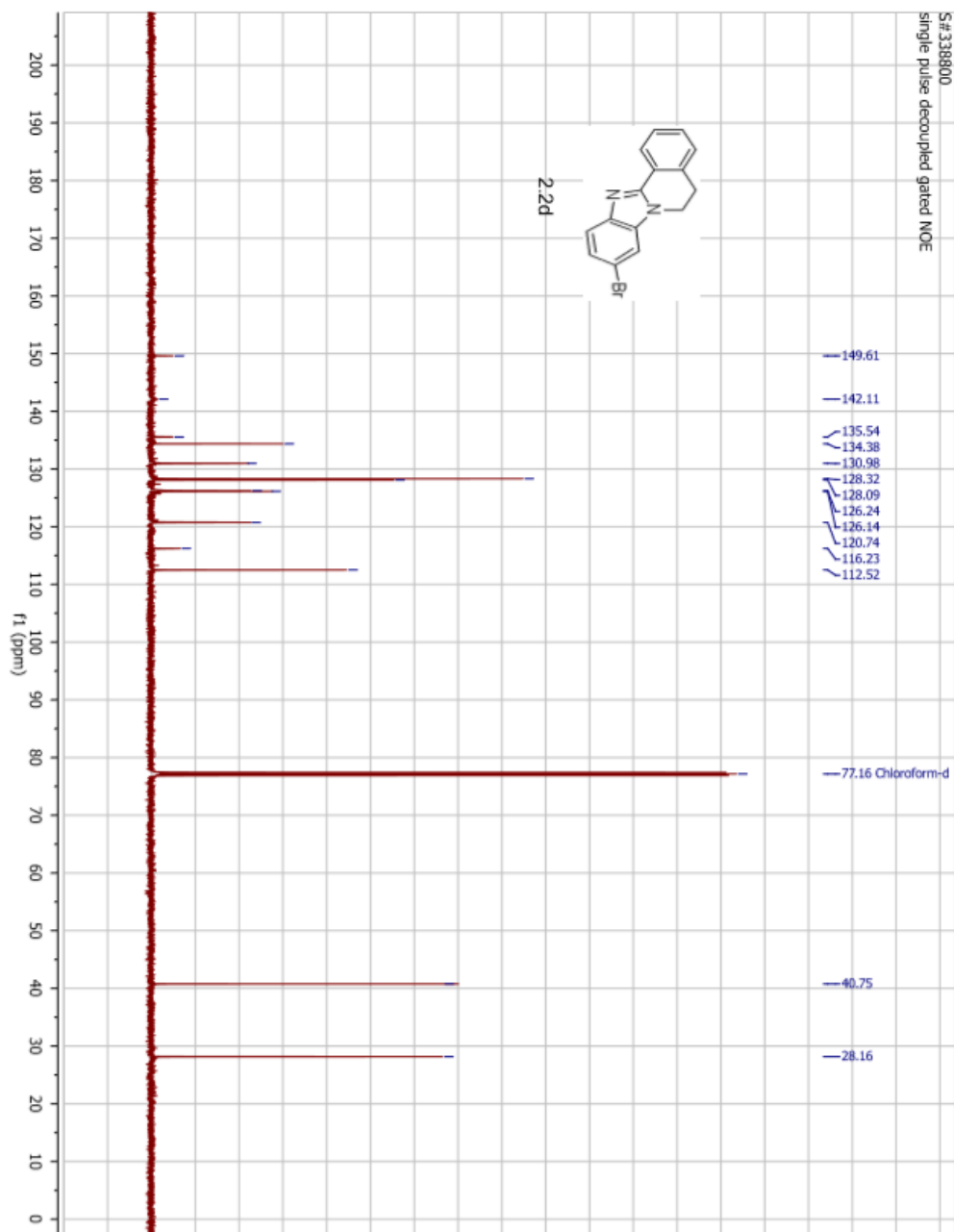


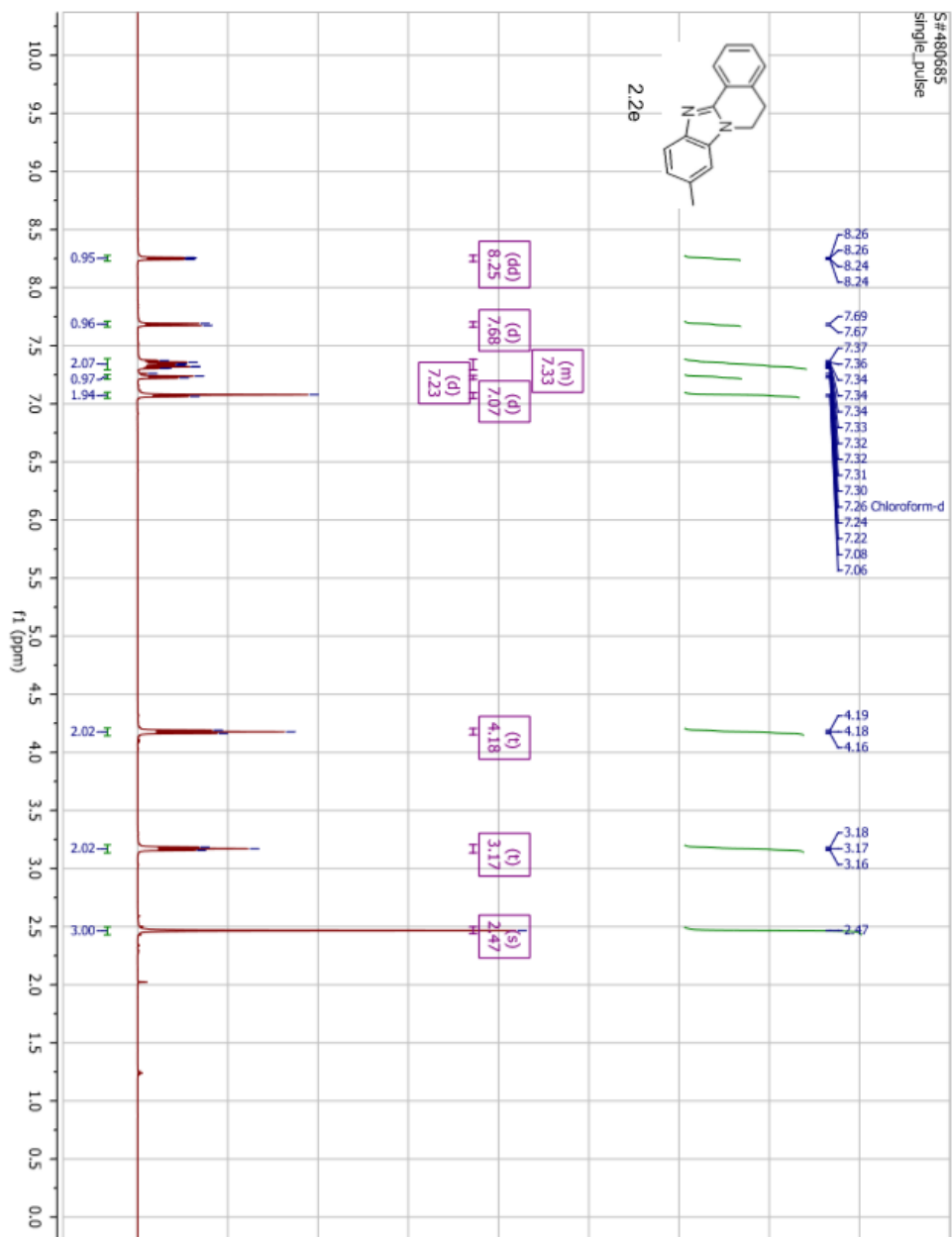


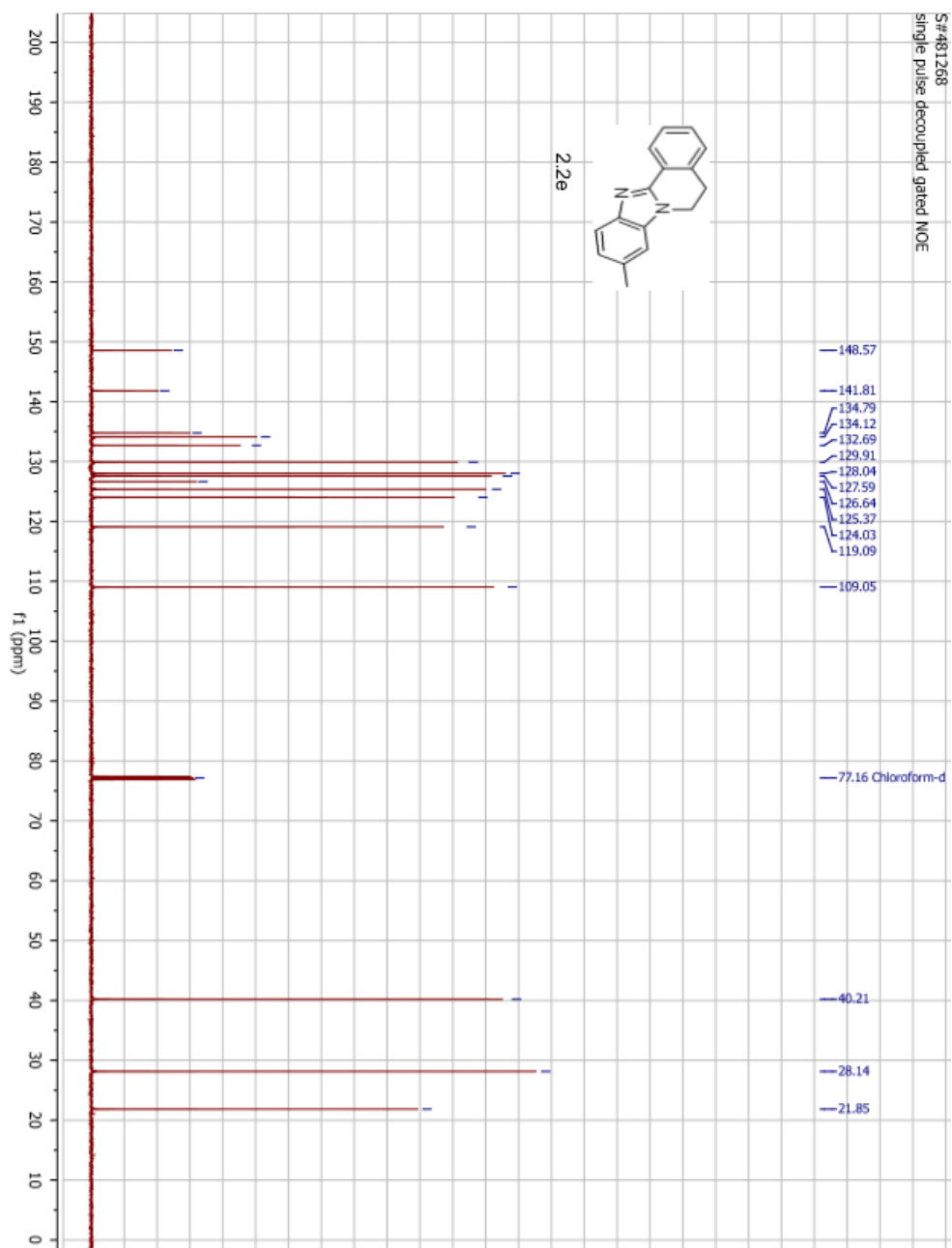
S# 338800
single pulse decoupled gated NOE

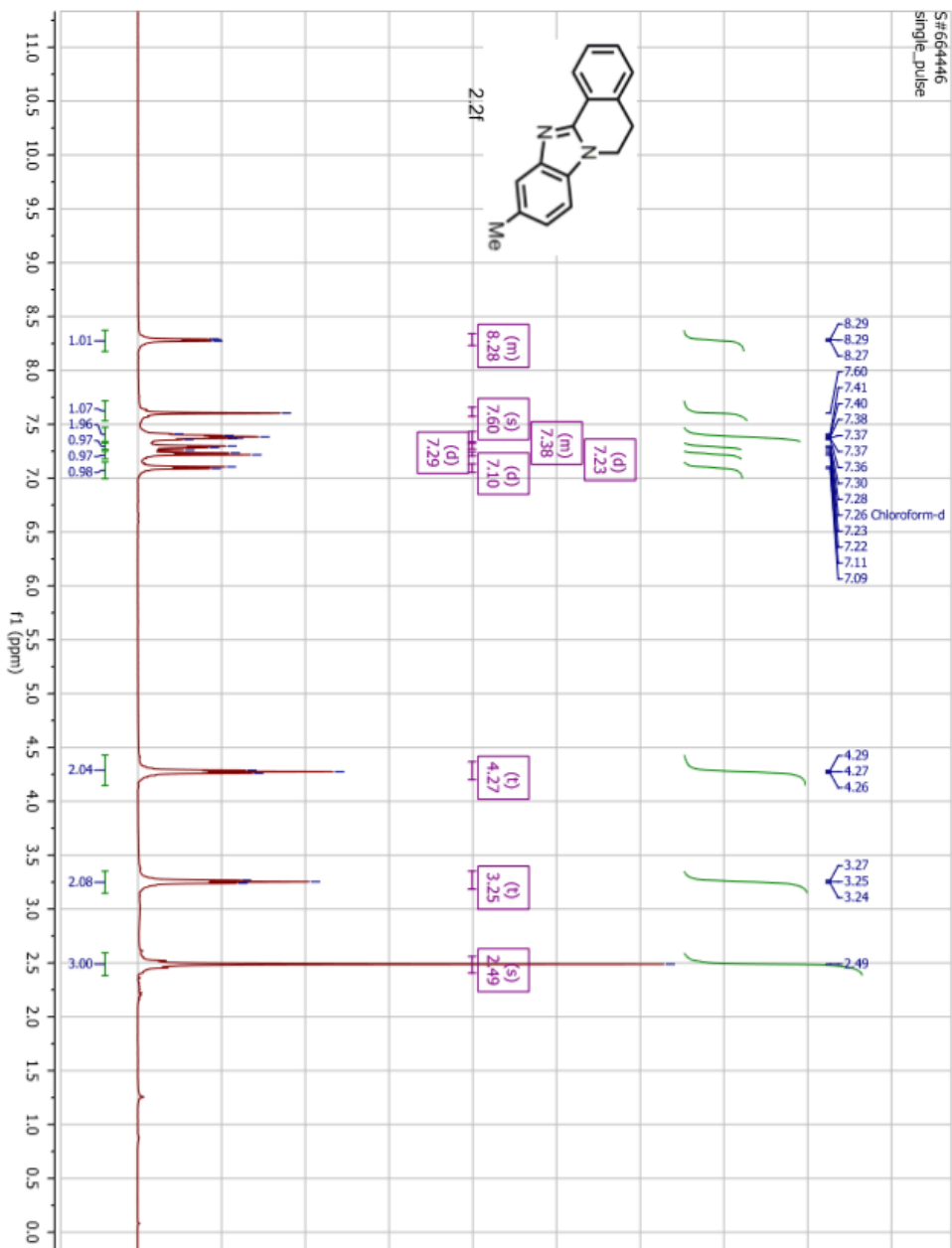


2.2d

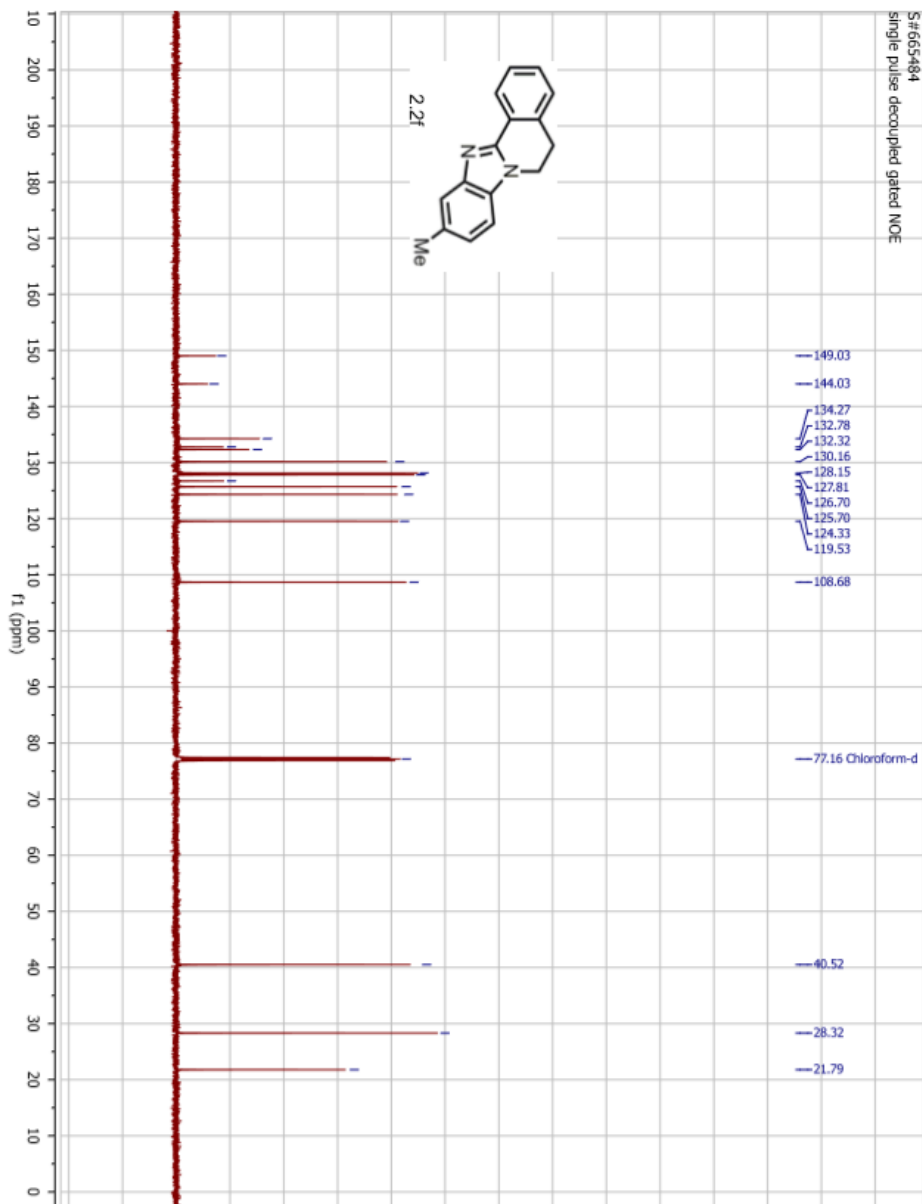
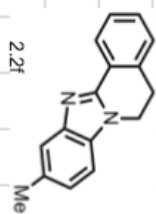


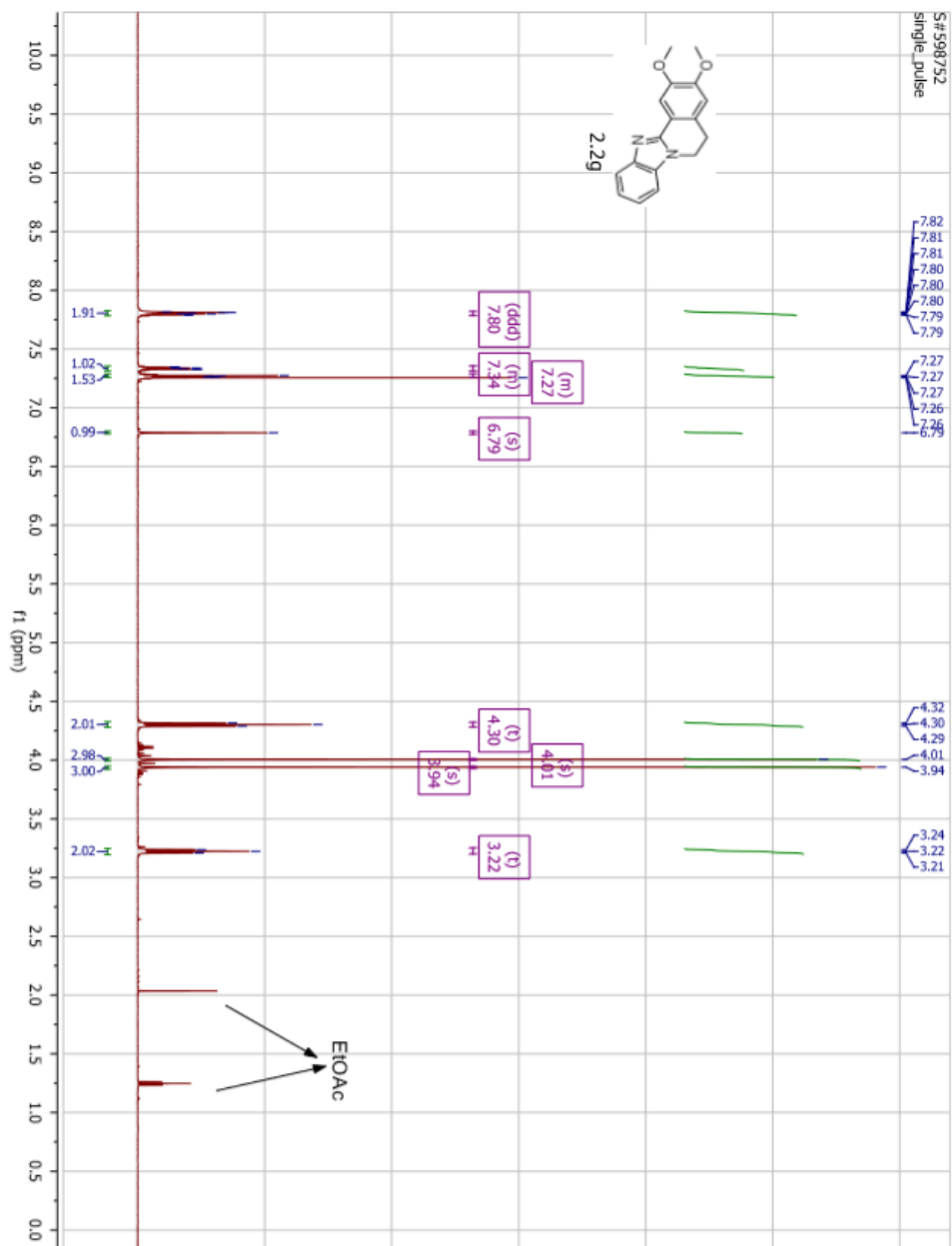


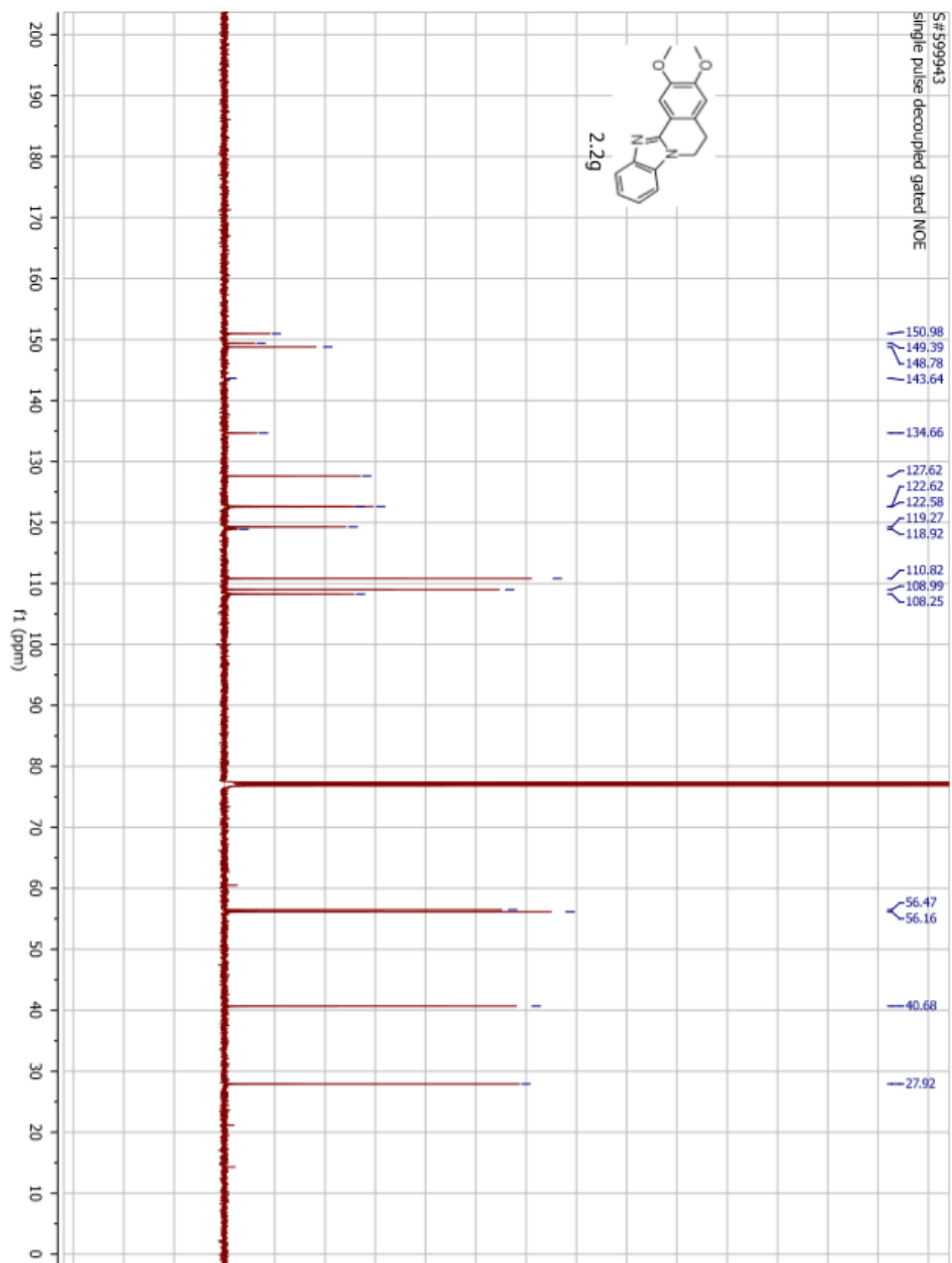


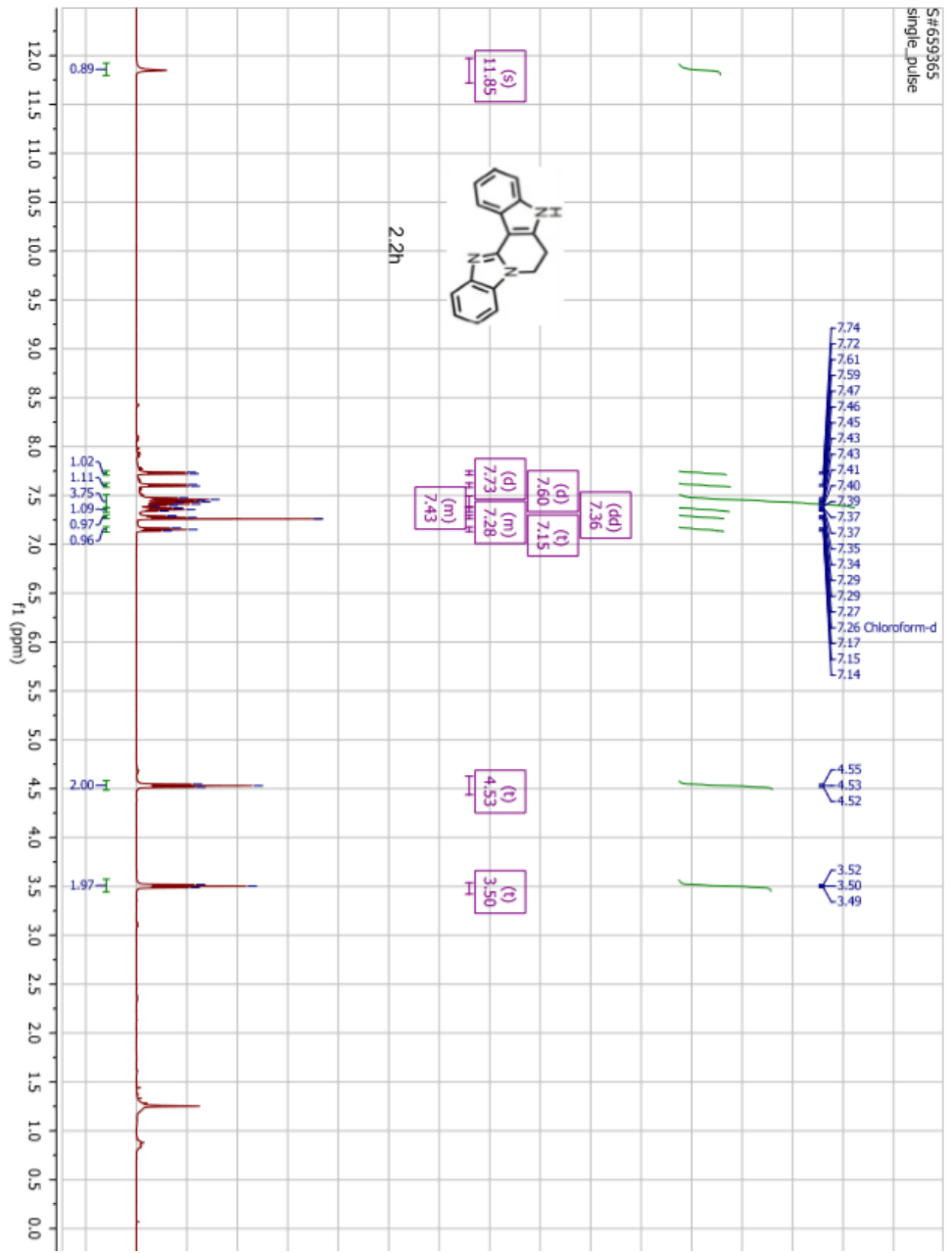


S#655484
Single pulse decoupled gated NOE

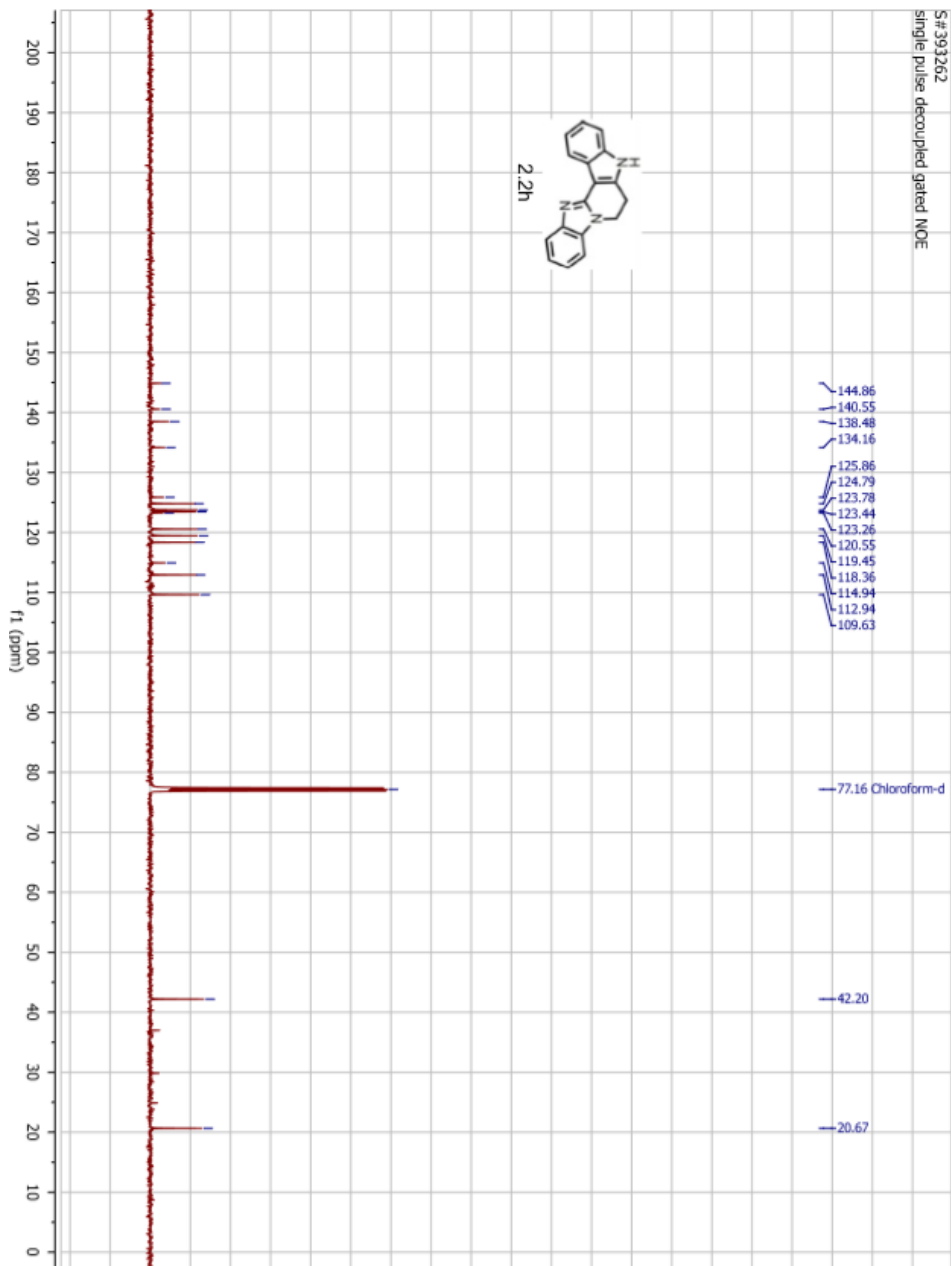
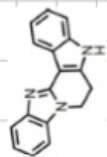


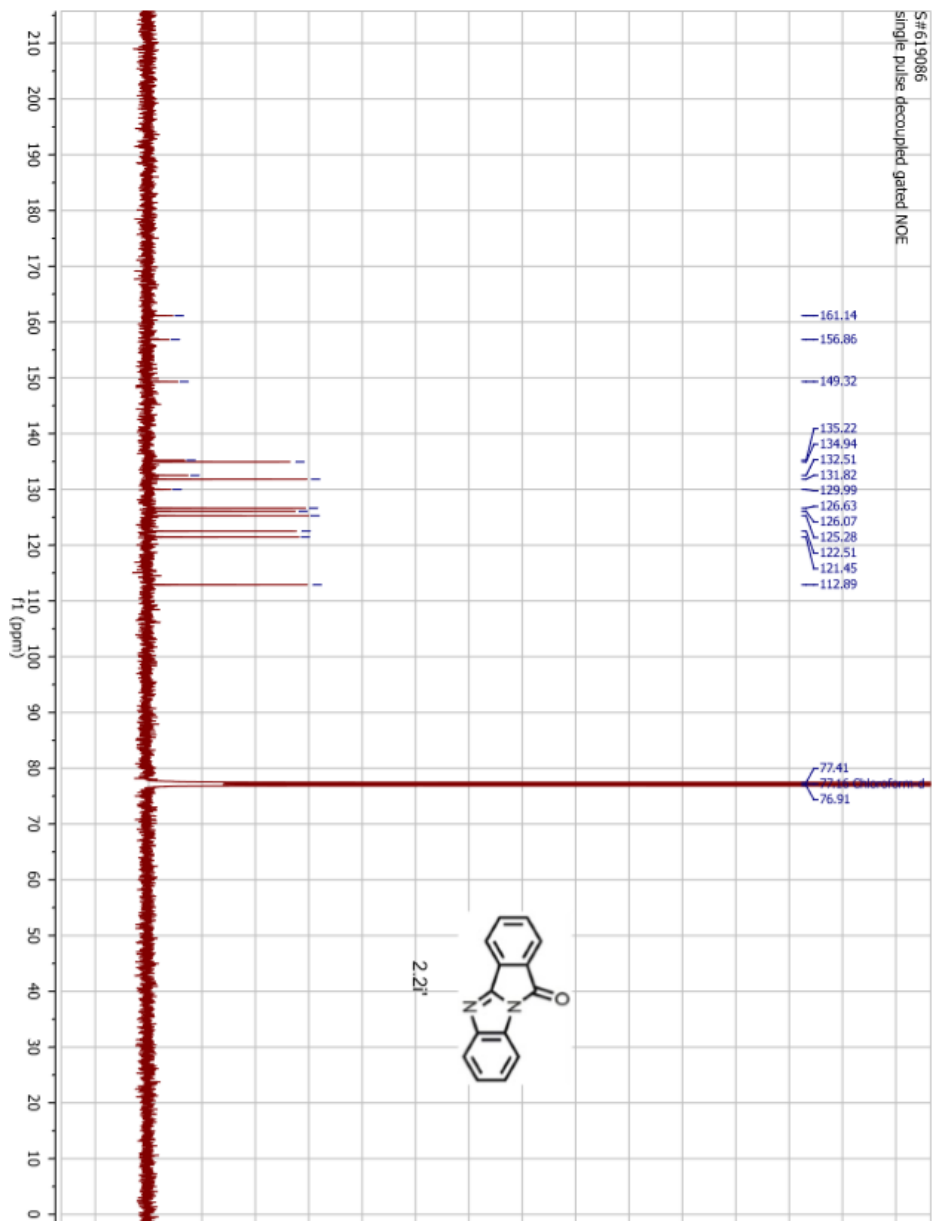


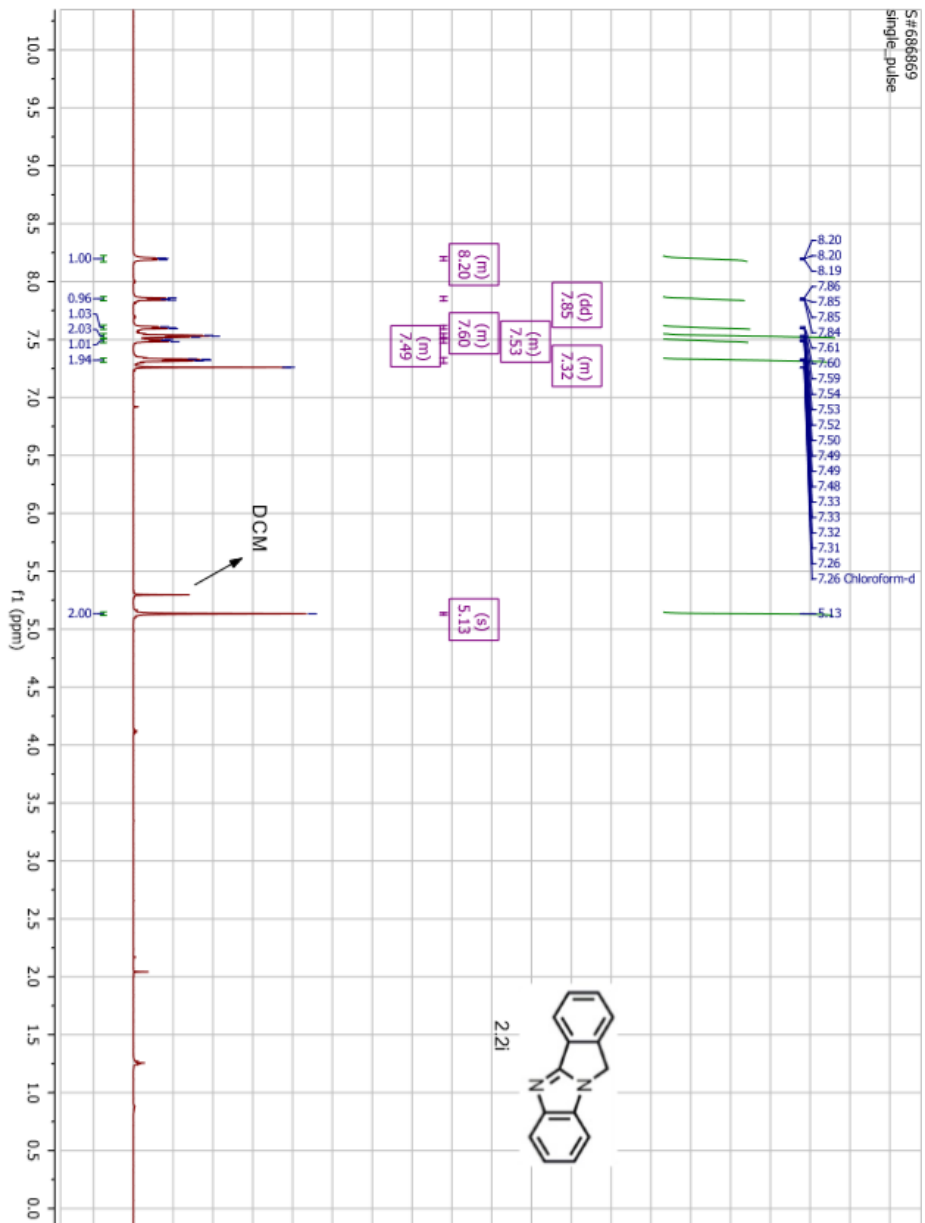


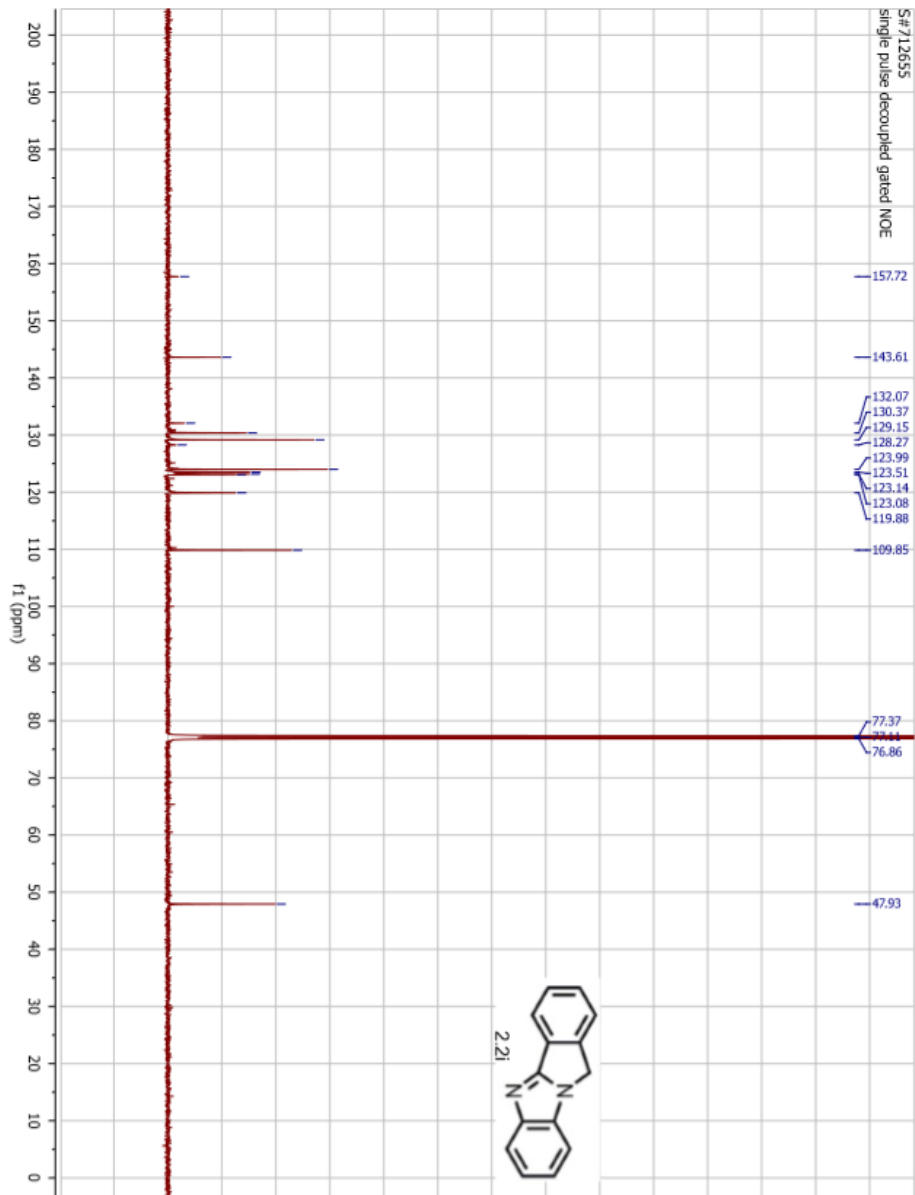


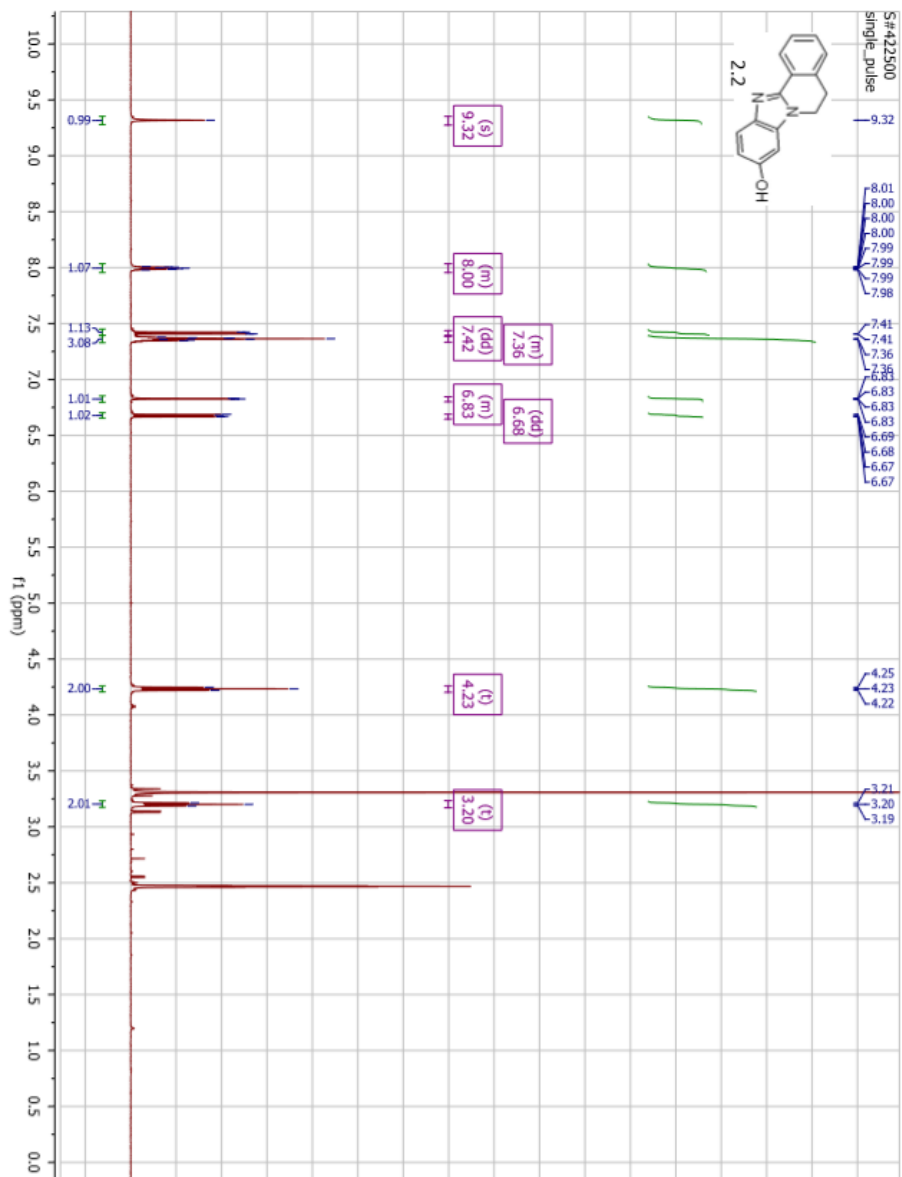
S# 393262
single pulse decoupled gated NOE

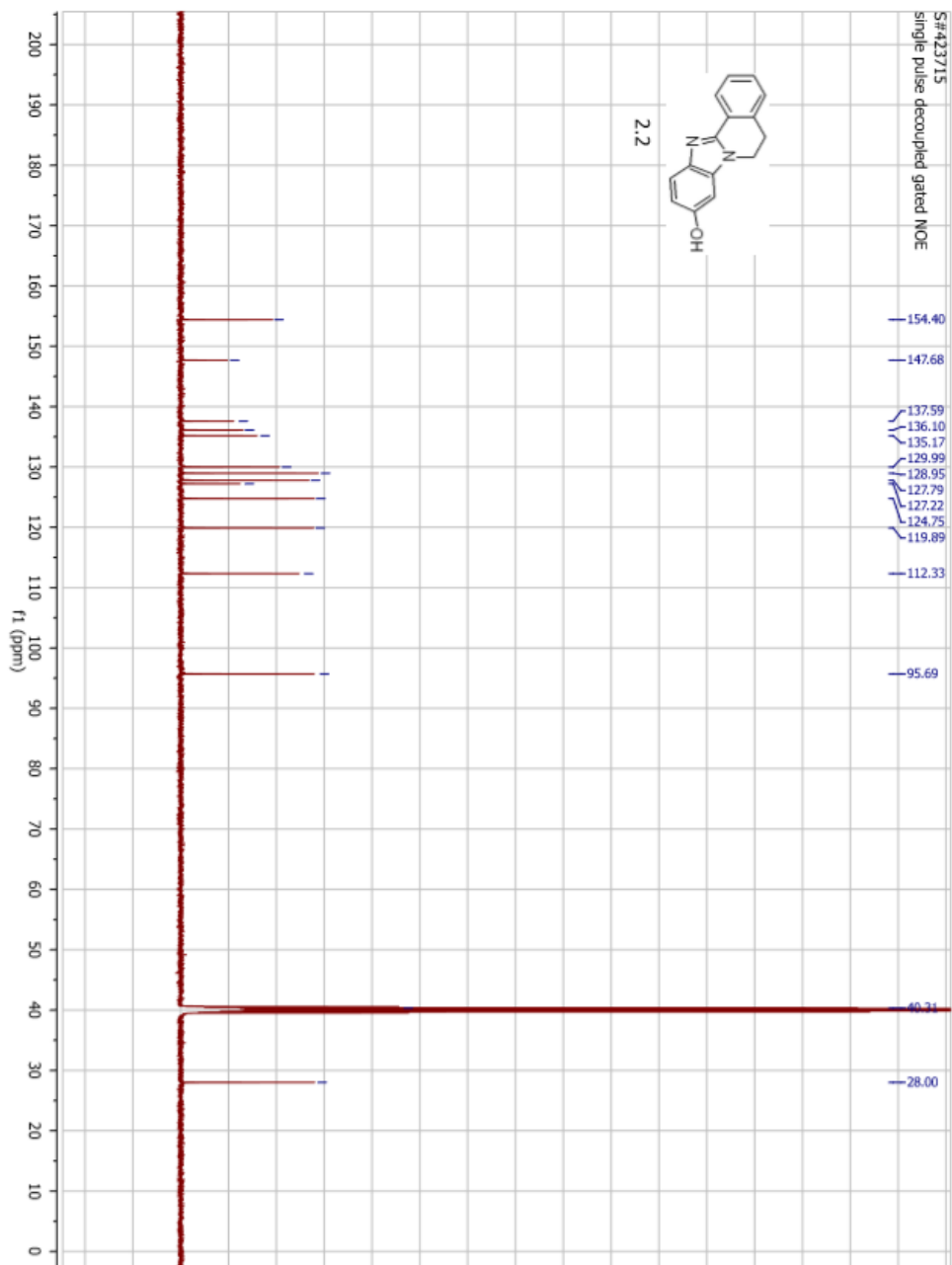


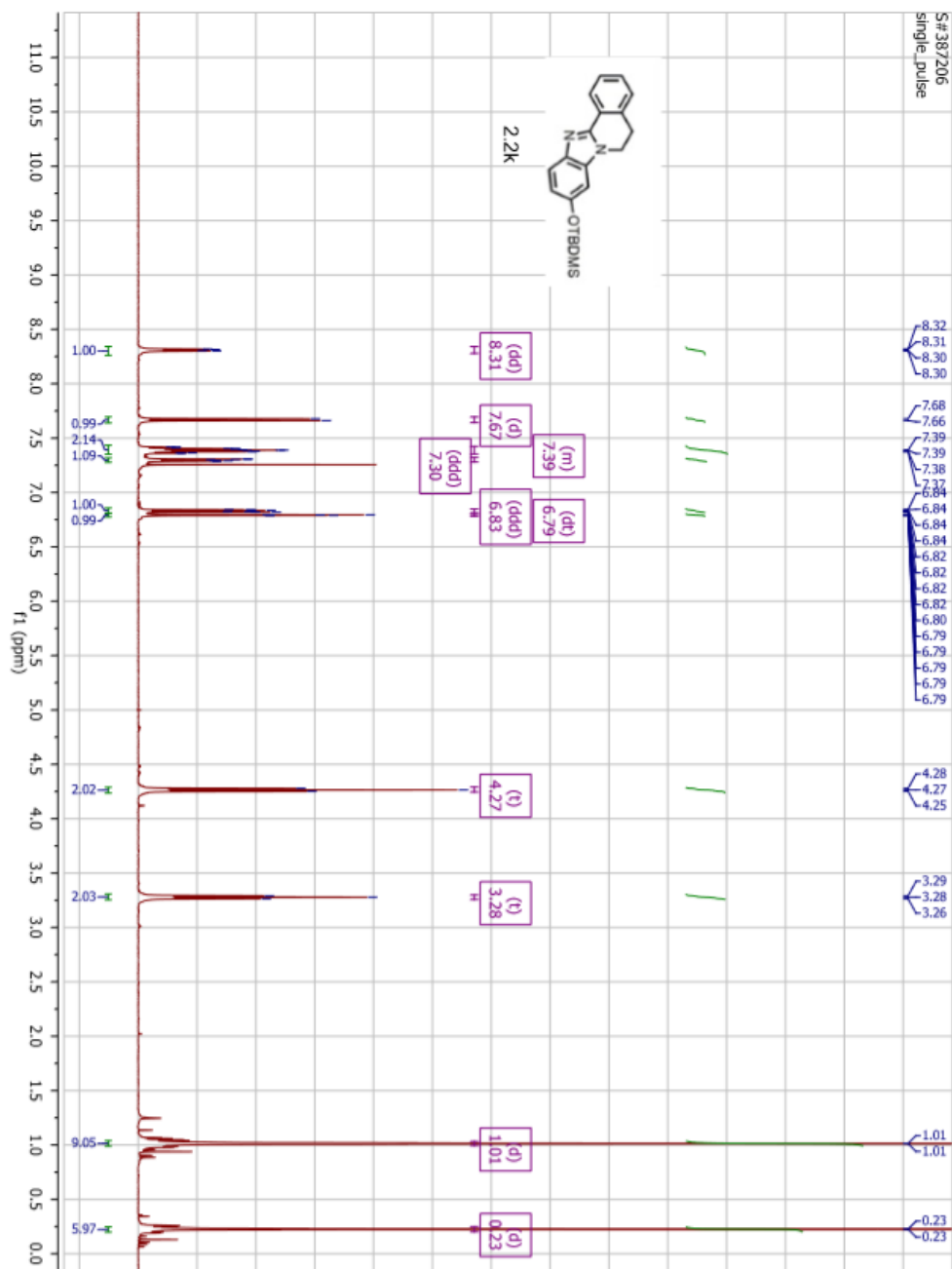


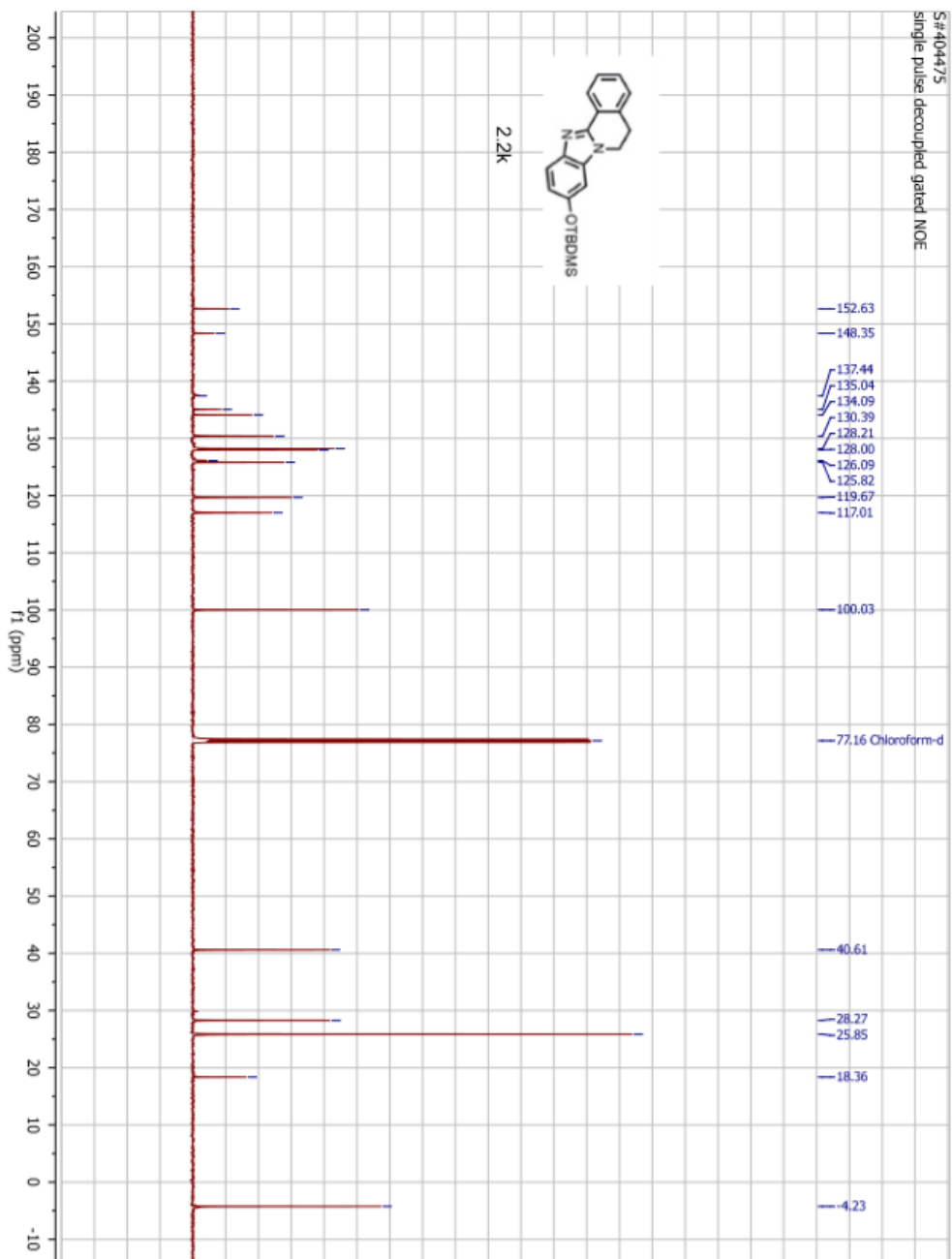


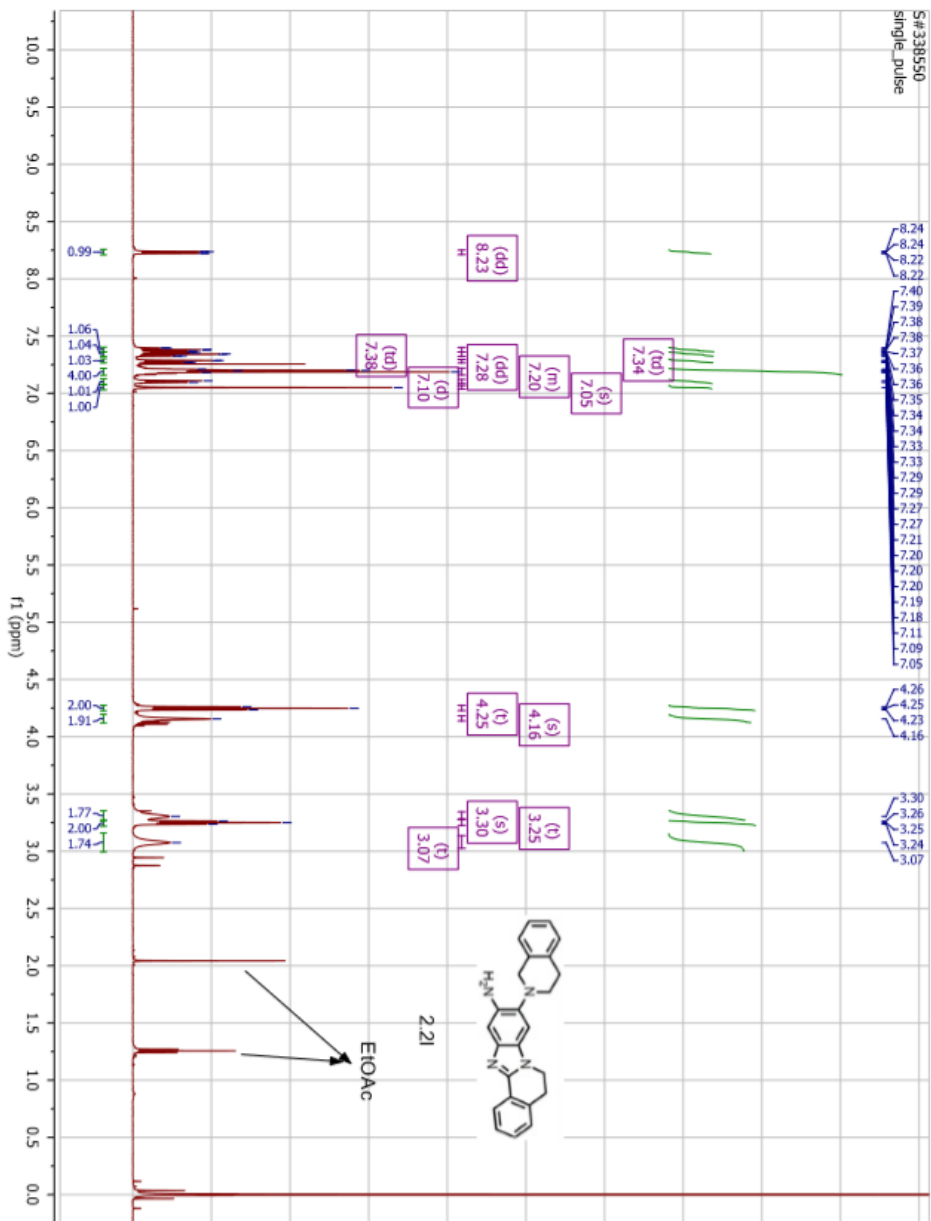




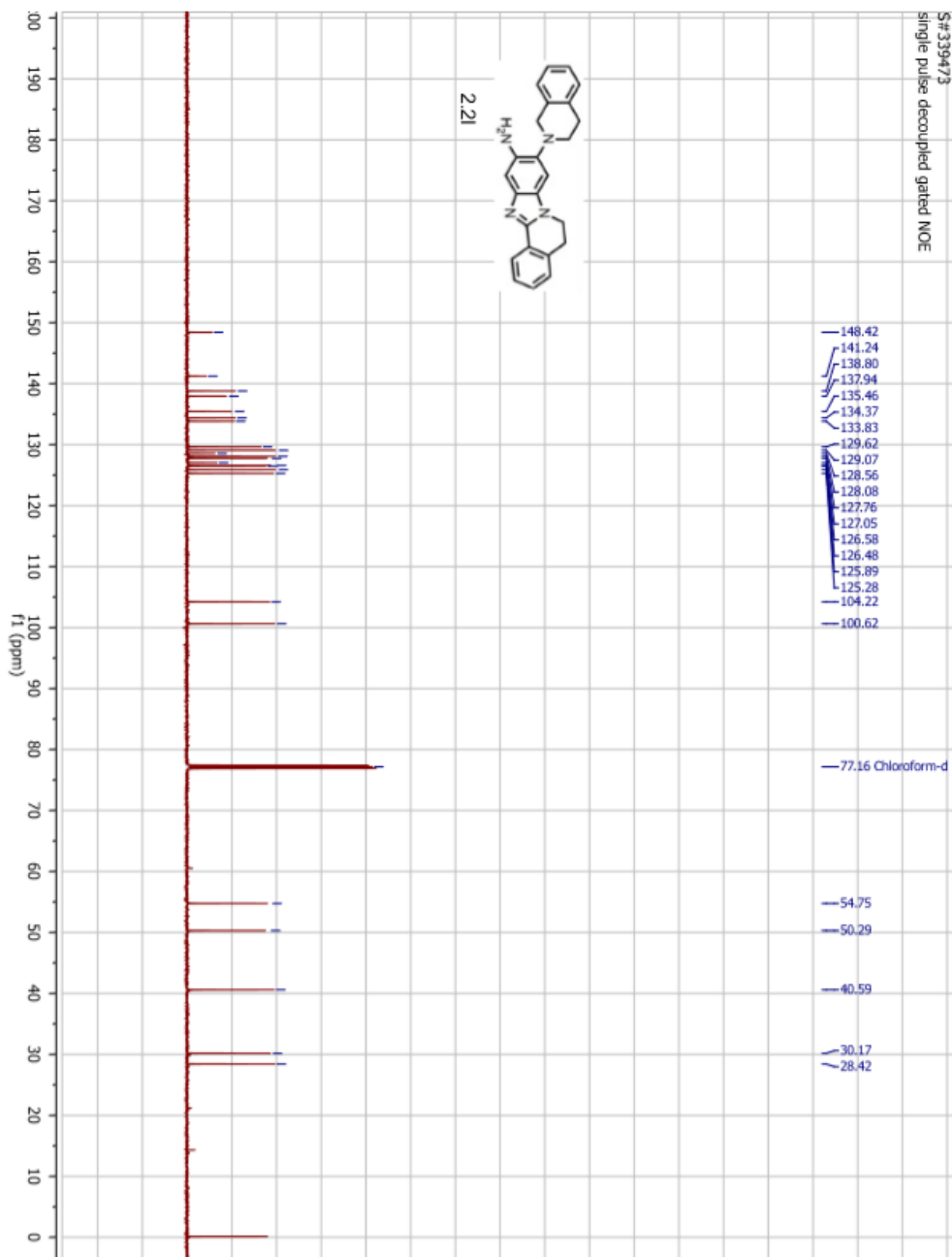
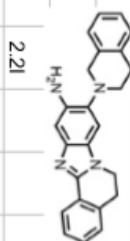




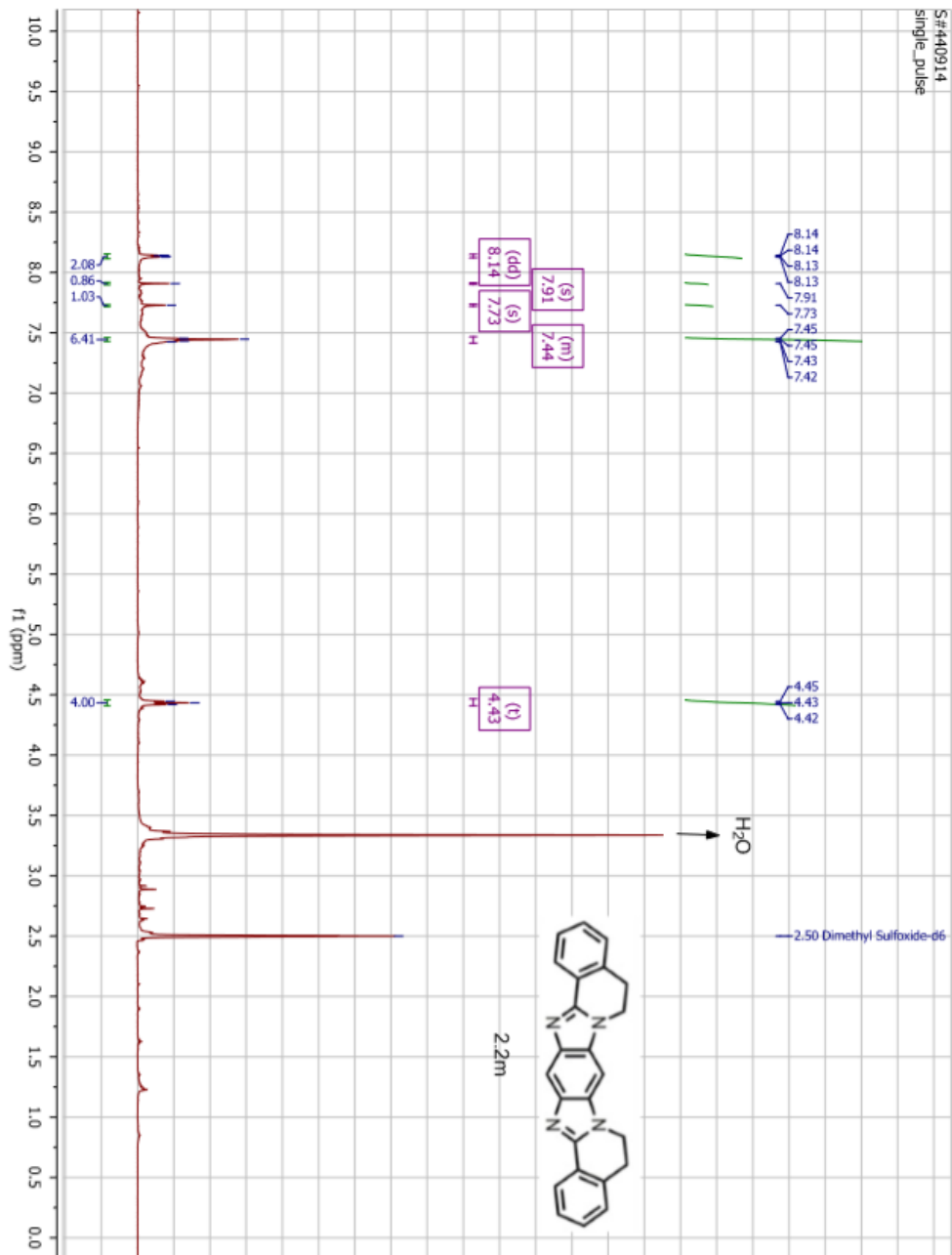




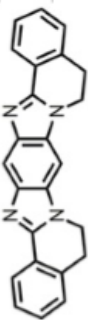
S#339473
single pulse decoupled gated NOE



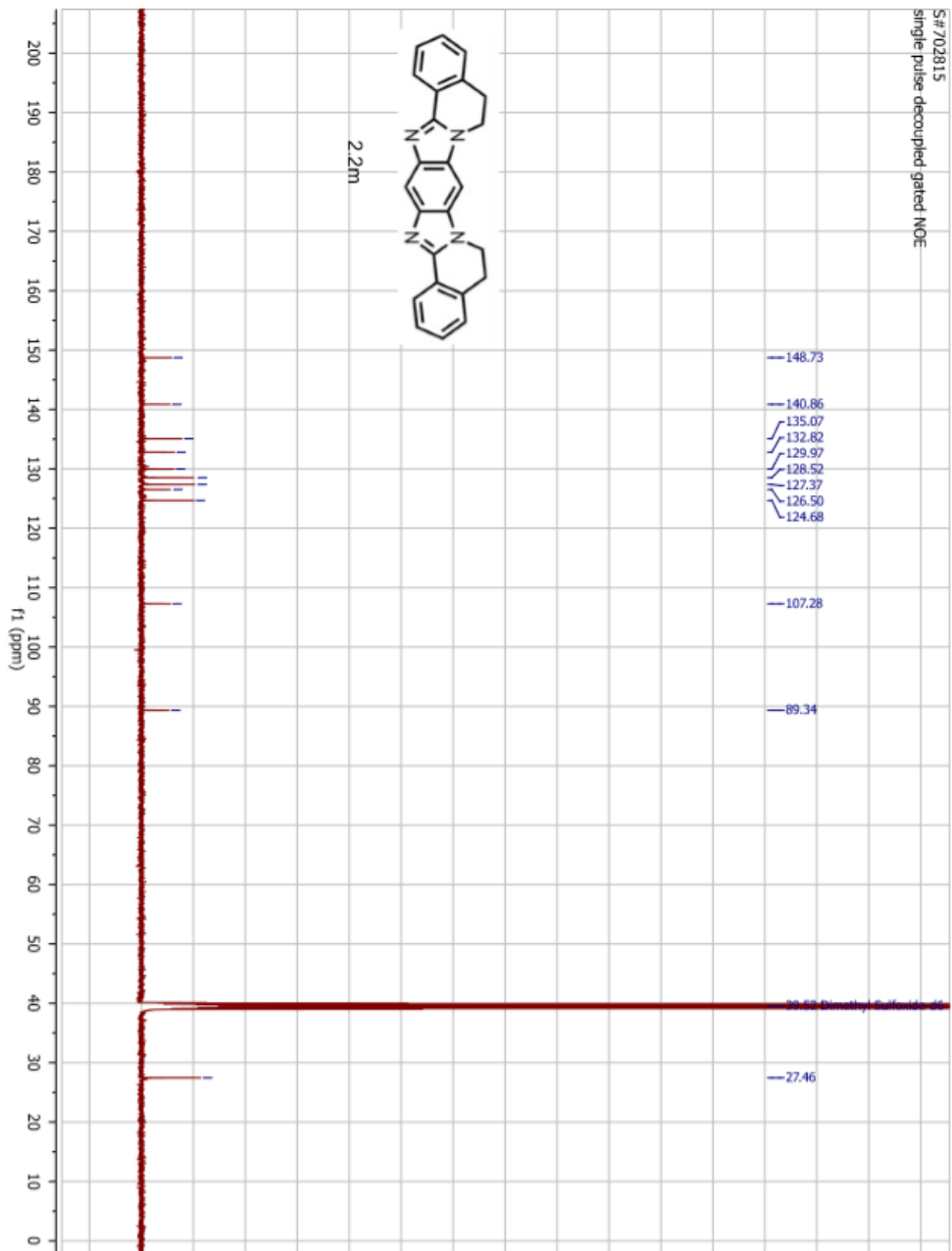
S#440914
single_pulse

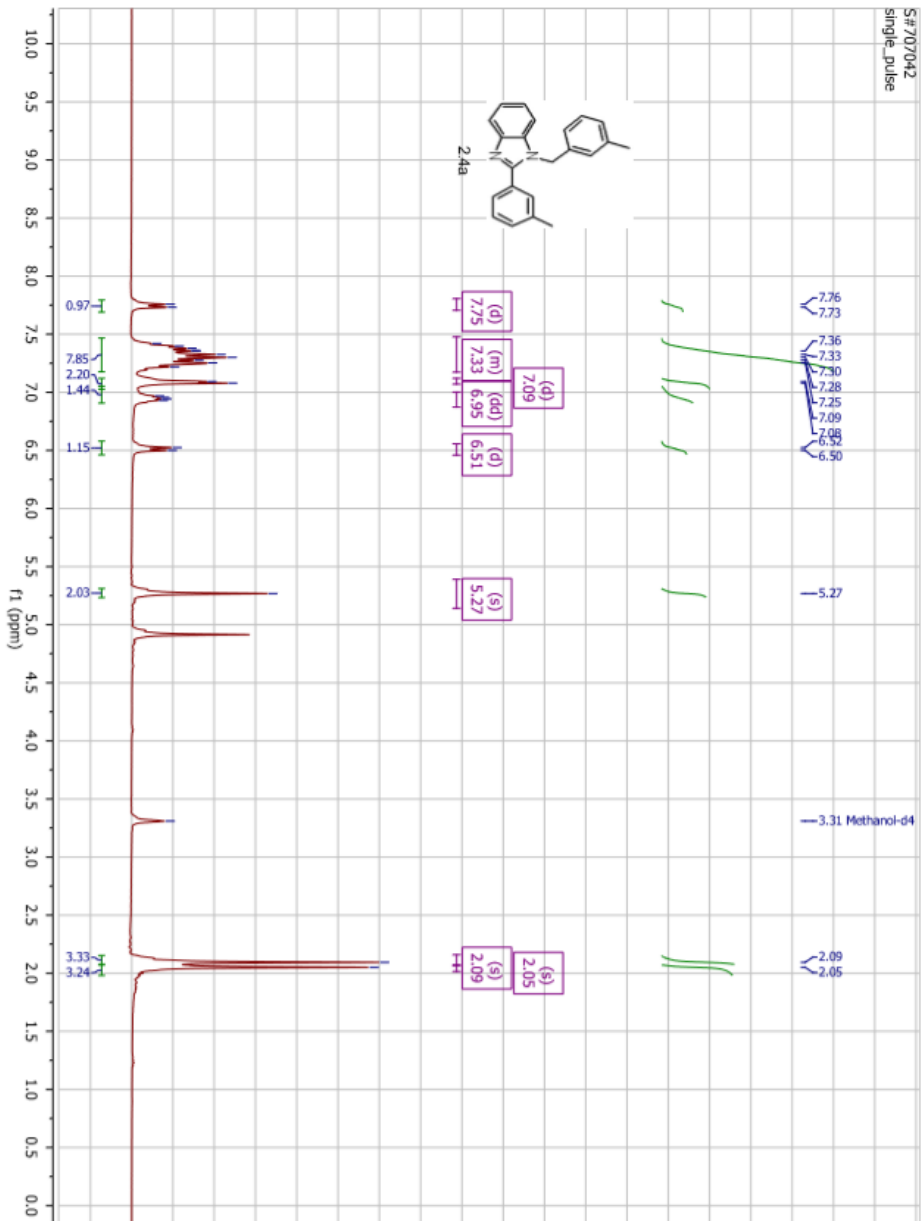


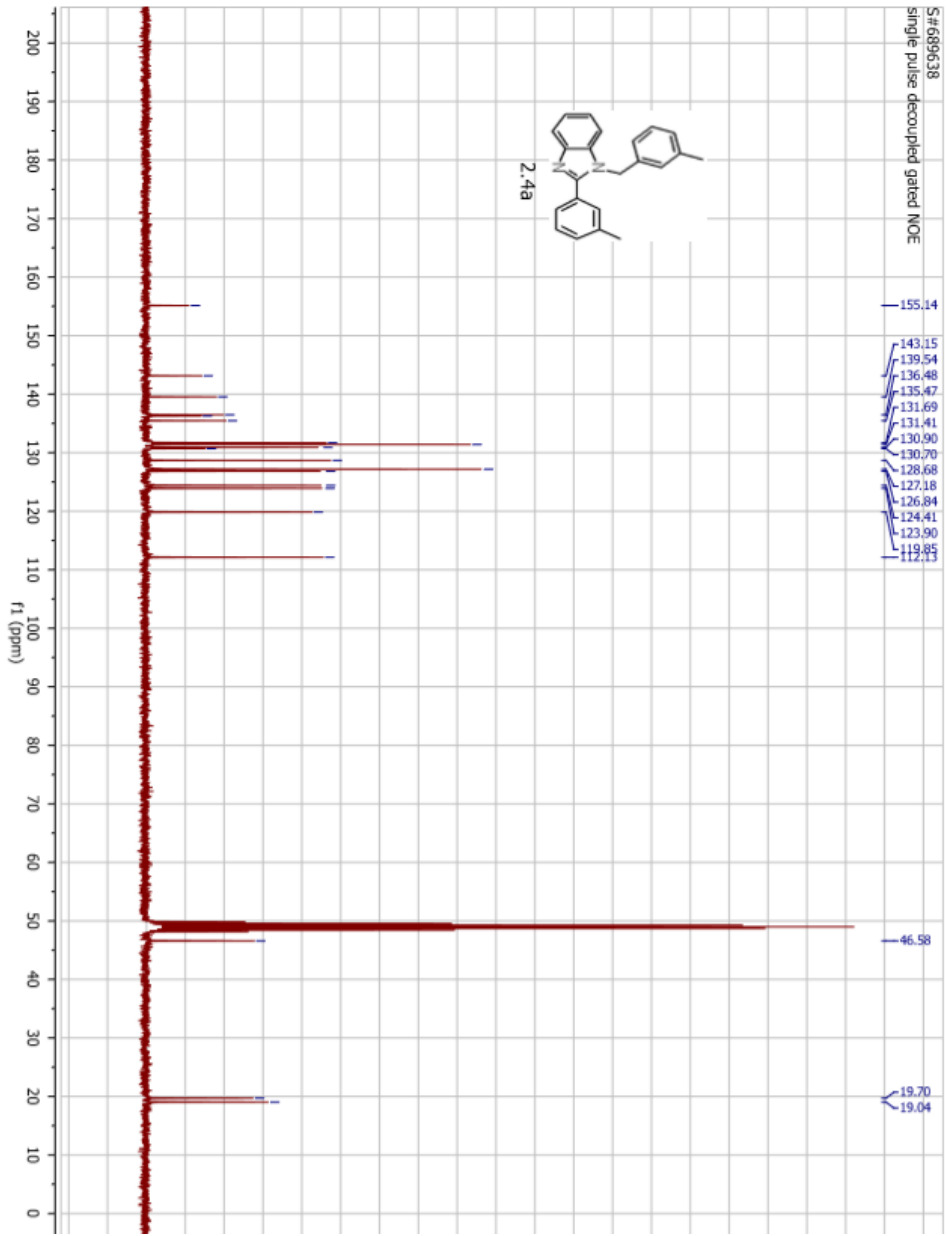
S# 702815
single-pulse-decoupled gated NOE

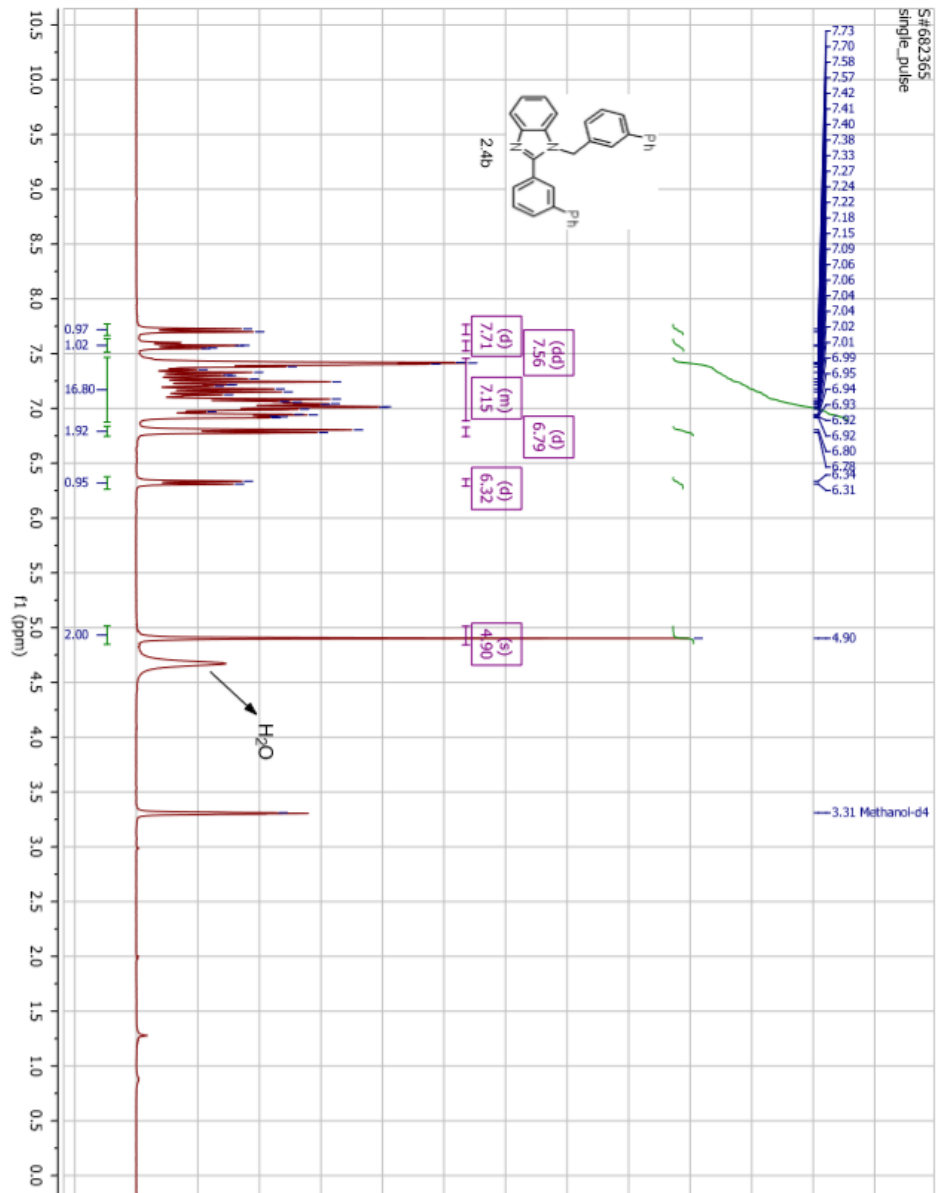


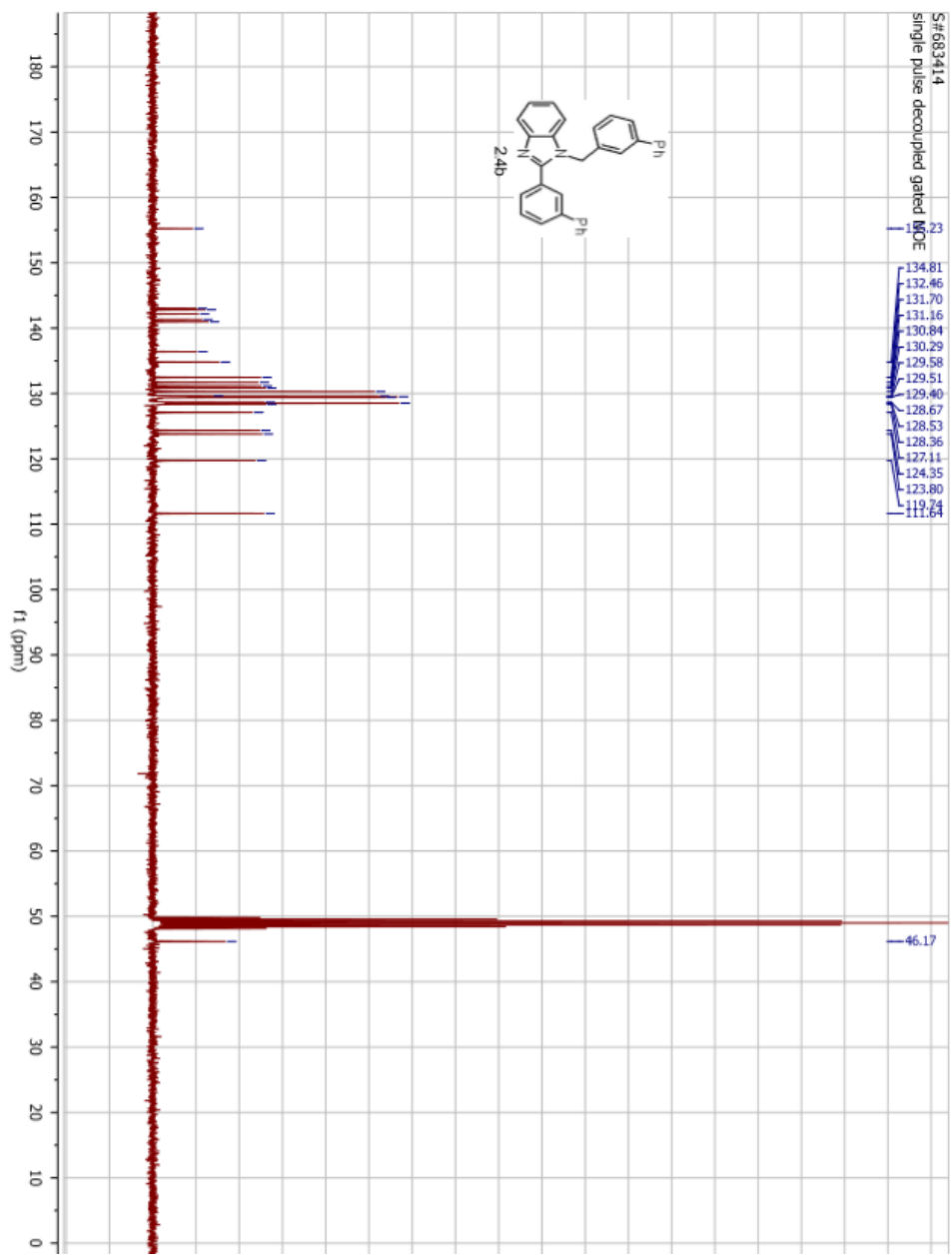
2.2m

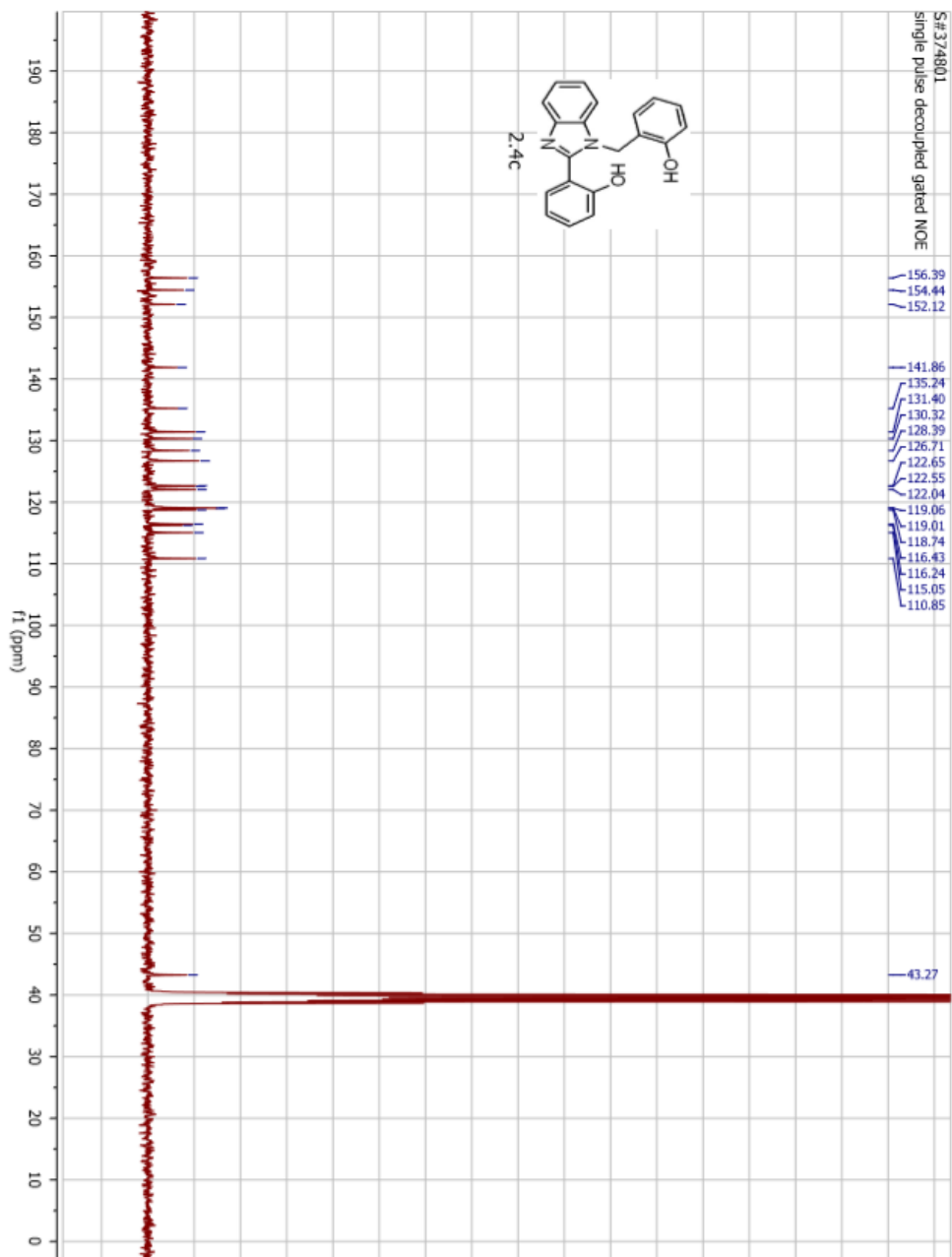


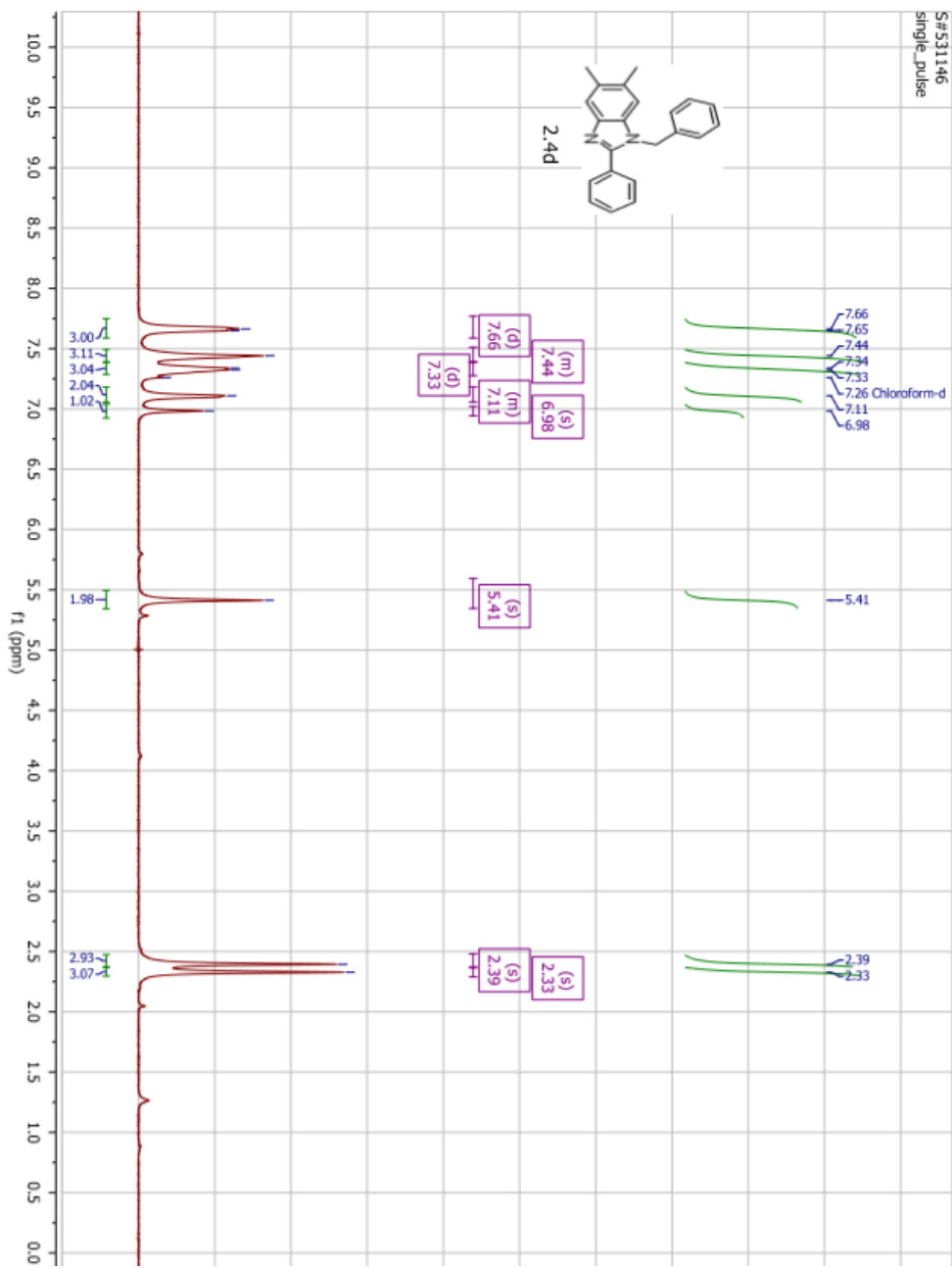


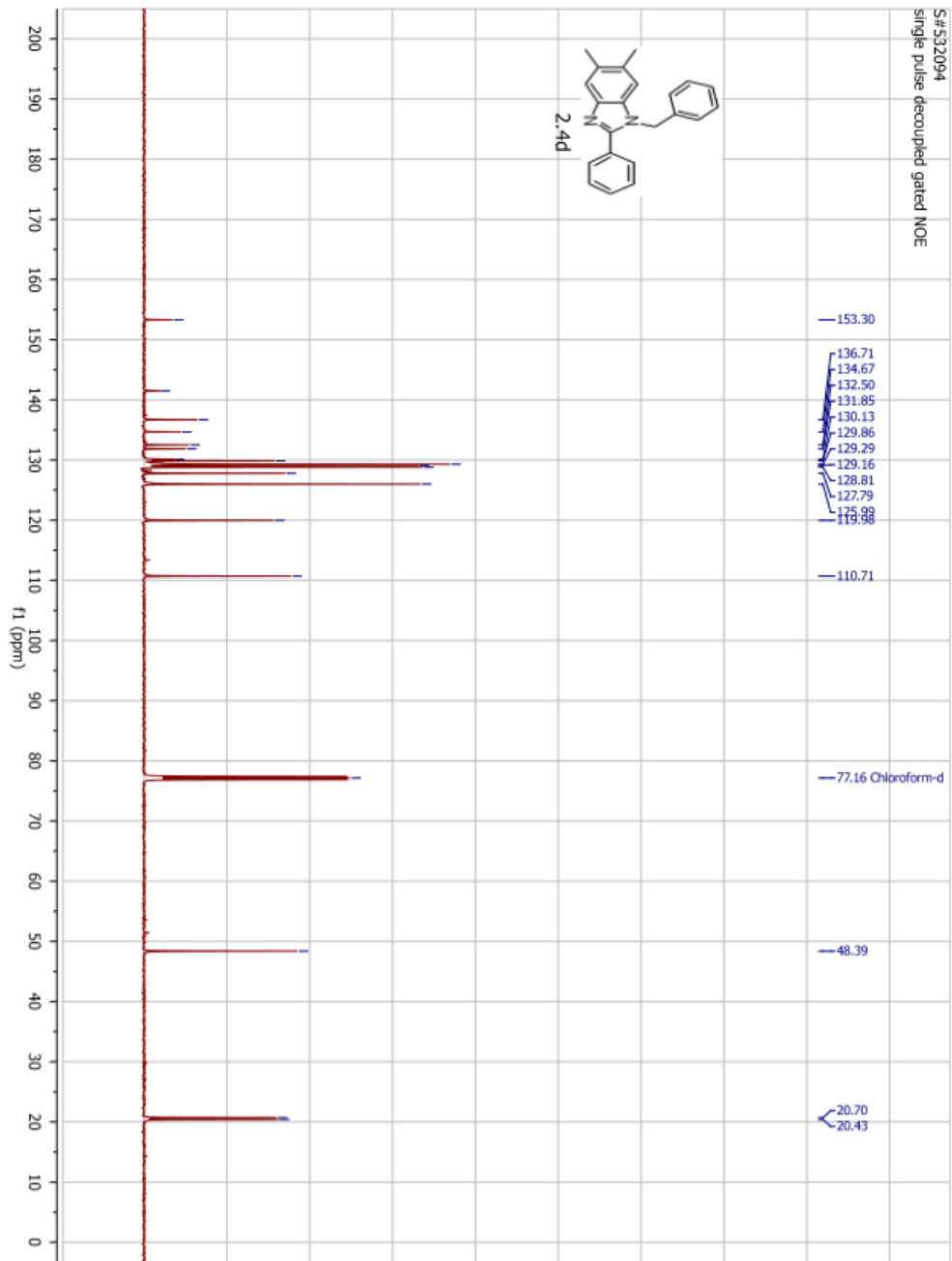


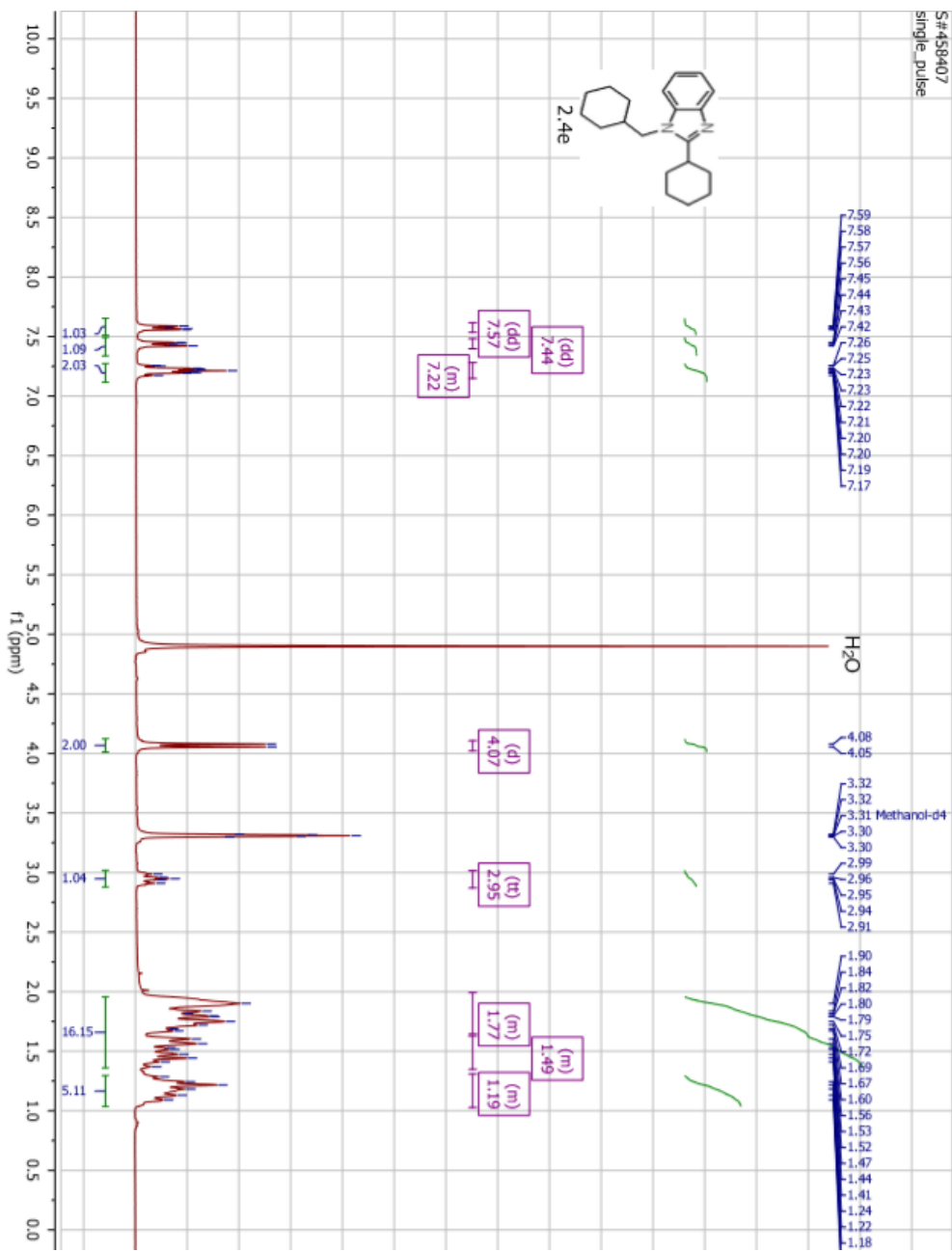


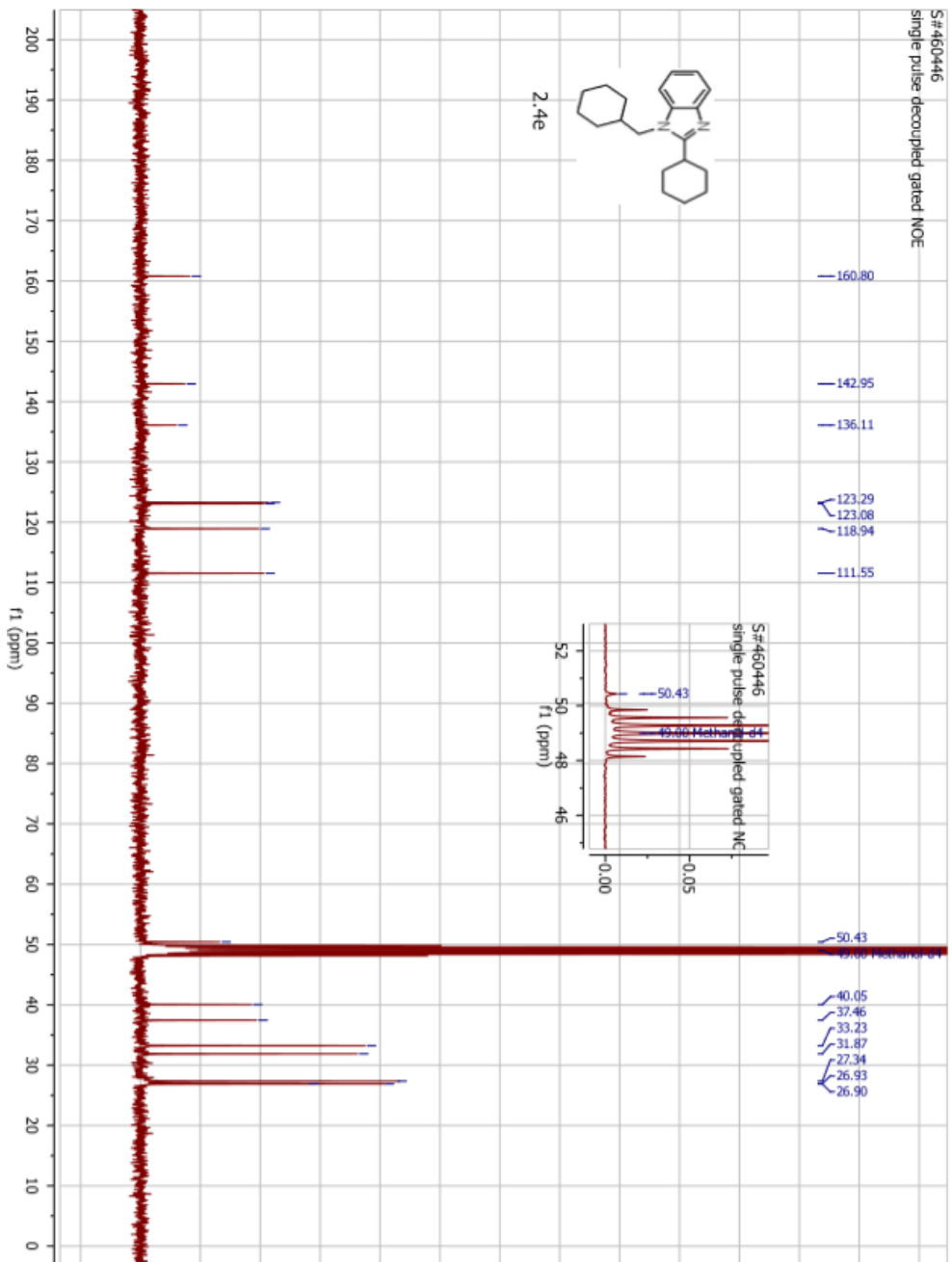


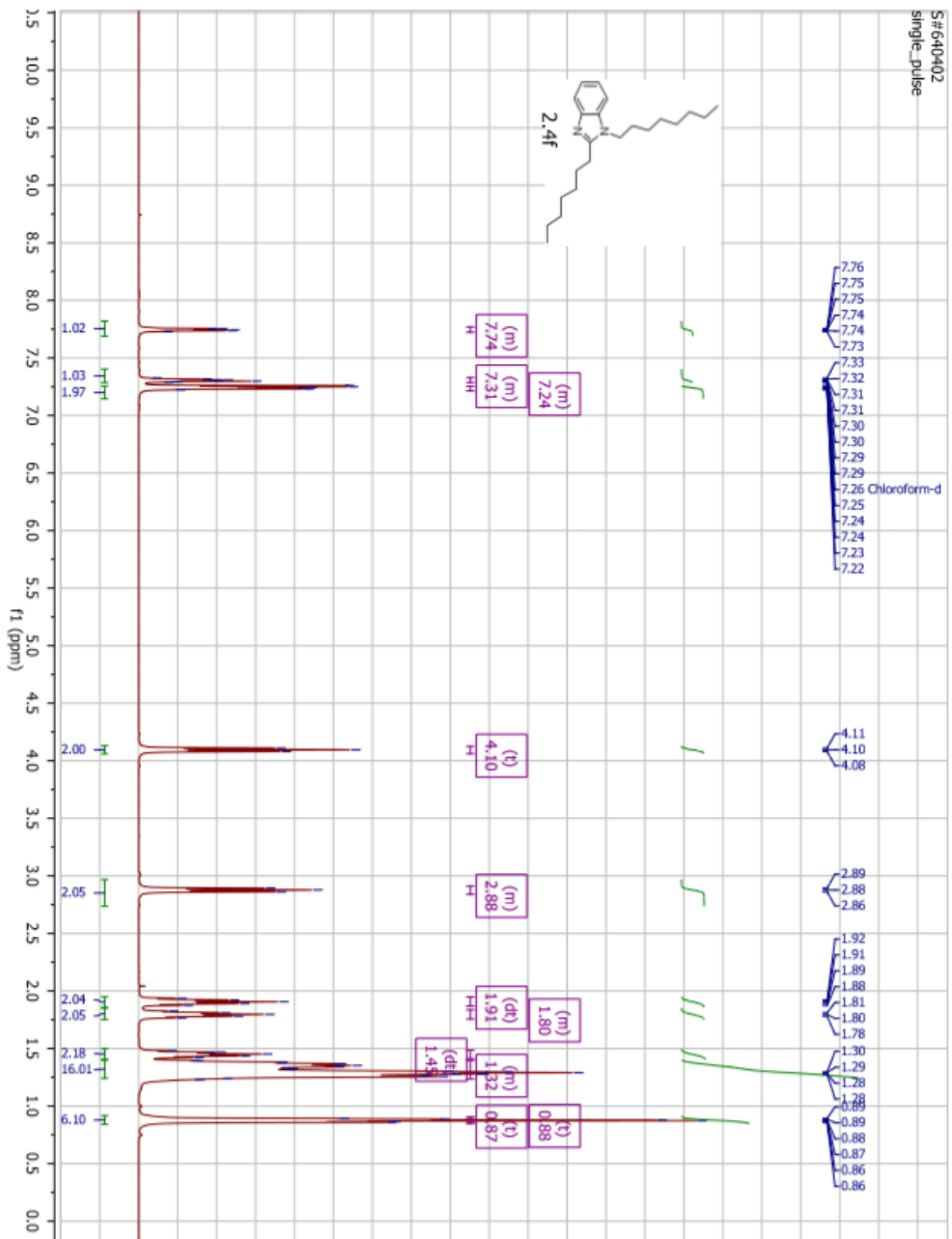


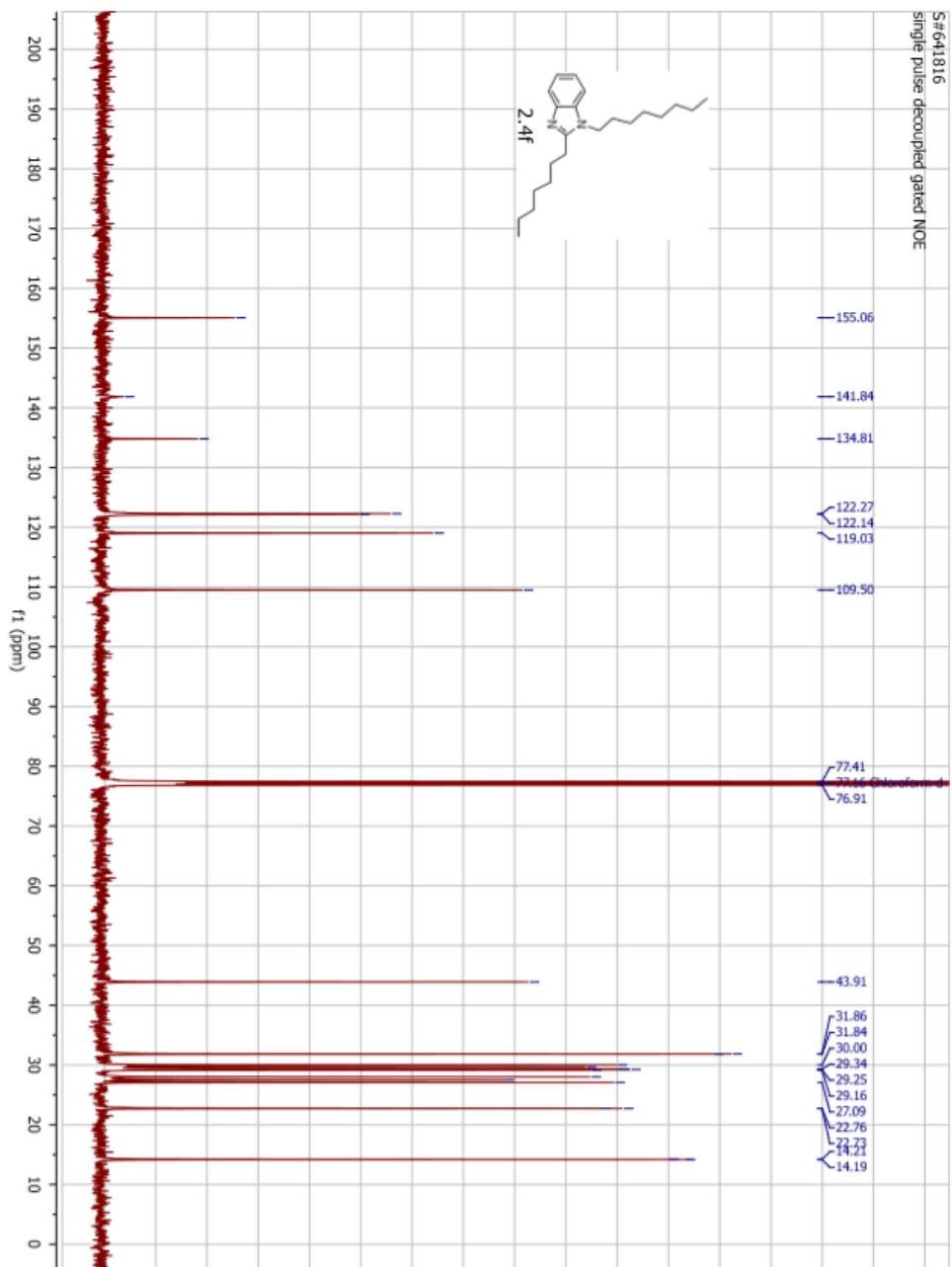


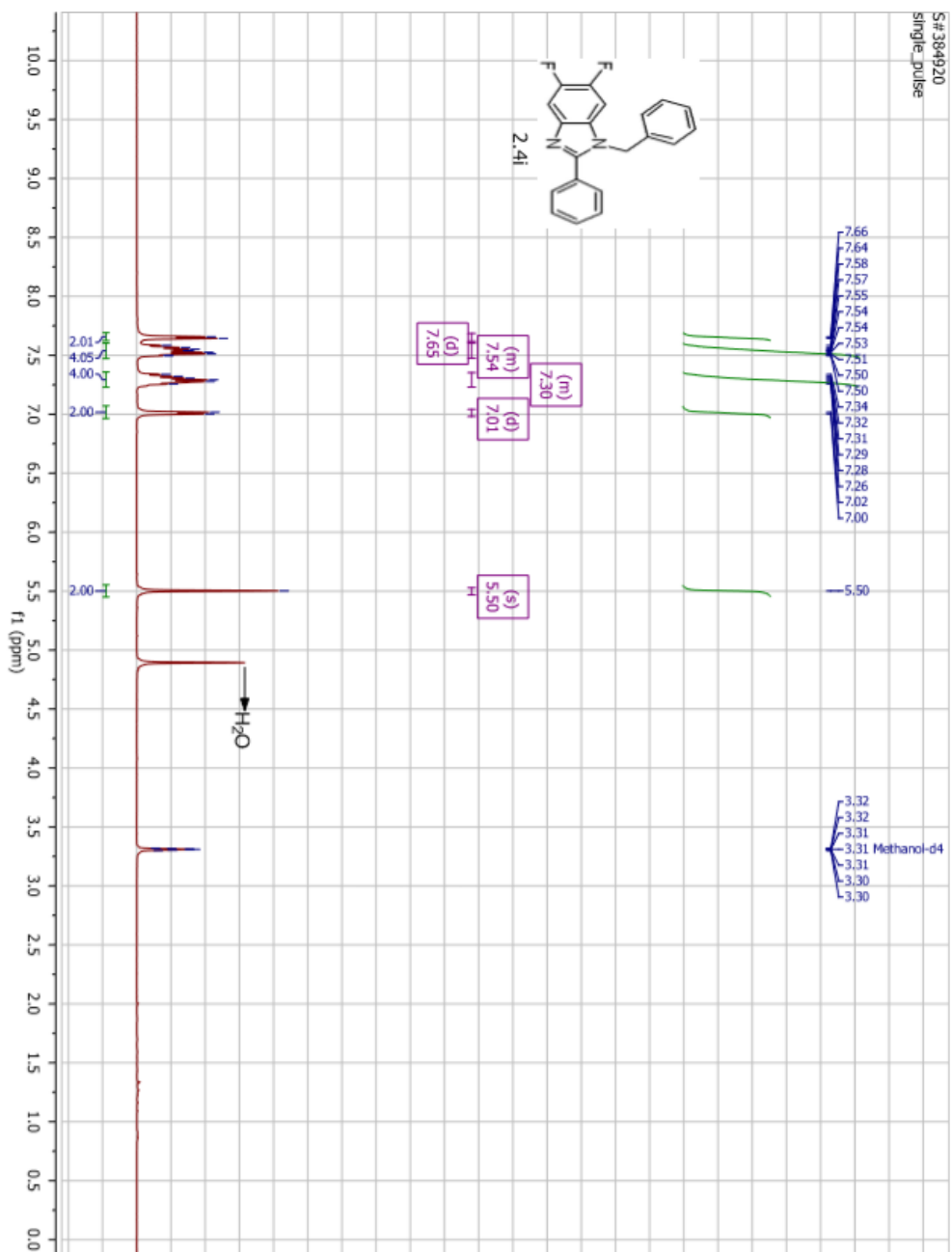


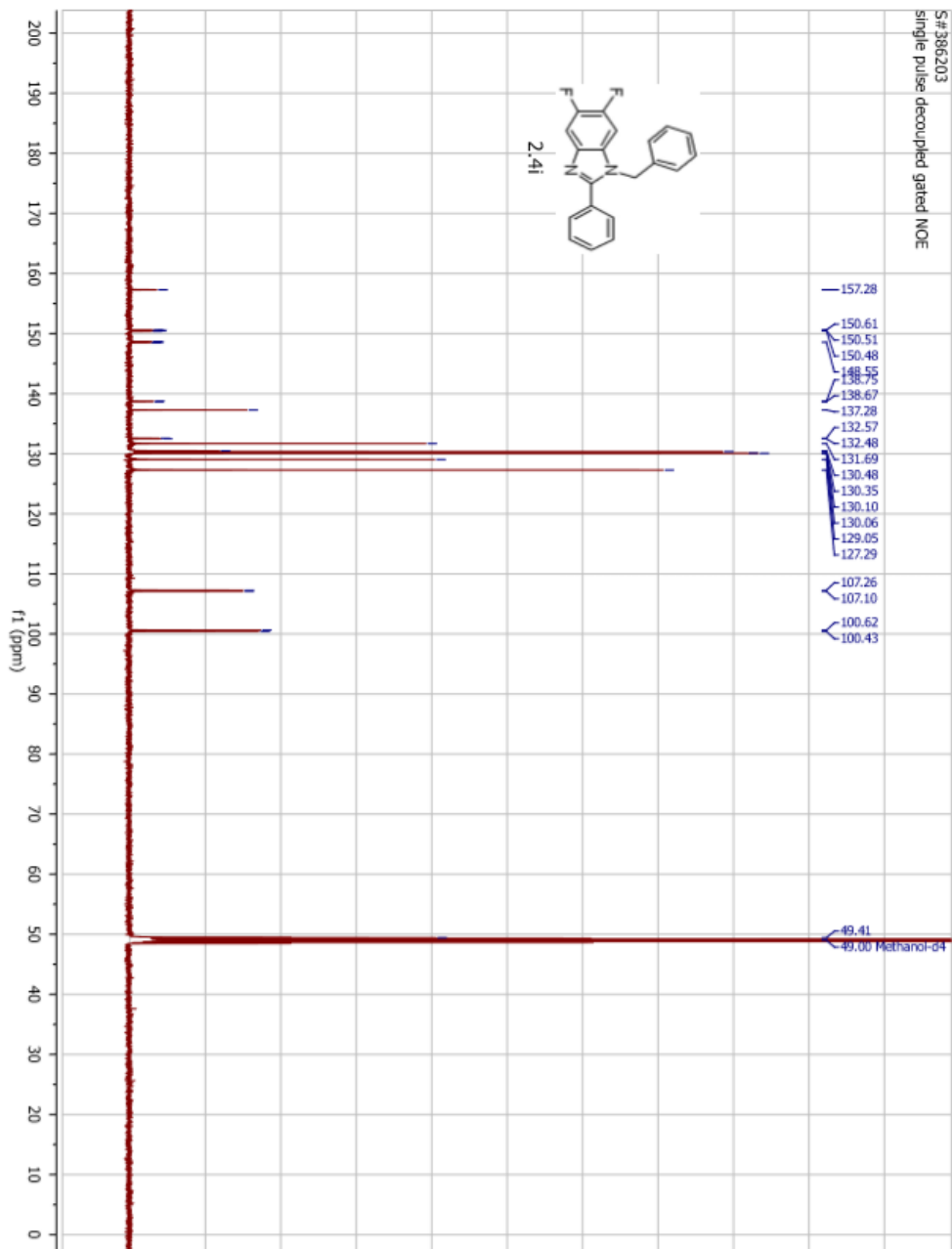




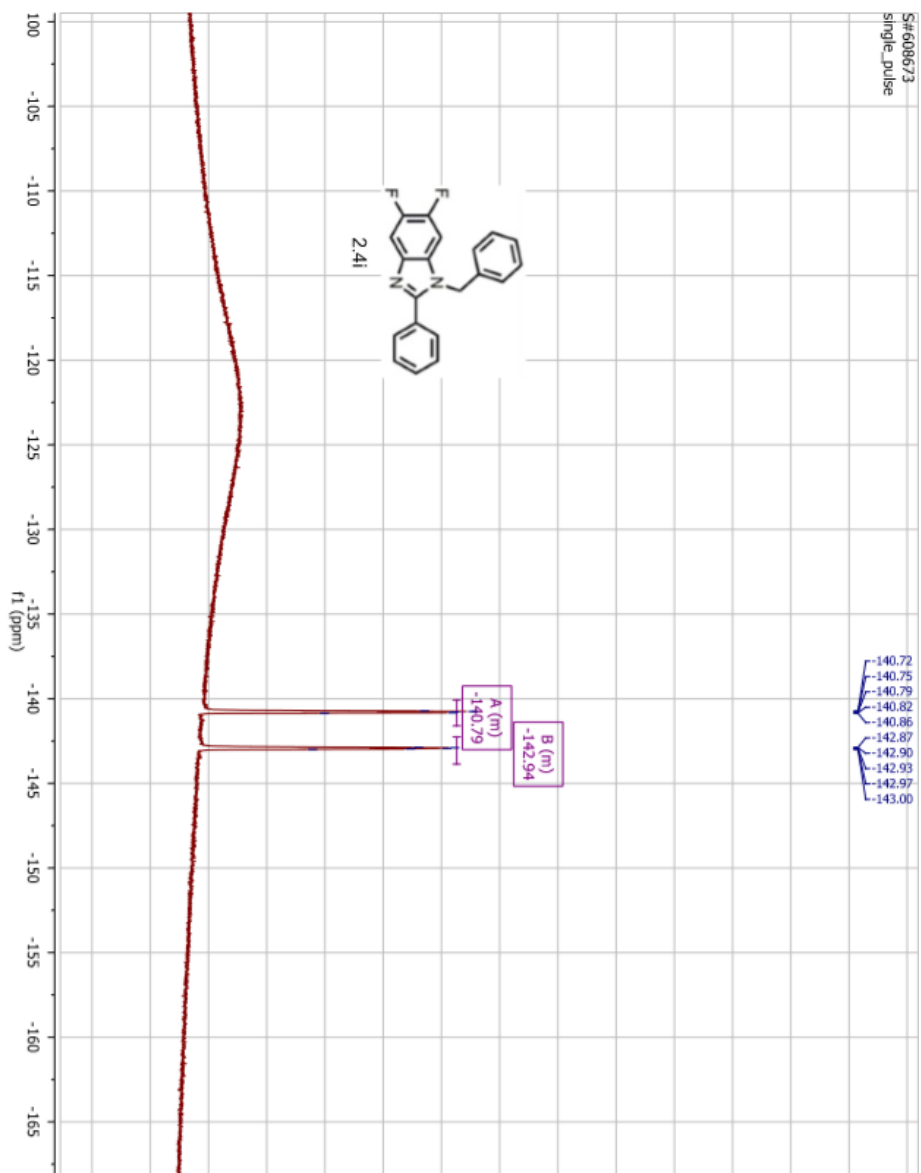


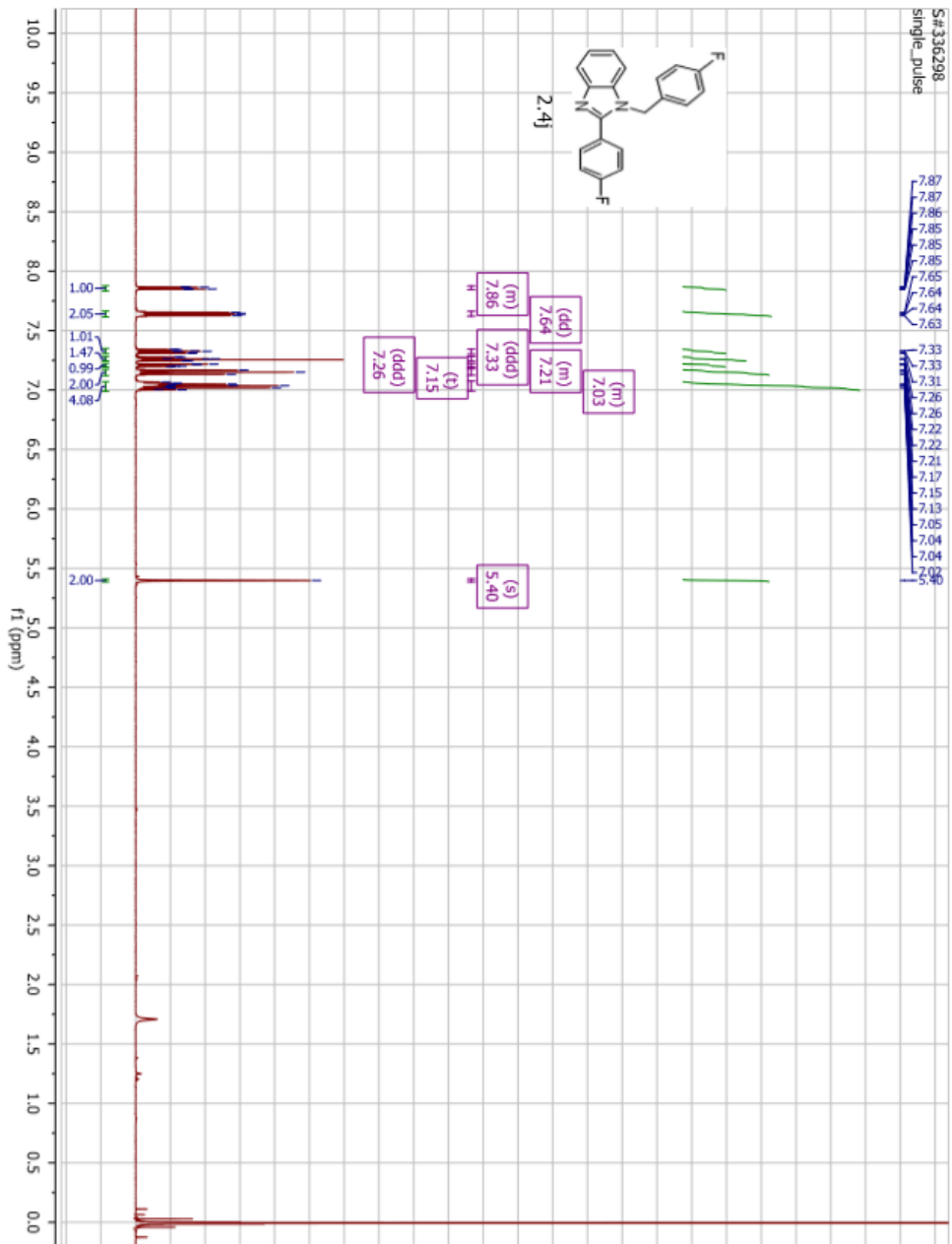


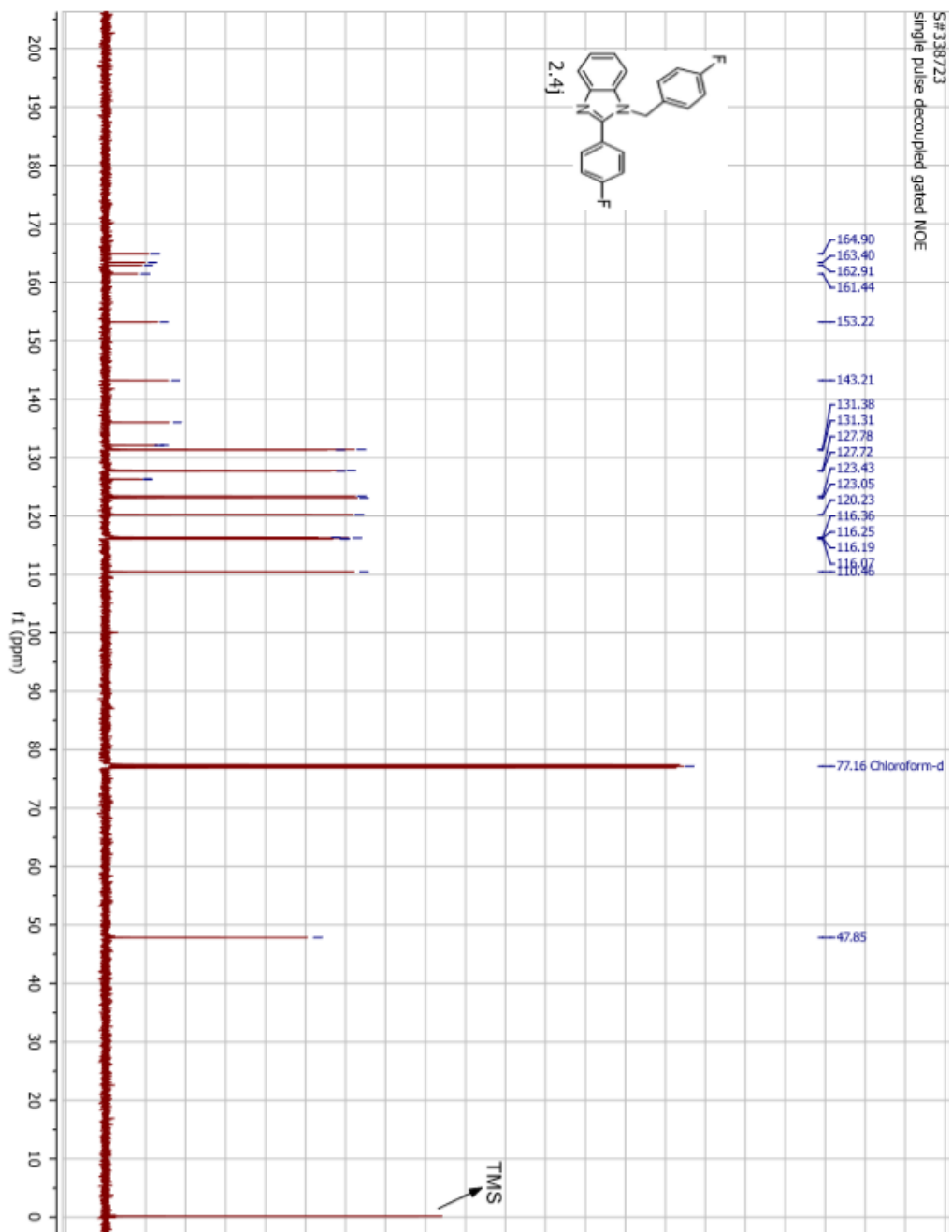


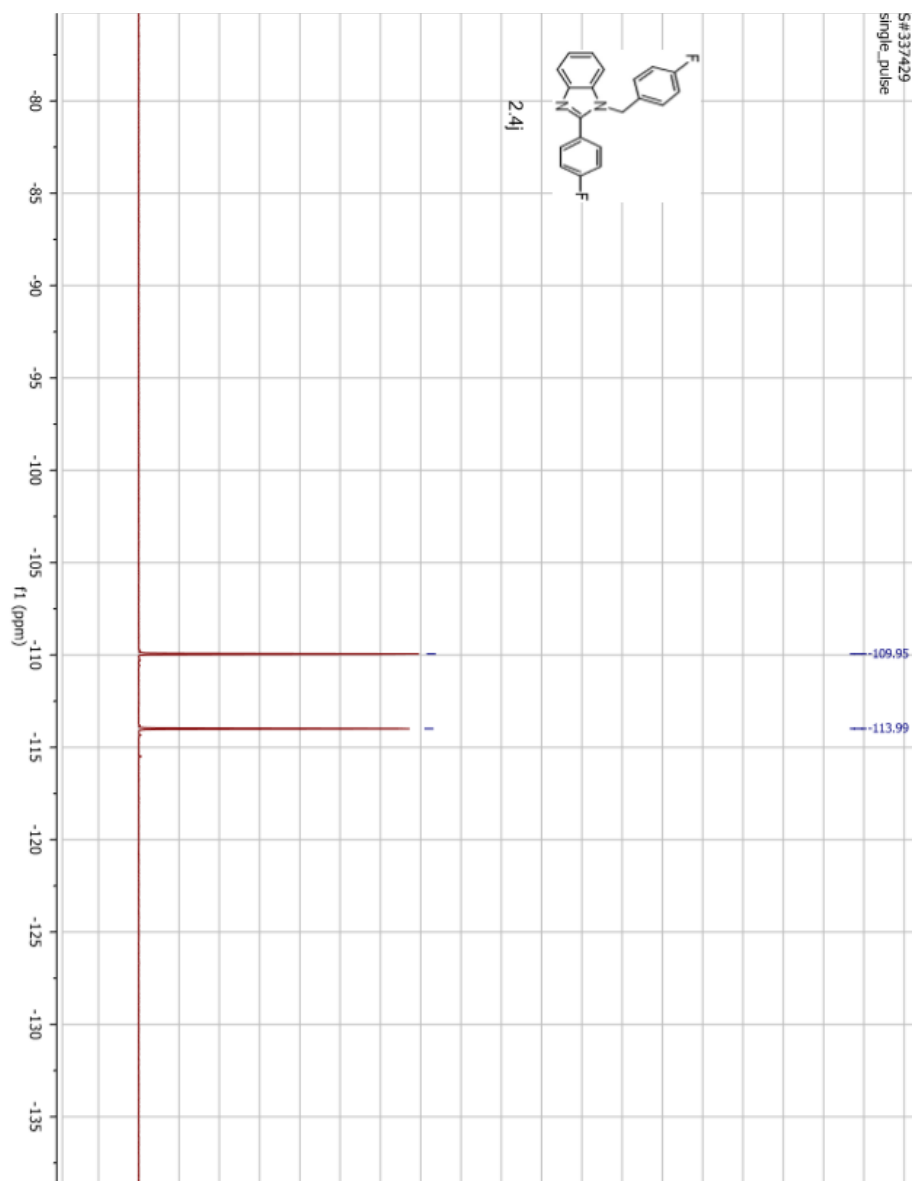


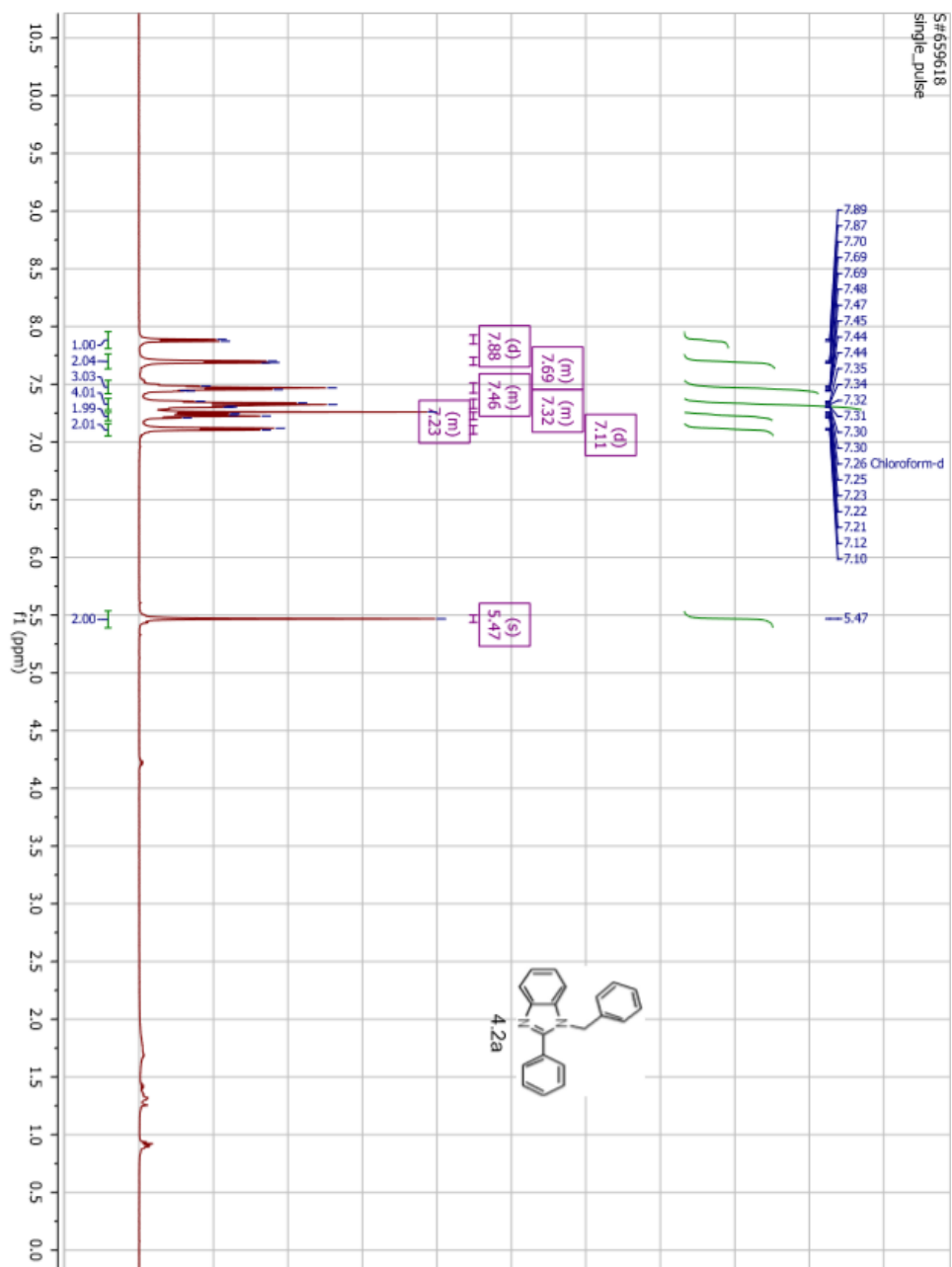
S#608673
single_pulse



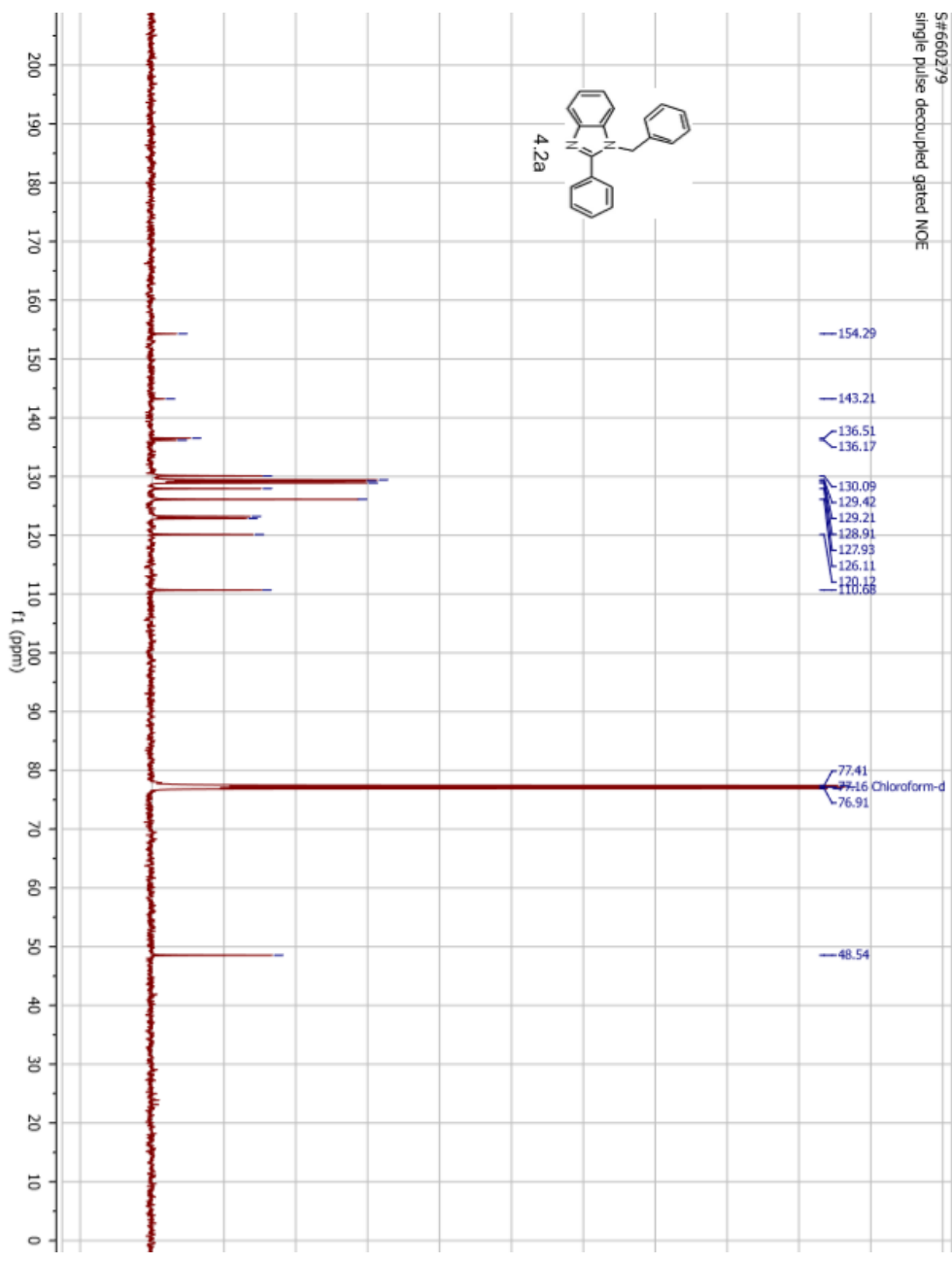
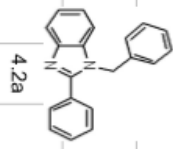


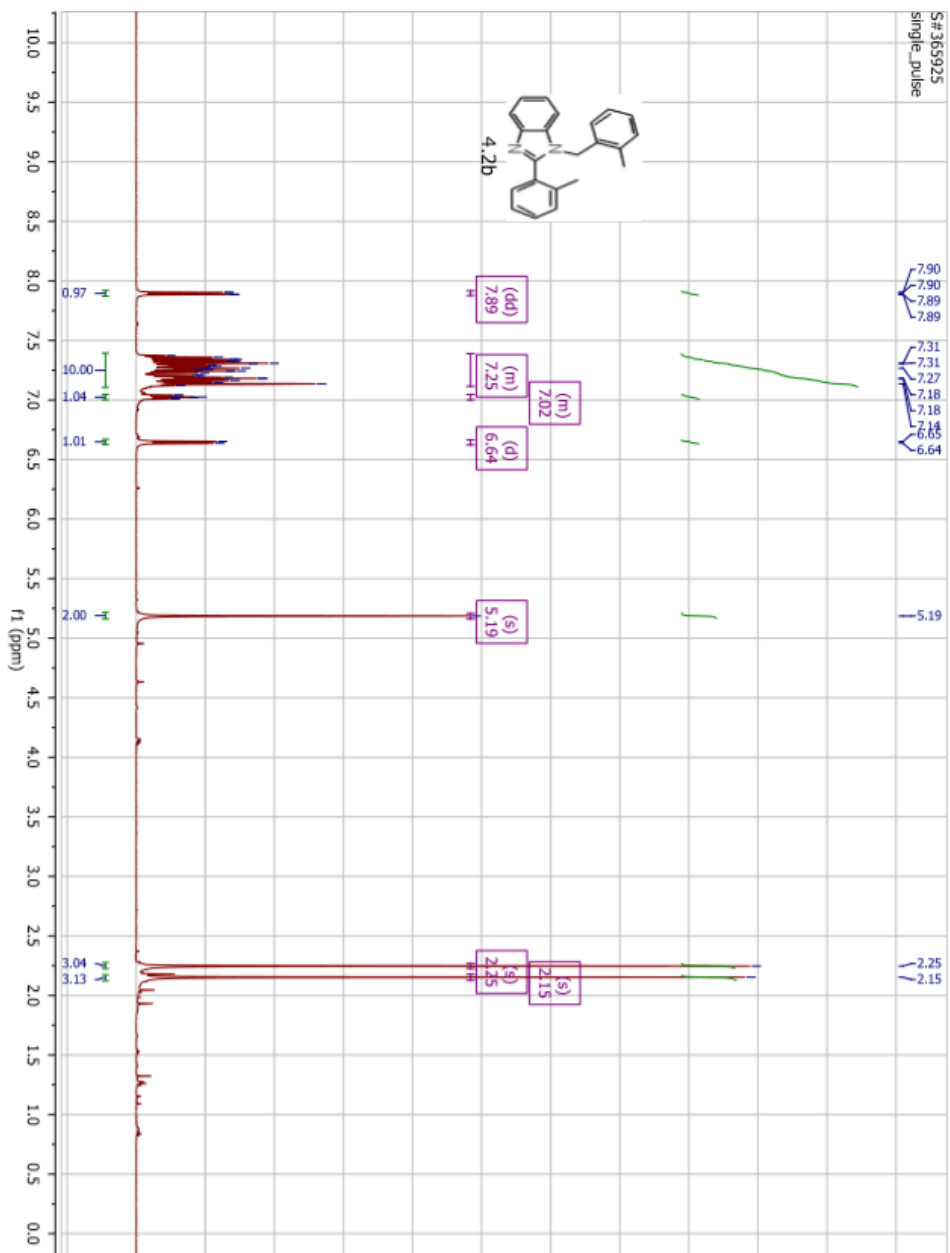


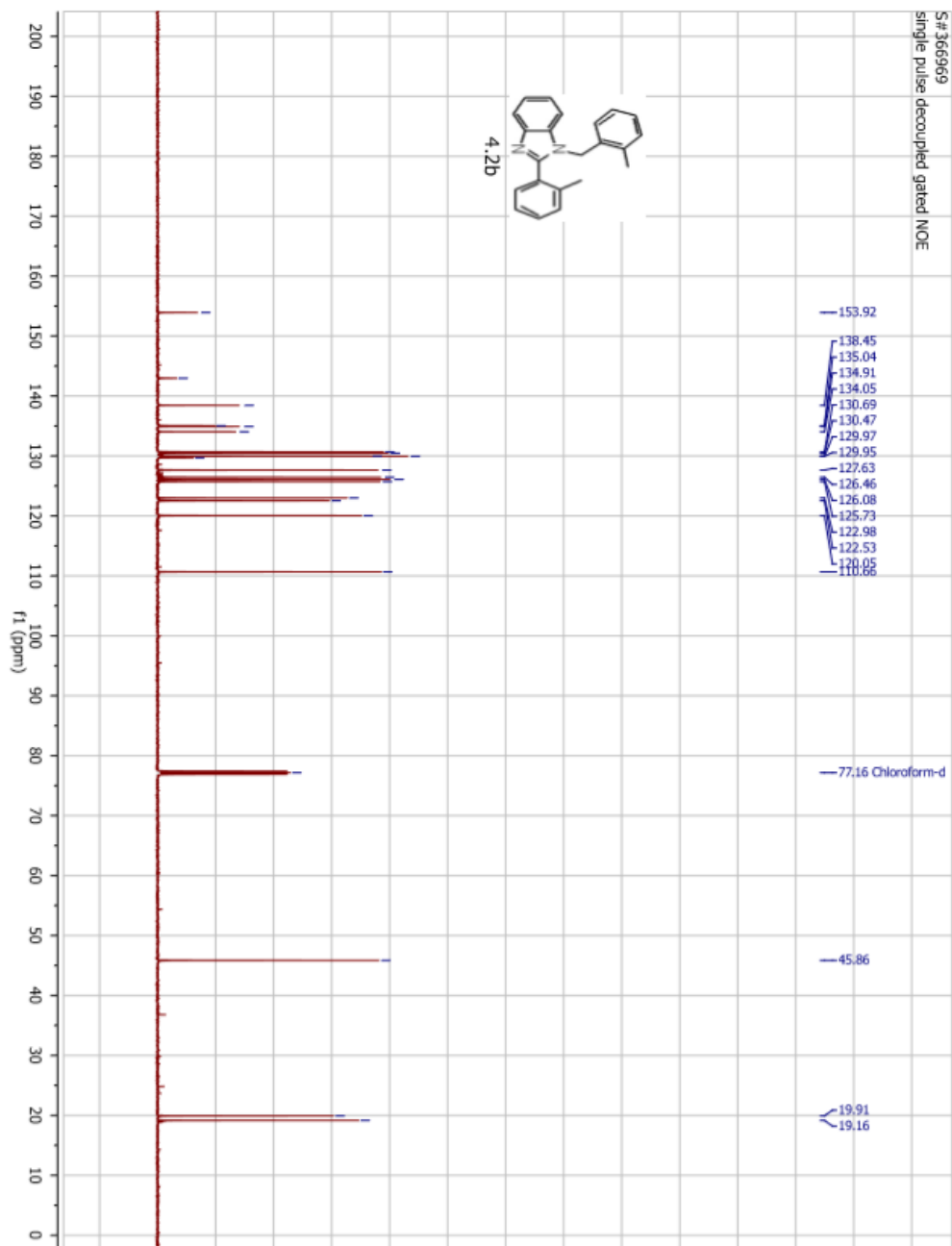


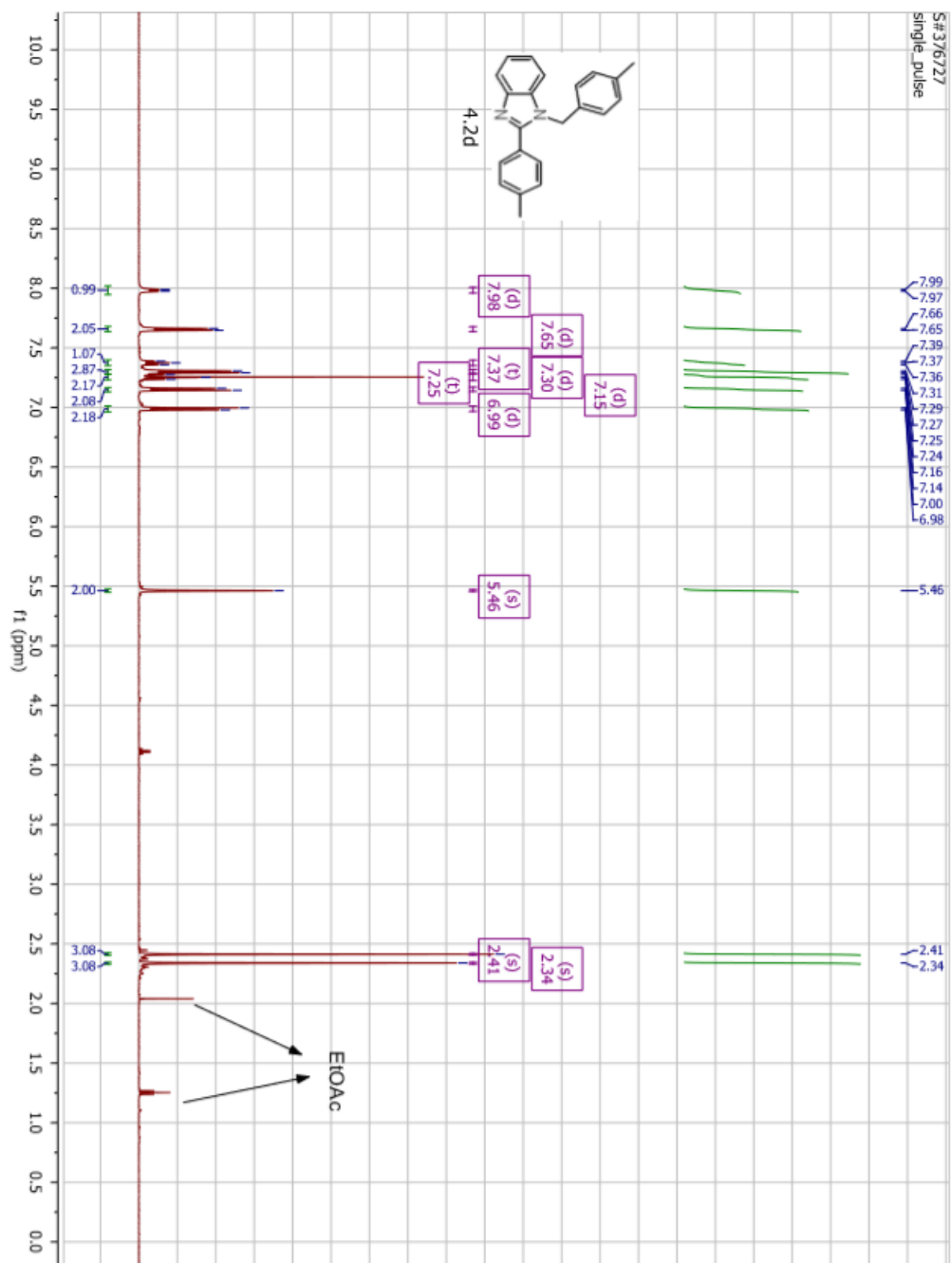


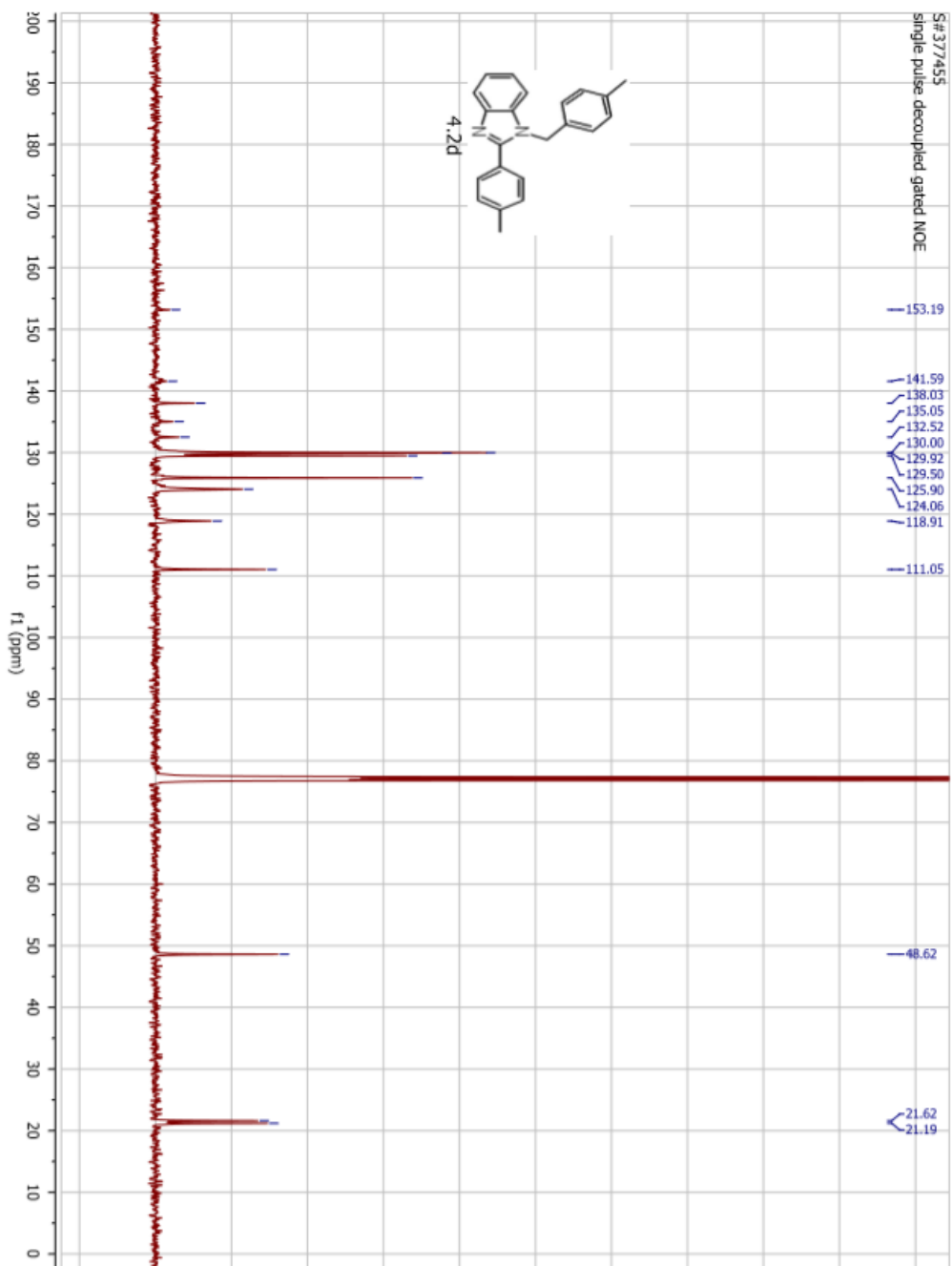
S#660279
single pulse decoupled gated NOE

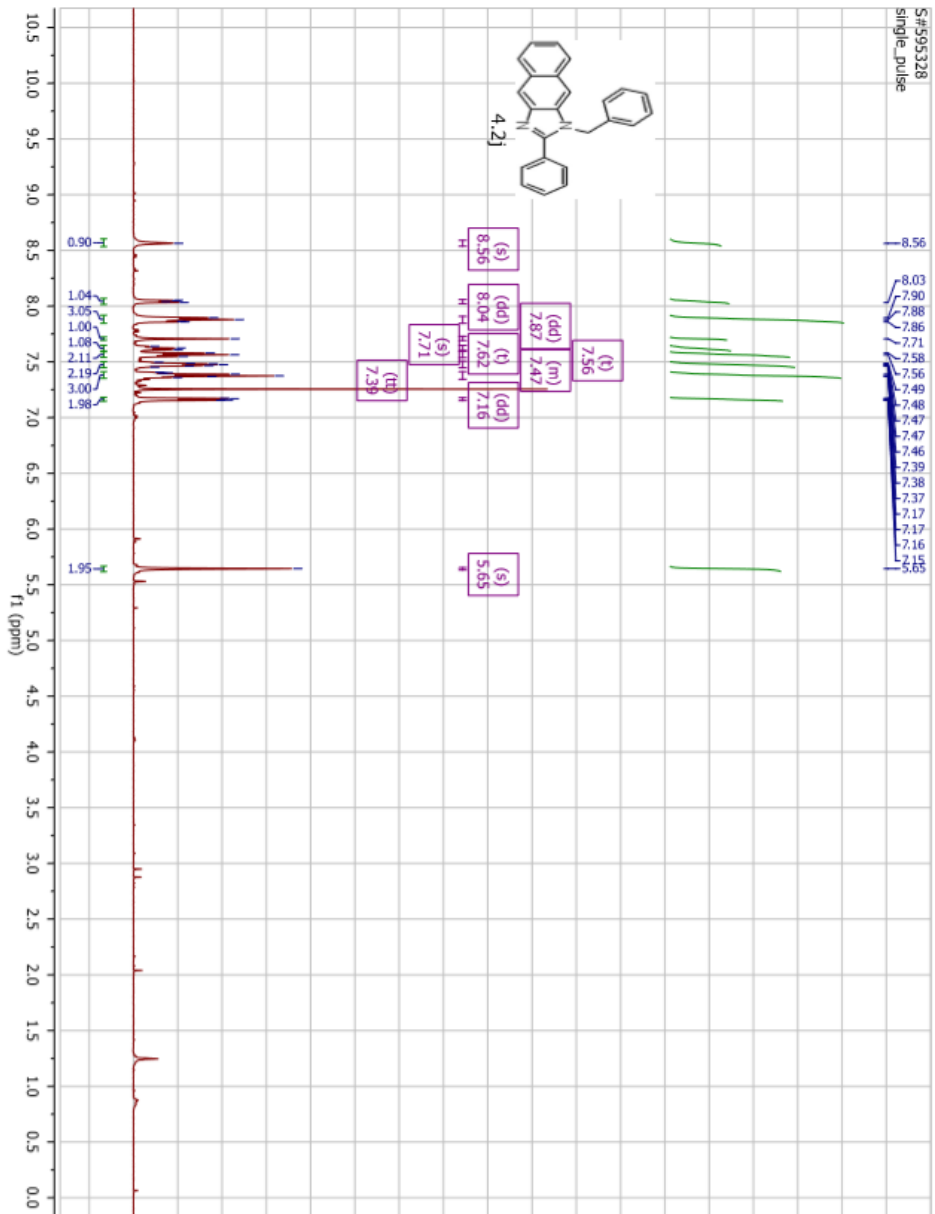


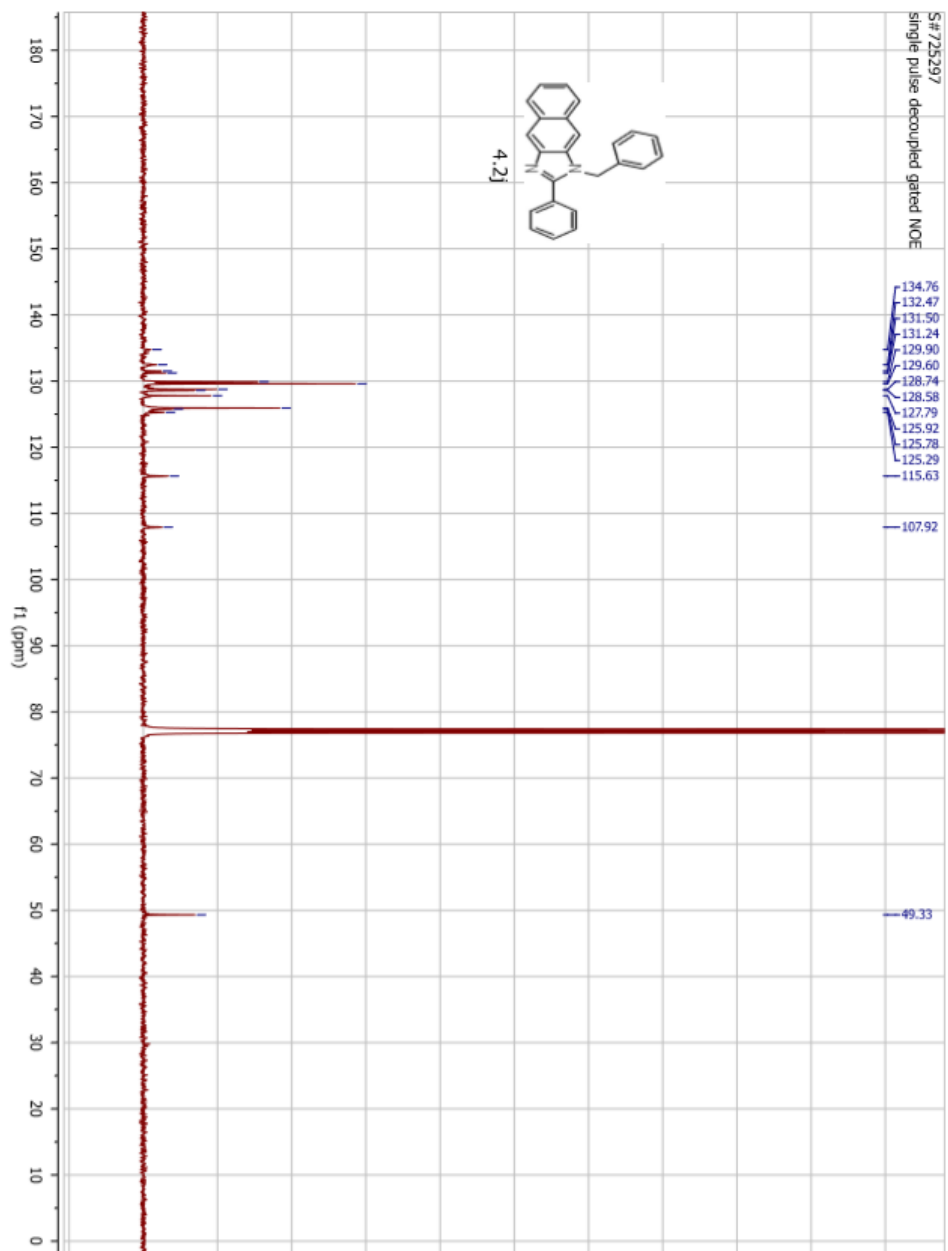


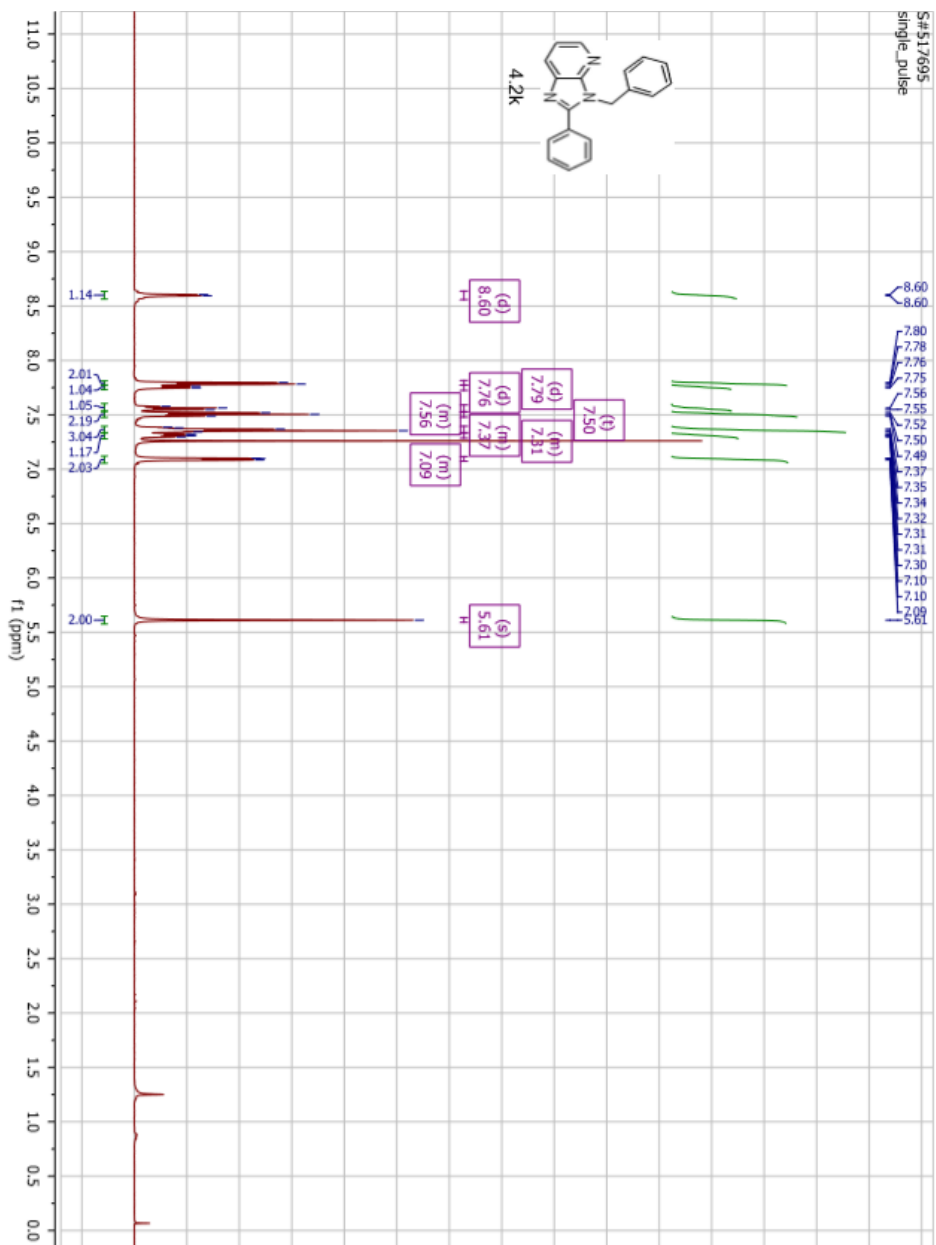


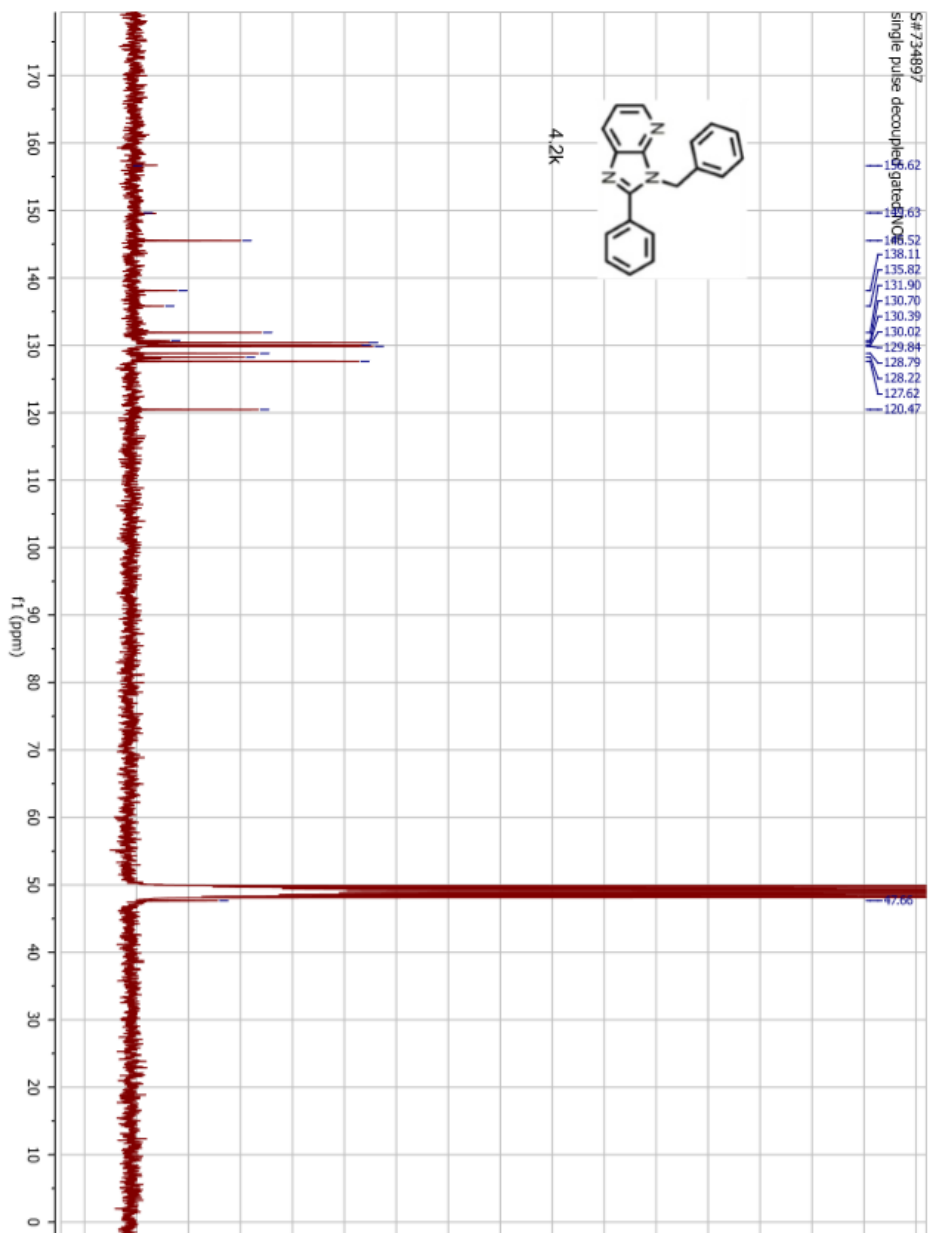


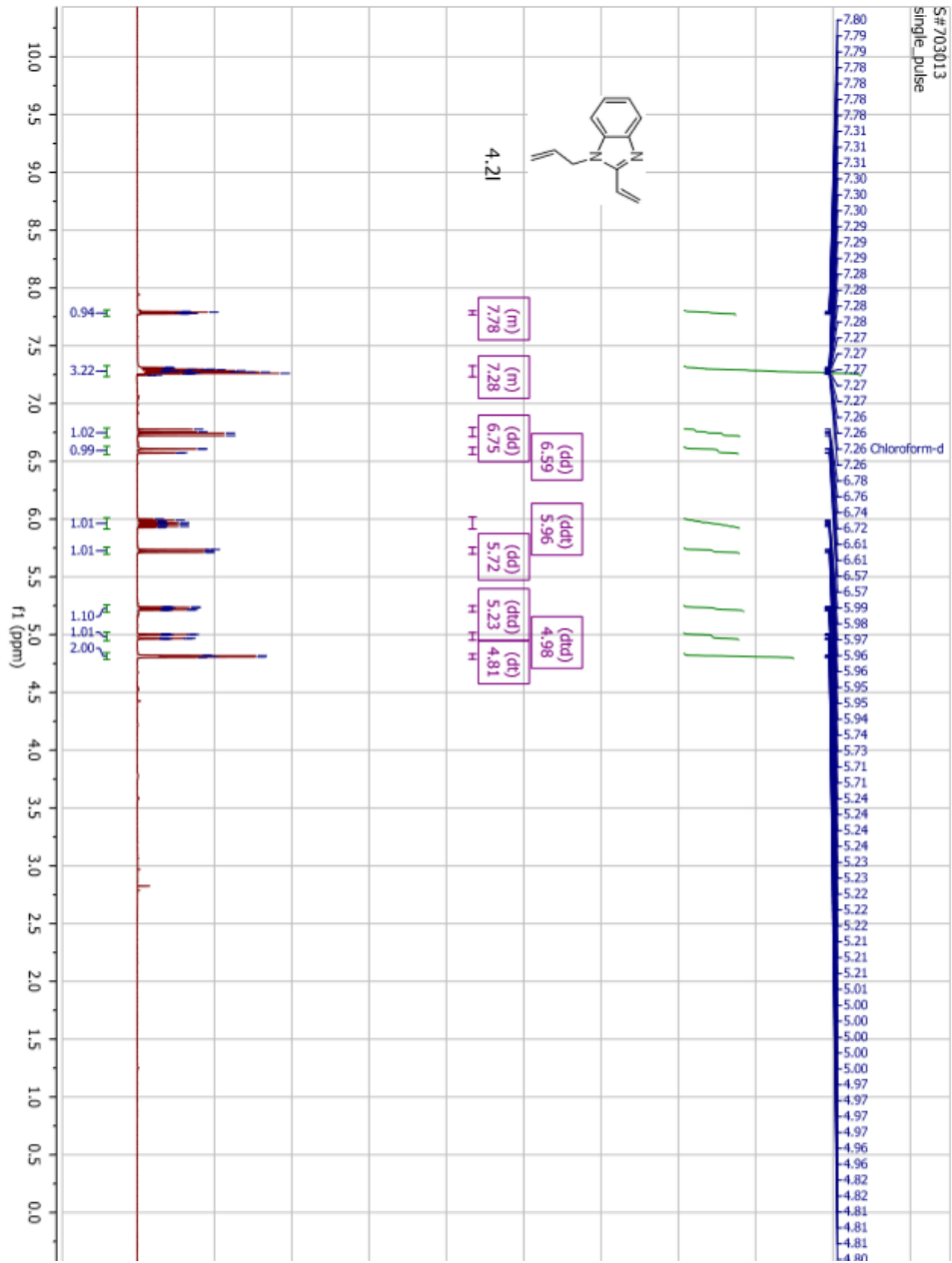


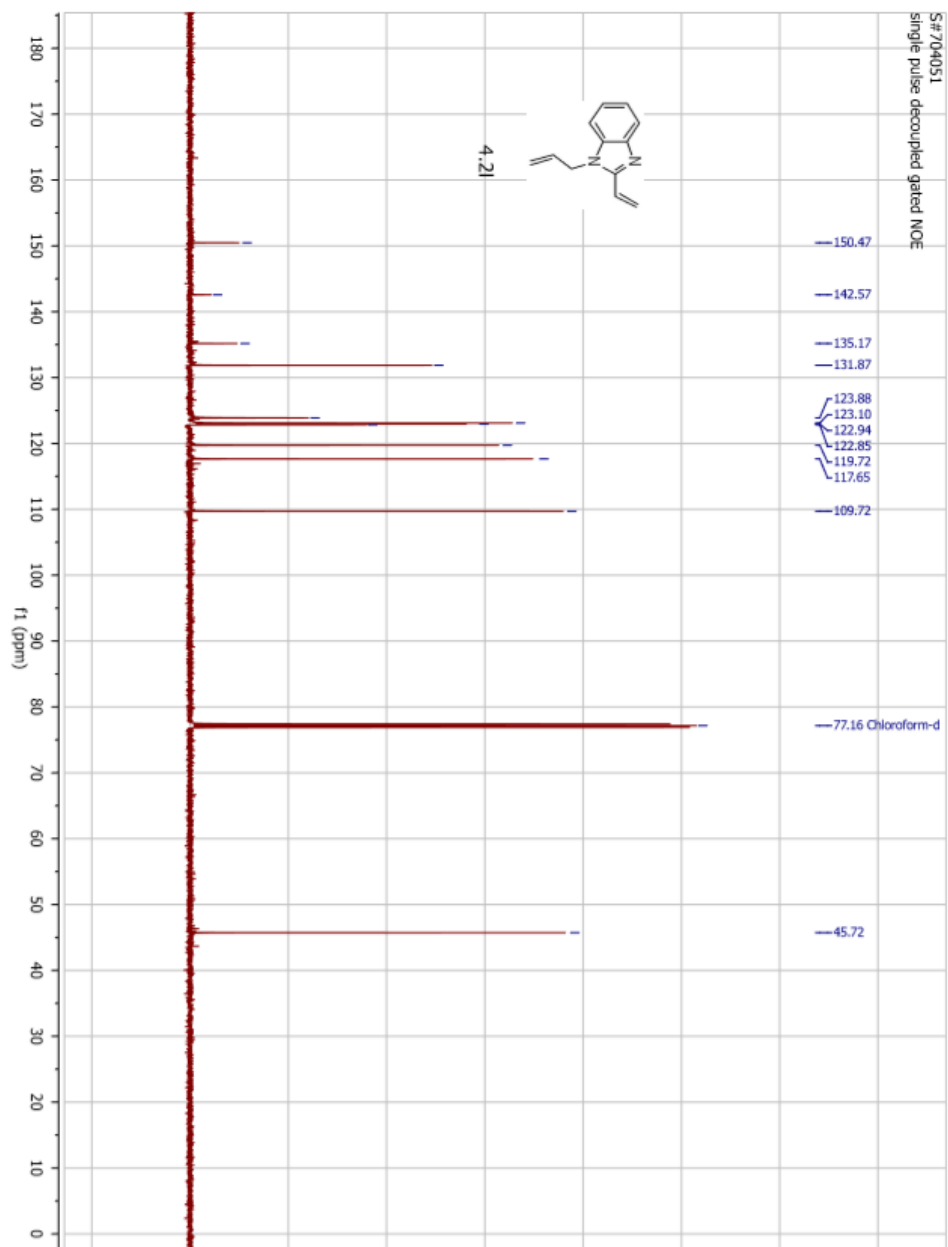


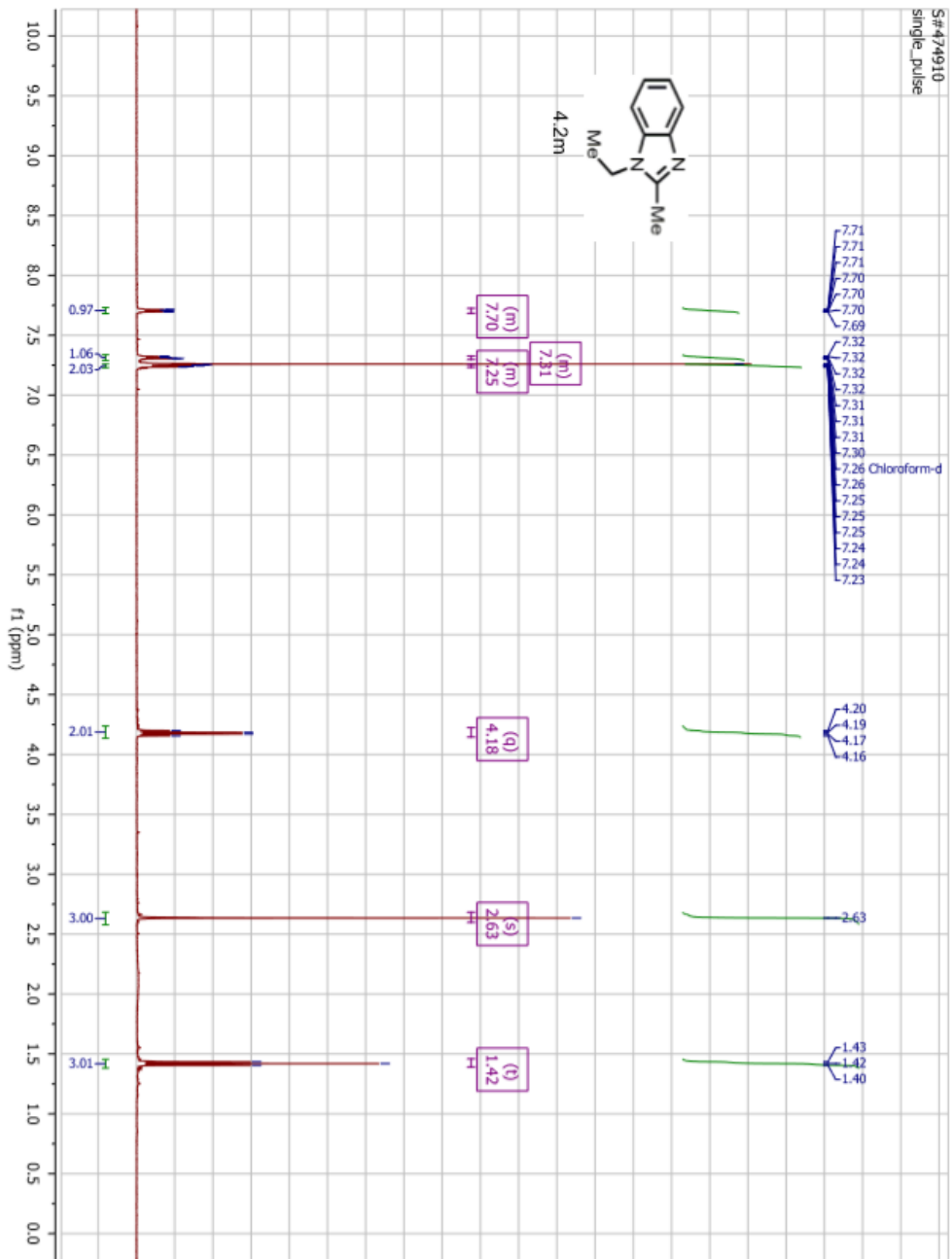


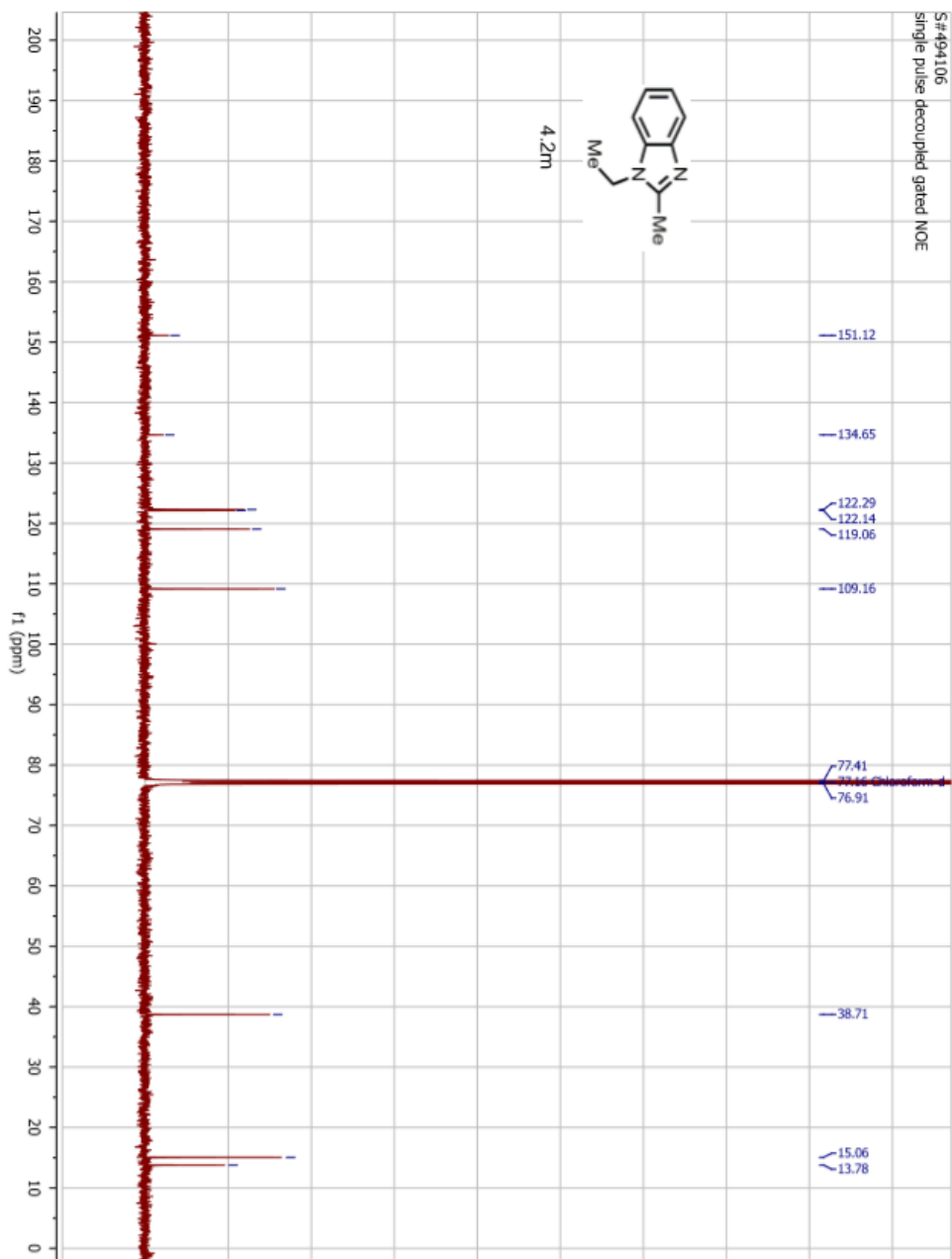


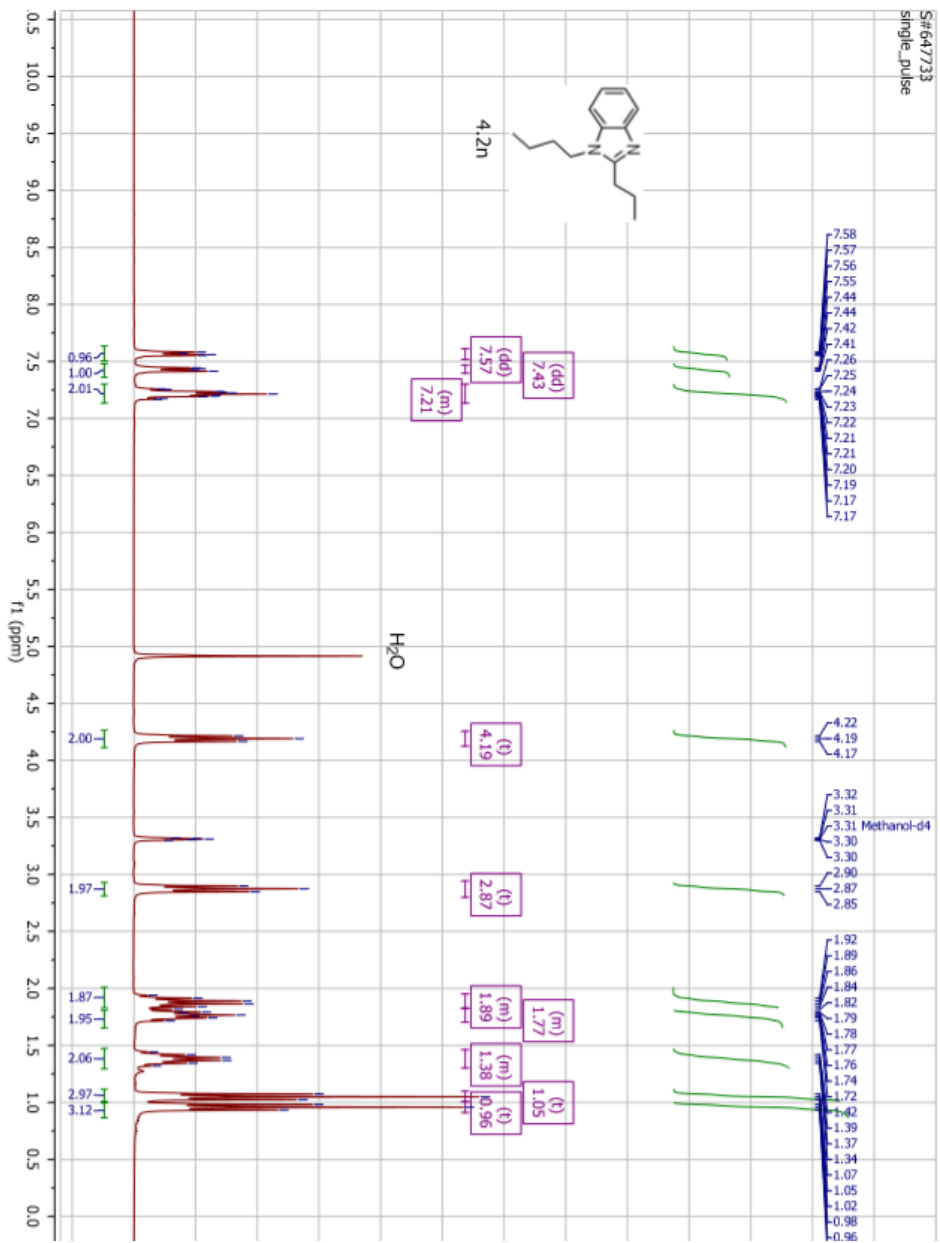




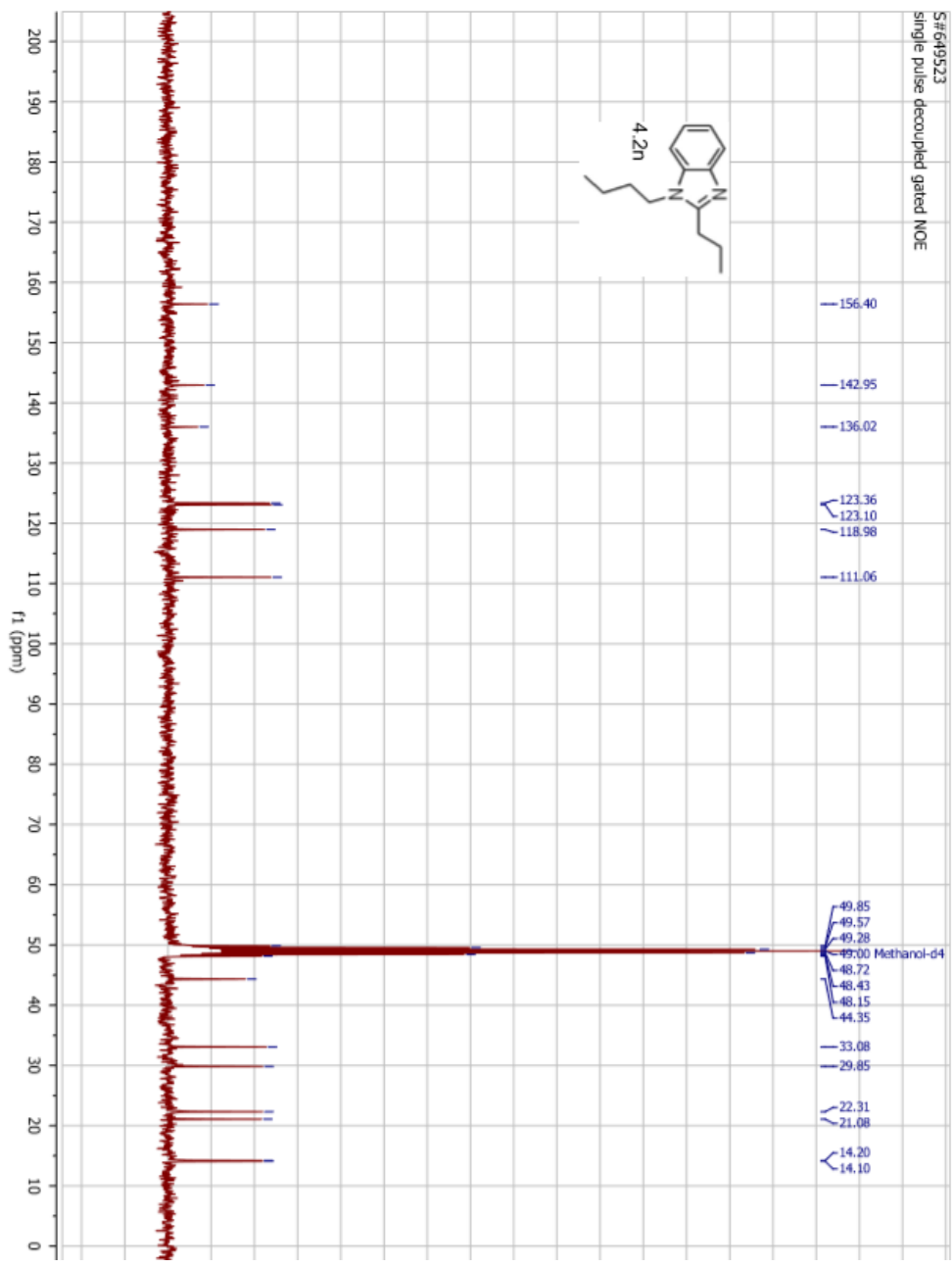
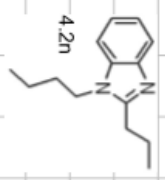


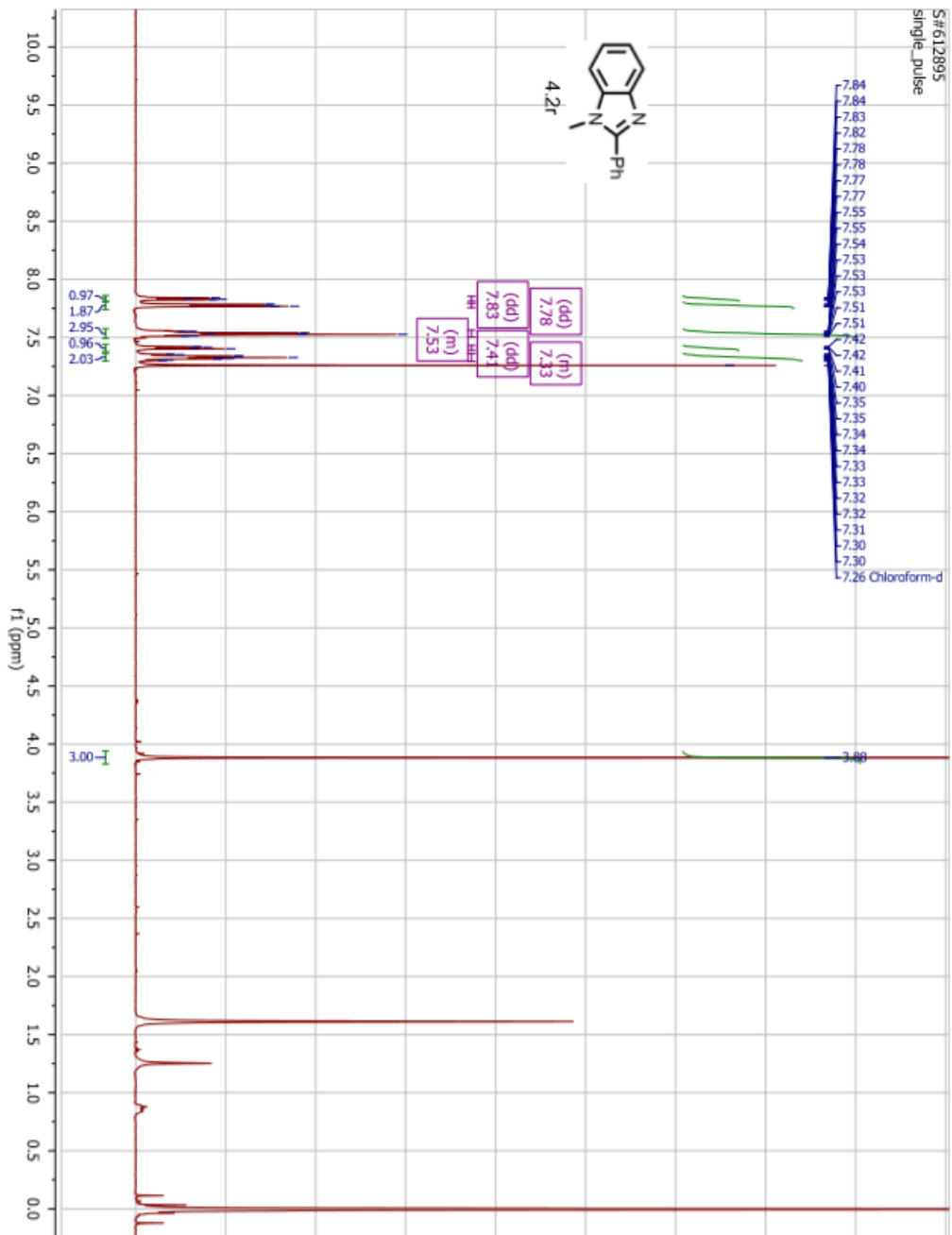




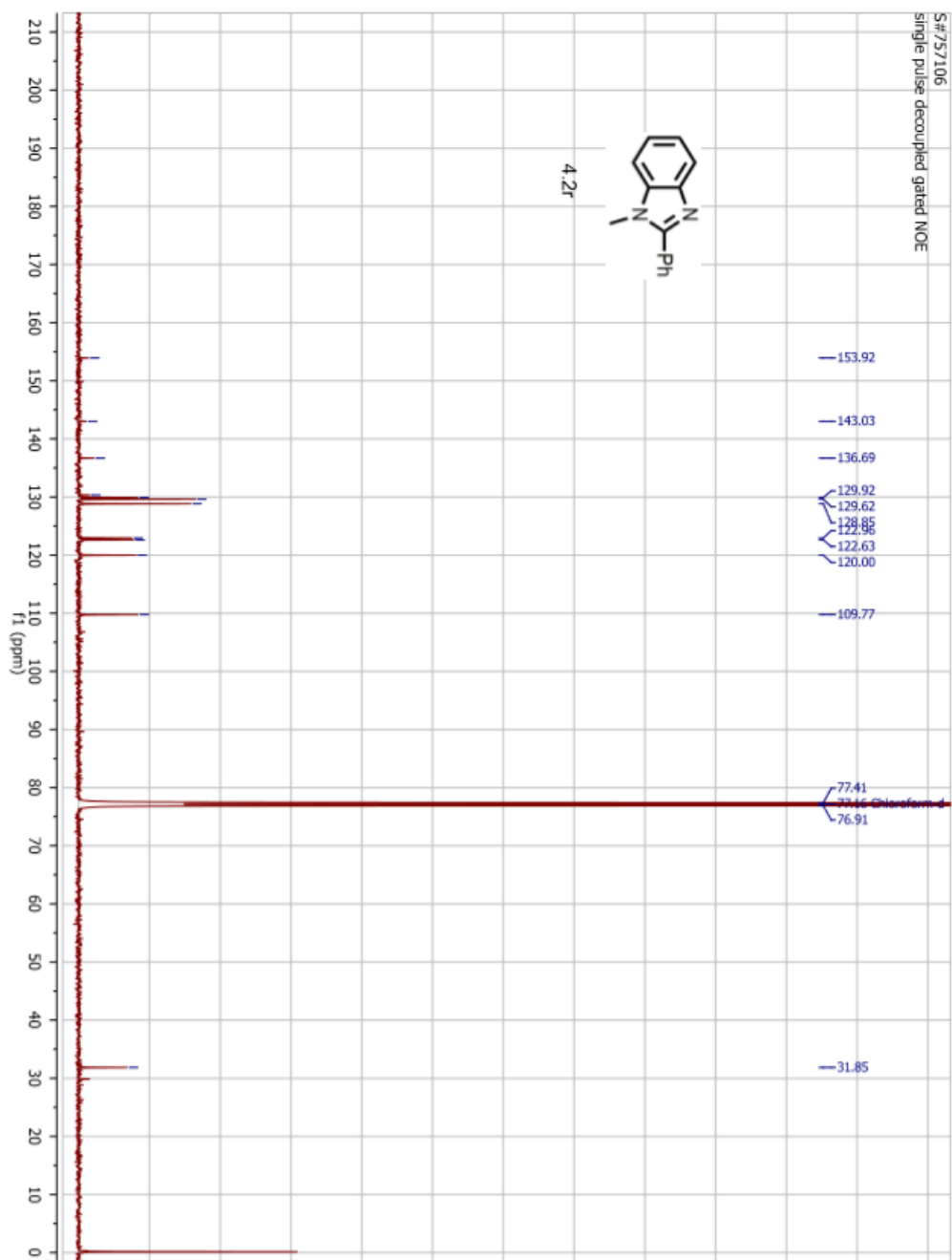


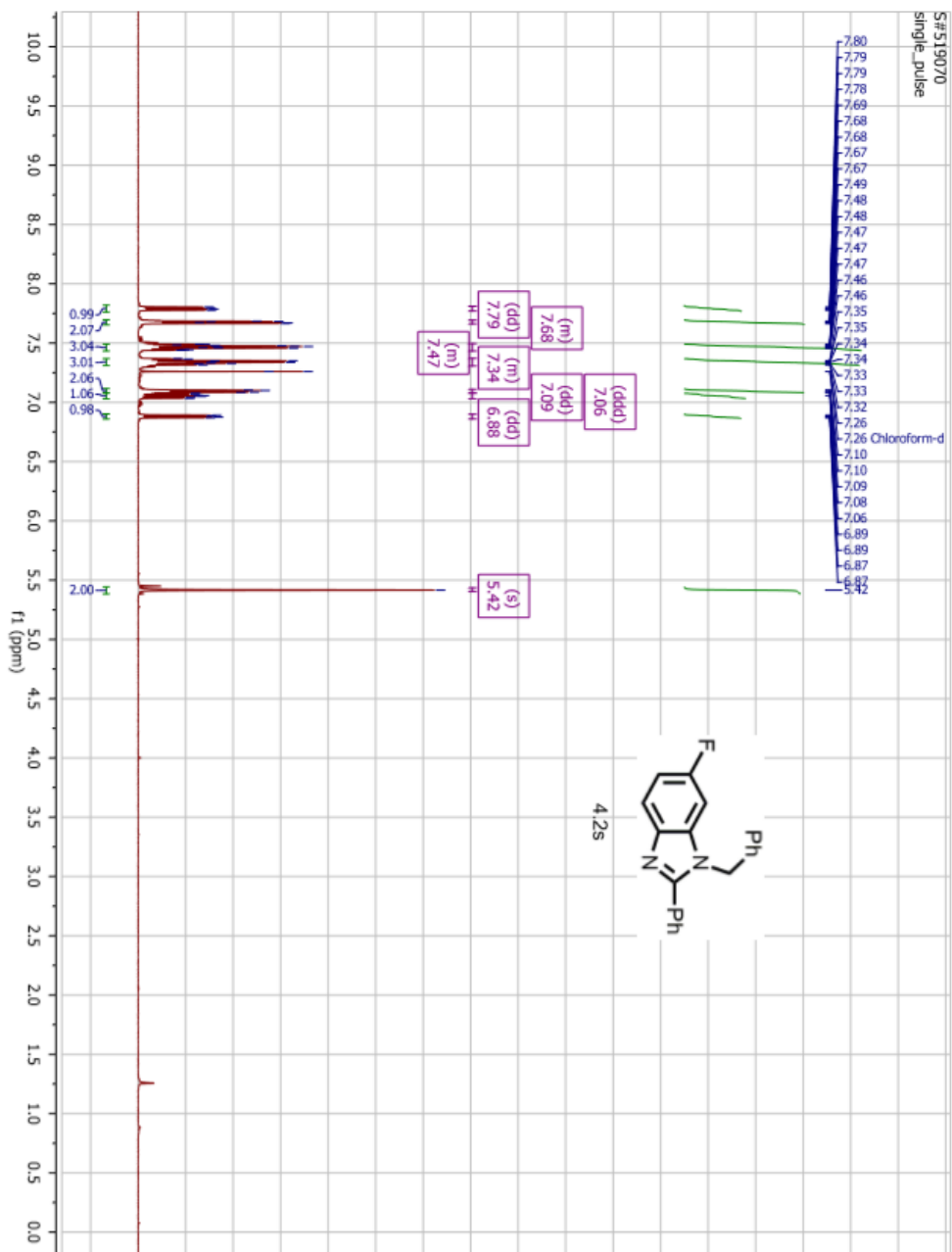
S#649523
single pulse decoupled gated NOE



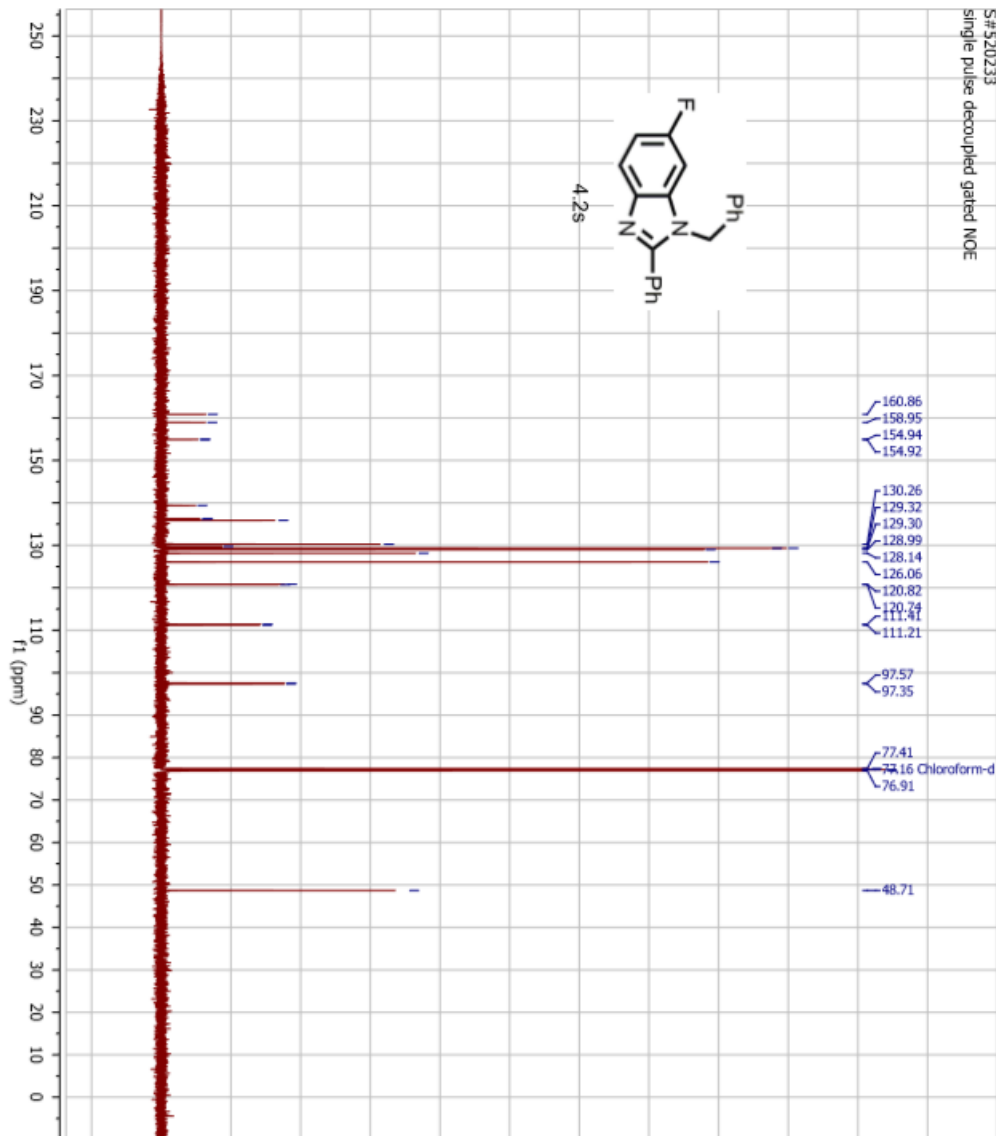
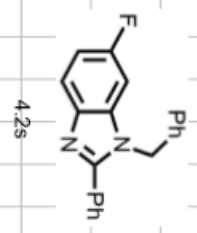


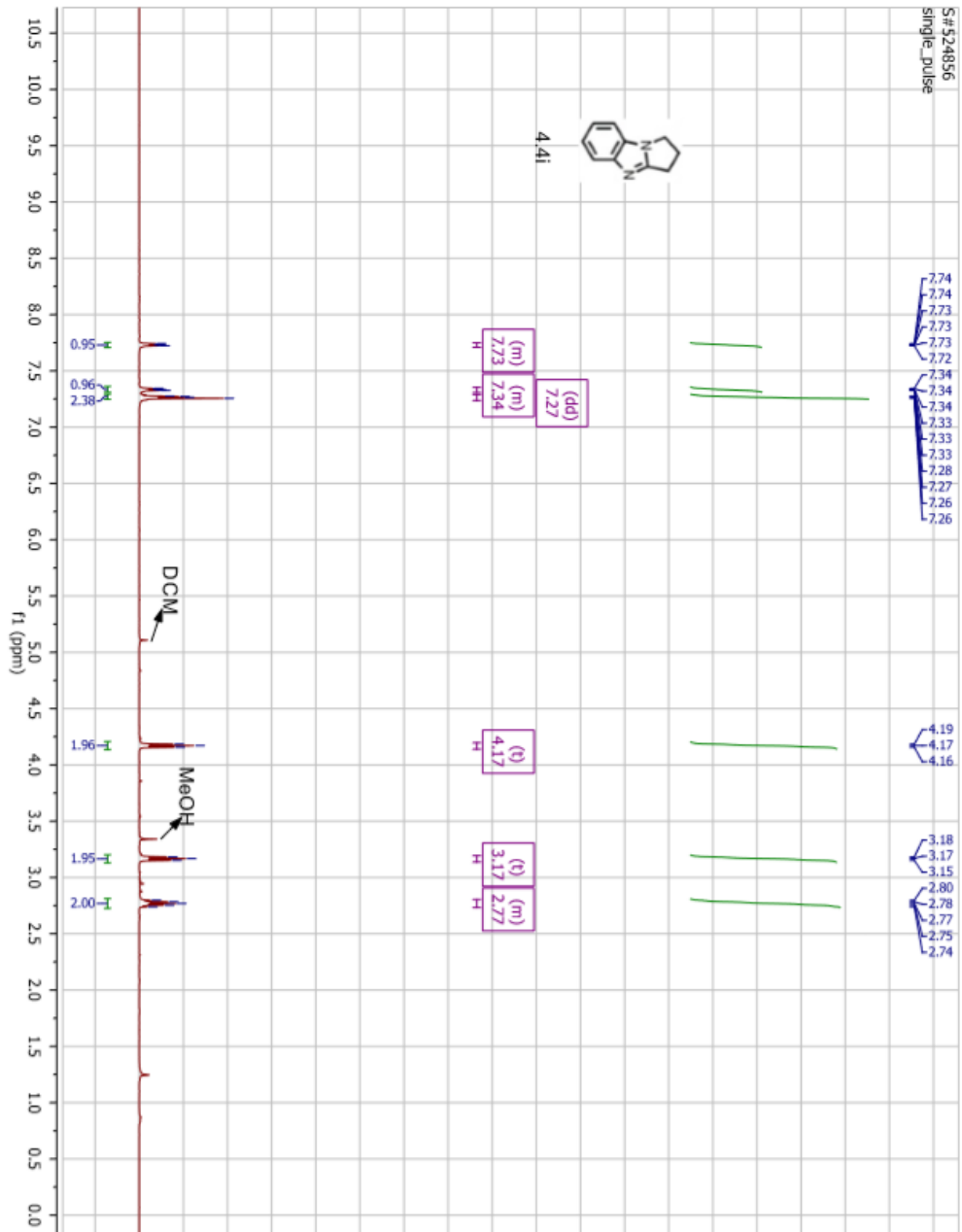
S#757106
single pulse decoupled gated NOE

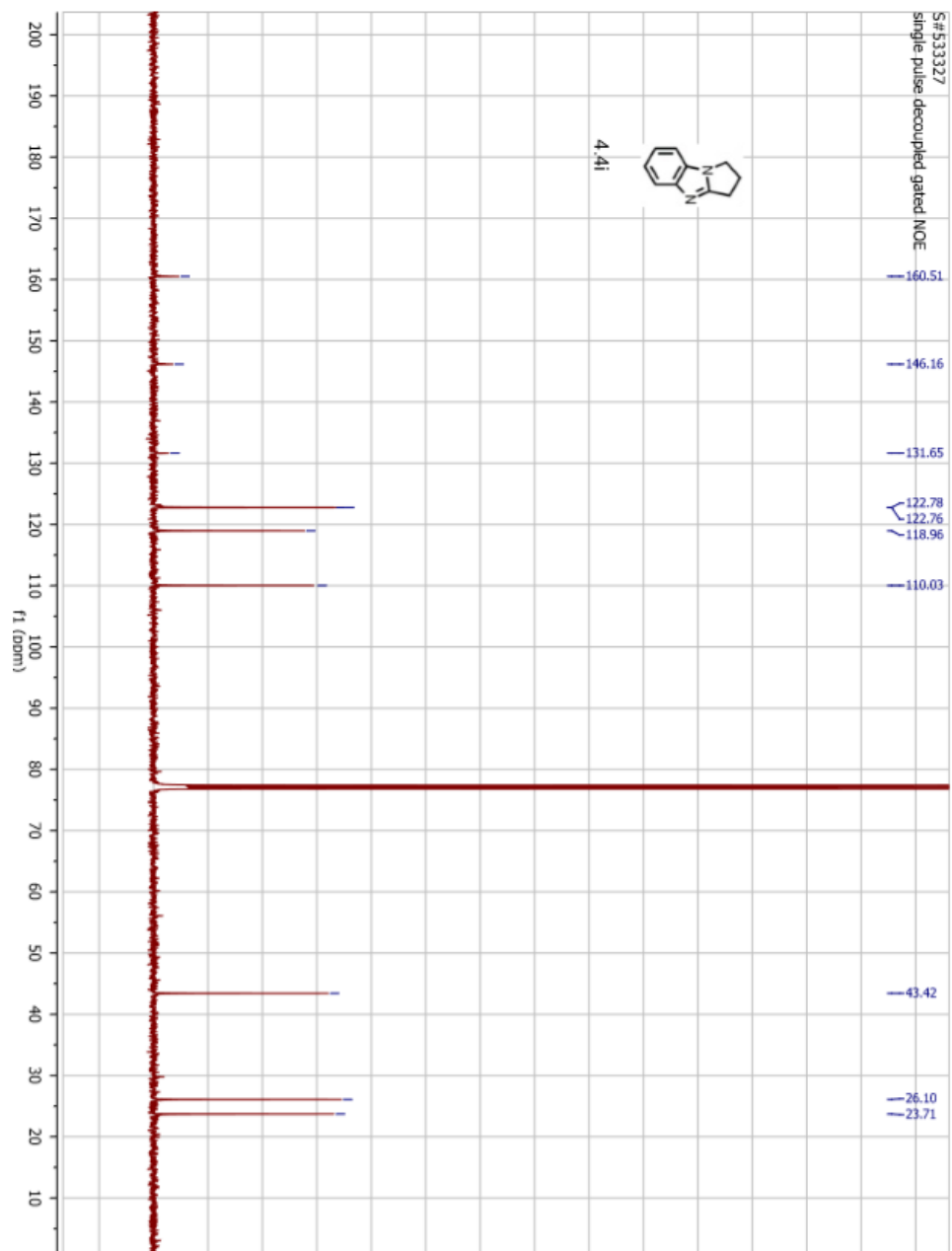


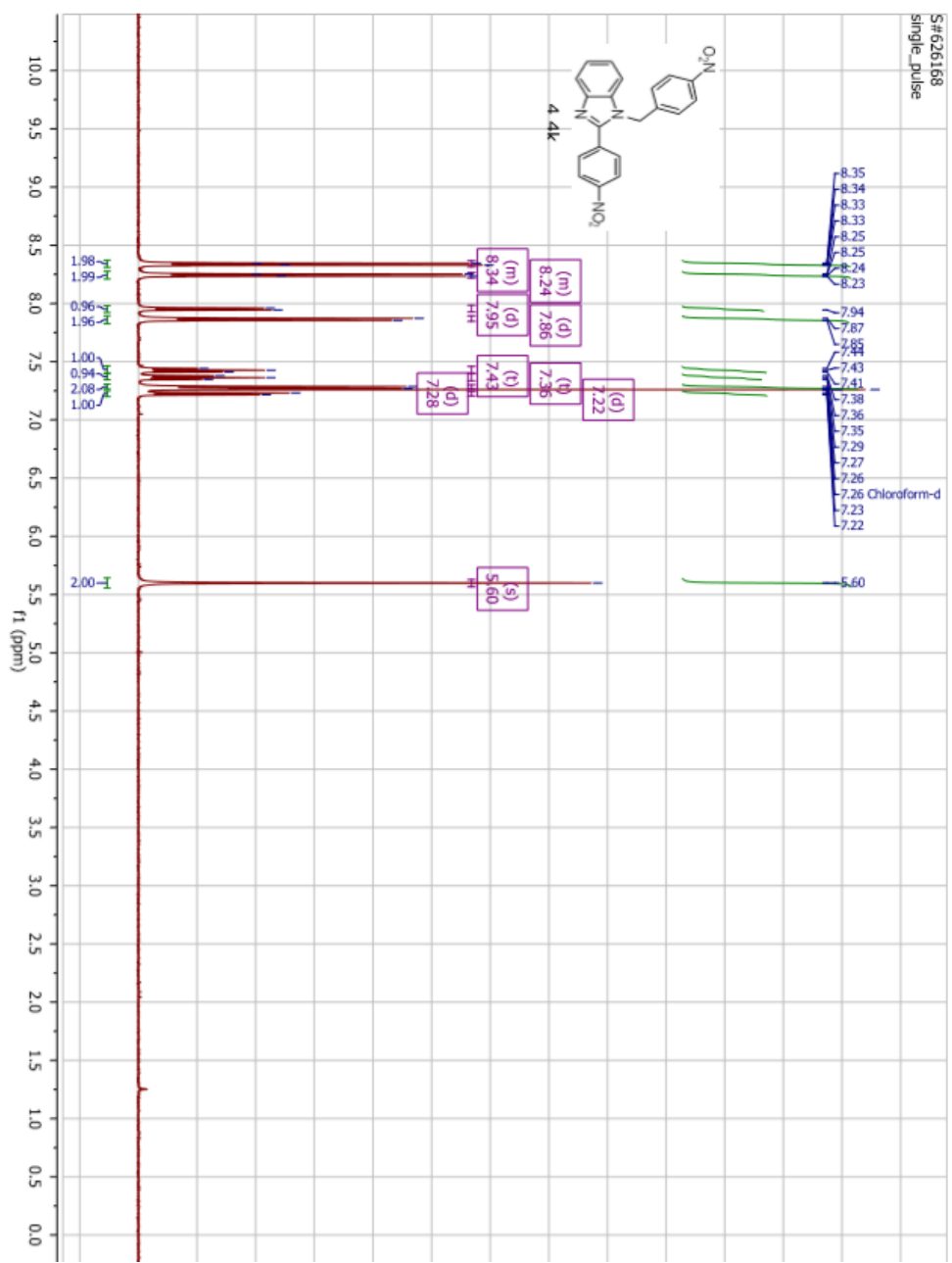


S#520233
single pulse decoupled gated NOE

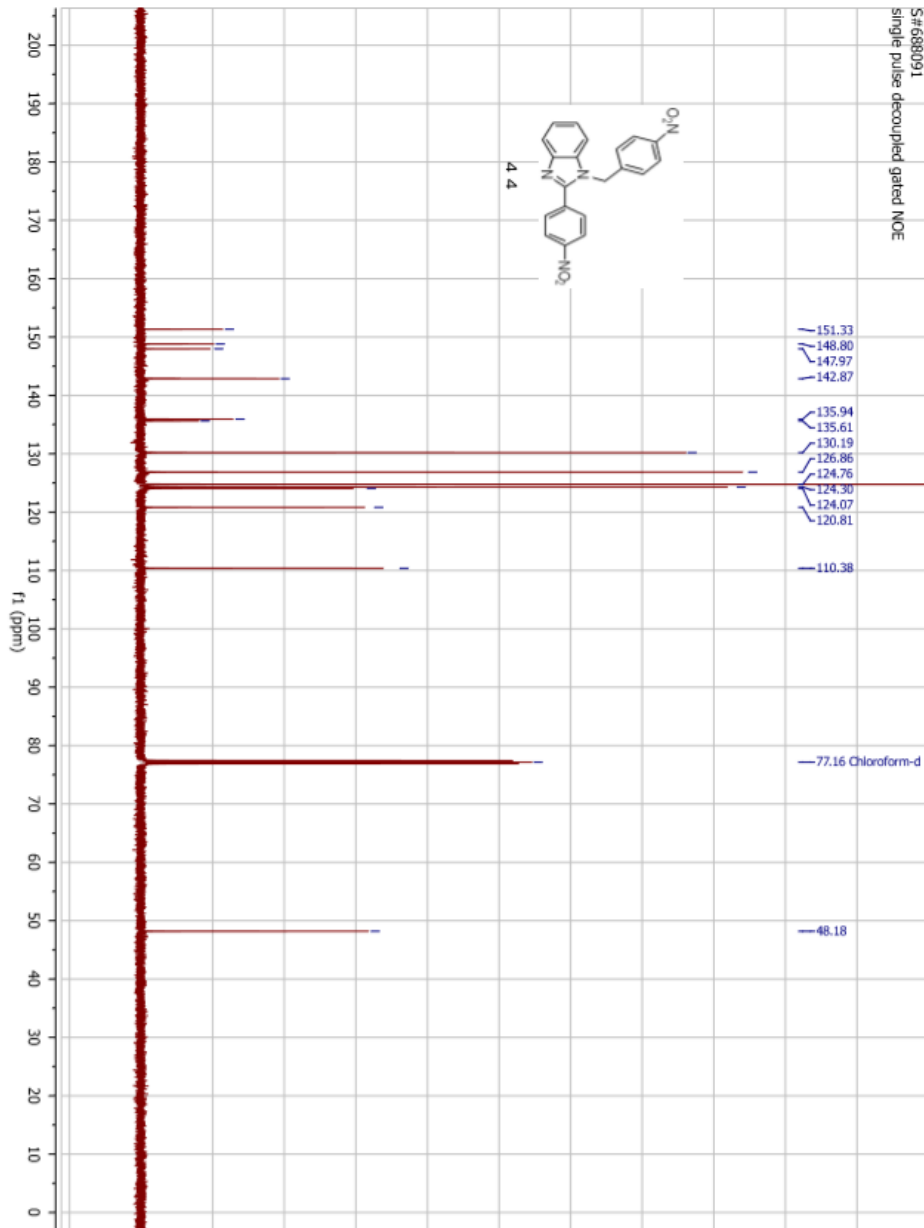
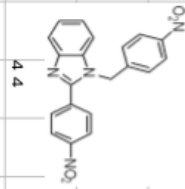


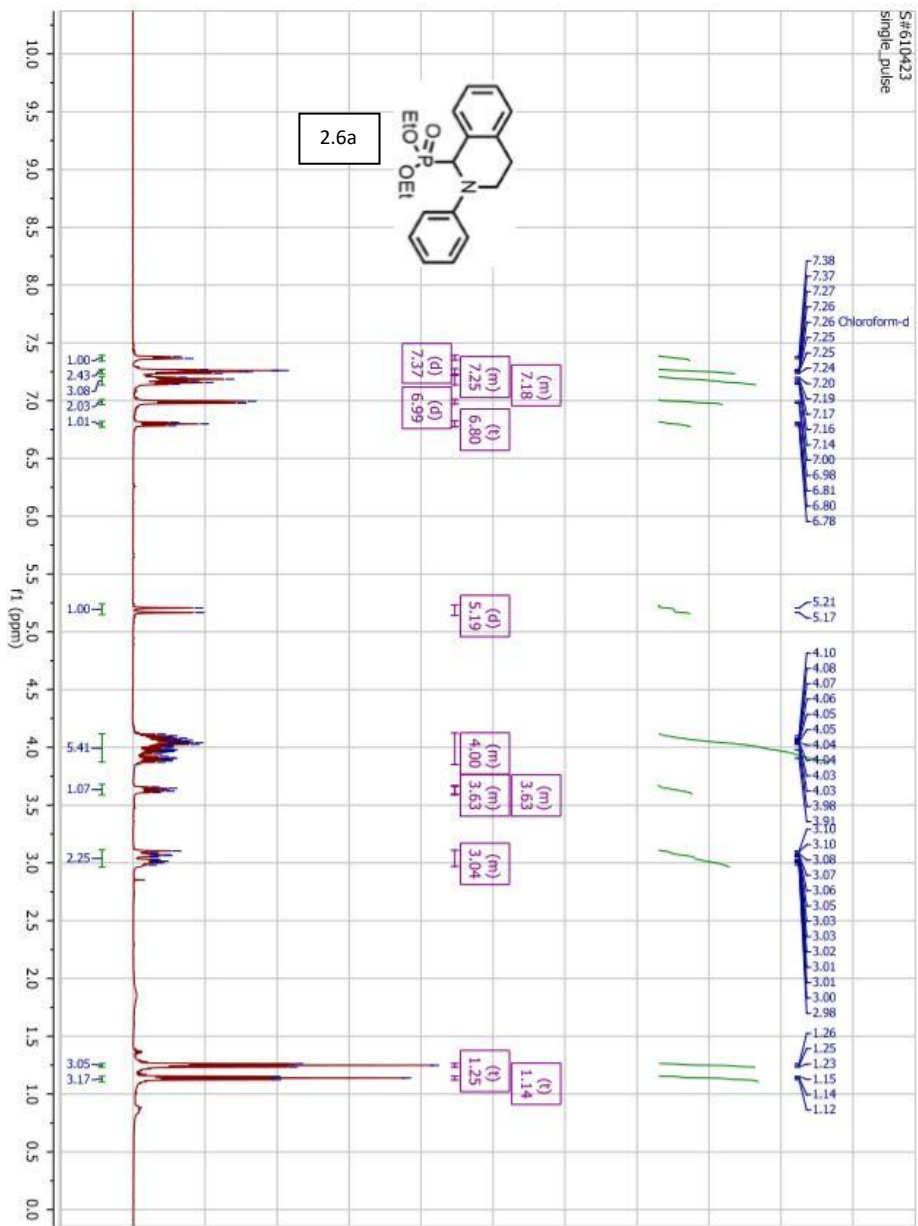


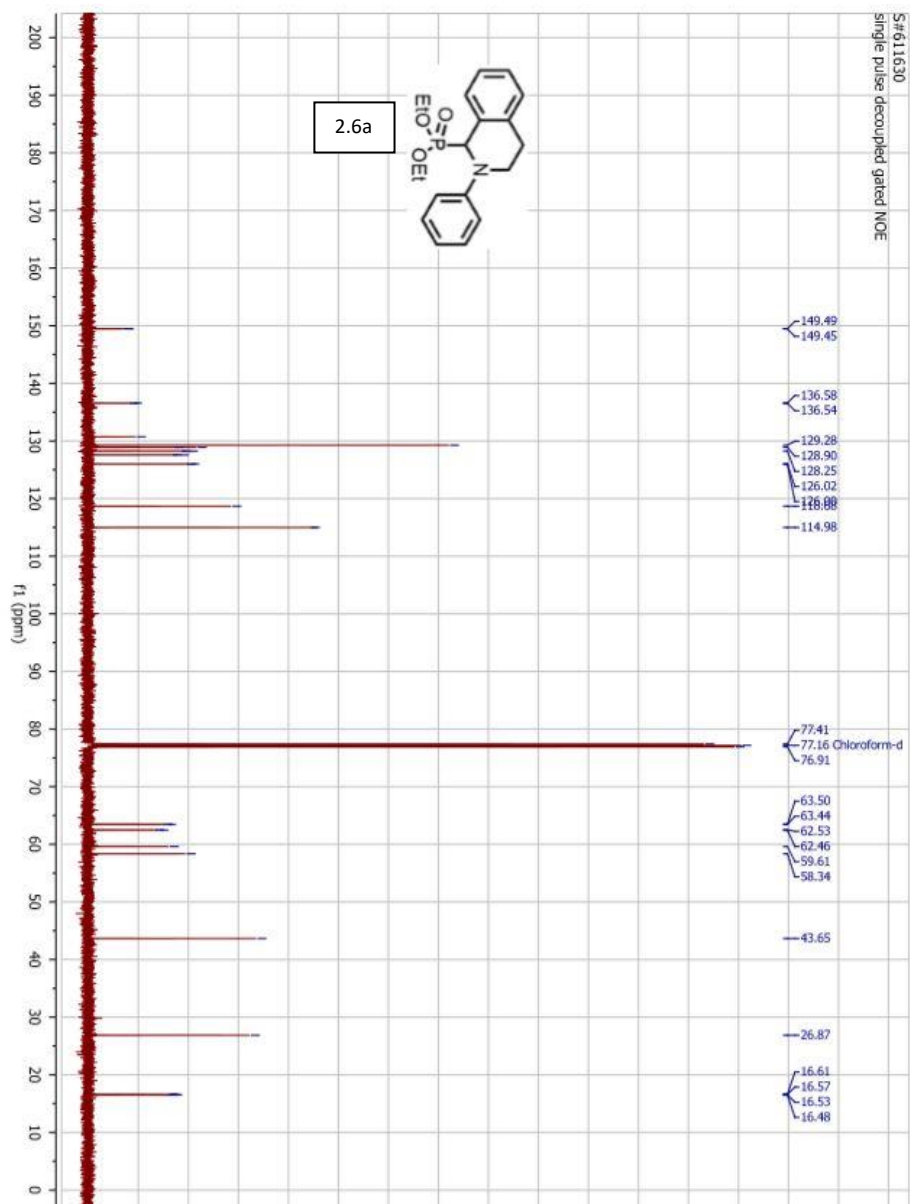




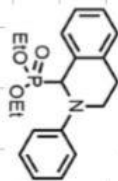
S#688091
single pulse decoupled gated NOE



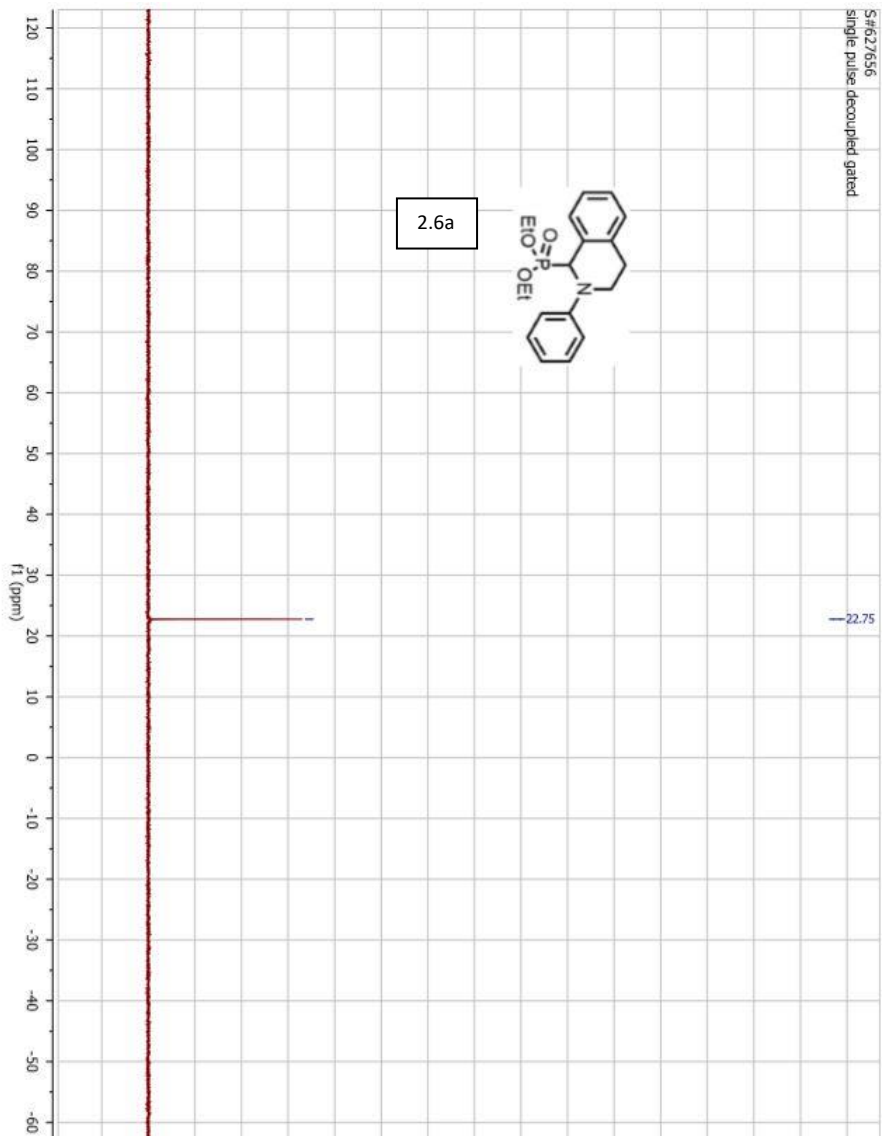


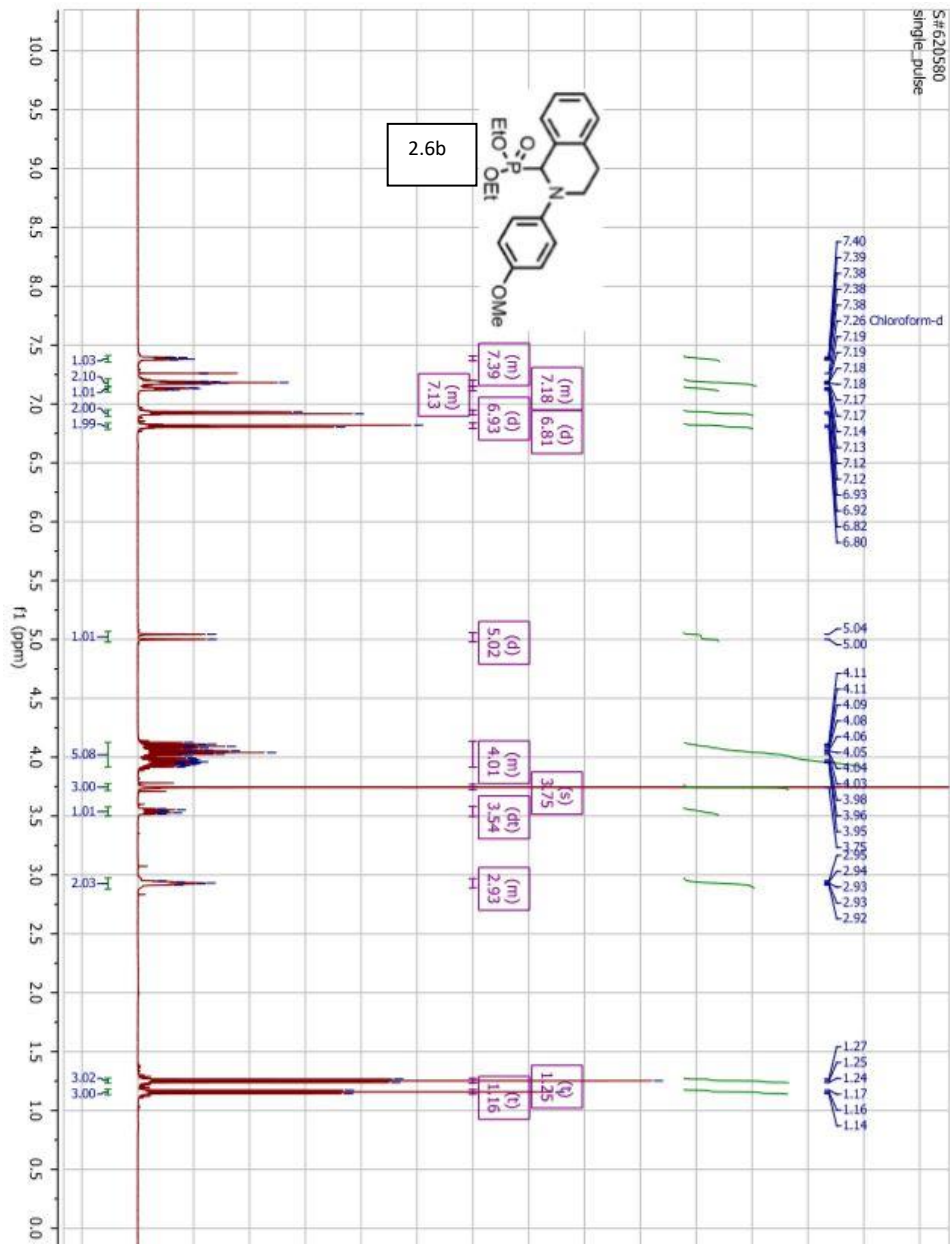


S#627656
single pulse decoupled gated

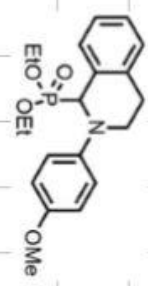


2.6a

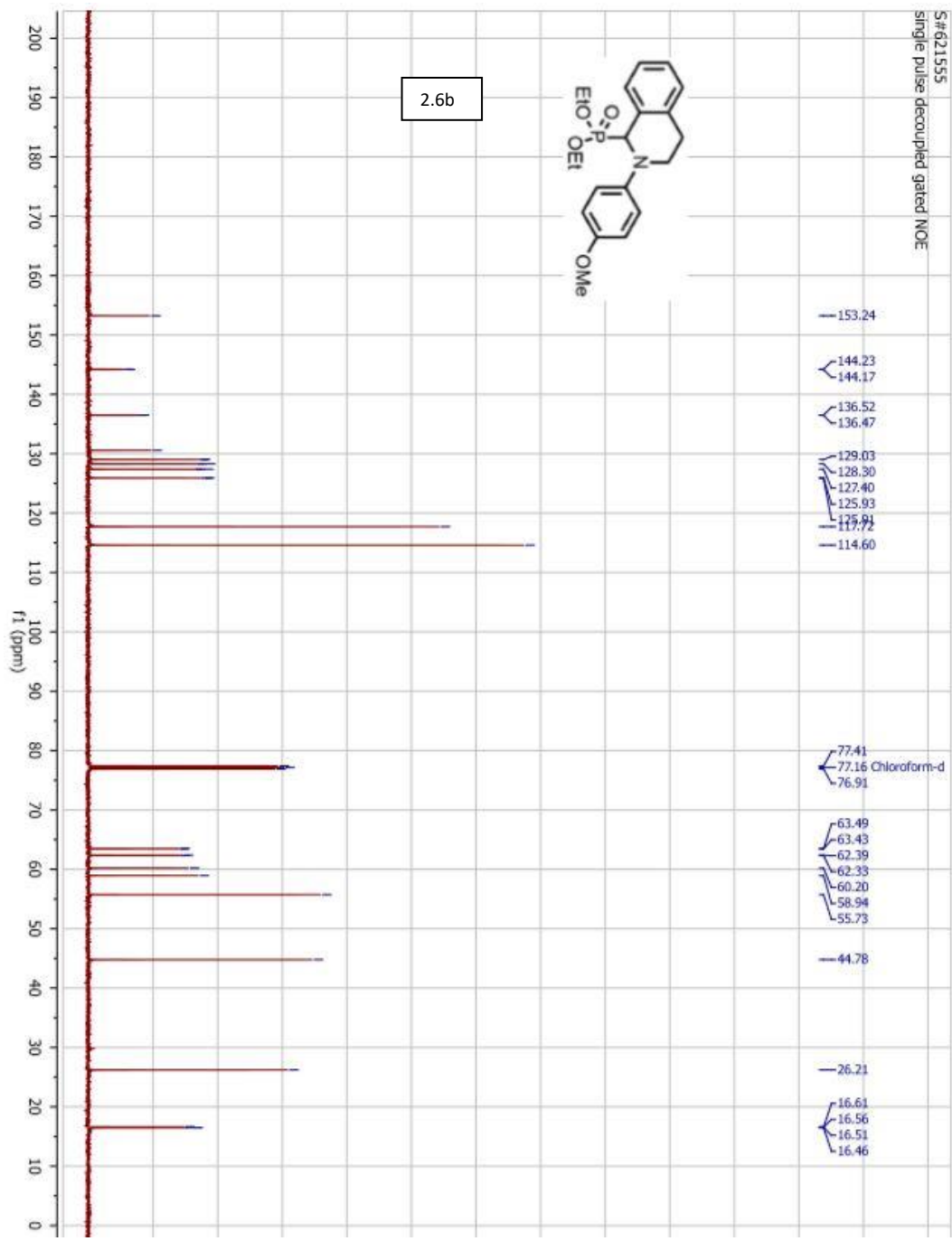




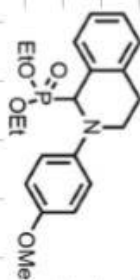
S#621555
single pulse decoupled gated NOE



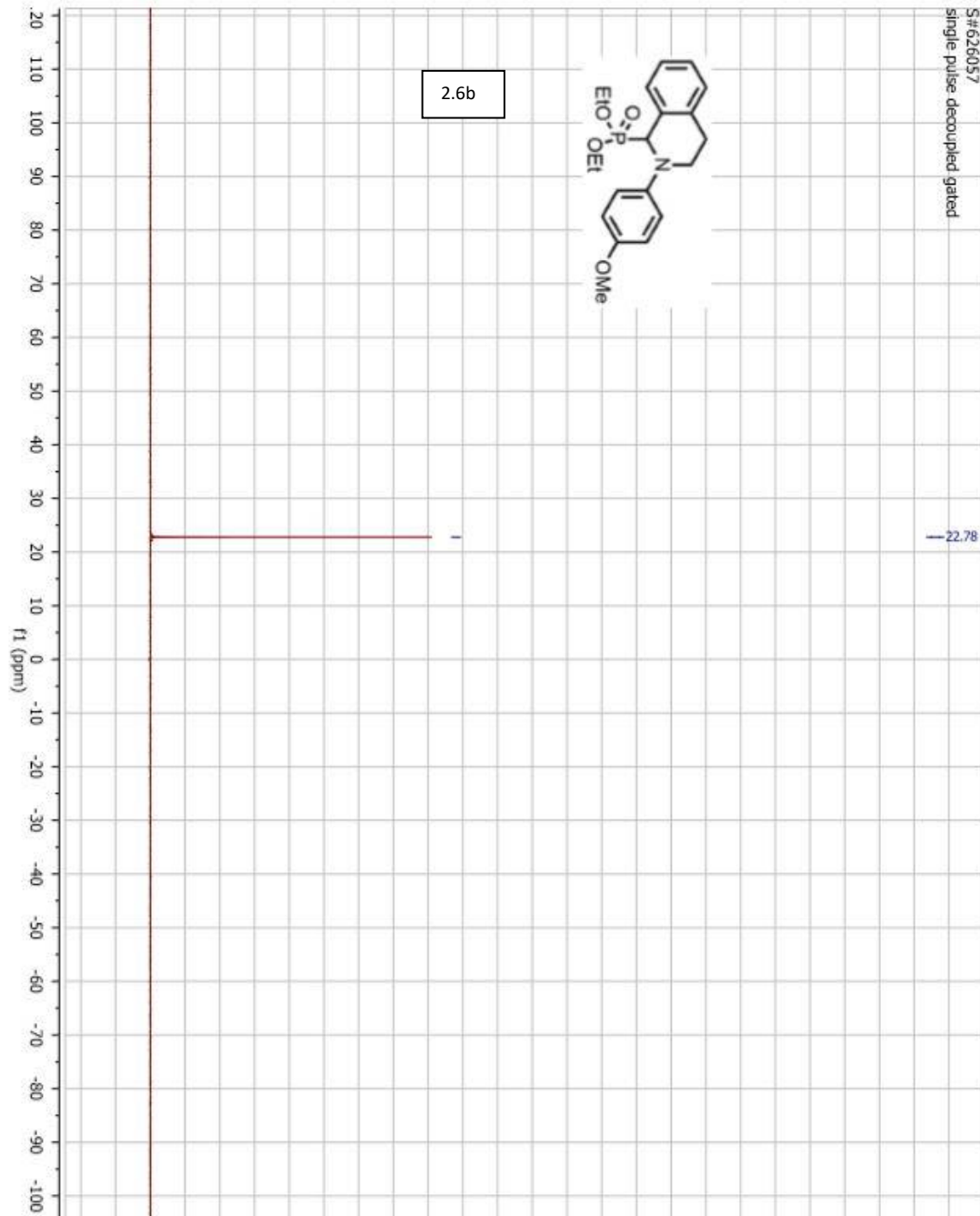
2.6b

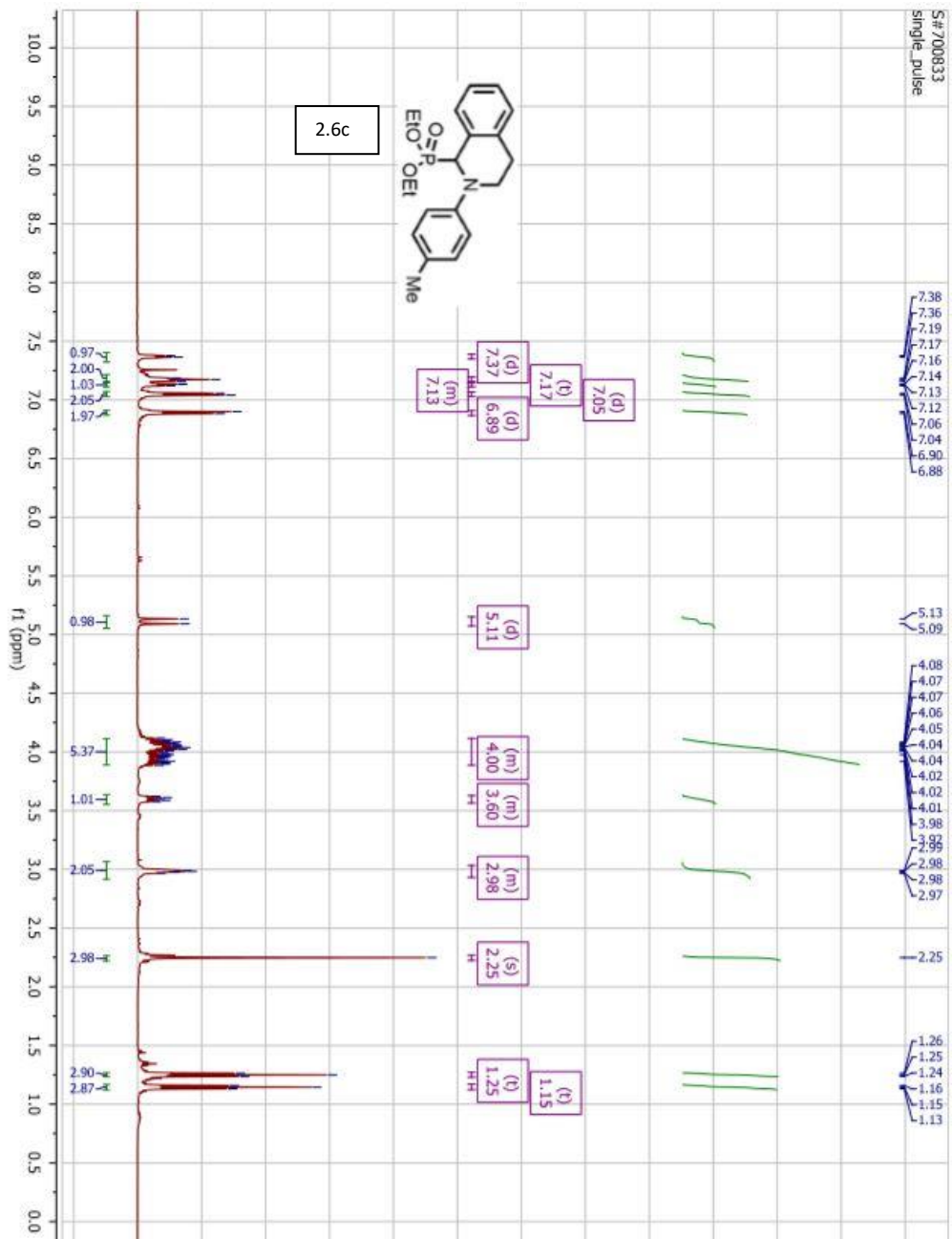


S#626057
single pulse decoupled gated

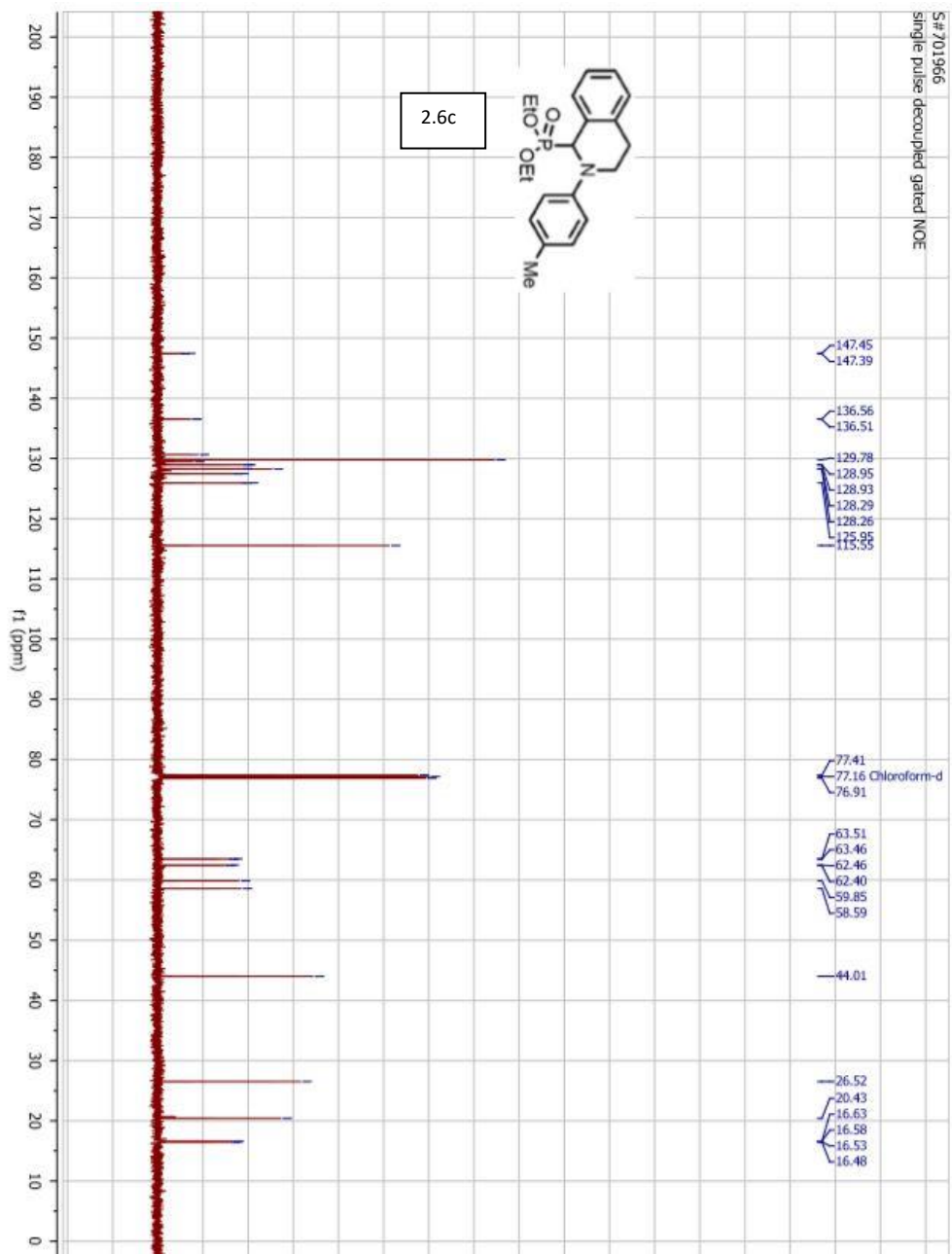


2.6b

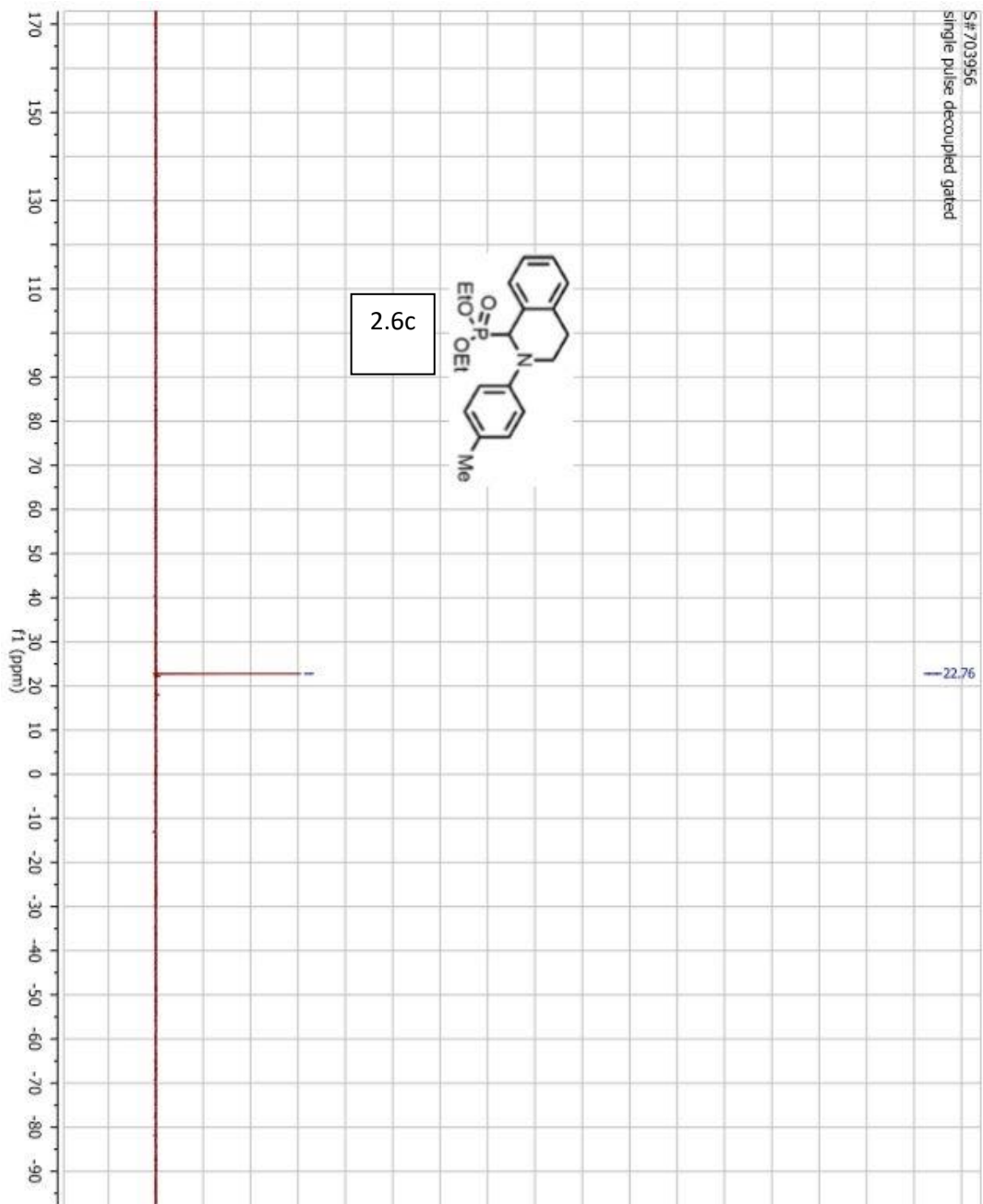


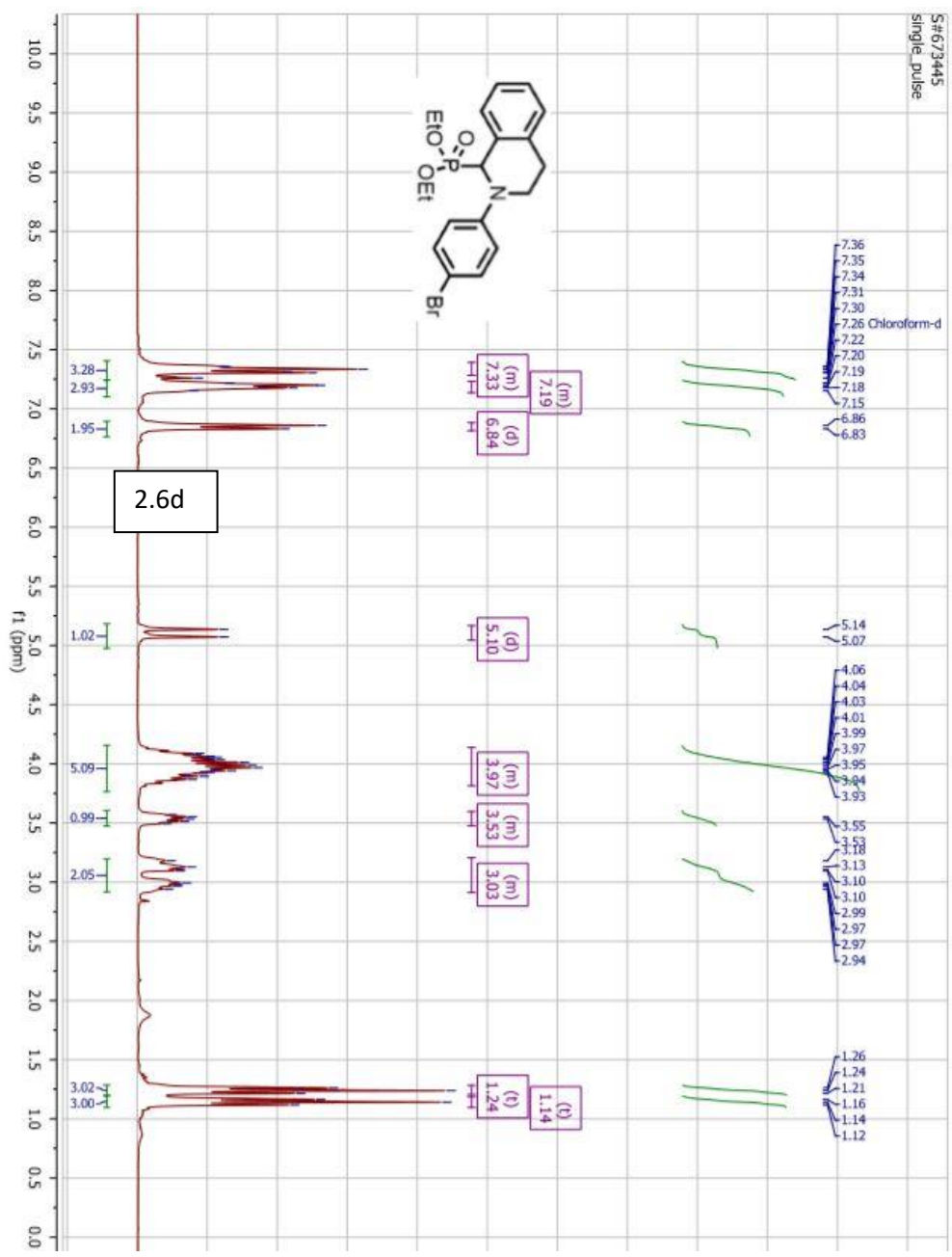


S# 701966
single pulse decoupled gated NOE



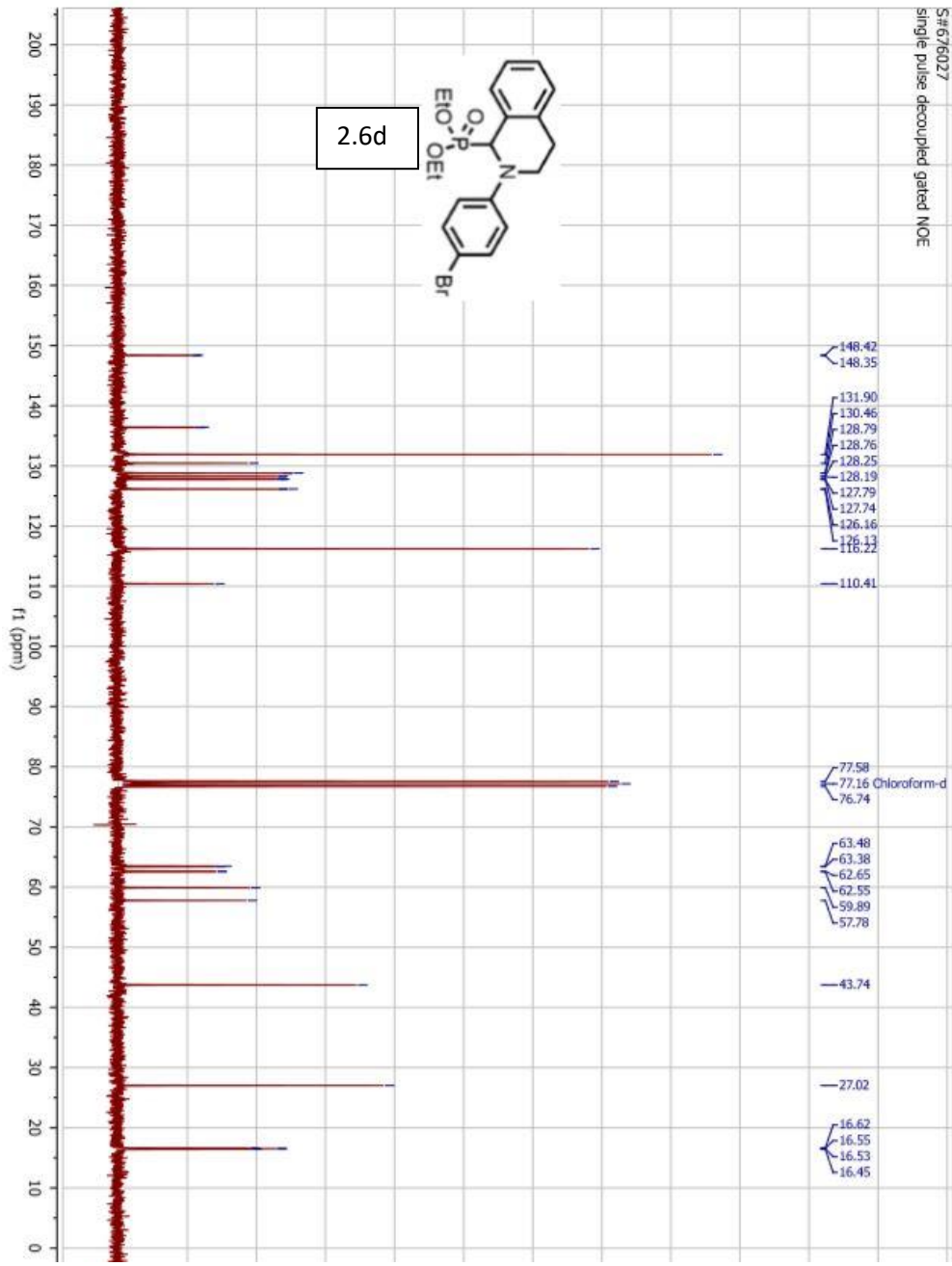
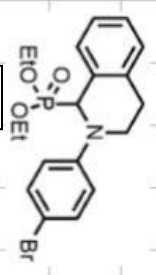
S# 703956
single pulse decoupled gated



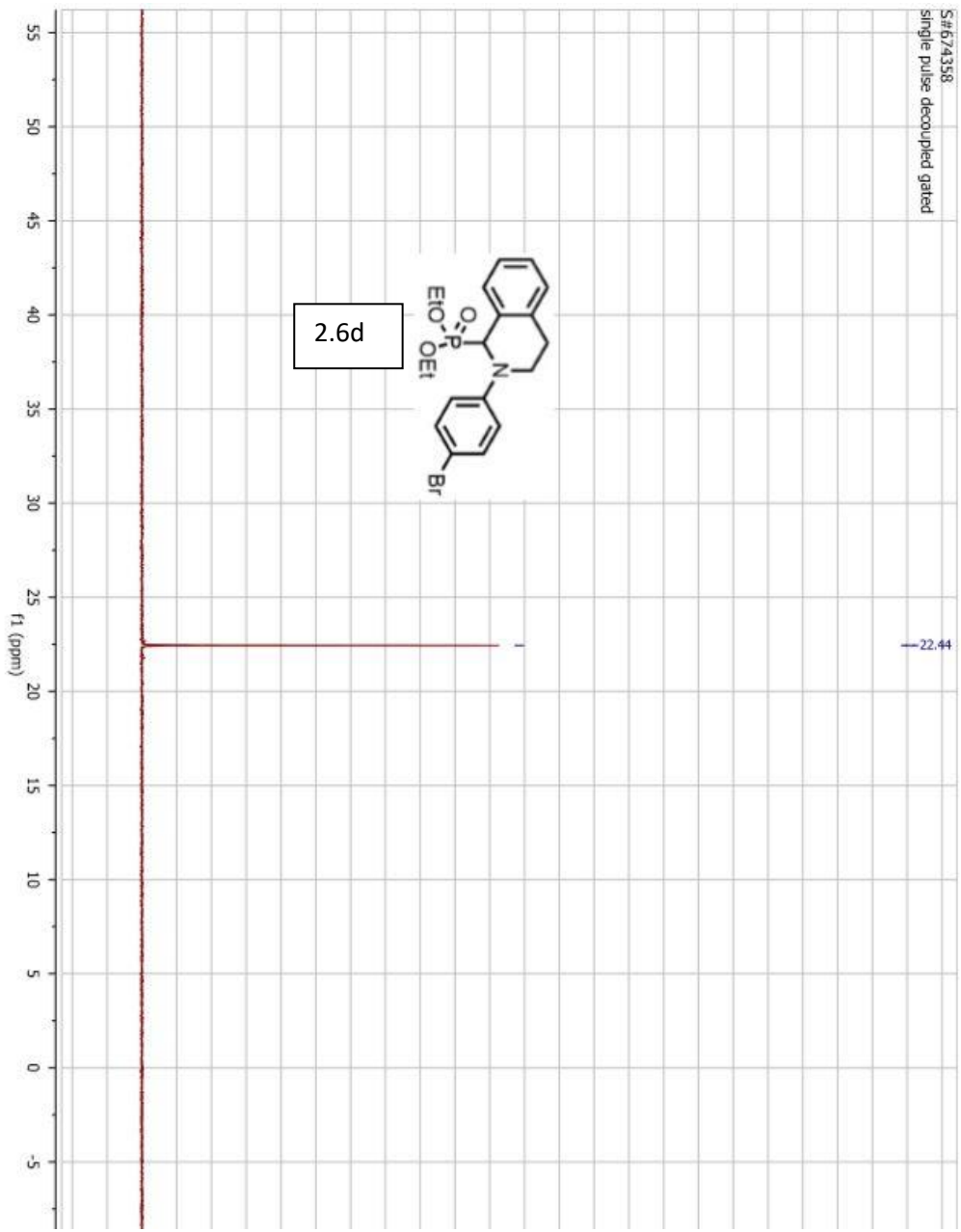


S#676027
single pulse decoupled gated NOE

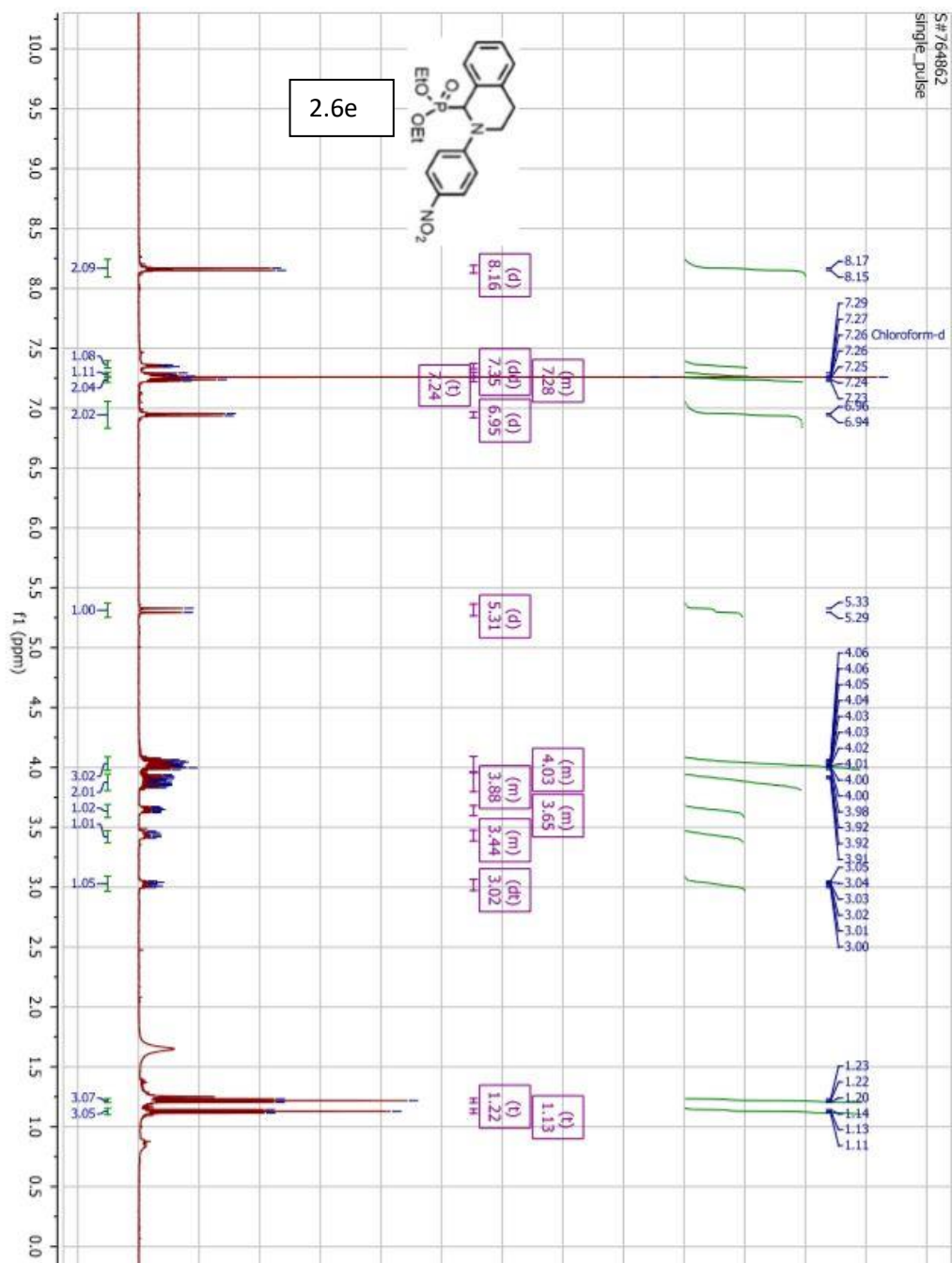
2.6d

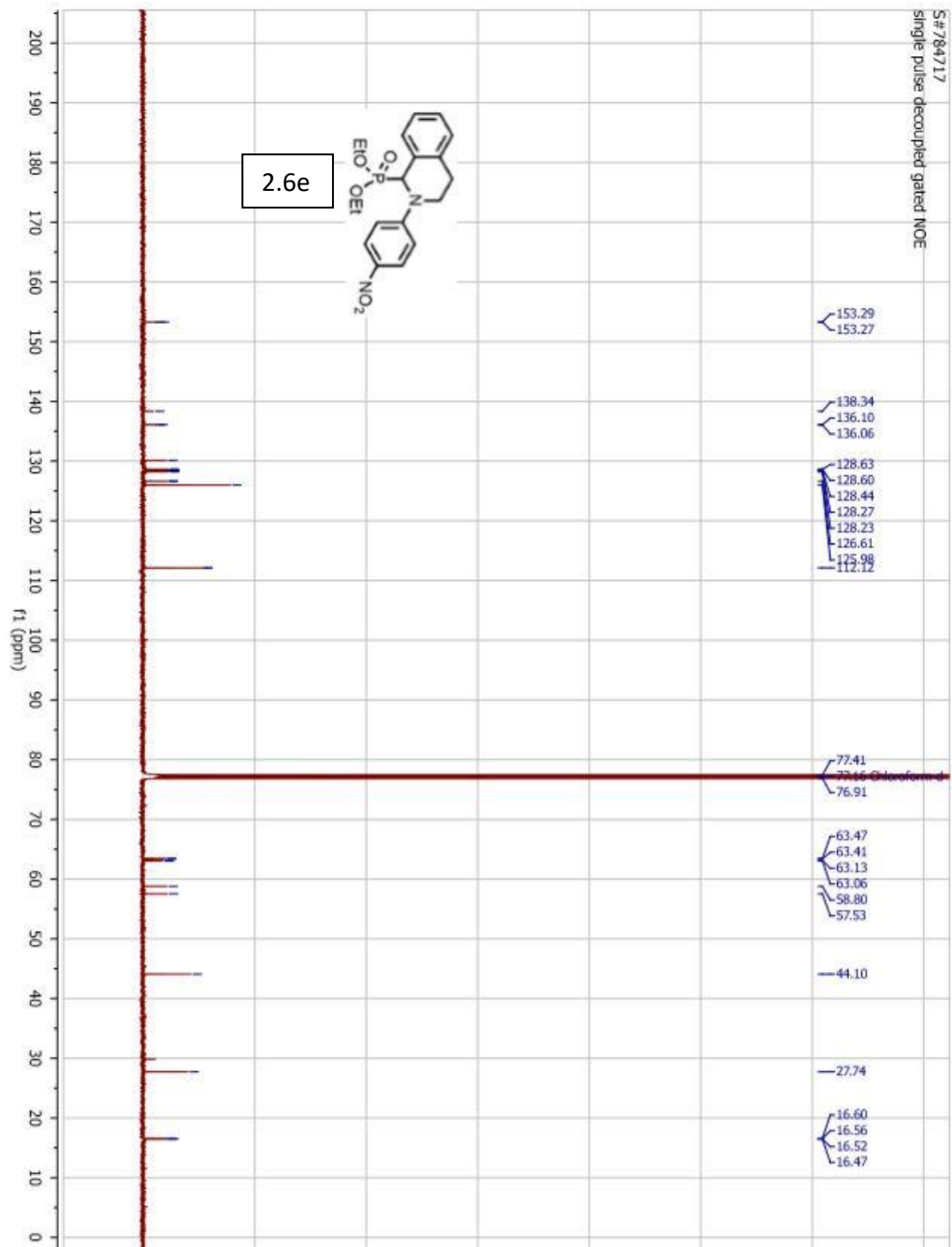


S#674358
single pulse decoupled gated

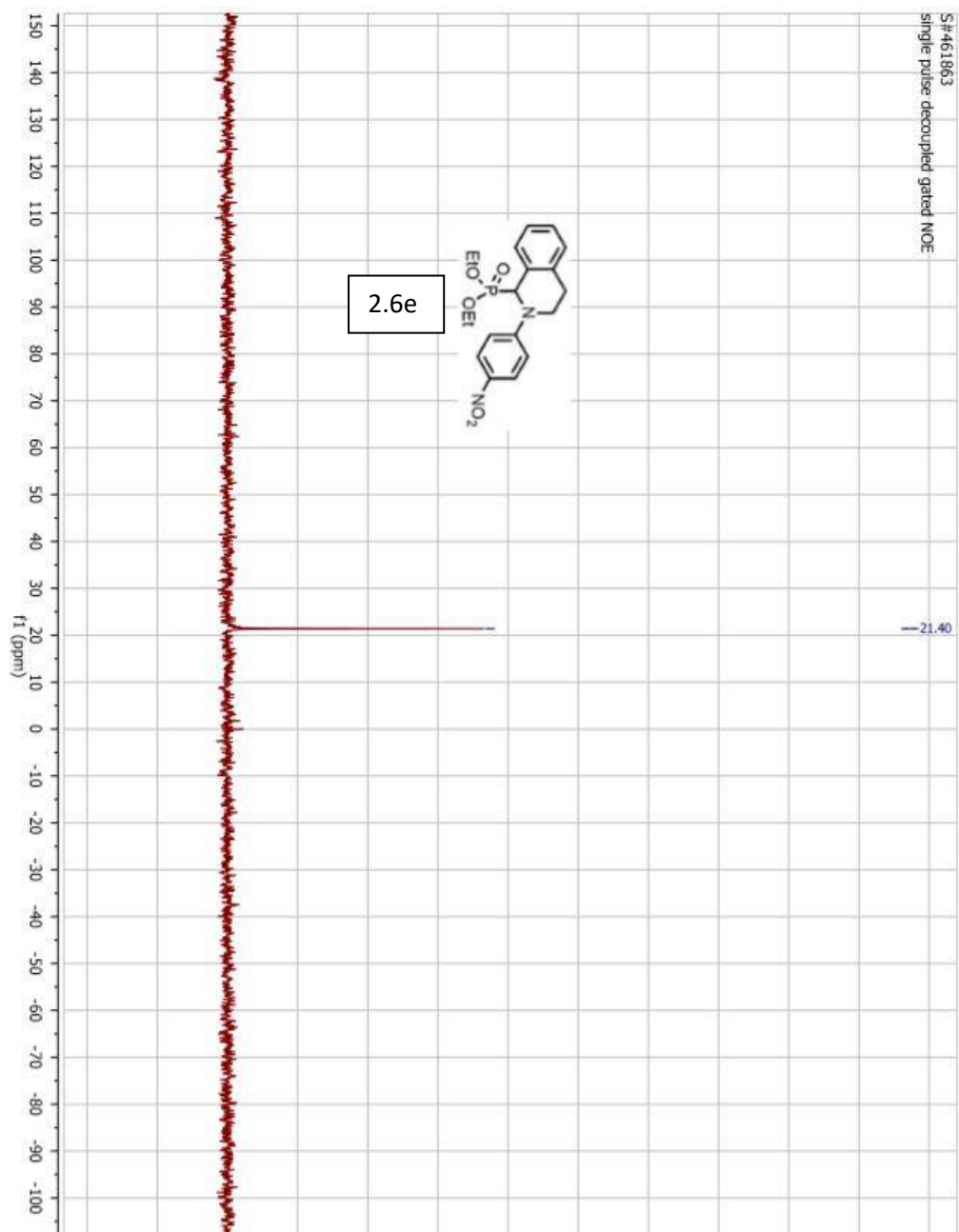


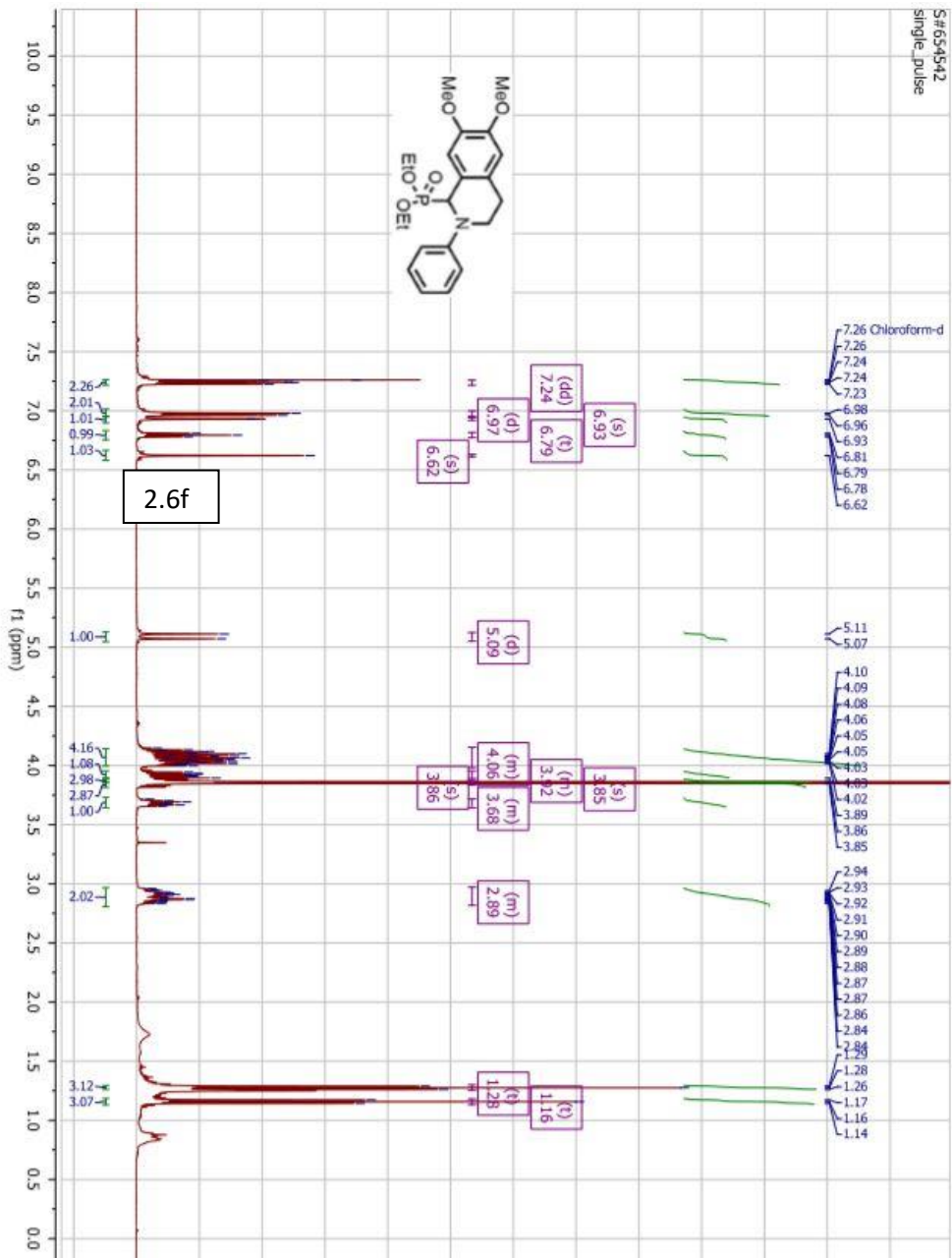
S#764862
single_pulse

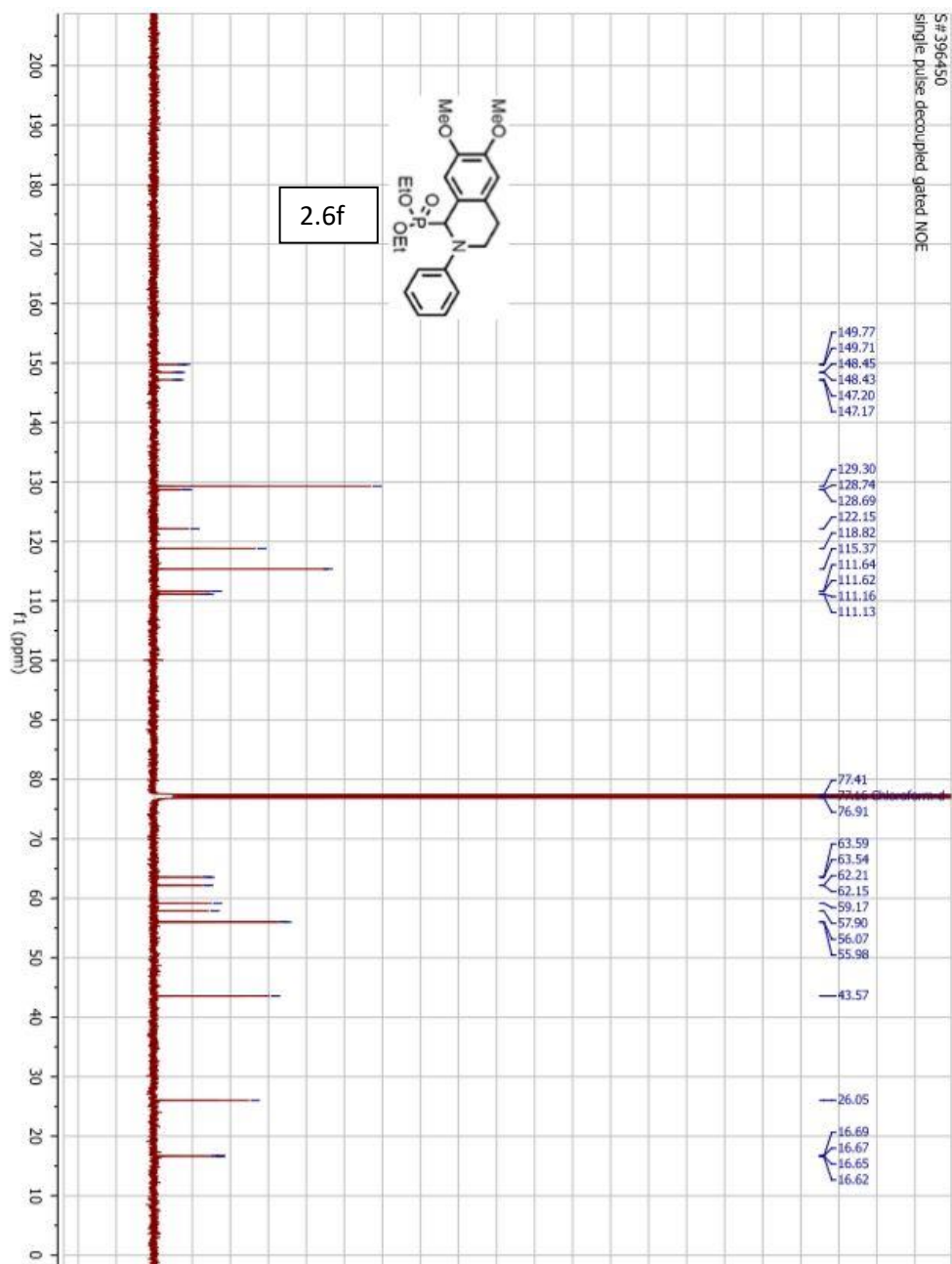




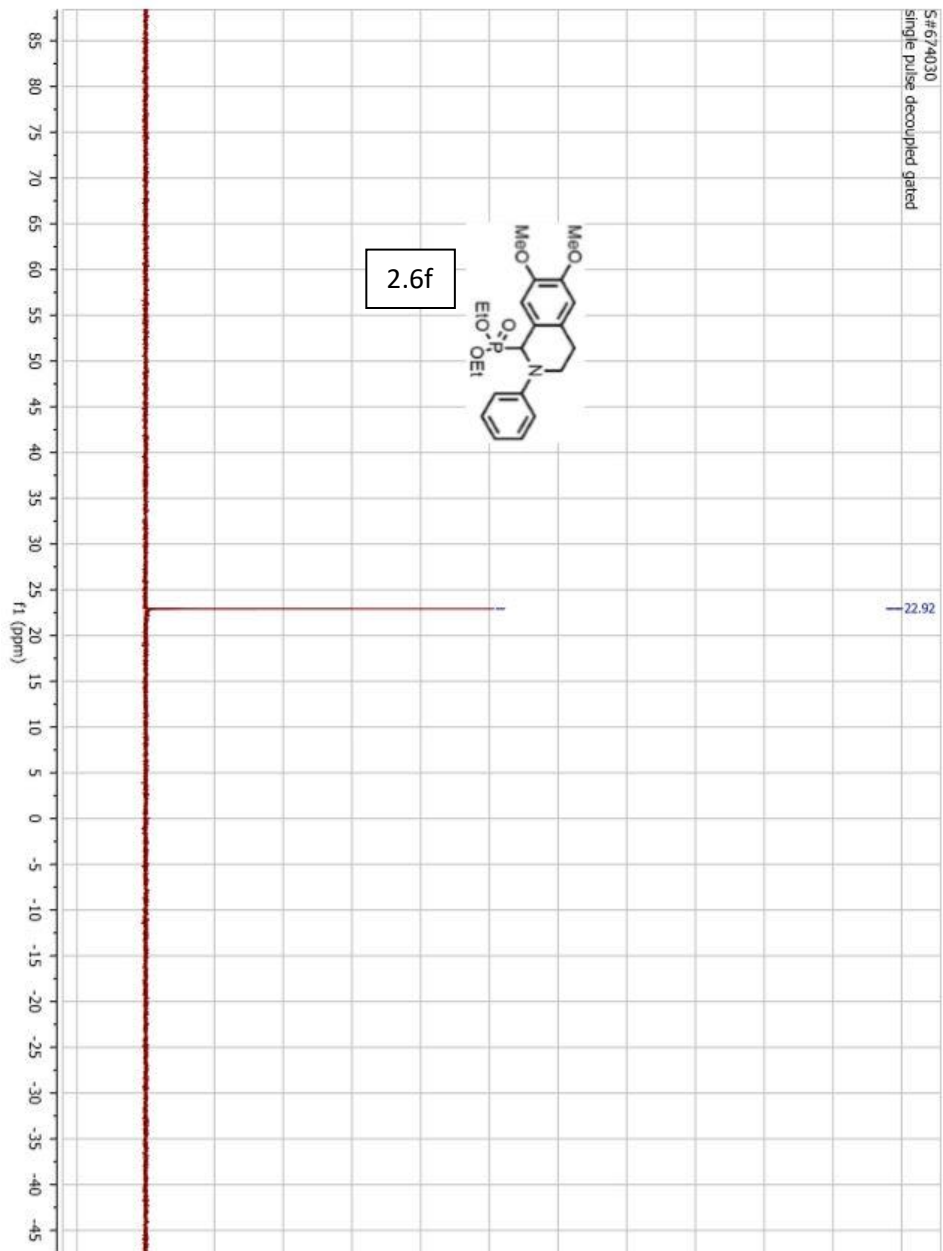
S#461863
single pulse decoupled gated NOE



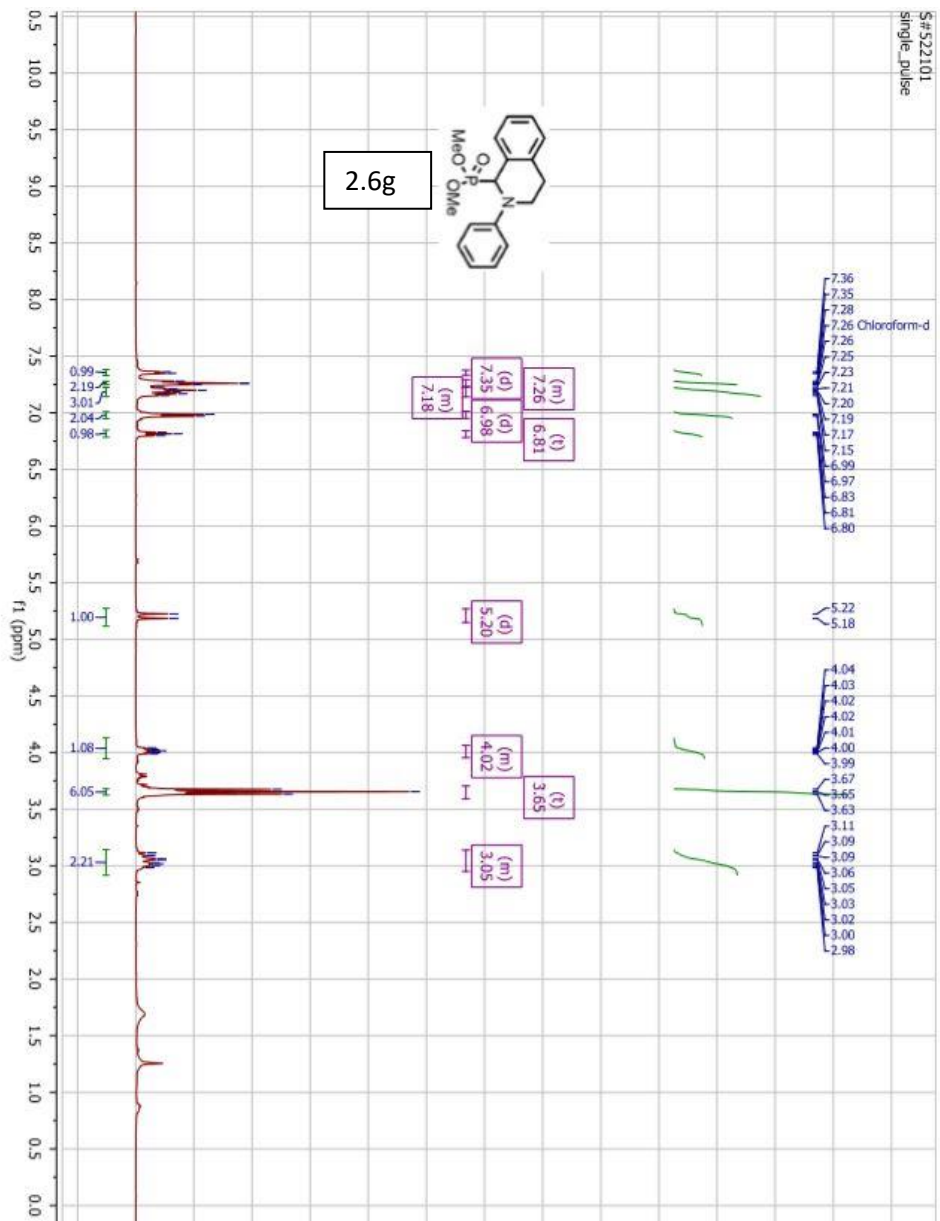


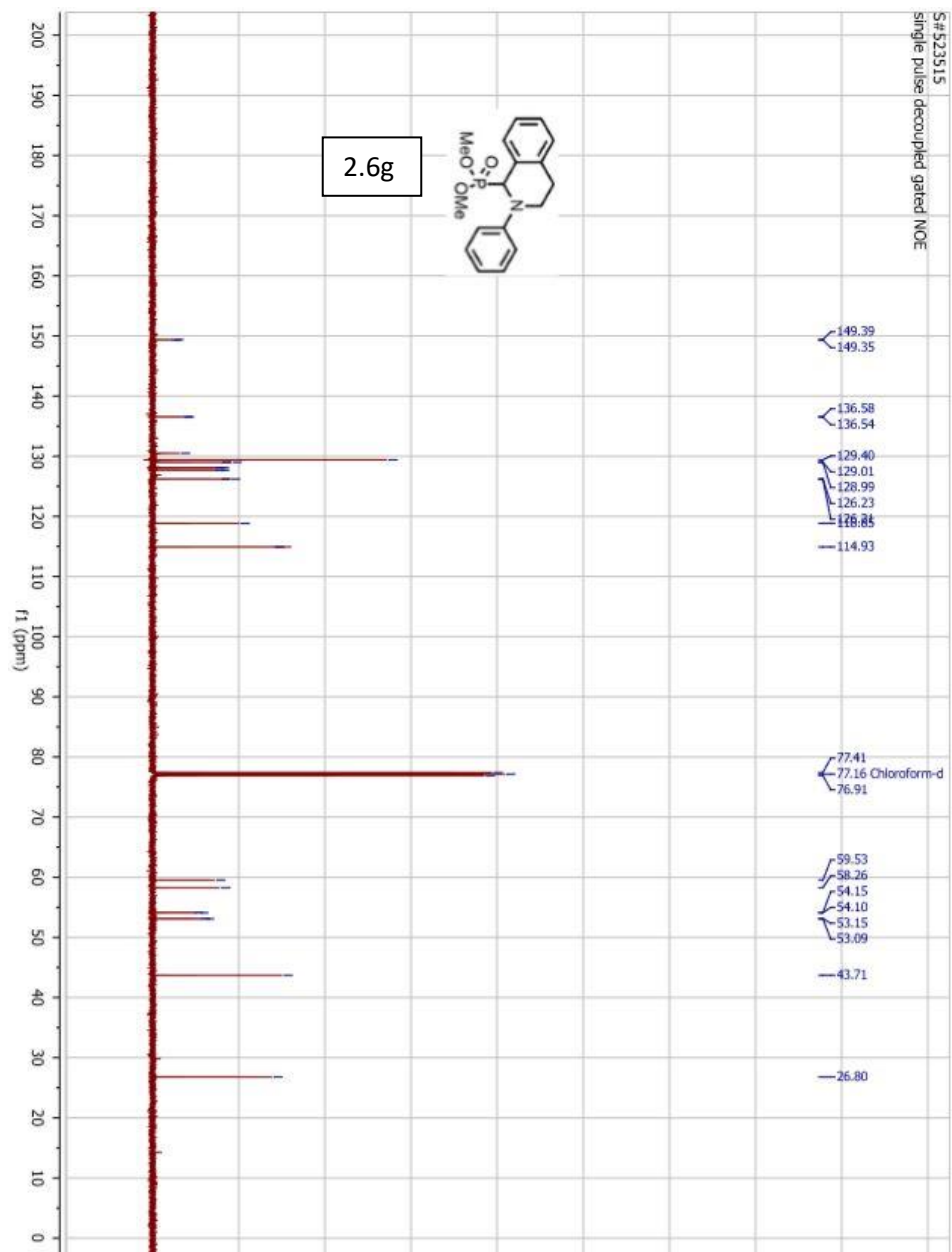


S#674030
single pulse decoupled gated

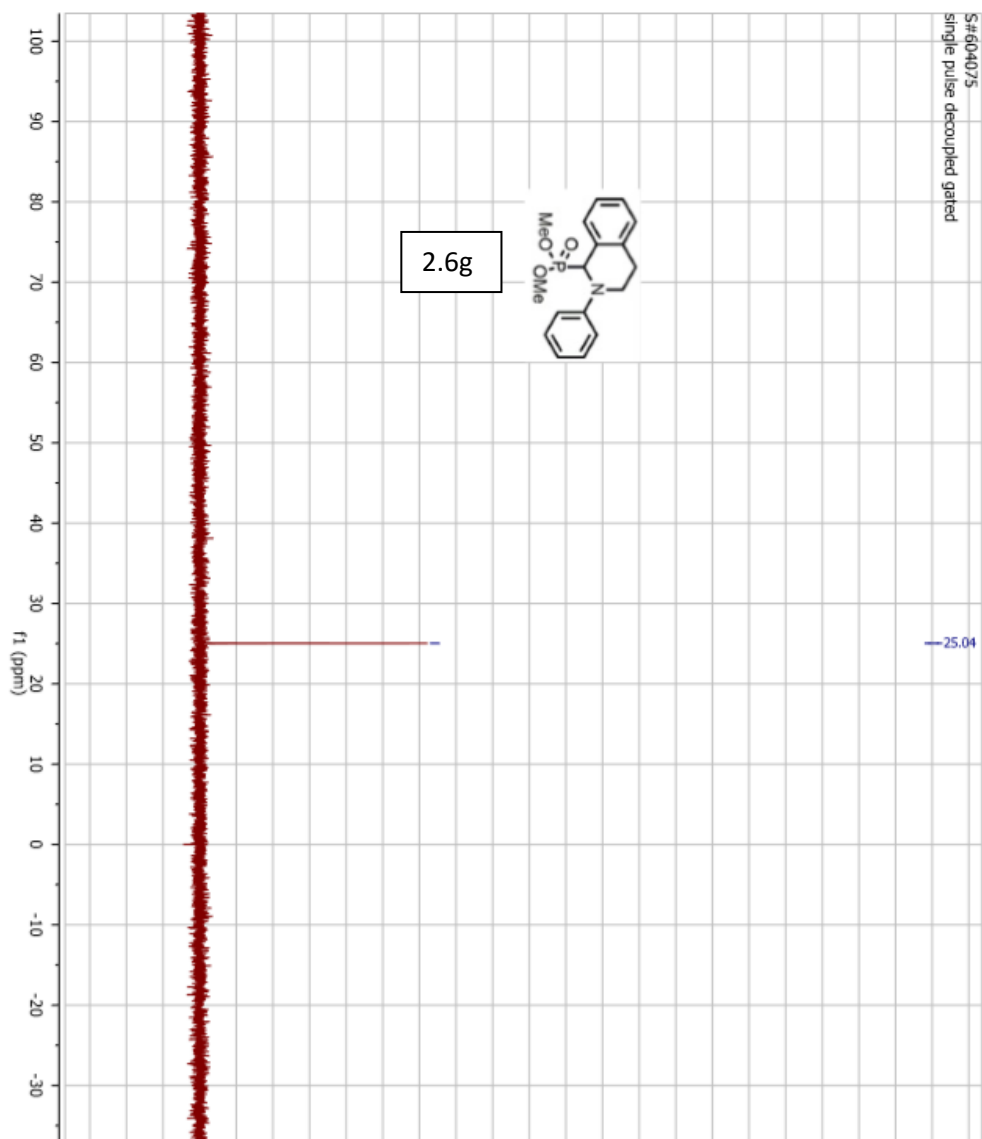


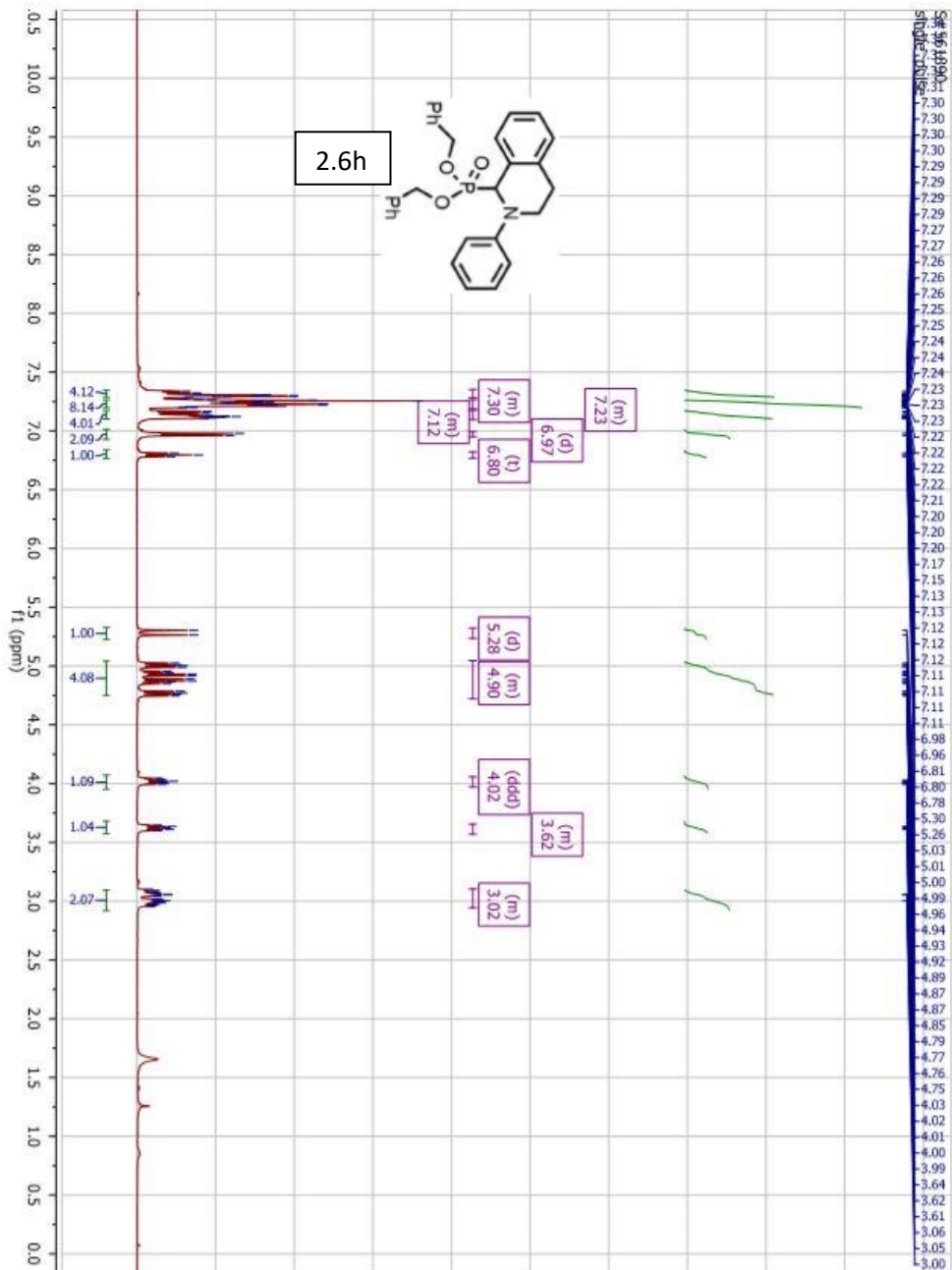
S#522101
single_pulse



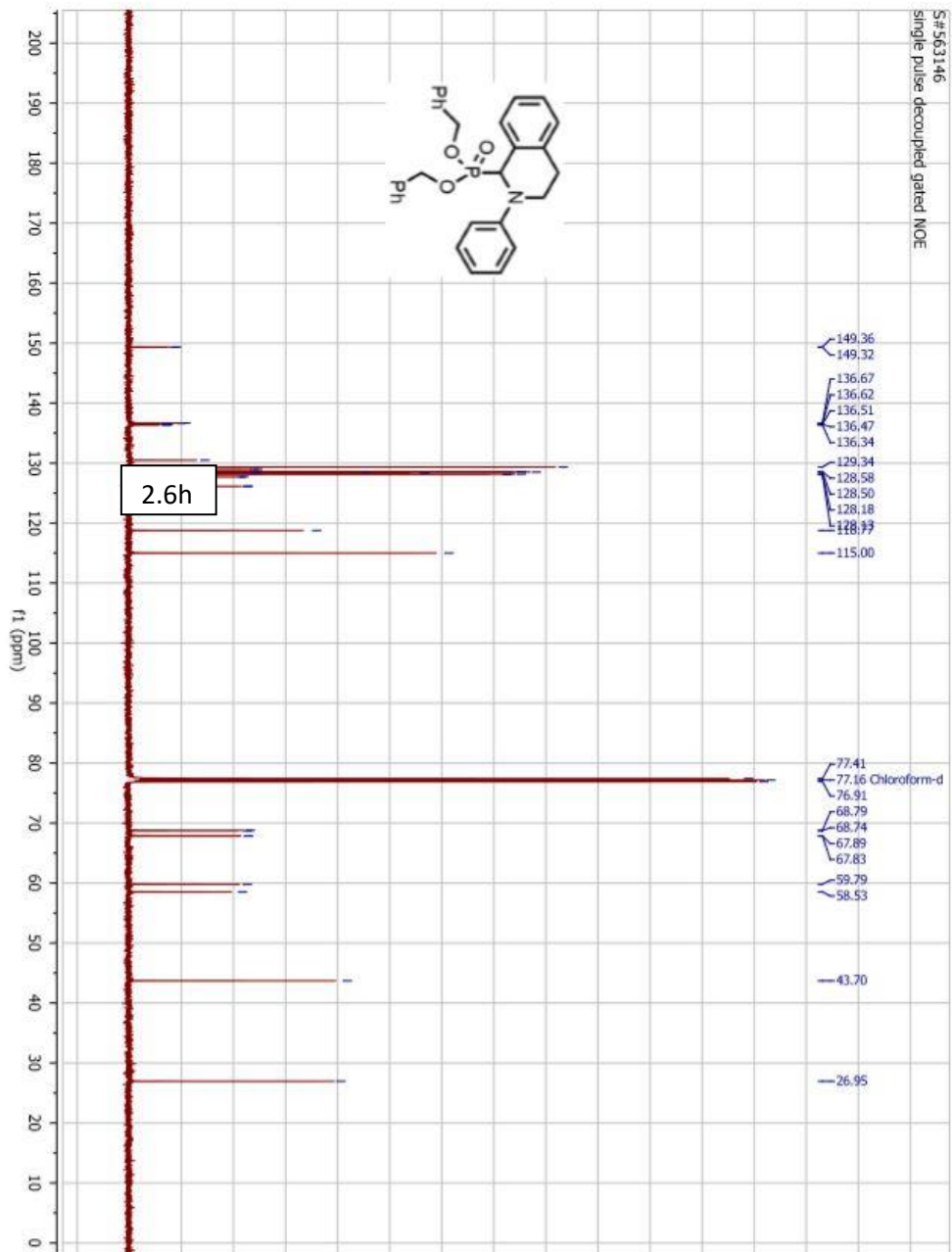


S#604075
single pulse decoupled gated

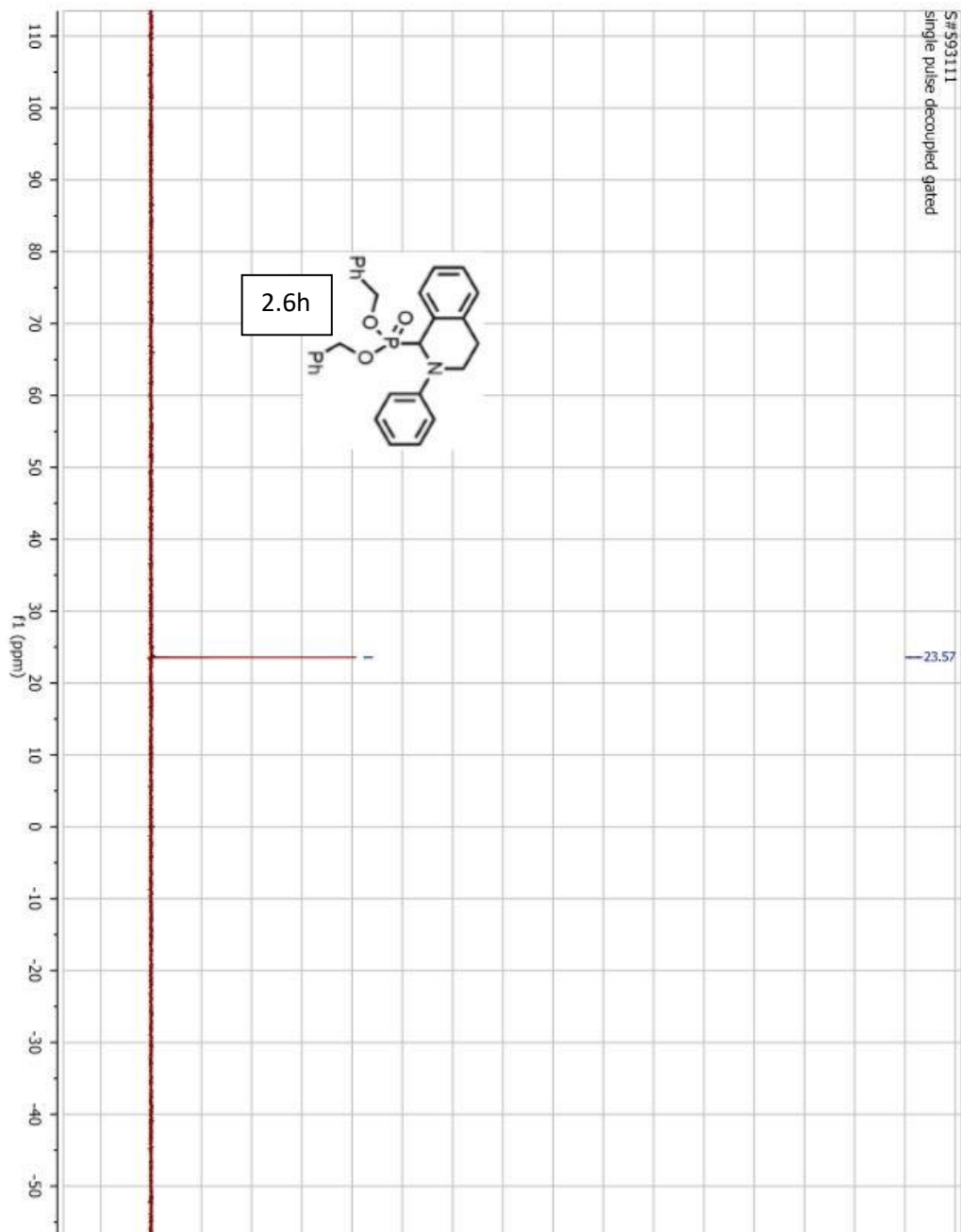


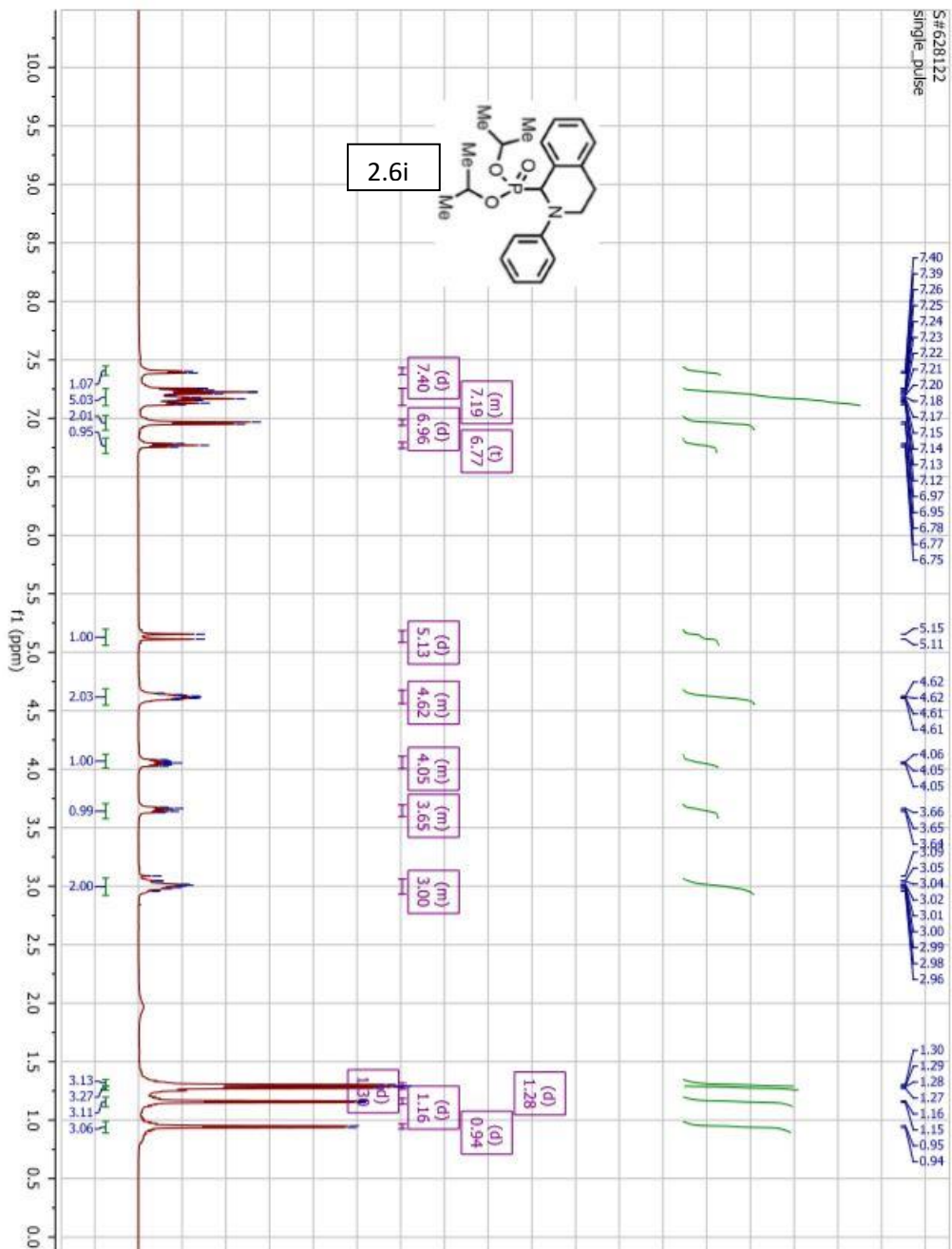


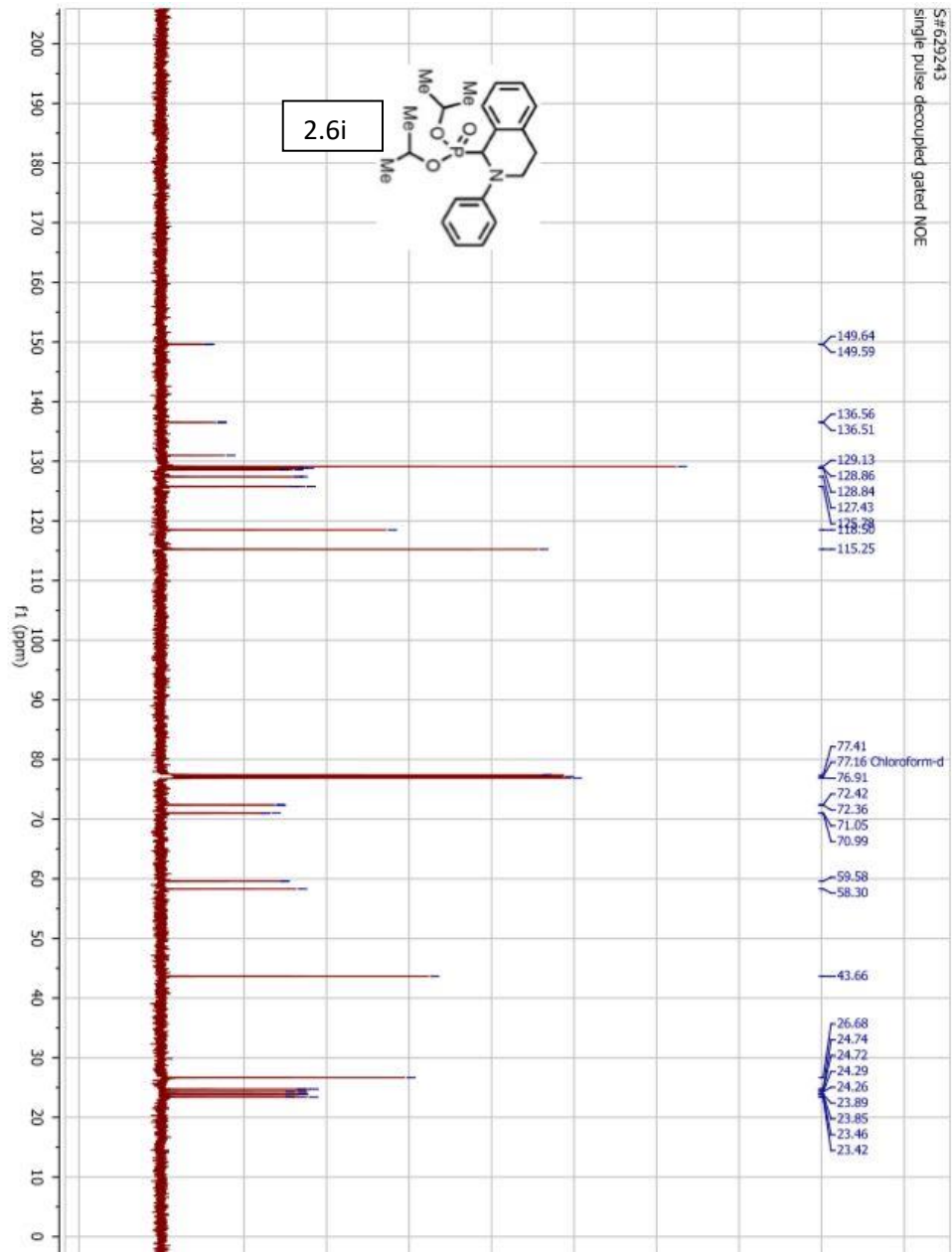
S#563146
single pulse decoupled gated NOE

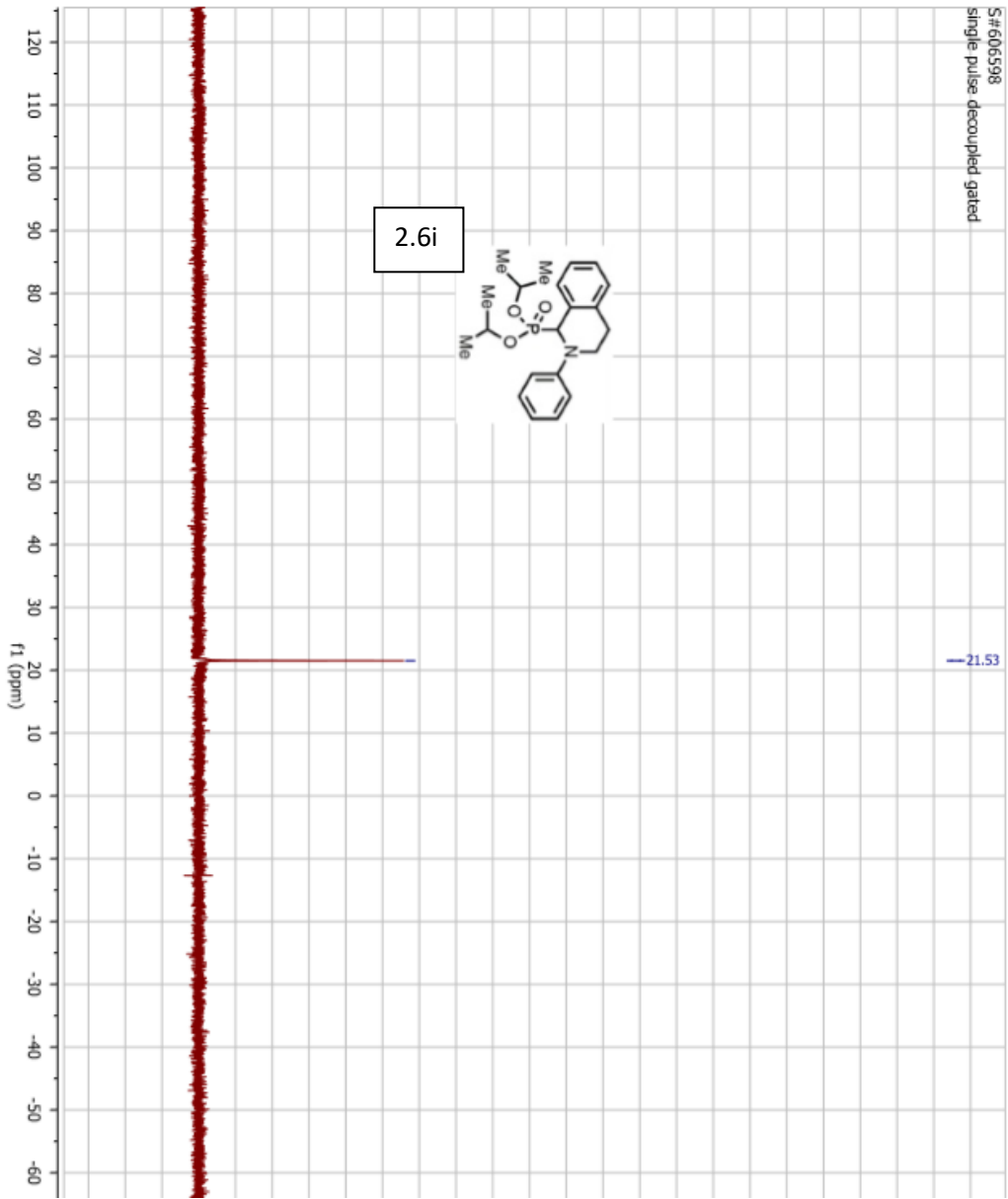


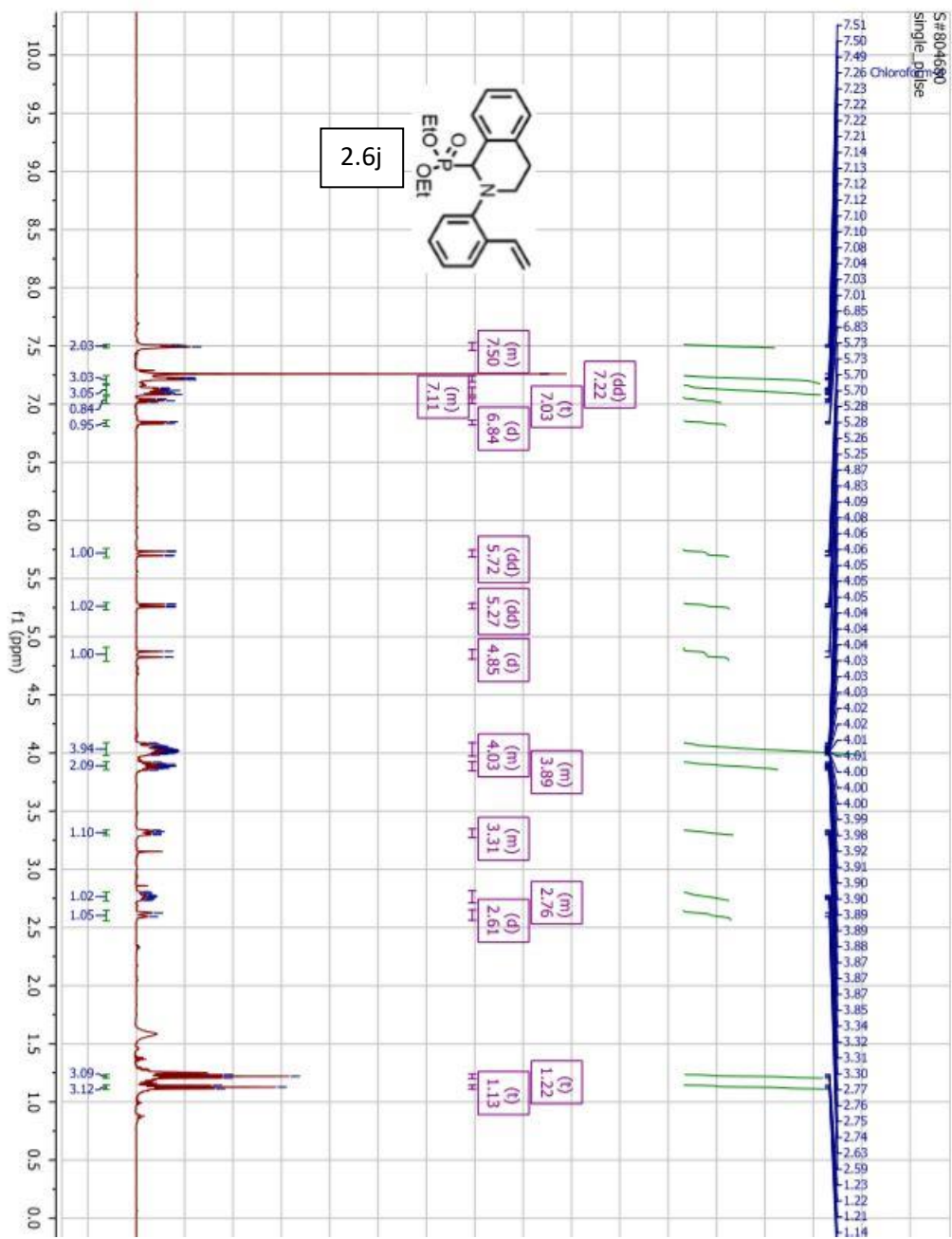
S#593111
single pulse decoupled gated





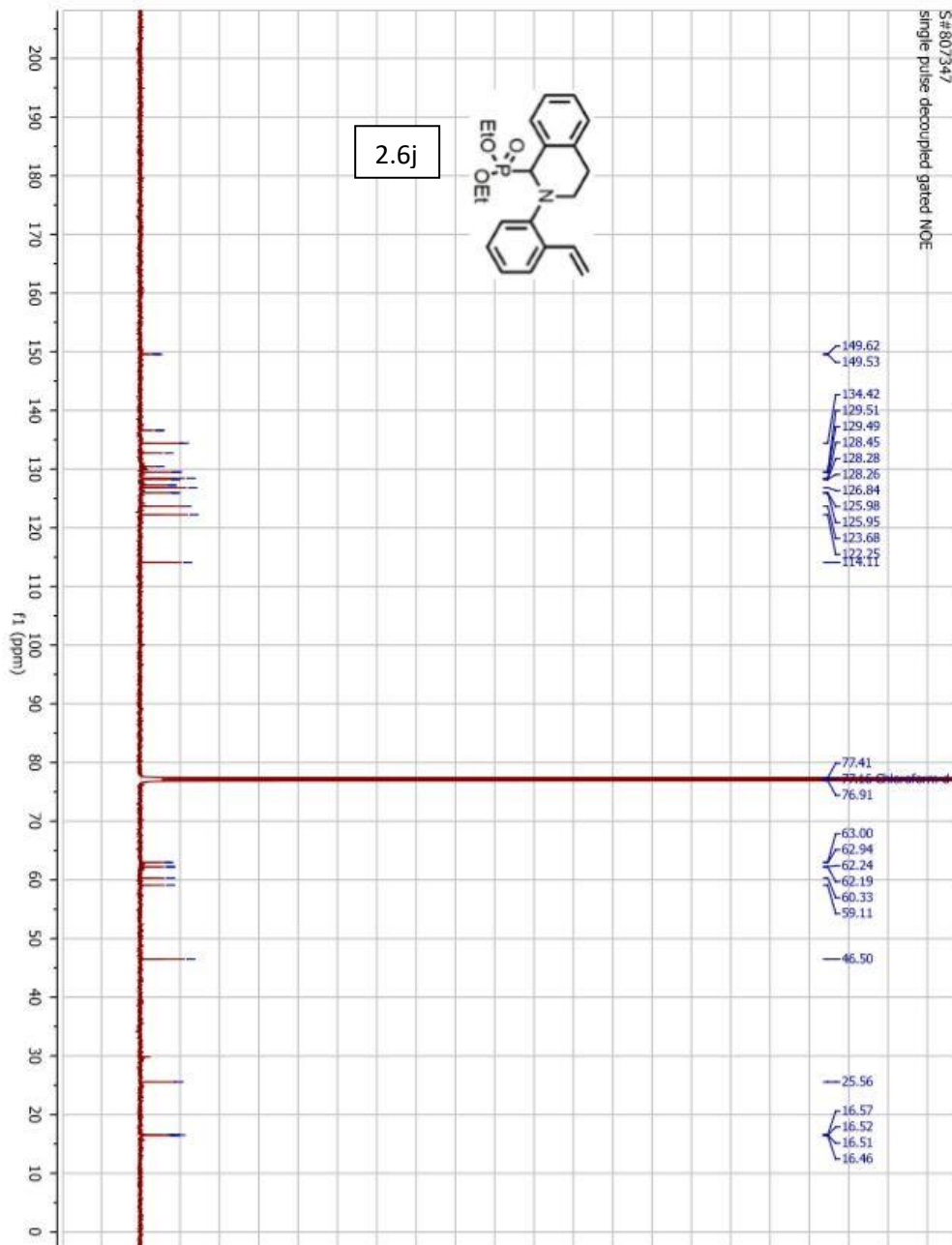
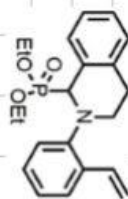




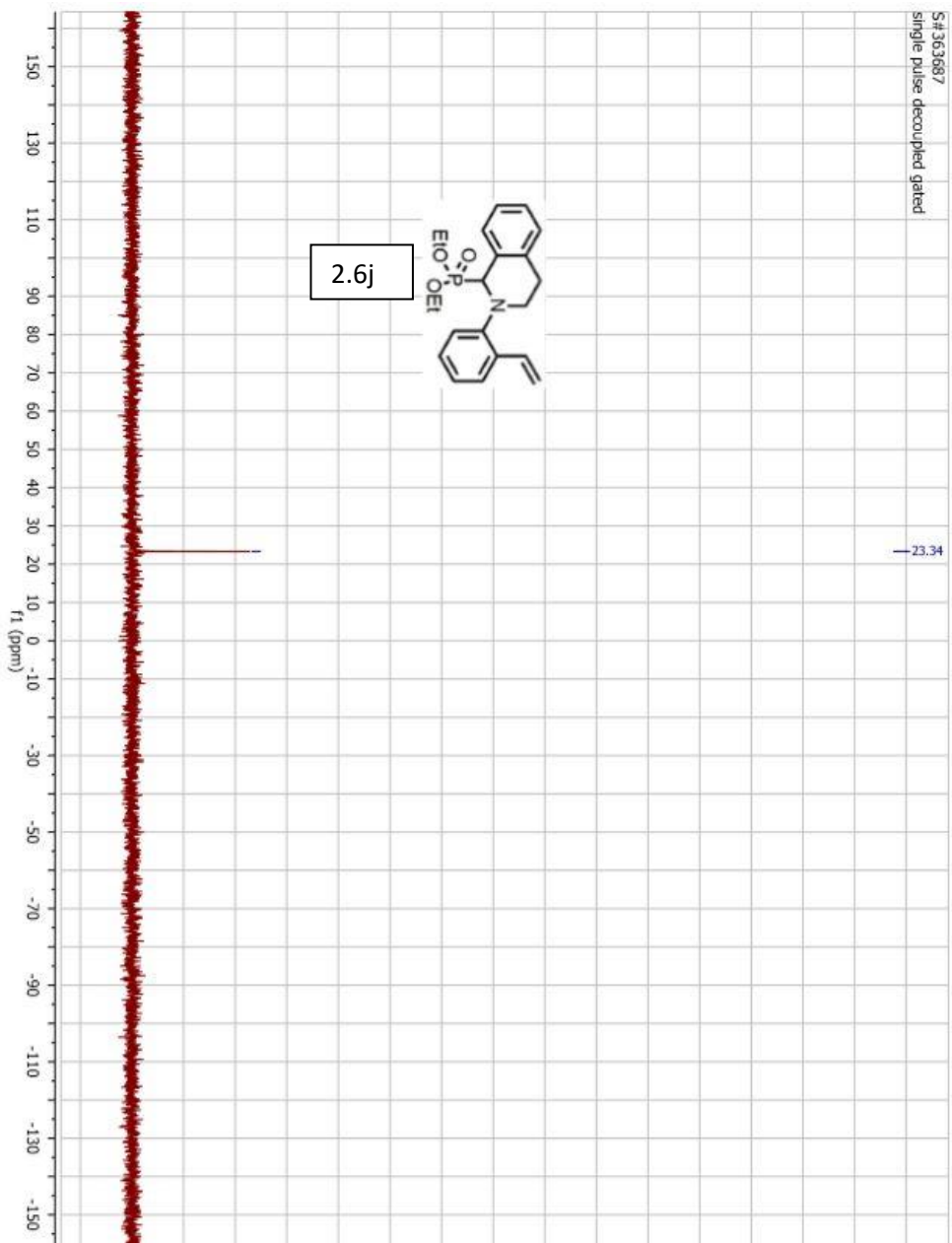


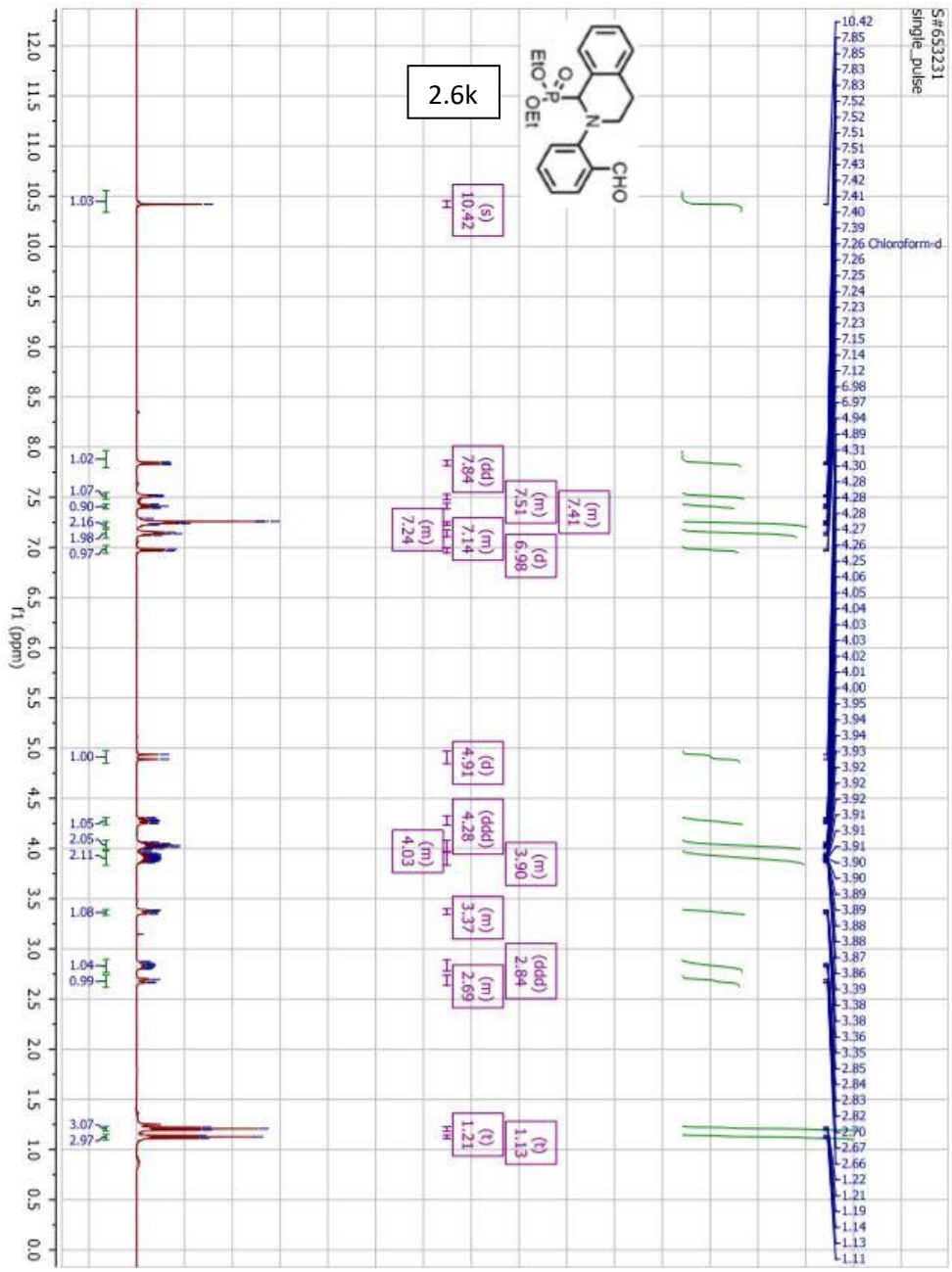
S#807347
single pulse decoupled gated NOE

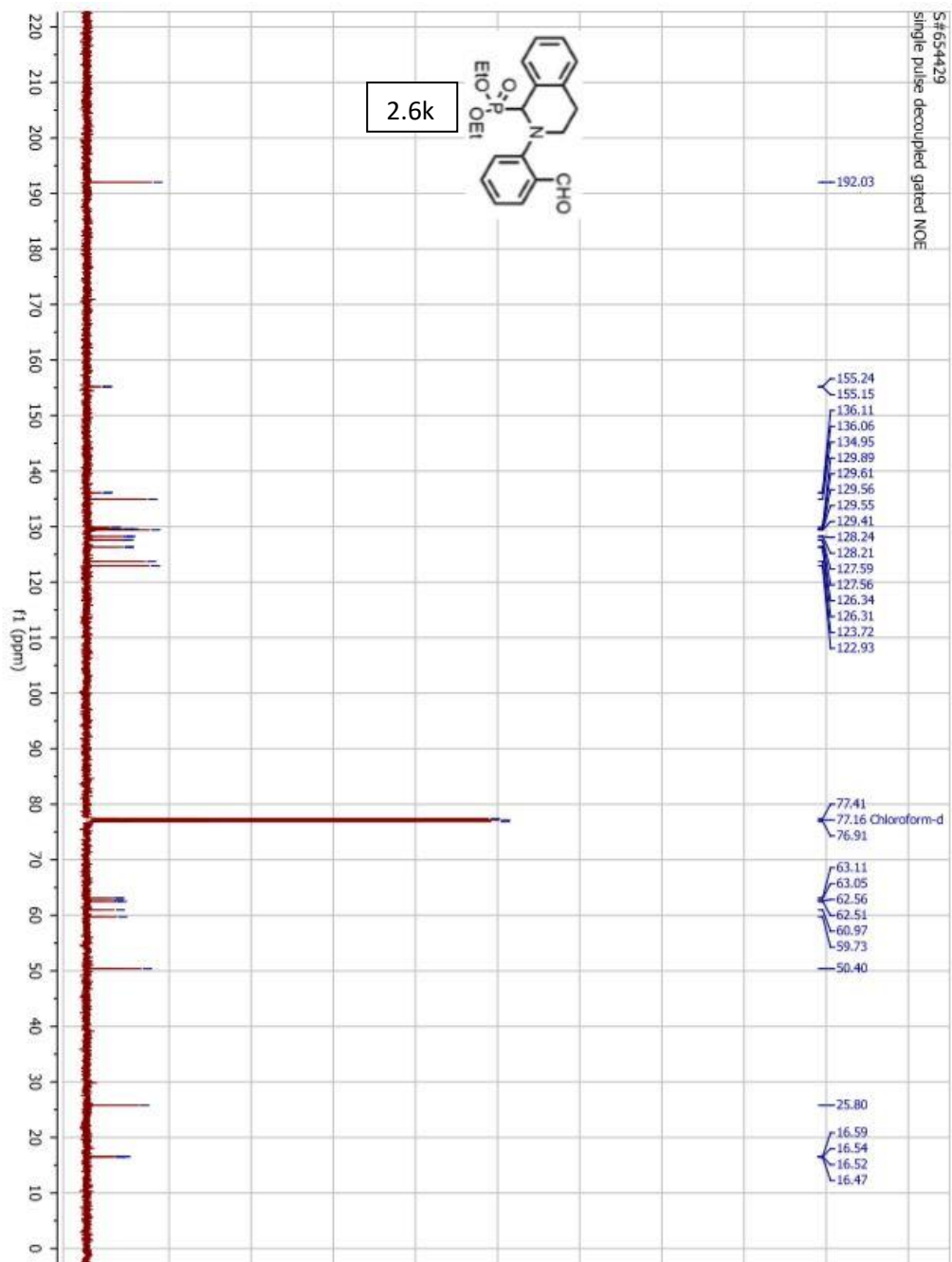
2.6j



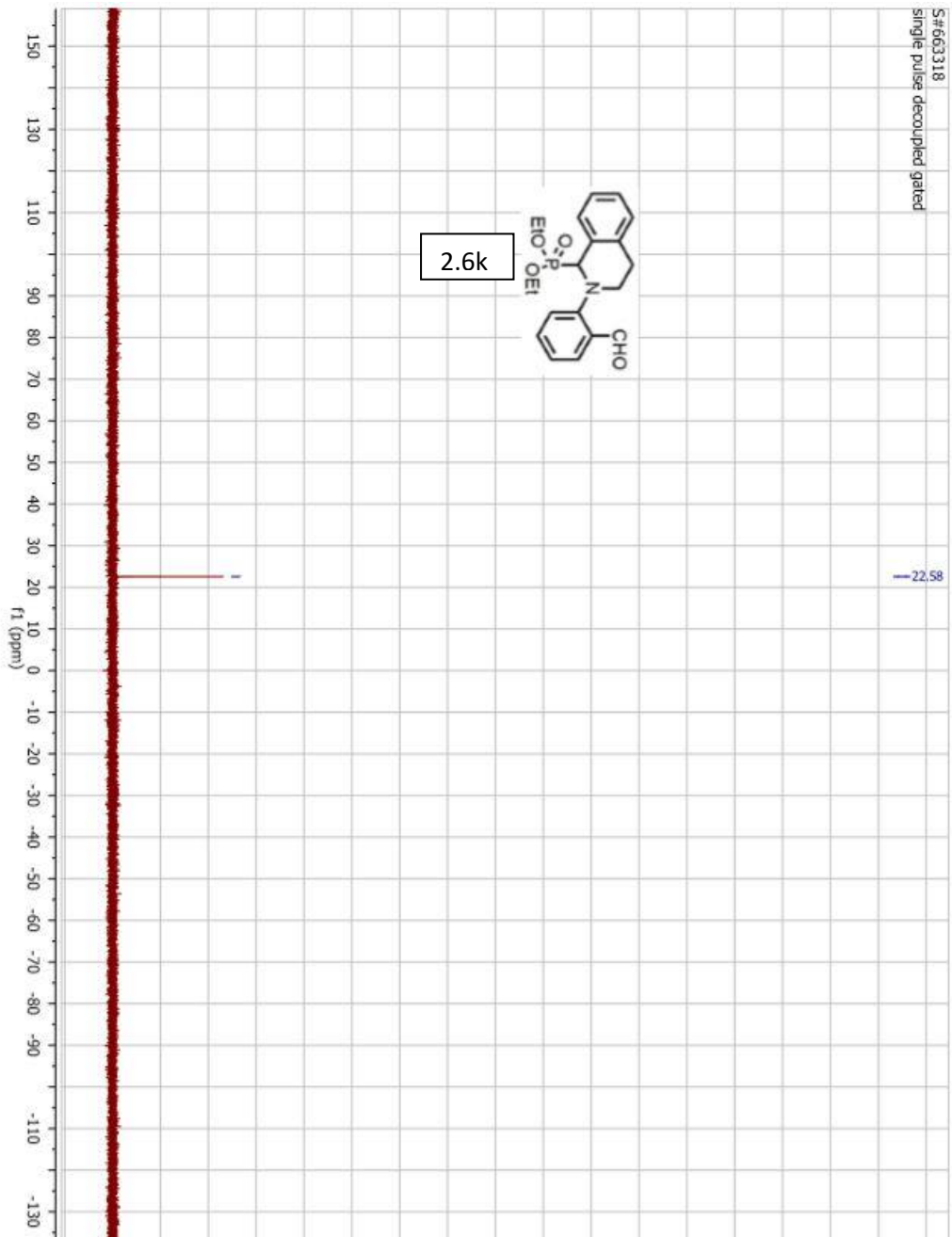
S#363687
single pulse decoupled gated

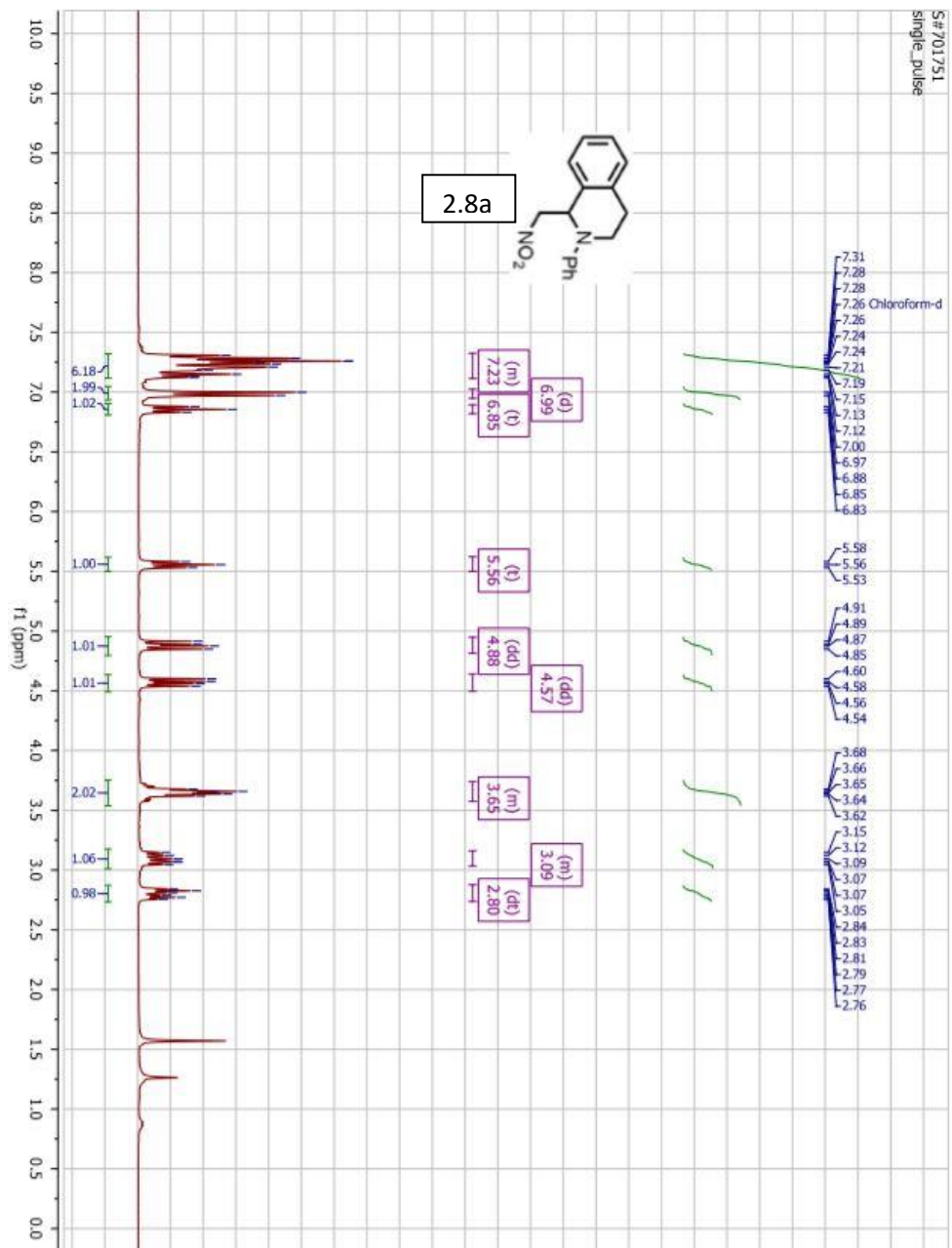


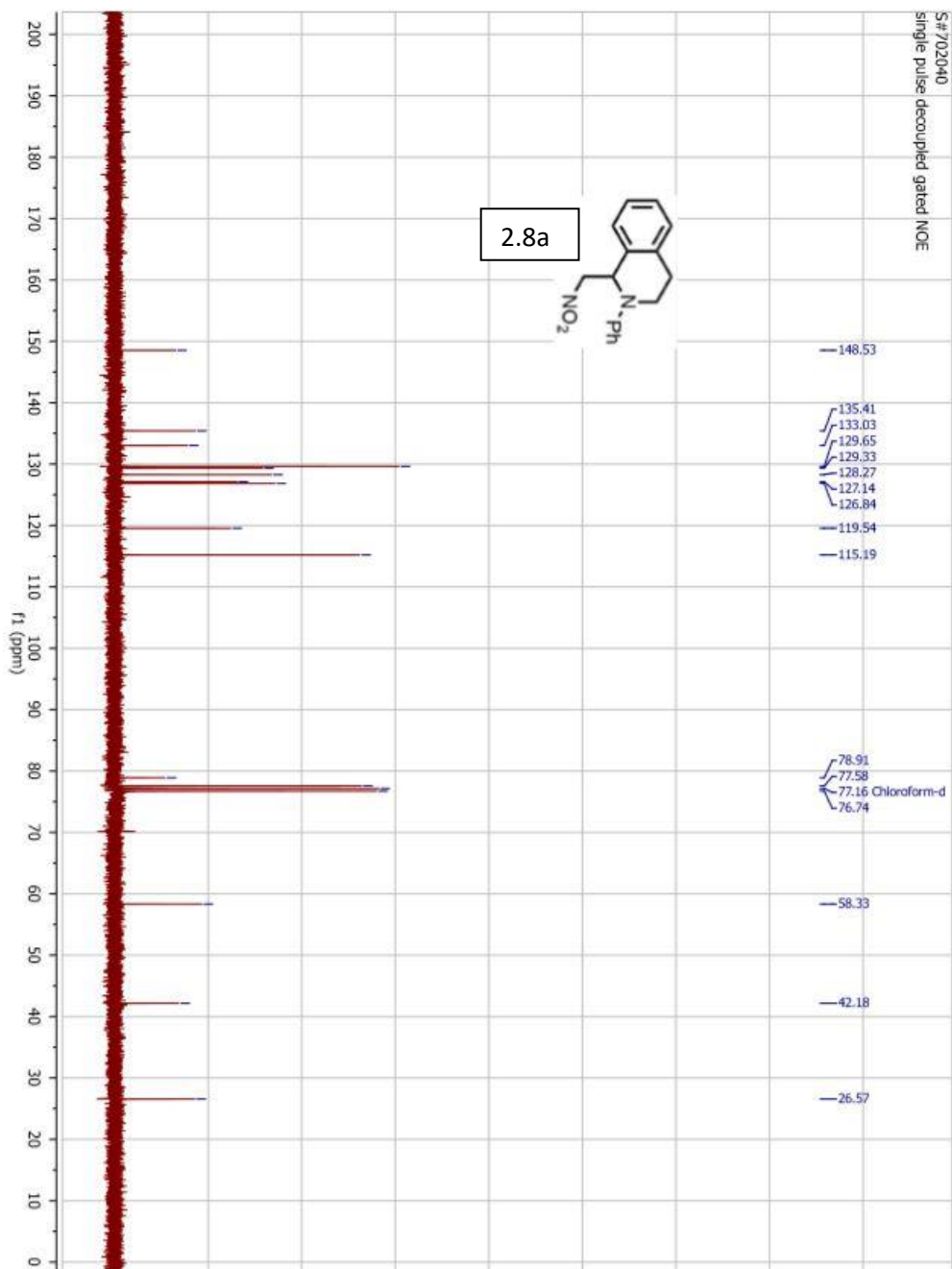


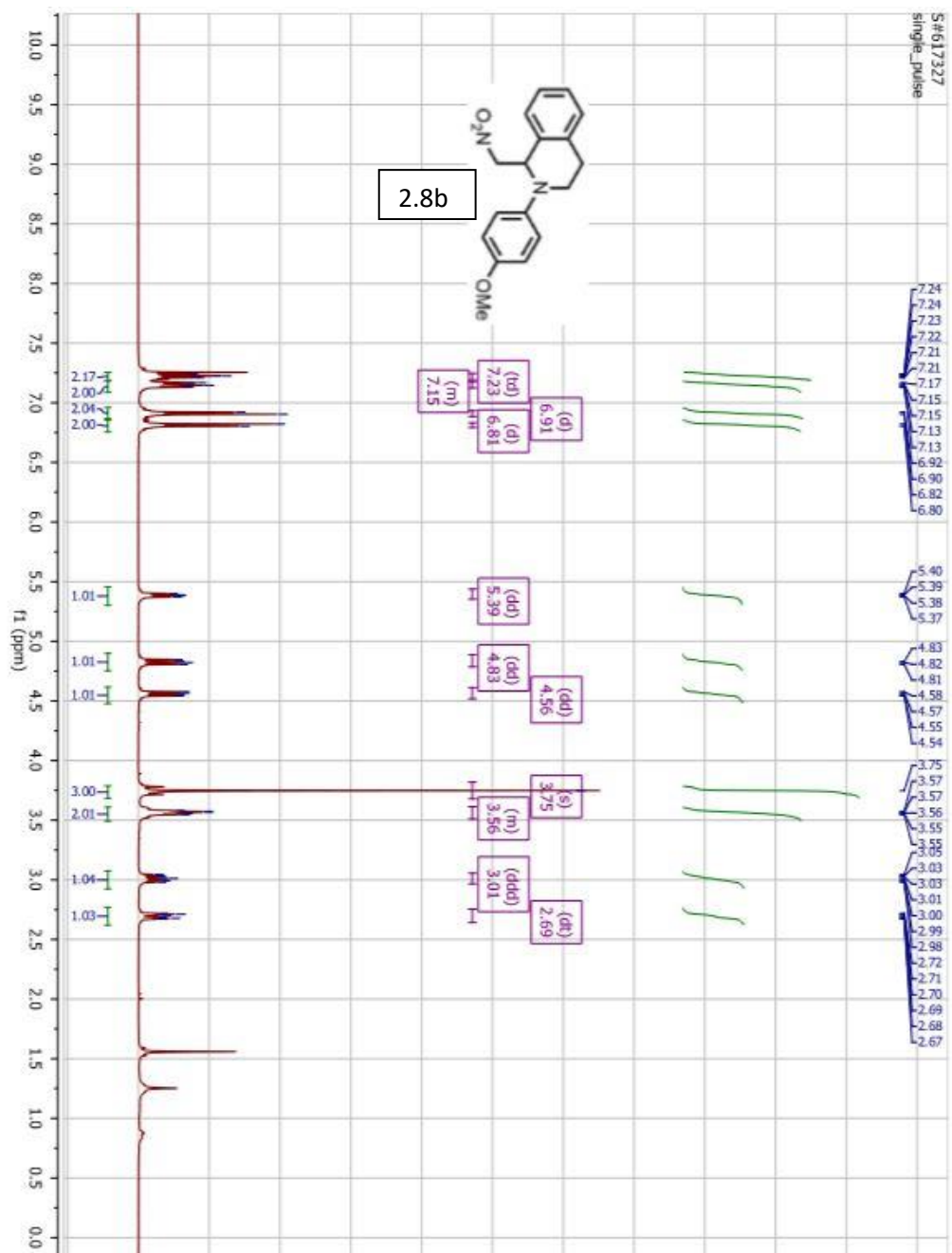


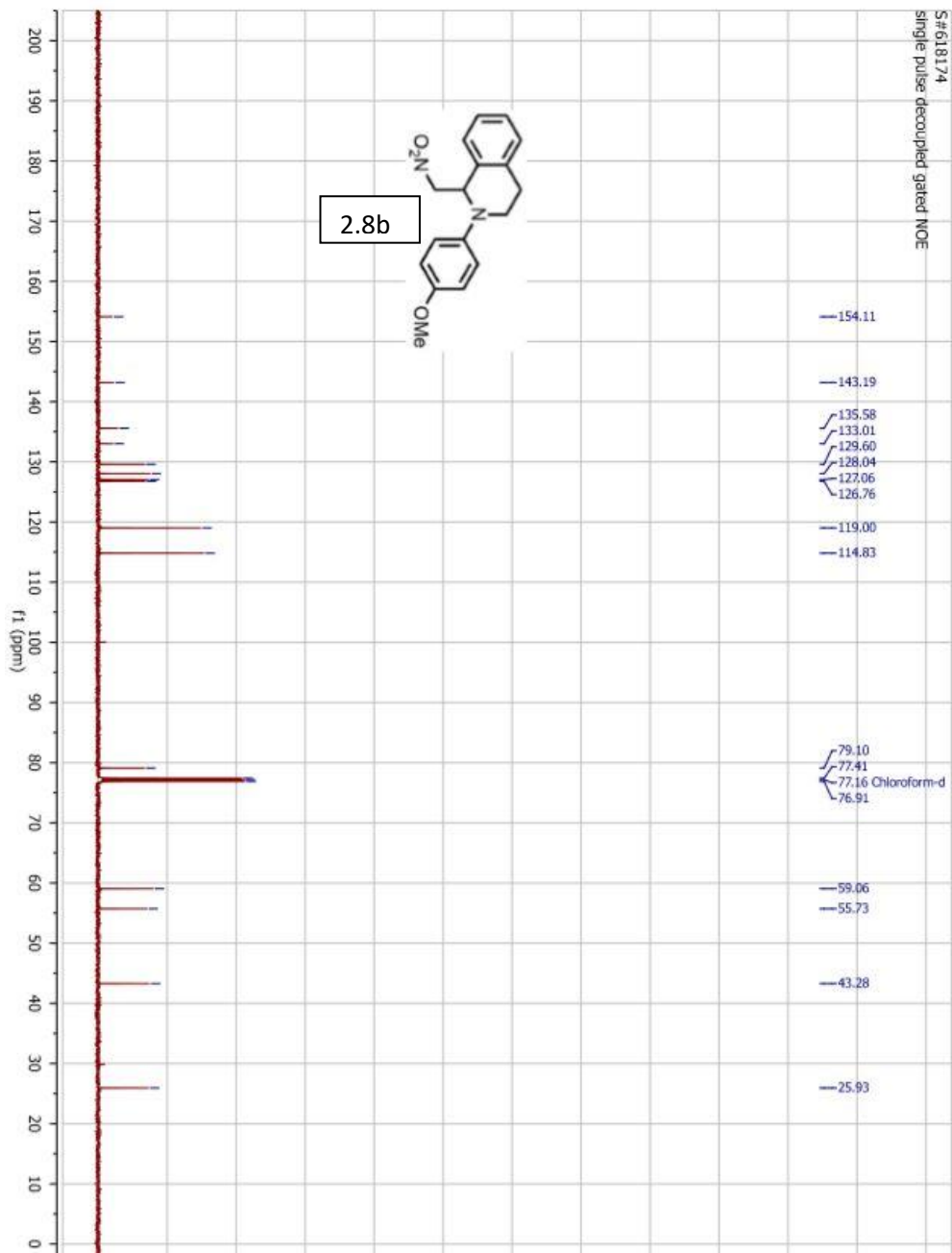
S#663318
single pulse decoupled gated

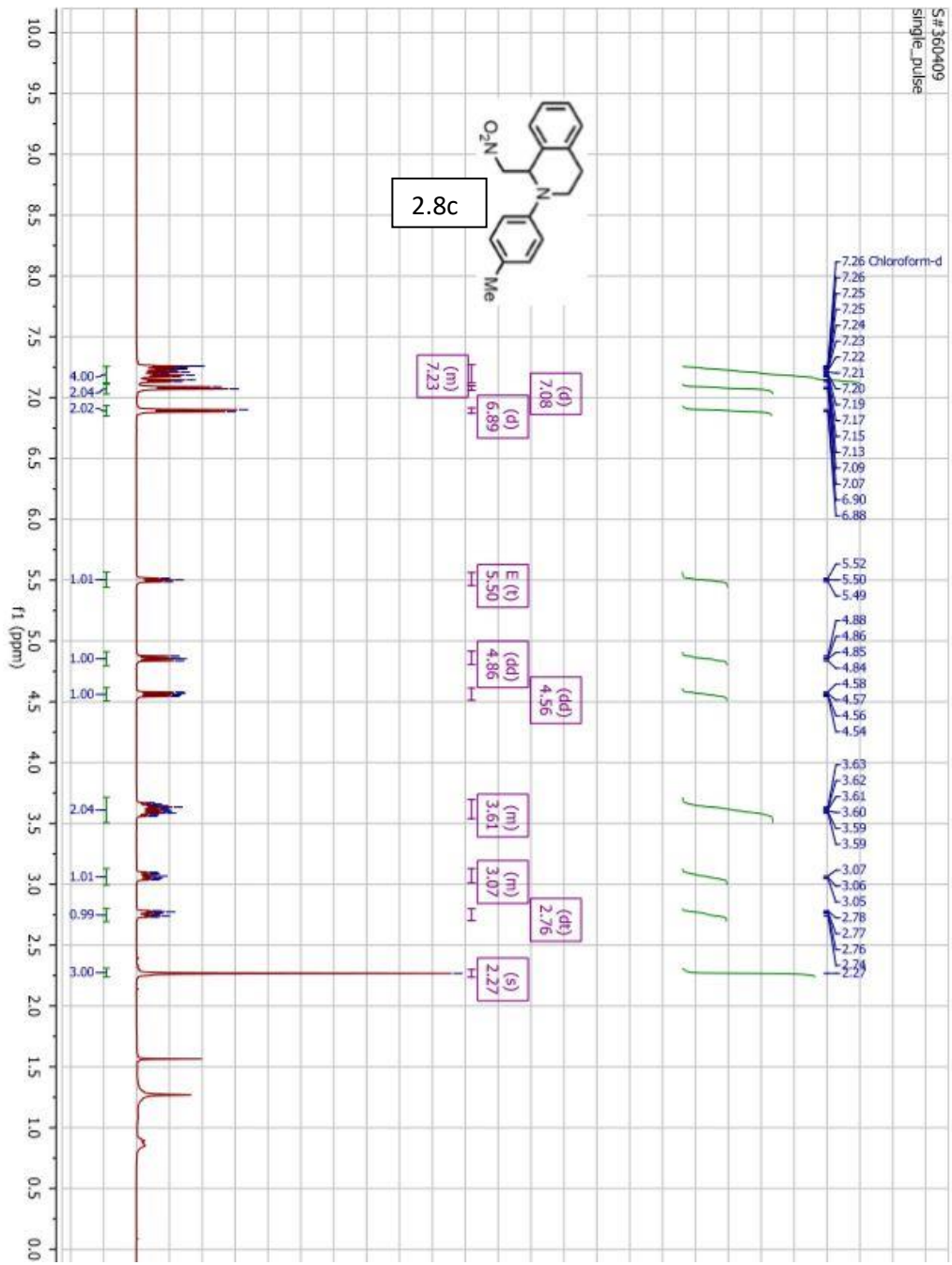


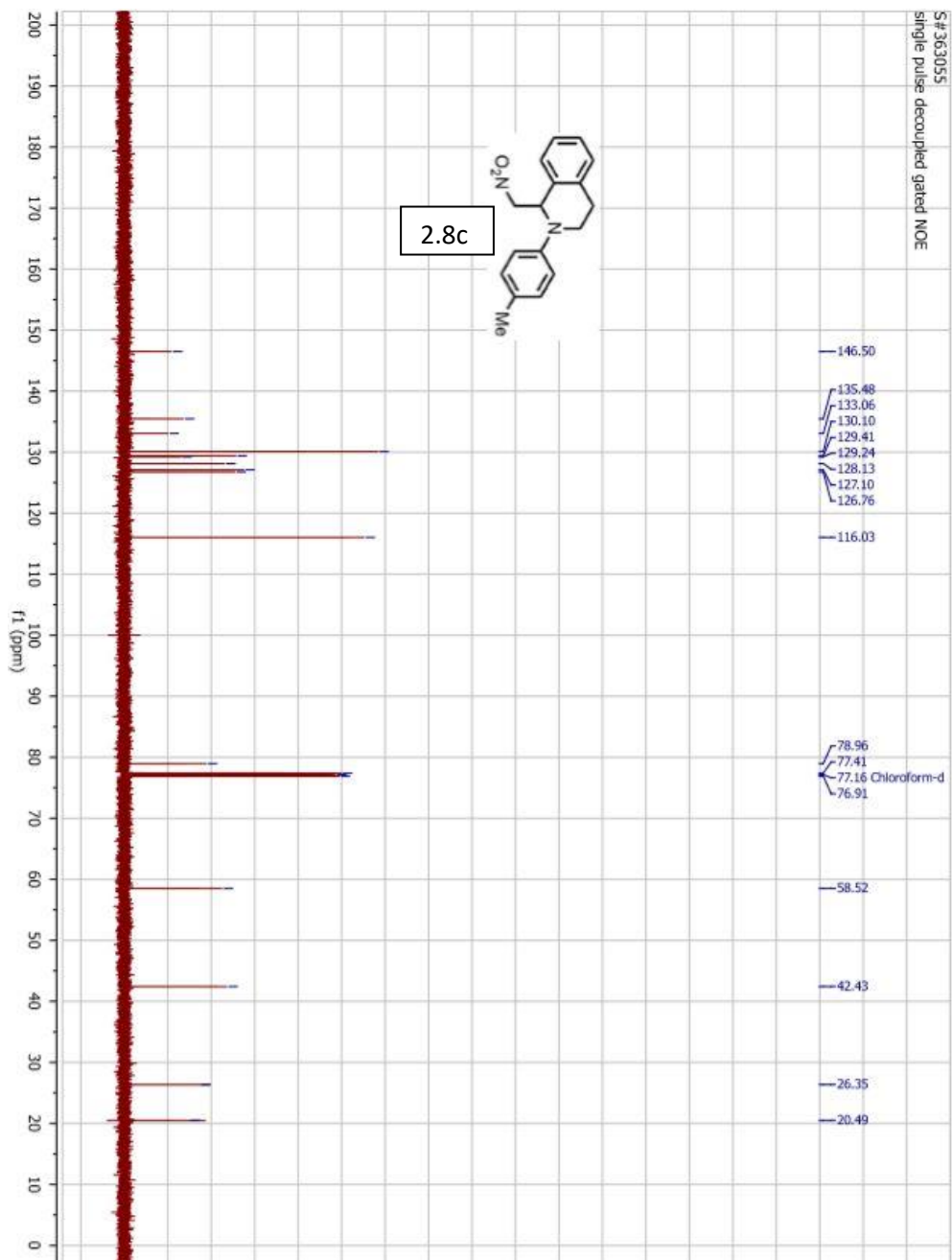


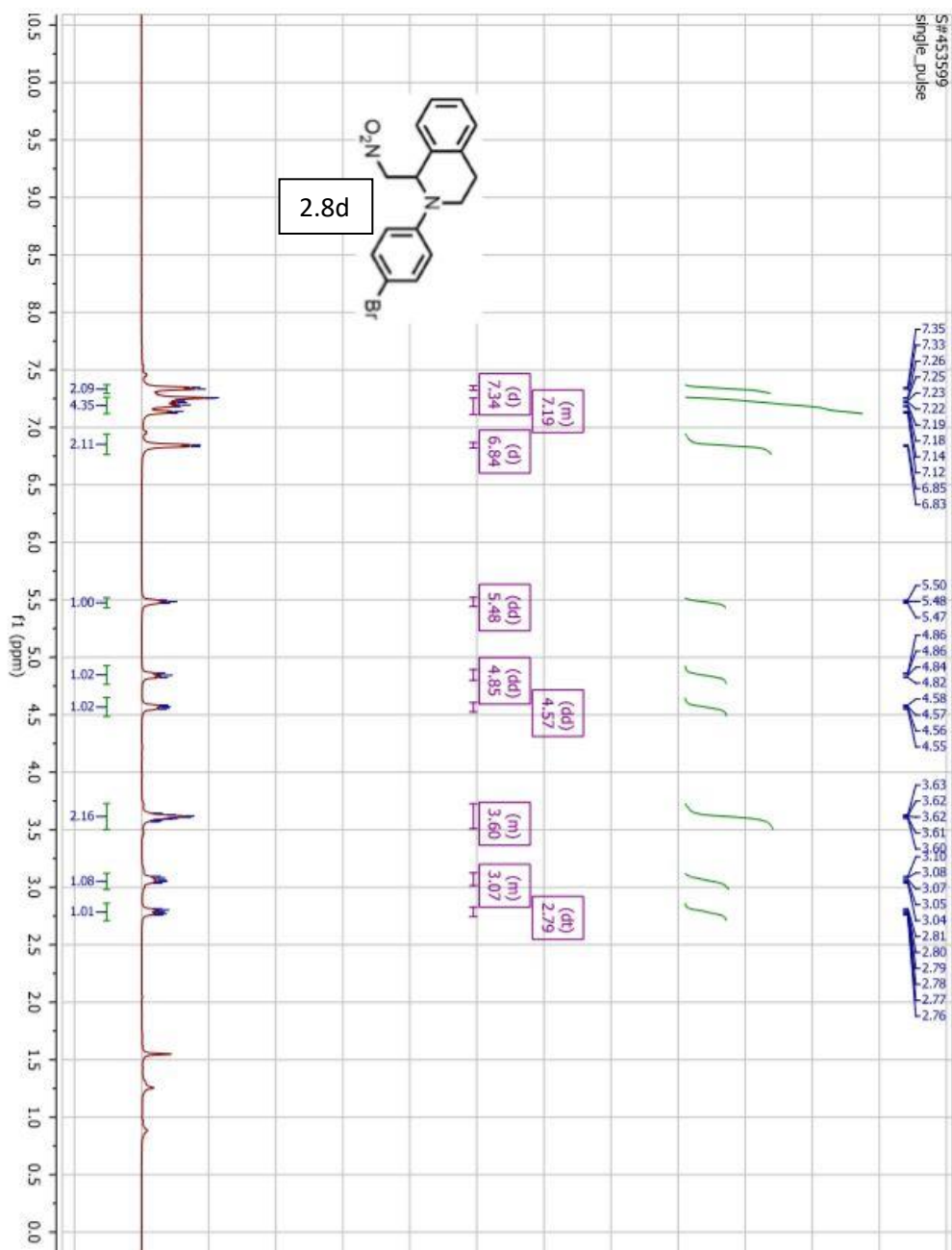


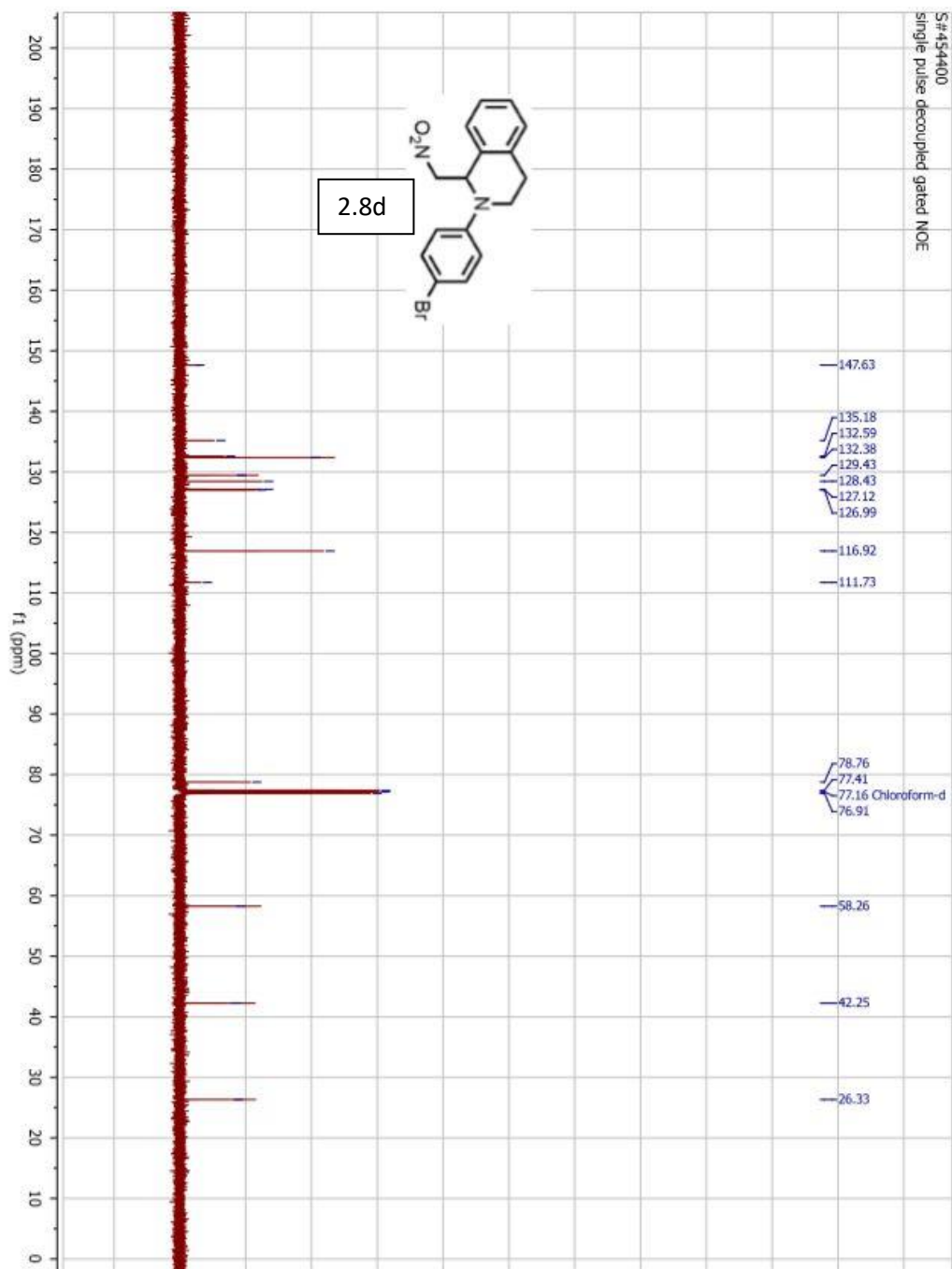


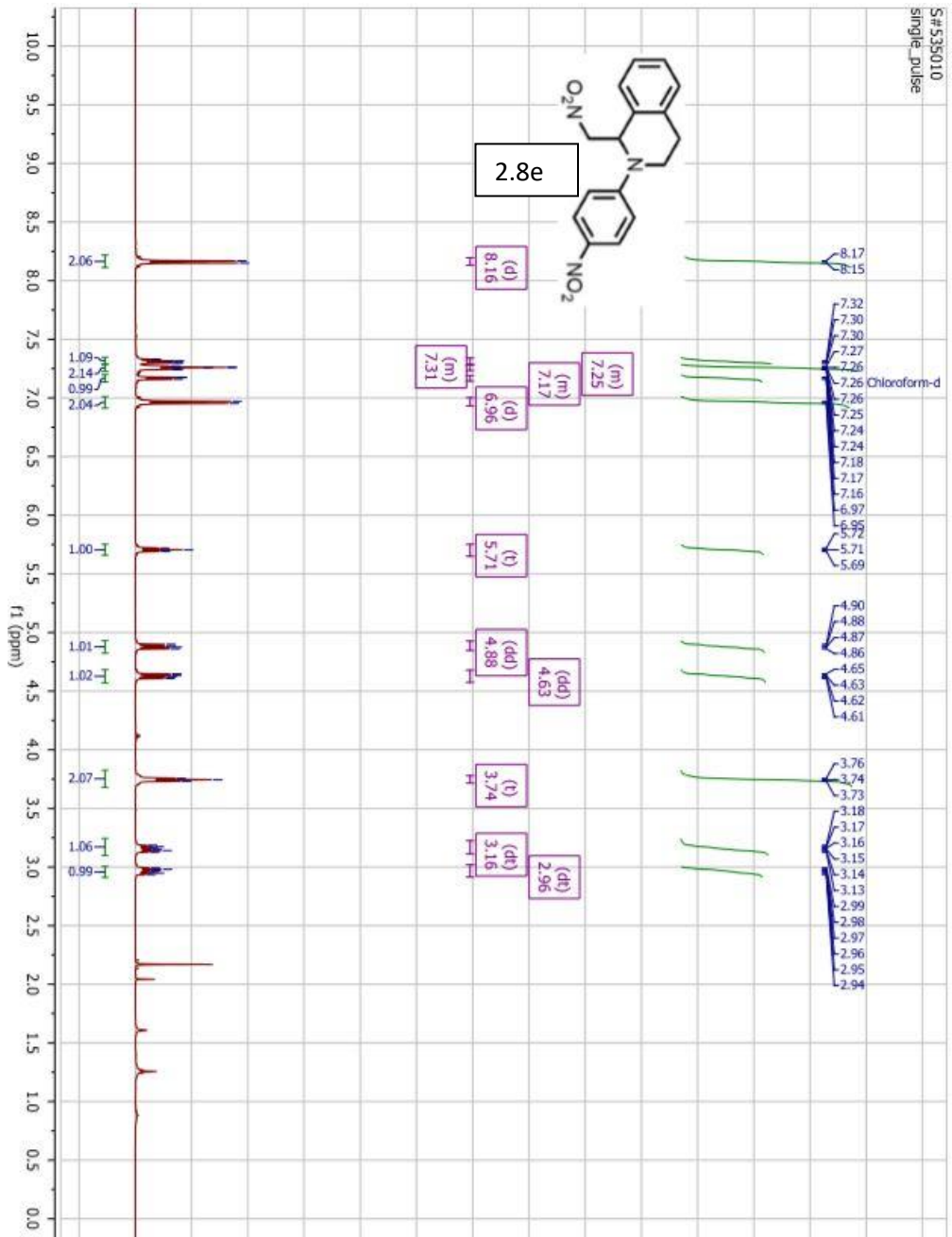


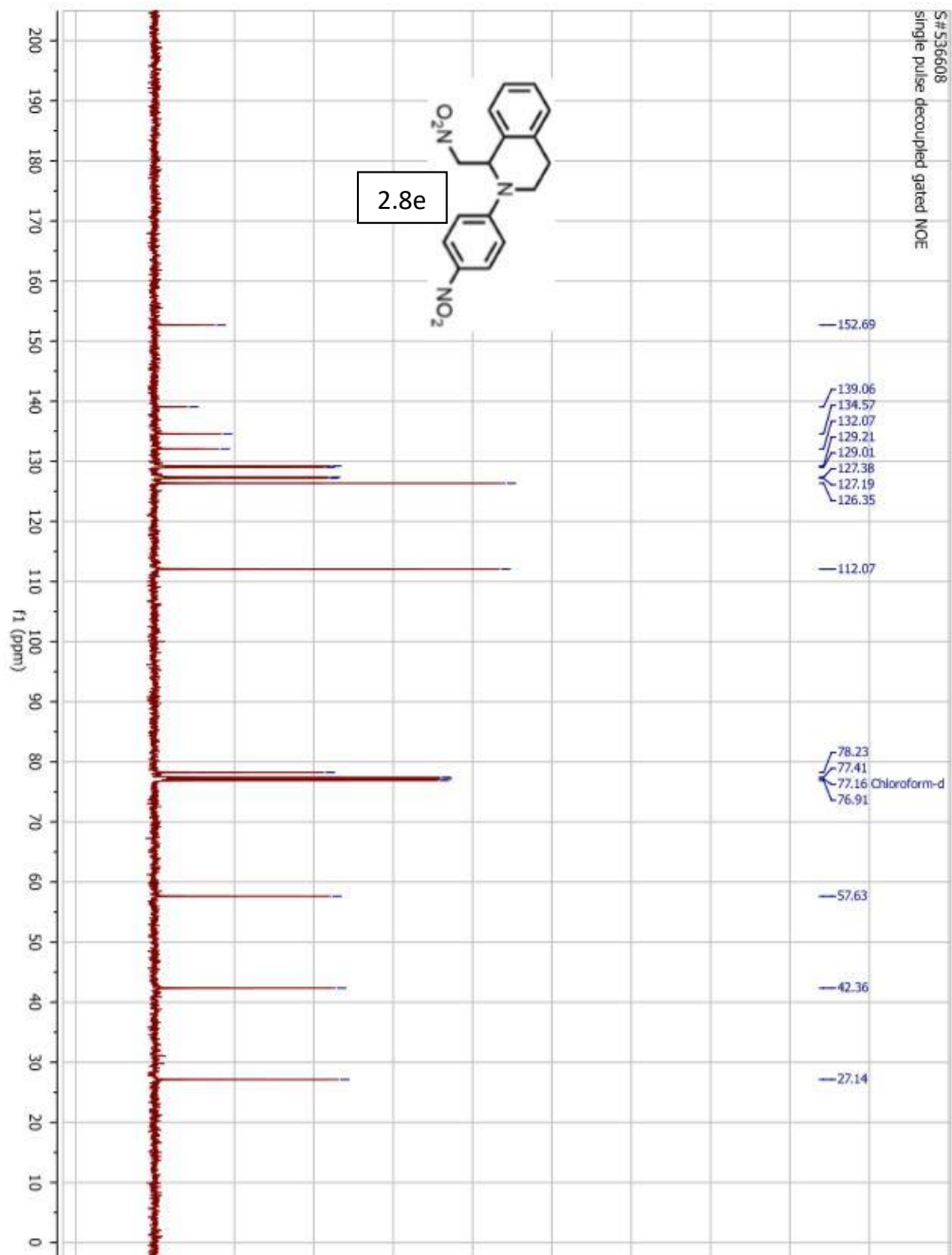


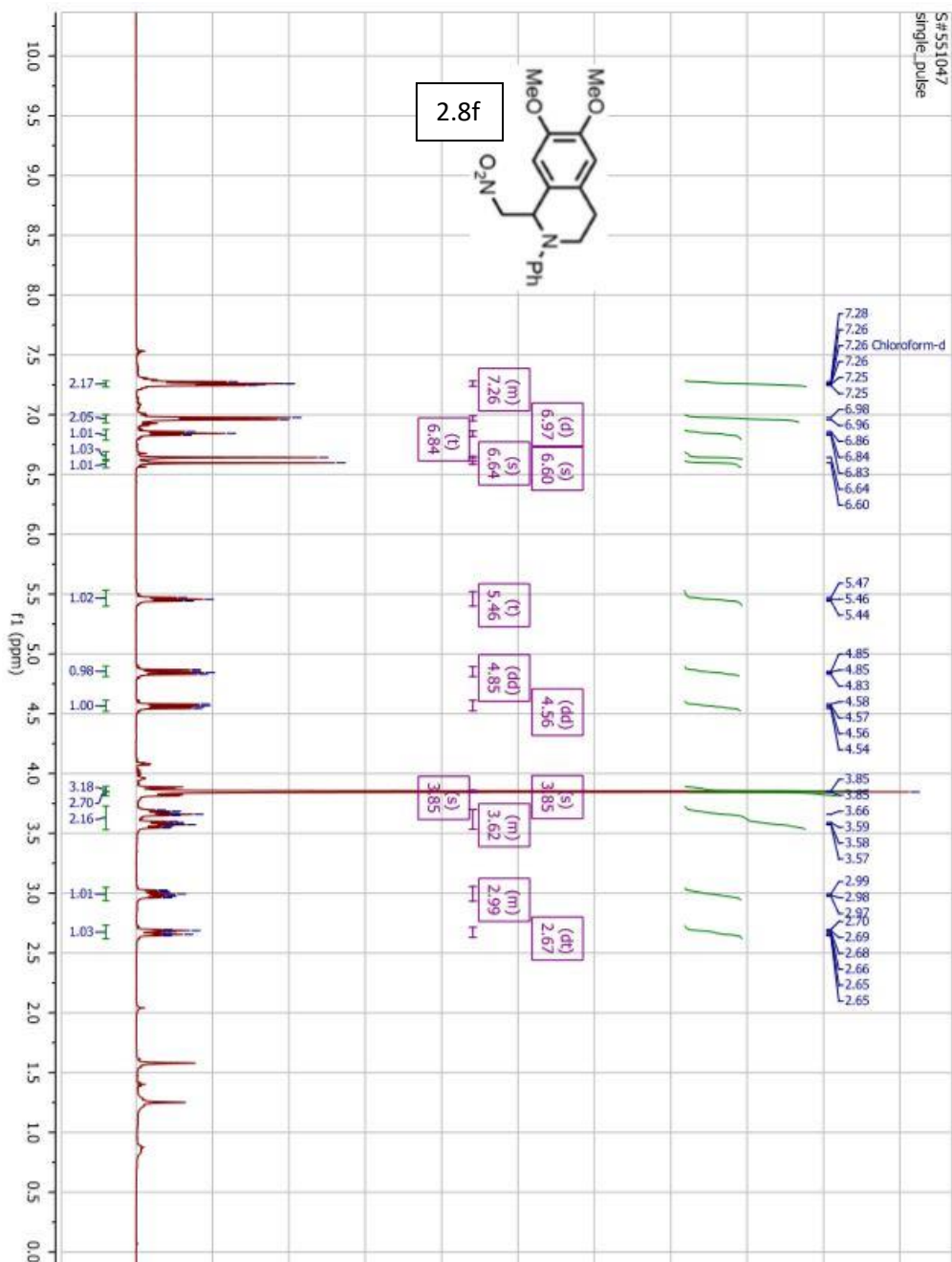


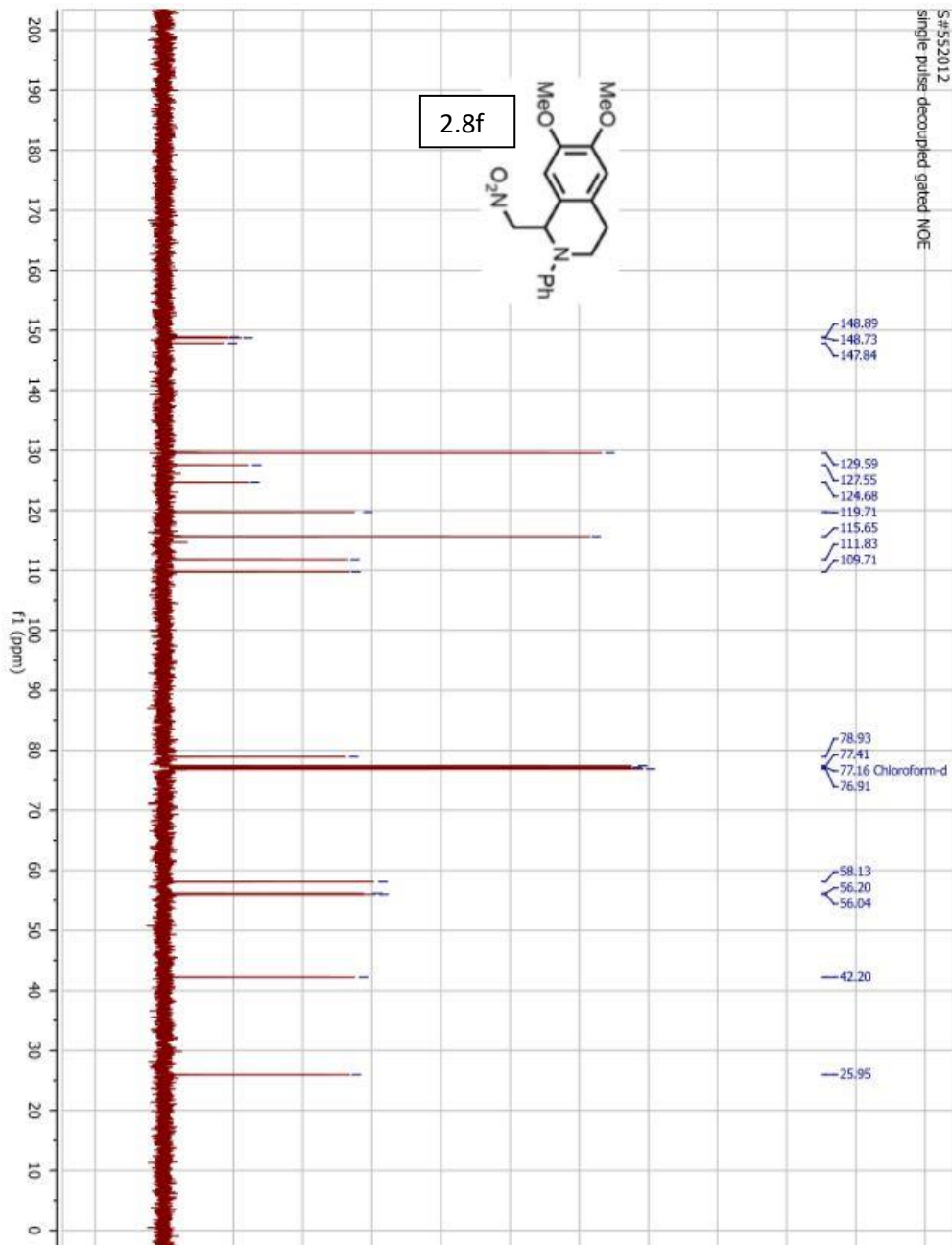


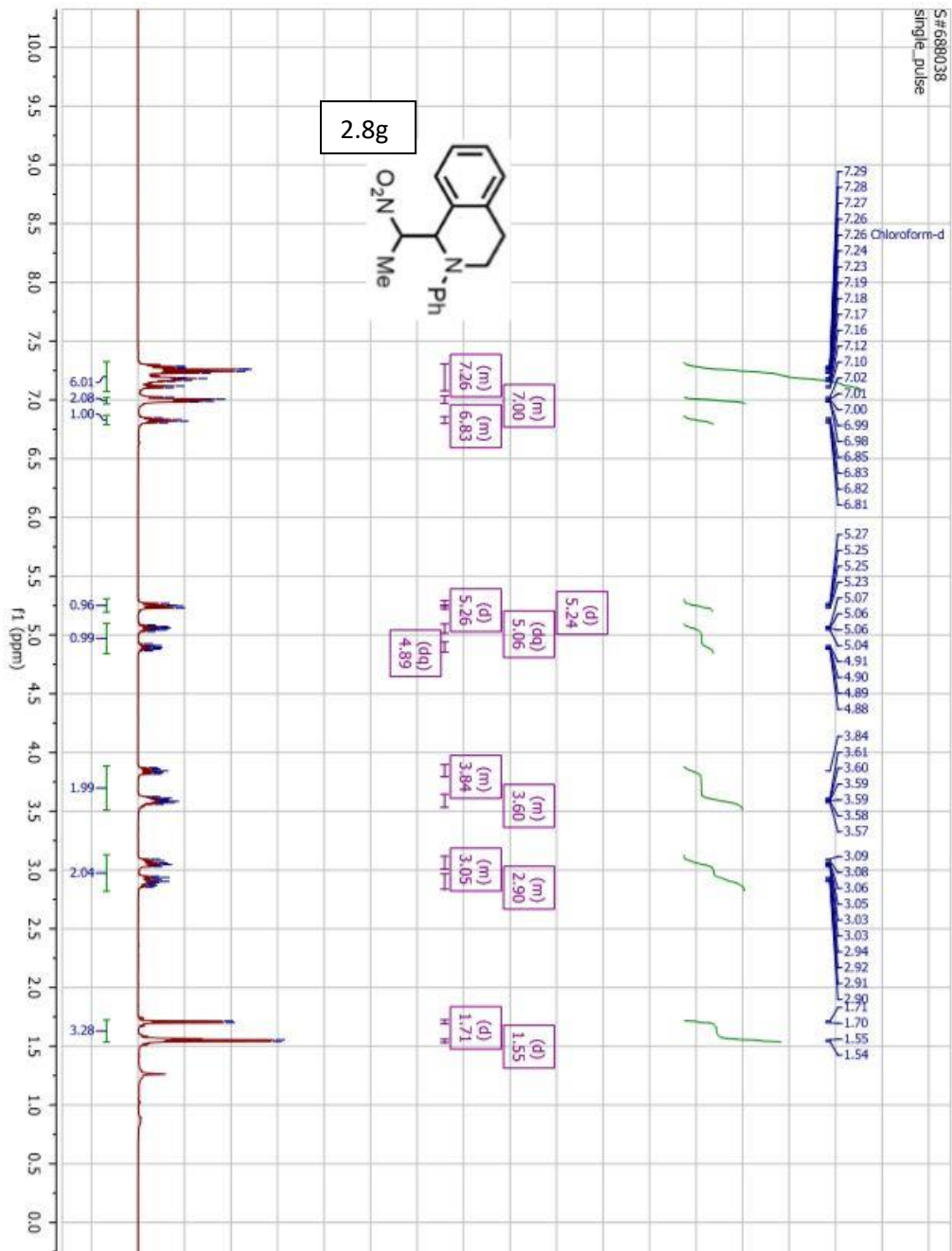




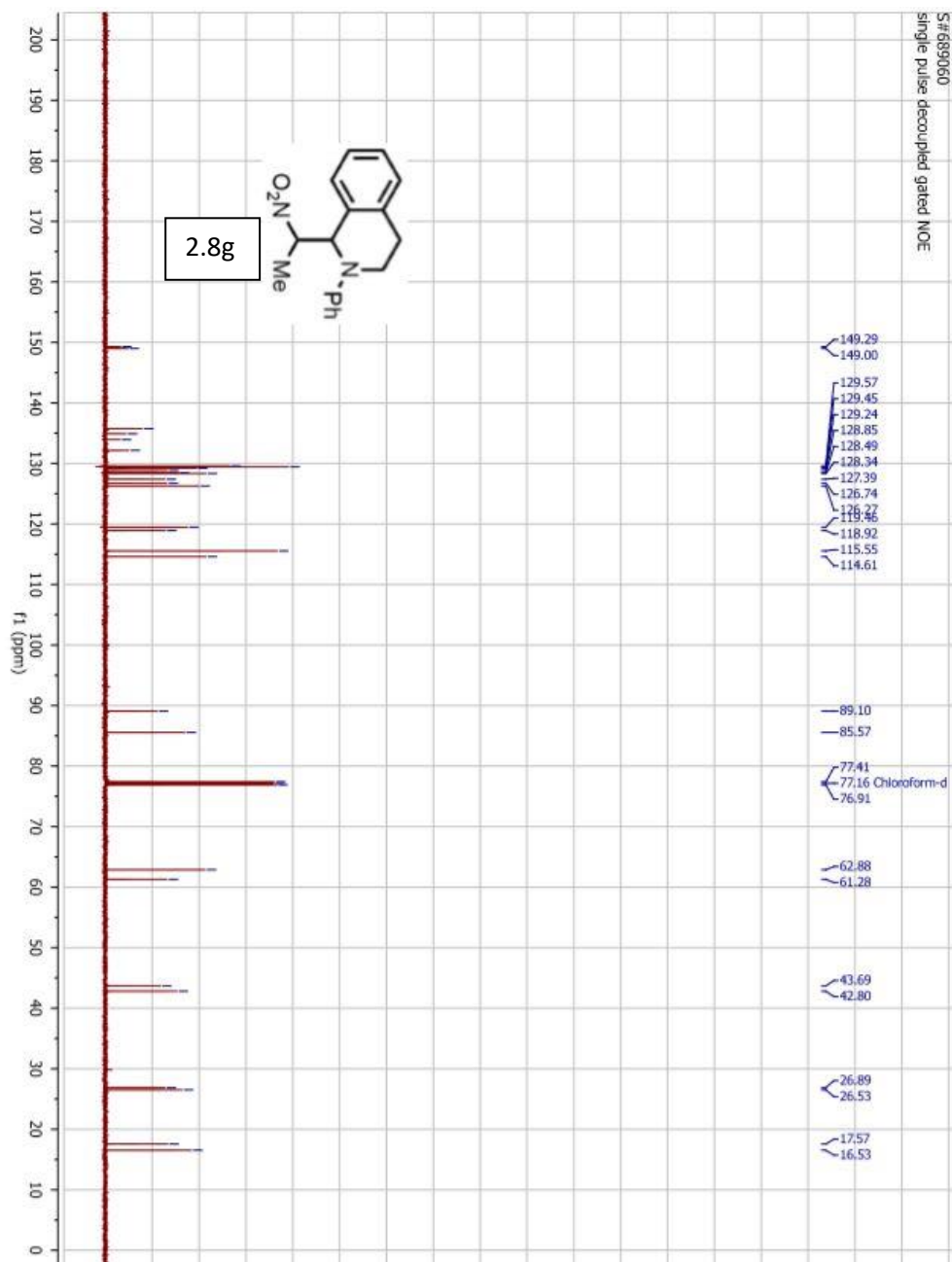


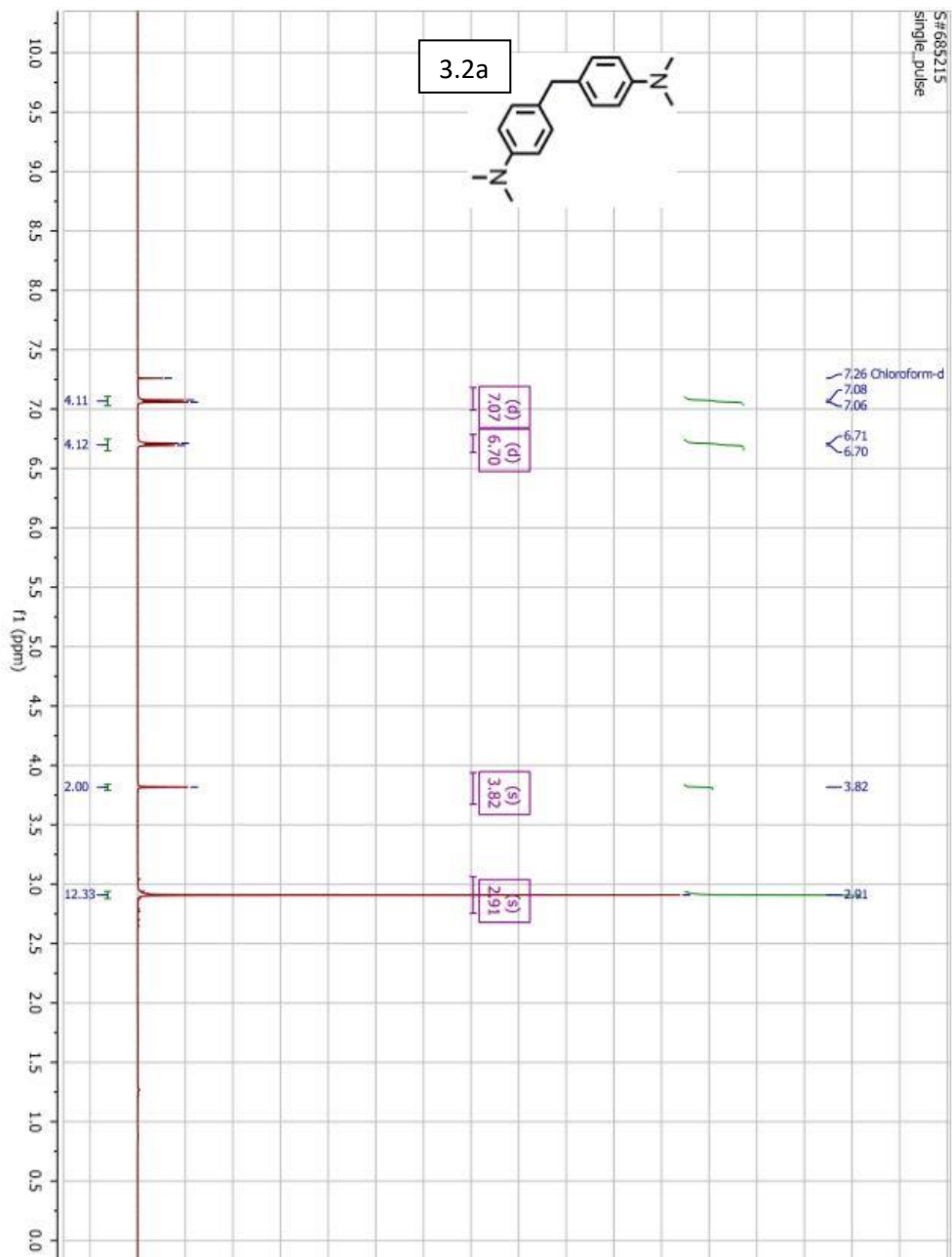


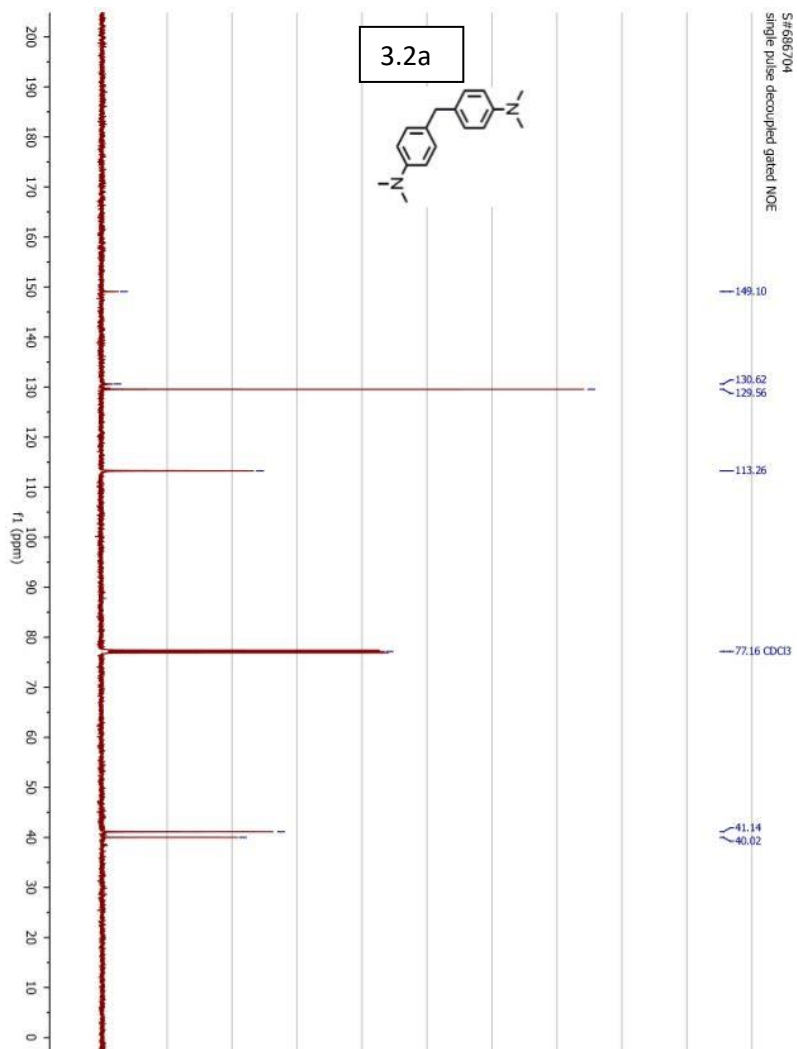


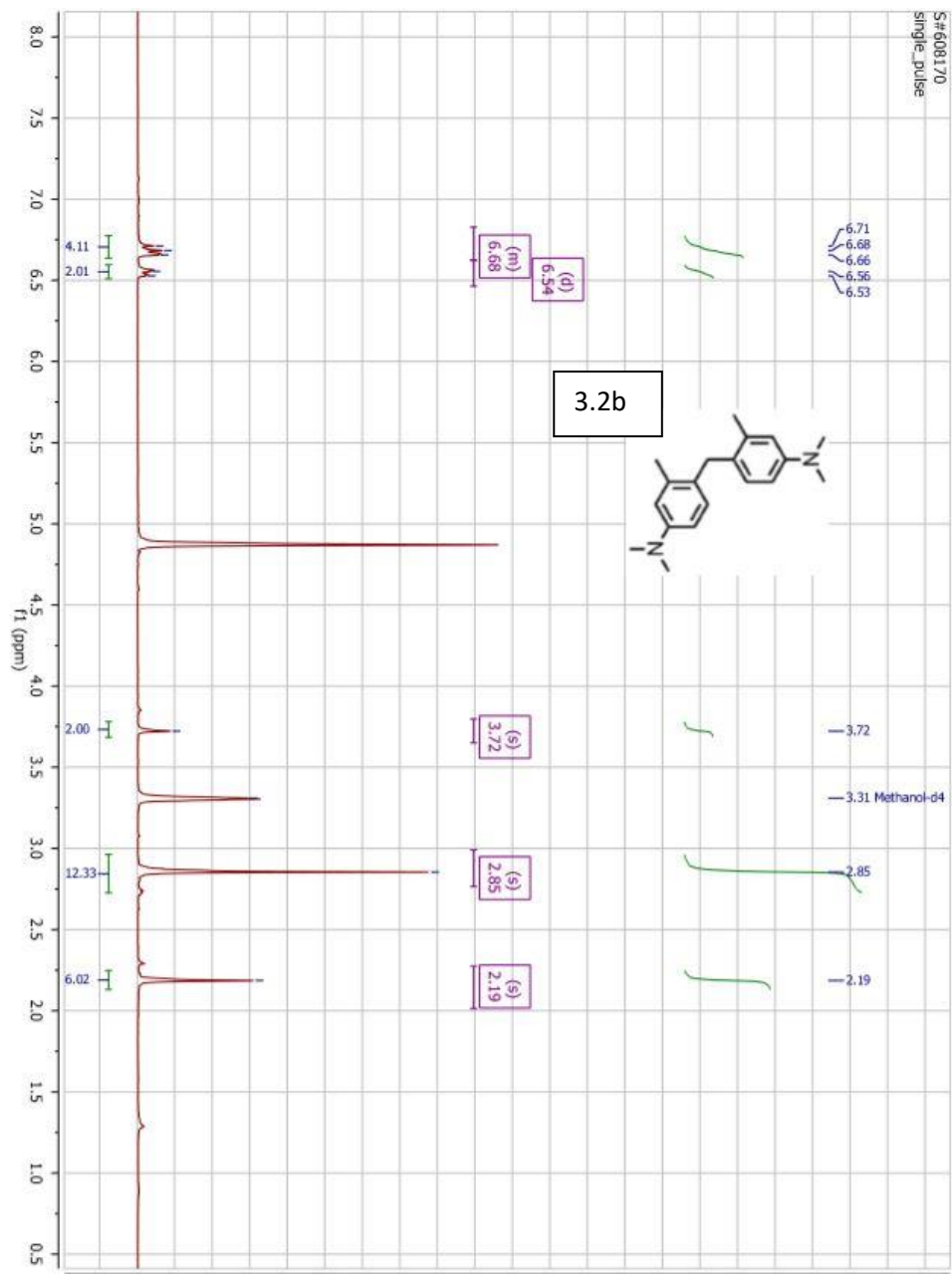


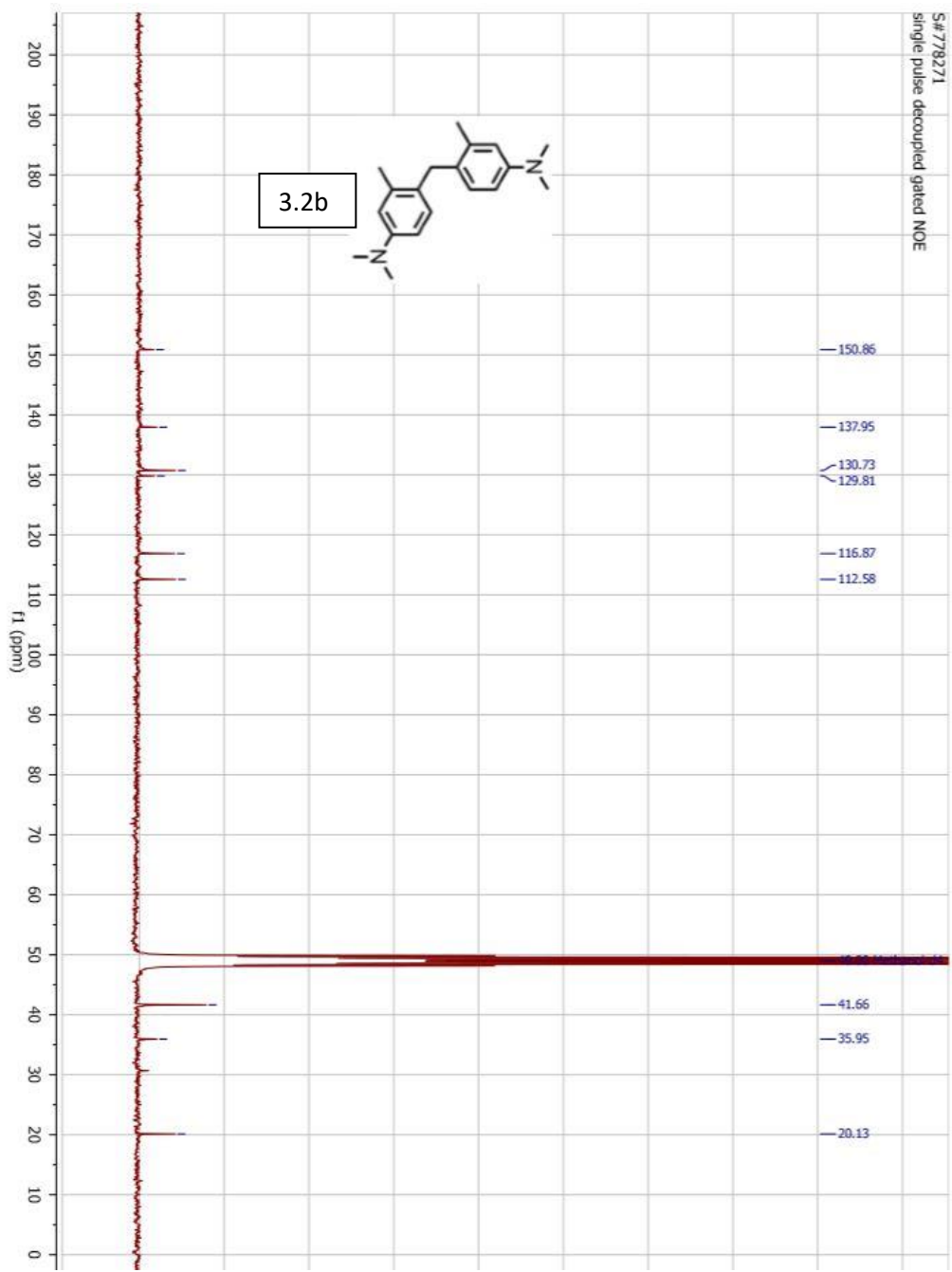
S#689060
single pulse decoupled gated NOE

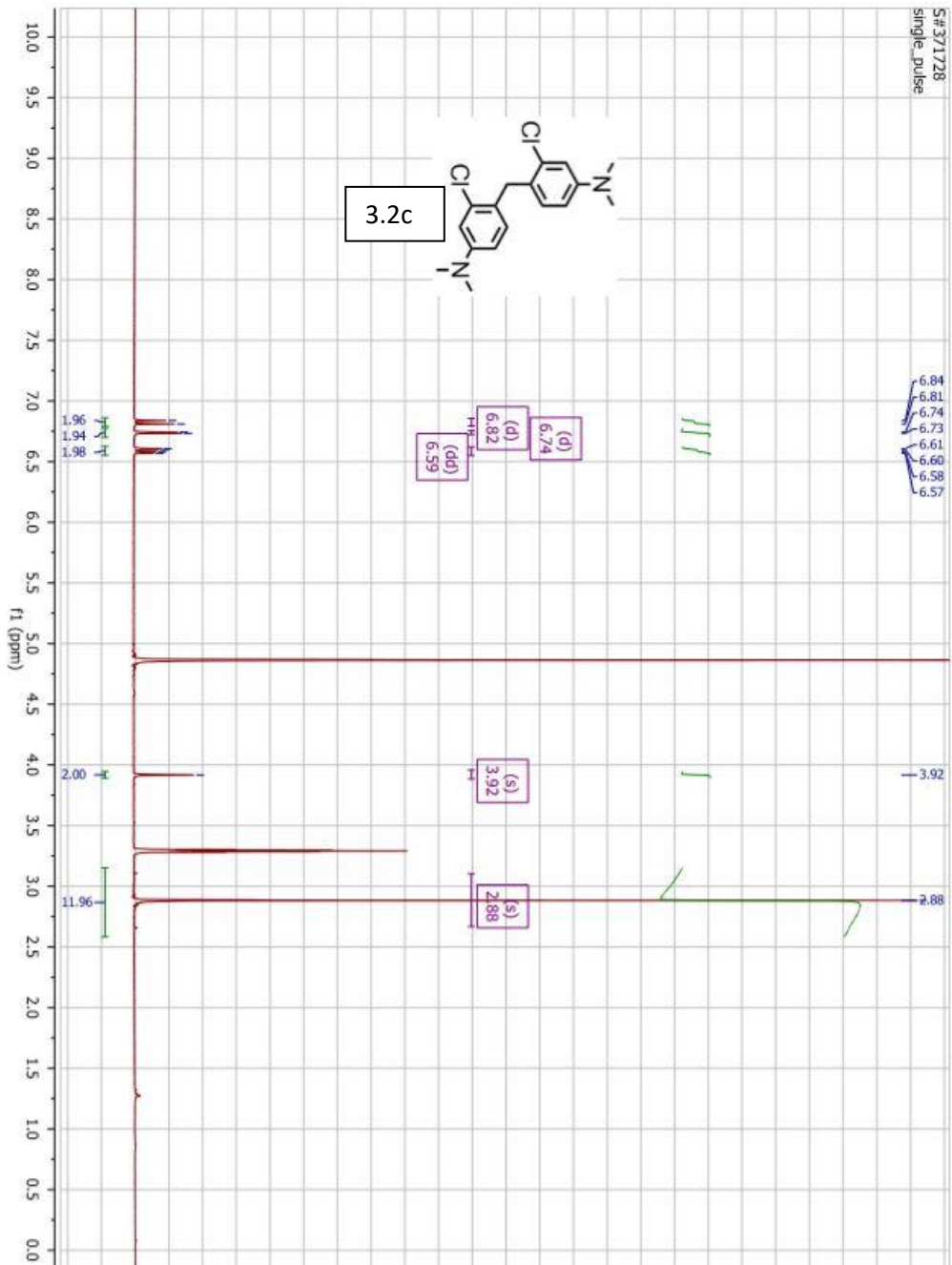


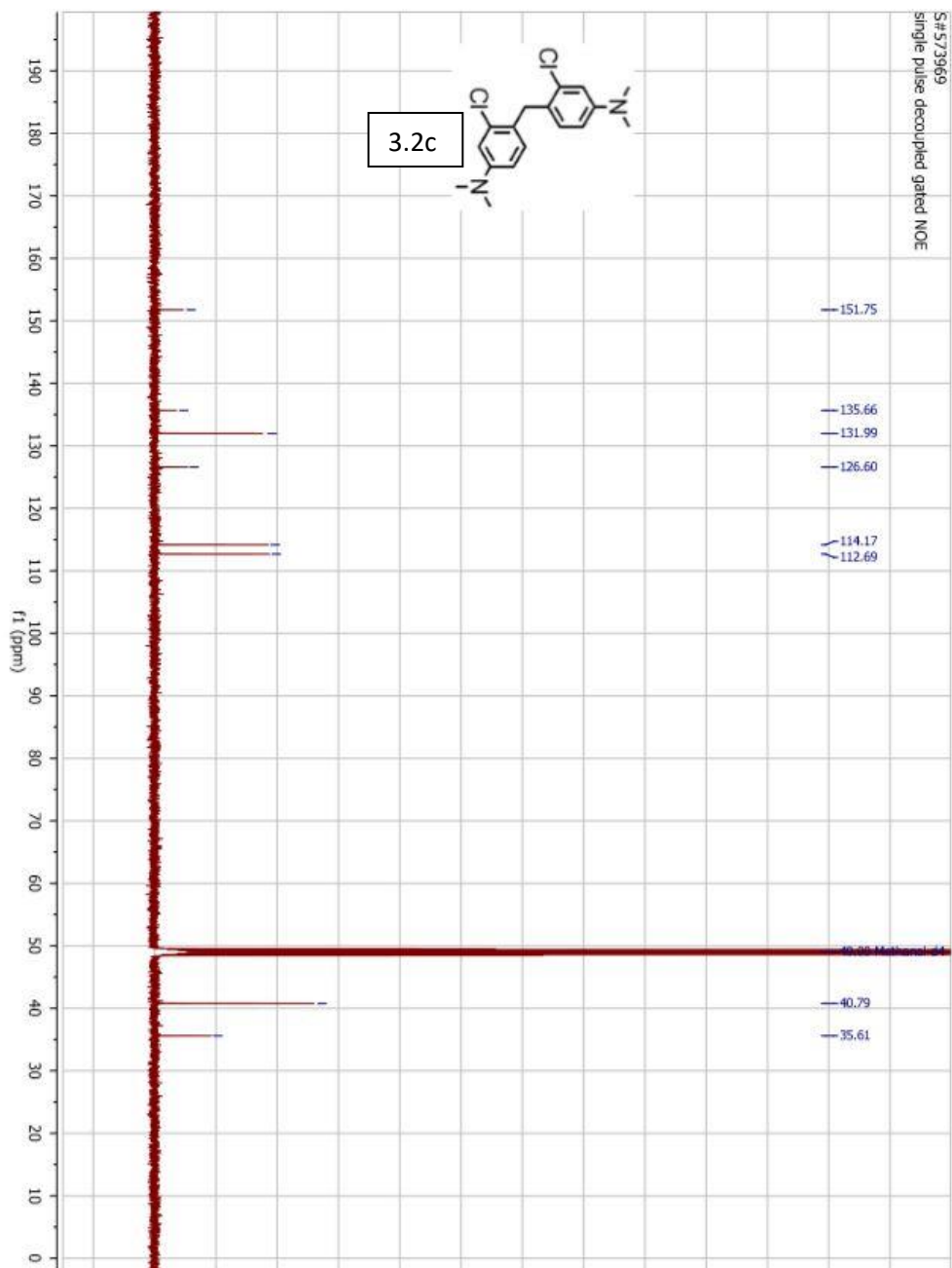


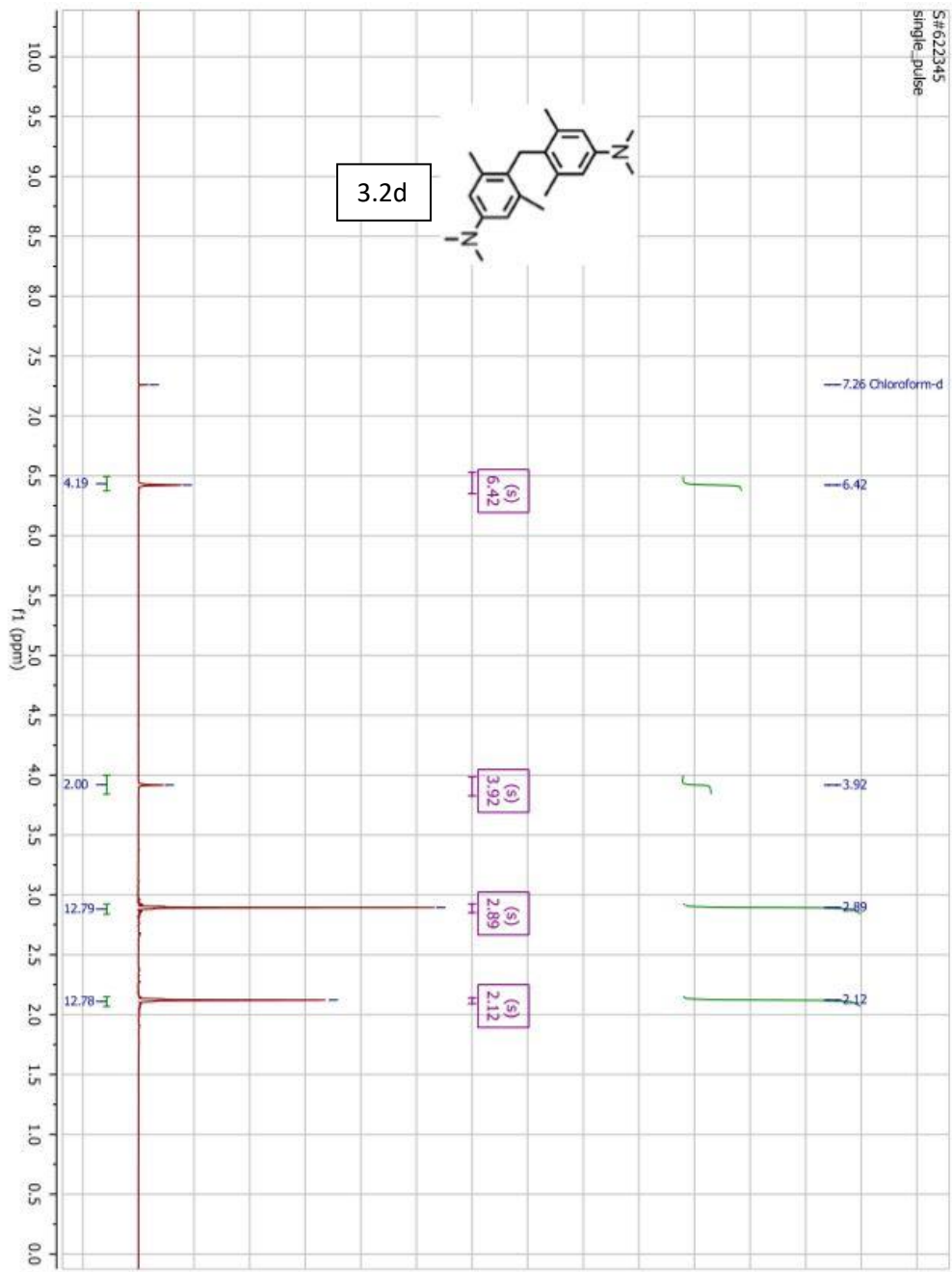




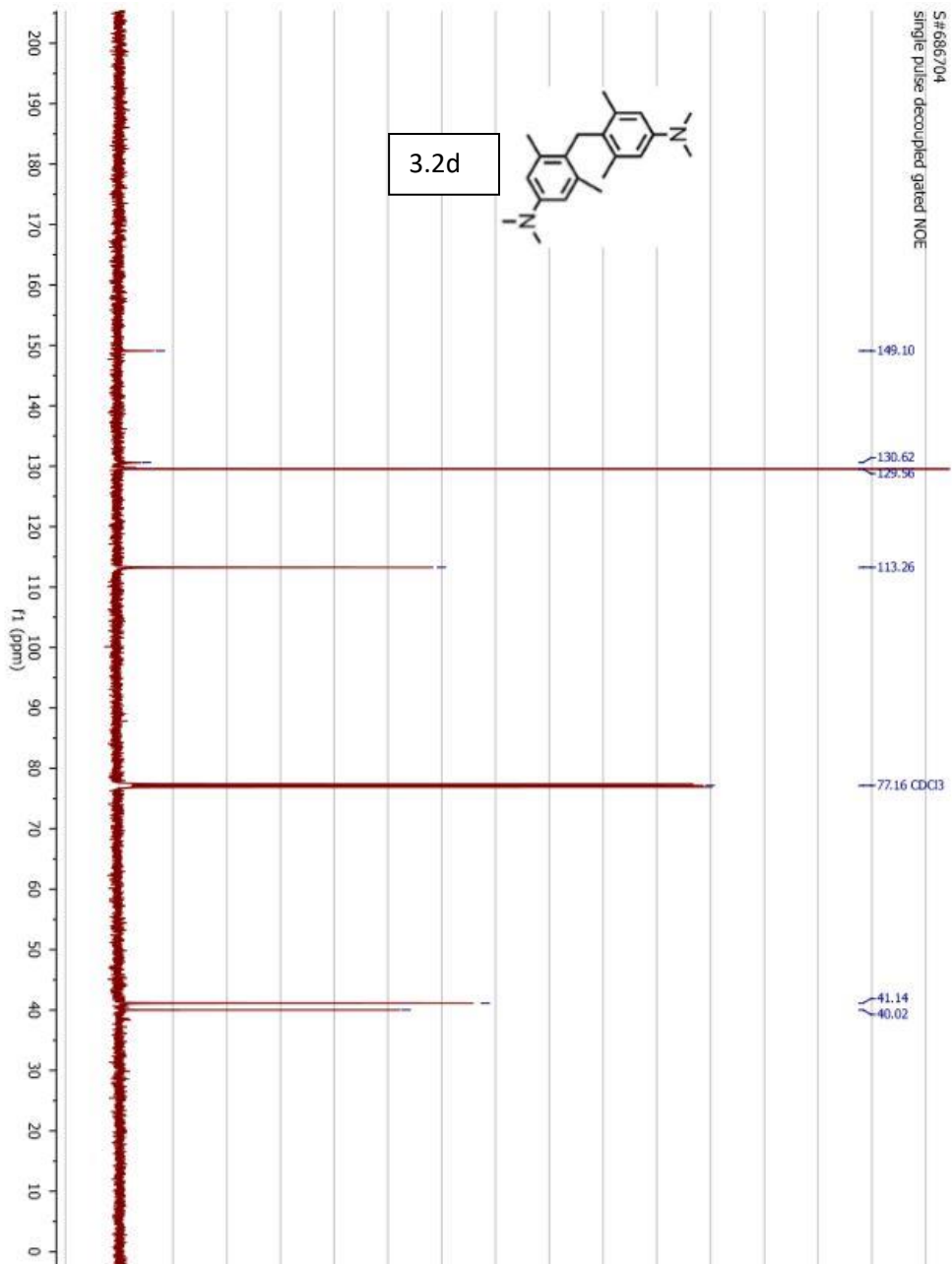


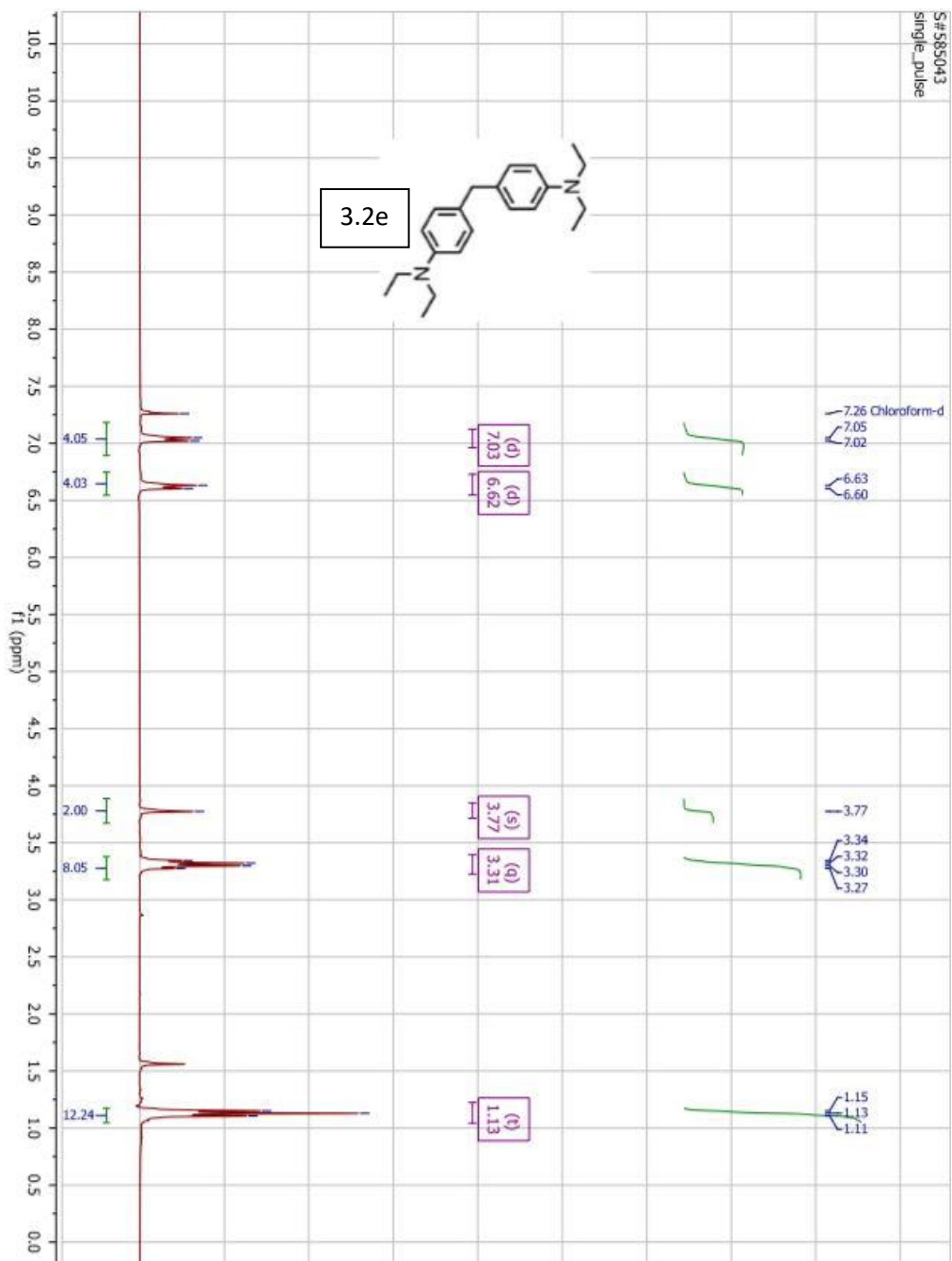


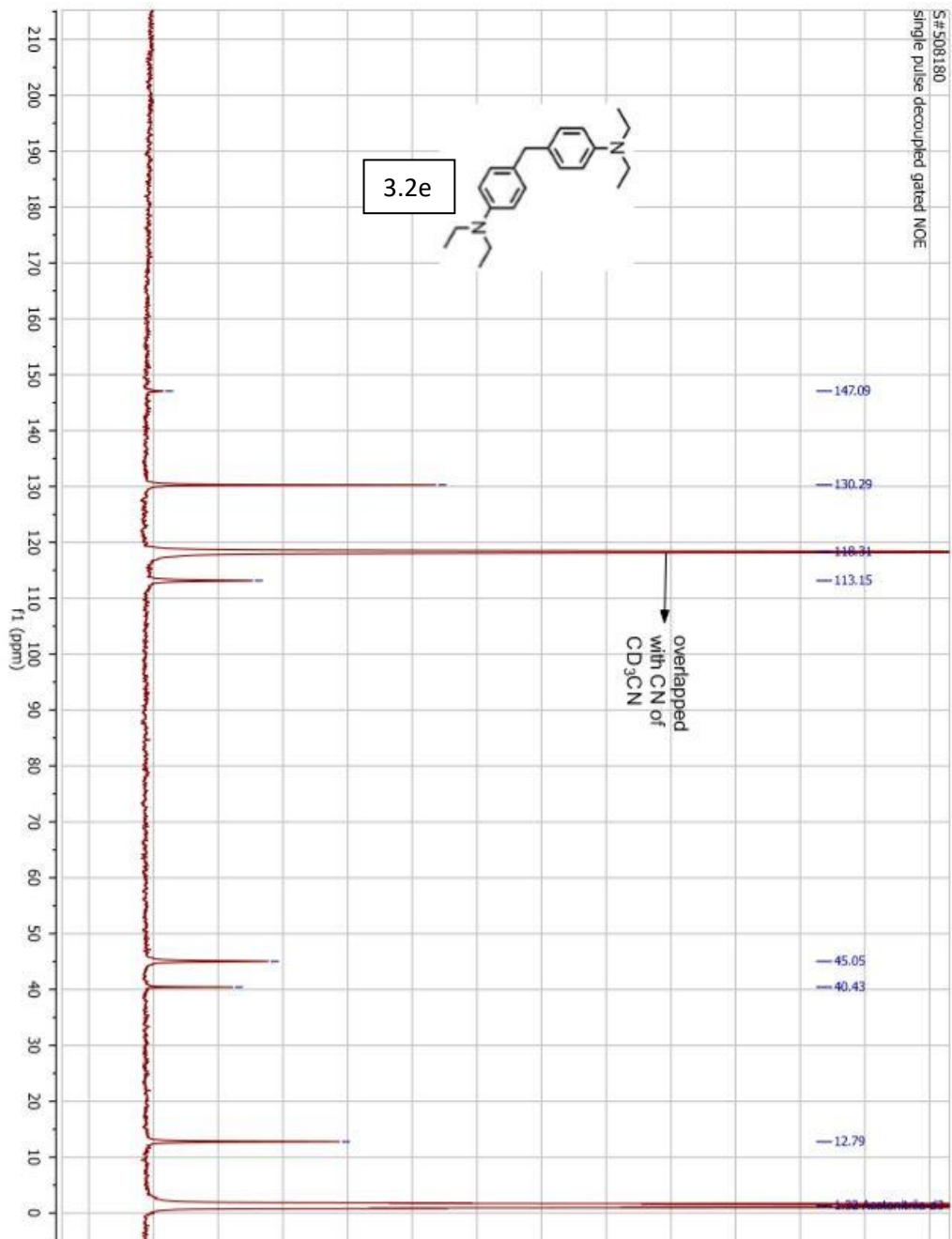


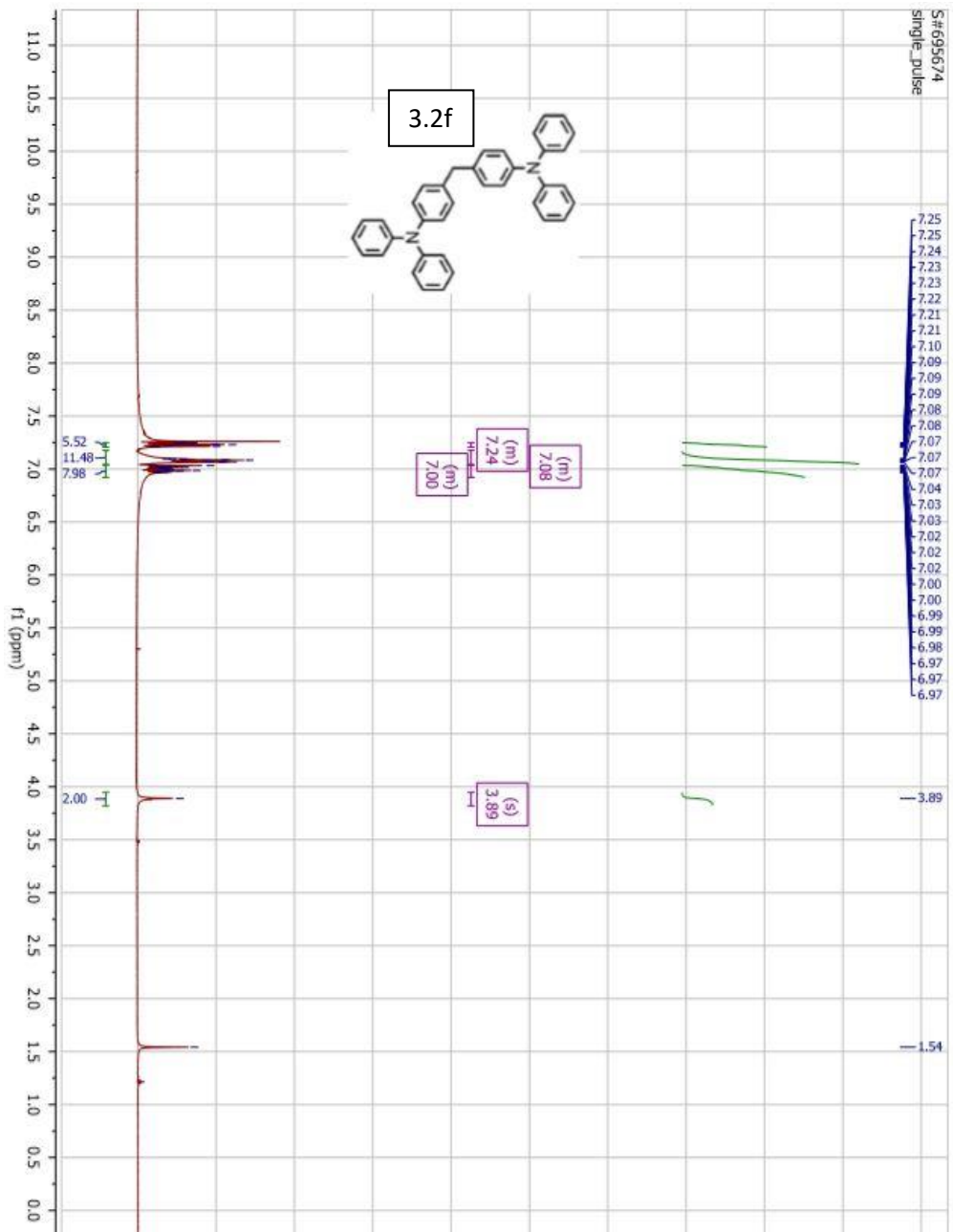


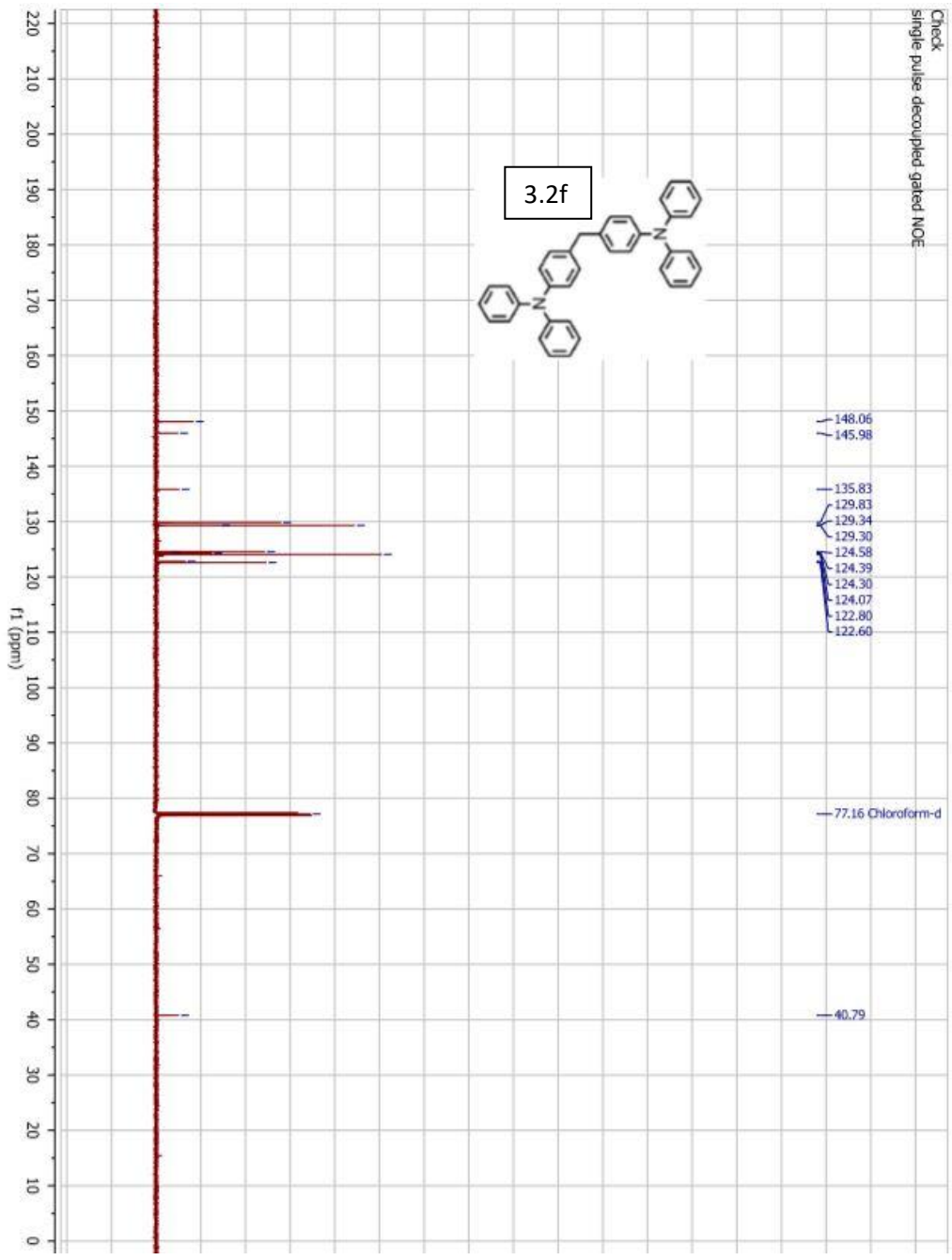
S#686704
single pulse decoupled gated NOE

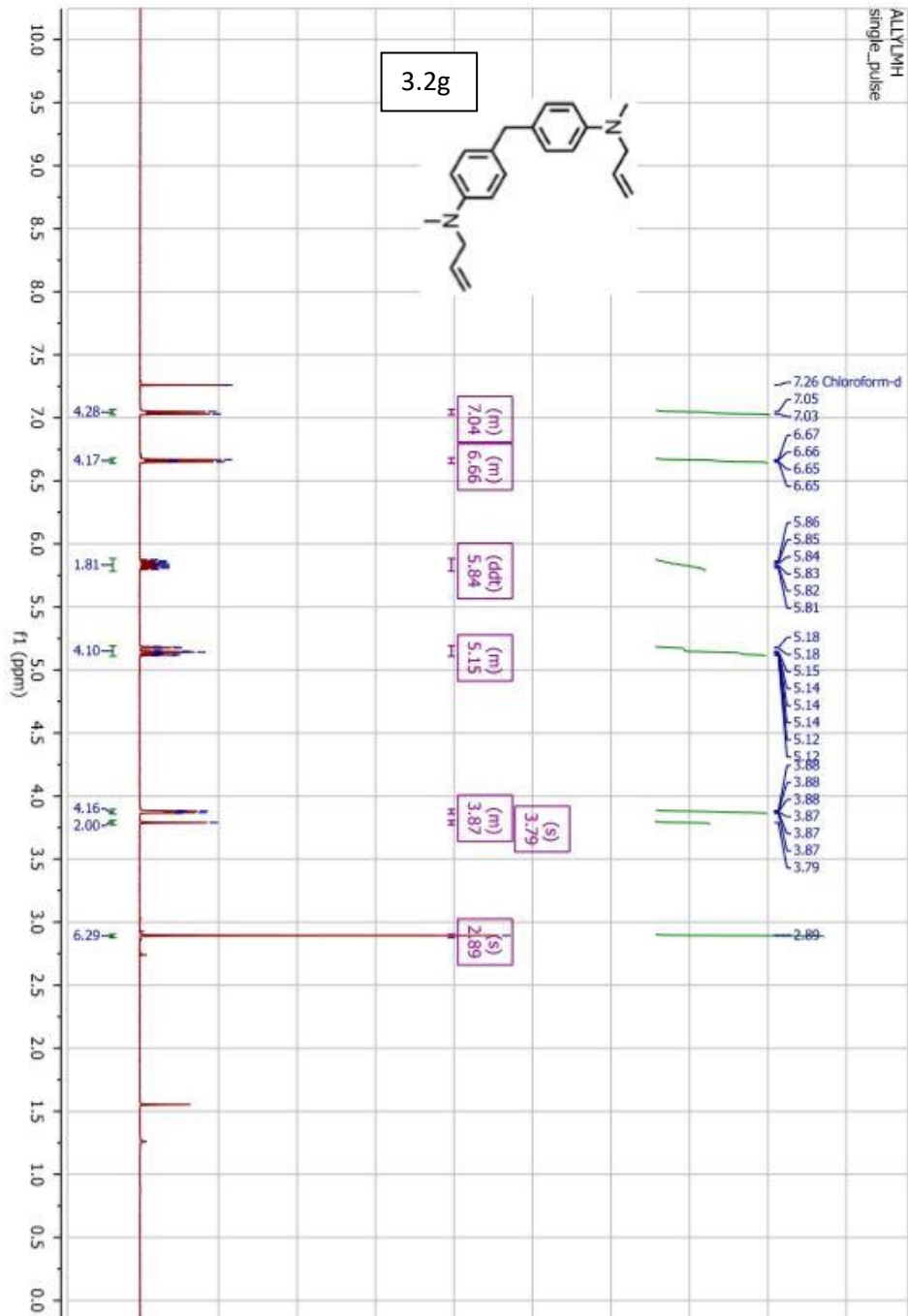


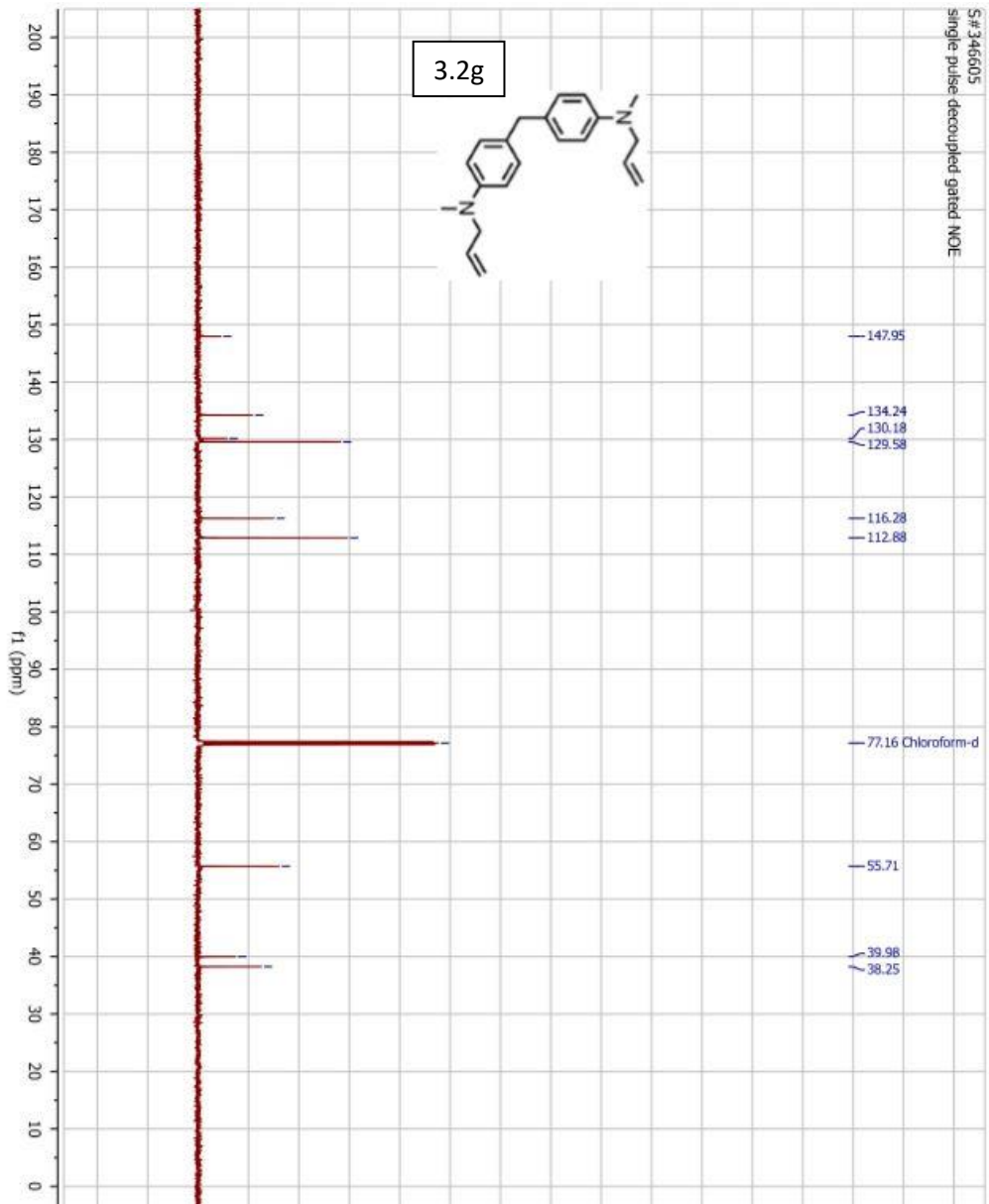


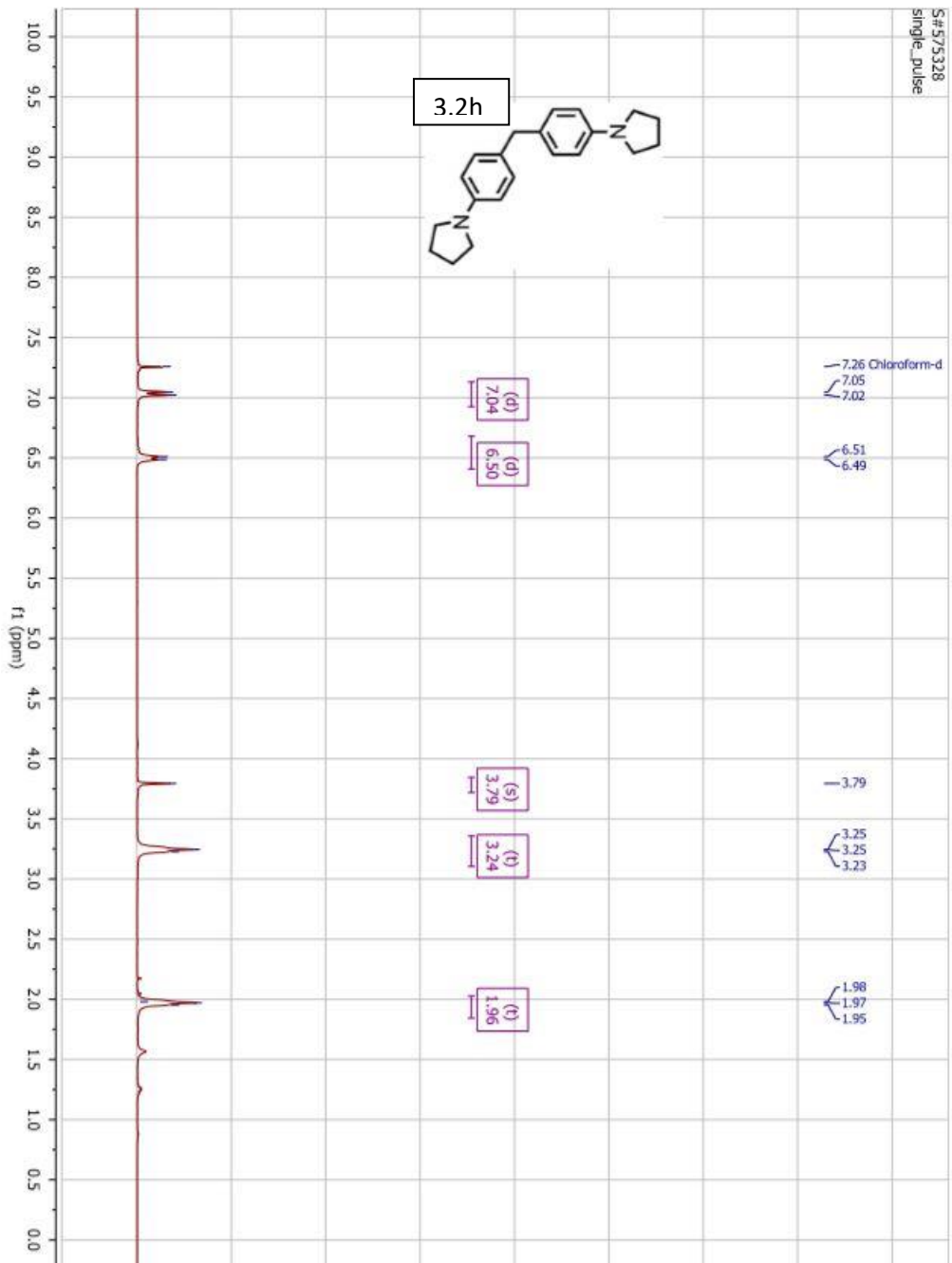


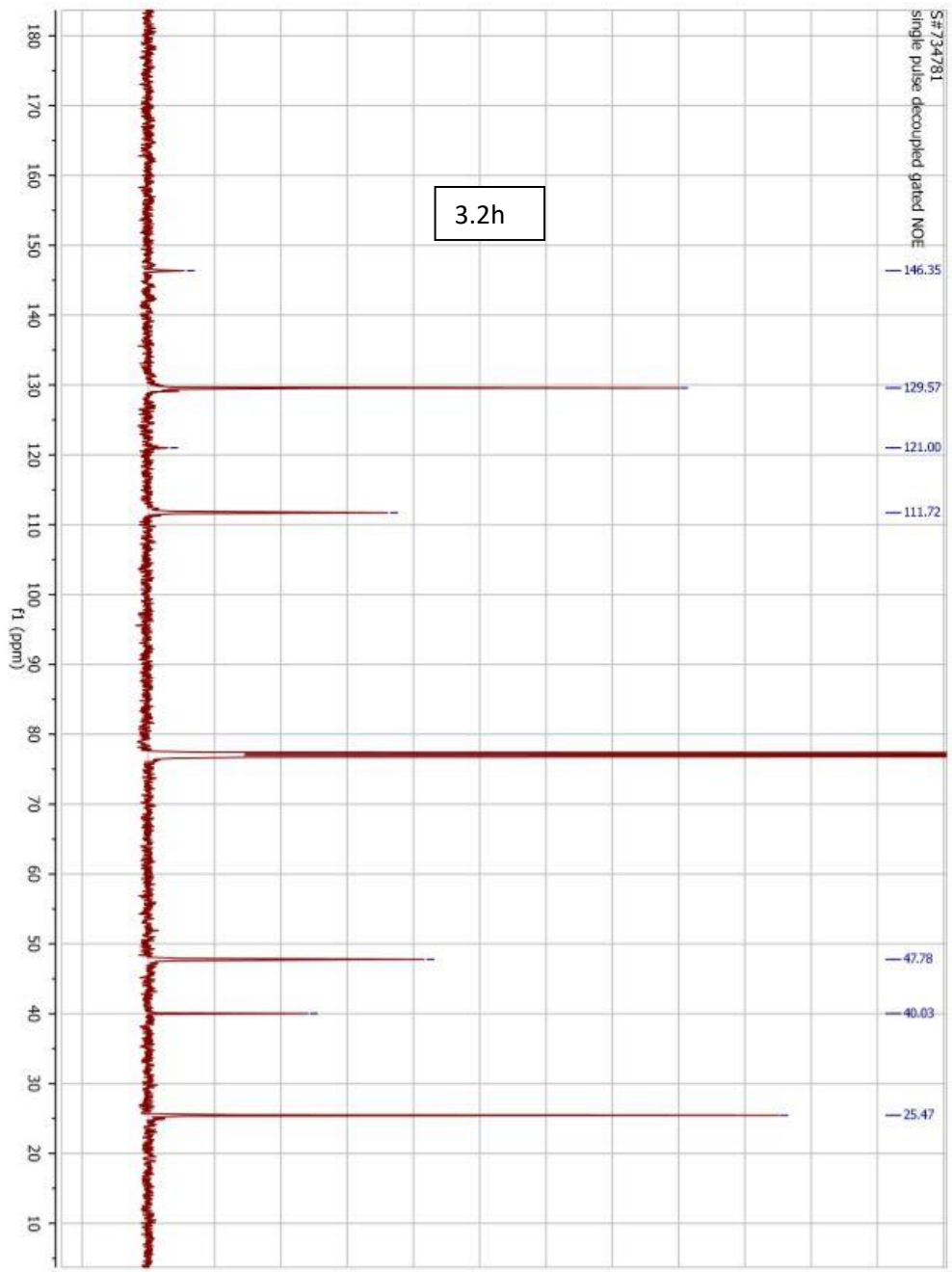






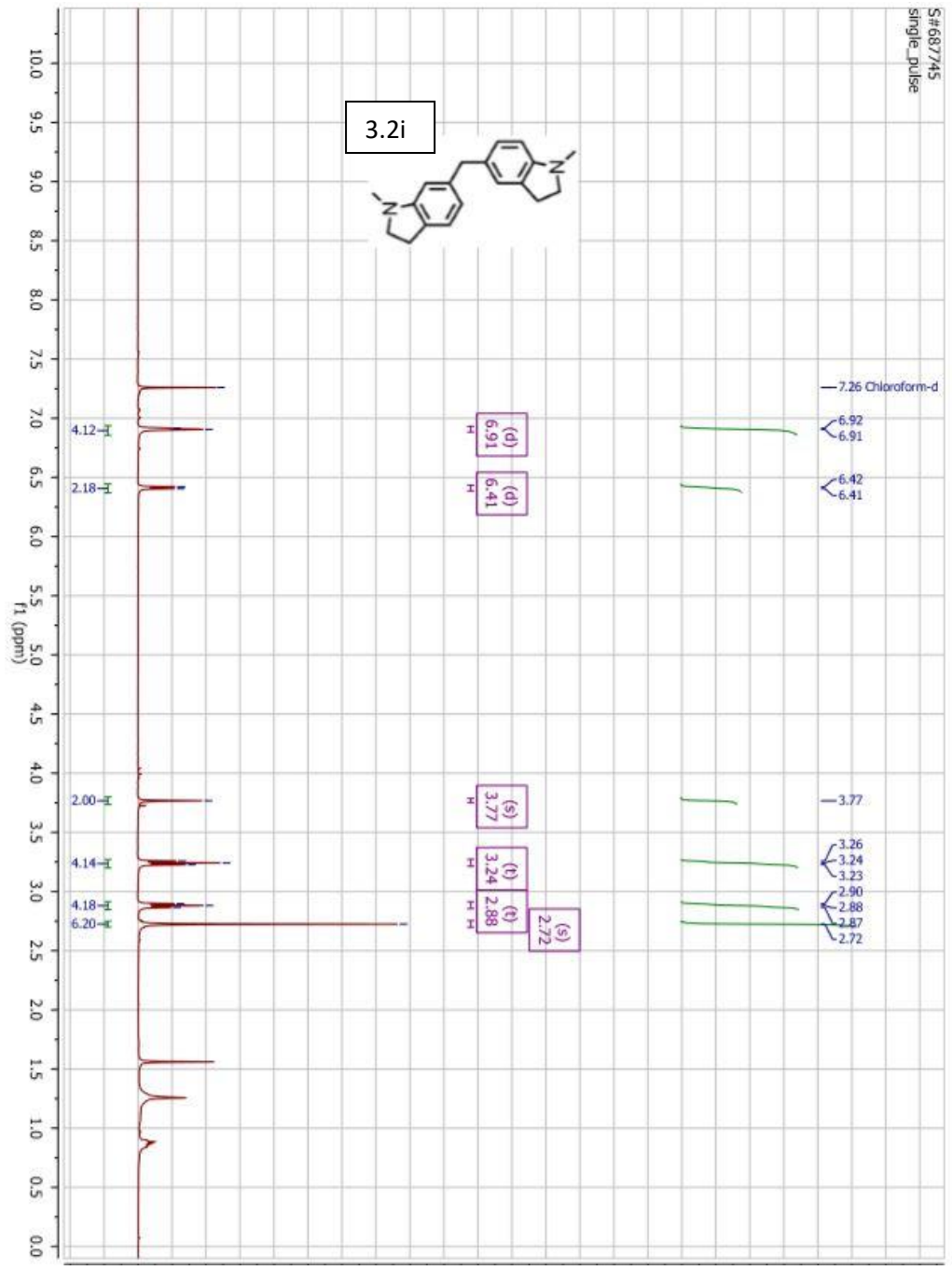
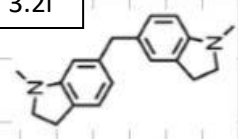


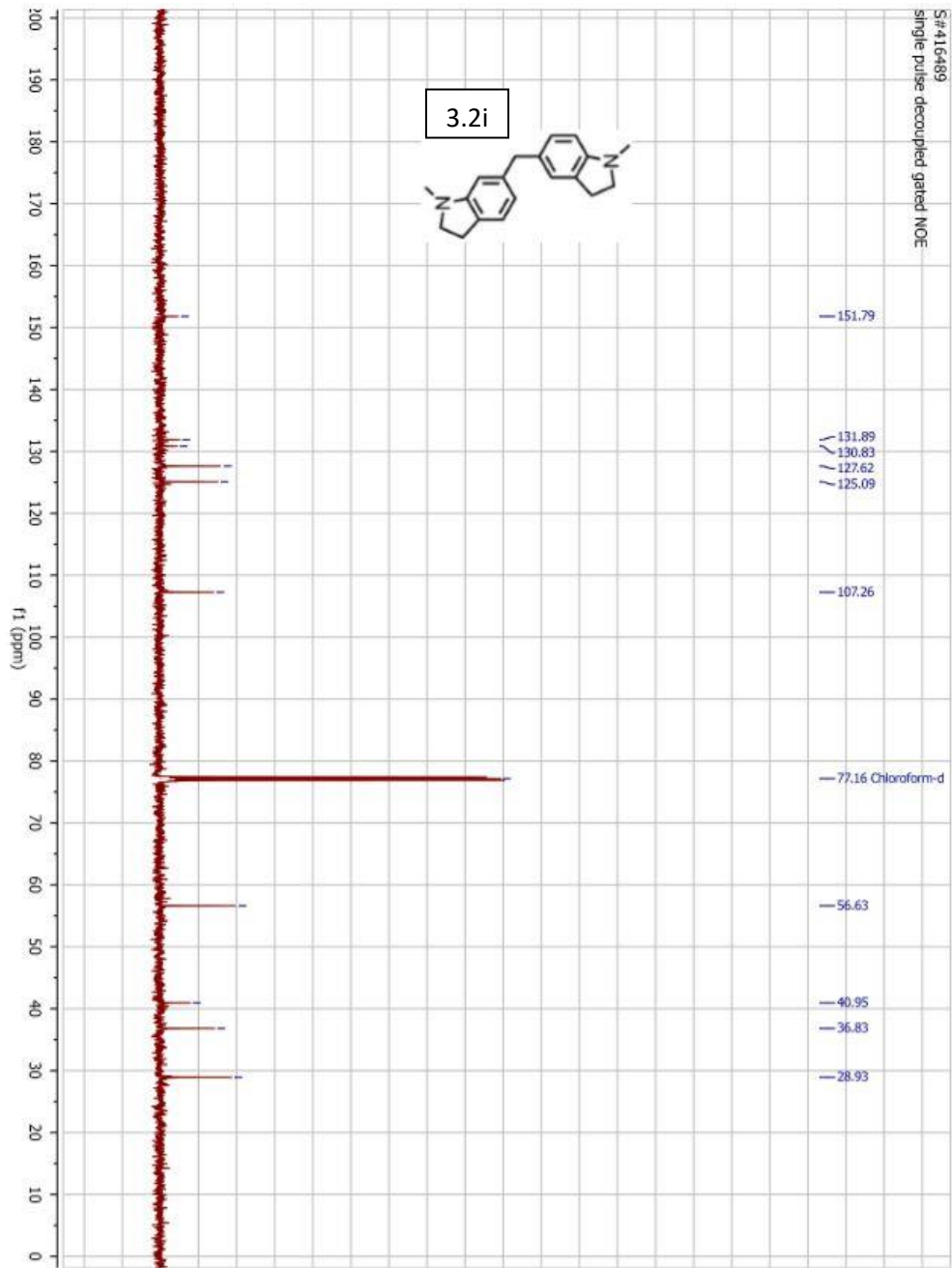


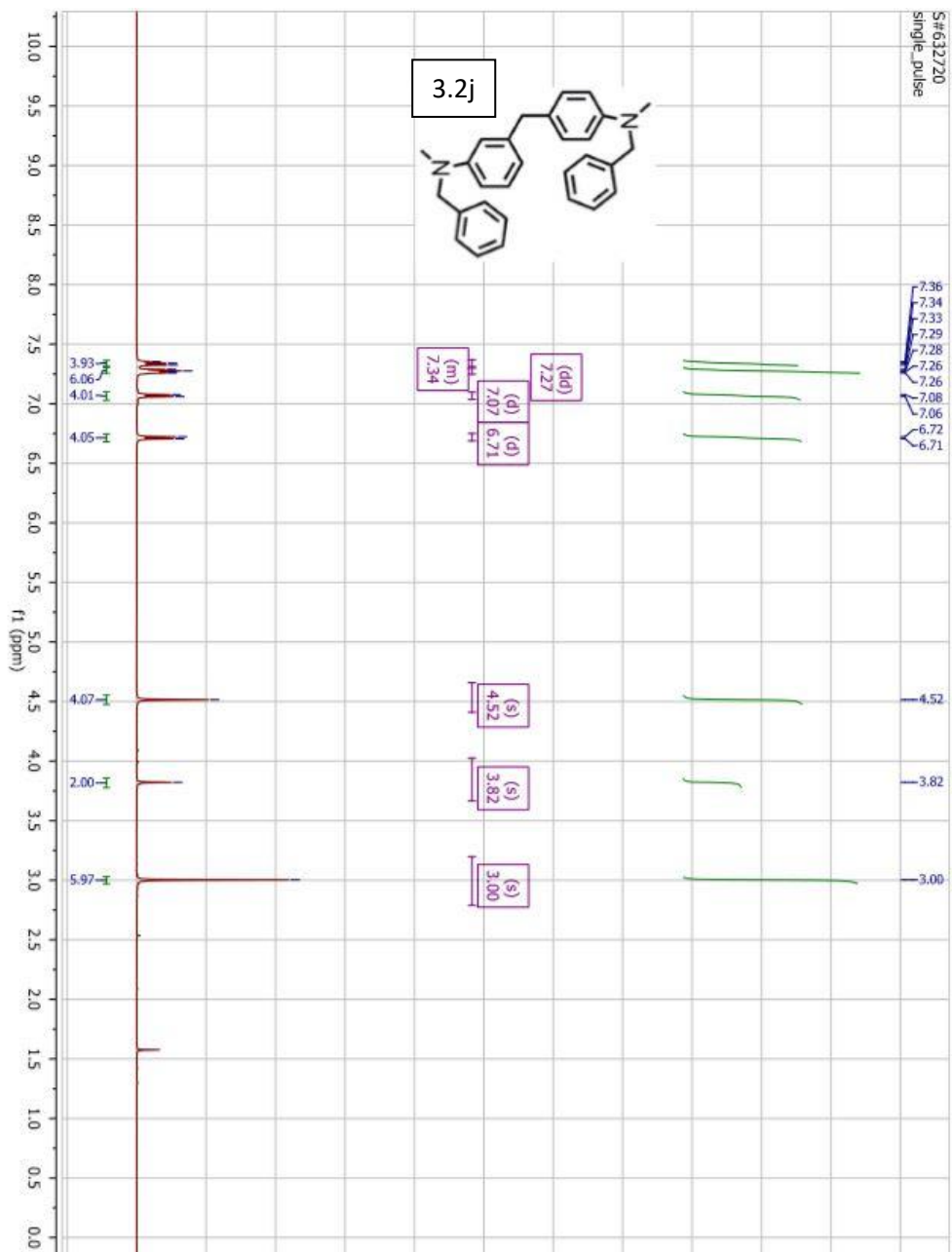


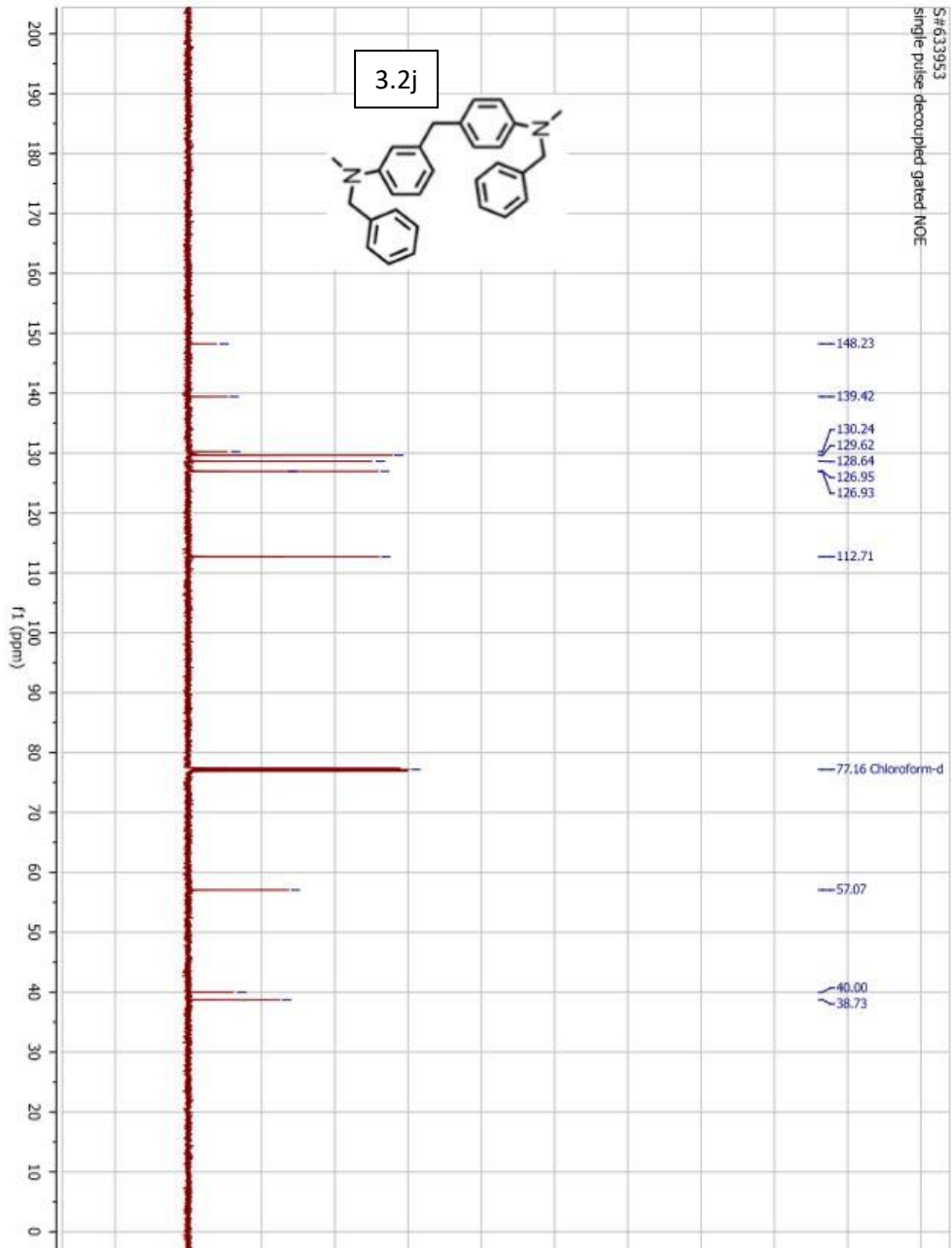
S#687745
single_pulse

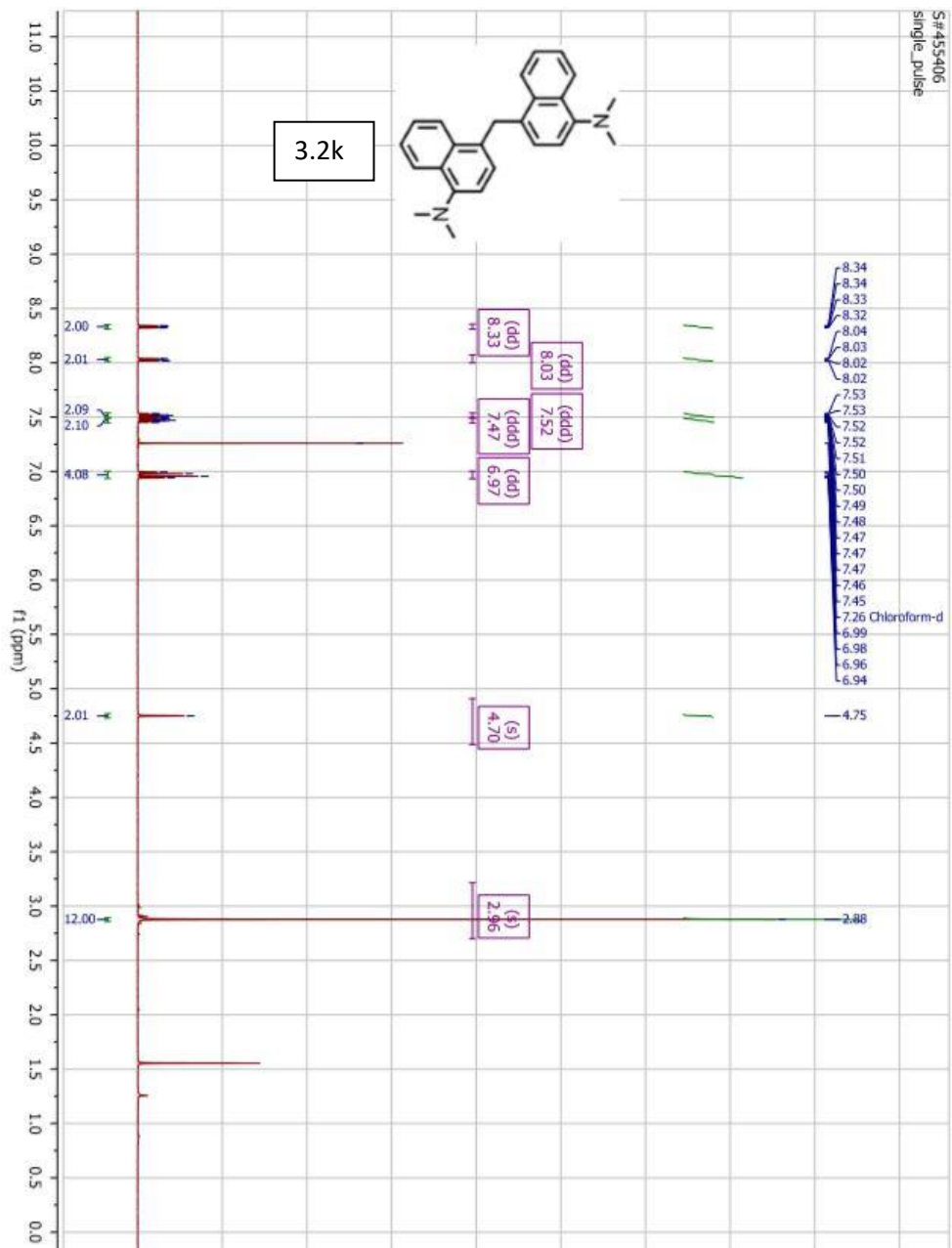
3.2i

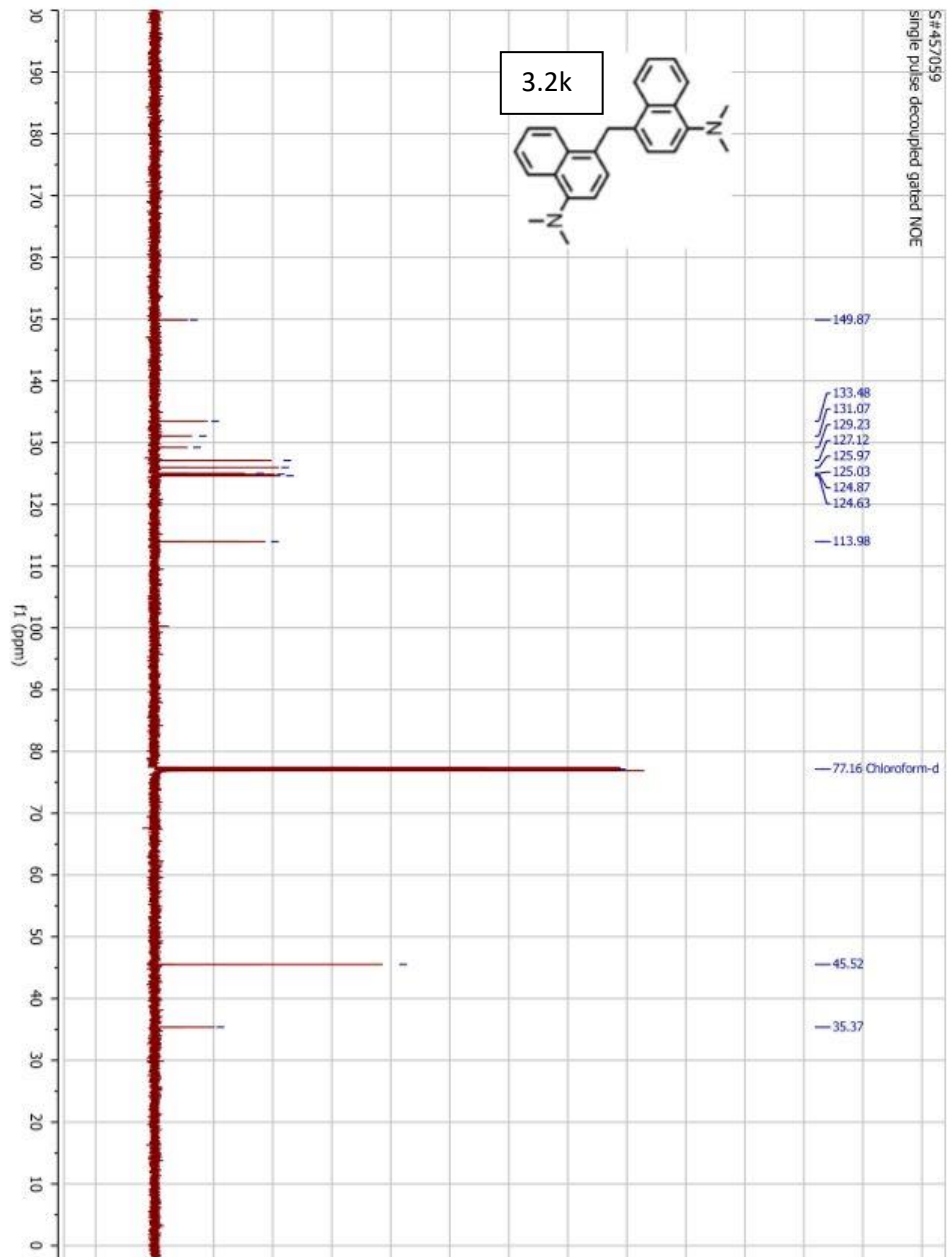


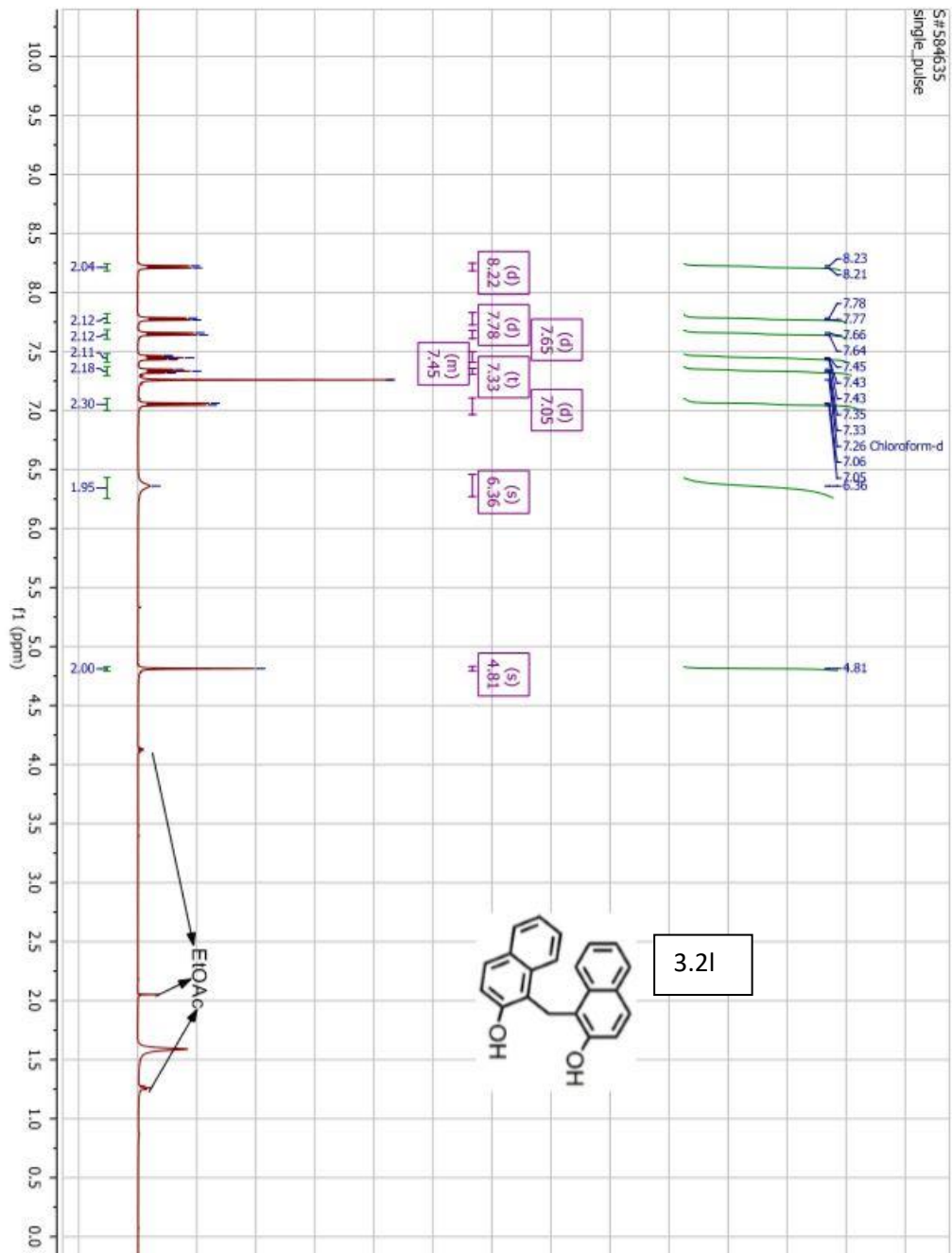


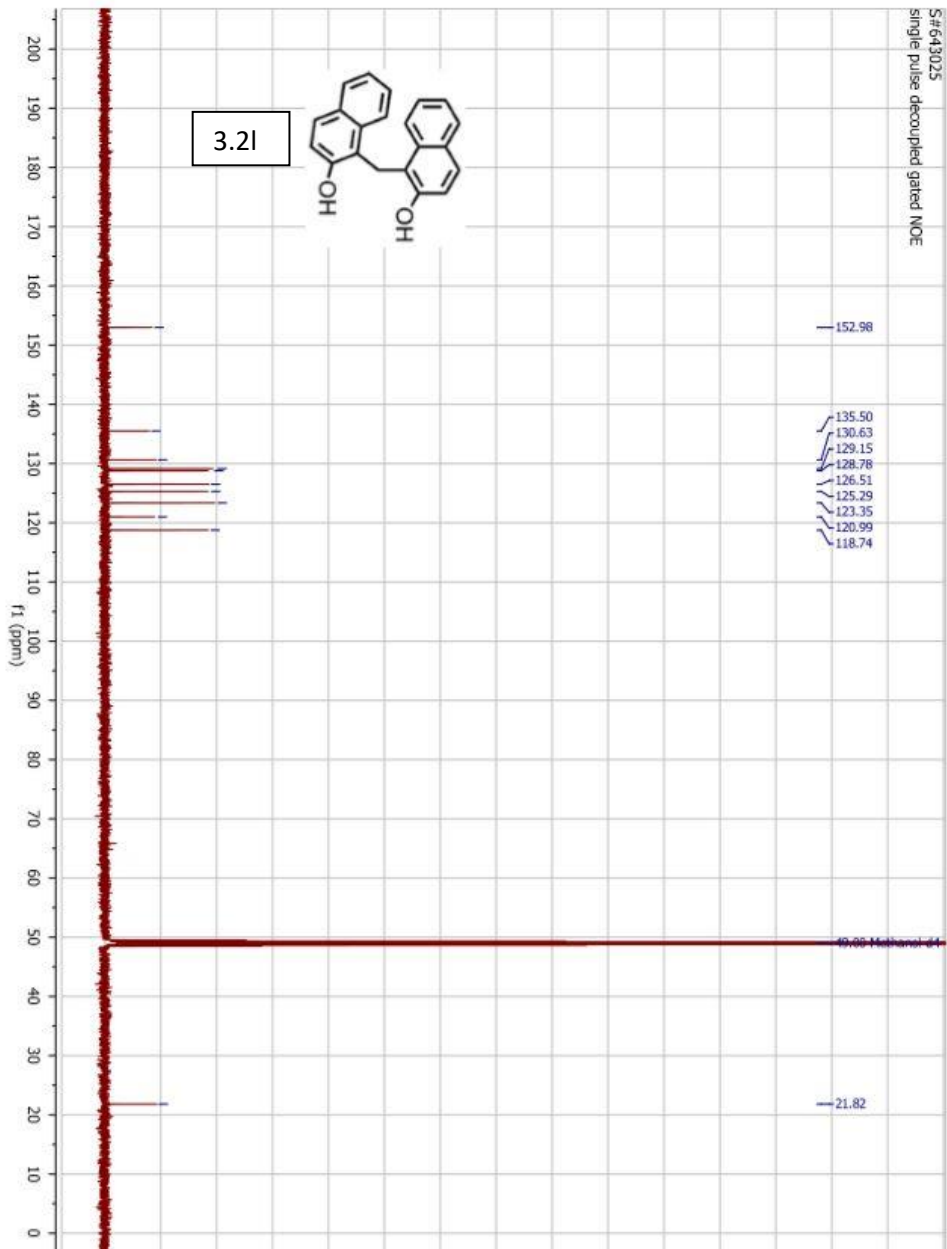


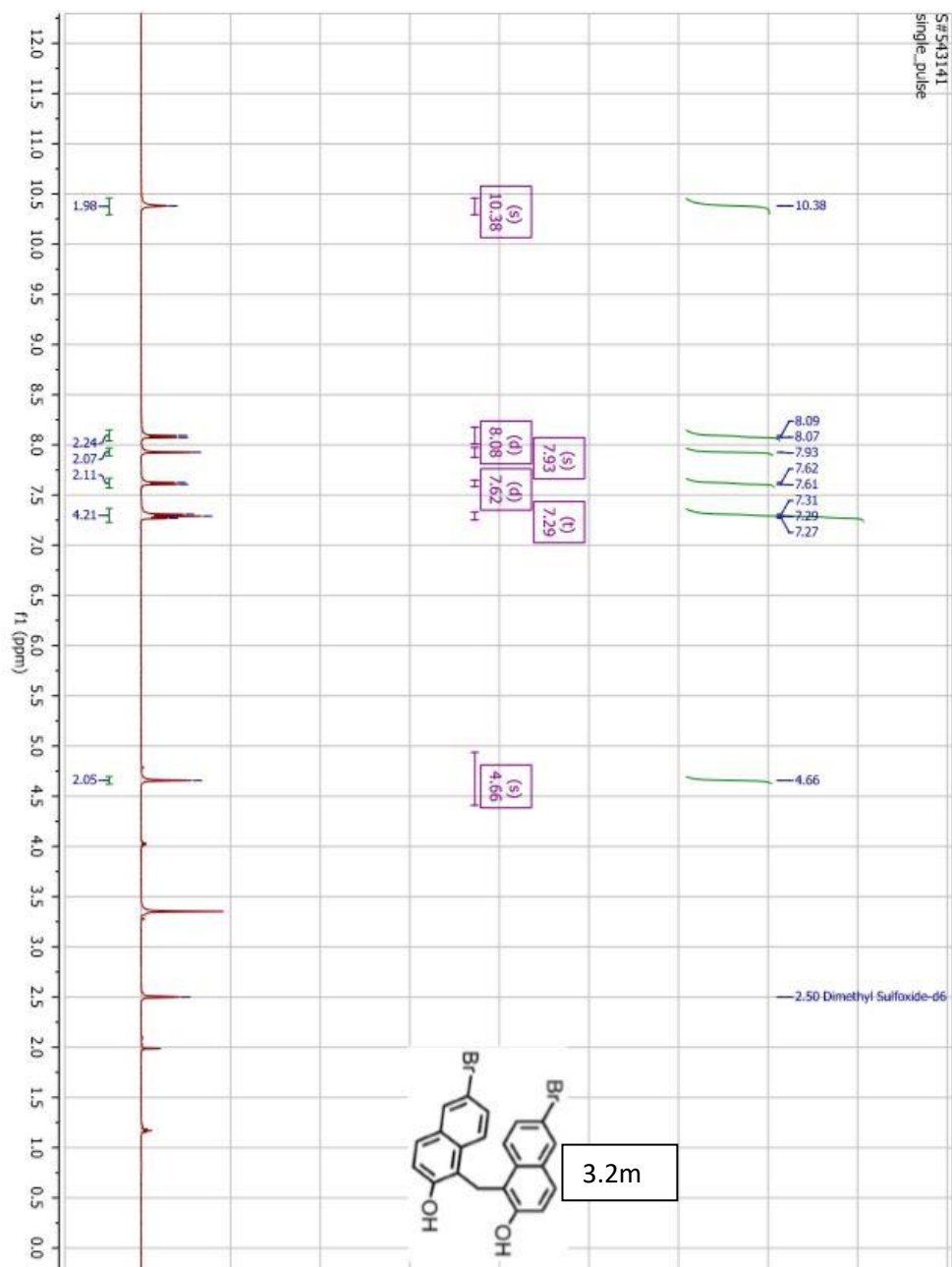




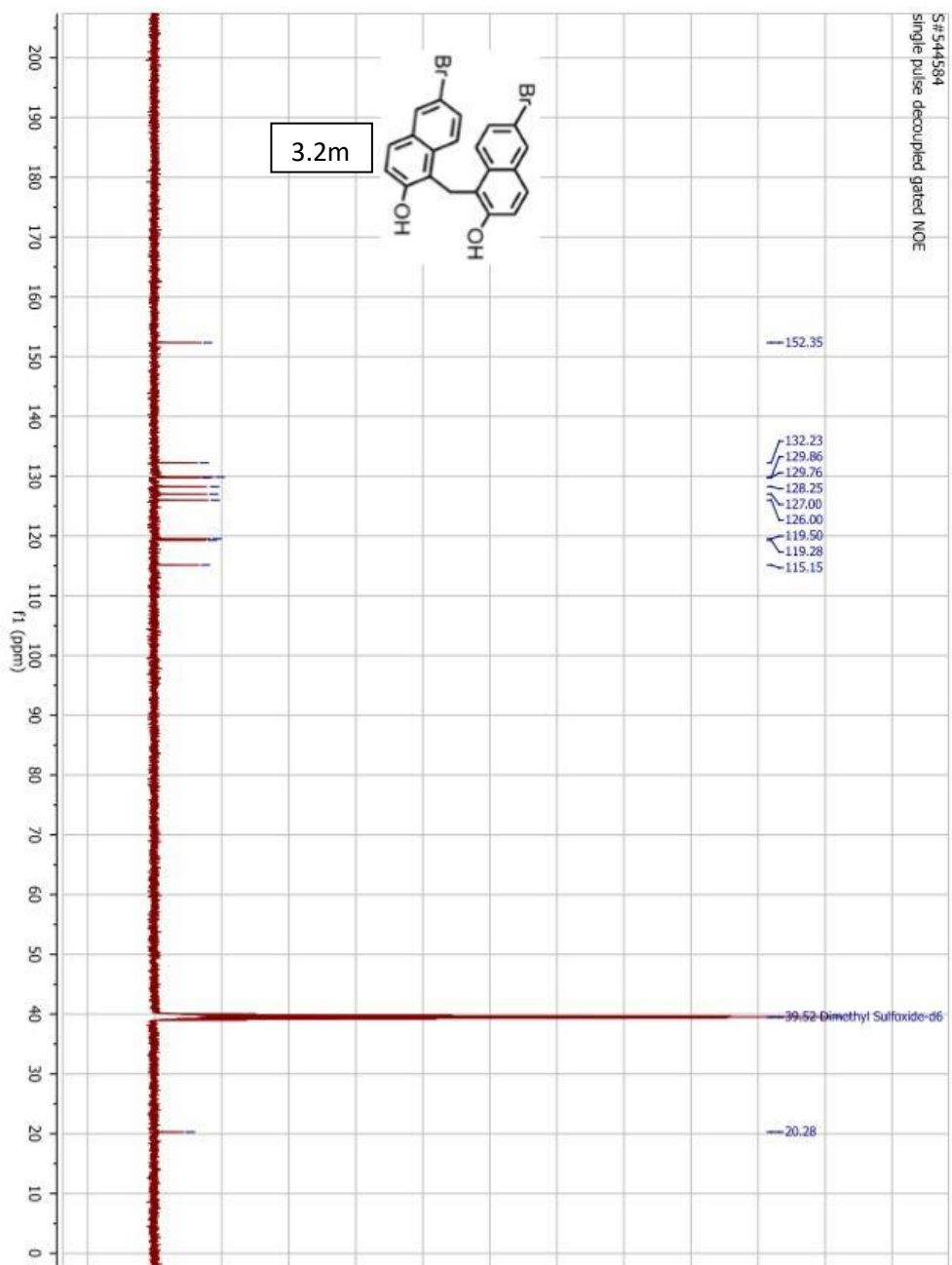


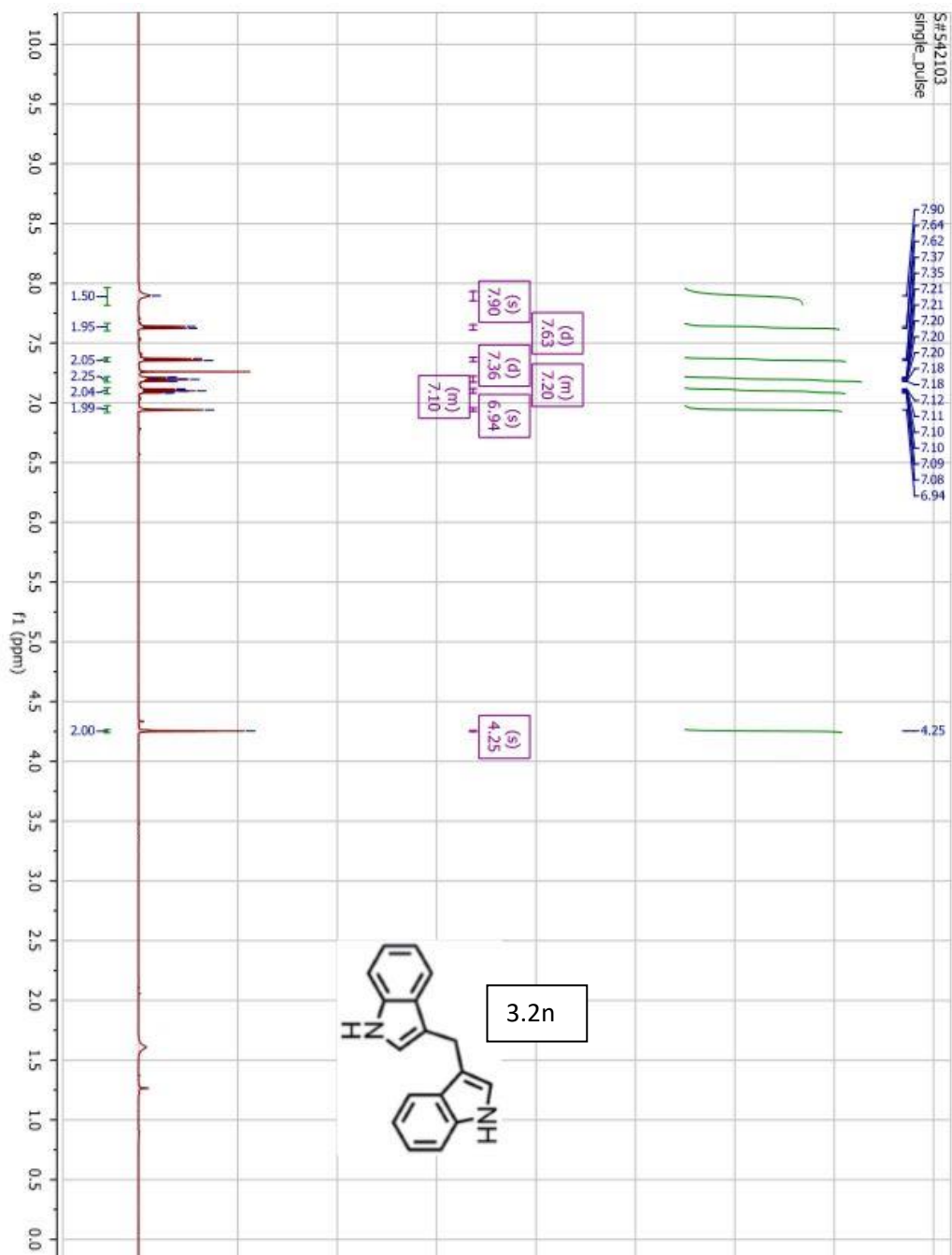


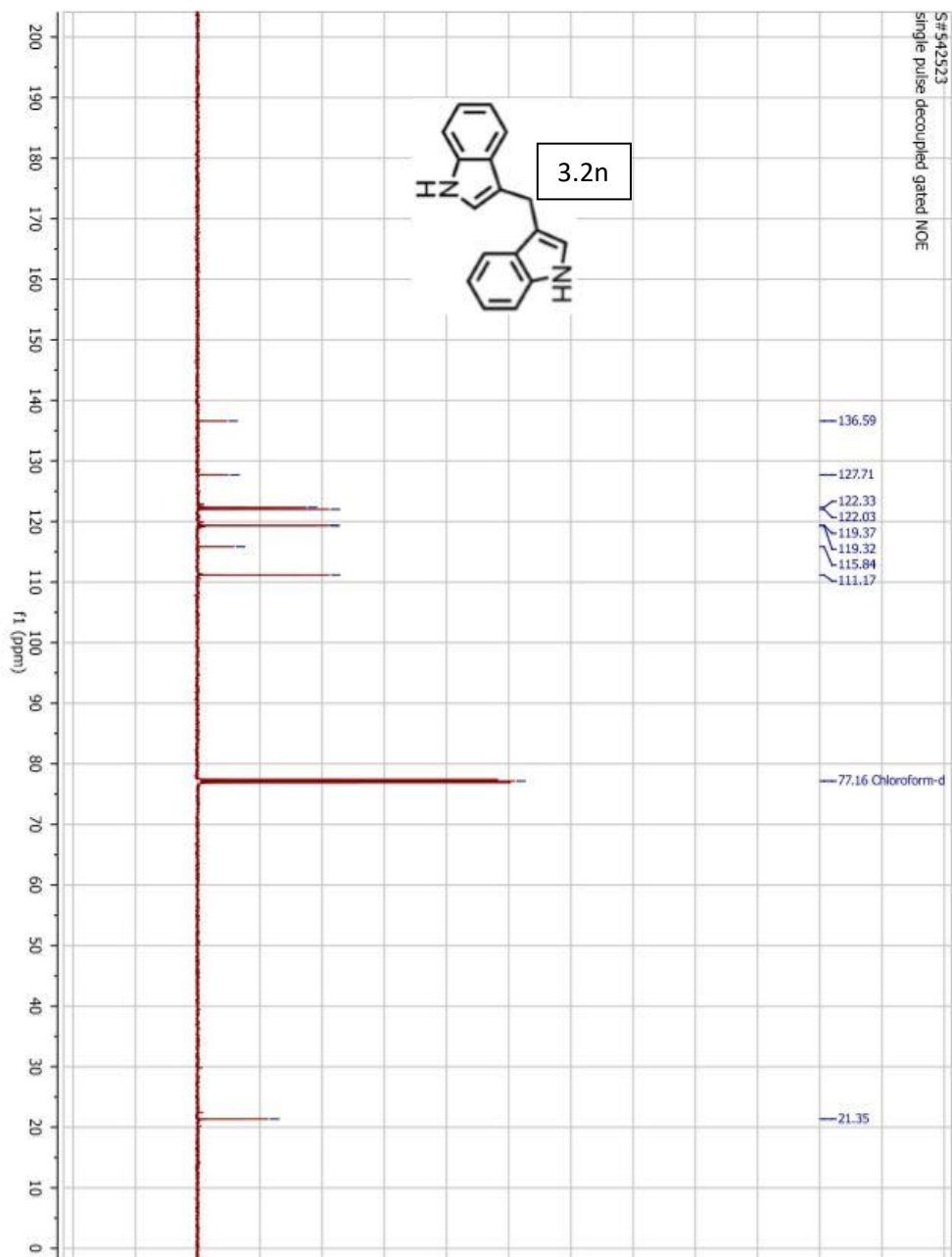




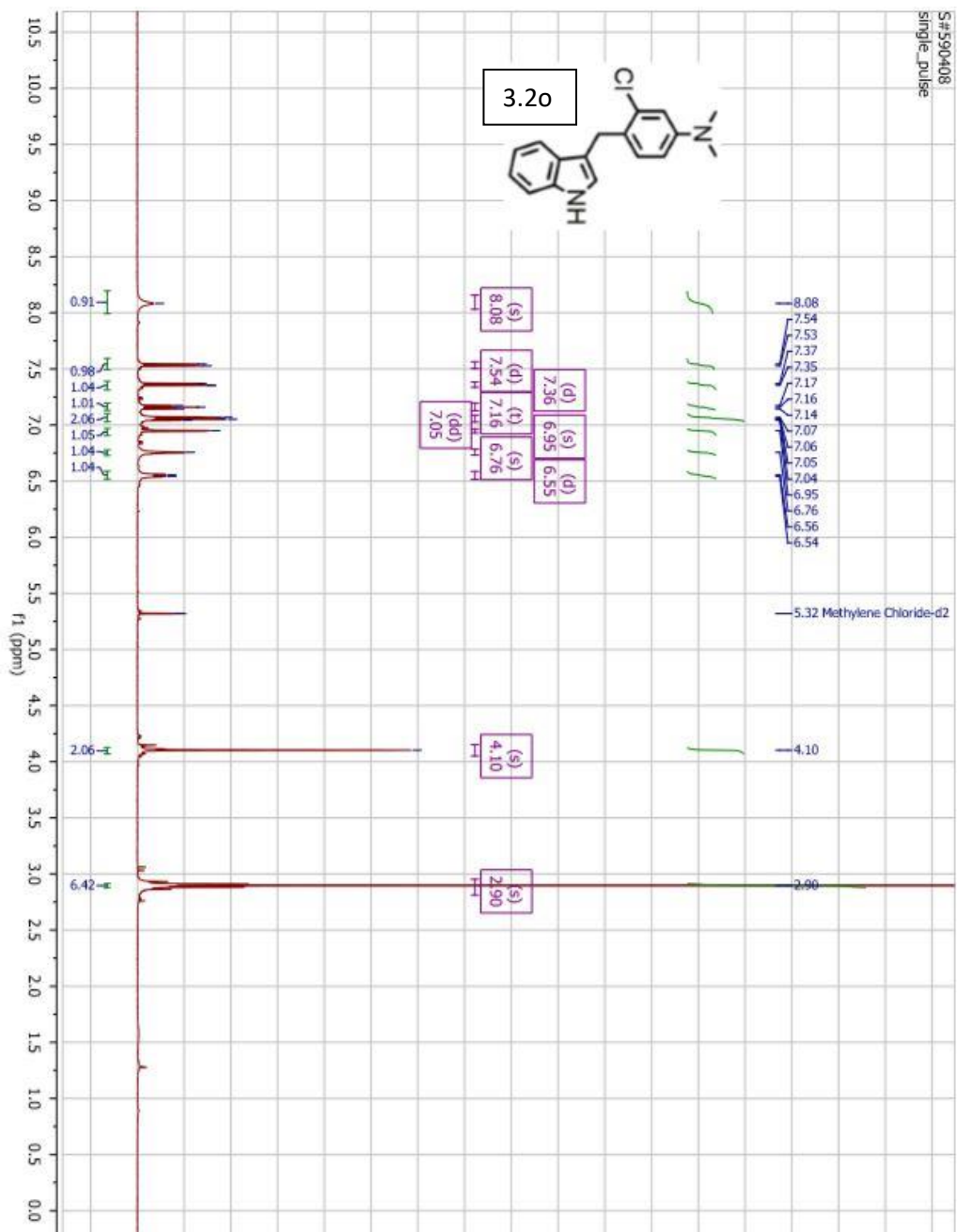
S#544584
single pulse decoupled gated NOE



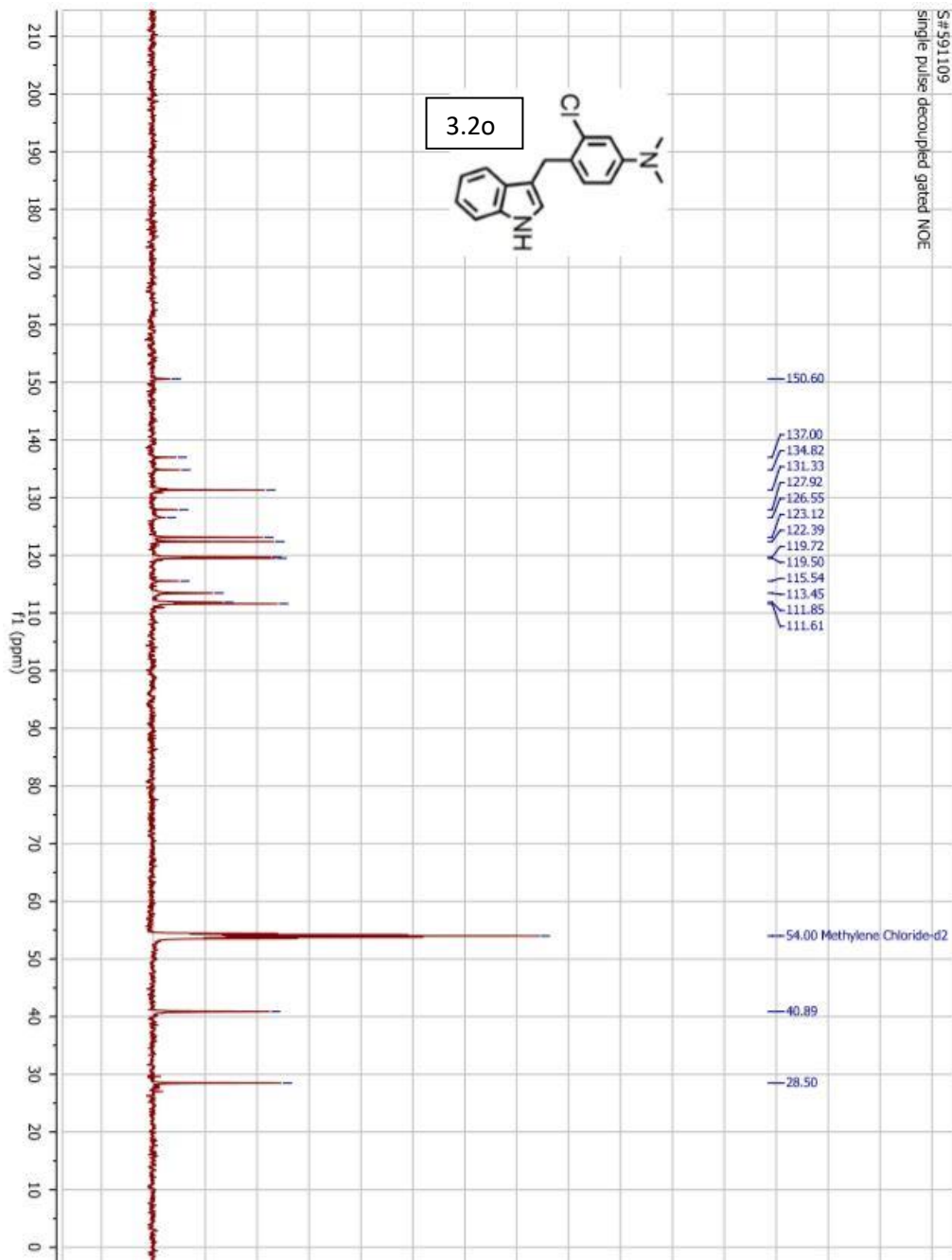
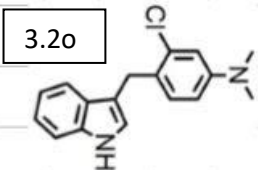


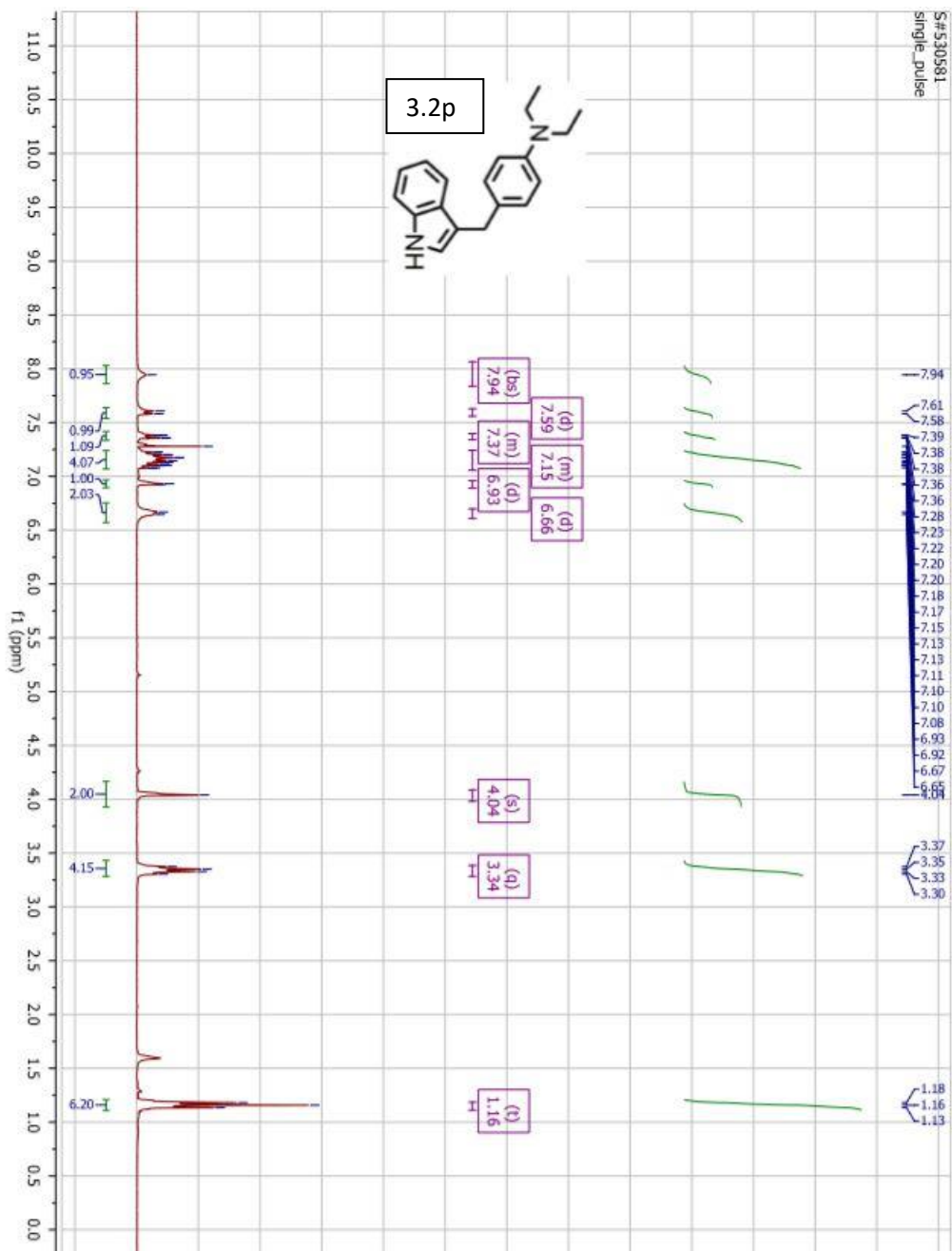


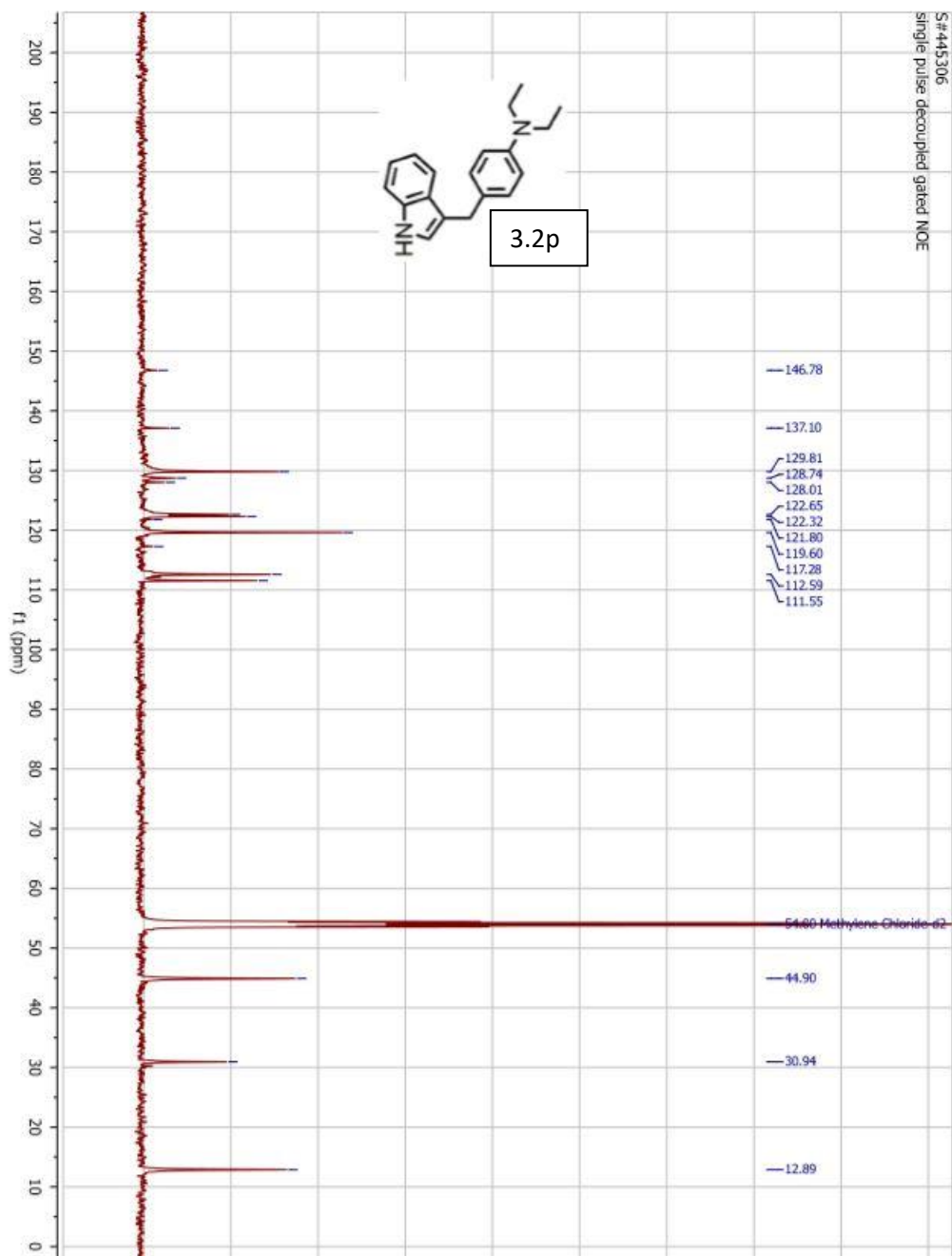
S#590408
single_pulse

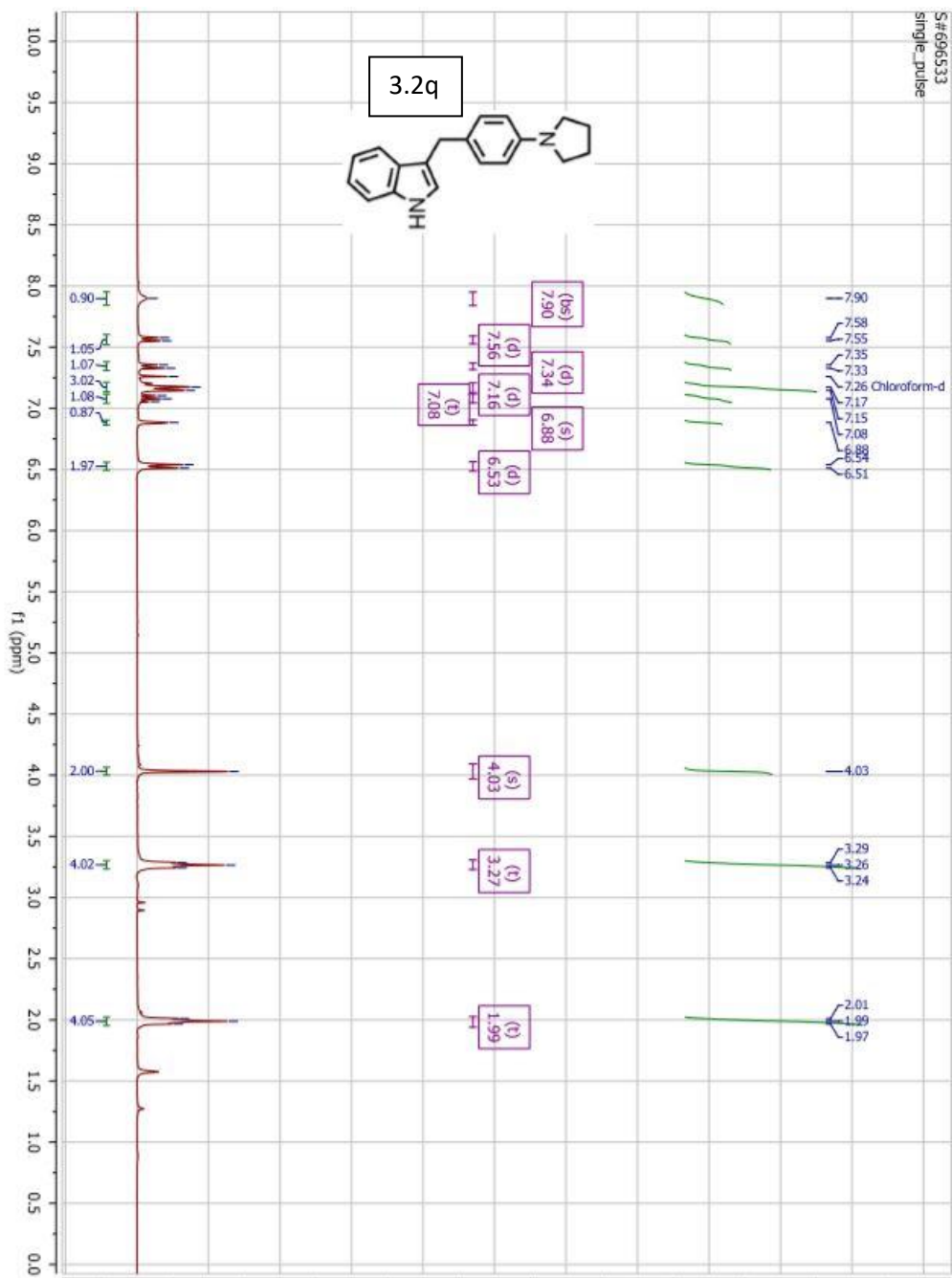


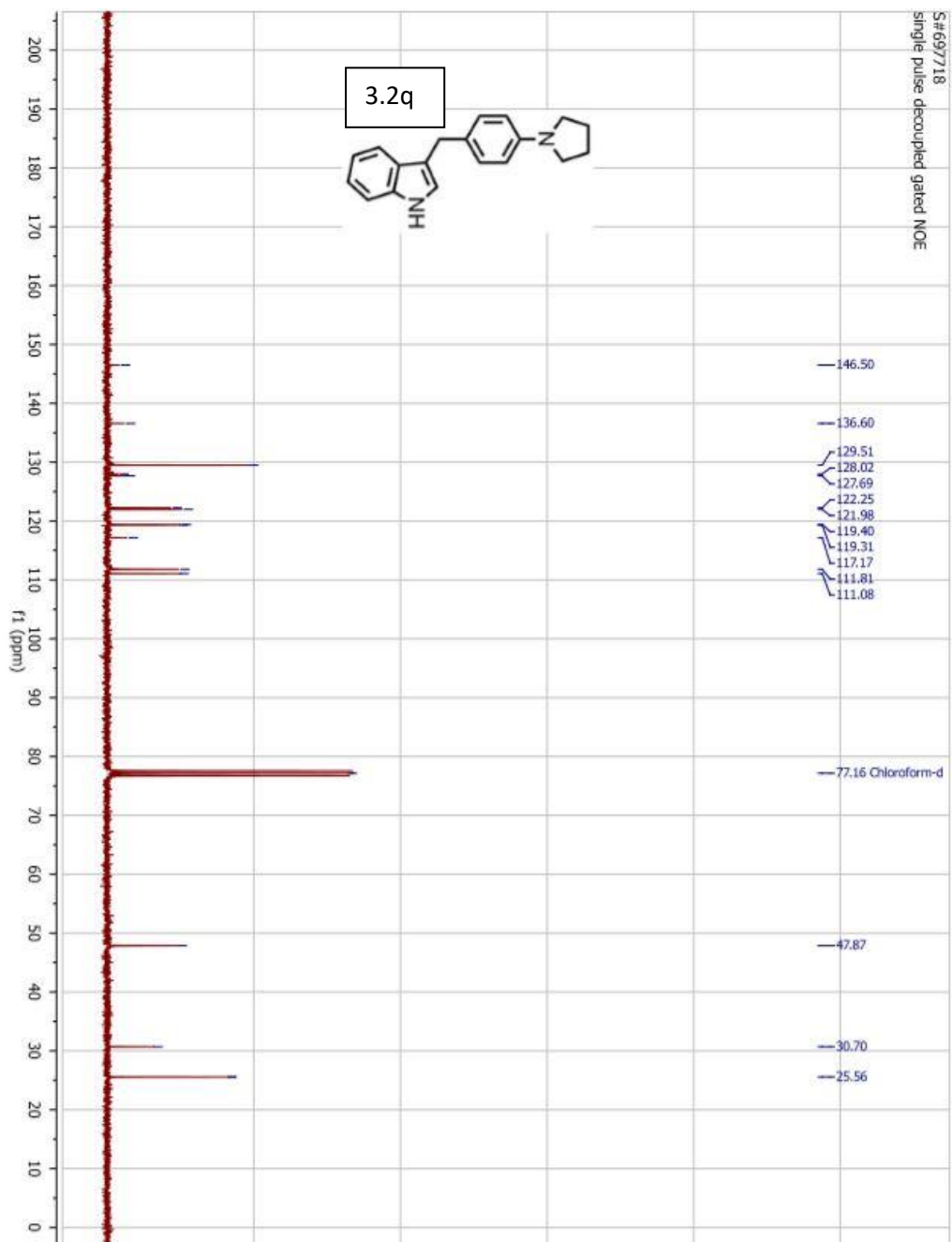
S#591109
Single pulse decoupled gated NOE

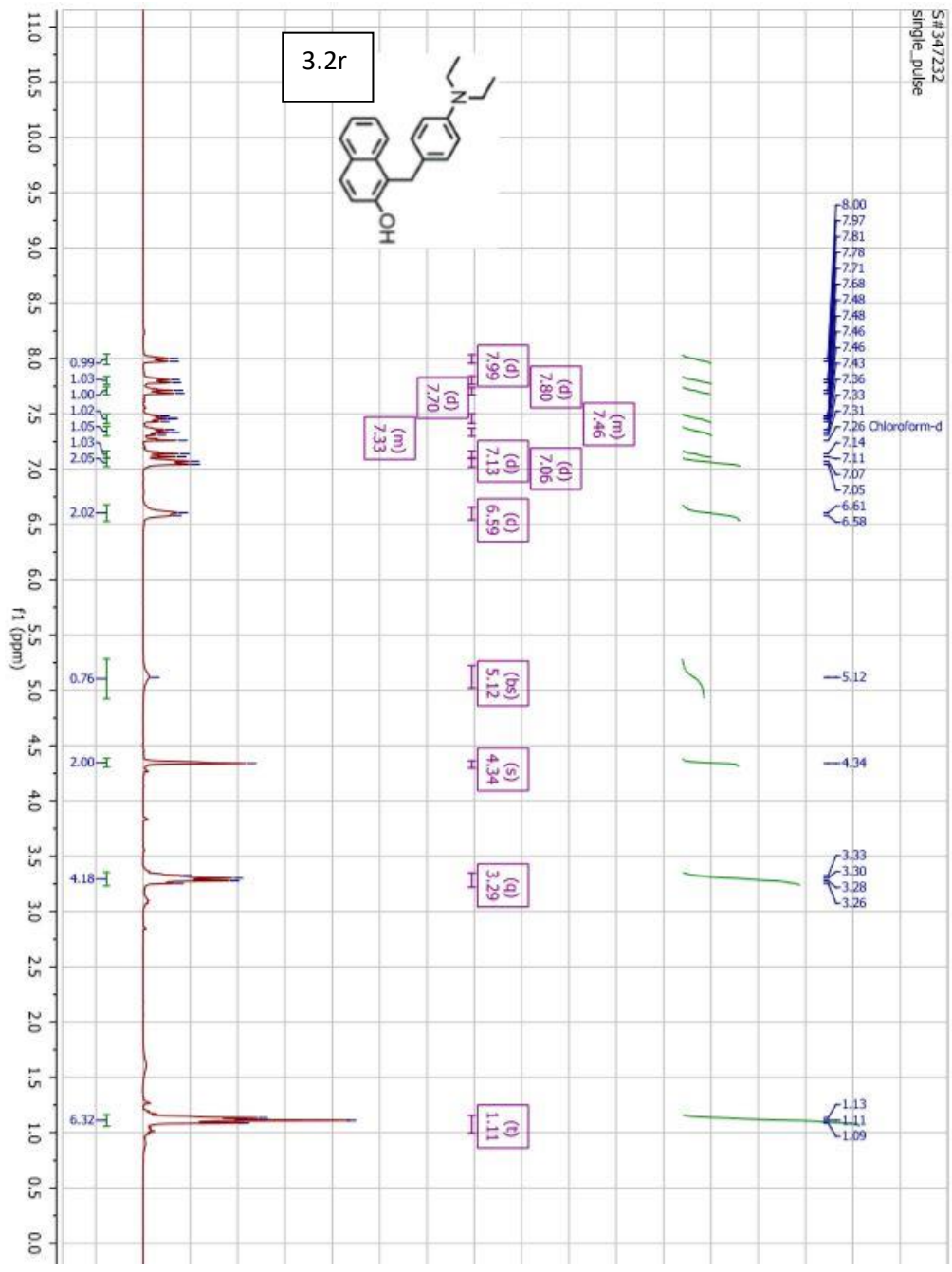


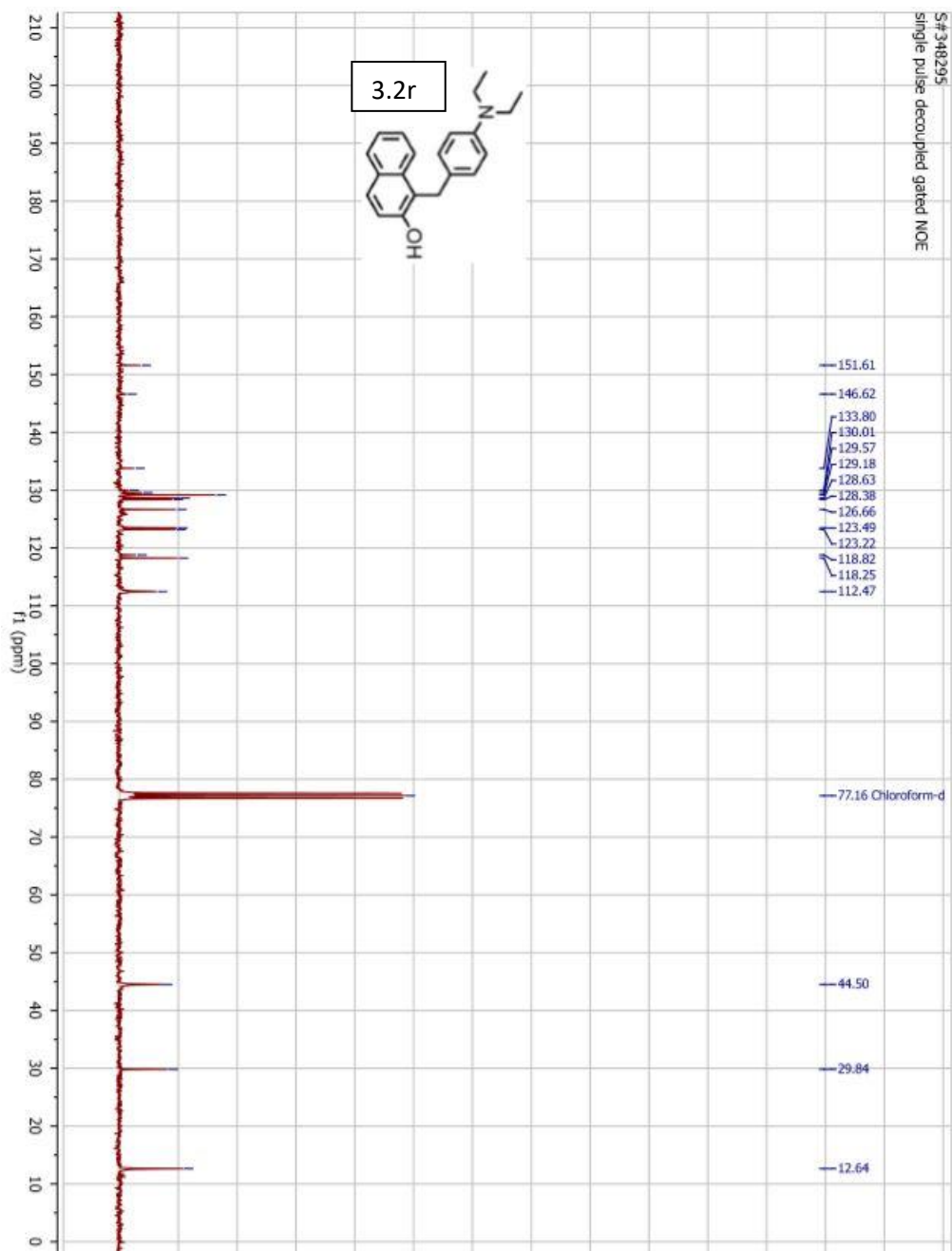


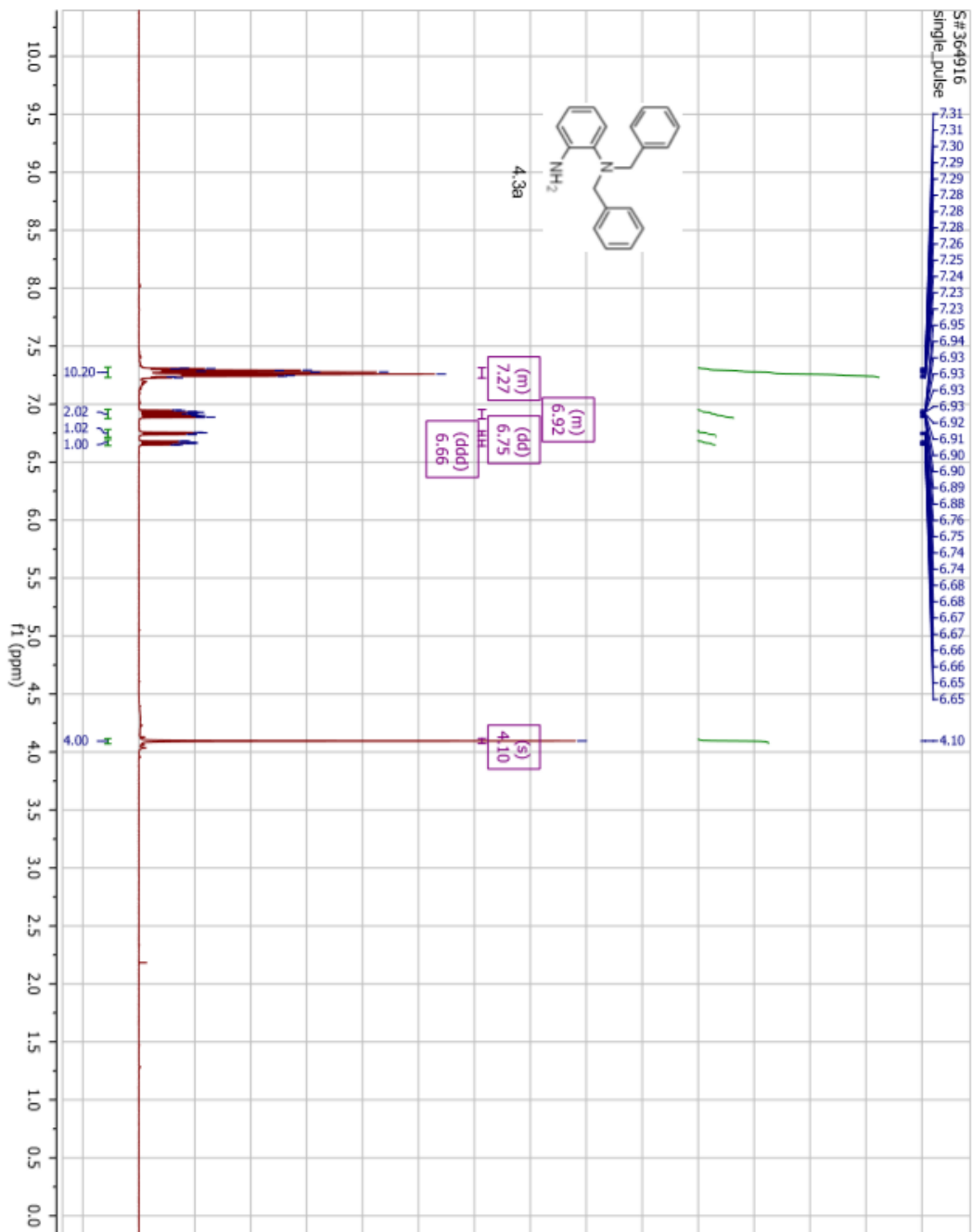


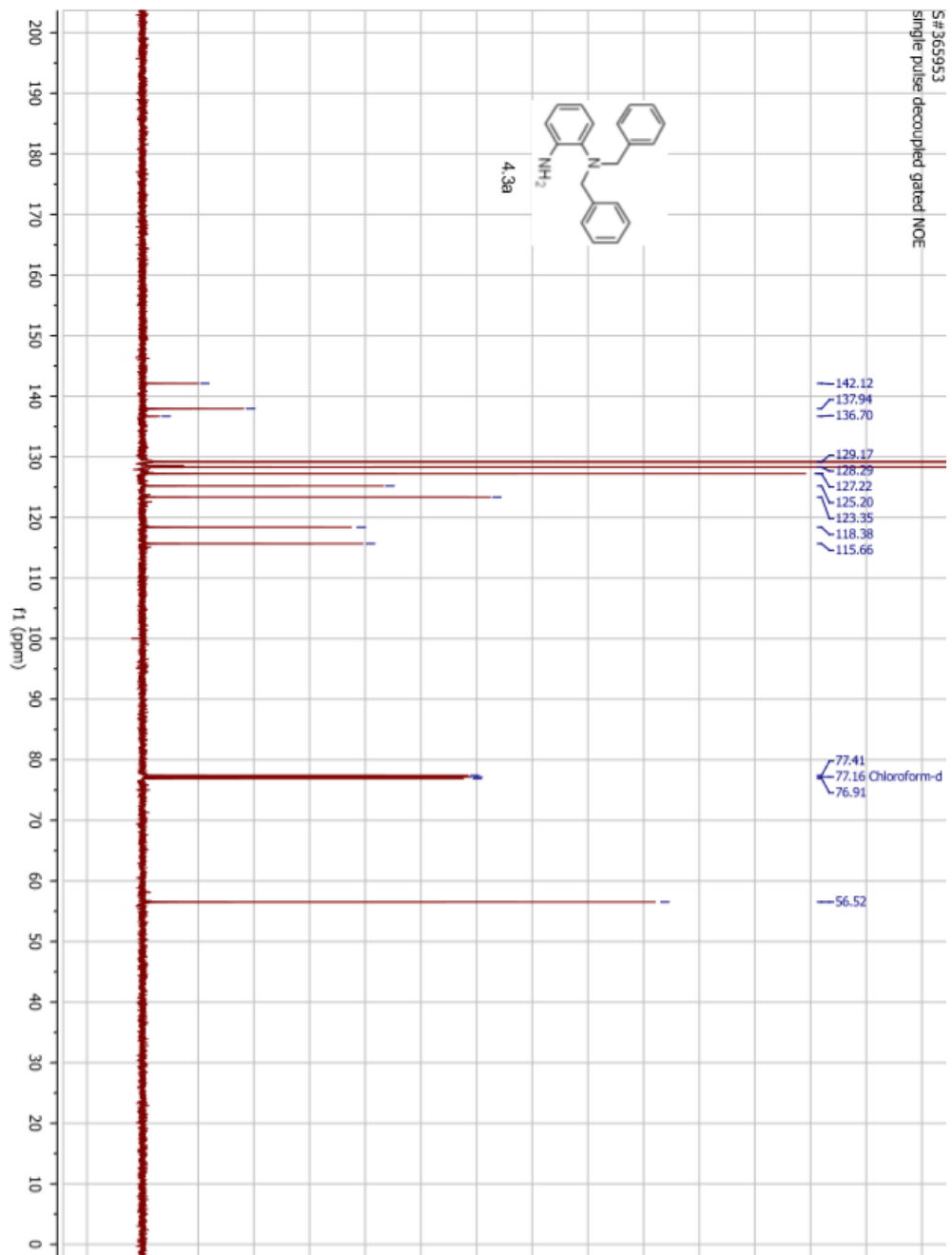


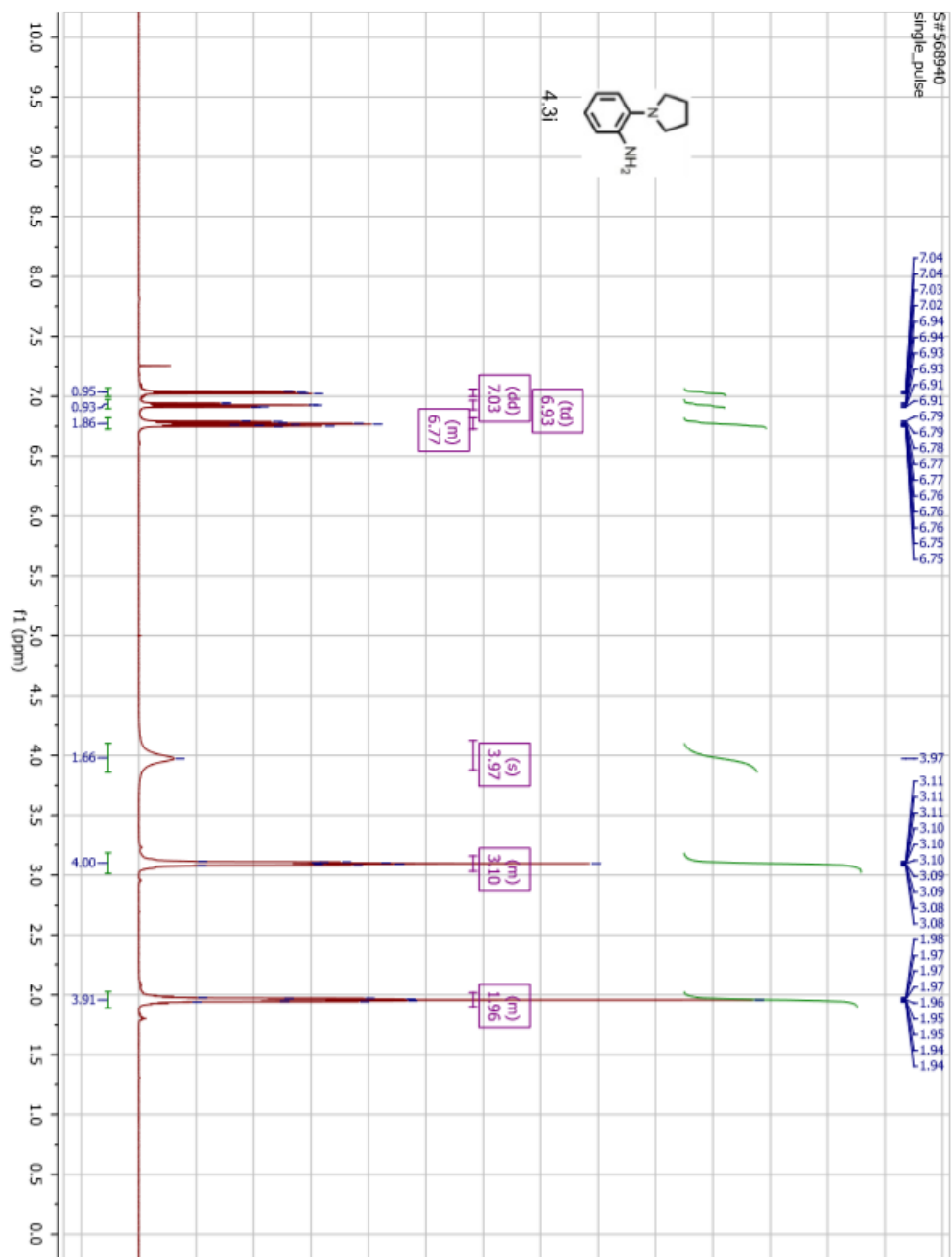


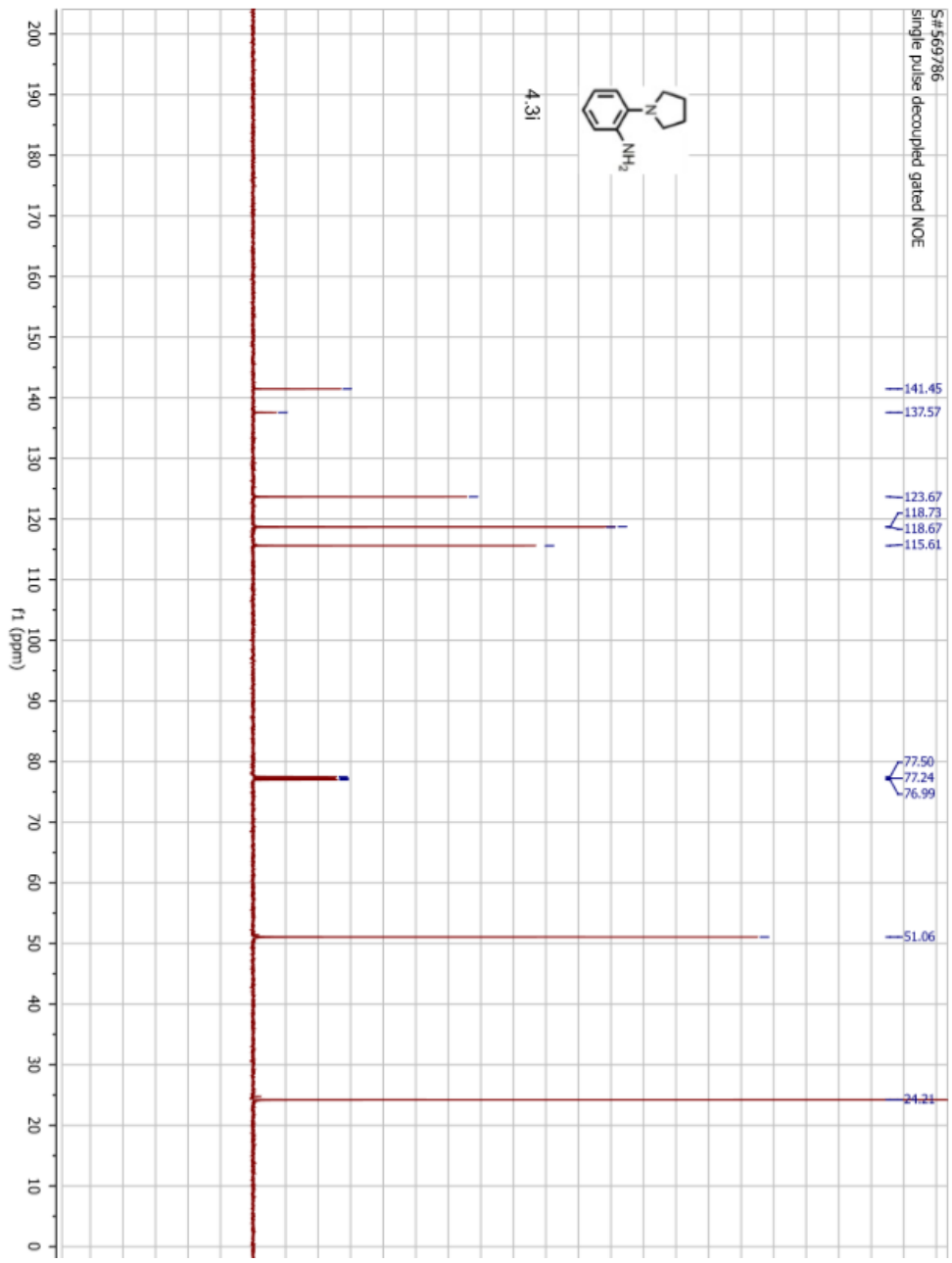


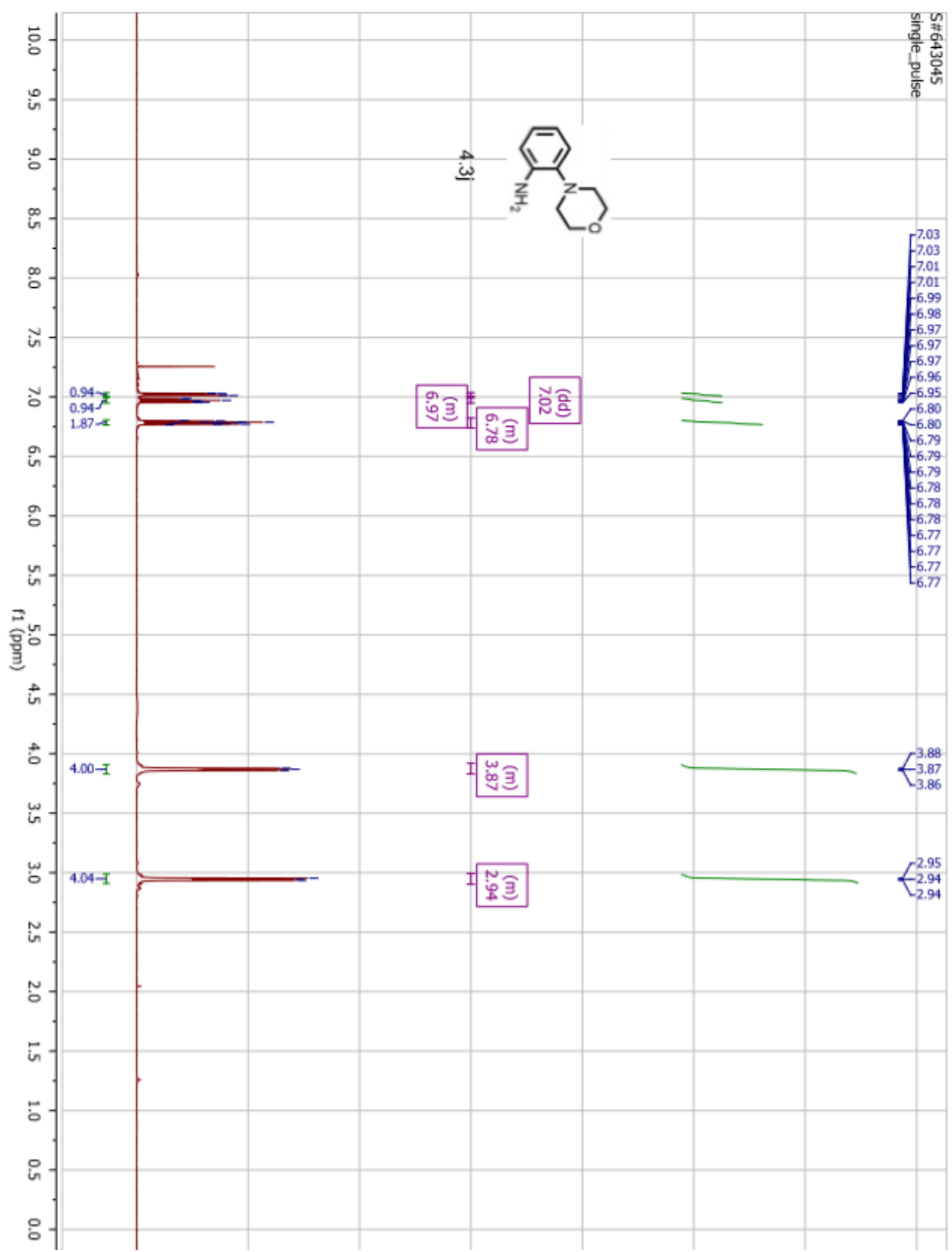


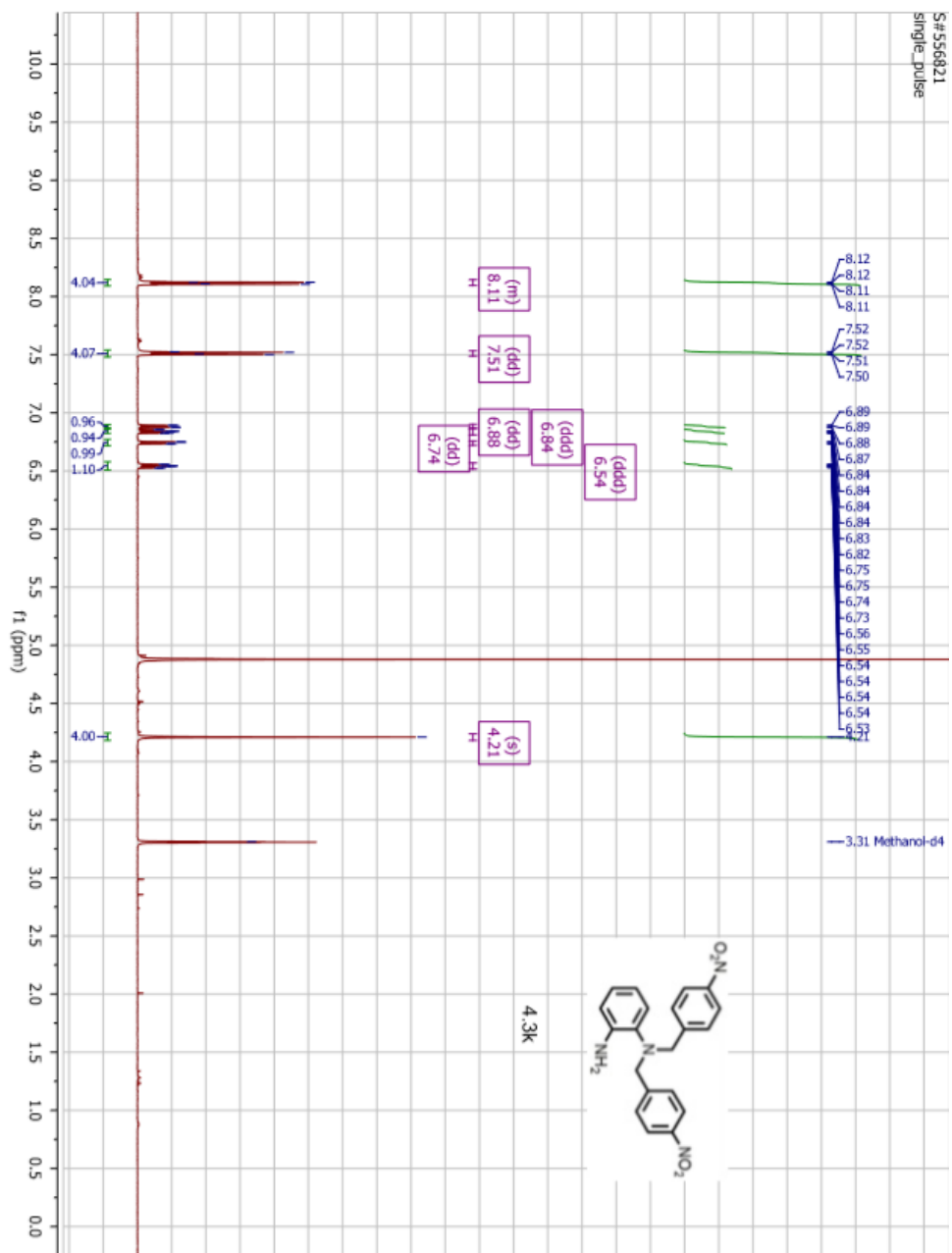


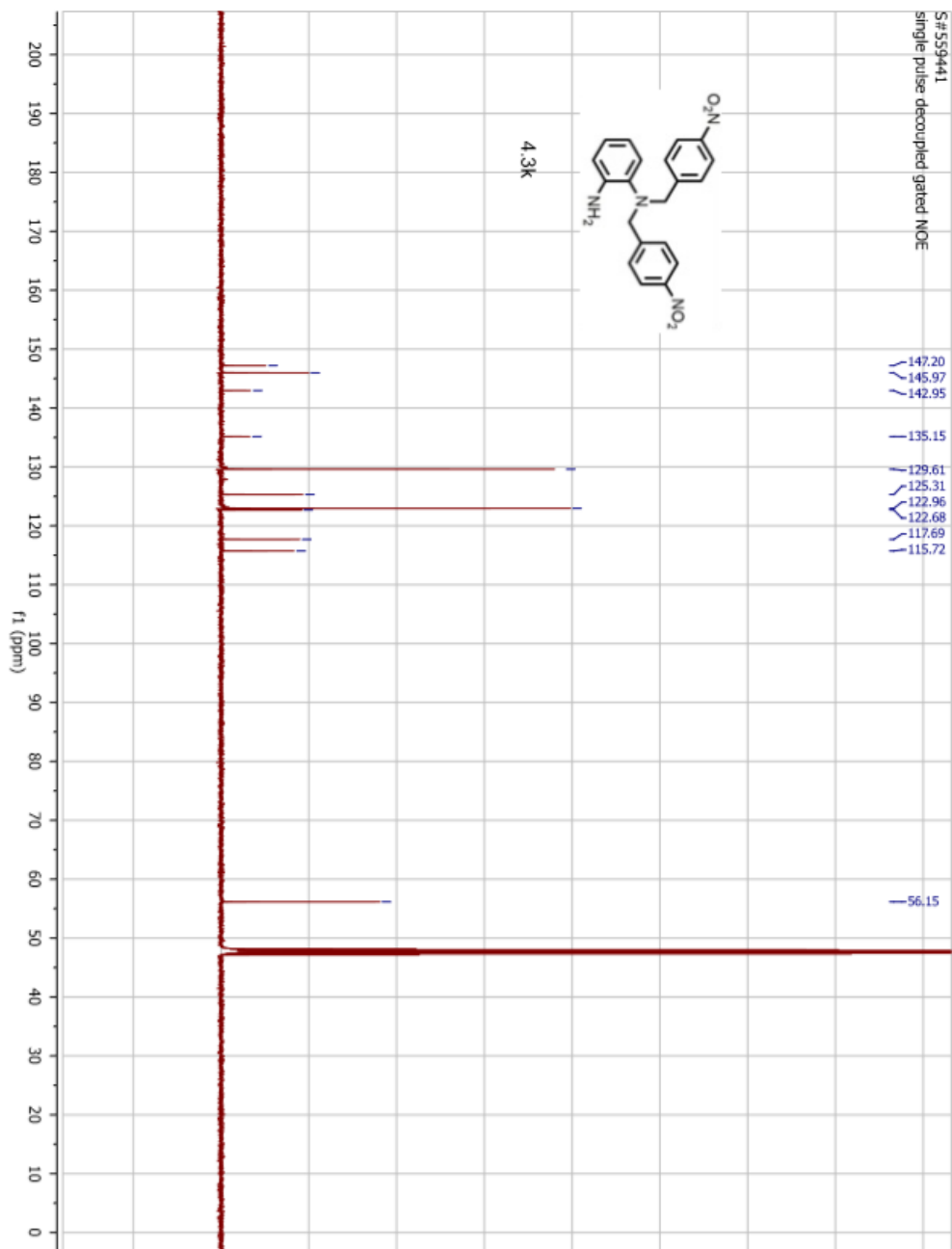


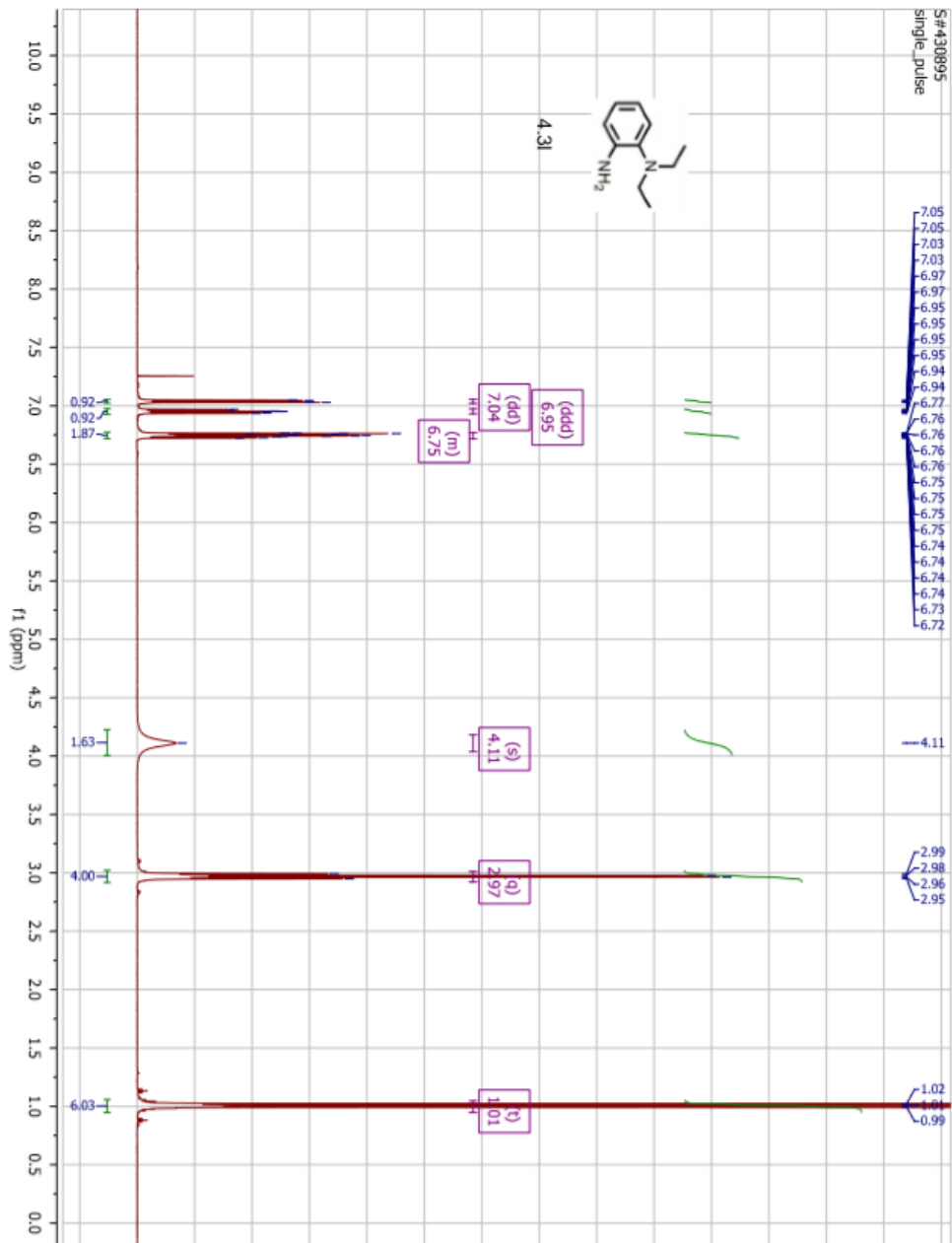




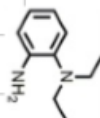




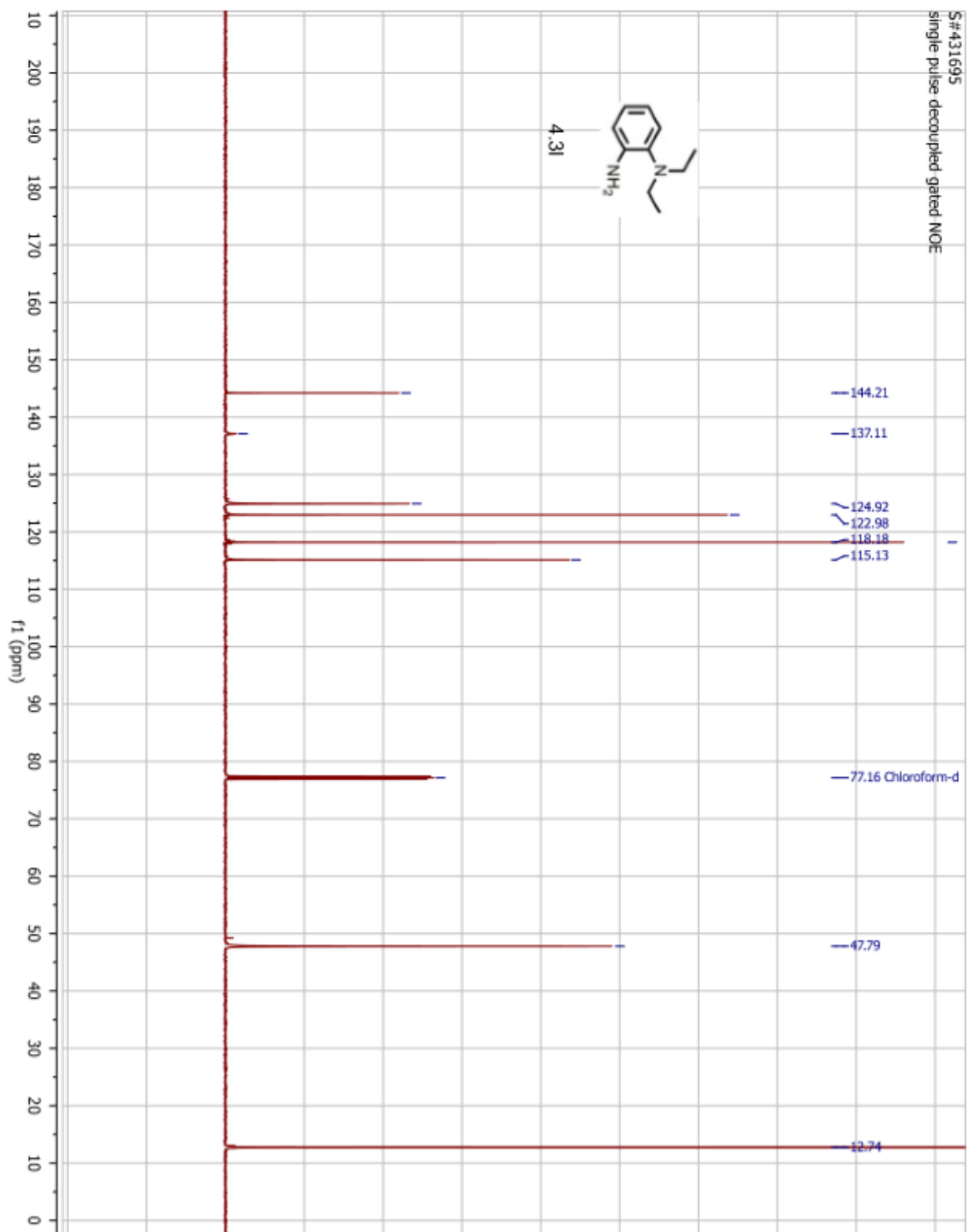




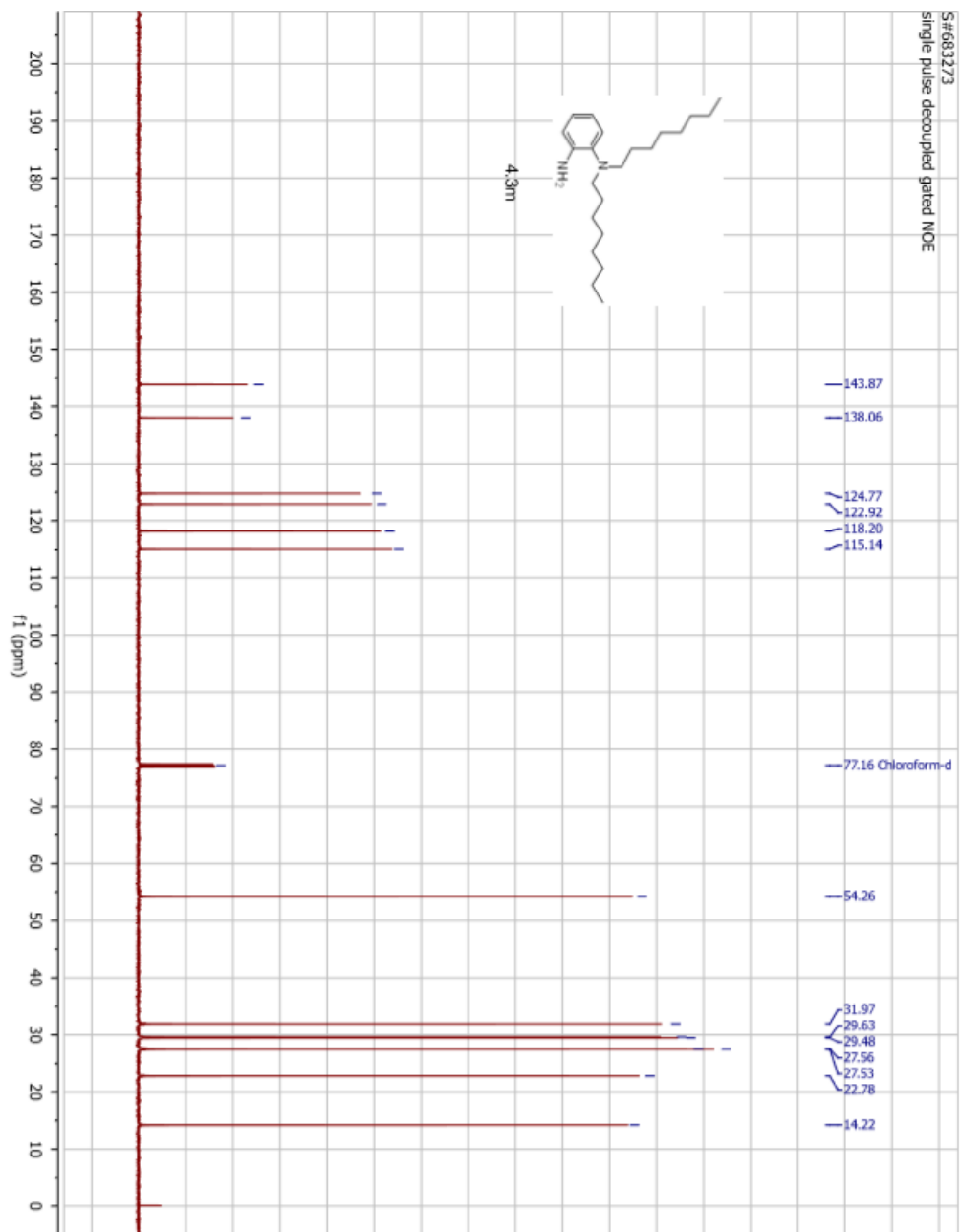
S#431695
single pulse decoupled gated NOE

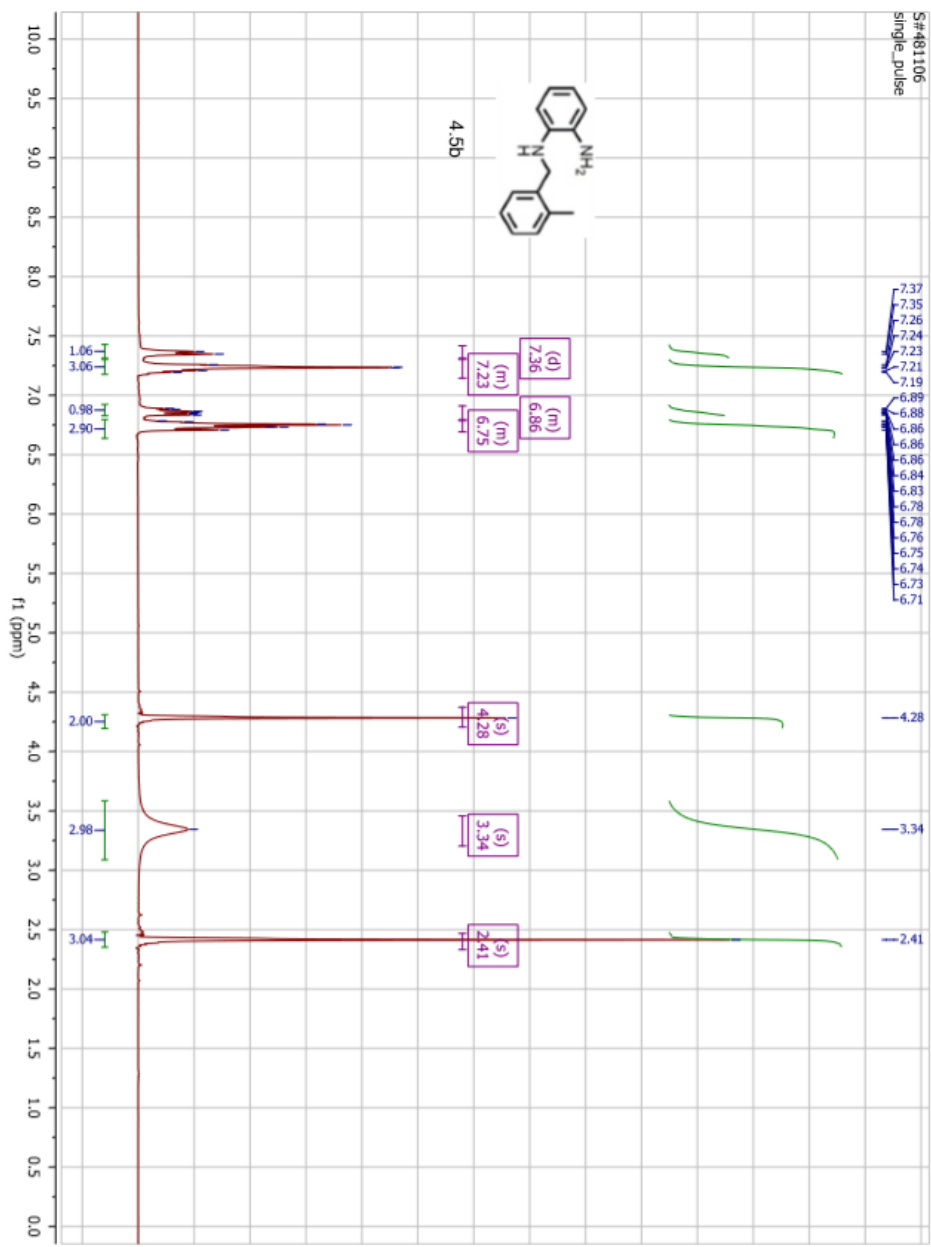


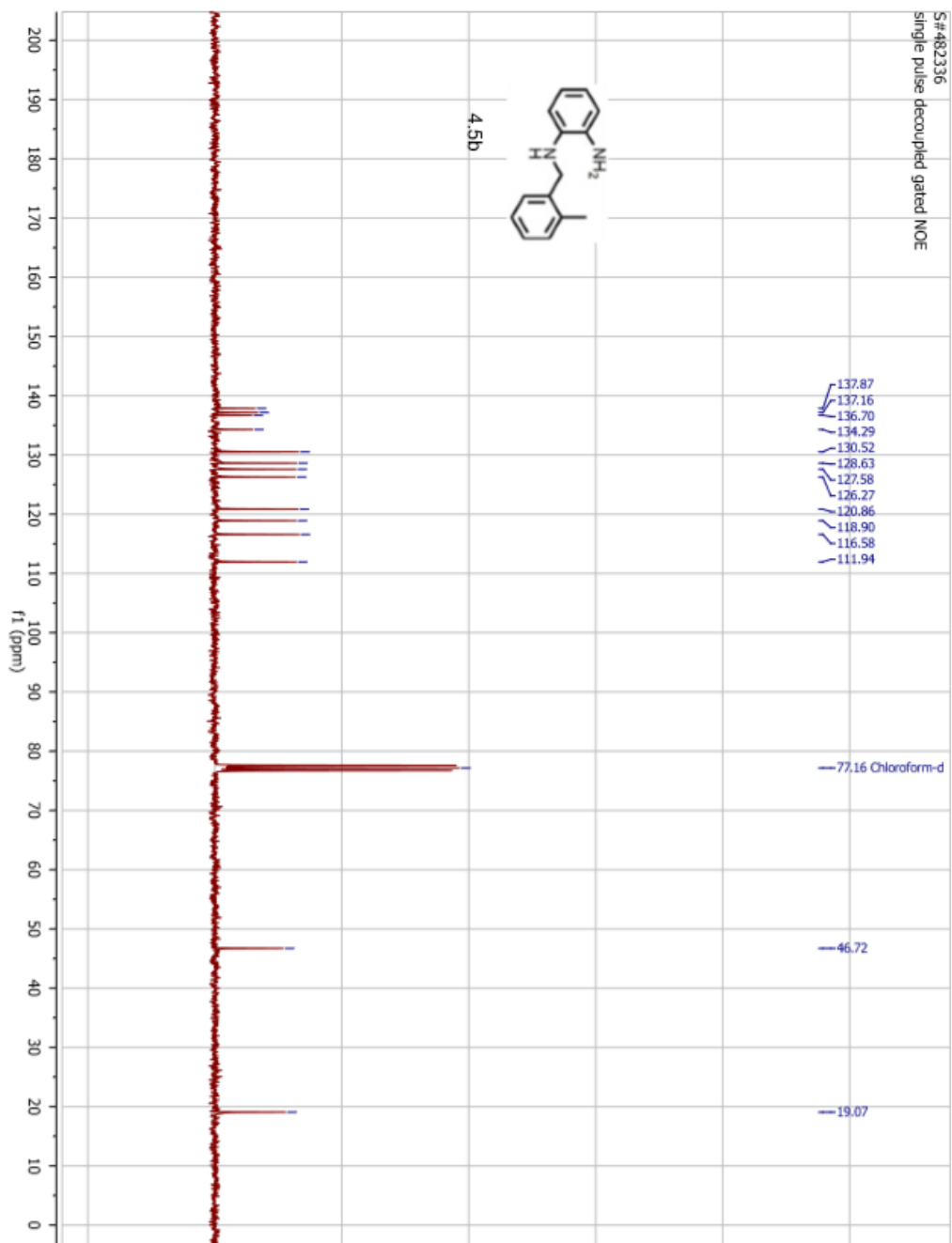
4.31

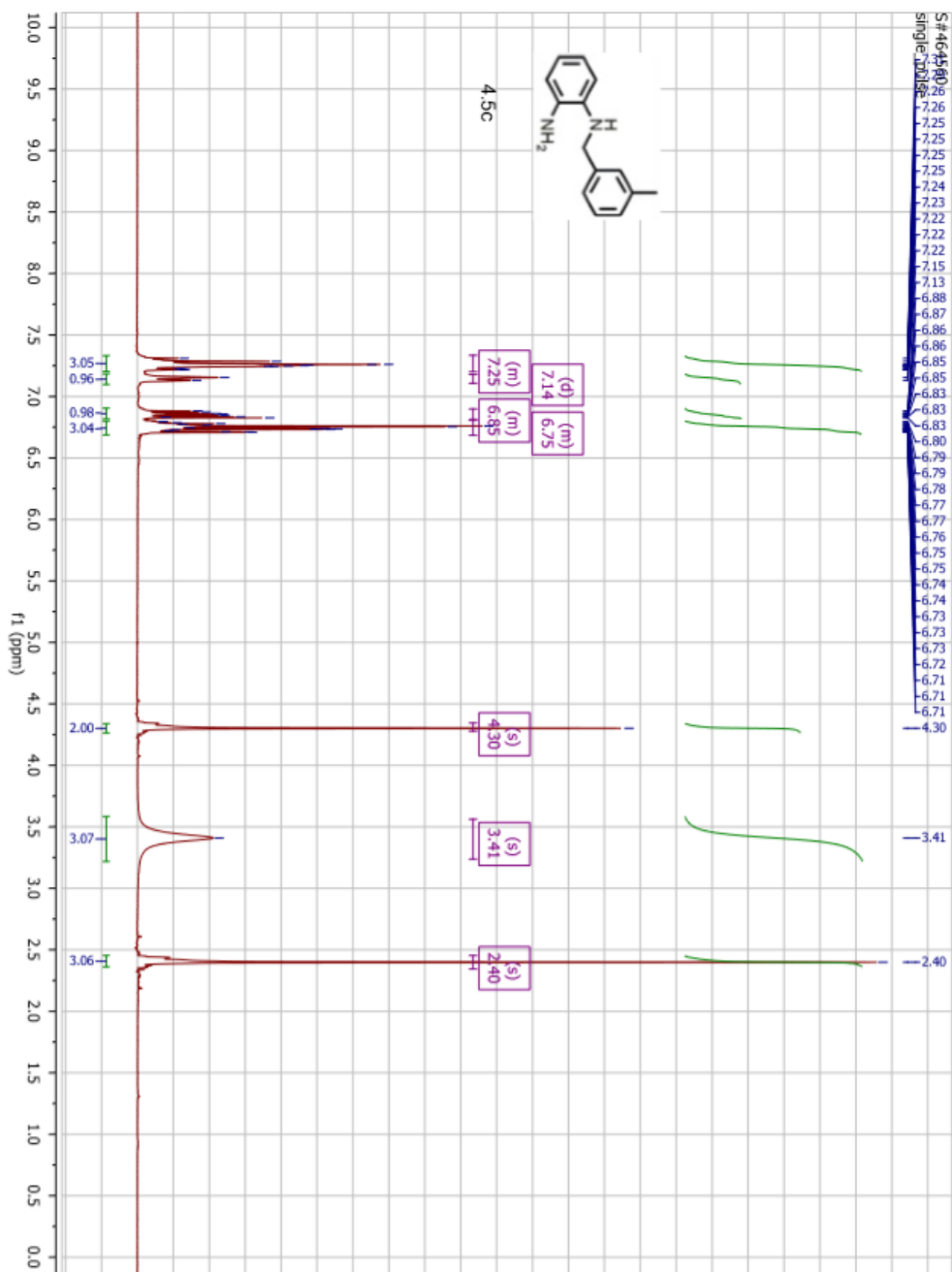


S#683273
single pulse decoupled gated NOE

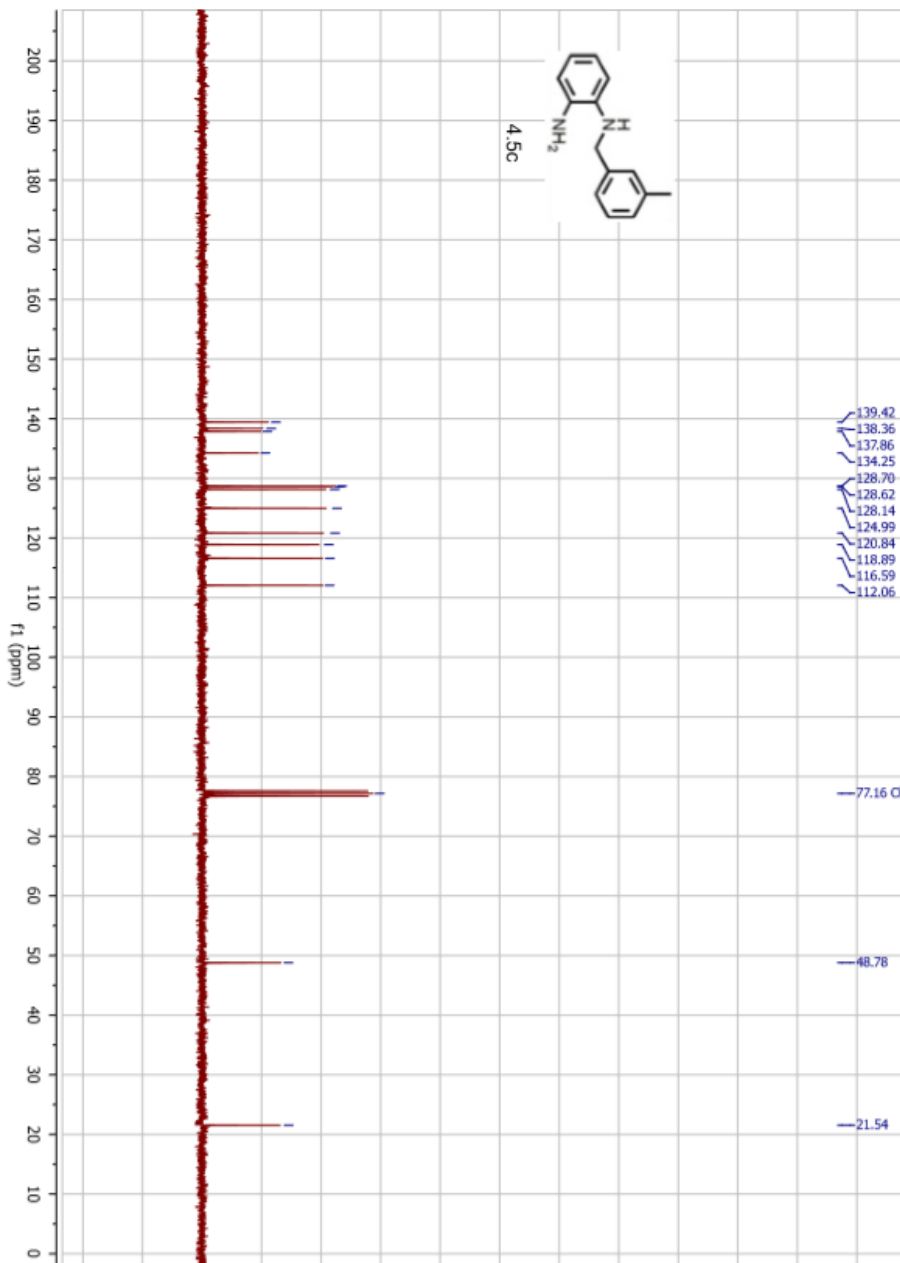
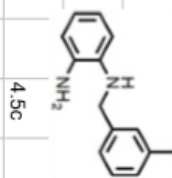




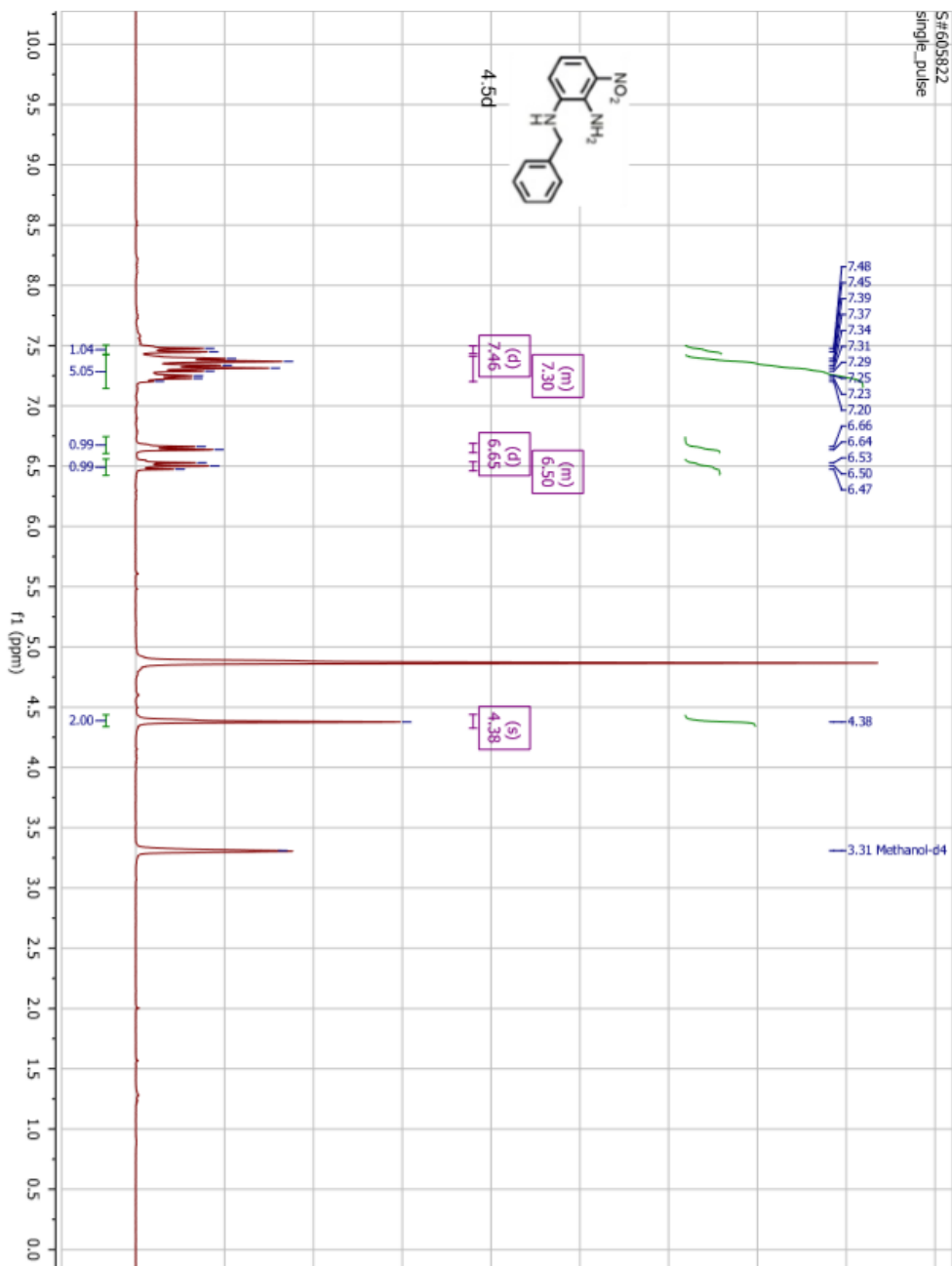




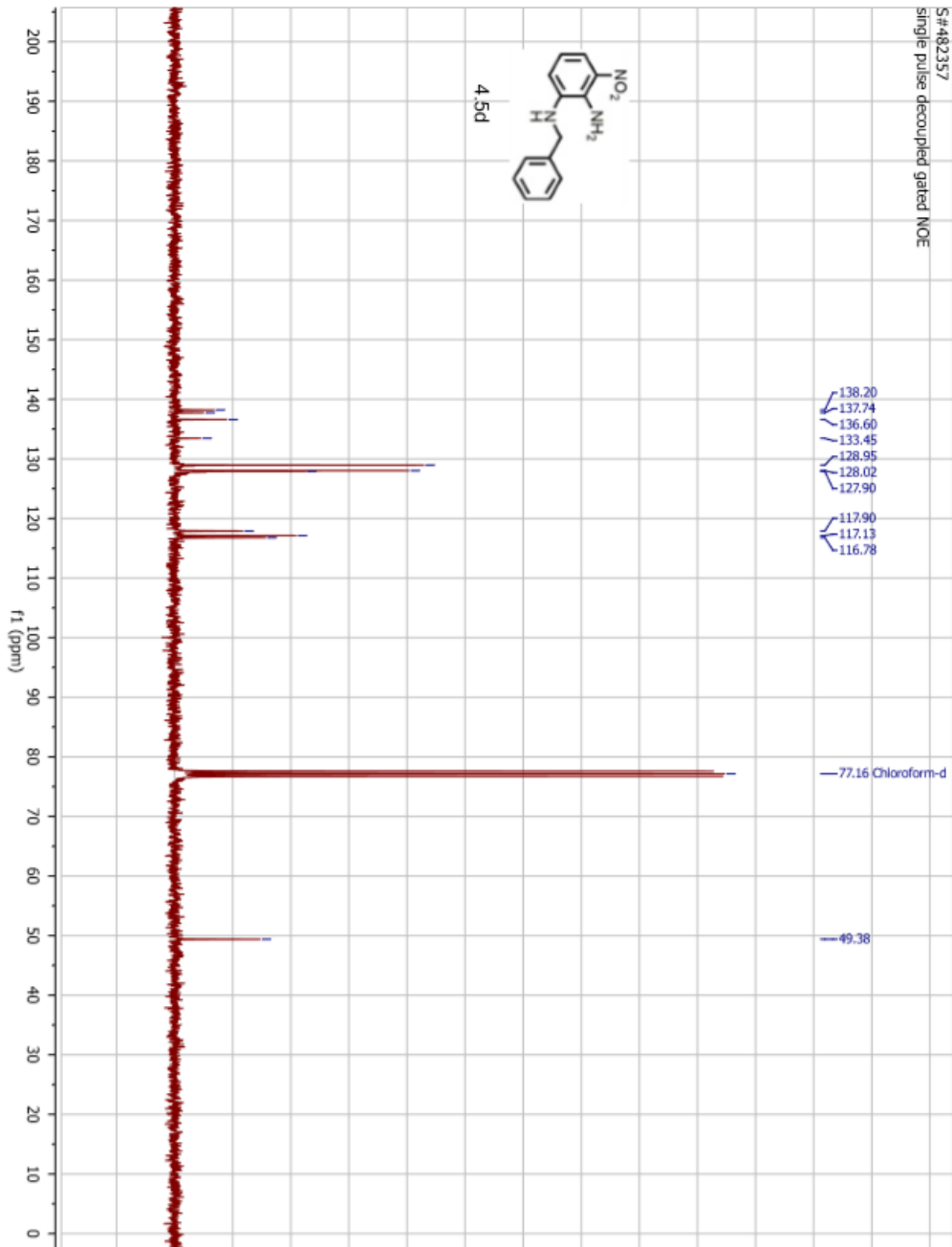
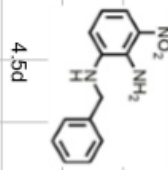
S#447596
single pulse decoupled gated NOE



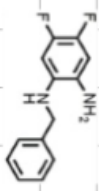
S:605822
single_pulse



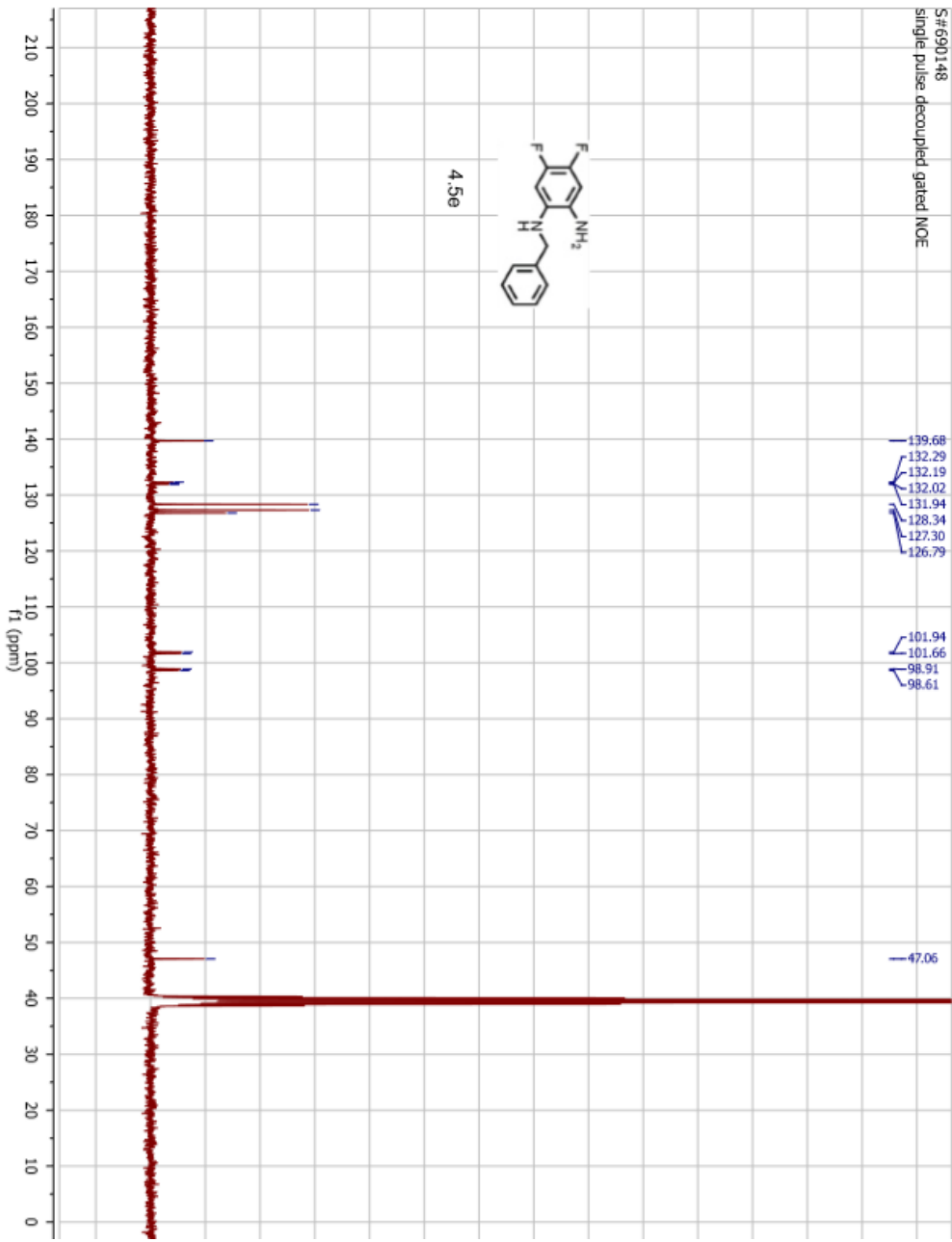
S#482357
single pulse decoupled gated NOE

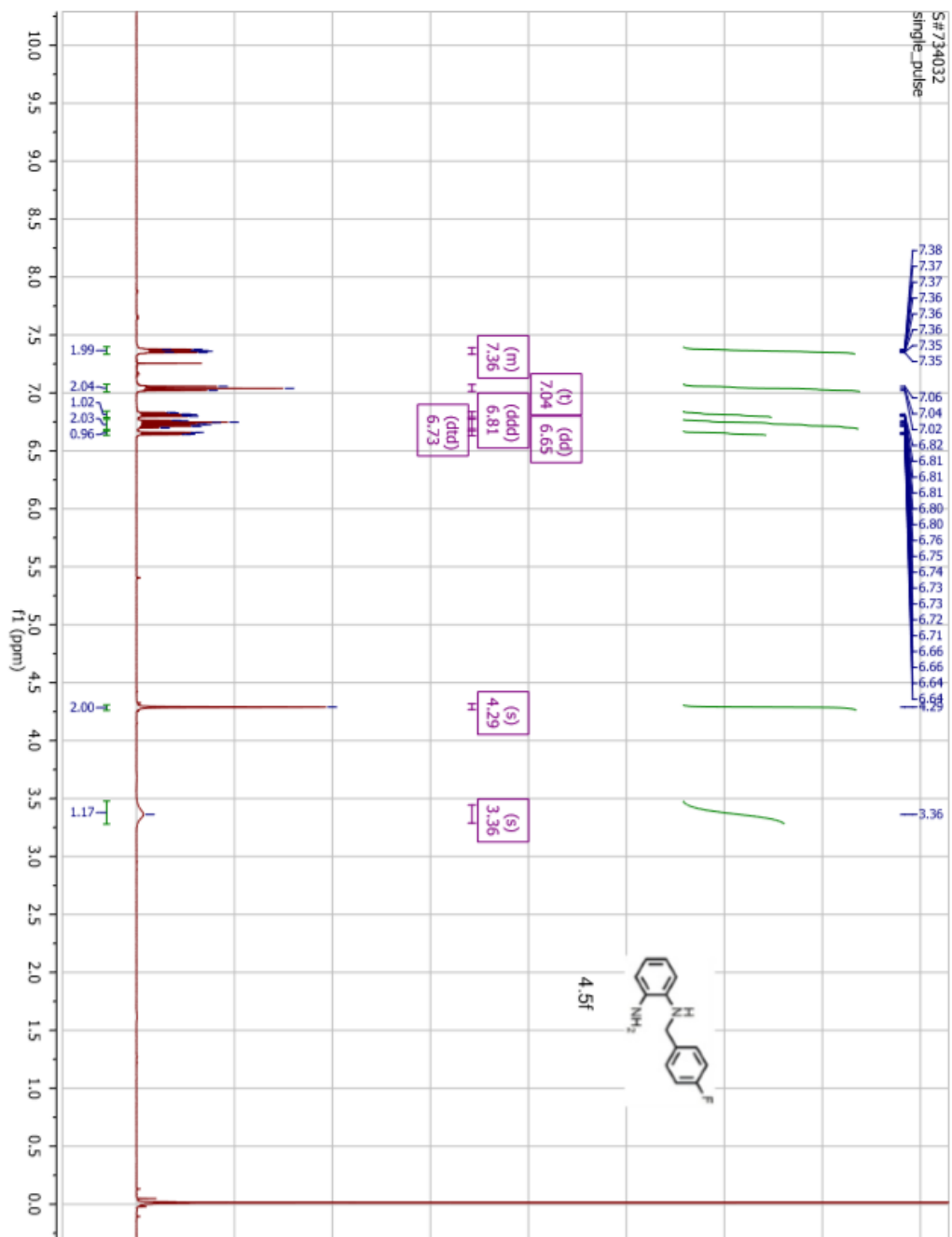


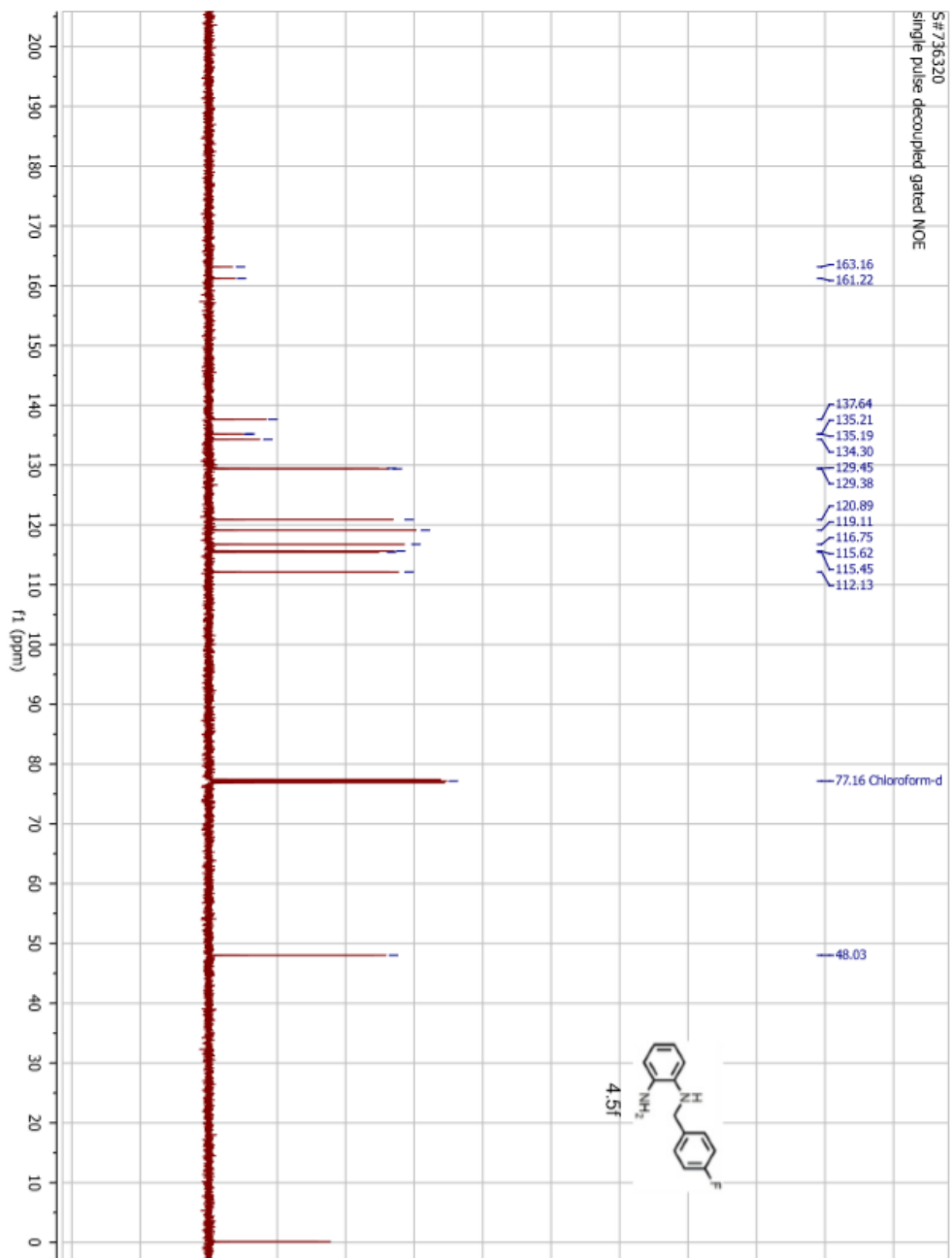
S#690148
single pulse decoupled gated NOE



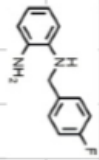
4.5e



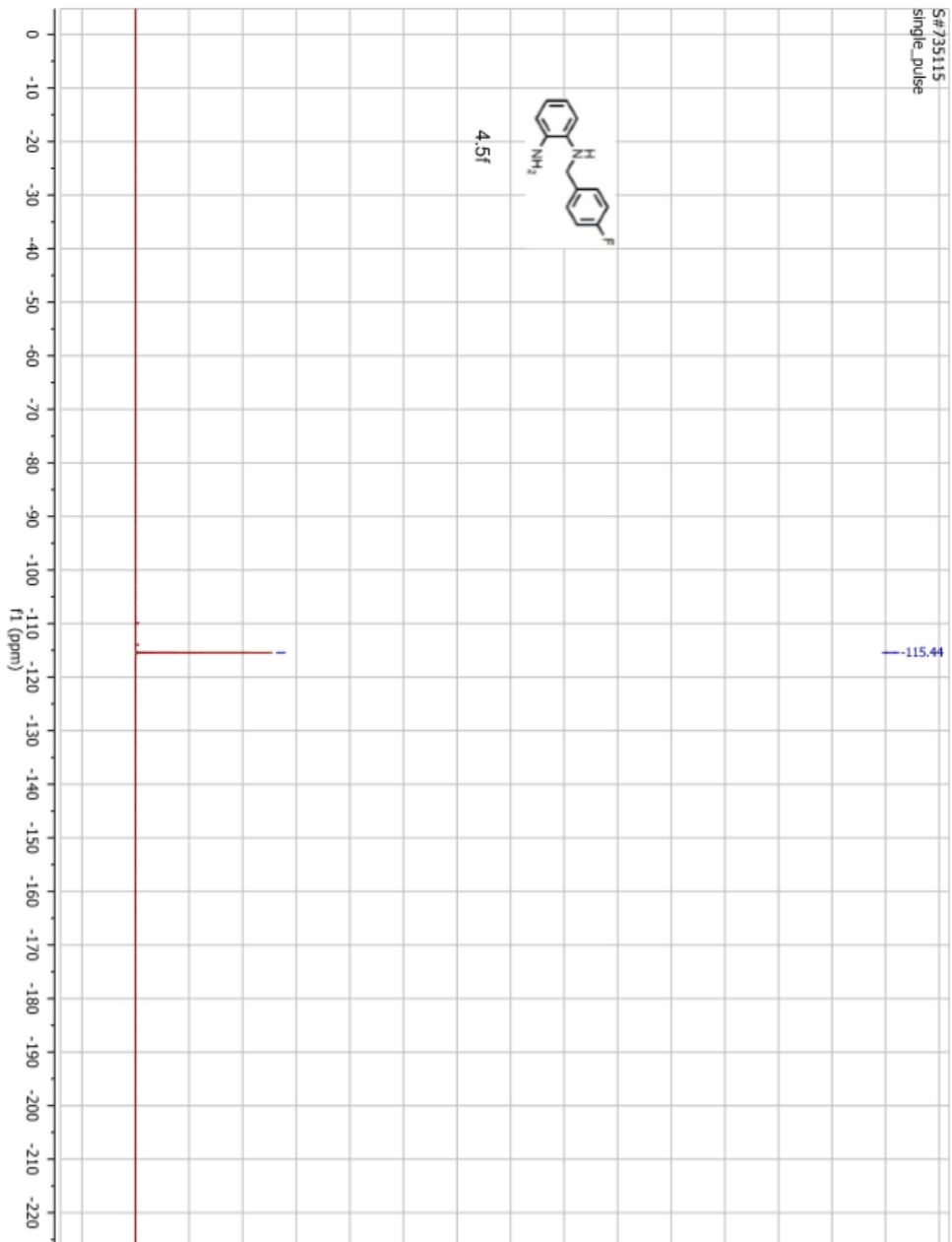


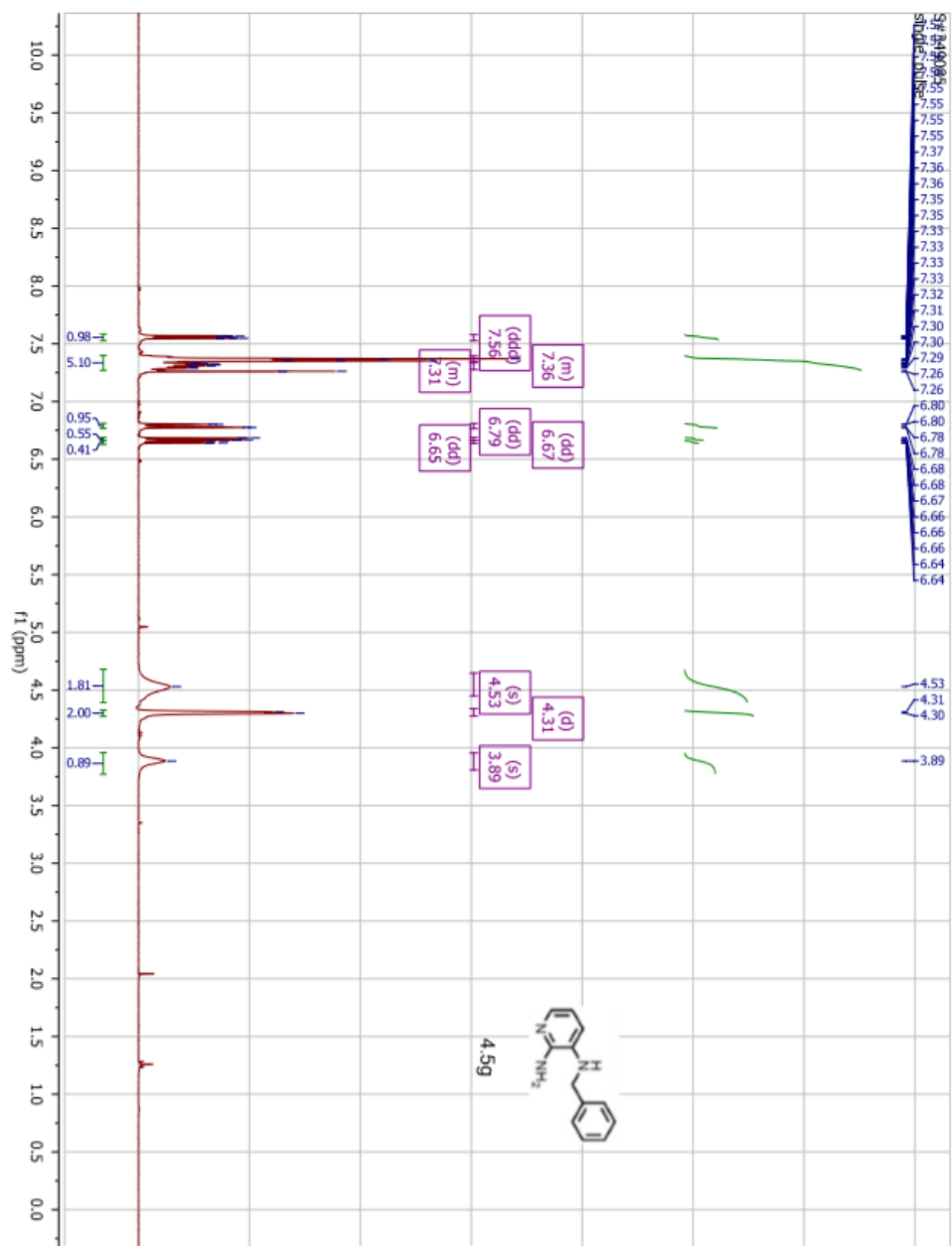


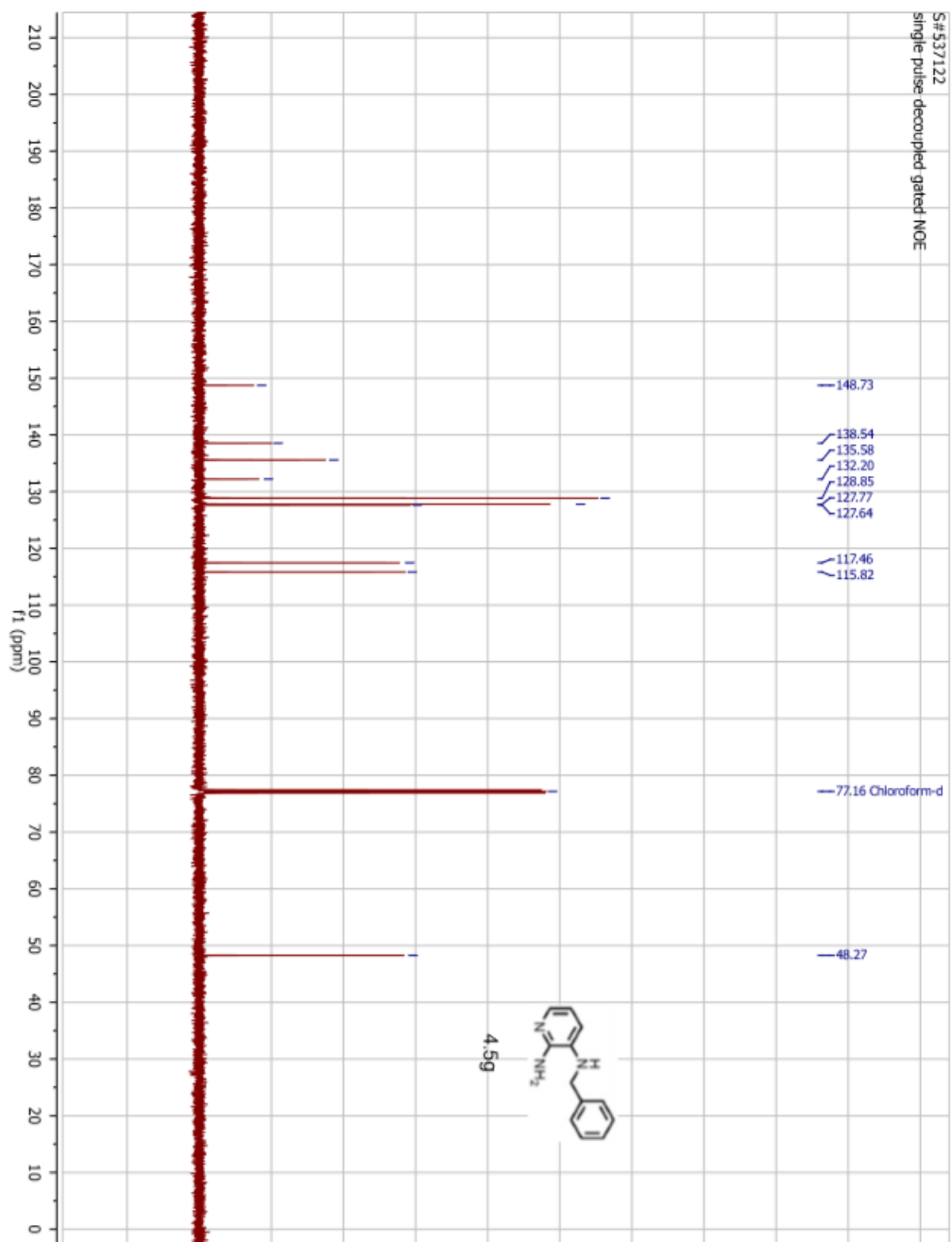
S#735115
single_pulse

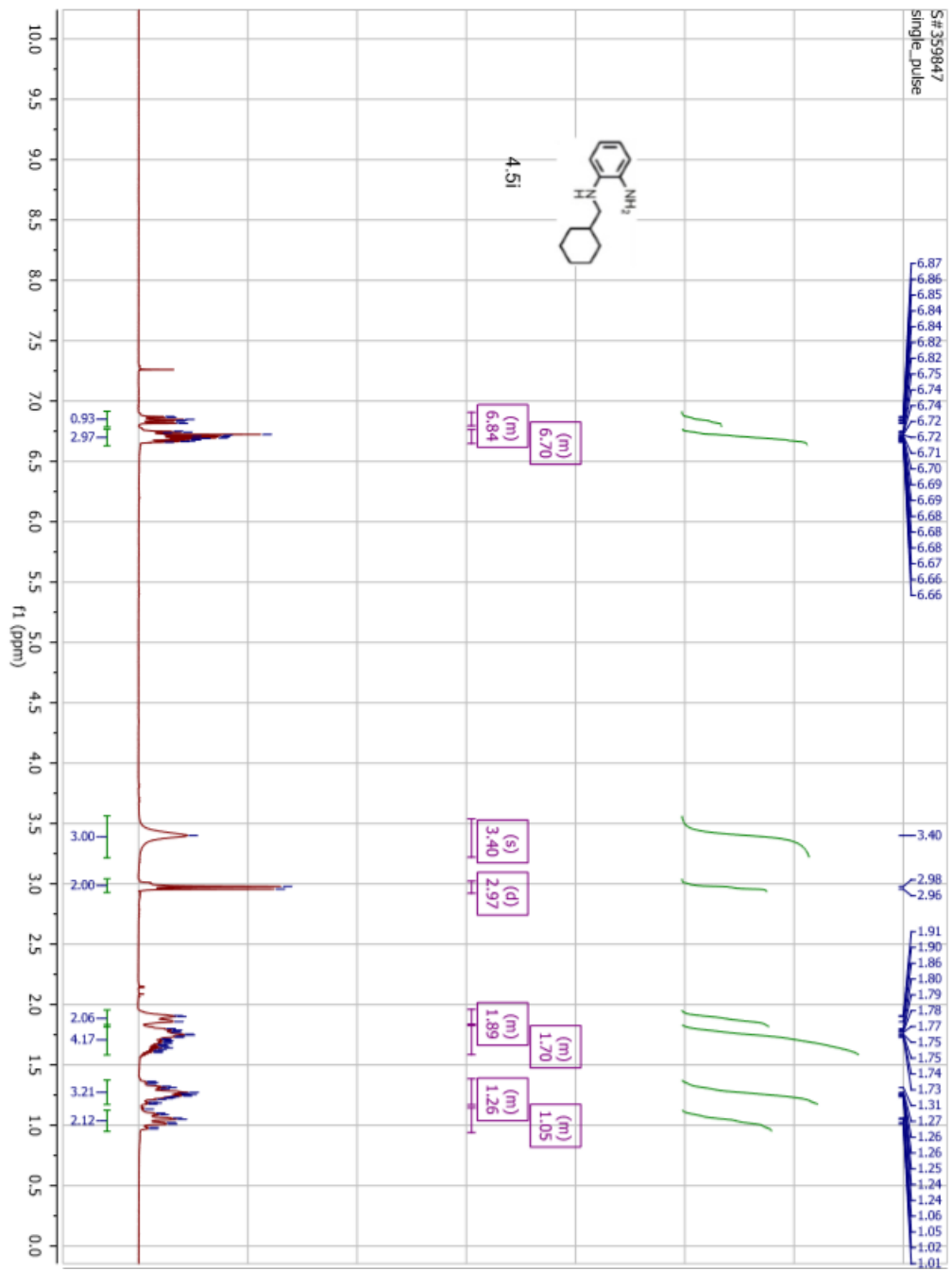


4.5f

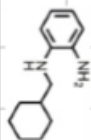




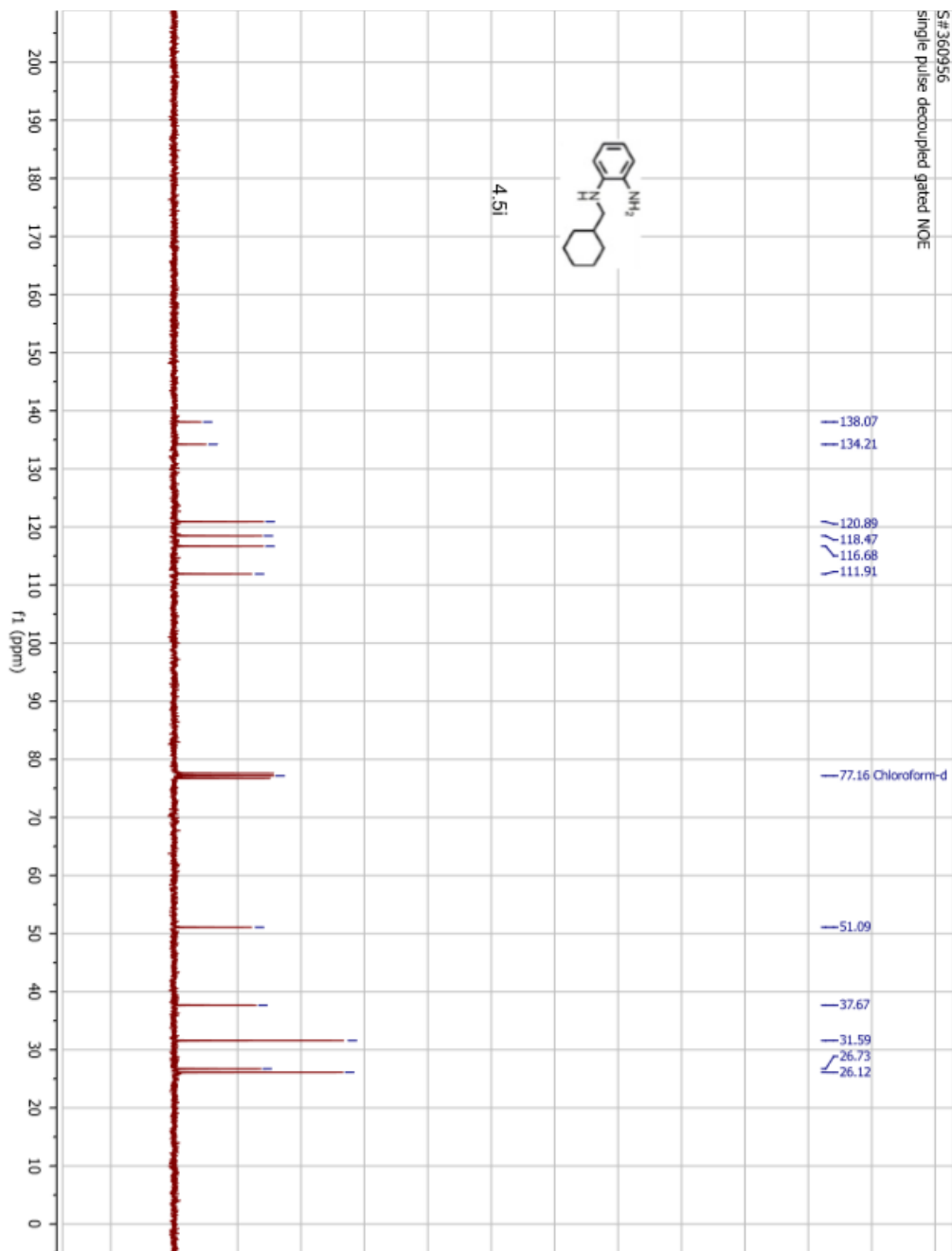


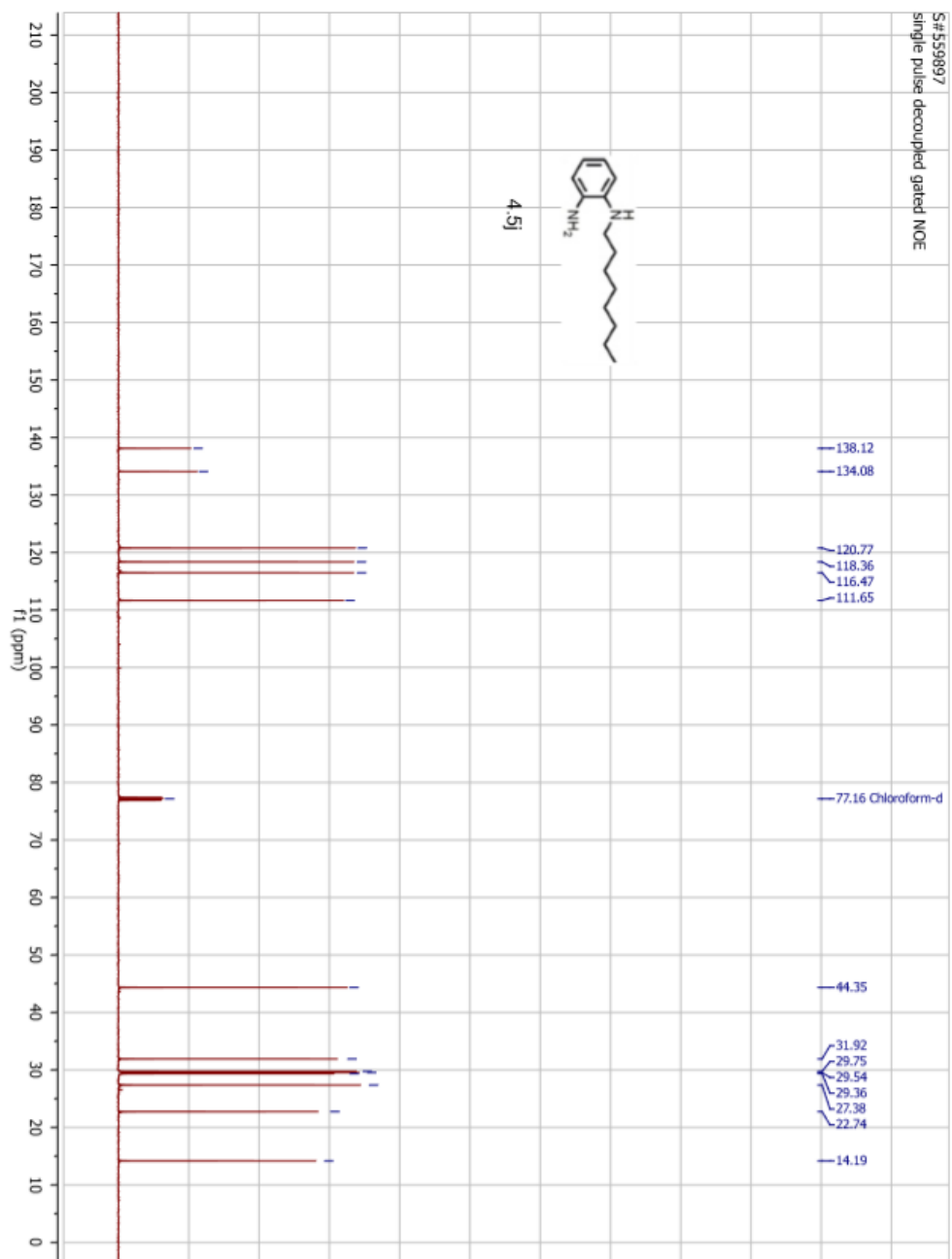


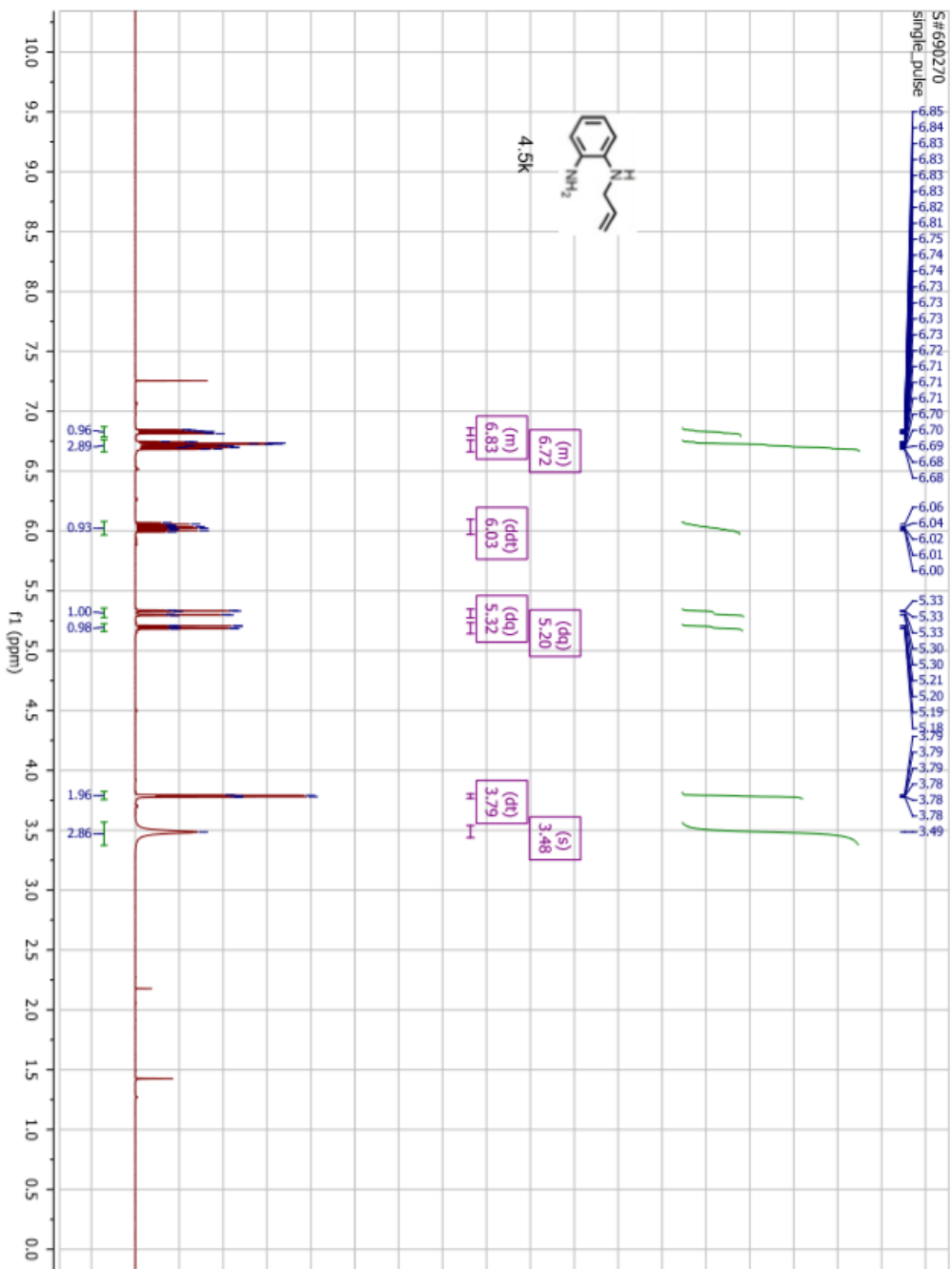
S# 360956
Single pulse decoupled gated NOE



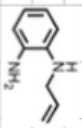
4.51



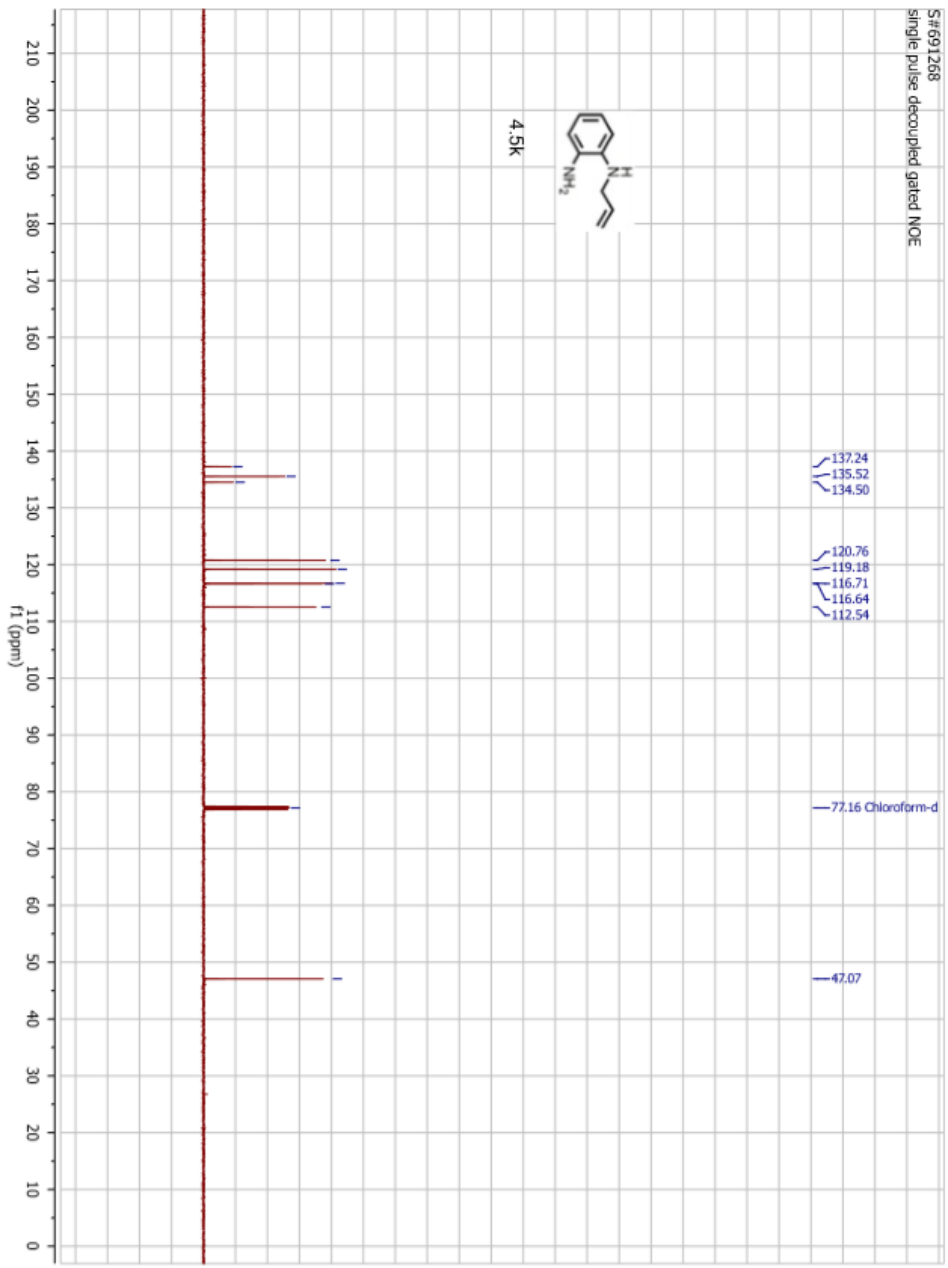


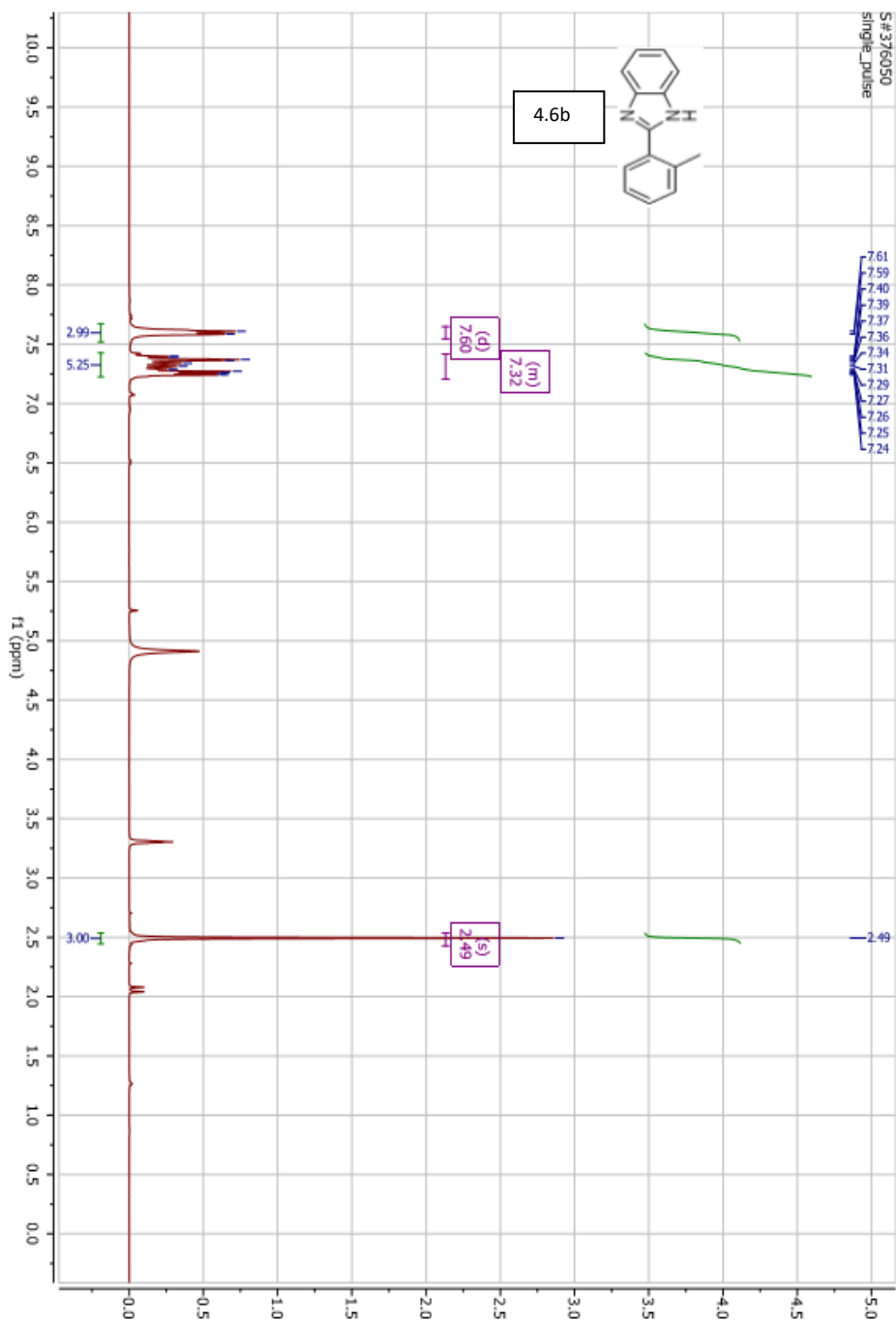


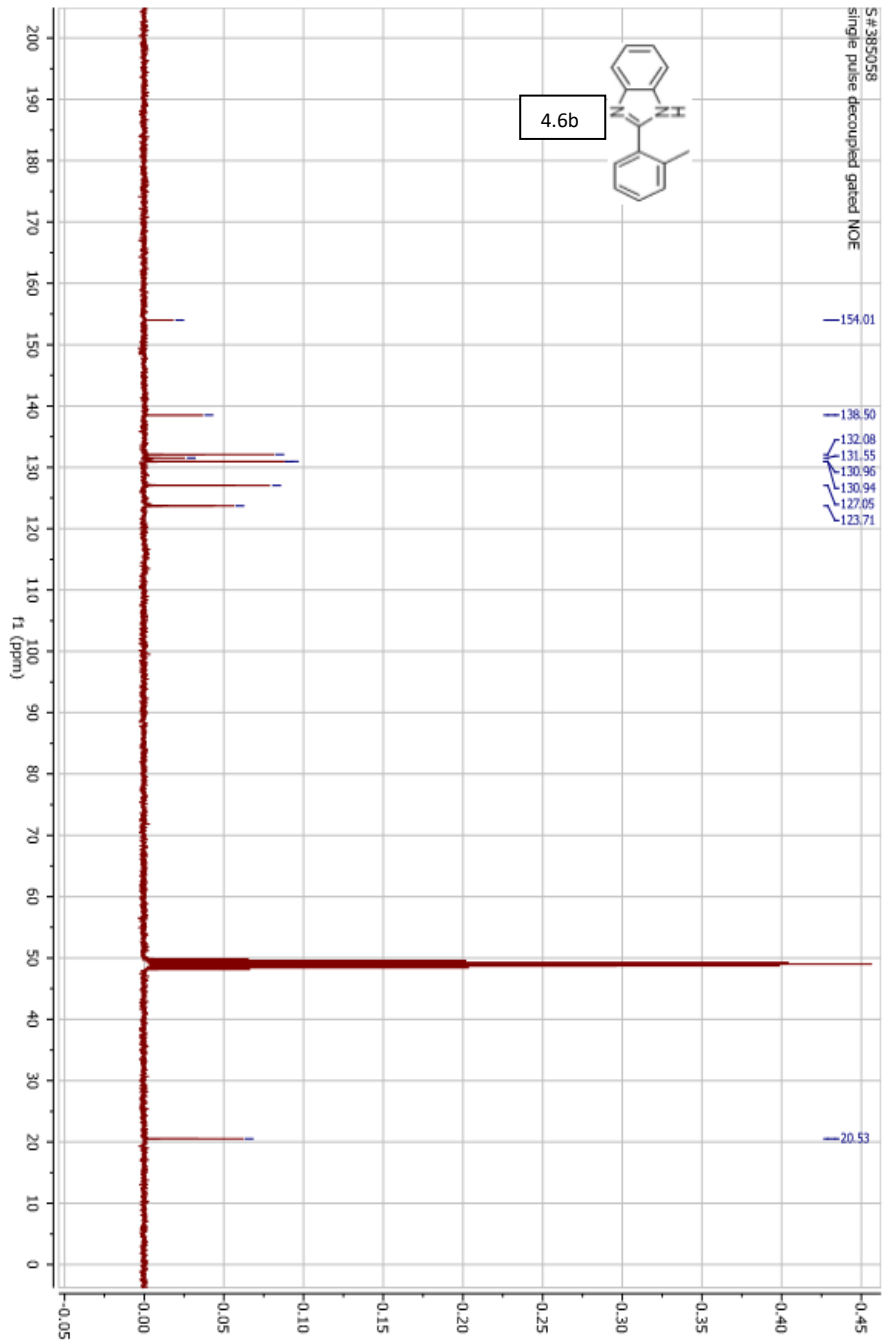
S#691268
single pulse decoupled gated NOE

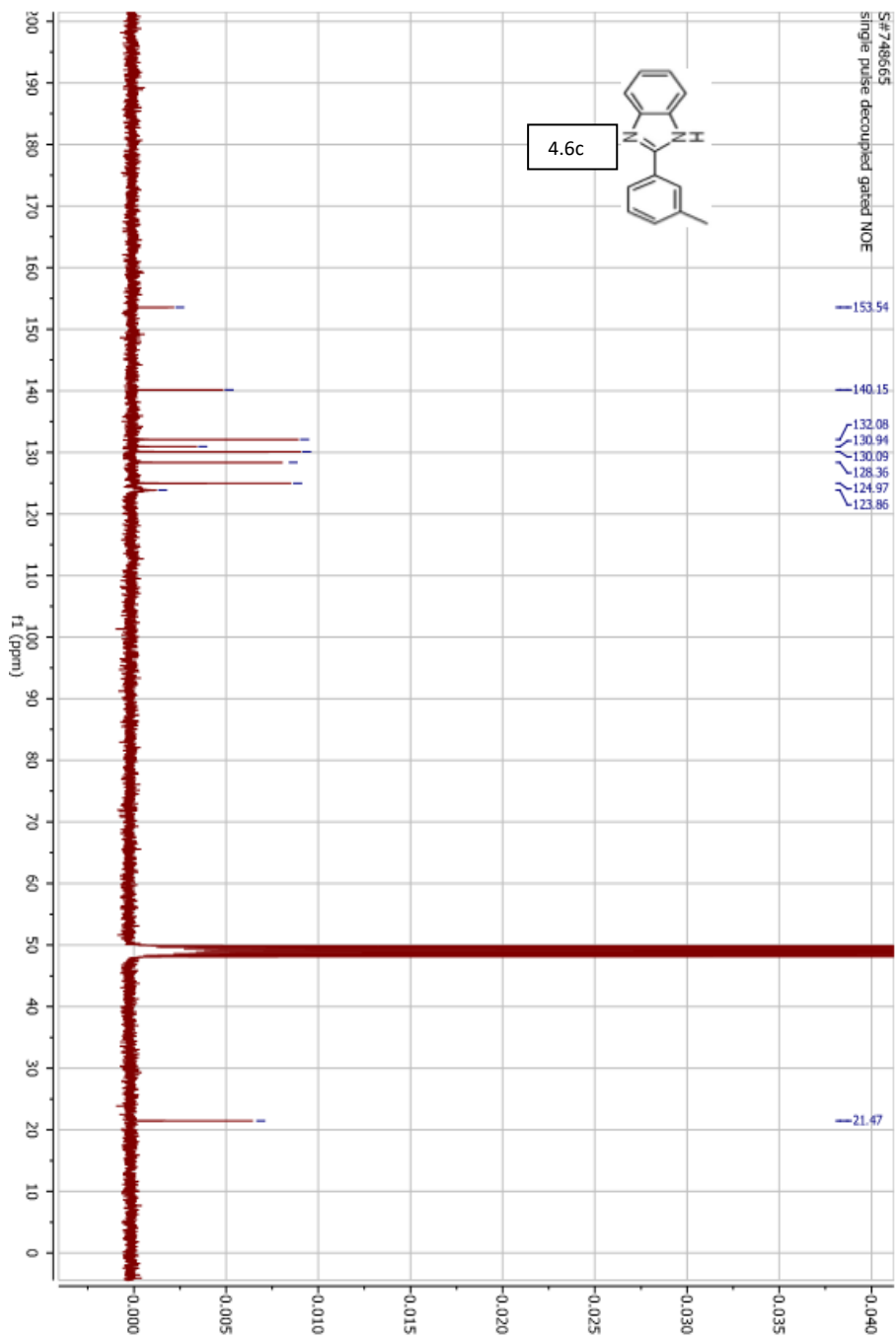


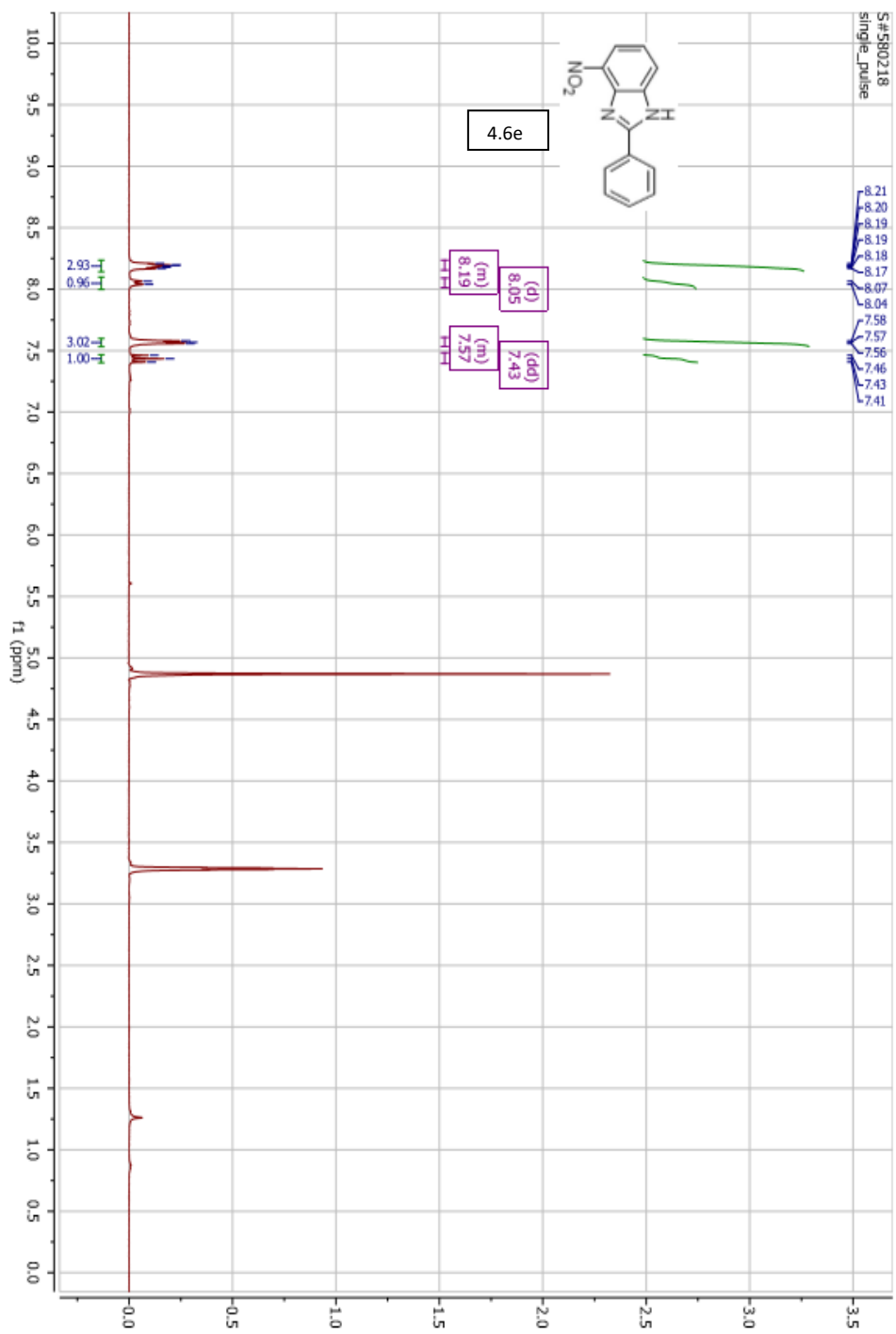
4.5K

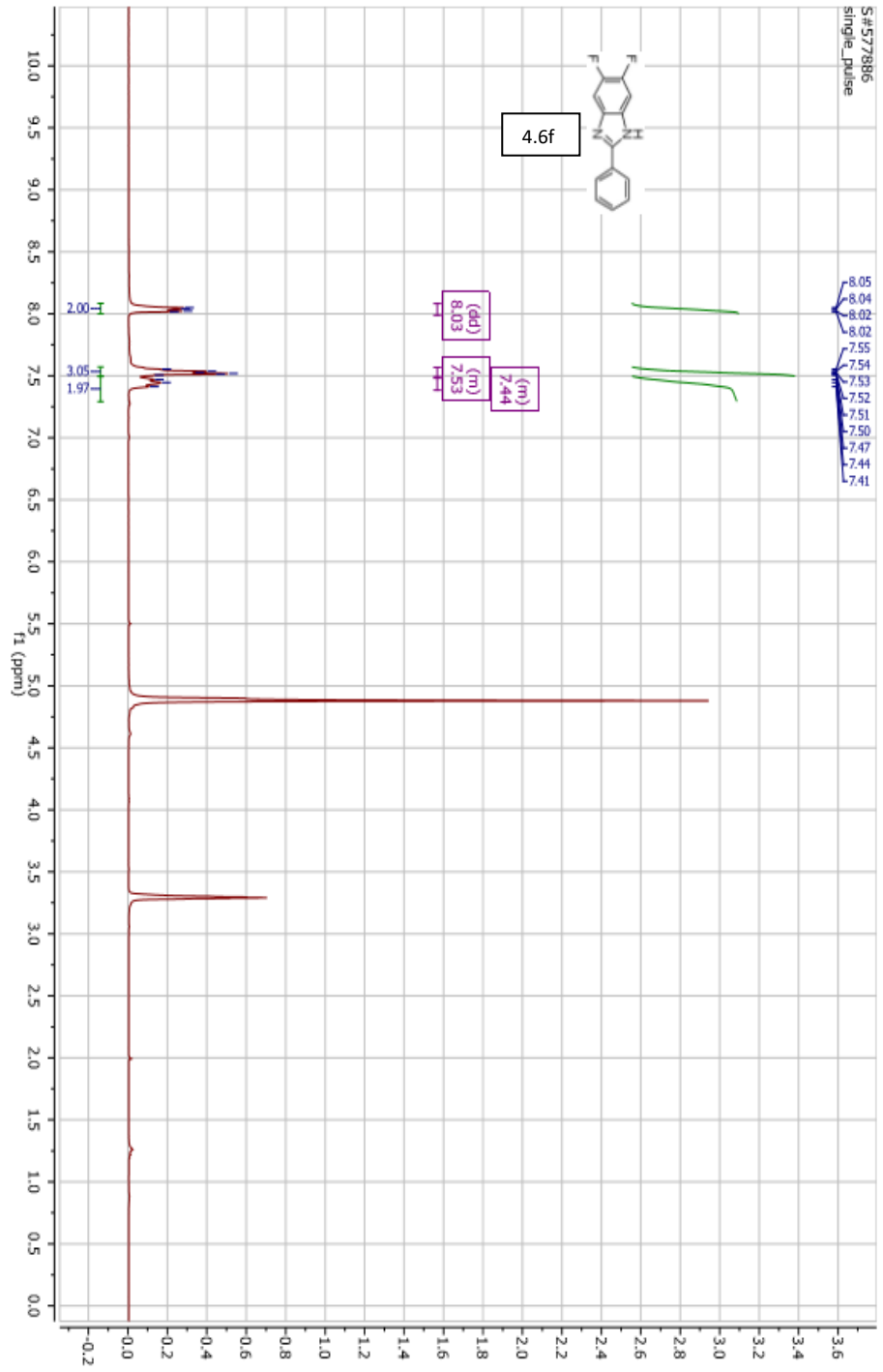


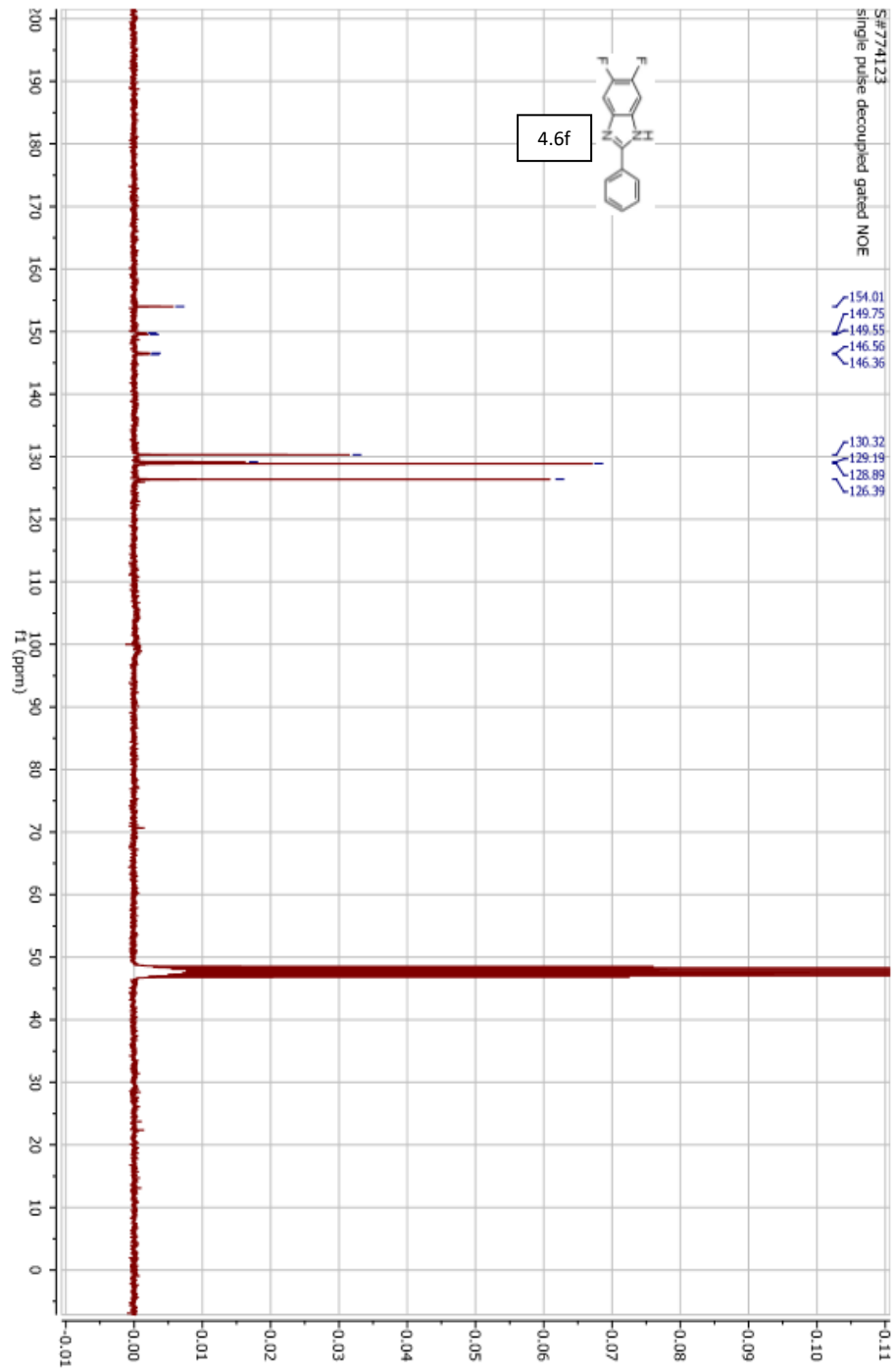


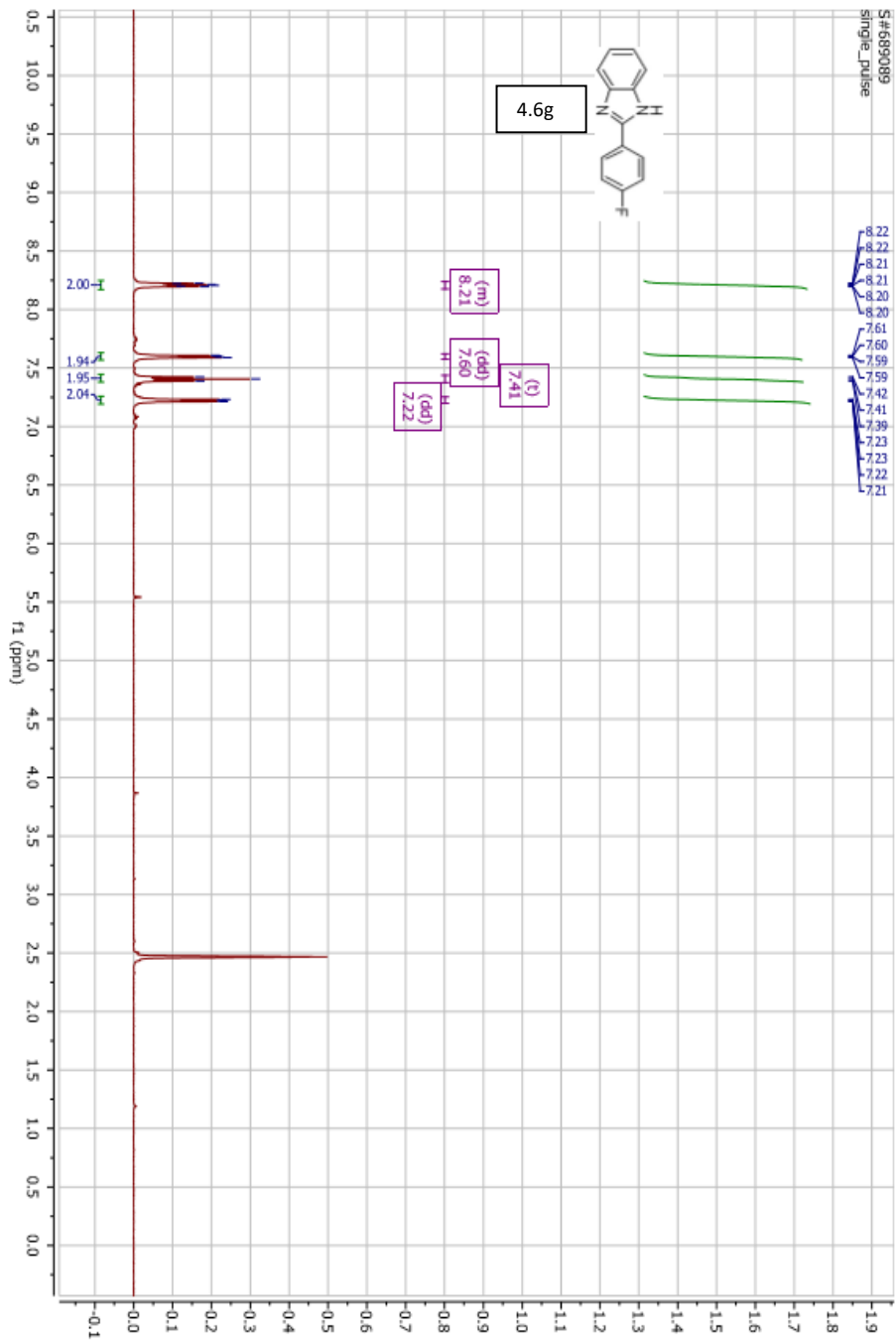


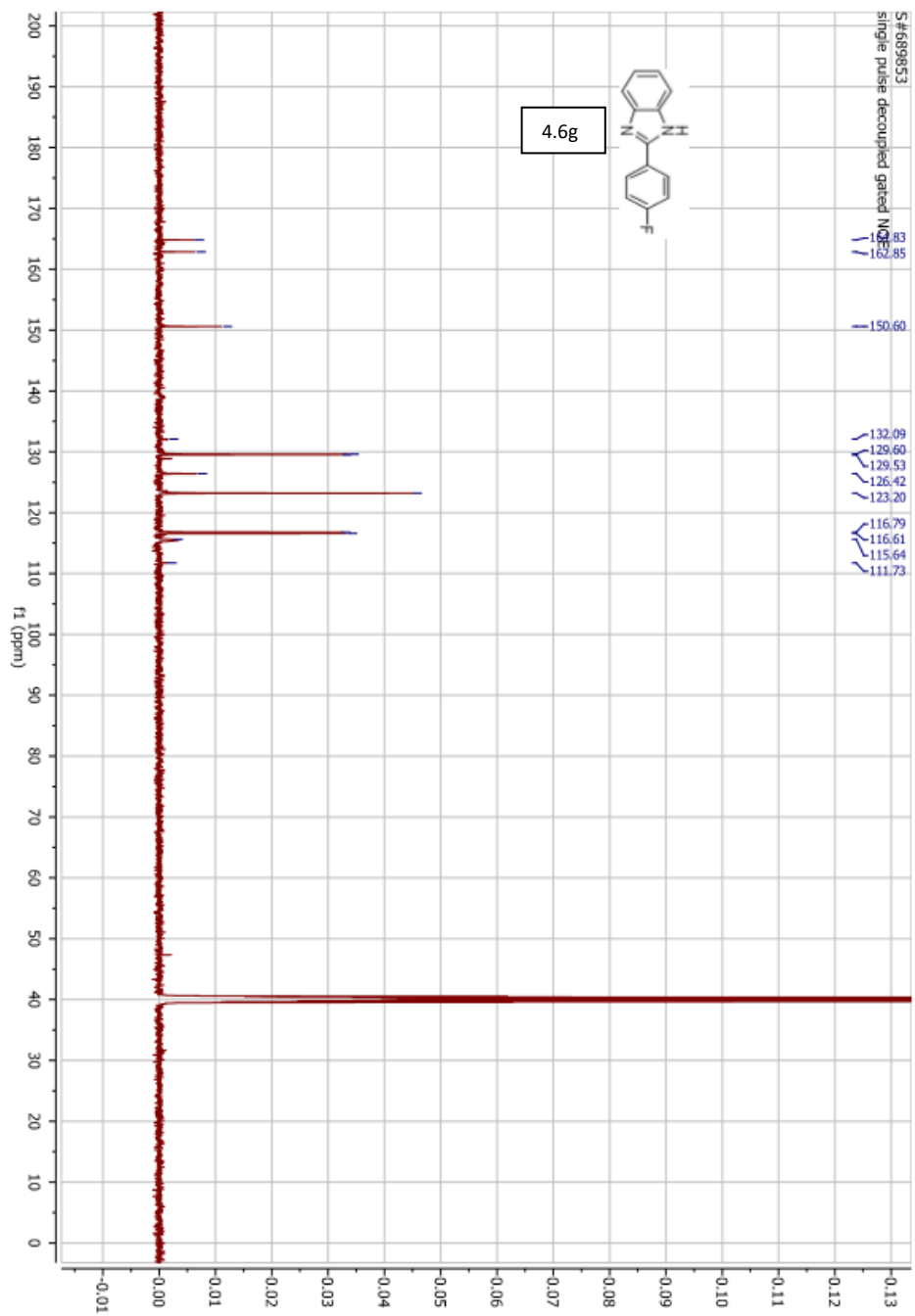


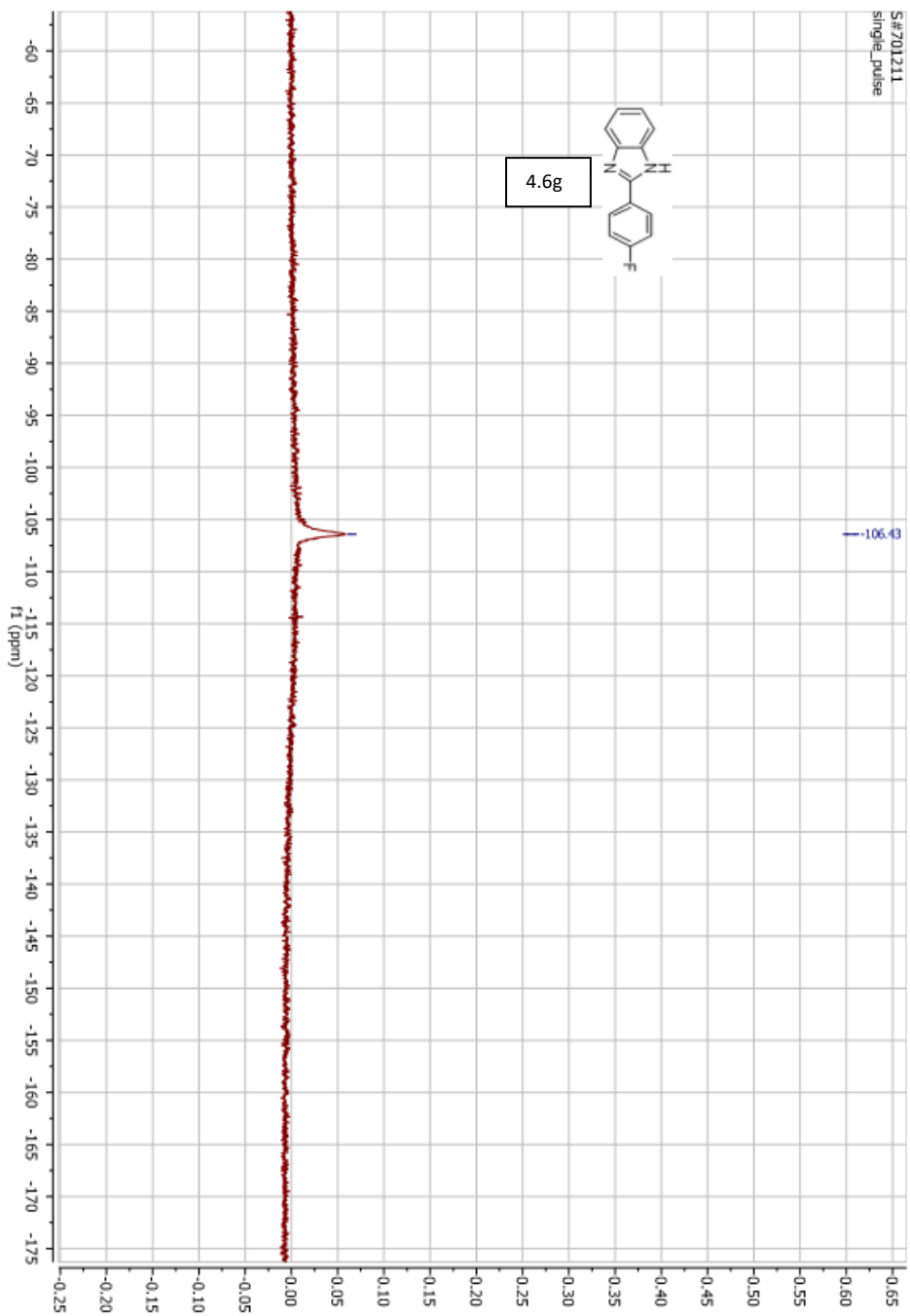


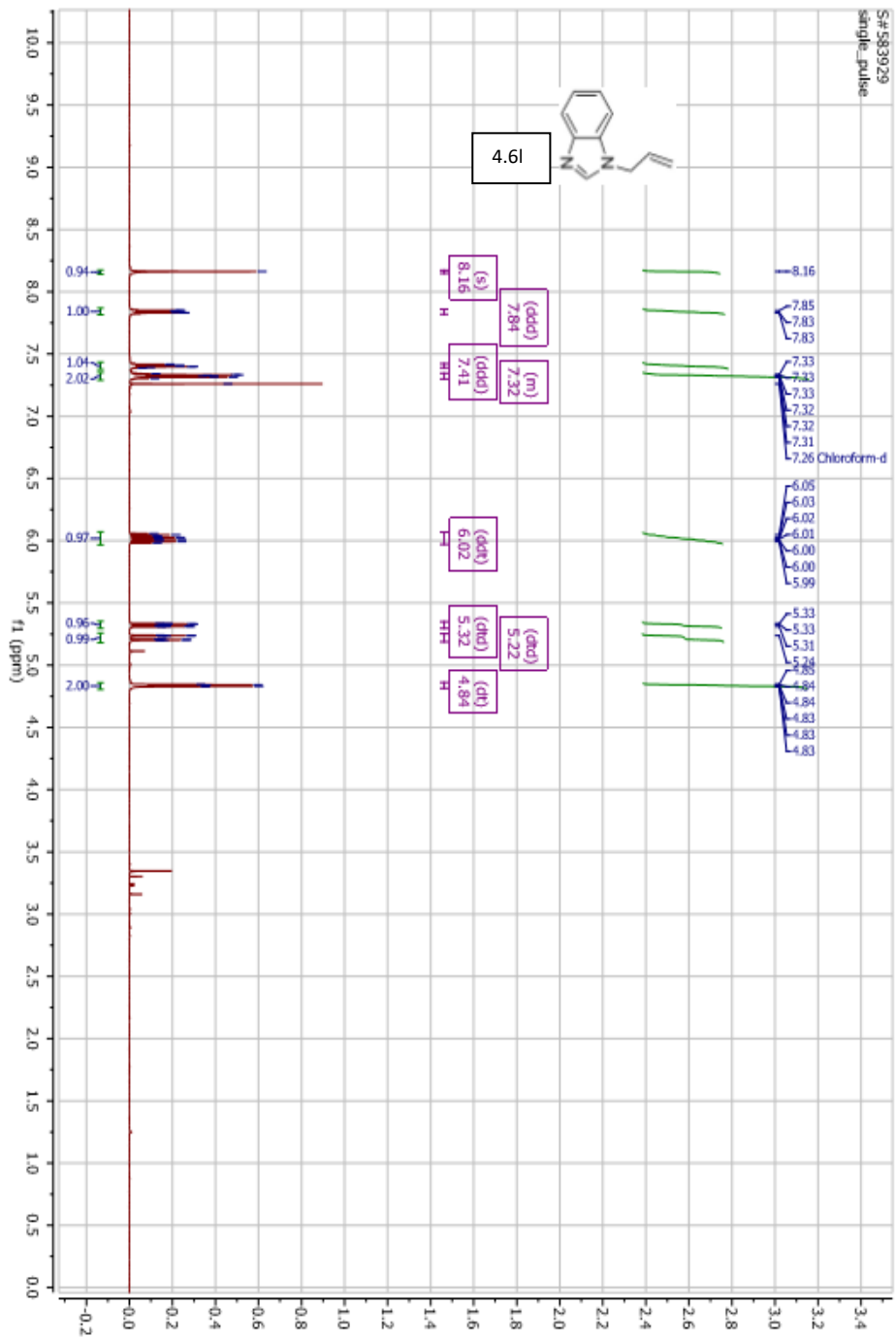


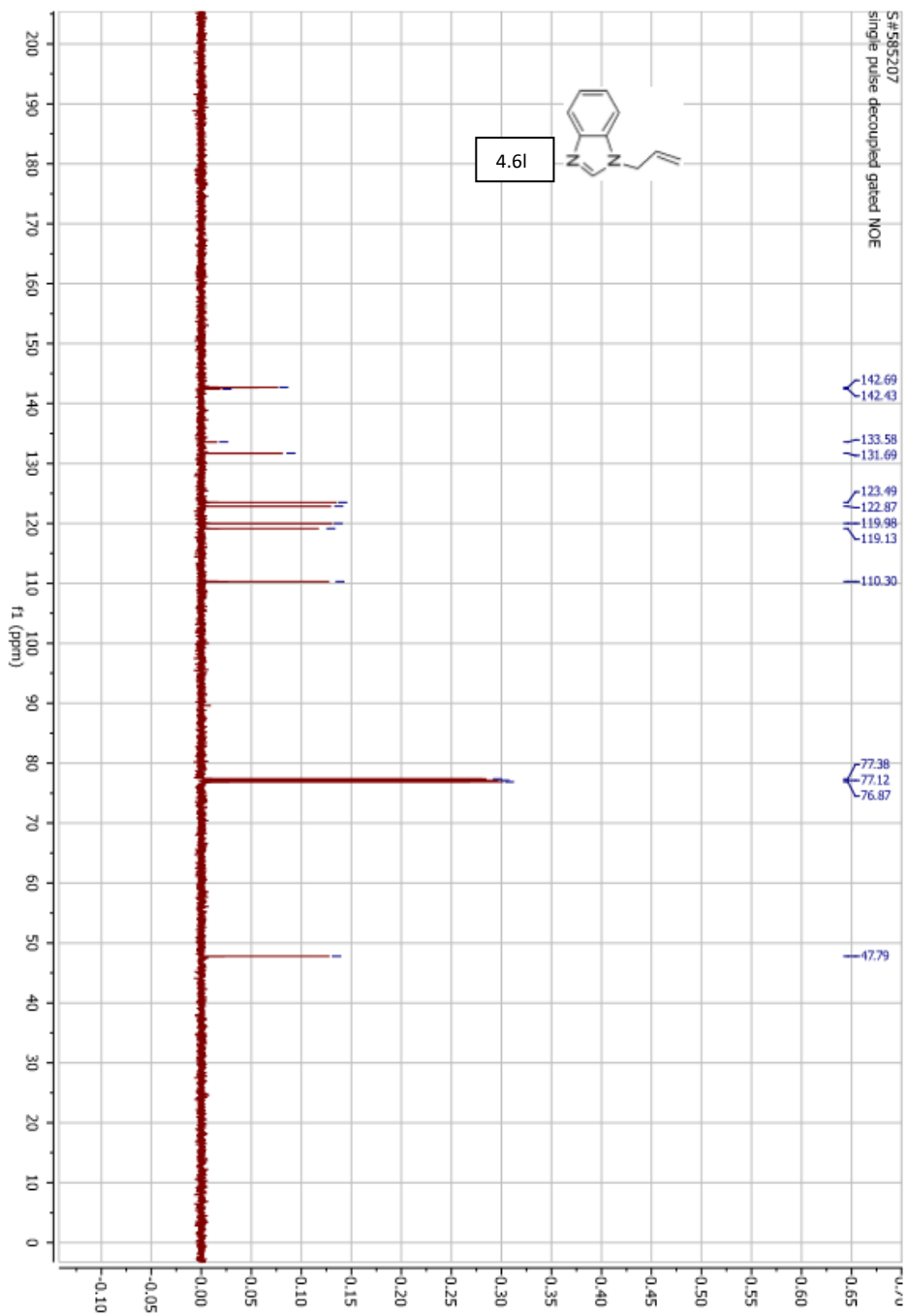


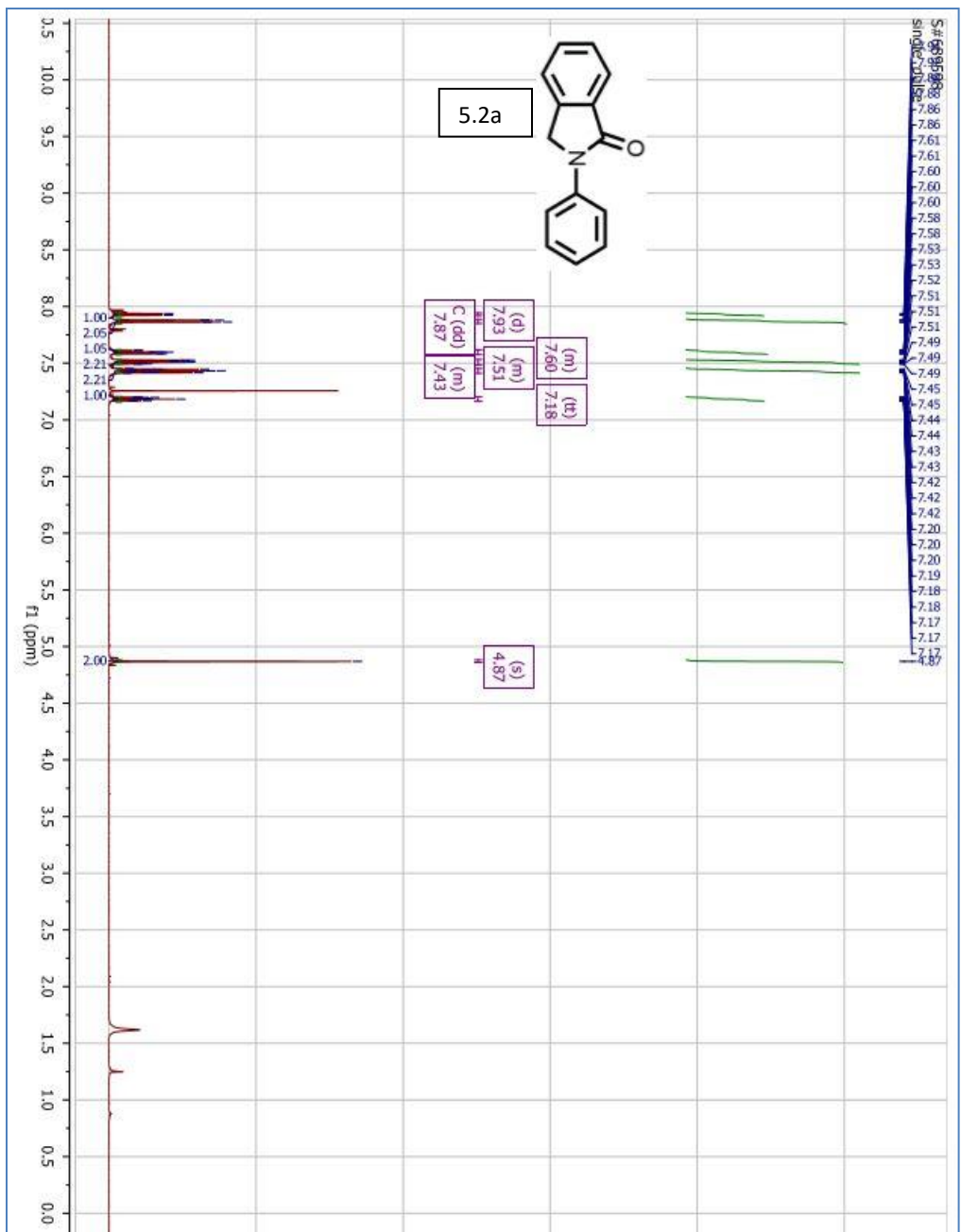


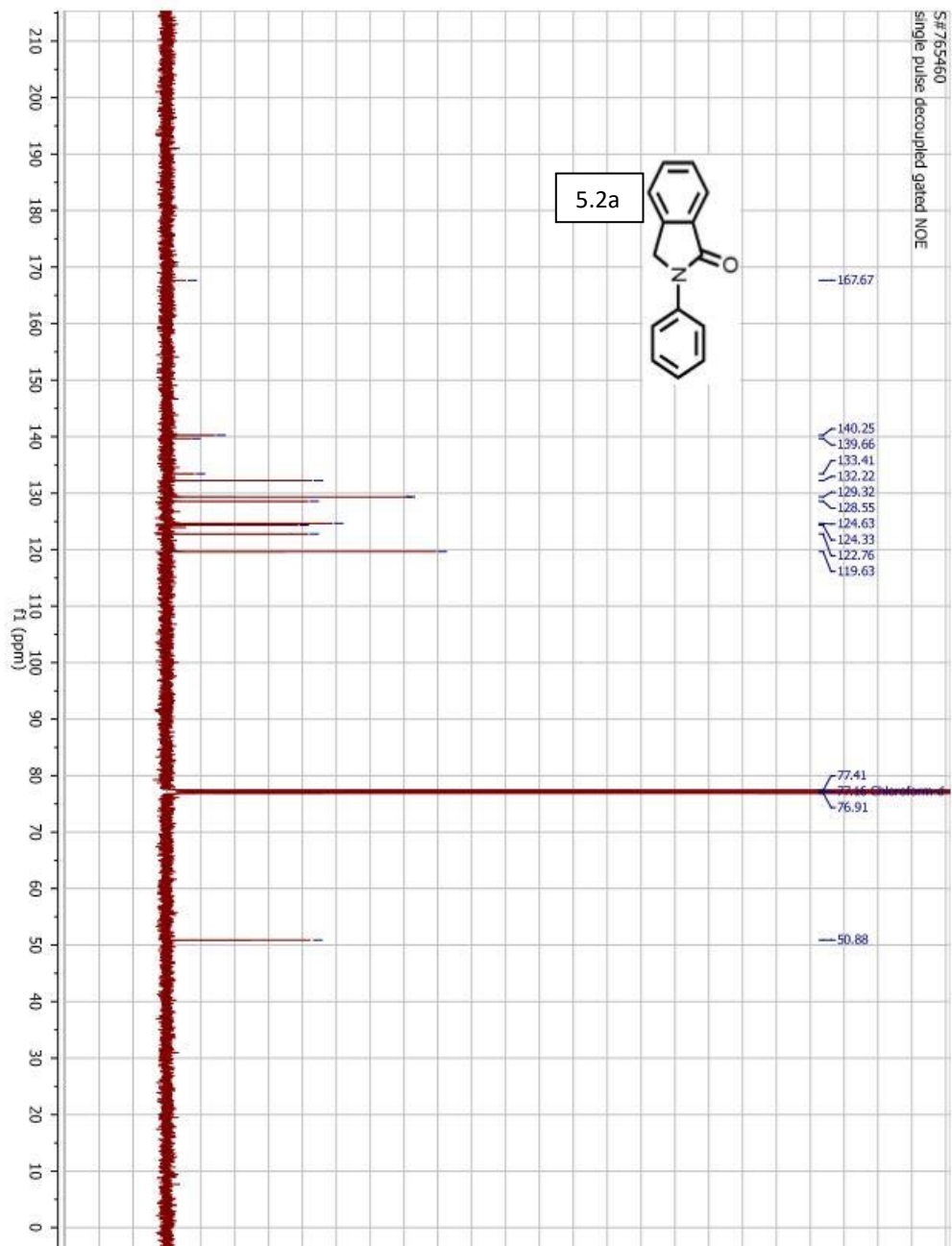


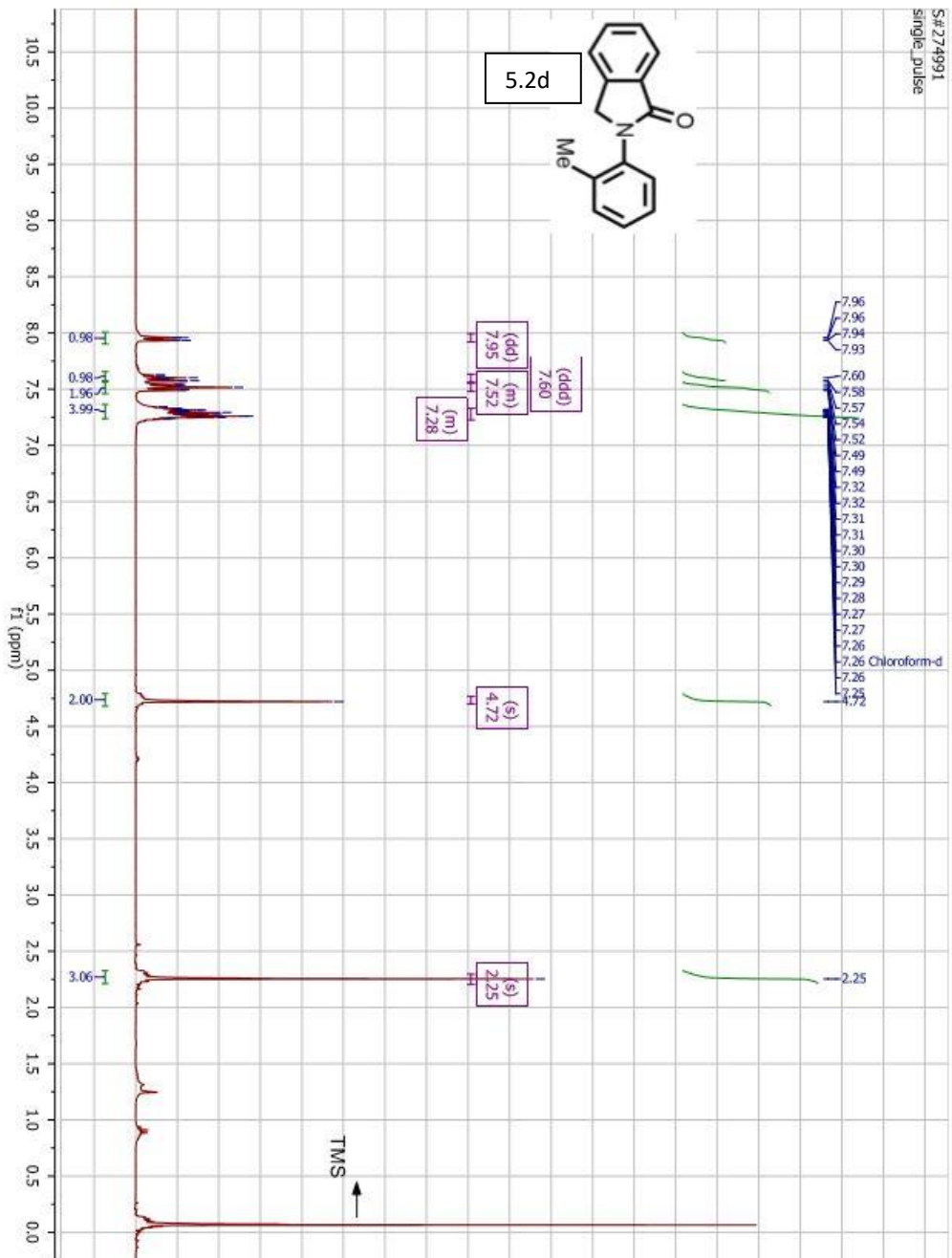


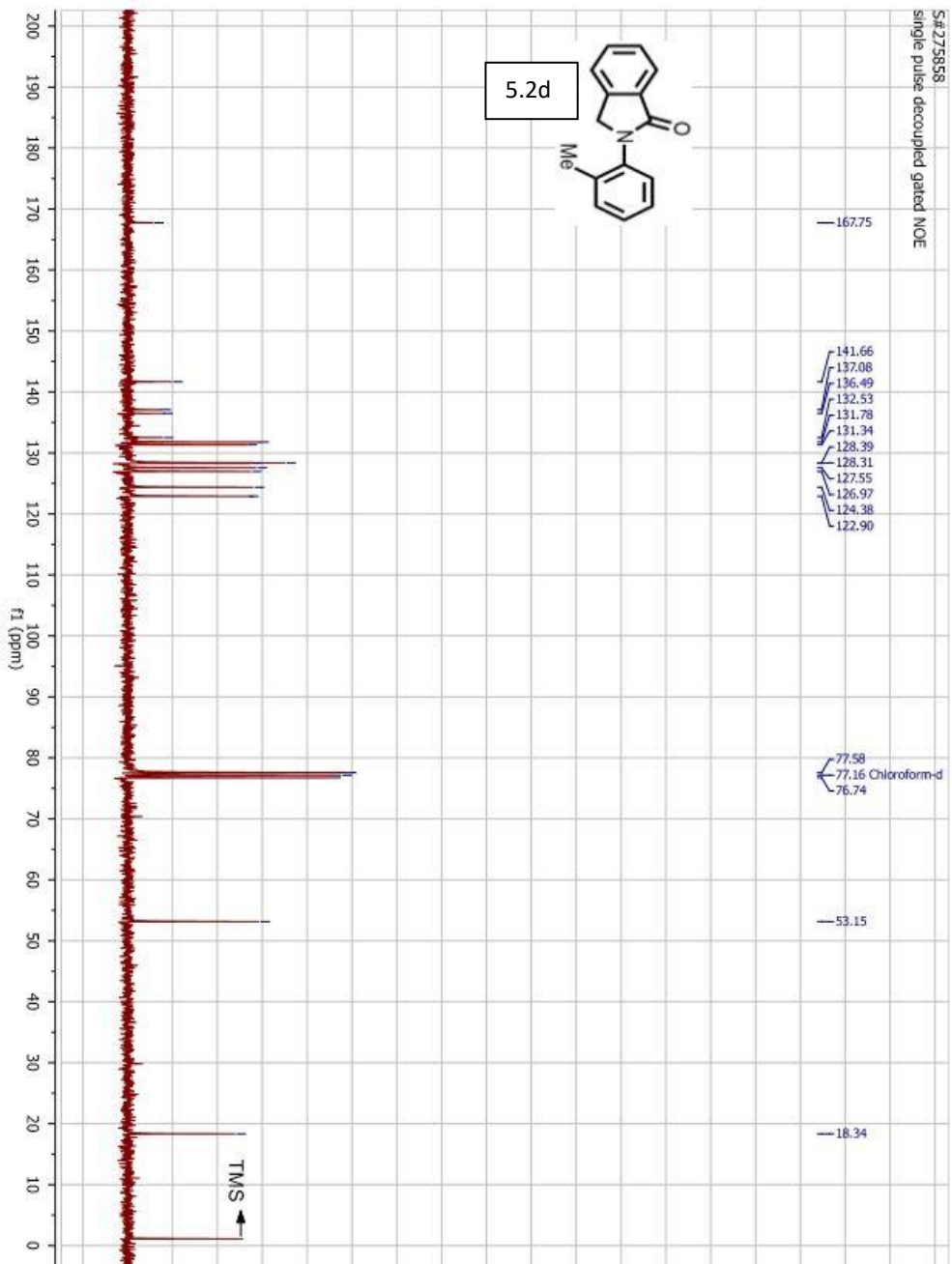


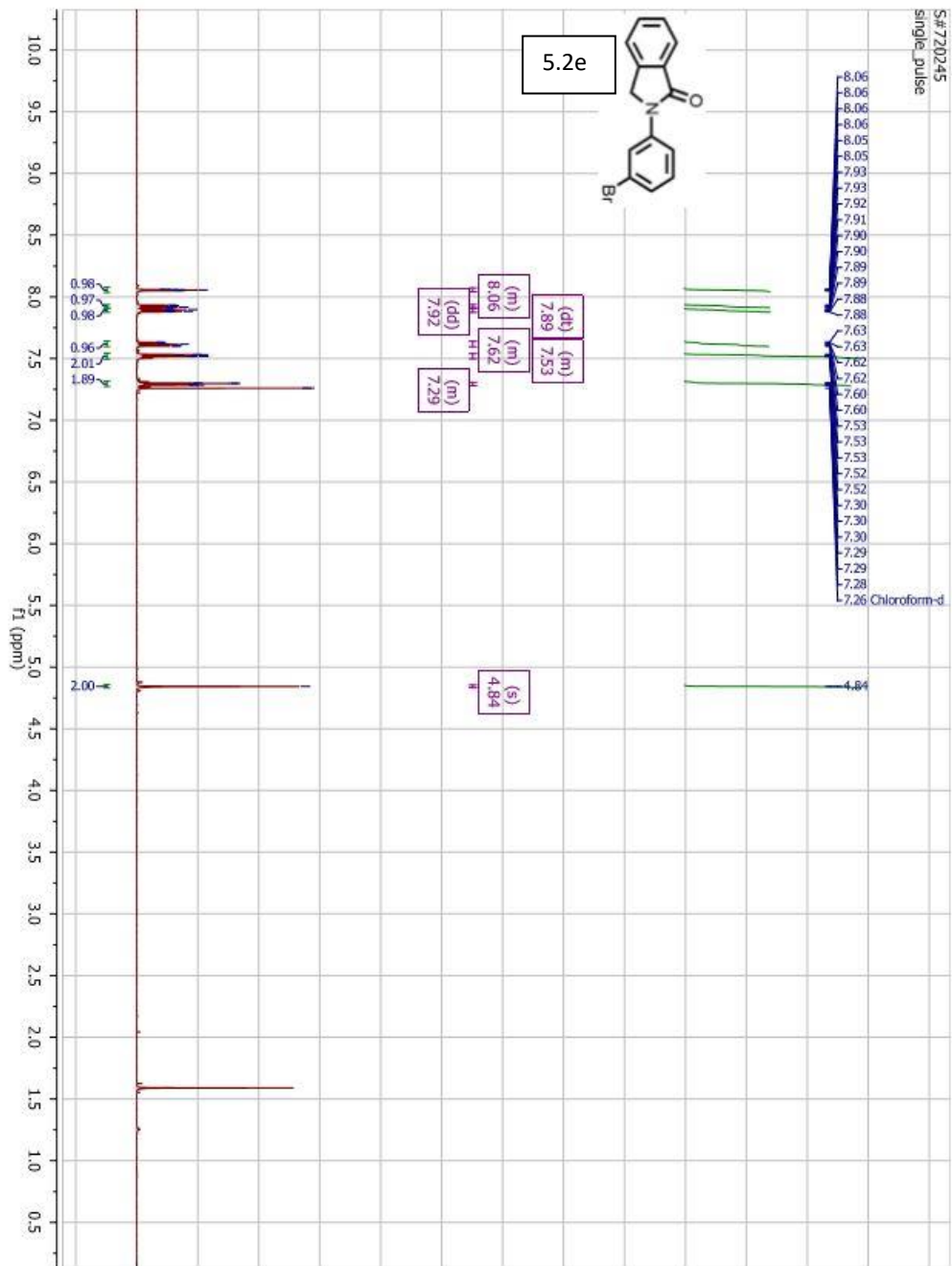




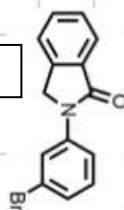




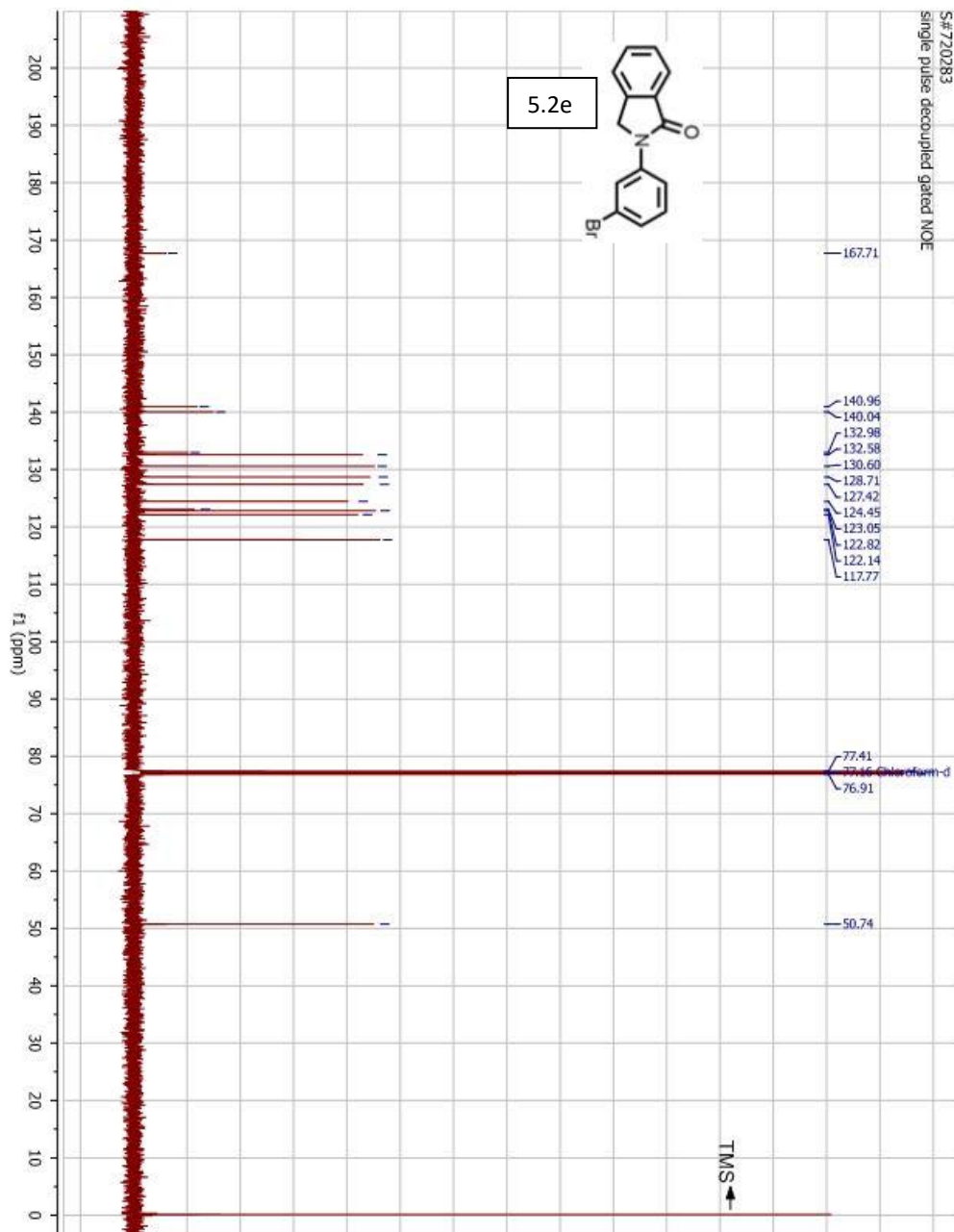


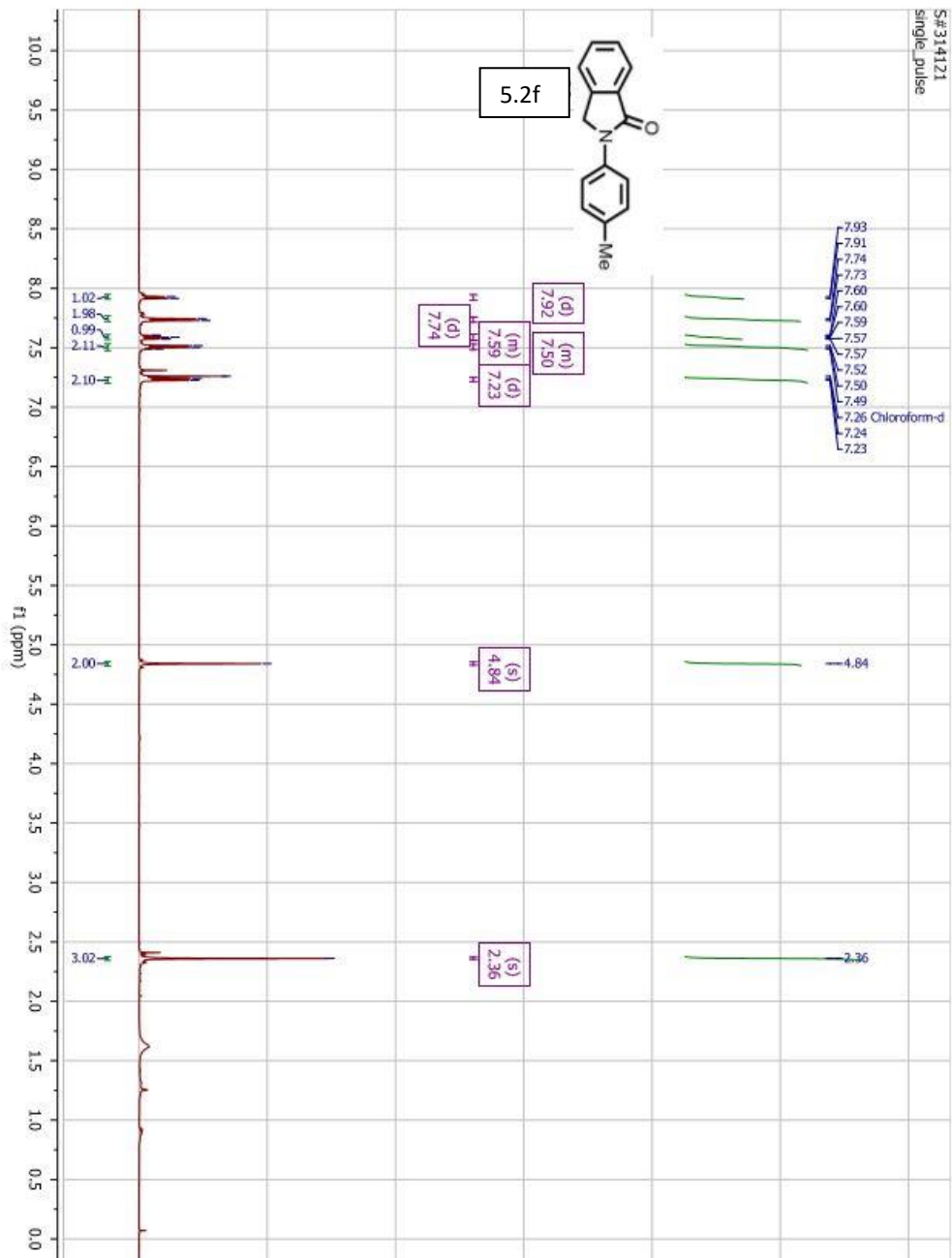


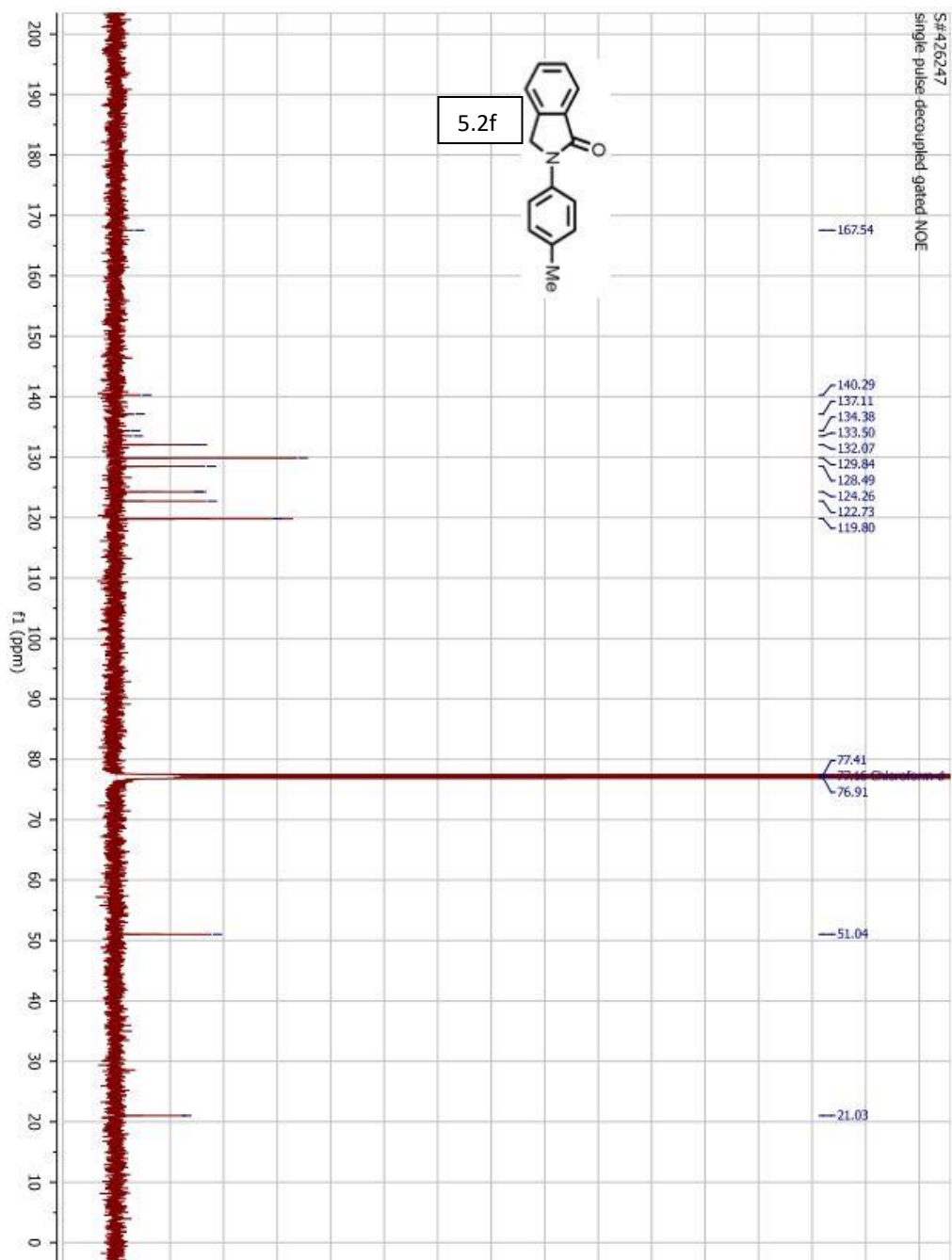
S# 720283
single pulse decoupled gated NOE

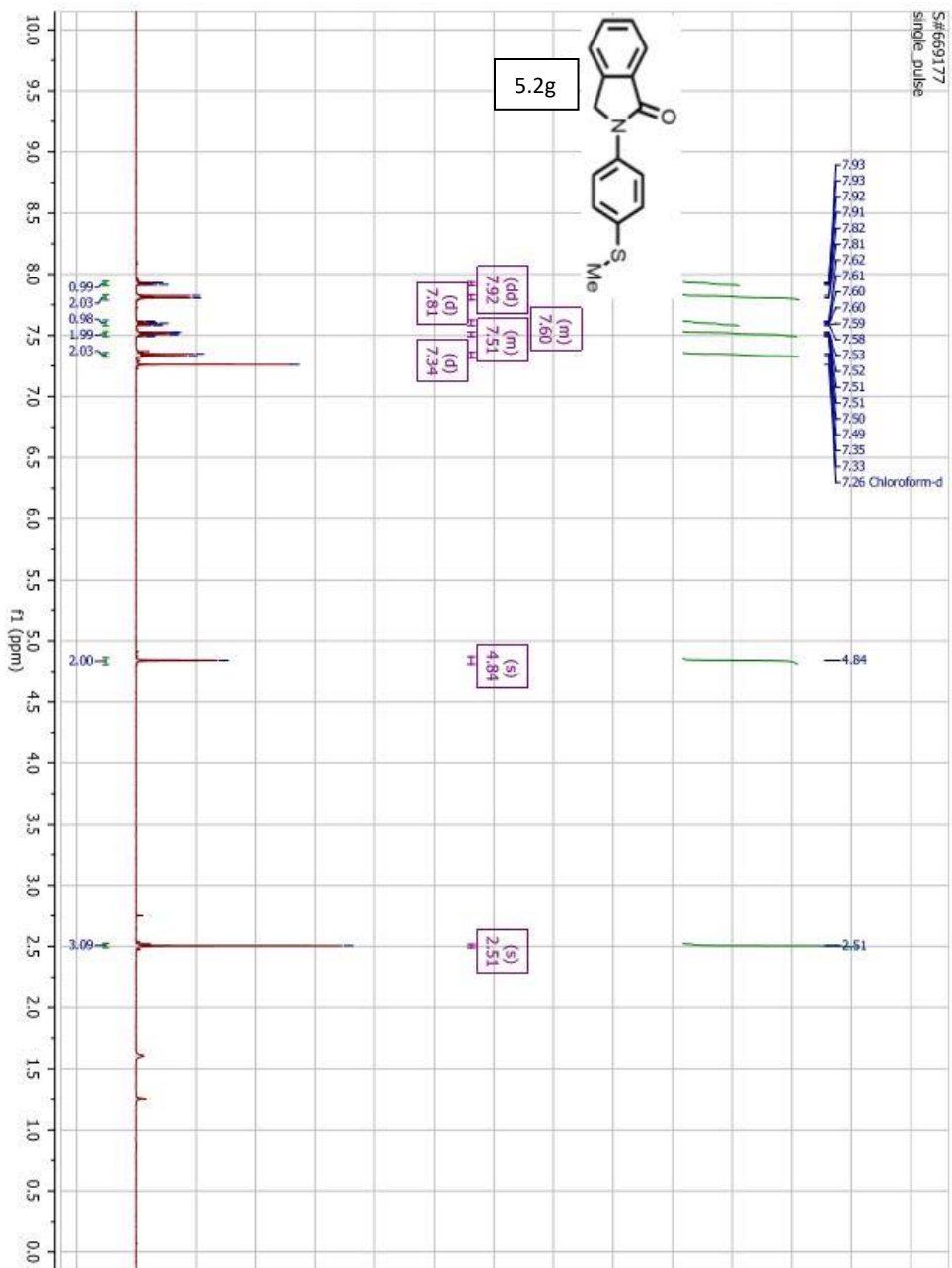


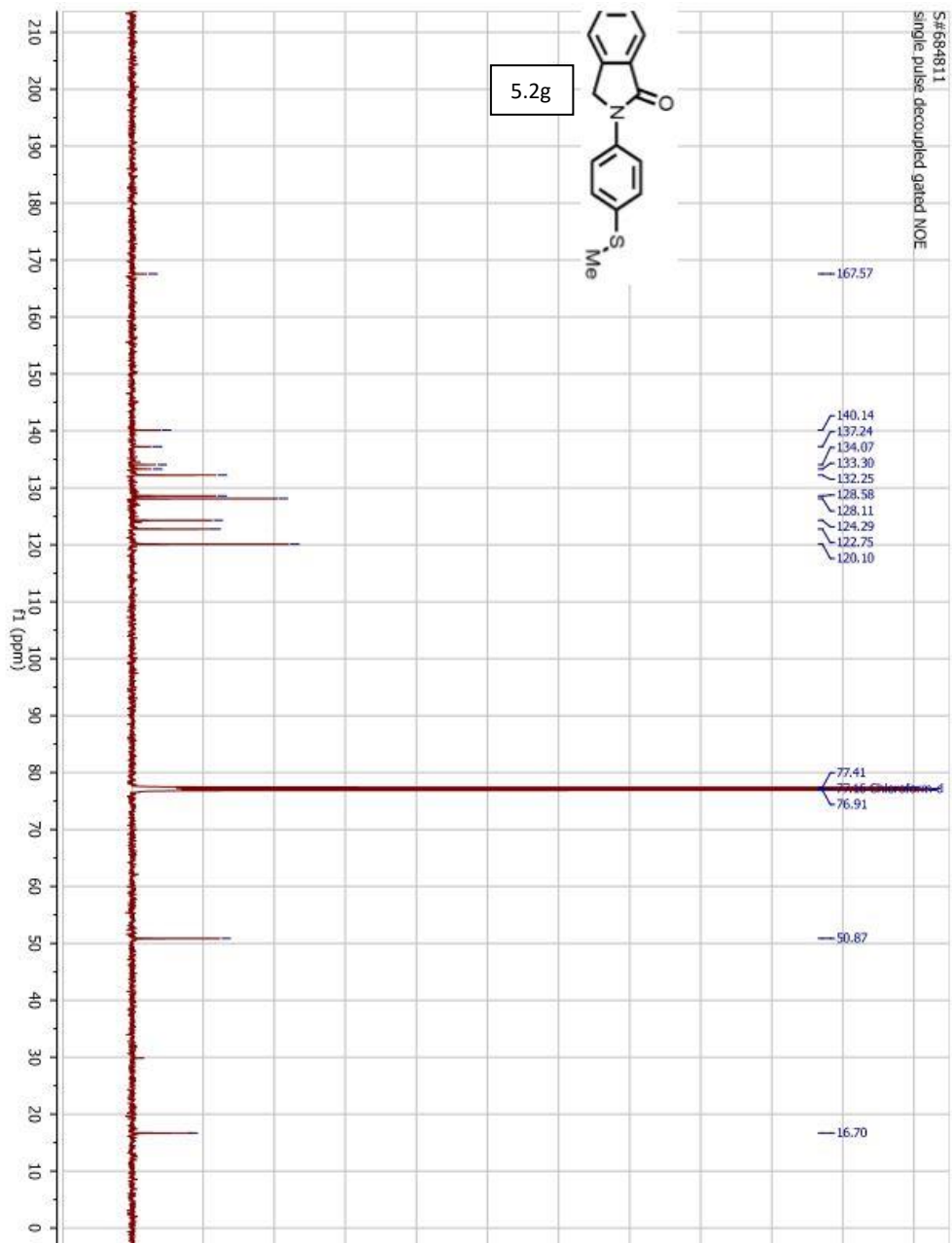
5.2e

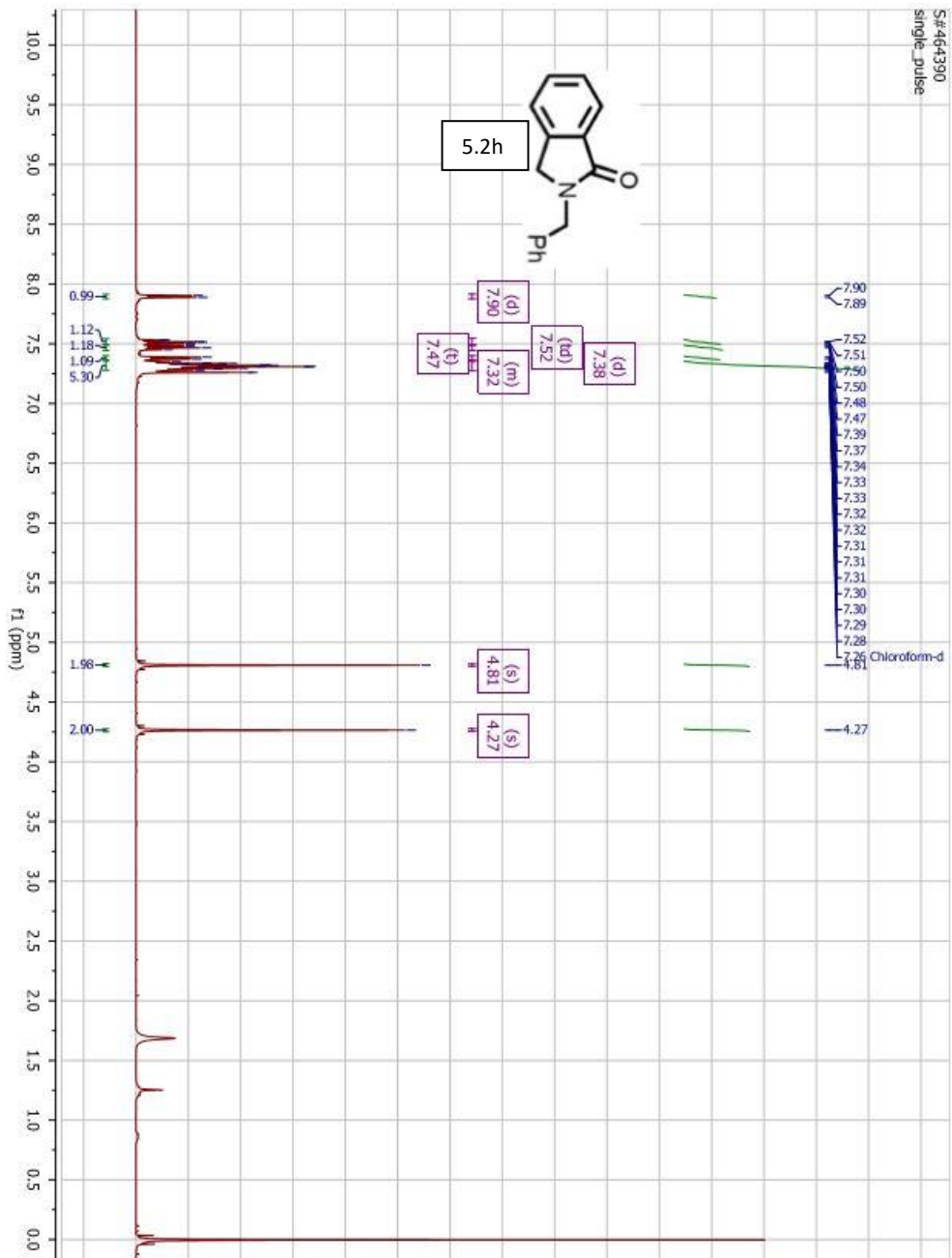




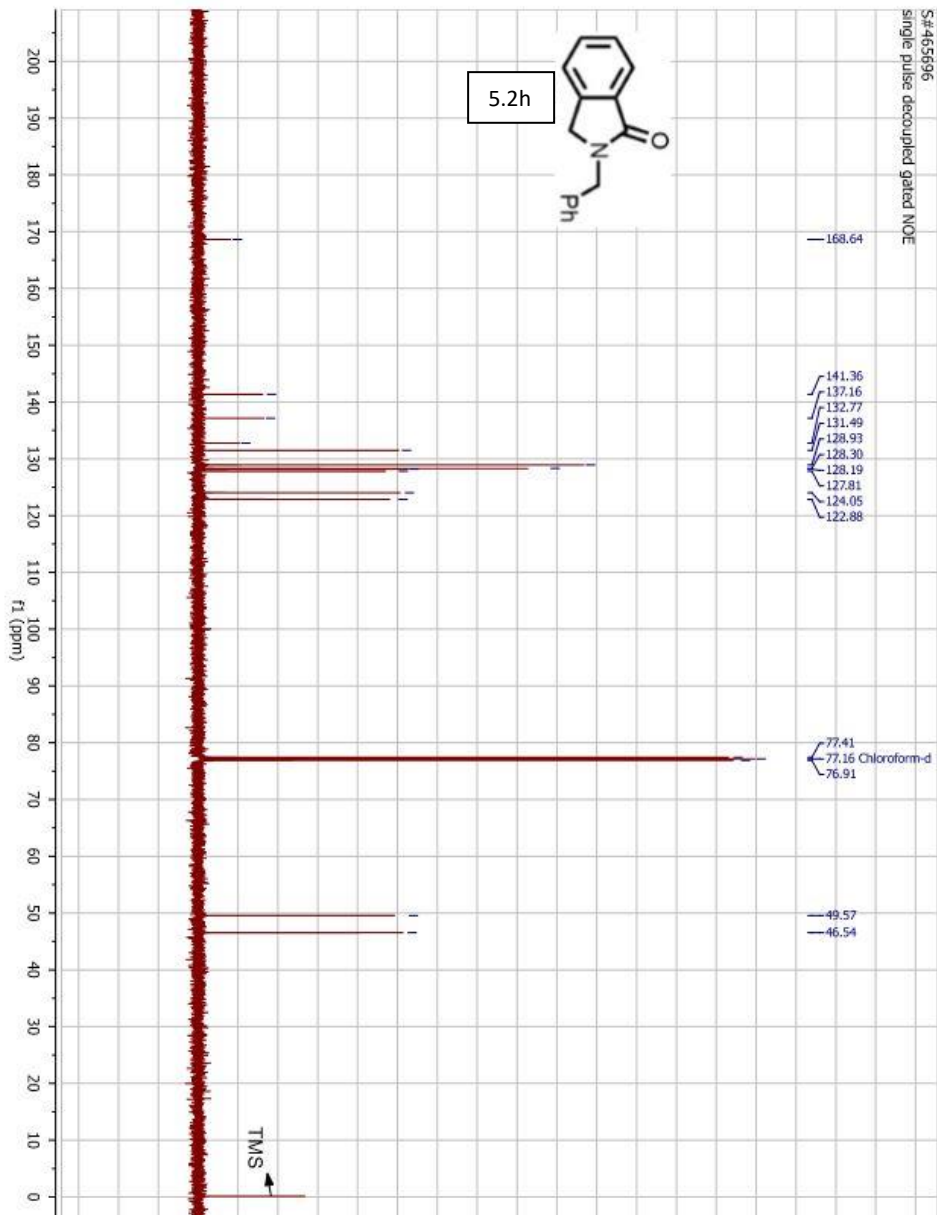


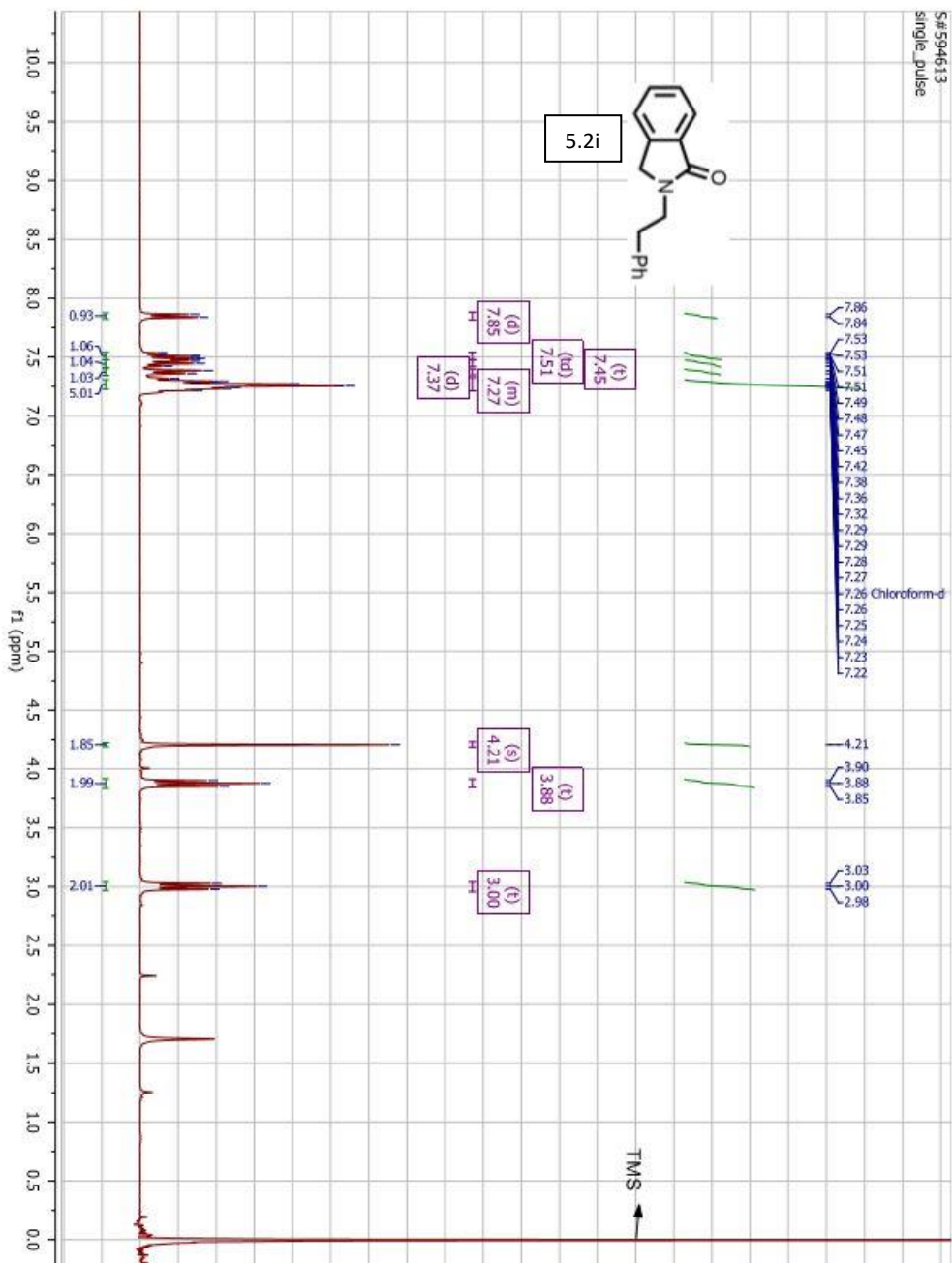


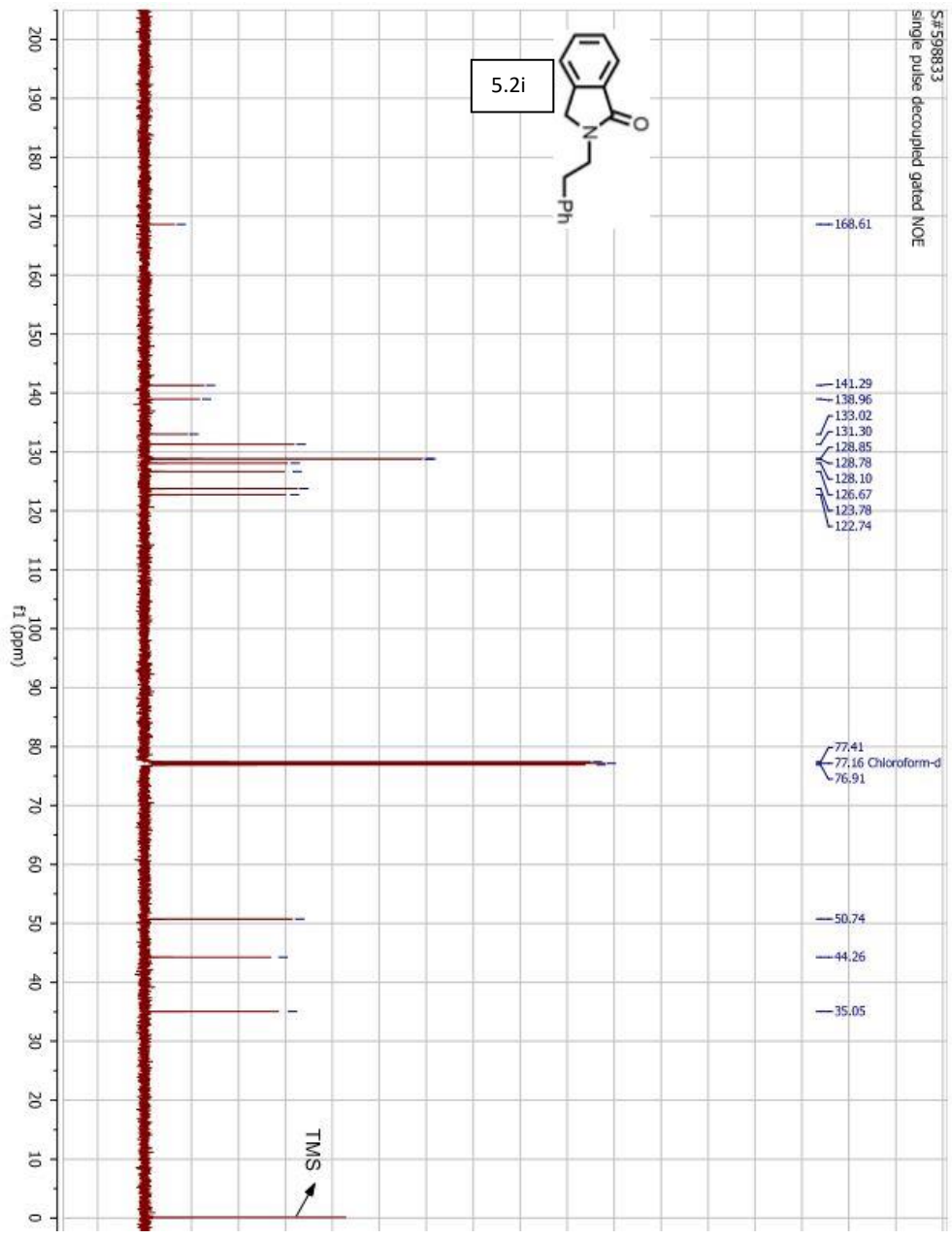


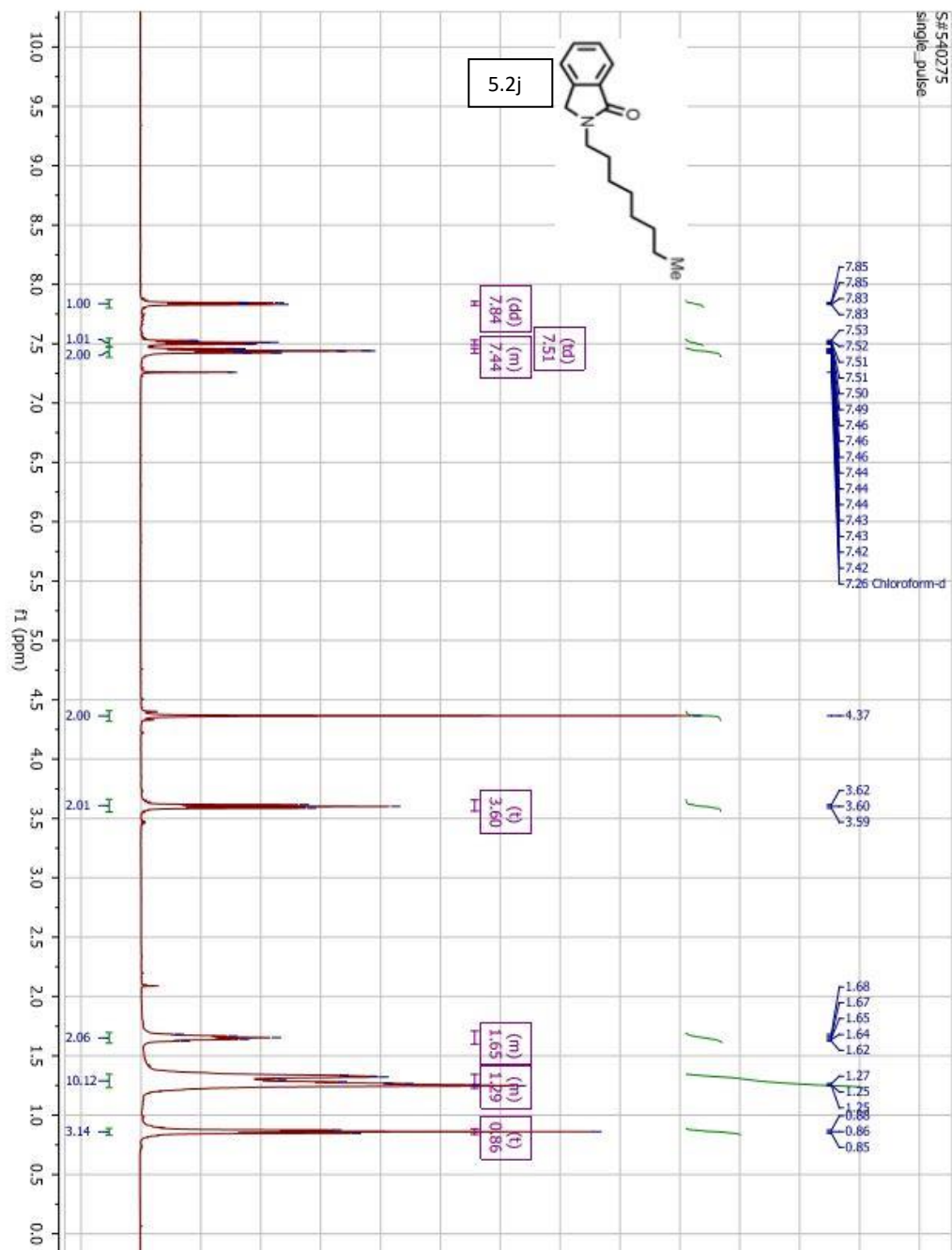


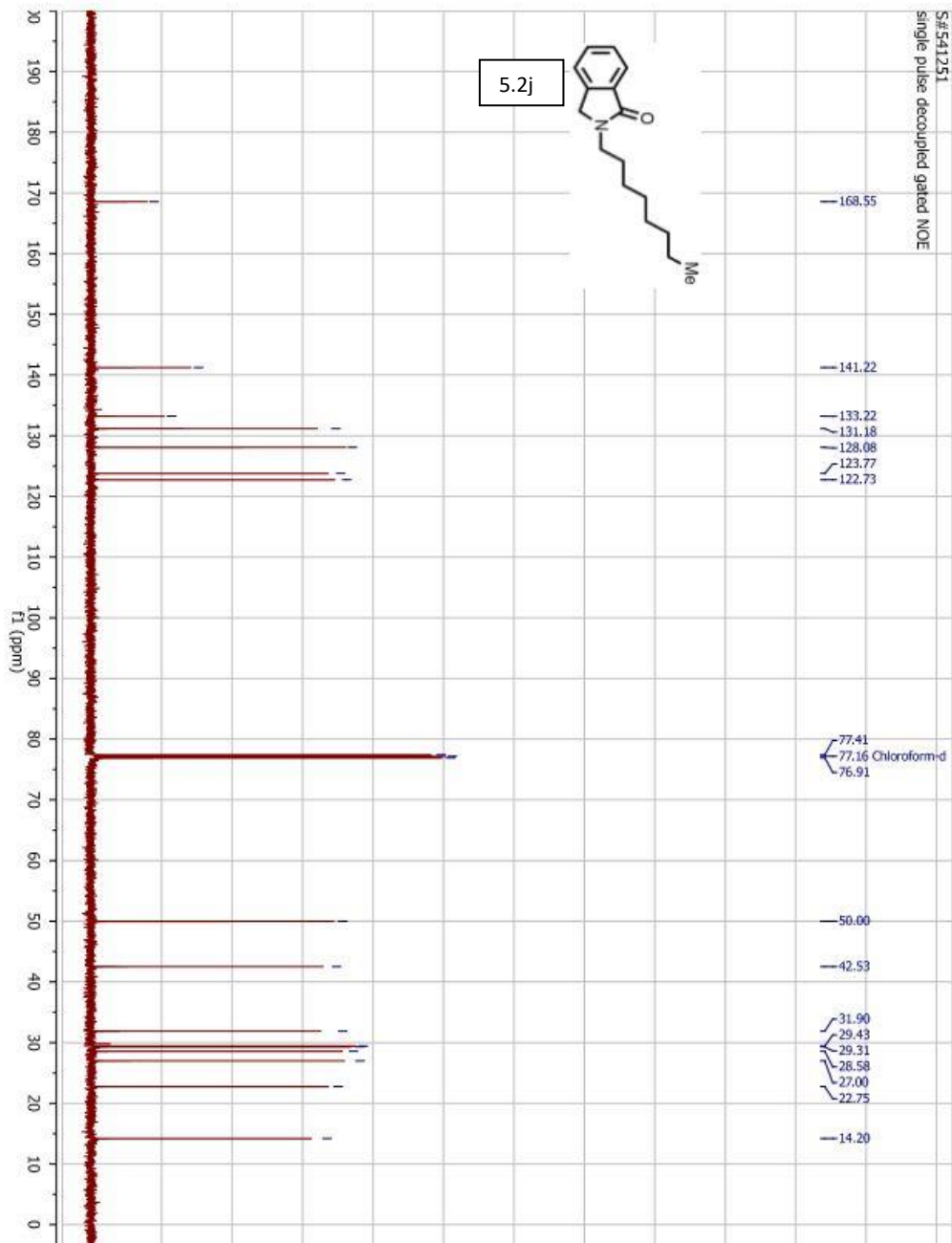
S#465896
Single pulse decoupled gated NOE

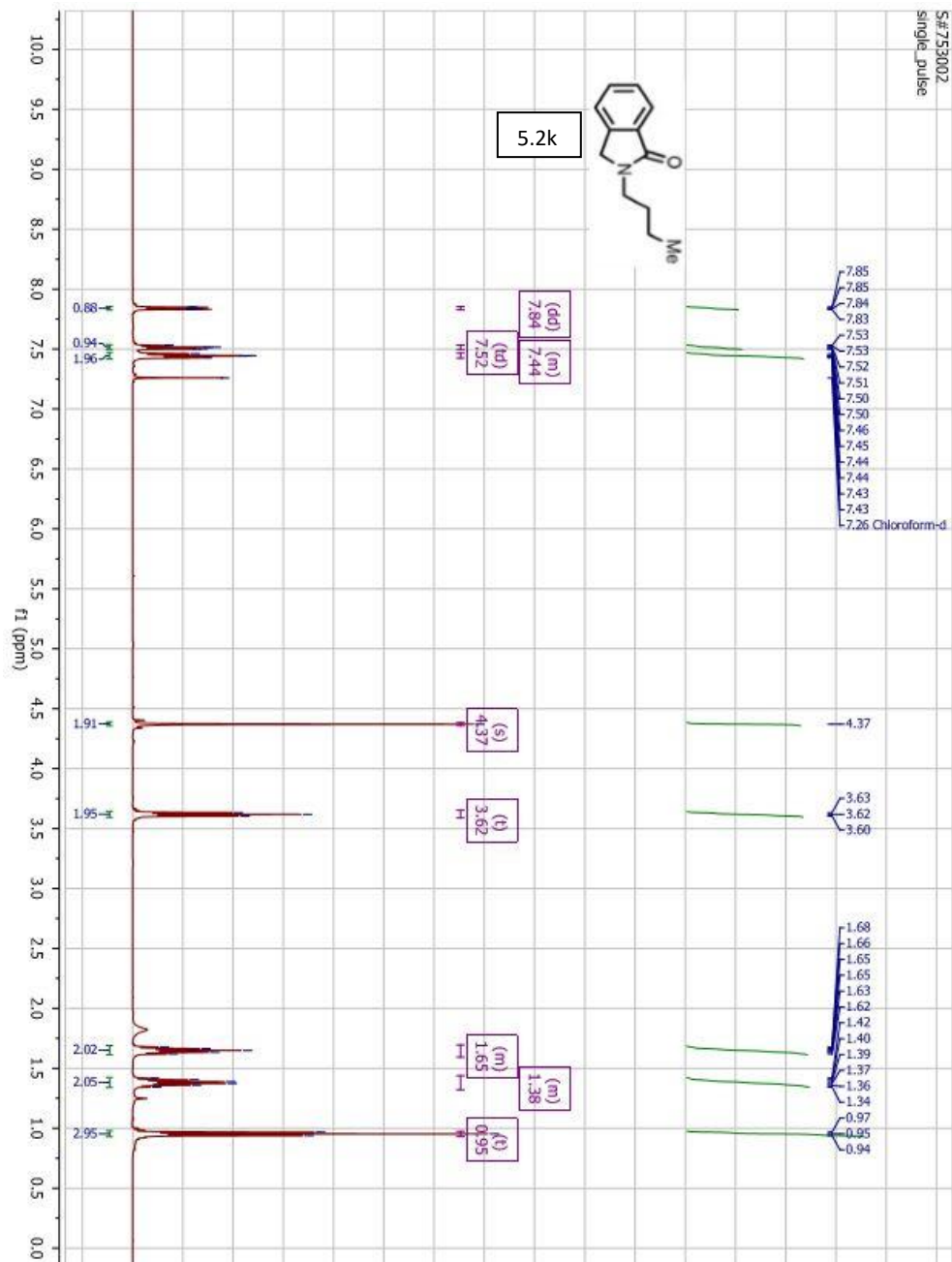


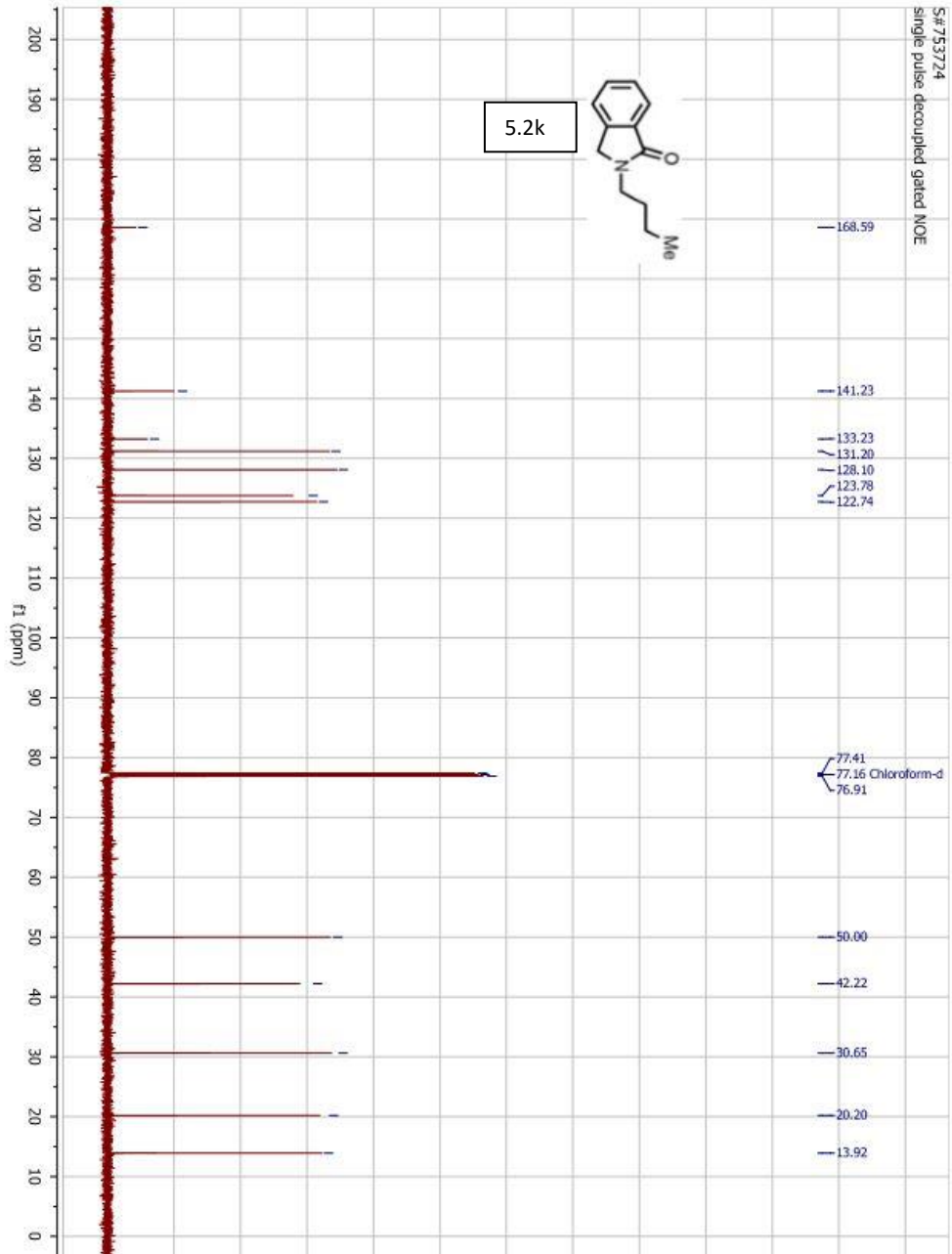


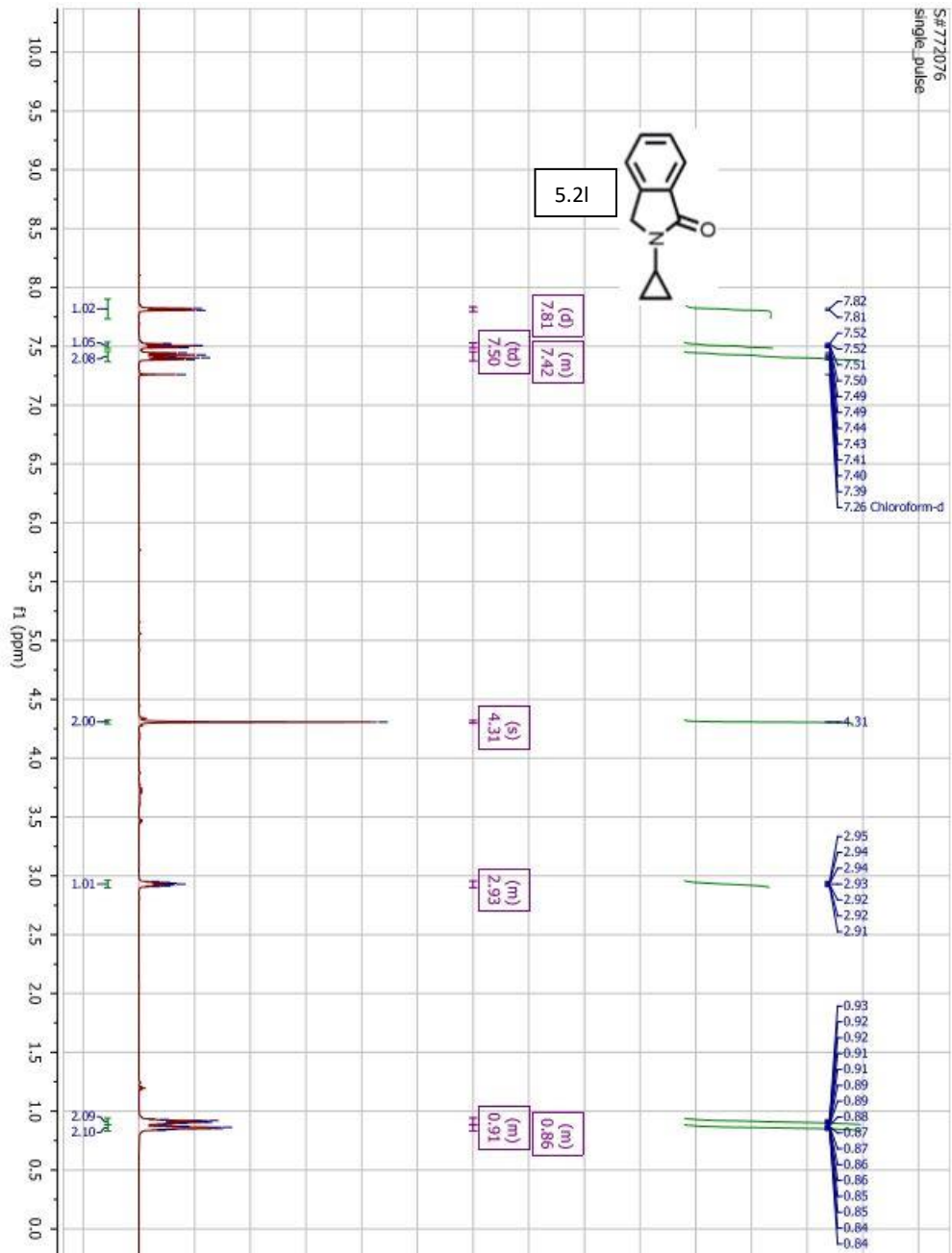


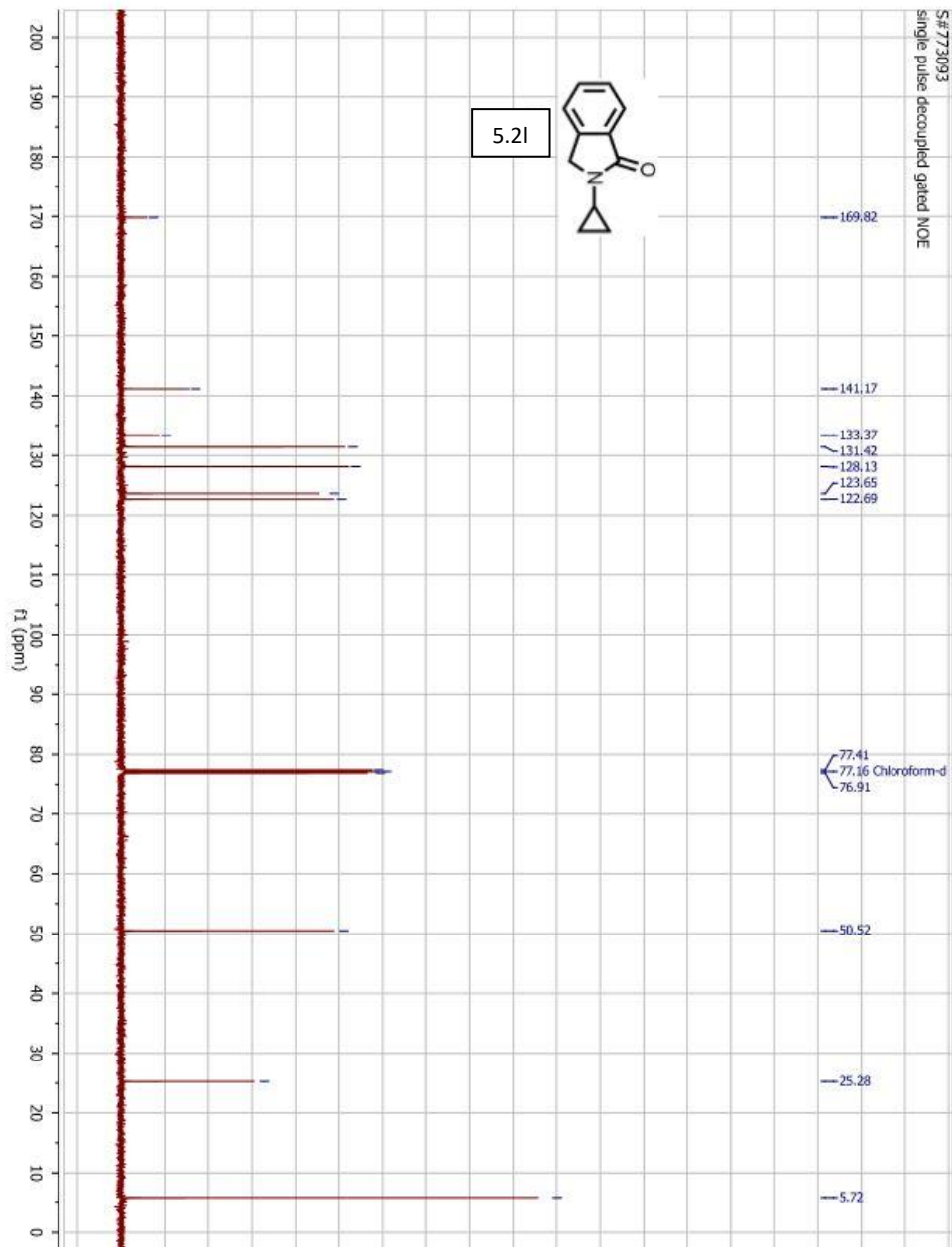




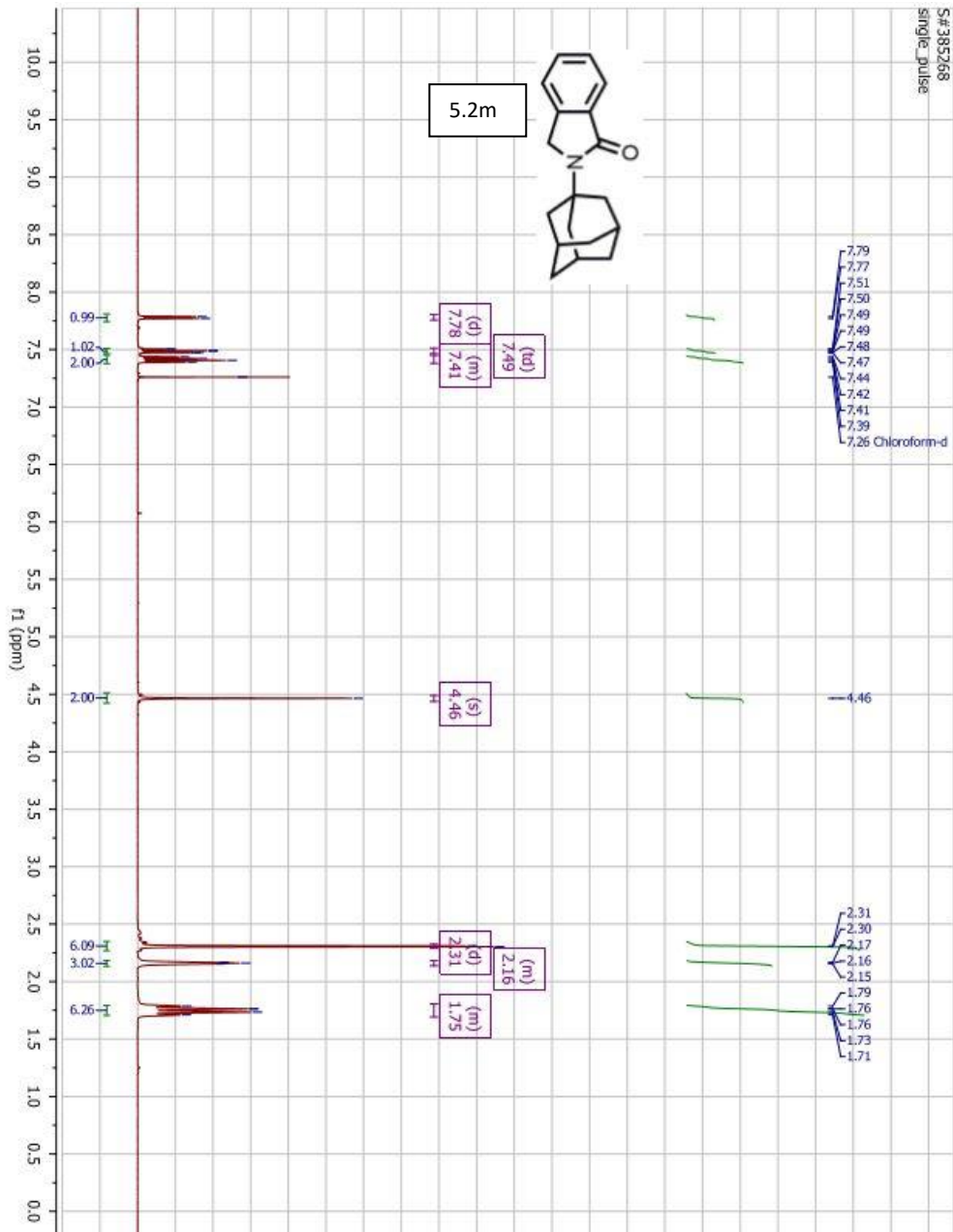


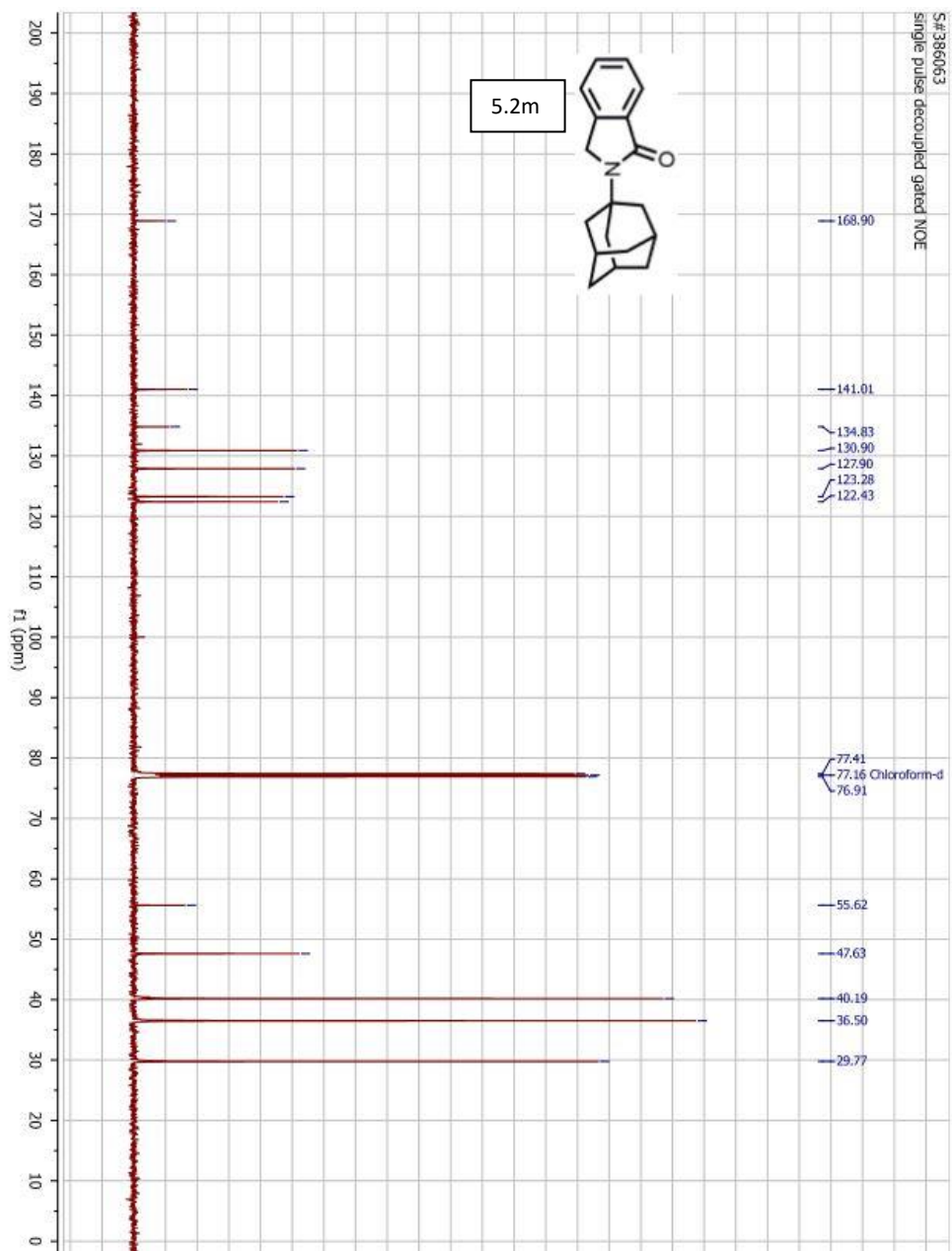


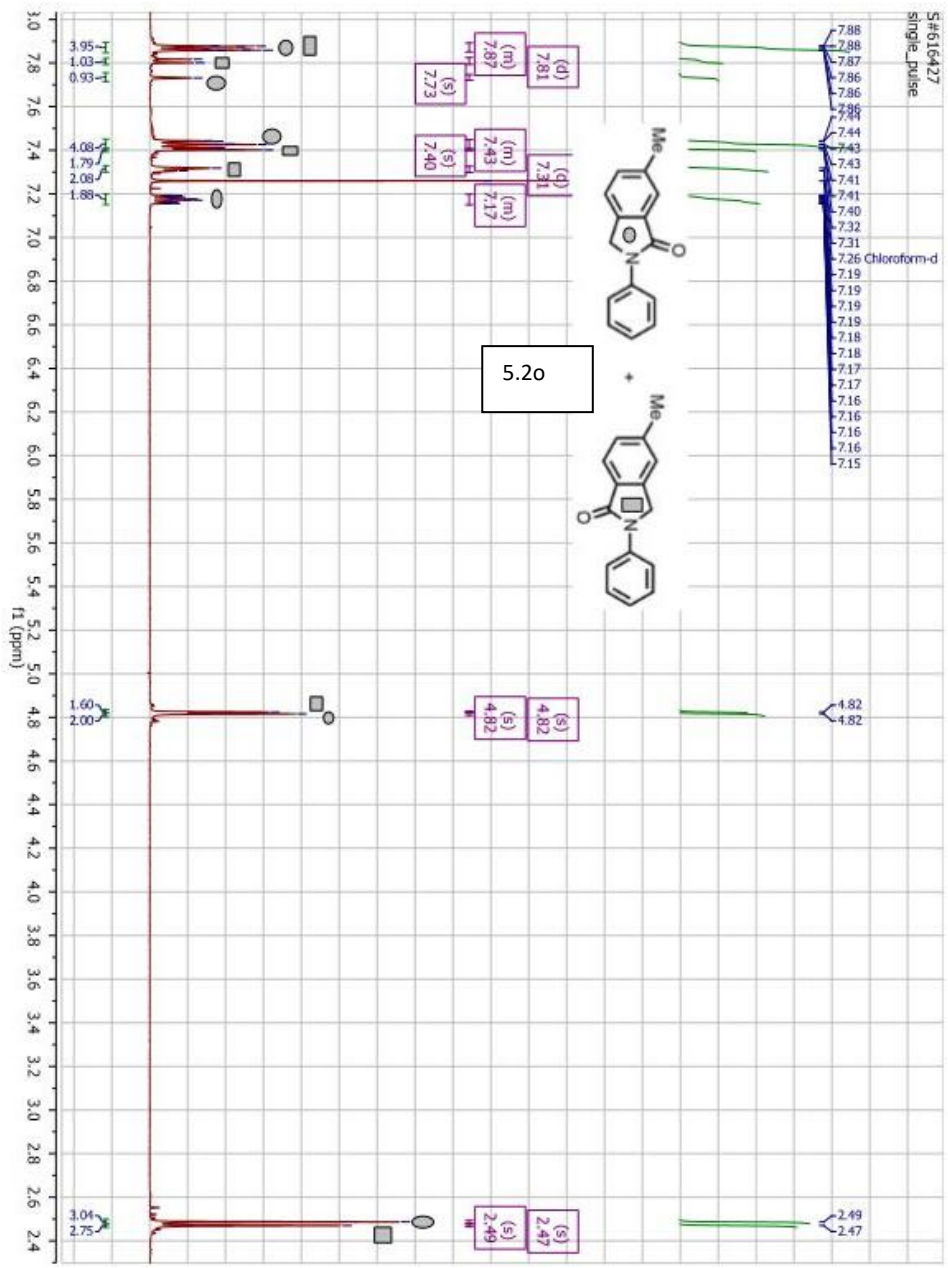


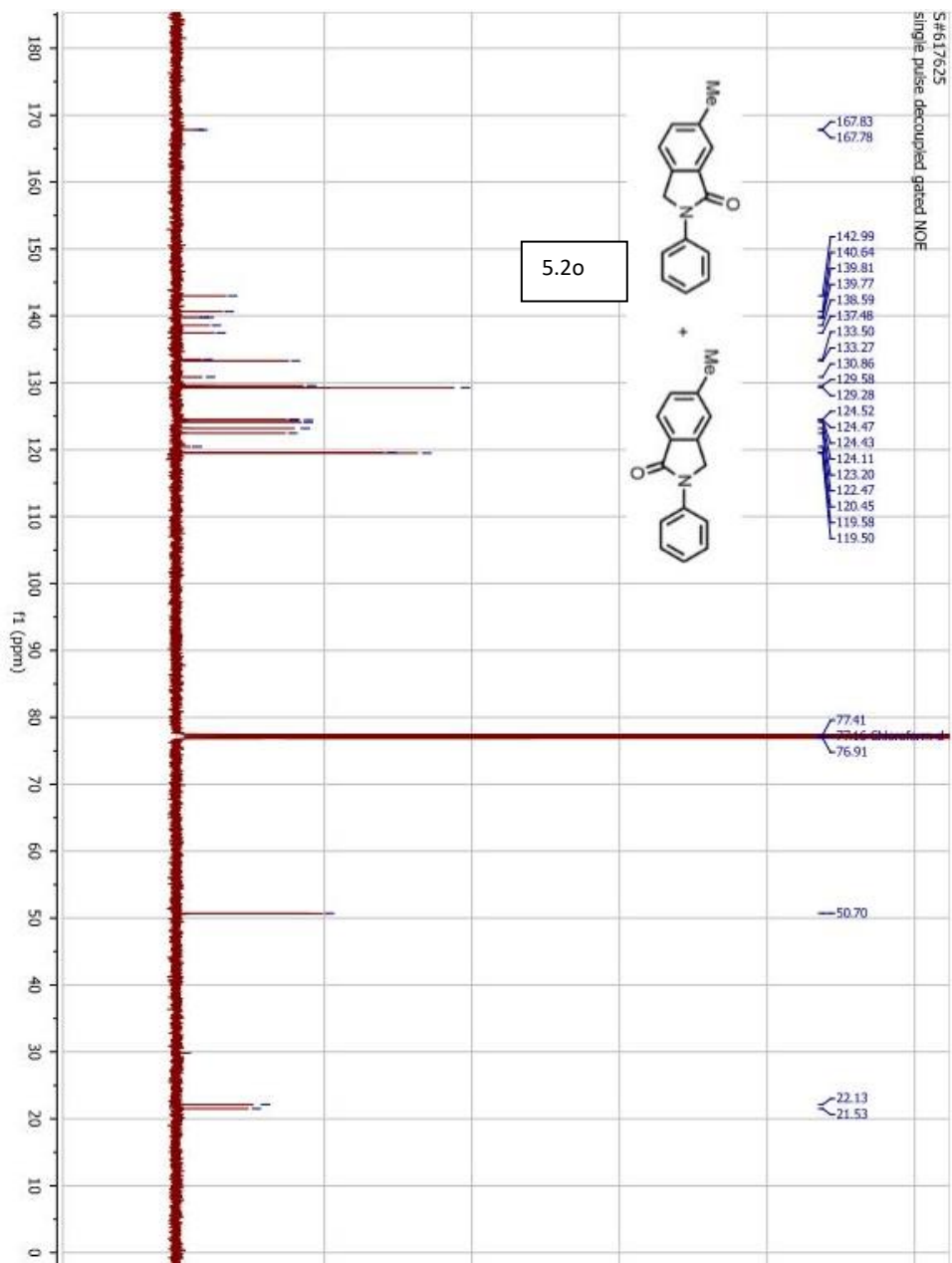


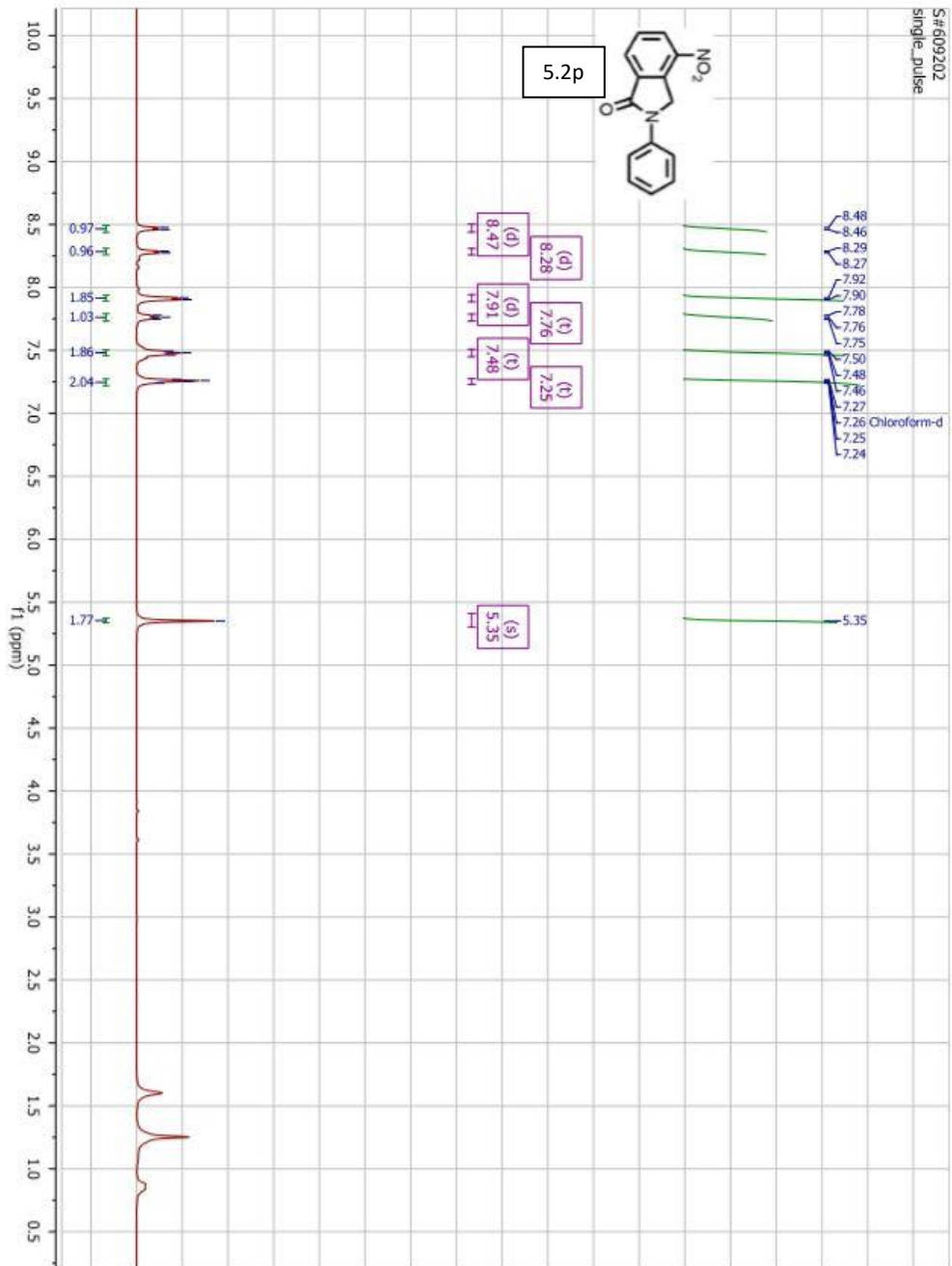
S#385268
single_pulse

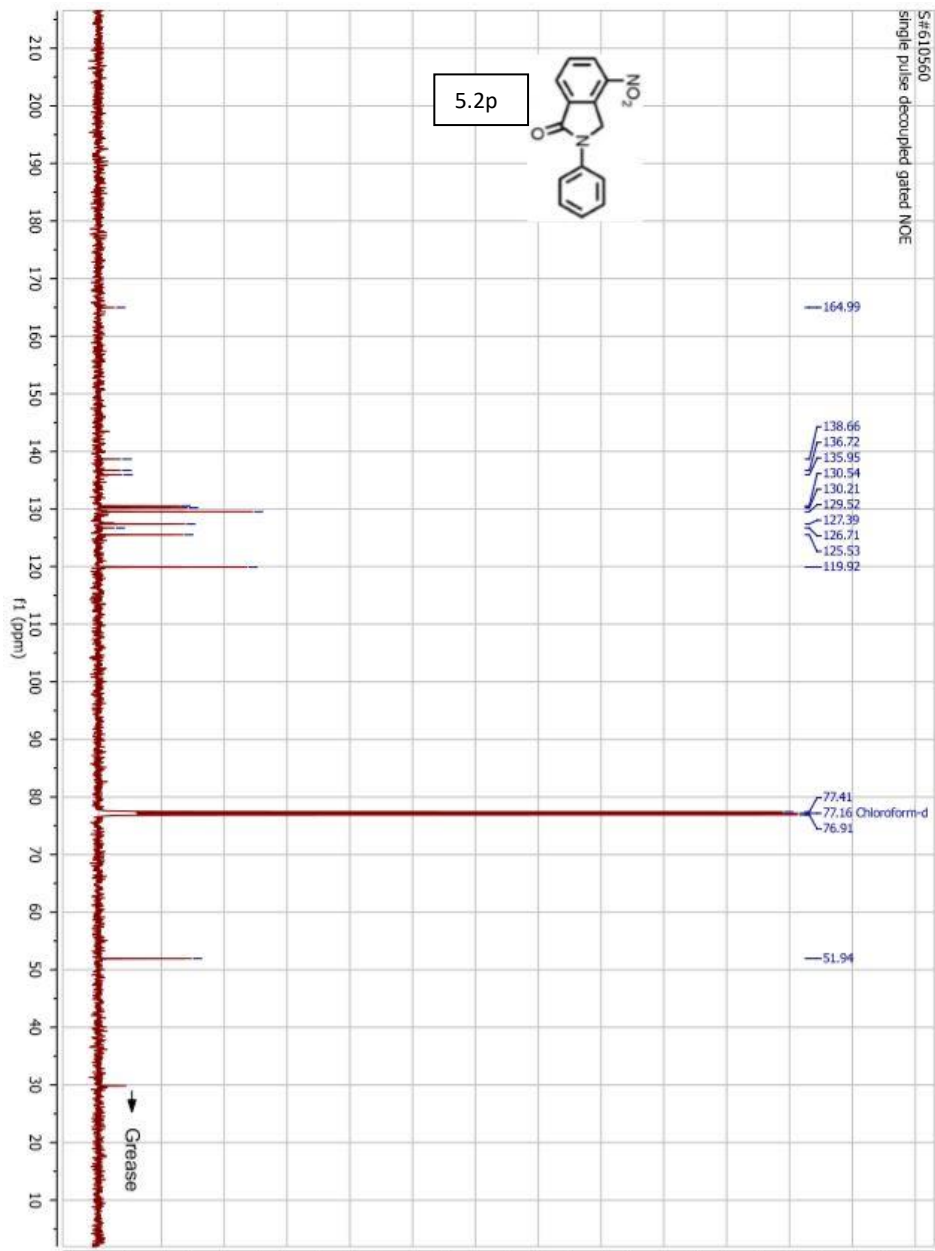


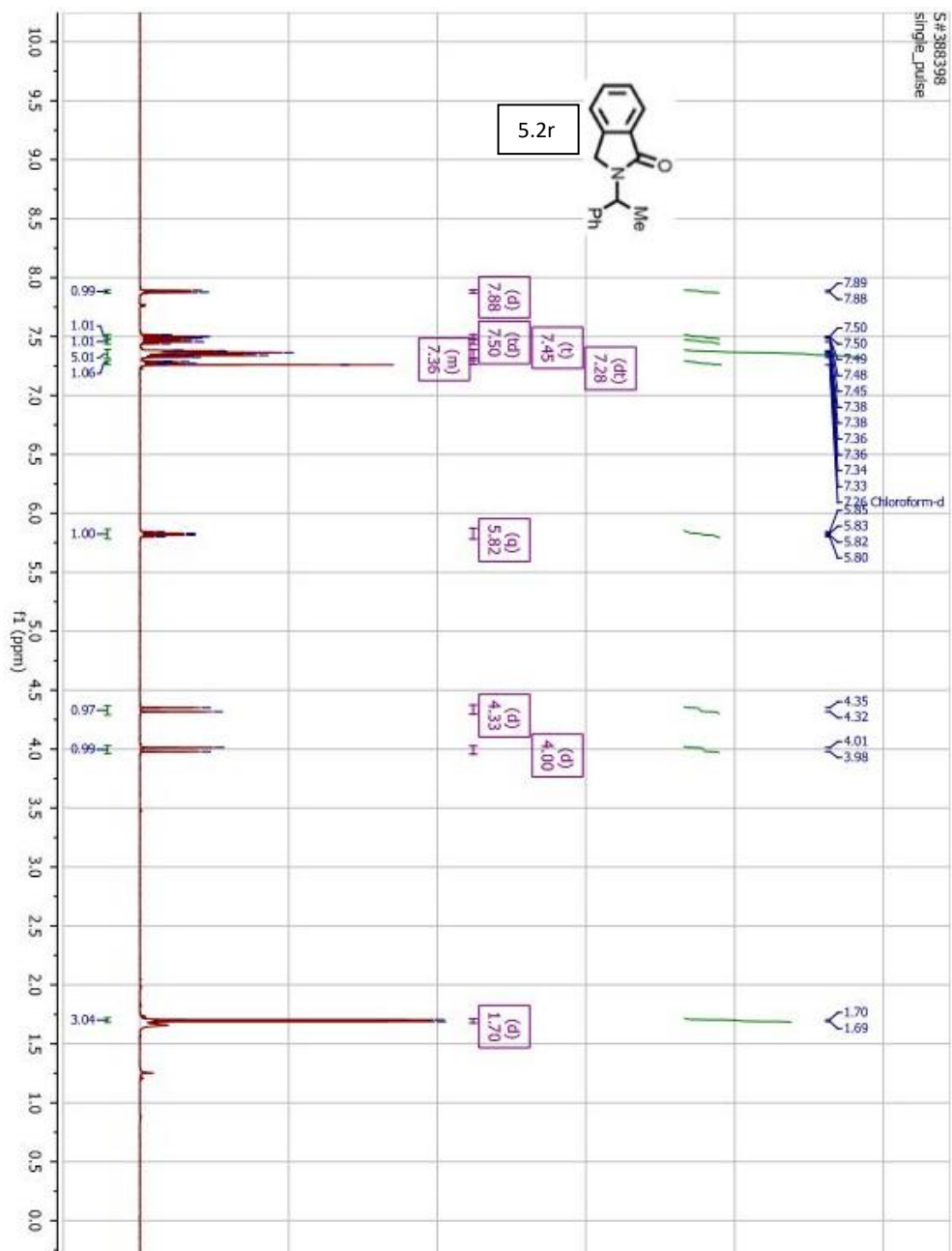






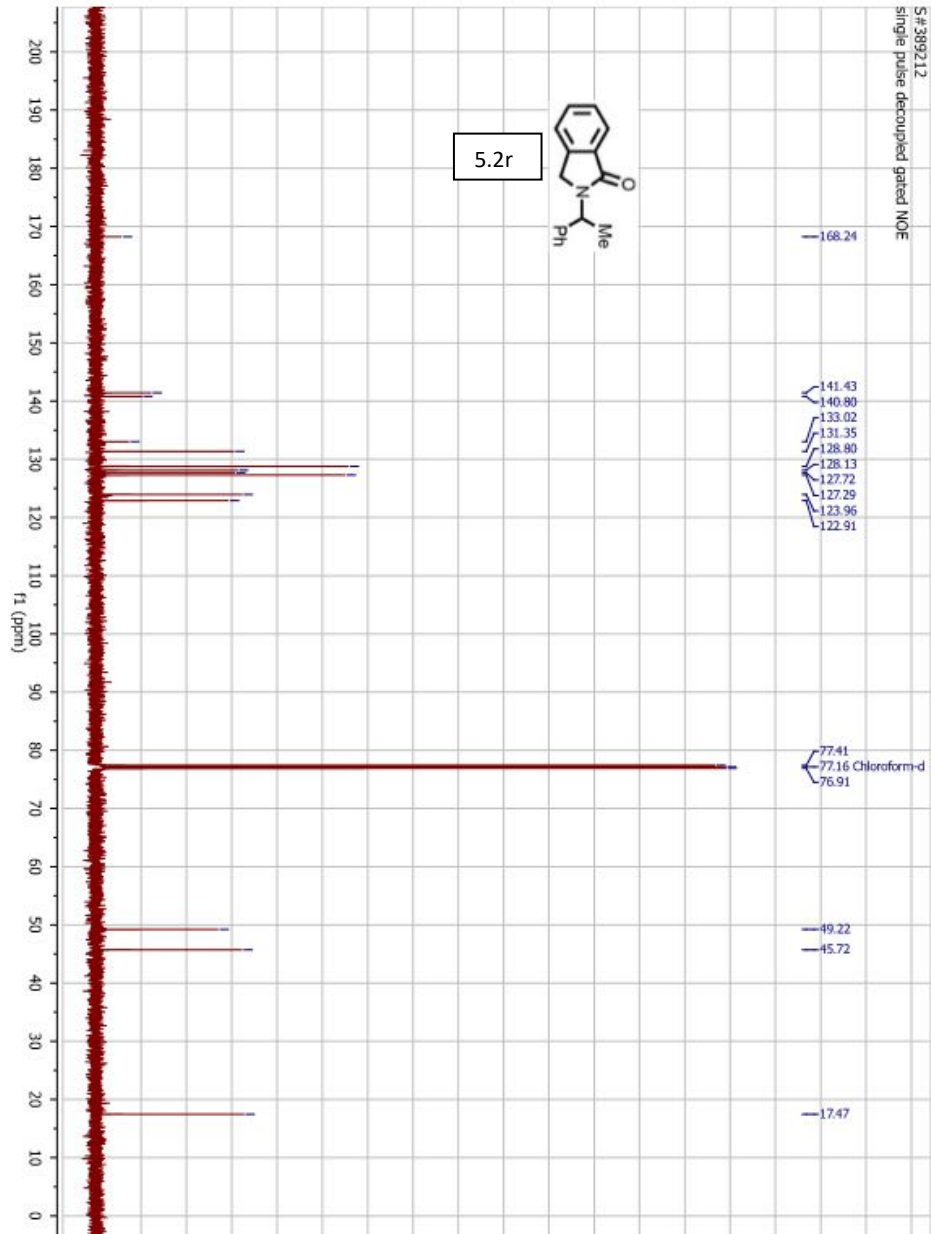
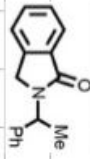


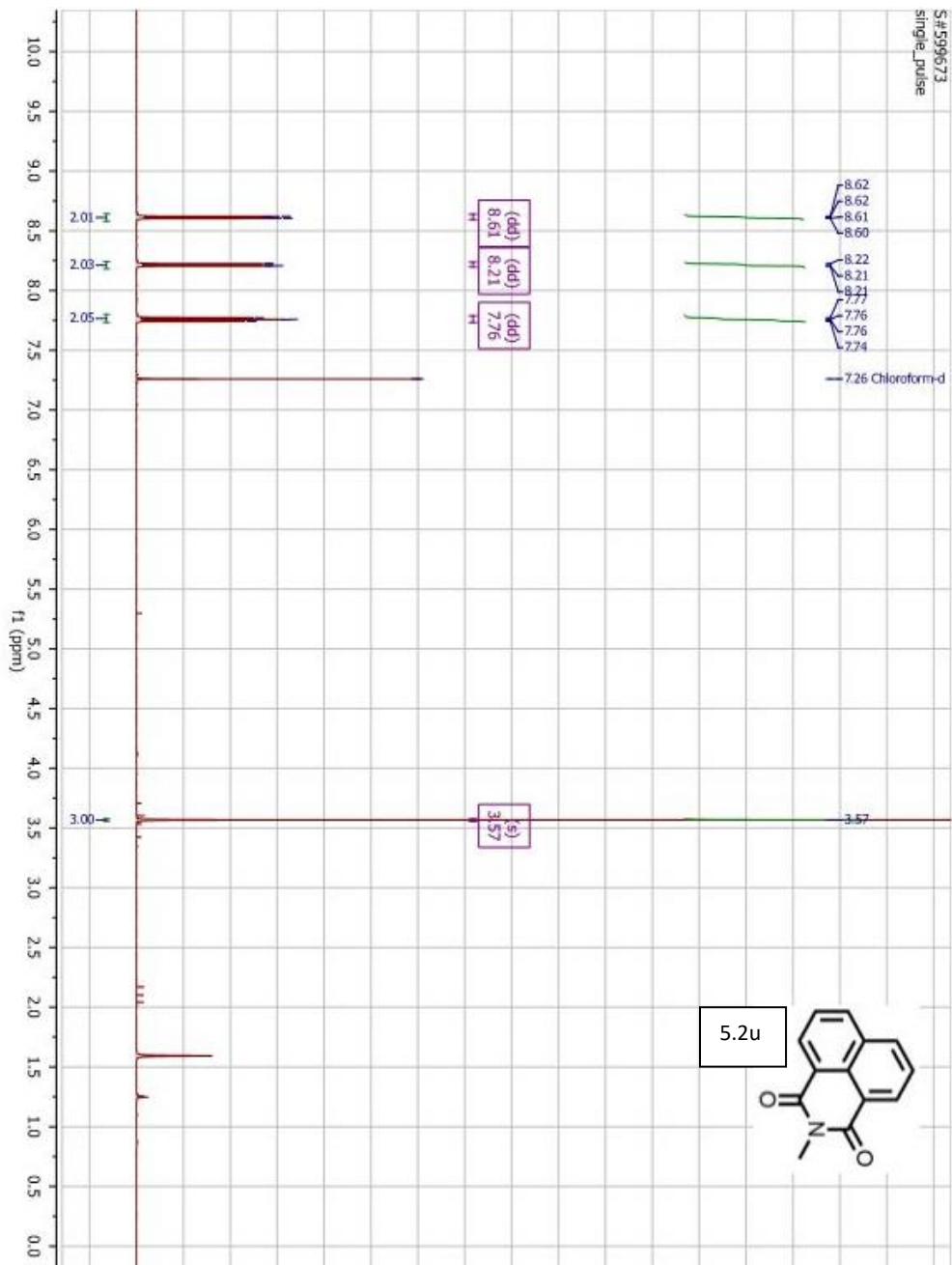


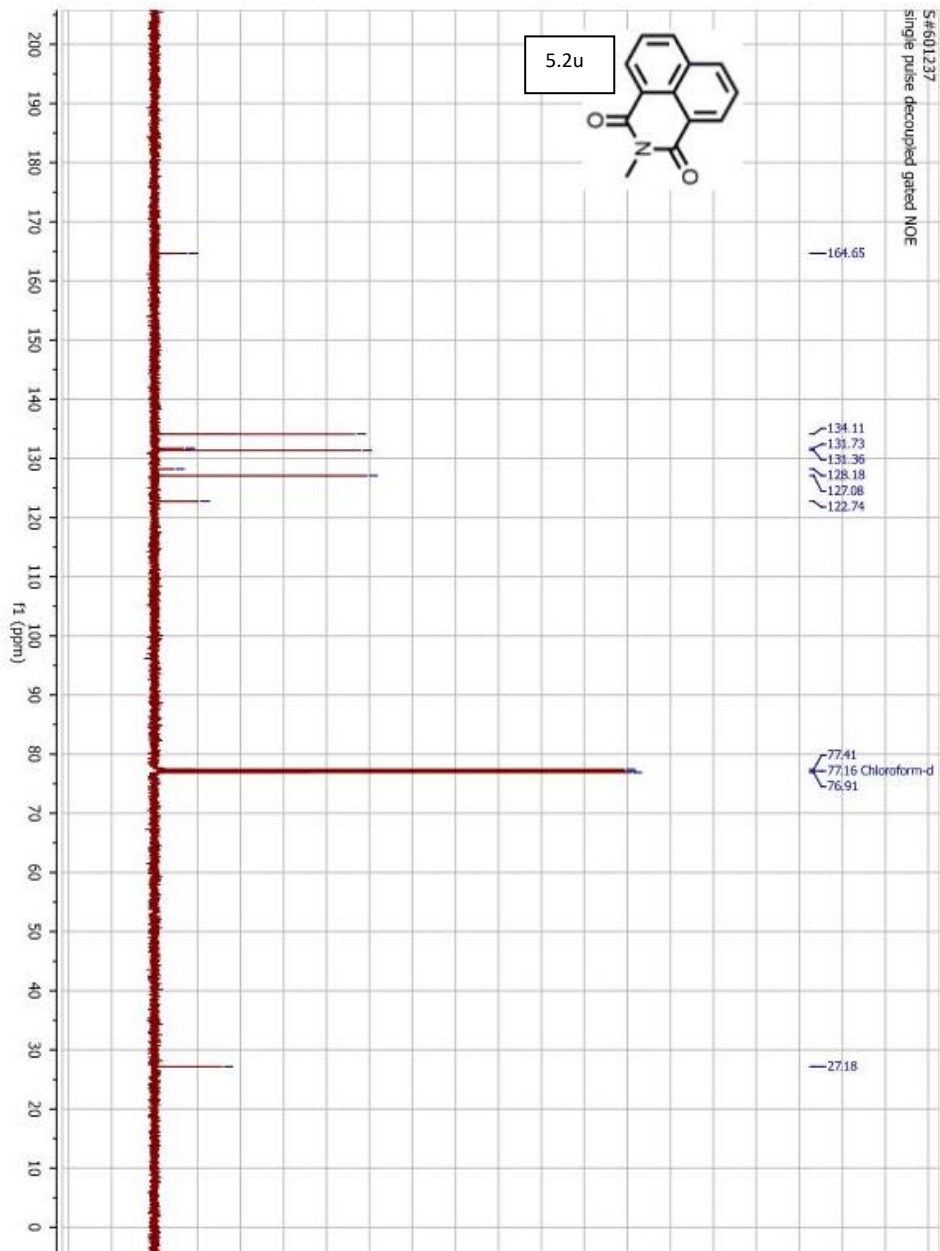


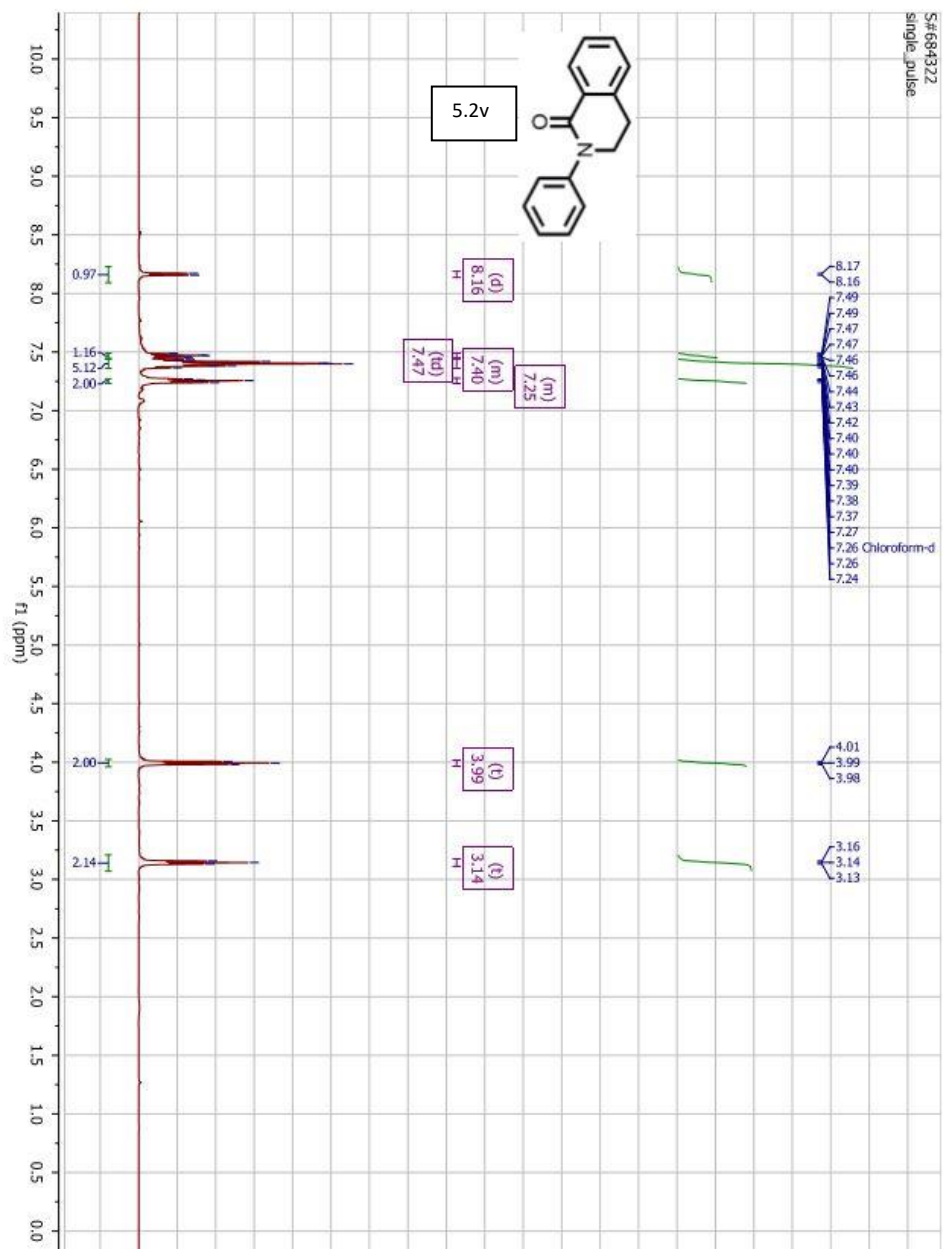
S# 389212
single pulse decoupled gated NOE

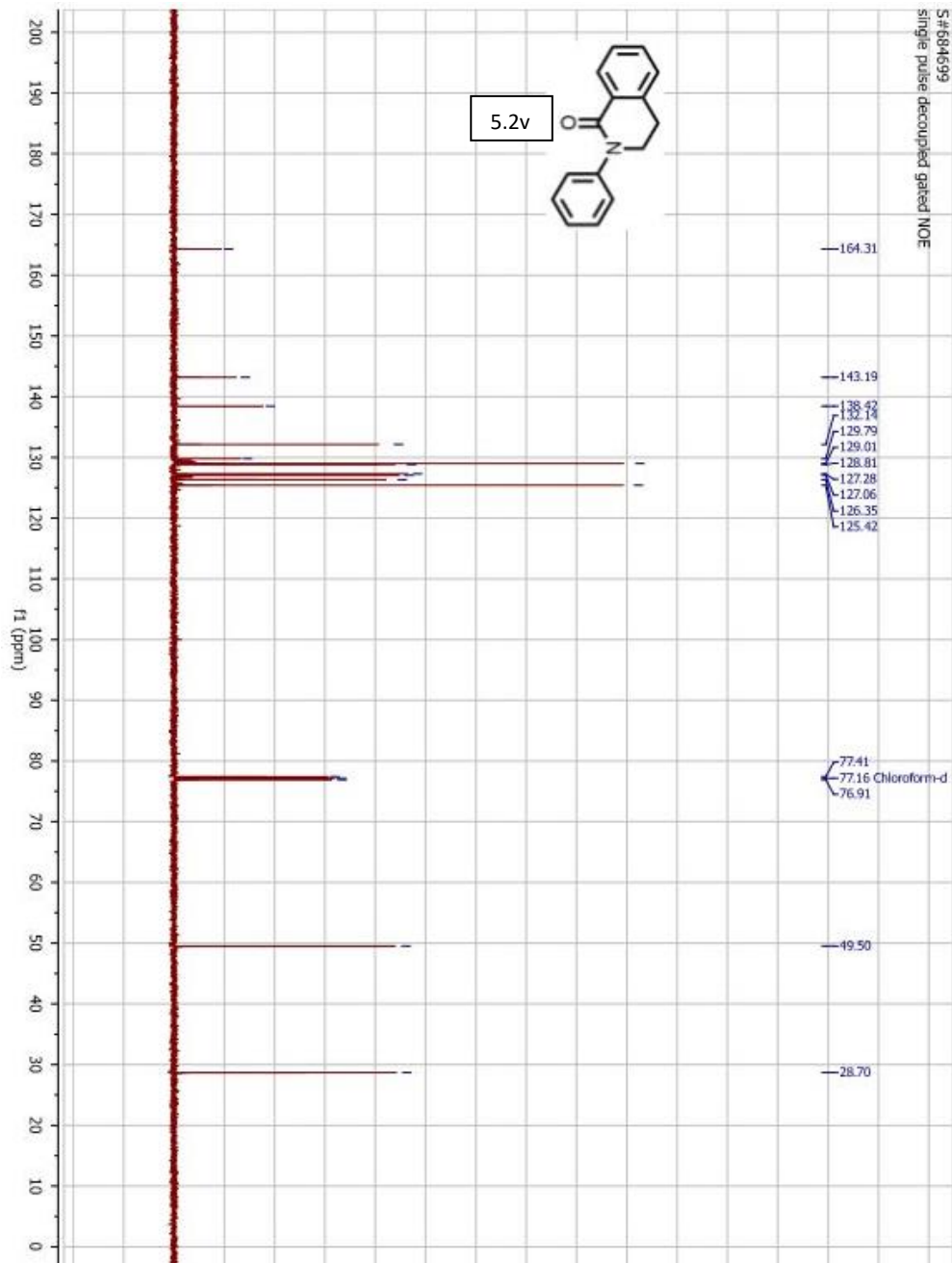
5.2r

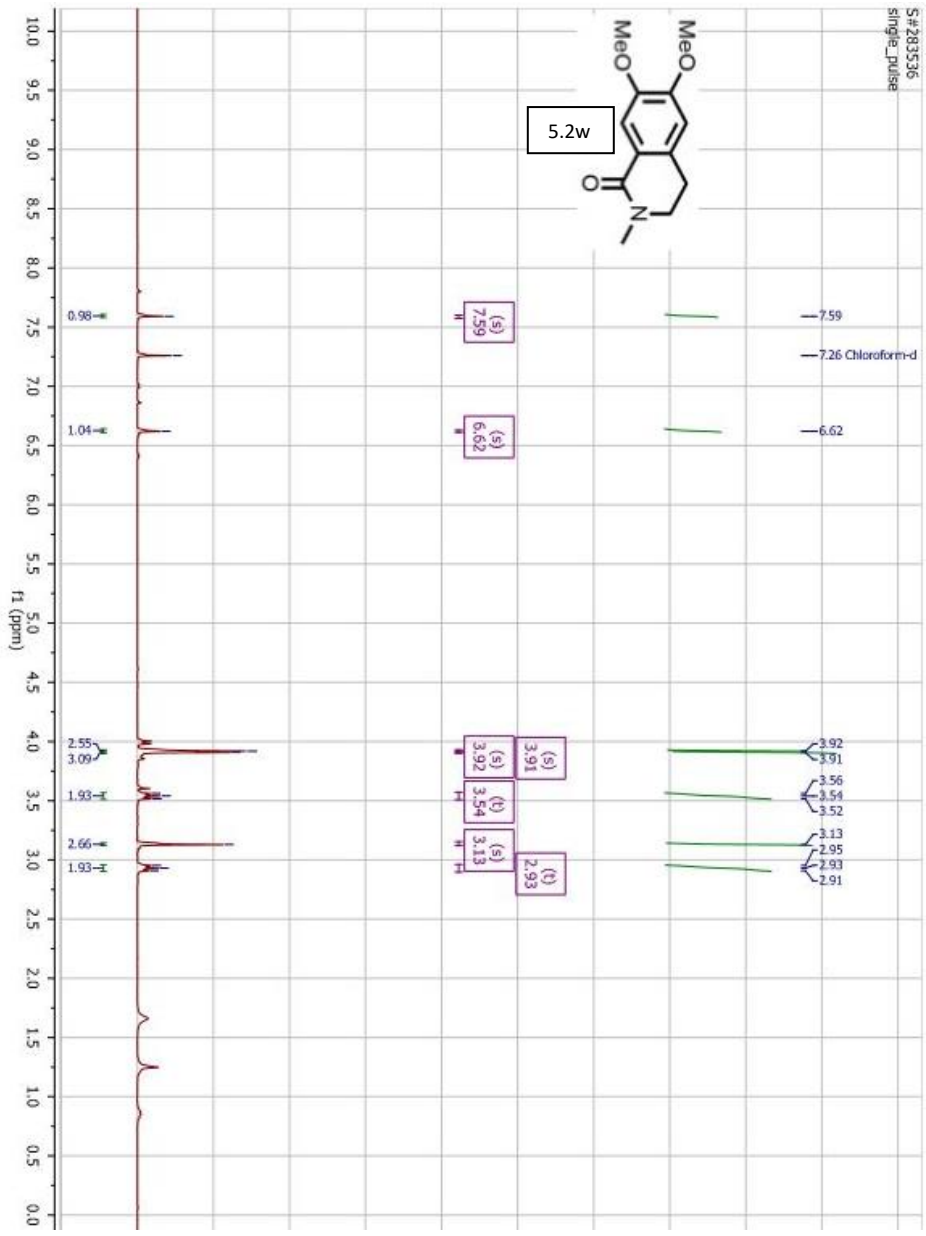


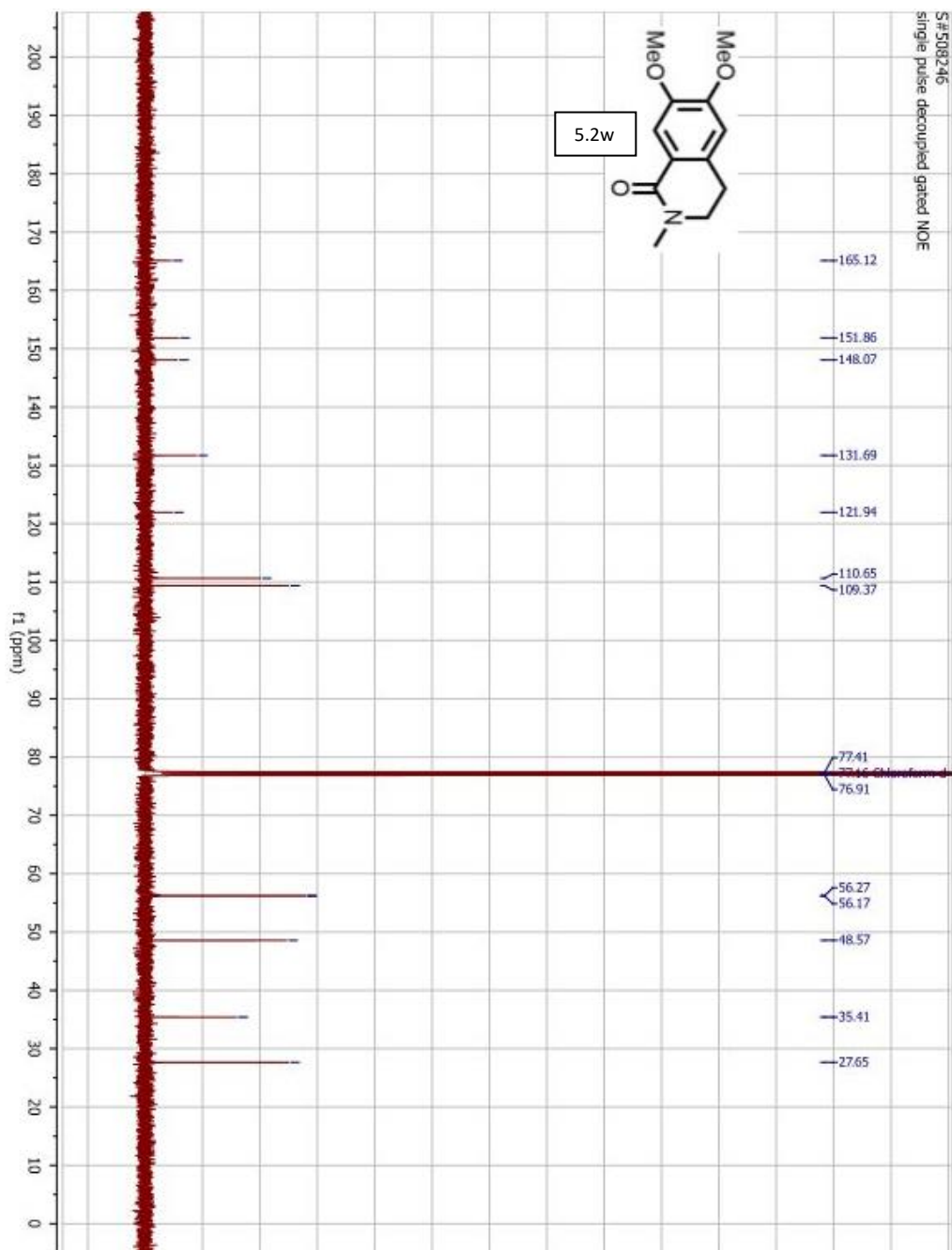


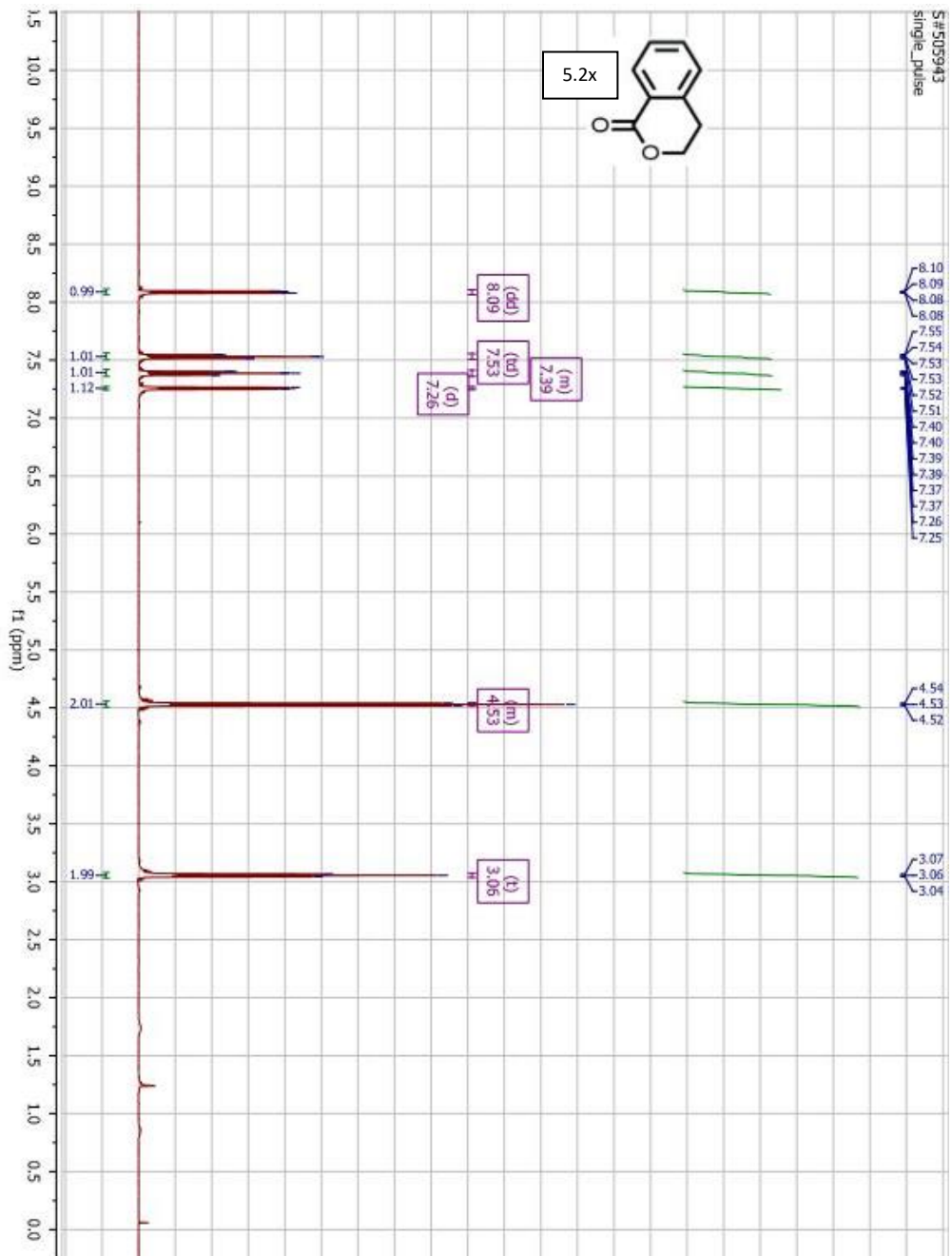


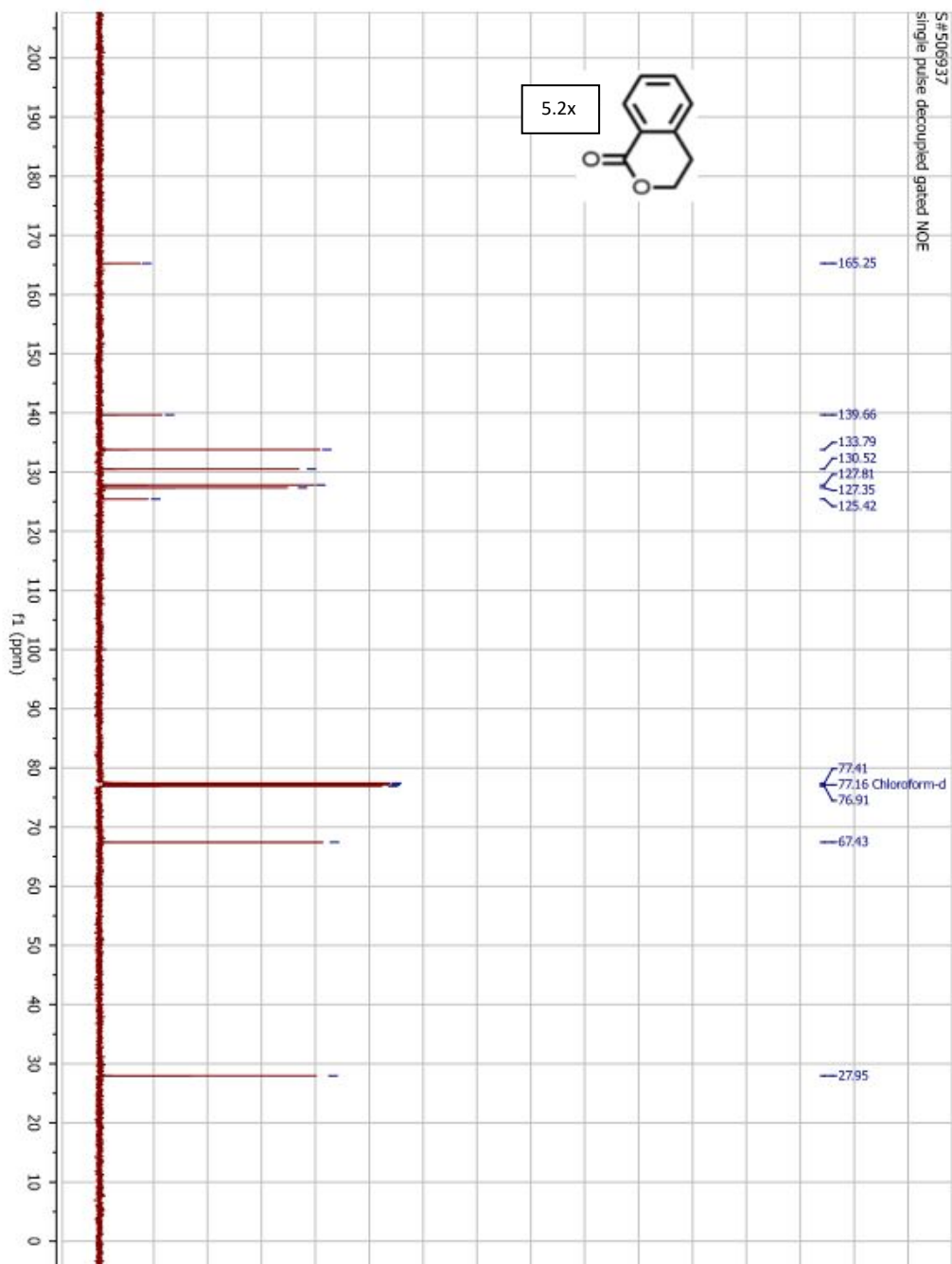


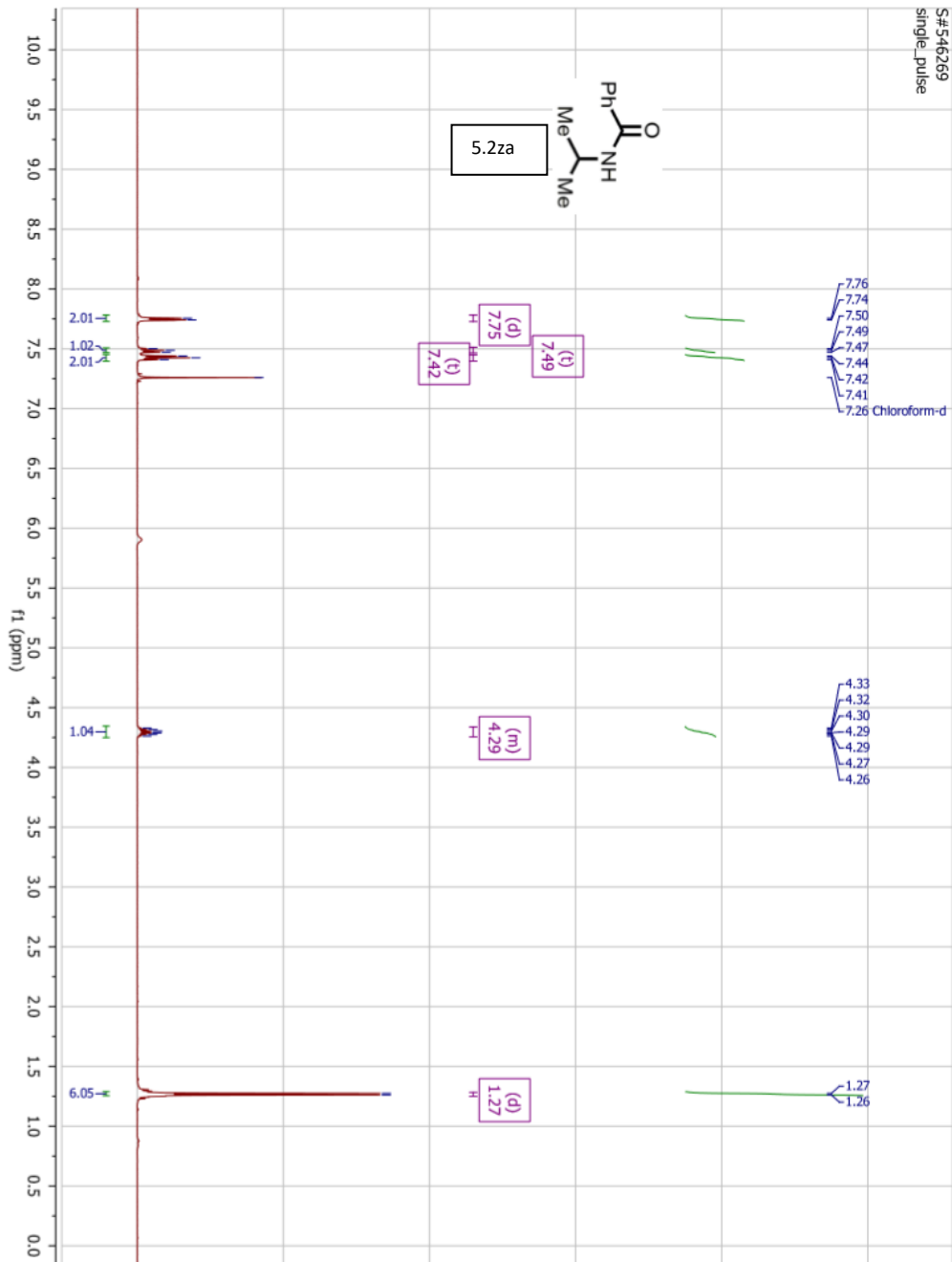


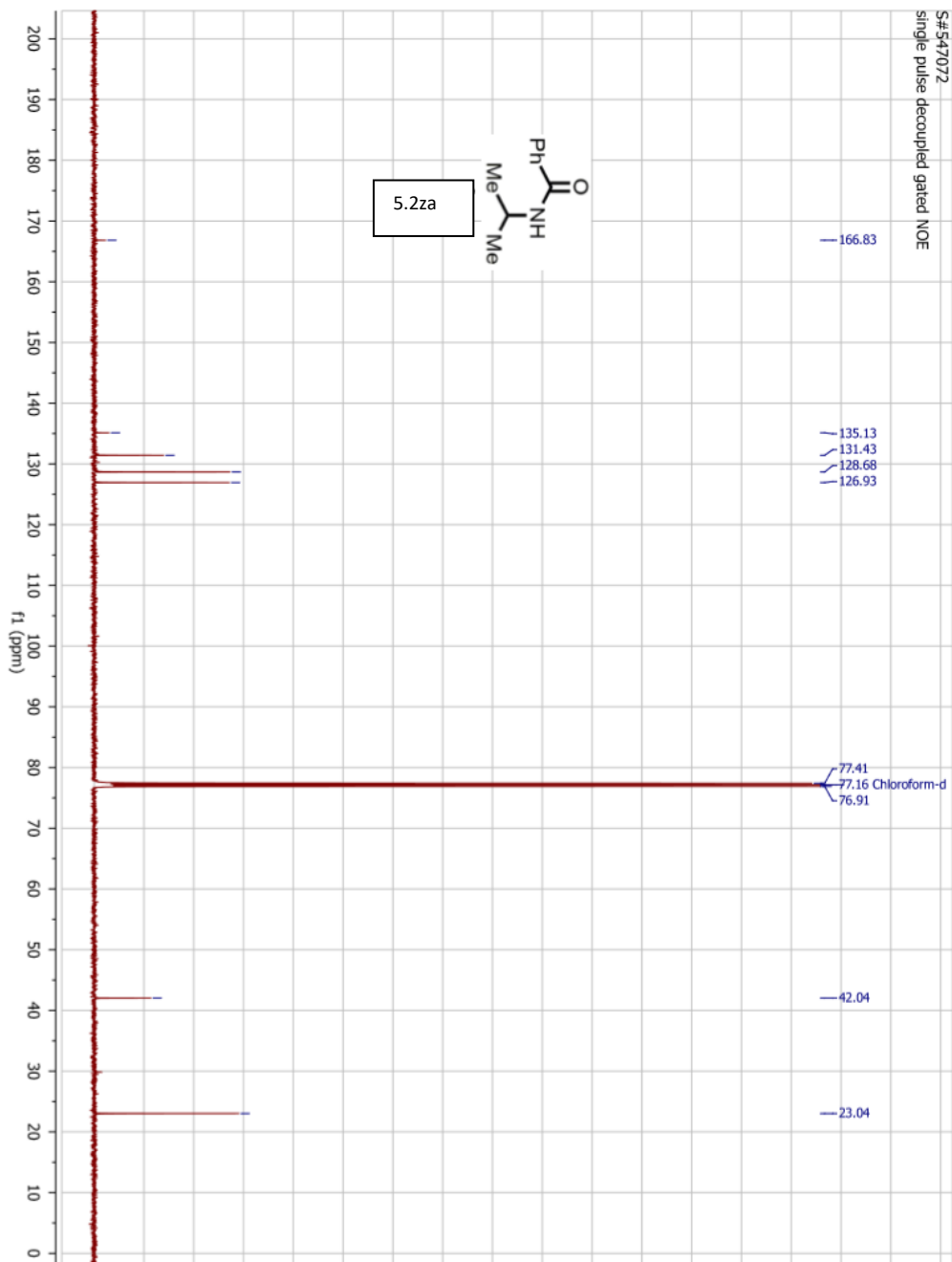


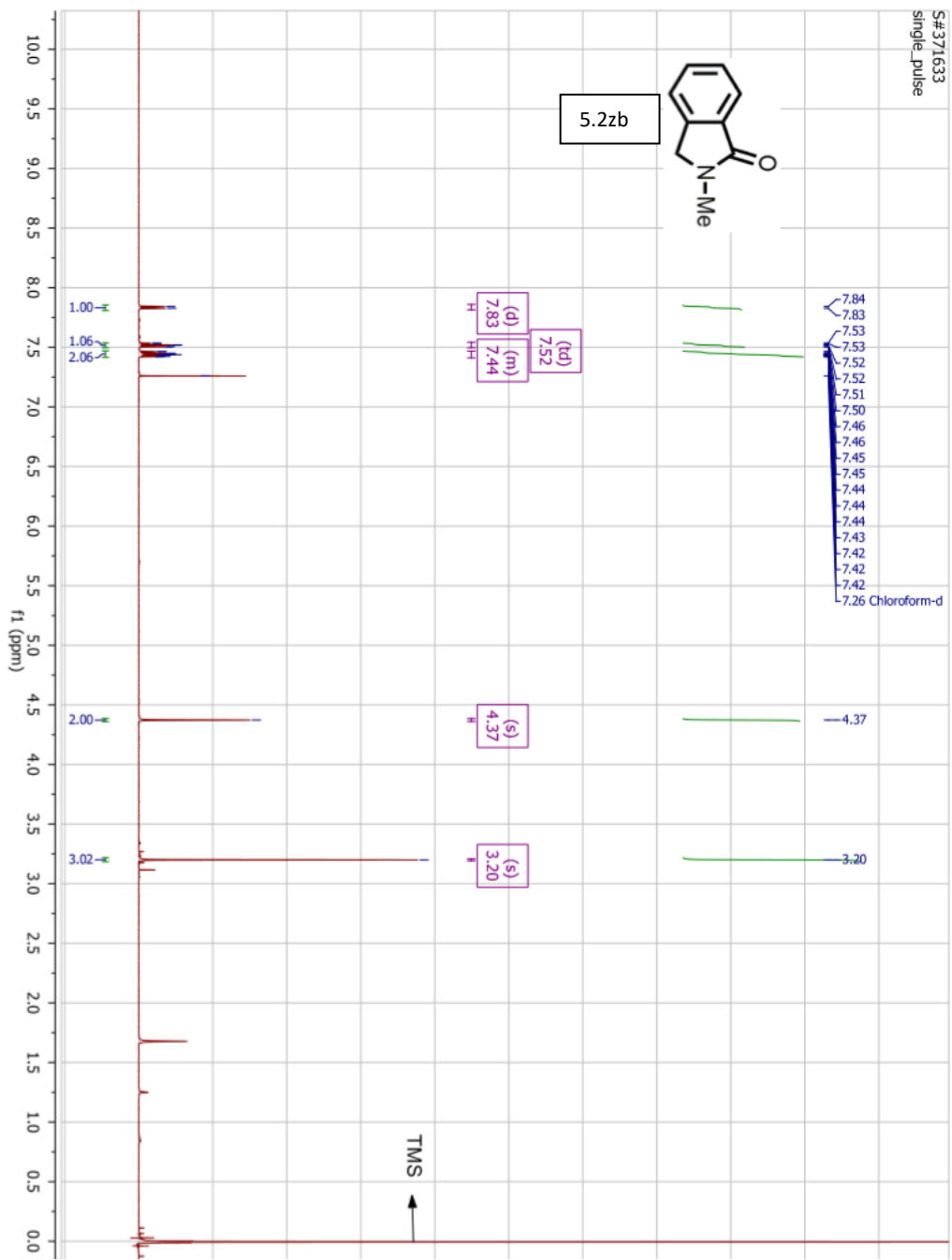


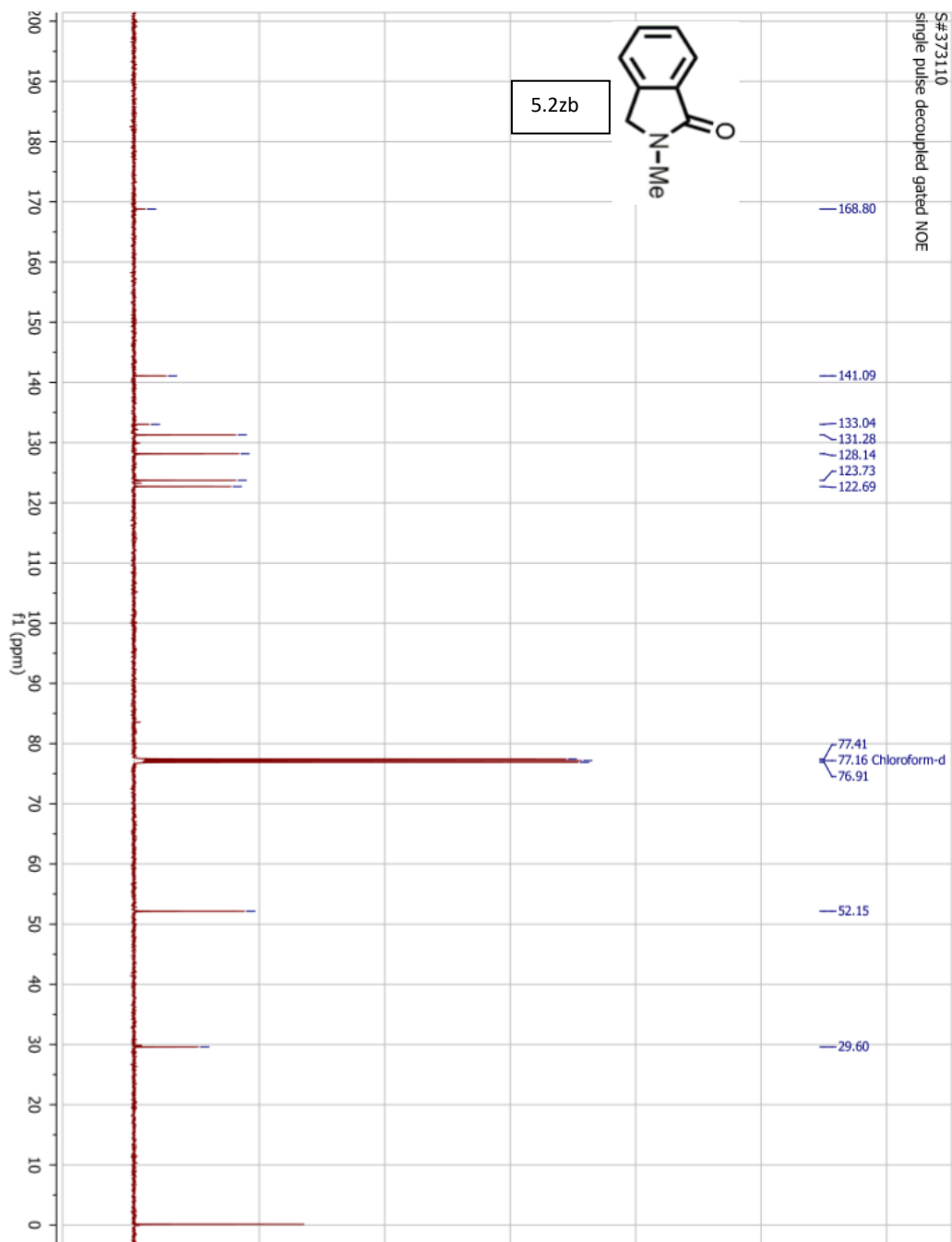


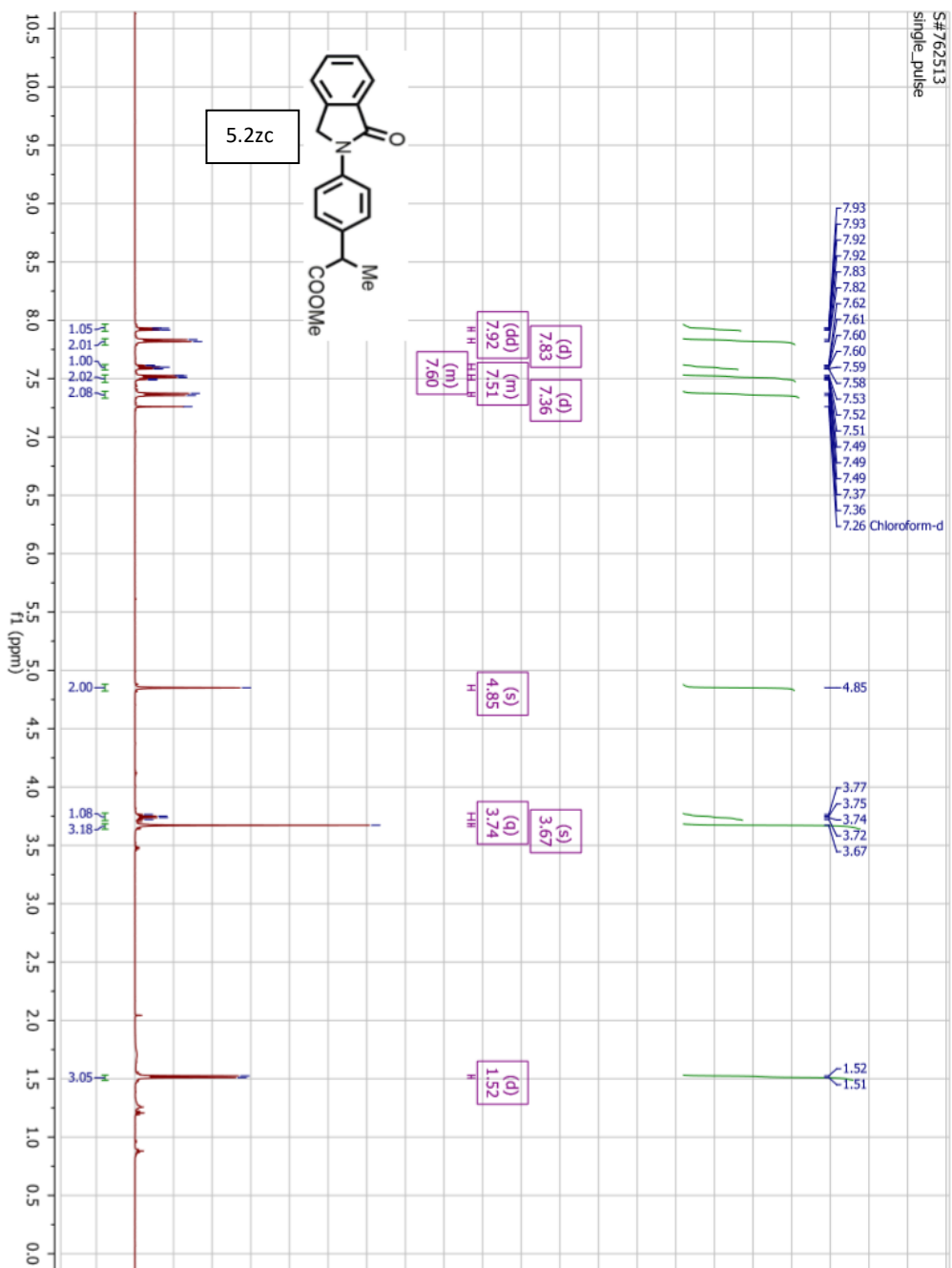


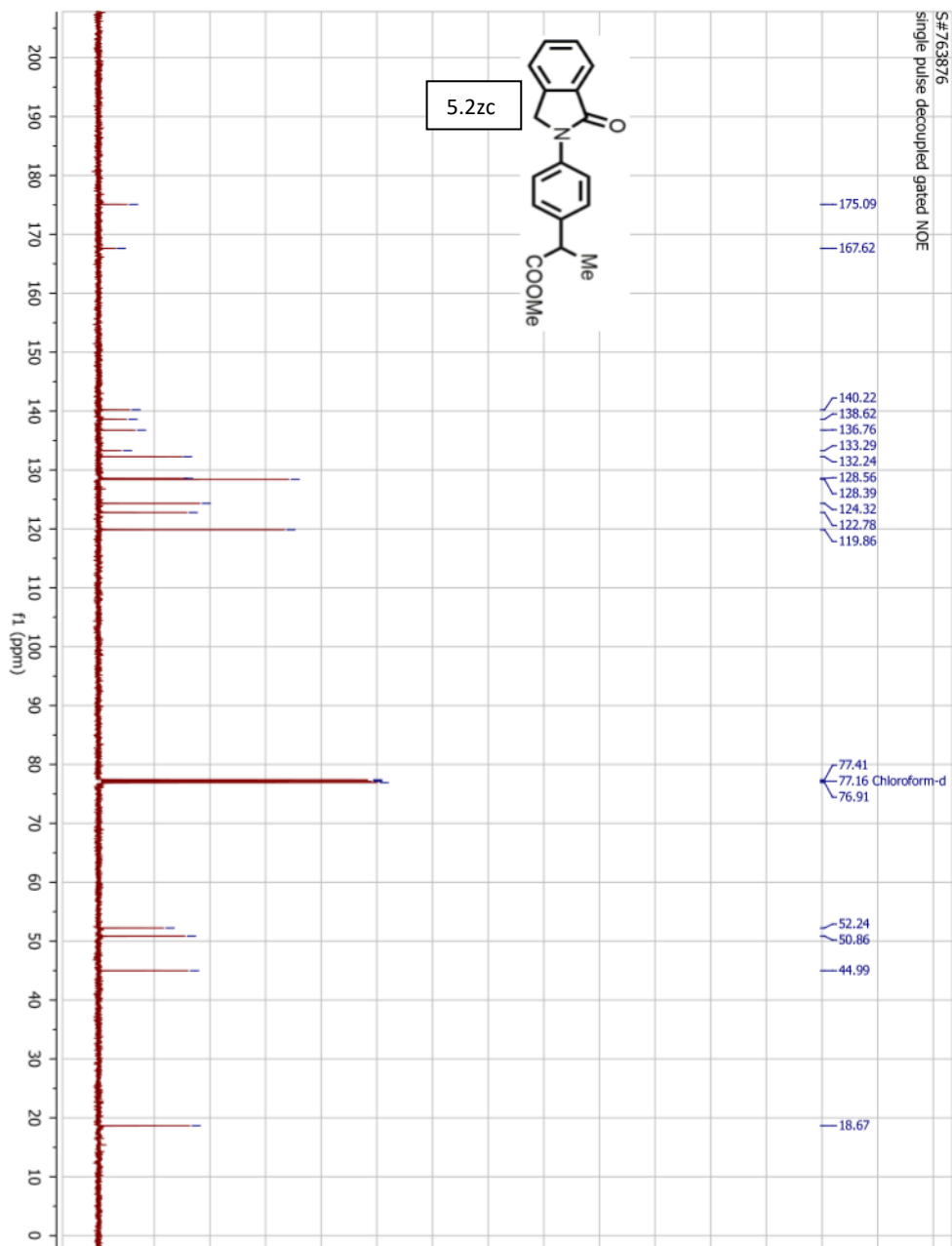








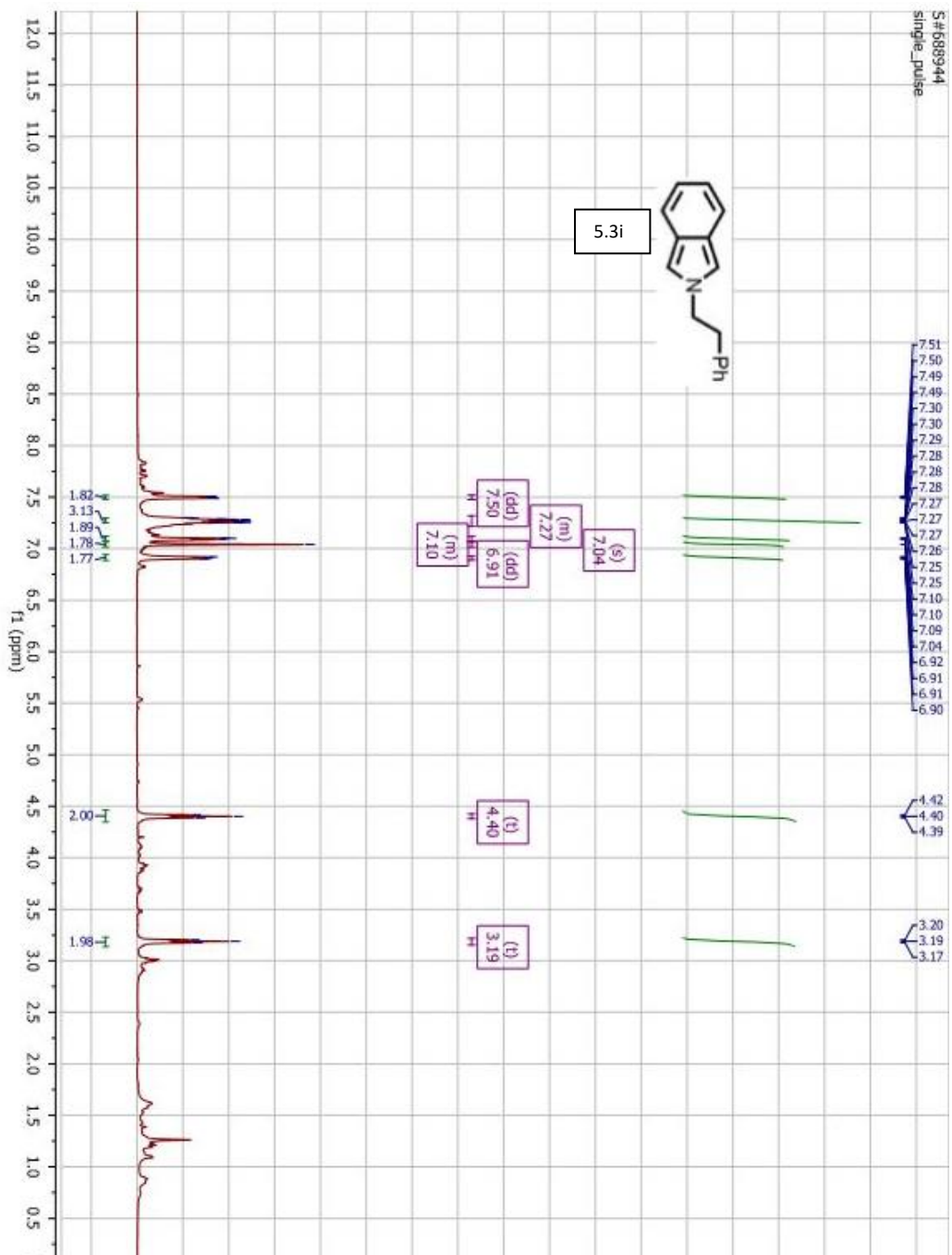




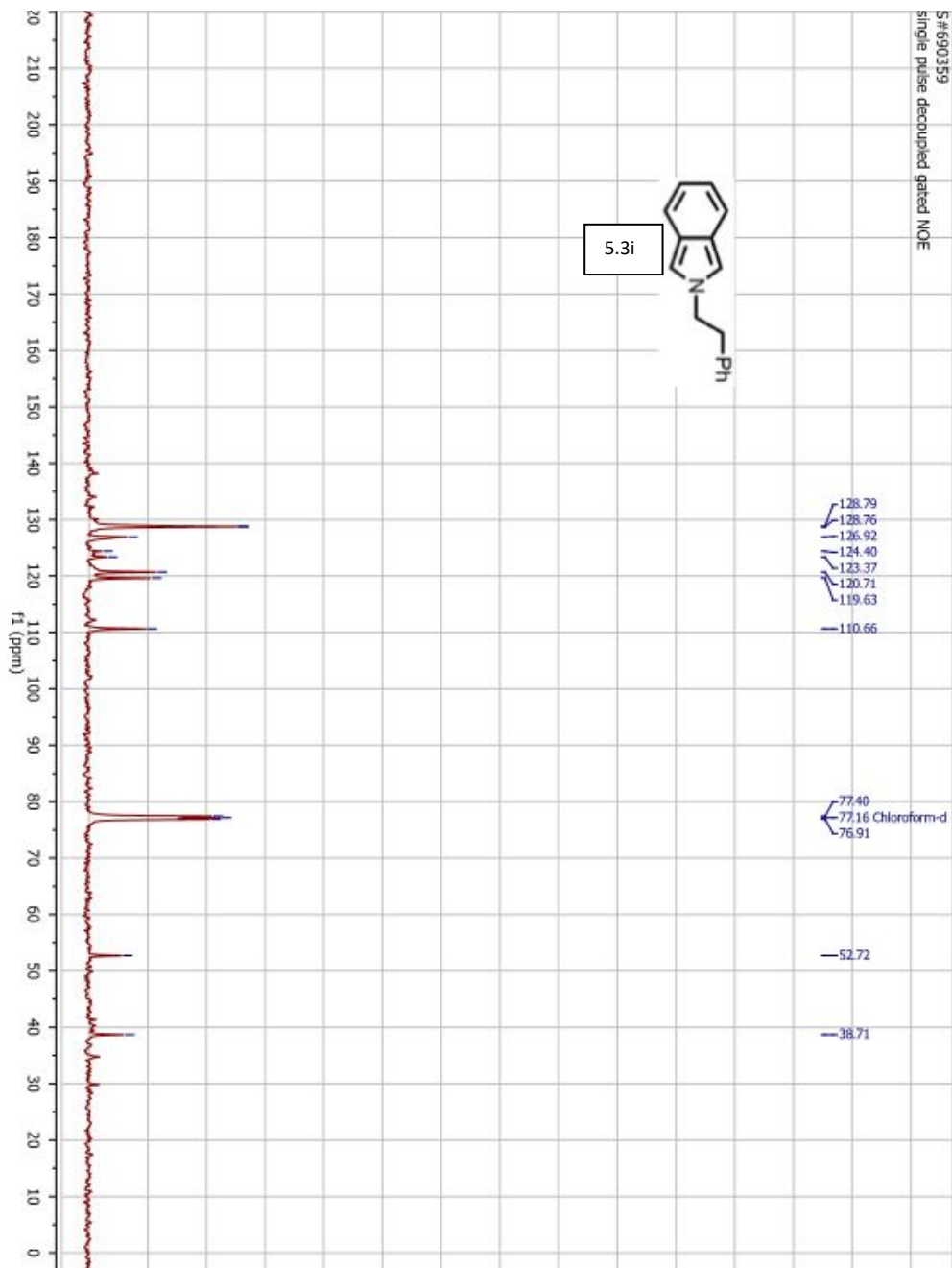
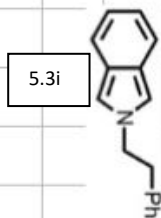
S#689344
single_pulse

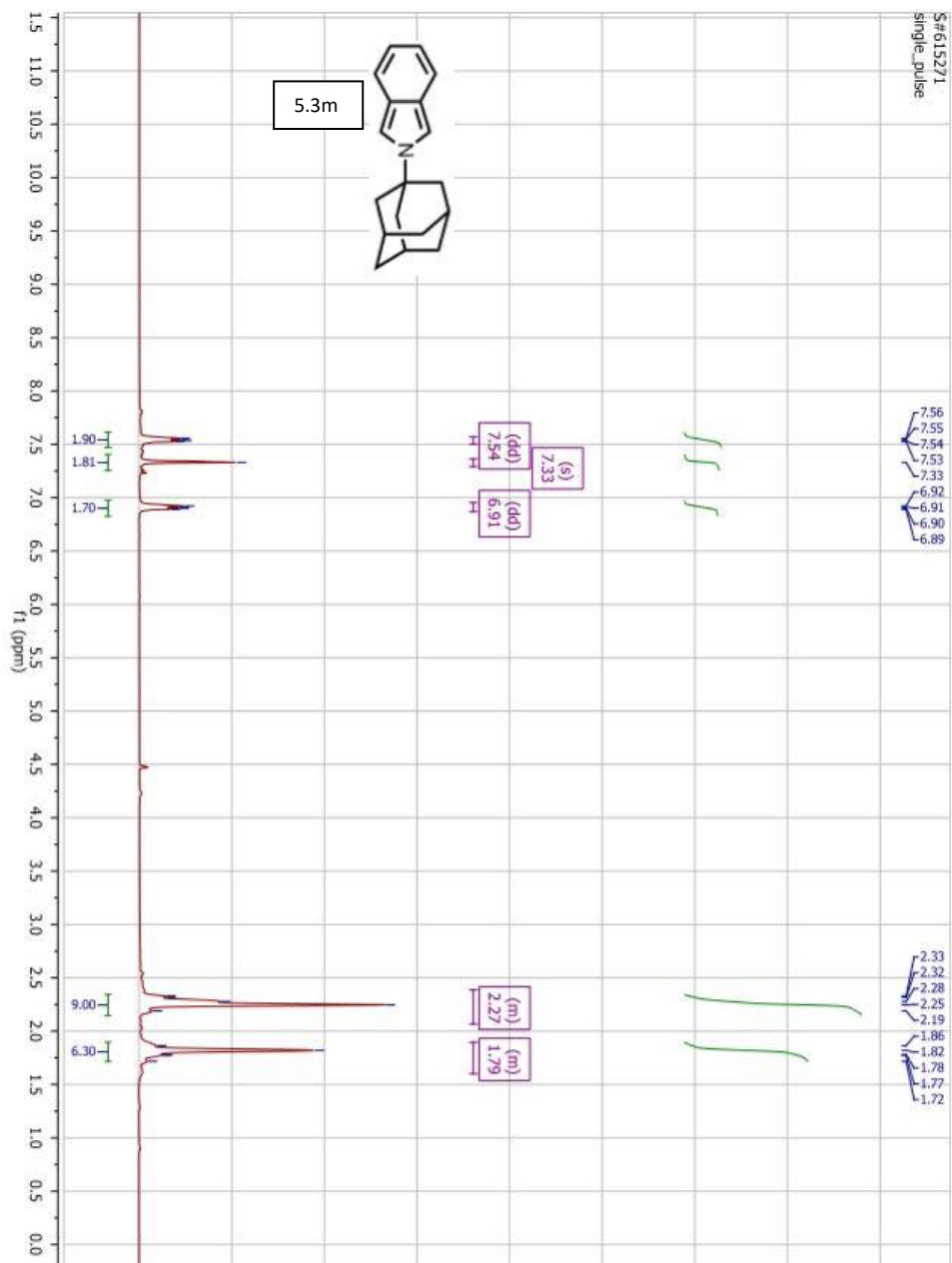


5.3i

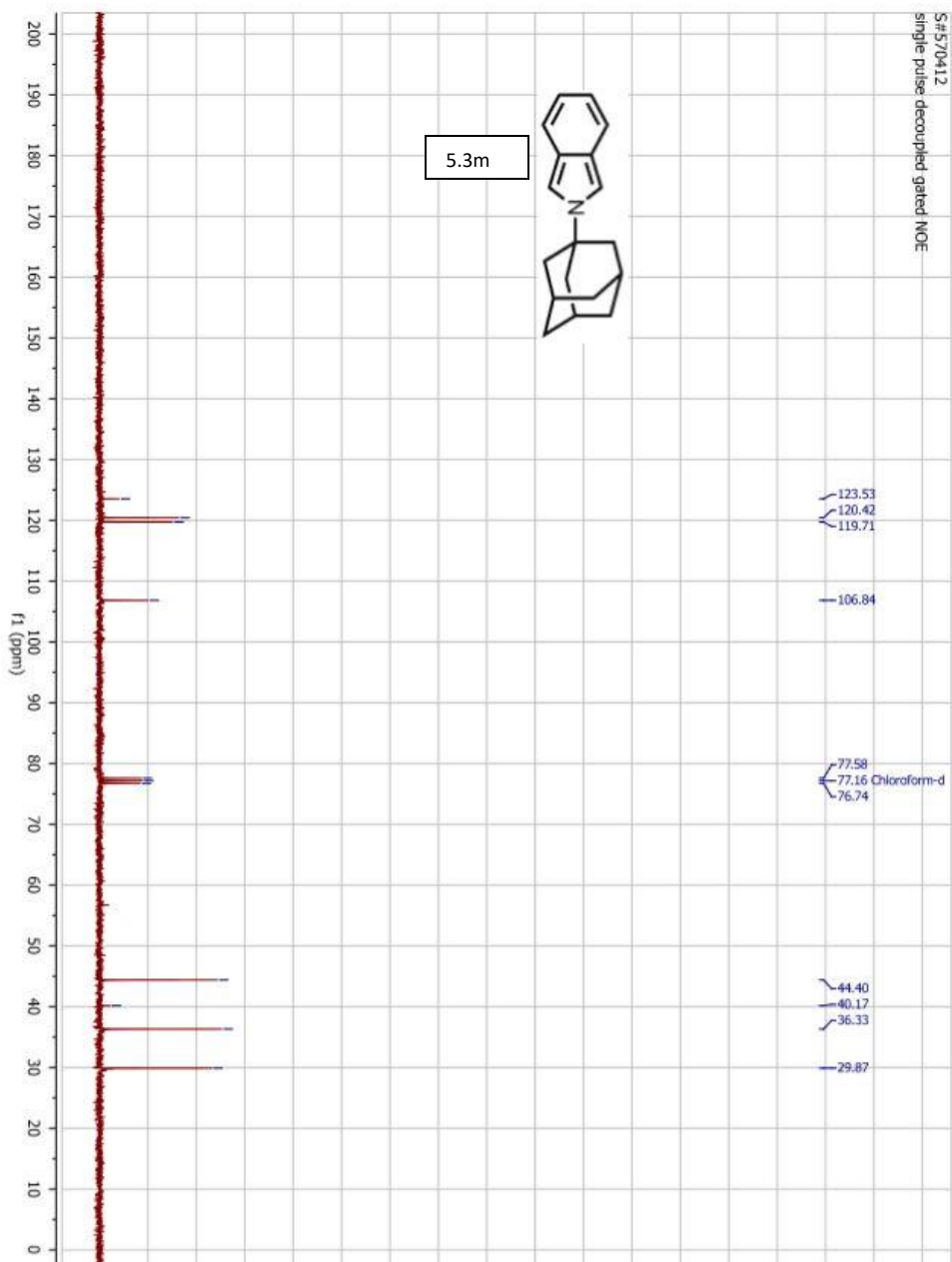


5:1690359
Single pulse decoupled gated NOE





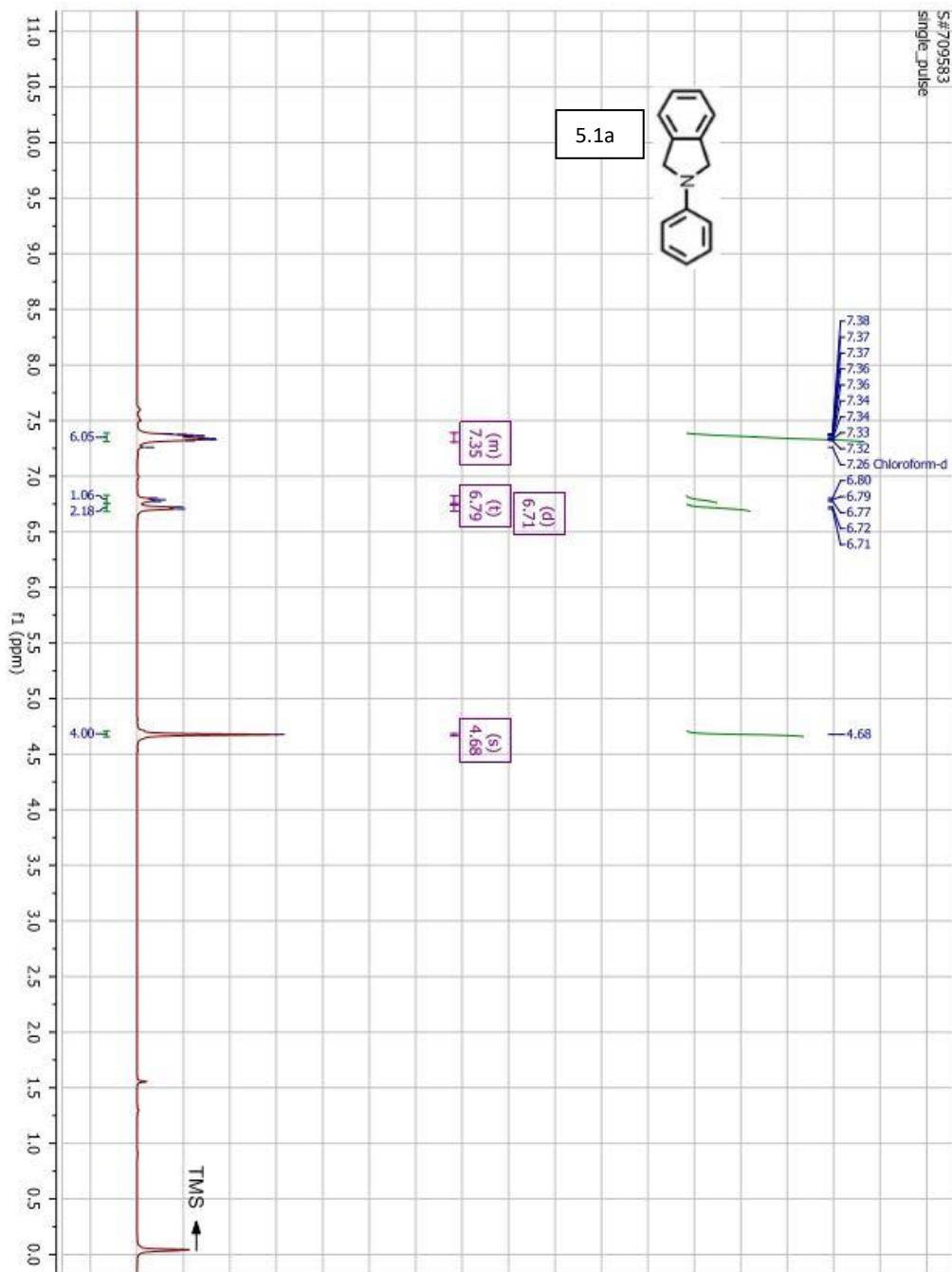
S#570412
single pulse decoupled gated NOE

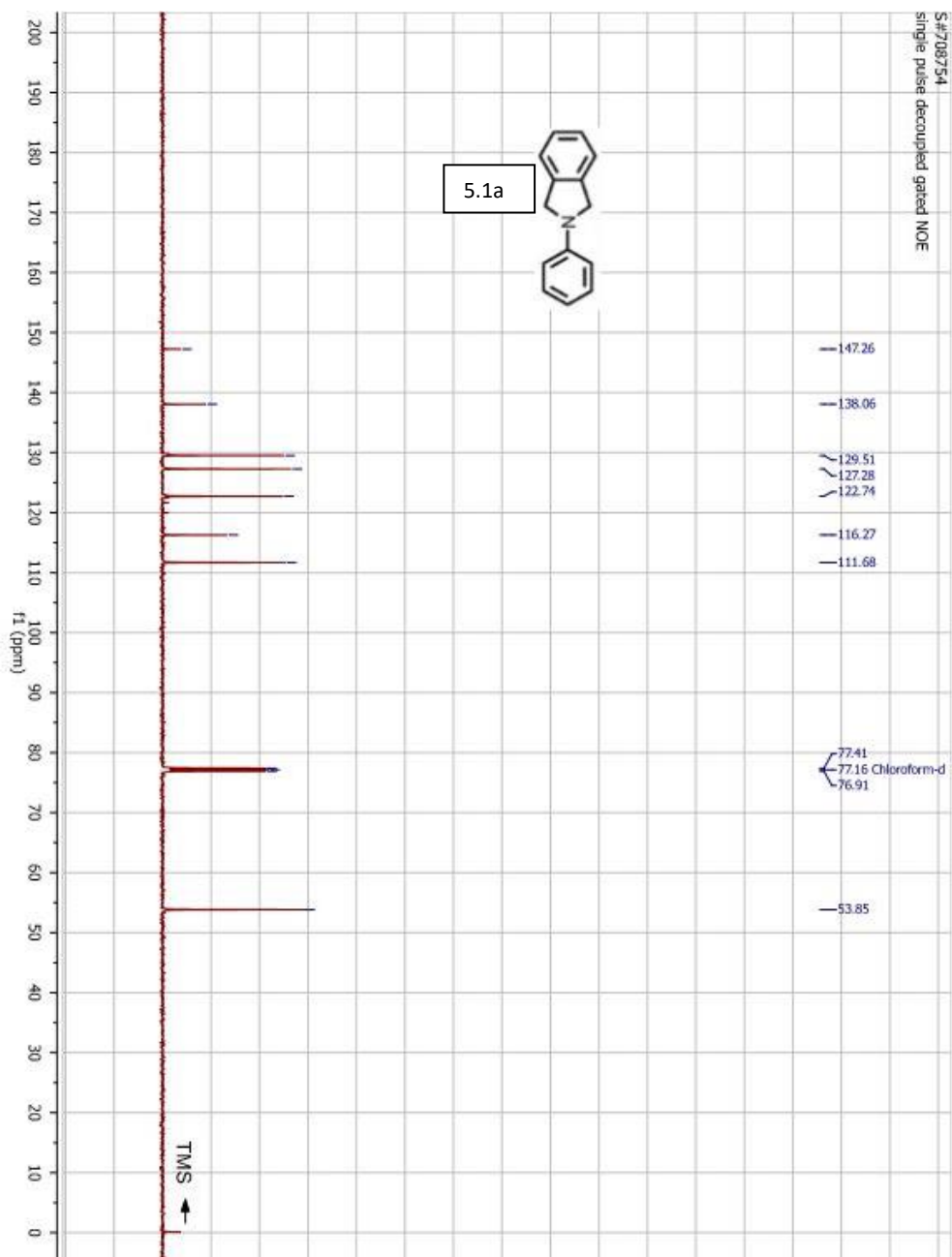


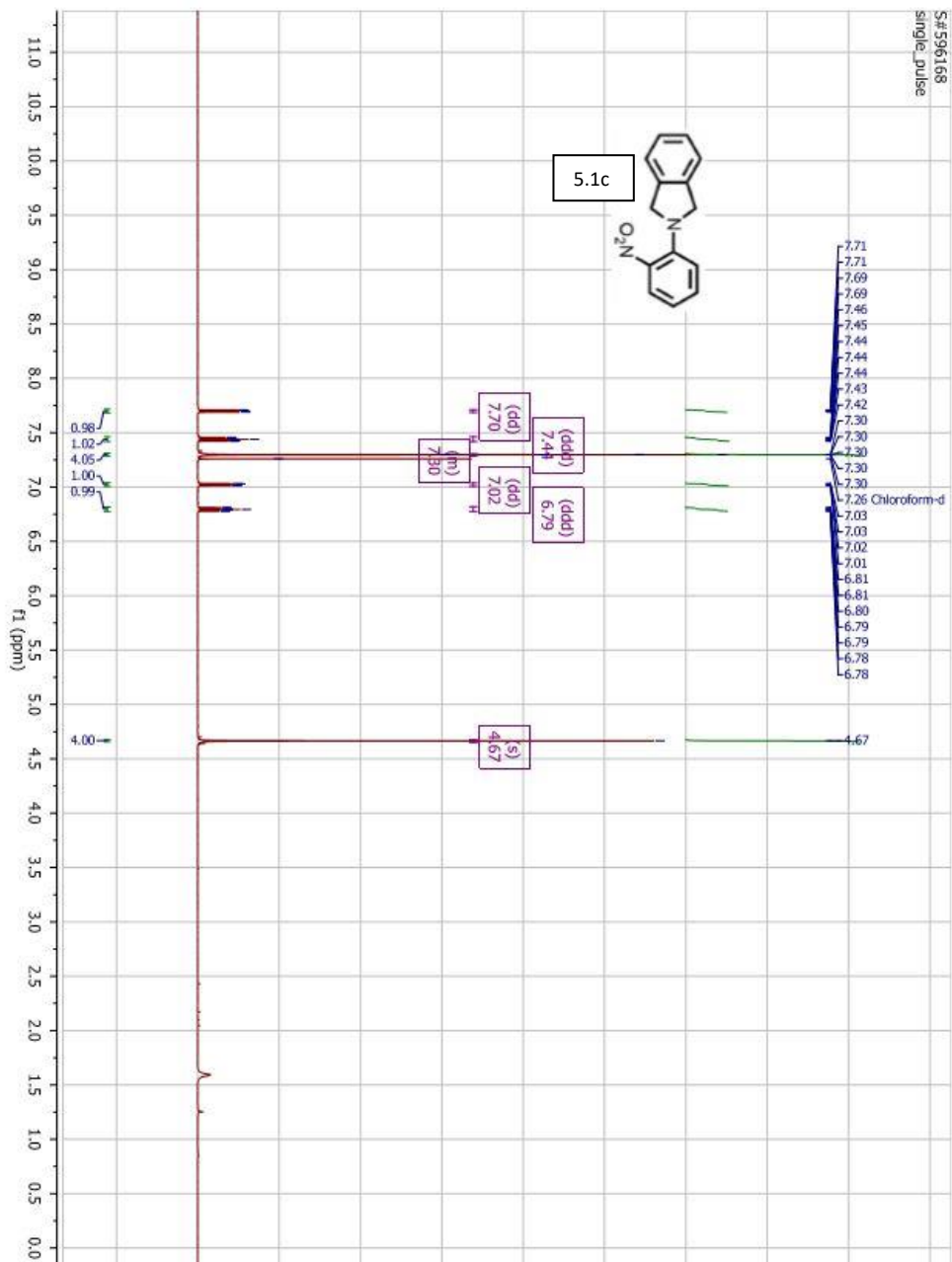
S#:709583
single_pulse



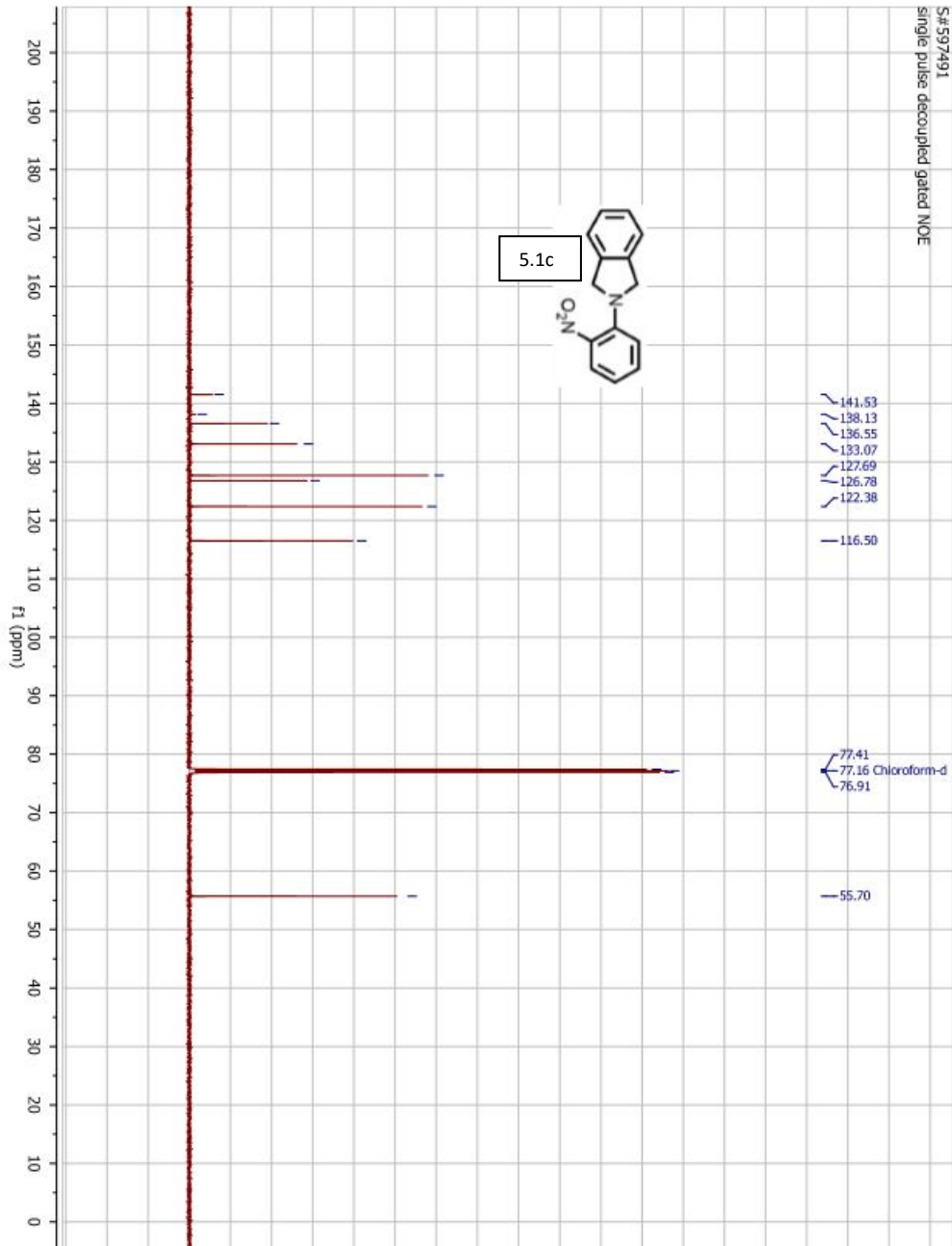
5.1a

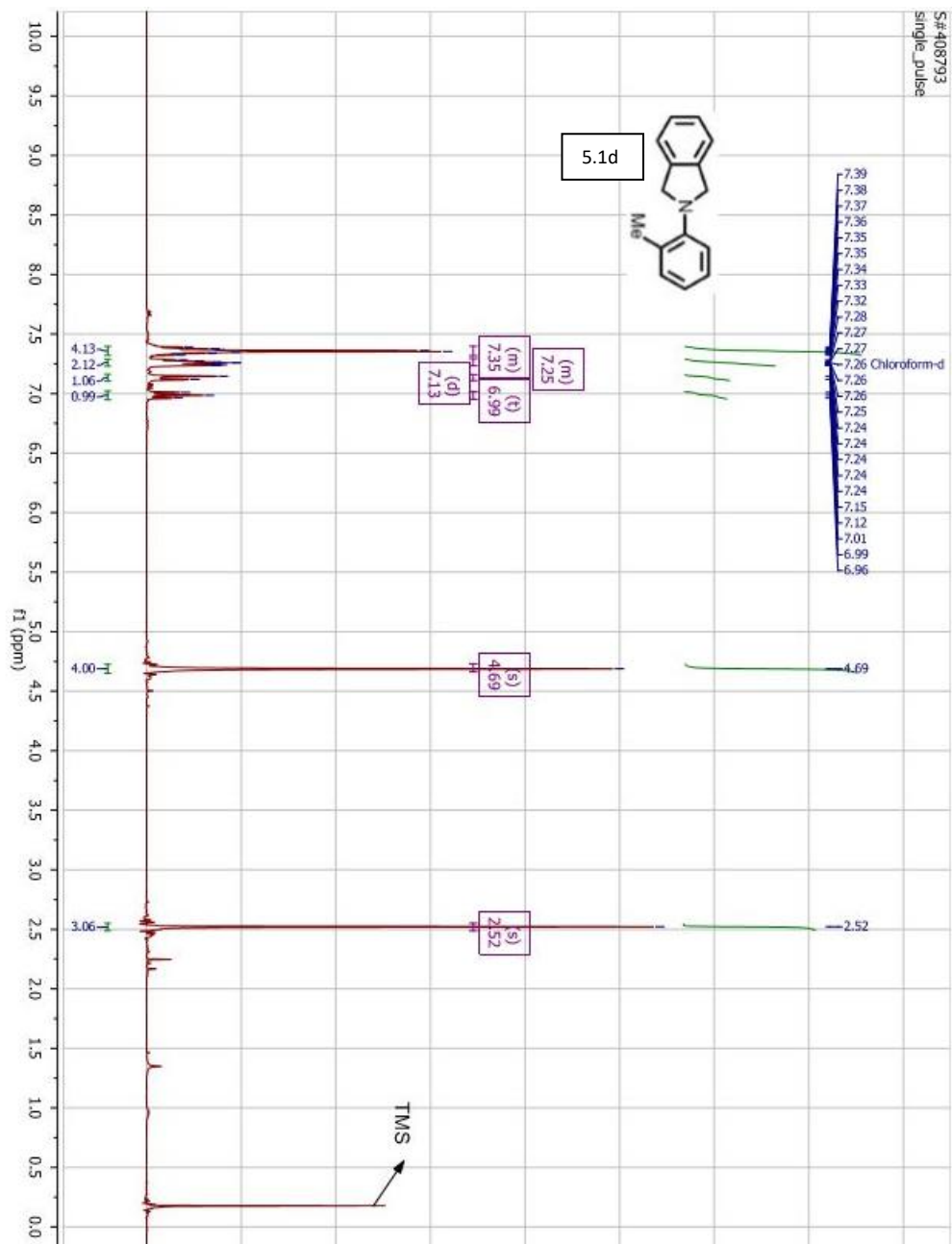


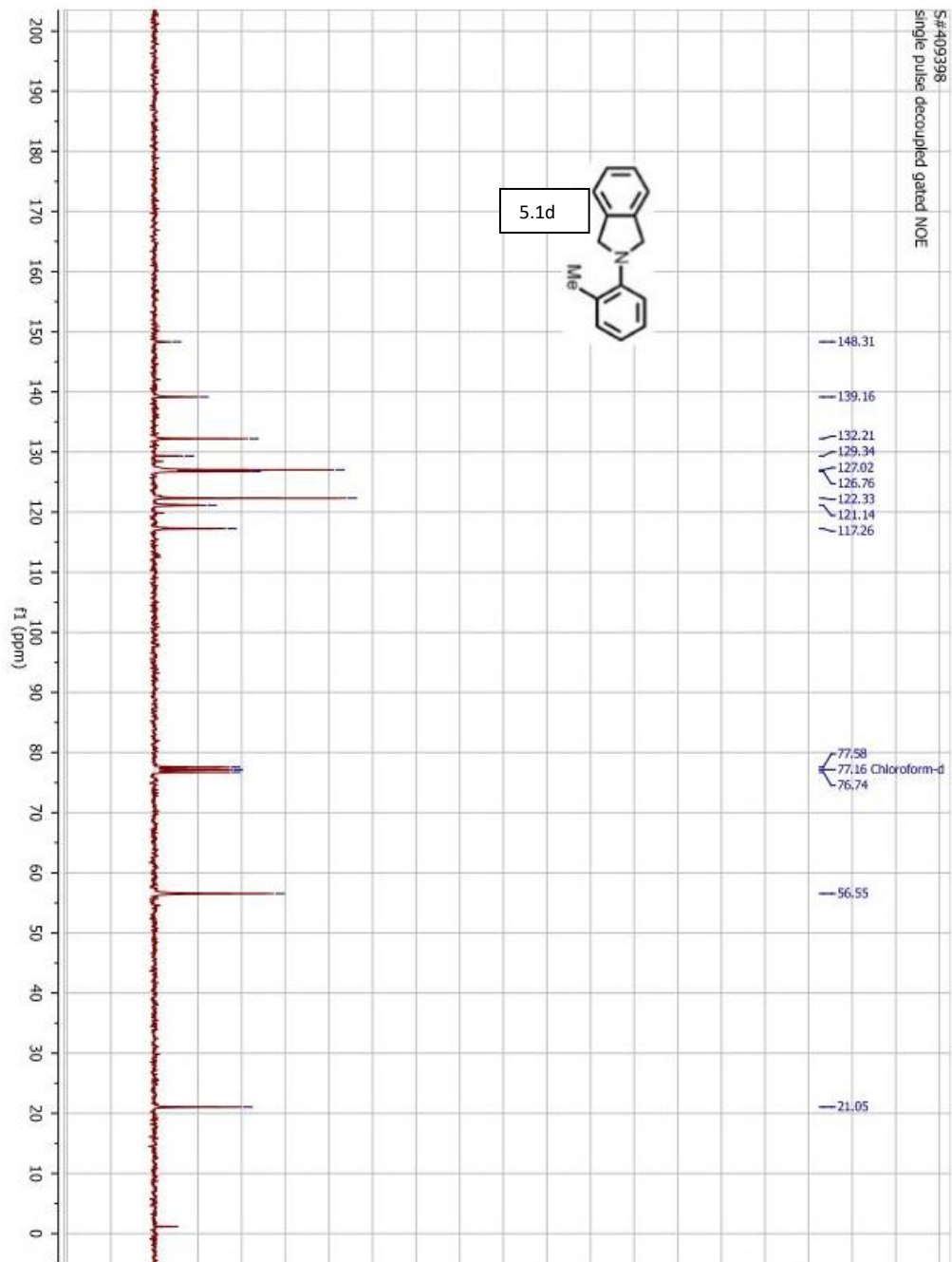


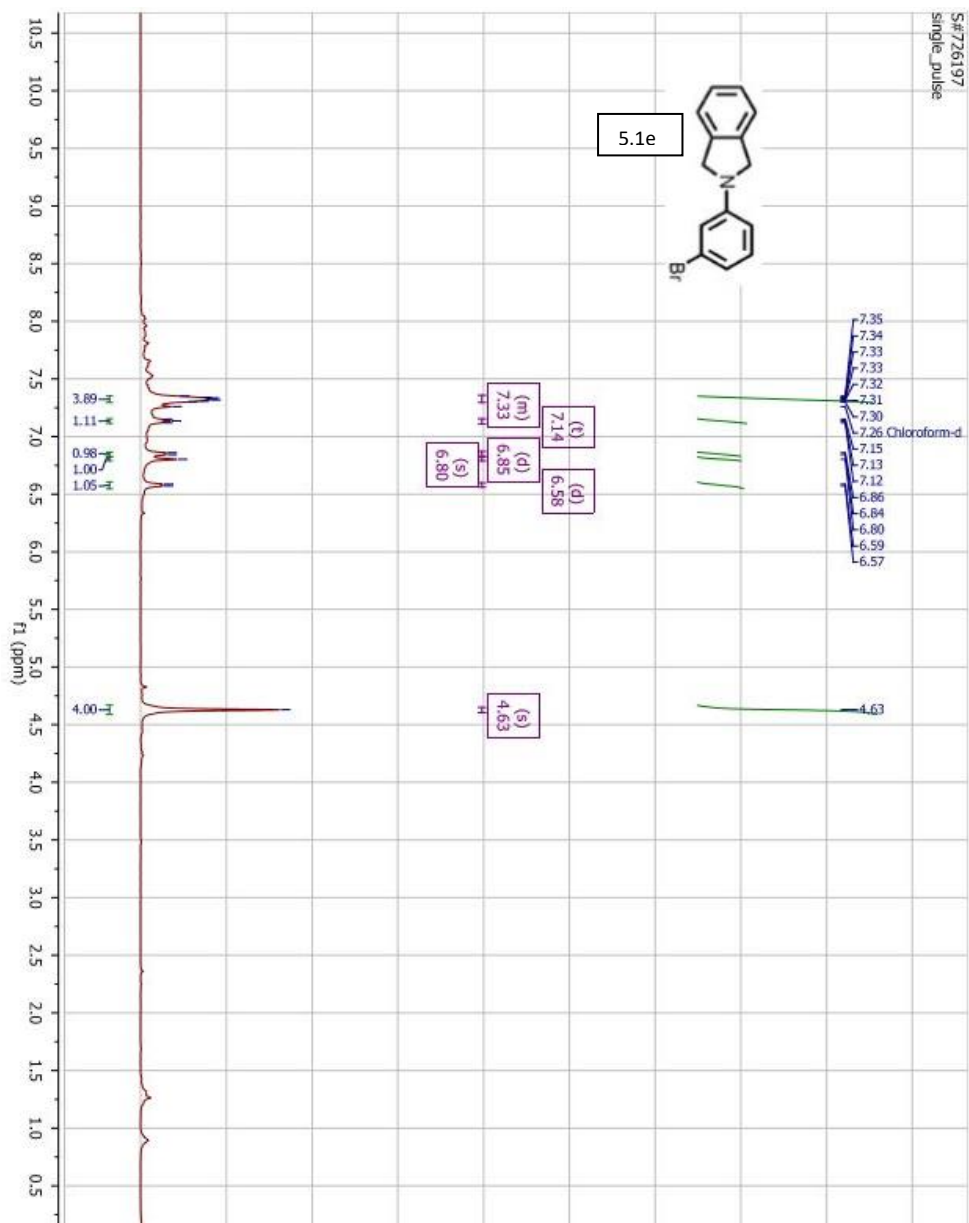


S#597491
single pulse decoupled gated NOE

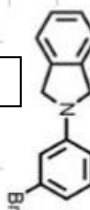




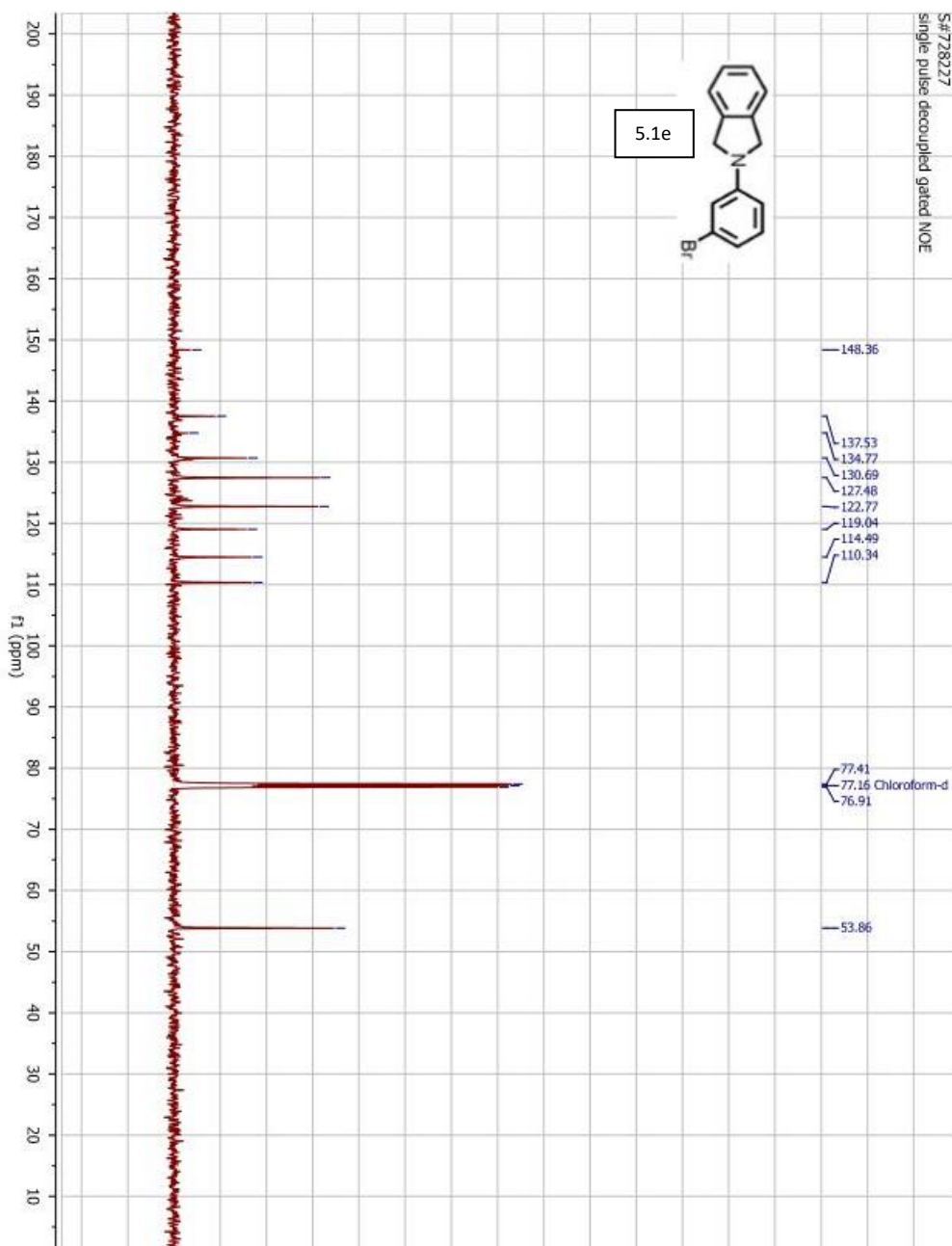


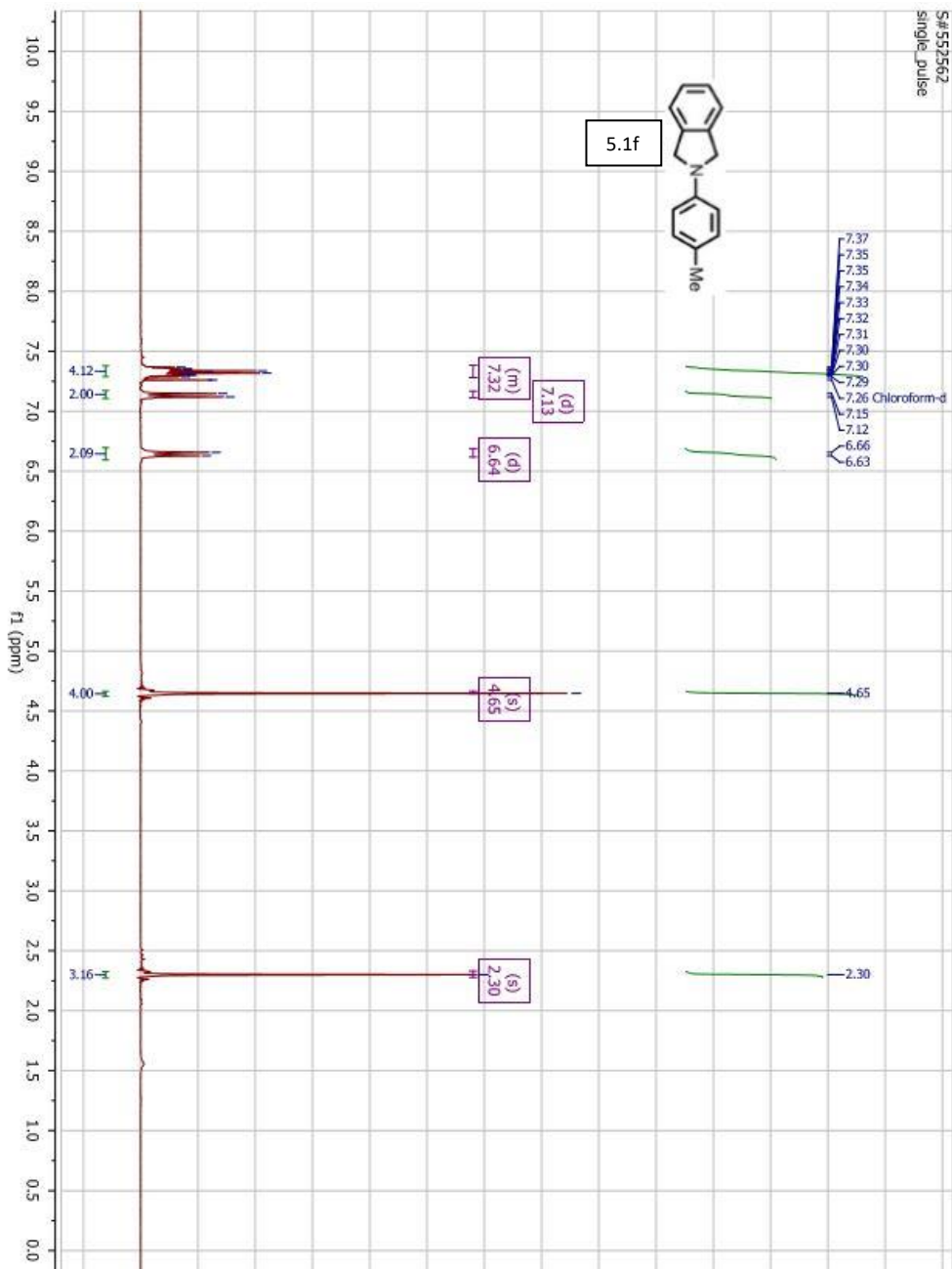


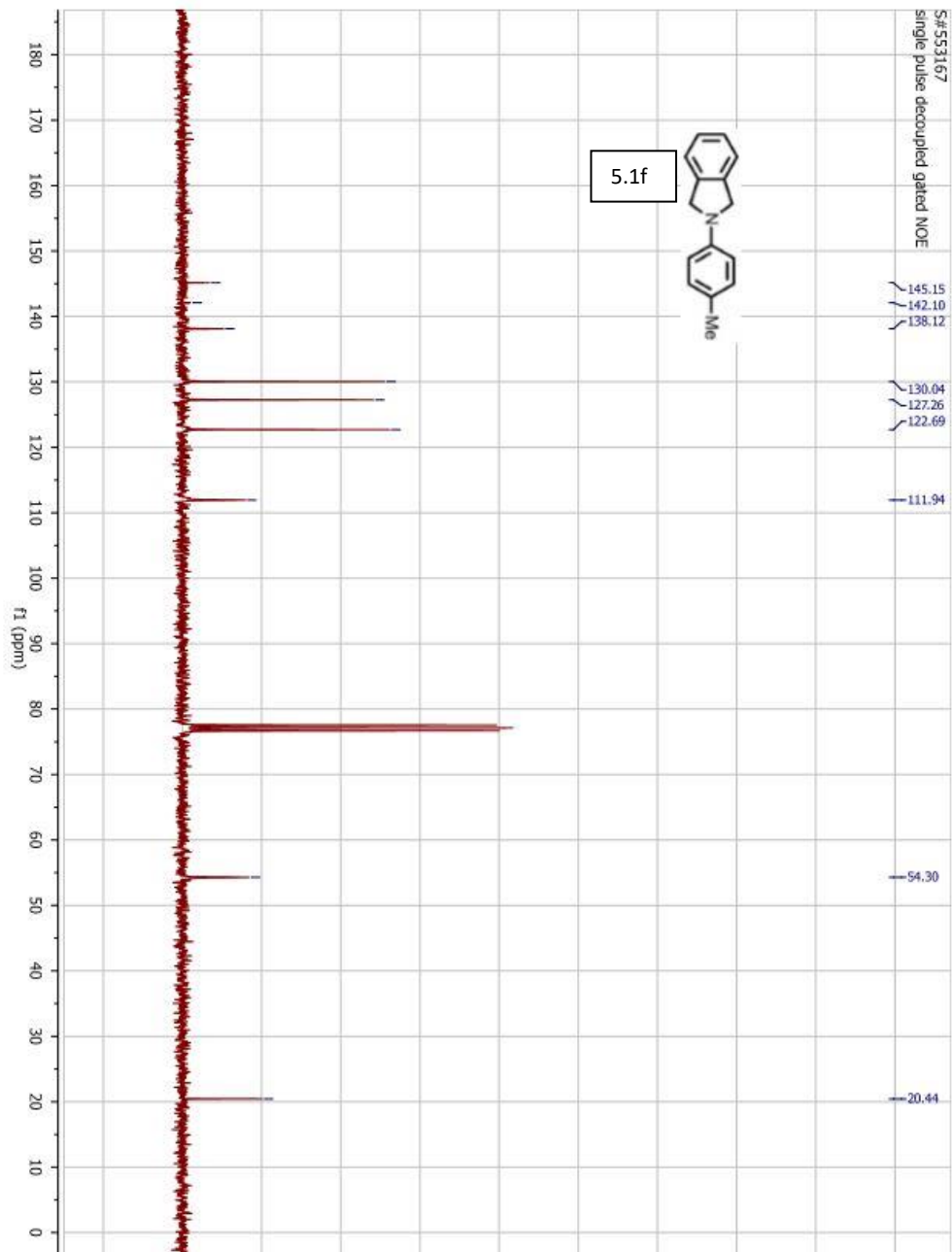
S# 728227
single pulse decoupled gated NOE

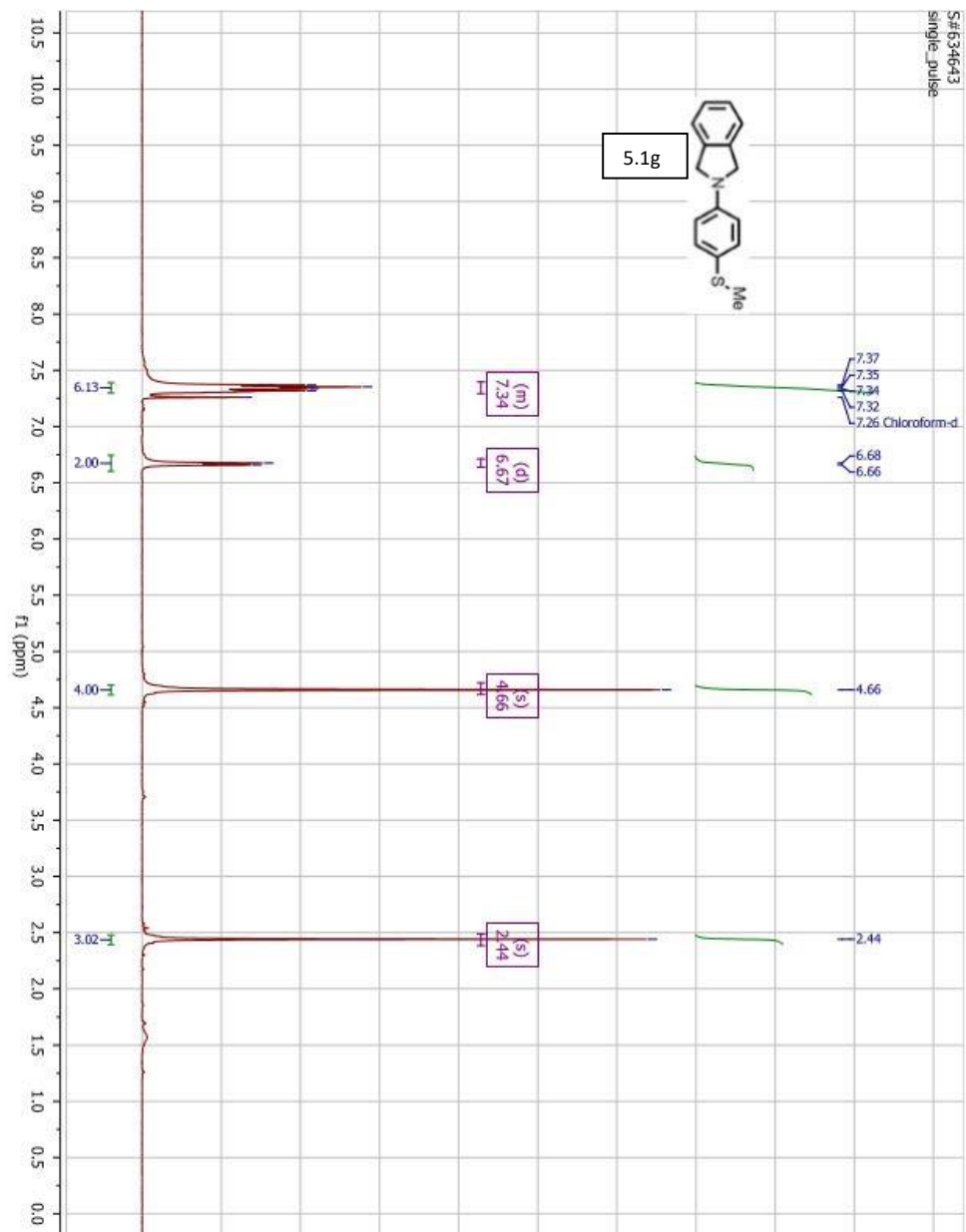


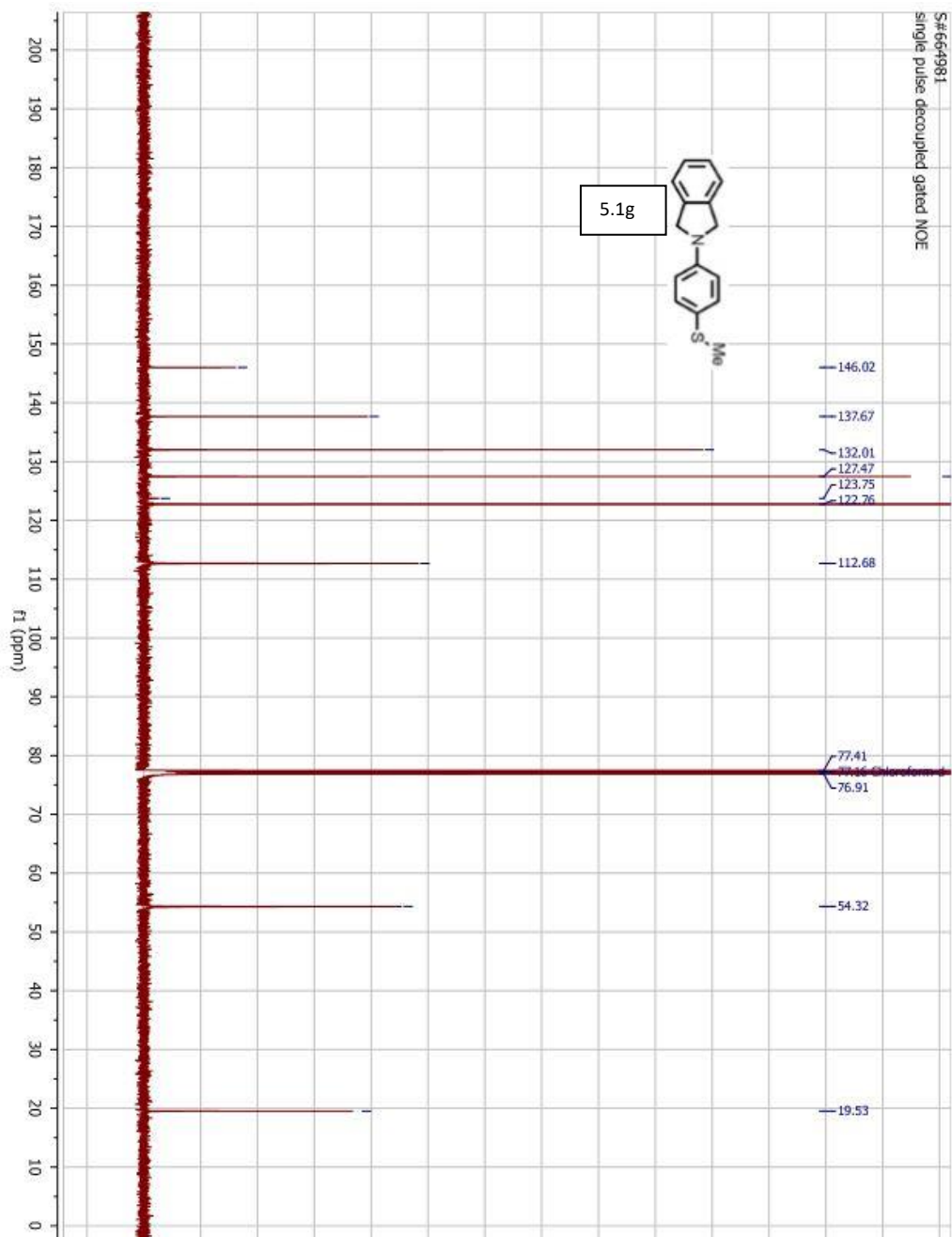
5.1e

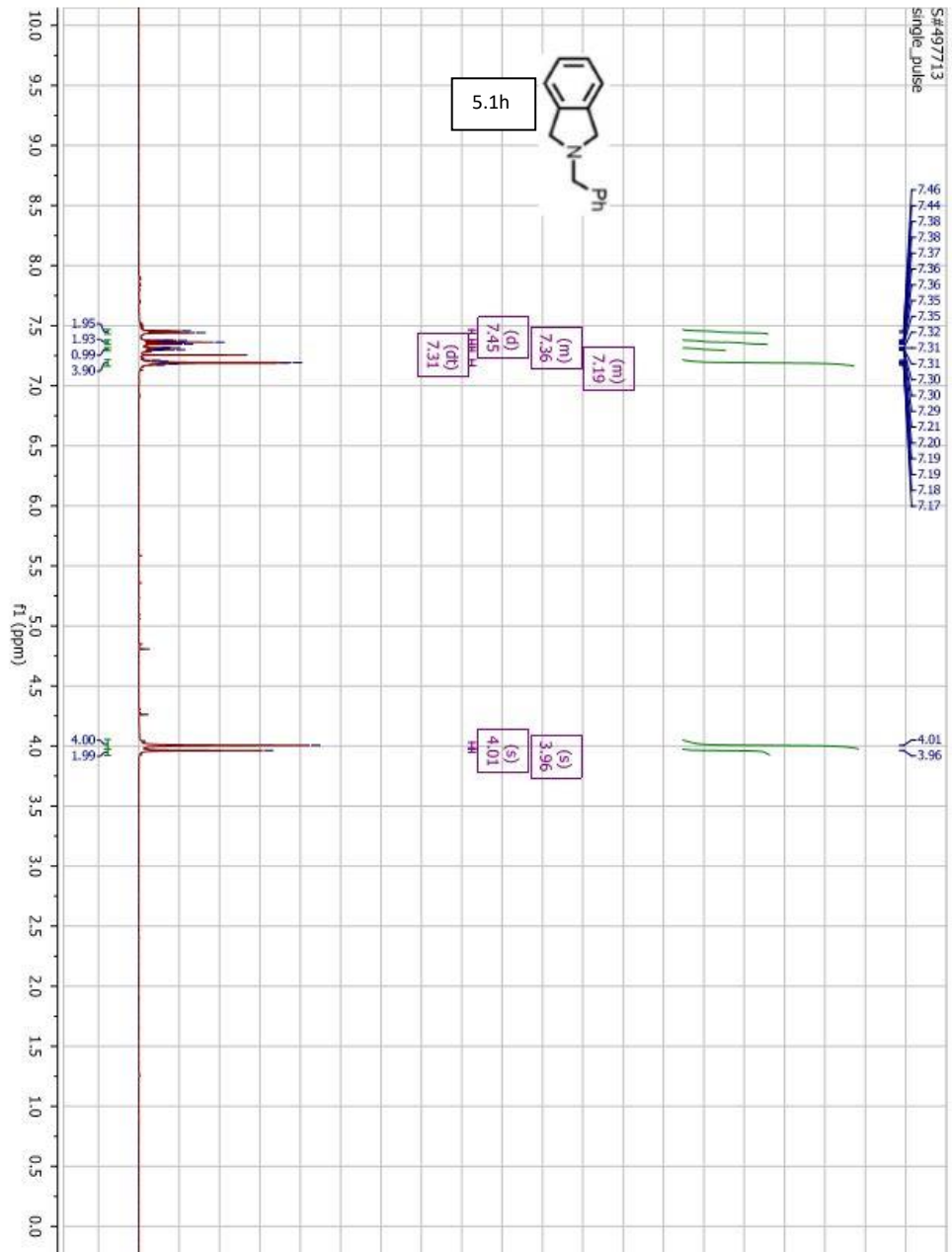




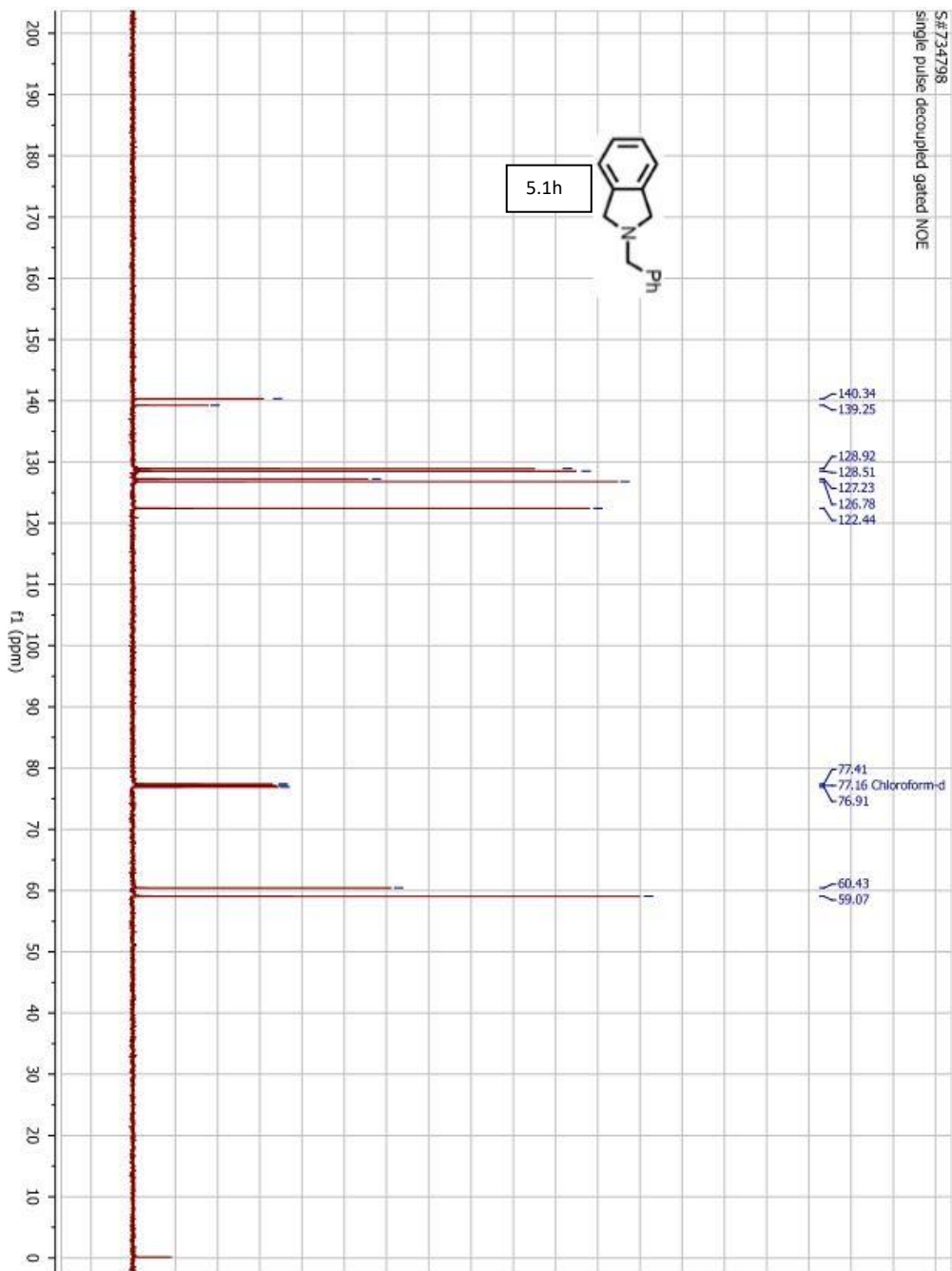


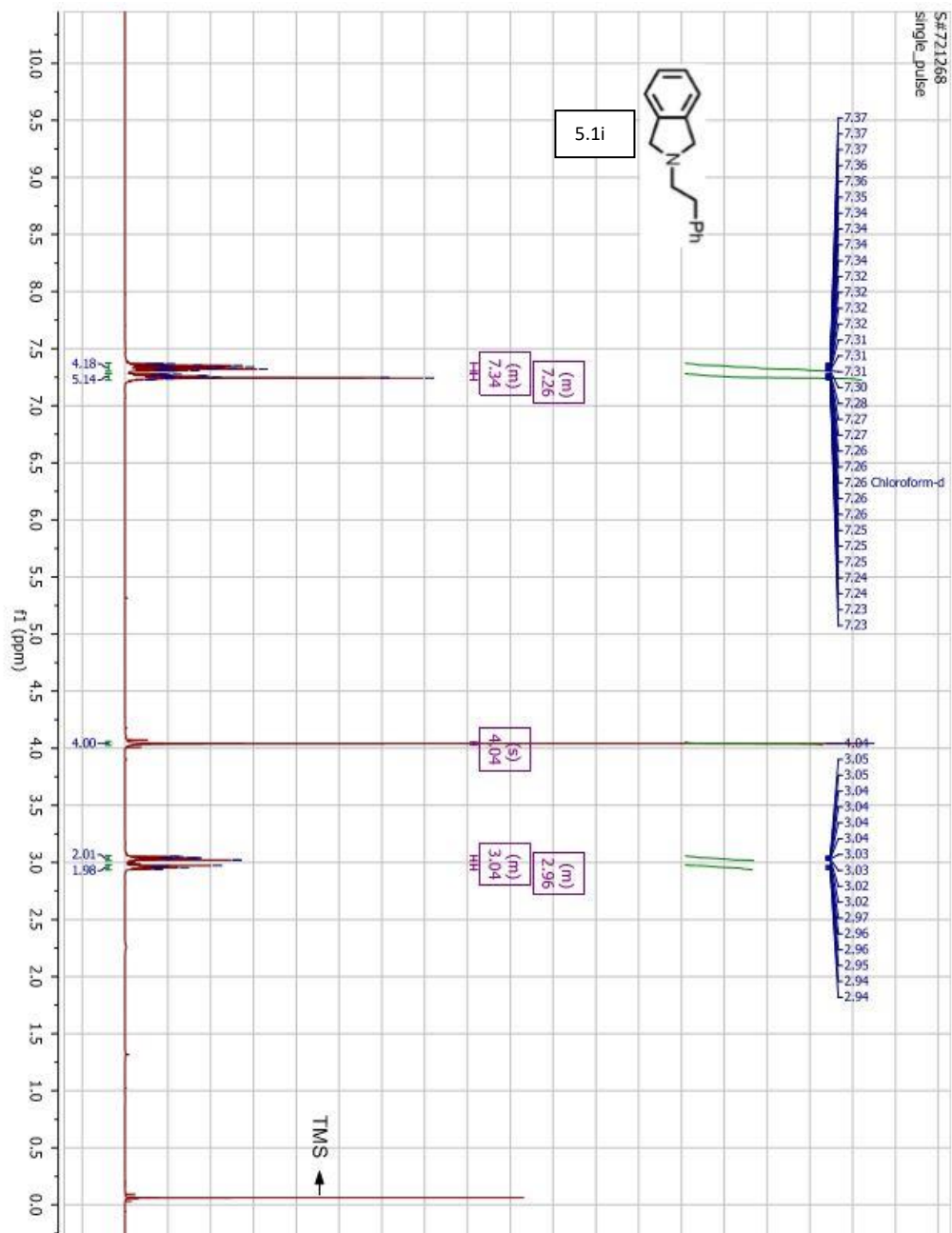




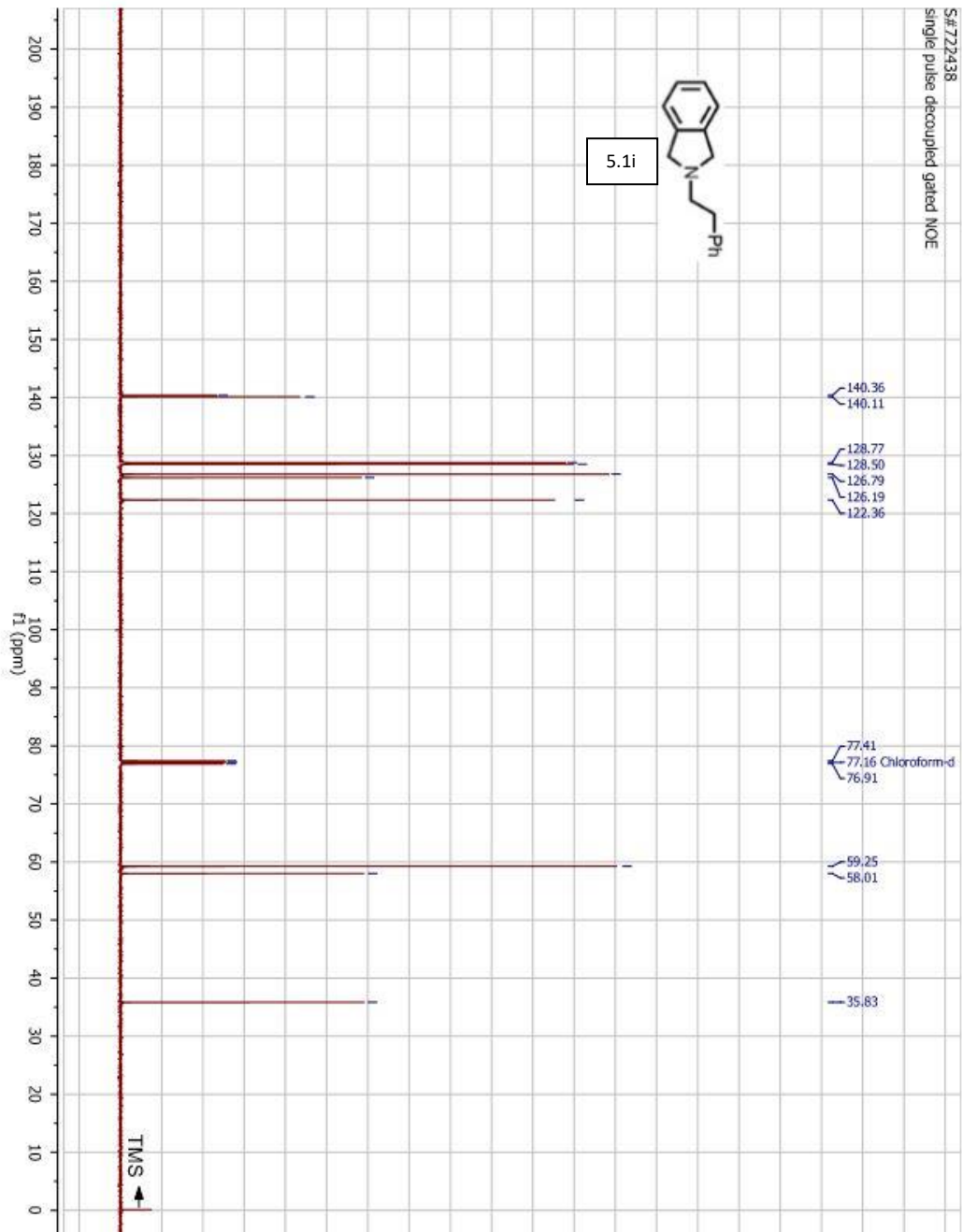
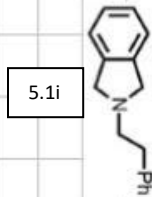


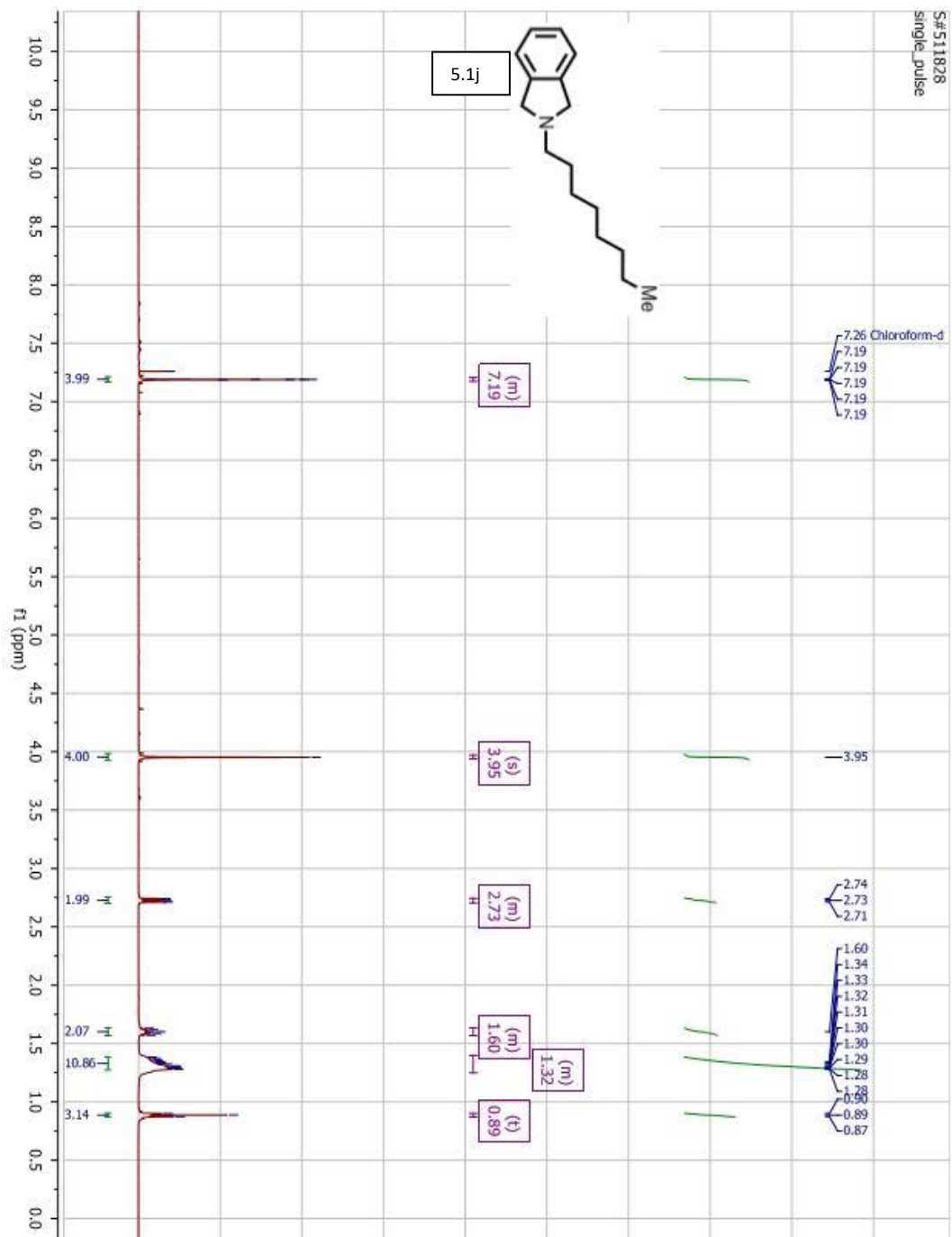
S# 734738
Single pulse decoupled gated NOE

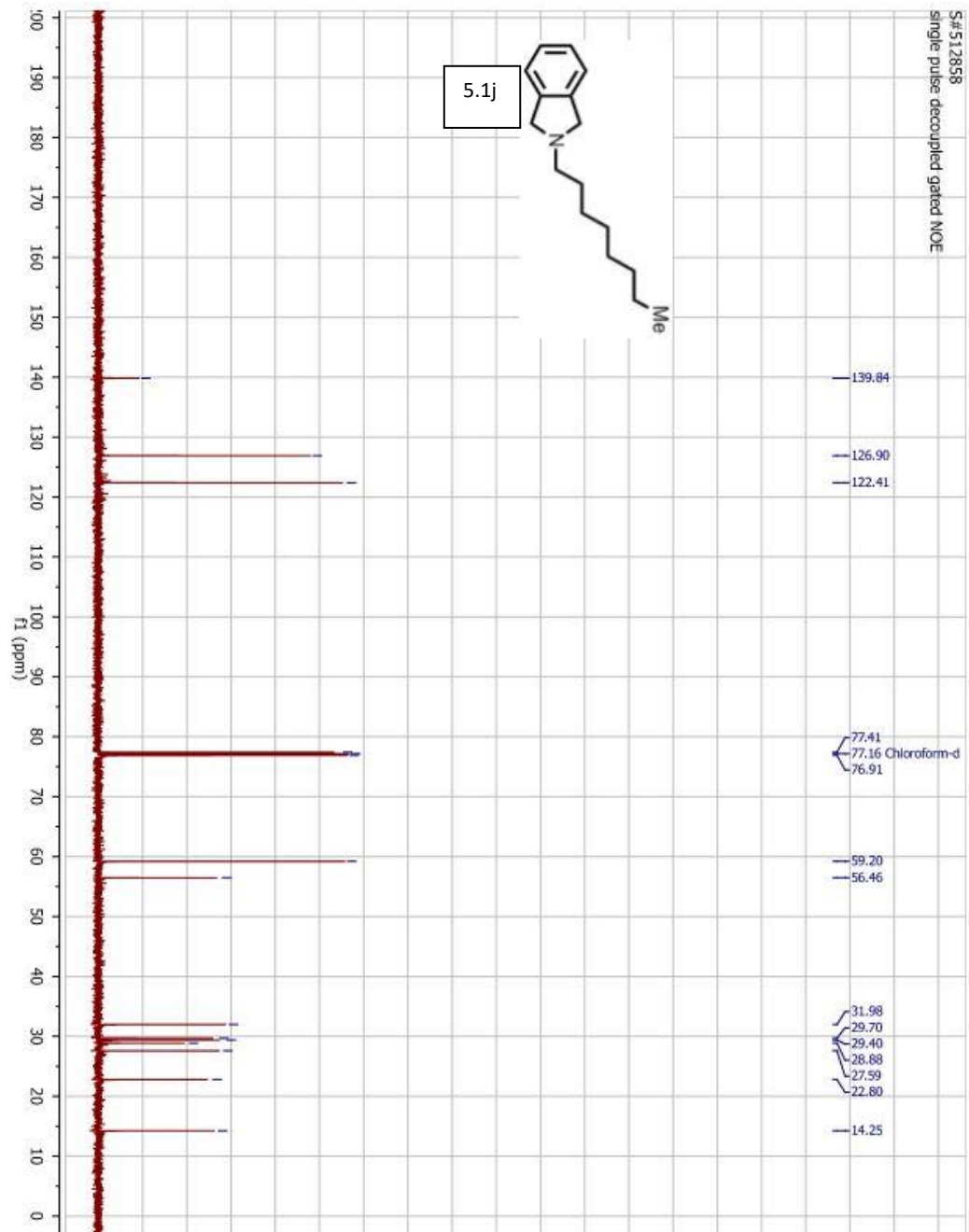


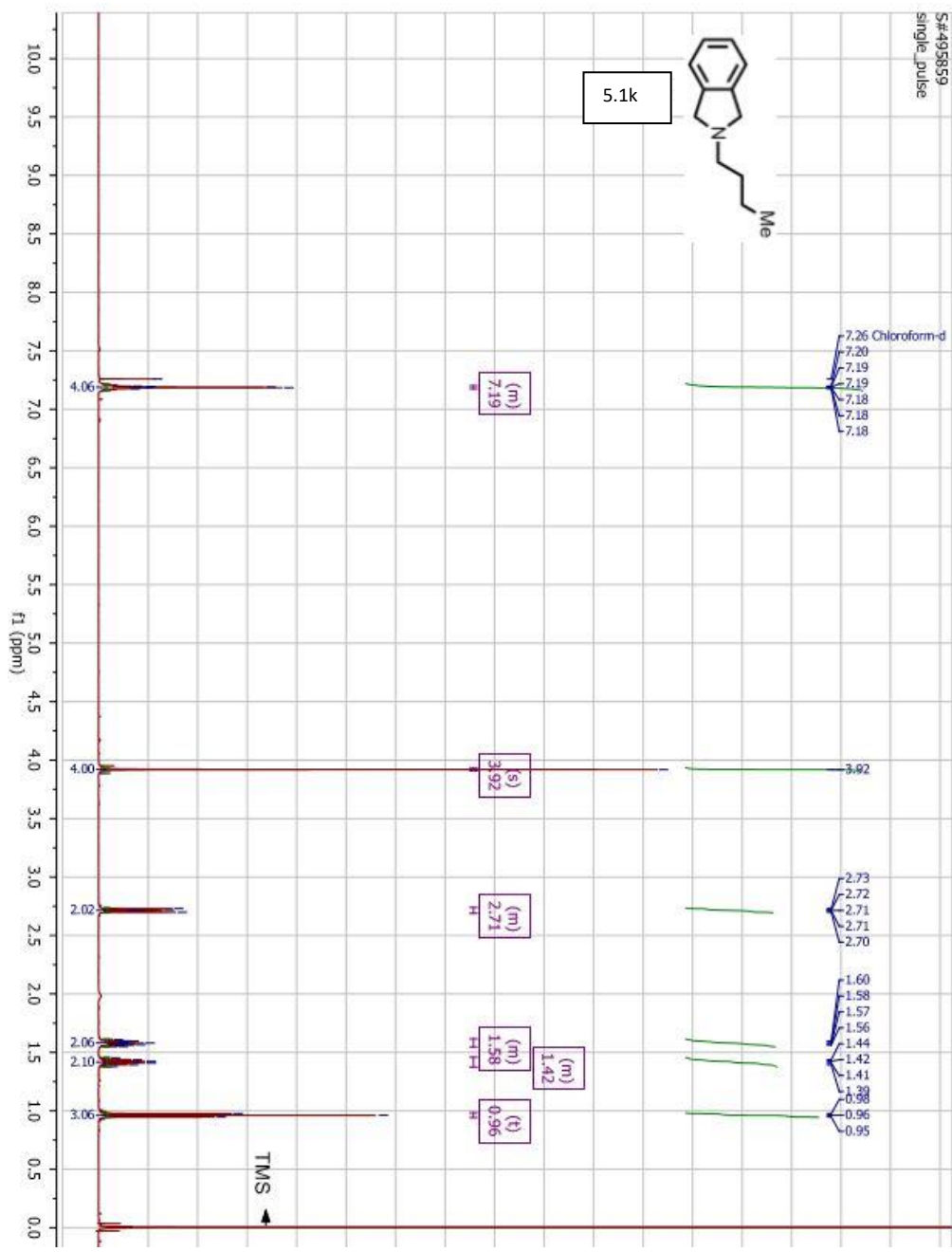


S#722438
Single pulse decoupled gated NOE

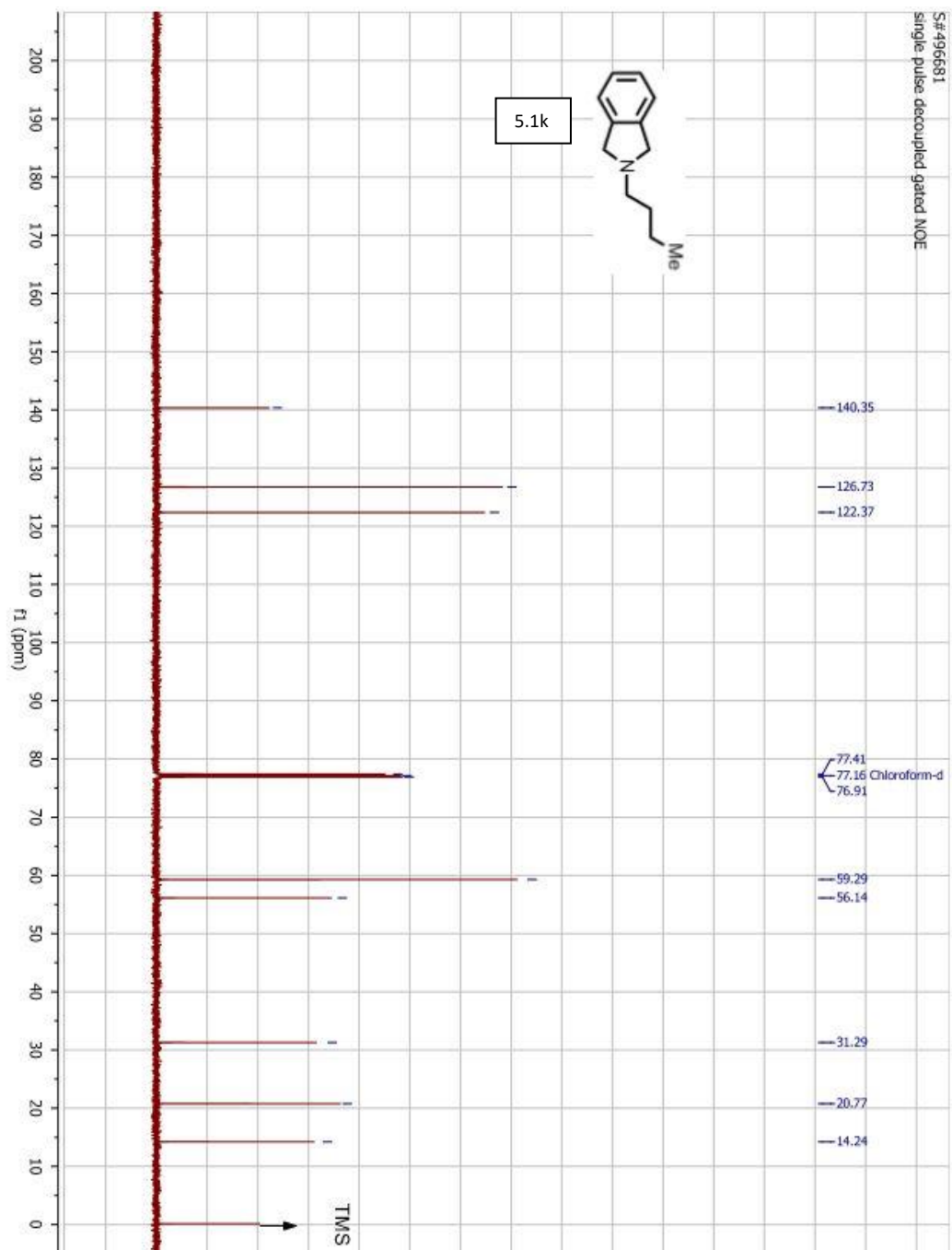




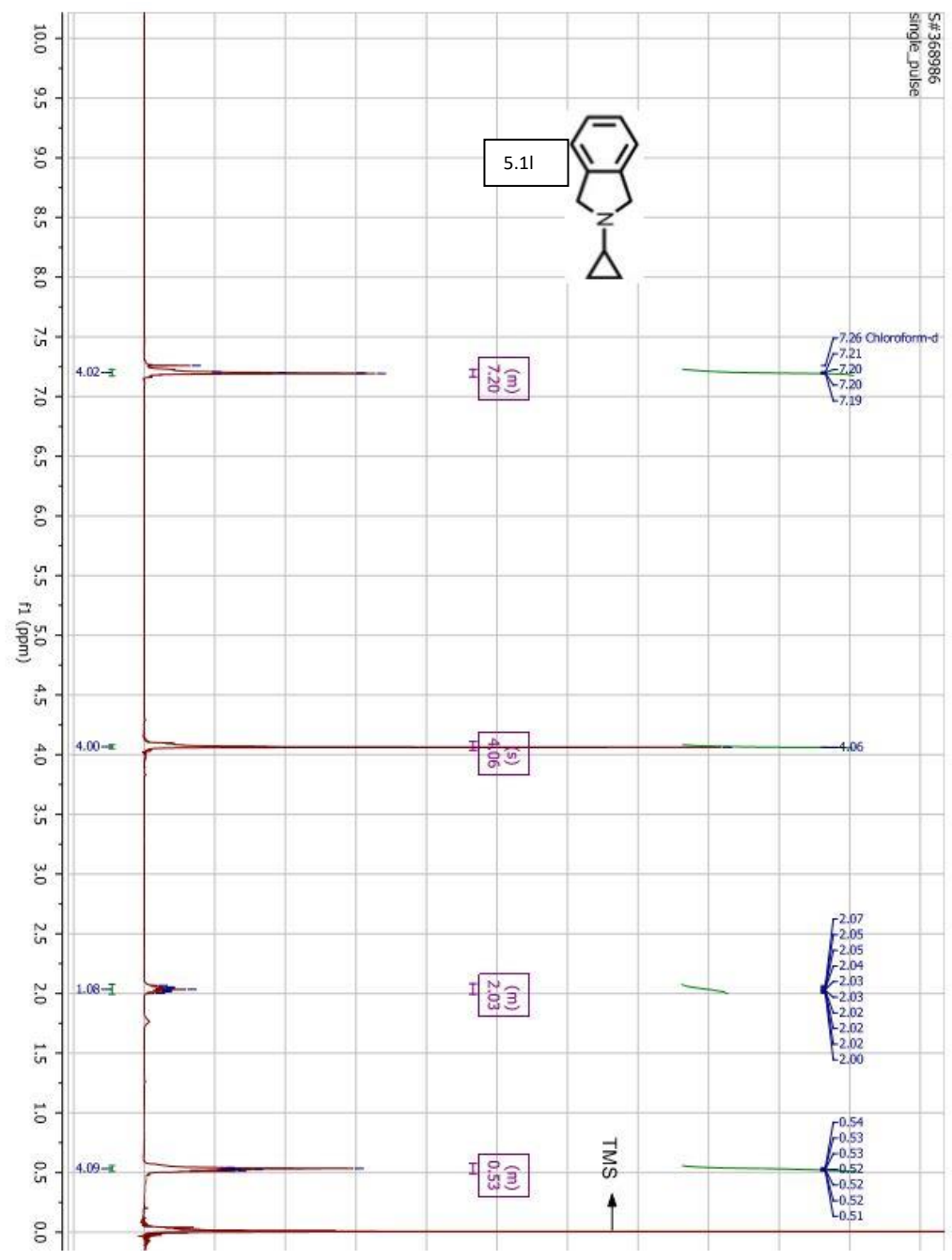




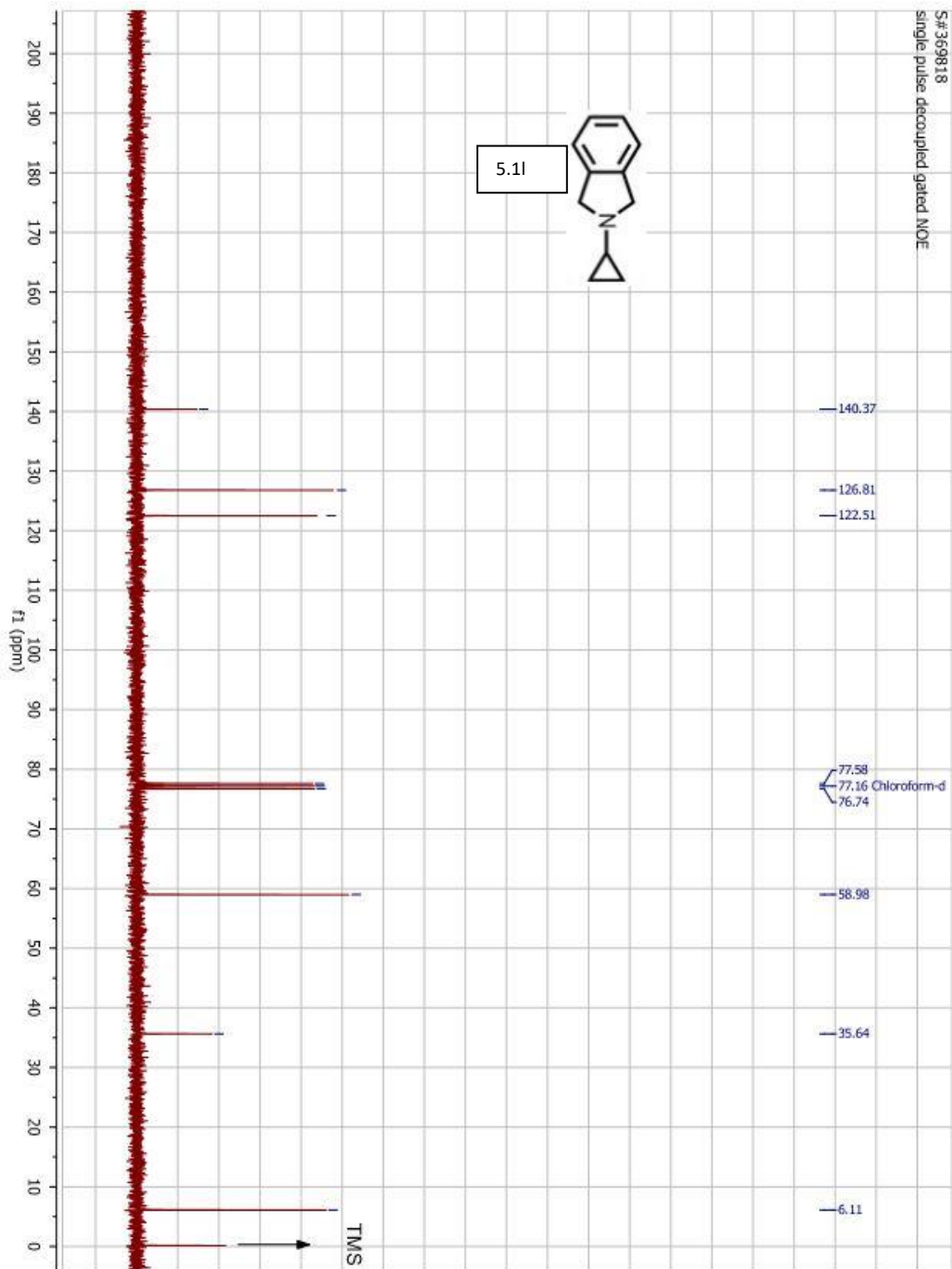
S#-496681
single pulse decoupled gated NOE



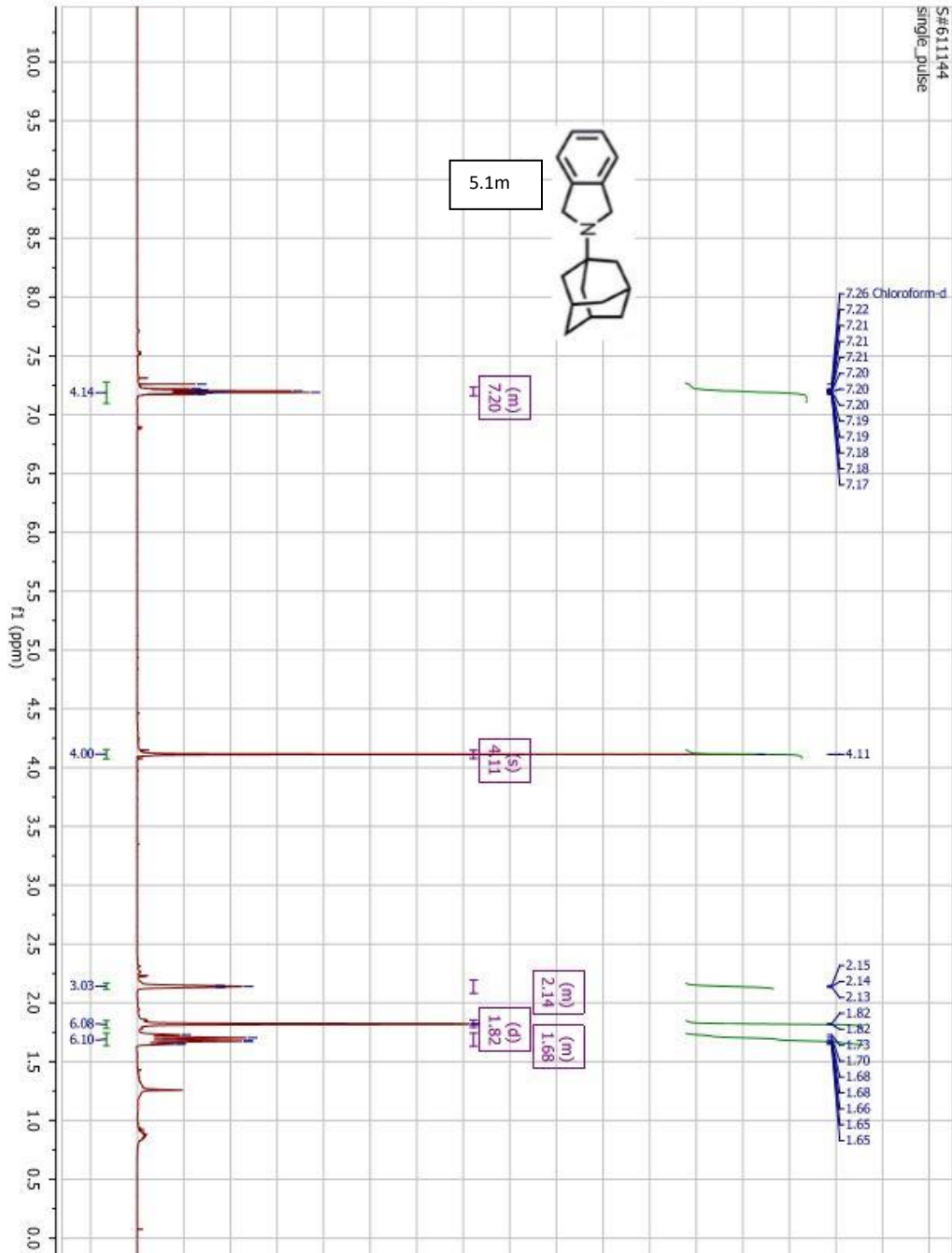
S#368986
single_pulse



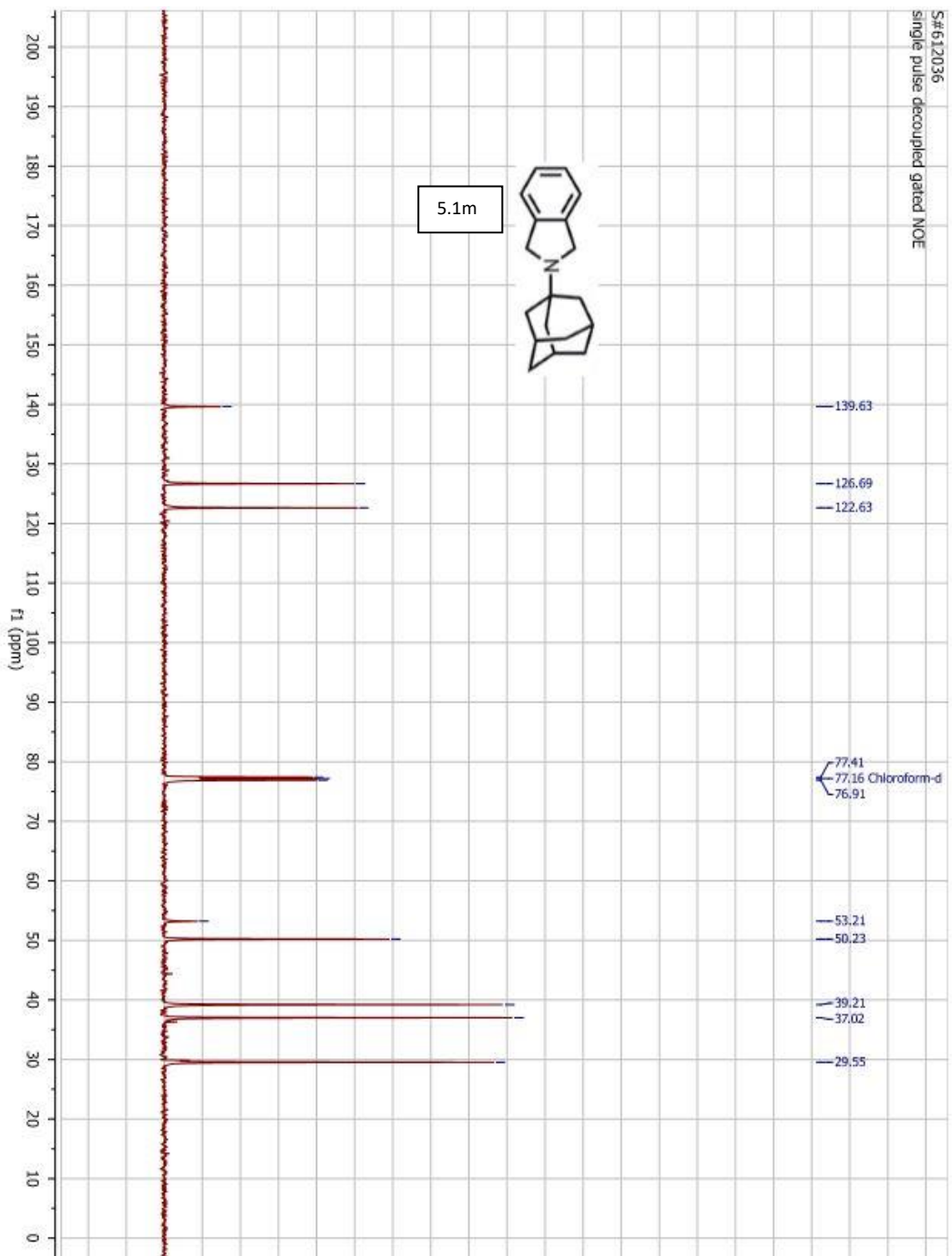
S#369818
Single pulse decoupled gated NOE

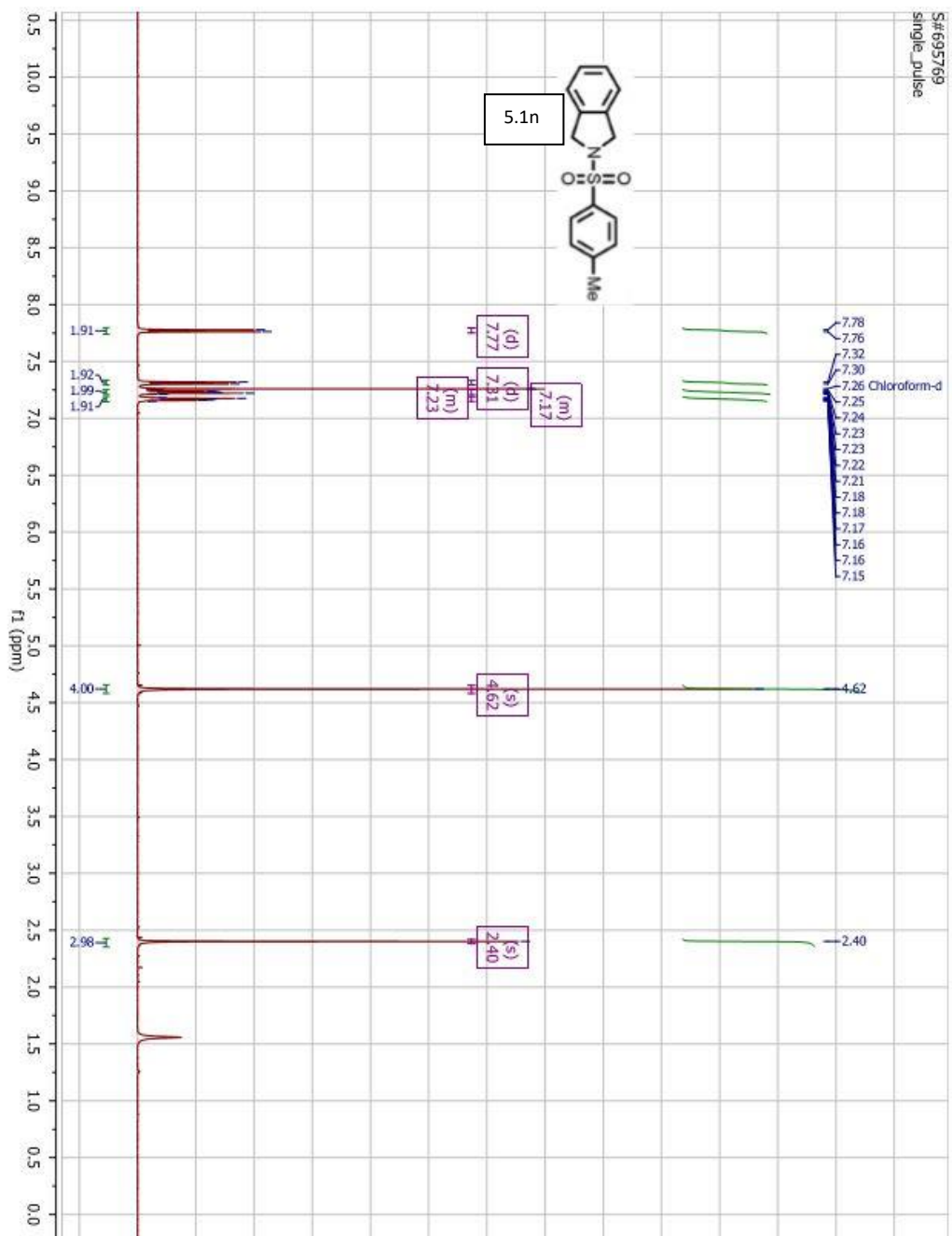


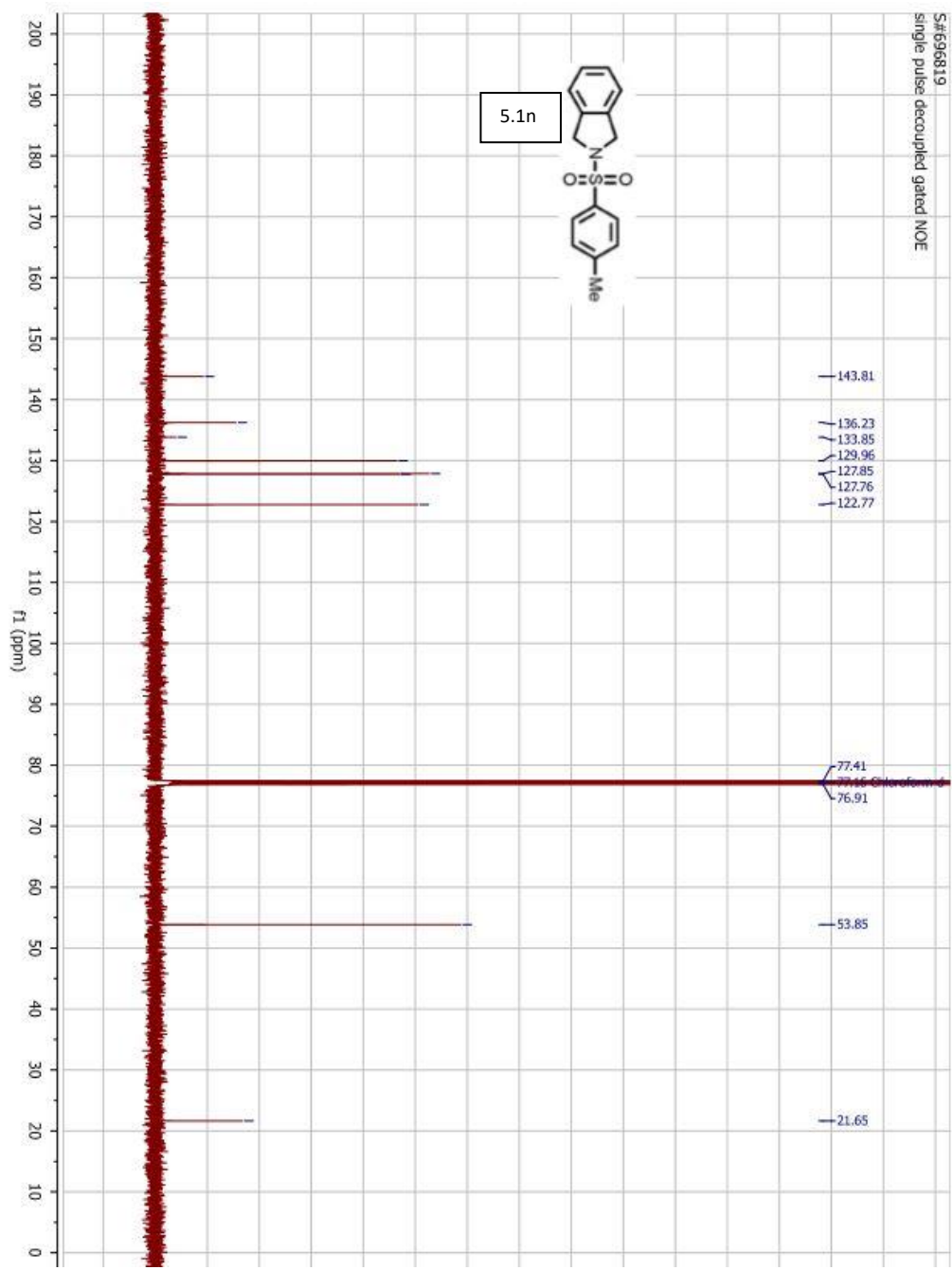
S#611144
single_pulse

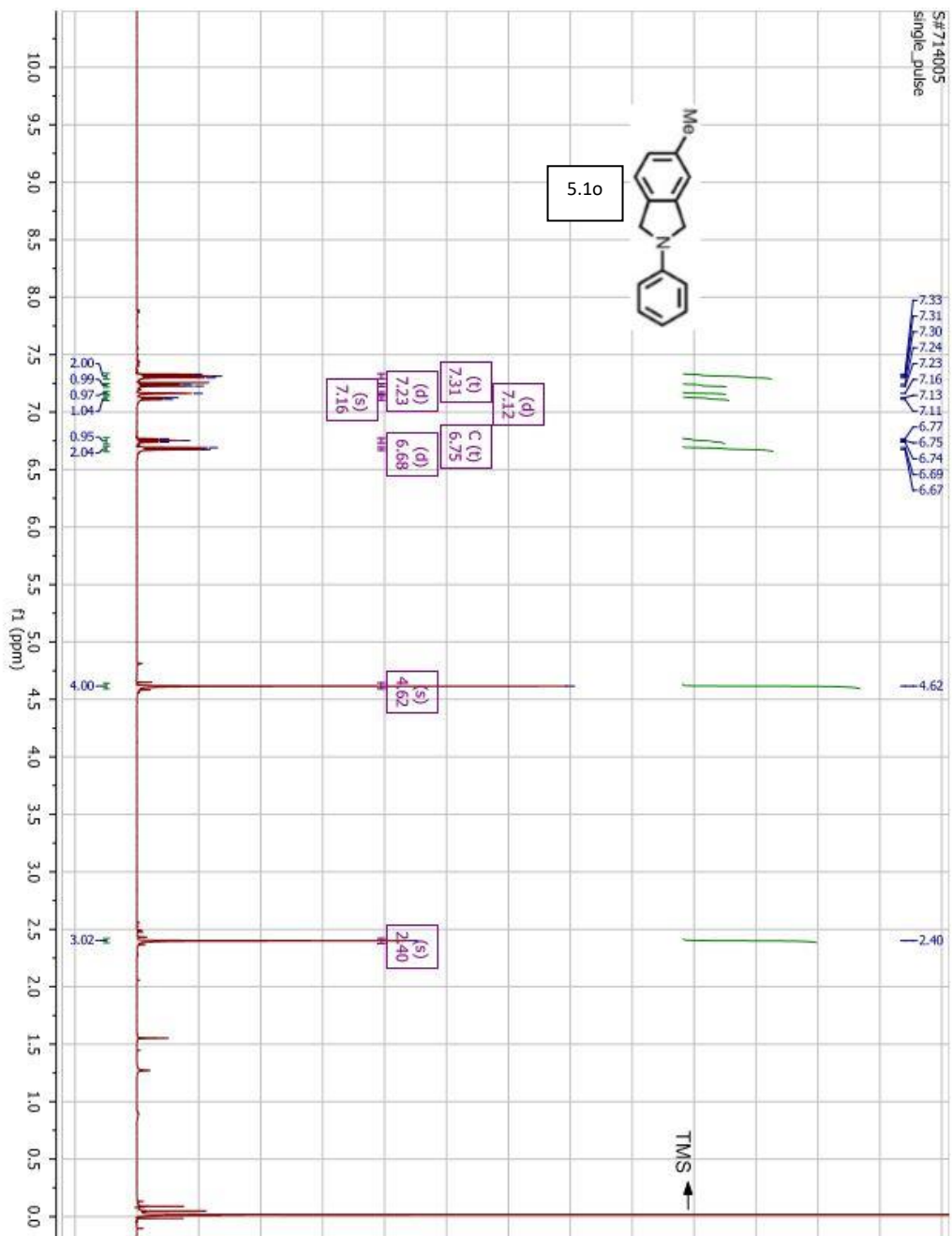


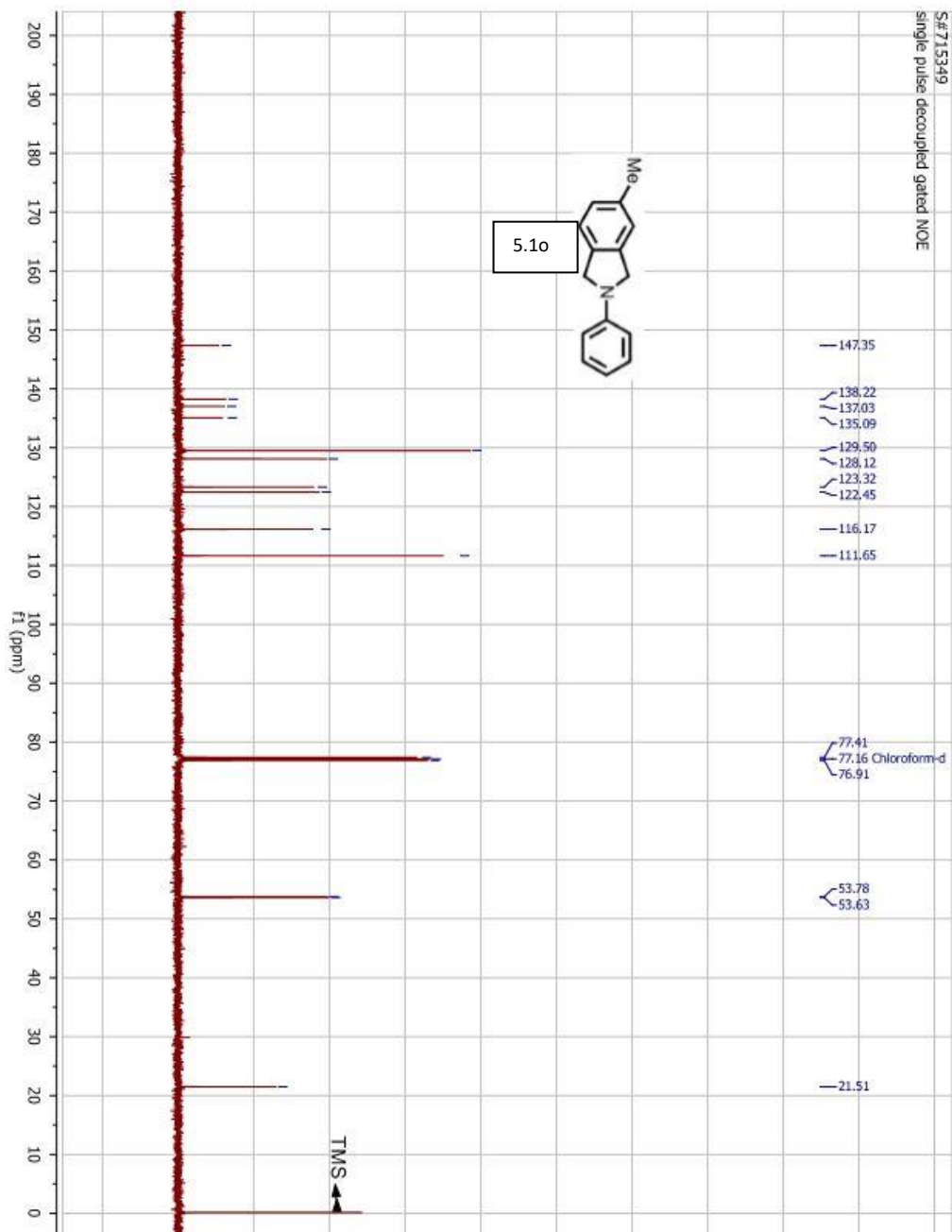
S#612036
single pulse decoupled gated NOE



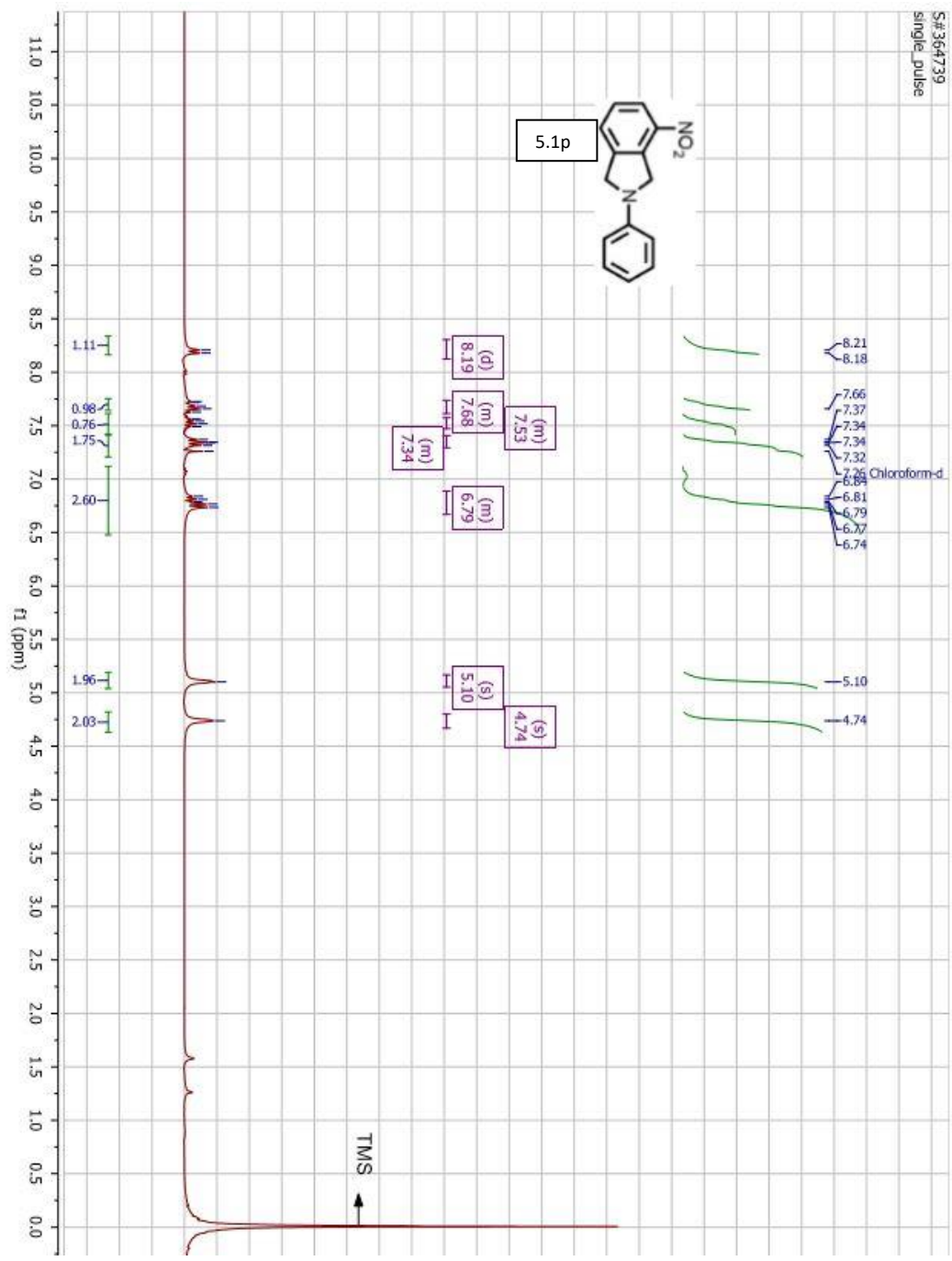
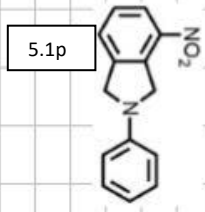




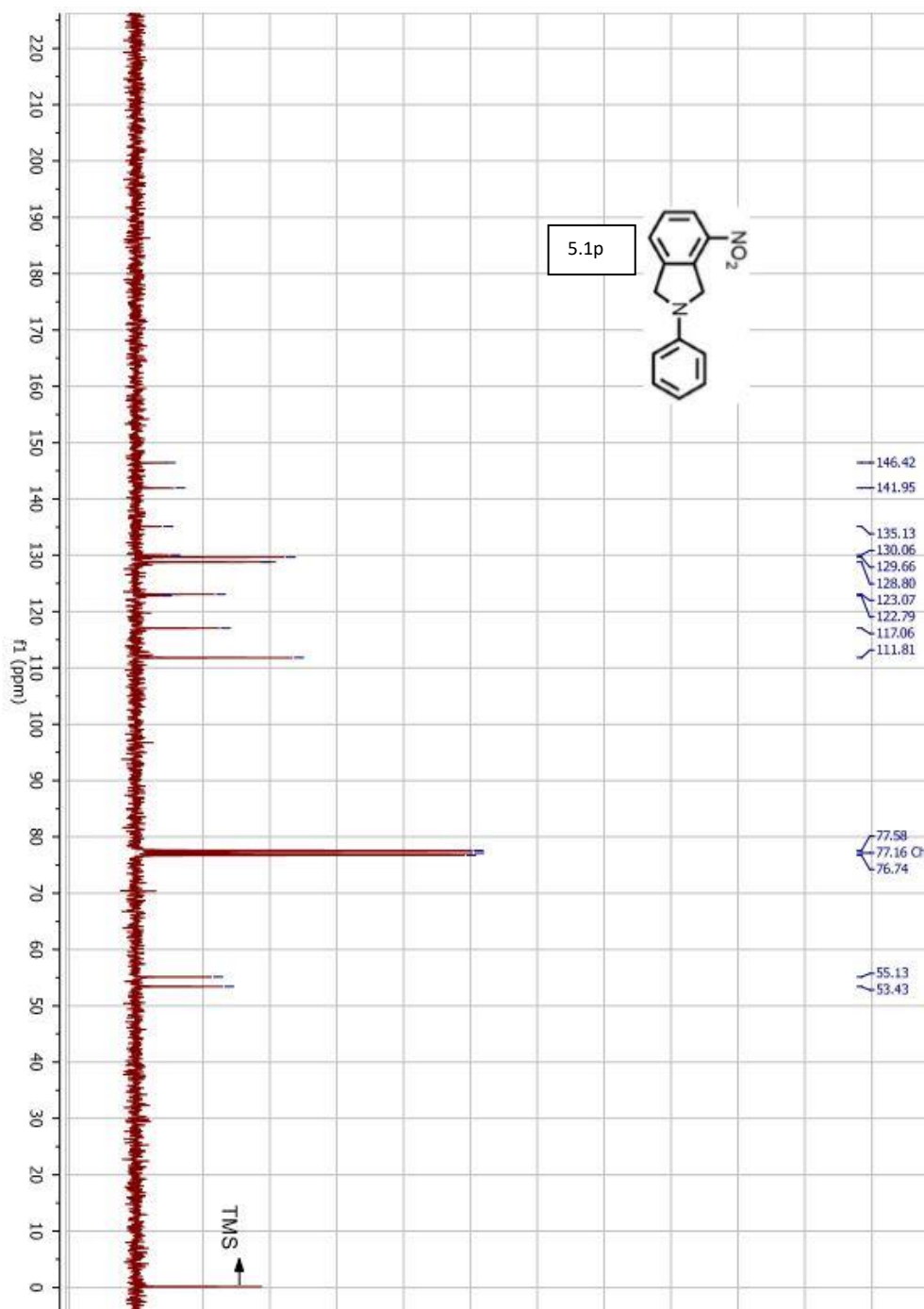
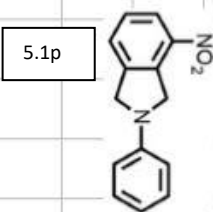




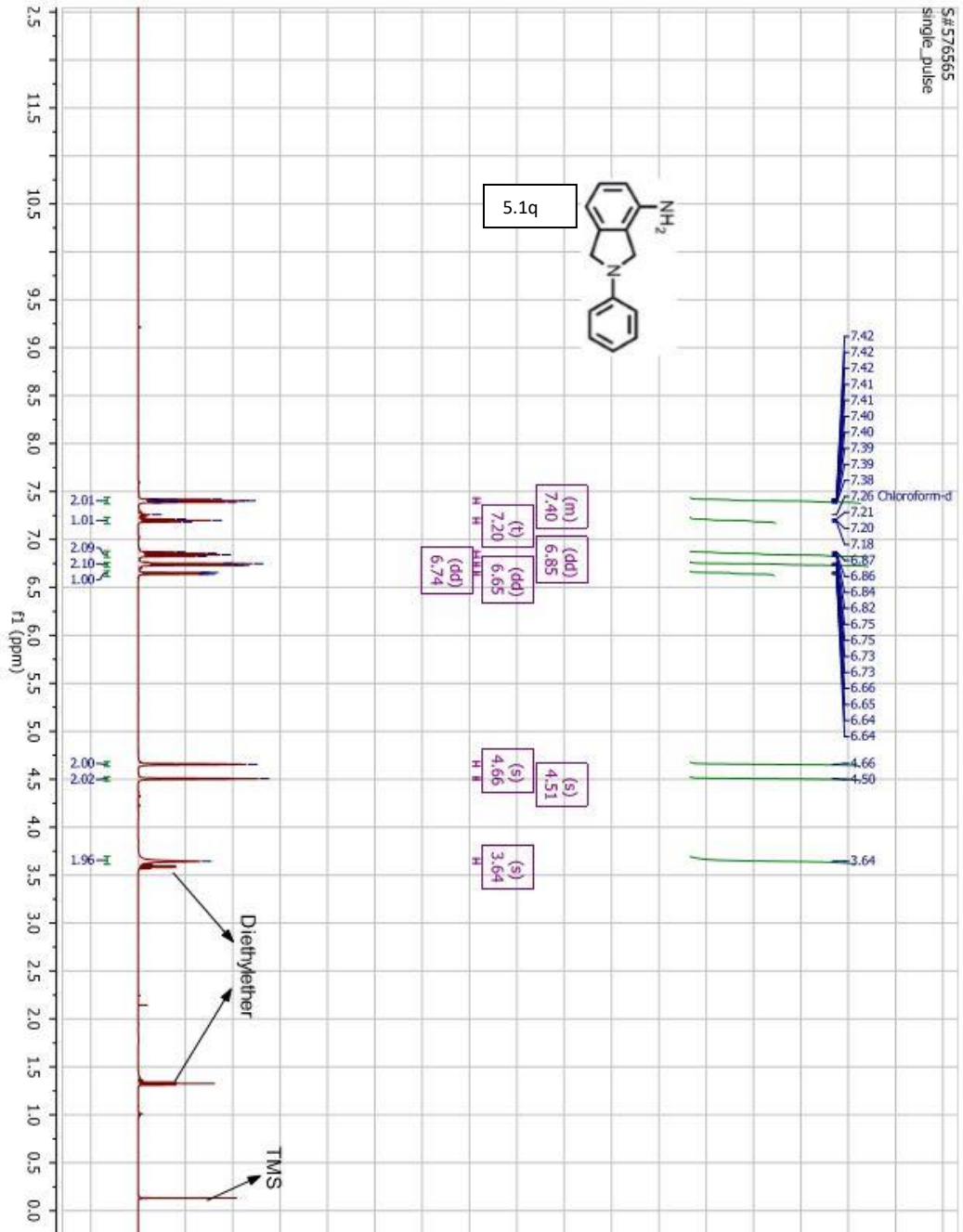
S#364739
single_pulse



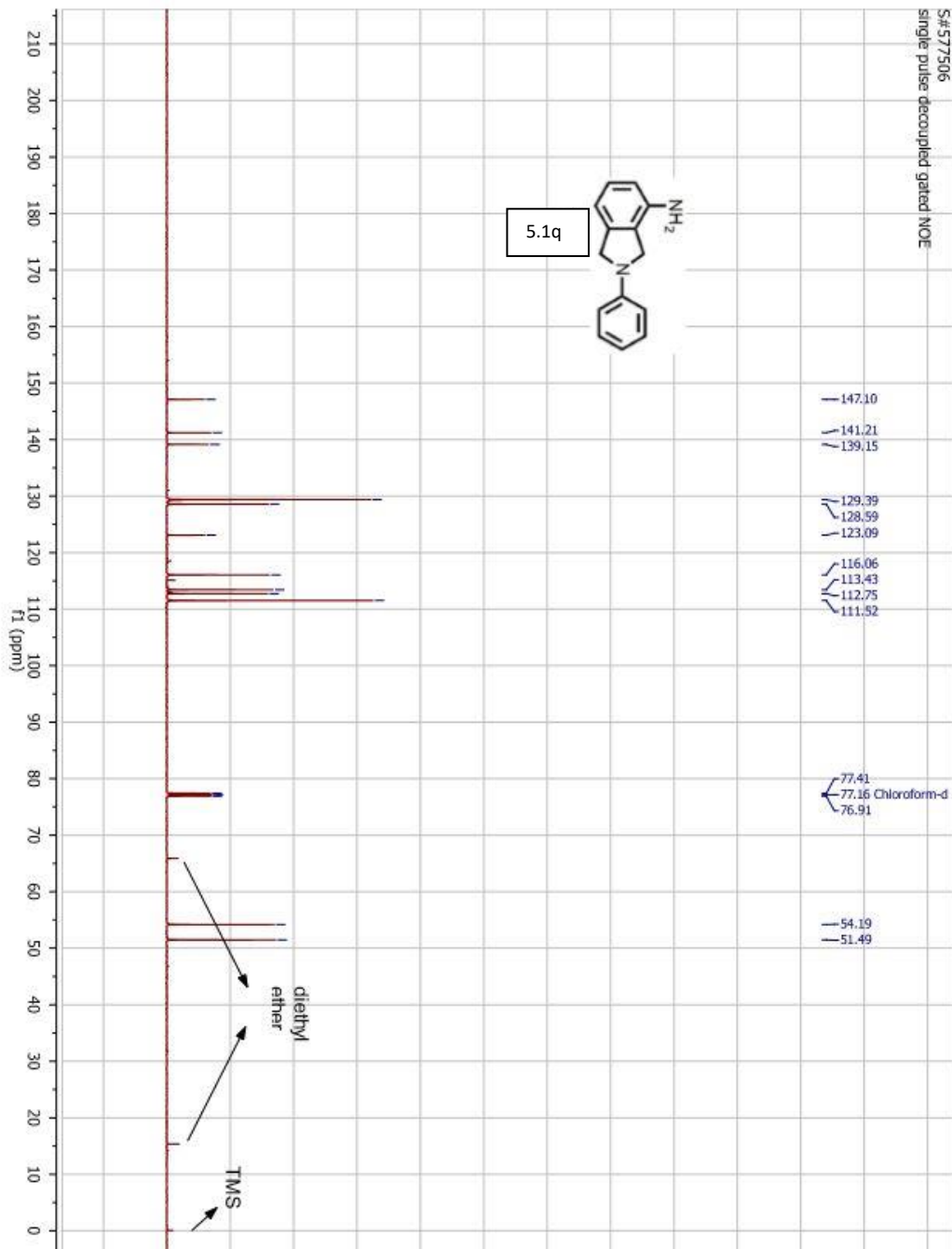
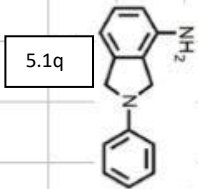
S#365751
single pulse decoupled gated NOE



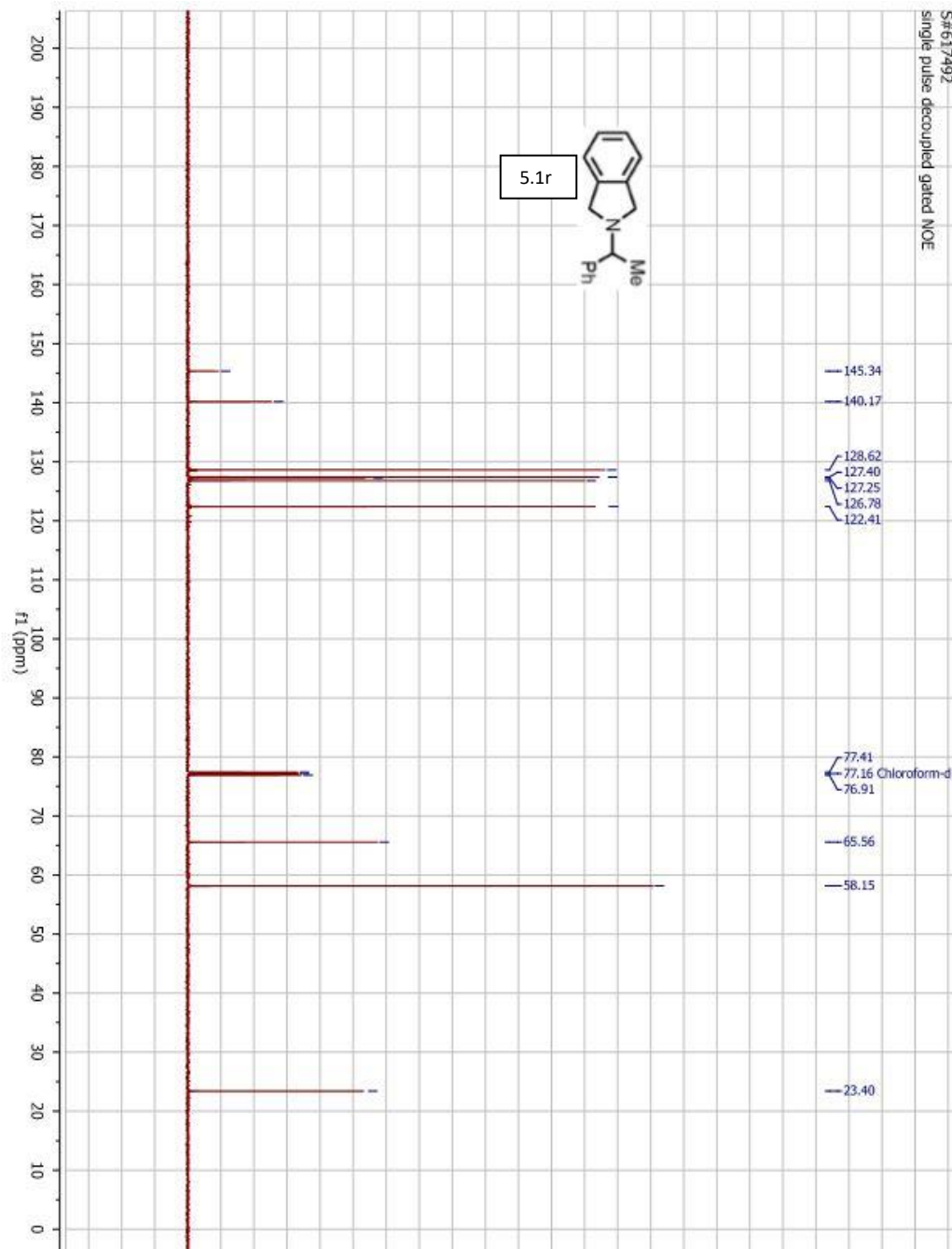
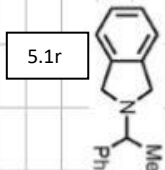
S# 576565
single_pulse



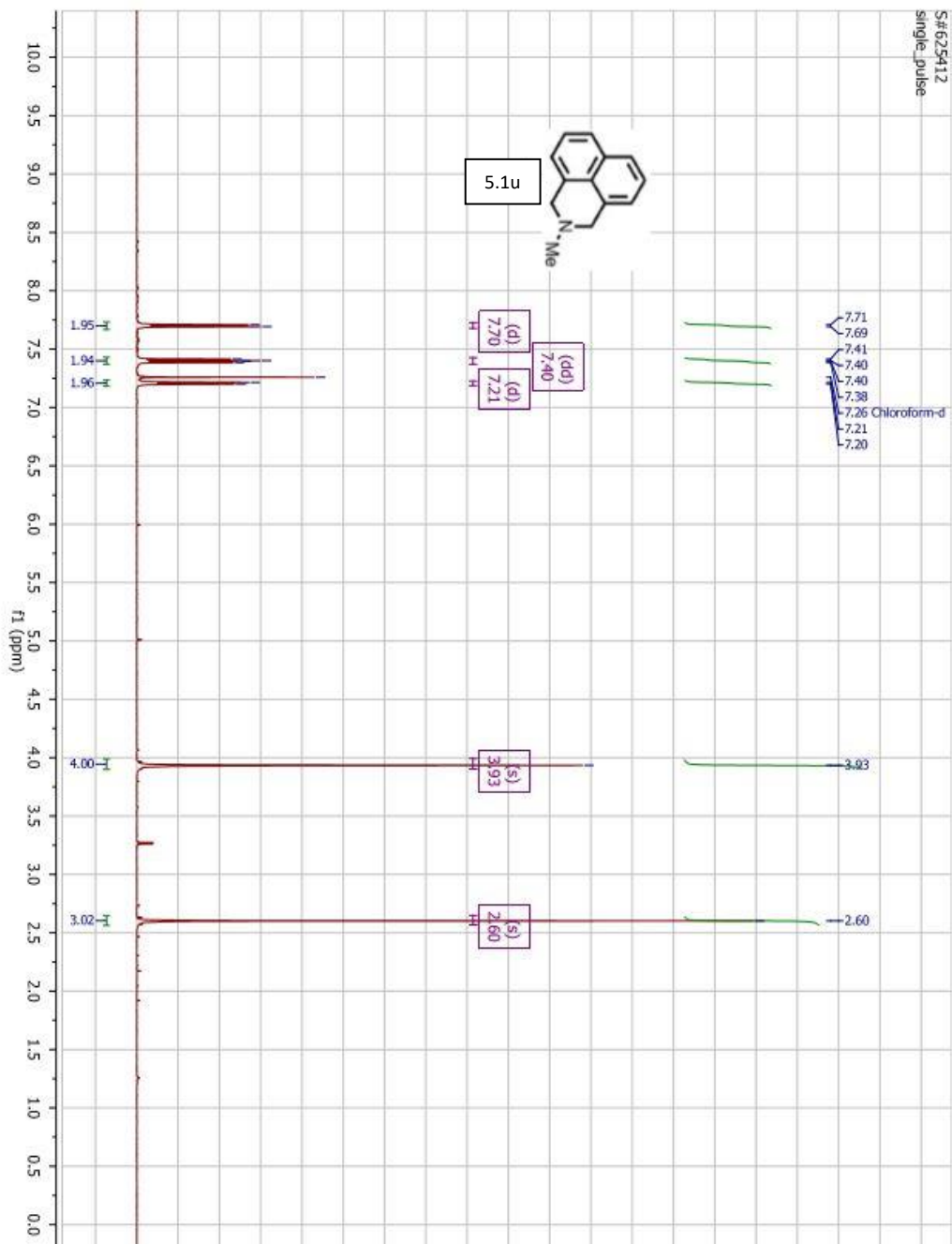
S# 577506
single pulse decoupled gated NOE



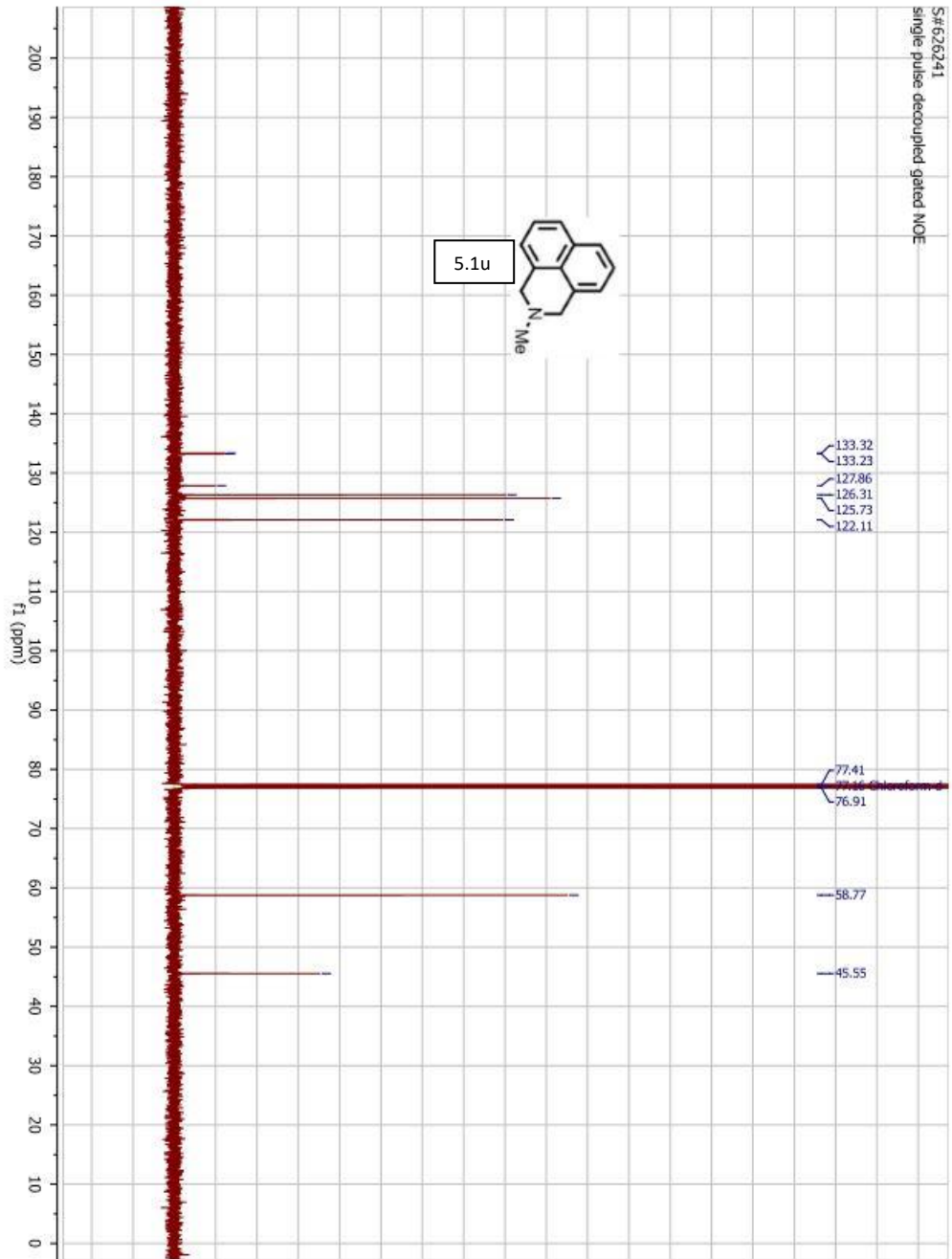
S#617492
single pulse decoupled gated NOE



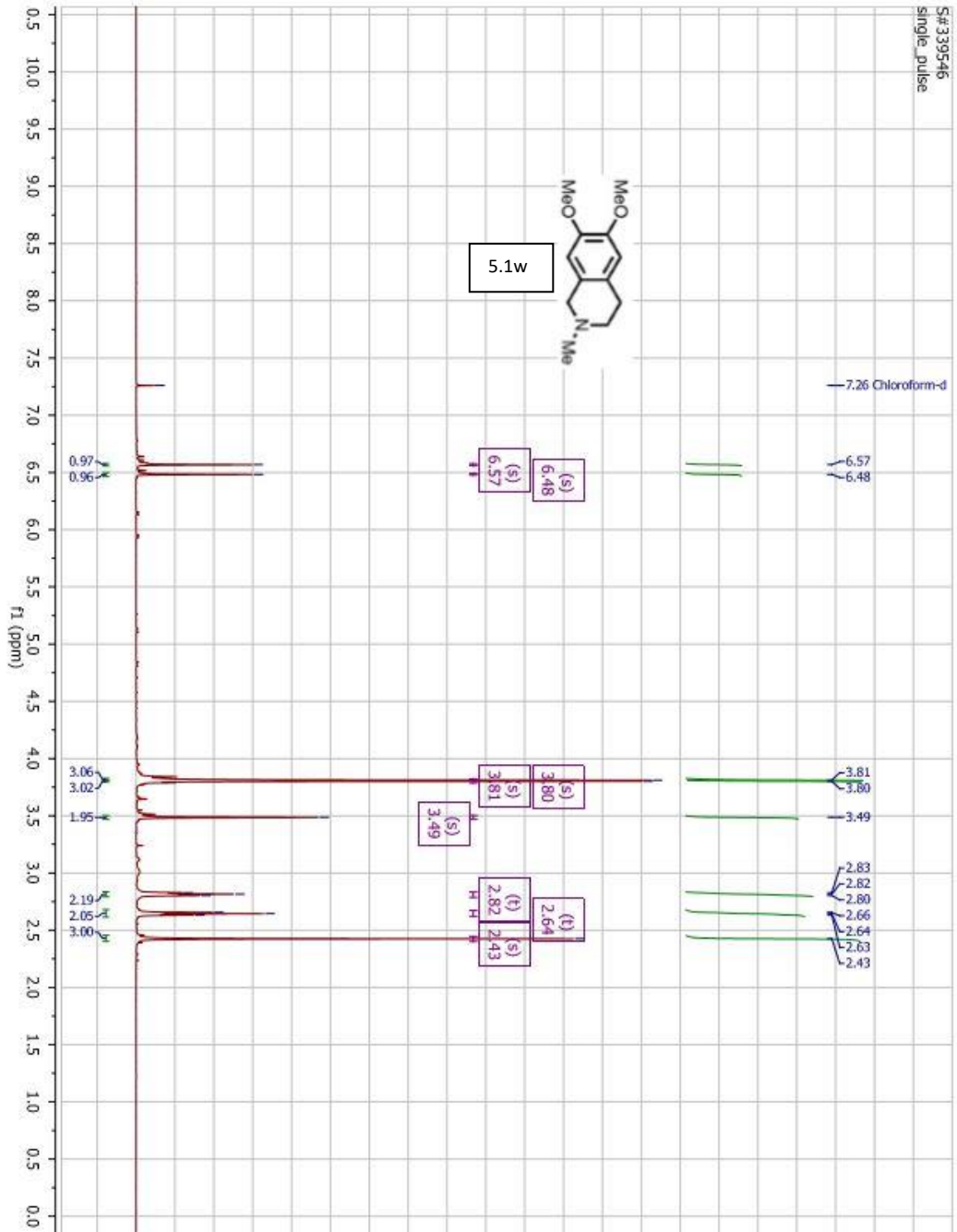
S# 625412
single_pulse



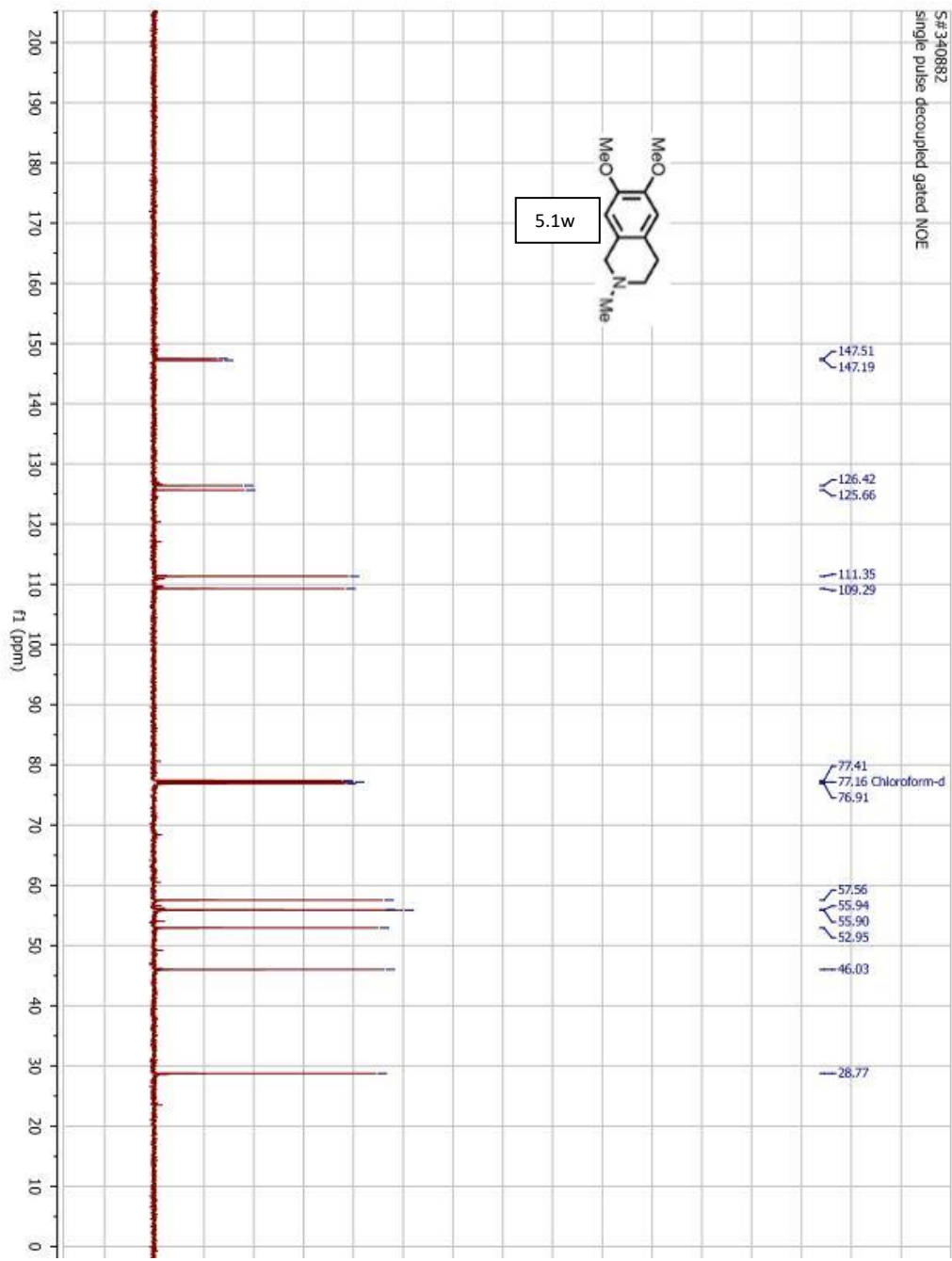
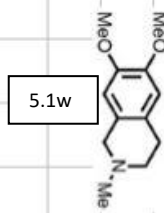
S#626241
single pulse decoupled gated NOE

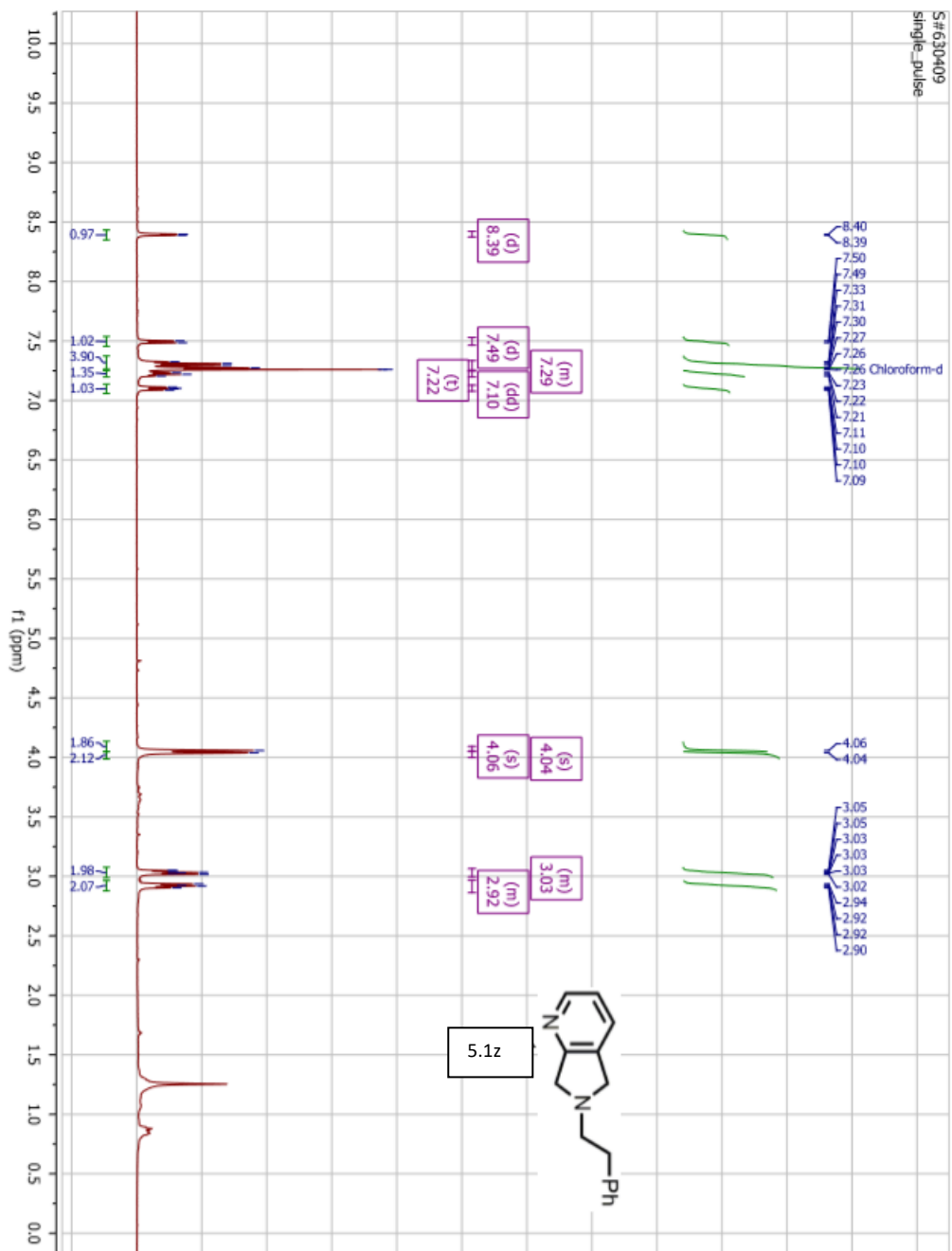


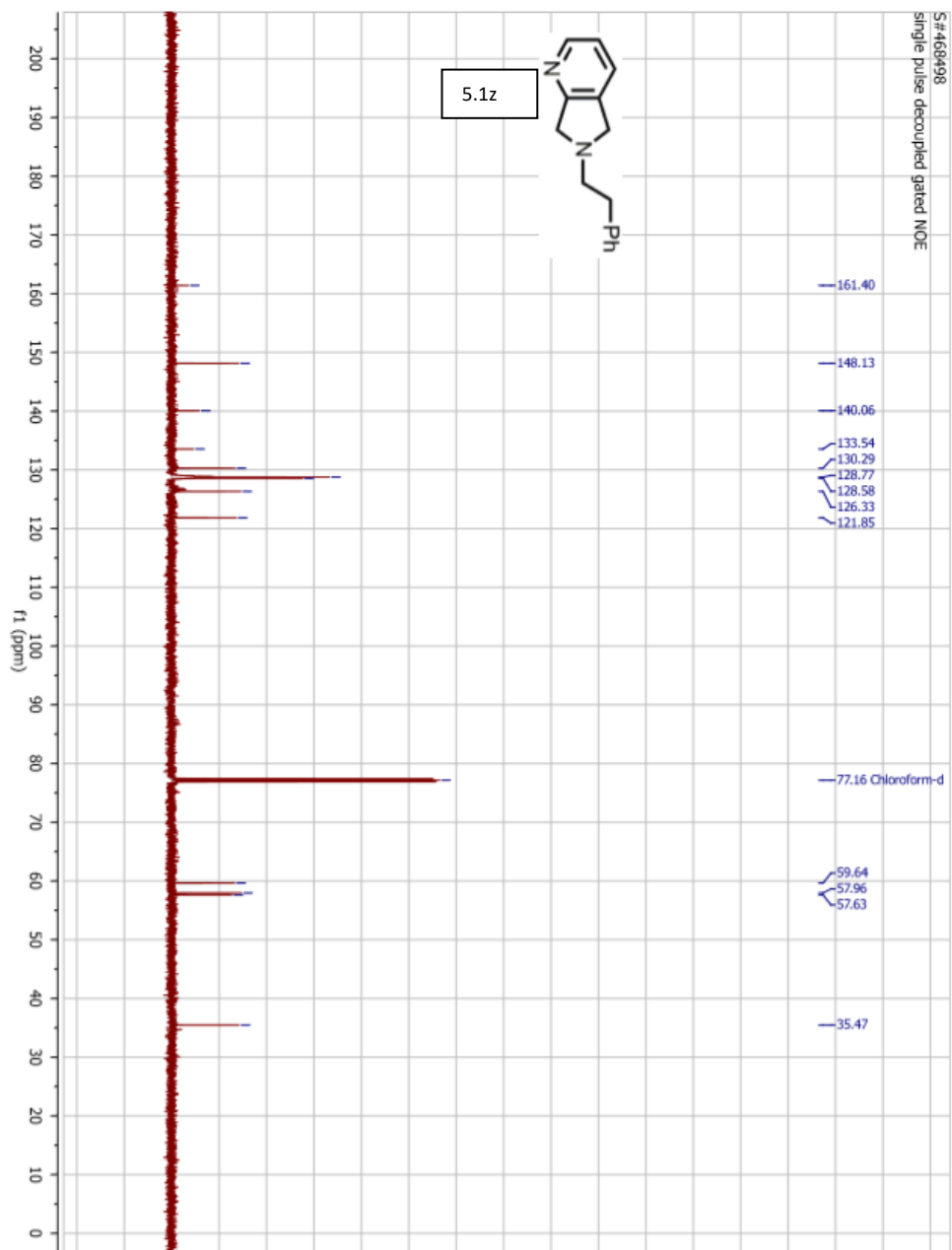
S#339546
single_pulse

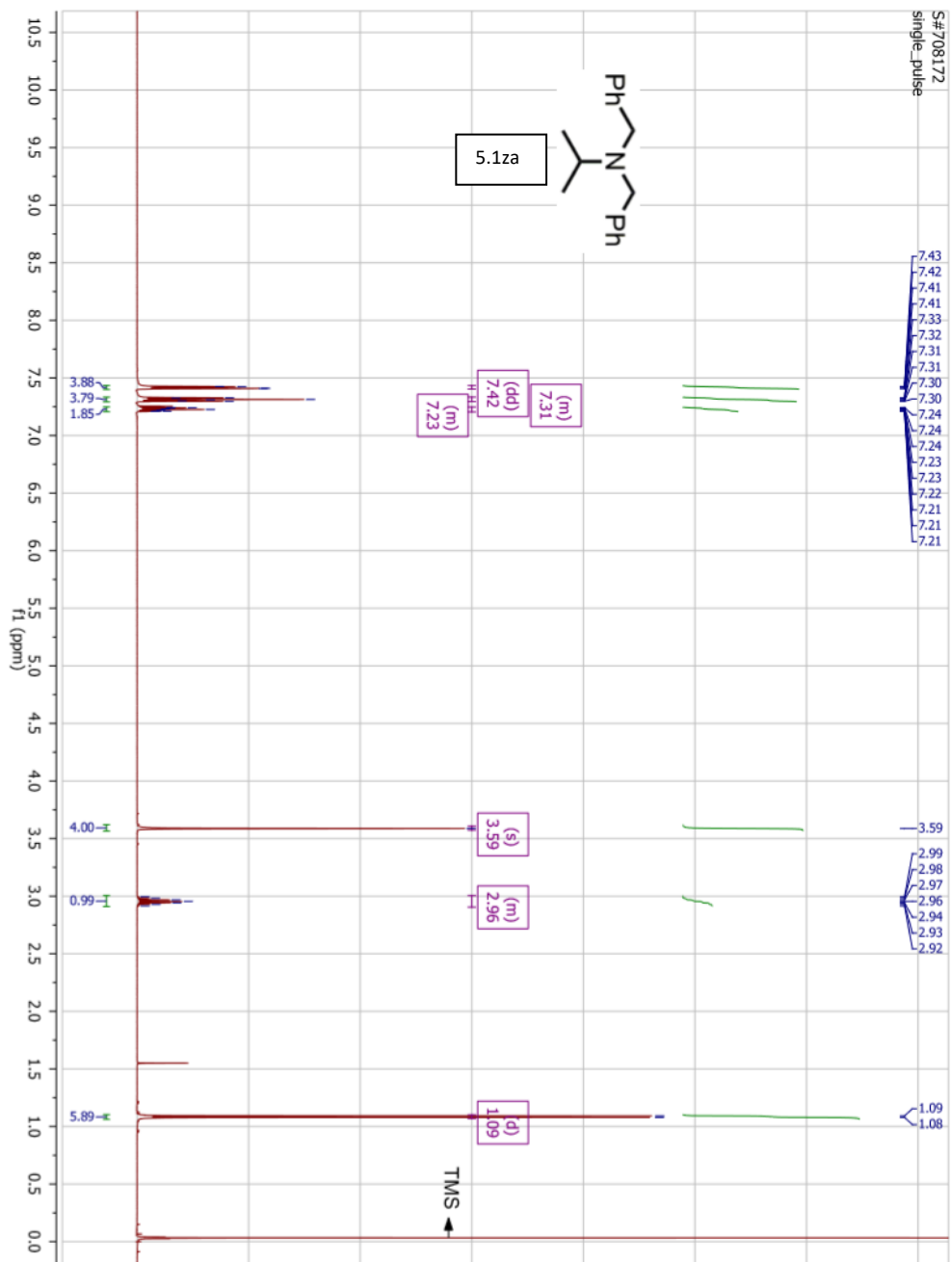


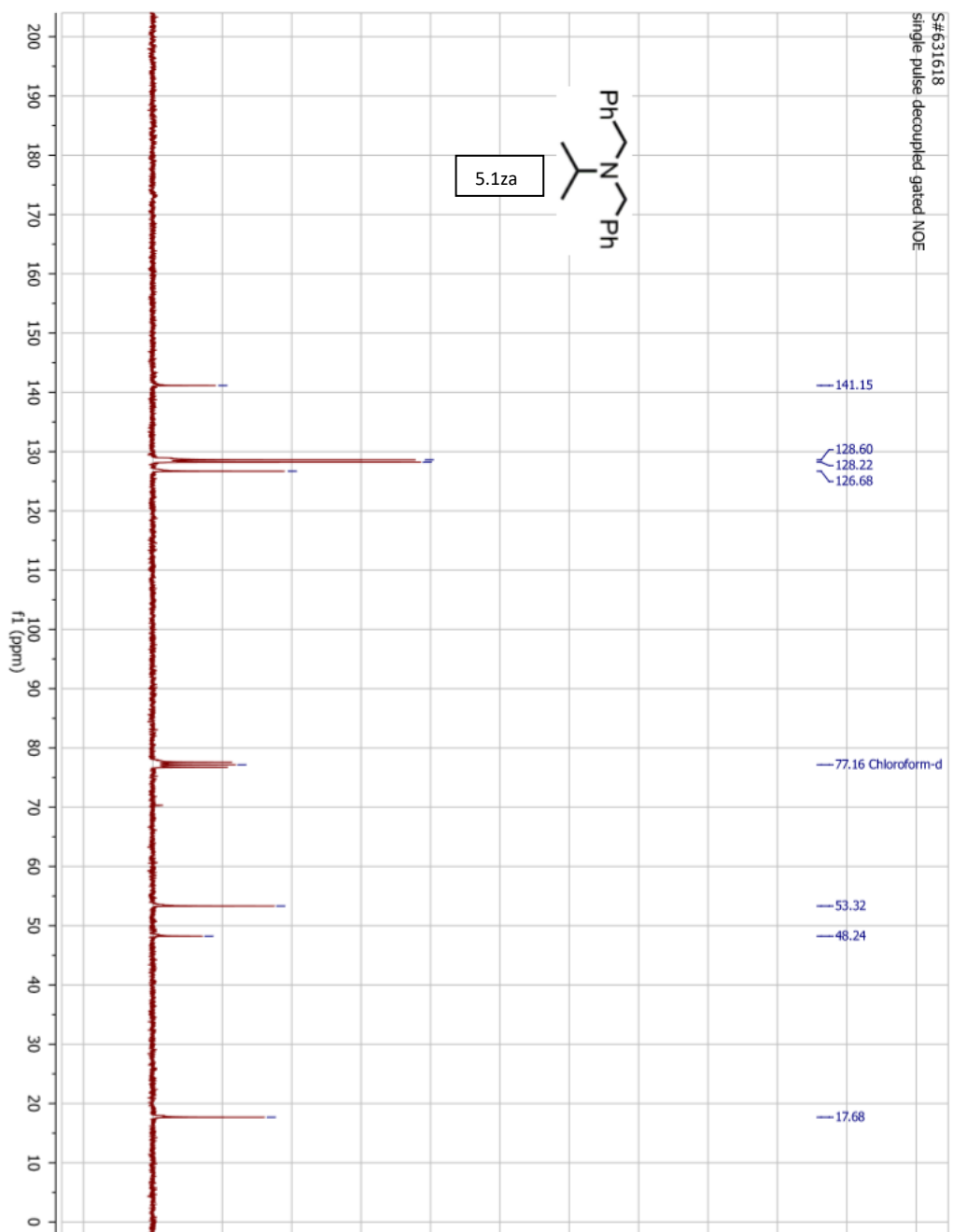
S#340882
single pulse decoupled gated NOE

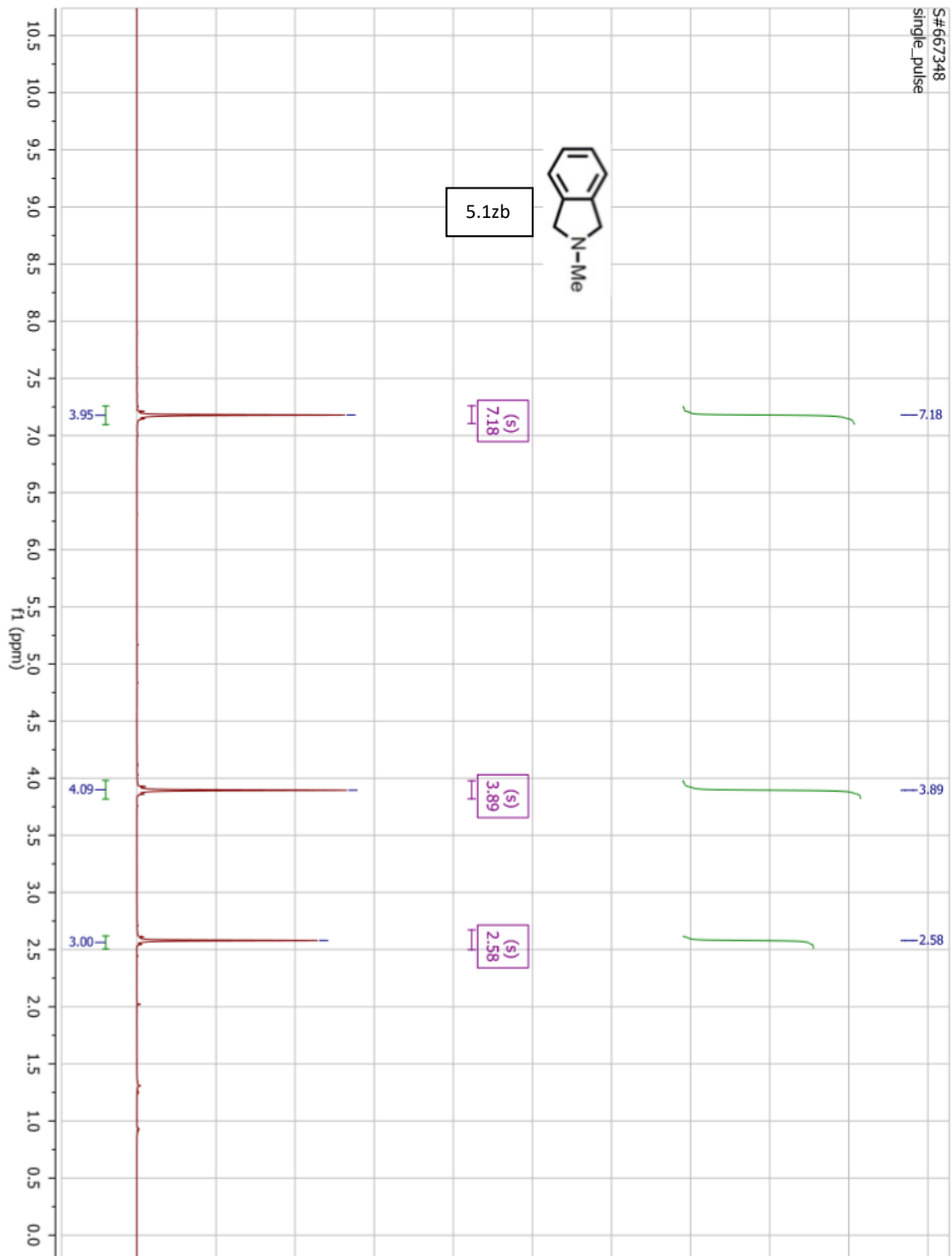


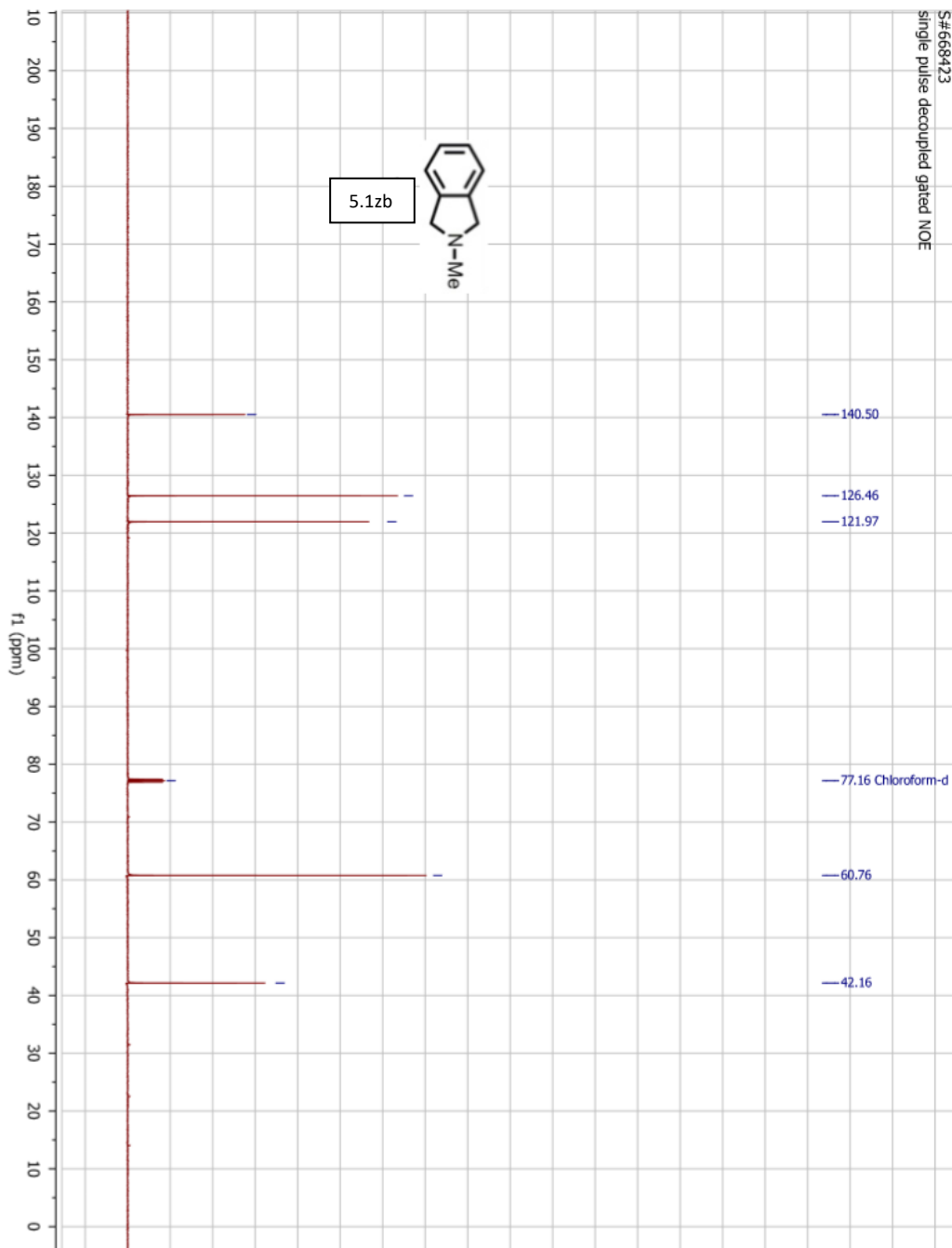


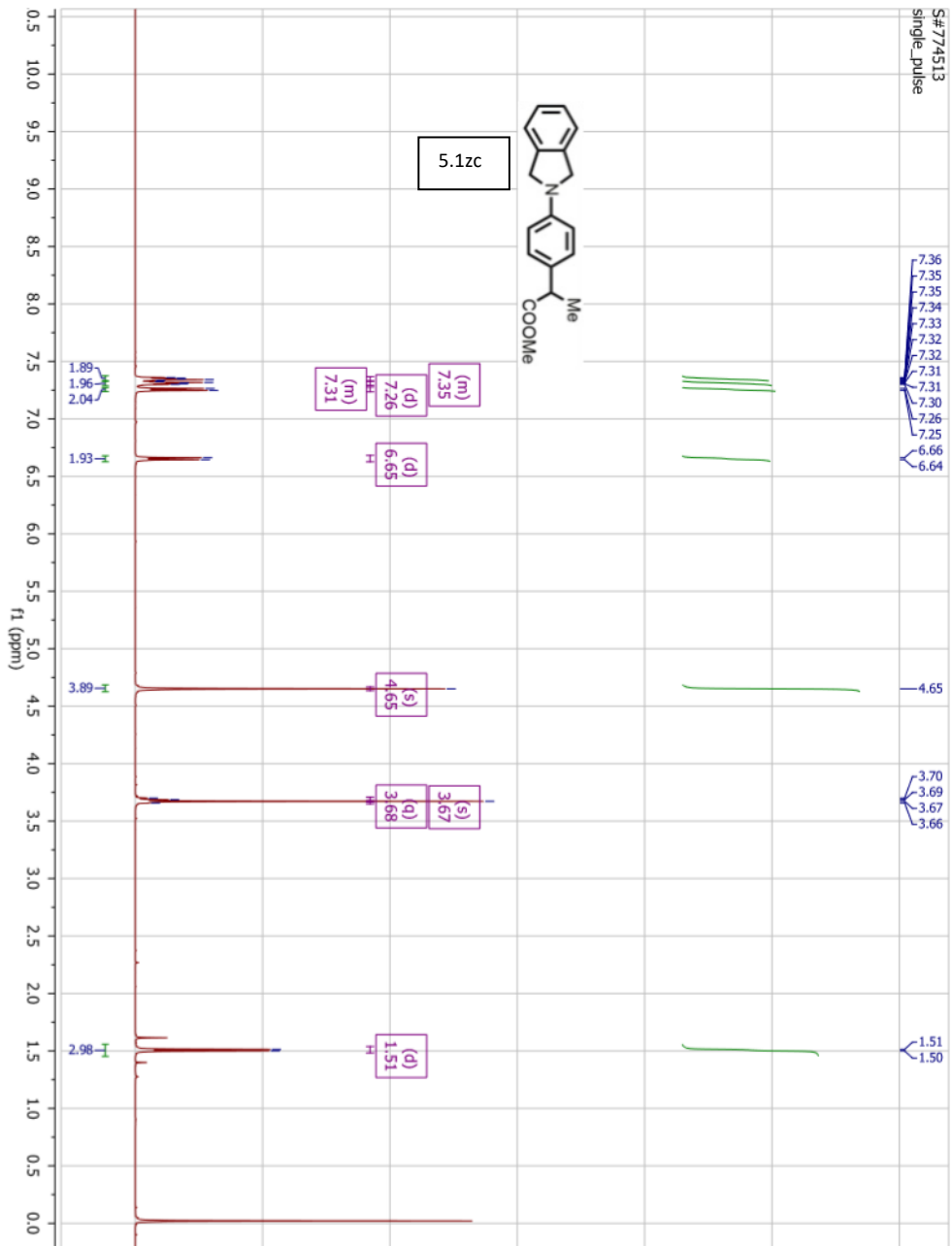


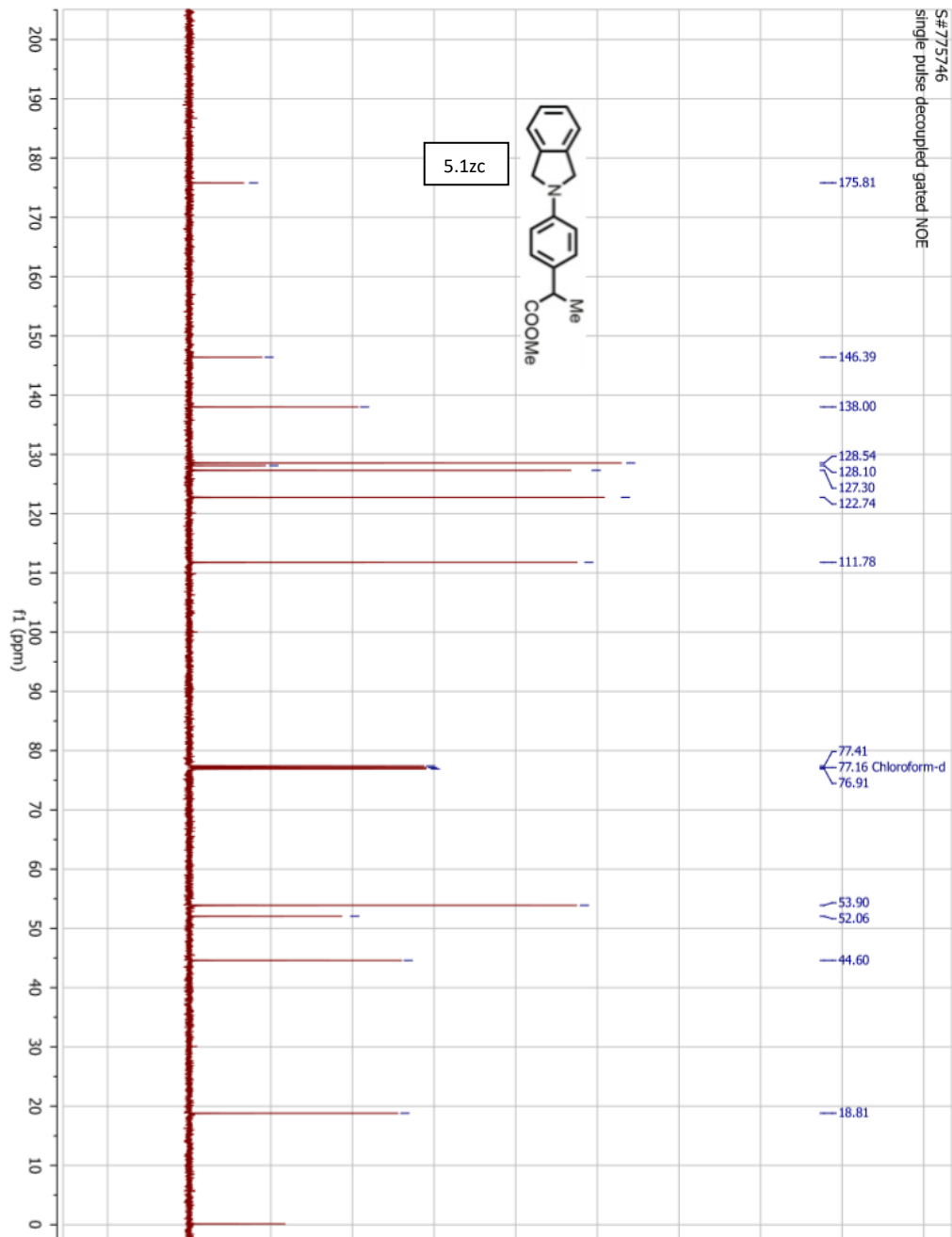




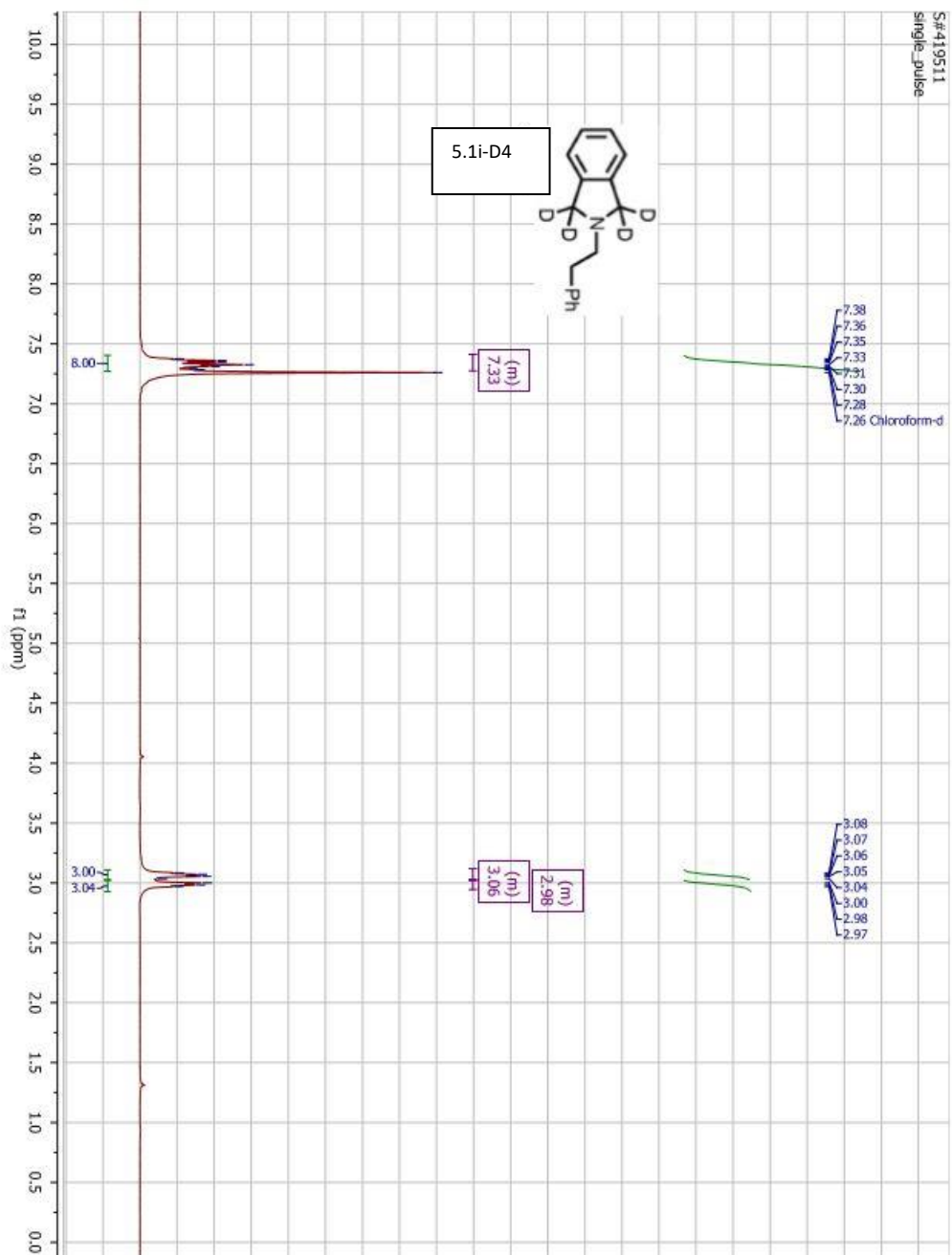




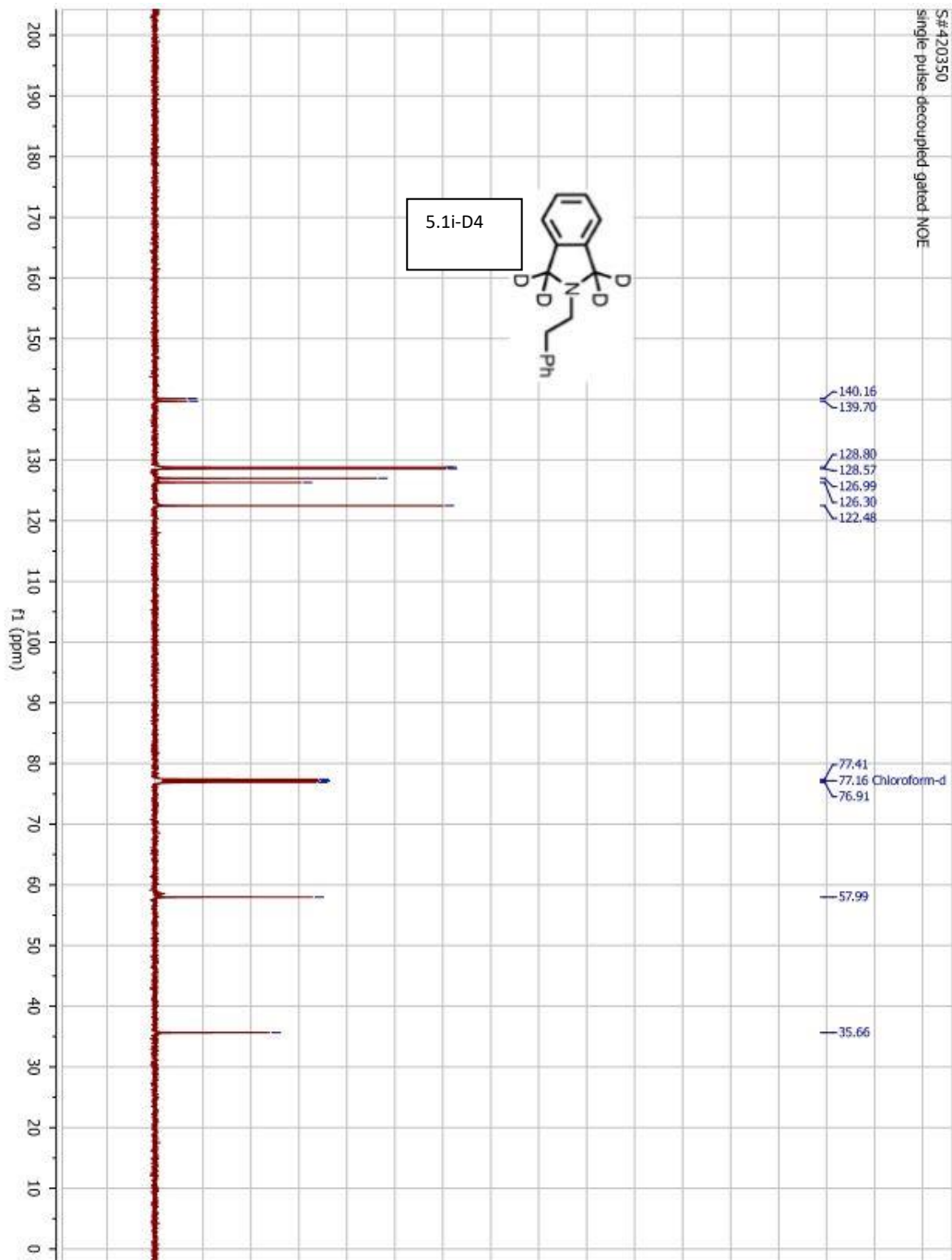


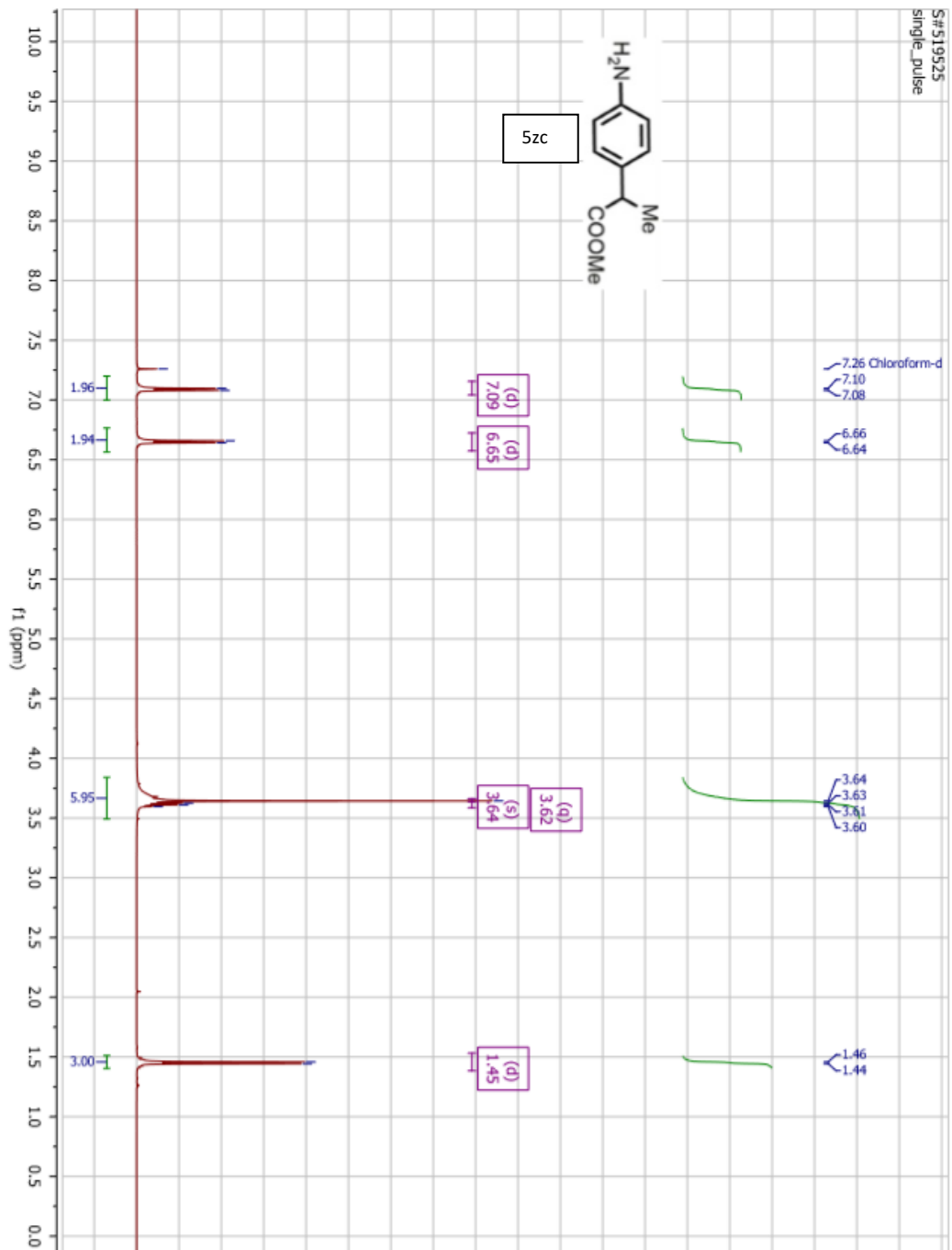


S:#419511
single_pulse

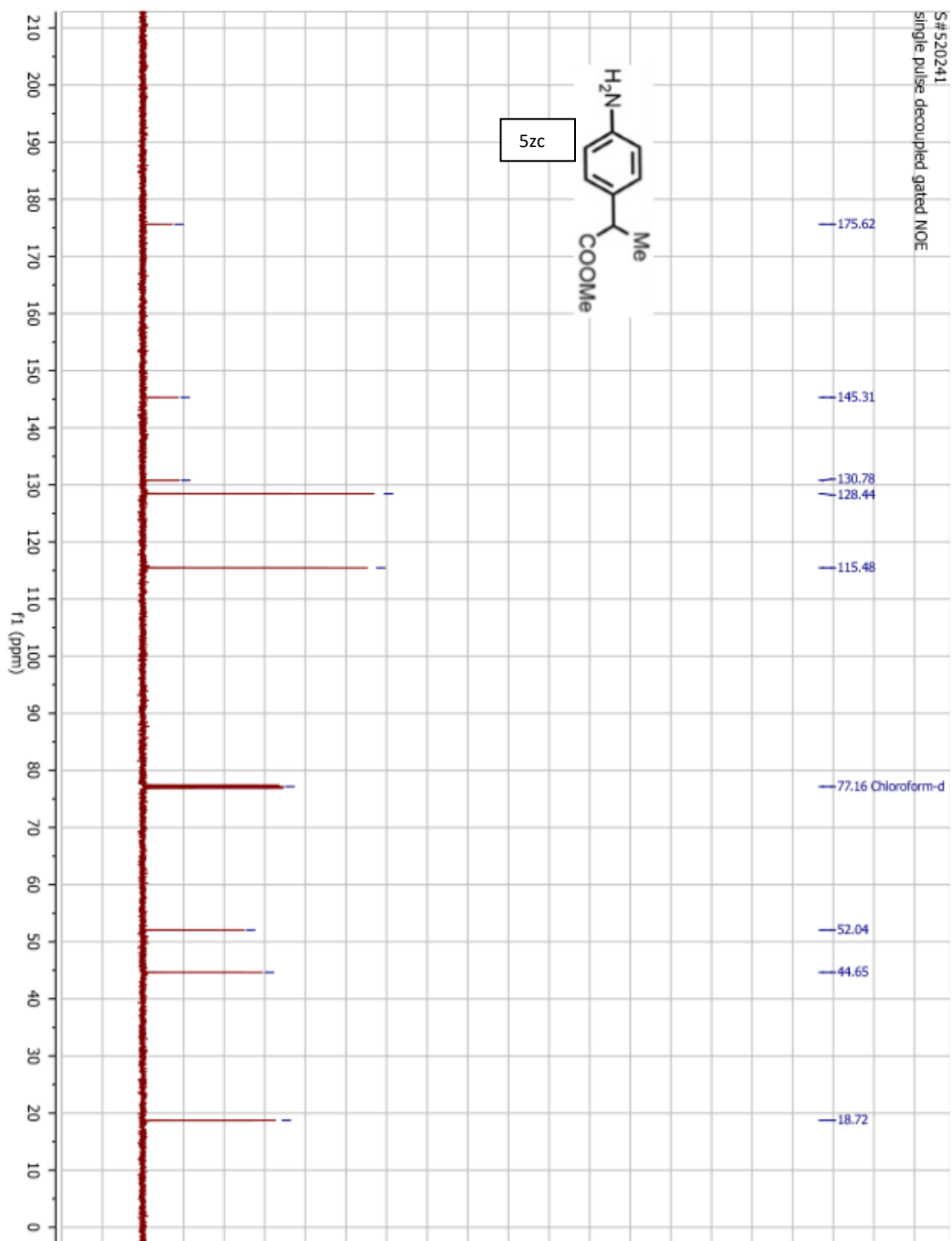
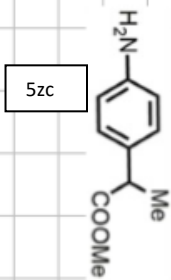


S#420350
single pulse decoupled gated NOE





S#520241
single pulse decoupled gated NOE



References

1. Blyth, A. W. *J. Chem. Soc., Trans.* **1879**, 35, 530-539.
2. Kuhn, R.; Reinemund, K.; Weygand, F. *Ber.* **1934**, 67, 1460-1463.
3. Karrer, P.; Schöpp, K.; Benz, F. *Helv. Chim. Acta.* **1935**, 18, 426-429.
4. Palfey, B. A. and Massey, V. Flavin-Dependent Enzymes. In *Comprehensive Biological Catalysis*, Volume III/Radical Reactions and Oxidation/Reduction; M. Sinnott, Ed.; Academic Press: London and San Diego, 1998; Chapter 29, pp 83–154.
5. Reid, G. A. Flavins, Flavoproteins, and Flavoproteomics. In *Flavin and Flavoproteins*; S. Chapman, R. Perham, N. Scrutton, Eds.; Rudolf Weber: Berlin, 2002; pp 3–10.
6. Massey, V.; Mueller, F.; Feldberg, R.; Schuman, M.; Sullivan, P. A.; Howell, L. G.; Mayhew, S. G.; Matthews, R. G.; Foust, G. P. *J. Biol. Chem.* **1969**, 244, 3999-4006.
7. Bruice, T. B. *Acc. Chem. Res.* **1980**, 13, 256-262.
8. Heasley, C. J.; Fitzpatrick, P. F. *Biochem. Biophys. Res. Commun.* **1996**, 225, 6-10.
9. Gadda, G.; Fitzpatrick, P. F. *Biochemistry* **2000**, 39, 1406-1410.
10. Nagpal, A.; Valley, M. P. Fitzpatrick, P. F.; Orville, A. M. *Biochemistry* **2006**, 45, 1138-1150.

11. Cesura, A. M. *Prog. Drug Res.* **1992**, *38*, 171–297.
12. Blaschko, H. *Pharmacol. Rev.* **1952**, *4*, 415–458.
13. Yamasaki; R. B. Silverman, R. B. *Biochemistry* **1985**, *24*, 6543–6550.
14. Silverman, R. B. *Acc. Chem. Res.* **1995**, *28*, 335–342.
15. Silverman, R. B.; Zhou; J. P.; Eaton, P. E. *J. Am. Chem. Soc.* **1993**, *115*, 8841–8842.
16. Brown; L. E.; Hamilton, G. E. *J. Am. Chem. Soc.* **1970**, *92*, 7225–7227.
17. Sharma, M.; Sharma, N. N.; Bhalla, T. C. *Enzyme Microb. Technol.* **2005**, *37*, 279-294.
18. Jorns, M. S. *Biochim. Biophys. Acta* **1980**, *613*, 203–209.
19. Kruse, C.G. Chiral cyanohydrins- their manufacture and utility as chiral building blocks Collins, A.N., Sheldrake, G.N. & Crosby. J (Eds.), *Chirality in Industry*, Wiley, London (1992), pp. 279-299.
20. Breslow, R. *Ann. N. Y. Acad. Sc.* **1962**, *98*, 445.
21. Breslow, R. *Pure Appl. Chem.* **1994**, *66*, 1573—1582.
22. Breslow, R. *Acc. Chem. Res.* **1980**, *13*, 170-177.
23. List, B. Introduction: Organocatalysis. *Chem. Rev.* **2007**, *107*, 5413-5415.
24. Osberger, T. J.; Rogness, D. C.; Kohrt, J. T.; Stephan, A. F.; White, M. C. *Nature* **2016**, *537*, 214-219.

25. Trost, B. M.; Brindle, C. S. *Chem. Soc. Rev.* **2010**, *39*, 1600-1632.
26. Cobb, A. J. A.; Shaw, D. M.; Longbottom, D. A.; Gold, J. B.; Ley, S. V. *Org. Biomol. Chem.* **2005**, *3*, 84-96.
27. Zheng, C.; You, S.-L. *Chem. Soc. Rev.* **2012**, *41*, 2498-2518.
28. Sheehan, J. C.; T. Hara, T. *J. Org. Chem.* **1974**, *39*, 1196-1199.
29. Flanigan, D. M.; Romanov-Michailidis, Fedor, R.-M.; White, N. A.; Tomislav, R. *Chem. Rev.* **2015**, *115*, 9307-9387.
30. Graham, D. W.; Rogers, E. F. U.S. Patent 4, 173, 631, 1979.
31. Noell, G.; Trawoeger, S.; Von Sanden-Flohe, M.; Dick, B.; Grininger, M. *ChemBioChem* **2009**, *10*, 834-837.
32. Korvinson, K. A.; Hargenrader, G. N.; Stevanovic, J.; Xie, Y.; Joseph, J.; Maslak, V.; Hadad, C. M.; Glusac, K. D. *J. Phys. Chem. A* **2016**, *120*, 7294-7300.
33. Insinska-Rak, M.; Sikorska, E.; Bourdelande, J. L.; Khmelinskii, I. V.; Prukala, W.; Dobek, K.; Karolczak, J.; Machado, I. F.; Ferreira, L. F. V.; Dulewicz, E.; Komasa, A.; Worrall, D. R.; Kubicki, M.; Sikorski, M. *J. Photochem. Photobiol. , A* **2007**, *186*, 14-23.
34. Stephan, D. W. *Science* **2016**, *354*, 1248.
35. Stephan, D. W. *J. Am. Chem. Soc.* **2015**, *137*, 10018–10032.

36. Welch, G. C.; San Juan, R. R.; Masuda, J. D.; Stephen, D. W. *Science* **2006**, *314*, 1124-1126.
37. Shang, M.; Wang, X.; Koo, S. M.; Youn, J.; Chan, J. Z.; Yao, W.; Hastings, B. T.; Wasa, M. *J. Am. Chem. Soc.* **2017**, *139*, 95-98.
38. Ren, X.; Du, F. *J. Am. Chem. Soc.* **2016**, *138*, 810–813.
39. Mummadi, S.; Unruh, D. K.; Zhao, J.; Li, S.; Krempner, C. *J. Am. Chem. Soc.* **2016**, *138*, 3286-3289.
40. Shima, S.; Pilak, O.; Vogt, S.; Schick, M.; Stagni, M. S.; Meyer-Klaucke, W.; Warkentin, E.; Thauer, R. K.; Ermler, U. *Science* **2008**, *321*, 572-575.
41. Kalz, K. F.; Brinkmeier, A.; Dechert, S.; Mata, R. A.; Meyer, F. *J. Am. Chem. Soc.* **2014**, *136*, 16626-16634.
42. Fagan, R. L. and Palfey, B. A. Flavin-Dependent Enzymes. *Comprehensive Natural Products II*. H.-W. Liu and L. Mander. Oxford, Elsevier, 2010: Chapter 3, pp 37-113.
43. Dittrich H.; Kutchan T. M. *Proc. Natl. Acad. Sci. U.S.A.* **1991**, *88*, 9969–73.
44. Clouthier, C. M.; Pelletier, J. N. *Chem. Soc. Rev.* **2012**, *41*, 1585–1605.
45. Li, C.-J. *Acc. Chem. Res.* **2009**, *42*, 335–344.
46. Luo, Y. R. Handbook of bond dissociation energies in organic compounds; CRC Press: Boca Raton, 2007.

47. Murahashi, S.; Komiya, N.; Terai, H.; Nakae, T. *J. Am. Chem. Soc.* **2003**, *125*, 15312–15313.
48. Li, Z.; Li, C.-J. *J. Am. Chem. Soc.* **2004**, *126*, 11810–11811.
49. Zhao, L.; Basle, O.; Li, C.-J. *Proc. Natl. Acad. Sci. U.S.A.* **2009**, *106*, 4106–4111.
50. Ibrahem, I.; Samec, J. S. M.; Bäckvall, J. E.; Córdova, A. *Tetrahedron Lett.* **2005**, *46*, 3965–3968.
51. Sud, A.; Sureshkumar, D.; Klusmann, M. *Chem. Commun.* **2009**, *45*, 3169–3171.
52. Zhang, J.; Tiwari, B.; Xing, C.; Chen, X.; Chi, Y. R. *Angew. Chem., Int. Ed.* **2012**, *51*, 3649–3652.
53. Zhang, G.; Ma, Y.; Wang, S.; Kong, W.; Wang, R. *Chem. Sci.* **2013**, *4*, 2645–2671.
54. Alagiri, K.; Devadig, P.; Prabhu, K.R. *Chem. Eur. J.* **2012**, *18*, 5160 – 5164.
55. Dhineskumar, J.; Lamani, M.; Alagiri, K.; Prabhu, K. R. *Org. Lett.* **2015**, *5*, 1092–1095.
56. Tanoue, A.; Yoo, W.-J.; Kobayashi, S. *Org. Lett.* **2016**, *9*, 2346–2349.
57. Pan, Y.; Kee, C. W.; Chen, L.; Tan, C.-H. *Green Chem.* **2011**, *13*, 2682–2685.
58. Freeman, D. B.; Furst, L.; Condie, A. G.; Stephenson, C. R. J. *Org. Lett.* **2012**, *14*, 94–97.
59. Chen, Y, Feng, G.; *Org. Biomol. Chem.* **2015**, *13*, 4260–4265.

60. Yoo, W-J.; Kobayashi, S. *Green Chem.* **2014**, *16*, 2438-2442.
61. Zhao, G.; Yang, C.; Guo, L.; Sun, H.; Chen, C.; Xia, W. *Chem. Commun.* **2012**, *48*, 2337-2339.
62. Ueda, H.; Yoshida, K.; Tokuyama, H. *Org. Lett.* **2014**, *16*, 4194-4197.
63. Pinter, A'; Sud, A.; Sureshkumar, D.; Klussmann, M. *Angew. Chem., Int. Ed.* **2010**, *49*, 5004.
64. Shu, X-Z.; Yang, Y-F.; Xia, X-F.; Ji, K-G.; Liu, X-Y.; Liang, Y-M. *Org. Biomol. Chem.* **2010**, *8*, 4077-4079.
65. Dhineshkumar, J.; Samaddar, P.; Prabhu K. R. *ACS Omega* **2017**, *2*, 4885-4893.
66. Iida, H.; Imada, Y.; Murahashi, S.-I. *Org. Biomol. Chem.* **2015**, *13*, 7599-7613.
67. Cibulka, R. *Eur. J. Org. Chem.* **2015**, *2015*, 915-932.
68. Murray, A. T.; Dowley, M. J. H.; Pradaux-Caggiano, F.; Baldansuren, A.; Fielding, A. J.; Tuna, F.; Hendon, C. H.; Walsh, A.; Lloyd-Jones, G. C.; John, M. P.; Carbery, D. R. *Angew. Chem., Int. Ed.* **2015**, *127*, 9125-9128.
69. Chen, S.; Hossain, M. S.; Foss, F. W., Jr. *Org. Lett.* **2012**, *14*, 2806-2809.
70. Murahashi, S.-I.; Oda, T.; Masui, Y. *J. Am. Chem. Soc.* **1989**, *111*, 5002-5003.
71. Imada, Y.; Iida, H.; Kitagawa, T.; Naota, T. *Chem.-Eur. J.* **2011**, *17*, 5908-5920.
72. Mazzini, C. Lebreton, J.; Furstoss, R. *J. Org. Chem.* **1996**, *61*, 8-9.

73. Pandiri, M.; Hossain, M. S.; Foss, F. W., Jr; Rajeshwar, K.; Paz, Y. *Phys. Chem. Chem. Phys.* **2016**, *18*, 18575–18583.

74. Rochkind, M.; Pandiri, M.; Hossain, M. S.; Foss, F. W., Jr; Rajeshwar, K.; Paz, Y. *J. Phys. Chem. C* **2016**, *120*, 16069–16079.

75. Effect of temperature on redox potential is governed by Nernst Equation as follow:

$$E = E^{\circ} + \frac{RT}{nF} \ln \frac{[\text{Ox}]}{[\text{Red}]}$$

76. Neel, A. J.; Hehn, J. P.; Triplet, P. F.; Toste, F. D. *J. Am. Chem. Soc.* **2013**, *135*, 14044–14047.

77. Sun, X.; Lv, X-H.; Ye, L-M.; Hu, Y.; Chen, Y-Y.; Zhang, X-J.; Yan, M. *Org. Biomol. Chem.* **2015**, *13*, 7381–7383.

78. Boess, E.; Schmitz, C.; Klussmann, M. *J. Am. Chem. Soc.* **2012**, *134*, 5317–5325.

79. Imada, Y.; Iida, H.; Ono, S.; Masui, Y.; Murahashi, S.-I. *Chem. -Asian J.* **2006**, *1*, 136–147.

80. Ménová, P.; Cibulka, R. *J. Mol. Catal. A: Chemical* **2012**, *363*, 362–370.

81. Kobayashi, S.; Sugiura, M.; Kitagawa, H.; Lam, W. W. L. *Chem. Rev.* **2002**, *102*, 2227–2302.

82. Corma, A.; Garcia, H. *Chem. Rev.* **2003**, *103*, 4307–4365

83. Sukumaran, J.; Hanefeld, U. *Chem. Soc. Rev.* **2005**, *34*, 530–542.

84. Chen, W.; Seidel, D. *Org. Lett.*, **2014**, *16*, 3158–3161.

85. J. T. Scanlan, *J. Am. Chem. Soc.*, **1935**, *57*, 890.

86. Shang, M.; Cao, M.; Wang, Q.; Wasa, M. *Angew. Chem., Int. Ed.* **2017**, *56*, 13338–13341.
87. Domilng, A. *Chem. Rev.* **2006**, *106*, 17. Reaction Polymers, ed. W. F. Gum, W. Riese and H. Ulrich, Hanser, New York, Oxford University Press, **1992**.
88. Ramon, D. J.; Yus, M. *Angew. Chem., Int. Ed.* **2005**, *44*, 1602.
89. Simon, C.; Constantieux, T.; Rodriguez, J. *Eur. J. Org. Chem.* **2004**, 4957
90. Isambert, N.; Cruz, M.; Arevalo, J.; Gomez, E.; Lavilla, R. *Org. Lett.* **2007**, *9*, 4199–4202
91. Wu, X.; Zhao, P; Geng, X.; Wang, C.; Wu, Y.; Wu, A. *Org. Lett.* **2018** *20*, 688–691.
92. Clark, E. R.; Ingleson, M. J. *Angew. Chem., Int. Ed.* **2014**, *53*, 11306–11309.
93. Scott, D. J.; Simmons, T. R.; Lawrence, E. J.; Wildgoose, G. G.; Fuchter, M. J.; Ashley, A. E. *ACS Catalysis* **2015**, *5*, 5540–5544.
94. Ghattas, G.; Bizzarri, C.; Holscher, M.; Langanke, J.; Gürtler, C.; Leitnerb, W.; Subhani, M. A. *Chem. Commun.* **2017**, *53*, 3205–3208.
95. Tofan, D.; Gabbai, F. P. *Chem. Sci.* **2016**, *7*, 6768–6778.
96. Dorko, E.; Szabl, M.; Kotai, B.; Papai, I.; Domjan, A.; Soos, T. *Angew. Chem., Int. Ed.* **2017**, *56*, 9512–9516.
97. Selmar, D.; Lieberei, R.; Conn, E. E.; Biehl, B. *Physiol. Plant* **1989**, *75*, 97–101.
98. Griengl, H.; Hickel, A.; Johnson, D. V.; Kratky, C.; Schmidta, M.; Schwabc, H. *Chem. Commun.* **1997**, 1933.

99. Williams, R. F.; Shinkai, S.; Bruice, T. C. *Proc. Nat. Acad. Sci. USA* **1975**, *72*, 1763-1767.
100. Wagner, U. G.; Hasslacher, M.; Griengl, H.; Schwab, H.; Kratky, C. *Structure* **1996**, *4*, 811-822.
101. Blankenhorn, G.; Ghisla, S.; Hemmerich, P. *Z. Naturforsch* **1972**, *27*, 1038-1040.
102. Hoegy, S. E.; Mariano, P. S. *Tetrahedron* **1997**, *53*, 5027-5046.
103. Guo, X.; Zipse, H.; Mayr, H. *J. Am. Chem. Soc.* **2014**, *136*, 13863-13873.
104. Deng, J.; Sanchez, T.; Neamati, N.; Briggs, J. M. *J. Med. Chem.* **2006**, *49*, 1684.
105. Baghel, G. S.; Ramanujam, B.; Rao, C. P. *J. Photochem. Photobiol., A: Chemistry* **2009**, *202*, 172-177.
106. Hiroyasu Takahashi, Nobuyuki Kashiwa, Yuichi Hashimoto and Kazuo Nagasawa. *Tetrahedron Lett.* **2003**, *42*, 2935-2938.
107. Li, W.-S.; Zhang, N.; Sayre, L. M. *Tetrahedron* **2001**, *57*, 4507-4522.
108. Leonard, N. J.; Leubner, G. W. *J. Am. Chem. Soc.* **1949**, *71*, 3408-3411.
109. Kumar, A.; Kumar, M.; Gupta, M. K. *Tetrahedron Lett.* **2009**, *50*, 7024-7027.
110. Ball, S.; Bruice, T. C. *J. Am. Chem. Soc.* **1980**, *102*, 6498-6503.
111. a) Sichula, V.; Kucheryavi, P.; Khatmullin, R.; Hu, Y.; Mirzakulova, E.; Vyas, S.; Manzer, S.F.; Hadad, C. M.; Glusac, K. D. *J. Phys. Chem.* **2010**, *114*, 12138-12147. b) Krzyminski, K.; Malecha, P.; Zadikowiz, B.; Wroblewska, A.; Blazejowski, J. *Spect. Acta* **2011**, *78*, 401-409.

112. Bolm, C.; Legros, J.; Paih, J. L.; Zani, L. *Chem. Rev.* **2004**, *104*, 6217–6254.
113. Sun, C. L.; Li, B. J.; Shi, Z. J. *Chem. Rev.* **2011**, *111*, 1293–1314.
114. Correa, A.; García Manchen, O.; Bolm, C. *Chem. Soc. Rev.* **2008**, *37*, 1108–1117.
115. Colombo, L.; Ulgheri, F.; Prati, L. *Tetrahedron Lett.* **1989**, *30*, 6435–6436.
116. Barrett, I. C.; Langille, J. D.; Kerr, M. A. *J. Org. Chem.* **2000**, *65*, 6268–6269.
117. Minisci, F.; Vismara, E.; Fontana, F. *J. Org. Chem.* **1989**, *54*, 5224–5227.
118. Fiandanese, V.; Miccoli, G.; Naso, F.; Ronzini, L. *J. Organomet. Chem.* **1986**, *312*, 343–348.
119. Fürstner, A.; Leitner, A.; Méndez, M.; Krause, H. *J. Am. Chem. Soc.* **2002**, *124*, 13856–13863.
120. Nagano, T.; Hayashi, T. *Org. Lett.* **2004**, *6*, 1297–1299.
121. Zhu, K.; Shaver, M. P.; Thomas, S. P. *Chem. Sci.* **2016**, *7*, 3031–3035.
122. Huehls, C. B.; Lin, A.; Yang, J. *Org. Lett.* **2014**, *16*, 3620–3623.
123. Noda, D.; Tahara, A.; Sunada, Y.; Nagashima, H. *J. Am. Chem. Soc.* **2016**, *138*, 2480–2483.
124. DalZotto, C.; Virieux, D.; Campagne, J. -M. *Synlett.* **2009**, 276–278.
125. Bauer, I.; Knolker, H. -J. *Chem. Rev.* **2015**, *115*, 3170–3387.
126. Dai, L. -X. Tu, T.; You, S. -L.; Deng, W. -P.; Hou, X. -L. *Acc. Chem. Res.* **2003**, *36*, 659–667.

127. Carvalho, L. C. R.; Fernandes, E.; Marques, M. M. B. *Chem. -Eur. J.* **2011**, *17*, 12544–12555.
128. Battershill, A. J.; Scott, L. J. *Drugs* **2006**, *66*, 51.
129. Bachert, C.; Vovolis, V.; Margari, P.; Murrieta-Aguttes, M.; Santoni, J. *P. Allergy* **2001**, *56*, 653–659
130. Falcó, J. L.; Piqué, M.; González, M.; Buira, I.; MÍndez, E.; Terencio, J.; Pérez, C.; Príncipe, M.; Palomer, A.; Guglietta, A. *Eur. J. Med. Chem.* **2006**, *41*, 985.
131. Wright, J. B. *Chem. Rev.* **1951**, *48*, 397–541.
132. Middleton, R. W.; Wibberley, D. G. *J. Heterocycl. Chem.* **1980**, *17*, 1757–1760.
133. Du, L. -H.; Wang, Y.-G. *Synthesis* **1995**, *51*, 5913–5818.
134. Vanden Eynde, J. J.; Delfosse, F.; Lor, P.; Haverbeke, Y. V. *Tetrahedron* **1995**, *51*, 5813–5818.
135. Ma, H. Q.; Wang, Y. L.; Wang, J. Y. *Heterocycles* **2006**, *68*, 1669–1673.
136. Itoh, T.; Nagata, K.; Ishikawa, H.; Ohsawa, A. *Heterocycles* **2004**, *63*, 2769–2783.
137. Chari, M. A.; Sadanandam, P.; Shobha, D.; Mukkanti, K. *J. Heterocycl. Chem.* **2010**, *47*, 153–155.
138. Cimarelli, C.; Nicola, M. D.; Diomedi, S.; Giovannini, R.; Hamprecht, D.; Properzi, R.; Sorana, F.; Marcantoni, E. *Org. Biomol. Chem.* **2015**, *13*, 11687–11695.

139. Chen, S.; Hossain, M. S.; Foss, F. W., Jr. *ACS Sustainable Chemistry & Engineering* **2013**, *1*, 1045–1051.
140. Cho, C. S.; Kim, J. U. *Bull. Korean Chem. Soc.* **2008**, *29*, 1097.
141. Mirza, B.; Zeeb, M. *Synth. Commun.* **2015**, *45*, 524–530.
142. Xue, D.; Long, Y-Q. *J. Org. Chem.* **2014**, *79*, 4727–4734.
143. Sun, X.; Lv, X-H.; Ye, L.-M.; Hu, Y.; Chen, Y-Y. ; Zhang, X.-J.; Yan, M. *Org. Biomol. Chem.* **2015**, *13*, 7381–7383.
144. Jaiswal, G.; Landge, V. G.; Jagadeesan, D.; Balaraman, E. *Green Chem.* **2016**, *18*, 3232-3238
145. Zhang, E.; Tian, H.; Xu, S.; Yu, X.; Xu, Q. *Org. Lett.* **2013**, *15*, 2704–2707.
146. Yu, J.; Lu, M. *Res. Chem. Intermed.* **2015**, *41*, 10017–10025.
147. Nguyen, T. B.; Bescont, J. L.; Ermolenko, L.; Al-Mourabit, A. *Org. Lett.* **2013**, *15*, 6218.
148. Brasche, G.; Buchwald, S. L. *Angew. Chem., Int. Ed.* **2008**, *120*, 1958–1960.
149. Peng, J.; Ye, M.; Zong, C.; Hu, F.; Feng, L.; Wang, X.; Wang, C.; Chen, C. *J. Org. Chem.* **2011**, *76*, 716–719.
150. Saha, P.; Ali, M. A.; Ghosh, P.; Punniyamurthy, T. *Org. Biomol. Chem.* **2010**, *8*, 5692–5699.
151. Ratnikov, M. O.; Xu, X.; Doyle, M. P. *J. Am. Chem. Soc.* **2013**, *135*, 9475–9479.

152. Yan, X.; Fang, K.; Liua, H.; Xi, C. *Chem. Commun.* **2013**, *49*, 10650–10652.
153. Bharate, S. B.; Mudududdla, R.; Sharma, R.; Vishwakarma, R. A. *Tetrahedron Lett.* **2013**, *54*, 2913–2915.
154. Chen, Y. L.; Hedberg, K. G.; Guarino, K. G. *Tetrahedron Lett.* **1989**, *30*, 1067–1068.
155. Marcazzan, P.; Abu-Gnim, C.; Seneviratne, K. N.; James, B. R. *Inorg. Chem.* **2004**, *43*, 4820–4824.
156. Mayilmurugan, R.; Sankaralingam, M.; Suresh, E.; Palaniandavar, M. *Dalton Trans.* **2010**, *39*, 9611-9625.
157. Pap, J. S.; Draksharapu, A.; Giogi, M.; Browne, W. R.; Kaizer, J.; Speier, G. *Chem. Commun.* **2014**, *50*, 1326-1329.
158. Bjornstad, L. G.; Giorgio Zoppellaro, G.; Tomter, A. B.; Falnes, P. O.; Andersson, K. K. *Biochem. J.* **2011**, *434*, 391-398.
159. Yatsunyk, L. A.; Walker, F. A. *Inorg. Chem.* **2004**, *43*, 757-777.
160. Chaudhuri, S.; Patra, S. C.; Saha, P.; Roy, A. S.; Maity, S.; Bera, S.; Sardar, P. S.; Ghosh, S.; Weyhermuller, T.; Ghosh, P. *Dalton Trans.* **2013**, *42*, 15028-15042.
161. Parsons, P. J.; Jones, D. R.; Walsh, L. J.; Allen, L. A. T.; Onwubiko, A.; Preece, L.; Board, J.; White, A. J. P. *Org. Lett.* **2017**, *19*, 2533.
162. Fouseki, M. M.; Damianakos, H.; Karikas, G. A.; Roussakis, C.; P Gupta, M.; Chinou, I. *Fitoterapia* **2016**, *115*, 9.
163. Hu, S.; Yuan, L.; Yan, H.; Li, Z. *Bioorg. Med. Chem. Lett.* **2017**, *27*, 4075.

- 164.** Flores, B.; Molinski, T. F. *Org. Lett.* **2011**, *13*, 3932.
- 165.** Augner, D.; Schmalz, H.-G. *Synlett* **2015**, *26*, 1395.
- 166.** Choomuenwai, V.; Beattie, K. D.; Healy, P. C.; Andrews, K. T.; Fechner, N.; Davis, R. A. *Phytochemistry* **2015**, *117*, 10.
- 167.** Lowinger, T. B.; Chu, J.; Spence, P. L. *Tetrahedron Lett.* **1995**, *36*, 8383.
- 168.** Link, J. T.; Raghavan, S.; Gallant, M.; Danishefsky, S. J.; Chou, T. C.; Ballas, L. M. *J. Am. Chem. Soc.* **1996**, *118*, 2825.
- 169.** Dominh, T.; Johnson, A. L.; Jones, J. E.; Senise, P. P. *J. Org. Chem.* **1977**, *42*, 4217–4221.
- 170.** Ghosh, U.; Bhattacharyya, R.; Keche, A. *Tetrahedron* **2010**, *66*, 2148–2155.
- 171.** Tian, Y.; Wei, J.; Wang, M.; Li, G.; Xu, F. *Tetrahedron Lett.* **2018**, *59*, 1866–1870.
- 172.** Das, S.; Addis, D.; Knöpke, L. R.; Bentrup, U.; Junge, K.; Brckner, A.; Beller, M. *Angew. Chem., Int. Ed.* **2011**, *50*, 9180–9184.
- 173.** Verma, A.; Patel, S.; Meenakshi, M.; Kumar, A.; Yadav, A.; Kumar, S.; Jana, S.; Sharma, S.; Prasad, C. D.; Kumar, S. *Chem. Commun.* **2015**, *51*, 1371–1374.
- 174.** Nozawa-Kumada, K.; Kadokawa, J.; Kameyama, T.; Kondo, Y. *Org. Lett.* **2015**, *17*, 4479–4481.
- 175.** Adachi, S.; Onozuka, M.; Yoshida, Y.; Ide, M.; Saikawa, Y.; Nakata, M. *Org. Lett.* **2014**, *16*, 358–361.

176. Wang, P. M.; Pu, F.; Liu, K. Y.; Li, C. J.; Liu, Z. W.; Shi, X. Y.; Fan, J.; Yang, M. Y.; Wei, J. F. *Chem. -Eur. J.* **2016**, *22*, 6262–6267.
177. Adachi, S.; Watanabe, K.; Iwata, Y.; Kameda, S.; Miyaoka, Y.; Onozuka, M.; Mitsui, R.; Saikawa, Y.; Nakata, M. *Angew. Chem., Int. Ed.* **2013**, *52*, 2087–2091.
178. Mori, M.; Chiba, K.; Ban, Y. *J. Org. Chem.* **1978**, *43*, 1684–1687.
179. Orito, K.; Horibata, A.; Nakamura, T.; Ushito, H.; Nagasaki, H.; Yuguchi, M.; Yamashita, S.; Tokuda, M. *J. Am. Chem. Soc.* **2004**, *126*, 14342–14343.
180. Zhang, C.; Ding, Y.; Gao, Y.; Li, S.; Li, G. *Org. Lett.* **2018**, *20*, 2595–2598.
181. Liu, B.; Wang, Y.; Liao, B.; Zhang, C.; Zhou, X. *Tet. Lett.* **2015**, *56*, 5776–5780.
182. Cho, C. K.; Ren, W. X. *Tetrahedron Lett.* **2009**, *50*, 2097–2099.
183. Han, J.; Wang, N.; Huang, Z.-B.; Zhao, Y.; Shi, D.-Q. *J. Org. Chem.* **2017**, *82*, 6831–6839.
184. Fujioka, M.; Morimoto, T.; Tsumagari, T.; Tanimoto, H.; Nishiyama, Y.; Kakiuchi, K. *J. Org. Chem.* **2012**, *77*, 2911–2923.
185. Ling, F.; Ai, C.; Lv, Y.; Z, W. *Adv. Synth. Catal.* **2017**, *359*, 3707–3712.
186. Li, H.-J.; Zhang, Y.-Q.; Tang, L.-F. *Tetrahedron* **2015**, *71*, 7681–7686.
187. Kobayashi, K.; Chikazawa, Y. *Tetrahedron* **2017**, *73*, 7245–7253.
188. Xu, Y.; Liu, X.-Y.; Wang, Z.-H.; Tang, L.-F. *Tetrahedron* **2015**, *71*, 7681–7686.
189. Speck, K.; Magauer, T. *Beilstein J. Org. Chem.* **2013**, *9*, 2048–2078.

- 190.** Heugebaert, T. S. A.; Roman, B. I.; Stevens, C. V. *Chem. Soc. Rev.* **2012**, *41*, 5626–5640.
- 191.** White, M. C. *Science* **2012**, *335*, 807–809.
- 192.** Sterckx, H.; De Houwer, J.; Mensch, C.; Caretti, I.; Tehrani, K. A.; Herrebout, W. A.; Van Doorslaer, S.; Maes, B. U. W. *Chem. Sci.* **2016**, *7*, 346–357.
- 193.** Niki, E.; Yokoi, S.; Tsuchiya, J.; Kamiya, Y. *J. Am. Chem. Soc.* **1978**, *105*, 1498–1503.
- 194.** Weinstein, A. B.; Stahl, S. S. *Catal. Sci. Technol.* **2014**, *4*, 4301–4307.
- 195.** Schweitzer-Chaput, B.; Sud, A.; Pinter, A.; Dehn, S.; Schulze, P.; Klussman, M. *Angew. Chem., Int. Ed.* **2013**, *52*, 13228–13232.
- 196.** Zelenka, J.; Hartman, T.; Klímová, K.; Hampl, F.; Cibulka, R. *ChemCatChem* **2014**, *6*, 2843–2846.
- 197.** Poudel, P. P.; Arimisu, K.; Yamamoto, K. *Chem. Commun.* **2016**, *52*, 4163–4166.
- 198.** Iida, H.; Ishikawa, T.; Nomura, K.; Murahashi, S.-I. *Tetrahedron Lett.* **2016**, *57*, 4488–4491.
- 199.** Chernick, E. T.; Ahrens, M. J.; Scheidt, K. A.; Wasielewski, M. R. *J. Org. Chem.* **2005**, *70*, 1486–1489.
- 200.** Ménová, P.; Hana Dvořáková, H.; Václav Eigner, V.; Jiří Ludvík, J.; Cibulka, R. *Adv. Synth. Catal.* **2013**, *355*, 3451–3462.
- 201.** Groysman, S.; Sergeeva, E.; Goldberg, I.; Kol, M. *Eur. J. Inorg. Chem.* **2005**, *2005*, 2480.

202. Woolley, D. W.; Stewart, John Morrow. *J. Med. Chem.* **1963**, *6*, 599–601.
203. Khanna, I. K.; Weier, R. M.; Lentz, K. T.; Swenton, L.; Lankin, D. C. *J. Org. Chem.* **1995**, *60*, 960.
204. Sabitha, G.; Reddy, B. V. S.; Srividya, R.; Yadav, J. S. *Synth. Commun.* **1999**, *29*, 2311–2315.
205. Zulfiqar, A. K.; Michio, I.; Thomas, W. *Tetrahedron* **2010**, *66*, 6639
206. Wei, W.-t.; Dong, X.-j.; Nie, S.-z.; Chen, Y.-y.; Shang, X.-j.; Yan, M. *Org. Lett.* **2013**, *15*, 6018–6021.
207. Nakao, A.; Suzuki, H.; Uena, H.; Iwasaki, H.; Setsuta, T.; Kashima, A.; Sunada, D. *Bioorg. Med. Chem.* **2015**, *23*, 4952–4969.
208. Tsang, A. S.-K.; Hashmi, A. S. K.; Comba, P.; Kerscher, M.; Chan, B.; Todd, M. H. *Chem. - Eur. J.* **2017**, *23*, 9313–9318.
209. Oss, G.; de Vos, S. D.; Luc, K. N. H.; Harper, J. B.; Nguyen, T. V. *J. Org. Chem.* **2018**, *83*, 1000–1010.
210. Mamada, M.; Perez-Bolivar, C.; Anzenbacher, P. Jr. *Org. Lett.* **2011**, *13*, 4882.
211. Cho, C. S.; Kim, J. U. *Bull. Korean Chem. Soc.* **2008**, *29*, 1097.
212. Senthilkumar, S.; Kumarajja, M. *Tetrahedron Lett.* **2014**, *55*, 1971–1974.
213. Chebolu, R.; Kommi, D. N.; Kumar, D.; Bollineni, N.; Chakraborti, A. K. *J. Org. Chem.* **2012**, *77*, 10158–10167.
214. Lin, J.-P.; Zhang, F.-H.; Long, Y.-Q. *Org. Lett.* **2014**, *16*, 2822–2825.
215. Hari, D. P.; Konig, B. *Org. Lett.* **2011**, *13*, 3852–3822.

- 216.** Gu, K.; Zhang, Z.; Zongbi, B.; Xing, H.; Yang, Q.; Ren, Q. *Eur. J. Org. Chem.* **2016**, 3939–3942.
- 217.** Zhang, L.; Peng, C.; Zhao, D.; Wang, Y.; Fu, H-J.; Shen, Q.; Li, J-X. *Chem. Commun.* **2012**, 48, 5928–5930.
- 218.** Chen, Y.-y.; Zhang, X.-j.; Yuan, H.-m.; Wei, W.-t.; Yan, M. *Chem. Commun.* **2013**, 49, 10974–10976.
- 219.** Mahajan, P. S.; Mahajan, J. P.; Mhaske, S. B. *Synth. Commun.* **2013**, 43, 2508–2516.
- 220.** Cano, R.; Ramon, D. J.; Yus, M. *J. Org. Chem.* **2011**, 76, 654–660.
- 221.** Murata, S.; Miura, M.; Nomura, M. *J. Org. Chem.* **1989**, 54, 4700–4702.
- 222.** Kito, T.; Yoshinaga, K.; Yamaye, M.; Mizobe, H. *J. Org. Chem.* **1991**, 56, 3336.
- 223.** Sun, C.; Zou, X.; Li, F. *Chem. - Eur. J.* **2013**, 19, 14030–14033
- 224.** Wang, A.; Yang, Z.; Liu, J.; Gui, Q.; Chen, X.; Tan, Z.; Shi, J-C. *Synth. Commun.* **2014**, 44, 280–288.
- 225.** Kosower, E. M. *J. Am. Chem. Soc.* **1955**, 77, 3883–3885.
- 226.** Mahesh, D.; Sadhu, P.; Punniyamurthy, T.; *J. Org. Chem.* **2015**, 80, 1644–1650.
- 227.** Mao, Z.; Wang, Z.; Li, J.; Song, X.; Luo, Y. *Synth. Commun.* **2010**, 40, 1963–1977.
- 228.** Tan, K. L.; Vasudevan, A.; Bergman, R. G.; Ellman, J. A.; Souers, A. J. *Org. Lett.* **2003**, 5, 2131–2134.

229. Kanhed, A. M.; Sinha, A.; Machhi, J.; Tripathi, A.; Parikh, Z. S.; Pillai, P. P.; Giridhar, R.; Yadav, M. R. *Bioorg. Chem.* **2015**, *61*, 7–12.
230. Jaouen, A.; Helissey, P.; Desbène-Finck, S.; Giorgi-Renault, S. *Heterocycles* **2008**, *75*, 2745–2759.
231. Chattopadhyay, P.; Rai, R.; Pandey, P. S. *Synth. Commun.* **2006**, *36*, 1857.
232. Lin, C.; Zhen, L.; Cheng, Y.; Du, H.J.; Zhao, H.; Wen, X.; Kong, L.Y.; Xu, Q. L.; Sun, H. *Org. Lett.* **2015**, *17*, 2684–2687.
233. Watanabe, Y.; Shim, S.C.; Uchida, H.; Mitsudo, T.; Takegami, Y. *Tetrahedron* **1979**, *35*, 1433–1436.
234. Ohmura, T.; Kijima, A.; Suginome, M. *J. Am. Chem. Soc.* **2009**, *131*, 6070–6071.
235. Subbarayappa, A.; Patoliya, P. U. *Indian J. Chem., Sect. B: Org. Chem. Incl Med. Chem.* **2009**, *48B*, 545–552.
236. Jeffrey, J.L.; Bartlett, E.S.; Sarpong, R. *Angew. Chem., Int. Ed.* **2013**, *52*, 2194–2197.
237. Benard, S.; Neuville, L.; Zhu, J. *Chem. Commun.* **2010**, *46*, 3393–3395.
238. Fenton, G. W.; Ingold, C. K. *J. Chem. Soc.* **1928**, *130*, 3295.
239. Azzena, U.; Demartis, S.; Pilo, L.; Piras, E. *Tetrahedron* **2000**, *56*, 8375–8382.
240. Crestey, F.; Jensen, A.; Borch, M.; Andreasen, J. T.; Andersen, J.; Balle, T.; Kristensen, J. L. *J. Med. Chem.* **2013**, *56*, 9673–9682.
241. Shi, L.; Hu, L.; Wang, J.; Cao, X.; Gu, H. *Org. Lett.* **2012**, *14*, 1876–1879.

- 242.** Orito, K.; Miyazawa, M.; Nakamura, T.; Horibata, A.; Ushito, H.; Nagasaki, H.; Yuguchi, M.; Yamashita, S.; Yamazaki, T.; Tokuda, M. *J. Org. Chem.* **2006**, *71*, 5951–5958.
- 243.** Ordóñez, M.; Tibhe, G.D.; Zamudio-Medina, A.; Viveros-Ceballos, J. *L. Synthesis* **2012**, *44*, 569–574
- 244.** Yan, X.; Fang, K.; Liua, H.; Xi, C. *Chem. Commun.* **2013**, *49*, 10650–10652.
- 245.** Ruiz Espelt, L.; Wiensch, E.M.; Yoon, T.P. *J. Org. Chem.* **2013**, *78*, 4107–4114.
- 246.** Huang, W. J.; Singh, O. V.; Chen, C. H.; Chiou, S. Y.; Lee, S. S. *Helv. Chim. Acta* 2002, *85*, 1069–1078.
- 247.** Ang, W. J.; Chng, Y. S.; Lam, Y. *RSC Adv.* **2015**, *5*, 81415–81428.
- 248.** Liu, Y.; Shi, S.; Achtenhagen, M.; Liu, R.; Szostak, M. *Org. Lett.* **2017**, *19*, 1614–1617.
- 249.** Mayer, U.; Gutmann, V.; Gerger, W. The Acceptor Number – A Quantitative Empirical Parameter for the Electrophilic Properties of Solvents, *Monat. Chem.* **1975**, *106*, 1235.

Biographical Information

Pawan Thapa was born in Sunsari, Nepal. He secured his BS in Chemistry and MS in Organic Chemistry from the Tribhuvan University, Nepal. During his MS thesis work, he studied the isolation of secondary metabolites from medicinal plants under supervision of Dr. Susan Joshi. In 2014, he joined Professor Frank Foss' group at the University of Texas, Arlington. His research focused on development of selective oxidation methods using redox active flavin and iron catalysts which are inspired by nature unique selectivity.